RF Energy Harvesting for INTERNET OF THINGS

K.J. Vinoy

ECE Dept
Indian Institute of Science
Bangalore 560012

ECE Dept, Indian Institute of Science

- **Vision Statement:** Excellence in Theoretical and Experimental Research in Communications, Signal Processing, Microelectronics and RF/Photonics.
- **Faculty: 24;** Fellows of IEEE: 4; Fellows of INAE: 8
- Active in Publications: Books, Book Chapters, Journal & Conference Papers; Patents; Standardization etc
- Collaborative research

People
Masters Students
[ME, MSc→ Mtech, Mtech(Res)]
PhD Students
Project Staff

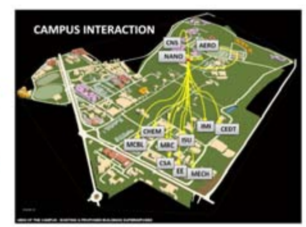

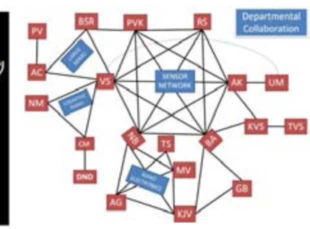

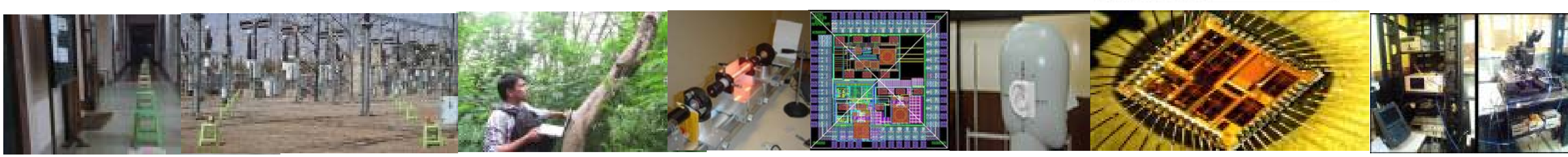

ECE: Microwave Engineering

K.J. Vinoy

- Low-Actuation Voltage Capacitive RF MEMS Switch (<10V)
  - Low-complexity fabrication process to enhance process yield
  - High reliability: no failure even up to 10 million cycles of operation tested
- Meso-scale Electrostatic Phase Shifter on microwave Laminate (MEPL)
  - Utilizes modern printed circuit board fabrication technology.
  - X-band monolithic antenna array system on the microwave laminate board demonstrated.

- Wideband group delay engineering in RF circuits for radar, medical imaging, and spectrum sensing.
  - Demonstration uses two stage All – Pass Networks; can be extended over multiple stages to obtain a higher bandwidth and/or higher group delay slope.
- RF energy harvesting circuits
  - Integrated with RF transmitters and sensors for practical IoT nodes
  - High efficiency RF-DC converter which can operate at input power of -20dBm (10µW) at 2.4GHz using UMC 130nm process MOSFETs.
- FEM based algorithms for Electromagnetic circuits & components (periodic structures such as metamaterials)
  - Fast computation of electromagnetic propagation characteristics
  - Especially suited for evaluation of processes uncertainties

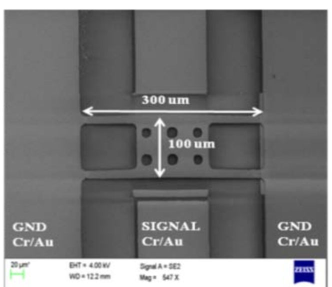

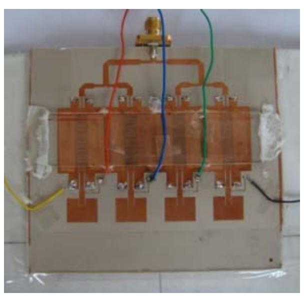
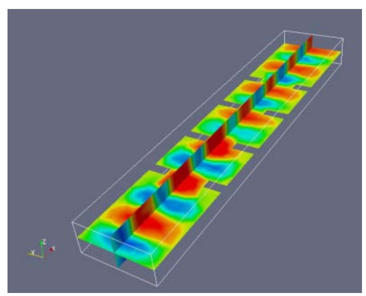
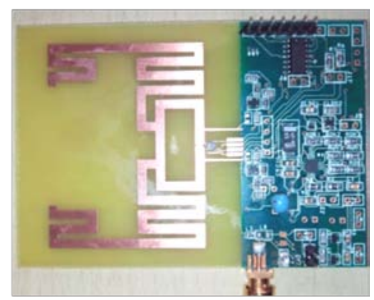
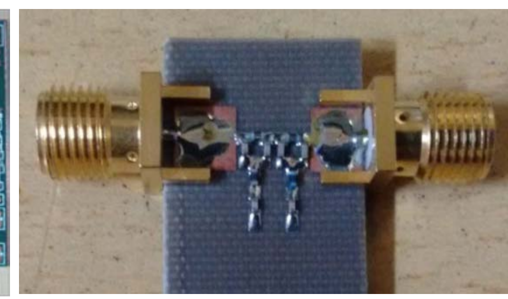

Setting the stage….

- **Introduction**
  - **Wireless Power Transfer**
    - **Energy Harvesting**
  - **Internet of Things**
- Highlights of Recent Development (Hardware)
  - Powering wireless terminals
  - RFID with integrated sensors

Ongoing Research Challenges

Wireless Power Transfer (WPT)

- Indicates transfer of electric energy remotely

- WPT has a long history!!
  - Tesla demonstrated it in 1899 by wirelessly powering fluorescent lamps 40 kms away from the power source.
  - Had multiple patents in early 1900s.

- In 1960s W.C. Brown coined the term Rectenna, which he used to directly converts incoming microwaves to DC.
  - He demonstrated its ability to power a helicopter solely through microwaves for 10 hours continuously.

- These demonstrations involved dedicated sources with **large power to transmit over long distances**.

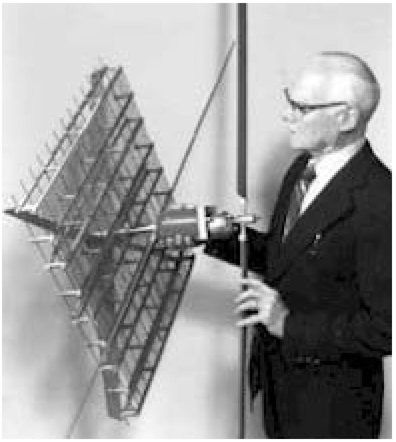

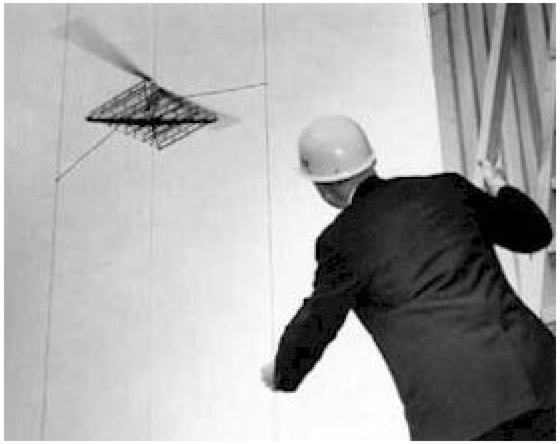

http://mainland.cctt.org/istf2008/brown.asp

SSPS

- Space Solar Power Satellites

- WPT is widely investigated for putting **solar power generating satellites** into space and transmitting power to Earth stations. (Mainly in Japan)

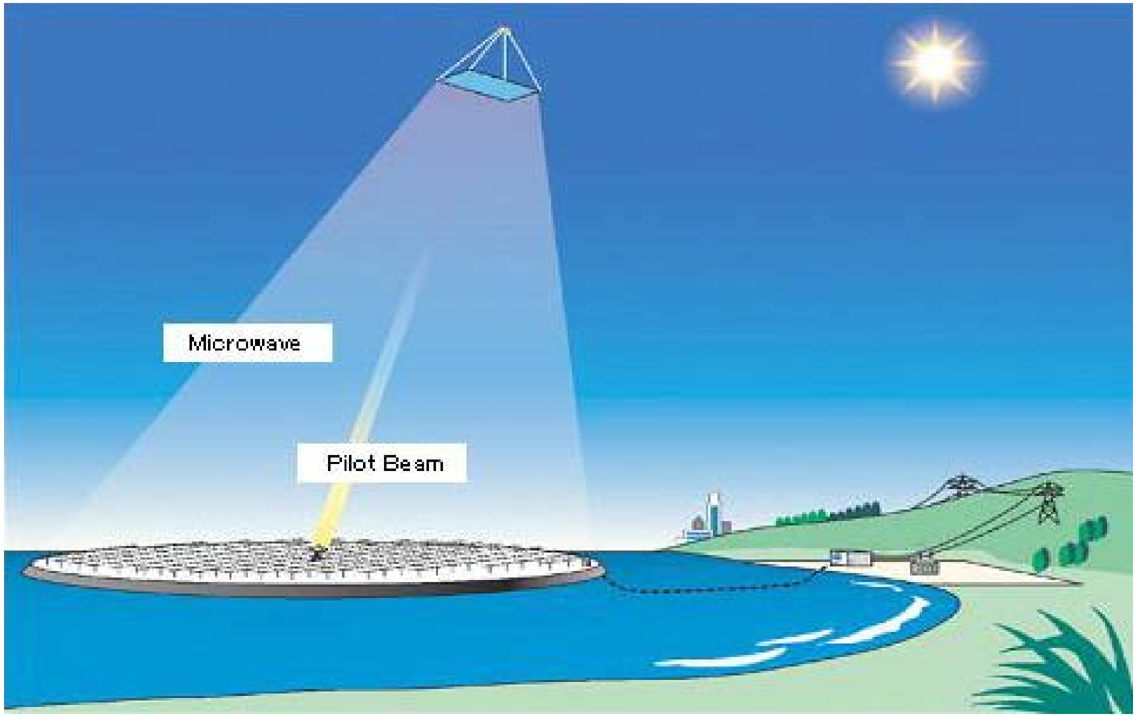

http://www.jspacesystems.or.jp/en_project_ssps/

Near field Wireless Power Transfer

- Recent demonstration by MIT to transfer high RF power (Watts) transferred across meters.
- Resonant coils are used
- Typically at 100 kHz to 10's of MHz
- Many new applications emerged

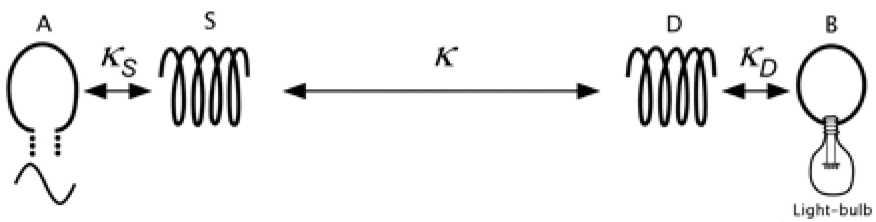

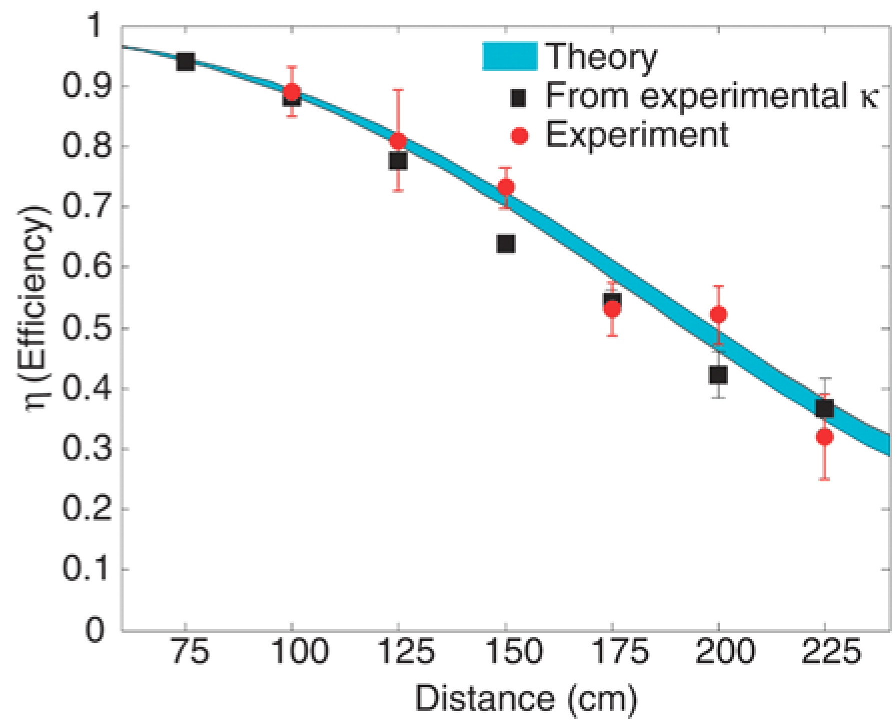

André Kurs et al, Wireless Power Transfer via Strongly Coupled Magnetic Resonances , Science, Vol. 317 no. 5834 pp. 83-86. 6 July 2007.

System Schematic Qi

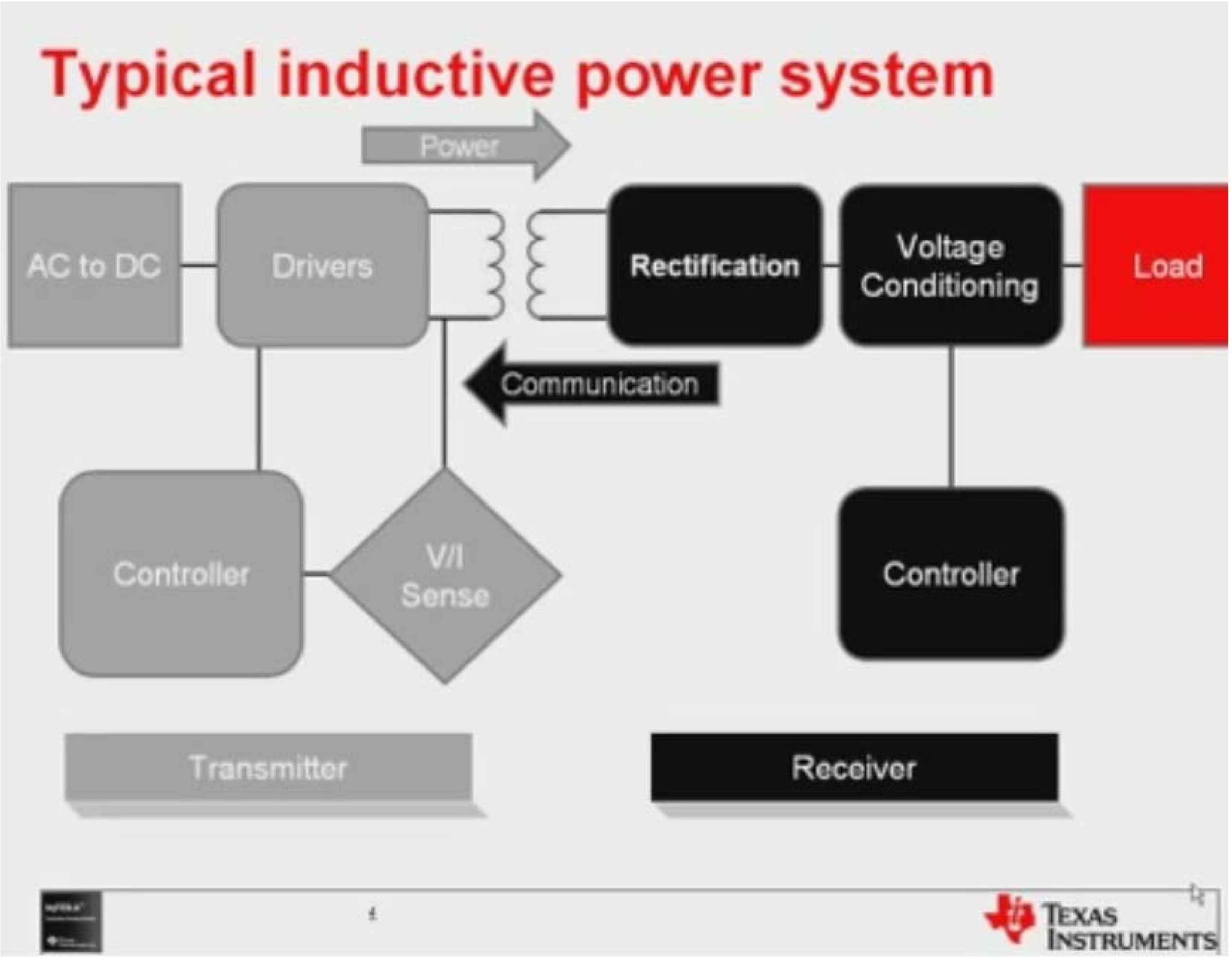

Source: Texas Instruments Qi Development kit

Far → Near in WPT

- Free space loss factor is a major bottleneck for power transfer at large distances

- Short distance/ Near field options
  - MIT demonstration (2007)
  - Qi Standard
  - Phone charging solutions
  - Vehicles running on wireless power
- Two extremes in WPT
  - mW ← → MW
  - mm ← → 1000s km
  - 100kHz ← → 2.4/5.8GHz
  - 10cm x 10cm ← → km x km
  - Commercial vs bluesky

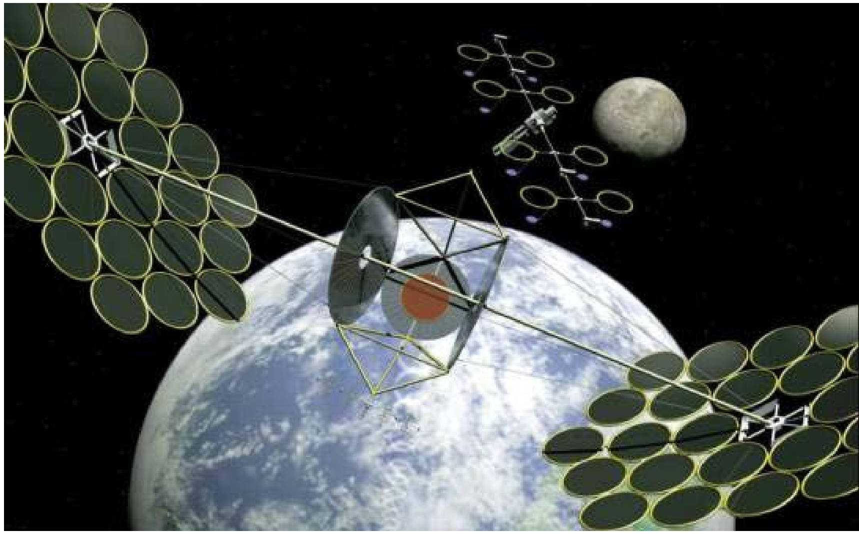

Far Field Transfer of RF Energy

- Focus of this talk
- Applications: RFID tags, Wireless Sensor Network nodes, biomedical equipment, home automation and structural monitoring can benefit from RF energy harvesting.
- Block diagram and a design example:

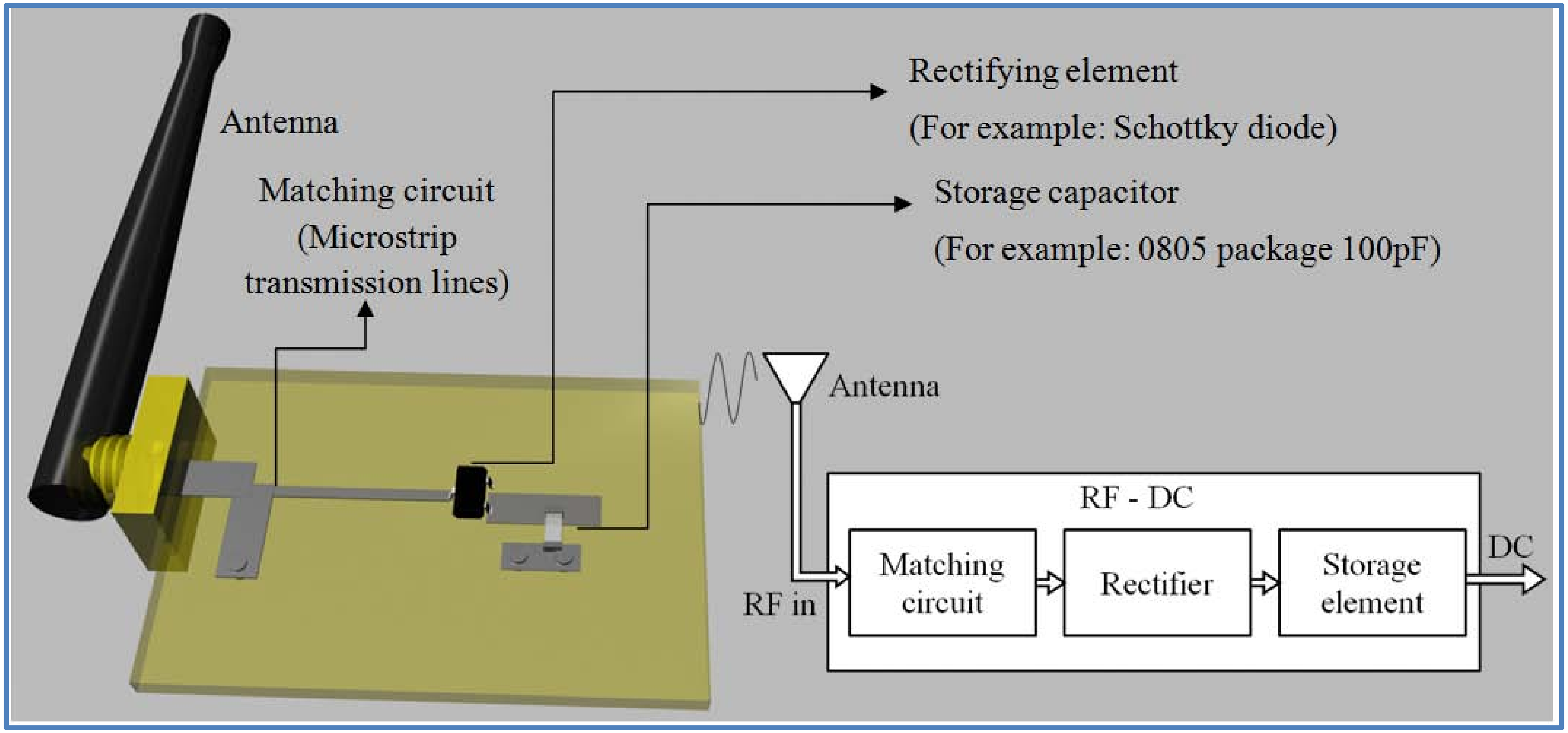

A New Paradigm: Internet of Things (IoT)

- IoT refers to uniquely identifiable objects and their virtual representations in an Internet-like structure.

Connects Anytime, Anyplace for Anyone (ICT)
AAA + for Anything (IoT)

- IoT is a scheme for connecting things: sensors, actuators, and other smart technologies, thus enabling person-to-object and object-to-object communications.

- **Continuous availability of power is crucial for their deployment**

IoT Applications

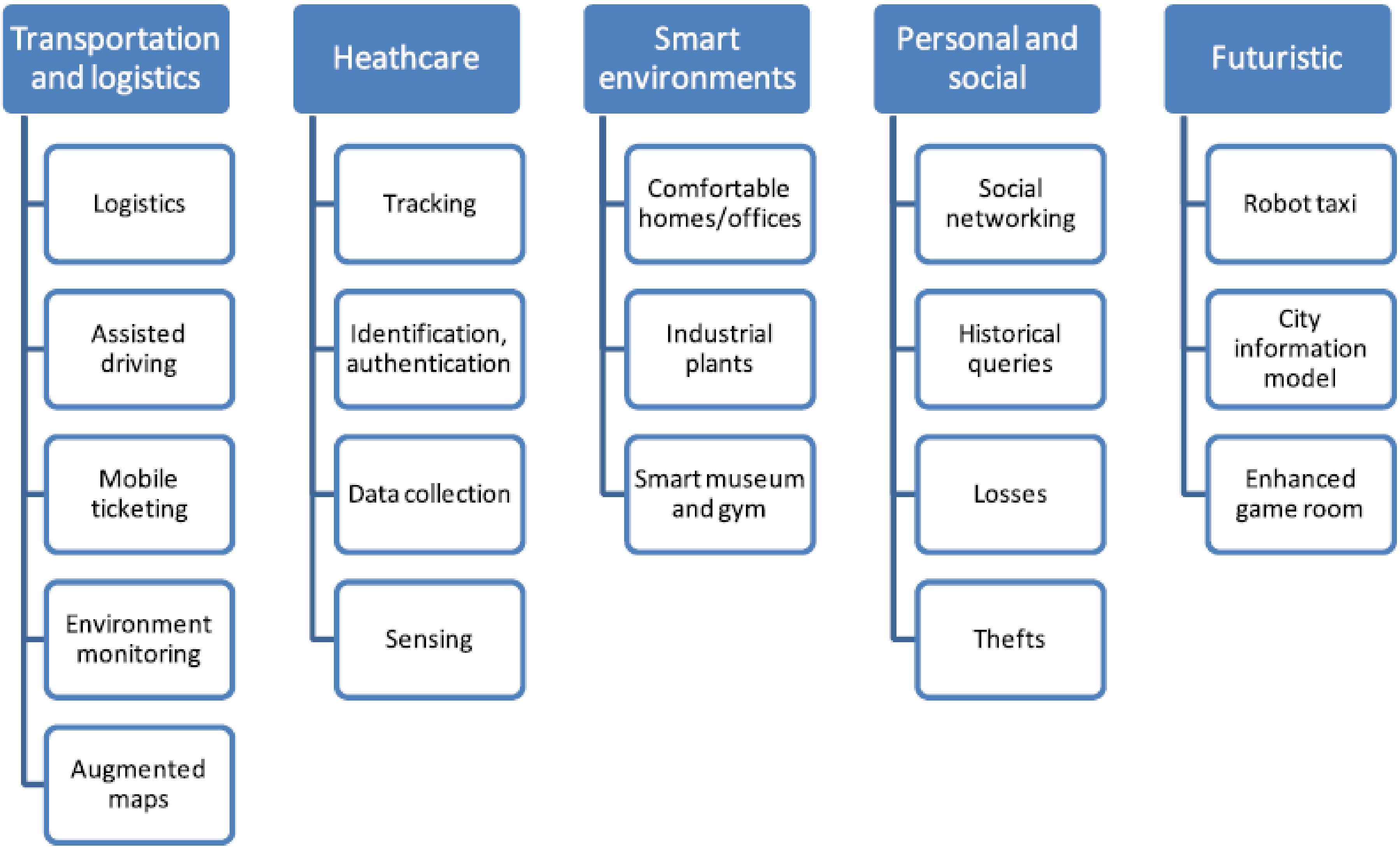

L. Atzori , A. Iera, G. Morabito, The Internet of Things: A survey Computer Networks 54 (2010) 2787–2805

Comparison of different wireless protocols

Today, a lot can be done at low power!!

Characteristics of key 2.4GHz ISM Band Radios studied :

	BLE	ANT	Zigbee	WLAN
Topologies	P2P , Star	P2P , Star, tree, mesh	P2P , Star, mesh	P2P , Star
Modulation	GFSK	GFSK	OQPSK	DSSS (802.11b)
Max data rate	1Mbps	12.8-60 Kbps	250Kbs (@2.4Ghz)	1- 11Mbps (802.11b)
Throughput	305 kbps	20Kbps	100Kbps	6Mbps (802.11b)
Range (in m)	10-100(0-10dBm)	30 (@ 0dBm)	10-100 (0-20dBm)	100+(20dBm)
Max nodes in piconet	7	65533	Star-65536	32-64
Battery life	1-2 years (coin cell)	1-2years (coin cell)	100-1000 days	0.5-5days

Key Aspects :

BLE is robust and has lowest power consumption but cannot natively form mesh networks,

Zigbee can support large mesh networks, power consumption is higher than BLE and throughput is lower: It is suitable for low data rate, low power, large size networks.

WLAN is primarily suitable for transferring bulk data at high speeds, Not suitable for low power applications.

Power Requirements in Common WSN

	Crossbow MICAz	Intel IMote2	Jennic JN5139
Radio standard	IEEE802.15.4/ZigBee	IEEE802.15.4	IEEE802.15.4/ZigBee
Typical range	100m (outdoor), 30m (indoor)	30m	1 km
Data rate (kbps)	250 kbps	250 kbps	250 kbps
Sleep mode (deep sleep)	15 μA	390 μA	2.8 μA (1.6μA)
Processor only	8mA active mode	31–53mA$\ast$	2.7+0.325mA/MHz
RX	19.7mA	44mA	34mA
TX	17.4mA (+0dbm)	44mA	34mA (+3 dBm)
Supply voltage (minimum)	2.7V	3.2V	2.7V
Average	2.8mW	12mW	3mW

JM. Gilbert$\ast$ F. Balouchi, Comparison of Energy Harvesting Systems for Wireless Sensor Networks, International Journal of Automation and Computing 05(4), October 2008, 334-347

	Jennic JN5148	**TI- CC430**	**BLE**	**Zarlink ZL70250**
Active mode current at 16MHz [mA]	6	4	6.7	3.2
Deep sleep current [nA]	100	1000	400	20
Transmission current [mA]@Tx-power [dBm]	15@2.5	18@0	36@2	2@-10
Transmit frequency	2.4 GHz	2.4 GHz	2.4 GHz	868 MHz
Wakeup time [ms]	1	3	0.12	0.16
Energy consumption for a transmission cycle of 2ms [µJ]	183	300	196	32
Power supply voltage [V]	2.2 – 3.6	1.8 -3.6	2-3.6	1.2 – 1.8

In perspective

- Energy requirements in different devices/systems
- 6 orders of magnitude variation!!!
- Energy requirements in WSN
  - Depends on the complexity/ standard/ range
  - eg 90 μW to power a pulse oxymeter sensor, to process data and to transmit them at intervals of 15 s

Device type	Power consumption
Smartphone	1W
MP3 decoder chip	58 mW
Hearing aid	1 mW
Wireless sensor node	100 μW*
RF receiver chip	24 mW
GPS receiver chip	15 mW
6D motion sensor	14.4 mW
Cell phone (standby)	8.1 mW
PPG sensor	1.473 mW
Humidity	1 mW
Pressure	0.5 mW
3D accelerometer	0.324 mW
Temperature	27 μW
Cardiac pacemaker	50 μW
Wristwatch	7 μW
Memory R/W	2.17 μW
A-D conversion	1 μW

J Yun, S. Patel, M.Reynolds, G. Abowd “A Quantitative Investigation of Inertial Power Harvesting for Human-powered Devices,” UbiComp’08, September 21-24, 2008, Seoul, Korea.

R.J.M. Vullers, et.al, Micropower energy harvesting, Solid-State Electronics 53 (2009) 684–693

Power Density from Various Harvesters

Ambient RF	< 1 μW/cm^2
Ambient light	100 mW/cm^2 (directed toward bright sun)
	100 μW/cm^2 (illuminated office)
Thermoelectric	60 μW/cm^2
Vibrational	4 μW/cm^3 (human motion ~Hz)
microgenerators	800 μW/cm^3 (machines ~kHz)
Ambient airflow	1 mW/cm^2
Push buttons	50 μJ/N
Hand generators	30 W/kg
Heel strike	Up tp 7 W for 1 cm deflection

Power requirements in conventional sensor network nodes may not be met by harvesting alone!

J Yun, S. Patel, M.Reynolds, G. Abowd "A Quantitative Investigation of Inertial Power Harvesting for Human-powered Devices," UbiComp'08, September 21-24, 2008, Seoul, Korea.

Electromagnetic: Solar → RF

- PV is a good source of energy. Recall,

Ambient light	100 mW/cm^2 (directed toward bright sun)
	100 μW/cm^2 (illuminated office)

- However, it light is not always available.
  - At night
  - Specific scenarios: in a closed chamber, or mine.

- RF is an alternative
  - Unlike others, RF sources may be ambient or intentional.
  - Ambient sources such as base stations or broadcast stations
  - Special sources: RF ID reader, Phone charger, special beacons

Demand and Supply

- The peak currents needed during transmit and receive operation is not achievable using the harvester alone.
- Buffering is also needed to ensure continuous operation during times without power generation.
- The combination of an energy harvester with a small-sized storage is the best approach to enable energy autonomy of the network over the entire lifetime.
  - Rechargeable battery
  - Thin film batteries
    - can be integrated directly in Integrated Circuit (IC) packages in any shape or size,
    - Flexible when fabricated on thin plastics
    - Thin film batteries have high impedance;
    - Low discharge efficiency compared to Li-ion batteries
  - super capacitor
    - Leakage in super capcitors depends on the voltage. Low at low voltage

Internet of Things (IoT)

Embedding short-range mobile transceivers into a wide array of gadgets and everyday items, enabling new forms of communication between people and things, and between things themselves.

RFID + Sensor + Smart Tech + Nano Tech = IoT

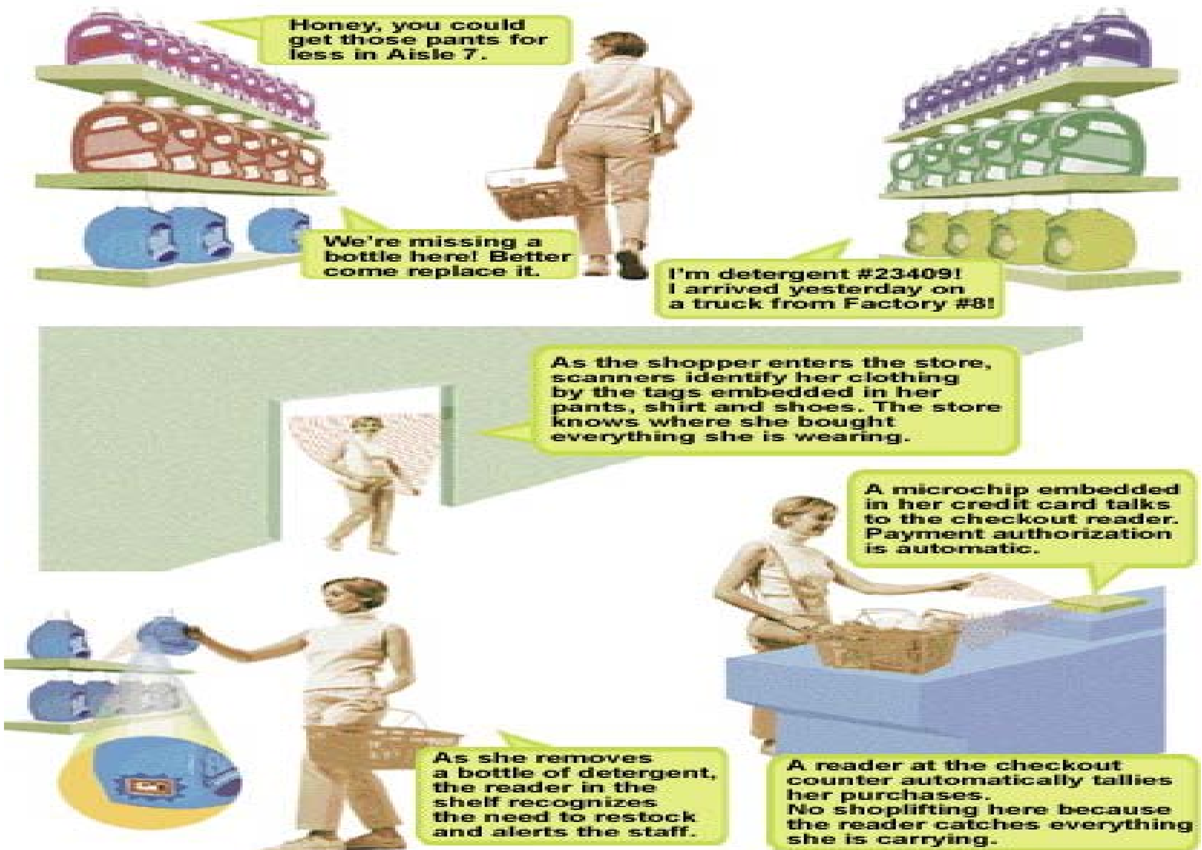

When shopping in the market, the goods will introduce themselves.

When entering the doors, scanners will identify the tags on clothing.

When paying for the goods, the microchip of the credit card will communicate with checkout reader.

When moving the goods, the reader will tell the staff to put a new one.

Introduction to RFID

- The reader converts incident field and returns useful data
- In passive RFID systems reader transmits EM energy that "wakes up“ the tag and provides power for the tag to respond to the reader.

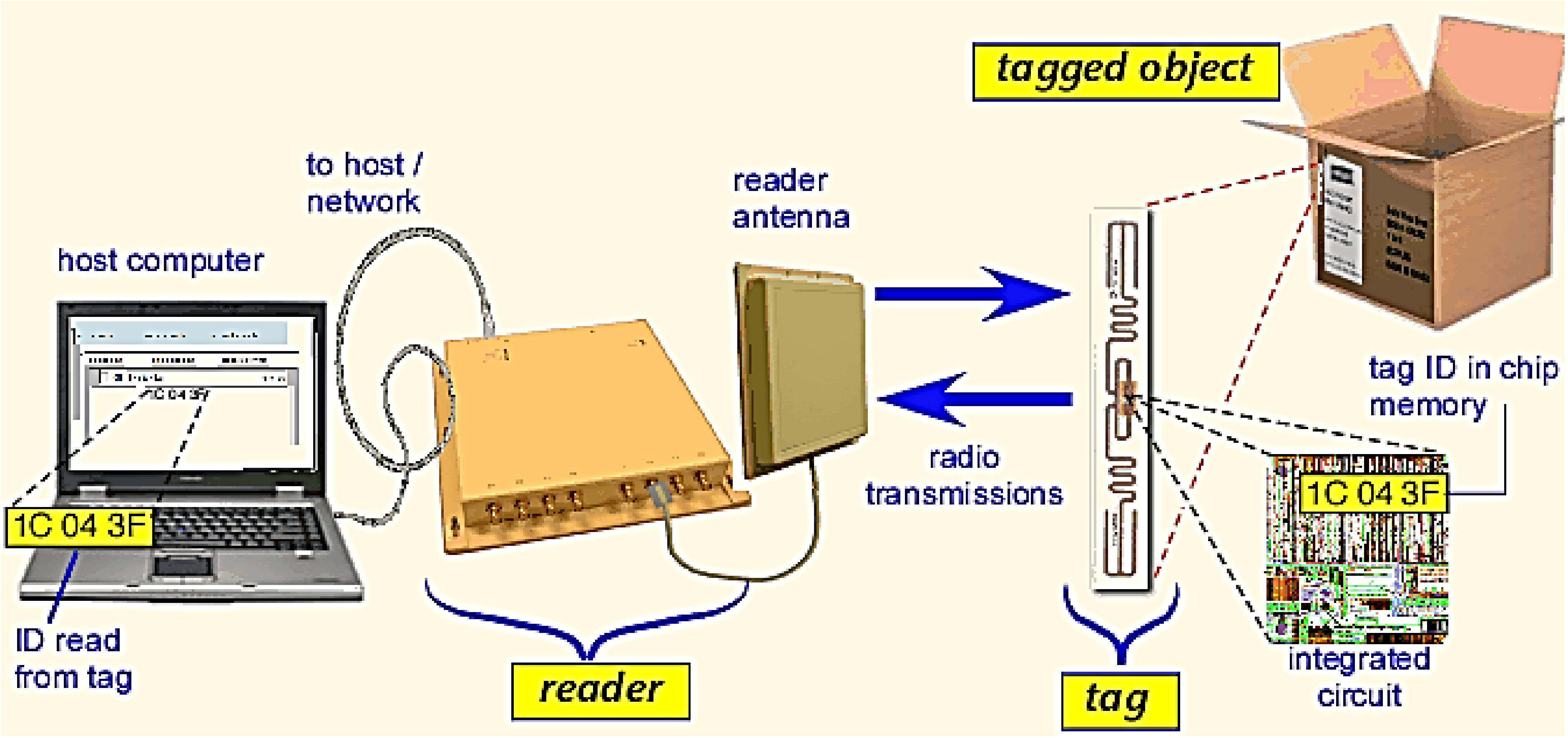

Backscatter Communication

- **Backscatter** is the reflection of signals back towards their source.
  - In this scheme, two devices communicate using incident (or ambient) RF as the source of power.
  - Backscattering is achieved by changing the impedance of a receiver in the presence of an incident signal.
  - When waves encounter a new media that have different impedances, a part of the wave is reflected.
  - The reflection depends on the difference in the impedances.
- By modulating the impedance at the receiver port, one can control the scattered RF energy, hence enabling information transmission.

abc.cs.washington.edu/files/comm153-liu.pdf

RFID → IoT

- RFID
  - Uses radio waves for identifying or tracking the object.
  - Proven to be a simple and cost effective system
  - Tags are very cheap and is possible to be attached to everyday objects.

- RFID is considered a prerequisite of **Internet of Things.**

- **Example: RFID tags can be integrated with sensors**
  - When a reader reads a tag, the sensor information will be sent to the reader along with the identity of the object.

Some Examples

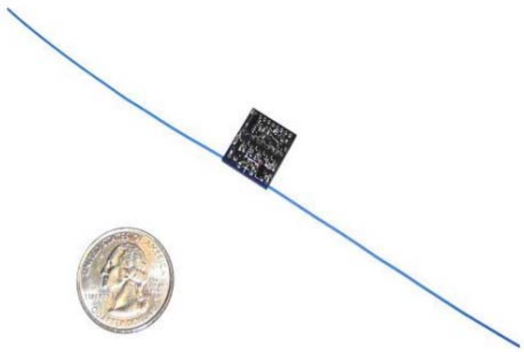

Discrete Element Based
WISP (Wireless Identification Sensing Platform)

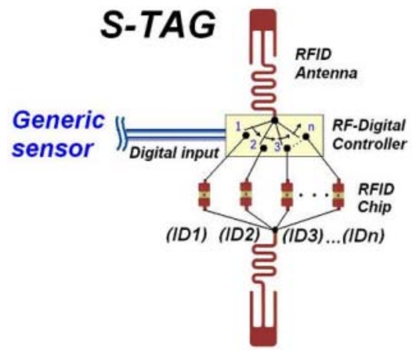

Multi-Chip Based S-tag

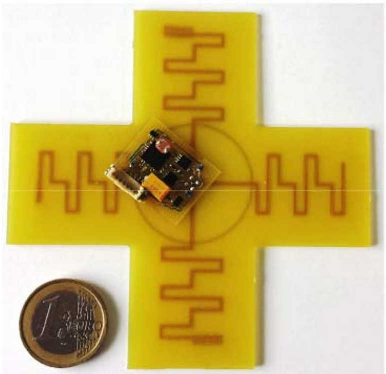

Chips with I2C / SPI
SPARTACUS / RAMSES (Self-Powered Augmented RFID Tag for Autonomous Computing and Ubiquitous Sensing / RFID Augmented Module for Smart Environmental Sensing)

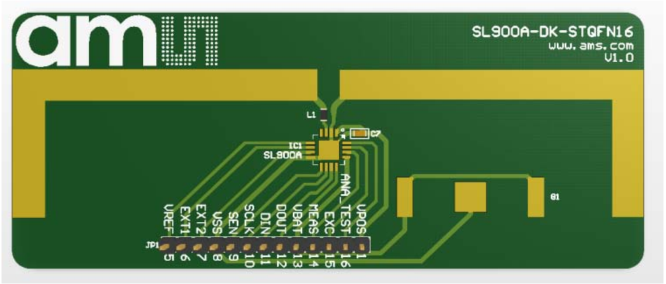

Single IC Based Sensing Tags

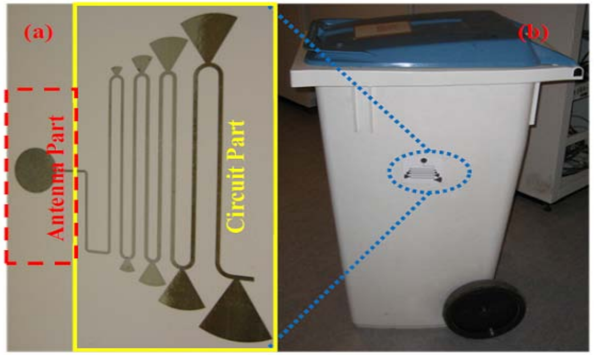

Printed Chipless RFID Tag

WISP

- Wireless Identification Sensor Platform (2009)
  - WISPs are a wireless, battery-free sensing and computation platform, powered by harvested energy from off-the-shelf UHF RFID readers.
  - To a RFID reader, a WISP is a EPC gen1 or gen2 tag; but inside the WISP, the harvested energy is operating a 16-bit general purpose microcontroller.
  - The microcontroller can perform computing tasks, including sampling sensors, and communicate to the RFID reader.
  - WISPs have been built with various sensors, WISPs can write to flash and perform cryptographic computations.

A collaboration between Intel Research Seattle and the University of Washington.

http://wisp.wikispaces.com/Wisp+4.1+DL

RFID Sensors (Products)

- ID operation is passive; yet most sensors require power sources

- Powercast has a wireless sensor that is battery-less. Uses RF energy harvesting.
- Harvesting schemes works at power as low as -12dBm. (RF-DC conversion efficiency above 40% only above -8dBm)
- Harvested power >0.4mW for RF in of >-1dBm.
- Multiple custom ICs and discretes

- Other suppliers include
  - Phase IV
  - RFID sensor systems
  - etc

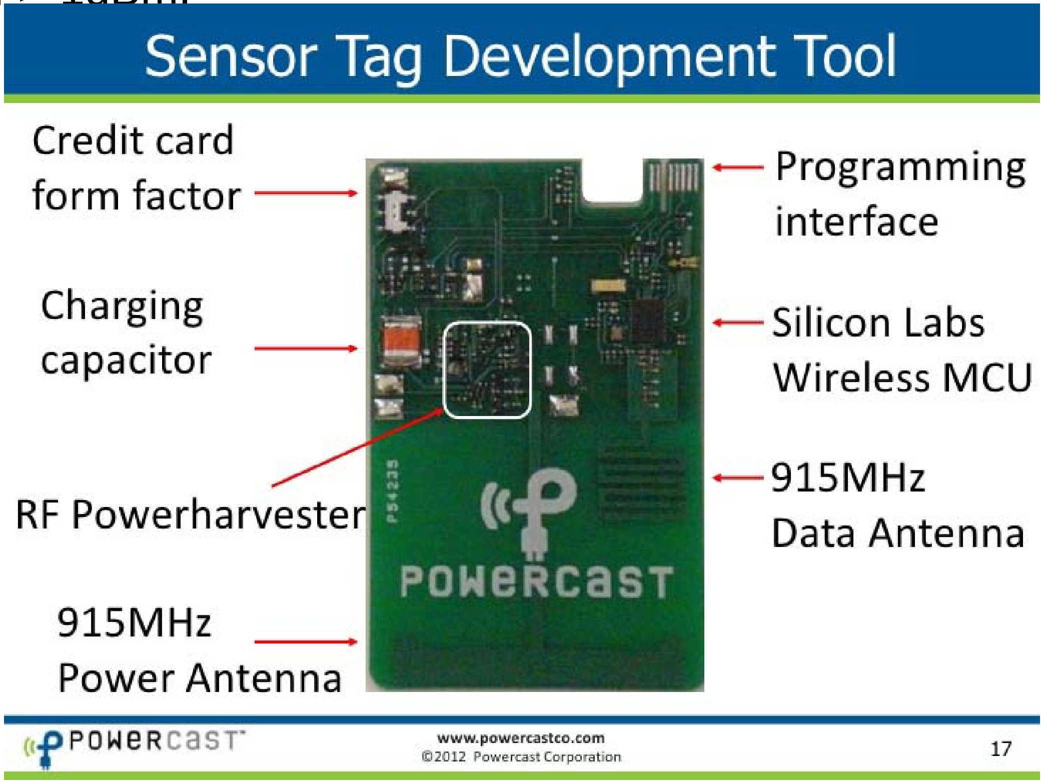

http://www.powercastco.com/uhf-rfid-sensing-passive-rfid-wireless-sensor-tags/

Battery-less Wireless Terminals

- Most of our work in this direction was towards battery-less terminals
- Long life terminals without wiring
- These are useful when
  - Terminals are embedded within structures (or body)
  - Devices to be deployed in hostile environments
  - Use of battery is not allowed (potential cause for explosion)
- Other factors
  - Cost, weight, etc.
- Primary focus: use of radio frequencies (ambient/intentional)

Ambient RF Sources

- Several sources:
  - WiFi Access points (mW) [2.4/.6GHz]
  - Cellular Tower (W) [900/1800 MHz]
  - TV Broadcast (MW) [150-450MHz]
  - FM broadcast (kW) [90-108MHz]
  - AM Radio broadcast (kW) [<1MHz]

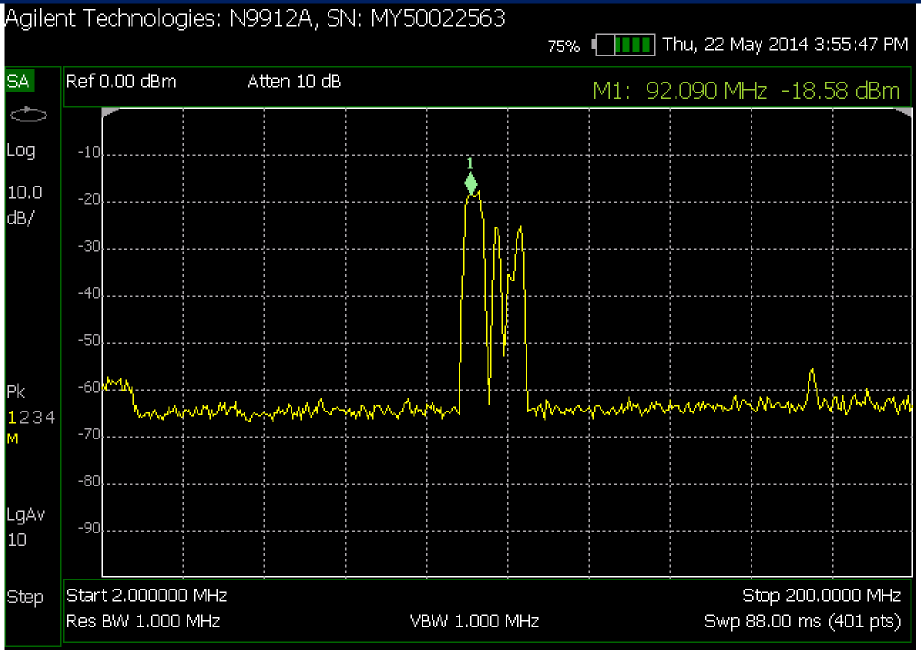

- In general
  - Lower frequencies help non-line-of sight propagation
  - Power availability from ambient sources is limited and varies from place to place.

- Note
  - Unlike other sources, most practical RF harvesters (eg in RF ID) depend on **intentionally generated energy**.
  - This is called **wireless power transfer (WPT)** in the conventional RF/Microwave parlance.

Wireless Communication System

- Power transfer scheme is no different!!

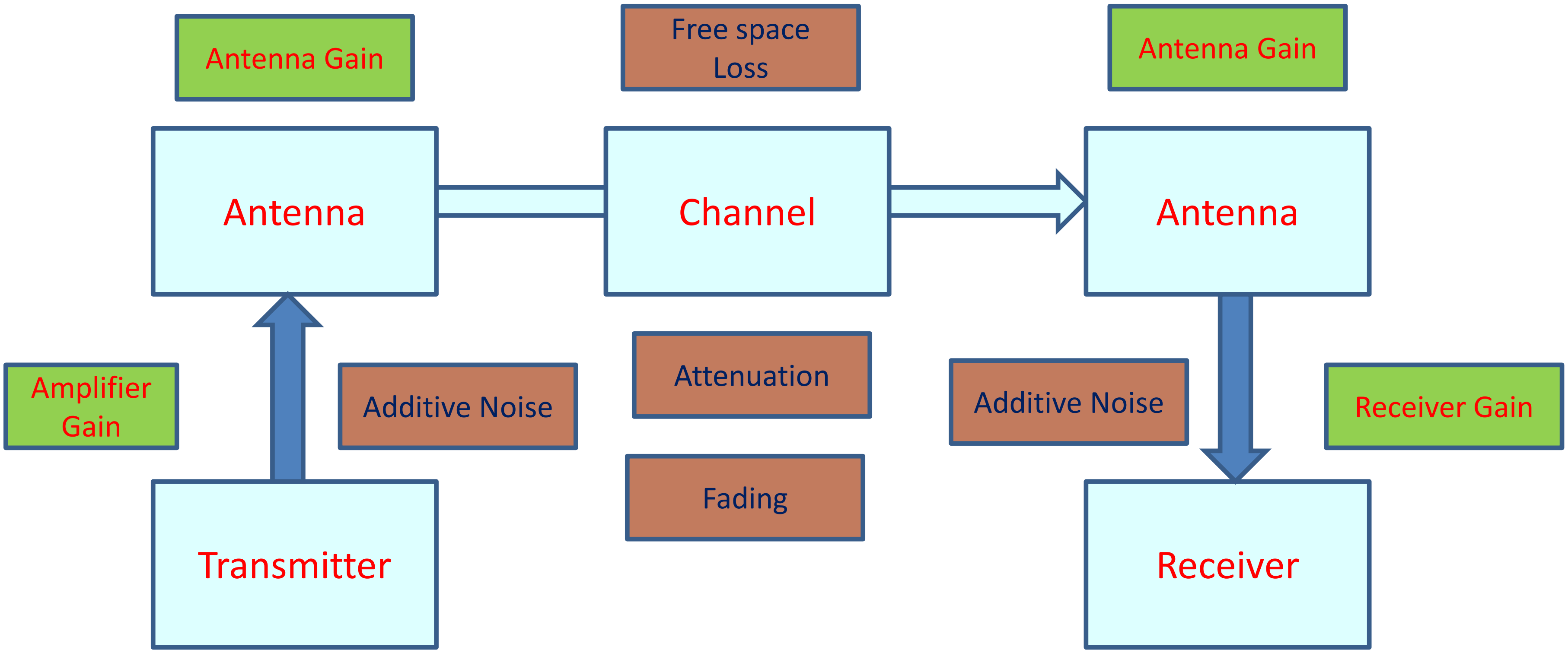

Antenna Fundamentals: Directivity

This is the ratio of the radiation intensity in a given direction to the radiation intensity averaged over all direction

Average radiation intensity, $U_0 = \dfrac{P_{rad}}{4\pi}$

Directivity,

$$D(\theta,\phi) = \frac{U(\theta,\phi)}{U_0} = \frac{4\pi U(\theta,\phi)}{P_{rad}}$$

- If direction is not specified, it implies the direction of maximum radiation intensity

$$D_{\max} = \frac{4\pi U_{\max}}{P_{rad}} \qquad D_{dB} = 10\log D$$

Maximum directivity and Maximum effective area

The radiated power density by a transmitter at a distance R

$$W_t = \frac{P_t D_t}{4\pi R^2}$$

Power received

$$P_r = W_t . A_r = \frac{P_t D_t A_r}{4\pi R^2}$$

$$or,\ D_t . A_r = \frac{P_r}{P_t} . 4\pi R^2$$

By reversing the transmission direction

$$D_r A_t = \frac{P_r}{P_t} \cdot 4\pi R^2$$

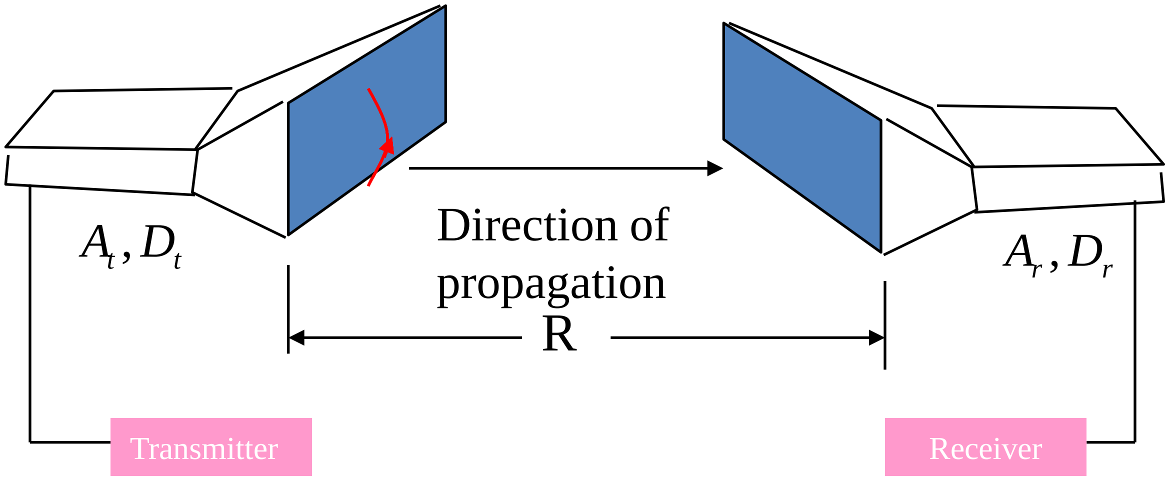

$$\therefore \frac{D_t}{A_t} = \frac{D_r}{A_r}$$

this can be generalized by

$$\frac{D_1}{A_1} = \frac{D_2}{A_2} = k = \frac{4\pi}{\lambda^2}$$

$if,\ D_0 = \text{max. directivity}$

$A_{em} = \text{max. effective area}$

$$\boxed{D = \frac{4\pi A_{em}}{\lambda^2}}$$

Frii's Transmission Equation

- The radiation intensity for an isotropic radiator is $W_0 = \frac{P_t}{4\pi R^2}$
- For an antenna of gain G_t (or directivity D_t)

$$W_t = \frac{P_t G_t(\theta_t,\phi_t)}{4\pi R^2} = e_t \frac{P_t D_t(\theta_t,\phi_t)}{4\pi R^2}$$

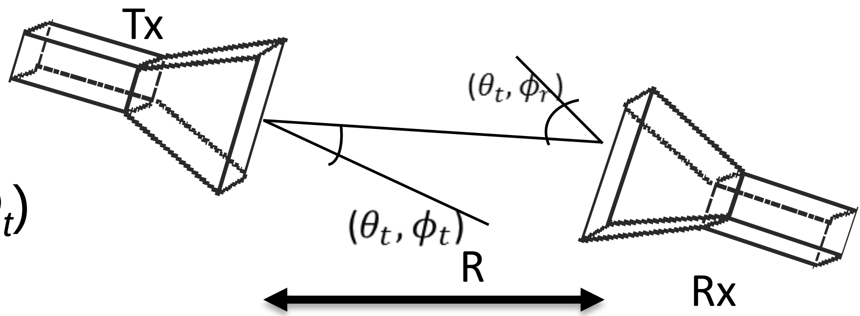

- The effective aperture of a receiving antenna is given by $A_r = e_r D_r(\theta_r,\phi_r)\frac{\lambda^2}{4\pi}$
- Therefore,

$$P_r = e_r D_r(\theta_r,\phi_r)\frac{\lambda^2}{4\pi} W_t = e_t\, e_r D_t(\theta_t,\phi_t) D_r(\theta_r,\phi_r)\frac{\lambda^2}{(4\pi R)^2}\,|\hat{\boldsymbol{\rho}}_t \cdot \hat{\boldsymbol{\rho}}_r|^2$$

$$\frac{P_r}{P_t} = e_t e_r D_t(\theta_t,\phi_t) D_r(\theta_r,\phi_r)\frac{\lambda^2}{(4\pi R)^2}\,|\hat{\boldsymbol{\rho}}_t \cdot \hat{\boldsymbol{\rho}}_r|^2$$

$$\frac{P_r}{P_t} = e_{cdt} e_{cdr}(1-|\Gamma_t|^2)(1-|\Gamma_r|^2) D_t(\theta_t,\phi_t) D_r(\theta_r,\phi_r)\frac{\lambda^2}{(4\pi R)^2}\,|\hat{\boldsymbol{\rho}}_t \cdot \hat{\boldsymbol{\rho}}_r|^2$$

- When the antennas are pointing towards each others' peak radiation direction,

$$\frac{P_r}{P_t} = G_{0t} G_{0r}\left(\frac{\lambda}{4\pi R}\right)^2$$

Note that includes a loss factor (usually called **Free space Loss factor)**
Does not include dissipation/attenuation in medium; caused by spreading

Some numbers on Radiative form of WPT…

- Practical systems will have
  - Operational frequencies in ISM bands.
  - Most terminals are compact.
  - Antenna efficiency is compromised.
  - Nearly isotropic radiations expected.

- Main bottleneck is the physical limits in transmission.

$$P_r = P_t * G_t * G_r * (\lambda/4\pi r)^2$$

  - At 1 GHz (λ=30cm) r=1m; Antenna gain @0dBm, free space loss factor is about **0.06%**
  - Even with a moderate gain transmitter antenna (6dBi) power received @1m for 1W transmission, is just 2mW.
    - Drops to 23μW at 10m !!
    - **The voltage of the signal is low!!**
- In radiative power transfer, Distance from transmitter is a major concern.

Some questions addressed in our work

- **Harvesting of ambient radiations or Radiative transfer of energy addressed**
  - Is it possible to harvest the RF energy from base stations
  - Are there other viable sources of RF energy

- Can low power communication systems be designed to operate entirely from harvested energy
  - Integrate sensors, control, etc

- Can we use RF EH/ WPT to increase the range of backscatter communication (RFID scenario)

Design of Rectifiers

Required for converting incoming RF into DC power.

The challenge lies in maximizing the power conversion efficiency for low input power and minimizing the dimensions.

- RF to DC conversion by rectification of the incident RF signal by a ***Schottky diode***
  - Most diodes have a finite cut-in voltage
  - Diode is a non-linear device (performance depends on current or load)
  - Impedance matching required between antenna and diode
  - In most cases, the input voltage needs to be boosted

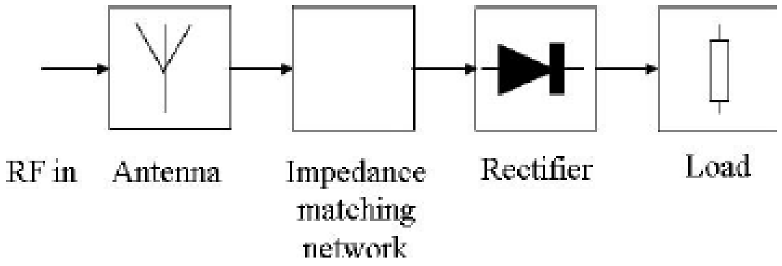

Conceptual diode based Rectenna

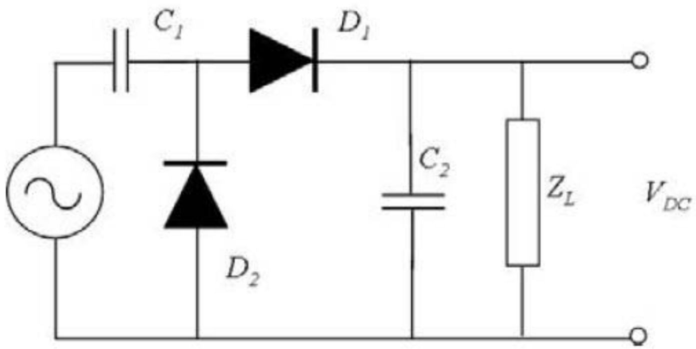

Voltage doubler

Voltage magnification in Matching circuit

- Matching circuit is required to provide impedance match between antennas (50Ω typical) to diode terminated with high impedance load (capacitor and/or high R in parallel).
  - LC matching networks provide voltage magnification.
  - This helps the diode conduct a good fraction of half cycle.
- The higher the voltage across the diodes, the more efficient the rectifier gets.
  - In practice Q is limited
  - Applications requiring higher voltages, a voltage multiplier configuration is used.

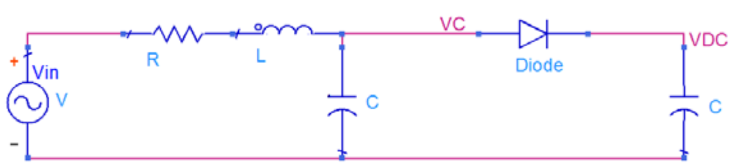

$$V_C = V_{in} \times \frac{\frac{1}{j\omega C}}{R + j\omega L + \frac{1}{j\omega C}}$$

At resonance,

$$V_C = V_{in} \times \frac{1}{j\omega_0 CR} = -jQV_{in}$$

Tuned Rectifier at RF

- A tuned rectifier implemented using discrete components

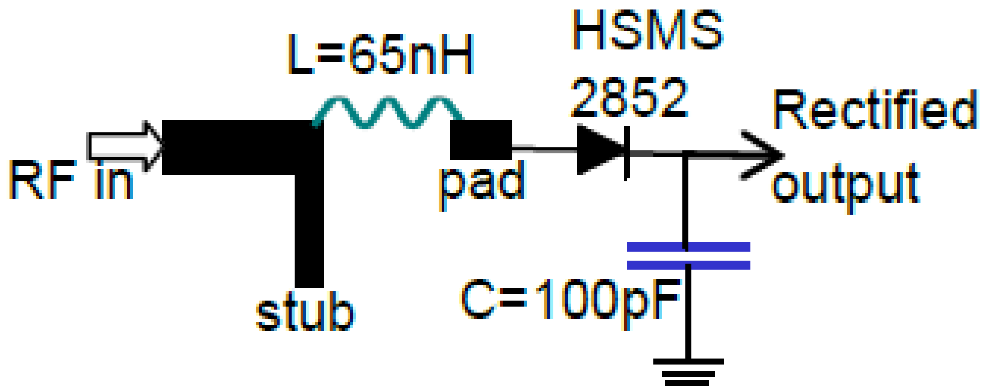

P_in→	-10dBm	-13dBm	-16dBm	-20dBm	-25dBm
Freq.↓					
930MHz	917mV	664mV	469mV	281mV	131mV
945MHz	1016mV	736mV	515mV	300mV	132mV
955MHz	1038mV	747mV	513mV	289mV	122mV
960MHz	1032mV	736mV	499mV	276mV	114mV
Peak efficiency	51%	47%	39%	33%	20%

K. J. Vinoy, T. V. Prabhakar, A Universal Energy Harvesting Scheme for Operating Low-Power Wireless Sensor Nodes Using Multiple Energy Resources, pp. 453-466, Micro and Smart Devices and Systems, Springer 2014.

Typical Performance of Rectifier

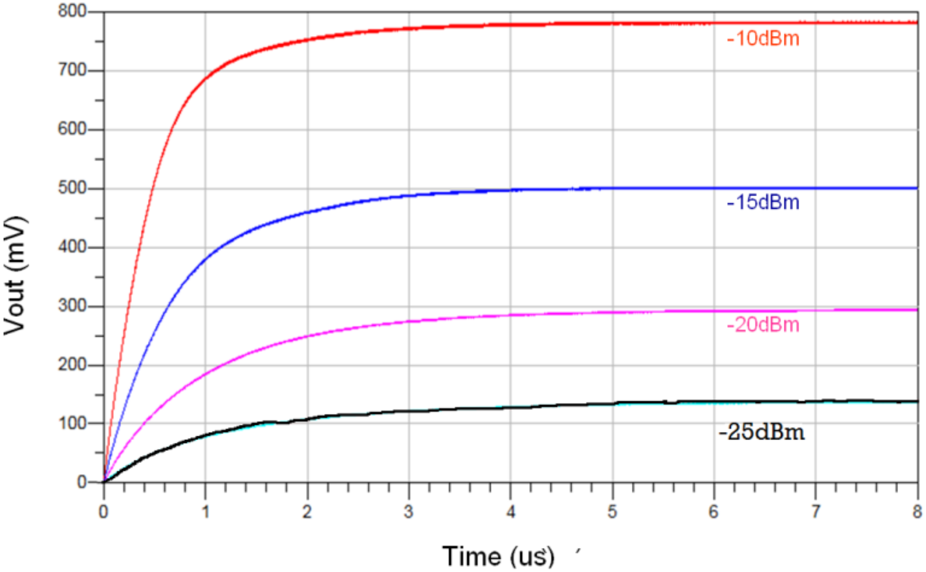

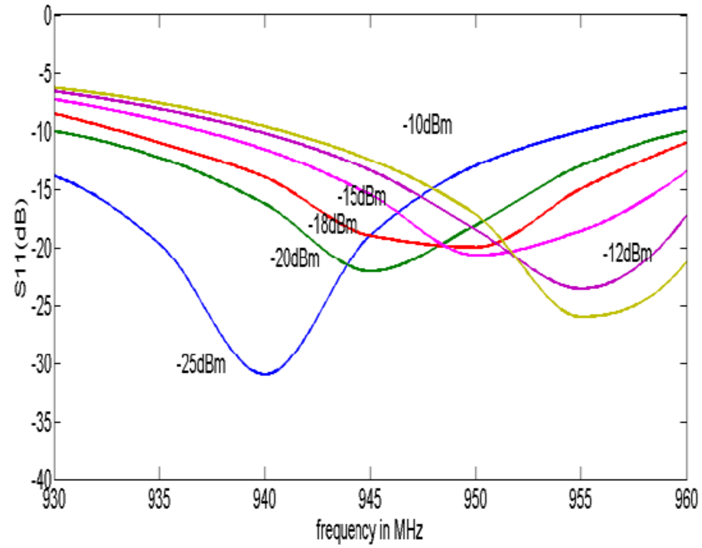

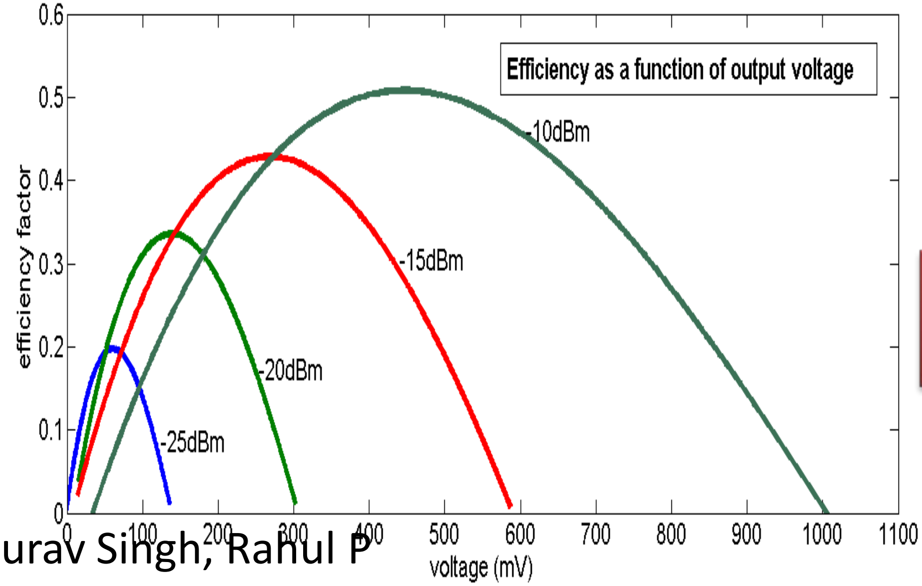

RF-DC Conversion efficiency depends on various conditions

Rectifier Circuit using 4 diodes

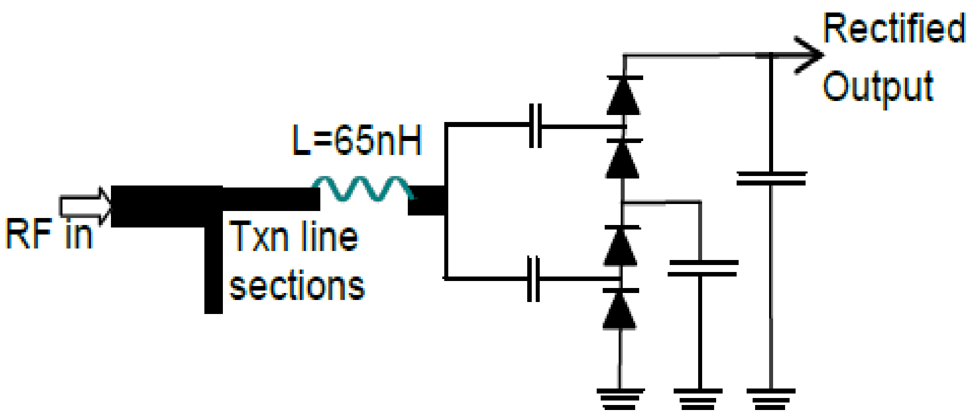

Power level (dBm)	Charging time (ms)	Efficiency (%)
0	40	64.11
-2	55	63.77
-3	67.5	63.5
-5	90	63
-7	230	59.89
-10	370	56.78
-12	500	53.89
-15	900	45
-18	2000	20.56

K. J. Vinoy, T. V. Prabhakar, A Universal Energy Harvesting Scheme for Operating Low-Power Wireless Sensor Nodes Using Multiple Energy Resources, pp. 453-466, Micro and Smart Devices and Systems, Springer 2014.

Aditya Mitra, Chaithanya (2011-12)

1: Scavenging Mobile Tower Radiations

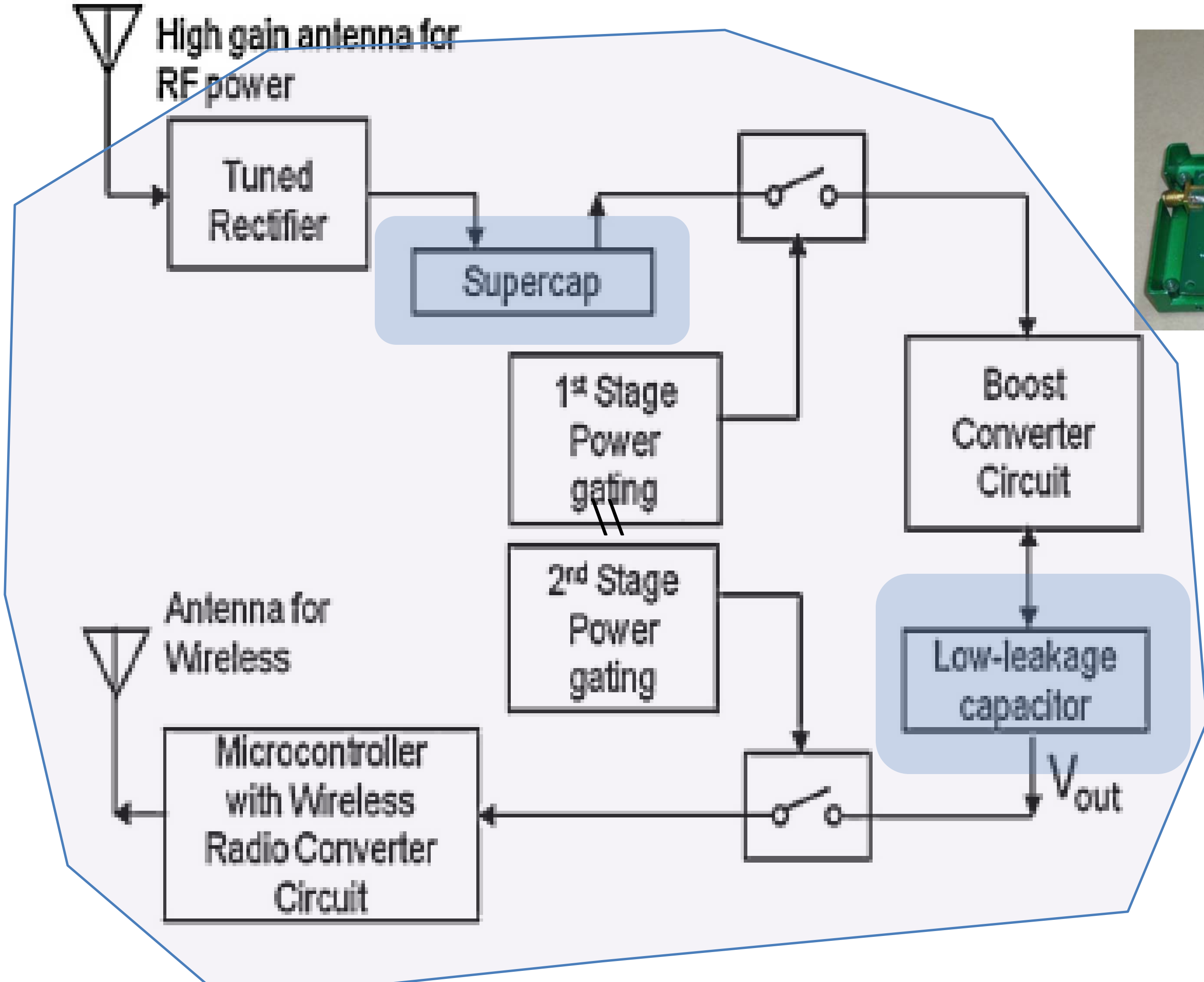

G. Singh, R. Ponnaganti, T. V. Prabhakar, and **K.J. Vinoy**, "A tuned rectifier for RF energy harvesting from ambient radiations," Int. J. Electronics & Communications, vol. 67, no. 7, pp. 564-569, July 2013

Gaurav Singh, Rahul P (2010-11)

Gaurav Singh, Rahul P (2010-11)

Characterization in Lab

- Using various antennas

Distance from Transmitter [m]	1.5	2	2.5	3
Power received by dipole antenna [dBm]	-20.5	-22.1	-23.9	-25.2
Calculated power density [uW/cm^2]	0.078	0.055	0.035	0.03
Power received by patch antenna [dBm]	-15.1	-16.1	-17.6	-19.2
Transmit interval [mm:ss]	07:26	12:13	25:00	never
Power received by biquad antenna [dBm]	-11.8	-13.2	-14.9	-15.9
Transmit interval [mm:ss]	02:20	03:25	7:10	10:33

G. Singh, R. Ponnaganti, T. V. Prabhakar, and **K.J. Vinoy**, "A tuned rectifier for RF energy harvesting from ambient radiations," Int. J. Electronics & Communications, vol. 67, no. 7, pp. 564-569, July 2013

Gaurav Singh, Rahul P (2010-11)

Incident power above -18dBm required for operation

2. Universal Energy Harvesting Platform

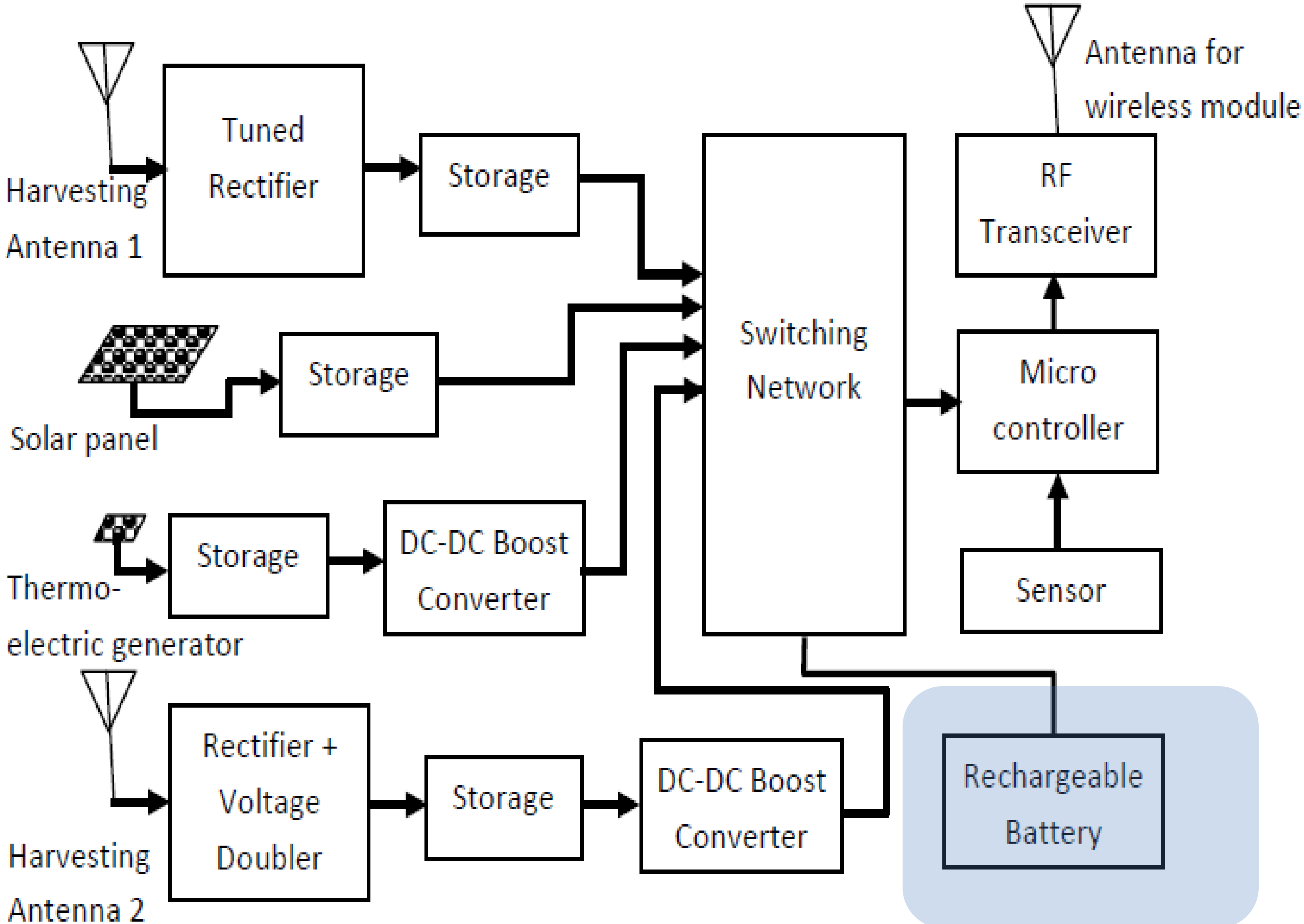

Only a small thin film battery is used

UEHP: Performance with different sources

Solar		RF		TEG	
Light Intensity (Lux)	Duty Cycle of operation (s)	Power Level (dBm)	Duty Cycle of Operation (s)	Temperature Differential (°C)	Duty Cycle of Operation (s)
1000	7	0	3	55	9
300	11	-5	6	45	13
200	**20**	**-7**	20	35	240
100	42	-10	50	-	-
-	-	-12	240	-	-

An incident RF power of -7dBm (~0.2mW) performs similarly as at low light PV.

An appropriately oriented 20mW source with a high gain antenna (~10dB) can reach this RF power at a low gain rectenna (eg using PIFA) at 1 m distance.
Power levels within emission guidelines…

K. J. Vinoy, T. V. Prabhakar, A Universal Energy Harvesting Scheme for Operating Low-Power Wireless Sensor Nodes Using Multiple Energy Resources, pp. 453-466, Micro and Smart Devices and Systems, Springer 2014.

Aditya Mitra, Chaithanya (2011-12)

Other Possibilities using Wireless Power Transfer

- Power transfer by radiation is not efficient
- Waveguiding systems can ensure better transmission of power
  - Loss in waveguide is a small fraction of a dB/m (~0.2dB/m)
  - Metal ducts may carry higher order modes with higher losses
  - Extended to conducting ducts, Tunnels, mine shafts etc with some compromise
- Other possibilities
  - Surface wave
  - Focusing of fields
- Empty enclosures with metallic walls
  - Containers, tanks, airplane cabin, trains, etc
  - Other objects in the path may reduce the efficiency!

3: Antenna for RFID sensors

- Work involved design of antenna for RF harvesting sensors
  - These fuel level sensors to be deployed in a fuel tank of aircrft.
  - Optimization of design should focus on efficiency
  - High gain or directivity is not required.

- EH platform to be used with RFID sensors deployed inside fuel tank

- Requirements/Assumptions:
  - Incident energy is of random polarity and direction.
  - Operating frequency is 902MHz-928MHz.
  - Antenna must operate in air (relative permittivity = 1) and fluid (relative permittivity = 2.1)
  - Dimensions of planar antenna board:
    - Target dimensions: 3 in. x 2 in.
    - Maximum dimensions: 6 in. x 4 in.

Antenna Design dimensions

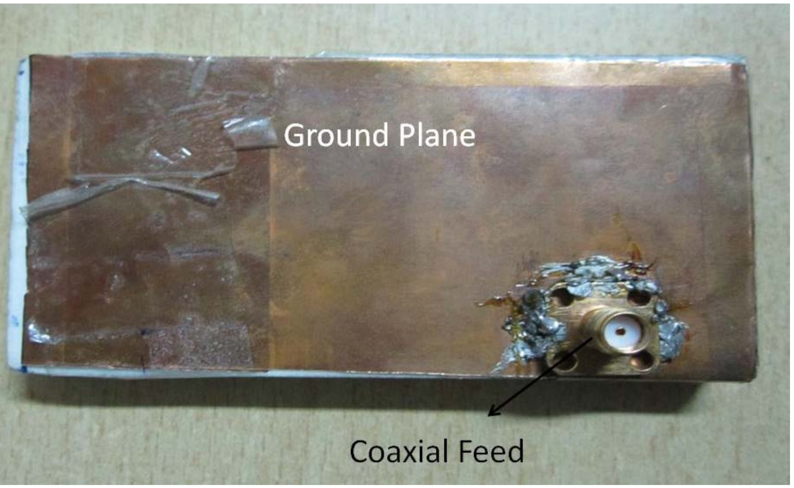

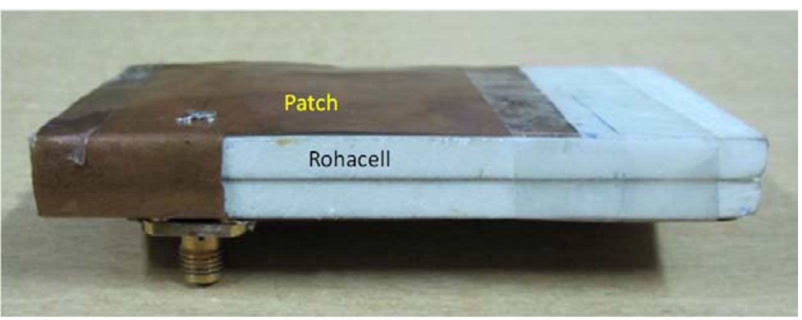

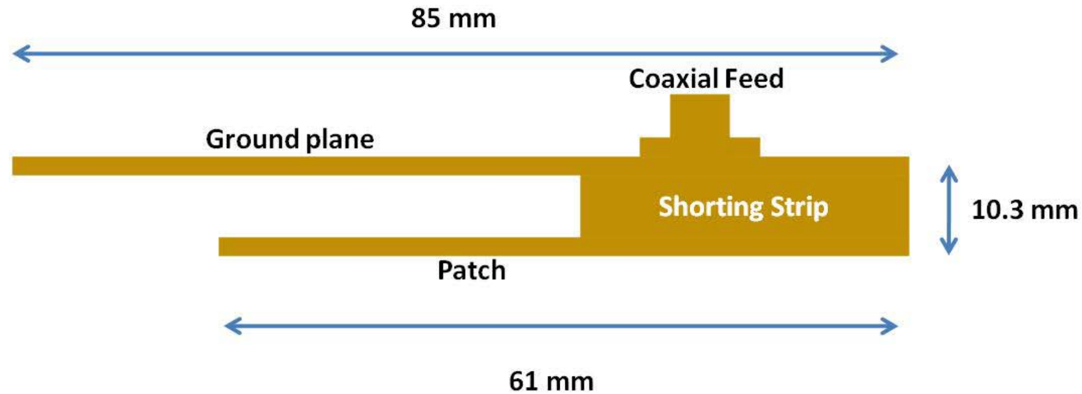

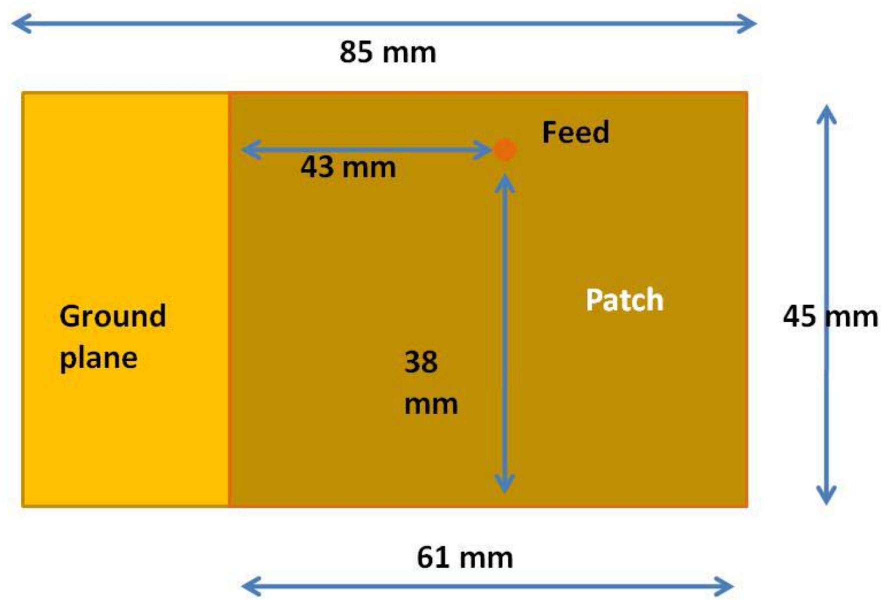

Vivekanand M, Harikiran M

Measurements at Boeing (Nov 2013)

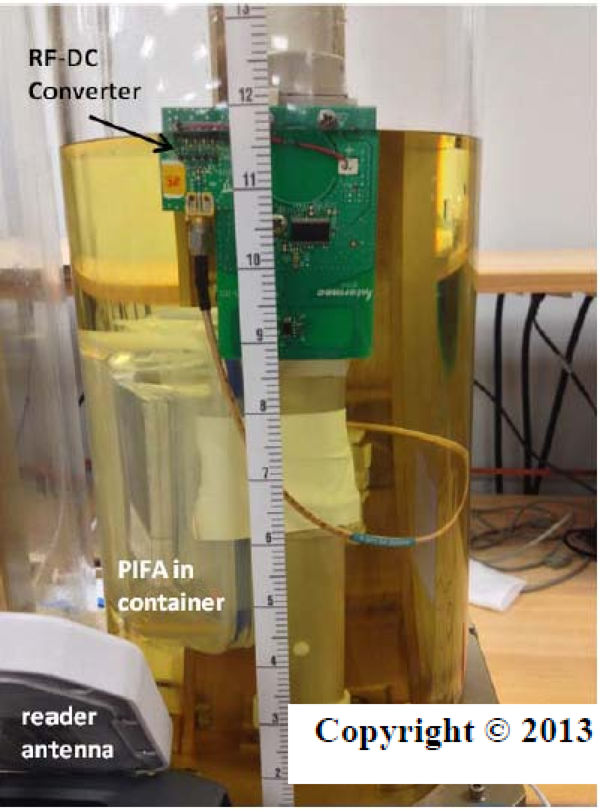

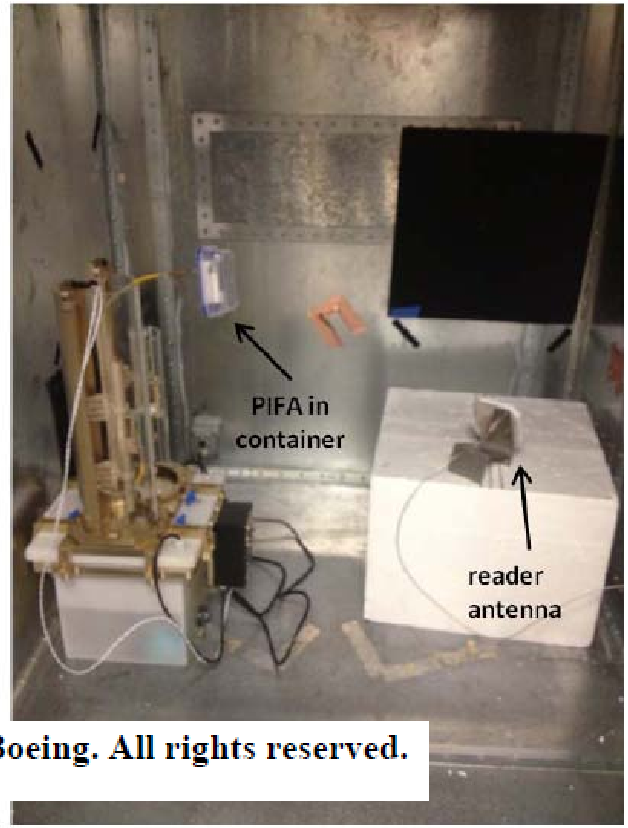

After Integrating with Sensor and RFID board;

Measured in a room and reverberation chamber

Resolution of fluid height measurement to within 0.25”.
1W maximum transmit power.
Uses a modified reader protocol.

A. Robb, J. Bommer, R. Martinez, J. Harrigan, S. Ramamurthy , H. Muniganti, V. Mannangi, and KJ Vinoy, “Wireless Aircraft Fuel Quantity Indication System,” 2014 IEEE Sensors Applications Symposium - , Feb 18-20, 2014, Queenstown, Newzealand.

4. RFID Integrated with Sensor

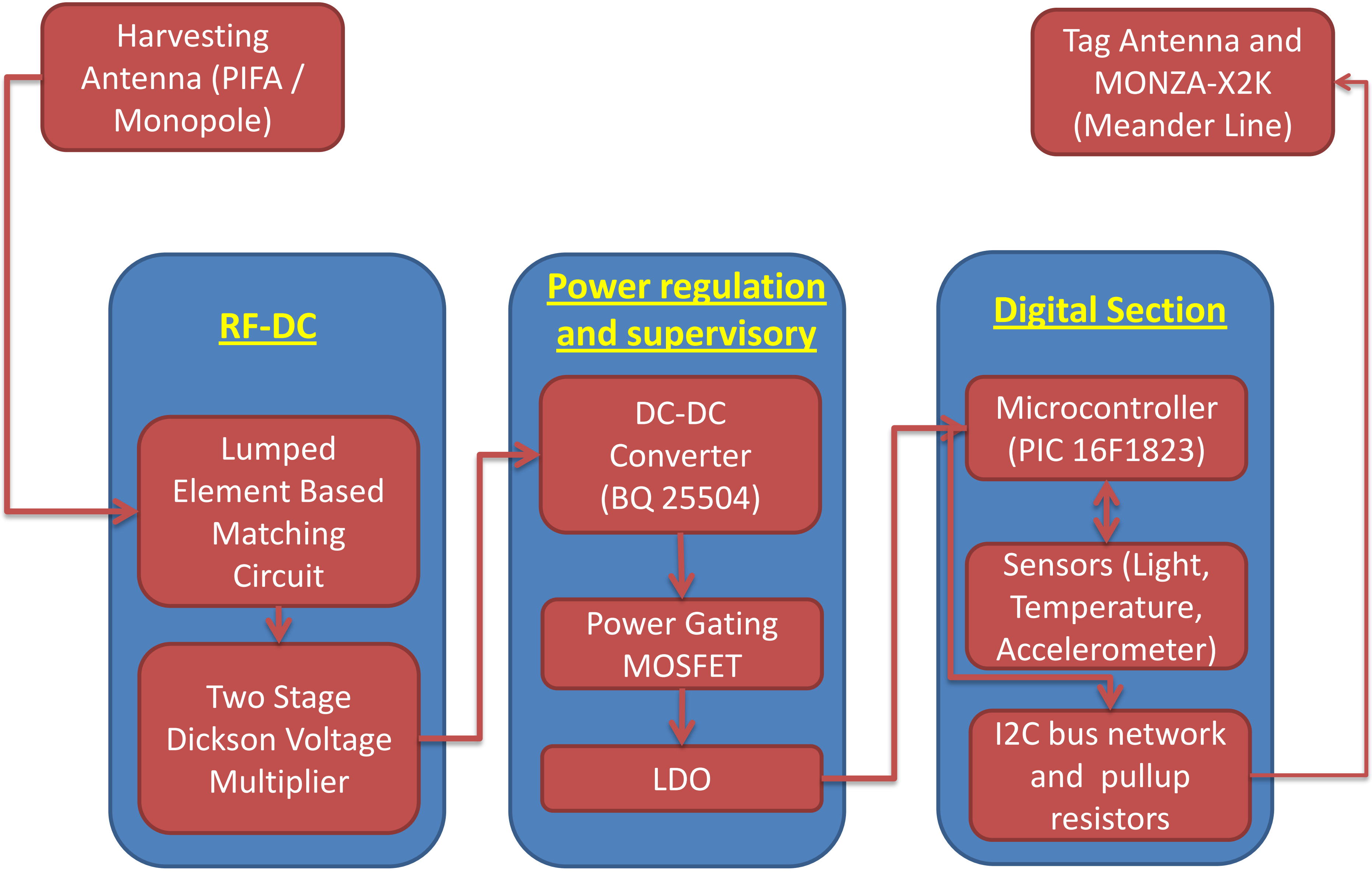

Parts of Fabricated System

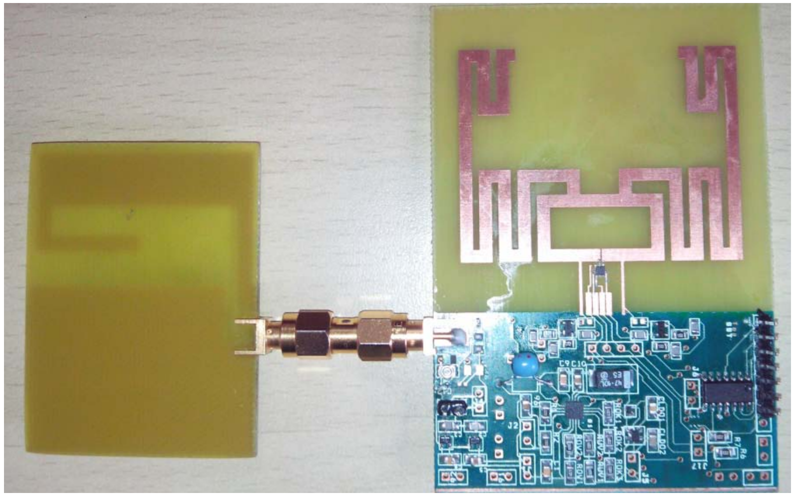

PIFA CONNECTED SENSING TAG

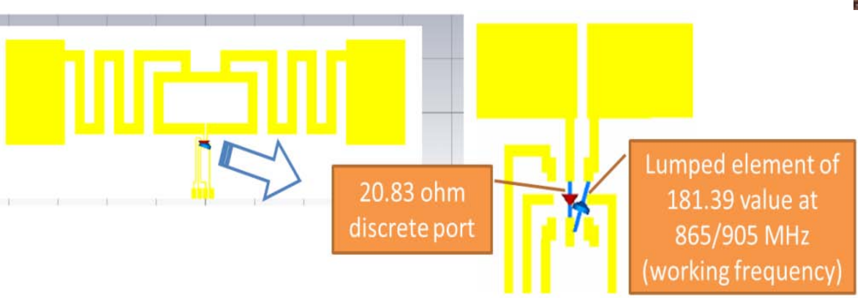

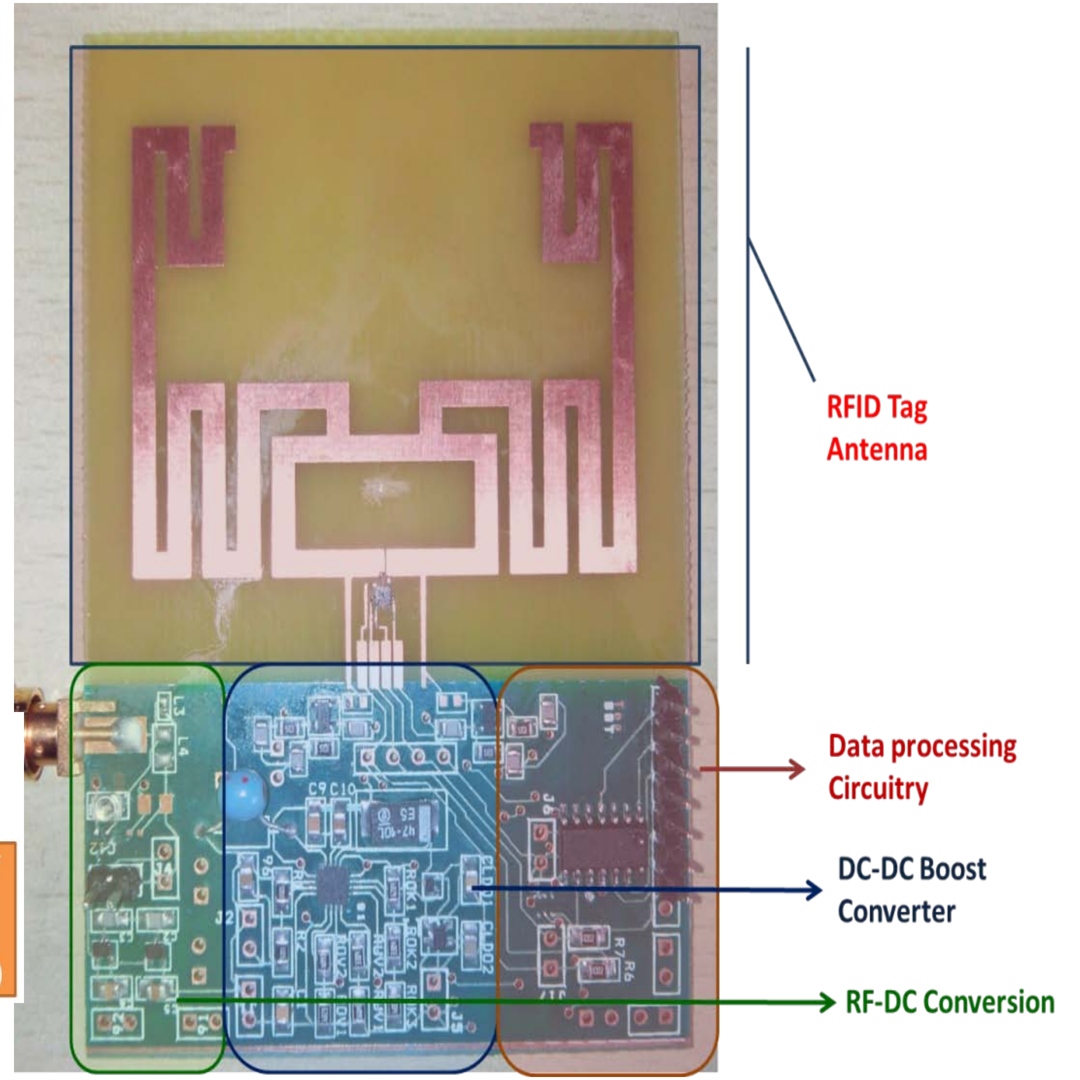

Sandeep Rana 2014-15

Sandeep Rana, TV Prabhakar, KJ Vinoy, An Efficient Architecture for Battery-less Terminals for Internet of Things, Applied Computational Electromagnetic Conference, Guwahati, Dec 28-21, 2015

Characterization of Performance

Source	Power
RFID Reader	30 dbm
Circularly polarized antenna	8 dbi
Polarization loss	3 dbi
Monopole Antenna	5 dbi
PIFA antenna	1 dbi
Meander Antenna	0.4 dbi

Tag Antenna	EIRP (dbm) + Gr	Rg Expected (-10 dbm) and 50 % overall efficiency	Range Achieved
Monopole	40	7.5 mtr	7 mtr
PIFA	36	5 mtr	5.5 mtr
Meander Line	35.4	4.5 mtr	4.5 mtr

$\lambda = 34.5\ cm$ $\quad$ Prx = $EIRP * Gr * \left(\frac{\lambda}{4*\pi*r}\right)^2$

Efficiency worked out for -10 dbm
RF-DC efficiency – 20 % and DC-DC efficiency – 80%
Overall efficiency – 16%

Sandeep Rana 2014-15

5. Harvesting at 2.4GHz

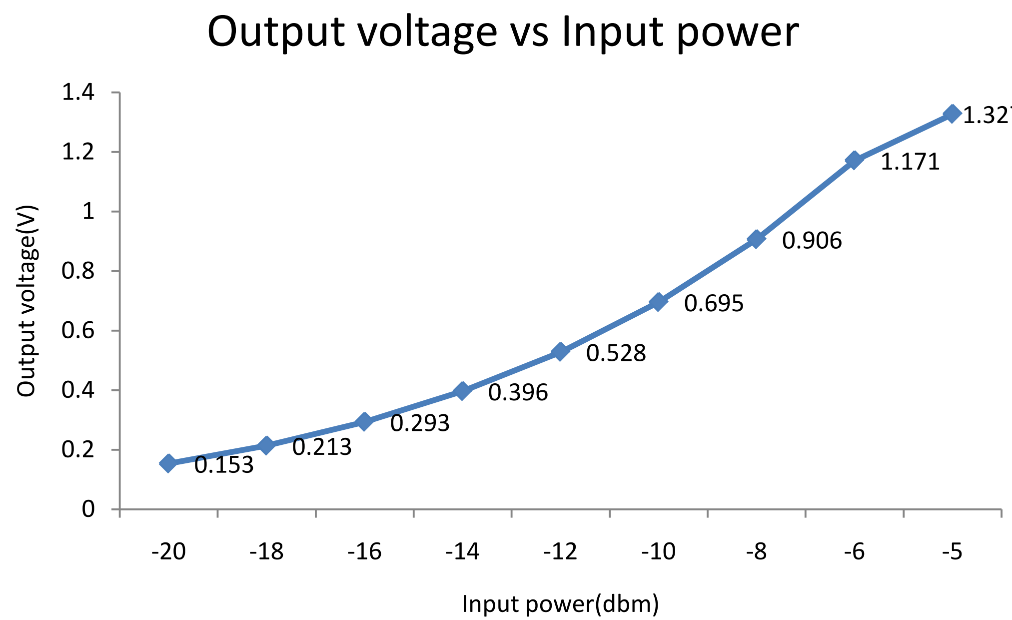

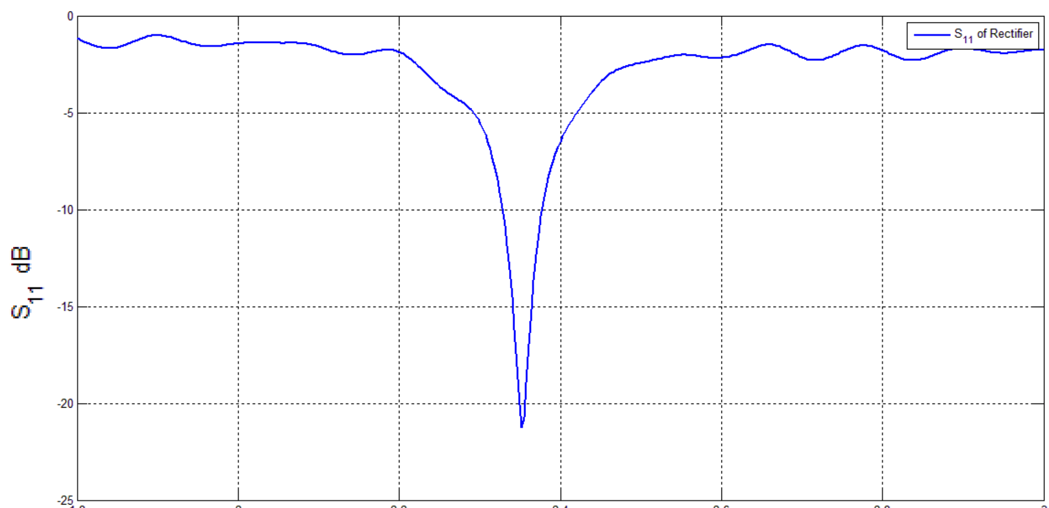

Sanjeev K. 2014-15

Frequency(GHz)

RICOH imagine. change.

Comparison of Efficiencies

Schottky diode

	900MHz	2400MHz
-15dbm	Efficiency=47% Output voltage=0.29V Load resistor=6K	Efficiency =17% Output voltage=0.2V Load resistor=6K
-20dbm	Efficiency=31% Output voltage=0.15V Load resistor=6K	Efficiency=5% Output voltage=0.1V (0.153V unloaded) Load resistor=6K
	Used HSMS 2852	Used HSMS 2862

Diode connected MOS with high Q matching

	900MHz	2400MHz
-14dbm	Efficiency=6.2% Output voltage=1.1V Load resistor=500K	Efficiency=2% Output voltage=0.632V Load resistor=500K
-20dbm	Efficiency=1.8% Output voltage=0.3V Load resistor=500K	Efficiency=0.2% Output voltage=0.118V Load resistor=500K

Zero V_{TH} CMOS

	900MHz	2400MHz
-15dbm	Efficiency=4.6% Output voltage=0.86V Load resistor=500K	Efficiency=3.79% Output voltage=0.774V Load resistor=500K
-25dbm	Efficiency=2.4% Output voltage=0.198V Load resistor=500K	Efficiency=1.7% Output voltage=0.165V Load resistor=500K

← Power

← Technologies

Frequencies →

Cross-coupled Rectifiers for Low Power

- CMoS integration requires diodes using MoSFETs.
- Simple diode connected configurations are not effective at low power/voltage levels
- In Cross Coupled Rectifiers
  - Biasing of MOSFETs by charge stored in capacitors. This is a way of threshold compensation.
  - Low ON resistance due to high overdrive voltage.
  - In both cycles of input, output capacitor is charged. Although DCP uses both cycles, only alternate cycles charges the output capacitor and the other cycle charges the input capacitor.

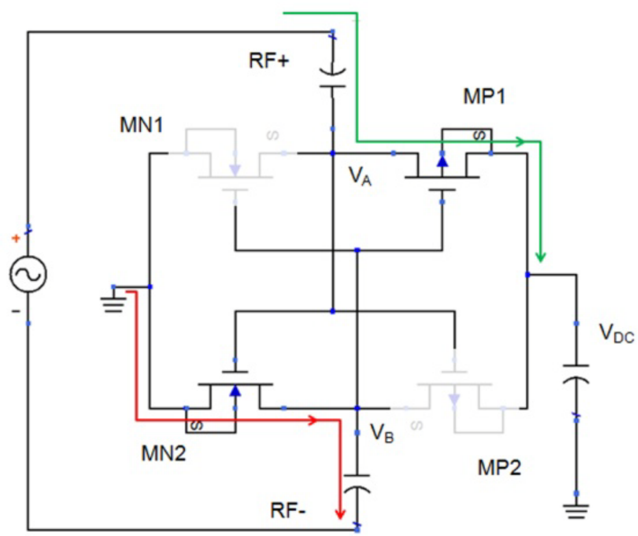

DC-DC converter

- Low loss switched capacitor DC-DC converter:

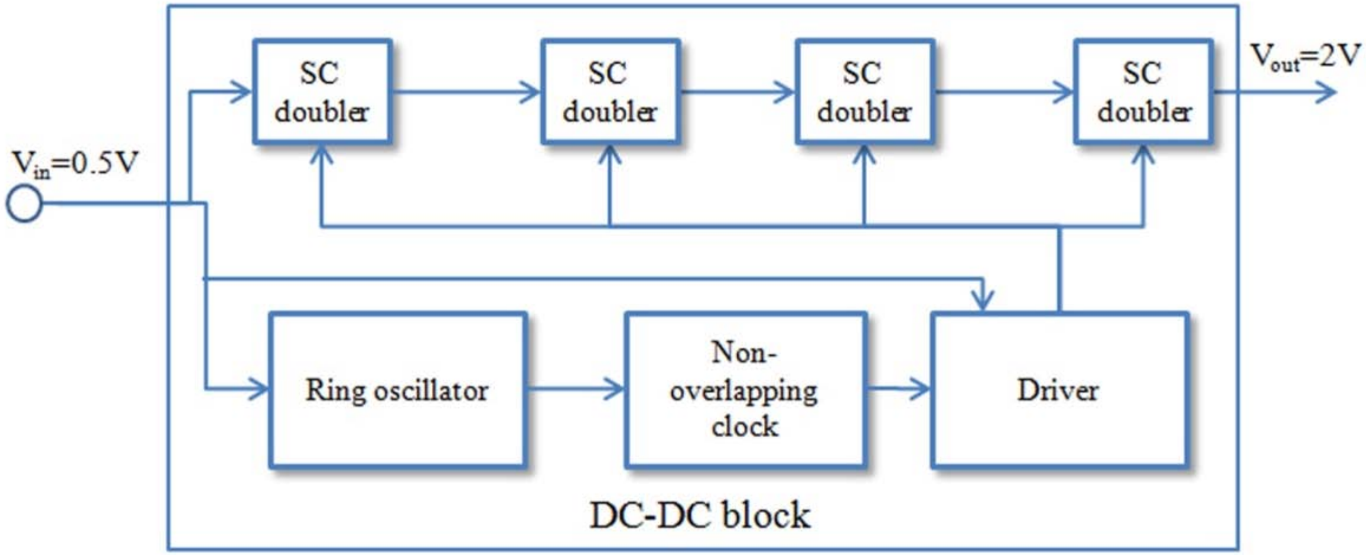

Full system block diagram

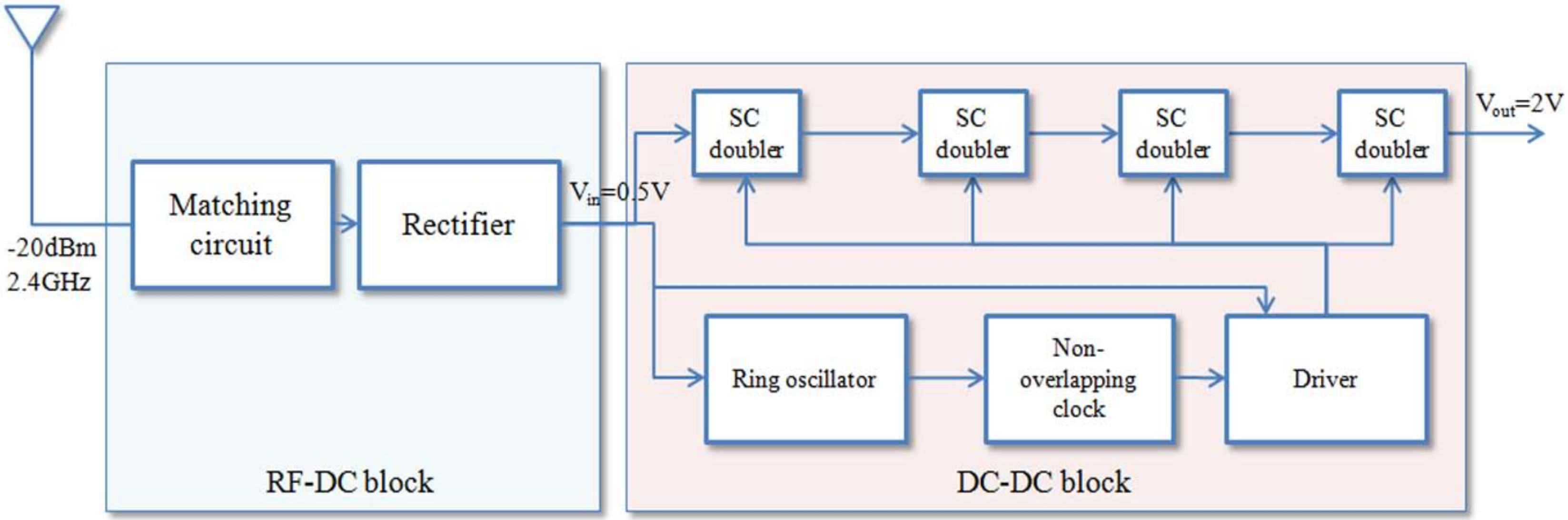

1. Output capacitor of RF-DC supplies DC-DC
2. Enable generator logic constructed using back to back inverters
3. 5 MOSFETs added to limit supply voltage to ring oscillator

RICOH imagine. change.

Sanjeev K, Manjunath M, TV Prabhakar, KJ Vinoy, Some Practical Considerations of RF to DC Converter using Low Vth CMOS Rectifier, Applied Computational Electromagnetic Conference, Guwahati, Dec 28-21, 2015

Full system simulations

- Output capacitor of RF-DC loaded heavily when clocks transition, so ripples exist in RF-DC output.
- Below 0.5V at clock transitions, above 0.5V between clock transitions
- Time step is 8ps for RF-DC simulation and DC-DC has to run for hundreds of µs or few ms, so simulations times are large.

Output voltage=2V across a load of 1.6MΩ, which gives

$$Efficiency = \frac{2^2 / 1.6 \times 10^6}{10^{-5}} = 25\%$$

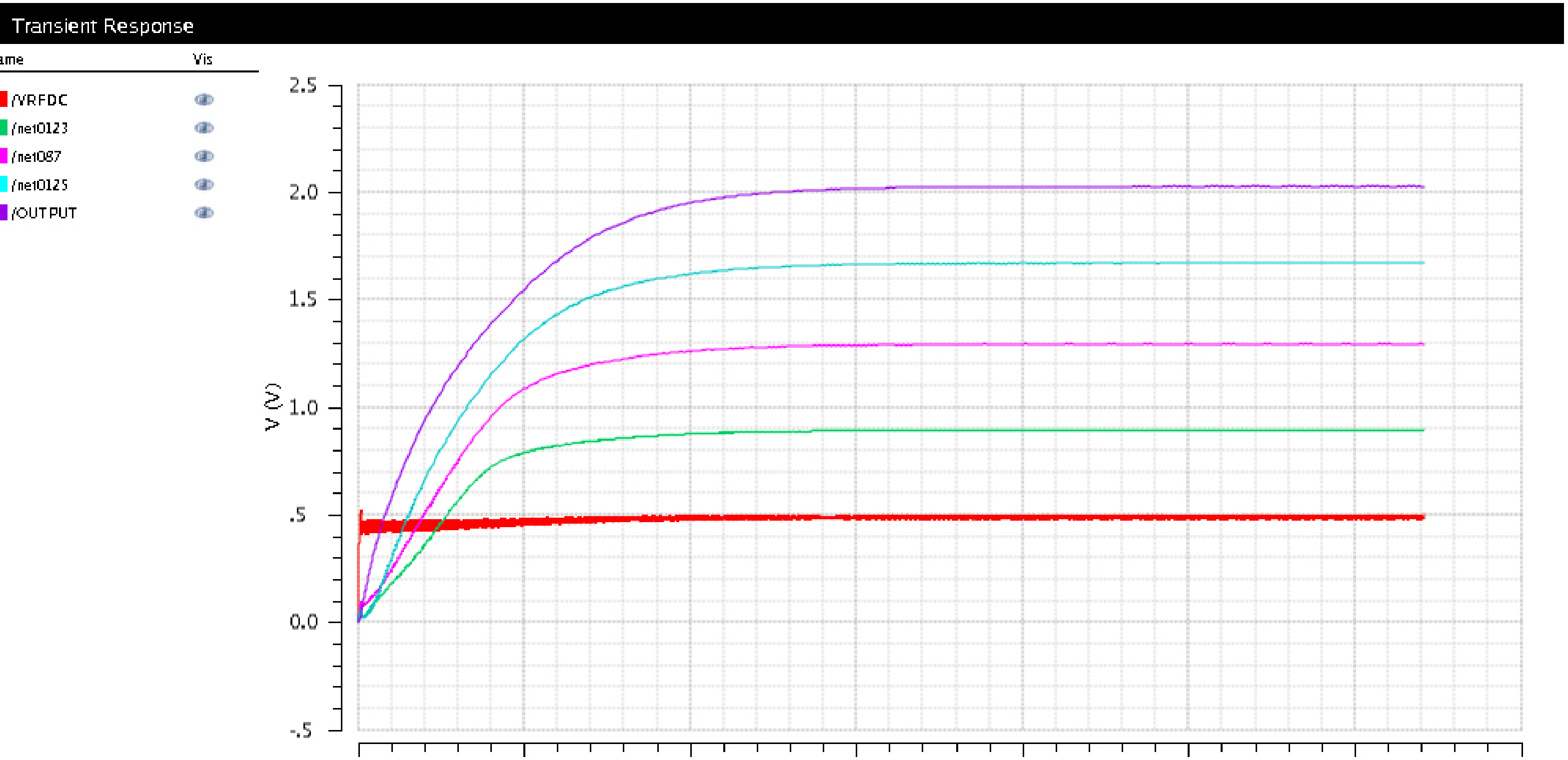

Summary with IC Design

- Low Vth NMOS based DCP gives 42.3% efficiency.
- FGCCR gives 55% efficiency.
- The overall system efficiency is 25%.
- Higher than efficiency reported in literature for RF-DC converter operating at -20dBm, 2.4GHz in 130nm technology.

Reference	This work	[5]	[7]	[6]
Power level	-20dBm	-25.7dBm	-22.6dB	-20dBm
Frequency	2.4GHz	2.45GHz	906MHz	2.4GHz
Efficiency	55%(simulated)	37%(measured)	10%(measured)	36%(simulated)
Rectifier	FGCCR in UMC 130nm CMOS	DCP in 0.5µm Silicon on Sapphire	DCP with floating gate transistors in 0.25µm CMOS	FGCCR in 130nm CMOS

6. ASIC Design for IOT

- Working on a 3-chip architecture
  - Our chip to enable sensing, and control functions
  - Communication using an external Monza chip
- Fabricated chip using commercial services!!

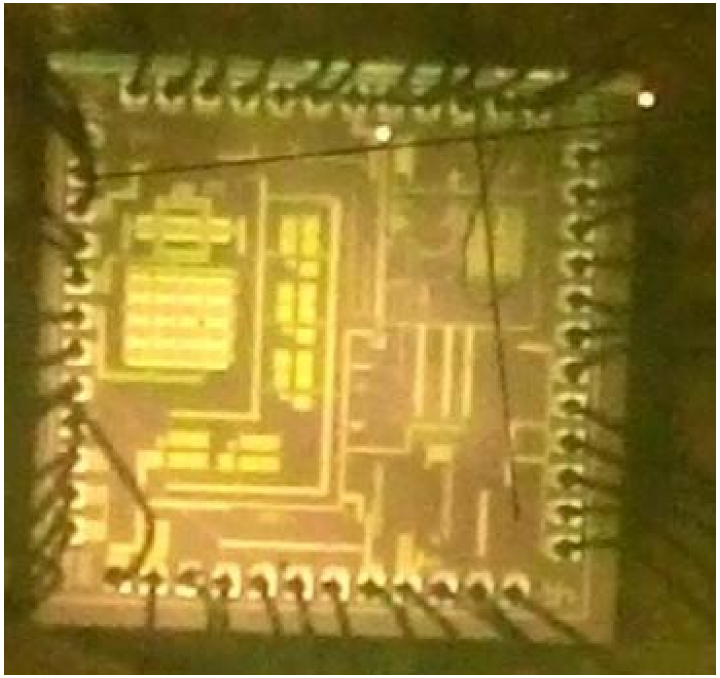

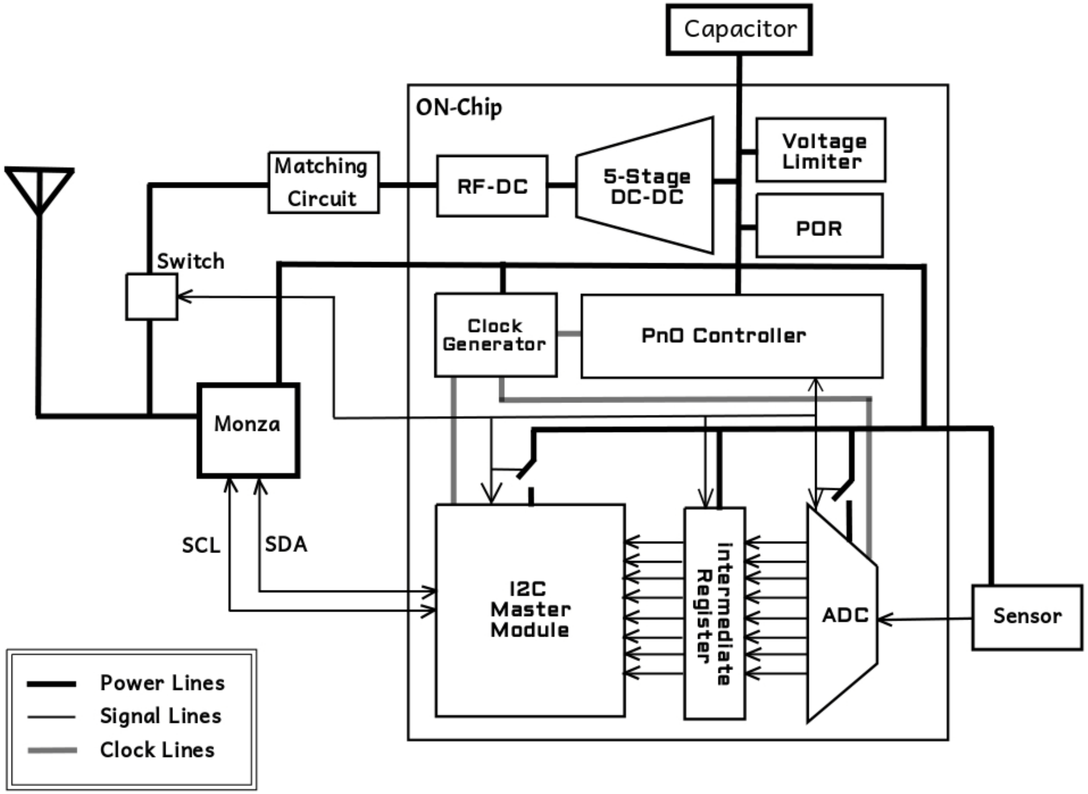

Battery-less Sensor node for BLE

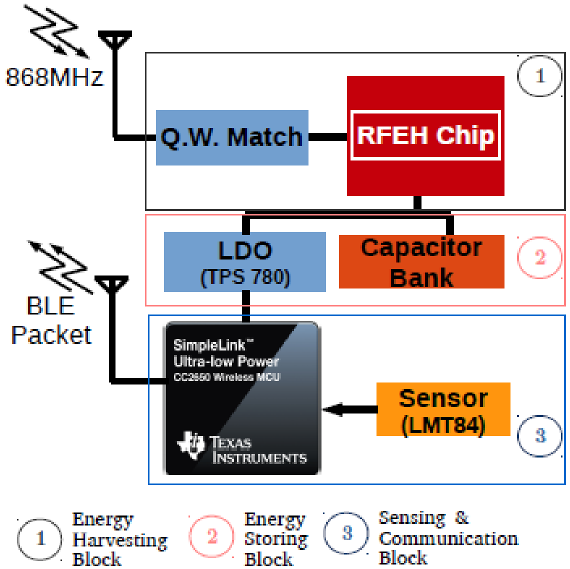

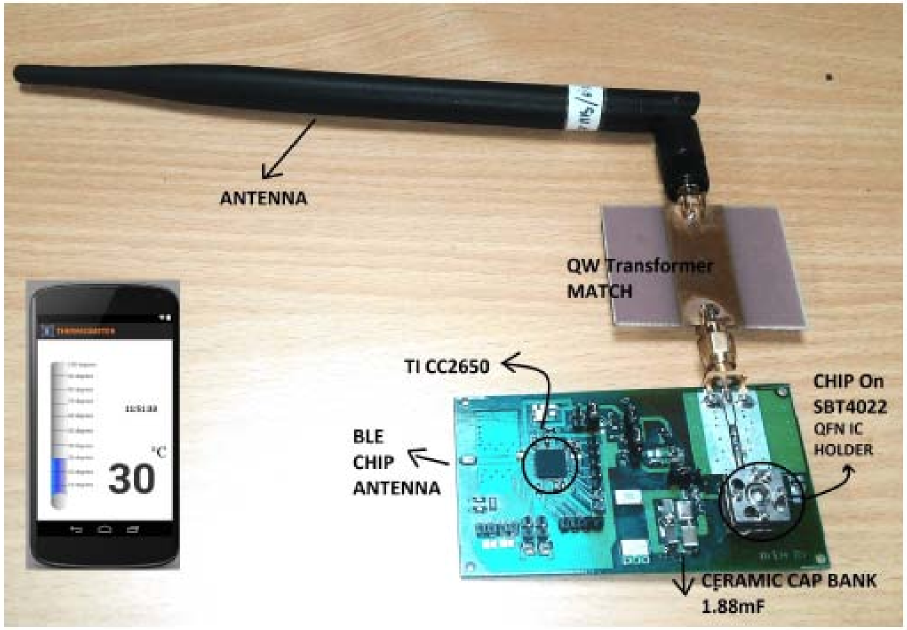

Distance from Reader (m)	Input Power (dBm)	Cold Start Time (min)	Packet Time (min)	Efficiency (%)
3	-2	15	1.75	2.2
4	-5	35	7	1.7
5	-8	120	32	1

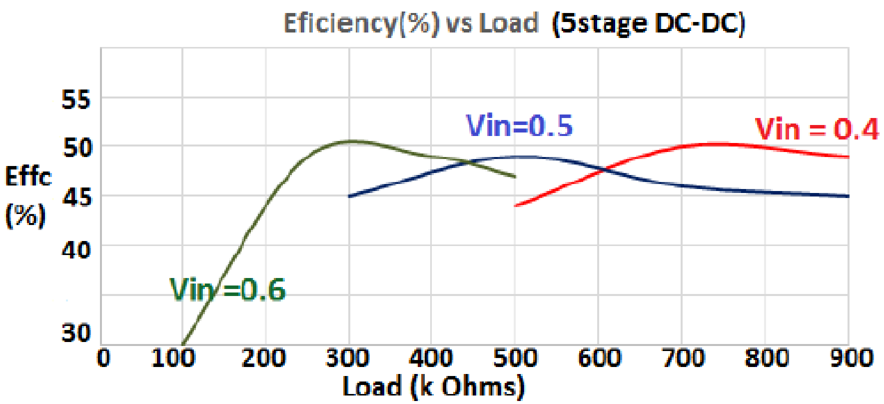

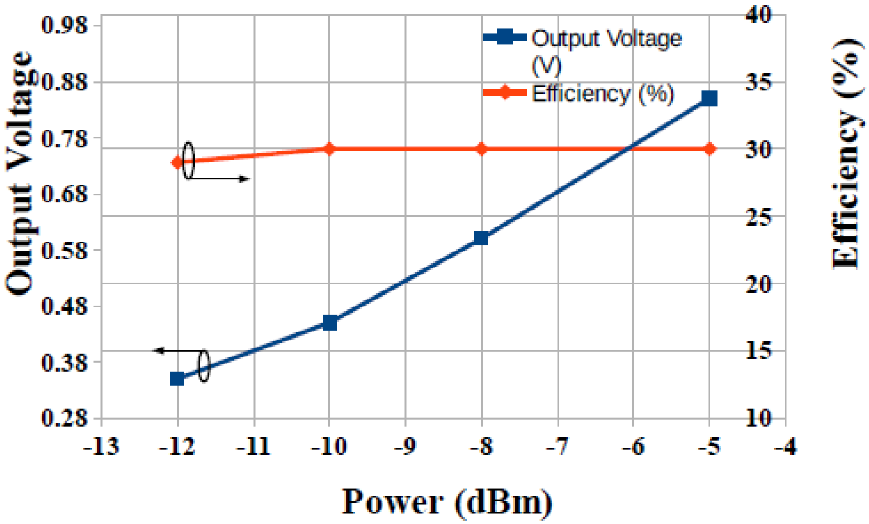

Bharat Hegde & Syed Younis 2015-16

Summary

- Most low power wireless terminals operate intermittently
- These require anywhere 50uW to about 10mW for their operation.
  - Batteries limited: cost, size, stored energy
  - Solar: not dependable through
- WPT and RF EH can enable wide use of IoT
  - Main challenges in the design is the low incident energy/power/voltage
  - High Quality factor components may help
- Several fabricated examples discussed here: All can transmit data to an aggregator wirelessly
  - Different standards implemented.

Acknowledgements

- Dr. TV Prabhakar, DESE, IISc
  - Gaurav Singh
  - Rahul P
  - Chaithanya C
  - Aditya Mitra
  - Prashuk Jain
  - Prashanth Raja
  - Nirmal John
  - Nithin Jose
  - Syed Younis
  - Bharat Hegde
  - Niharika Thakuria
- Prof Bharadwaj Amrutur
  - Uday S
  - NS Sreeram
- Others
  - Vivekanand M
  - Harikiran M
  - Manjunath M
  - Sanjeev K
  - Sandeep Rana
- Partial Funding From
  - ANRC (Boeing, Wipro, HCL)
  - Ricoh Research, India

Thank YOU

Free Energy From Air Circuit

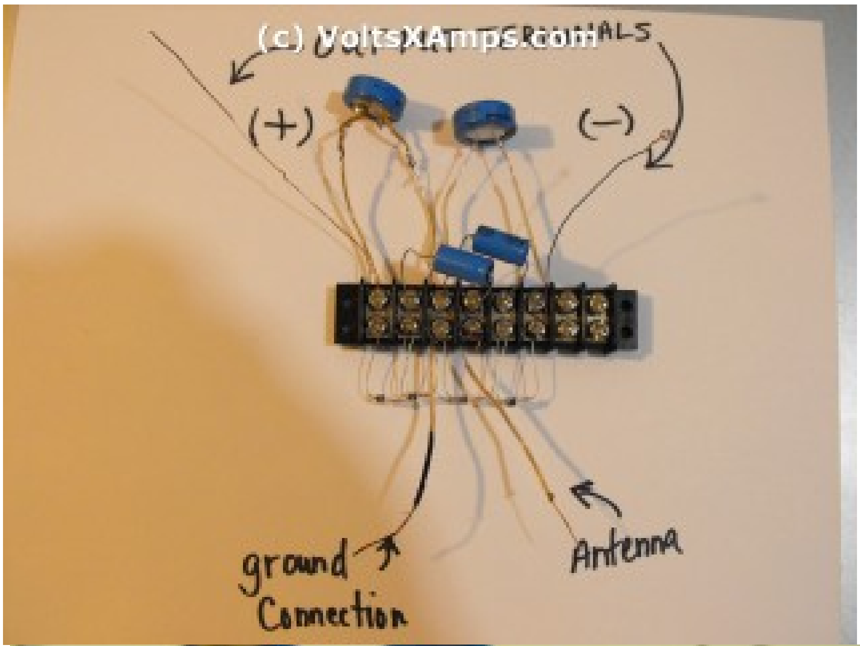

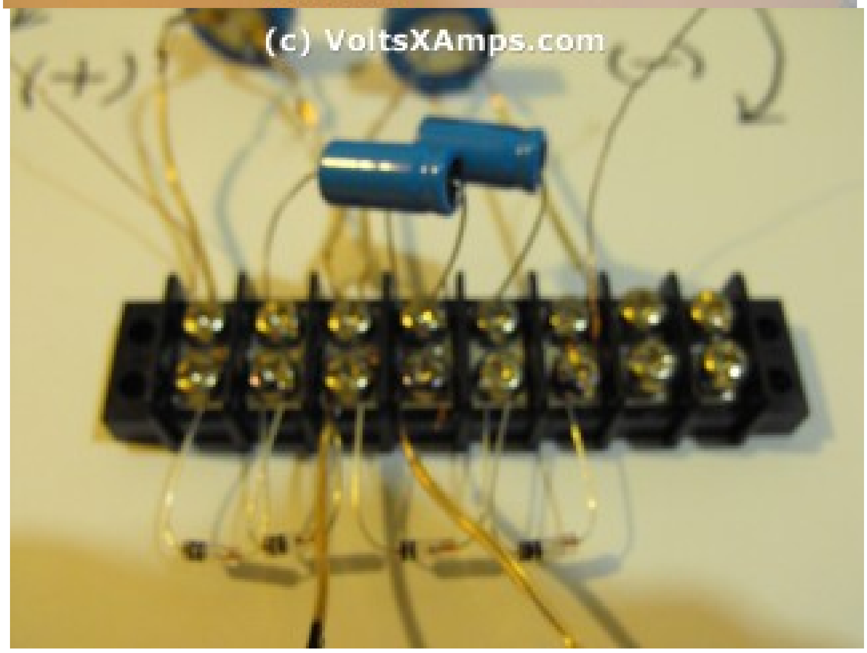

Last year I found a United States Patent that showed how to collect ambient energy right from the air. I finally decided to build this curcuit just to see what it could do.

[protected]

The above images are from the circuit I built. Most of the text and info comes direct from the US4628299filed by Joseph Tate.
US4628299

The Amazing Ambient Power Module

Parts List for the APM-2

Four 1N34 germanium diodes (Radio shack #276-1123) ~ Figure 1, X1, X2, X3, & X4
Two 0.2 mfd 50 V ceramic capacitors ~ Figure 1, C1 & C2
Two 100 mfd 50V electrolytic capacitors (Radio Shack #272-1016) ~ Figure 1, C3 & C4
Copper wire for antenna & ground connections

Introduction

The Ambient Power Module (APM) is a simple electronic circuit which, when connected to antenna and earth ground, will deliver low voltage up to several milliwatts. The amount of voltage and power will be determined by local radio noise levels and antenna dimensions

Generally a long wire antenna about 100' long and elevated in a horizontal position about 30' above ground works best. A longer antenna may be required in some locations. Any type copper wire, insulated or not, may be used for the antenna. More details about the antenna and ground will be discussed further on.

The actual circuit consists of two oppositely polarized voltage doublers (Figure 1). The DC output of each doubler is connected in series with the other to maximize voltage without using transformers. Single voltage doublers were often found in older TV sets for converting 120 VAC to 240 VDC. In the TV circuit the operating frequency is 60 Hz.

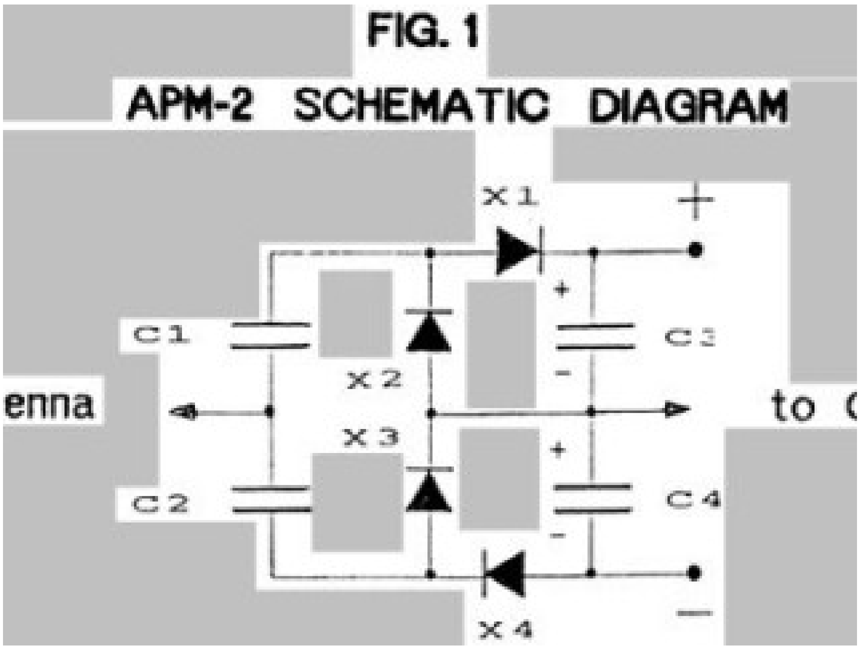

The APM operates at radio frequencies, receiving most of its power from below 1 MHz. The basic circuit may be combined with a variety of voltage regulation schemes, some of which are shown in Figure 2. Using the APM-2 to charge small NiCad batteries provides effective voltage regulation as well as convenient electrical storage. This is accomplished by connecting the APM-2 as shown in Figure 2B.

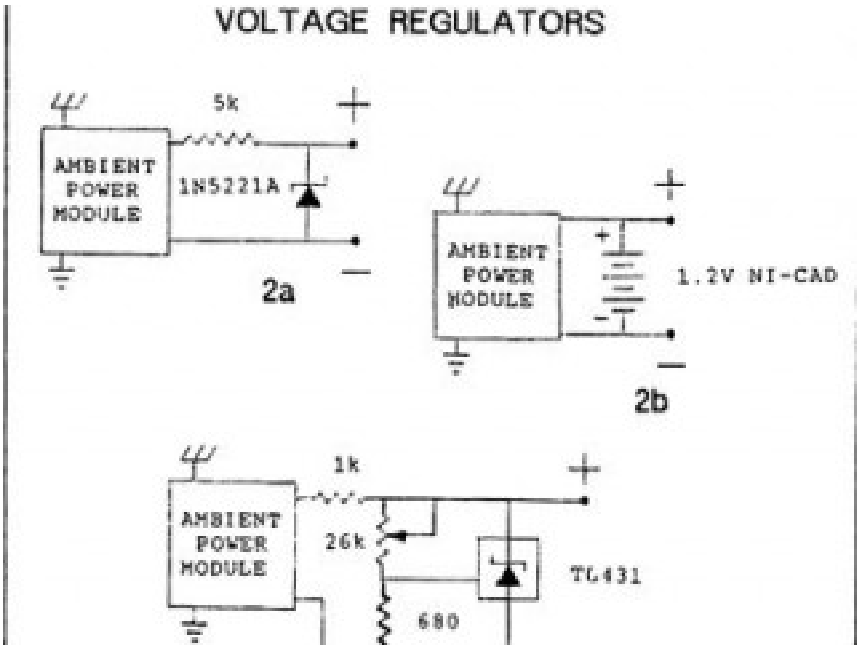

Charging lead acid batteries is not practical because their internal leakage is too high for the APM to keep up with. Similarly, this system will not provide enough power for incandescent lights except in areas of very high radio noise.

It can be used to power small electronic devices with CMOS circuitry, like clocks and calculators. Smoke alarms and low voltage LEDs also can be powered by the APM.

Figure 3 is a characteristic APM power curve measured using various loads from 0-19 kOhm. This unit was operating from a 100' horizontal wire about 25' high in Sausalito CA. As can be seen from the plot, power drops rapidly as the load resistance decrease from 2 kOhm. This means that low voltage, high impedance devices, like digital clocks, calculators and smoke alarms are the most likely applications for this power source. Some applications are shown in Figures 4 through 7.

FIG. 3 AMP Power Envelope

Volts vs. Resistance

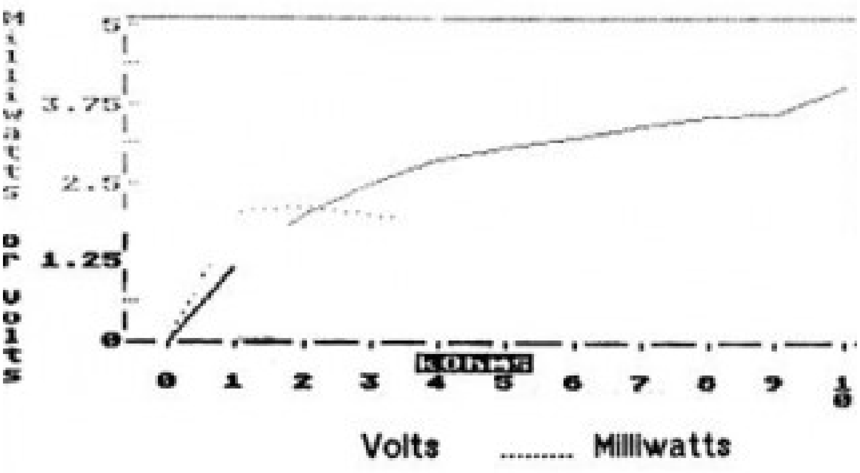

Figure 4 ~ A digital clock is shown powered by the APM-2. The 1.5 volt clock draws 28 microamps. Its position on the power envelope curve would be off the scale to the right and almost on the bottom line, dissipating only 42 microwatts.

FIG. 4 Clock powered by APM

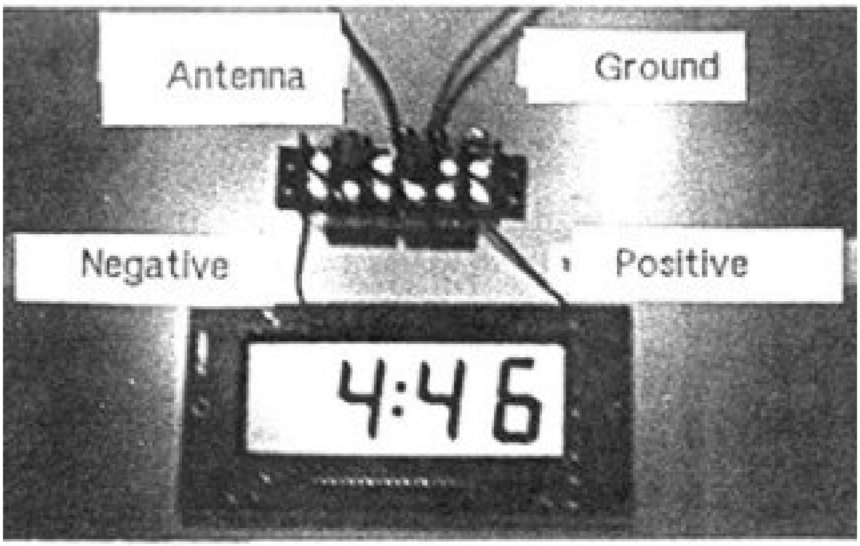

FIG. 5 APM charging a battery

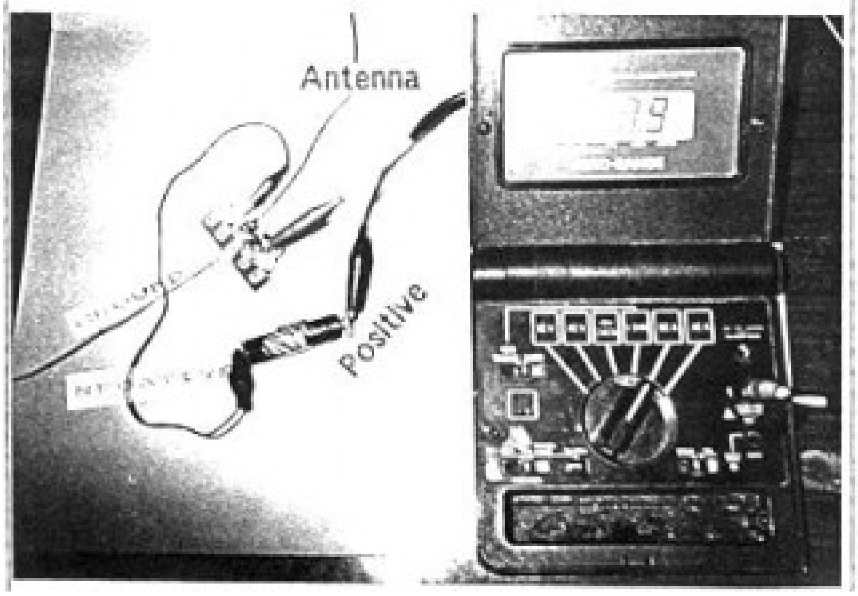

Figure 6 shows a clock which has the APM-2 built into it so it is only necessary to connect the antenna and ground wires directly to the clock. The antenna for this clock, which is a low frequency marine type, is shown in Figure 7.These antenna are expensive, not generally available, and usually don't work any better than the long wire mentioned above. But it may be necessary to use them in urban areas where space is limited and radio noise is high.

FIG. 6

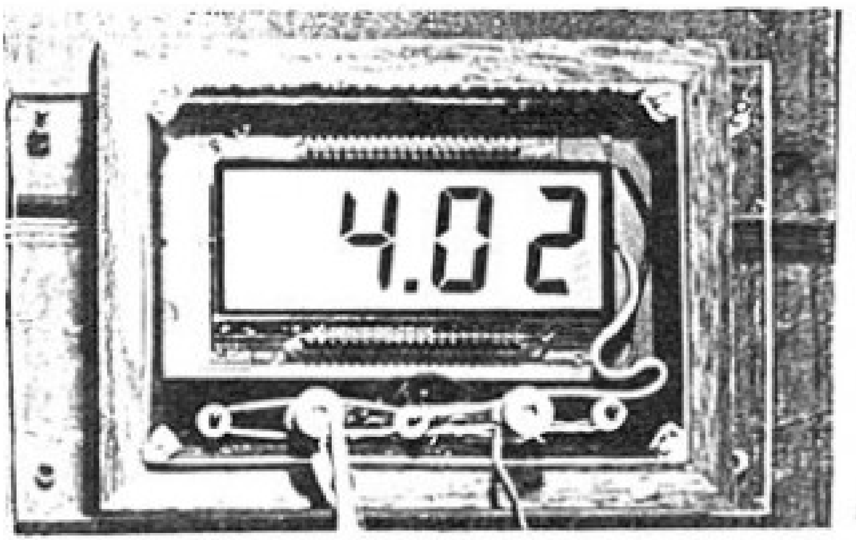

Building the Module

The builder has a choice of wiring techniques which may be used to construct the module. It may be hand wired onto a terminal strip, laid out on a bread board, experiment board, or printed circuit. Figure 8 shows some of the different ways of constructing the APM-2.

Figure 8A is constructed on a screw strip terminal; Figure 8B is constructed on a perforated breadboard; Figure 8C is built on a standard experiment board; Figures 8D, 8E, and 8F are all printed circuits; Figure 8F is made up on a solder strip terminal.

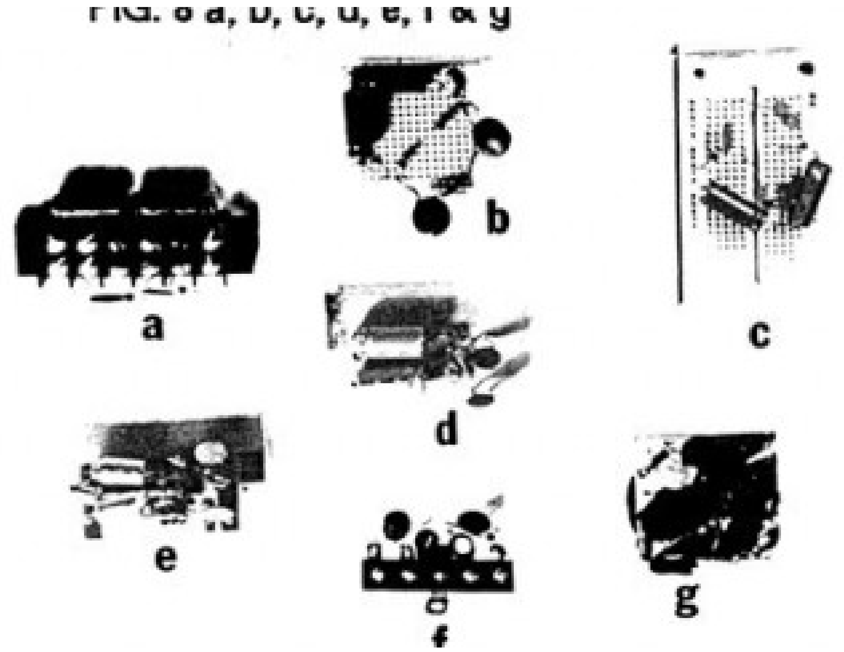

If you wish to make only one or two units, hand wiring will be most practical, either on a terminal strip or breadboard. Assembly on the terminal strip (Figure 8A) can be done easily and without soldering. It is important to get the polarity correct on the electrolytic capacitor. The arrow printed on the side of the capacitor points to negative.

Figure 9 is a closer view of the terminal strip with an illustration of the components and how they are connected.

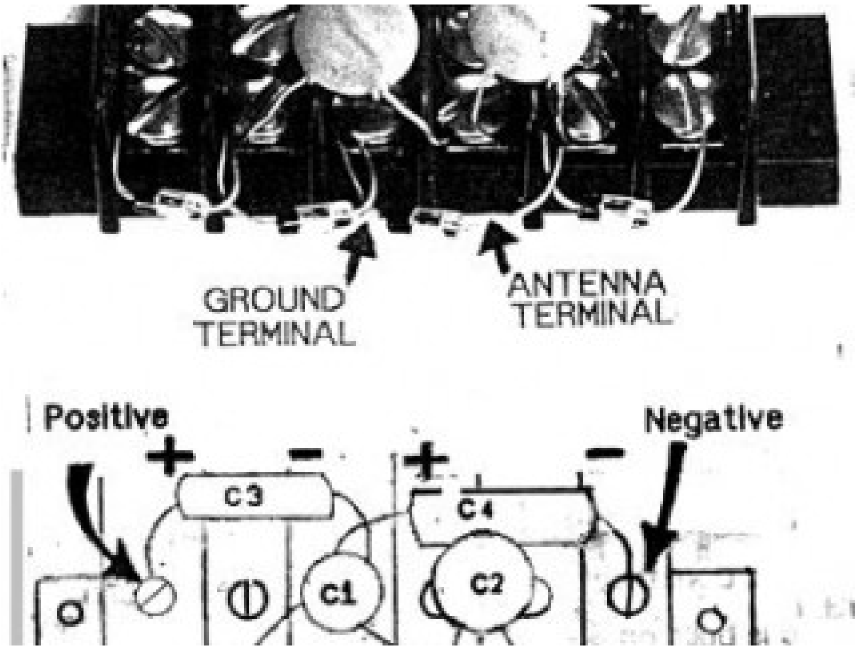

The breadboard unit is shown in Figure 10 with all components on one side and all connections on the other. All you need is a 2" x 2" piece of perforated breadboard (Radio Shack #276-1395) and the components on the parts list. Push component wires through the holes and twist them together on the other side. Just follow the pattern in the photo, making sure to observe the correct polarity on the electrolytic capacitors and the diodes. The ceramic capacitors may be inserted in either direction.

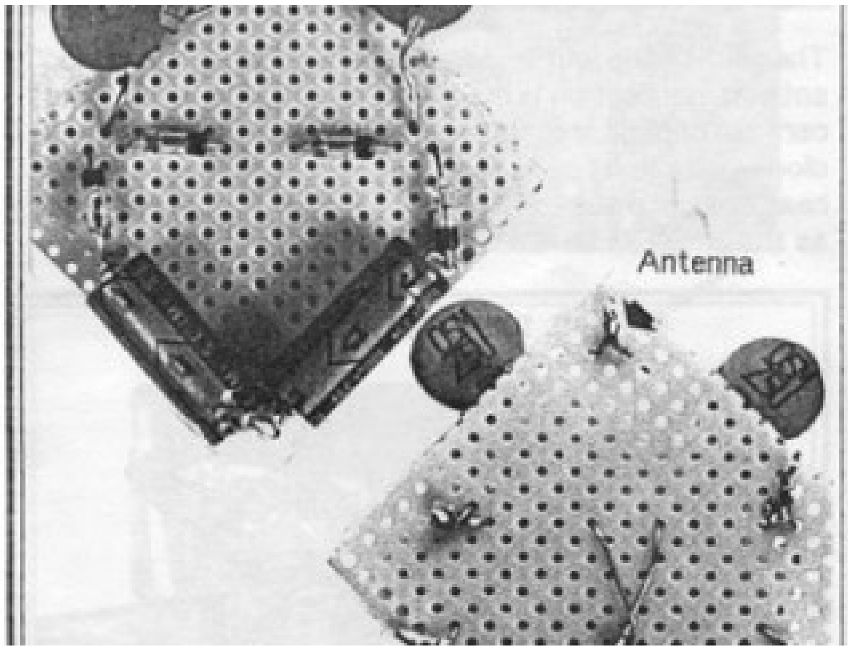

The experiment board unit is assembled by simply pushing the component leads into the board as shown in Figure 11. This unit is powering a small red LED indicated by the arrow.

FIG. 11 EXPERIMENT BOARD

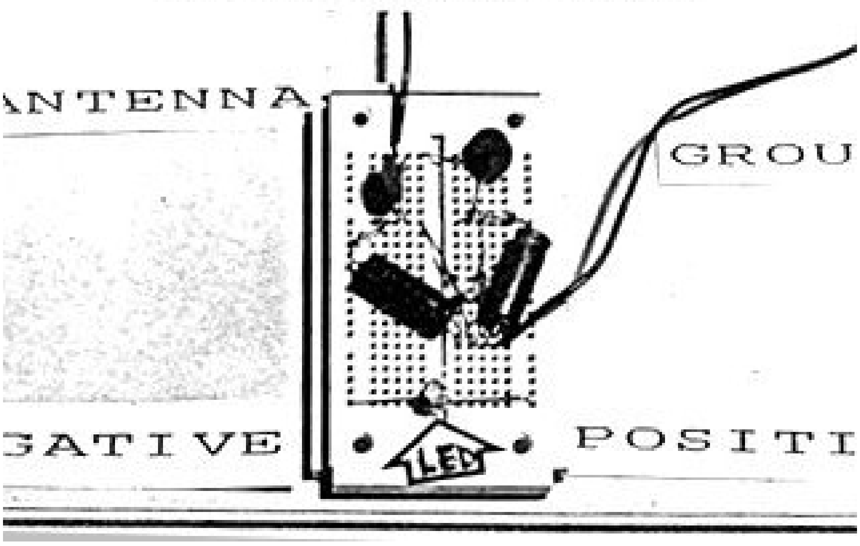

The solder strip unit is made up on a five terminal strip. The antenna connection is made to the twisted ends of the ceramic capacitors. When soldering the leads of the 1N34 diodes, care must be taken to avoid overheating. Clip a heat sink onto the lead between the diode and the terminal as shown in Figure 12.

FIG. 12 SOLDER STRIP UNIT

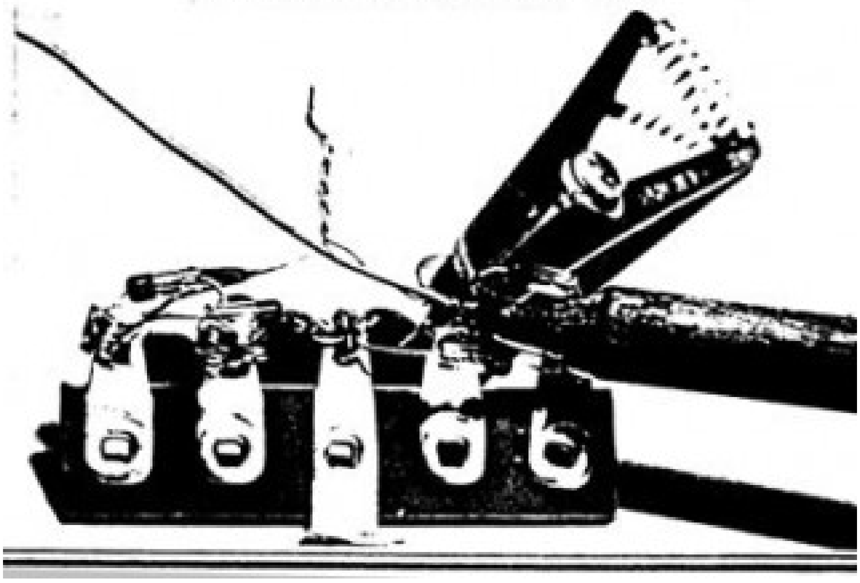

FIG. 13

Figure 14 shows the front and back view of the completed printed circuit.

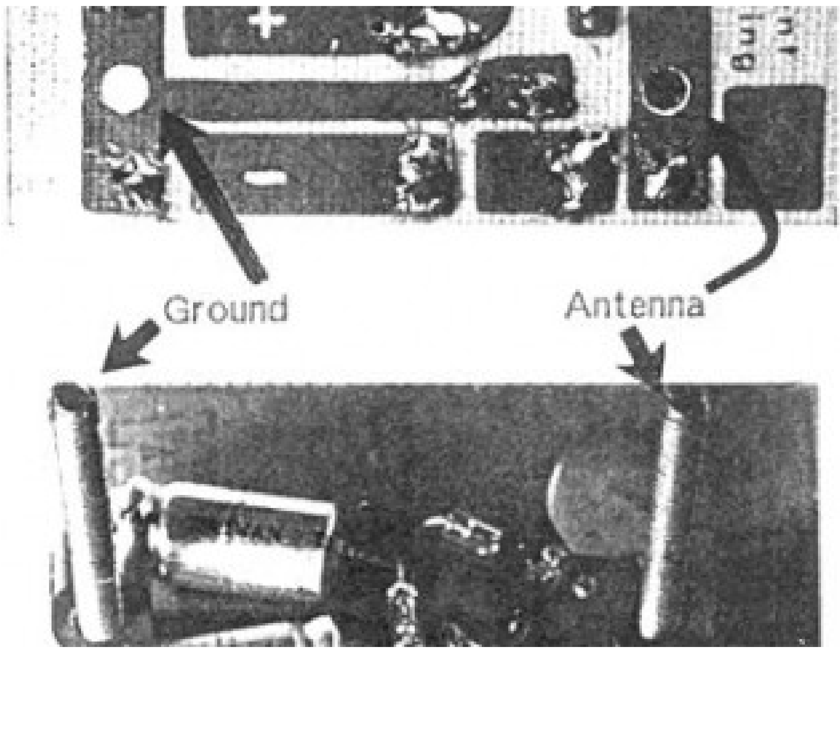

A small switch may be installed on the board to activate the zener regulator (Figure 15). This board was designed for use in clocks.

FIG. 15

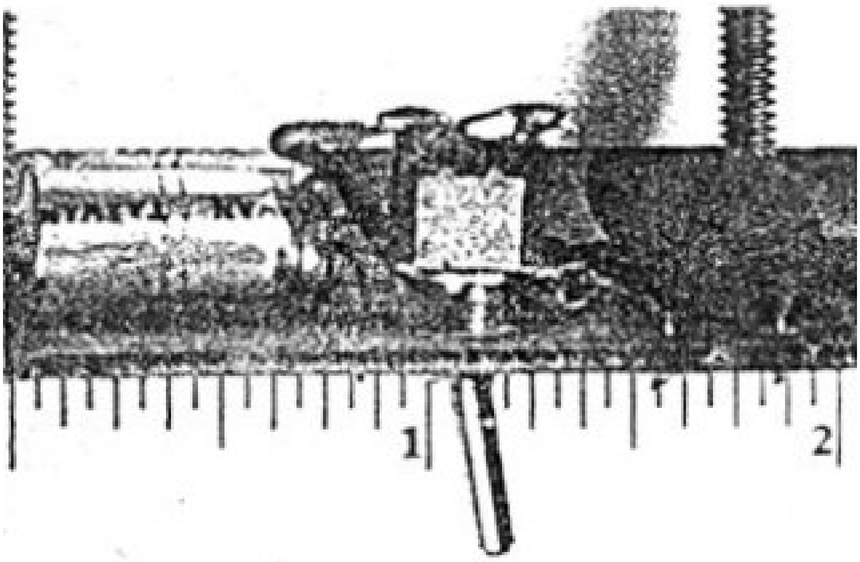

Antenna Requirements

The antenna needs to be of sufficient size to supply the APM with enough RF current to cause conduction in the germanium diodes and charge the ground coupling capacitors. It has been found that a long horizontal wire works best. It will work better when raised higher. Usually 20-30 feet is required. Lower elevations will work, but a longer wire may be necessary.

In most location, possible supporting structures already exist. The wire may be stretched between the top of a building and some nearby tree or telephone pole. If live wires are present on the building or pole, care should be taken to keep your antenna and body well clear of these hazards.

To mount the wire, standard commercial insulators may be sued as well as homemade devices. Plastic pipe makes an excellent antenna insulator. Synthetic rope also works very well, and has the advantage of being secured simply by tying a knot. It is convenient to mount a pulley at some elevated point so the antenna wire may be pulled up to it using the rope which doubles as an insulator (Figure 16).

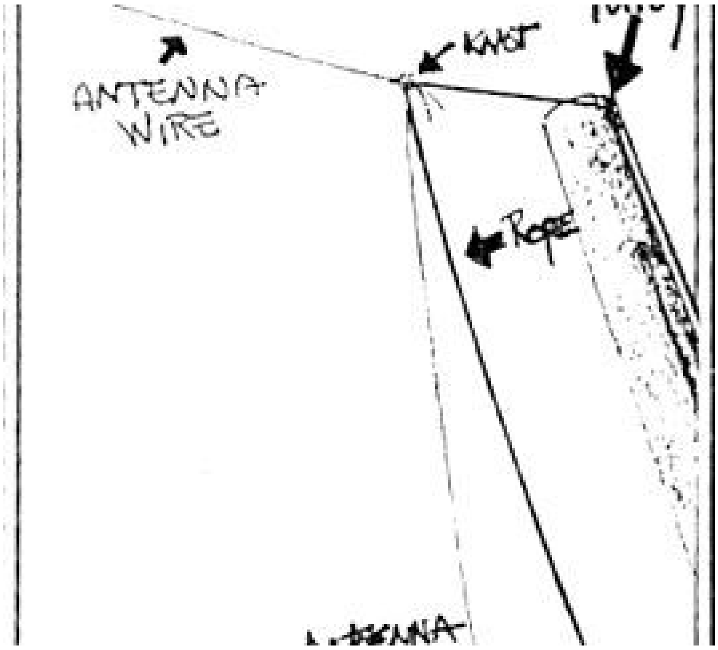

Figure 17 is an illustration of a horizontal wire antenna using a building and tree for supports.

FIG. 17

Horizontal Wire Installation

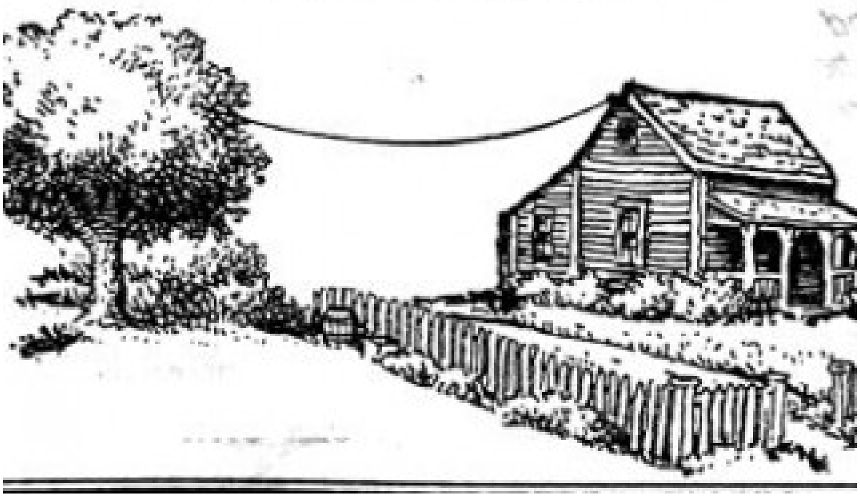

Grounding

Usually a good ground can be established by connecting a wire to the water or gas pipes of a building. Solder or screw the

wire to the APM-2 ground terminal. In buildings with plastic pipes or joints, some other hookup must be used. A metal rod or pipe may be driven into the ground in a shady location where the earth usually is damper. Special copper coated steel rods are made for grounds which have the advantage of good bonding to copper wire. A ground of this type usually is found within the electrical system of most buildings.

Conduit is a convenient ground provided that the conduit is properly grounded. This may be checked with an ohmmeter by testing continuity between the conduit and system ground (ground rod). Just as with the antenna, keep the ground wire away form the hot wires. The APM's ground wire may pass through conduit with other wires but should only be installed by qualified personnel.

Grounding in extremely dry ground can be enhanced by burying some salts around the rod. The slats will increase the conductivity of the ground and also help retain water. More information on this subject may be found in an antenna handbook.

Good luck getting your Ambient Power Module working. It is our hope that experimenters will find new applications and improve the power capabilities of the APM.

Inventors: Tate, Joseph B. (Sausalito, CA)
Brown, David E. (Mill Valley, CA)

Application Number: 06/695632

Publication Date: 12/09/1986

Filing Date: 01/28/1985 NOTE: The images maybe hard to see as they were originally scanned and uploaded in black and white. If it helps you to replicate this device you may want to check the images of the one I built at the very top (in color) Here are some more photos of my completed unit for your review.

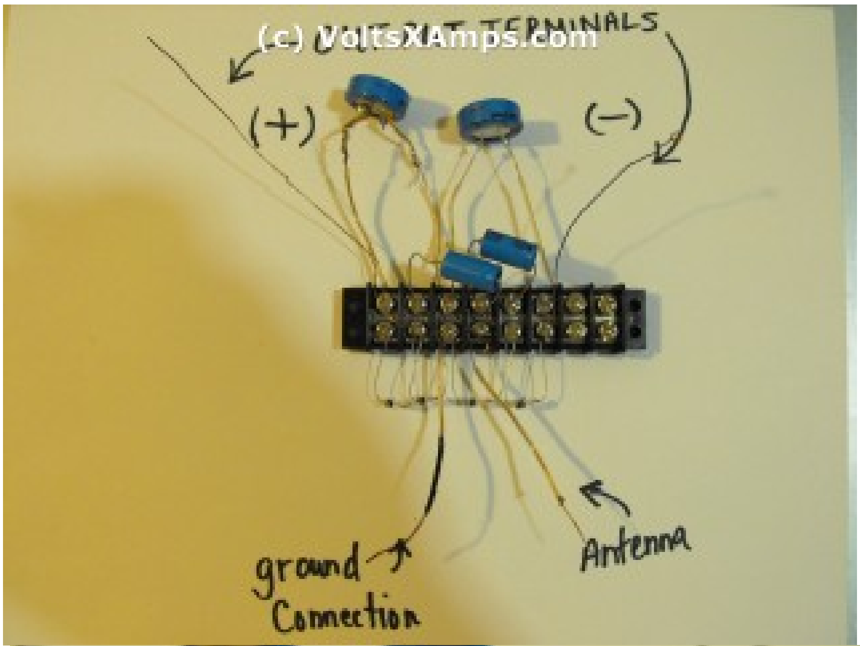
(c) VoltsXAmps.com
TERMINALS
(+)
(−)
Antenna
ground
Connection

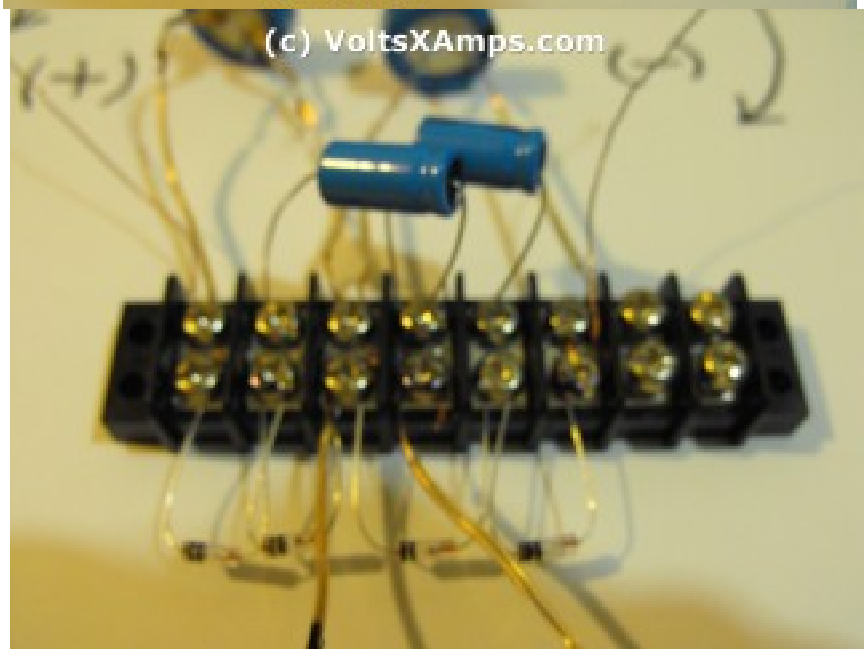
(c) VoltsXAmps.com
(+)

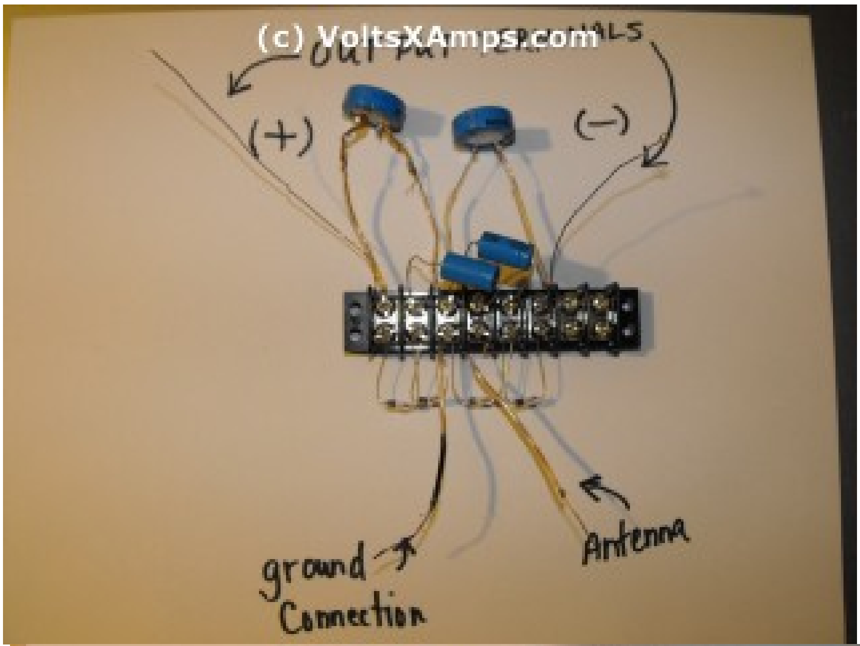
(c) VoltsXAmps.com
(+)
(–)
ground
Connection
Antenna

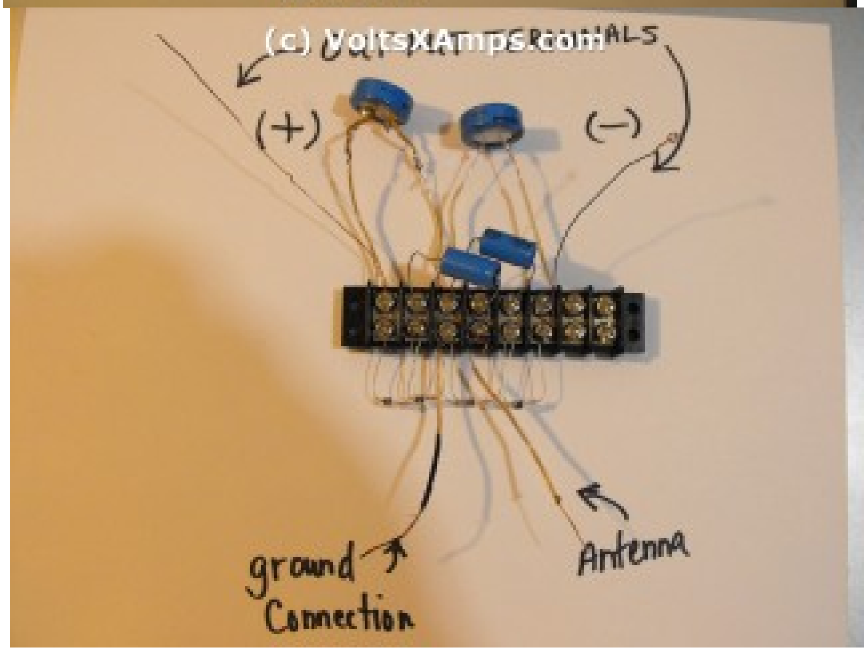
(c) VoltsXAmps.com
(+)
(–)
ground
Connection
Antenna

[/protected]

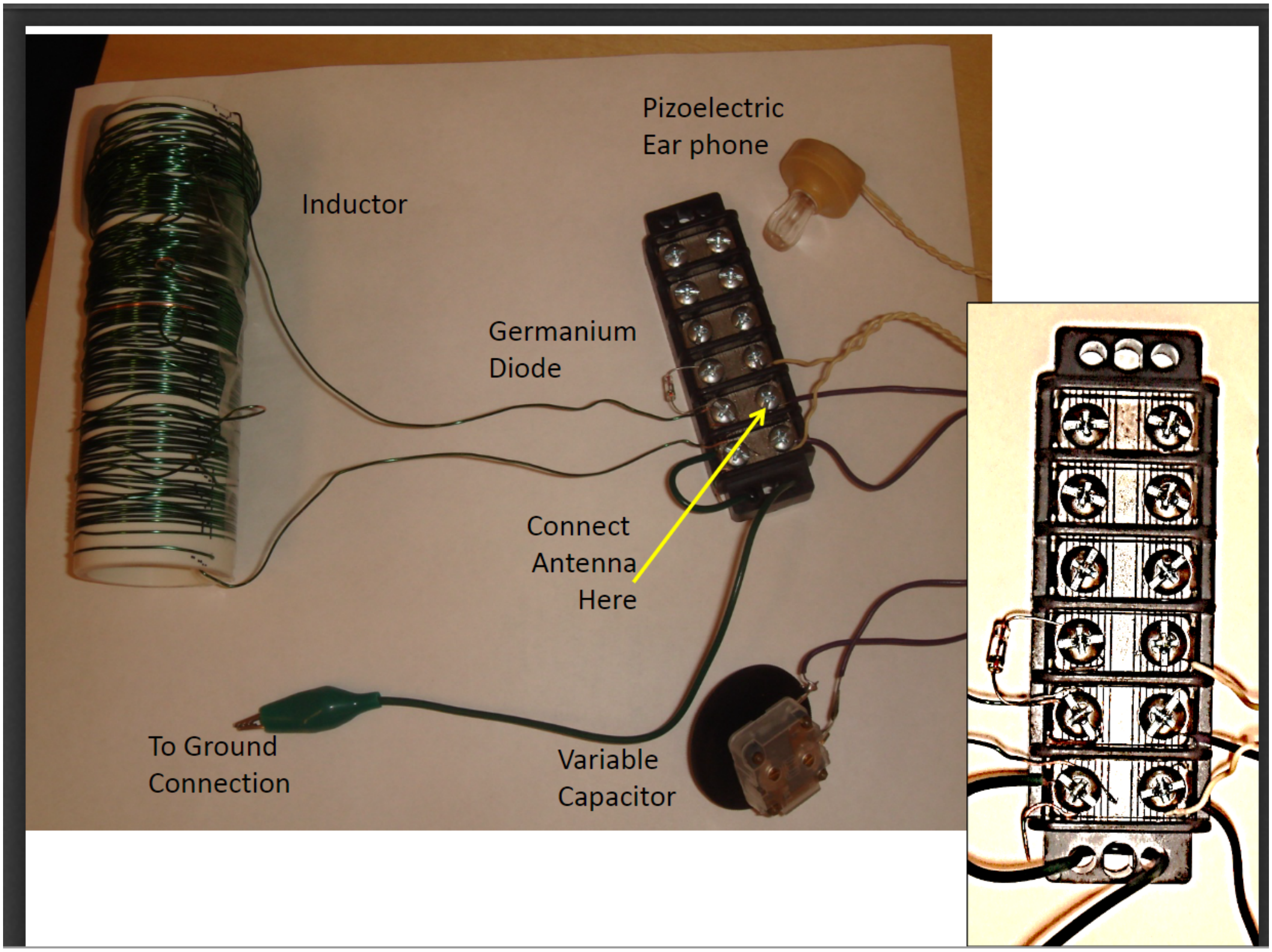
Pizoelectric
Ear phone
Inductor
Germanium
Diode
Connect
Antenna
Here
To Ground
Connection
Variable
Capacitor

FM Crystal Radios?

I have heard, even from a physicist, that it is impossible to build FM crystal radios. On the other hand some experimenters claim that they have built them. This argument intrigued me to try and build an FM crystal radio, which I have done successfully. To my surprise, the result is an astounding performer, pulling in four local stations in Tucson. When connected as a receiver to a good sound system the sound fidelity is as good or better than more expensive AM radios. In fact, it sounds "high-fidelity".

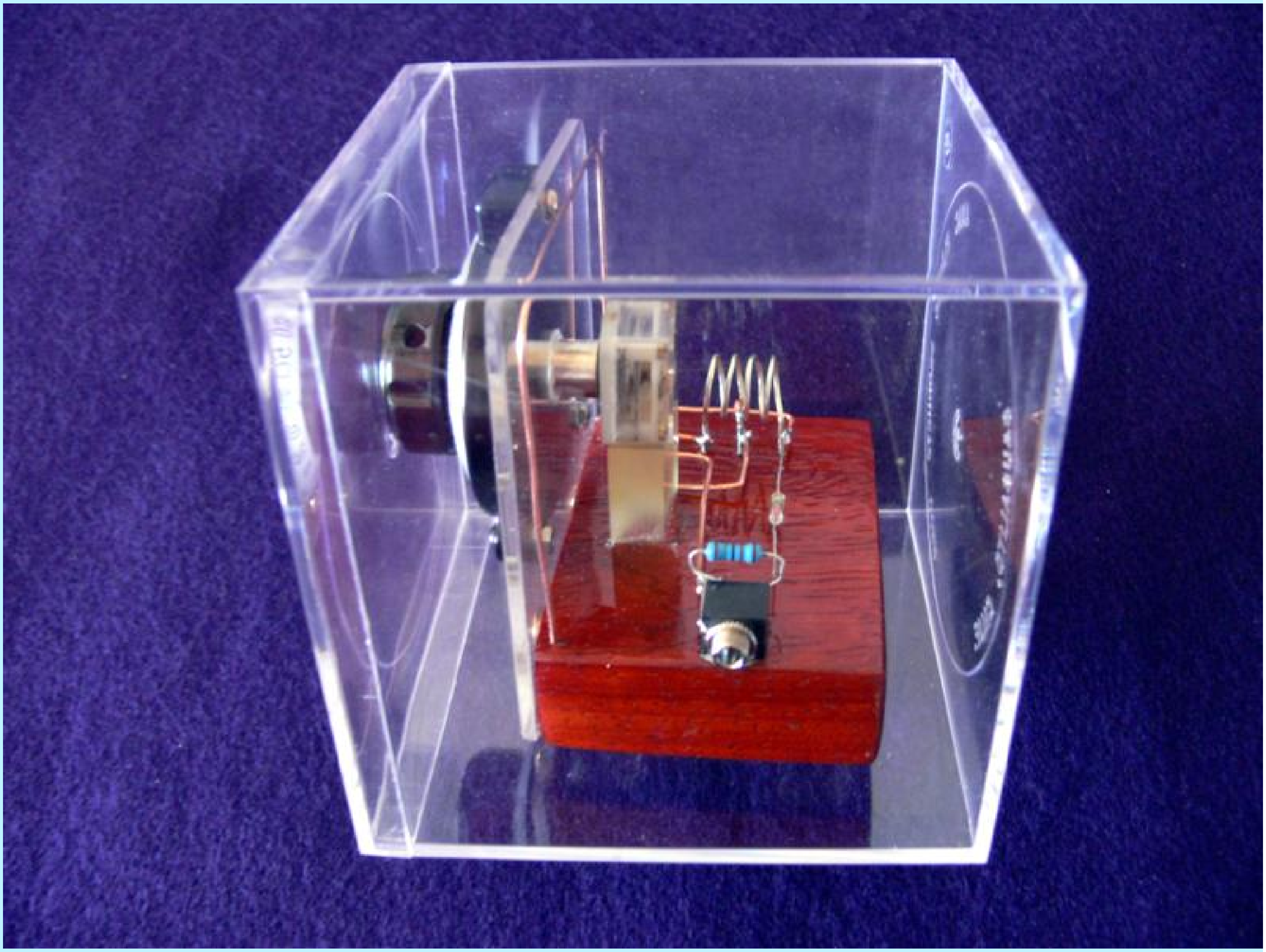

This picture shows the Solomon FM Crystal Set in an acrylic display case. I made the set specifically to fit inside this case (the case came first).

My definition of a crystal radio is one that is not powered, except by the radio transmission itself and employs a crystal detector. So, it should work without any batteries or AC power. An FM crystal receiver must be able to detect and receive FM signals well enough to be heard in earphones without any such extra power.

This FM receiver is an amazing performer. It has crystal clear reception (pun intended), good sensitivity, but only fair selectivity. This set was a discovery for me. I started out by designing and building the normal AM sets. Then one day while testing the "Mystery" set (see my other web links), to my surprise, in addition to the expected panoply of AM stations, I heard a very faint signal that I could not tune out. At first, it seemed too weak to identify. When I tuned out all the AM stations, I was astonished to hear the announcement "KiiM FM, 99.5"! This is a

country music FM station here in Tucson. It was all over the dial, untunable, but the much louder AM signals masked it when they were tuned in.

I set myself the task of trying to improve the FM reception. I tried some simple circuit modifications that did not seem to improve anything. Then I connected a dipole antenna instead of the AM antenna I normally use. Suddenly, the FM signal was much clearer, although still weak. By using the audio output and sound system amplifier, I was even more amazed that four different FM stations came in loud (or rather medium) and clear. I found that changing the telescoping antenna length and position I could tune the stations in and out. They were KRQ, KLPX, KiiM, and KHYT all local FM stations with transmitters nearby. Their reception was also affected by the length and position of the audio output cable.

After doing some research, I discovered that there was a physical theory that claimed that FM reception was possible and even probable using the same circuit as an AM receiver. The theory is called "slope detection". So, I set out to find circuit improvements. A web search yielded little, mostly theory. But there was enough information that I thought I could make some modifications to the AM circuits to make them more tunable to FM signals and less tunable to AM. Since FM operates at higher frequencies, all I had to do, I thought, was make the coil and caps smaller. After much "tinkering" I arrived at the current circuit.

The circuit looks identical to a classic AM crystal circuit but is even simpler to build. The components were reduced in dimension to resonate at higher frequencies. This was done by experimenting with smaller and smaller coils and capacitors. The antenna is also much reduced in size (from that of AM) to resonate at higher frequencies (the antenna is crucial). The air variable capacitor I used has two trimmers in it which should be adjusted for best reception.I have found that a commonly available vernier dial and knob will fit the capacitor nicely. See end of article for a picture of the variable. C3 is a ceramic capacitor of 18 pf, but may be anywhere from 10 to 50pf. A detected FM signal is converted to AM due to an effect called slope detection that modulates amplitude.

This FM Crystal Set works best near the transmitter (I have not tested it beyond about 10 miles). Secondly, the sound level is quiet, especially without an amplifier. A quiet room is needed for listening with earphones. One must be willing to move the set around to find a location for the best reception of signals. However, in addition to listening with high impedance earphones (crystal or otherwise), the set can be connected directly to an audio amplifier's low level magnetic input which can then play amplified through a sound system at any volume -- sounds GREAT. In fact, I recommend starting tests with the FM crystal set by connecting it to the low-level phono inputs of a receiver or preamplifier. (Nowadays, many receivers don't even have a phono input!) That way you can crank up the volume, which makes it more likely to find the FM stations. If no signals are detected, I also recommend connecting an external "rabbit ear" antenna or hanging a short wire (12 inches or so) in various positions next to the internal antenna. The variable length of rabbitt ears can help to tune in stations.

No additional wiring or antenna is necessary (the antenna is optimized in length for FM.)

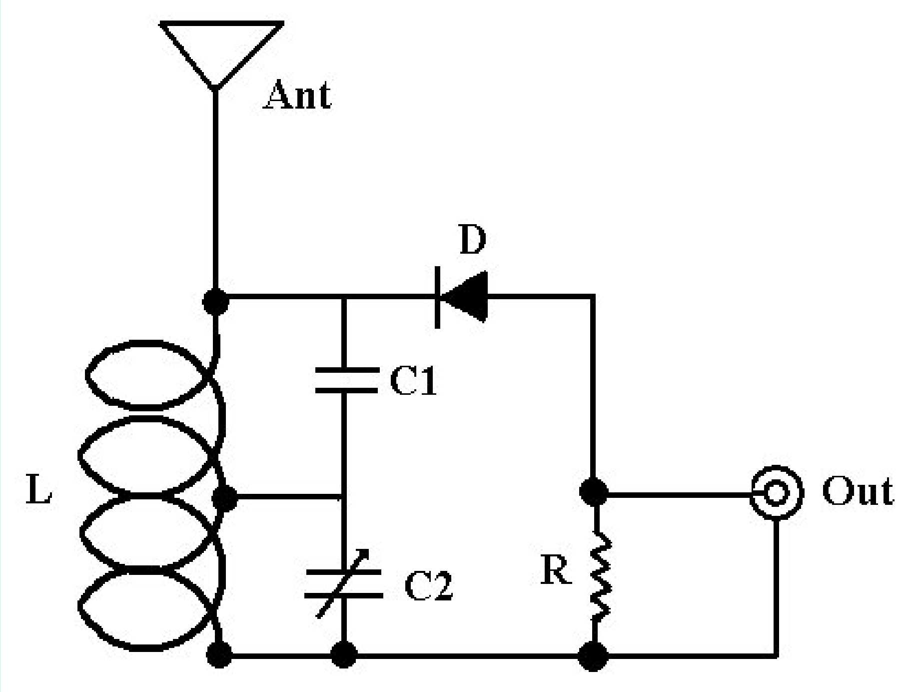

L - 4 turns #18 copper or silver wire, 12mm inside diameter, tapped at 2.5 turns
Ant - 7 inches of #18 bare copper wire
C1 - 18 pf ceramic capacitor
C2 - 50 pf air variable capacitor
D - 1N34 diode or rock crystal
R - 150K resistor

The diode is tapped directly to the antenna. The vernier dial fits directly on the tuning capacitor. The antenna parallels the perimeter of the acrylic face plate. "Military style" #18 AWG wiring is used without any insulation. It is important to keep the components physically close together. The component specifications are the same as in circuit #2. The coil is silver rather than copper, but copper does just as well. I think that the contrast of the silver and copper is beautiful. The coil was wrapped around a Sharpie Permanent Marker, then slipped off and expanded slightly. The wooden base is made from lacquered, polyurethane padouk.

I consider this set a work of art as well as science and think it is the most elegant crystal receiver I have created. I love the contrast of the silver coil, the copper antenna, the clear acrylic faceplate, the black vernier dial, the white and transparent variable capacitor, and the subtle colorings on the resistor, the diode, and the lucite base. Yet the circuit is so ridiculously simple that some will not believe it is possible without building it themselves. No shielding is necessary, and there is no problem with hand capacitance. However, the output cable position may affect reception sensitivity.

Photos of wired circuit

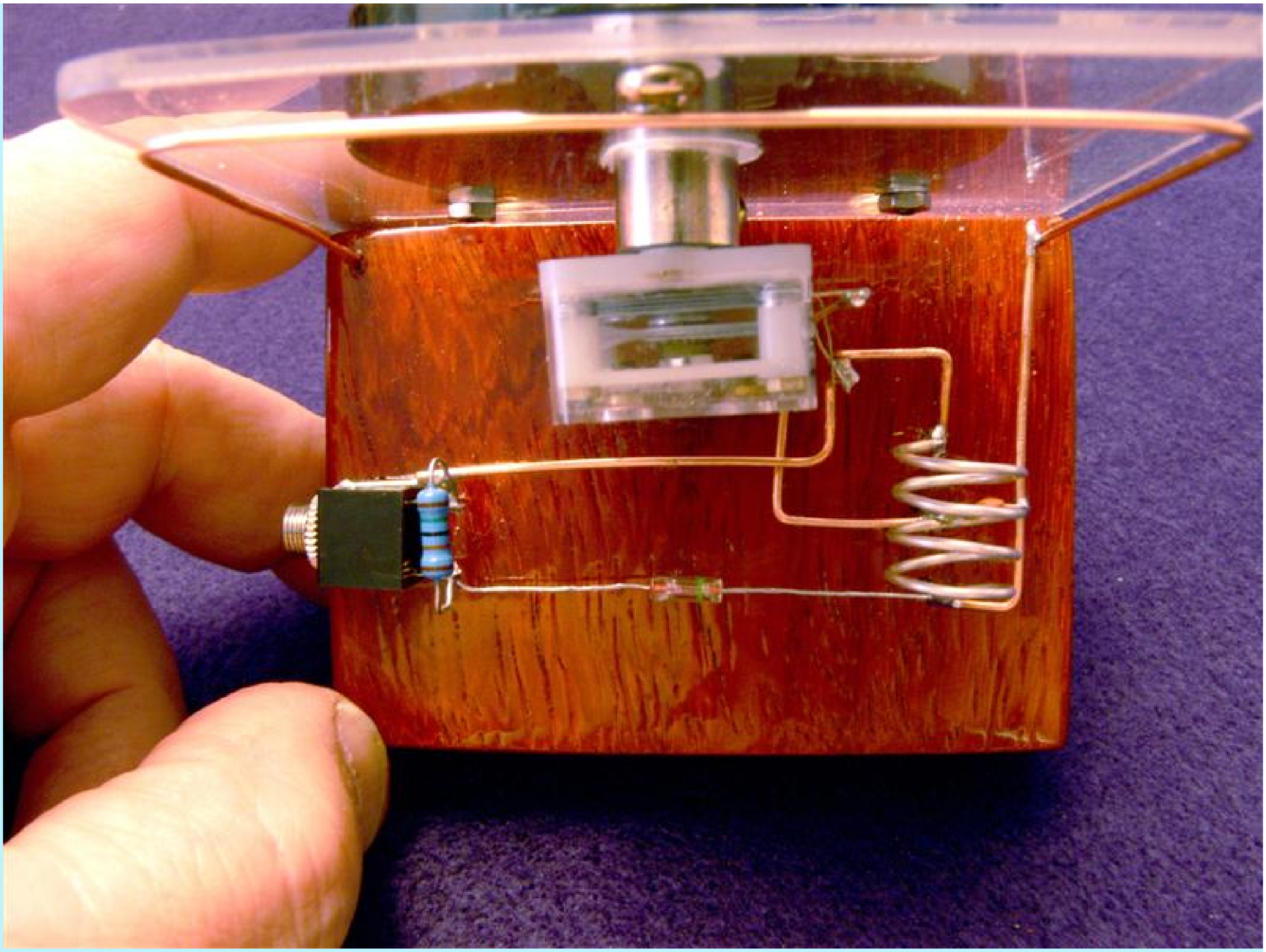

A hand is included in this photograph to show scale. Note the military style wiring, diode, and antenna. I wanted the wiring to create a modern design similar to a Mondrian painting. Not only is this set beautiful, it works! No power and no long antenna! It looks like a work of fiction.

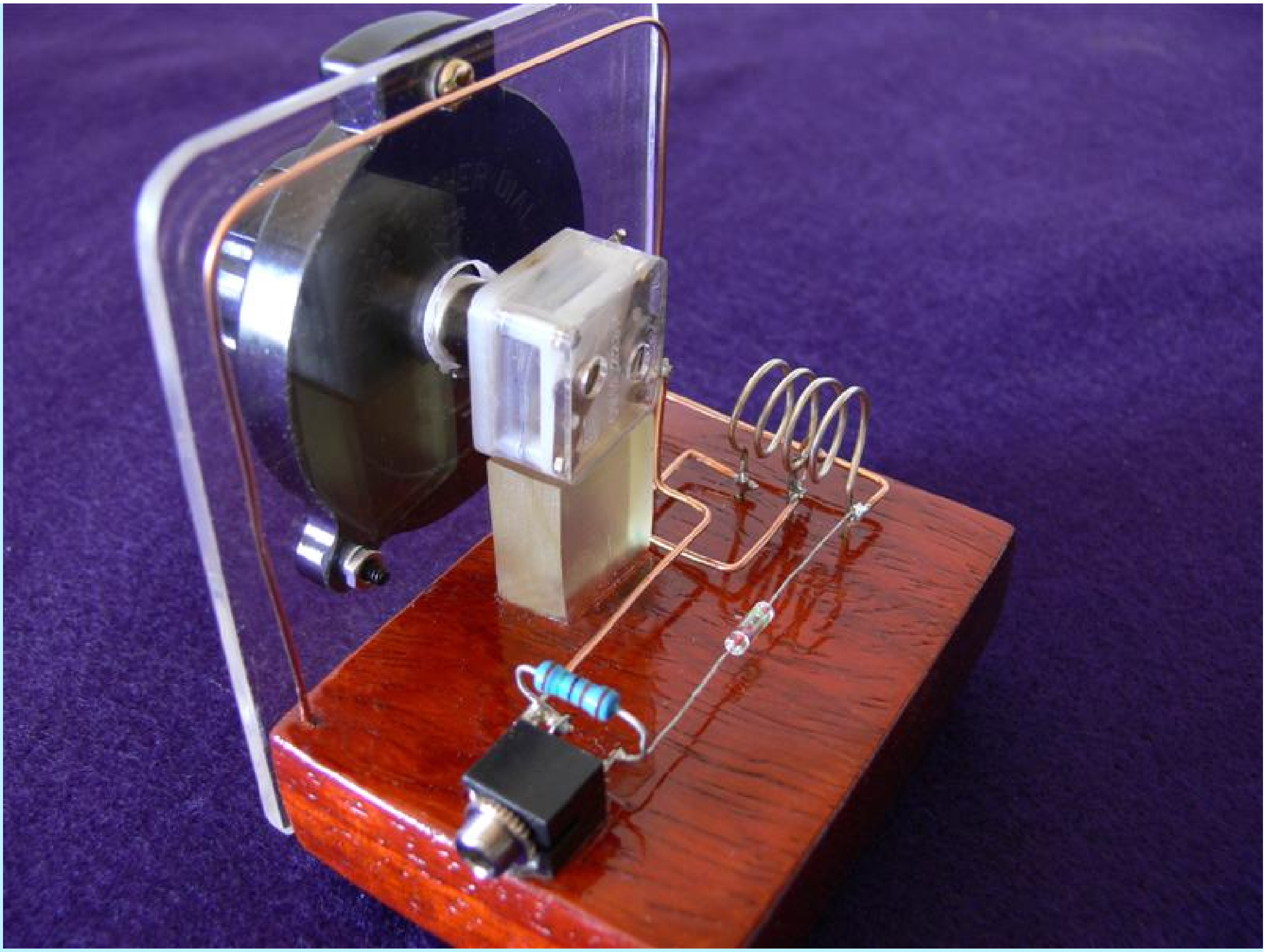

Is this thing imaginary -- science fiction? Well, imagination did play a part, but it is definitely not science fiction. This shot shows the elegance of the FM set best, I think. There is only one resistor and one fixed capacitor.

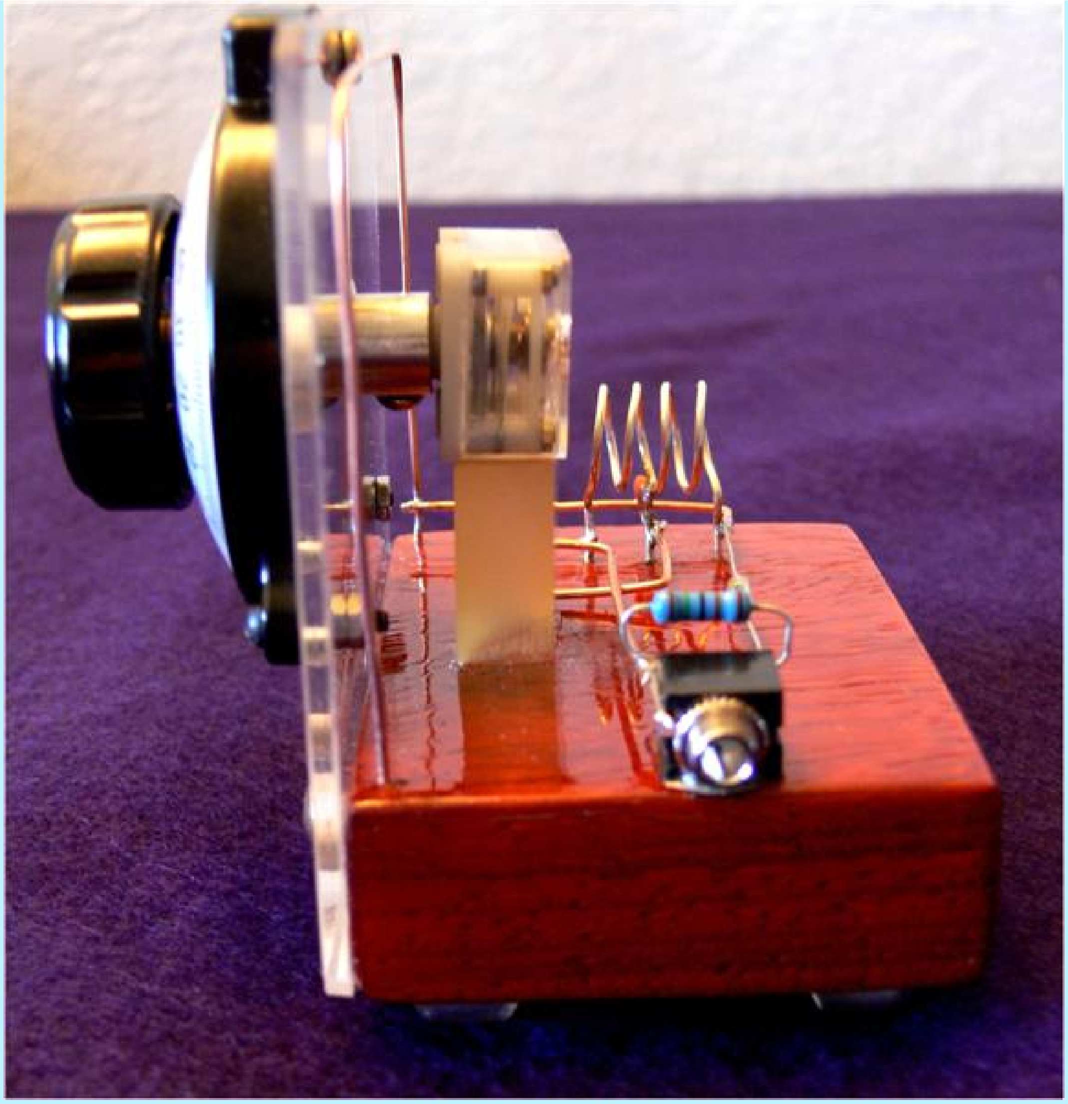

The inside of the tuning capacitor and the phono jack/output can be seen here. Can you spot the fixed ceramic capacitor? Note the polished edge of the face plate and the reflection in the wooden base.

A quarter-inch piece of lucite was fitted under the tuning capacitor to anchor it. Note the two tiny trimmers on the back of the tuning capacitor. Brass screws were used to enhance appearance.

The vernier dial is large to accomodate ease of tuning, and the vernier makes it easy to separate stations. Two golden (brass) wood screws fix the face plate to the base. Holes for the face plate were made with special plastic drills, but ordinary drills may be used if drilled very SLOWLY. The knob is removable.

FM Crystal Circuit #2

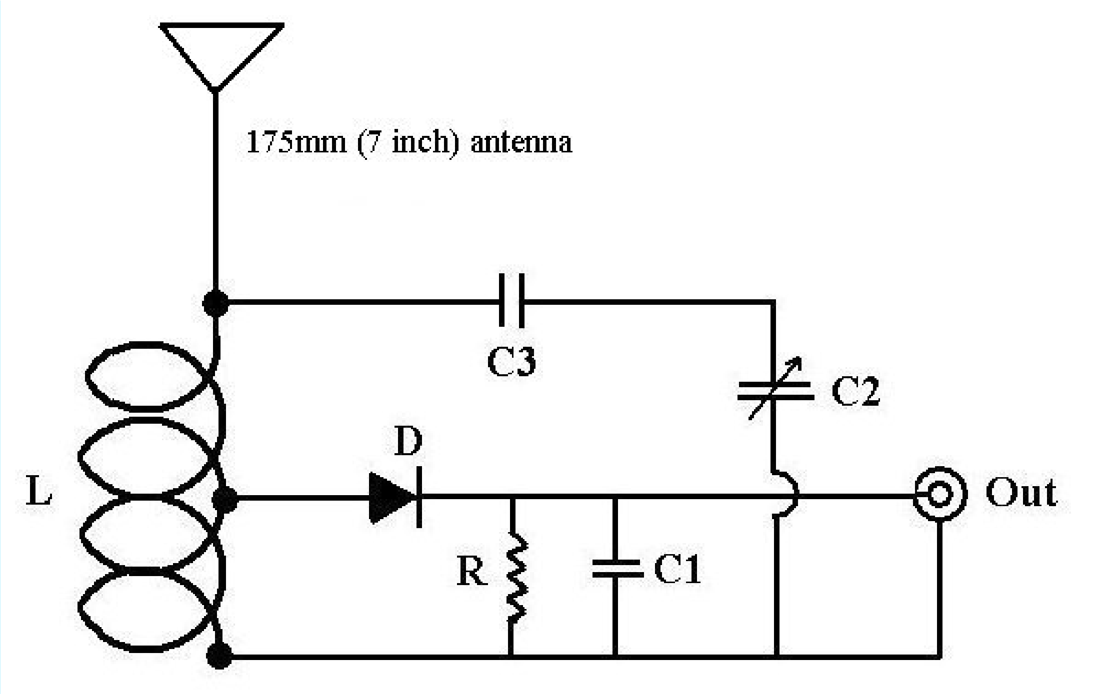

L - 5 turns AWG#18 bare copper or silver wire, 12mm inside diameter, tapped at 2.5 turns
D - 1N34 or rock crystal diode
C1 - 82 pf capacitor
C2 - 80 pf air variable capacitor
C3 - 18 pf capacitor
R - 150K resistor

The following photographs show the circuit wired with the handmade Saturn Dial. and knob. It is perhaps not as visually striking as set No. 1, but it works just as well. In fact, this set was the original version. Notice that all the wiring and coil are copper.

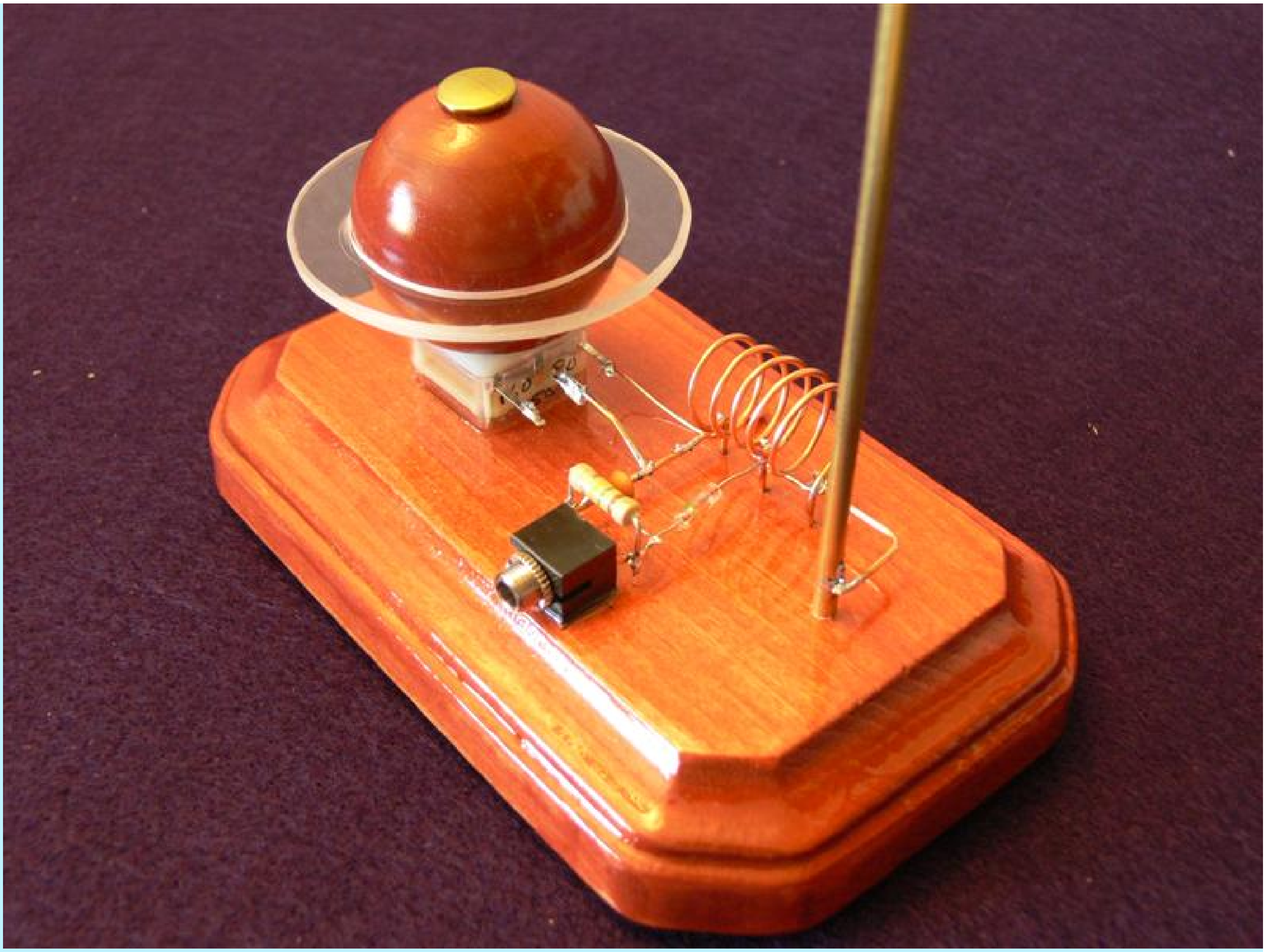

The Saturn dial and knob were fashioned from a "doll's head" from Michael's Arts and Crafts, a piece of lucite cut with two circle cutters, and a brass paper fastener. The knob is fixed to the tuning capacitor with a small machine screw that fits in the hole below the brass fastener. The most difficult part of this was fashioning "Saturn's rings". This must be done very carefully and slowly. The inside edge should be cut slightly undersized and then sanded with a drum sander to fit snugly. The outside edges can be sanded with fine sandpaper and polished with a plastic polisher.

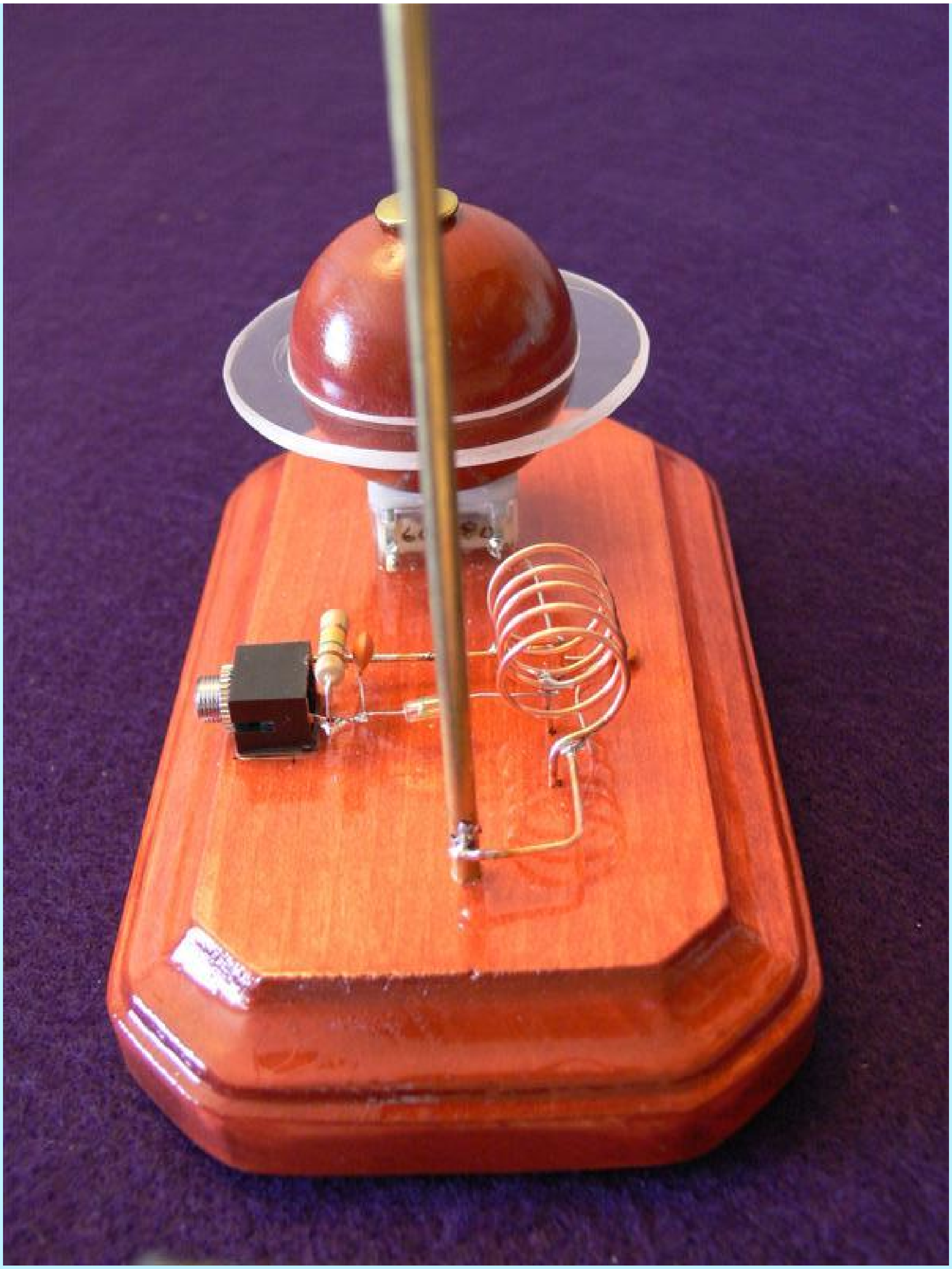

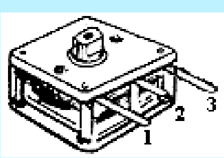

The air variable capacitor may be obtained from Electronix Express at http://www.elexp.com/. Part number 14VCRF10-280P. The 80 pf side is recommended for the second circuit, contacts 2-3. Contacts 1 and 3 were used for the first circuit (50pf).

- OSC: 5-59 pf
- ANT: 5-142 pf
- OSC and ANT Trimmer 10pf range

Home -- If you want to contact me go to the home page and go through the Music Clinic link.

FREE ENERGY FROM THIN AIR!

Technology (/technology/) > Science | by DrewPaulDesigns (/member/DrewPaulDesigns/) Follow

79,181 1,078 230

Posted May. 24, 2016 |

(https://cdn.instructables.com/FAT/Z4RR/IOKRVYWL/FATZ4RRIOKRVYWL.LARGE.jpg)

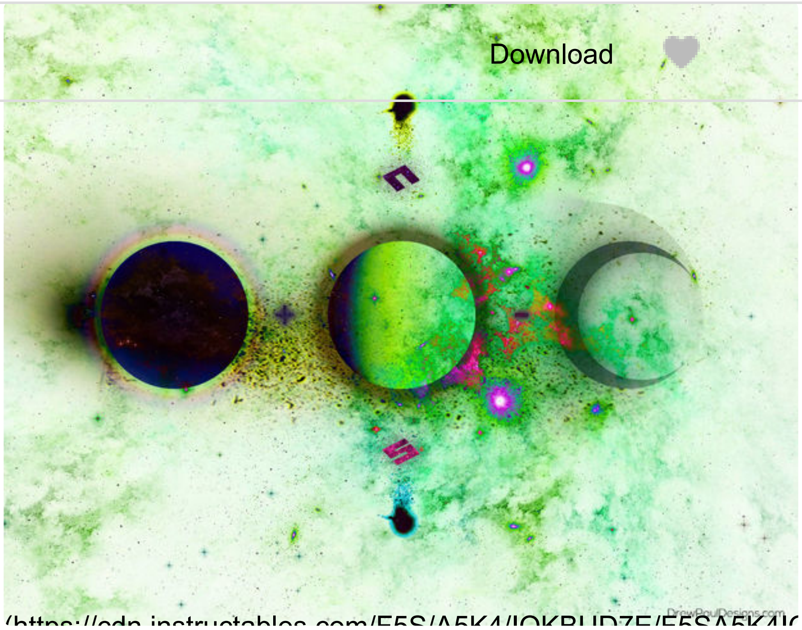

(https://cdn.instructables.com/F5S/A5K4/IQKBUDZE/F5SA5K4IC (https://cdn.instructables.com/FOH/L0OF/IQKBVTOS/

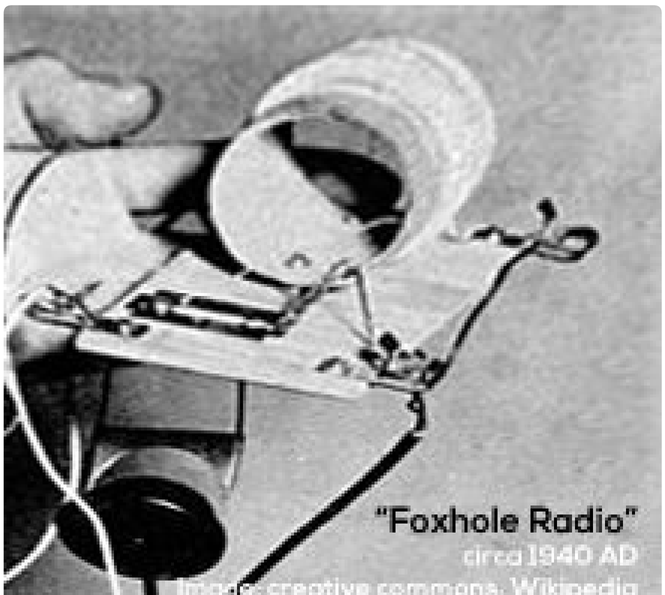

(https://cdn.instructables.com/FGE/GJG9/IQKBVTOT (https://cdn.instructables.com/FHS/HM1V/IQKBT6GY/FHSHM1V/

"Free energy from the air?, Yea, right!" Sardonic skepticism was my first reaction to this unusual concept, as well.

Though, its not so far out there, in fact. Light can be converted to DC current with solar panels, electricity can be converted to magnetism as I did in my last article (https://www.instructables.com/id/DIY-Electro-Magnetic-Levitation/), in a microphone sound waves are converted to an electrical signal (by vibrating a magnet near a coil (http://hyperphysics.phy-astr.gsu.edu/hbase/audio/mic.html)), solar rays can even be focused and converted to heat in awesome devices like this! (http://www.gosunstove.com/) When we think about it, energy is all around us and can be harvested in an enumerable many of ways.

Today, we are going to take a rather novel approach. We are going to build a device specifically designed to sense and capture a particular band of energy which is all around us.

The earth is magnetic and anyone who has ever used a compass knows this. Magnetic bodies in motion produce electricity, we can see this in any alternator, like the one in your car. So, therefore the earth is electric as well as magnetic, by definition.

Can we detect this energy? Yes, we sure can! Ever turn on a radio in the middle of nowhere and heard static? That is your radio picking up naturally occurring energy in the RF spectrum!

Can we use this energy to do work? Absolutely! This has been known for a long time. Crystal radios (https://en.wikipedia.org/wiki/Crystal_radio) have been around since before the 1930's and can run with no input energy other than the radio signal. Even when completely isolated, but from the atmosphere, a crystal radio will produce a voltage in the earpiece resulting in a sound (albeit and undesirable one).

Well, this is where it gets interesting...

Can we replicate this effect? Yea, and with modern components like the high quality crystals found in germanium diodes, we can even increase efficiency. By applying this concept as a Crystal Energy Receiver we can take advantage of a wide range of energetic frequencies rather than tuning in to just one.

Can we scale it up? Definitely. Things like micro germanium diodes, high efficiency antennas and compact contemporary capacitors make the components that are required to build a crystal receiver fit in the palm of your hand. While there may or may not be a more efficient way, this renewable energy solution is simple to employ

and can be scaled up, or down, indefinitely.

Download

It sounds like we can build a Crystal Energy Receiver. Let's give it a shot...

Add Tip Ask Question

Step 1: What You'll Need

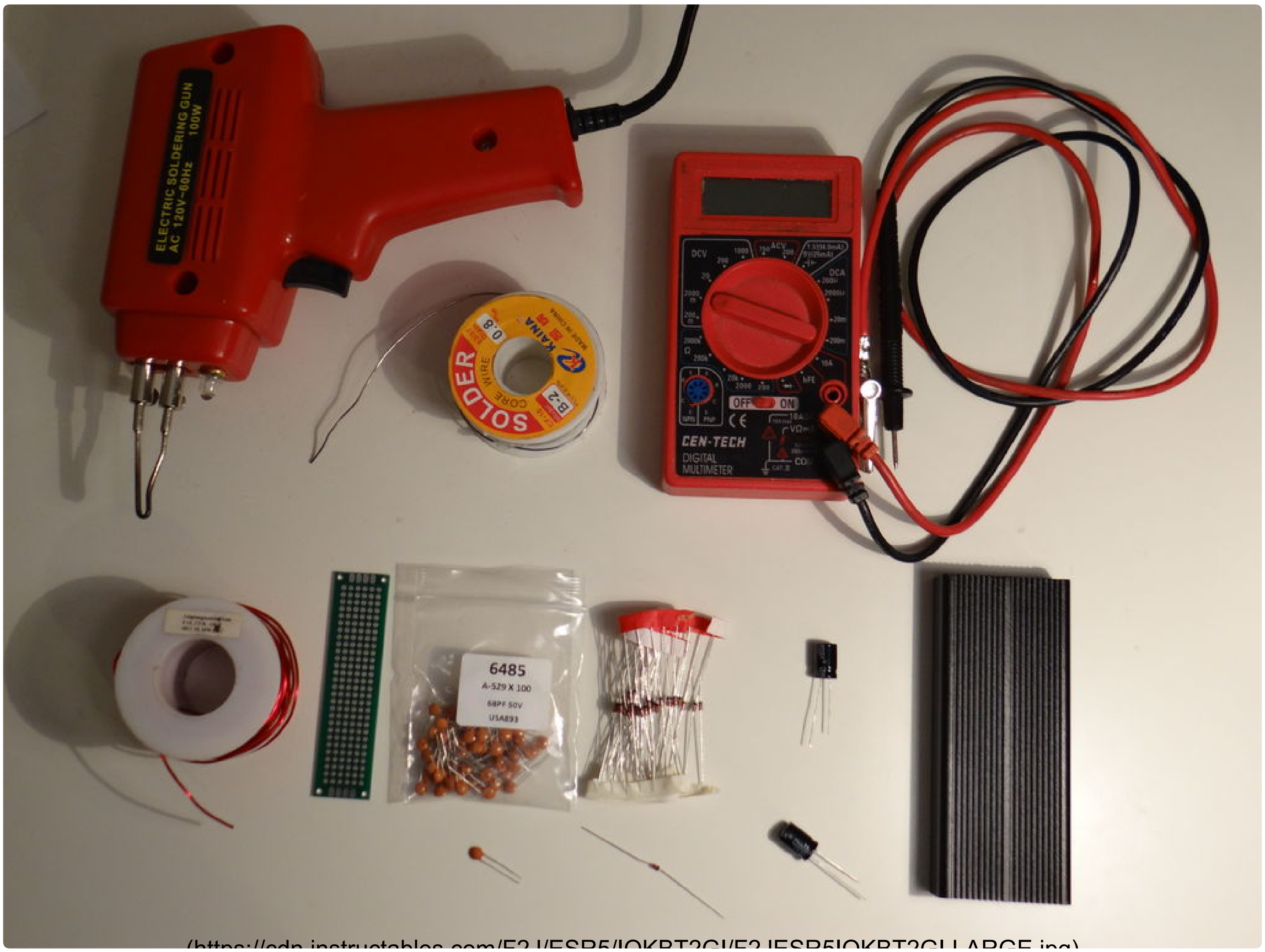

(https://cdn.instructables.com/F2J/FSP5/IOKBT2GI/F2JFSP5IOKBT2GI.LARGE.jpg)

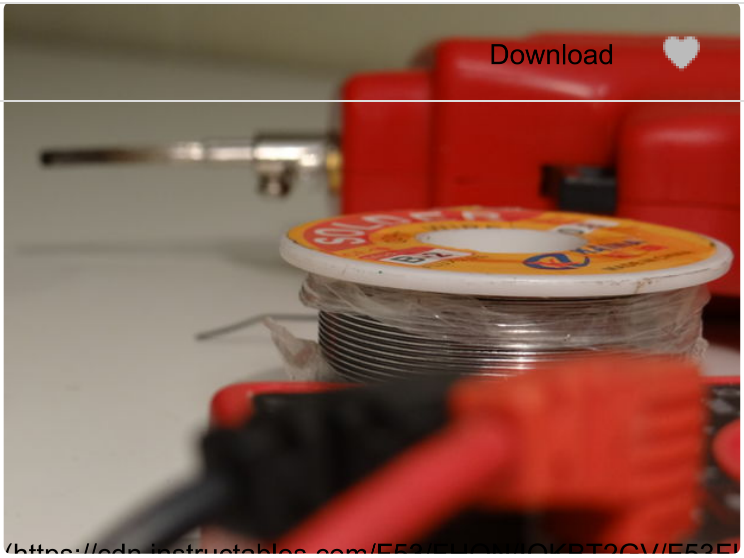

(https://cdn.instructables.com/F53/EUGM/JQKBT3GV/F53E

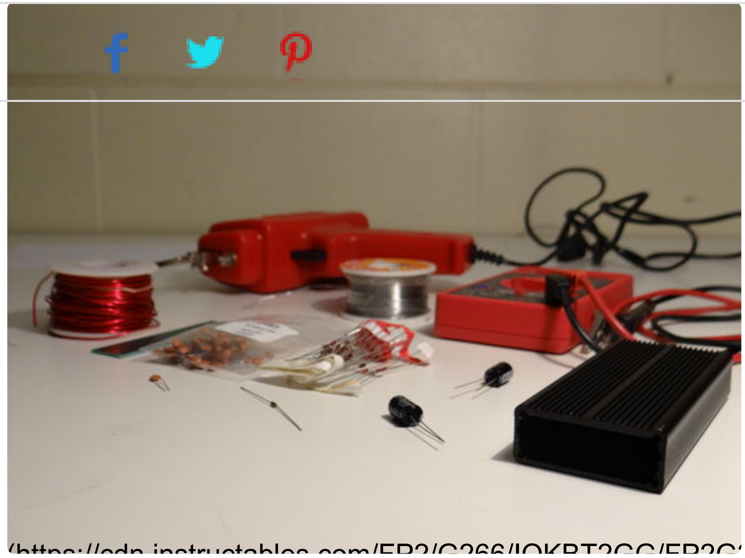

(https://cdn.instructables.com/FP2/G266/JQKBT3GG/FP2G

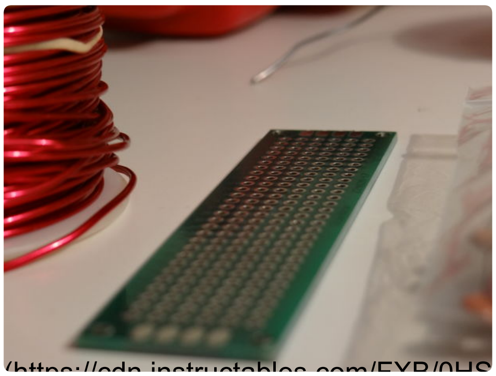

(https://cdn.instructables.com/FXB/0HS

(https://cdn.instructables.com/FYS/DZC

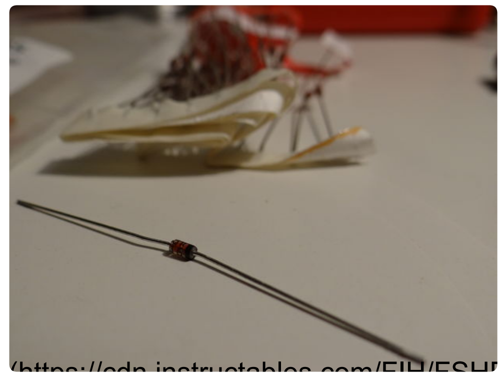

(https://cdn.instructables.com/FIH/FSHI

Download

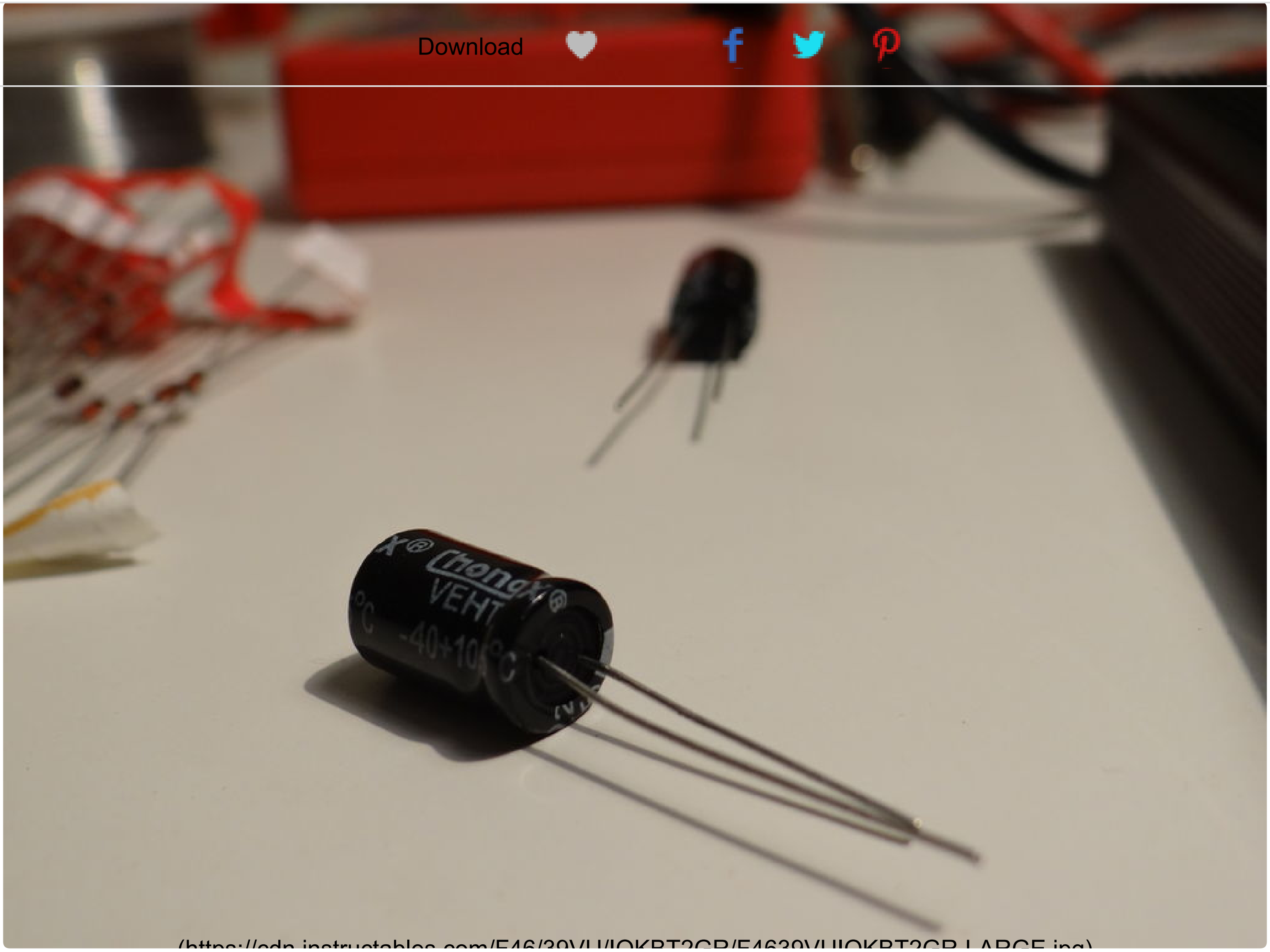

(https://cdn.instructables.com/F46/39VU/IQKBT2GB/F4639VUIQKBT2GB.LARGE.jpg)

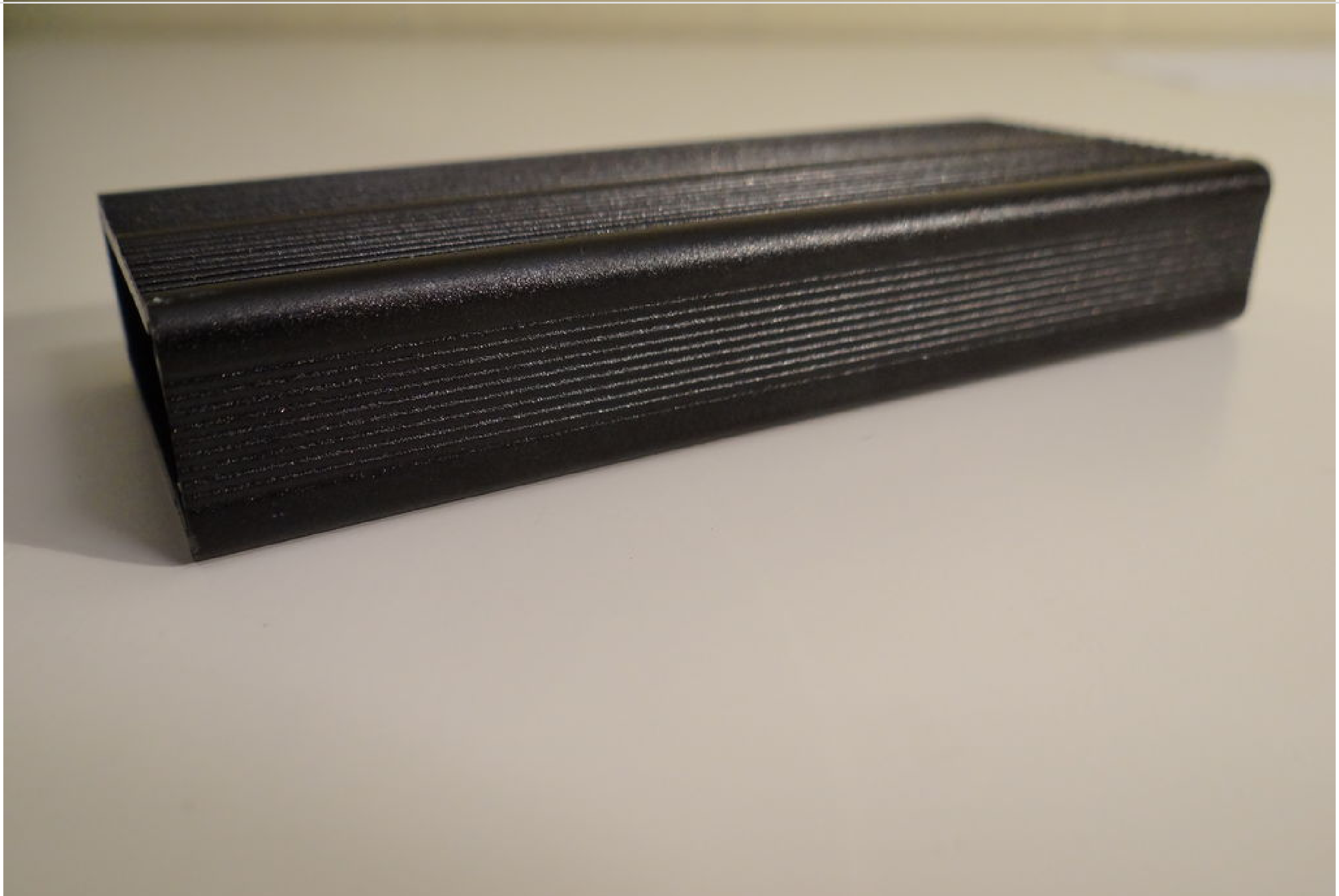

(https://cdn.instructables.com/FKY/5NKQ/IQKRT2GU/FKY5NKQIQKRT2GU.LARGE.jpg)

One of the reasons this particular renewable energy harvesting method is so viable is the relatively few and easy to obtain materials required.

The simplest crystal receiver design needs no power and can be built with only three parts: a coil, a crystal and a resistor. We're going to optimize that design in order to produce a cleaner and more reliable output signal by first polarizing the input amplitude, then rectifying and filtering the signal. Then we'll add an antenna, case and connections.

Get the circuit diagram here (http://www.drewpauldesigns.com/crystal-energy-receiver-kit.html)
Get the kit here (http://www.drewpauldesigns.com/crystal-energy-receiver-kit.html)

The parts for the circuit include:

(1) Circuit Board (http://www.drewpauldesigns.com/crystal-energy-receiver-kit.html)

(1) 10-18 gauge Copper Wire

(2-12+) Ceramic Capacitors (matched)

(2-6+) Electrolytic Capacitors (matched)

*note various types of capacitors can be used

(4) Germanium Crystal Diodes (1A+)

Total Unit Cost: +/- $0.40 (USD, scaled for volume of 1,000+ units)

In addition, you'll probably want to get:

(1) Project box (optional)

(1) Antenna (a loop antenna or elevated antenna is recommended and can be made with copper wire)

The tools you'll need are:

Soldering Iron/ Solder (optional)

Multimeter

Oscilloscope (http://www.seeedstudio.com/depot/DSO-Nano-v3-p-1358.html?cPath=63_65) (optional)

That's it. Yup, that's all. Once we've got it all, let's begin.

Step 2: Build the Circuit

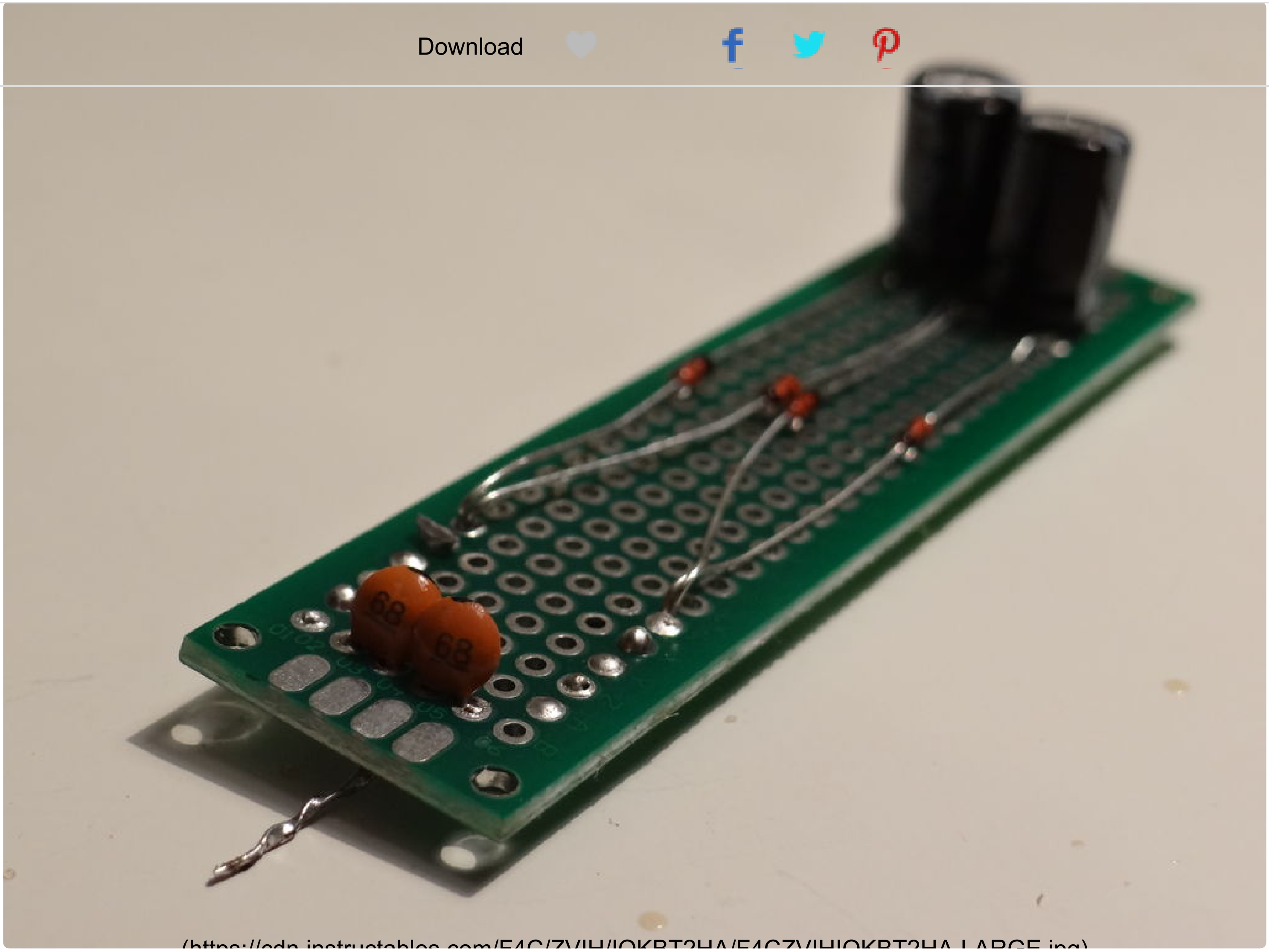

(https://cdn.instructables.com/F4C/ZVIH/IOKBT2HA/F4CZVIHIOKBT2HA.LARGE.jpg)

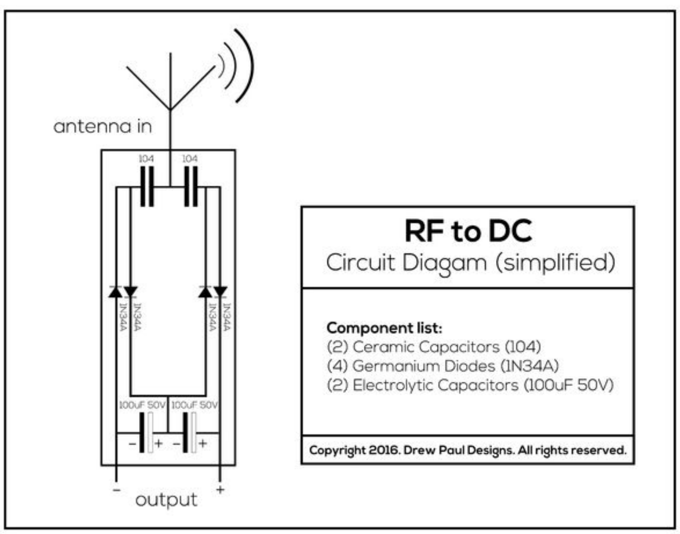

(https://cdn.instructables.com/FAW/ABS2/IOKBUKAD/FAV

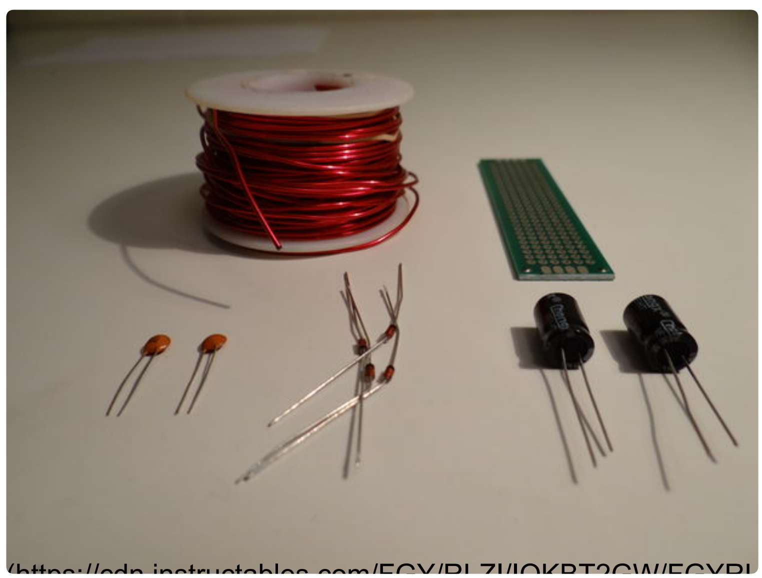

(https://cdn.instructables.com/FCY/PLZI/IOKBT2GW/FCYPI

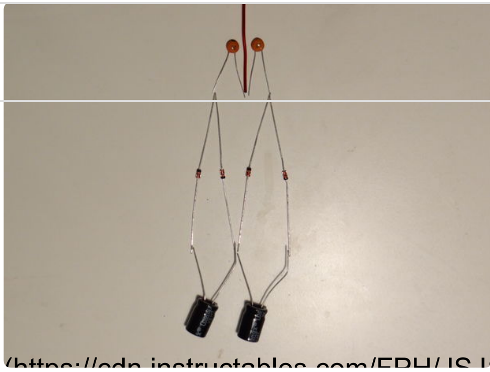

(https://cdn.instructables.com/FPH/JS k

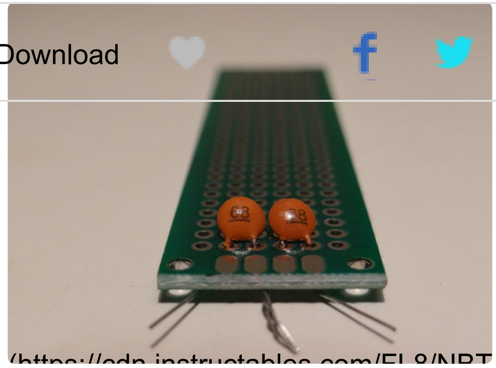

(https://cdn.instructables.com/FL8/NBT

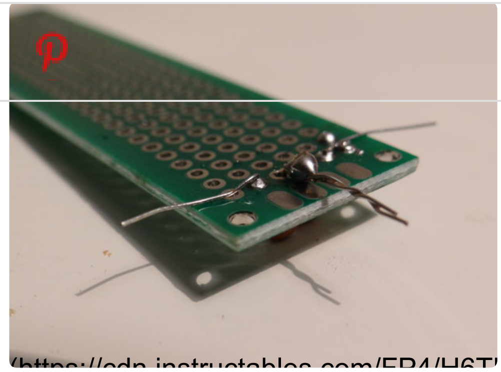

(https://cdn.instructables.com/FP4/H6T

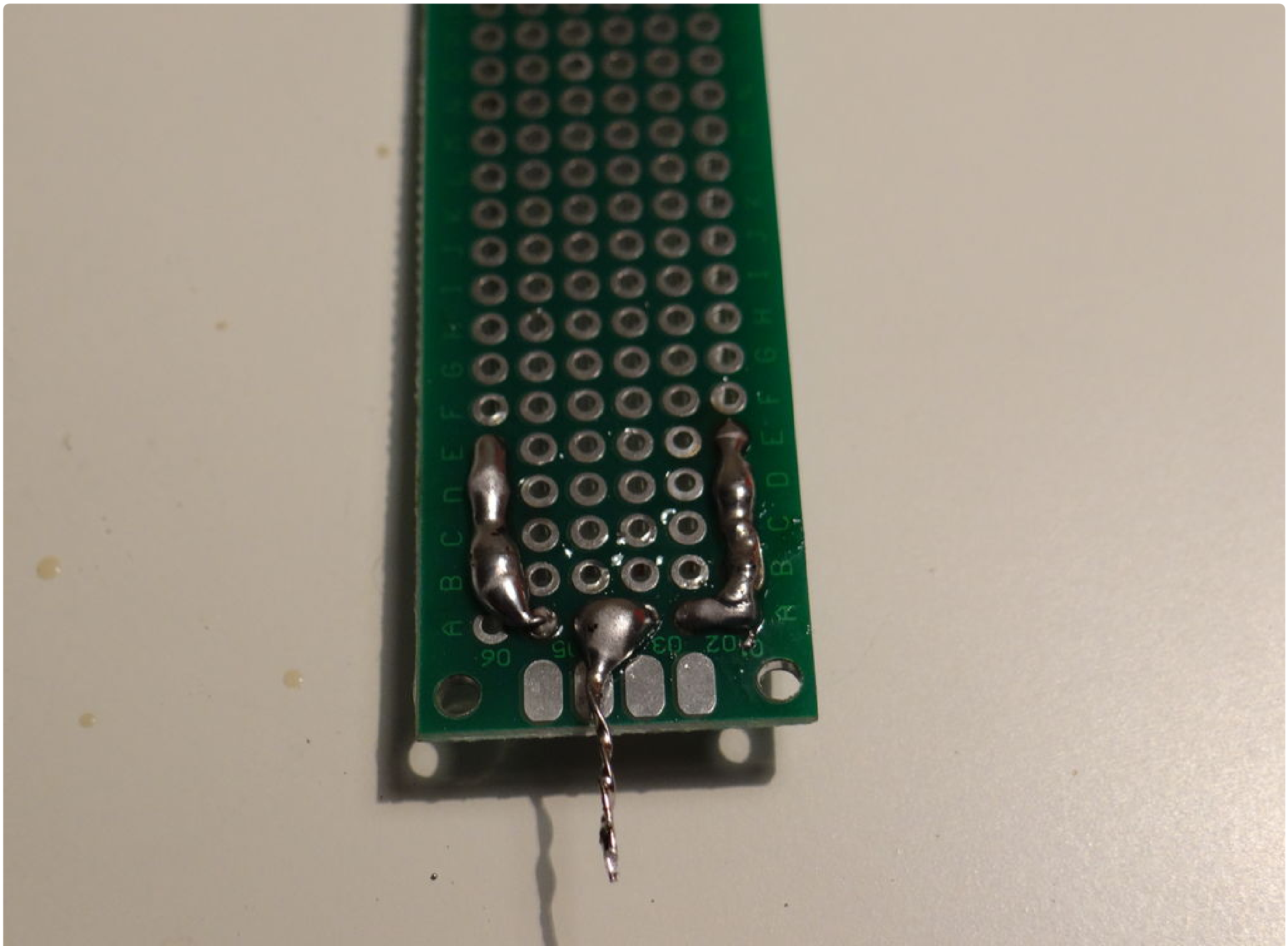

(https://cdn.instructables.com/FN2/OSG1/JQKBT2H5/FN2OSG1JQKBT2H5.LARGE.jpg)

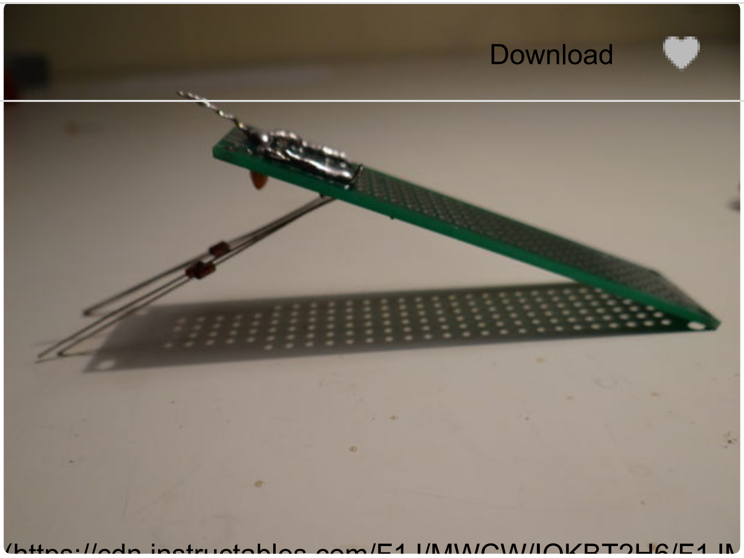

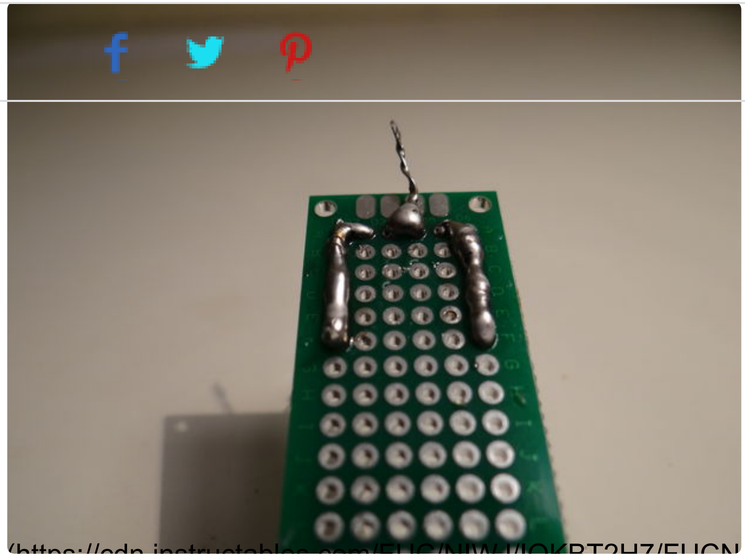

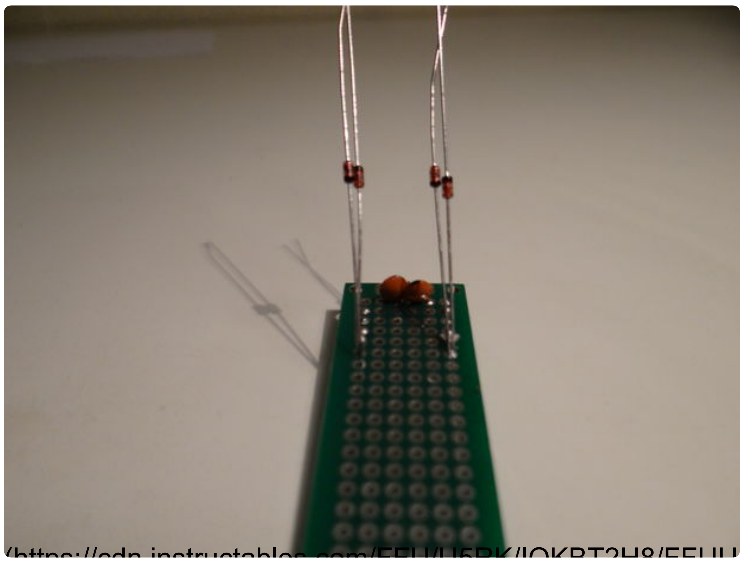

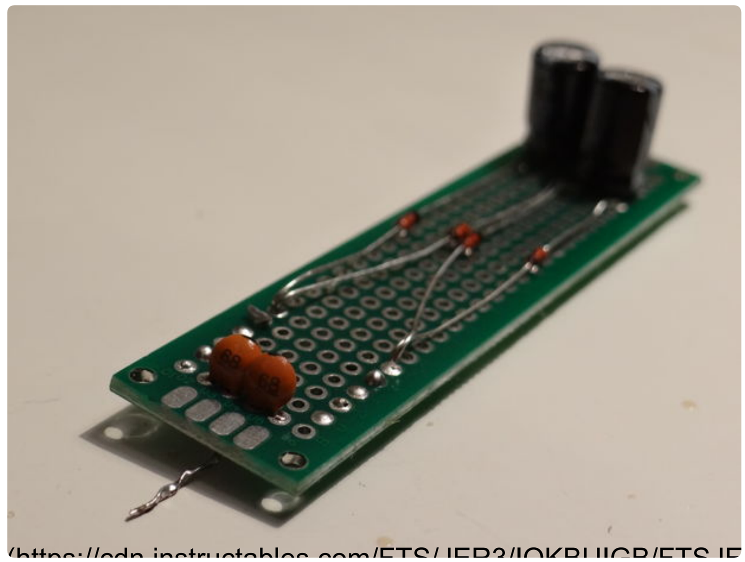

We're going to build the simplest version of this circuit variation in order to understand how each component interacts and as a proof of concept.

There are three simple systems at work in the circuit that are composed of capacitors, which store energy, and diodes that direct it.

Energy in the band of radio waves, among others, will vibrate a wire antenna on an atomic level, sending a discernible signal to its lead. This signal will then meet the junction between two ceramic capacitors wired in series. This junction will force positive charge from the wave to travel in one direction and negative charge in the other direction which, when collected again, makes the signal uniform and polar. Connecting the two capacitors in series creates leads on each end; the now positively charged side of one and the now negatively charged side of the other

creates a two cell battery.

This next stage of the circuit takes a signal with a net value of zero, adds the absolute values of the positive and negative amplitudes with respect to the origin and produces a positive integer. This concept can be thought of as taking:

(+1) + (-1) + (+1) + (-1) = 0

and converting it to:

| [(+1) + (+1)] | = 2
+
| [(-1) + (-1)] | = 2
= 4

Isn't math fun?

To each of these leads from our two capacitors in series, we will connect two crystal diodes, one facing each direction, to form what is called a bridge rectifier. A bridge rectifier is a configuration which will convert an alternating current to a direct one by cleverly rerouting the signal.

By connecting the bridge rectifier as shown in the circuit diagram, this direct current from the diodes then charges the electrolytic capacitors. This stage normalizes the amplitude, making the current constant and usable.

Components can easily be twisted together for testing and then soldered to a circuit board to secure.

Step 3: Test and Optimize Your Circuit

Download

(https://cdn.instructables.com/F...LTBCLAVIOKBT2HC.LARGE.jpg)

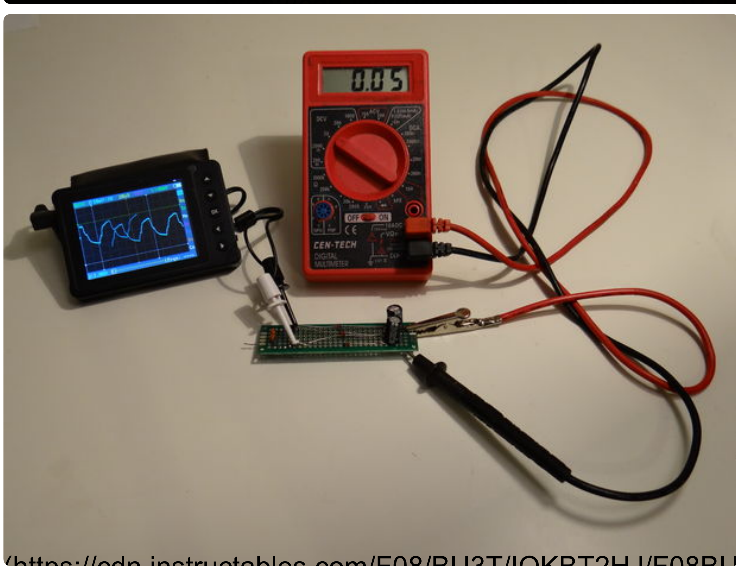

(https://cdn.instructables.com/F08/RU3T/IOKBT2HJ/F08RU

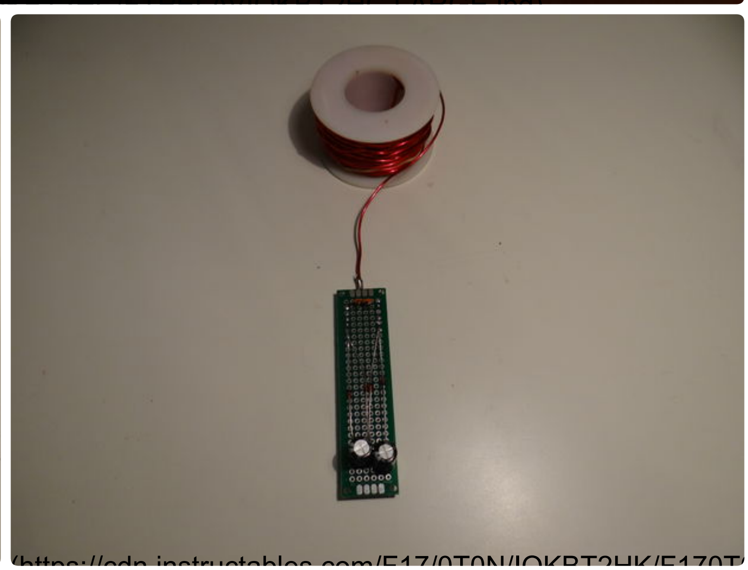

(https://cdn.instructables.com/F17/0T0N/IOKBT2HK/F170T

Download

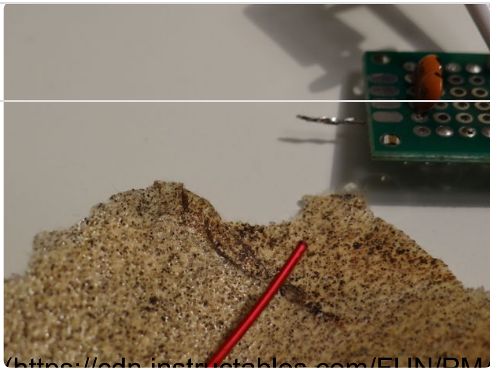

(https://cdn.instructables.com/FUN/PM

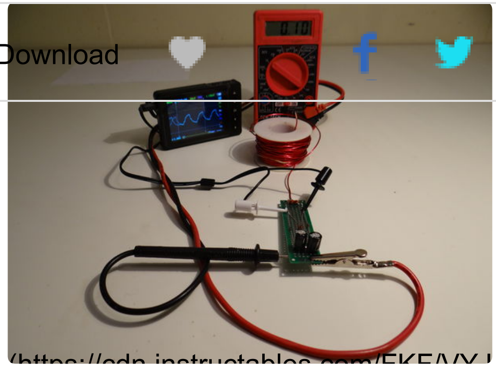

(https://cdn.instructables.com/FKF/VX

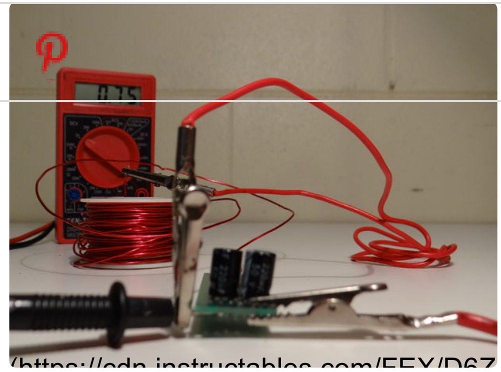

(https://cdn.instructables.com/FEY/D6Z

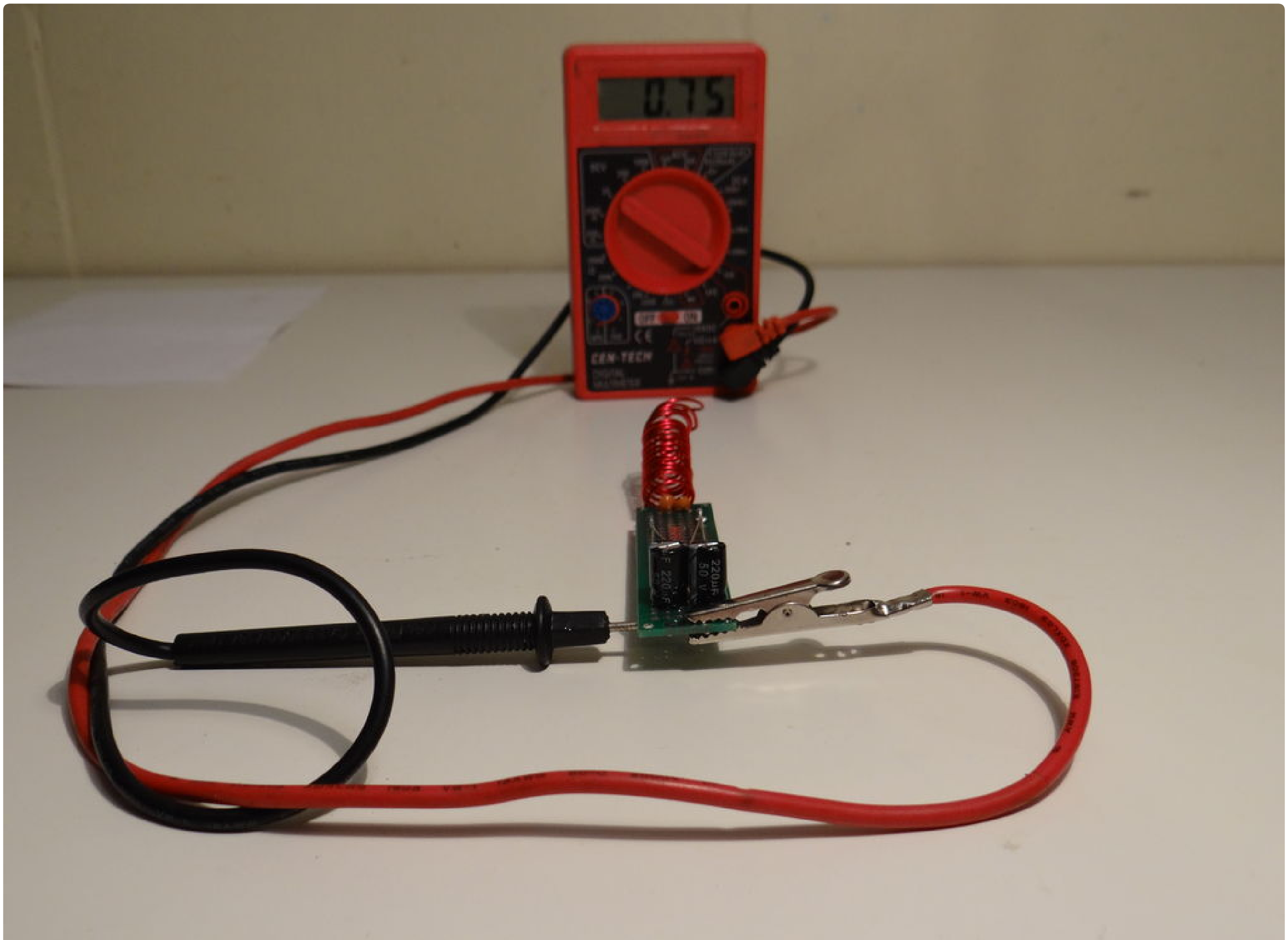

(https://cdn.instructables.com/F9A/XB15/IQKBT4X3/F9AXB15IQKBT4X3.LARGE.jpg)

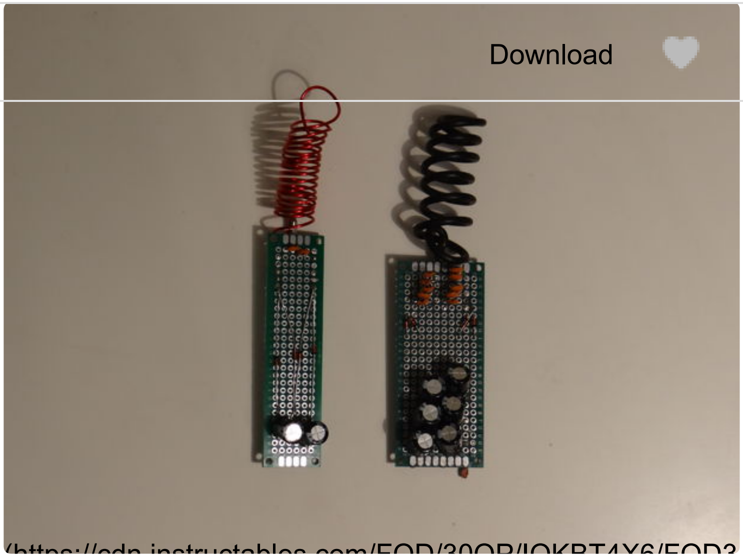

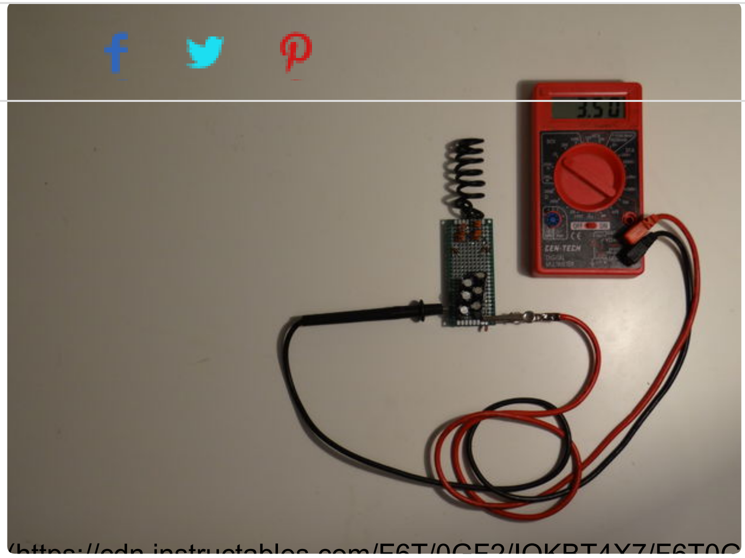

To test and analyze our circuit, we'll be using a digital voltmeter and oscilloscope.

By connecting a voltmeter to the output, we'll immediately begin to see a small voltage climbing in the 10-100mV range. If not, we'll want to check our connections and make sure the circuit is not isolated from the environment by taking it outside to a clear area.

Then, by connecting an oscilloscope to the outside leads of our two ceramic capacitor bank, we will see the the polarized signal being captured from the air around us. We can then connect after the diodes to see our varying direct current and then to after the electrolytic capacitors to see a normalized, usable direct current at our output.

We can then optimize the input resistance in two ways. Firstly, we can add additional ceramic capacitors in parallel to our original two and make sure our soldered connections are consistent and thick in this area.

We can optimize the circuit's capacity by adding electrolytic capacitors in parallel to our original two which will allow this circuit to charge slightly when not in use. For this purpose, a charging circuit can also be added here in order to incorporate an optional battery bank.

We can optimize the antenna by attaching loops and coils of copper wire in various positions, store-bought antennas or by stringing some wire up to the highest point you can reach.

We don't have to stop there, either. We can now connect multiple circuits in series to increase voltage or in parallel to increase current. This can be done indefinitely.

Add Tip

Ask Question

Step 4: Add a Case and Antenna

(https://cdn.instructables.com/FK6/6YAF/IQKBT4XC/FK66YAFIQKBT4XC.LARGE.jpg)

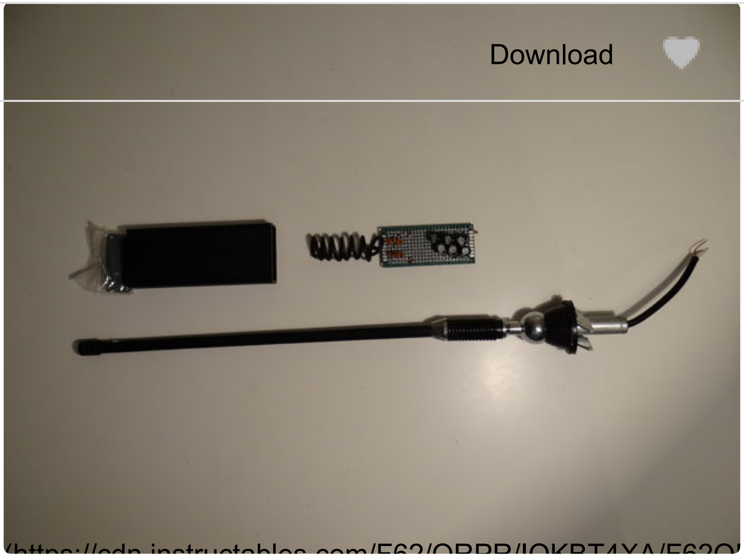

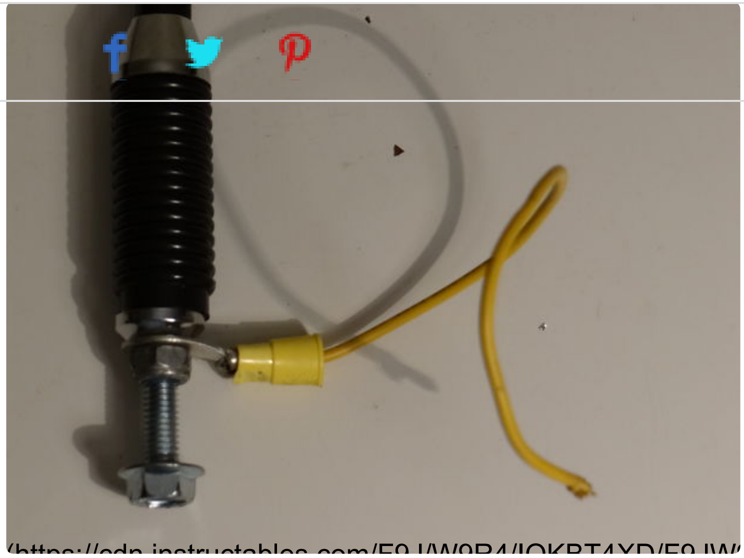

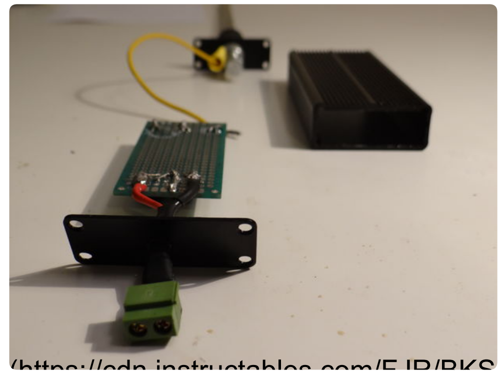

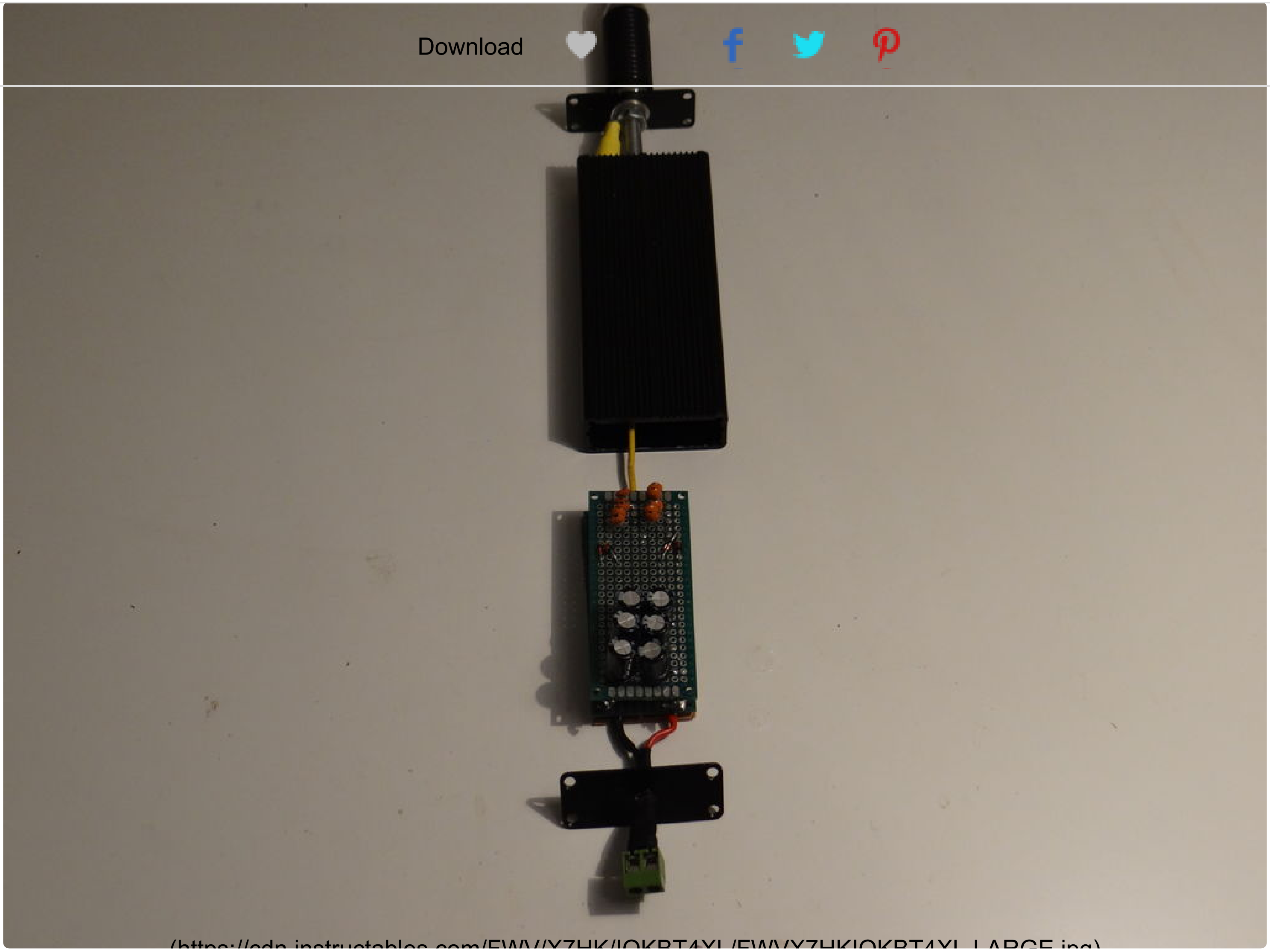

(https://cdn.instructables.com/FWV/YZHK/IOKRT4XL/FWVYZHKIOKRT4XL.LARGE.jpg)

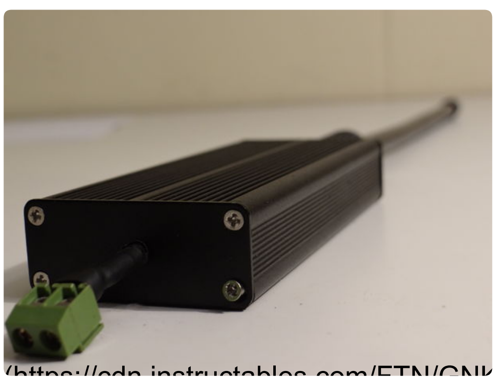

(https://cdn.instructables.com/FTN/GNK

(https://cdn.instructables.com/FM8/8IF

(https://cdn.instructables.com/FD9/OGS

After choosing an antenna in the last step we'll now want to permanently wire it. Whether you choose a compact antenna for portability or a tall fixed antenna for power and range, we will wire it in the same manner according to the diagram in the previous step. Note that the input on the configuration here is grounded to the metallic case, and thus the users hand, and incorporation of longer antennas will require proportionally more substantial grounding.

We will then attach a terminal to the output to allow us to connect this circuit to an electrical device or charging circuit and battery bank.

Next, we will add a case, making sure to isolate exposed leads with non-conductive material especially if mounting in a conductive case. A piece of cardboard secured with glue is sufficient for the circuit's bottom and shrink wrap or electrical tape can be used in the case of any additional exposed leads. Drill two holes in your enclosure, one for the antenna or antenna lead and another for your output terminals. You can then insert your components, fasten the enclosure and your device is ready to use!

Add Tip Ask Question

Step 5: Your Crystal Energy Receiver Is Complete!

Download

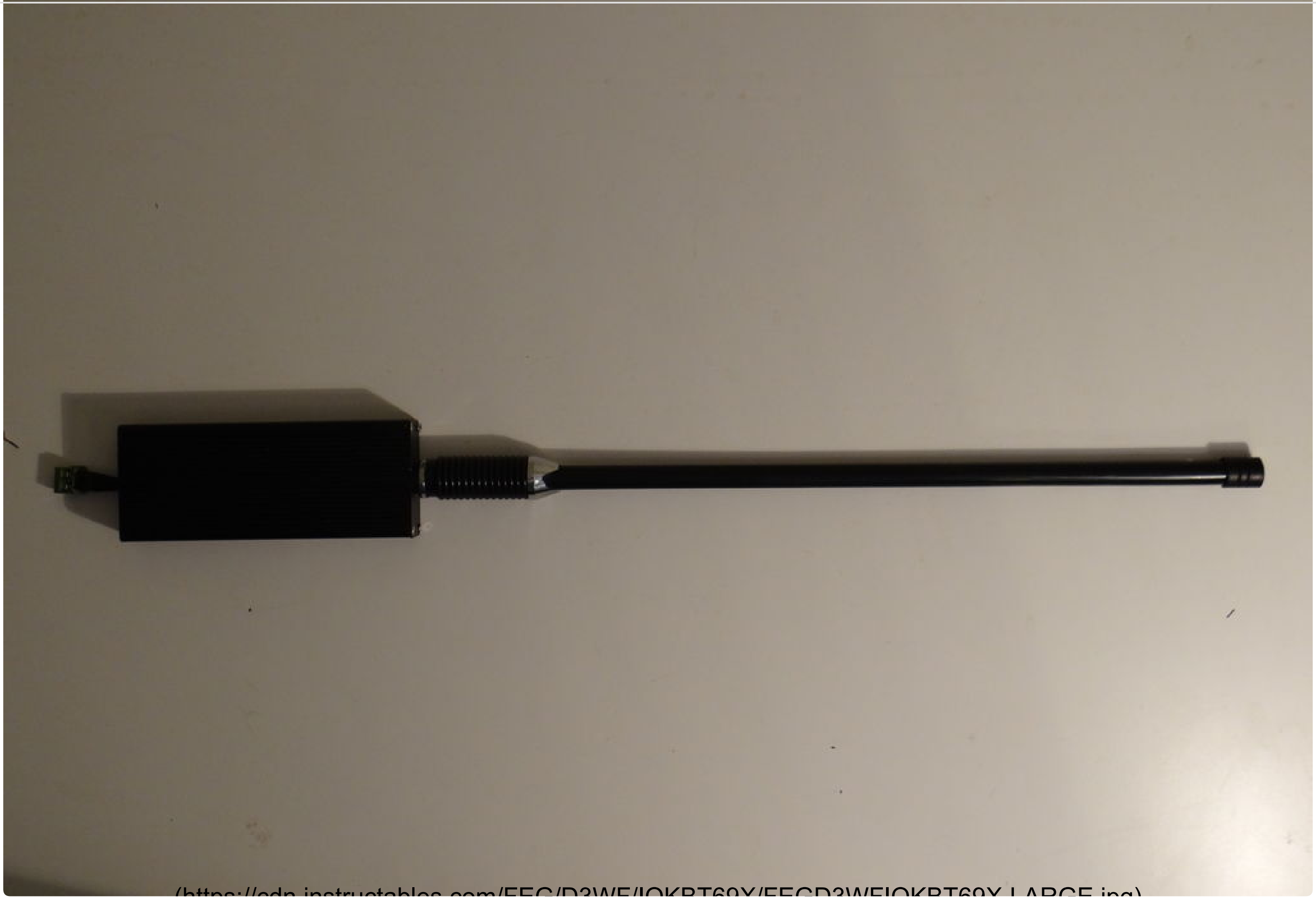

(https://cdn.instructables.com/FEC/D3WF/IOKBT69X/FECD3WFIOKBT69X.LARGE.jpg)

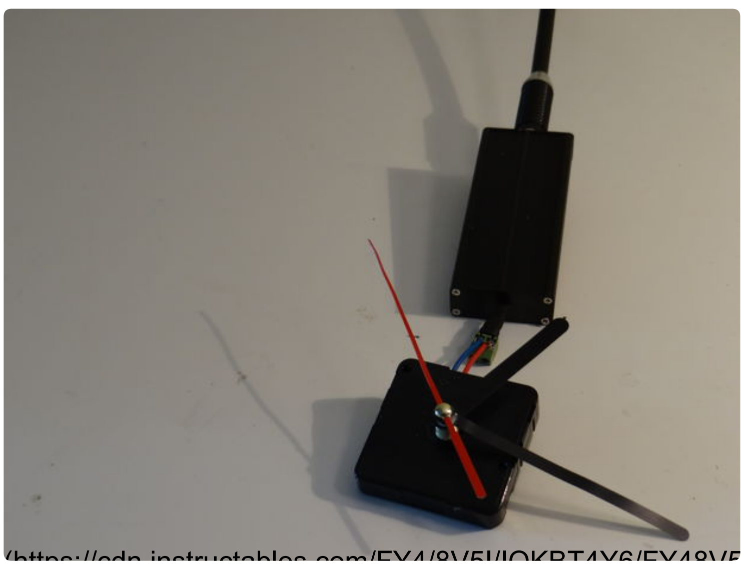

(https://cdn.instructables.com/FX4/8V5I/IOKBT4X6/FX48V5

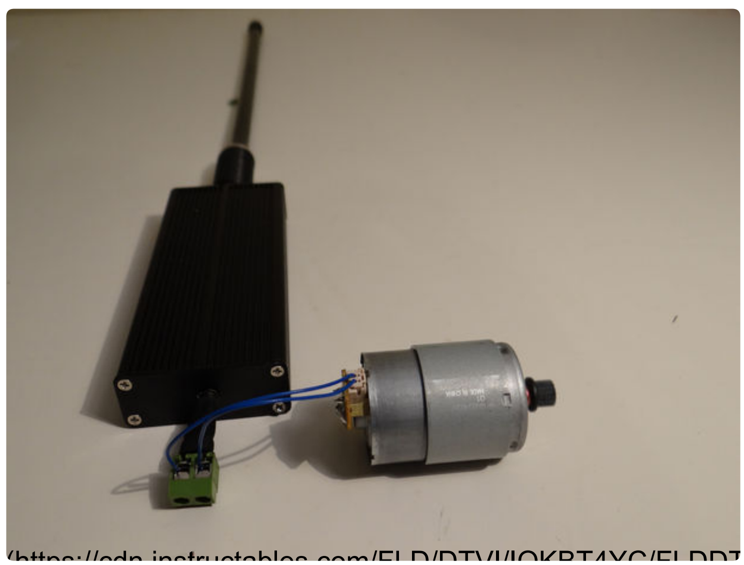

(https://cdn.instructables.com/FLD/DTVI/IOKBT4XC/FLDDT

Your Crystal Energy Receiver is now complete and ready to use!

I built a portable version, for proof of concept and demonstration purposes. However, you can go as big as you want- to passively charge batteries or run equipment remotely; or go as small as you want- to power sensors, RFID devices, small electronics and more.

I used this harvested energy to easily power a low-consumption quartz clock, a digital chronograph with integrated circuits and LCD and was even able to momentarily rotate a small dc motor.

Because of its simplicity this device is a durable, efficient and reasonably effective method of harvesting radiant energy in a simple, replicable and sustainable way. I humbly hope that the contributions made here, and by those reading, can be one day used by people worldwide to conveniently capture free energy.

Thanks for checking out my project and I look forward to seeing everyone's variations, suggestions and improvements!

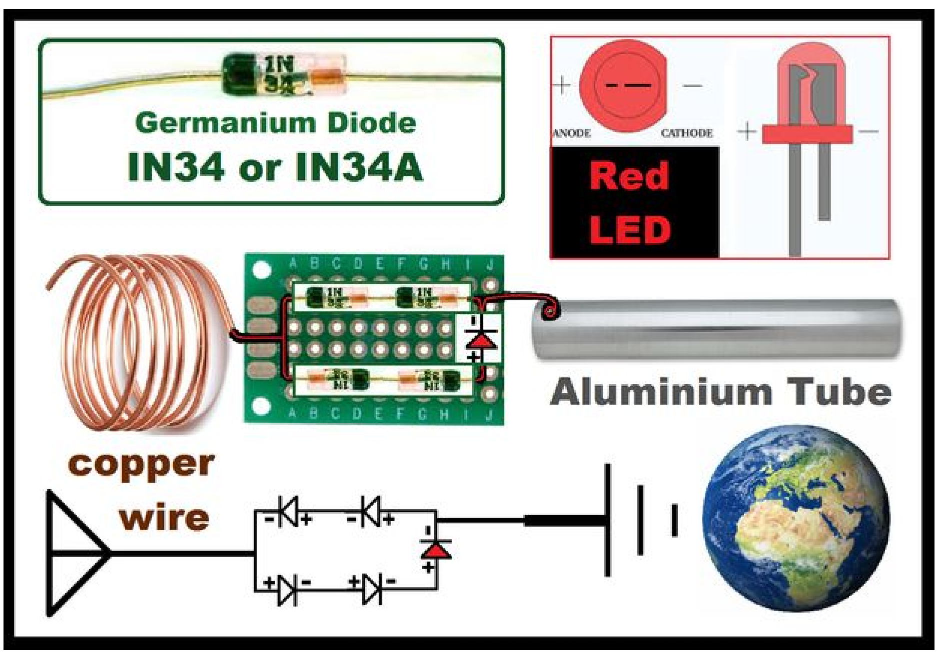

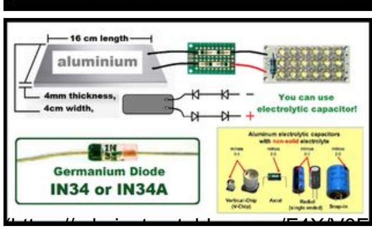

(https://cdn.instructables.com/FUD/RBY8/IRBC73B/FUDR

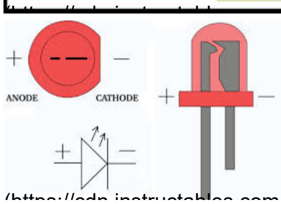

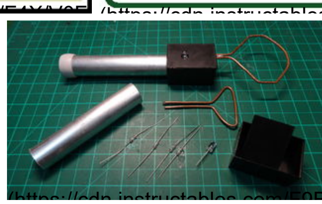

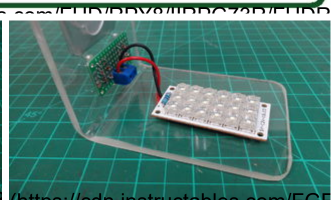

(https://cdn.instructables.com (https://cdn.instructables.com/F9F (https://cdn.instructables.com/FCF

About This Instructable

2,351 views

46 favorites

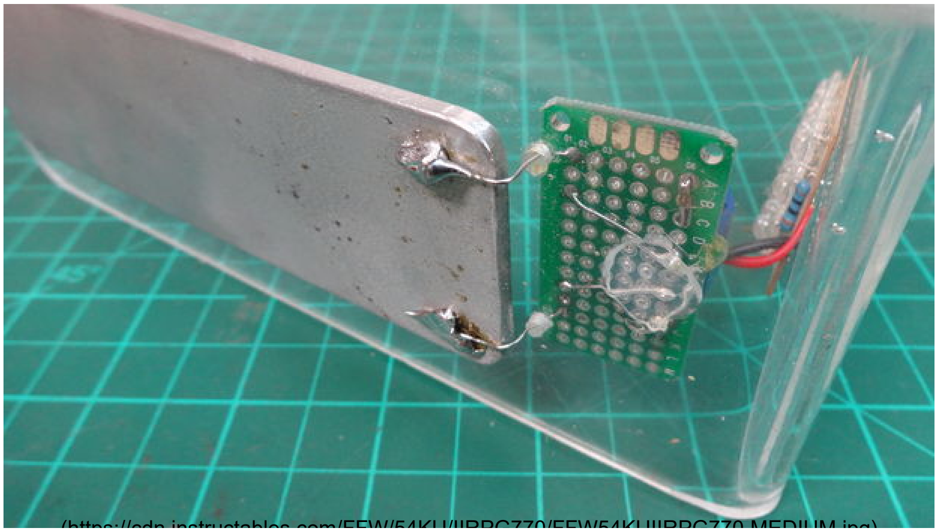

(https://cdn.instructables.com/FEW/54KU/IBPC770/FEW54KUIBPC770.MEDIUM.jpg)

(https://cdn.instructables.com/FB2/K73U/IBPC78S/ ... MEDIUM.jpg)

How to Make a Electrostatic RF Detector or Ghost Detector, Hunting Solution. Much cheaper and easier than you may think For Under $5 ! A simple description is that IN34 or IN34A RF Germanium Diodes for Crystal Radio can take "Ambient" or "Radio Waves" to turns them into DC energy. I would like to show the Tesla Coil Transmitter, where I made an homemade "RF Detector" this is the simplest detector! without any batteries or hardships circuit, only with IN34 diodes and Ether to Earth!.. Stay Tuned and Enjoy! Please click the "like" button, subscribe my channel, and share this with your friends... To support my "work" every little bit helps! Watch the "ADS" THANKS

- See the original video https://www.youtube.com/watch?v=cSxqeGVC9t0

Step 1:

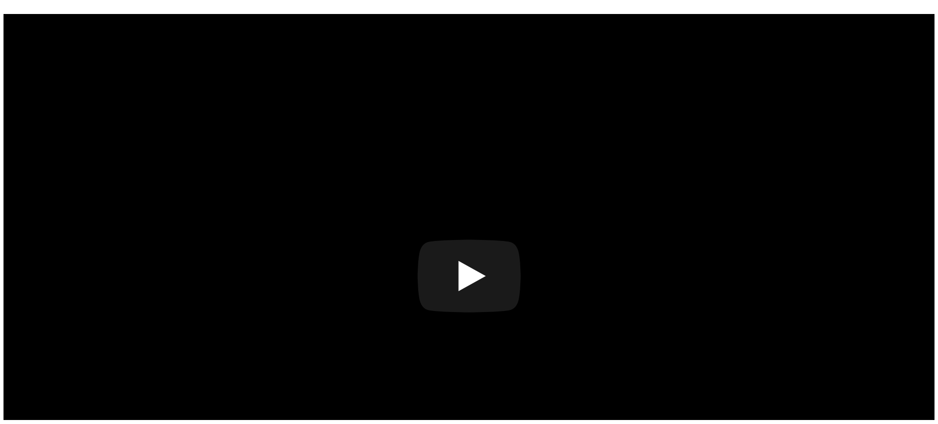

GEORGE CHANIOTAKIS (/member/GEORGE+CHA
(http://https://www.youtube.com/
Follow 84
(/member/GEORGE+CHANIOTAKIS/)

Bio: A big hello to all mankind! This is my channel I hope you can find here various interesting things on in Renewable Energy Technologies and ... More » (/member/GEORGE%20CHANIOTAKIS/)

More by GEORGE CHANIOTAKIS:

(/id/MAKE-PERMANENT-MAGNET-SYNCHRONOUS-MOTOR-GENERATOR/)

(/id/Make-Wind-Turbine/)

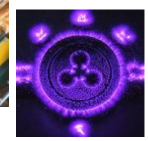

(/id/High-Voltage-Die/)

Comments

be nice

We have a be nice comment policy.
Please be positive and constructive.

I Made it! Add Images Post Comment

LazaroG4 (/member/LazaroG4/) 2017-11-14 Reply

I can't download and I was doing it before. I now need to go premium. This why i do not give any of my own files for the idea i have posted for free on You Tube. sorry for the not using of file and I have integrity and will not copy and paste as many do for free.

More Comments

How to Make a Electrostatic RF Detector or Ghost Detector by

Build a Homebrew Radio Telescope

Explore the basics of radio astronomy with this easy to construct telescope.

Mark Spencer, WA8SME

There are many ham radio related activities that provide a rich opportunity to explore and learn more about the science of radio. One of those opportunities is radio astronomy.

All matter emits radio frequency (RF) energy dependent on the temperature and makeup of the matter, including the matter in space. The foundation of radio astronomy is to study the heavens by collecting and analyzing the RF energy that is emitted by bodies in space, very much as optical astronomers use light energy collected by telescopes. It sounds complicated. While professionals use very sophisticated and expensive equipment, you can, with some simple equipment and a little investment, build a radio telescope that will allow you to learn and explore the fundamentals of radio astronomy.

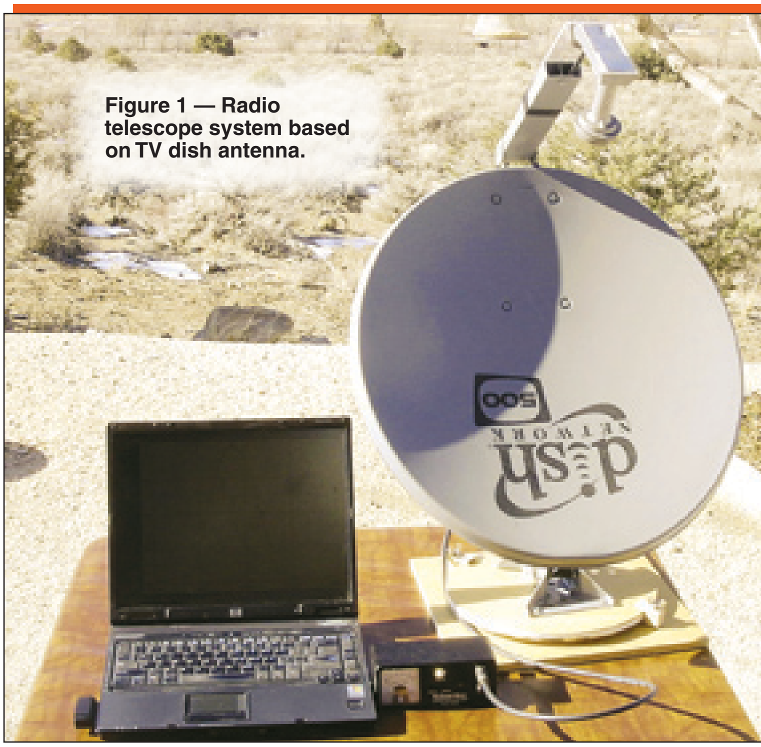

Figure 1 — Radio telescope system based on TV dish antenna.

A Homemade Radio Telescope

In this article, I will build on an existing design of a radio telescope made from one of those ubiquitous TV dish antennas that you see around your neighborhood. The radio telescope (RT) project described here can easily be reproduced. Although this is not a fully capable RT, it can provide a wonderful learning opportunity for you, or perhaps students in your local school.

Figure 1 shows the radio telescope set up. The major components include a modified TV dish antenna mounted on a wooden support structure to allow pointing the antenna, a commercial satellite signal strength detector that displays the signal strength of signals collected by the dish on a meter and an interface that converts the signal strength into a amplitude modulated tone. The tone is fed into a computer sound card and finally a computer and software graphically displays the signal strength as a function of time.

The TV dish modifications are structural, and any available TV dish system can be used. The signal strength detector costs between $40 and $65 and is widely available from Web retailers. The interface circuit, which will be described shortly, is easily duplicated and costs approximately $20. Finally, the display software is free.

Figure 2 — Dual LNB mount. Note two coax connectors.

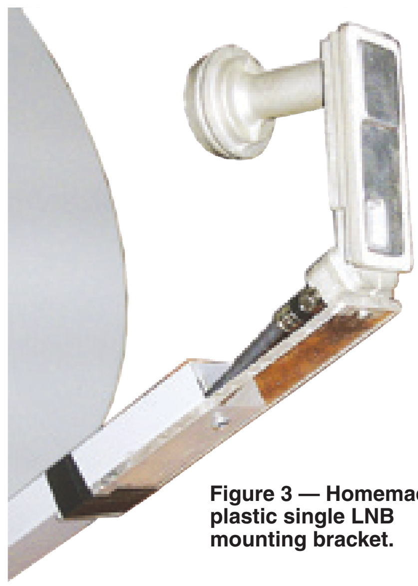

Figure 3 — Homemade plastic single LNB mounting bracket.

What it Can Do

The following is just a sample of what you can do with this simple RT:

- Use the sun to study and determine the beamwidth of the dish and verify the mathematic formula that is used to predict dish antenna performance.
- Measure the radiation intensity of the Sun and perhaps detect changes in solar activity.
- Measure the relative changes in the surface temperature of the moon.
- Learn about and explore a common radio astronomy collection technique called the *drift scan*.

Figure 4 — Dual coax connector configured LNB. Terminate one connector with a dummy load.

- Explore the fundamental principle of energy emission as a function of temperature by detecting the relative differences between the temperatures of emitting bodies.
- Detect satellites parked along the Clarke Belt in geosynchronous orbit and illustrate how crowded space has become.

Figure 5 — CM satellite signal strength meter.

- Detect the Earth's rotation around the Sun and the Earth's spin on its axis by comparing daily drift scans of the horizon.

Antenna Subsystem

The basic RT system is based on the "Itty-Bitty" design that is described in two Web pages.[1,2] The TV dish is an offset 18 inch dish that has down converter(s) mounted at the focal point of the dish. The down converter is called a low noise block (LNB). The LNB is a preamplifier/down converter that converts the satellite signals from around 12 GHz down to around 2.4 GHz. Most modern dishes have two or more LNBs to access more than one TV satellite at a time without changing the pointing of the dish

[1]Notes appear on page 45.

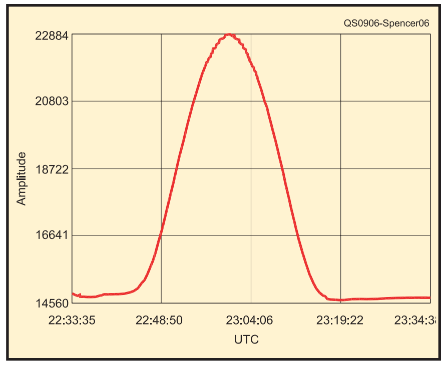

Figure 6 — *SkyPipe* screen showing antenna response.

(Figure 2). The LNBs are mounted to share the focal point of the dish. Since only one LNB is required for the RT, I made a minor adjustment to the published Itty-Bitty design to position the single LNB at the dish focal point. Mounting the single LNB at the focal point really helps in pointing the antenna.

I used the existing LNB housing and mounting bracket as a template to determine the distance between the edge of the mounting arm to the mounting hole of the LNB. I then used a piece of plastic to fabricate a new mounting bracket for the LNB as shown

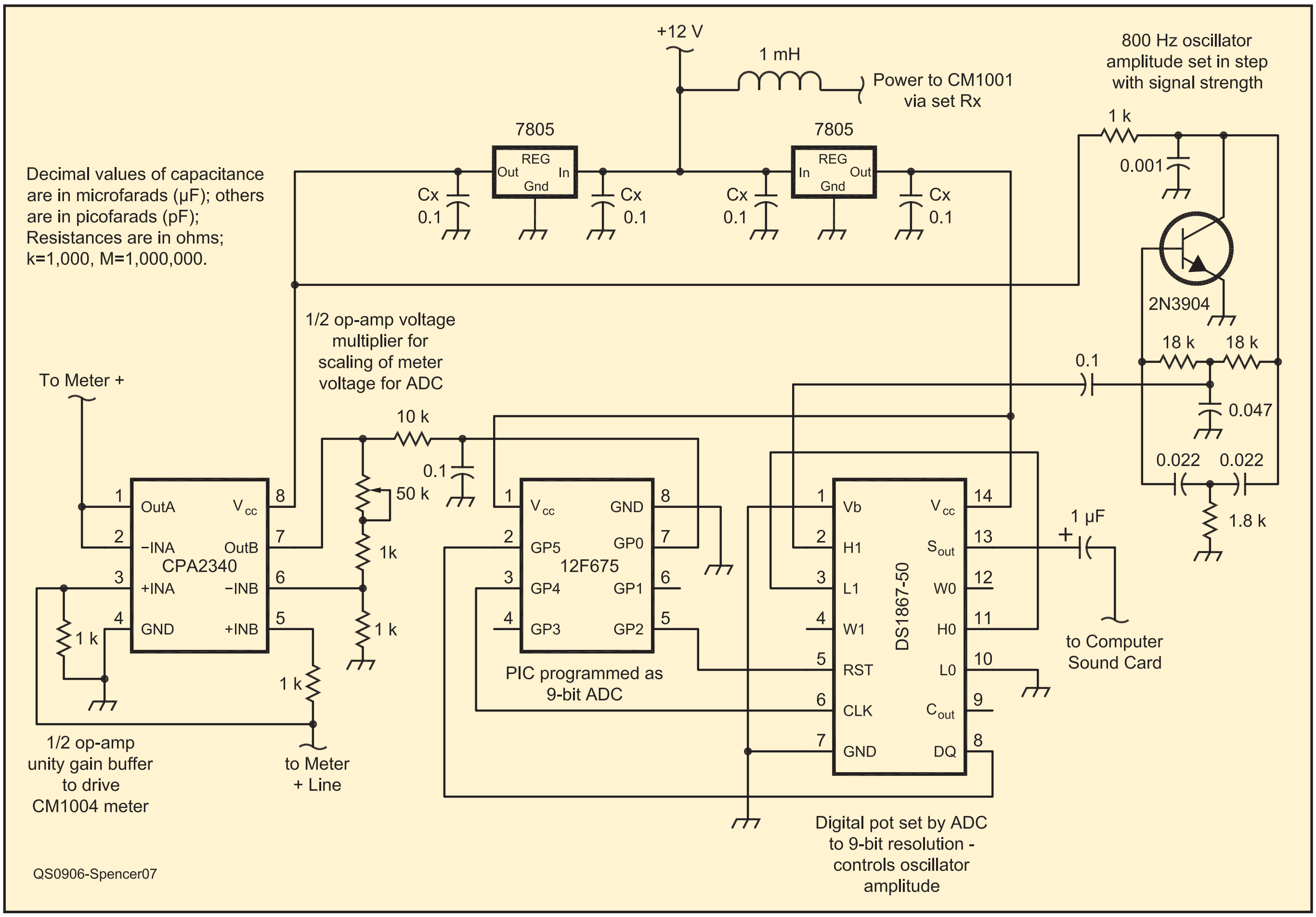

Figure 7 — RT Interface circuit diagram.

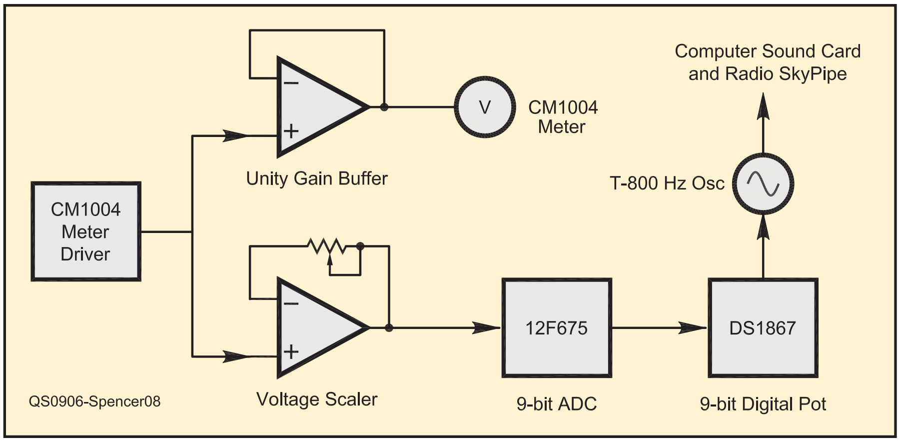

Figure 8 — RT Interface block diagram.

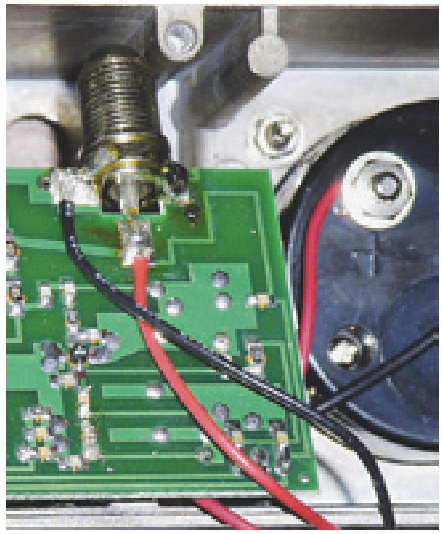

Figure 9 — Power and ground connection to CM board.

in Figure 3. The dimensions are not super critical, but careful placement certainly will improve the RT performance.

Some LNBs have two coax connectors. Only one will be used in the RT (Figure 4). It is a good idea to terminate the extra coax connector with a 75 Ω dummy load plug to balance the load on the LNB. The dummy loads for F type TV coax connectors are readily available from electronic parts retailers.

Note that the dish is mounted upside down. Though this orientation is not ideal for receiving satellite signals, this arrangement helps with pointing the dish in its radio telescope role.

Satellite Detector

The detector used in this project is the Channel Master (CM) satellite signal level meter model 1004IFD (Figure 5).[3] The CM is connected to the LNB. Power is supplied to the LNB through the coax connection from the CM. The CM detects the signal coming from the LNB and gives a meter indication of the signal strength and also varies the frequency of an audio tone to help technicians point the dish at the desired satellite. As you move the dish through the beam coming from the satellite, the meter indication will increase and then decrease coincident with the pitch of the audio tone.

The Itty-Bitty plans detail how to connect power to the CM and in turn connect power to the LNB (this power connection is handled by the interface in this project). Though somewhat effective, the CM meter and variable frequency tone indications provide limited utility in detecting changes in signal strengths required for radio astronomy.

Display

To really study the signals received by the RT, you will need to see them displayed graphically on a strip chart. There is an excellent software package called *Radio-SkyPipe* that is posted on radio astronomy Web sites.[4] The free version of this software is a good place to start. *SkyPipe* uses the computer sound card to measure the incoming signal strength and graphically displays the signal strength as a function of time. Figure 6 is illustrative of a signals detected by the RT. *SkyPipe* is very easy to use but some study of the HELP files will make it easier for you to fully tap into the capabilities of this software.

SkyPipe requires audio signals to be fed into the sound card MICROPHONE jack. The output of the CM detector is either an analog meter reading or a frequency modulated (constant amplitude) tone that is not really compatible with *SkyPipe*. An interface is required.

Interface

What is required to make the CM output work with *SkyPipe* and a sound card is to convert the signal level into an amplitude varying audio tone. The interface designed to do this is shown in Figure 7 and as a block diagram in Figure 8. Refer to the block diagram during the description of the interface function.

The unity-gain op-amp is used as a buffer between the CM meter driver circuit and the analog meter. The other op-amp is used as a voltage multiplier to scale the CM meter driver output voltage to match the 5 V reference voltage of the following analog to digital converter (ADC). The variable resistor in this voltage multiplier circuit is used to calibrate the CM to *SkyPipe*. The voltage from the multiplier is fed to a programmable interface controller (PIC) that is programmed as a 9-bit ADC to covert the analog voltage that is a function of received signal strength to a 9-bit digital word that is used to control a digitally controlled variable resistor. The interface includes a simple Twin-T audio oscillator circuit that provides a tone of approximately 800 Hz that is fed to the computer sound card. The amplitude of this audio oscillator is varied by the digital pot that is being controlled by the PIC. The result is the audio amplitude being varied in step with the signal strength detected by the CM.

The circuit provides power to the CM and the LNB. A 12 V source in the CM is tapped through an RF choke and this is connected to the LNB coax connector inside the CM (Figure 9). The 12 V is also regulated to 5 V to provide power to the interface. Though probably not required, there are two 5 V sources, one for the digital components of the interface, and the other for the analog components with one common ground point. This arrangement is used to isolate potential digital and analog noise sources within the circuit.

The interface is built on a circuit board and mounted right inside the CM box

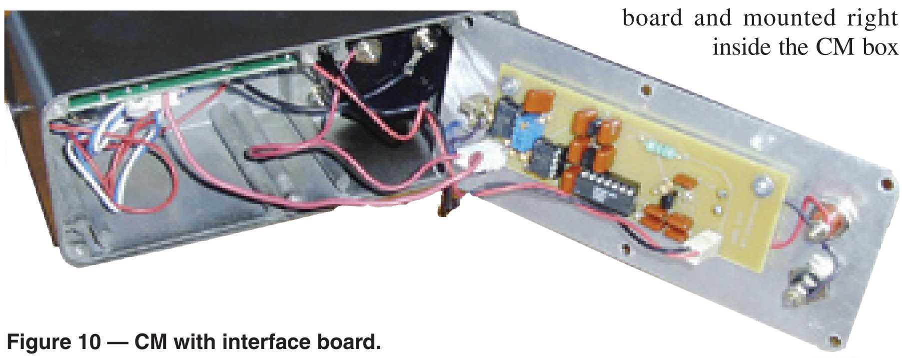

Figure 10 — CM with interface board.

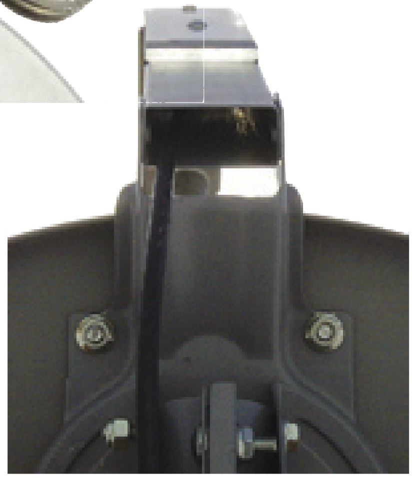

Figure 11 — Aiming the RT at the Sun, note LNB shadow location.

(Figure 10). Though I made an etched circuit board for the circuit, the hand wired prototype worked equally well for those who would rather roll their own. The PIC firmware is available on the *QST* Web site.[6]

RT in Action

The first thing you need to do is learn how to point the RT antenna. The best place

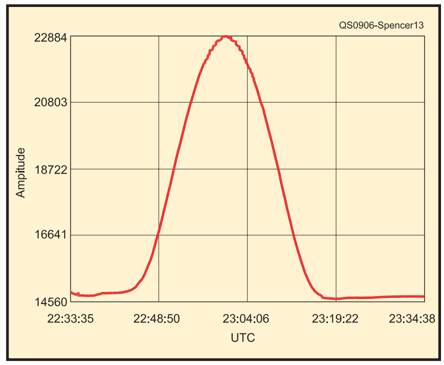

Figure 13 — Drift scan of the Sun indicating antenna's azimuth pattern.

to start is to connect the CM to the antenna and point the antenna at the Sun. *Caution*: Do not look into the Sun as you do this, or at any time. Adjust the pointing angle and elevation until you get peak signal strength as indicated on the CM meter or hear the highest pitch audio tone. With the antenna pointed directly at the Sun, take note of the position of the shadow of the LNB on the surface of the dish (left in Figure 11). If you look from behind the dish, along the LNB

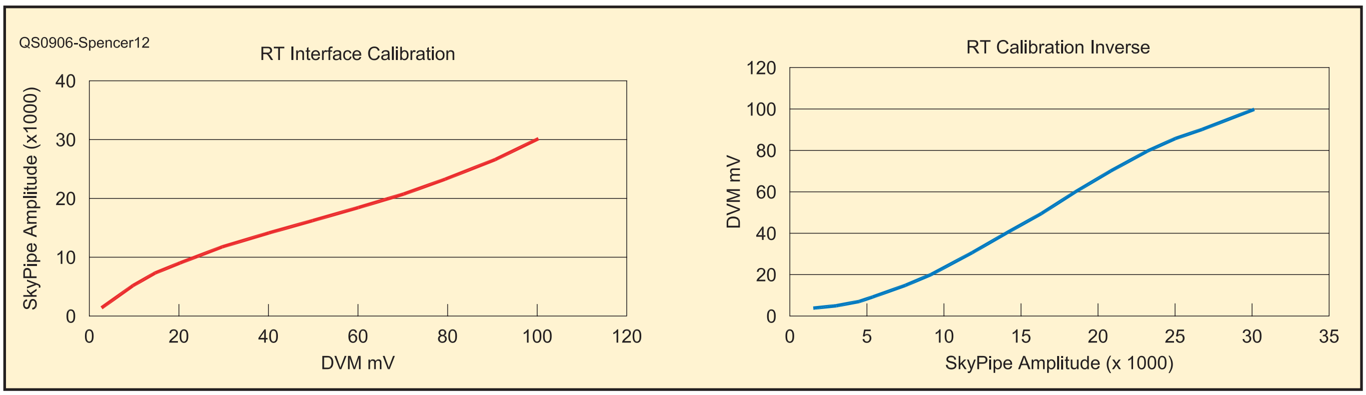

Figure 12 — Example calibration curves.

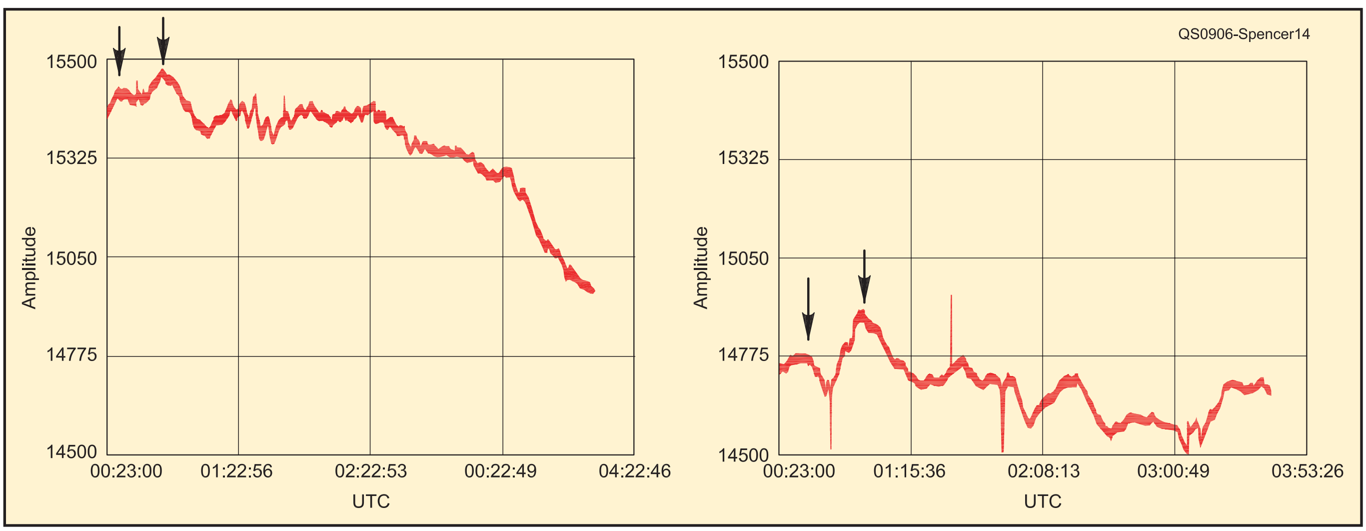

Figure 14 — Sequential drift scans. Note the time offsets between the peaks.

supporting arm (between the arm and the rim of the dish), you will see the Sun being blocked by the LNB.

Once you have the RT set up, it needs to be calibrated to match the output of the CM to *SkyPipe*. I have developed an *Excel* spreadsheet template to help with the calibration and a few of the other activities that you can accomplish with the RT (also available from the *QST* Web site). Turn the RT to a signal source, the Sun, or the side of a building would work. Turn the gain control of the CM to set the meter to maximum. Run *SkyPipe* and adjust the variable resistor on the interface board until you get a reading on the *SkyPipe* graph vertical (y) axis of approximately 32,000. With the maximum value set, adjust the CM gain control through the voltage range (0 to 100 mV) in 10 mV steps and record the corresponding y axis value on *SkyPipe*. This data is entered into the *Excel* spreadsheet to compute the calibration curve between voltage and y axis value. Both voltage and y axis values are used in analyzing recorded signal strength data (Figure 12).

A good first activity is to do a drift scan of the Sun. A drift scan means that you set the antenna azimuth (AZ) and elevation (EL) to some fixed pointing angle and allow the Earth to serve as the rotator to drag the antenna across the sky. To do a drift scan of the Sun, first set the elevation and azimuth to point directly at the Sun (maximum signal) and then move the azimuth toward the west

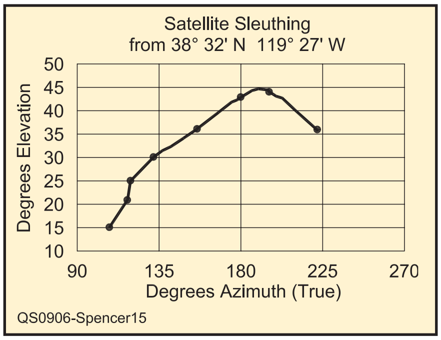

Figure 15 — Clarke Belt plot — tracking down satellites.

(leave the elevation set) until you are off the peak signal. Now start *SkyPipe*. In about 15 minutes, the Sun will pass through the antenna pattern beam width and the result will be as illustrated in Figure 13. You can also use this collection technique to explore the antenna performance parameters.

A good second activity is to do two drift scans of the night sky on two consecutive nights (beginning the scans at the same time each night) using the same fixed antenna azimuth (AZ) and elevation (EL). Figure 14 shows two such drift scans. Although at first glance they may not seem similar, there are some interesting features that are pointed to by arrows. If you compare the time that these two peaks occurred, the time difference is about 4.5 minutes. This shift is the result of the distance the Earth had traveled during the 24 hours between collections. This illustrates that the Earth's rotation as well as its travel in orbit needs to be considered when comparing drift scans. Enough to make your head spin (pun intended)?

A final good starting activity is to point the antenna toward the Clarke Belt and find all the satellites in geosynchronous orbit transmitting on 12 GHz. If you record signal strength peaks and AZ and EL for each peak, you will develop a graph of the Clarke belt as illustrated in Figure 15.

I have only scratched the surface, and the sky is the limit of this little project. The RT project can certainly broaden your horizons and expand your understanding of our universe. If you would like more detail than can be presented here, please contact the author.

Notes

[1]**www.setileague.org/articles/lbt.pdf**.
[2]**www.aoc.nrao.edu/epo/teachers/ittybitty/procedure.html**.
[3]**www.pctinternational.com/channelmaster/0612/satellite.html**.
[4]**radiosky.com/skypipeishere.html**.
[5]**en.wikipedia.org/wiki/Geostationary**.
[6]**www.arrl.org/files/qst-binaries/**.

Mark Spencer, WA8SME, is ARRL Education and Technology Program Coordinator. He is an ARRL member and holds an Amateur Extra class license. You can reach Mark at 774 Eastside Rd, Coleville, CA 96107 or at **wa8sme@arrl.org**.

Simple demonstration to explore the radio waves generated by a mobile phone.

Dr Jonathan Hare, Sussex University, Department of Physics, Falmer, Brighton. BN1 9QH

Note: this article has been published: Simple demonstration to explore the radio waves generated by a mobile phone J P Hare, 2010, Journal of Physics Education, Institute of Physics, 45, p. 481 45 481

Also see the brief full article at: mobile phone detector

IMPORTANT NOTE: this device works very well on the old style mobile phones (as shown in the photo above). However, it does not always work well with modern smart phones. This may be because modern phones use higher frequencies, less power and use the power in a slightly different way (e.g. spread spectrum). Some smart phones do work and success may be due to the signal strength of the local mobile phone mast nearby. If you are in a low signal area the phone will create more power to ensure reliable communications. If you are in a very strong signal area (very near the local network) your phone will drop its output power and consiquently there will be less power to pick-up and to convert to a voltage to light the LED.

Described is a simple low cost home-made device that converts the radio wave energy from a mobile phone signal into electricity to light an LED. No battery or complex circuitry is required. The device can form the basis of a range of interesting experiments on the physics and technology of our mobile phones.

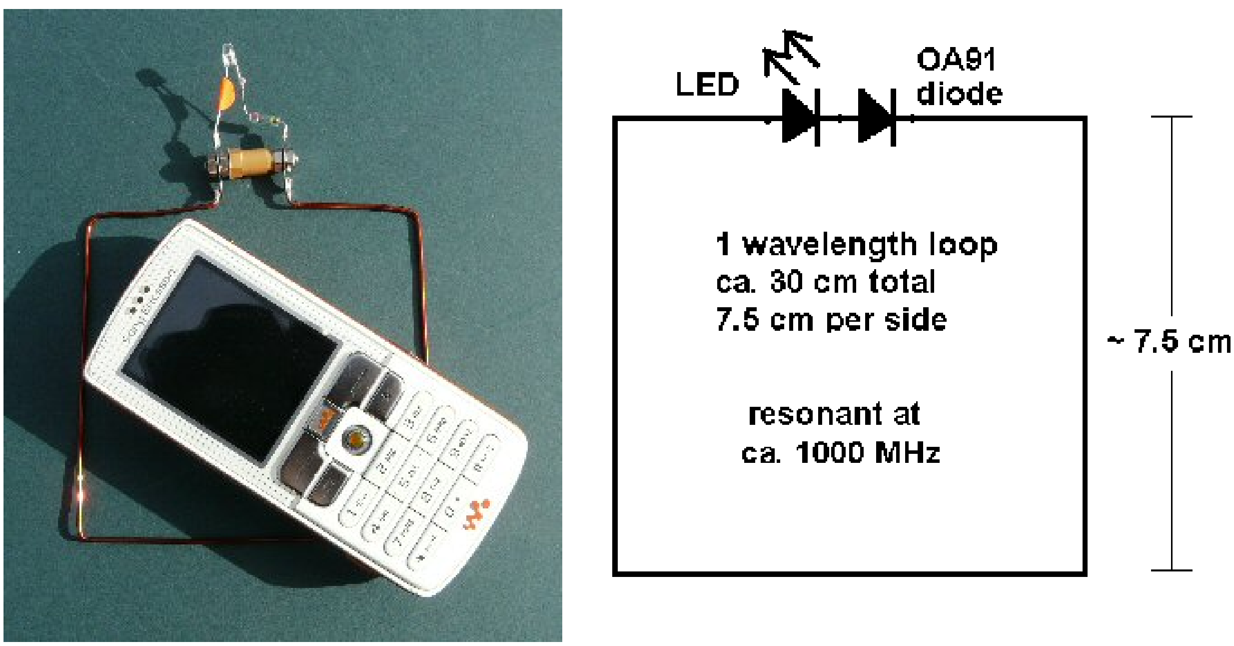

Fig. 1: left: mobile phone radio wave detector and right: the simple schematic

Introduction

Electromagnetic radiation (EMR) is at the heart of modern mobile phone data communications networks. The way a mobile phone and local base stations (the antenna covered masts you see dotted all around the place) communicate between each other is by using EMR in the radio wave part of the spectrum [1,2,3]. On switch-on your mobile sends digital information pulses by rapidly switching on and off the radio waves rather like a fast Morse code signal. Your text or voice is also converted into a series of digital pulses and sent across the network to be decoded (reassembled) by another mobile phone you dialled.

EM radiation and radio waves

Mobiles make use of various bands of radio frequencies to communicate between the mobile to base and the base to mobile: in Europe these include 900 and 1800 MHz (850 and 1900 MHz in the USA and Canada) [2, 3].

The relationship between wavelength, speed of light and the frequency follows the well known formula:
Wavelength λ (m) = speed / frequency = c (ms^{-1}) / ν (Hz)
λ (m) = 300,000,000 / ν (Hz) or approximately:
λ (m) = 300 / ν (MHz) ..... Equation 1.

So for a mid-range of about 1000 MHz (1 GHz) we get a typical mobile phone wavelength of about:
λ = 300/ 1000 = 0.3 m = 30 cm.

Simple radio wave detector

The loop consists of about a wavelength of wire, ca. 30 cm so each side is about 30/4 = 7.5 cm. The dimensions are not critical. The two ends are connected directly to a simple series circuit consisting of a high brightness LED and a germanium diode. They need to be connected correctly. All these components are cheap and readily available from electronic stores [4]. The loop can be made from a piece of copper wire roughly bent into a square (although a circular loop or rectangle will also work). If the wire is insulated remember to scrap off the insulation and solder-tin the ends. Simply solder the germanium diode and LED into circuit as shown in the diagram.
On a new LED the long lead is the positive (anode) while the short lead is the negative (cathode). The germanium diode has a line (band) around the end which is the cathode. When correctly wired the LED and the germanium diodes are connected so they both allow current to pass in the same direction, i.e. in the circuit diagram the arrows point in the same direction. In practice this means the LED and germanium diode are joined at the cathode of one and the anode of the other.
In my prototypes I used an insulator between the loop ends (light coloured cylinder in the photo) to make the whole thing more sturdy but this was purely for mechanical reasons and is not needed for the circuit to function properly. Note: a much more sensitive version using a x10 and x100 DC amplifier is described on my web site [6].

How it works and how to use it

When a radio wave passes across a metal object the EM fields cause the charged electrons in the metal to oscillate and this causes small AC currents at the same frequency to be induced into the metal. If a mobile is brought near to the loop and a call or text is made [5] the radio waves emitted from the phone pass across the loop. This induces a voltage into the antenna (the loop) and if it is close enough will be large enough to light the LED. As the loop is about one wavelength in size it is resonant and so there is a good transfer of power (low reactance) between the radio wave and LED.

The mobile phone automatically tests the network and adjusts its transmission power to maximise the battery life and minimise network interference. As a result the brightness of the LED will depend on the data being sent (the average signal), the local signal strength and how close the loop is to the phone. Why the second diode? - It's curious why the germanium diode is needed at all. The LED is a Light Emitting Diode after all and one would not think that another diode would help. However my initial experiments failed because I had not included it. The LED will have a relatively high capacitance which at these frequencies will tend to de-tune the loop and short out the LED. The germanium diode however is made up of a tiny wire which only makes a point-of-contact onto a piece of semiconducting germanium so it's 'self' capacitance is very low keeping the loop resonant.

The germanium diode will rectify the AC signal from the loop forming a series of DC pulses that will be nicely smoothed by the LED's capacitance. Without the diode however the raw AC signal from the loop will tend to be averaged to zero by the LED's capacitance.

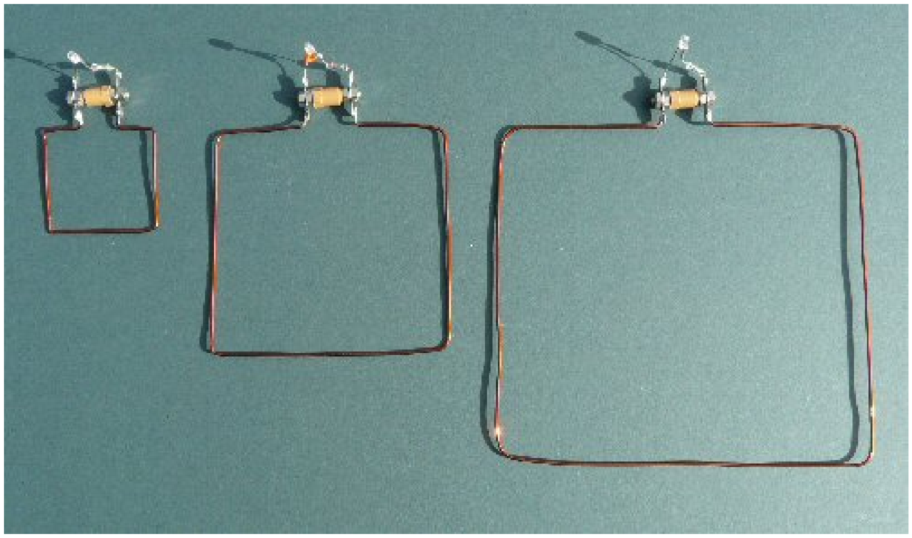

Fig. 2: Three loops in a row of varying size. The one described here and shown in Fig. 1 is shown in the middle. Smaller ones may well work better for higher frequencies such as the 3G networks (see below).

Other size loops
Fig. 2 shows a set of three loop devices with edge lengths of roughly 3.7, 7.5 and 15 cm. You can find out for yourself that the best match to the mobile signal is with the full wave loop of ca. 7.5cm per side. The other loops do work to varying degrees however (smaller ones may work better for the 3G network). The larger loop works well for the '70 cm' amateur radio bands.

Polarisation
The electric and magnetic fields making up the EM wave are orthogonal (they are at right angles to each other as they pass through space) to each other but depending how they are generated by the transmitting antenna can arrange themselves in any orientation with respect to the ground. If the electric field is parallel with the ground we say the wave is 'horizontally polarised' while if its normal to the ground we say its 'vertically polarised'. The loop antenna will respond best to one type of polarisation (depending on its orientation) so it's worth experimenting with the orientation of the mobile (or the loop) to get the strongest signal - brightest LED.

Mobile antenna
Inside your mobile phone is a transmitter / receiver and antenna. Many mobiles have this antenna at the top of the phone but some of the PDA type phones have it at the bottom. As a result you can locate the position of the antenna by moving it around the center of the loop till you get maximum LED brightness.

Networks
There are various different networks that a mobile may use both in the UK and abroad. It may be that you need to adjust the network phone settings on your mobile i.e. change from "automatic select" to set for "GSM" so as it get the strongest signal to light the LED. Note: the 3G network might not be powerful enough to light the LED. As the GMS network is currently the main network over the UK the device should work anywhere where you can get a signal as long as you check the correct selection on your mobile menus [5, 7]. The 3G network operates on a higher frequency (smaller wavelength) so you might find a smaller loop will work better than the main one described here. See 'other experiments' section below.

Test signals
In order to pick up the radio wave energy from the phone it obviously needs to be transmitting a signal. There are a few ways to do this:

1) On switch 'on' (or change of network) you can see that the mobile initially transmits for a few seconds to the network to tell it it's there (especially if you have moved since turning it off). You don't actually need to dial a number to detect these signals.
2) Even if don't text or call, throughout the day the mobile will send out data to 'keep up' with the network, especially if you are moving around (going through train tunnels etc. see below).

3) When you make a phone call you will transmit. Initially there is quite a lot of data being sent but in a few seconds data / power only gets transmitted when you speak. So to light the LED continuously you need to talk or provide some background sound continuously. Your service provider voicemail might be a good free phone number to try for these experiments [5].

4) Texting is the easiest way to show the radio wave power being transmitted. Long texts will light the LED for longer than short texts.

5) Finally set up the mobile on the loop and use another phone to text or phone the mobile. Even though you are not directly using the phone you will see that even on 'receive' the mobile phone transmits data to and fro. Ring off before you get charged.

Note: If you can use a free phone number it will save you money [5].

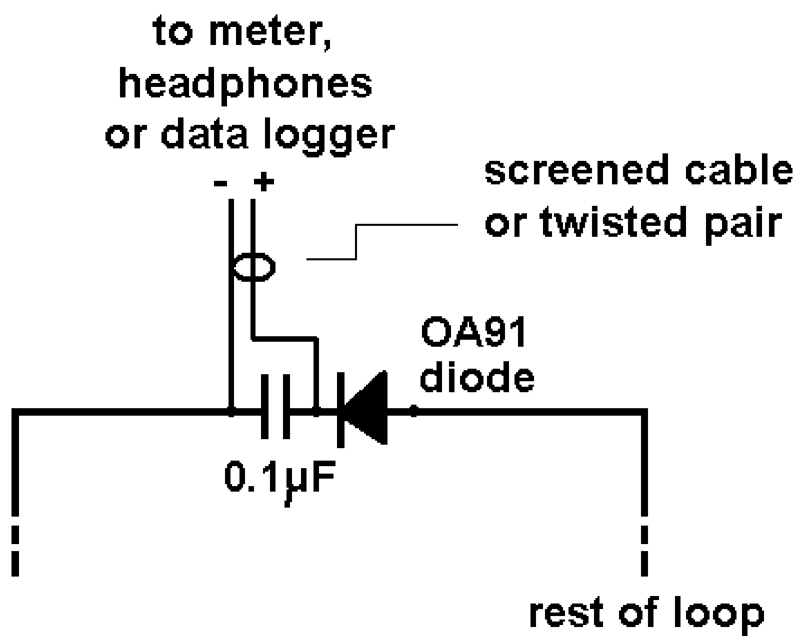

Fig. 3: Adding a capacitor and coax (or twin) lead so that headphones, a meter or a data logger can be connected (Note: diode is reverse wired compared to Fig. 1).

Other experiments:
Hearing data - if headphones are wired across the LED they will convert the voltages into sound and you can 'hear' the clicks of the digital data being transmitted. These are the same clicks that so easily get picked up by sensitive electronics such as a stereo amp or recording equipment when making a video for example. Hence - 'no phones on' when filming.

Logging data - if a meter, or better still a stand-alone data logger, is attached across the LED then one can monitor the EMR from the phone. For example even if you are not making a call your mobile will send signals too (and receive signals from) the network while travelling around. Fig. 3 shows a simple modification using a de-coupling capacitor so that a coax cable (or twisted pair) can be used to go to headphones, meter or data logger. Note the diode has been reversed so that the logger has the correct + and – connections for a unipolar input logger. The capacitor should help average the signal and stop radio frequencies going down to the logger. If one is available a few turns of the wire can be wound within a ferrite ring near to the logger so that maximum immunity to the mobile phone signal can be obtained for the logger electronics.

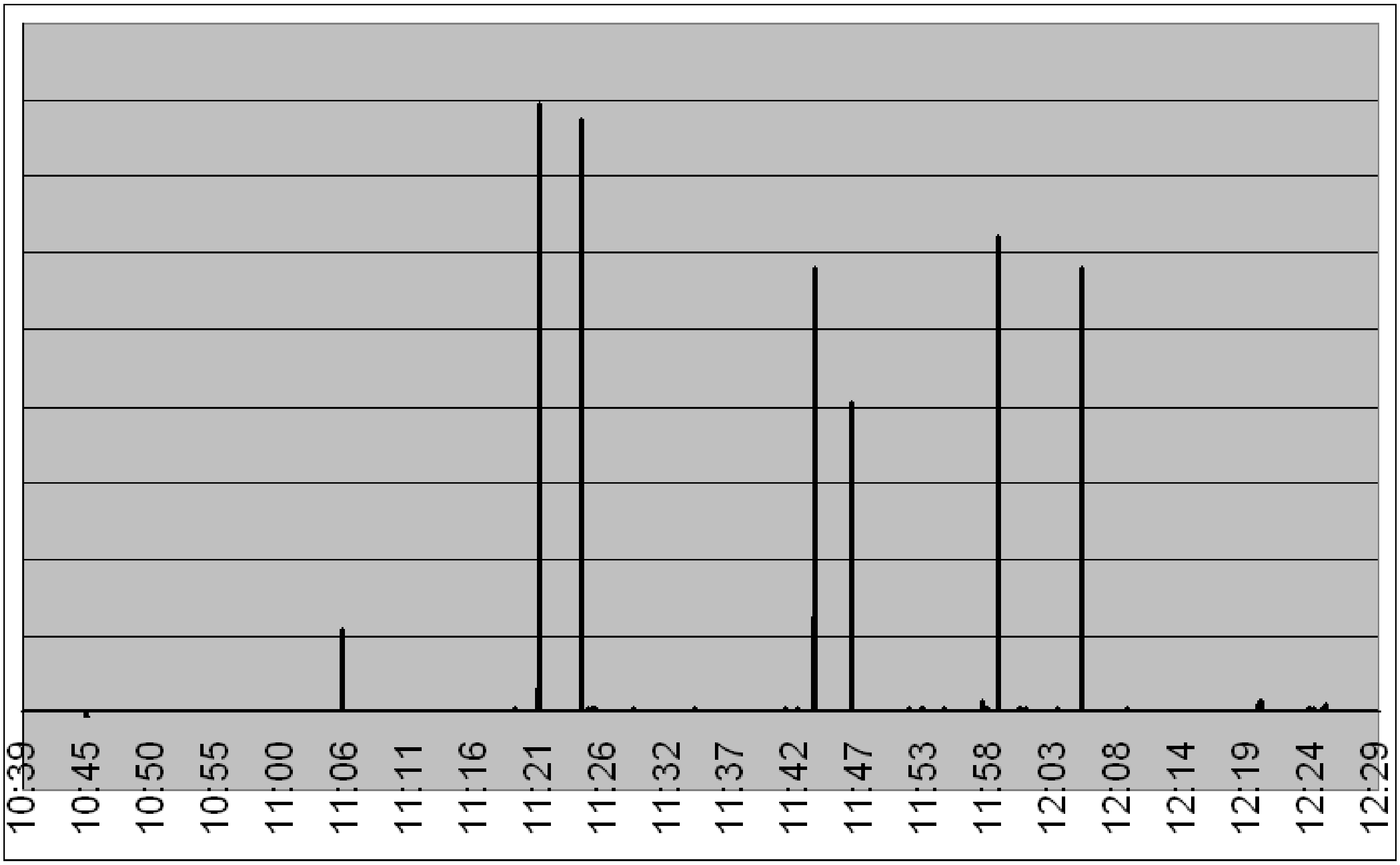

Fig. 4: Typical mobile phone data signals sent out onto the network while travelling around. These were recorded by a data logger from a mobile using the loop (no calls or text were made) while travelling on the train from Brighton to London Victoria (and then around London and return). Many of these peaks were the phone sending out 'I am here' data after coming out of one of the many long tunnels under the South Downs during the journey.

Out and about - Once you can log data you can discover all sorts of interesting things your mobile phone is doing without you realising it. Fig. 4 shows the plot over a few hours of travelling between Brighton and London (and within London) on the train. The detector was simply placed near to a phone that was not making or receiving a phone call or text, but was turned on.

The graph shows that the mobile sends out signals to tell the network where it is as it travels along and in particular goes in and out of long train tunnels. The peak heights vary because of the different powers the mobile transmits at depending on the signal strength of the local network and also because of the way the data logger 'snatches' a reading from the circuit every few seconds. As your phone sends out data onto the network to ensure the very best communications as you move around, so your mobile and the network obviously knows where you are and where you have been. Thieves and criminals beware the police can track you!

The inverse square law - If the transmitting mobile phone is moved away from the loop one would expect the signal to drop off. Unfortunately because both diodes need a certain threshold before they conduct the detector is not sensitive to small signals and not very linear. Therefore it's not very easy to use the device to measure the inverse square law (drop in signal v distance away) but of course you can see the signal go down. You could perhaps use the device to plot isobars - i.e. plot the equal intensity signals around the phone / nearby objects.

Changing the resonant frequency of the loop - you might be able to make some simple sliding mechanism (e.g. a small trombone-like mechanism) out of metal tube for example to tune the loop device for different frequencies. Then you can use it to find the average wavelength and so determine the center frequency by adjusting the size for maximum brightness of the LED. The wavelength can be determined by measuring the total distance around the loop. If we assume the antenna is one wavelength in total length then the frequency can be established by rearranging Equation 1, i.e. ν (MHz) = 30,000 / L (cm), where L is the length around the loop (cm).

Note: You will need to allow the transmitted digital signal to 'settle down' i.e. make measurements only after a few seconds after dialling / pick up so that only the sound data is being transmitted rather than the initial connection data. A constant sound will also need to be made so that the mobile phone continuously transmits data. It's worth playing music near to the phone or constantly whistling to keep sound coming into the phones microphone.

Mobile phone detector - teachers who want to know if the students / pupils really have turned-off their mobile phones (rather than just put on 'silent') can wire the loop device into the class room white-board speakers. Any mobile that is on in the class will send out signals which (if you are close enough) you will hear the data going to and fro - you will have your very own 'who's got their mobiles on' device which might be useful for exams etc.

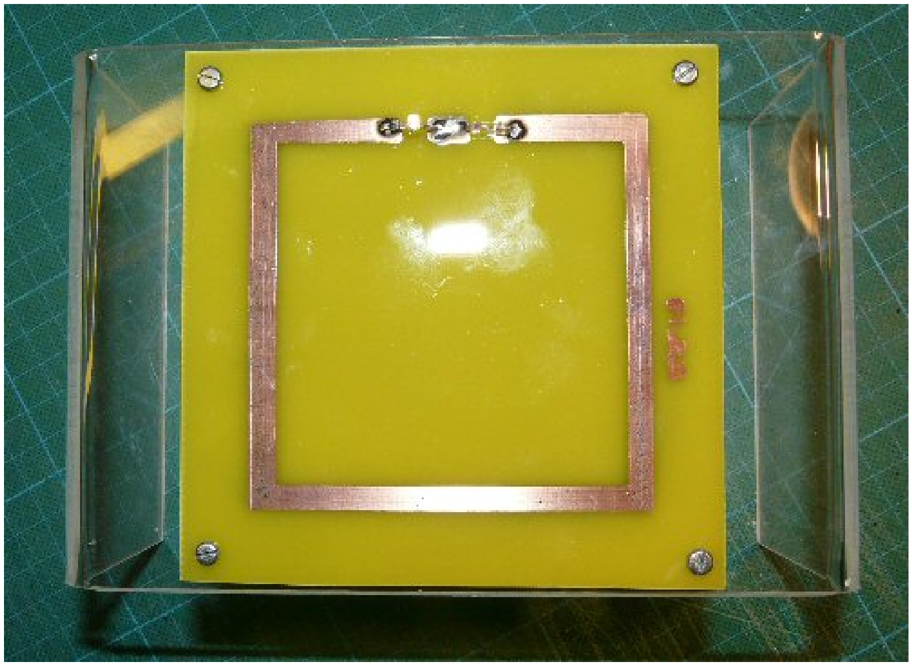

Fig. 5: The SEPNet 'deluxe' printed circuit board version (pcb) on a perspex stand where the loop is composed of a pcb copper track and the diode and LED soldered onto the board (top) [8,9].

Summary

All in all then, for such a simple easy to make device I hope you agree that there is a lot of scope for interesting science / technology investigations with your mobile phone. The device would make a good science week project (for radio amateur clubs etc.) A 'deluxe' pcb version (Fig. 5) on a perspex display case (Fig. 5) is currently going around the southern UK as part of the SEPnet outreach work, see the 'Radiation Exhibition' [8] and also as part of my on-going lecture series [9].

Post publication additions

(What follows was not included in the published article as this calculation was worked out later). A full wave loop is resonant and so looks purely resistive to the radio waves. Such a loop will have a resistance of about 100 ohms (Note: this is the AC resistance and not the DC resistance which will be very low). Now power P = V x I (V = voltage and I = current) and resistance = R = V/ I therefore $P = V^2 / R$ or rearranging $V = \sqrt{(P \times R)}$ which means that the voltage created by a power level of say 50mW (say for argument that roughly half the mobile phone power) arriving at the antenna will be about $V = \sqrt{(100 \times .05)}$ which is aprox. V = 2V, enough to light an LED.

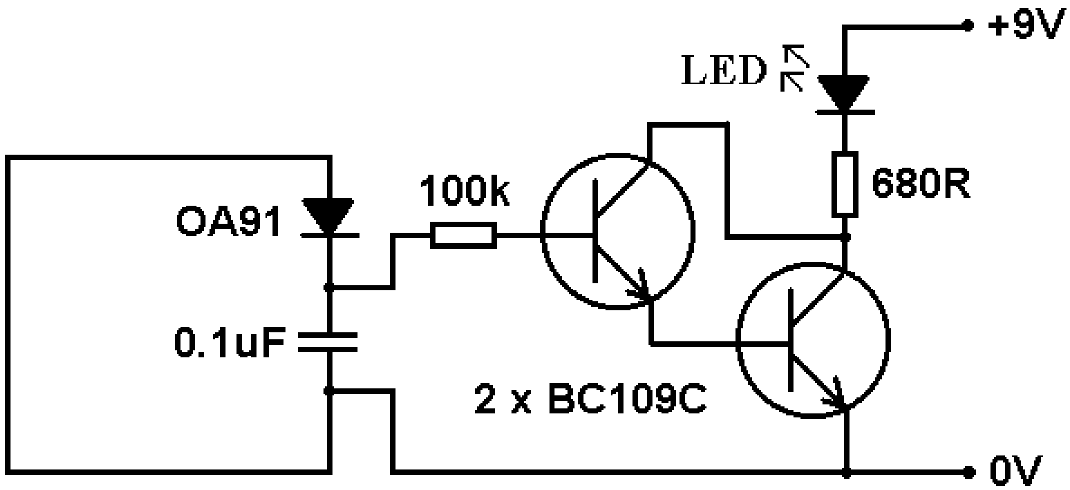

This circuit uses a two transistor darlington driver to amplify the signal from the loop and diode making the detector much more sensitive. The LED will be much brighter using this circuit. Note: the circuit needs a battery to power it (e.g. a PP3 9V)

References

[1] These ultra high frequencies (UHF, > 1000 MHz) are also often called microwaves.
[2] wiki pages
[3] Elektor Electronics magazine, June 2005
[4] order codes for the germanium diode and LED are:
e.g. Germanium diode: Maplin Electronics: QH71N, Rapid Electronics: 47-3114
e.g. LED: Maplin Electronics: UF72P , Rapid Electronics: 55-0085
[5] to save money use your voice mail service (often you simply dial 121).
[6] for details of an amplified detector see: wavemeter
[7] select 'network setting' from the mobile phone 'settings' menu and then go to 'network mode' and select 'GSM 900/1800' rather than 'automatic'.
[8] SEPnet mobile phone device on display throughout southern UK. [9] for details of my talks see: talks and workshops

THE CREATIVE SCIENCE CENTRE

Dr Jonathan Hare, Brighton, East Sussex. BN1 9QJ.

Simple demonstration to show mobile phones emit radio waves

Dr Jonathan Hare, Sussex University, Department of Physics, Falmer, Brighton. BN1 9QH
Note: this article is in press: Elektor Magazine, July-August 2010, p. 56-57

For other experiments with this device please see my full article at: mobile phone detector

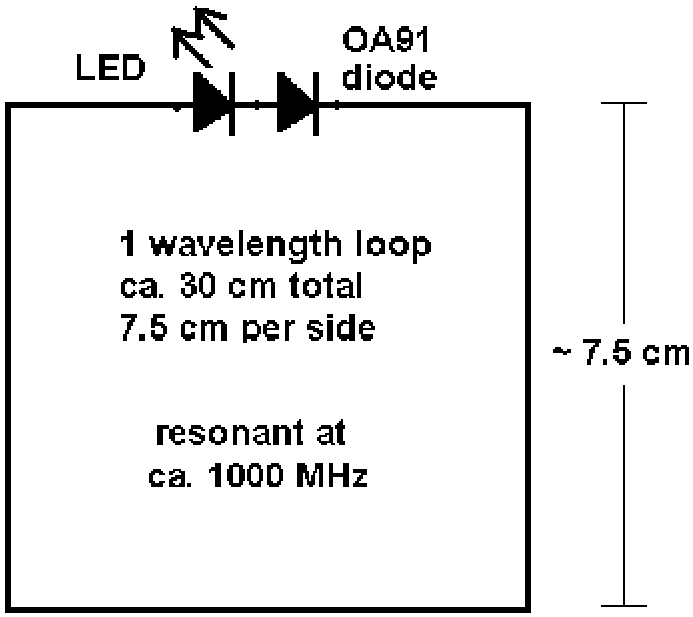

left: mobile phone radio wave detector and right: the simple schematic. Below: detail of the LED and germanium diode.

IMPORTANT NOTE: this device works very well on the old style mobile phones (as shown in the photo above). However, it does not always work well with modern smart phones. This may be because modern phones use higher frequencies, less power and use the power in a slightly different way (e.g. spread

spectrum). Some smart phones do work and success may be due to the signal strength of the local mobile phone mast nearby. If you are in a low signal area the phone will create more power to ensure reliable communications. If you are in a very strong signal area (very near the local network) your phone will drop its output power and consiquently there will be less power to pick-up and to convert to a voltage to light the LED.

This is a very simple and cheap device that demonstrates mobile phones ('cell phones' or 'handies') generate radio waves. We have a 30 cm (7.5 cm per side) full-wavelength loop antenna (a 'Quad' to radio amateurs) connected to a germanium diode and a hyper-bright LED. The loop can be made of copper wire, thin sheet metal or a track on a pcb. The diodes need to be wired correctly. I think the germanium diode is needed as the LED probably has too great a self-capacitance to perform at the very high AC frequencies generated by the phone (ca. 900 or 1800 Hz) but will work well with the DC pulses from the germanium diode (which has a very small capacitance).

To show the mobile generates radio waves put the mobile near to the loop and dial a number (use a free phone number, e.g. your voice mail) or text. The radio waves will induce a voltage into the loop, large enough to light the LED. The LED will flash indicating the digital data being sent by the mobile phone transmitter. You may need to set your phone to 'GSM 900/1800' rather than the '3G' network in the settings menu.

parts:
germanium diode: Maplin Electronics: QH71N or Rapid Electronics: 47-3114
LED: Maplin Electronics: UF72P or Rapid Electronics: 55-0085

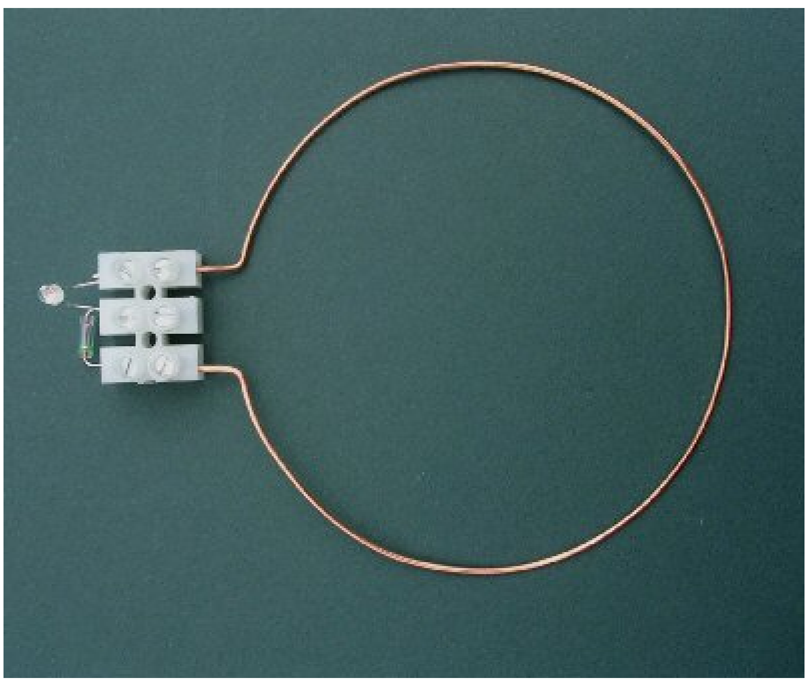

A very simple connector block version and a circular 1 wavelength loop

THE CREATIVE SCIENCE CENTRE

Dr Jonathan Hare, Brighton, East Sussex. BN1 9QJ.

home | diary | whats on | CSC summary | latest news

BACK TO G1EXG RADIO PAGE

EPAD MOSFET - 'near zero' and 'zero' threshold devices (e.g. the ALD110900)

I will add more details to this page later on but for the moment it gives links to important and inspiring sites.

ARTICLES
1) High Sensitivity Crystal sets, Technical Topics, Pat Hawker, Rad Com, p. 77-78, May 2007.
2) A novel kind of 'crystal set' radio, Giles Read, Rad Com, p. 60-61, June 2007.
3) also see Pat Hawker, Technical Topics, Rad. Com. January 200, page 53-57.
4) High Sensitivity Crystal Set by By Bob Culter (N7FKI)
5) Next-generation Zero-Threshold Voltage EPAD™ design enables circuits with greater operating range in low voltage supply environments

LINKS ABOUT THE CHIPS / DEVICES
1) Advanced Linear Devices web site
2) EPAD MOSFET (ALD web site)
3) ALD110800 and ALD110900 page (ALD web site)
4) ALD110802 and ALD110802 page (ALD web site)

ORDERING THE CHIPS / DEVICES
1) mouser.com (USA)

'CRYSTAL SET' RADIO'S - DIFFERENT DETECTORS

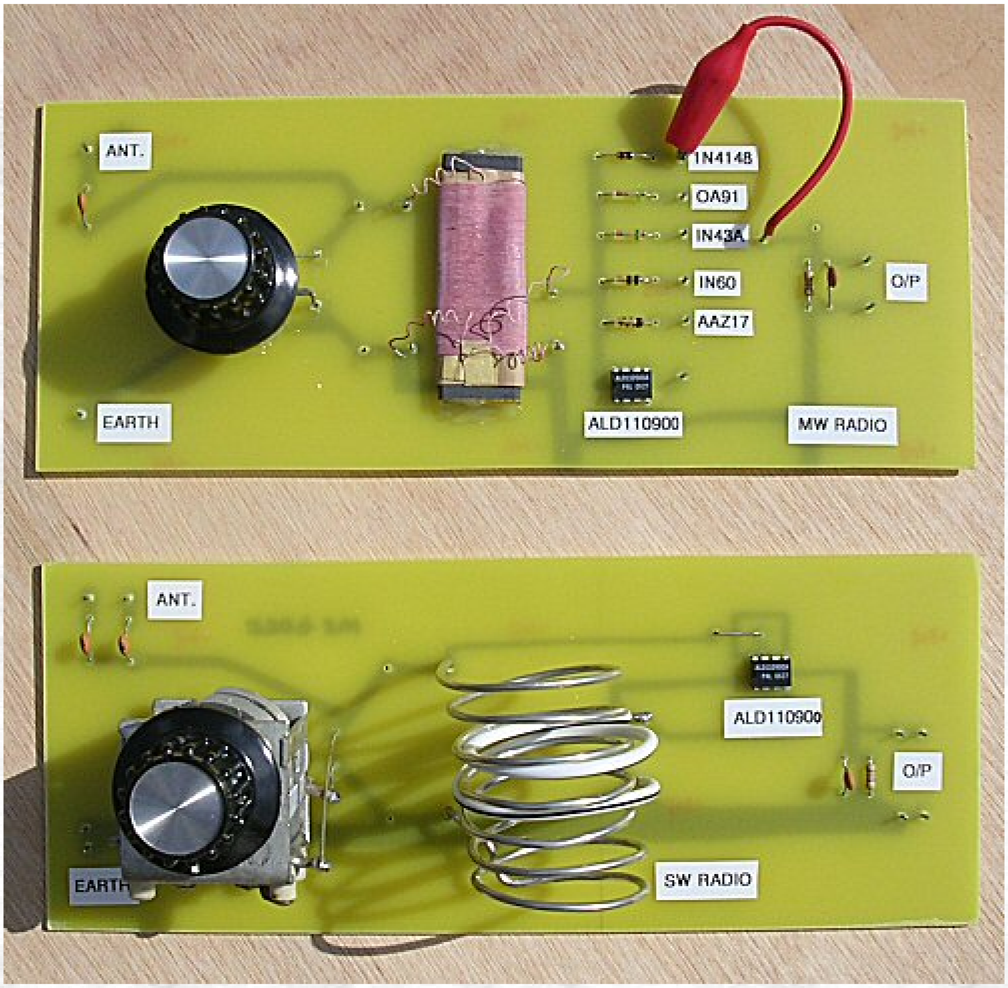

Top: the medium wave (MW) test radio with a selection of 'detectors' (selected by the croc clip lead)
Bottom: the short wave (SW) version with a ALD110900 detector
(on each circuit board the connections are: antenna - top left, Earth - bottom left, audio output (heaphones / amp) - far right.)

RADIO AND RADIO WAVES

The simplest 'radio' can be a piece of wire attached to the input of an amplifier. Why does this pick up radio signals? Well in principle it should not be able to pick up anything but in reality poor solder joints in the amplifier circuitry, as well as point contact effects between the ends of the anenna wire going into the input socket of the amp as well as other effects mean that you do often hear radio signals.

Radio waves are electromagnetic waves as they pass through a metal they induce small voltages into it. Any piece of metal e.g. metal fram specs, tape measures, metal window frames, a piece of wire etc. will act as an antenna and have tiny voltages induced into them. These voltages will be due to natural radio waves (from Space as well as the Sun and Earth), radio stations, satellites, mobile phones, garage door remote controls, microwave ovens .... the list goes on and on.

In the case of long, medium and short wave radio stations the amplitude of the radio wave signal is modified by the music, voice or program - we call it Amplitude modulation AM. Here the strength of the radio waves varies as the tones, loudness and pitch of the program vary. As a result the voltages induced in the metal object antennas distant from the radio wave stations also vary in accord this program information or modulation.

To actually hear the programs on the radio waves you cant actually take this tiny signal and listen to it directly (say with headphones or an amplifier). This is because the signal is a very high frequency signal out of the range of human hearing. To get the audible information - the program - 'off' the radio signal you need a device known

as a 'detector'. This is usually a diode but lots of other things can act as inefficent detectors for example a mineral called galena, coke (burnt coal) ... as well as rusty screws and bad solder joints which is how the ampilfier mentioned above apparently picks up radio signals.

In the early days of radio crystals of galina were used as diodes and so these radios became known as 'crystal set radios'. They did not have any amplifiers and did not require any battery to work. They got all their power from that induced into the (of very long) antenna by the radio signal(s). The radio detector is an extremely important part of the radio and its proper function determines how well the radio works.

The radio signal is an AC signal. A speaker or headphones can not resonate at such high frequencies as radio waves and if you try to wire in the RF to the headphones the diaphram just averages the power. As half the time the RF is positive and half the time negative, in an AC signal, the average is zero and so you dont hear anything. The diode or detector is a device called a diode which only conducts electricity in one direction. So it only allows the positive, or negative half (one half but but not both) of the AC signal to go through (depending on which way it is wired). After the diode the average is now no longer zero its actually a changing signal dependant on the modulation of the radio wave - which is the information we want to hear. As this is at audio frequencies, and as the diaphram can move at audio frequencies, you hear the information on the detected RF signal - the music, voice or what ever.

Why should some detectors (diodes) be 'better' than others? The answer is not that some are better at 'magnifying' the signals but rather that each diode requires a certain threshold voltage in order to start conducting (one way). Signals below this level will not get passed through and a signal only slightly larger will therefore only pass through weekly (the diode unfortunatly absorbing the majority of the signal). As a result for large signals you wont expect to see much difference between different detectors but for weak signals there can be a great deal of difference. In an ideal world the diode would start to (forward) conduct at just above zero volts and this ideal detector (which does not conduct at all in reverse) would produce the greatest signal possible for the particular strength signal applied to it.

Recently I was playing around with OA91 germanium diodes for a mobile phone detector. I made a simple 10cm per side square loop and wired it directly to an LED. I was hoping that if I brought the mobile near to the loop and texted, or made a phone call, the RF should be picked up by the loop (which is almost resonant) and the LED should light - it didnt work! But putting an OA91 in series I did get it to work. So why did I need the OA91 diode when the LED is itself a diode?

It can't be due to the threshold voltage in this case as I am still using the LED and I did get it to work with the same signal! So I guess it because the capacitance of the LED is very high compared to the point-contact germanium diode. If we extend this thinking to the crystal set radio I guess the germanium diodes have very little capacitance and so dont allow any of the 'wrong' half of the AC signal through and so act as a more perfect detector. An LED would have a high capacitance and so let some of the wrong half of the AC signal through which on averaging by headphones would be nearer zero (see above) - hence less sound.

A low threshold (turn-on) voltage and a low self capacitance are crucial things in a good detector. Point contact germanium diodes having a very small area (a point of contact) have low capacitance and the germanium semiconductor-metal junction of the contact has a low turn on voltage. EPAD Mosfets also have low capacitance, high input resistance (low loading of the signal) and low turn on voltage.

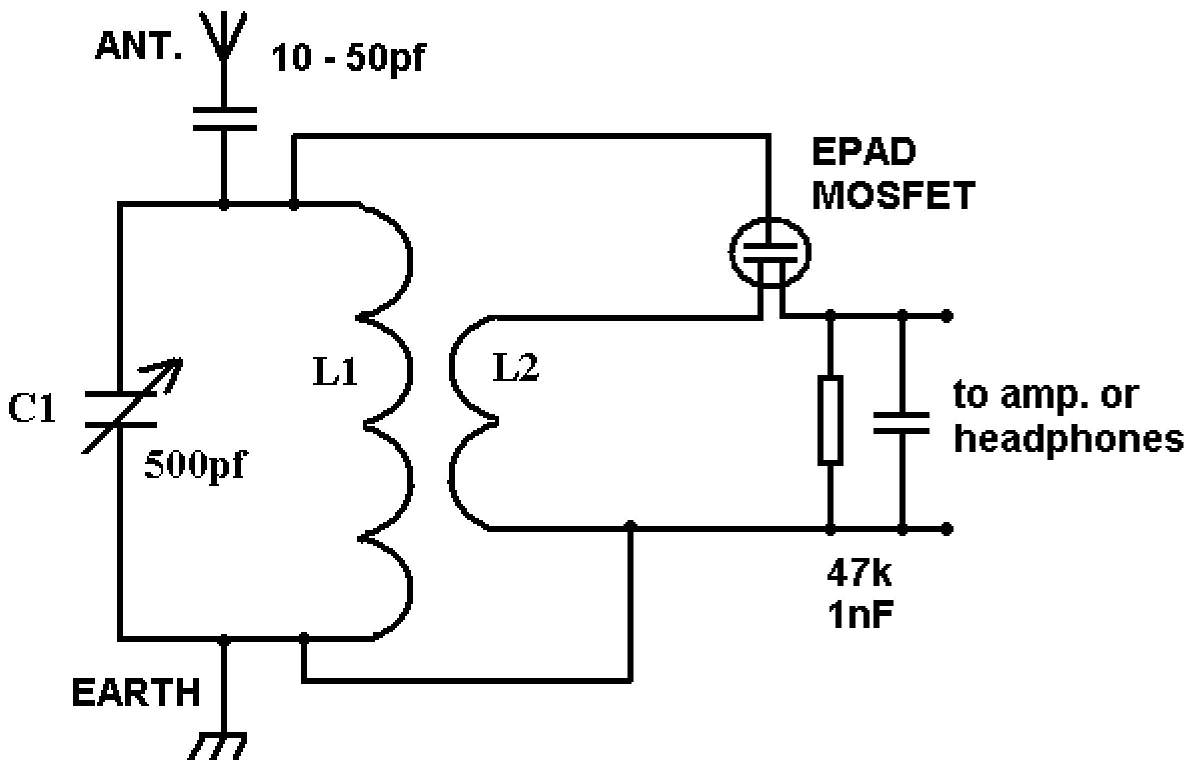

MEDIUM WAVE TEST CIRCUIT (top in photo)
As a simple test circuit to compare detectors I made up a simple 'crystal set' radio from a ferrite rod coil from an old radio, tuning capacitor an array of diodes (crystals) and a simple RF filter composed of a 47k resistor and 1nF capacitor. The coil and capacitor formed the resonant circuit which was fed via a 10 - 50pf capacitor by the antenna (long wire). This capacitor helps to reduce the effect of the antennas own capacitance and inductance from modifying the resonant frequency of the tuned circuit. Ideally this should be as small a capacitance as you can get away with but too small a value will reduce the radios sensitivity ....

An earth was connected to the ground connection of the circuit. Instead of taking the antenna end of the resonant circuit to a diode detector (as many simple crystal sets do) I used a ca. 10 turn coupling coil around the coil. This was done to limit the loading on the resonant circuit by the detector. It should help keep the tuning sharp and also help to keep the overall (band) spread of tuning as large as possible.

Because of the reduction in turns (ca. 100 turns : 10 turns, i.e. 10:1) the coupling coil reduces the signal that is available to drive the detector. For example if I use a standard silicon diode (e.g. a 1N4148) which requires about 0.6V to conduct then we might need ca. 10 x 0.6 = 6V of RF to be developed in the resonant circuit! A high Q resonant circuit might do this with a long antenna coupled to it but without such a generious antenna such a set-up wont be very sensitive.

RESULTS
I tried an array of 'crystal set' type diodes to campare them. Typical rough results are shown in the table below. This was with an Earth and about 3-4m of antenna wire randomly strung near to ground level (so its a pretty bad set up really - a good test).

The EPAD MOSFET data sheets described how the gate and drain of one of the MOSFETS can be joined together to form the anode of a diode the source then forms the cathode. I tried this arangement with the ALD110900 in order to make up a 'crystal set' diode from this MOSFET but it didnt perform well.

Then I tried the alternative arrangement as described in the references above. In these articles they dont use the MOSFETS as diodes but connect the gate directly to the resonant circuit. As the input resistance is extremely high (c.a. 1E12 ohms) and the input capacitance is very low (c.a 3pf) it does not load the tuned circuit by any appreciable amount. The source and drain are then wired between the coupling coil and filter just as the usual diode detector is in a crystal set radio. In this configuration the MOSFET is working more as a gate voltage controlled resistor rather than a diode i.e 'off' for half an RF cycle and 'on' for the rest - this lets the envelope through and you hear the music or sound. One article describes the arrangement as a synronious detector. As there are two MOSFETS in one package the two are wired in parallel i.e. gate to gate, drain to drain (there is a common source) etc.

DETECTOR TYPE	AF voltage produced after filtering
1N4148 silicon	no signal
OA91 germanium	1mV
1N43A germanium	1mV
1N60 germanium	1mV
AAZ17 germanium	1.5mV
ALD110900 EPAD MOSFET wired as diode	<1mV
ALD110900 EPAD MOSFET wired as sync. detc.	10mV

Typical results of the AF voltages produced by the detector (for use by headphones or amplifier) for an Earth connection, small (ca. 3-4m antenna wire near ground level) and the prototype 'crystal set' radio.

For the simple set-up described above there was not enough signal to get the silicon diode to work at all (although a much longer wire did provide a very small signal). A simple listening test and measurement of the AF prodiced by each diode showed that their was very little difference between the various germanium diodes. The MOSFET simply wired as a diode (gate wired directly the drain) was a poor detector - better than a silicon but not nearly so good as any of the germanium diodes. Finally the EPAD MOSFET wired as a syncronious detector worked really very well apparently producing ca. 10 times the signal (in other words it has much less loss than a germanium diode) for this particular set up and station than the germanium diodes.

As the syncronious arrangement was so succesful it got me thinking about this circuit. As the gate goes straight in on the main resonant circuit where the voltages, in a good Q circuit, might well be relatively high I thought I would try a standard FET (2N3819) and MOSFET (VN10KM) instead - and they worked! (they are a lot cheaper than an EPAD MOSFET chip and easier to get). Some FETS have a larger input capacitance so it helped to put a 10pf capacitor in series to the gate (a 10M ohm from gate to earth might reduce 50Hz pick up).

They were not as good as the EPAD MOSFET (although I only tried a single device) but the arrangment was still better than a simple 'crystal set' diode. For weak signals the EPAD MOSFET should perform better as it is able to keep going while the FET and the standard MOSFET will start to trail off as the resonant circuit voltage drops below the relatively higher gate voltage required for these devices. However it was interesting to see that it seems to be possible to get a more efficent set-up for a 'crystal' radio using a standard FET or MOSFET than with the standard germanium diode detector.

By the way I recently re-tried the 1N4148 diode but wired a 1.5V AA battery with a 100k resistor across it to forward bias it - and it worked ! It seemed to work better than a OA91!

SHORT WAVE 'CRYSTAL SET RADIO (bottom in photo)
The bottom circuit shown in the photo above is my own short wave version of the 'crystal set' radio but based on the references above. It's the same circuit as the MW radio but has a reduction drive tuning capacitor and different coil. I used about 7 turns (ca. 4cm diameter) for the resonant circuit and a couple of turns of insulated wire (white) for the coupling coil. I guess the radio tunes from about 3-8 MHz - I havent tried a sig gen on it yet.

I made this in the summer months (not the best time for listening on this part of the spectrum). Using an Earth and few meters of wire for antenna I heard 2 or 3 stations from around the world during the day while at night there were at least 7 including the voice of Russia world service, Radio Thailand as well as German and French speaking stations.

BACK TO G1EXG RADIO PAGE

THE CREATIVE SCIENCE CENTRE

Dr Jonathan Hare, The University of Sussex
Brighton, East Sussex. BN1 9QJ

home | diary | whats on | CSC summary | latest news

Design Issues in Radio Frequency Energy Harvesting System

Chomora Mikeka and Hiroyuki Arai
Yokohama National University
Japan

1. Introduction

Emerging self powered systems challenge and dictate the direction of research in energy harvesting (EH). State of the art in energy harvesting is being applied in various fields using different single energy sources or a combination of two or more sources. In certain applications like smart packaging, radio frequency (RF) is the preferred method to power the electronics while for smart building applications, the main type of energy source used is solar, with vibration & thermal being used increasingly. The main differences in these power sources is the power density; for example RF (0.01 ~ 0.1 $\mu W/cm^2$), Vibration (4 ~ 100 $\mu W/cm^2$), Photovoltaic (10 $\mu W/cm^2$ ~ 10mW/cm^2) and Thermal (20 $\mu W/cm^2$ ~ 10mW/cm^2). Obviously RF energy though principally abundant, is the most limited source on account of the incident power density metric, except when near the base stations. Therefore, in general, RF harvesting circuits must be designed to operate at the most optimal efficiencies.

This Chapter focuses on RF energy harvesting (EH) and discusses the techniques to optimize the conversion efficiency of the RF energy harvesting circuit under stringent conditions like arbitrary polarization, ultra low power (micro or nanopower) incidences and varying incident power densities. Harvested power management and application scenarios are also presented in this Chapter. Most of the design examples described are taken from the authors' recent publications.

The Chapter is organised as follows. Section 2.1 is the introduction on RF energy sources. Section 2.2 presents the antenna design for RF EH in the cellular band as well as DTV band. The key issue in RF energy harvesting is the RF-to-DC conversion efficiency and is discussed in Section 2.3, whereas Section 2.4 and 2.5 present the design of DTV and cellular energy harvesting rectifiers, respectively. The management of micropower levels of harvested energy is explained in Section 2.6. Performance analysis of the complete RF EH system is presented in Section 3.0. Finally, conclusions are drawn in Section 4.0.

1.1 RF energy sources

These include FM radio, Analogue TV (ATV), Digital TV (DTV), Cellular and Wi-Fi. We will present a survey of the measured E-field intensity (V/m) for some of these RF sources as shown in Table 1, [1]-[2]. Additionally, measured RF spectrums for DTV and Cellular signals are presented as shown in Fig. 1 to show on the potential for energy-harvesting in

these frequency bands. In general, many published papers on RF-to-DC conversion, have presented circuits capable of converting input or incident power as low as -20dBm. This means that, if an RF survey or scan finds signals in space, with power spectrum levels around -20dBm, then, it is potentially viable to harvest such signal power. In Fig. 1 (left side), the spectrum level is well above -20dBm and hence, a higher potential for energy harvesting. In Fig. 1 (right side), while the spectrum level is below -20dBm, what we observe is that the level increases with decrease in the distance toward the base station (BTS). Using free space propagation equation with this data, it was calculated that at a distance 1.4 m from the BTS, the spectrum level could measure 0dBm. An example calculation and plot for the estimated received power level, assuming 0dBi transmitter (BTS) and receiver antenna gains and free space propagation loss (FSPL) for FM and DTV is presented in Section 2.1.1. For the example estimation in Section 2.1.1, we select FM and DTV because they measured with a higher level than cellular and Wi-Fi for example.

Source	V/m	dBm	Reference	
FM radio	0.15~3		Asami et al.	
Analogue TV	0.3~2			
Digital TV	0.2~2.4	-40~0.0	Asami et al.	Arai et al.
Cellular		-65~0.0	Mikeka and Arai	
Wi-Fi		≅ -30		

Table 1. RF energy sources, measured data.

In Table 1, FM radio has the highest E-field intensity implying the highest potential for energy harvesting. However, due to the requirements for a large antenna size and the challenges for simulations and measurements at the FM frequency i.e. 100 MHz or less (See Section 2.2.3, example FM antenna at 80 MHz), this Chapter will focus on DTV (470~770 MHz band) and Cellular (2100 MHz band) energy harvesting.

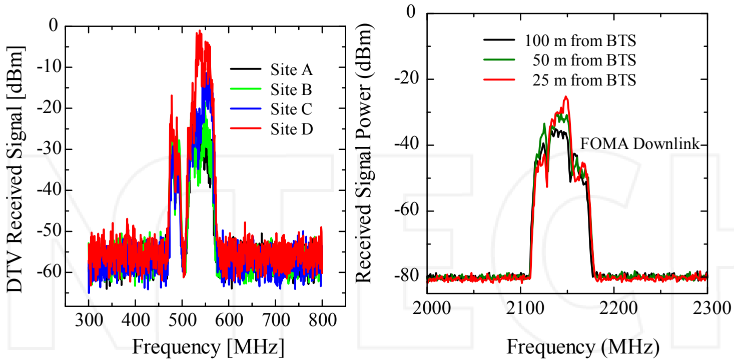

Fig. 1. DTV signal spectrum measured in Tokyo City (left side graph) and Cellular signal spectrum measured in Yokohama City (right side graph).

The received DTV signal power is high and also wide band, presenting high potential for increased energy harvesting unlike in cellular signals. We demonstrated in [2] that the total RF-to-DC converted power is roughly the integral over the DTV band (1), and is significantly larger than in the case of narrow band cellular energy harvesting.

$$P_{DC(DTV)} = \alpha \int_{470}^{770} \delta P_{DC}(f)\, df \,, \tag{1}$$

where α is the attenuation factor on the rectifying antenna's RF-to-DC conversion efficiency due to multiple incident signal excitation. δP_{DC} is the small converted DC power from each of the single DTV signals in the 470 MHz to 770 MHz band.

In detail, we derive (1) from fundamentals as follows.

The incident power density on the rectifying antenna (rectenna), $S(\theta,\phi,f,t)$, is a function of incident angles, and can vary over the DTV spectrum and in time. The effective area of the antenna, $A_{eff}(\theta,\phi,f)$, will be different at different frequencies, for different incident polarizations and incidence angles. The average RF power over a range of frequencies at any instant in time is given by:

$$P_{RF}(t) = \frac{1}{f_{high} - f_{low}} \int_{f_{low}}^{f_{high}} \int_{0}^{4\pi} S(\theta,\phi,f,t) A_{eff(\theta,\phi,f)} d\Omega df \tag{2}$$

The DC power for a single frequency (f_i) input RF power, is given by

$$P_{DC}(f_i) = P_{RF}(f_i,t) . \eta\left(P_{RF}(f_i,t), \rho, Z_{DC}\right), \tag{3}$$

where η is the conversion efficiency, and depends on the impedance match $\rho(P_{RF}, f)$ between the antenna and the rectifier circuit, as well as the DC load impedance. The reflection coefficient in turn is a nonlinear function of power and frequency.

The estimated conversion efficiency is calculated by P_{RF}/P_{DC}. This process should be done at each frequency in the range of interest. However, DC powers obtained in that way cannot be simply added in order to find multi-frequency efficiency, since the process is nonlinear. Thus, if simultaneous multi-frequency or broadband operation like in DTV band is required, the above characterization needs to be performed with the actual incident power levels and spectral power density. In this Chapter, we shall demonstrate DTV spectrum power harvest, given a rectenna than has been characterised in house at each single frequency in the DTV band.

1.1.1 An example calculation and plot for the estimated received power level

In this example we consider Tokyo's DTV and FM base stations (BS) as the RF sources. Both DTV and FM BS transmitter power (P_t) equals 10 kW (70dBm). The antenna gains are assumed 0dBi in both cases but also at the points of reception for easiness of calculation but with implications as follows. Assuming 0dBi antenna at each reception point, demands that we specify the frequency of the transmitted signal. For this reason we specify DTV signal frequency to be equal to 550 MHz while the FM signal frequency equals 80 MHz (Tokyo FM).

The received power, P_r is calculated using the simplest form of Friis transmission equation given by

$$P_r = P_t + G_t + G_r + FSPL\,, \tag{4}$$

where P_t = 70dBm, $G_t = G_r$ = 0dBi. G_r is the receiving antenna gain while FSPL is the free-space path loss given by

$$FSPL(dB) = 20\log(d) + 20\log(f) + 32.45\,, \tag{5}$$

where ***d*** is in (km) and ***f*** is in (MHz). The plot for the received power as a function of distance from the DTV and FM base stations is shown in Fig. 2.

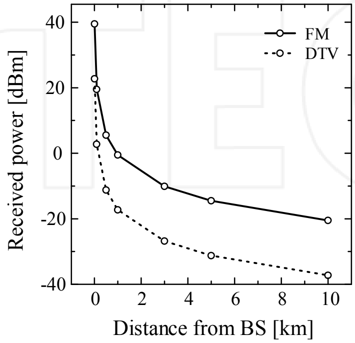

Fig. 2. DTV and FM received signal power level against distance.

With respect to Fig. 2, FM registers higher received power level than DTV at every reception point due to its lower transmit frequency and hence lower free-space path loss. For example at 1 km distance, FM received power level is -0.51dBm while for DTV, the received power is -17.26dBm. The important thing however, is that the received power level is frequency independent. It means that P_t is the transmitter power and the received power level at the position of distance ***d*** is $\frac{P_t}{4\pi d^2}$. However, if we assume 0dBi antenna at each reception point as in the above example, the power level is different because the antenna size of 0dBi is frequency dependent. As a result, high transmit power level is favorable for RF energy harvesting. Also near the base station is favorable.

1.2 Antenna design for the proposed RF energy harvesting (EH) system

It is well known that RF EH system requires the use of antenna as an efficient RF signal power receiving circuit, connected to an efficient rectifier for RF-to-DC power conversion. Depending on whether we want to harvest from cellular or DTV signals, the antenna design requirements are different. We will discuss the specific designs in the following sub sections.

1.2.1 Cellular energy harvesting antenna design

We propose a circular microstrip patch antenna (CMPA) for easy integration with the proposed rectifier (Section 2.5.1). However, the use of circular microstrip patch antennas (CMPA) is often challenged by the need for impedance matching, circular polarization (CP) and higher order harmonic suppression.

To address the above concerns, we create notches on the circular microstrip patch antenna. In our approach, we use only two, thin, fully parameterized triangular notches to achieve higher order harmonic suppression, impedance matching and circular polarization, all at once. This is the novelty in our proposed antenna. Our proposed CMPA is shown in Fig. 3. We study the behaviour of CMPA surface current vectors when notches (triangles ABC) are created on the structure at $\alpha = 45^0$ and $\alpha = 225^0$.

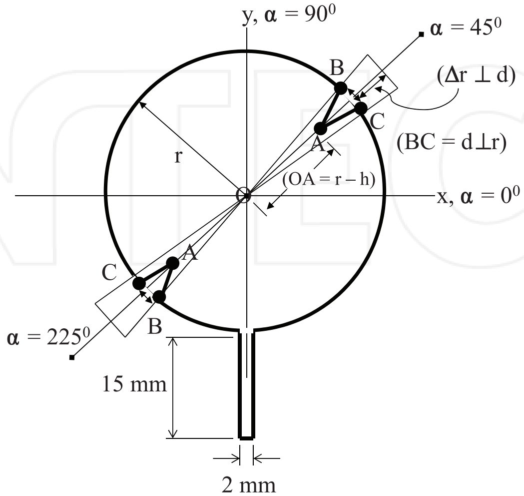

Fig. 3. Cellular energy harvesting antenna structure.

Notch parameters ***d*** and ***h*** in Fig. 3 were investigated by calculation using CST microwave Studio.

Without notches, the CMPA's input is not matched at f_c= 2.15 GHz as shown in Fig. 4 (left side). However, with notches, matching is achieved. The parameter combination ***d*** = 7 and ***h*** = 6 offers a matched and widest band input response and hence we adopt it for cellular energy harvesting applications.

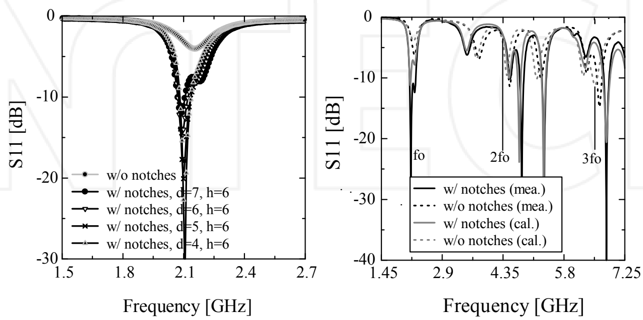

Fig. 4. *Left side:* ***d*** and ***h*** parameter investigation. *Right side:* Comparison between (cal.) and (mea.) S_{11} at f_0 = 2.175 GHz, $2f_0$ = 4.35 GHz and $3f_0$ = 6.53 GHz. The adopted notch parameters are ***d***=7 mm while ***h***= 6 mm.

The comparison between calculated and measured S_{11} is shown in Fig. 4 (right side). The 2nd and 3rd harmonics are suppressed as required by design. The comparison between calculated and measured radiation patterns is shown in Fig. 5, where $E_{\vartheta} \cong E_{\varphi}$ due to the 45^0 tilted surface current vector. Ordinarily, without notches, the surface current vector is parallel to the microstrip feeder axis. In conclusion, our proposed CMPA is sufficiently able to suppress higher order harmonics while simultaneously radiating a circularly polarized (CP) wave. The CP is required to efficiently receive the arbitrary polarization of the incident cellular signals at the rectenna.

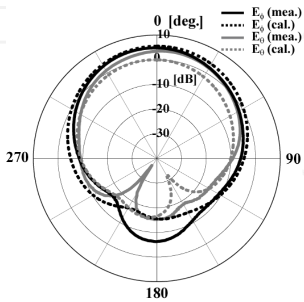

Fig. 5. Cellular energy harvesting antenna pattern at f_c= 2.15 GHz.

1.2.2 DTV energy harvesting antenna design

Unlike in the cellular energy harvesting antenna, the DTV energy harvesting antenna must be wideband (covering 470 MHz to 770 MHz), horizontally polarized and omni-directional.

The proposed antenna is typically a square patch (57 mm x 76 mm) with a partial ground plane (9 mm x 100 mm). The patch is indirectly fed by a strip line (9 mm x 3 mm). The proposed antenna geometry is shown in Fig. 6. The partial ground plane is used to achieve omni-directivity and a certain level of wide bandwidth. To tune the impedance of this antenna as well as to adjust the bandwidth within the target band, a "throttle" with stepped or graded structures is used between the microstrip feed line and the square patch, as shown in Fig. 6 (left side).

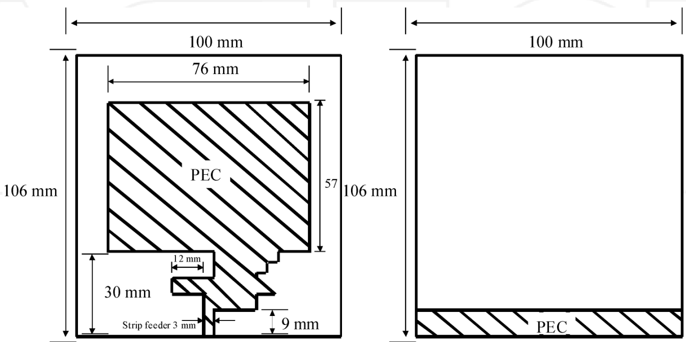

Fig. 6. Proposed DTV antenna geometry. *Left side:* Front view. *Right side:* Back view. The antenna is printed on FR4 substrate; t = 1.6 mm, ε_r = 4.4.

The input response for the proposed antenna is shown in Fig. 7 (left side). The omni directivity is confirmed by measurement at 500 MHz, 503 MHz, and 570 MHz as shown in Fig. 7 (right side). The radiation patterns shown in Fig. 7 are for the xz plane, which happens to be the vertical polarization for the antenna. DTV signals are horizontally polarized and therefore, when using this antenna, the orientation must be in such a way as to efficiently receive the DTV signal. Simply a 90 degree rotation of the antenna along the z axis achieves this requirement.

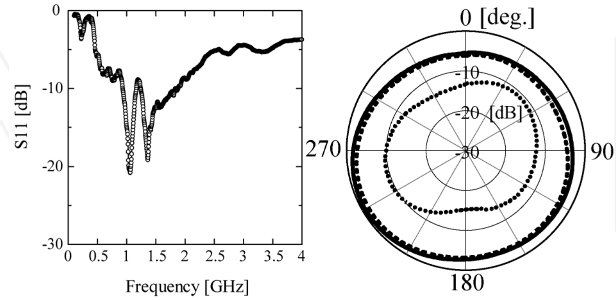

Fig. 7. Proposed DTV antenna performance. *Left side:* The antenna's measured input performance. *Right side:* The omni directivity in the vertical plane is confirmed at 500 MHz, 503 MHz, and 570 MHz. The outermost, black solid and dotted line patterns represent 503 MHz and 500 MHz directivity, respectively. The innermost dotted line pattern is the directivity at 570 MHz.

1.2.3 Example design for an 80 MHz FM half-wave dipole antenna

A half-wave dipole is the simplest practical antenna designed for picking up electromagnetic radiation signals, see Fig. 8 (courtesy of Highfields Amateur Radio Club). Calculating the optimal antenna length to pick up a certain frequency signal is fairly straightforward because antenna physics demand that the total length of wire used in the antenna be equal to one wavelength of the type of electromagnetic radiation it will be picking up. This means that the total length of the antenna should be equal to half the desired wavelength. By converting the 80 MHz frequency into a wavelength, you can thus obtain your antenna length as 1.875m by using the magic equation, $\lambda = \frac{c}{f}$. However, the actual length is typically about 95% of a half wavelength in free space, hence a half-wave dipole for this frequency should be 1.788m long, which would make each leg of the dipole 0.894m in length.

1.3 RF-to-DC conversion efficiency improvement techniques

A Schottky diode circuit connected to an antenna is used for RF-to-DC power conversion. To convert more of the antenna surface incident RF power to DC power, high RF-to-DC conversion efficiency is required of the rectifying circuit. Many authors have shown that the efficiency depends on several factors like Schottky diode type, harmonics suppression capability, load resistance selection, and the capability to handle arbitrary polarized incident waves. What is missing in most of these published works is the efficiency optimization for

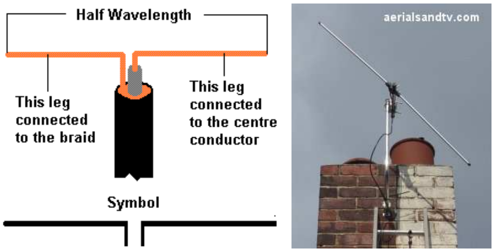

Fig. 8. Half-wave dipole. *Left side:* Antenna structure. *Right side:* Typical deployment.

ultra low power incident waves and the explanation of the physical phenomena behind most of the recommended efficiency optimization approaches.

This Chapter will show for example that a Schottky diode that delivers the highest efficiency at 0dBm incidence may not necessarily deliver the highest efficiency at lower power incidence e.g. –20dBm. We will therefore classify which diodes perform better at given power incidences; of course, this will also be compared to the diode manufacturers' application notes. Simulations in Agilent's ADS using SPICE and equivalent circuit models will compare the performance of few selected Schottky diodes namely; HSMS-2820, HSMS-2850, HSMS-2860, HSC-276A, and SMS7630. Moreover, the effect of the Schottky diode's junction capacitance (C_j) and junction bias resistance (R_j) on the conversion efficiency will be shown from which, special techniques for Schottky diode harmonic suppression and rectifying circuit loading for maximum efficiency point tracking will be presented.

1.3.1 The schottky diode

The classical *pn* junction diode commonly used at low frequencies has a relatively large junction capacitance that makes it unsuitable for high frequency application [3]. The Schottky barrier diode, however, relies on a semiconductor-metal junction that results in a much lower junction capacitance. This makes Schottky diodes suitable for higher frequency conversion applications like rectification (RF-to-DC conversion) [3]. We will demonstrate the effects of junction capacitance and resistance in the following sub section.

1.3.2 The effect of Schottky diode's C_j and R_j on the conversion efficiency

We have studied Schottky diode's C_j and R_j and published our results in [4]. In this work, we designed a rectifying antenna tuned for use at 2 GHz. The circuit proposed in [4] is a voltage doubler by configuration, but we replaced the amplitude detection diode (series diode) with its equivalent circuit adapted from [5]. The results of this investigation show that variation of C_j shifts the tuned frequency position and also introduces a mismatch in the resonant frequency, see Fig. 9 (left side graph). Therefore for this circuit at 2 GHz, we recommend using a Schottky diode having C_j = 0.2pF. In general, a smaller value of C_j is desirable at higher frequencies. Similarly, for R_j investigation, a smaller value is desirable for better matching at 2 GHz for example. If the R_j is increased towards 10kΩ, there is a mismatch in the resonant frequency but no shift in the frequency, see Fig. 9 (right side graph). Another approach to the study of Schottky diodes for higher frequency and efficiency rectenna design is presented in [6].

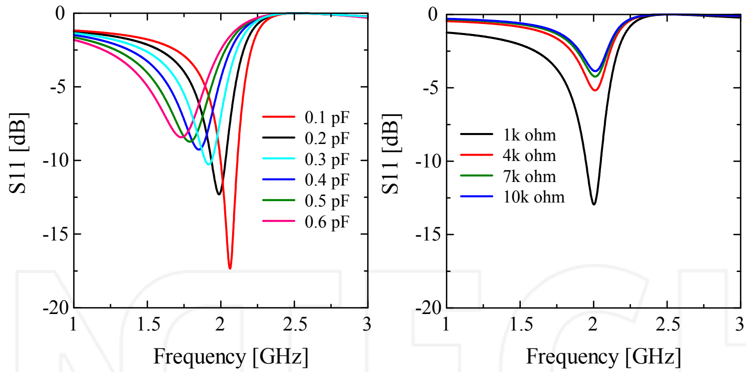

Fig. 9. Schottky diode's C_j effect (Left) and R_j effect (Right) on 2 GHz rectenna's input response.

1.4 Rectifying circuit for DTV energy harvesting

In the design of a DTV energy harvesting circuit, several basic design considerations must be paid attention to. First is the antenna; it must be wideband (covering 470 MHz to 770 MHz), horizontally polarized and omni-directional. Secondly is the rectifier; it must also be wideband, and optimized for RF-to-DC conversion for incident signal power at least -40dBm. Until recently, very few authors have published on DTV energy harvesting circuit. For the few publications, the antenna could not meet all those three requirements and a discussion on the performance of the harvesting circuit for ultra low power incidences has been neglected. In this Chapter we will present such a rectenna with conversion efficiencies above 0.4% at -40dBm, above 18.2% at -20dBm and over 50% at -5dBm signal power incidence. We will closely compare simulated and measured performance of the rectenna and discuss any observed disparities.

Agilent's ADS will be used to simulate the nonlinear behaviour of the rectifying circuit based on harmonic balance tuning methods. To simulate the multiple incident waves, a multi-tone excitation in the DTV band will be invoked. The wideband input characteristic will be achieved by the input matching inductors and capacitors.

The generic version of our proposed DTV energy harvesting circuit is shown below in Fig. 10. The implementation, however, is in two phases or scenarios as follows. First, we investigate the class called "ultra low power" DTV band rectenna. Secondly, we introduce the "medium power" DTV band rectenna.

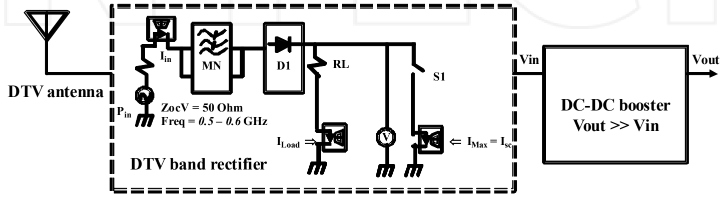

Fig. 10. Generic version of our proposed DTV energy harvesting circuit.

1.4.1 Ultra low power DTV rectenna

We define an ultra low power rectenna as one impinged by RF power incidence in the range between – 40dBm and -15dBm. Below in Fig. 11 is the circuit we designed; optimized for -20dBm input. The matching network is complex so as to achieve a wide band input characteristic. The fabricated circuit was well matched for the frequency range between 470 MHz and 600 MHz. More details about the circuit design can be found in [7].

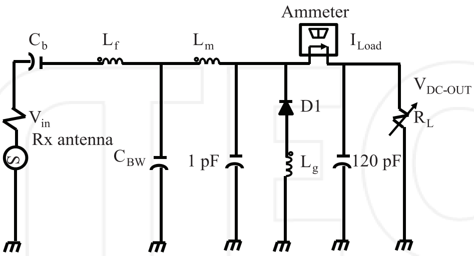

Fig. 11. Ultra low power DTV band rectenna circuit. SMS7630 Schottky diode by SKYWORKS offered the best performance.

The RF-to-DC conversion efficiency for this circuit is shown in Fig. 12 where at input power equal to -40dBm, efficiency is at least 0.4% and rectified voltage equals 1mV; at -20dBm, we have at least 18.2% by measurement and a rectified voltage of 61.7mV. The level of rectified voltage is too low and disqualifies this circuit for purposes of charging capacitors or batteries to accumulate such micropower over time. Instead, boosting the low voltage to usable levels is the option available and we shall discuss this at a later stage, (in Section 2.6).

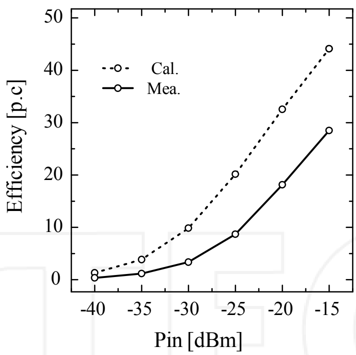

Fig. 12. Ultra low power DTV band rectenna efficiency.

1.4.2 Medium power DTV rectenna

We define a medium power rectenna as one impinged by RF power incidence in the range between – 5dBm and 0dBm. Below in Fig. 13 is the circuit we designed, optimized for -5dBm input. The matching network is simpler than as shown in section 2.4.1 since we require a narrow band around 550 MHz, with received peak power spectrum levels at least -5dBm. The circuit in Fig. 13 is a modification of Greinacher's doubler rectifier. In the circuit, C_b equals 1 pF and is used to block DC current against flowing towards the source. The shunt

capacitance, C_{BW} equals 3300 pF and is used to set the input bandwidth. The grounding inductance, L_g equals 56nH (optimal) and is used to improve the RF-to-DC conversion efficiency by cancelling the Schottky diodes (D_b and D_D) capacitive influence; thereby minimizing the harmonic levels (harmonic suppression). We used HSMS2850 diodes in these circuits for their better performance at this level of incident power.

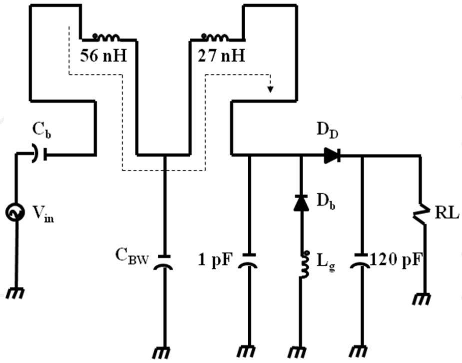

Fig. 13. Medium power DTV rectenna circuit. HSMS 2850 or 2820 from Hewlett-Packard offered the best performance.

The RF-to-DC conversion efficiency for this circuit is shown in Fig. 14 where at input power equal to -5dBm, we achieve at least 50% conversion efficiency by measurement, equivalent to 1.2 V DC rectified at 8.2kΩ optimal load. If we change the load to 47kΩ, over 2 V DC is rectified. This rectenna circuit is ideal for powering small sensors that run on 1.5 V or 2.2 V and draw around 6μA nominal current. If we need to power sensors demanding more power, say at least 2.2 V and 0.3mA to 1.47mA current consumption, we have to accumulate the power in a capacitor over time.

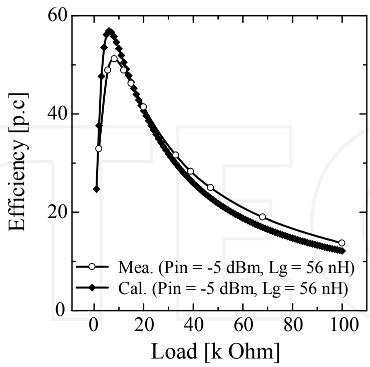

Fig. 14. Medium power DTV band rectenna efficiency.

1.4.3 DTV energy harvesting scenario and application demo

Using the medium power DTV band rectenna, connected to a gold capacitor as an accumulator, energy harvesting was initiated as shown in Fig. 15. Details about the gold

capacitor, which include its charge function, backup time and leakage losses are presented in [8]. For the scenario shown in Fig. 15, the accumulated voltage by measurement i.e. capacitor charge function follows the path;

$$V_{acc} = 0.5388\ln(t) + 1.4681 \tag{6}$$

where V_{acc} is the accumulated voltage in volts and t the time in hours. It takes 4.5 hours to accumulate 2.25 V, given a rectified charging voltage and current of 2.4 V and 51μA, respectively, supplied by the DTV band rectenna instantaneously.

With this rectenna, it was possible to power up many different kinds of sensors. Sensors with ultra low power consumption were powered directly, without need to accumulate the power in a capacitor, as shown in Fig. 16.

Fig. 15. DTV energy harvesting in a park at some line of sight from the base station.

Fig. 16. Directly powering a thermometer mounted on a car park wall (right picture). The maximum instant voltage rectification on record equals 3.7 V (left picture).

1.5 Rectifying circuit for cellular energy harvesting

Unlike in the DTV energy harvesting circuit, for cellular energy harvesting, the antenna must be narrowband (50 MHz bandwidth is acceptable), and circularly polarized even

though cellular signals are vertically polarized. The circular polarization is desired to maximize the RF-to-DC conversion efficiency of the arbitrary polarization incident signals in the multipath environment. Similarly, the rectifier must be narrowband, and optimized for RF-to-DC conversion over a wide range of incident signal power.

Thinking about the potential applications for cellular energy harvesting is useful. Other authors have reported on powering a scientific calculator or a temperature sensor from GSM energy harvesting. In this Chapter we will present a special application for energy harvesting in the vicinity of the W-CDMA cellular base station and analyze the system performance by calculation from experimental data. A cellular energy harvesting circuit optimized for over 50% RF-to-DC conversion efficiency given approximately 0dBm incidence will be presented.

1.5.1 Cellular band rectenna

Below in Fig. 17 is the circuit we designed, optimized for 0dBm input. Simple input matching network is ideal since we require a narrow band response around 2.1 GHz. The optimum value for L_g equals 5.6nH, where L_g is used to improve the RF-to-DC conversion efficiency as earlier discussed. HSMS2850 diode was used.

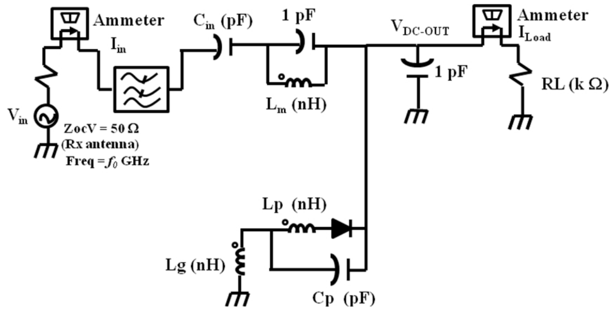

Fig. 17. Shunt rectifier configuration for the cellular band. The matching elements L_m = 3.2nH, while C_{in} =2.5pF. The load resistance is fixed at R_L = 2.1kΩ.

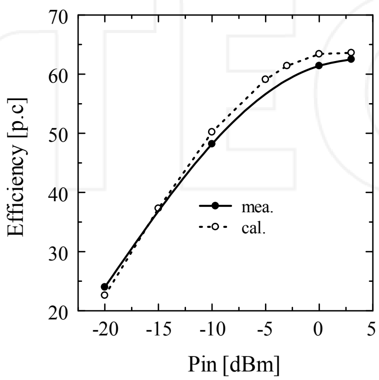

Fig. 18. Conversion efficiency as a function of input power (P_{in}) in the cellular band.

The RF-to-DC conversion efficiency for this circuit is shown in Fig. 18 where at input power equal to 0dBm, we achieve at least 60% conversion efficiency by measurement, given a 2.1kΩ optimal load. This rectenna circuit is ideal for powering small sensors that run on 1.5 V or 2.2 V and 6μA nominal current consumption. If we need to power sensors demanding more power, say at least 2.2 V and 0.3mA to 1.47mA, we have to accumulate the power in a capacitor over time as discussed in section 2.4.3 above.

1.5.2 Cellular energy harvesting application example

Environmental power generation in the neighbourhood of a cellular base station to power a temperature sensor is proposed as shown in Fig. 19 below. Electric field strength measurements in the base station neighbourhood have demonstrated the potential for environmental power generation, and the proposed temperature sensor system is designed based on these values. The rectenna described in Section 2.5.1 is used as the RF-to-DC rectifying circuit with the notched circular microstrip patch antenna (CMPA) proposed in Section 2.2.1. RF-to-DC conversion efficiency equal to 53.8% is obtained by measurement. The temperature sensor made for trial purposes clarifies the capability for temperature data wireless transmission for 20 seconds per every four hours in the base station neighbourhood.

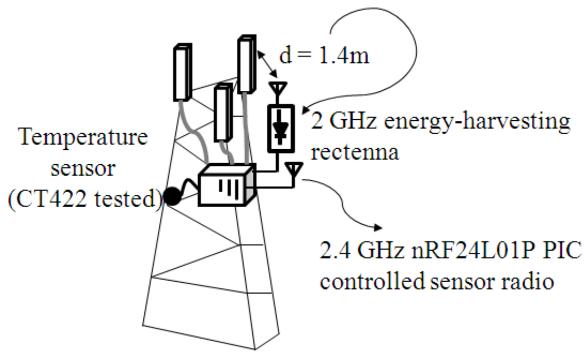

Fig. 19. Application example in the vicinity of the cellular base station.

1.6 Micropower energy harvesting management

A rectifying antenna circuit for -40dBm incident power harvesting generates 1mV at 2kΩ load, given 0.4% efficiency as presented in Section 2.4.1. At -20dBm incidence and at least 18.2% efficiency, 61.7mV is generated given a 2kΩ load [7]. The generated DC power in both of these two cases is in the μW range, hence the micropower definition. To manage such micropower, power accumulation or energy storage is required. Storage devices may either be a gold capacitor, super capacitor, thin film battery or the next generation flexible paper batteries. These storage devices have specific or standard maximum voltage and trickle charging current minimum requirements. Typically, gold capacitors have voltage ratings like 2.7 V, 5.5 V for 100 μA, 10mA or 100mA maximum discharge current. On the other hand, standard ratings for batteries are 1.8 V, 2 V, 3.3 V and 4.1 V. Therefore, to directly charge any of these storage devices from 1mV, or 61.7mV DC is impractical.

Published works have demonstrated the need for a DC-to-DC boost converter placed between the rectifying antenna circuit (rectenna) and the storage device. Recent efforts have demonstrated that a 40mV rectenna output DC voltage could be boosted to 4.1 V to trickle charge some battery. A Coilcraft transformer with turns ratio ($N_s : N_p$) equal to 100 was used in the boost converter circuit. An IC chip leading manufacturer (Linear Technology Corp., LT Journal, 2010) has released a linear DC-to-DC boost regulator IC chip capable of boosting an input DC voltage as low as 20 mV and supplying a number of possible outputs, specifically suited for energy harvesting applications. While this IC is a great milestone, readers and researchers need to understand the techniques to achieve such ICs and also the limitations that apply. In the following sub section, we will describe the methods toward designing a DC-DC boost converter, suitable for micropower RF energy harvesting.

In the design, we will attempt to clarify the parameters that affect the DC-DC conversion efficiency. For this design, Envelope simulation in Agilents's ADS is used. This simulation technique is the most efficient for the integrated rectenna and DC-DC boost converter circuits.

1.6.1 DC-DC boost converter design theory and operation

The DC-DC boost converter design theory and actual implementation are presented in this section. The inequality $V_{in} \ll V_{out}$ defines the boost operation. In this Chapter, our boost converter concept is illustrated in Fig. 20. A small voltage, V_{in} is presented at the input of the boost converter inductive pump which as a result, generates some output voltage, V_{out}. The output voltage is feedback to provide power for the oscillator. The oscillator generates a square wave, F_{OSC} that is used for gate signalling at the N-MOSFET switch.

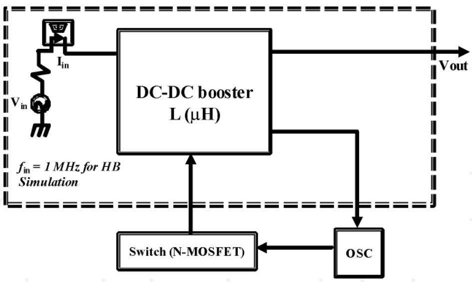

Fig. 20. Boost converter concept.

The drain signal of the N-MOSFET is used as the switch node voltage, V_{sn} at the anode of the diode inside the boost converter circuit block. From the concept presented in Fig. 20, the actual implemented circuit is shown in Fig. 21. The circuit was designed in Agilent's ADS and fabricated for investigation by measurement.

The circuit in Fig. 21 is proposed for investigation. Since a DC-DC boost converter is supposed to connect to the rectenna's output, it therefore, becomes the load to the rectenna circuit. This condition demands that the input impedance of the boost converter circuit emulates the known optimum load of the rectenna circuit. This has the benefit of ensuring

maximum power transfer and hence higher overall conversion efficiency from the rectenna input (RF power) to the boost converter output (DC power). In this investigation, as shown in [7], the optimum load for the rectenna is around 2kΩ. In general, emulation resistance R_{em} is given by

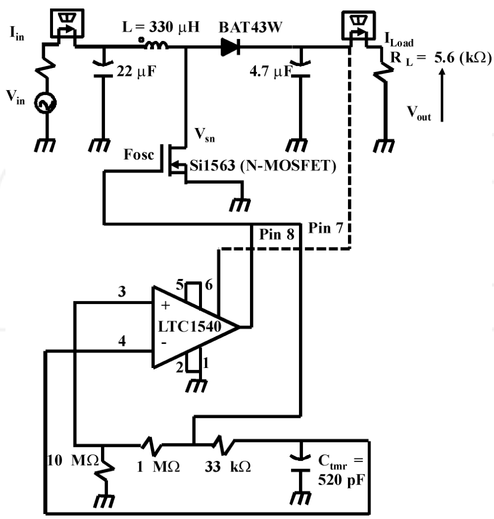

Fig. 21. The proposed boost converter circuit diagram. Designed in Agilent's ADS and fabricated for investigation by measurement.

$$R_{em} = \frac{2LT}{t_1^2 k}\left(\frac{M-1}{M}\right) \tag{7}$$

where ***L*** is the inductance equal to 330μH as shown in Fig. 20, $M = \frac{V_{out}}{V_{in}}$, ***T*** is the period of F_{OSC}, t_1 is the switch"ON" time for the N-MOSFET, and ***k*** is a constant that according to [3] is a low frequency pulse duty cycle if the boost converter is run in a pulsed mode and typically, ***k*** may assume values like 0.06 or 0.0483. With reference to (7), we select L as the key parameter for higher conversion efficiency while V_{in} = 0.4 V DC is selected as the lowest start up voltage to achieve oscillations and boost operation. Computing the DC-DC boost conversion efficiency against different values of L, we have results as shown in Fig. 22.

From the results above, L = 100μH is the optimum boost inductance that ensures at least 16.5% DC-DC conversion efficiency, given R_L = 5.6kΩ.

Now having selected the optimum boost inductance given some load resistance, the emulation resistance shown in Fig. 23 is evaluated from the ratio of voltage versus current at the boost converter circuit's input.

The results show a constant resistance value against varying inductance. In general, we can say that this boost converter circuit has a constant low input impedance around 82.5Ω. This impedance is too small to match with the optimum rectenna load at 2kΩ. This directly affects the overall RF-to-DC conversion efficiency.

The results show a constant resistance value against varying inductance. In general, we can say that this boost converter circuit has a constant low input impedance around 82.5Ω. This impedance is too small to match with the optimum rectenna load at 2kΩ. This directly affects the overall RF-to-DC conversion efficiency.

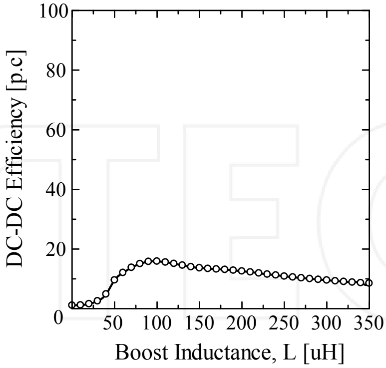

Fig. 22. Boost inductance variation with DC-DC conversion efficiency for a 5.6 kΩ load.

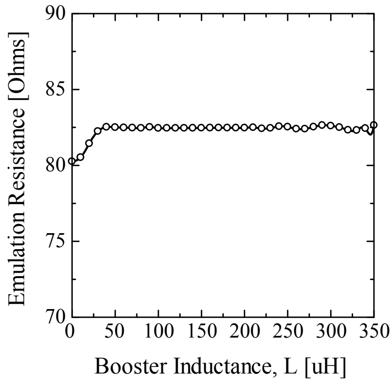

Fig. 23. Boost converter's input impedance: the emulation resistance.

Another factor, which affects the overall conversion efficiency is the power lost in the oscillator circuit. Unlike the circuit proposed in [9], which uses two oscillators; a low frequency (LF) and high frequency (HF) oscillator; in Fig. 21, we have attempted to use a single oscillator based on the LTC1540 comparator, externally biased as an astable multivibrator.

The power loss in this oscillator is the difference in the DC power measured at Pin 7 (supply) to the power measured at pin 8 (output). We term this loss, L_{osc}; converted to heat or sinks through the 10MΩ load. A comparison of the oscillator power loss to the power available at the boost converter output is shown in Fig. 24.

Looking at Fig. 24; we notice that the power loss depends on whether the oscillator output is high or low. The low loss corresponds to the quiescent period where the power lost is

almost negligible. However, during the active state, the lost power (power consumed by the oscillator) nearly approaches the DC power available at the boost converter output. This results in low operational efficiency.

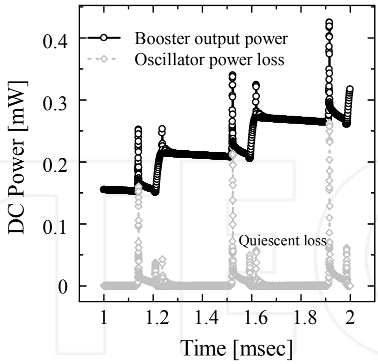

Fig. 24. The power loss in the oscillator.

To confirm whether or not the circuit of Fig. 21 works well, we did some measurements and compared them with the calculated results. Unlike in calculation (simulation), during measurement, L = 330μH was used due to availability. All the other component values remain the same both in calculation and measurement. In Fig. 25 (left side graph) and (right side graph), we see in general that the input voltage is boosted and also that the patterns of F_{osc} and V_{sn} are comparable both by simulation and measurement. To control the duty cycle of the oscillator output (F_{osc}), and the level of ripples in the boost converter output voltage (V_{out}), we change the value of the timing capacitance, C_{tmr} in the circuit of Fig. 21. Simulations in Fig. 25 (left side graph) show that C_{tmr} = 520pF realizes a better performance i.e. nearly constant V_{out} level (very low ripple).

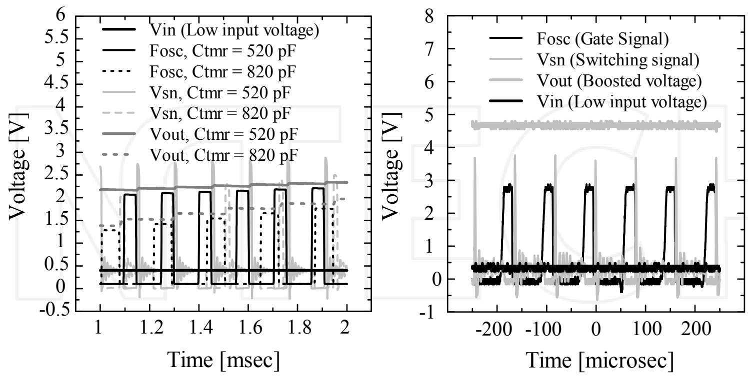

Fig. 25. Voltage characteristics of the developed boost converter circuit. The left side graph represents simulation while the right side graph is for measurements.

Generally, we observe that with this kind of boost converter circuit topology, it is difficult to start up for voltages as low as 61.7mV DC generated by the rectenna at -20dBm power

incidence and at least 18.2% rectenna RF-to-DC conversion efficiency. Self starting is the issue for this topology at very low voltages.

At least 11.3% DC-DC conversion efficiency was recorded by measurement and is comparable to the calculation in Fig. 22. During measurement it was clearly revealed that the boost converter efficiency does depend on the value of **L** and the duty cycle derived from $\mathbf{t_1}$. To efficiently simulate the complete circuit, from the RF input to the DC output, envelope transient simulation (ENV) in Agilent's ADS was used. The (ENV) tool is much more computationally efficient than transient simulation (Tran). This simulation is appropriate for the boost converter circuit's resistor emulation task. Moreover, the boost converter's DC-DC conversion efficiency, and the overall RF-to-DC conversion efficiency can be calculated at once with a single envelope transient simulation.

In summary, though not capable to operate for voltages as low as 61.7mV DC, the proposed boost converter has by simulation and measurement demonstrated the capability to boost voltages as low as 400mV DC, sufficient for battery or capacitor recharging, assuming that the battery or the capacitor has some initial charge or energy enough to provide start-up to the boost converter circuit.

The limitations of our proposed boost converter circuit include; low efficiency, lack of self starting at ultra low input voltages, and unregulated output. To address these limitations, circuit optimization is required. Moreover, alternative approaches which employ a flyback transformer to replace the boost converter inductance must be investigated. A regulator circuit with Low Drop Out (LDO) is necessary to fix the boost converter output voltage commensurate with standard values like 2.2 V DC for example. For further reading, see [7]

2. Performance analysis of the complete RF energy harvesting sensor system

To demonstrate how one may analyze the performance of an RF energy harvesting system including its application, we extend the discussion of Section 2.5.2 to this Section. We propose a transmitter assembled as in Fig. 26 for temperature sensor wireless data transmission.

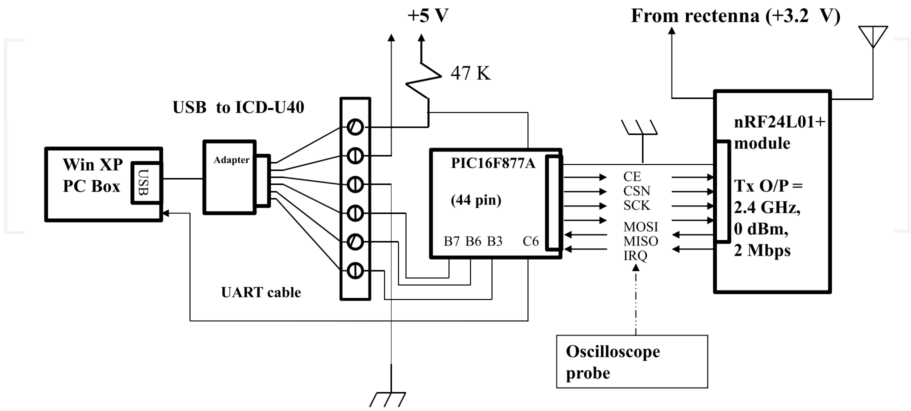

Fig. 26. The assembly and test platform for the proposed battery-free sensor transmitter.

The transmitter consists of one-chip microcomputer (MCU) PIC16F877A and wireless module nRF24L01P for the control, and MCU can be connected with an outside personal computer using ICD-U40 or RS232 cable. The wireless module operates in transmission and reception mode, and controls power supply on-off, transmitting power level, the receiving mode status, and transmission data rate via Serial Peripheral Interface (SPI). Figure 27 shows the operation flow when transmitting.

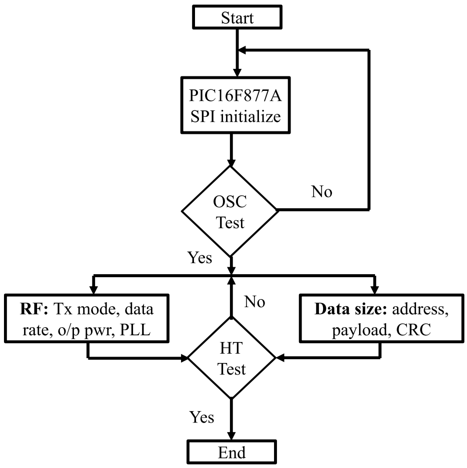

Fig. 27. Operation flow during transmission.

The experimental system composition is shown in Fig. 28 to transmit acquired data by the temperature sensor with WLAN at 2.4 GHz (ISM band). An ISM band sleeve antenna is used for the transmission. Using the cellular band rectenna shown and discussed in Section 2.5.1, at least 3.14 V is stored in the electric double layer capacitor over a period of four hours. To harvest a maximum usable power for the overall system, we charge the capacitor up to 5V. The operation voltage for the wireless module presented in Fig. 26 above is between 1.9V and 3.6V.

The signal was transmitted from the wireless module while a sleeve antenna, same like the one for transmission was used with the spectrum analyzer and the reception experiment was performed. Received signal level equal to -43.4dBm was obtained at a distance 3.5m between transmitter and reception point. The capacitor's stored voltage was used to supply the wireless module in the above-mentioned experiment. Successful transmission was possible for 5.5 minutes after which, the capacitor terminal voltage decreased from 3.16V to 1.47V, and the transmission ended. The sending and receiving distance of data can be estimated to be about 10m when the sensitivity of the receiver is assumed to be -60dBm, given 0dBm maximum transmit power.

Hereafter, the overall system examination is done by environmental power generation using the transmitted electric waves from the cellular phone base station, proposed based on the above-mentioned results. First of all, the power consumption shown in Fig. 29 is based on the fact that 120mW (5V, 24mA) is saved in the electric double layer capacitor by environmental power generation, achieved by calculation as discussed earlier.

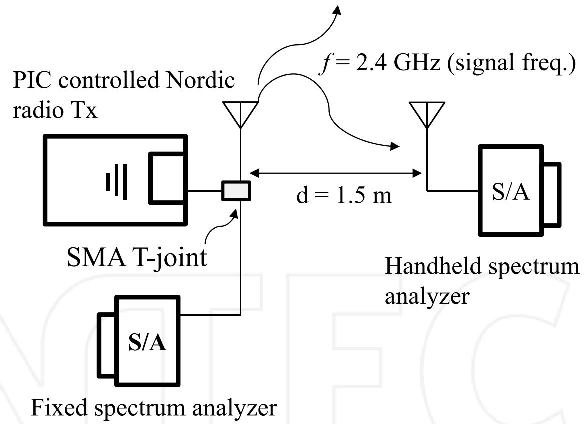

Fig. 28. Indoor measurement setup for received traffic from the sensor radio transmitter.

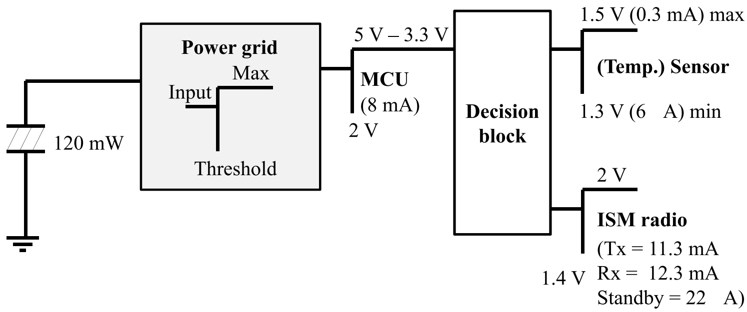

Fig. 29. Power management scheme for the cellular energy-harvesting sensor node.

The sensor data packet is transmitted wirelessly in ShockBurst mode for energy efficient communication. The data packet format includes a pre-amble (1 byte), address (3 bytes), and the payload i.e. temperature data (1 byte). The flag bit is disregarded for easiness, and cyclic redundancy check (CRC) is not used.

The operation of the proposed system is provisionally calculated. When the rectenna is set up in the place where power incidence of 0dBm is obtained in the base station neighbourhood (as depicted in Section 2.5.2), an initially discharged capacitor accumulates up to 3.3V by a rectenna with 53.8% conversion efficiency (presented in Section 2.5.1). At this point, it takes 1.5 minutes to start and to initialize a wireless module, and the voltage of the capacitor decreases to 2V. This trial calculation method depends on the capacitor's back up time discussed in [8]. After this, when the wireless module is assumed to be in sleep mode, the capacitor is charged by a 0.28mA charging current for four hours whereby the capacitor's stored voltage increases up to 5V. The power consumption in the sleep mode or standby is 33μW (1.5V, 22μA).

When the wireless module starts, after data transmission and the confirmation signal is sent, the voltage of the capacitor decreases by 0.6V, and consumes the electric power of 7.4mW.

The voltage of the capacitor decreases to 2V when 3.2mW is consumed to the acquisition of the sensor data, and the operation time of MCU is assumed to be one minute to the data storage in the wireless module etc. As for the capacitor voltage, when the wireless module continuously transmits data for 20 seconds, it decreases from 2V to 1.4V and even the following operation saves the electric power. Therefore, a temperature sensing system capable of transmitting wireless data in every four hours becomes feasible by environmental power generation from the cellular phone base station if we consider intermittent operation by sleep mode.

3. Conclusion

This Chapter has given an overview of the present energy harvesting sources, but the focus has stayed on RF energy sources and future directions for research. Design issues in RF energy harvesting have been discussed, which include low conversion efficiency and sometimes low rectified power. Solutions have been suggested by calculation and validated by measurement where possible, while highlighting the limitations of the proposed solutions. Potential applications for both DTV and cellular RF energy harvesting have been proposed and demonstrated with simple examples. A discussion is also presented on the typical performance analysis for the proposed RF energy harvesting system with sensor application.

4. Acknowledgment

The authors would like to thank Prof. Apostolos Georgiadis of Centre Tecnològic de Telecomunicacions de Catalunya (CTTC, Spain) for the collaboration on the design and development of the DC-DC boost converter circuit. Further thanks go to all those readers who will find this Chapter useful in one way or the other.

5. References

[1] Keisuke, T.; Kawahara, Y. & Asami, T. (2009). *RF Energy Intensity Survey in Tokyo..,* (c)2009 IEICE, B-20-3, Matsuyama-shi, Japan

[2] Mikeka, C.; Arai, H. (2011). *Dual-Band RF Energy-Harvesting Circuit for Range Enhancement in Passive Tags,* (c)2011 EuCAP, Rome, Italy

[3] Pozar, D. (2005). *Microwave Engineering,* Wiley, ISBN 978-0-471-44878-5, Amherst, MA, USA

[4] Mikeka, C.; Arai, H. (2010). Techniques for the Development of a Highly Efficient Rectenna for the Next Generation Batteryless System Applications, *IEICE Tech. Rep.,* pp. 101-106, Kyoto, Japan, March, 2010

[5] http://www.secomtel.com/UpFilesPDF/PDF/Agilent/PDF_DOCS/SKYDIODE/ 03_SKYDI/HSMS2850.PDF (Last accessed on 13 July, 2011)

[6] McSpadden, J. et al., H. (1992). Theoretical and Experimental Investigation of a Rectenna Element for Microwave Power Transmission, *IEEE Trans., on Microwave Theory and Tech., Vol. 40, No. 12.,* pp. 2359-2366, Dec., 1992

[7] Mikeka, C.; Arai, H. ; Georgiadis A. ; and Collado A. (2011). DTV Band Micropower RF Energy-Harvesting Circuit Architecture and Performance Analysis, *RFID-TA Digest,* Sitges, Spain, Sept., 2011

[8] Mikeka, C.; Arai, H. (2009). Design of a Cellular Energy-Harvesting Radio, *Proc. 2 nd European Wireless Technology Conf.,* pp. 73-76, Rome, Italy, Sept., 2009

[9] Popovic Z., et al., (2008). Resistor Emulation Approach to Low-Power RF Energy Harvesting, *IEEE Trans. Power Electronics, Vol. 23, No. 3*, 2008

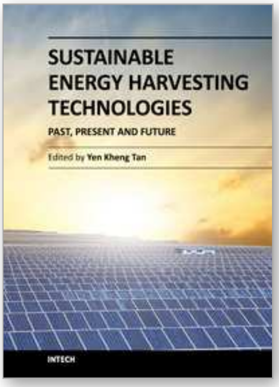

ISBN 978-953-307-438-2
Hard cover, 256 pages
Publisher InTech
Published online 22, December, 2011
Published in print edition December, 2011

SCIENTIFIC REPORTS

OPEN

SUBJECT AREAS:
ELECTRICAL AND ELECTRONIC ENGINEERING
ELECTRONIC AND SPINTRONIC DEVICES

Received
4 September 2014

Accepted
19 February 2015

Published
7 May 2015

Correspondence and requests for materials should be addressed to N.S. (negin.shariati@rmit.edu.au)

Multi-Service Highly Sensitive Rectifier for Enhanced RF Energy Scavenging

Negin Shariati, Wayne S. T. Rowe, James R. Scott & Kamran Ghorbani

School of Electrical and Computer Engineering, RMIT University, Melbourne, VIC 3001, Australia.

Due to the growing implications of energy costs and carbon footprints, the need to adopt inexpensive, green energy harvesting strategies are of paramount importance for the long-term conservation of the environment and the global economy. To address this, the feasibility of harvesting low power density ambient RF energy simultaneously from multiple sources is examined. A high efficiency multi-resonant rectifier is proposed, which operates at two frequency bands (478–496 and 852–869 MHz) and exhibits favorable impedance matching over a broad input power range (−40 to −10 dBm). Simulation and experimental results of input reflection coefficient and rectified output power are in excellent agreement, demonstrating the usefulness of this innovative low-power rectification technique. Measurement results indicate an effective efficiency of 54.3%, and an output DC voltage of 772.8 mV is achieved for a multi-tone input power of −10 dBm. Furthermore, the measured output DC power from harvesting RF energy from multiple services concurrently exhibits a 3.14 and 7.24 fold increase over single frequency rectification at 490 and 860 MHz respectively. Therefore, the proposed multi-service highly sensitive rectifier is a promising technique for providing a sustainable energy source for low power applications in urban environments.

AMBIENT energy harvesting is attracting widespread interest as it has the potential to provide a sustainable energy source for future growth and protection of the environment. Considerable research effort has been directed toward low-profile, low-power, energy efficient and self-sustainable devices aiming to harvest energy from inexhaustible sources such as solar energy, thermal, biomass, mechanical sources (e.g. wind, kinetic, vibration, and ocean waves) wastewater, and microwave energy. A thorough set of reviews is given in the literature[1–4]. Among these green energy sources, there has been a growing interest for radio frequency (RF) energy scavenging, as the availability of ambient RF energy has increased due to advancements in broadcasting and wireless communication systems. Furthermore, the development of wireless power transmission (WPT) technologies[5] that allow micro sensors[6], mobile electronic devices[7], wireless implantable neural interfaces[8] and far-field passive RFID (Radio-Frequency Identification) systems[9–11] to operate without batteries has triggered impetus for RF energy harvesting.

Efficient RF energy harvesting is a very challenging issue, as it deals with the very low RF power levels available in the environment. Furthermore, the scavengeable power level can vary unpredictably, depending on several factors such as the distance from the power source, the transmission media, the telecommunication traffic density and the antenna orientation. The majority of available literature on RF rectification has been dedicated to narrowband rectennas, which essentially operate at a single frequency and hence provide low DC output power[12,13]. Various topologies, such as voltage doublers or multipliers have been employed in order to increase the RF to DC conversion efficiency and the output DC voltage for specific applications[14–16]. However, from an ambient RF scavenging perspective, harvesting energy from various available frequencies could maximize power collection and hence increase the output DC power. Ultra-wideband and broadband rectenna arrays have been proposed as a potential solution[17,18]. However in some cases, simulation and experimental results were not provided to demonstrate the findings[17]. A broadband rectenna consisting of a dual-circularly polarized spiral rectenna array operating over a frequency range of 2–18 GHz was demonstrated[18]. The rectified DC power was characterized as a function of DC load, RF frequency and polarization for power densities between 10^{-5} and 10^{-1} mW/cm^2. However, the proposed rectenna was matched at a single input RF power level for a specified load resistance for the characterization. Also, due to the low Q value of the rectifier circuit, the conversion efficiency was a fraction of 1% at −15.5 dBm. From a design point of view, while it is relatively easy to achieve a broadband antenna, it is very challenging to realize a broadband rectenna due to the non-linearity of the rectifier impedance with input power across the frequency band[19].

To address this, a promising approach is to use a dual-band or multi-band configuration. This can maximize the power conversion efficiency (PCE) at the specific frequencies where the maximum ambient signal level is

available. Various dual-band RF energy harvesting systems has been demonstrated[20–24], however a large signal analysis of the rectifier was commonly not provided over a broad input power range. A dual-band RF energy harvesting using frequency limited dual-band impedance matching has been proposed[20] and the PCE was shown over a high power range of 0 to 160 mW, however it was only matched at a single input power level (10 dBm). A CMOS dual-narrowband energy harvester circuit was modeled at environmental power levels[21]. Again, the rectifier efficiency was demonstrated with only single input power levels of −19 and −19.3 dBm at 2 GHz and 900 MHz respectively, and a large signal analysis was not presented. A compact dual-band rectenna operating at 915 MHz and 2.45 GHz has been demonstrated[22] and the PCE was shown for input power levels of −15, −9 and −3 dBm. However, the reflection coefficient was evaluated at a single incident power level. Furthermore, the efficiency results with dual-tone excitation simultaneously and single-tone excitation (at 915 MHz) are very similar, hence the impact of applying a dual-band technique does not demonstrate a clear advantage over a single band. A dual-frequency rectenna for WPT has been proposed[23] which achieved a conversion efficiency of 84.4% and 82.7% at 2.45 and 5.8 GHz with a high input power level of 89.84 and 49.09 mW respectively. These power levels far exceed ambient levels in the environment[19]. A conformal hybrid solar and electromagnetic (EM) energy harvesting rectenna has been presented[24] and the PCE was provided with −30 to 5 dBm input power, achieving an efficiency up to 40% at 1.85 GHz for higher input power levels (above −5 dBm). However the reflection coefficient was not provided at low input power range.

A multi-resonant rectenna that uses a multi-layer antenna and rectifier has been evaluated for a −16 dBm to +8 dBm RF received power level, but the rectifier circuit layout and large signal analysis were not provided to clarify the findings[25]. Furthermore, a rectenna for triple-band biotelemetry communications has been proposed using a triple-band antenna and single frequency rectifier[26]. However, this rectenna is not suitable for RF energy scavenging due to the low efficiency at lower input power levels. Another triple band rectenna presented an RF-DC efficiency over the input power range of −14 to +20 dBm[27], however the reflection coefficient results were only evaluated at a single input power level. This rectenna was shown to harvest 7.06 μW of DC power from three sources simultaneously at a high input power level of +10 dBm. A multi-band harvesting system has also been proposed where four individual harvesters are designed to cover four frequency bands[28]. However, a large signal analysis was not provided over a broad input power range. Furthermore, the proposed harvesting system has a minimum sensitivity of −25 dBm, whilst in a real environment more sensitive systems are required as the available RF power levels are very low[19].

Tunable impedance matching networks have been demonstrated in order to collect RF signals from various sources and convert them to DC power[29]. However from an application point of view, this is still single frequency rectification and it is not widely applicable to environmental RF energy scavenging where the available power is very low.

In order to increase the amount of RF energy scavenged by a rectenna, it is crucial to identify and harvest multiple ambient frequency sources over their realistic available energy range. Our previous research has demonstrated the feasibility of RF energy harvesting through RF field investigations and maximum available power analysis in metropolitan areas of Melbourne, Australia[19]. The maximum available power for different frequency bands based on antenna aperture and number of antennas in a given collection area was analyzed. Measured results and analysis indicated that cellular systems and broadcast sources are well suited to harvesting, with scavengeable RF power ranging from −40 to −10 dBm. This identifies two important considerations in the design of efficient rectenna for RF energy harvesting: the scavengeable ambient RF power sources available, and the significant variance of this power.

The RF to DC rectifier solutions proposed in recent literature have focused on maximizing the system efficiency at a given, and often quite high, input power level. This neglects the issues related to input power variation which can lead to unexpected variations in the matching network due to diode non-linearity. Also, the scavangeable levels of ambient RF power have been shown to be orders of magnitude lower. Therefore, based on our previous research outcomes and recommendations[19], an efficient power harvesting solution could encompass a multi-band matching circuit at the specific frequencies where maximum signal power is available, enabling greater power harvesting due to the combination of RF signals. This also results in a higher power being fed to a single rectifier, utilizing the diode function more efficiently.

This paper presents an RF energy harvesting method that can scavenge a wide range of ambient power levels which are orders of magnitude lower than previous reported techniques in the literature. An efficient dual resonant rectifier circuit is proposed, matched to a 50 Ω input port at 490 and 860 MHz over a broad low input RF power range from −40 to −10 dBm. The proposed dual resonant matching network operates efficiently at two identified harvesting frequency bands over a wide input power range, maximizing DC power by scavenging two sources simultaneously.

The remainder of this paper is organized as follows. First, the key results for the reflection coefficient and output DC power are presented. Subsequently, the Discussion section summarizes the results and demonstrates their potential implications, the limitations of this study, open questions and future research. Finally, the Method section describes the proposed rectifier design.

Results

A dual resonant rectifier was fabricated on a 1.58 mm FR-4 substrate with a dielectric constant $\varepsilon_r \approx 4.5$ and a loss tangent $\delta \approx 0.025$. These substrate parameters were measured using the Nicolson-Ross method[30] so accurate values could be used in the rectifier design. A photograph of the fabricated dual resonant rectifier is shown in Fig. 1 which depicts input RF port, dual-band matching network lumped components, Schottky diodes and the output terminal. The performance of the rectifier was verified by measuring the input reflection properties, and the output power was calculated from the measured output DC voltage for the input powers from −40 to −10 dBm.

Reflection Coefficient. The $|S_{11}|$ of the rectifier was evaluated using a vector network analyzer (VNA). The VNA was re-calibrated for each input power level. Figure 2 compares the simulated and measured $|S_{11}|$ versus frequency for the dual resonant rectifier circuit at four different input power levels from −40 to −10 dBm. The measured results show very good agreement to the simulations. Slightly higher reflection was observed for the resonant frequencies at the lower part of the input power range (due to the diode characteristics). However, the proposed rectifier circuit is well-matched ($|S_{11}| < -10$ dB) at the desired frequency bands of

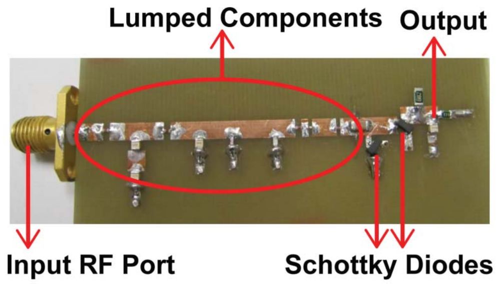

Figure 1 | **Fabricated rectifier prototype.**

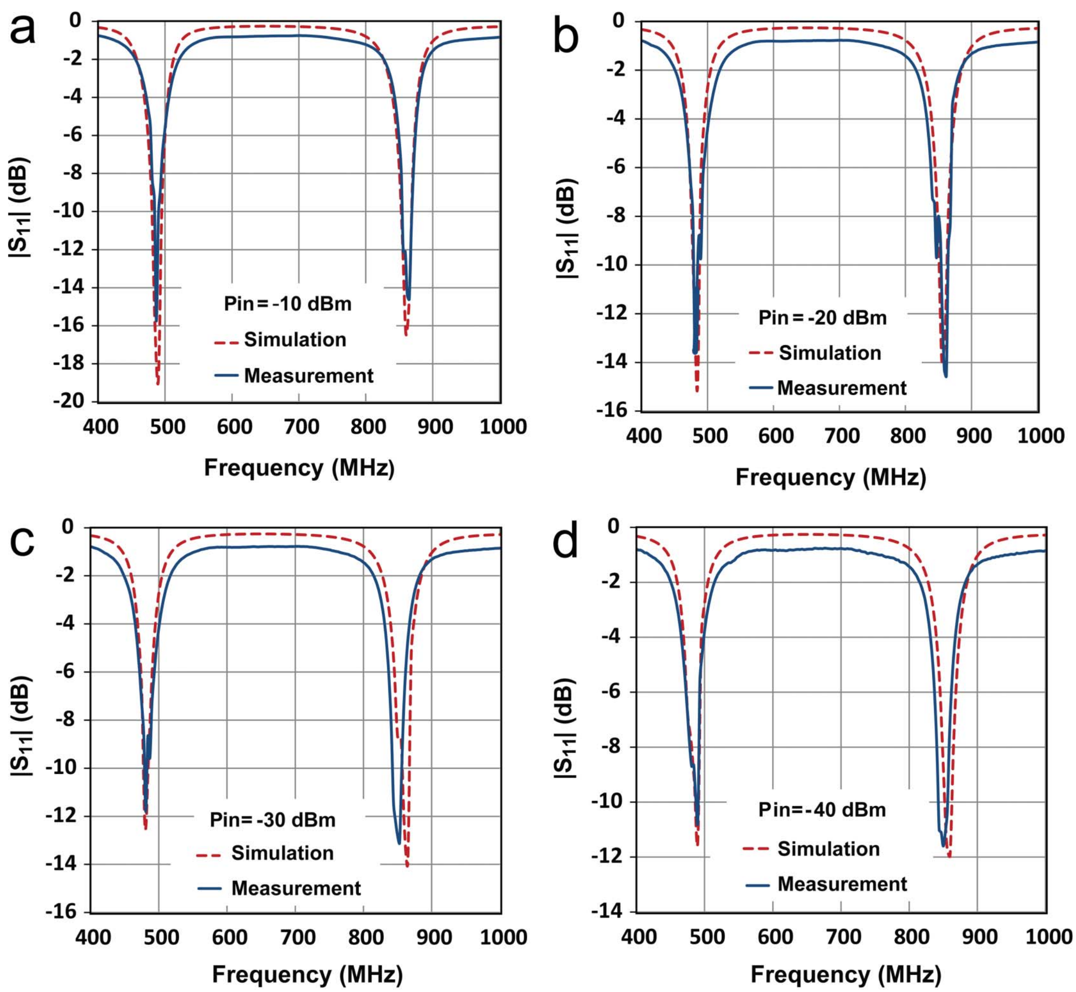

Figure 2 | Simulated and measured $|S_{11}|$ as a function of frequency and input RF power for the proposed dual resonant rectifier circuit. (a) −10 dBm. (b) −20 dBm. (c) −30 dBm. (d) −40 dBm.

478–496 MHz and 852–869 MHz over the broad range of input powers from −40 to −10 dBm. The small difference between simulation and measurement is due to the parasitic extraction accuracy.

Output DC Power. In the frequency domain, the Harmonic Balance method of analysis provides a comprehensive treatment of a multispectral problem[18]. The method intrinsically takes into account the DC component and a specified number of harmonics, while allowing the ability to specify the source impedance and harmonic terminations. A Harmonic Balance simulation was used to numerically evaluate the output DC voltage of the dual resonant rectifier for both a single and two tone input. The output DC voltage across the load resistor was also measured and used to calculate output DC power. Measurements were performed using a Wiltron 68247B synthesized signal generator as a RF power source for the rectifier circuit. Recording of the output DC voltage across the load resistance was achieved with a Fluke 79III digital voltage meter. The RF source power was initially set at −10 dBm, and decreased in 2 dB steps. In the dual-band measurement case, two RF signal generators were fed to the rectifier circuit simultaneously via a power combiner.

The simulation and measurement results for single and dual input tones are summarized in Fig. 3(a) and (b). A measured DC voltage of 772.8 mV is achieved with two simultaneous input tones at an input power of −10 dBm. For single tone measurements, DC voltages of 436 mV and 286 mV at 490 MHz and 860 MHz respectively are produced. The comparison between the 490 and 860 MHz single rectifiers highlights the impact of the input frequency on the PCE. A higher amount of DC voltage can be generated at the lower frequency. This difference comes from decreasing diode performance at the higher frequency due to the higher junction capacitance of the diode[31].

Importantly, a slightly higher DC voltage can be generated with the dual resonant rectifier as compared to the sum of output voltage from the two single bands, particularly at the lower input power levels as can be seen in Fig. 3(b) which shows the lower power section of Fig. 3(a) in more detail. By maximizing power collection from various sources of different frequencies and delivering the combined power to the rectification circuit, the diode conversion efficiency is enhanced which results in a higher level of rectified voltage. Figure 4 compares the simulated and measured output DC power for the dual resonant rectifier circuit with both single and dual input tones. A measured DC power of 17.3 μW and 7.5 μW can be generated at 490 MHz and 860 MHz respectively with a single tone input of −10 dBm (100 μW). This represents true efficiencies of 17.3% and 7.5% for the individual single band rectification (see Fig. 5). However, the measured DC output power with two concurrent input tones of −10 dBm is 54.3 μW which corresponds to an effective efficiency of 54.3% for the dual-band rectifier (see Fig. 6). This represents a 3.14 and 7.24 times increase in output DC power over the single tone excitation at 490 MHz or 860 MHz respectively. This trend is evident down to low input power levels (around 40 μW). Furthermore, there is a significant increase in the PCE of the dual resonant rectifier for lower input power levels (<40 μW).

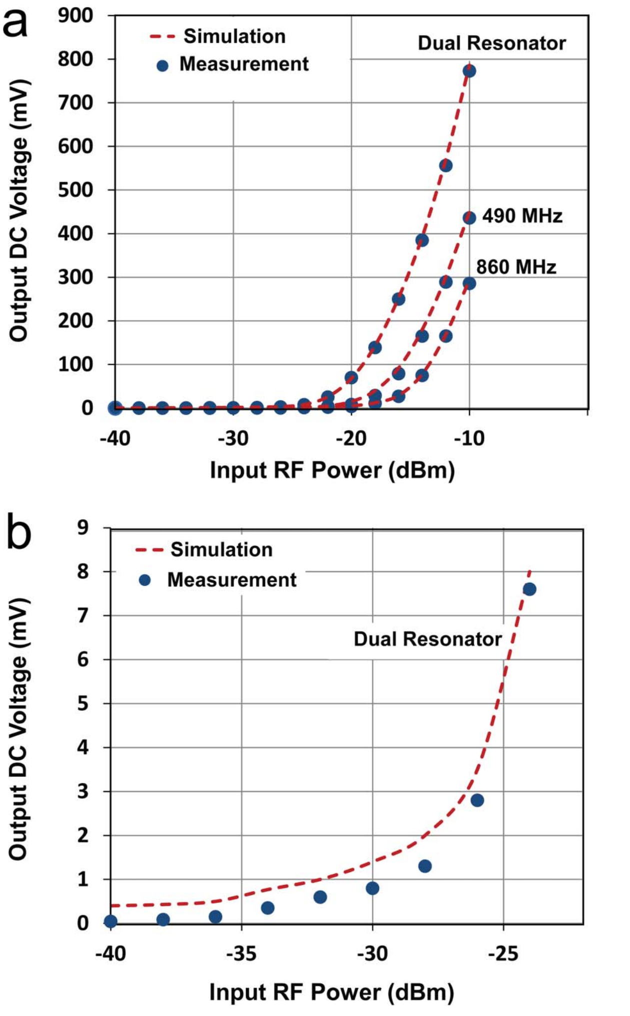

Figure 3 | Output DC voltage as a function of input RF power for single input tone at both 490 MHz and 860 MHz and for dual input tones (a) with −40 to −10 dBm input RF power (b) with −40 to −25 dBm input RF power. (This power range is associated with the signal source).

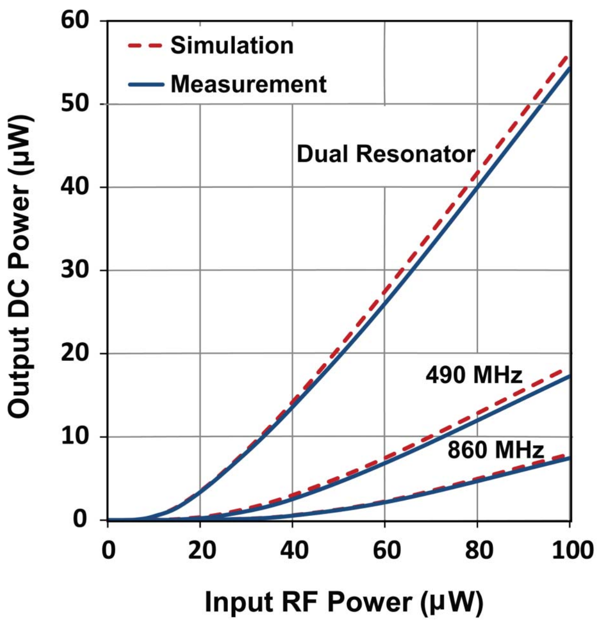

Figure 4 | Output DC power as a function of input RF power for single and dual input tones.

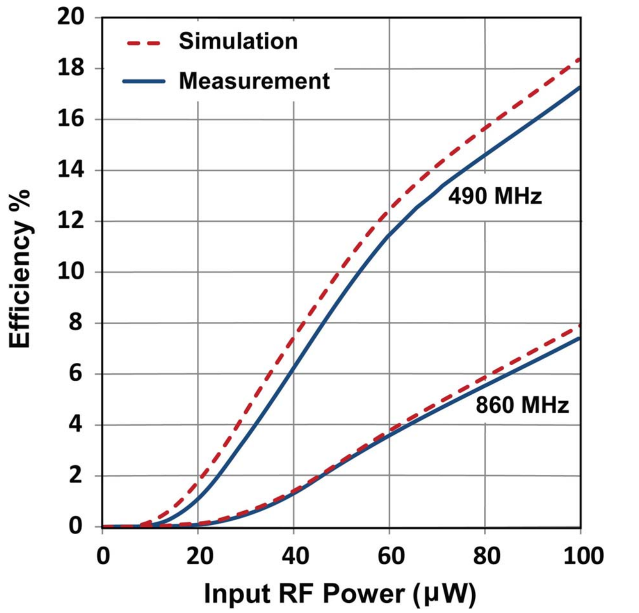

Figure 5 | RF to DC conversion efficiency as a function of input RF power for single band rectification.

Here, the effective efficiency is defined as the ratio of output DC power to the available input RF power rather than the power delivered to the diodes (equation (1)). The available power level is associated with the signal source. For the single resonator, the available input power is −10 dBm and the delivered power is also −10 dBm (assuming no loss). However, by creating a dual resonant matching network the power delivered to the diodes is −7 dBm (combined total input power from two signal generators) but the available power is still −10 dBm.

$$\eta = \frac{p_o}{p_i} = \frac{\left(\frac{V_o^2}{R_L}\right)}{p_i} \tag{1}$$

Therefore, combining input RF signals into a single rectification stage results in high sensitivity rectifier, which is widely applicable to

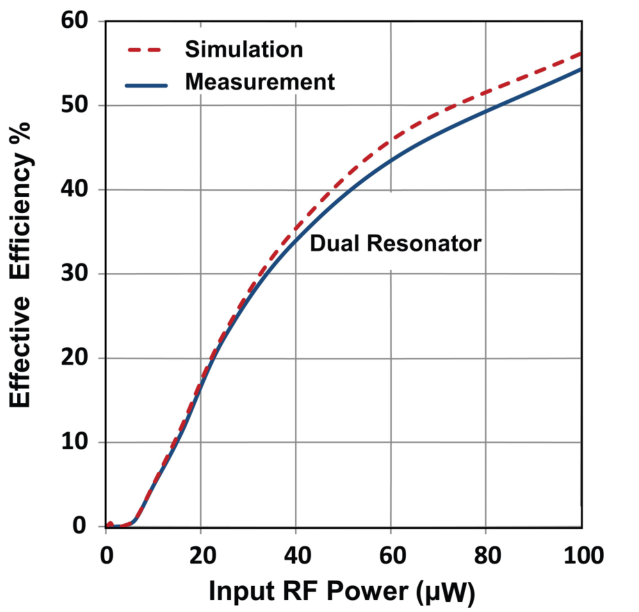

Figure 6 | Effective RF to DC conversion efficiency as a function of input RF power for dual resonant rectification.

Table 1 | Rectifier performance comparison

Ref.	Technology	Measured Efficiency (%)	RF power variation (in PCE evaluation)	Rectification Technique
13	Schottky diode	82@50 mW	N/A	Single resonator
16	Schottky diode	44@−10 dBm	N/A	Single resonator
18	Schottky diode	20@0.07 mW/cm^2 0.1@5×10^{-5} mW/cm^2	10^{-5} to10^{-1} mW/cm^2	Broad band
20	Schottky diode	77.13@22 dBm (158.49 mW)	0 to 160 mW	Dual resonator
21	CMOS	9.1@−19.3 dBm (900 MHz) 8.9@−19 dBm (2 GHz)	N/A	Dual resonator
22	Schottky diode	37 (915 MHz)@−9 dBm 30 (2.45 MHz)@−9 dBm	−40 to 0 dBm	Dual resonator
23	Schottky diode	84.4@89.84 mW (2.45 GHz) 82.7@49.09 mW (5.8 GHz)	0 to 100 mW	Dual resonator
27	Schottky diode	80@10 dBm (940 MHz) 47@8 dBm (1.95 GHz) 43@16 dBm (2.44 GHz)	−14 to 20 dBm	Triple resonator
29	Schottky diode	50@−5 dBm	−25 to 0 dBm	Dual resonator with tunable input response
This work	Schottky diode	54.3@−10 dBm 11.25@−18 dBm (490 and 860 MHz)	−40 to −10 dBm	Dual resonator

Table 2 | Environmental measurement results

Suburb	Available frequencies (MHz)	Respective available RF power (dBm) [μW]	Measured DC power (μW)
Bayswater	486, 488, 489, 490, 491, 867, 868, 869, 870, 871, 872, 873, 874	−19[12.5], −20[10], −17[19.95], −15[31.62], −22[6.3], −37[0.199], −37[0.199], −30[1], −24[3.98], −20[10], −30[1], −37[0.199], −40[0.1]	39.38
Bentleigh	491, 492, 494, 495, 865, 866, 867, 868, 869, 870, 871	−12[63.09], −46[0.02], −42[0.063], −57[0.001], −27[1.99], −27[1.99], −30[1], −37[0.199], −40[0.1], −40[0.1], −41[0.07]	30.9
RMIT University (Melbourne CBD)	487, 488, 489, 490, 491, 851, 861, 862, 866, 867, 868, 869	−30[1], −22[6.3], −29[1.25], −22[6.3], −20[10], −23[5.01], −21[7.94], −21[7.94], −30[1], −35[0.31], −40[0.1], −40[0.1]	14.5

real environmental RF energy scavenging. This multi-band technique can provide higher DC power than combining two separate single frequency rectifier circuits operating at the same frequencies. This is due to the fact that harvesting RF energy from various available sources simultaneously increases the delivered power to the rectifier, which improves the diode conversion efficiency and consequently enhances the output DC power. Table 1 summarizes this work as compared to previous published work.

In order to provide a realistic scenario for the proposed dual-band rectifier, measurement results were taken in three suburbs of Melbourne, Australia, congruent with our previous research outcomes[19]. Table 2 summarizes these environmental measurement results. It should be noted that the lower band (478–496 MHz) has a 3.67% fractional bandwidth and the higher band (852–869 MHz) has around 2% fractional bandwidth. Hence, various RF frequencies from different sources can be harvested within these two bands. The environmental measurement results demonstrate the feasibility of harvesting ambient EM energy from multiple sources simultaneously.

Discussion

The feasibility of harvesting ambient EM energy from multiple sources simultaneously is investigated in this paper. The proposed dual resonant rectifier operates at two frequency bands (478–496 and 852–869 MHz), which are used for broadcasting and cellular systems respectively. The dual resonant rectifier exhibits favorable impedance matching over a broad input power range (−40 to −10 dBm) at these two bands. The achieved sensitivity and dynamic range demonstrate the usefulness of this innovative low input power rectification technique. Simulation and experimental results of input reflection coefficient and rectified output power are in excellent agreement. The measurement results demonstrate that a two tone input to the proposed dual-band RF energy harvesting system can generate 3.14 and 7.24 times more power than a single tone at 490 or 860 MHz respectively, resulting in a measured effective efficiency of 54.3% for a dual-tone input power of −10 dBm. It is evident that this dual resonant rectification technique increases the RF to DC effective conversion efficiency, and hence the recoverable DC power for low power applications. Furthermore from a design and economic perspective, utilizing a large number of components (e.g. antennas, diodes) to realize individual rectifier circuits for each frequency band creates additional expense. In order to provide more realistic measurement results, the proposed dual-band rectifier was tested in three suburbs of Melbourne, Australia. Therefore, this dual-band technique offers a simple and cost-effective solution which is of paramount importance for environmental power harvesting systems. This innovative technique has the potential to generate a viable perpetual energy source for low power applications in urban environments.

Limitation of the study, open questions and future work

Utilizing diodes which are more suitable to low power applications ($P_i < -20$ dBm) could increase the voltage sensitivity, resulting in a higher RF-DC conversion efficiency[32]. Applying a power optimized waveform excitation to the rectifier circuit in these frequency bands, a higher amount of DC power can be generated when compared with a single and dual tone excitations with the same input power[33,34]. However this technique is not applicable to energy harvesting where the input waveform is arbitrary.

Utilizing our proposed dual resonant rectification technique to combine resonant circuits for any other arbitrary frequency bands could lead to PCE improvement, provided that suitable diodes for the desired frequency bands are selected. Note that by increasing the operating frequency the rectification performance degrades due to

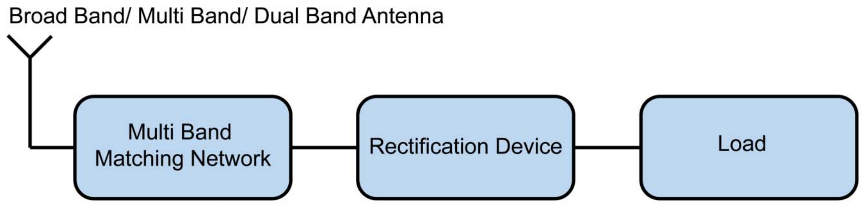

Figure 7 | General block diagram of the RF energy harvesting system.

the higher junction capacitance of the diode. Hence, lower output voltage is expected at higher frequency bands.

It is the object of our future work to design a multi-band rectenna array for enhanced RF energy harvesting. Furthermore, increasing the bandwidth, sensitivity and efficiency will also be investigated.

Methods

The major goal in designing an efficient RF harvesting system is to produce high DC output power. Toward this goal, a high sensitivity rectifier is crucial for optimum RF scavenging. A significant factor governing the sensitivity of a rectifier is the threshold voltage of the diode used for rectification. The diode must be able to "switch on" for very low ambient energy levels.

To address this sensitivity issue, a system that scavenges power from multiple frequency bands and combines them to activate a rectification circuit is proposed. The general block diagram of the proposed system is depicted in Fig. 7. Various environmental RF energy sources of different frequencies are collected by an appropriately designed antenna, and delivered to the rectification circuit via a multi-band matching network. The rectification circuit converts the combination of RF signals into DC power for low-power applications. The embodiment in this paper realizes a dual resonant matching circuit as a transition between a 50 Ω nominal antenna output and the non-linear rectification device at 490 and 860 MHz. Based on the Australian Radiofrequency Spectrum Plan[35], these bands are allocated to broadcasting services and cellular systems.

Device Selection. Due to the very low ambient power available in a real environment[19], a very low threshold voltage rectification device is required in order to increase sensitivity. For this reason, Schottky diodes (GaAs or Si) are commonly employed for RF energy harvesting. In this work, a microwave Schottky detector HSMS2820 ($C_{j0} = 0.7$ pF, $R_s = 6$ Ω, $I_s = 2.2e^{-8}$ A) is chosen due to its excellent high frequency performance, low series resistance (R_s) and junction capacitance (C_j), and low threshold voltage with high-saturation current[31]. This low threshold voltage (0.15–0.3 V) supports rectification at low input power levels.

Proposed Rectifier Design. In order to design an efficient RF harvesting system, the non-linearity of the rectifier impedance with frequency and input power should be matched to the 50 Ω output of the antenna at the desired frequency bands. Therefore, the diode input impedance as a function of frequency and different power levels were calculated and analyzed[36]. In order to match the input impedance of the rectifier to the 50 Ω output of the antenna, the total load impedance for different input power and frequencies should be determined. A circuit consisting of a pair of Schottky Barrier Diodes (SBD) terminated with a load resistor ($R_{Load} = 11$ kΩ) and an output bypass capacitor ($C2 = 6.8$ pF) was simulated using Agilent ADS software. Figure 8 shows the proposed geometry of the voltage-doubler topology[31,37]. The voltage doubler rectifier structure is employed for the design of the RF-DC power conversion system as this topology is well suited to low power rectification. The resistor and capacitor at the output will filter high frequencies. The high load resistor (11 kΩ) was chosen to observe a reasonable output voltage at very low currents. Using Large Signal S-Parameters analysis in Agilent ADS software, the load impedance and bypass capacitor were determined and optimized.

The voltage doubler rectifier in Fig. 8 consists of a peak rectifier formed by *D2* and bypass capacitor *C2* (6.8 pF) and a voltage clamp formed by *D1* and *C1* (total capacitance of the transmission lines and diode's parasitic capacitance (C_p)). In the negative phase of the input, current flows through *D1* while *D2* is cutoff. The voltage across *D1* stays constant around its threshold voltage and the voltage at node 1 is charged to $-V_{th1}$ (where $-V_{th1}$ is the threshold voltage of the *D1*). At the negative peak, the voltage across *C1* is $V_{amp} - V_{th1}$ (where V_{amp} is the amplitude of the input signal). In the positive phase of the input, current flows through *D2* while *D1* is cutoff. The voltage across *C1* remains the same as the previous phase because it has no way to discharge. At the positive peak, the voltage across *D1* is $2V_{amp} - V_{th1}$. Since *D2* is conducting current to charge *C2*, the voltage at the output is $V_{out} = 2V_{amp} - V_{th1} - V_{th2}$.

The DC equivalent circuit of the SBD is a voltage source in series with the junction resistor R_j which is obtained by differentiating the diode voltage–current characteristic and is given by equation (2)[31,38]:

$$R_j = \frac{nKT}{q(I_s + I_b)} \tag{2}$$

Where n is the diode ideality factor, *K* is the Boltzmann's constant, *T* is the temperature in degrees Kelvin, *q* is the electronic charge, I_s is the diode saturation current and I_b is the external bias current. At low power levels, the saturation current is very small ($I_s = 2.2\ e^{-8}$ A) and for a zero-biased diode, $I_b = 0$. Therefore, the resulting value of junction resistance at room temperature is approximately 1.7 MΩ. Since, the saturation current is highly temperature dependent, R_j will be even higher at lower temperatures which tends to decrease the output voltage. As the input power increases, some circulating rectified current will cause a drop in the value of R_j and this phenomenon will increase the value of the DC output voltage. Furthermore, it is worth to highlight that the rectified current produced by the first diode (*D1*) in Fig. 8 constitutes the external bias current of the second diode (*D2*) which will help to reduce the R_j and hence the detection sensitivity is improved. Therefore, depending on the amount of available bias current, R_j is varying (equation (2)), hence the matching network is changing which impacts the amount of delivered power to the diode and results in different values of PCE.

A Schottky barrier diode can be modeled by the linear equivalent circuit shown in Fig. 9, where L_p and C_p are the diode's parasitic inductance and capacitance respectively due to packaging ($L_p = 2$ nH and $C_p = 0.08$ pF) which are generally unwanted[39]. This linear model is used for determining the diode impedance at a given input power.

The diode impedance analyzed using a Harmonic Balance simulator and a non-linear model of the diodes over the frequency range of 400 to 900 MHz at various input power levels (Fig. 10). Due to the large junction resistor at low input RF power levels, the rectification device is turned off in absence of an appropriate matching network. Large Signal S-parameter analysis was conducted and higher input power (associated with the signal source) is applied directly to the Schottky diodes configuration of Fig. 8 which does not include a matching network in order to turn on the diodes (reduce the value of R_j) and extract approximate input impedance value as our starting point in design of a matching network. As it can be seen in Fig. 10, with increasing the source power, the diode impedance is varying and it is beginning to switch on. Hence, the input impedance needs to be determined when the diode is

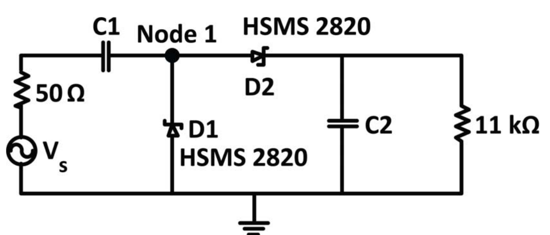

Figure 8 | Schematic of a voltage-double rectifier without matching network.

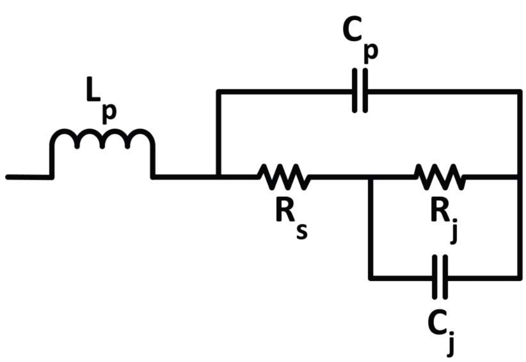

Figure 9 | HSMS 2820 Schottky diode equivalent circuit.

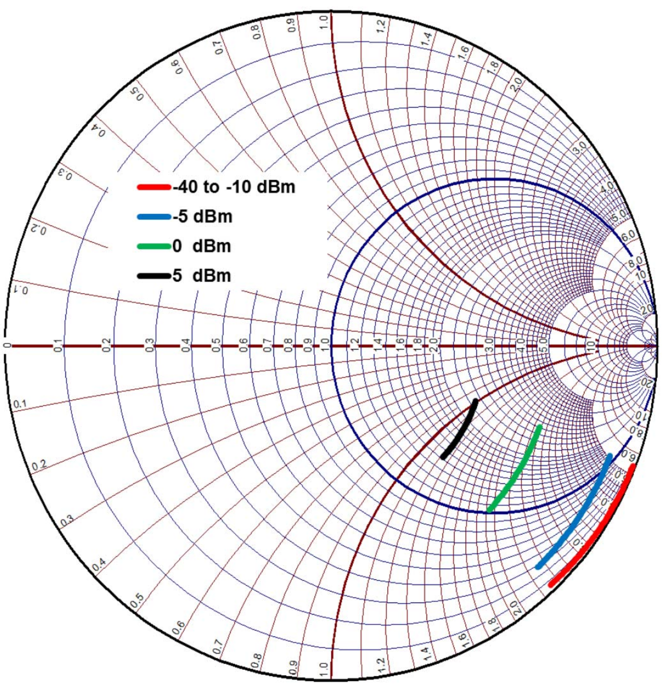

Figure 10 | Diode input impedance calculated with Large Signal S-parameter analysis over the frequency range of 400 to 900 MHz with various unmatched input power levels.

turned on to realize the matching network for a rectifier circuit. Obviously, in the presence of an appropriate matching network the rectification device can be turned on at lower power levels, whilst in the absence of a matching network a higher input power should be applied to switch on the diode. (Note that, with an unmatched rectifier the total applied input power from the signal source cannot be delivered to the diode due to the high reflection in the circuit).

The aim is to match the input impedance of the device to 50 Ω at 478–496 MHz and 852–869 MHz bands over a broad range of input RF powers. The procedure commences by matching the diode input impedance at high unmatched source power and shifting the diode input impedance at various power levels to within the voltage standing wave ratio (VSWR) <2 circle on the Smith chart. This procedure assumes that diode input impedance does not drastically change in this low power range. The simulation results of Fig. 10 prove that this is the case.

In order to provide maximum power transfer from the antenna to the rectifier circuit, a dual resonant rectifier network is designed as a transition between a 50 Ω nominal antenna output and the non-linear rectification device over the power range of -40 to -10 dBm (see Fig. 11). Hence, a coupled-resonator structure with both series and shunt resonators is designed to achieve a dual-band network[40]. The linear equivalent circuit model of the SBD chip[39] has been taken into consideration to design the dual band match at the desired frequency bands. In Fig. 11, $C_{equivalent}$ represents the total capacitance of the diodes and bypass capacitor and $L_{equivalent}$ is the overall parasitic inductance of the diodes. The series L-C resonator ($L4 + L_{equivalent}$ and $C_{equivalent}$) and the parallel L-C resonator ($C3$ and $L3$) define the dual resonant circuit. The series resonator corresponds closely to the higher band specification of 852–869 MHz, whilst the parallel resonator approximates the lower 478–496 MHz band. A minimum number of components were used in order to reduce the ohmic and parasitic losses.

The resonant frequency of each sub-circuit was determined in isolation using the following equation:

$$f = \frac{1}{2\pi\sqrt{LC}} \tag{3}$$

The 852–869 MHz band resonator circuit components were calculated. Here, $C = C_{equivalent} \cong 1.3$ pF consists of the combination of the bypass capacitor (6.8 pF) and

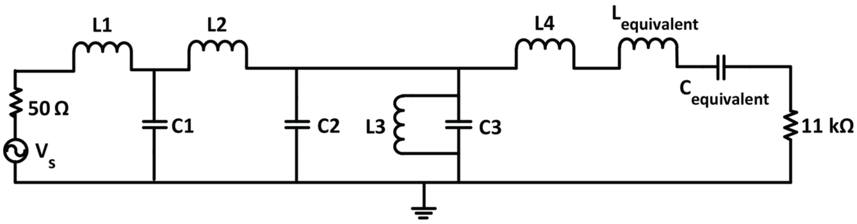

Figure 11 | Schematic of a dual resonant rectifier (optimized parameters of the chip components are: $L1 = 3.9$ nH, $C1 = 0.2$ pF, $L2 = 12$ nH, $C2 = 1.8$ pF, $L3' = 3.9$ nH, $C3' = 7.5$ pF, $L4' = 11.6$ nH, $L_{equivalent} \cong 1$ nH, $C_{equivalent} \cong 1.3$ pF).

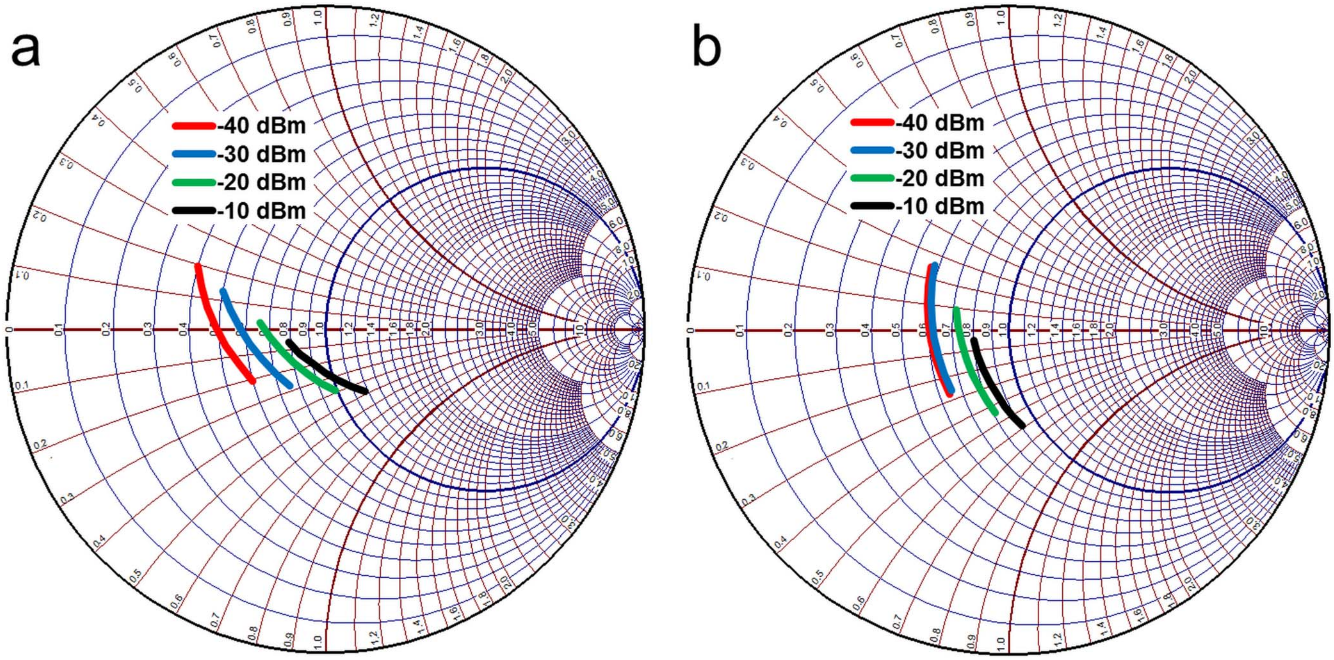

Figure 12 | Dual resonant impedance matching with -40 to -10 dBm input RF power. (a) 478–496 MHz. (b) 852–869 MHz.

the overall junction ($C_{j0} = 0.7$ pF) and parasitic capacitance ($C_p = 0.08$ pF) of *D1* and *D2*. Thus, *L* is calculated to be 26.5 nH in order to achieve an appropriate resonant frequency. Note that, *L* consists of L_4 and the overall parasitic inductance ($L_{equivalent} \cong$ 1 nH) of *D1* and *D2*. The 478–496 MHz band resonator circuit components were calculated as $C3 \cong 15$ pF and $L3 \cong 7.2$ nH. Hence, the initial component values are determined for the two resonant circuits.

Initially these resonators were combined to achieve a dual-band structure. Then standard *LC* matching technique[40] is utilized to determine *C1*, *C2*, *L1*, and *L2* to achieve minimum reflection at the resonant frequencies. The substitution of realistic chip component values with their associated parasitics, and addition of 50 Ω microstrip lines and T-junctions introduce delay and shift the imaginary part of the input impedance. The via-holes also contribute to extra inductance in the circuit. Hence minor circuit adjustments are made in order to fine tune the resonant frequencies to the desired values. The final optimized values of the standard chip components are: $L3' = 3.9$ nH, $C3' = 7.5$ pF and $L4' = 11.6$ nH. Large Signal S-parameter analysis is also performed to demonstrate the matching network performance as the input power is varied. Simulation results for the input impedance of the circuit depicted in Fig. 11 are illustrated in Fig. 12. The proposed dual-resonant matching circuit achieves a VSWR <2 at 478–496 MHz and 852–869 MHz for input power ranging from −40 to −10 dBm. It should be noted that the matching circuit was designed based on the input impedance of two diodes and the output resistor and capacitor (Fig. 10). Therefore, selecting a different value for the load resistor requires a new matching circuit to be designed.

1. Paradiso, J. A. & Starner, T. Energy scavenging for mobile and wireless electronics. *IEEE Pervasive Comput.* **4**, 18–27 (2005).
2. Singh, R., Gupta, N. & Poole, K. F. Global green energy conversion revolution in 21st century through solid state devices. 26th International Conference on Microelectronics, Nis, Serbia. *IEEE.* DOI:10.1109/ICMEL.2008.4559221. 45–54 (11–14 May, 2008).
3. Wang, Y. K., Sheng, G. P., Shi, B. J., Li, W. W. & Yu, H. Q. A Novel electrochemical membrane bioreactor as a potential net energy producer for sustainable wastewater treatment. *Sci. Rep.* **3**, DOI:10.1038/srep01864 (2013).
4. Inayat, S. B., Rader, K. R. & Hussain, M. M. Nano-materials enabled thermoelectricity from window glasses. *Sci. Rep.* **2**, DOI:10.1038/srep00841 (2012).
5. Brown, W. C. The history of power transmission by radiowaves. *IEEE Trans. Microw. Theory Tech.* **32**, 1230–1242 (1984).
6. Le, T., Mayaram, K. & Fiez, T. Efficient far-field radio frequency energy harvesting for passively powered sensor networks. *IEEE J. Solid-State Circuits.* **43**, 1287–1302 (2008).
7. Paolo, J. & Gaspar, P. D. Review and future trend of energy harvesting methods for portable medical devices. Proceedings of the World Congress on Engineering (WCE). London, U. K. 909–914 (30 June–2 July, 2010).
8. Matsuki, H., Yamakata, Y., Chubachi, N., Nitta, S. & Hashimoto, H. Transcutaneous DC-DC converter for totally implantable artificial heart using synchronous rectifier. *IEEE Trans. Magn.* **32**, 5118–5120 (1996).
9. Scorcioni, S. *et al.* RF to DC CMOS rectifier with high efficiency over a wide input power range for RFID applications. Microwave Symposium Digest (IMS), *IEEE MTT-S.* Montreal, QC, Cabada. DOI:10.1109/MWSYM.2012.6259760. 1–3 (17–22 June, 2012).
10. Shameli, A., Safarian, A., Rofougaran, A., Rofougaran, M. & De Flaviis, F. Power harvester design for passive UHF RFID tag using a voltage boosting technique. *IEEE Trans. Microw. Theory Tech.* **55**, 1089–1097 (2007).
11. Mandal, S. & Sarpeshkar, R. Low-power CMOS rectifier design for RFID applications. *IEEE Trans. Circuits Syst. I, Reg. Papers.* **54**, 1177–1188 (2007).
12. Sun, H., Guo, Y. X., He, M. & Zhong, Z. Design of a high-efficiency 2.45-GHz rectenna for low-input-power energy harvesting. *IEEE Antennas Wireless Propag. Lett.* **11**, 929–932 (2012).
13. McSpadden, J. O., Fan, L. & Chang, K. Design and experiments of a high-conversion-efficiency 5.8-GHz rectenna. *IEEE Trans. Microw. Theory Tech.* **46**, 2053–2060 (1998).
14. Din, N. M., Chakrabarty, C. K., Bin Ismail, A., Devi, K. K. A. & Chen, W. Y. Design of RF energy harvesting system for energizing low power devices. *PIER.* **132**, 49–69 (2012).
15. Barnett, R. E., Liu, J. & Lazar, S. A RF to DC voltage conversion model for multi-stage rectifiers in UHF RFID transponders. *IEEE J. Solid-State Circuits.* **44**, 354–370 (2009).
16. Kanaya, H. *et al.* Energy harvesting circuit on a one-sided directional flexible antenna. *IEEE Microw. Wireless Compon. Lett.* **23**, 164–166 (2013).
17. Buonanno, A., D'Urso, M. & Pavone, D. An ultra wide-band system for RF energy harvesting. 5th European Conference on Antennas and Propagation (EUCAP). Rome, Italy. *IEEE.* 388–389 (11–15 April, 2011).
18. Hagerty, J. A., Helmbrecht, F. B., McCalpin, W. H., Zane, R. & Popovic, Z. B. Recycling ambient microwave energy with broad-band rectenna arrays. *IEEE Trans. Microw. Theory Tech.* **52**, 1014–1024 (2004).
19. Shariati, N., Rowe, W. S. T. & Ghorbani, K. RF field investigation and maximum available power analysis for enhanced RF energy scavenging. 42nd European Microwave Conference (EuMC). Amsterdam RAI, The Netherlands. *IEEE.* 329–332 (29 October–1 November, 2012).
20. Kim, P., Chaudhary, G. & Jeong, Y. A dual-band energy harvesting using frequency limited dual-band impedance matching. *PIER.* **141**, 443–461 (2013).
21. Li, B. *et al.* An antenna co-design dual band RF energy harvester. *IEEE Trans. Circuits Syst. I, Reg. Papers.* **60**, 3256–3266 (2013).
22. Niotaki, K. *et al.* A compact dual-band rectenna using slot-loaded dual band folded dipole antenna. *IEEE Antennas Wireless Propag. Lett.* **12**, 1634–1637 (2013).
23. Suh, Y. H. & Chang, K. A high-efficiency dual-frequency rectenna for 2.45- and 5.8-GHz wireless power transmission. *IEEE Trans. Microw. Theory Tech.* **50**, 1784–1789 (2002).
24. Collado, A. & Georgiadis, A. Conformal hybrid solar and electromagnetic (EM) energy harvesting rectenna. *IEEE Trans. Circuits Syst. I, Reg. Papers.* **60**, 2225–2234 (20013).
25. Rizzoli, V., Bichicchi, G., Costanzo, A., Donzelli, F. & Masotti, D. CAD of multi-resonator rectenna for micro-power generation. European Microwave Integrated Circuits Conference (EuMIC). Rome, Italy. *IEEE.* 331–334 (228–29 September, 2009).
26. Huang, F. J. *et al.* Rectenna application of miniaturized implantable antenna design for triple-band biotelemetry communication. *IEEE Trans. Antennas Propag.* **59**, 2646–2653 (2011).
27. Pham, B. L. & Pham, A. V. Triple bands antenna and high efficiency rectifier design for RF energy harvesting at 900, 1900 and 2400 MHz. Microwave Symposium Digest (IMS), *IEEE MTT-S.* Seattle, WA. DOI:10.1109/MWSYM.2013.6697364. 1–3 (2013).
28. Pinuela, M., Mitcheson, P. D. & Lucyszyn, S. Ambient RF energy harvesting in urban and semi-urban environments. *IEEE Trans. Microw. Theory Tech.* **61**, 2715–2726 (2013).
29. Mikeka, C. & Arai, H. Microwave Tooth for sensor power supply in battery-free applications. Proceedings of the Asia-Pacific Microwave Conference (APMC). Melbourne, VIC. *IEEE.* 1802–1805 (5–8 December, 2011).
30. Baum, T., Thompson, L. & Ghorbani, K. Complex dielectric measurements of forest fire ash at X-band frequencies. *IEEE Geosci. Remote Sens. lett.* **8**, 859–863 (2011).
31. Avago Technologies, *Surface Mount RF Schottky Barrier Diodes HSMS-282X Series. Data sheet.* (2005). Available at: http://www.avagotech.com/docs/AV02-1320EN. (Accessed: 22/11/2014).
32. Avago Technologies, *Surface Mount Zero Bias Schottky Detector Diodes HSMS-285X Series. Data sheet.* (2005). Available at: http://www.avagotech.com/docs/AV02-1377EN. (Accessed: 22/11/2014).
33. Valenta, C. R. & Durgin, G. D. Rectenna performance under power-optimized waveform excitation. IEEE International Conference on RFID. Penang. DOI:10.1109/RFID.2013.6548160. 237–244 (30 April–2 May, 2013).
34. Trotter, M. S. & Durgin, G. D. Survey of range improvement of commercial RFID tags with power optimized waveforms. IEEE International Conference on RFID. Orlando. DOI:10.1109/RFID.2010.5467265. 195–202 (14–16 April, 2010).
35. Australian Government, *Australia Radio Frequency Spectrum Plan (ACMA).* (January 2013). Available at: http://acma.gov.au/~/media/Spectrum%20Transformation%20and%20Government/Information/pdf/Australian%20Radiofrequency%20Spectrum%20Plan%202013.pdf. (Accessed: 22/09/2014).
36. Keyrouz, S., Visser, H. J. & Tijhuis, A. G. Rectifier analysis for radio frequency energy harvesting and power transport. 42nd European Microwave Conference (EuMC). Amsterdam RAI, The Netherlands. *IEEE.* 428–431 (29 October–1 November, 2012).
37. Avago Technologies, *Schottky Diode Voltage Doubler. Application Note 956-4.* (2005). Available at: http://c1233384.r84.cf3.rackcdn.com/UK_HPA_HSCH-5331_7AN.pdf. (Accessed: 22/11/2014).
38. Eriksson, H. & Waugh, R. W. *A temperature compensated linear diode detector. Design Tip.* Agilent Technologies. (2000). Available at: http://electronix.ru/forum/index.php?act=Attach&type=post&id=13726. (Accessed: 22/11/2014).
39. Avago Technologies, *The Zero Bias Schottky Diode Detector at Temperature Extremes-Problems and Solutions. Application Note AN 1090.* (2005). Available at: http://www.efo.ru/download/Zero_bias_shottky_over_temperature.pdf. (Accessed: 22/11/2014).
40. Mattaei, G., Young, L. & Jones, E. M. T. *Microwave Filters, Impedance-Matching Networks and Coupling Structures.* Artech house books, Dedham, MA. (1980).

Acknowledgments

The authors would like to acknowledge Dr. Khashayar Khoshmanesh for valuable advice. The authors also acknowledge Mr. David Welch for assistance in fabrication of the rectifier circuit.

Author contributions

N.S. designed and simulated the rectifier, carried out the measurements, interpreted results and wrote the paper. K.G. directed the research, contributed to perform the simulation and measurement and validation of design and results. W.S.T.R. supervized the research, analyzed the data and contributed to the general concept, validation of design and results. J.R.S. analyzed the data and contributed to the general concept, validation of design and results. All authors reviewed the manuscript.

Additional information

Competing financial interests: The authors declare no competing financial interests.

How to cite this article: Shariati, N., Rowe, W.S.T., Scott, J.R. & Ghorbani, K. Multi-Service Highly Sensitive Rectifier for Enhanced RF Energy Scavenging. *Sci. Rep.* **5**, 9655; DOI:10.1038/srep09655 (2015).

Sensors **2012**, *12*, 13636-13663; doi:10.3390/s121013636

OPEN ACCESS

sensors

ISSN 1424-8220
www.mdpi.com/journal/sensors

Article

Optimization of Passive Low Power Wireless Electromagnetic Energy Harvesters

Antwi Nimo *, Dario Grgić and Leonhard M. Reindl

Department of Microsystems Engineering, Laboratory for Electrical Instrumentation,
University of Freiburg, IMTEK, Georges-Köhler-Allee 106, 79110 Freiburg, Germany;
E-Mails: grgic@imtek.de (D.G.); leonhard.reindl@imtek.uni-freiburg.de (L.M.R.)

* Author to whom correspondence should be addressed; E-Mail: antwi.nimo@imtek.de;
Tel.: +49-761-203-7223; Fax: +49-761-203-7222.

Received: 13 August 2012; in revised form: 28 September 2012 / Accepted: 28 September 2012 / Published: 11 October 2012

Abstract: This work presents the optimization of antenna captured low power radio frequency (RF) to direct current (DC) power converters using Schottky diodes for powering remote wireless sensors. Linearized models using scattering parameters show that an antenna and a matched diode rectifier can be described as a form of coupled resonator with different individual resonator properties. The analytical models show that the maximum voltage gain of the coupled resonators is mainly related to the antenna, diode and load (*remote sensor*) resistances at matched conditions or resonance. The analytical models were verified with experimental results. Different passive wireless RF power harvesters offering high selectivity, broadband response and high voltage sensitivity are presented. Measured results show that with an optimal resistance of antenna and diode, it is possible to achieve high RF to DC voltage sensitivity of 0.5 V and efficiency of 20% at −30 dBm antenna input power. Additionally, a wireless harvester (*rectenna*) is built and tested for receiving range performance.

Keywords: RF energy harvesting; wireless power transmission; coupled resonators; Schottky diode; RF to DC power converter; impedance matching; PI-matching; L-matching; rectenna

---

1. Introduction

For autonomous powering of sensor nodes in remote or inaccessible areas, wireless power transfer provides the only viable option to power them from an energy source. Due to the low power density of ambient RF at far-field from transmitters, there is a need to optimize each aspect of a wireless RF energy harvester for possible realistic applications. Today remote autonomous sensors are mostly powered by batteries, which have limited lifespan. Renewable powering has the potential to power autonomous sensors perpetually. Due to the expansion of telecommunications technology ambient electromagnetic (EM) power is among the most common sources of ambient energy. There are power transmitters/receivers scattered in practically any society, ranging from television transmission stations to cell phone transmitters and even wireless routers in our homes/offices or mobile phones. These transmitters in our environment and others which are on special dedicated frequencies produce ambient RF power (on the order of microwatts) which can be used as a source for powering remote microwatt budget sensors through wireless energy harvesting. This work presents different matching techniques based on different application requirements using Schottky diode-based RF to DC power converting circuits for wireless remote EM energy harvesting around 434 MHz and 13.6 MHz. Generalized analytical models and limitations of the matched RF to DC power converters are discussed. A wireless RF energy harvester consisting of an antenna and a matched diode rectifier is then realized and its performance tested. Passive wireless energy harvesting also finds applications in near field communications (NFC) [1], RFID tags [2–5], implantable electronics [6,7], and environmental monitoring [8], among others.

1.1. State of the Art

Hertz was the first to demonstrate the propagation of EM waves in free space and to demonstrate other properties of EM waves such as reflection using parabolic reflectors [9]. Wireless power transmission was then investigated and demonstrated for possible wireless remote powering by Tesla. Electromagnetic power beaming for far field wireless power transfer using collimated EM waves was proposed in the 1950s [9]. Recent advances in ultralow power sensors means ambient omni-directional EM power can be used as a source for powering remote sensors without the need to collimate the EM power through the wireless space. Mickle [10] and McSpadden [11] have presented earlier work on wireless energy harvesting systems using Schottky diodes and rectennas where the usability of ambient RF power into DC power was shown. Sample [12] presented a wireless harvester which can harvest EM power from TV and radio base stations transmitting 960 kW of effective radiated power; 60 μW was harvested at a range of about 4 km. Umeda [13] and Le [14] have presented more integrated wireless energy harvesters based on CMOS RF to DC rectifying circuits. CMOS-based rectifying power converters provide full compatibility with standard CMOS technologies and have advantages in batch processes for mass production. The drawback of CMOS-based diode connected transistors is the need to bias the gate of the transistors for the rectifying circuits to effectively function. This gate bias is provided externally, which makes the system not passive. Without the injection of external charges or a biasing of the transistor gate, the circuit has low efficiency, especially when the amplitude of the input voltage is low [15]. Shameli [2] presented a passive CMOS RF to DC power converter with a

voltage sensitivity of 1 V at −14.1 dBm input, but the circuit efficiency was only 5 %. Zbitou [16] presented an RF to DC converter based on Schottky diodes and achieved 68 % efficiency at 20 dBm RF input power. Ungan [17,18] presented antennas and high quality factor RF to DC power converters at 24 MHz and 300 MHz for RF wireless energy harvesting at -30 dBm input power. The power converter used high quality factor resonators for impedance matching the EM source and the diodes and achieved high open circuit voltage sensitivity of 1 V/µW. Boquete [19] presented a risk assessment system for calculating insurance premiums by monitoring mobile phone usage while driving. This was done by harvesting EM power from detected mobile phone usage during driving for risk assessment. Heikkinen [20] presented rectennas on different substrates at 2.4 GHz using transmisson lines to match the antennas output resistance (*at resonance*) to the rectifying diodes. Akkermans [21] presented a rectenna design by complex conjugating impedance provided by a microstrip structure to a diode so that resonance may be achieved for a working frequency. This design approach may need sophisticated tools to realize and the dominant resonance frequency of the rectenna can be unpredictable in practice. Hagerty [22] presented rectenna arrays for broadband ambient EM harvesting and characterized the harvesters from 2 GHz to 18 GHz; rectennas combine impedance matching the RF rectifying circuit and the antenna into one compact device, but an array of rectennas may increase the overall size of an EM harvester. Herb [23] and Vullers [24] have provided a comprehensive state of the art for micro energy harvesting and have explored the various techniques used for harvesting ambient renewable energy.

2. RF to DC Power Converter

2.1. Diode Rectifier

A junction diode equivalent circuit and simple Schottky diode rectifier are shown in Figure 1. R_{DS} is the diode resultant series resistance, C_{DS} is the diode resultant series capacitance, R_{DP} is the diode resultant parallel resistance, C_{DP} is the diode resultant parallel capacitance, V_S is the sinusoidal source voltage and V_C is the voltage across the capacitor.

Figure 1. (**a**) Diode series equivalent model, (**b**) Diode parallel equivalent model, (**c**) Simple diode detector.

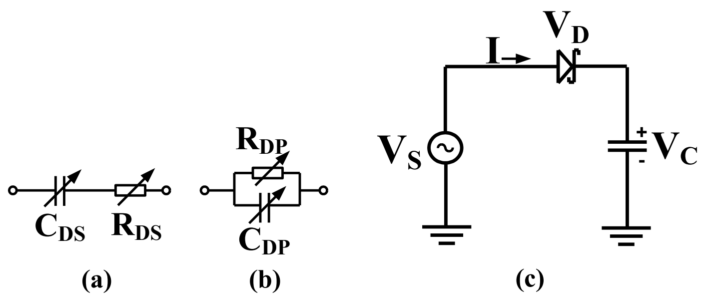

The diode capacitive impedance is mainly due to the junction capacitances provided by the metal, its passivation and the semiconductor forming the diode. AC power incident on a forward biased diode input is converted to DC power at the output. The current-voltage behavior of a single metal/semiconductor diode is described by the Richardson equation [25] as in Equation (1):

$$I = I_S\left(e^{\left(qV_D/_{nKT}\right)} - 1\right) \tag{1}$$

where I is the current through the diode, I_S is the saturation current, q is the charge of an electron, V_D is the voltage across the diode, T is the temperature in degrees Kelvin and K is Boltzmann constant. The voltage equation around the loop can be derived from Figure 1(c) and is given in Equation (2):

$$V_D = V_S - V_C \tag{2}$$

Since the same current flows through the diode and the capacitor, one can find the average current through the circuit by integrating Equation (1) over a time period. By substituting Equation (2) into Equation (1), V_C can be expressed in terms of V_S by averaging the diode current to zero. This is given in Equation (3) [26]:

$$V_C = \frac{KT}{q}\ln\left[\vartheta_0\left(\frac{qV_S}{KT}\right)\right], \tag{3}$$

where ϑ_0 is the series expansion of the sinusoidal source voltage. Equation (3) can further be simplified for very small amplitude V_S as Equation (4):

$$V_C \approx \frac{qV_S^2}{4KT} \tag{4}$$

Equation (4) shows that for a small voltage source, the circuit output voltage is proportional to the square of the input sinusoidal voltage; hence it's so-called square law operation. Extensions of this model for voltage multipliers and other input signals are presented in [27] and [28]. Equation (4) further confirms that for low input voltage (power $\leq$ 10 dBm), an impedance matching network between the source and the diode is necessary to improve the detected output voltage and efficiency.

2.2. Impedance Matching

The maximum power transfer theorem states that the highest power is transferred to the load when the source resistance is the same as the load resistance. For systems with both resistive and reactive impedances from source and load, the source and the load impedance should be adjusted in a way that they are the complex conjugate of each other through impedance matching. For the purposes of this work, a 50 Ω resistive source is chosen as reference for load impedance matching. The antenna which captures the ambient RF signals is tuned to provide this source resistance at resonance for the rectifying circuit in a complete EM wireless remote harvester. The load is the resistance of the Schottky diodes and the actual connected resistance (*remote sensor*). The specific type of matching network which can be used for complex conjugation depends on the nature of load or source impedance, the desired RF to DC converter functionality and other factors like circuit size, cost, *etc.* The response of a matched RF to DC power converter depends on the matching network used as well as the source or load component quality factors and impedances.

2.3. Diode Impedance

Schottky diodes HSMS-285C and HSMS-286C from Avago [29,30] are used to build the RF to DC power converters. The HSMS-285× or 286× series diodes can be operated as zero biased with relatively low forward junction potential. This allows for the realization of completely passive RF to DC power converters for wireless energy harvesting. The HSMS-285C or 286C is a pair of series connected Schottky diodes in a SOT-323 package. The impedance of the HSMS-285C and HSMS-286C diodes was first measured so it can be matched to the resistance (50 Ω) of the antenna source. This is done by connecting the input of the diodes to a network analyzer and measuring the scattering parameters. These scattering parameters are then converted to the corresponding impedances. The input impedance of a diode depends mainly on the resistive and capacitive impedance provided by the junction of the diode and its connected load. For a couple of diodes arranged in a package such as the HSMS-285C or 286C, the input impedance is the vector sum of the impedances provided by each diode in the package arrangement, the extra impedance associated with the packaging and the connected load. The diode measuring board is as shown in Figure 2. The diodes were measured at room temperature for an input power of -30 dBm at a diode connected load of 1 MΩ with a 100 pF filter capacitor. For the sake of this work, the input impedance of the diodes will always be referred to at these connected load conditions.

Figure 2. (**left**) Reference circuit layout for measuring diodes input impedance, (**right**) measuring printed circuit board (PCB) for diodes input impedance on 1 mm FR4 substrate.

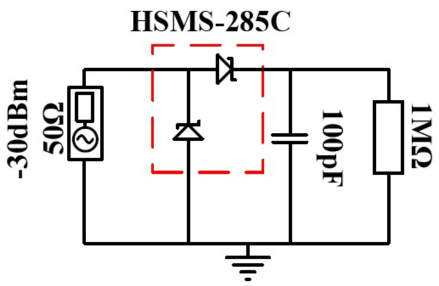

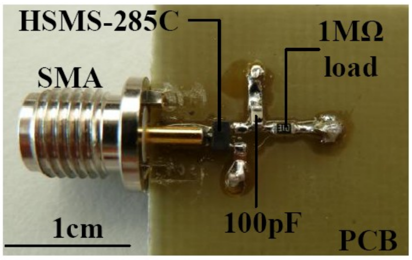

Figure 3. Measured input impedance (Δ resistive, □ capacitive) of HSMS-285C (**left**) and HSMS-286C (**right**) diodes at −30 dBm input with 1 MΩ load and 100 pF filter.

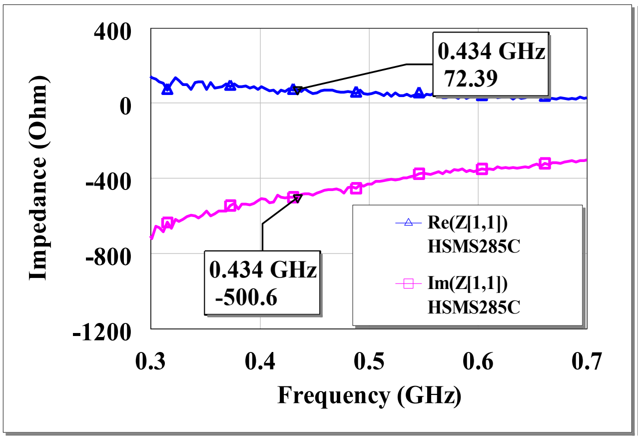

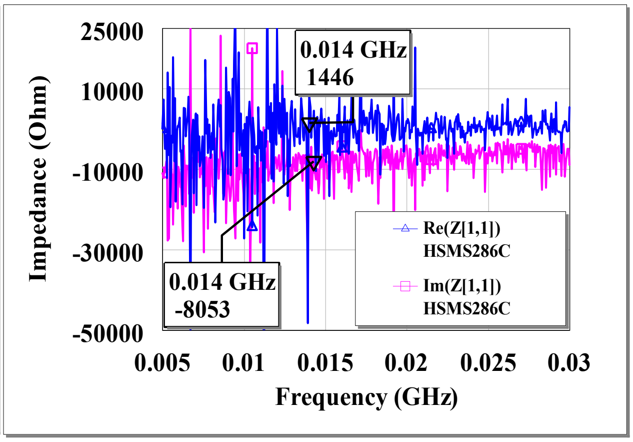

The board is fabricated such that components are soldered directly one into another to prevent additional impedances introduced by copper route. The PCB backside had the ground layer. An example of measured input impedance for HSMS-285C and HSMS-286C is shown in Figure 3.

The diodes quality factor is given by $X_{DS}R_{DS}^{-1}$, where X_{DS} is the resultant series capacitive impedance of the diodes. At an input power of −30 dBm, the measured input impedance of the HSMS-285C diodes is 72–j501 Ω at 434 MHz and 587–j1239 Ω at 13.6 MHz. For HSMS-286C diodes, it is 10–j503 Ω at 434 MHz and ~1.5–j8.1 kΩ at 13.6 MHz for −30 dBm input. The measured impedance of the HSMS-286C diodes at low frequencies (< 60 MHz) shows pronounced fluctuations. The low-frequency excess flicker noise and the shot noise observed in the HSMS-286C have been studied by several authors [31–33]. The pronounced presence of trap states in the depletion region of the semiconductor, mobility fluctuations in carriers, edge effects among other reasons is reported to cause deviations from the ideal Schottky diode behavior and hence generation-recombination noise for some diodes such as the HSMS-286C [34]. When a diode rectifier is matched at a reference operating condition, the matching network may function less effectively at other input power levels, connected load and other operating frequencies. This is due to possible changes in the diode input impedance. Throughout this work the imperfections of the matching circuit at other operating conditions away from the matched reference conditions are accepted without changes to the matching network.

2.4. Voltage Doubler

The Delon voltage doubler and Greinacher doubler are both used to realize the RF to DC power converters presented in this work. The Delon voltage doubler and Greinacher doubler are shown in Figure 4. The diodes output voltage (V_{out}) is doubled what is detected by a simple detector circuit shown in Figure 1. Both doublers produce the same output performance, the only difference is that the Delon doubler has an instantaneous input ground which is not shared with the output.

Figure 4. Circuit diagram of voltage doubler, (**a**) Delon doubler and (**b**) Greinacher doubler.

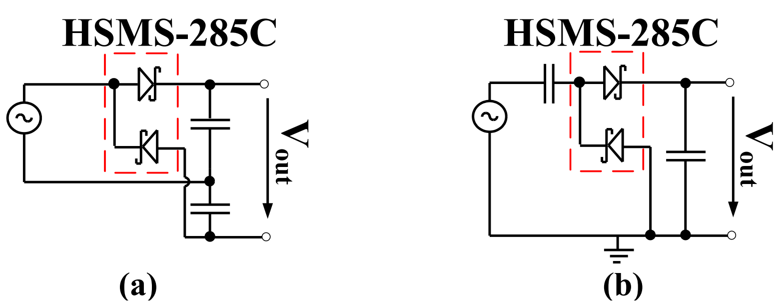

2.5. Matching Techniques for Antenna Source and RF to DC Power Converter

2.5.1. L-match RF to DC Power Converter

An L-match network converts a source series impedance to its equivalent load parallel impedance or *vice-versa* and tunes out by subtracting or adding any surplus reactance from the load or source with the counter impedance. Series impedance is converted to its parallel equivalent impedance using Equations (5–7):

$$Q_S = \frac{X_S}{R_S} \tag{5}$$

$$Q_P = \frac{R_P}{X_P} \tag{6}$$

where *Xs* is the total series reactive impedance, *Rs* is the total series resistance, R_P is the total parallel resistance, *Xp* is the total parallel reactive impedance, Q_S and *Qp* are the series and parallel quality factors respectively:

$$R_S + jX_S = \frac{R_P \times jX_P}{R_P + jX_P} \tag{7}$$

Equation (7) is the equation of a series sum of impedances and a parallel sum of impedances. It is interesting to note that Q_S and Q_P from an L-matched network may be different from the individual component quality factors as a result of the inherent resistive and reactive impedances in that component. By virtue of Equation (7), Q_S and Q_P must be equal in an L-matched network. Using Equations (5,6) and (7), the ratio of the parallel resistance (*or reactance*) to the series resistance (*or reactance*) can be derived in terms of the quality factors Q_P or Q_S [35]. Since at match conditions, only the resistive impedances dissipate power, the loaded quality factor *Q,* of the L-matched network can be expressed as in Equation (8):

$$R_P = (Q^2 + 1)R_S \tag{8}$$

Using Equations (5,6) and (8), series impedance can be converted to its parallel equivalent for a fixed frequency and power level. As an example; a series impedance 72–j501 Ω (HSMS-285C at 434 MHz for −30 dBm input power) is easily converted to −*j*510(3519)/(−*j*510 + 3519) Ω as its parallel equivalent with a component quality factor of 6.96. The source resistance is taken as part of the parallel matching network in an L-match circuit if the source series equivalent resistance is greater than the load series equivalent resistance. On the other hand, the load resistance is taken as part of the parallel matching network if the load series equivalent resistance is greater than the source series equivalent resistance. For the purpose of this work, inductors were only used for series impedance matching and capacitors as shunts. This prevents power seeping through any shunt inductor used for impedance matching due the short circuit provided by a shunt inductor to ground and resulting in less output efficiency. Resistors were not used for impedance matching.

2.5.2. L-match RF to DC Converter Generalized Analytical Model

The classical matching technique using Equations (5,6) and (8) is first used to L-match the 50 Ω resistance of the antenna to the resistance of the HSMS-286C diodes (and load) at 434 MHz for −30 dBm input and then the generalized model is discussed. The antenna source resistance was L-matched to the resistance of the diodes (and load). The 50 Ω resistance of the antenna is taken as the parallel matching component and the diodes 10 Ω resistance is the series matching component. The loaded *Q* is found as 2 between the 50 Ω antenna source resistance and the 10 Ω diode series resistance using Equation (8). From this loaded *Q*, a shunt capacitive impedance of 25 Ω (14.6 pF at 434 MHz) using Equation (6) and a series inductive impedance of 20 Ω (7.3 nH at 434 MHz) using Equation (5)

will match the 50 Ω source to the 10 Ω HSMS-286C diodes (and load) series resistance at −30 dBm input. Since the HSMS-286C diodes inherently provides 503 Ω series capacitive impedance at −30 dBm, a resultant series inductive impedance of 523 Ω (192 nH at 434 MHz) is needed to tune the 50 Ω resistive source to the complete HSMS-286C diodes impedance at 434 MHz for −30 dBm input. The L-matched HSMS-286C diodes rectifier is as shown in Figure 5(a).

Figure 5. (**a**) L-match RF to DC harvester using the HSMS-286C diodes at 434 MHz for −30 dBm input. (**b**) Small signal impedance model of a generalized L-matched RF to DC power converter as capacitive coupled series RLC resonator with different resonator elements.

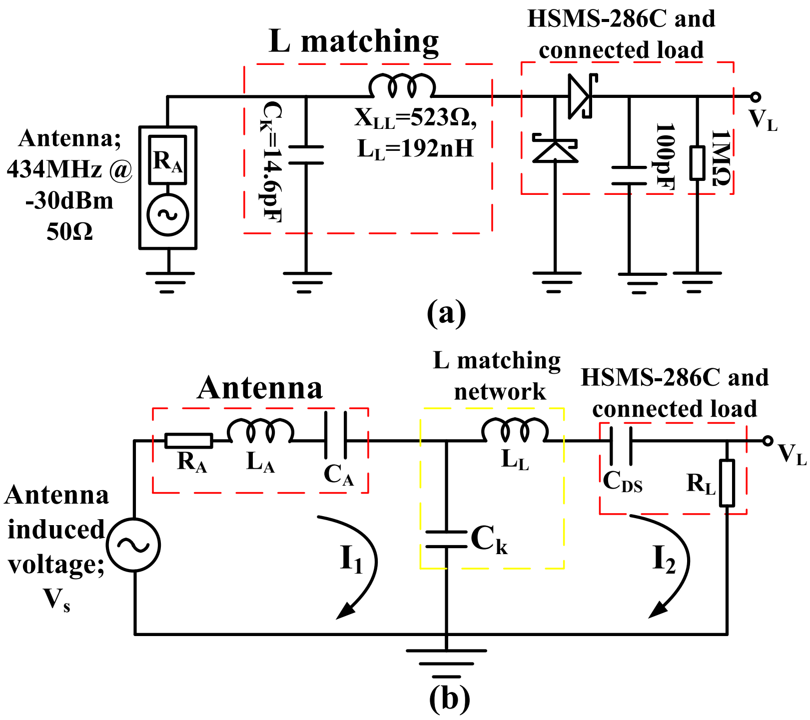

C_K is the tuning capacitance, L_L is the tuning inductance, X_{LL} is the tuning inductive impedance, C_{DS} is the diodes series capacitance, X_{DS} is the diodes series capacitive impedance, V_S is the antenna captured ambient EM voltage, R_A is the resistance of antenna, L_A is the inductance of antenna, C_A is the capacitance of antenna, R_L is the resultant series resistance from the diodes and the connected load resistance, V_L is the resistive load voltage. From Figure 5(a) the power dissipated in the resistance of the diodes (and connected load); P_L is given by Equation (9), where R_L is the series resistance of the diodes and load:

$$P_L = \frac{V_L{}^2}{R_L} \tag{9}$$

The source power; P_S is given by Equation (10), where V_S* is the root mean squared (RMS) antenna captured source voltage. Half of the source power is transferred to the resistance of the diodes (and connected load) at match conditions as described by the maximum power transfer theorem:

$$P_S = \frac{V_S{}^2}{R_A} \quad \text{or} \quad P_S = \frac{V_{S*}{}^2}{2R_A} \tag{10}$$

Equating P_L and half RMS P_S gives a condition of maximum voltage gain for the matched RF to DC power converter shown in Figure 5(a):

$$\frac{V_L}{V_{S*}} = \frac{1}{2}\sqrt{\frac{R_L}{R_A}} \tag{11}$$

From Equation (8), substituting the series and parallel resistance ratio into Equation (11) the voltage gain can be expressed in terms of the loaded quality factor as in Equations (12) and (13), where Q is the loaded quality factor of the RF to DC power converter:

$$\frac{V_L}{V_{S*}} = \frac{1}{2}\sqrt{\frac{1}{1 + Q^2}} \tag{12}$$

Equation (12) is the voltage gain in-terms of the loaded Q if the resistance of the diodes (and connected load) is part of the series matching network and the resistance of the antenna source is part of the parallel matching network as in Figure 5(a). If the resistance of the diodes is part of the parallel matching network, then Equation (13) may be written as the voltage gain in-terms of the loaded Q in an L-matched circuit:

$$\frac{V_L}{V_{S*}} = \frac{1}{2}\sqrt{1 + Q^2} \tag{13}$$

Equations (12) and (13) shows that the maximum voltage gain is directly related to the relative differences between the diodes (and connected load) resistance and source resistance at matched conditions or the circuit loaded quality factor. It is interesting to note that the circuit shown in Figure 5(a) has a loaded Q of 2, but an HSMS-286C unloaded quality factor of 50 (at 434 MHz for −30 dBm).

Figure 5(a) is generally modeled as capacitive coupling of two series RLC resonators with a voltage source. This linearized model can be made at any defined frequency and power level. The model however neglects the metal/semiconductor physics of the diode's junction potentials which results in a Schottky barrier. The first series RLC resonator is modeled as impedance from the antenna with or without some passive matching components. The voltage source V_S, is the antenna captured electromagnetic voltage. The second series RLC resonator is the impedance from the diodes (at a defined condition), connected resistance and some passive matching components. Ck is modeled as the coupling element between the two series RLC resonators. Figure 5(b) gives a more general look at the special scenario shown in Figure 5(a). The voltage equations in the two loops are given by Equations (14,15) according to Kirchhoff's voltage loop laws, where ω is the angular frequency and I_1, I_2 are the currents in the first loop and second loop, respectively:

$$V_S = I_1\left[R_A + j\omega L_A - \frac{j}{\omega C_A} - \frac{j}{\omega C_K}\right] + \frac{jI_2}{\omega C_K} \tag{14}$$

$$0 = \frac{jI_1}{\omega C_K} + I_2\left[R_L + j\omega L_L - \frac{j}{\omega C_{DS}} - \frac{j}{\omega C_K}\right] \tag{15}$$

Using Cramers rule, I_2 can be expressed as:

$$I_2 = \frac{\frac{-jV_S}{\omega C_K}}{\left[R_A + j\omega L_A - \frac{j}{\omega C_A} - \frac{j}{\omega C_K}\right]\left[R_L + j\omega L_L - \frac{j}{\omega C_{DS}} - \frac{j}{\omega C_K}\right] + \frac{1}{\omega^2 C_K^2}}. \tag{16}$$

The voltage across R_L is V_L; given by I_2R_L:

$$V_L = \frac{\frac{-jV_S}{\omega C_K} R_L}{\left[R_A + j\omega L_A - \frac{j}{\omega C_A} - \frac{j}{\omega C_K}\right]\left[R_L + j\omega L_L - \frac{j}{\omega C_{DS}} - \frac{j}{\omega C_K}\right] + \frac{1}{\omega^2 C_K^2}} \tag{17}$$

The voltage gain of the coupled resonator can be expressed as in Equation (18):

$$\frac{V_L}{V_S} = \frac{\frac{-jR_L}{\omega C_K}}{\left[R_A + j\omega L_A - \frac{j}{\omega C_A} - \frac{j}{\omega C_K}\right]\left[R_L + j\omega L_L - \frac{j}{\omega C_{DS}} - \frac{j}{\omega C_K}\right] + \frac{1}{\omega^2 C_K^2}} \tag{18}$$

At resonance, there is no resultant reactance in the RLC resonators or the capacitive and inductive impedances become equal; hence Equation (19) can be written:

$$\omega L_A - \frac{1}{\omega}\left\{\frac{1}{C_A} + \frac{1}{C_K}\right\} = 0 \text{ and } \omega L_L - \frac{1}{\omega}\left\{\frac{1}{C_{DS}} + \frac{1}{C_K}\right\} = 0 \tag{19}$$

Equations in Equation (19) can be used to find the resonant frequencies of the series coupled resonator. The voltage gain of the coupled resonator at resonance can then be expressed as in Equation (20):

$$\frac{V_L}{V_S} = V_{gain} = \frac{\frac{-jR_L}{\omega C_K}}{R_A R_L + \frac{1}{\omega^2 C_K^2}} \tag{20}$$

where V_{gain} is the voltage gain. V_{gain} at resonance is a function of the resistance of the source and load and the coupling element. The maximum of Equation (20) is obtained when:

$$\frac{dV_{gain}}{dC_K} = 0. \tag{21}$$

This gives the results as in Equation (22):

$$\frac{dV_{gain}}{dC_K} = \frac{j2R_L}{\omega^3 C_K^4} - j\left\{R_A R_L + \frac{1}{\omega^2 C_K^2}\right\}\frac{R_L}{\omega C_K^2} = 0 \text{ or } R_A R_L^2 = \frac{R_L}{\omega^2 C_K^2} \tag{22}$$

Equation (22) can be simplified to find $C_{K(max)}$:

$$C_{K(\max)} = \pm\frac{1}{\omega}\sqrt{\frac{1}{R_A R_L}} \tag{23}$$

where C_{Kmax} is the value of the coupling element where maximum power transfer from the first resonator to the second resonator occurs. Using Equations (19) and (23) the unknown optimal matching impedances can be found from the known impedances just like the classical L-matched procedure using Equations (5,6) and (8). By substituting $C_{K(max)}$ into Equation (20) and taking the magnitude of V_{gain}, gives the maximum voltage gain of the coupled series resonator at resonance:

$$\left|\frac{V_L}{V_S}\right| = \frac{1}{2}\sqrt{\frac{R_L}{R_A}} \text{ or simply } \frac{V_L}{V_{S*}} = \frac{1}{2}\sqrt{\frac{R_L}{R_A}} \tag{24}$$

For wireless harvesters consisting of an antenna and a diode rectifying circuit, the diode resistive impedance at any condition is dependent on the diode realized parameters, signal frequency, connected load and the input power level. The source impedance is determined by the impedance of the antenna. For maximum efficiency, the ratio of the source resistance to the load resistance must tend to zero at matched conditions. The efficiency η of the circuit is given by Equation (25):

$$\eta = \frac{P_L}{P_S}; \eta \rightarrow 1 \ \ when \ \frac{R_A}{R_L} \rightarrow 0 \tag{25}$$

2.5.3. L-Match RF to DC Converter Experimental Results and Discussion

The presented circuit was L-matched between the 50 Ω resistance of the antenna source and the resistance of the HSMS-285C diodes (and load) at 434 MHz for −30 dBm input as shown in Figure 6. Since the series equivalent resistance of the HSMS-285C diodes and load (72 Ω) is greater than the 50 Ω series resistive antenna source, the diode is taken as parallel matching network with a parallel equivalent impedance of $-j510(3519)/(-j510 + 3519)$ Ω. The analysis follows the same procedure as in Section 2.5.2 after this step. Figure 6(b) shows the resultant L-matched RF to DC power converter. C_{DP}* is the resultant shunt matching capacitance.

Figure 6. (**a**) L-matched impedance circuit for matching the HSMS-285C diodes at 434 MHz for −30 dBm input. (**b**) Resultant network, (**c**) PCB layout of the L-matched Delon doubler with adjusted values on FR4 substrate (**d**) Fabricated PCB of the L-network matched Delon voltage doubler.

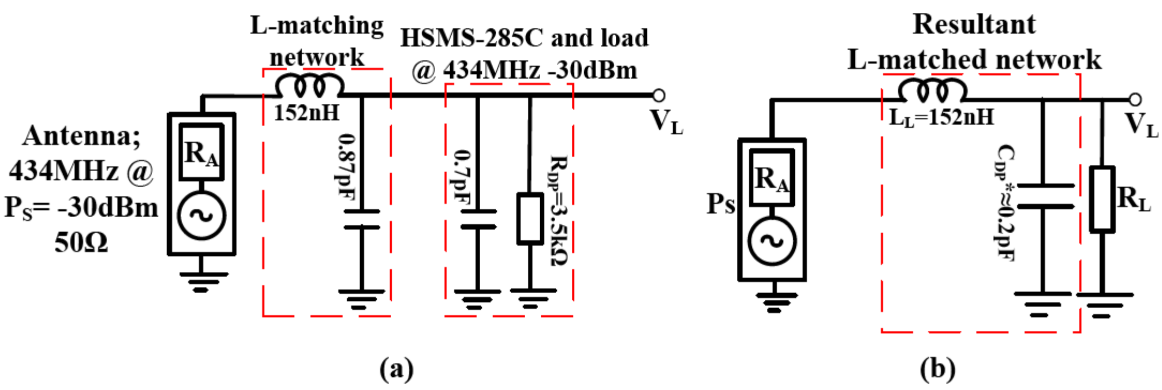

Figure 6. *Cont.*

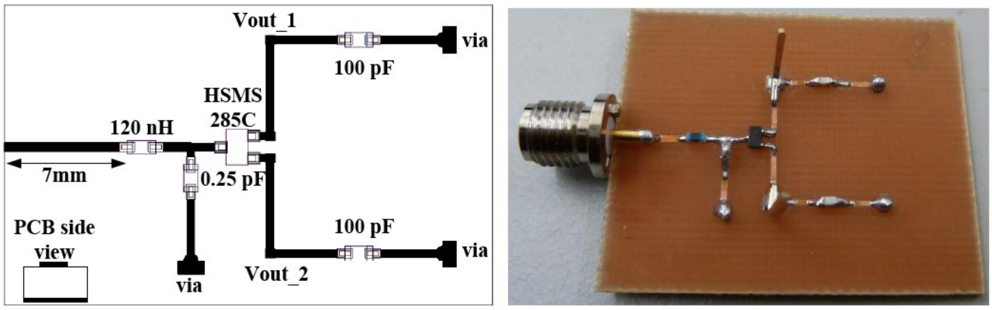

(c) (d)

Figure 6(a,b) assume perfect characteristic impedance between the various components in the matched circuit. When a copper route is introduced between components and on a material substrate, it must be accounted for in the total impedance as seen by the source or load. This PCB impedance compensation is carried out in Advance Design Systems (ADS) from Agilent [36]. ADS has extensive models for microstrip substrates to account for its impedances. The optimized layout using ADS microstrip models and its compensated values in the passive tuning components for a Delon doubler is shown in Figure 6(c).

The circuit reflection coefficient (S_{11}) and input impedance at open circuit are shown in Figure 7. There is high return loss and resonance around 434 MHz. The circuit input impedance at open circuit conditions is ~38 Ω at resonance for −40 dBm and ~17 Ω at −10 dBm input.

The measured L-matched circuit efficiency and voltage sensitivity is shown in Figure 8. The maximum measured L-matched efficiency at −30 dBm is 22% at ~20 kΩ load and an open circuit voltage of 124 mV. At −10 dBm, the maximum efficiency and open circuit voltage is 47% and 2 V respectively. At the optimal load of ~20 kΩ, the detected voltage is 58 mV and 1 V at −30 dBm and −10 dBm respectively.

Figure 7. Measured open circuit S_{11} of the L-matched Delon circuit at different input power levels from a 50 Ω source (**left**), measured open circuit input impedance at −10 dBm and −40 dBm of the L-matched circuit (**right**).

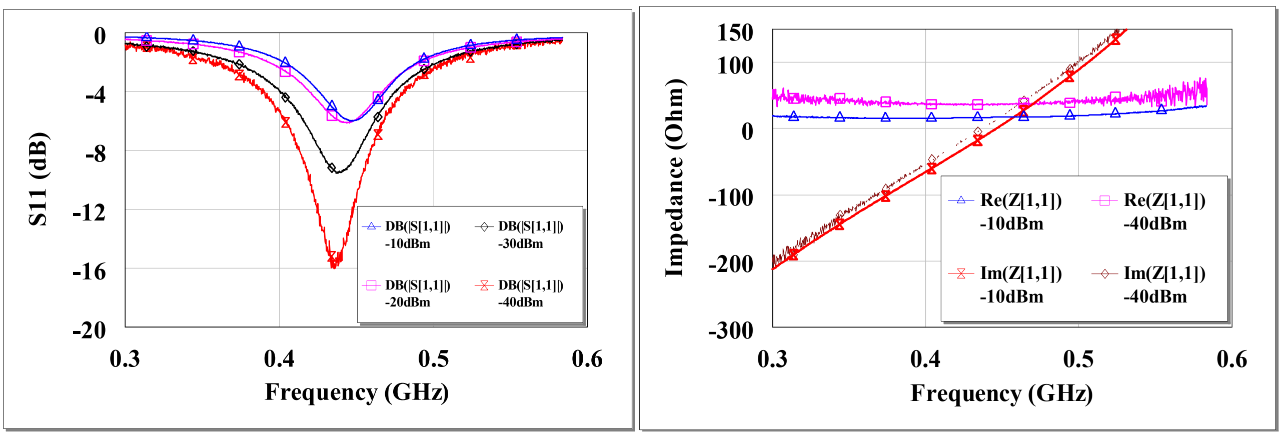

The open circuit voltage gain is 25 at −30 dBm and 40 at −10 dBm. The maximum measured efficiency at −35 dBm is 27%. This is higher than that of −30 dBm due to the better matched circuit

impedance at −35 dBm (35 Ω) than at −30 dBm (27 Ω) input. The L-matched RF to DC power converter has a loaded Q, sensitivity and efficiency determined mainly by the diodes resistance, diodes junction potential, connected resistance and antenna source resistance at matched conditions.

Figure 8. Measured L-matched circuit efficiency *versus* resistive load at various input power levels at 434 MHz (**left**), measured open circuit voltage and at 17 kΩ load *versus* input power at 434 MHz (**right**).

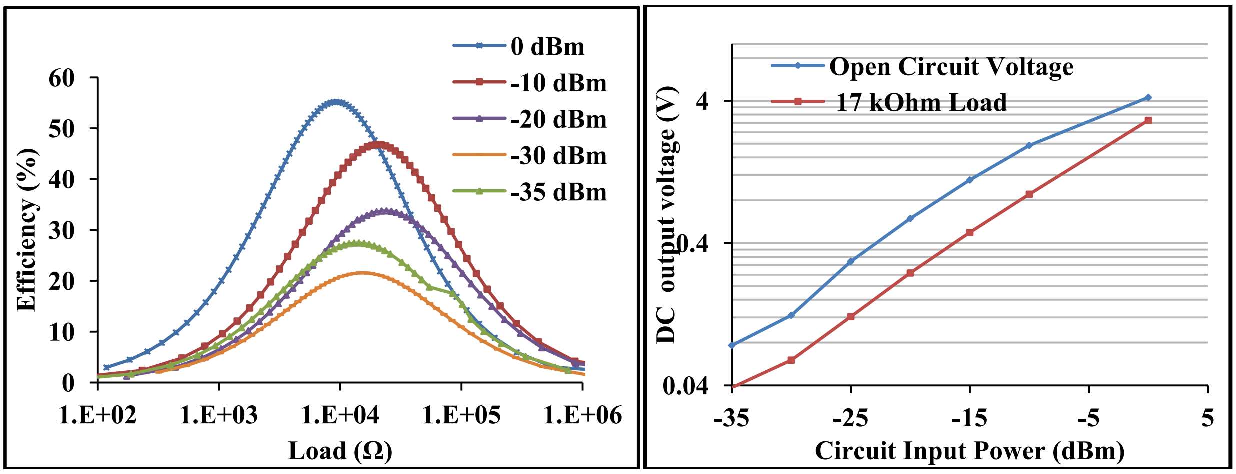

2.5.4. PI-match RF to DC Power Converter

A highly selective or small frequency bandwidth RF power converter is realized with a PI-network in-between the source impedance from the antenna and the diode rectifier. A PI-network is a 'back to back' L-network that are both configured to match the load and source impedance to an invisible resistance located at the junction between the two L-networks [37]. The quality factor of the L-network with the parallel resistance is given by Equation (26):

$$Q_P^* = \sqrt{\frac{R_P}{R^*} - 1}, \tag{26}$$

where R_P is the parallel resistance, R^* is a virtual resistance and Q_P^* is the quality factor of the L-network with the parallel resistance. The quality factor of the L-network with the series resistance is given by Equation (27):

$$Q_S^* = \sqrt{\frac{R_S}{R^*} - 1}, \tag{27}$$

where Q_S^* is the quality factor of the L-network with the series resistance. The unloaded quality factor; Q_S^* or Q_P^* is set higher than what is normally achieved with a single L-network [37] to realize the small frequency bandwidth circuit. The resistance of the load is assigned the parallel network in a PI-matched circuit if its series equivalent resistance is higher than the source series equivalent resistance; the opposite is true if the source is higher than the load. Equation (26) and Equation (27) are synonymous to Equation (8), except the lowest resistive impedance in Equation (8) is substituted with the virtual resistance which is dependent on the newly desired circuit selectivity. From Equations (26) and (27) the loaded quality factor of the PI-matched circuit can be written as Equation (34) in terms of Q_S^* and Q_P^*:

$$Q^2 = \left[\left(\frac{Q_P^{*2} + 1}{Q_S^{*2} + 1}\right) - 1\right], \tag{28}$$

where Q is the loaded quality factor of the PI-network. Q_S* or Q_P* are the unloaded quality factors of the PI-matched network. The larger value among the unloaded quality factors result in small frequency bandwidth response which is desired when matching a source and load impedance with a PI-network. Some authors approximate the highest value of Q_S* or Q_P* or their algebraic sum as the loaded quality factor of the PI-network as in [35] and [37], but Equation (28) gives the exact loaded Q of the PI-matched circuit in terms Q_S* and Q_P*. This allows for the correct estimation of the maximum voltage gain from the loaded quality factor.

2.5.5. Selectivity RF to DC Converter Generalized Analytical Model

An example of a PI-matched RF to DC converter using the HSMS-285C diodes operating at 434 MHz for −30 dBm input is presented first and then the generalized model is discussed. The circuit is matched for Q_P* of 60 between the antenna and the resistance of the diodes as shown in Figure 9.

Figure 9. Impedance diagram of PI-matched RF power converter; (**a**) Impedance diagram of 50 Ω source and the HSMS-285C diodes at 434 MHz, (**b**) Resultant PI matched network between the antenna source and load resistance.

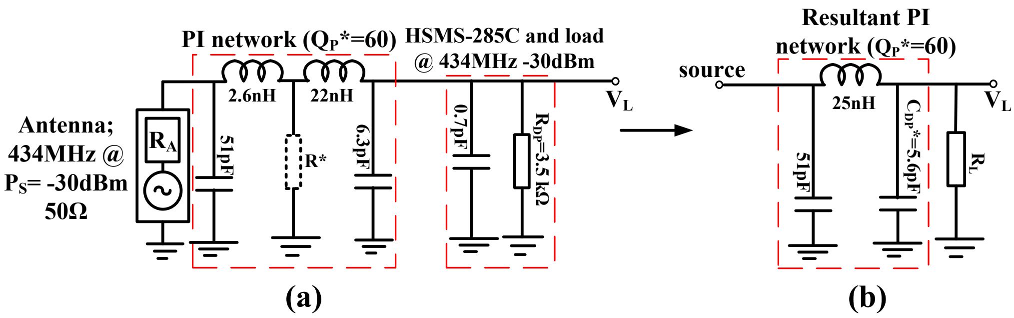

Figure 9(b) can also be modeled as an inductive coupling of two parallel RC circuits. A more general look at such a circuit is shown in Figure 10, as an inductive coupling of two parallel RLC resonators with a current source.

Figure 10. Inductive coupled parallel RLC small signal model of a generalized PI-matched antenna and diode rectifier.

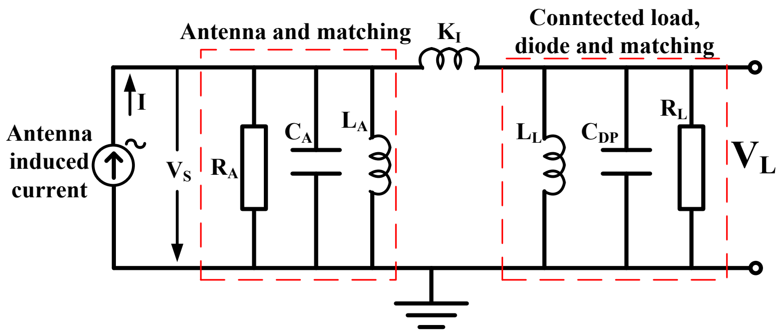

The first parallel RLC resonator is modeled as impedance from the antenna and some passive matching components. The second parallel RLC resonator is modeled as impedance from the linearized diodes, its connected load and some passive matching components. I is the antenna induced current, V_S this time is the voltage across the parallel R_A and K_1 is the coupling element between the two parallel resonators. Using Kirchoff's current laws, the node equations can be expressed as Equations (29) and (30):

$$I = V_S\left[\frac{1}{R_A} + j\omega C_A - \frac{j}{\omega L_A} - \frac{j}{\omega K_1}\right] + \frac{jV_L}{\omega K_1} \tag{29}$$

$$0 = \frac{jV_S}{\omega K_1} + V_L\left[\frac{1}{R_L} + j\omega C_{DP} - \frac{j}{\omega L_L} - \frac{j}{\omega K_1}\right] \tag{30}$$

Load voltage (V_L) and the source voltage (V_S) at resonance are given by the equations in Equation (31). The resonance frequencies are given by Equation (32):

$$V_L = \frac{\frac{-jI}{\omega K_1}}{\left[\frac{1}{R_A R_L} + \frac{1}{\omega^2 K_1^2}\right]} \quad \text{and} \quad V_S = \frac{\frac{I}{R_L}}{\left[\frac{1}{R_A R_L} + \frac{1}{\omega^2 K_1^2}\right]} \tag{31}$$

$$\omega C_A - \frac{1}{\omega}\left\{\frac{1}{L_A} + \frac{1}{K_1}\right\} = 0 \text{ and } \omega C_{DP} - \frac{1}{\omega}\left\{\frac{1}{L_L} + \frac{1}{K_1}\right\} = 0 \tag{32}$$

From V_L and Vs in Equation (31), the voltage gain at resonance can be expressed as:

$$\frac{V_L}{V_S} = \frac{R_L}{j\omega K_1} \tag{33}$$

The maximum of Equation (33) is obtained when:

$$j\omega K_1 \to 0 \quad or \quad R_L \to \infty \tag{34}$$

Since $j\omega K_1$ is restricted by the conditions in Equation (32) to attain resonance, one cannot manipulate $j\omega K_1$ alone without changing the resonance conditions. What can drive the voltage gain is if R_L is very large at resonance conditions. If the input impedance (V_S/I) of the coupled resonator is maximum at resonance, conditions in Equation (35) hold:

$$\left(\frac{Vs}{I}\right) \to maximum \quad when \ \frac{R_L}{\omega^2 K_1^2} \to 0 \tag{35}$$

Equation (36) may be assumed when $\frac{R_L}{\omega^2 K_1^2} \to 0$:

$$\frac{V_S}{I} = R_A \tag{36}$$

Under these conditions and an optimal coupling coefficient K_{1max}, the maximum voltage gain of the parallel coupled resonator can be written as in Equation (37), where K_{1max} is given by Equation (38):

$$\left|\frac{V_L}{V_S}\right| = \left|V_{gain}\right| = \left|\frac{1}{2}\sqrt{\frac{R_L}{R_A}}\right| \quad (37)$$

$$K_{1(\max)} = \mp \frac{1}{\omega}\sqrt{R_A R_L} \quad (38)$$

The analysis of Section 2.5.2 and parallel coupled RLC resonators show that any antenna and matched rectifying diode can be described as an equivalent circuit of a coupled resonator at a defined operating point. This general model can be applied to optimize other harvesters with complex output impedance such as piezo-harvesters or vibration harvesters for maximum transfer of power or voltage to its connected load. The model can also be applied to near field magnetically coupled antennas/coils for optimization.

2.5.6. Broadband RF to DC power converter

A broadband network is preferred when an RF to DC power converter is to be operated for a wide range of frequencies. A broadband converter is realized by connecting successive L-networks together in a multi-network between the antenna source and the rectifying diodes. The result is broadband or multiband RF power converter around certain frequencies. This can be deduced from the general model of a coupled resonators that by choosing certain passive components between a source and the load, it is possible to have more frequencies (ω) fulfilling Equation (32) and hence a result of multiple resonant frequencies or broader bandwidth at match conditions. For a two stage L-connected match, the quality factor of the L-network with the parallel resistance is given by Equation (39):

$$Q_P^{*} = \sqrt{\frac{R_P}{R^{*}} - 1} \quad (39)$$

The quality factor of the L-network with the series resistance is given by Equation (40):

$$Q_S^{*} = \sqrt{\frac{R_{*}}{R_S} - 1} \quad (40)$$

From Equations (39) and (40) the loaded quality factor of the two stage L-connected broadband network may be written as Equation (41) in terms of the unloaded quality factors; Q_S* and Q_P*:

$$Q^2 = \{(Q_P^{*2} + 1)(Q_S^{*2} + 1)\} - 1 \quad (41)$$

R^* in this case may be chosen if it is larger than R_S and lower than the R_P. The highest possible bandwidth between a resistive source and resistive load is found for a virtual resistance (R^*) given in Equation (42) [37]:

$$R^{*} = \sqrt{R_S R_P} \quad (42)$$

For complex loads such as rectifying diodes or transistors, the largest achievable bandwidth prescribed by Equation (42) is limited by the load or source component quality factor, since Equation (42) does not take into account reactive impedance associated with the source or load.

2.5.7. Broadband-Match RF to DC Converter Results and Discussion

The antenna source resistance was broadband matched to the HSMS-285C diodes (and load) resistance at −30 dBm input around 434 MHz. For a desired Q_P* and Q_S* of 2.7 there is ~0.4 pF inherent diode capacitance which is un-tuned using a two stage L-matching network [Figure 11(b)]. This is because the HSMS-285C diodes provides an inherent component quality factor of 6.96 at 434 MHz for −30 dBm input, hence a broadband circuit with Q_P* lower than this inherent component quality factor of the diodes (and load) is difficult to achieve without trade-offs. However, connected L-networks with Q_P* as high as the diode component quality factor may perform worse than a single L-matched network with similar loaded quality factor. This is due to redundant components of the connected L-networks which have inherent losses.

Figure 11. Impedance diagram of broadband RF power converter; (**a**) Broadband match around 434 MHz with loaded Q of 2.7, (**b**) Resultant impedance matching network with un-turned capacitance of 0.4 pF.

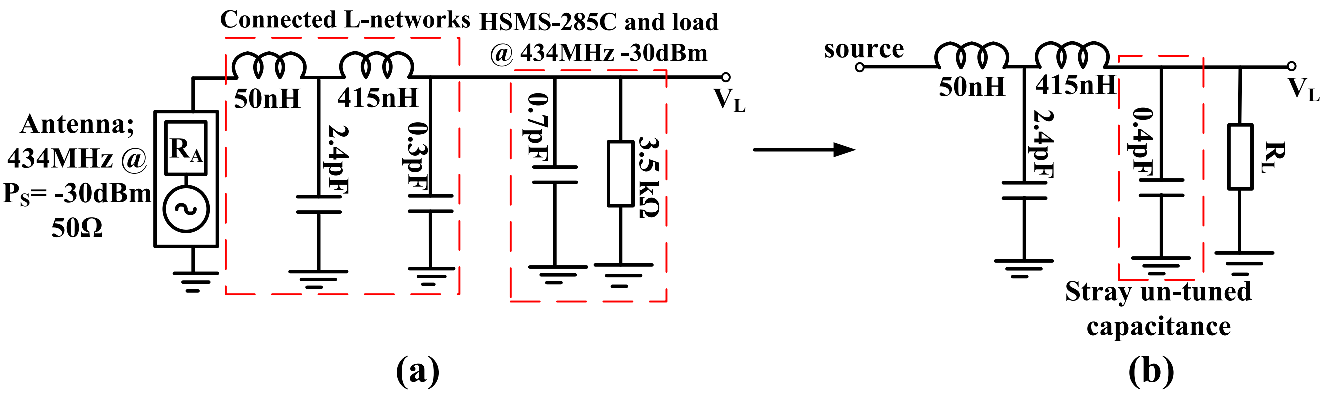

Figure 12. Measured open circuit S_{11} of the broadband circuit around 434 MHz at different input power levels from a 50 Ω source (**left**), measured open circuit input impedance at −10 dBm and −40 dBm of the broadband circuit (**right**).

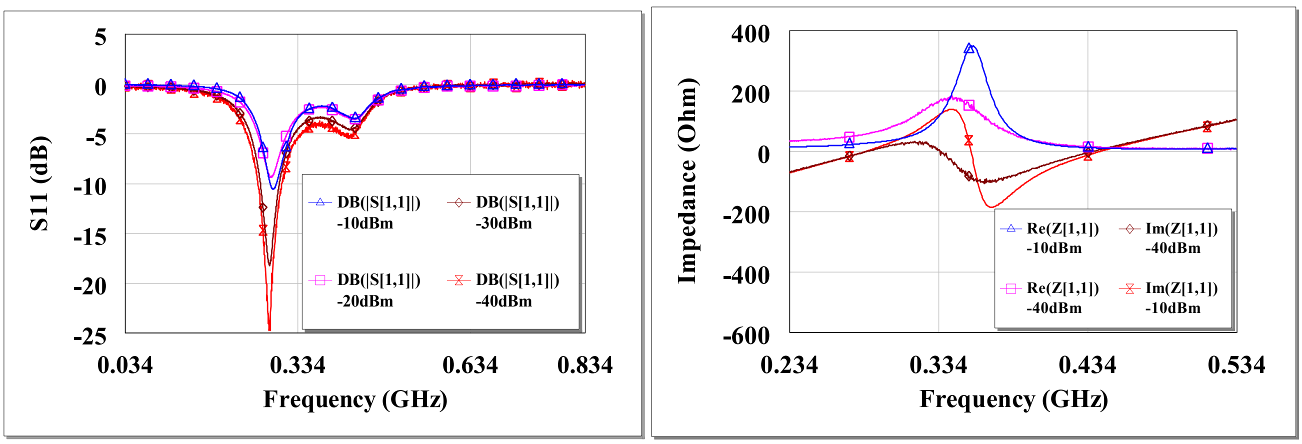

Therefore the broadband circuit is matched for Q_P* of 2.7, notwithstanding the un-tuned shunt capacitance as can be seen in Figure 11(b). Figure 12 shows the circuit S_{11} at various input power levels and input impedance at open circuit conditions. From Figure 12 (left) there is ~−5 dB return loss

from 200 MHz to 500 MHz providing an operating band of ~300 MHz. The impedance of the circuit shows resonances at ~290 MHz and ~450 MHz as shown in Figure 12(right). A third resonance occurs around 356 MHz at −10 dBm as the frequency of highest harvester input resistance (~350 Ω) and where the reactive impedances approach their extremes. Figure 12 show that a wireless EM harvester can exhibit different resonance scenarios depending on the dominant instantaneous conditions. The efficiency and voltage sensitivity of the broadband matched wireless EM harvester are shown in Figure 13. The average open circuit voltage is 47 mV and 1.1 V at −30 dBm and −10 dBm, respectively, when operating from 200 MHz to 500 MHz.

Figure 13. Measured open circuit voltage *versus* frequency sweep from 200 MHz to 500 MHz for −10 dBm and −30 dBm (**left**), measured efficiency at 17 kΩ load *versus* frequency sweep for −10 dBm and −30 dBm (**right**).

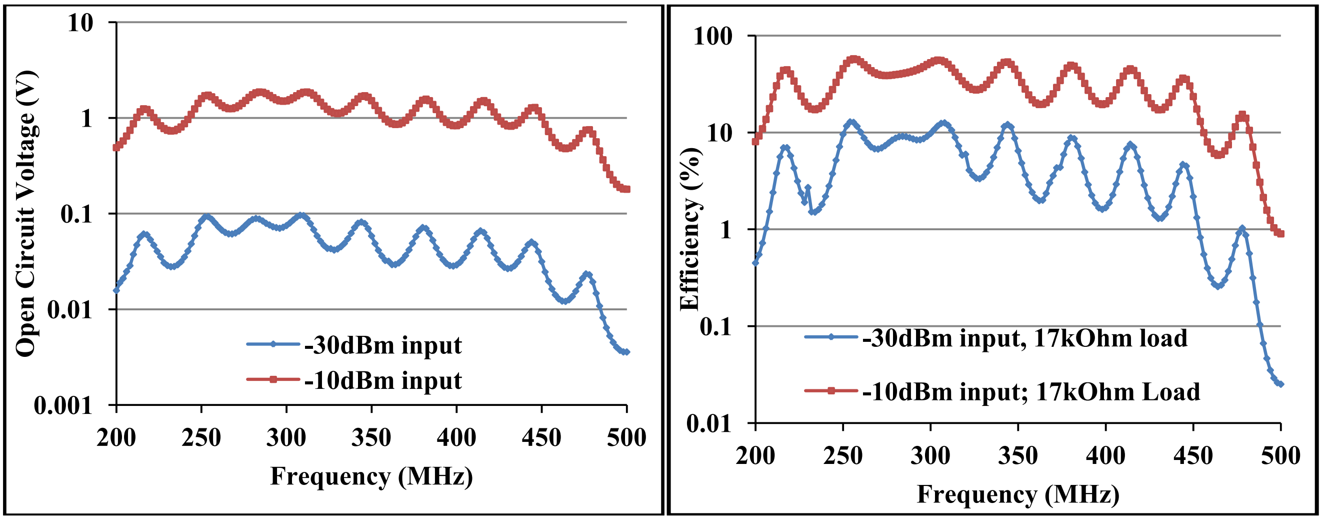

The broadband circuit achieves average efficiency of 5% at 17 kΩ load for −30 dBm and 30% at 17 kΩ load for −10 dBm input power from 200 MHz to 500 MHz. Figure 13 further confirm a direct link between frequency response and the unloaded quality factors. For Q_S* and Q_P* of ~2.7, the circuit response is broadband around 434 MHz.

2.6. High Voltage Sensitive RF to DC Converter

The current state of the art low power remote sensors would require a DC voltage supply of about 1 V and DC current of about 30 μA for operation. Therefore, the issue is not only how efficient a wireless EM harvester is in converting RF to DC power, but also what the output DC voltage and current of the EM harvester are at the RF input power level [38]. Equations (11,24) and (33) show that the maximum voltage sensitivity of a coupled resonator system or an RF to DC power converter is mostly related to the load and the source resistances at resonance. Therefore high voltage sensitive wireless EM harvester can be achieved with a diode voltage doubler with a very high input resistance relative to the antenna source without the need to cascade the diodes as in voltage multipliers. If the diodes been used for the RF to DC power conversion cannot provide high resistive impedance at the working frequency relative to the antenna source, then a DC-DC converter can be applied after the EM harvester as presented in [39] or the diodes may be cascaded by way of multipliers as presented in our

earlier work [40] and by several other authors [3,5,14]. In case of multipliers, the input voltage ought to be high enough to overcome the junction potential of the several diodes in the multiplier network. If frequency is not a constraint, then a frequency sweep *versus* impedance for the diodes can be made and the frequency where the diodes exhibits high resistive impedance can be used to realize high voltage sensitive wireless RF harvester. For Schottky diodes, high resistive impedance occurs mostly at lower frequencies (see Figure 3). The measured voltage gain of a high resistive diode pair (voltage doubler) is presented in the next results.

2.6.1. High Voltage Sensitive RF to DC Converter Results and Discussion

The presented result was L-matched using 50 Ω resistance of the antenna source and the resistance of the HSMS-286C diodes (and load). The HSMS-286C diodes do provide high resistive impedance at low frequencies; notwithstanding the flicker noise which causes its resistive (and reactive) impedance to fluctuate. The HSMS-286C has low forward junction potential (~350 mV at 1 mA) per diode and series impedance of ~1.5–j8.1 kΩ or parallel impedance of ~$-j8.3(46.3)/(-j8.3 + 46.3)$ kΩ at 13.6 MHz for −30 dBm input. Even though the HSMS-286C diodes unloaded component quality factor at 13.6 MHz is similar to that of the HSMS-285C diodes at 434 MHz, the elevated resistive impedance at 13.6 MHz fulfills the condition for high voltage sensitivity relative to a 50 Ω antenna source at resonance conditions.

Figure 14. (**a**) L-matched impedance diagram for matching the HSMS-286C diodes at 13.6 MHz at -30 dBm input. (**b**) Resultant network, (**c**) PCB layout of the L-matched Greinacher doubler with adjusted values due to impedances provided by copper route on FR4 substrate with thickness of 1 mm. (**d**) Fabricated PCB of the L-matched RF to DC power converter.

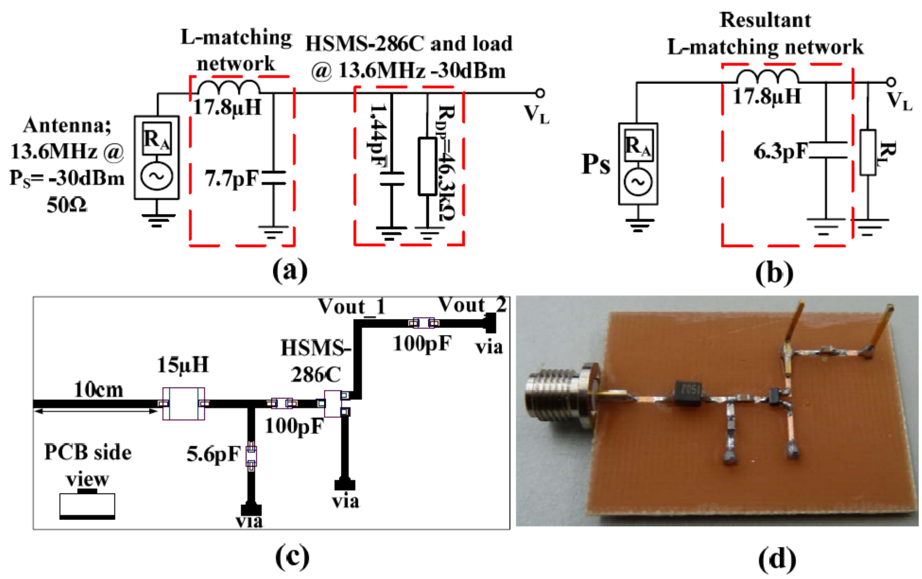

The high voltage sensitive EM harvester operating at 13.6 MHz is as shown in Figure 14. On the realized PCB is a Greinacher doubler. An inductance of 15 µH and a shunt capacitance of 5.6 pF were the adjusted values after the microstrip contributions.

The measured S_{11} and input impedance at open circuit are shown in Figure 15. There is high return loss and resonance around 13.6 MHz. The circuit input impedance at open circuit conditions is 58 Ω at resonance for both −40 dBm and −10 dBm.

Figure 15. Measured open circuit S_{11} of the L-matched HSMS-286C diodes at 13.6 MHz for different input power levels from a 50 Ω source (**left**), measured open circuit input impedance at −10 dBm and −40 dBm of the L-matched HSMS-286C diode at 13.6 MHz (**right**).

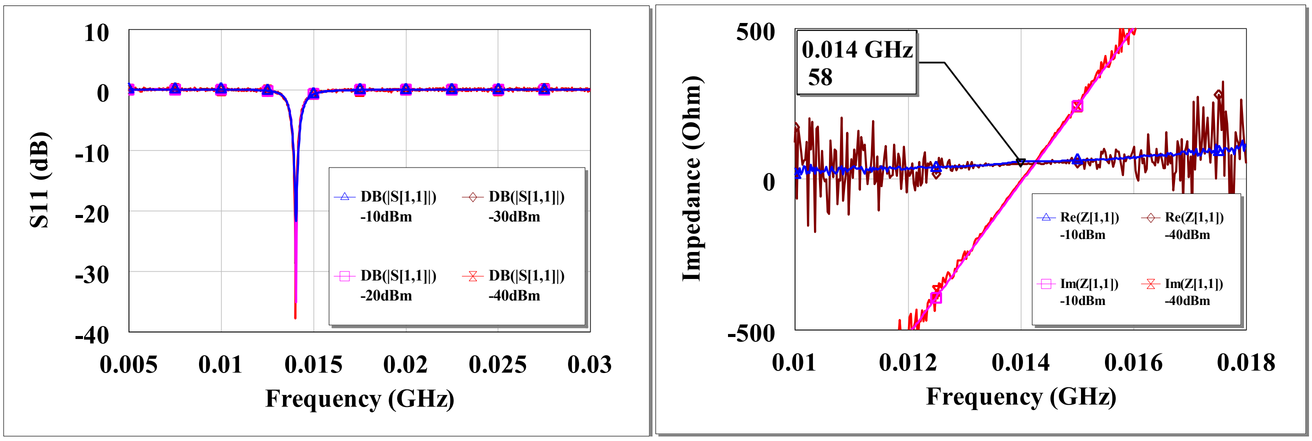

The efficiency and voltage sensitivity of the high voltage sensitive wireless EM harvester are shown in Figure 16.

Figure 16. Measured circuit efficiency *versus* load at various input power levels at 13.6 MHz (**left**), measured open circuit voltage and at 200 kΩ load *versus* input power at 13.6 MHz (**right**).

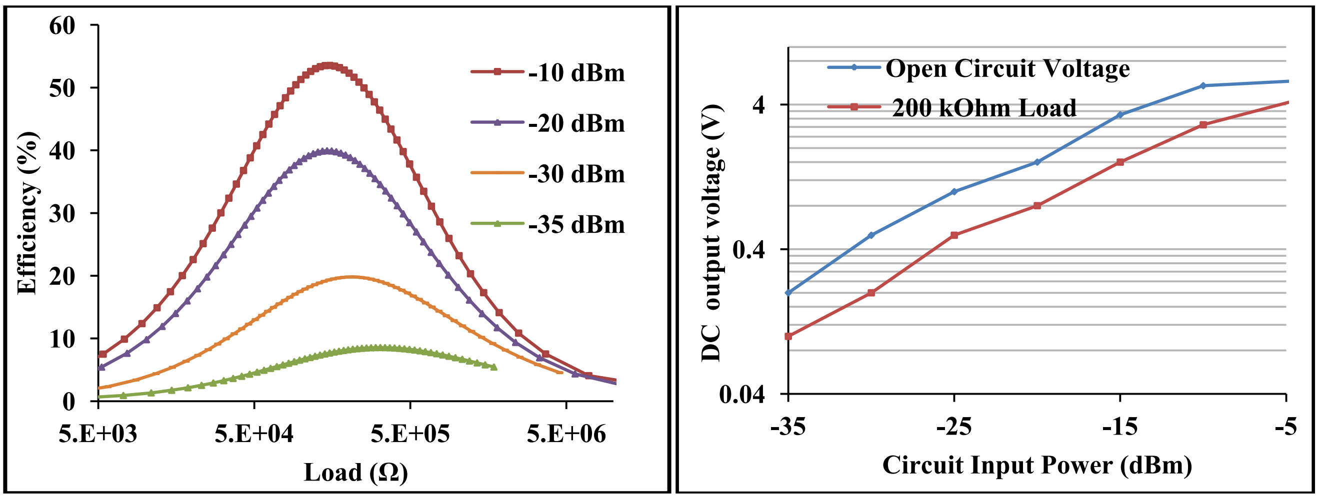

The maximum measured efficiency at −30 dBm is 20% for ~200 kΩ load and an open circuit voltage of 0.5 V. At −10 dBm, the maximum efficiency and open circuit voltage are 54% and 5.4 V respectively. At the optimal load of ~200 kΩ, the detected voltage is 0.2 V and 2.9 V at −30 dBm and −10 dBm respectively. The open circuit voltage gain is 100 at −30 dBm and 108 at −10 dBm.

Even though the RF to DC converter presented in Section 2.5.3 is the same as the L-match circuit realized with the HMSM-286C diodes at 13.6 MHz, the voltage gain is increased by a factor of 4 due to the large difference between the diodes (and load) resistance and source resistance so that at matched conditions high voltage gain occurs. The loaded Q of the L-matched circuit is 30 which results in small frequency bandwidth just like a PI-matched diode rectifier presented in our earlier work [40]. From this result and the results from our earlier presented PI-matched EM harvester, it can be inferred that all high loaded Q RF to DC circuits have high selectivity but not all highly selective RF to DC circuits have high loaded Q. The voltage sensitivity of the matched HSMS-286C diode at 13.6 MHz can be improved if its resistive impedance is not lowered by the flicker noise.

3. Wireless EM Power Harvester

A wireless EM harvester, consisting of a rectifying antenna (*rectenna*) was designed to find a compromise between size and performance of its antenna. The rectenna is shown in Figure 17.

Figure 17. Rectenna realized on a Duroid 5880, 1.57 mm substrate. (**a**) Backside of the rectenna, (**b**) cross-section of antenna output coplanar stripline dimensions (**c**) frontside of the rectenna.

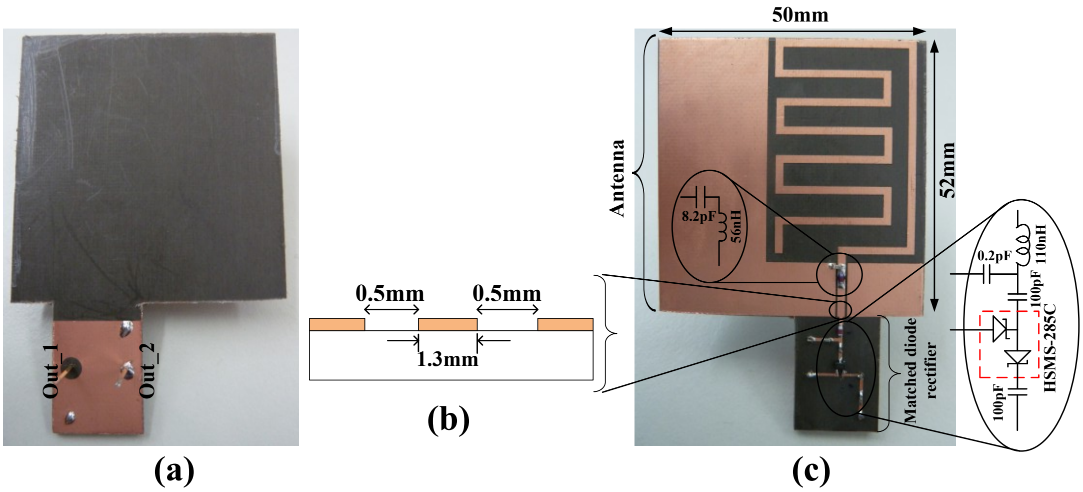

The antenna (planar) part of the rectenna is based on our earlier work [41]. In contrast to the earlier presented antenna, this rectenna is realized on a Duroid [42] substrate of thickness 1.57 mm. Duroid 5880 has lower loss tangent of 0.0004 at 1 MHz compared to 0.025 at 1 MHz for FR4. This means there is less loss in the transmission of signals on a Duroid PCB at this frequency range. The antenna part is fabricated to resonate around 434 MHz; hence its dimensions of 5 × 5.2 cm make it electrically small. The antenna is tuned with a chip inductor and a capacitor to achieve the resonance frequency around 434 MHz [Figure 17(c)]. This is done at a cost of reduced antenna radiation efficiency. An antenna is one of the few components the size of which is related to the operating frequency. Thus, if the size of an antenna is fixed, resonance frequency reduction of the antenna can only be achieved with penalty factors [10]. The antenna's output impedance is tuned with the dimensions of the coplanar stripline as shown in Figure 17(b).

HFSS [43] was used to simulate the presented antenna and to find the correct capacitive and inductive components for frequency tuning before the optimized design was fabricated. The simulated antenna resonances occur at 438 MHz and 445 MHz. At these frequencies, the radiation efficiency is 20% and a peak gain of −6 dBi. The rectifying part of the rectenna consists of L-matched HSMS-285C diodes (Figure 17(c)). The L-matched HSMS-285C part of the rectenna can be engineered to be as small as possible if required. The separate parts of the rectenna were characterized by terminating their ends and measuring the individual reflection coefficients just like the power converters presented in Section 2. Figure 18 shows the measured antenna and matched rectifier individual S_{11} and impedance. Figure 18 (left) also show the HFSS simulated S_{11} results. From Figure 18 (right), the measured antenna resonance where the input impedance is at maximum is ~434 MHz. At ~434 MHz, the antenna input resistance is 376 Ω and the reactive impedances approach their extreme (*so called anti-resonance*). The other resonance occurs when the input resistance is 'finite' and the reactive impedance is zero; at ~441 MHz. The input resistance is 57 Ω at ~441 MHz. The rectifier circuit is matched for the antenna's resistance at ~441 MHz.

Figure 18. Antenna HFSS simulated, antenna measured, and measured L-matched diode rectifier S_{11} on a Duroid 5880 PCB for −30 dBm input (**left**), Measured open circuit input impedance of antenna and rectifier at −30 dBm input (**right**).

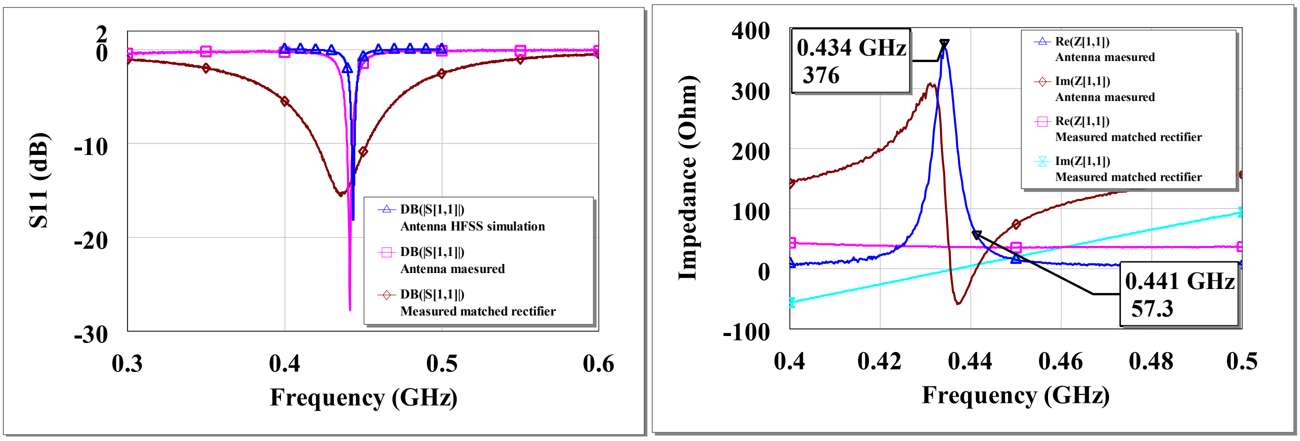

3.1. EM Range Results and Discussion

At far field between wireless EM transmitting and receiving antenna, the coupling mechanism between the transmitting and receiving antenna is neither capacitive nor inductive as is the case for the RF to DC converters. The coupling is radiative which can be described by the Friis equation of transmission on the assumption that the transmitting and receiving antenna are in free space [44]. A modified Friis equation for a transmitting and receiving antenna at far-field (R >> λ and R >> transmitting antenna largest dimension) to each other at a specified direction is given by Equation (43) [45]. Equation (43) assumes real world open space conditions:

$$\frac{P_r}{P_t} = F_{envt} G_t G_r \left(\frac{\lambda}{4\pi R} \right)^2, \tag{43}$$

where *Pr* is the power at the receiving antenna port, *Pt* is the power supplied at the transmitting antenna port, F_{envt} is a factor accounting for environmental effects as such ground reflections among others, *Gt and Gr* are the transmitting and receiving antenna gain (*at specified direction*) respectively. *R* is the distance between the transmitting and receiving antenna and λ is the wavelength of the transmitting EM wave. The rectenna receiving range measurements were carried out in an open space (*hall*) with the antennas 2 m above ground level. The transmitting and receiving antennas were arranged in the direction of their peak gain. The rectenna range performance is shown in Figure 19. According to Equation (43), the efficiency of RF power transferred between a sending and receiving antenna depends on controllable factors like the gain of the antennas in the arranged direction and the radiation efficiency of the antennas. Since the receiving/transmitting antenna's incorporated in remote harvesters for sensor powering are normally small in relation to their operating frequencies, they tend to be less efficient.

Figure 19. Rectenna receiving range performance by sending 17 dBm (50 mW) at a gain of −6 dBi at 437 MHz. Output DC voltage *versus* receiving distance for different loads (**left**), loads output power *versus* receiving distance (**right**).

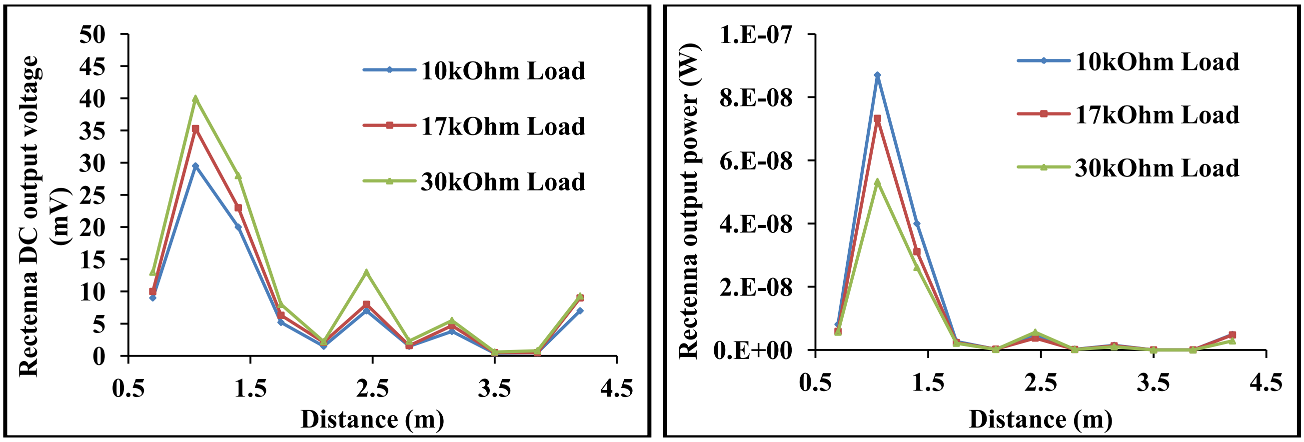

The efficiency of the rectenna's antenna is ~20% at resonance. A 'perfectly' matched RF to DC power converter operating in its square law region has efficiencies in the region of 20% as depicted in Section 2. The transmitting antenna was the same as the antenna incorporated in the rectenna. By transmitting the EM power with a small antenna (5 cm × 5.2 cm) at 437 MHz with efficiency of ~20% and at a gain of −6 dBi, the power delivered by the rectenna is generally low at far-field from the transmitter as can be seen in Figure 19. A mediocre transmitting antenna was used to transmit the EM waves due to limitations in the European Union about transmitting EM power at certain frequencies; so the goal in the rectenna range experiment is to show the lowest limit functionality of such a harvester. At 4.2 m from the electrically small transmitting antenna transmitting at 17 dBm, the rectenna harvested DC voltage and power are 9 mV and 5 nW respectively for 10 kΩ load. It can be seen from Figure 19 that the harvested voltage/power generally degrades as an inverse square of distance from transmitter as described by Friis equation. The measured received power however alternate along this R^{-2} fit as shown in Figure 19. This anomaly is accounted for by F_{envt} [Equation (43)] as influence of ground reflections and polarization in real world open field measurements [45]. For any particular distance *R*, the signals reflected from ground can be constructive with the direct signal to the rectenna,

in which case the measured power may be higher than that predicted by the original Friss equation as in [44]. The ground effect can also be destructive, in which case the measured power will be lower than what is predicted by the original Friis equation.

4. Conclusions

Optimization of Schottky diode-based RF to DC power converters using different matching techniques for wireless EM energy harvesting applications is presented. Using scattering parameters for small signal modeling, it is shown that wireless EM harvesters can be generally described as coupled resonators with efficiencies and maximum voltage sensitivity depending mostly on the source and load resistances under matched conditions. The analytical models allow systematic control in the design of passive wireless EM harvesters. Based on these analyses, a rectenna is built and tested for lower limit functionality from harvesting ambient EM waves. The analysis presented in this work may also be applied to optimize derivatives of wireless EM harvesters like RFID tags, NFC, wireless chargers *etc.*, for efficient powering of their sensors or integrated circuits. Generally, most energy harvesters and their matched loads can be described as coupled resonators and thus may be optimized with the methods presented in this work.

Acknowledgments

This work is part of the graduate program GRK 1322 Micro Energy Harvesting at IMTEK, University of Freiburg, funded by the German Research Foundation (DFG). Special thanks to Daniela Ohnemus for the PCB preparations and Uwe Burzlaff for antenna range measurements.

References

1. Fischer, J. NFC in cell phones: The new paradigm for an interactive world [Near-Field Communications]. *IEEE Commun. Mag.* **2009**, *47*, 22–28.
2. Shameli, A.; Safarian, A.; Rofougaran, A.; Rofougaran, M.; de Flaviis, F. Power harvester design for passive UHF RFID tag using a voltage boosting technique. *IEEE Trans. Microw. Theor. Tech.* **2007**, *55*, 1089–1097.
3. Karthaus, U.; Fischer, M. Fully integrated passive UHF RFID transponder IC with 16.7-µW minimum RF input power. *IEEE J. Solid-State Circuits* **2003**, *38*, 1602–1608.
4. Lee, S.H.; Jin, I.S. Interoperation of an UHF RFID reader and a TCP/IP device via wired and wireless links. *Sensors* **2011**, *11*, 10664–10674.
5. Mandal, S.; Sarpeshkar, R. Low-power CMOS rectifier design for RFID applications. *IEEE Trans. Circuits Syst. I: Regul. Papers* **2007**, *54*, 1177–1188.
6. Yu, H.; Bashirullah, R. A Low Power ASK Clock and Data Recovery Circuit for Wireless Implantable Electronics. In *Proceedings of IEEE Custom Integrated Circuits Conference, CICC '06*, San Jose, CA, USA, September 2006; pp. 249–252.
7. Hannan, M.A.; Abbas, S.M.; Samad, S.A.; Hussain, A. Modulation techniques for biomedical implanted devices and their challenges. *Sensors* **2011**, *11*, 297–319.

8. Cho, N.; Song, S.-J.; Lee, J.Y.; Kim, S.; Kim, S.; Yoo, H.-J. A 8-μW, 0.3-mm2 RF-powered Transponder with Temperature Sensor for Wireless Environmental Monitoring. In *Proceedings of IEEE International Symposium on Circuits and Systems, ISCAS*, Kobe, Japan, May 2005; Volume 5, pp. 4763–4766.
9. Brown, W.C. The history of power transmission by radio waves. *IEEE Trans. Microw. Theor. Tech.* **1984**, *32*, 1230–1242.
10. Mickle, M.H.; Mi, M.; Mats, L.; Capelli, C.; Swift, H. Powering autonomous cubic-millimeter devices. *IEEE Antennas Propag. Mag.* **2006**, *48*, 11–21.
11. McSpadden, J.O.; Chang, K. A Dual Polarized Circular Patch Rectifying Antenna at 2.45 GHz for Microwave Power Conversion and Detection. In *Proceedings of IEEE MTT-S International Microwave Symposium Digest*, San Diego, CA, USA, May 1994; Volume 3, pp. 1749–1752.
12. Sample, A.; Smith, J.R. Experimental Results with Two Wireless Power Transfer Systems. In *Proceedings of the 4th International Conference on Radio and Wireless Symposium*, San Diego, CA, USA, January 2009; pp. 16–18.
13. Umeda, T.; Yoshida, H.; Sekine, S.; Fujita, Y.; Suzuki, T.; Otaka, S. A 950-MHz rectifier circuit for sensor network tags with 10-m distance. *IEEE J. Solid-State Circuits* **2006**, *41*, 35–41.
14. Le, T.; Mayaram, K.; Fiez, T. Efficient far-field radio frequency energy harvesting for passively powered sensor networks. *IEEE J. Solid-State Circuits* **2008**, *43*, 1287–1302.
15. Yuan, F. *CMOS Circuits for Passive Wireless Microsystems*; Springer: New York, NY, USA, 2011.
16. Zbitou, J.; Latrach, M.; Toutain, S. Hybrid rectenna and monolithic integrated zero-bias microwave rectifier. *IEEE Trans. Microw. Theor. Tech.* **2006**, *54*, 147–152.
17. Ungan, T.; Le Polozec, X.; Walker, W.; Reindl, L. RF Energy Harvesting Design Using High Q Resonators. In *Proceedings of IEEE MTT-S International Microwave Workshop on Wireless Sensing, Local Positioning and RFID, IMWS 2009*, Cavtat, Croatia, September 2009; pp. 1–4.
18. Ungan, T.; Freunek, M.; Muller, M.; Walker, W.D.; Reindl, L.M. Wireless Energy Transmission Using Electrically Small Antennas. In *Proceedings of IEEE Radio and Wireless Symposium, RWS '09*, San Diego, CA, USA, January 2009; pp. 526–529.
19. Boquete, L.; Rodríguez-Ascariz, J.M.; Barea, R.; Cantos, J.; Miguel-Jiménez, J.M.; Ortega, S.; Data acquisition, analysis and transmission platform for a pay-as-you-drive system. *Sensors* **2010**, *10*, 5395–5408.
20. Heikkinen, J.; Salonen, P.; Kivikoski, M. Planar Rectennas for 2.45 GHz Wireless Power Transfer. In *Proceedings of Radio and Wireless Conference, RAWCON 2000*, Denver, CO, USA, 10–13 September 2000; pp. 63–66.
21. Akkermans, J.A.G.; van Beurden, M.C.; Doodeman, G.J.N.; Visser, H.J. Analytical models for low-power rectenna design. *IEEE Antenn. Wireless Propag. Lett.* **2005**, *4*, 187–190.
22. Hagerty, J.A.; Helmbrecht, F.B.; McCalpin, W.H.; Zane, R.; Popovic, Z.B. Recycling ambient microwave energy with broad-band rectenna arrays. *IEEE Trans. Microw. Theor. Tech.* **2004**, *52*, 1014–1024.
23. Harb, A. Energy harvesting: State-of-the-art. *Renew. Energ.* **2011**, *36*, 2641–2654.
24. Vullers, R.J.M.; van Schaijk, R.; Doms, I.; van Hoof, C.; Mertens, R. Micropower energy harvesting. *Solid-State Electron.* **2009**, *53*, 684–693.

25. Sah, C.-T. *Fundamentals of Solid-State Electronics*; World Scientific: Singapore, Singapore, 1991.
26. Wetenkamp, S. Comparison of Single Diode *vs.* Dual Diode Detectors for Microwave Power Detection. In *Proceedings of IEEE MTT-S International Microwave Symposium Digest*, Boston, MA, USA, June 1983; pp. 361–363.
27. Cardoso, A.J.; Schneider, M.C.; Montoro, C.G. Design of Very Low Voltage CMOS Rectifier Circuits. In *Proceedings of Circuits and Systems for Medical and Environmental Applications Workshop (CASME)*, Merida, Mexico, December 2010; pp. 1–4.
28. Cardoso, A.J.; de Carli, L.G.; Galup-Montoro, C.; Schneider, M.C. Analysis of the Rectifier Circuit Valid Down to Its Low-Voltage Limit. *IEEE Trans. Circuits Syst. I: Regul. Papers* **2012**, *59*, 106–112.
29. Data sheet HSMS-285x. Avago Technologies. Available online: http://www.avagotech.com (accessed on 28 September 2012).
30. Data sheet HSMS-286x. Avago Technologies. Available online: http://www.avagotech.com (accessed on 28 September 2012).
31. Hsu, T.S. Low-frequency excess noise in metal—Silicon Schottky barrier diodes. *IEEE Trans. Electron Devices* **1970**, *17*, 496–506.
32. Hastas, N.A.; Dimitriadis, C.A.; Dozsa, L.; Gombia, E.; Amighetti, S.; Frigeri, P. Low frequency noise of GaAs Schottky diodes with embedded InAs quantum layer and self-assembled quantum dots. *J. Appl. Phys.* **2003**, *93*, 3990.
33. Gomila, G.; Reggiani, L.; Rubí, J.M. Shot-noise suppression in Schottky barrier diodes. *J. Appl. Phys.* **2000**, *88*, 3079.
34. Kleinpenning, T.G.M. Low-frequency noise in Schottky barrier diodes. *Solid-State Electron.* **1979**, *22*, 121–128.
35. Lee, T.H. *The Design of CMOS Radio-Frequency Integrated Circuits*; Cambridge University Press: Cambridge, UK, 2004.
36. Advanced Design System. Agilent Technologies: Santa Clara, CA, USA.
37. Bowick, C.; Blyler, J.; Ajluni, C.J. *RF Circuit Design*; Newnes/Elsevier: Amsterdam, The Netherlands, 2008.
38. Joe, J.; Chia, M.; Marath, A.; Ang, C. Zero Bias Schottky Diode Model for Low Power, Moderate Current Rectenna. In *Proceedings of Defence Electronics Technology Seminar (DETS 97)*, Singapore, Singapore, November 1997; pp. 1–5.
39. Visser, H.J.; Vullers, R.J.M.; Veld, B.O.h.; Pop, V. Remote RF Battery Charging. In *Proceedings of Power MEMS 2010*, Leuven, Belgium, December 2010; pp. 37–40.
40. Nimo, A.; Grgic, D.; Reindl, L.M. Impedance optimization of wireless electromagnetic energy harvester for maximum output efficiency at μW input power. *Proc. SPIE* **2012**, *8341*, 83410W:1–83410W:14.
41. Nimo, A.; Grgic, D.; Reindl, L.M. Electrically small Planner Antenna for Compact Electromagnetic (EM) Wireless Energy Harvester. In *Proceedings of Power MEMS 2011*, Seoul, Korea, November 2011; pp. 310–313.
42. RT-duroid-5870–5880-Data-Sheet; Rogers Corporation: Rogers, CT, USA, 2011.

43. *HFSS*; Ansys Corporation. Ansys, Inc: Canonsburg, PA, USA, 2005.
44. Friis, H.T. A Note on a Simple Transmission Formula. *Proc. IRE* **1946**, *34*, 254–256.
45. Kvaksrud, T.I. *Range Measurements in an Open Field Environment*, *Design Note DN018*; Texas Instrum. Incorporated: Dallas, TX, USA, 2008.
46. *LabView*; National Instruments: Austin, TX, USA, 2009.

Appendix A: Measuring Setup for RF Rectifier Efficiency and Voltage Sensitivity

The measuring setup is as shown in Figure A1.

Figure A1. RF to DC Power converter characterization setup.

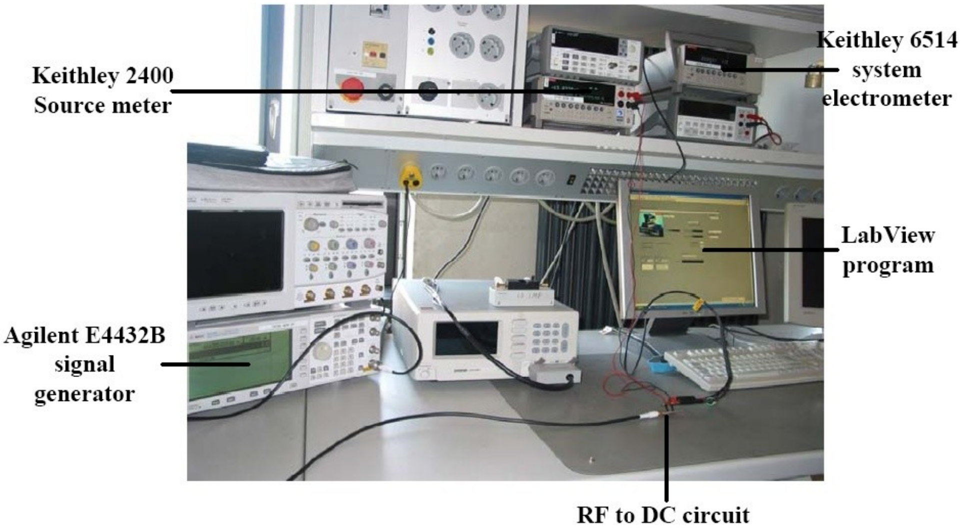

The RF to DC circuit efficiency and voltage sensitivity measurements were made with a Keithley 2400 source meter and Keithley 6514 system electrometer with an Agilent E4432B signal generator providing 50 Ω RF signal into the circuit board.

The closed circuit current drawn by the RF to DC power converter (*without load*) from the generator is first determined by the Keithley 2400 source meter; then starting from this current, the value of the current is decreased at set intervals to creates virtual load resistances to the circuit for up to a lowest current of 0.1 µA. The 6514 system electrometer is used to measure the output voltage. The number of data point is set through LabView [46] as well as the measurements. Additionally open circuit voltage or at specific loads and frequency sweep can be made through the LabView program. At −40 dBm input power and below, the detected voltages and currents were difficult to measure accurately with the measuring setup; hence measurements were made up to a minimum of -35 dBm input power. The circuit layout for the efficiency and voltage sensitivity measurements is schematically shown in Figure A2.

Figure A2. RF to DC power converter characterization circuit.

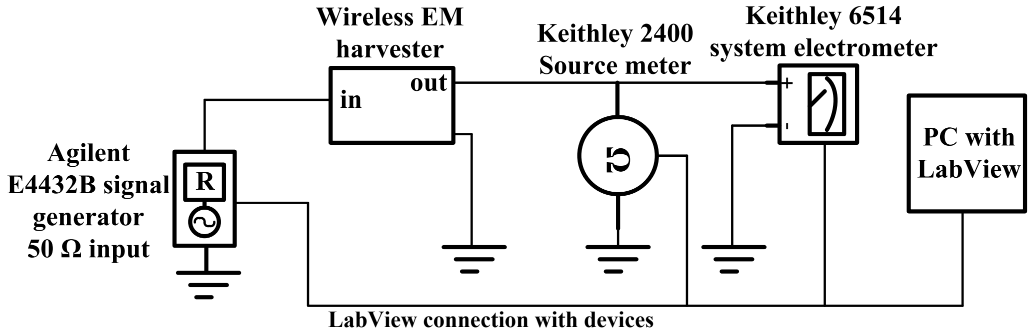

STANDARD ANTENNA TERMS AND RELATED FORMULAS

The "IEEE Standard Definitions of Terms for Antennas" (IEEE STD-145) represents a consistent and comprehensive vocabulary suited for the effective communication and understanding of antenna theory. General use of these definitions of terms would eliminate much of the wide-spread inconsistency concerning antenna characteristics, particularly with regard to the basic parameters of gain, beamwidth, polarization and efficiency. For convenience, IEEE antenna terms of general interest are listed here. Wherever these terms appear in this catalog, the definitions given below apply. Other commonly used terms, not covered by the IEEE standard, are shown with an "*."

ANTENNA APERTURE. A surface, near or on an antenna, on which it is convenient to make assumptions regarding the field values for the purpose of computing fields at external points. **Note:** The aperture is often taken as that portion of a plane surface near the antenna, perpendicular to the direction of maximum radiation, through which the major part of the radiation passes.

ANTENNA EFFICIENCY OF APERTURE - TYPE ANTENNA. For an antenna with a specified planar aperture, the ratio of the maximum effective area of the antenna to the aperture area.

*** ANTENNA FACTOR.** That quantity by which the voltage developed across the output of an antenna is related to the incident field strength in which the antenna is immersed. **Note:** Applicable to low frequency antennas and usually refers to a 50 ohm output.

$$\mathrm{AFE\ (dB\ m^{-1}) = E\ (dB\ V/m)\ -\ V\ (dB\ V)}$$

AFE = Electric Field Antenna Factor
E = Electric Field Strength at antenna
V = Voltage at terminals of antenna

$$\mathrm{AFH\ (dB\ AV^{-1}\ m^{-1}) = H\ (dB\ A/m) - V(db\ V)}$$

AFH = Magnetic Field Antenna Factor
H = Magnetic Field Strength at antenna
V = Voltage at terminals of antenna

$$\mathrm{AFE\ (dB\ m^{-1})\ =\ AFH\ (dB\ AV^{-1}\ m^{-1}) + 51.53}$$

for a plane wave in free space.

$$\mathrm{AFB\ (dB\frac{pT}{\mu V})\ =\ B\ (dBpT)\ -\ V_o\ (dB\mu V)}$$

AFB = Magnetic flux Antenna Factor
B = Magnetic flux at the antenna
pT: picoTesla units
V = Voltage at the terminals of the antenna

$$\mathrm{AFB\ (dB\frac{pT}{\mu V}) = AFH\ (dB\frac{A}{Vm})\ + 2}$$

APERTURE ILLUMINATION. The field over the aperture as described by amplitude, phase, and polarization distributions.

APERTURE ILLUMINATION EFFICIENCY. For a planar antenna aperture, the ratio of its directivity to the directivity obtained when the aperture illumination is uniform.

BEAM. The major lobe of the radiation pattern.

CIRCULAR POLARIZATION. It may be either right hand circular polarization (RHCP) or left hand circular polarization (LHCP). The sense of polarization is determined by observation of the direction of rotation of the electric field vector from a point behind the source, RHCP and LHCP correspond to clockwise and counter-clockwise respectively. **Note:** RHCP transmit requires a like polarization to receive.

CO-POLARIZED. The polarization which the antenna is intended to radiate or receive. Also "like polarization".

*** CROSS POLARIZATION DISCRIMINATION (XPD).** Cross polarization discrimination is the measure of the antenna’s ability to differentiate between the vertical and the horizontal polarization of an antenna. This difference, shown in relative signal level, is indicated on directional pattern envelopes (DPE’s).

Antenna Research

STANDARD ANTENNA TERMS AND RELATED FORMULAS

* **DIRECTIONAL PATTERN ENVELOPES (DPE'S).** In accordance with standard practice, radiation characteristics in any given plane of polarization are measured and plotted using 360-degree polar coordinate systems. The resultant Directional Pattern Envelope is the smoothed composite of all these measurements. The purpose of these DPE's is to emphasize the worst composite condition.

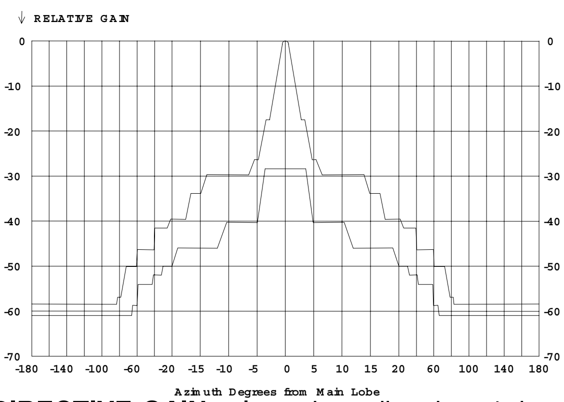

DIRECTIVE GAIN. In a given direction, 4 times the ratio of the radiation intensity in that direction to the total power radiated by the antenna.

DIRECTIVITY. The value of the directive gain in the direction of its maximum value.

EFFECTIVE AREA OF AN ANTENNA. In a given direction, the ratio of power available at the terminals of a receiving antenna to the power per unit area of a plane wave incident on the antenna from that direction, polarized coincident with the polarization that the antenna would radiate.

FAR FIELD REGION. That region of the field of an antenna where the angular field distribution is essentially independent of the distance from a specified point in the antenna region.

* **FRONT-TO-BACK RATIO**. The ratio of the maximum directivity of an antenna to its directivity in a specified rearward direction.

* **Gain, dBi**. The gain expressed in decibels relative to an isotropic radiator that is linearly polarized.

$$G(dBi) = 10\log(G) \qquad G = 10^{\frac{G(dBi)}{10}}$$

* **GAIN, dBic**. The gain expressed in decibels relative to an isotropic radiator that is circularly polarized.

HALF-POWER BEAMWIDTH. In plane containing the direction of the maximum of a beam, the angle between the directions in which the radiation intensity is one half the maximum value of the beam.

HALF-WAVE DIPOLE. A half wavelength antenna, center fed so as to have equal current distribution in both halves. Mounted vertically, it has a doughnut shaped pattern, circular in the horizontal plane. It is an antenna that can be constructed. It has some inherent losses. When used as a gain reference, the half-wave dipole has a power gain of about 1.7 dBi.

* **ISOLATION.** Refers to the ability of one port of a dual polarized feed to discriminate against a signal fed into the other port.

ISOTROPIC RADIATOR. A hypothetical antenna having equal radiation intensity in all directions. Note: An isotropic radiator represents a convenient reference for expressing the directive properties of actual antennas.

NEAR-FIELD REGION. The spherical region of space between the antenna and the far field region.

NULL. The region of a radiation pattern, either computed or measured, where the amplitude goes through a minimum value. Note: (1) It represents the angular position where the phase or the far field pattern crosses the zero axis if the pattern is plotted as a phasor instead of a scalar value. Note: (2) The region outside the main beam of a directive antenna pattern consists of a series of minor lobes separated by nulls.

PARALLEL POLARIZATION. The condition where the electric vector is parallel to the local conducting surface. Note: Over the earth, this is usually referred to as being horizontal polarization.

PHASE CENTER. The location of a point associated with an antenna such that, if it is taken as the center of a sphere whose radius extends into the far-field, the phase of a given component over the surface of that radiation sphere is essentially constant, at least over the portion of the sphere where the radiation is significant.

Phone: 301-937-8888 ● Fax: 301-937-2796 ● http://www.ara-inc.com ● sales@ara-inc.com

STANDARD ANTENNA TERMS AND RELATED FORMULAS

POLARIZATION. The polarization of an antenna is defined as the polarization of the electromagnetic wave as described by the shape and orientation of an ellipse, which is the locus of the extremity of the field vector, and the sense in which the ellipse is traversed with time. The elliptical locus is called the polarization ellipse and the wave is said to elliptically polarized. Circular polarization and linear polarization are degenerate cases of elliptical polarization.

POWER DENSITY AT A POINT

$$S_{av} = \frac{GP_t}{4\pi r^2}$$

S_{av} = Time average power density in W/m^2
P_t = Power transmitted in watts
G = Antenna gain relative to an isotrope
r = Distance from antenna to point in meters

POWER DENSITY TO VOLTS/METER IN FREE SPACE

$$E^2 \ (V/m) = 377 \ S_{av} \ (W/m^2)$$

$$S_{av} \ (W/m^2) = E^2 \ (V/m) / 377$$

$$1 \ V/m = 2.65 \ mW/m^2$$

POWER GAIN. In a given direction, 4 times the ratio of the radiation intensity in that direction to the net power accepted by the antenna from the connected transmitter. **Note:** (1) When the direction is not stated, the power gain is usually taken to be the power gain in the direction of its maximum value. (2) Power gain does not include reflection losses arising from mismatch of impedance.

POWER GAIN IN PHYSICAL MEDIA. In a given direction and at a given point in the far field the ratio of the power flux per unit area from an antenna to the power flux per unit area from an isotropic radiator at a specified location with the same power input as the subject antenna.

Note: The isotropic radiator must be within the smallest sphere containing the antenna. Suggested locations are antenna terminals and points of symmetry, if such exist.

POWER GAIN REFERRED TO A SPECIFIED POLARIZATION. The power gain of an antenna, reduced by the ratio of that portion of the radiation intensity corresponding to the specified polarization to the radiation intensity.

POWER TRANSMISSION FORMULAS

$$P_r = P_t \frac{G_t G_r \lambda^2}{(4\pi r)^2}$$

P_r (dB W) = P_t (dB W) + G_t (dBi) + G_r (dBi) - 20 log r - 20 log f + 27.56

P_r (dB W) = P_t (dB W) - AFE_t (dB m^{-1}) - AFE (dB m^{-1}) - 20 log r + 20 log f - 32

P_r = Power received
P_t = Power transmitted
G_r = Gain of receiving antenna
G_t = Gain of transmitting antenna
f = Frequency in MHz, λ = Wavelength
r = distance between antennas in meters
AFE_r = AFE of receiving antenna
AFE_t = AFE of transmitting antenna

RADIATOR. Any antenna or radiation element that is a discrete physical and functional entity.

RADIATION, ELECTROMAGNETIC. The emission of energy in the form of electromagnetic waves.

RADIATION INTENSITY. In a given direction, the power radiated from an antenna per unit solid angle.

RADIATION LOBE. A portion of the radiation pattern bounded by regions of relatively weak radiation intensity

RADIATION PATTERN (ANTENNA PATTERN). A graphical representation of radiation properties of the antenna as a function of space coordinates. **Note:** (1) In the usual case the radiation pattern is

determined in the far-field region and is represented as a function of directional coordinates. (2) Radiation properties include power flux density, field strength, phase, and polarization.

*** RADIATION RESISTANCE OF AN ELECTRICALLY SMALL LOOP ANTENNA.** The resistive component of an antenna's input impedance that results from the coupling of the antenna to its environment. This resistance dissipates the power that is actually radiated from the antenna.

$$R_r = 20\,(2\pi/\lambda)^4\, n^2 A^2 \text{ ohms}$$

n = number of turns
A = area of the loop

REALIZED GAIN. The power gain of an antenna in its environment, reduced by the losses due to the mismatch of the antenna input impedance to a specified impedance.

*** REALIZED RADIATOR EFFICIENCY.** The efficiency of an antenna in its environment reduced by all losses suffered by it, including: ohmic losses, mismatch losses, feedline transmission losses, and radome losses.

RELATIVE POWER GAIN. The ratio of the power gain in a given direction to the power gain of a reference antenna in its reference direction. **Note:** Common reference antennas are half-wave dipoles, electric dipoles, magnetic dipoles, monopoles, and calibrated horn antennas.

RETURN LOSS. The reflection coefficient of a mismatch expressed in decibels. **Note:** Modern swept VSWR techniques actually sense the reflected component which is normalized to the forward component to yield return loss. A 2:1 VSWR is equivalent to 9.5 dB return loss.

VSWR. The voltage standing wave ratio of a component such as an antenna. It is referred to the characteristic impedance of the transmission line being used. **Note:** The most common characteristic impedance is 50 ohms, but 75 and 300 ohms are frequently used in coaxial or twin lines for VHF, UHF applications.

NOTES:

THE HANDYMAN'S GUIDE TO OSCILLOSCOPES (Part 2 of 2)

by Paul Harden, NA5N

Making some advanced measurements with your Oscilloscope

Print as .pdf file
4 pages
8½ x 11 or A4

In Part 1, oscilloscope operation was covered for making basic voltage, time and frequency measurements. In this part, we'll continue with some more advanced uses of a scope, and in particular, how to use a scope for testing and troubleshooting ham radio QRP transceivers in the homebrewer's workshop.

Receiver Filter Bandwidth.

This procedure uses a scope (a DVM can be used with less accuracy) for determining the overall filter bandwidth (or selectivity) of a receiver. It is basically measured by plotting output voltage vs. audio frequency to construct a picture of the filter response.

Connect scope to the receiver audio output (speaker or phone jack); measurement will be based on peak-to-peak voltages (Vpp) on a scope, or rms voltage (Vrms) on a DVM.

Using a signal generator, set the frequency for the band of interest on your radio. For example, on a general coverage shortwave receiver, you might set it for 10 MHz (top end of the 31M band), or perhaps to 7.040 MHz on a 40M ham radio receiver/transceiver. Tune the receiver to the signal generator signal. If you don't have a signal generator, you can also tune to a steady carrier or station to produce a hetrodyne audio "pitch." Tune in the signal to the pitch that causes the maximum peak-to-peak display. Adjust the scope and volume control to produce a 2Vpp display (4 divisions). This is the peak response of the overall filtering stages as shown in **Fig. 13**.

Now determine the audio frequency at this peak response by measuring the time period between cycles and covert to frequency. In the example to the right, the period of one cycle is 1.7mS, which is an audio tone of 750Hz (1/.0017sec). A frequency counter on the output can also be used.

Next, tune the receiver such that the sidetone pitch goes UP in frequency and the peak-to-peak signal will decrease in magnitude. Tune to the point where the signal is exactly 1Vpp on the scope. See **Fig. 12**.

This is the –6dB point of the high end of the filter (20log 1v/2v =–6dB). Determine the frequency of the audio pitch as before. In the example, this is 1100 Hz. Record the data.

From these two data points, the –6dB bandwidth can be estimated. The bandwidth from the filter peak (750 Hz) to the –6dB point (1100 Hz) is 350 Hz. The bandwidth (BW) between the two –6dB points is usually twice this value, or 700 Hz. A filter with a –6dB BW of 700Hz is a mediocre filter for CW reception, and way too narrow for SSB or AM.

Of course you can determine the exact –6dB BW by tuning the receiver back to the 2Vpp peak response, and continue tuning DOWNward in frequency until the audio is again exactly 1Vpp. Determine this frequency and record. In this example, it should occur around 400 Hz if the filter shape is symmetrical.

Plot these three data points on a sheet of graph paper as shown in **Fig. 15** to construct the filter shape. Return to the upper –6dB point (1100Hz in the example) and continue tuning upwards in audio pitch, recording the frequency at 0.5v (–12 dB), 0.25v (–18 dB), 125mV (–24 dB), etc. Everytime you "halve the voltage," it is a 6 dB change. The more points you collect, the more accurate your filter response plot will be.

Fig. 13 – Displaying Filter Peak Response

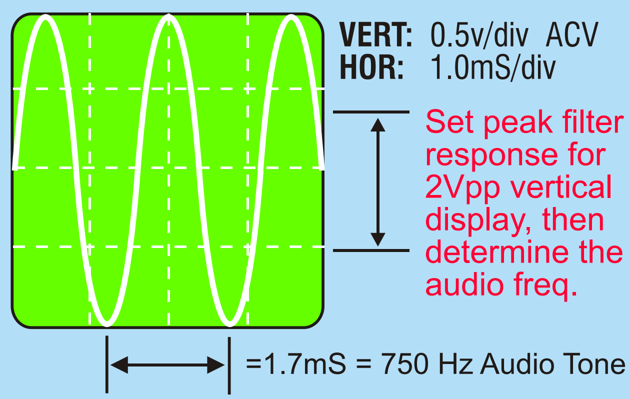

Fig. 14 – Displaying –6dB Frequency

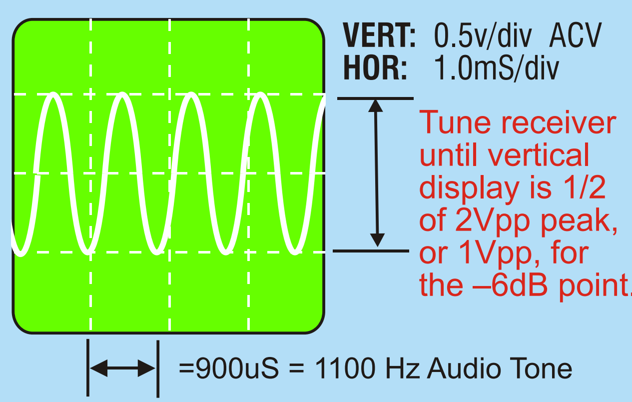

Of interest to proper rig alignment is to repeat the above using the output of the product detector. To maximize the effectiveness of the filtering, the receive offset frequency set by the BFO should be adjusted to the same frequency as the peak frequency response of the audio. In this example, with the peak audio response occuring at 750Hz, if your BFO is set for a sidetone frequency of 700 Hz, you are loosing 2–3 dB, since this is in your filter skirt. This is shown on the response plot in **Fig. 15** by the dashed lines. By adjusting your BFO for a sidetone frequency of 750 Hz, you will pick up 3-4dB of overall gain in your receiver, plus increase the selectivity a bit as well. Why? Because nearby stations, such as one at 800–900Hz tone, could actually be louder than the 700Hz tone signal you are trying to copy, since the gain of the receiver is greater at those tones than at 700Hz, as shown in the plot.

Fig. 15 – Plotting Audio Response

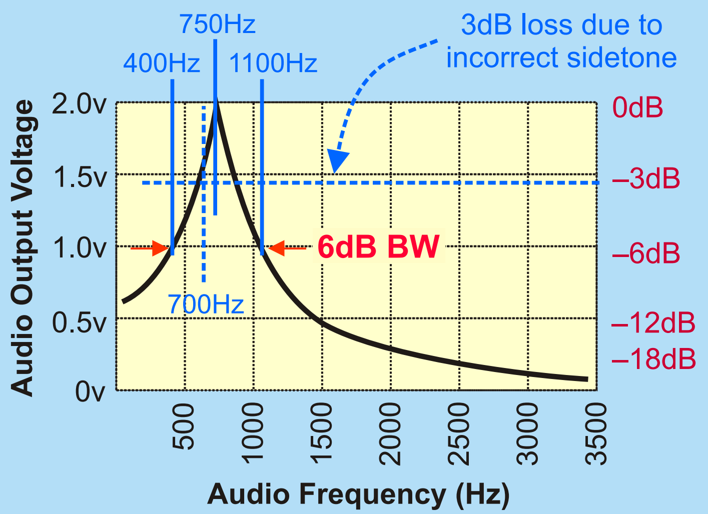

Opposite Sideband Rejection

A superhet receiver is supposed to pass just one sideband and reject the other. Poor opposite sideband rejection could indicate the crystals in your IF filter are not well matched or other problems. It is measured almost identical to plotting the filter response just described. First, you tune the receiver to the test signal to find the peak response frequency, or 750Hz in this example. Set the scope display for 2Vpp. Now tune downward in audio pitch, passing zero-beat, and continue tuning and you should hear the test signal, much weaker, now rising again in tone. This is the *opposite sideband*. Measure the peak-to-peak voltage, if you can. For example, say it is 80mVpp, as shown in **Fig. 16**. Calculate the opposite sideband rejection by:

$$\text{rejection} = 20\log\frac{80\text{mV}}{2.0\text{v}} = \frac{80\text{mV}}{2000\text{mV}} = -28\text{dB}$$

Fig. 16
Calculating Opposite Sideband Rejection

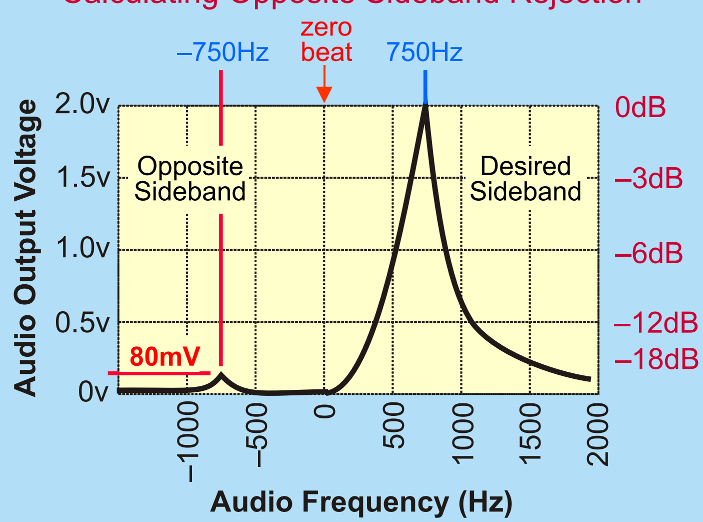

If you can't hear the opposite sideband, then obviously you have excellent filter rejection. If you can just barely hear it, you may have to increase the sensitivity of your scope (set vertical gain to 20 or 50 mV/div). In this example, –28dB rejection of the opposite sideband is quite good. A –30dB rejection means the opposite sideband is only 1/1000th of the desired sideband, a very suitable attenuation of the opposite sideband.

These tests are important to perform on your rig for documenting it's current performance, and repeated periodically to detect unfavorable changes or for troubleshooting when a problem is evident. For homebrewing, these tests can allow you to evaluate different circuits or when experimenting with different components or part values.

Oscillator Phase Noise

When homebrewing a basic oscillator circuit, such as a VFO, looking at the oscillator output on a scope can reveal several problems. One is to check for excessive phase noise. Phase noise is small variations of the oscillator frequency that causes power in the close-in sidebands, usually measured on laboratory equipment within 100KHz, or even within 10 KHz.

To check for oscillator phase noise, connect the oscilloscope to the oscillator output, loading the output of the oscillator as little possible. Most scopes have sufficiently high input impedances where this shouldn't be a problem, but some cheaper scopes can load an oscillator circuit. If you suspect your scope is loading the oscillator, couple the scope to the circuit with a small value capacitor, less than 20pF.

Display 2–3 cycles of the oscillator output as shown on the scope display shown in **Fig. 17**. Properly focus the scope and carefully observe if the waveform appears in focus at the peaks, but slightly out-of-focus at the zero-crossing points, that is, on the rising and falling edges of the sine wave.

Fig. 17 – Checking Oscillator Phase Noise

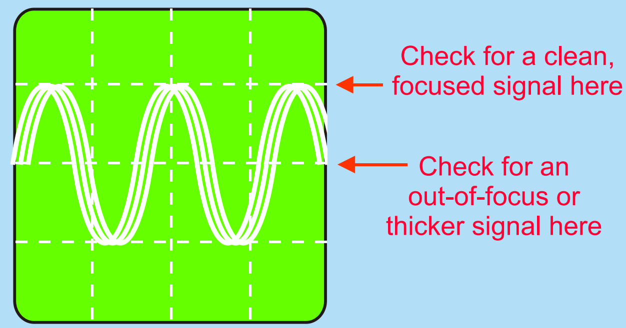

If it appears out-of-focus, this is excessive phase noise jittering the signal and "smearing" the waveform along the time (horizontal) axis. Extreme phase noise may show 2-3 sine waves very close to each other, as shown in the exagerated waveform to the right — assuming you have your scope properly triggered.

Phase noise is random, instantaneous changes in the oscillator frequency that smears the display. If you can see this on a scope, the phase noise is excessive! If you can't see it, it doesn't mean the oscillator has no phase noise (all oscillators have some phase noise), it just means it is not excessive enough to see on a scope. A scope is not a good instrument for checking phase noise, but for homebrew circuits, it is a check to ensure you do not have a serious oscillator problem.

Excessive oscillator phase noise in receivers can cause IMD products and noise in the audio range at the output of the mixer(s), including the product detector. In a transmitter, excessive oscillator phase noise will put power in the close-in sidebands of your carrier, not only wasted power for lower transmitter efficiency, but may produce strange sounds (buzzing or chirping) to the receiving station. A few causes of phase noise are excessive current in the oscillator transistor, low-Q coil(s), high dissipation in the tuning caps or poor power supply filtering at the oscillator frequency.

AM (Amplitude) Noise

Another oscillator problem may be AM noise, or amplitude modulated noise. It is an opposite effect on a scope when displaying the oscillator output — the sine wave appears out-of-focus or thicker at the peaks, and in-focus elsewhere as shown in **Fig. 18**.

If you detect AM noise, slow down the scope's sweep rate to the audio frequencies or slower to see if you can notice a lower frequency component. A common cause of AM oscillator noise is 60 Hz from the power mains leaking into the circuits. This is particularly true if using a power supply off of 120v 60 Hz, or sometimes it can be due to the AC lighting above your head! If the AM noise seems to be at the same frequency as the audio output tone, it means audio is getting into the Vcc bus, likely due to poor bypass filtering at the audio amplifier stages (particular if using an LM386 or similar).

Fig. 18 – Checking for AM Oscillator Noise

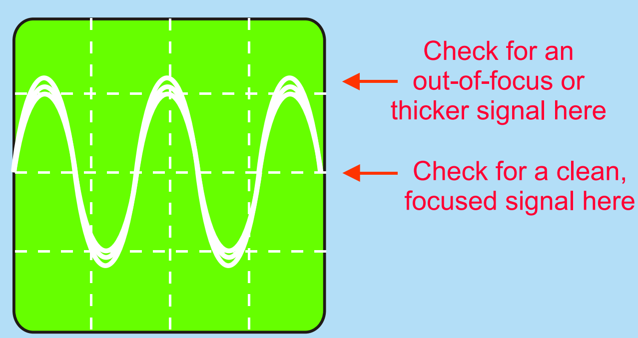

If you can't find a low frequency component, the AM noise may be random, which may indicate poor voltage regulation, a noisy voltage regulator, or perhaps a circuit in VHF oscillation. If the AM noise seems to occur on key-down only on a transmitter, the transmit current may be loading the power supply, the voltage regulator is under-rated, or just simply loading the oscillator. In the case of loading the power supply or regulator(s), perhaps a separate voltage regulator or zener circuit should be used, dedicated for the oscillator(s). In the case of transmit loading, adding a buffer amplifier or emitter follower to isolate the load from the oscillator may help.

Much of this can be diagnosed also with the scope, by looking at the AC ripple on the DC power lines. You should have less than 50mV of any AC component on the 8-12v DC wiring, whether 60Hz, audio or RF. If >50mV, then additional low or high frequency filtering on the DC power is needed.

Monitoring Transmitter RF Output

RF Power (in watts) is E^2/R, where E is in rms and R=50 . The voltage displayed on the scope (peak-to-peak) must be converted to rms by Erms=.707(Epp/2). To measure properly, the transmitter should be on a 50 dummy load using the normal hi-Z scope input. If your scope has a selectable "50 "input, it can be the transmitter dummy load directly, providing it can tolerate the 50Vpp input. (Always know what the maximum p-p input voltage your oscope will tolerate. It is often stated on your scope at the vertical channel inputs. 50Vpp to 100Vpp are typical).

Measuring Transmitter RF Output Power

Figure 19 shows how you can use an oscilloscope to fairly accurately measure output power from a low power transmitter (generally 10W or less with a 1X probe and 20-30W with a 10X probe). Connect transmitter output to a 50 dummy load. Connect the scope lead to the transmitter output (after the low pass filters) or directly to the dummy load. Do not connect the scope leads to the collector or drain of the final PA transistor. The displayed voltage in this case will be erroneous.

In the example, the output transmit voltage across the dummy load measures 24Vpp. Convert this voltage to Vrms, then use the equation (Vrms squared divided by the load resistance) to calculate the power in watts. In the example, 24Vpp, the output power is 1.4 watts. A 5W QRP transmitter should produce about 45Vpp.

The accuracy of your power measurements depend upon the condition of your oscilloscope:

1) Ensure your scope's vertical sensitivity (volts/division) is properly calibrated (see Part I)
2) Ensure your vertical sensitivity is properly calibrated with the 1X or 10X probe you are using.
3) Ensure that the transmitter frequency is well within the bandwidth of your scope. A 100 MHz scope should give reliable readings on all HF bands. A 50 MHz scope should be reliable on all HF bands except slight errors at 28MHz.

Fig. 19 –Oscilloscope as a Power Meter

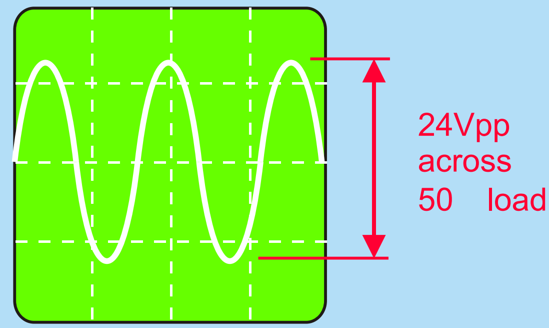

1. Measure output voltage. 24Vpp
2. Convert Vpp to Vrms

   Vrms=.707(Vpp/2) 8.5Vrms

3. Calculate power in watts

$$\frac{Vrms^2}{R} = \frac{8.5v^2}{50} = 1.4W$$

Checking Transmitter Purity

Phase Noise of the transmitter is measured identically to the phase noise checks on page 2–3. With the scope properly triggered and focused, you are looking for an out-of-focus "fuzziness" around zero crossing. If it appears phase noise exists, the fault is generally at the beginning of the transmit chain. That is, seldom does the PA transistor add phase noise; it's merely amplifying what it is given. Phase noise on the transmitter output is more likely due to the transmit oscillator, or the transmit mixer if used.

Harmonic Power can also be detected on a scope while looking at the transmitter RF output power. In **Fig. 20**, notice the "dips" or the two "peaks" on the top and bottom of each sine wave. This is caused by excessive 2nd harmonic output power. The rule-of-thumb is – if you can see any 2nd harmonic power (a dip or flattening at the peaks), then you are right at or exceeding the –30dBc FCC harmonic specification. A clean sine wave implies FCC compliance, providing the 2nd harmonic is within your scope's bandwidth. Obviously, a spectrum analyzer should be used for accurate harmonic evaluation, but a scope can be used to indicate if you have a problem. If you build your own transmitter, it is your responsibility to ensure it is compliant. An approximate method of estimating 2nd harmonic attenuation is shown.

–30dBc means the 2nd harmonic power is 1/1000th of the fundamental power. For a 5W transmitter, this means the 2nd harmonic power should be 5mW or less, or about 1Vpp. In displaying a 5W signal on a scope (45Vpp), it would be difficult to resolve much less than a 1Vpp dip or ripple.

Fig. 20 –Checking 2nd Harmonic Power

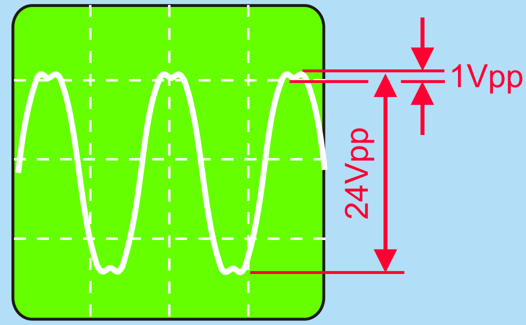

1. Measure output voltage. 24Vpp
2. Measure ripple voltage. 1Vpp
3. Calculate dBc of 2nd harmonic ripple

$$20\log\frac{V2}{V1} = 20\log\frac{1v}{24v} = -27.6\text{ dBc}$$

or, not quite FCC compliant!

Conclusion. This concludes the NA5N "Handiman's Guide to Oscilloscopes." Hopefully, it has helped you to understand your oscilloscope to make simple measurements, and with some practice, perform the more advanced measurements discussed. An oscilloscope is a very powerful tool that is invaluable on the homebrewer's workbench. If there is a particular measurement you feel I omitted, please let me know and I will add it when time permits.

73, Paul Harden, NA5N (na5n@zianet.com or pharden@nrao.edu)

THE HANDYMAN'S GUIDE TO OSCILLOSCOPES (Part 1 of 2)

by Paul Harden, NA5N

Getting Acquainted with your Scope and making some measurements

Updated May 2004 with actual oscope waveforms

Print as .pdf file
5 pages
8½ x 11 or A4

When in the course of human events, it becomes necessary to look at neat signals floating around your radio, you go to a hamfest and buy that $50 o-scope. Now what? This two part article will attempt to explain basically how an oscilloscope works, operator functions, basic measurements, and some advanced applications. An o-scope is a powerful tool in any shack – even a real "cheapie" with limited bandwidth.

HOW AN OSCILLOSCOPE WORKS

A block diagram of a typical o-scope is shown in **Fig. 1**. The test probe usually plugs into the scope via a BNC connector, then passes through a switch to determine whether the input signal will be dc or ac coupled (to remove any dc component). Often this switch will have a "ground" position for setting the zero-volts reference. Next is the input attenuators. The vertical input amplifier is quite sensitive, designed for 20-50mV of input. For larger input voltages, the signal is applied to attenuators comprised of simple voltage dividers. This is the first area of concern for cheap o-scopes, as the input attenuators may not be very linear or accurate. For example, if you appy a 10Vpp signal on the 10v/division setting, the signal should be 1 division high. Switching to 1v/div., the signal should be 10 divisions (usually full-scale) high. If it is not exactly 10 divisions, the attenuator for that setting needs adjusting. Some scopes have internal adjustments for fine-tuning each attenuator setting.

Following the attenuators, the signal is applied to the first vertical amplifier, which converts the input to a differential signal. This differential signal is amplified up to high voltages for the oscilloscope deflecting plates – moving the beam up and down (in the vertical axis).

The sweep generator is usually a constant current source charging a capacitor to make a sawtooth waveform that eventually deflects the beam in the horizontal axis. The frequency of the sawtooth determines how fast the beam travels from the left to the right side of the tube, and is controlled by the sweep control, usually calibrated in seconds, milli-seconds or micro-seconds per division. This is the second area of concern for an oscilloscope – how linear the sawtooth waveform is generated. For example, a sawtooth with a nonlinear ramp will cause the signal displayed in the central portion of the tube to be expanded or compressed compared to the signal at the ends.

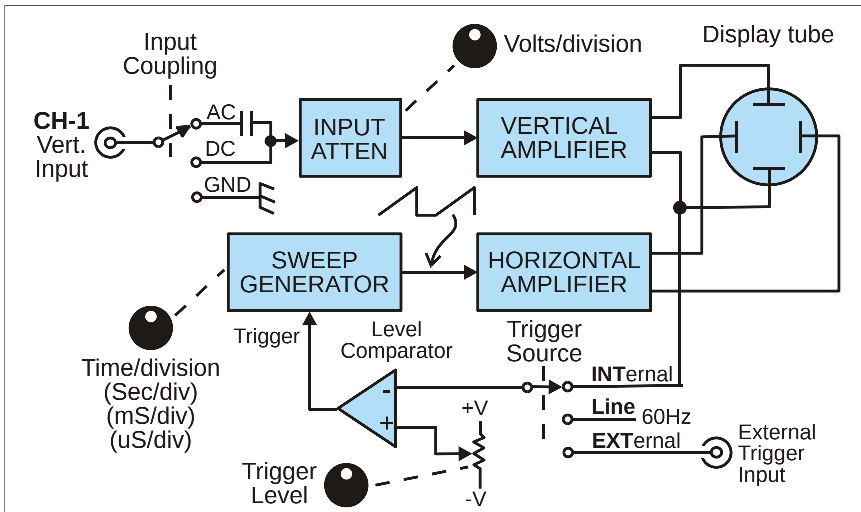

FIG. 1 - Basic block diagram of an Oscilloscpe

The sawtooth ramp is amplified to high voltages, applied to the oscope tube, to deflect the beam from left to right. An important task of an oscope is when the horizontal deflection begins. Normally a switch labeled "Trigger Source" determines what initiates the sawtooth ramp. In the "Internal" position, a sample of the input signal (in the vertical amplifiers) is sampled, with a variable resistor setting the level. When the input signal exceeds the "Trigger Level," a pulse is generated to start the sawtooth ramp and hence the horizontal sweep. The purpose of triggering is to keep the input waveform synchronized to the sweep so it appears stationary on each sweep. The trigger source usually has a "Line" position, which simply triggers the sweep off of 60Hz from the power supply. This synchronizes the sweep to the AC power frequency and is useful for checking television signals, which are synchronized to the power mains. Also, an "External" position may be present, which connects an external input signal (via a BNC connector) to trigger the sweep generator.

Other features your oscope may have are two vertical channels for dual trace operation, various modes to display both waveforms (alternate, chopped, A+B added, etc.), delayed sweep features, dual sweep time bases, built in calibrators, etc.

CALIBRATING YOUR OSCILLOSCOPE

The first thing you should do upon acquiring an o-scope is to check its calibration.

The vertical amplfiers can be checked with a known voltage source or 9v transistor radio battery. Measure the output voltage of the battery with an accurate voltmeter. Let's say it just happens to be +9v exactly. Set the input coupling to ground (0v) and move the trace to the bottom division. Switch the input coupling to DC and set the attenuators to 1v/div. The deflection should be 9

divisions. Switching to 10v/div., deflection should be 0.9 divisions. Internal to the oscope (or perhaps accessible from the outside) are adjustments for the vertical amplifier gain. Adjust this for 9 divisions of deflection in the 1v/div. range. Procedure can be repeated with a 1.5v flashlight battery (assuming you know the exact voltage from a DVM).

The horizontal amplifiers should be checked/calibrated using a signal generator. For example, a 1MHz signal has a period of 1uS. Setting the sweep rate to 1.0uS/div., a 1MHz signal should take exactly 1 division per cycle. Set the horizontal width control properly to ensure the beam starts at the first division and ends at the last division. If the sweep rate appears incorrect, an internal adjustment (Sweep gain or similar) can be set for proper display of the test signal.

The main operator controls are:

- **Intensity** - controls the brightness of the beam. **NOTE: Too bright a beam can damage to the CRT tube!**
- **Focus** - adjusts the beam for the thinnest and sharpest display.
- **VERT & HOR Position** - controls the vertical and horizontal position of the display respectively
- **VERT V/div** - controls the vertical sensitivity of the display, i.e., how many volts (or mV) per division.
- **HOR Sweep Speed** - sets the horizontal sensitivity, i.e., how many mS or uS per division.
- **VERT & HOR vernier** - allows the vertical and horizontal sensitivity settings to be varied in small steps.

Other adjustments you may find on your scope are:

Astigmatism - With the scope intensity and focus properly set, this adjustment compensates for the curvature of the CRT tube by making it in-focus across the sweep. If your trace is out-of-focus in certain areas, but in-focus elsewhere, the astigmatism needs to be adjusted. See ***Fig. 2***.

Trace Rotation - is a small coil around the CRT that skews the trace to ensure it is perfectly horizontal. On scopes without this adjustment, the trace is leveled by physically rotating the CRT to align the trace to the graticle grid. See ***Fig. 2***.

DC BAL (DC Balance) - is a dc offset in the vertical amplifiers that causes a shift in the trace baseline when changing vertical scales. It is most obvious when measuring ac voltages. For example, you are displaying a 10Vpp sine wave, centered on the center graticle, at 2v/div. Changing to 5v/div, the sine wave shifts off the center graticle ... that is, it assumes a dc bias error. The DC BAL is adjusted until the shift no longer occurs when changing vertical scales.

HV ADJ. - is the high voltage that controls the intensity of the trace. Turn up the **Intensity** control to its brightest position, then adjust the HV ADJ for a trace slightly brighter than normal intensity. The **Intensity** control now has the proper range. The HV ADJ might have to be re-adjusted to acquire proper focus.

NOTE: Very bright trace displays can cause permanent damage to the CRT, particularly on a well-used scope.

Fig. 2 – Effects of Astigmatism & Trace Rotation

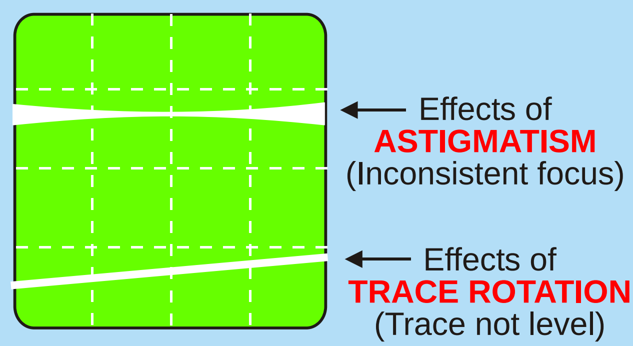

Fig. 3 – Triggering

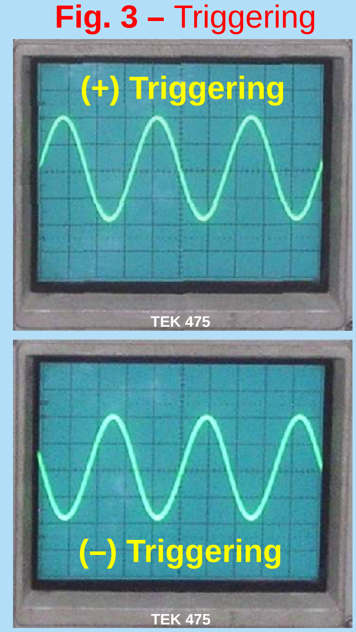

LET'S MAKE SOME MEASUREMENTS

It is assumed you have your scope relatively calibrated and familiar with the front panel controls. The sample o-scope displays are based on eight vertical and ten horizontal divisions on the CRT screen, typical to most oscilloscopes. Most waveforms are actual displays of the signal cited, photographed from my trusty Tektronix 475 oscilloscope.

First ... a word on TRIGGERING.

Most oscilloscopes have a knob or two for "Triggering." This tells the oscilloscope when to start the sweep. When the **Triggering Slope** is placed in the **(+)** position, the scope will begin its trace when the *input* signal goes positive. Likewise, when **(–)** triggering is selected, the trace will begin when the input signal goes negative, as shown in **Fig. 3**. Often there will be the option to chose the **Triggering Source**, such as "CH.1" or "LINE." Line means the scope is triggered off the 60Hz line voltage, and is useful when synchronizing on television signals or looking at 60Hz power supply noise. CH.1 or CH.2 means the scope will trigger off the signal on channel 1 or 2 respectively. **Trigger Level** is at what voltage of the input signal triggering begins. For example, if set high, triggering may not begin until the input signal reaches several volts. When set around zero, it will trigger the moment the signal goes positive (if set for (+) triggering). This setting can be troublesome if noise exists on the signal. Adjust for stable triggering.

DC Voltages.

Say you want to check the transmit-receiver (T-R) switch in your QRP rig, or other digital signal. See ***Fig. 4.*** The key line is the input to the HCT240 inverter to form the 0v TX– on key- down and the 0v RX– on key- up. This switches the rig between transmit and receive (T-R Switch). It is a logic function, that is, a voltage to represent ON or OFF.

Place the scope lead on pin 13 at 10v/div. and you should see the waveform like the top trace in ***Fig. 4*** ... about +6v on key-up and 0v on key down. Move the scope lead to pin 7 and you should see 0v on key-up and about +8v on key-down (bottom trace). If the output does not go "HI" (+8v) on key-down, or does not go to a solid "LO" (<1v) on key-up, the inverter is not working properly. (It's busticated). Many shortwave receivers use similar schemes for switching filters or attenuators.

While this test could be done with a DVM, the integration time is slow, requiring long key-downs to get the voltages. A scope will also show you how clean the switching is, or if there is an ac voltage (or RF noise) riding on the T-R voltage.

Scopes are thus good dc voltmeters, with about a 5% reading accuracy.

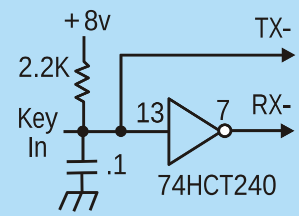

Fig. 4 - 38-Special T-R Switch

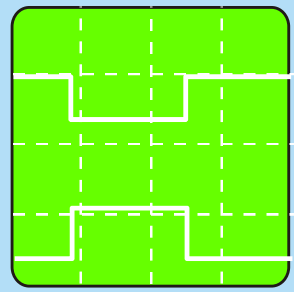

VERT: 10v/div DC
HOR: 500mS/div

AC Voltages.

Here is where an oscilloscope pays for itself by making AC voltage (and frequency) measurements. You must remember, AC voltages are displayed on a scope as ***peak-to-peak* voltages**, while a voltmeter measures in ***rms***. RMS voltages are about 1/3 the p-p voltage read on a scope, or specifically:

Vrms=½(.707 x Vpp) = 0.354 x Vpp

For example, let's measure the output voltage and frequency from the sidetone oscillator in your QRP rig. Place the scope lead on the audio amplifier output. On key-down, you get the waveform shown in ***Fig. 5***. The transmit sidetone audio is 1.9Vpp.

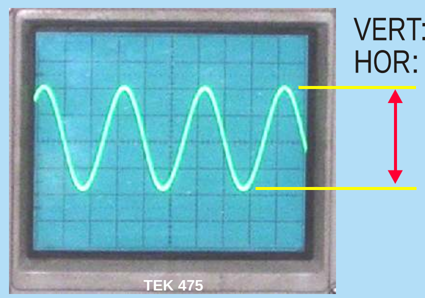

VERT: 0.5v/div ACV
HOR: 0.5mS/div

3.8 divisions
peak-to-peak
times 0.5v/div
= 1.9 Vpp
= 0.67 Vrms

Fig. 5

AC Frequency Measurement.

With this waveform, we might as well see what frequency our sidetone or transmit-offset frequency is. Most operators prefer the sidetone to be about 700–750Hz. Trigger the scope for a stable waveform and set the time-base (sweep) to display 2 or 3 cycles, as shown in ***Fig. 6***. Center the waveform between two horizontal divisions so zero volts on the waveform is on a graticule line, then move the horizontal position so the first "zero– crossing" is also on a division line.

Fig. 6

VERT: 0.5v/div ACV
HOR: 0.5mS/div

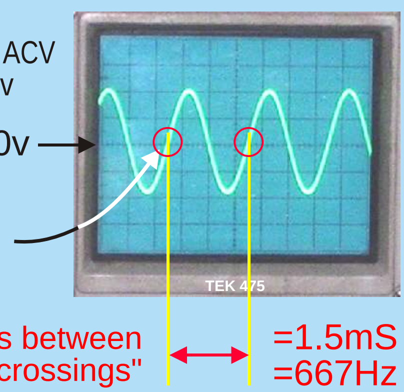

3 divisions between
"zero-crossings"
=1.5mS
=667Hz

Measure the time it takes to make one complete sine wave from one zero-crossing to the next. In this example, it is 1.5 divisions, at 1mS per division, or 1.5mS. Frequency is simply the reciprocal of time, such that the sidetone frequency is:

$$f = \frac{1}{t} = \frac{1}{1.5mS} = 667\ Hz$$

For some, this may be about right. For others, this may be a little low to your liking. To raise it to 700Hz, calculate the time period of 700Hz (1/700 = 1.4mS). At 1.0mS/div, you can adjust your sidetone or transmit offset until zero-crossings for a single sinewave is 1.4 divisions. This will be about 700 Hz. (Sidetone may not be adjustable on some rigs).

All frequency measurements are made in this fashion, by measuring the distance between zero-crossings (or from one peak to the next) and converting the time period to frequency. This should emphasize the importance of ensuring your sweep speed is calibrated; as any error in the time base will cause a corresponding error in the accuracy of your time or frequency measurements.

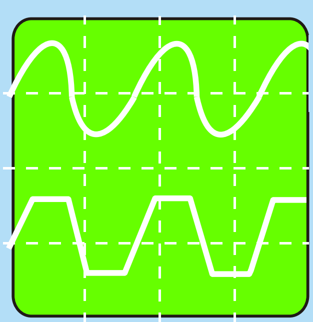

Fig. 7

Example of
Waveform Quality

VERT: 2v/div ACV
HOR: 1.0mS/div

Quality of the waveform is another feature of a scope that is unsurpassed since you are "seeing" the waveform in real time. Two examples of waveform quality are shown in ***Fig. 7***.

The top trace shows the sidetone frequency with distortion, perhaps due to improper time-constant on the coupling capacitors or improperly biased audio amplifiers. The bottom trace would be a raspy sounding side tone, due to the amplifier being over-driven and in compression (clipping). The o-scope is an invaluable tool for detecting and diagnosing such impurities in the signal quality.

FIG. 8 – Full Scale Signal Display

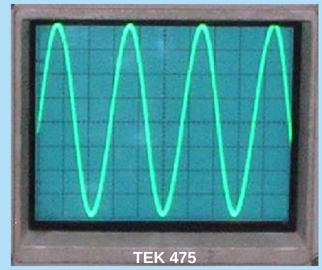

Actual display
Tektronix 475

MORE NIFTY MEASUREMENTS

Amplifier Gain.

The gain of an amplifier can be measured in terms of voltage or decibels (dB). For voltage gain, it is simply Vout/Vin of the amplifier. For example, if the input is 1Vpp and the output is 4Vpp, then the amplifier has a voltage gain of 4.

Gain in dB is often more useful and is how the gains of amplifiers are usually expressed. With dB's, every-time you double the AC voltage, you add 6dB of gain. It is the **ratio** of output to the input, and this **ratio** is easy to measure on a scope.

It is often easier to start with the output. Set the vertical amplifier gain to display the amplifier **output** as a full-scale signal as shown in ***Fig. 8***. Now move the scope probe to the amplifier **input** without disturbing the scope gain. You will of course have a much smaller signal, and the ratio of the input to the output will be the gain in dB. In our example of using eight divisions for full-scale, then four divisions would be 6db, 2 divisions 12dB, etc. as shown in **Fig. 9.** You may want to add your own dB scale along your scope display to remind you of this relationship. Note: this is ***voltage gain*** (Av=20log x Vout/Vin). In this example, with 4Vpp output and 1Vpp input (Av=4), then the gain is dB=20log(4) = 20(0.602) = 12dB, or as shown directly on the CRT tube. Since this is a relative measurement, the absolute Vin or Vout voltage does not need to be determined.

Fig. 9 – Volt. vs. dB relationship

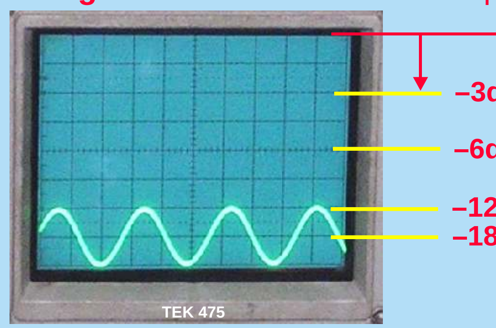

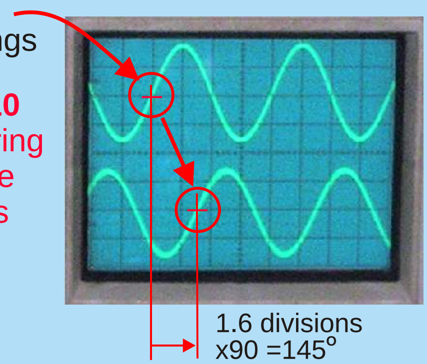

Fig. 10 Measuring Phase Shifts

Insertion Loss.

In some circuits, such as filters or attenuators, the ***loss*** in the circuit needs to be measured, and like circuit gain – expressed in dB. The loss through a circuit is called the ***insertion loss***. It is determined in the same way as amplifier gain just presented, except start with the input (the highest AC voltage) as the full-scale or reference display, then measure the output AC voltage (the lowest level). **The ratio is the insertion loss in dB.**

Fig. 11 –Phase Shift by imposition

For example, with a signal generator connected to your receiver, you want to measure the insertion loss through the IF crystal filter. At the filter input, you can just barely squeek out 2 divisions of input signal on your scope at its most sensitive setting. The output from the crystal filter is 1.5 divisions. The insertion loss would be 20log(1.5/2.0 div.) = –2.5 dB. If the output were only 1.0 division (50% reduction), the insertion loss would be 6dB.

Measuring Phase Shifts.

Phase relationships between two signals at the same frequency can be measured with 2-5^{o} accuracy with a scope, although more suited for a dual-trace scope. The reference signal is applied to CH. 1 and the signal to be measured to CH. 2. For proper phase measurements, ensure your dual trace display is in the **chopped** mode, not **alternate** mode for proper phased referenced triggering.

There are many methods to do this. One is to stretch out the signal so it takes 4 horizontal divisions, such that each division is 90^{o} of phase, as shown in **Fig. 10**. By measuring from a common point on one signal (zero-crossing or from peak-to-peak) to the next, the phase can be measured. For example, say you are making a phased-array antenna in which one feedline must cause a 90^{o} delay. You calculate the electrical length for a ¼λ [L=(246/f) x Velocity Factor] and cut the coax to that length. You are now working on blind faith that you have exactly 90^{o}. With a scope, you can measure it fairly accurately by injecting a signal into one end with a signal generator (at the frequency of interest) and a 50Ω load on the other. Connect the scope CH.1 to the coax (signal) input and CH.2 to the load end and measure the phase. In the **Fig. 10** example, the CH.2 signal is delayed by 1.6 divisions, at 90^{o} /div is 145°. ***Your delay line is too long!*** Cut off an inch or two at a time until the CH.2 signal is 90^{o} from CH.1 for precise tuning of the delay

line. (While departing from o-scopes for a moment, the sharp null of a phased array is astounding when exactly 90^o delay is achieved. More than $10\text{-}15^o$ in error causes a very "mushy" null with little difference over a single vertical antenna. Most errors in achieving exactly 90° by the "measure-and-cut" method are due to uncertainties in the stated velocity factor of the coax).

Another method is to superimpose the two signals on top of eachother. Make one signal larger than the other so you know which one is what, as shown in **Fig. 11**. In this example, the smaller signal lags the larger signal by about 100^o, estimated by where they cross. For more accurate determination, use the time base to measure the time period of one cycle (T1), then the time period one signal lags (or leads) the other (T2). The phase shift is then $\theta = (T2/T1) \times 360^o$.

Phase measurements can be made on a single trace scope as well. First, connect the reference signal, uisng a BNC "T," to both the *external trigger* and the normal *vertical input*. Adjust the trigger level so the zero-crossing occurs at the beginning of the trace (left-hand graticle). Remove the reference from the vertical input, but not the e*xternal trigger,* and apply the signal to be tested to the vertical input – without altering the time base or trigger level. The distance of zero-crossing of the test signal is from the left-hand graticle can now be measured to determine the phase, though with slightly less accuracy than using a dual-trace scope.

An interesting experiment is to measure the phase shift of the audio signal at different frequencies as it travels through the stages in a CW, SSB or AM active filter. What is the phase shift of the wanted vs unwanted frequencies?

Measuring Rise and Fall Times.

In digital circuits, it is sometimes important to know the rise and fall times of a signal through a gate. In amateur radio transceivers, this same interest could be applied to how fast the T-R switch switches. On key-down, if the transmitter turns on slightly before the receiver is turned off, it can produce an annoying "thump" in the receiver. Rise and fall times are measured by triggering on the edge of the signal of interest, then increase to a faster sweep speed to measure the time it takes the signal to reach 90% of its final level. The signal to be measured is shown in **Fig. 12** on the top trace, and the expanded version on the bottom. For proper rise times, the signal being measured should be well within the bandwidth of your scope and using a low capacity probe.

For example, in **Fig. 12** (bottom trace), the rise time is about 1/4th of a division. If the sweep speed is 100nS/division, the rise time would then be about 25nS.

Fig. 12 –
Rise and Fall Times

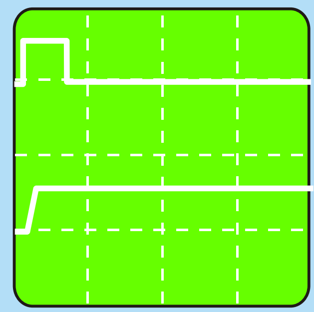

USING LIMITED BANDWIDTH SCOPES

Today's scopes have 200–500MHz bandwidths. Likely your scope is much less than that. A limited bandwidth scope is still very useful to the amateur or homebrewer. Say the bandwidth of your scope is 5MHz. This does not mean you can't see 7MHz signals. It just means the peak-to-peak value has lost meaning, and will likely be very weak, since it is beyond the bandwidth of the scope. (Like other bandwidth measurements in electronics, the "bandwidth" of a scope is usually based on the "3dB bandwidth." That is, at the maximum bandwidth, you are already at the –3dB point, or a 25% reduction in the peak-to-peak voltage display). You can still resolve individual cycles higher than the cited bandwidth to a certain degree and make gain and phase measurements, since they are based on ***ratios.***

Most of the examples in this article explore many regions of a communications receiver or ham transceiver without the benefit of any great bandwidth. Experiment with your scope to learn its limitations. ***Use a good scope probe and make measurements with a good ground to get the most out of the bandwidth you have.***

For the homebrewer building circuits in the HF bands, a 50 MHz scope **with good calibration** will yield fairly accurate measurements up to 30 MHz with little concern for accuracy. The old 465 or 475 series of Tektronix scopes, with 100/200 MHz bandwidths, make an excellent oscilloscope for the amateur or experimenter. They can often be found at hamfests today for $100–150, and tend to maintain a fairly good calibration almost regardless of how much use they have seen.

In Part 2 - we'll probe (bad pun) into some advanced measurement techniques, even with a simple scope ... such as measuring sideband rejection, filter responses, VCO phase noise, etc. (and what it all means).

72, Paul NA5N

na5n@zianet.com
pharden@nrao.edu

Colophon:
Article prepared by NA5N using CorelDraw 11

NIC NAC TIC TAC CRYSTAL RADIO SET - AN IDEAL PRIMARY SCHOOL PROJECT...

Technology (/technology/) > Science | by mk484 (/member/mk484/) Follow

Posted Jul. 4, 2014 |

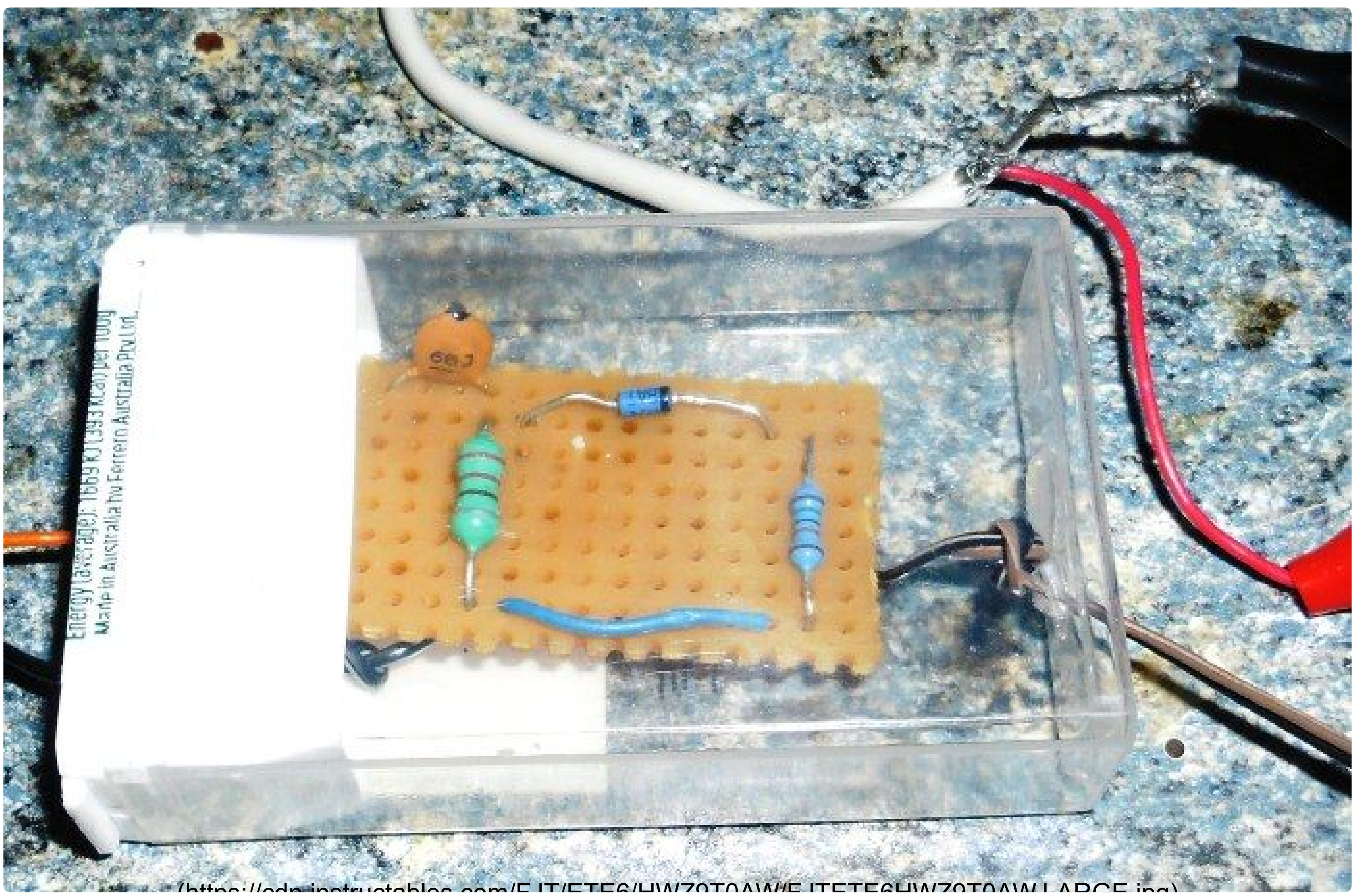

(https://cdn.instructables.com/F1T/FTF6/HWZ9T0AW/F1TFTF6HWZ9T0AW.LARGE.jpg)

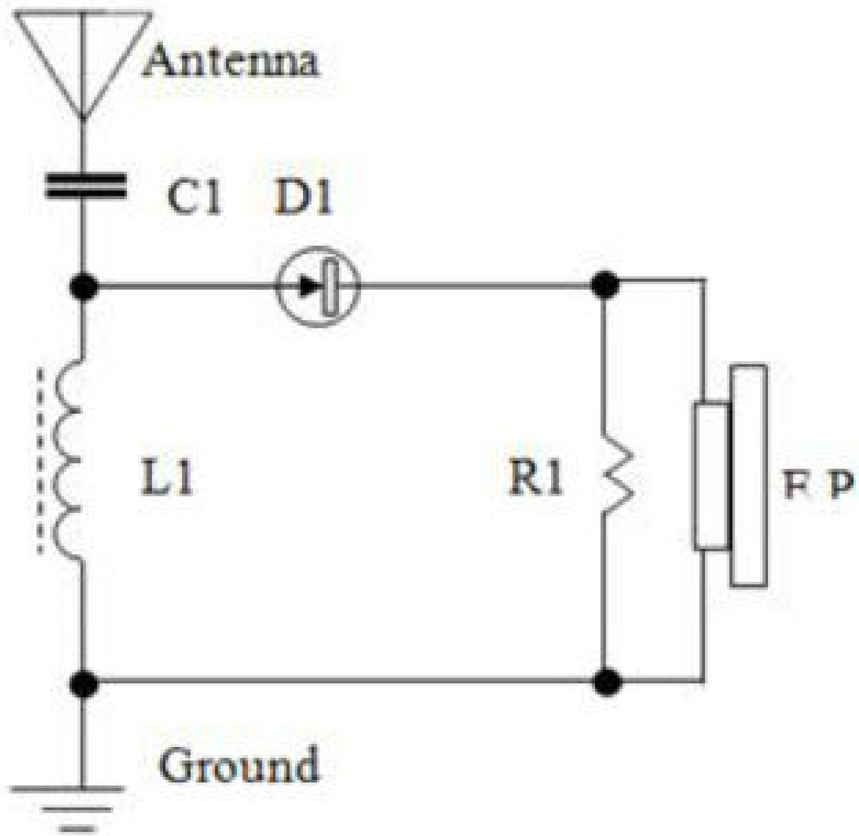

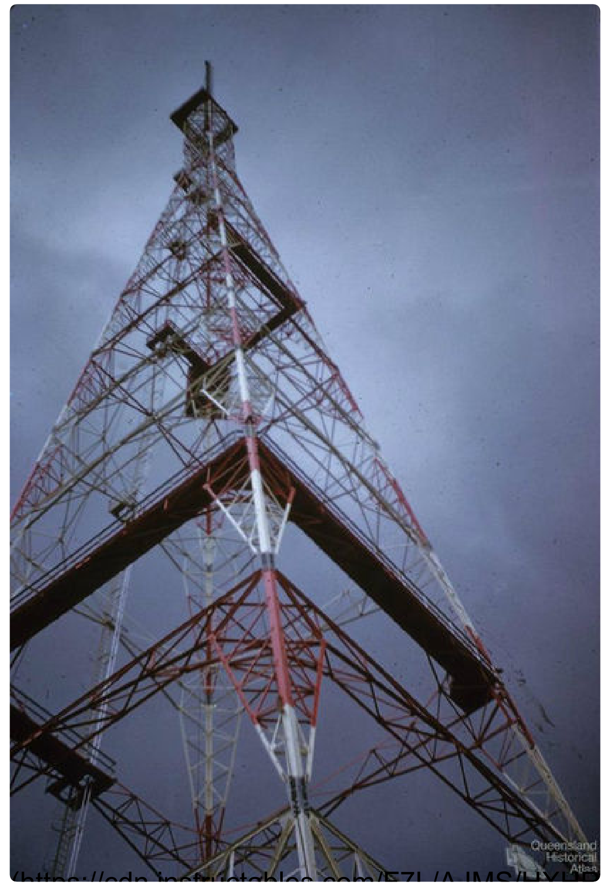

Hi there! This Instructable is all about building a basic crystal radio set that is so simple to build and understand, that a child could do it - with help from mum or dad - or even at school, as a class project. Parts can be bought "off the shelf" at Jaycar Electronics and other suppliers, or purchased online via Ebay and Paypal.

I built my first ever crystal set when I was 9 years old, but that was a different world. We're going to build a 21st century style radio with all modern components which are relatively easy to obtain at your local electronics store or on the Internet.

The radio is contained inside a Tic Tac box, and is called "The Nic Nac Tic Tac Radio". It is built on a square of matrix board, with the component leads poked through the holes in the board, and joined underneath. It is a very simple crystal set, designed to initially receive only one station, but you can expand the tuning range with the addition of only one extra component.

The Tic Tac radio can be constructed by simply twisting the component leads together, underneath the matrix board and attaching antenna/ground wires as well as the earphone wires to the board, using that same technique. You don't have to

solder any wires, but there is another way to join them all together - more on that later.

The Tic Tac Radio is a very easy set to put together - you don't need to wind bulky coils or use heavy tools and screw strange looking parts onto a large breadboard. See step 1 for the parts list you will need.

Add Tip   Ask Question

Step 1: Parts and Tools You Will Need

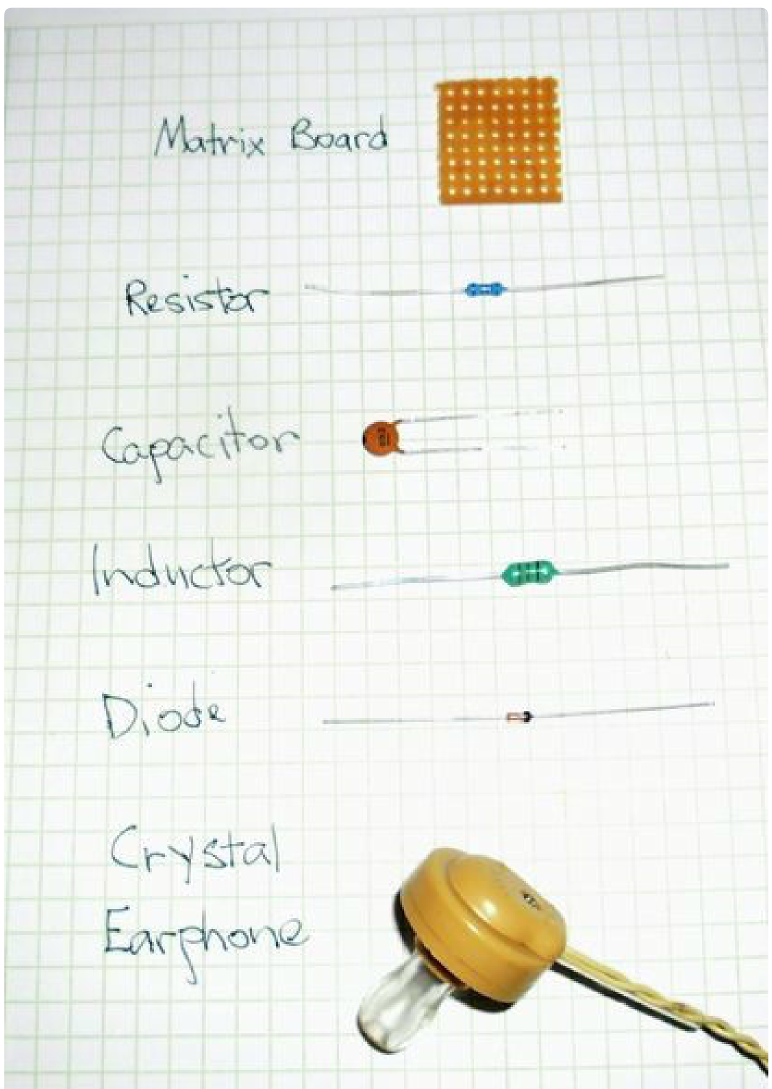

(https://cdn.instructables.com/F9B/WLF.I/HY5H54TY/F9BWLF


(https://cdn.instructables.com/F99/H0BC/H\

(https://cdn.ins


(https://cdn.instructables.com/FXV/F

You will need to acquire the following components from a local electronics shop or an online electronics business.

I am adding the catalogue numbers for Jaycar Electronics, so if you live in Australia or North America, you may be able to visit a Jaycar store and buy the parts over the counter, if not then you may be able to do an online mail order via Paypal:

Parts List

Resistor - 47k - yellow-purple-black-red and brown - RR 0612 (pkt of 8)

Capacitor - 68pF - ceramic x 2 - RC 5322 (pkt of 2) and a 100 or 120 pF value as well for experiments.

Inductor - 220 uH - red-red-brown silver - LF 1538 (resistive type)

Polyvaricon tuning capacitor - 220 pF - RV 5728 - with knob and mounting screws

Diode - BAT46 - ZR 1141 (You can also use a 1N34A Germanium Diode too if you have one at home)

Ceramic Earphone - AS 3305 *

A 25 meter roll of yellow hook up wire for the Antenna wire and a 3 meter length of wire for the Ground wire.

Please note that some Jaycar parts come in multiples of 2 or more per packet. And please note the following:

PLEASE NOTE: THIS PROJECT/KIT CONTAINS SMALL PARTS THAT MAY FORM A CHOKING HAZARD FOR SMALL CHILDREN OR PETS. NOT SUITABLE FOR CHILDREN UNDER FIVE (5) YEARS OLD.

*A normal crystal radio earphone is OK, but if you can't get one of these, or if the one you bought goes dead (as they sometimes do,) you can use a substitute, such as the Murata PKM44EW passive transducer (see picture above) which is available from an old Telstra TF200 touchphone, (the one on the left in the diagram above,) or an equivalent, such as the ARIO transducer, from an old Telstra T1000 pushbutton phone.

The ARIO unit is soldered to the phone's pc board so you'll need to be able to unsolder the three mounting pins underneath the board, or find someone in the neighbourhood who is able.

Take the back off the TF200 (if you've obtained one of these phones,) and you'll see a black disc shaped object 2" round by 1/2' thick - with a red and black wire. Unplug the wires from the circuit board, and unscrew any retaining screws and remove the transducer. Cut the mini plug off, carefully strip the insulation from the ends of the wires and extend them by about 18" with 2 thin lengths of hookup wire. These pietzo devices make good earphones for crystal sets and can be housed in an old pair of ear muffs.

Miscellaneous Materials:

A Tic Tac box (smaller size)

A piece of matrix board at least 7 holes long by 8 holes across. Cut the board to fit neatly inside the Tic Tac box.

A short length of 2 differently coloured wires 60 mm in length and 2 crocodile clips with red and black plastic covers

A length of antenna wire at least 25 metres long and a 3 metre length of a different colour for the Ground wire.

A metal rod or cold water pipe for the ground stake. Be careful which pipes you connect your Ground wire to.

You will need a small sharp object for punching holes in the Tic Tac box.

A small pair of wire cutters for cutting and stripping wires.

Step 2: How a Crystal Radio Works

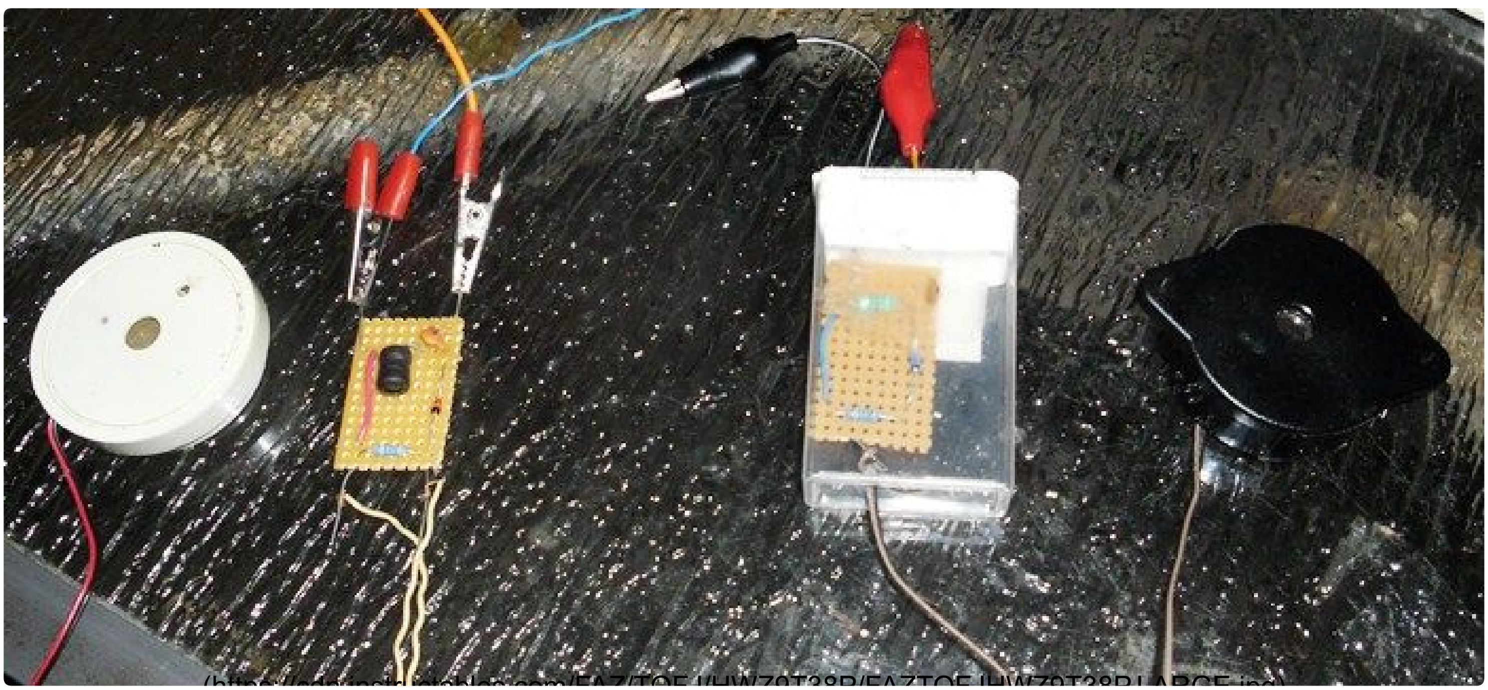

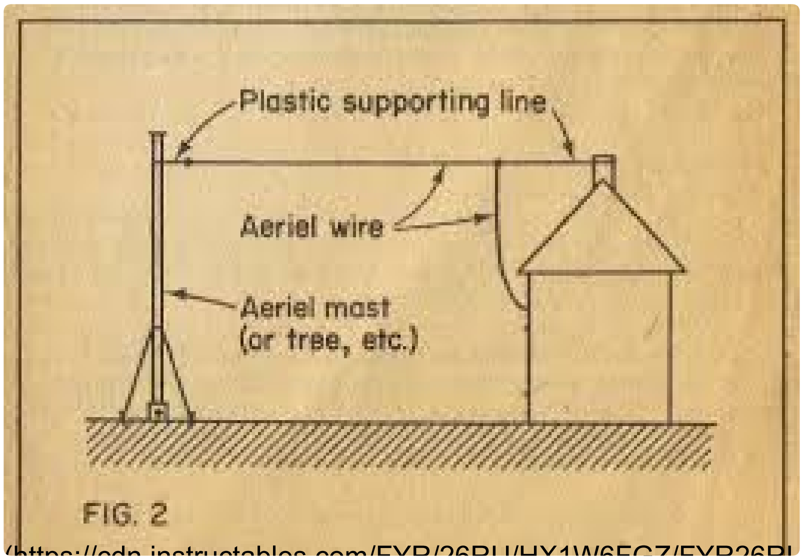

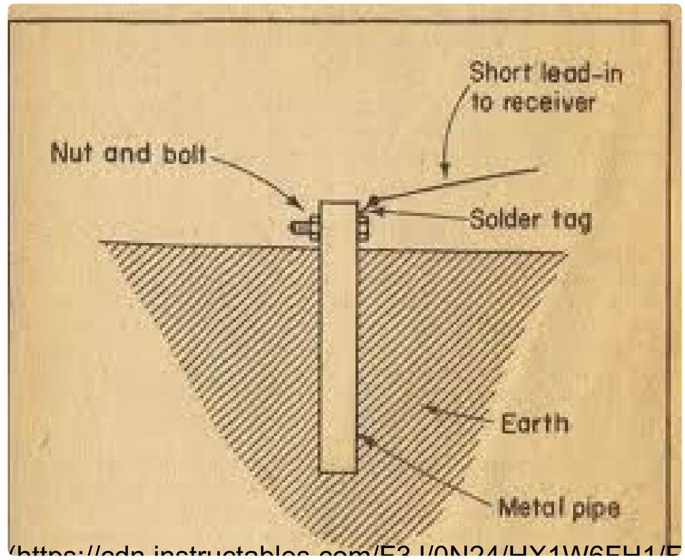

Radio signals consists of two parts - the 'carrier wave' which is the AM radio station's frequency of operation, and the 'program signal' which is mixed with the carrier wave for transmission.

Radio waves travel out from the AM transmitter tower through the atmosphere. We want to capture one specific frequency so we can listen to it, so we need the antenna/ground wire system to capture that signal. We also need a 'tuned circuit' that will filter out the desired AM signal, and discard the rest, so that all the other unwanted radio signals pass out through the ground wire to earth.

Two components in our circuit will perform that task for us. The capacitor C1, together with L1 inductor, form a basic 'series tuned' circuit. Their respective values will determine just which local AM radio station we will capture.

We also need a diode to 'detect' the voice and music, so we can hear them in our earphone, which transduces electrical signals into sound waves that we can hear.

In the photo above you can see a completed Tic Tac crystal radio. It is already inside the box. The other set is connected to the antenna/ground wire circuit, undergoing a 'soak test'. It is necessary to do this to ensure that the radio will work once inside the box!

The first diagram shows a typical antenna wire installation. Coming out of a window, the wire is anchored to the building and then over some distance (10 metres +) to a nearby tree or other building.

You must take great care not to erect antenna wires near to power or telephone cables, near your home!

The ground wire comes out the same window and is anchored to a metal pipe/water pipe or metal ground stake, embedded in soft, moist soil.

You must not connect ground wires to electrical mains wiring installations, including wall power outlets!

Another electrical hazard to consider is lightning strikes! Although it is very rare for anyone to be seriously injured or die from a lightning strike it is not impossible. So, if you hear a thunderstorm coming your way (you may hear the lightning 'crashes' in your earphone first,) then disconnect your antenna wire immediately, connect it to the ground wire and put it well up out of the way. Stay well clear of this temporary antenna/ground connection until the storm has completely passed away from your general area - miles away!

Step 3: How to Build the Tic Tac Crystal Radio Set

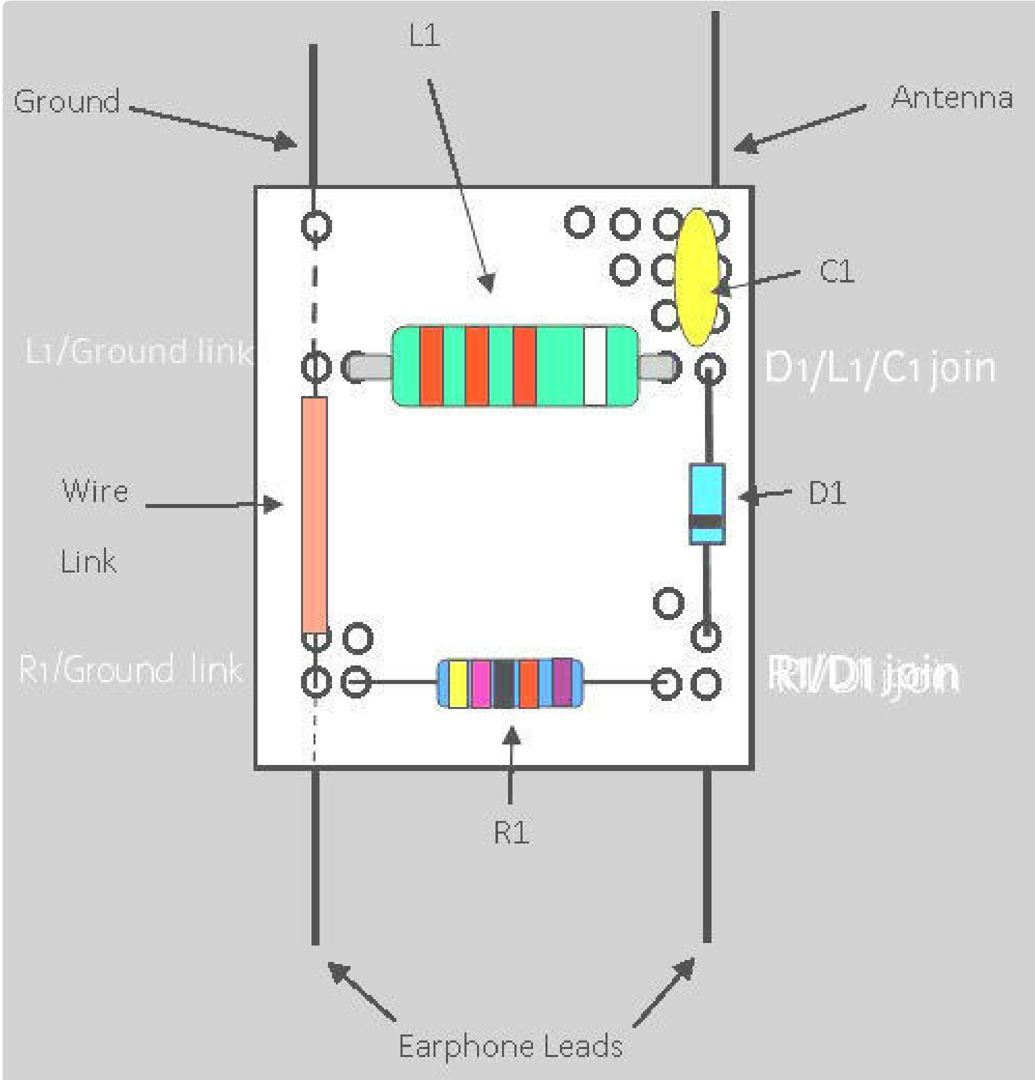

(https://cdn.instructables.com/FA5/FW4F/HXA9BXF0/FA5FW4FHXA9BXF0.LARGE

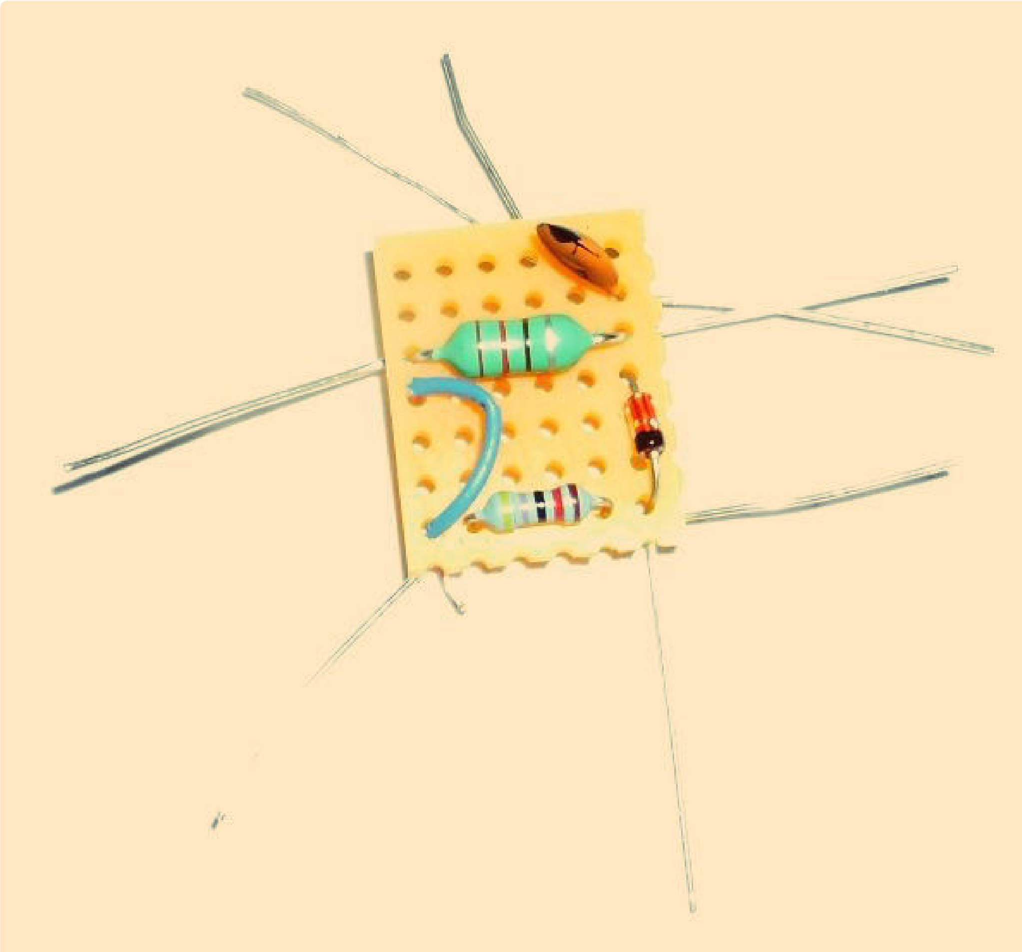

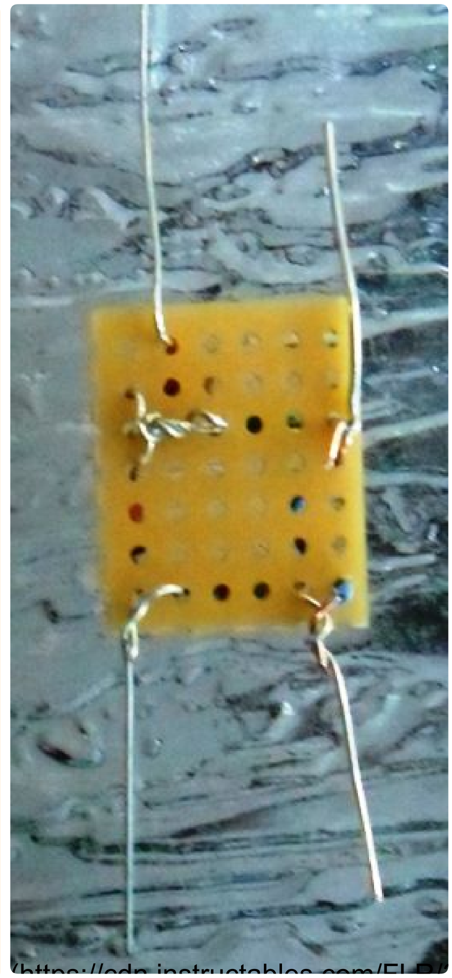

(https://cdn.instructables.com/FS8/N068/HXA9RY3O/FS8N068HXA9RY3O.LARGE (https://cdn.instructables.com/FLP/

1. Take the components and lay them out on a clean surface.

2. Take the square of matrix board (this is also called 'perf board' because of all the holes or perforations in the material) and beginning with the 220uH (uH = micro-Henry) and place it as shown in the diagram.

3. Then take the diode, capacitor and resistor and place them in the places shown for them, making sure that the coloured band at one end of the diode joins with the resistor wire, as shown

4. Then take each junction where wires come together through their respective holes and gently twist them together, until they form a neat, tight bundle. Take your side cutters and cut off any excess length, taking care not to cut any one wire too short, so that it comes undone from the join.

.5. Take the link wire, strip 2 centimetres of insulation from each end of the wire and install that wire between the free ends of the inductor and resistor, and the matrix board construction is complete.

6. Then take the ceramic earphone, cut the plug off the end, and strip the 2 wire ends about 1.5 centimetres in length. Wrap each earphone wire around each end of the resistor component, underneath the matrix board.

7. Finally, strip the insulation off both ends of the 60mm long differently coloured wires, and attach them to the matrix board - one goes to the inductor/link wire junction and this will be the Ground connection wire. Attach the other one to the free end of capacitor C1 and this will be the antenna wire connection. Both connections are made underneath the matrix board. The Nic Nac Tic Tac Crystal Radio is now ready for testing.

Step 4: Final Checks and Installation of Wires

(https://cdn.instructables.com/FX9/8RCY/HX8HJEU3/FX98RCYHX8HJEU3.LAR

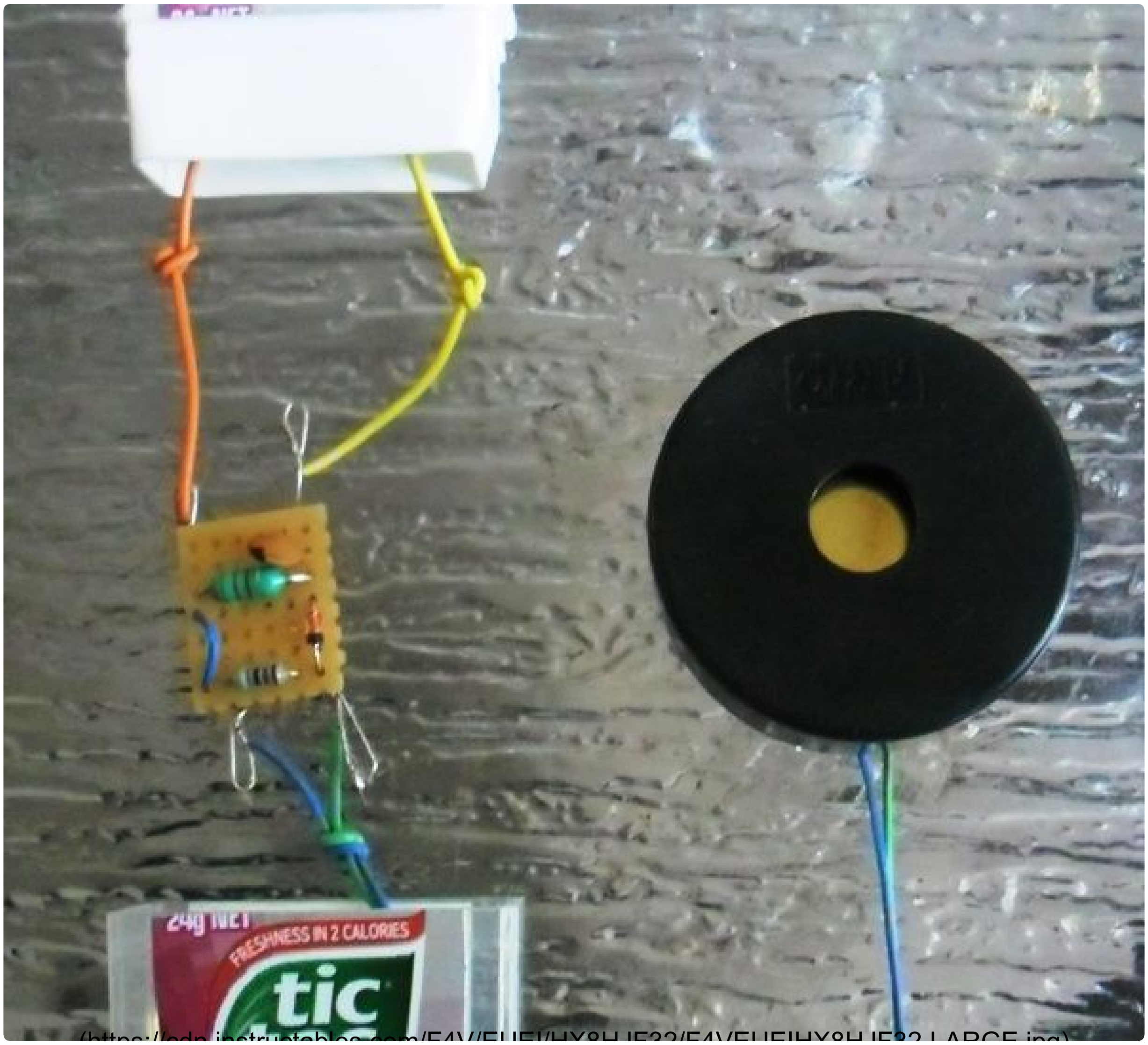

(https://cdn.instructables.com/F4V/FHEI/HX8HJF32/F4VFHEIHX8HJF32.LARGE.jpg)

When you've finished constructing the matrix board circuit and have clipped all the excess component leads off, puncture three (3) holes in the Tic Tac box - 2 small holes on the top lid of the box, about an inch (24mm) apart, so that your antenna and ground wire leads can come through the box lid, and be connected to the matrix board at those 2 points.

Feed the wires through the holes and then tie small knots in each one, near the underside of the box lid, so that they won't pull back out if strained, and disconnect themselves from the matrix board.

Then make one larger hole in the centre of the bottom of the box (clear part) so that your earphone wires can be fed through to the connecting points on that part of the matrix board. Tie a larger knot in the earphone lead so as to prevent it from pulling

out of the box if it is strained. Strip the insulation off the earphone leads, and wrap them around the matrix board leads at those 2 points. You are now ready to test out the Nic Nac Tic Tac Crystal Radio.

Add Tip Ask Question

Step 5: Testing Out the Tic Tac Radio

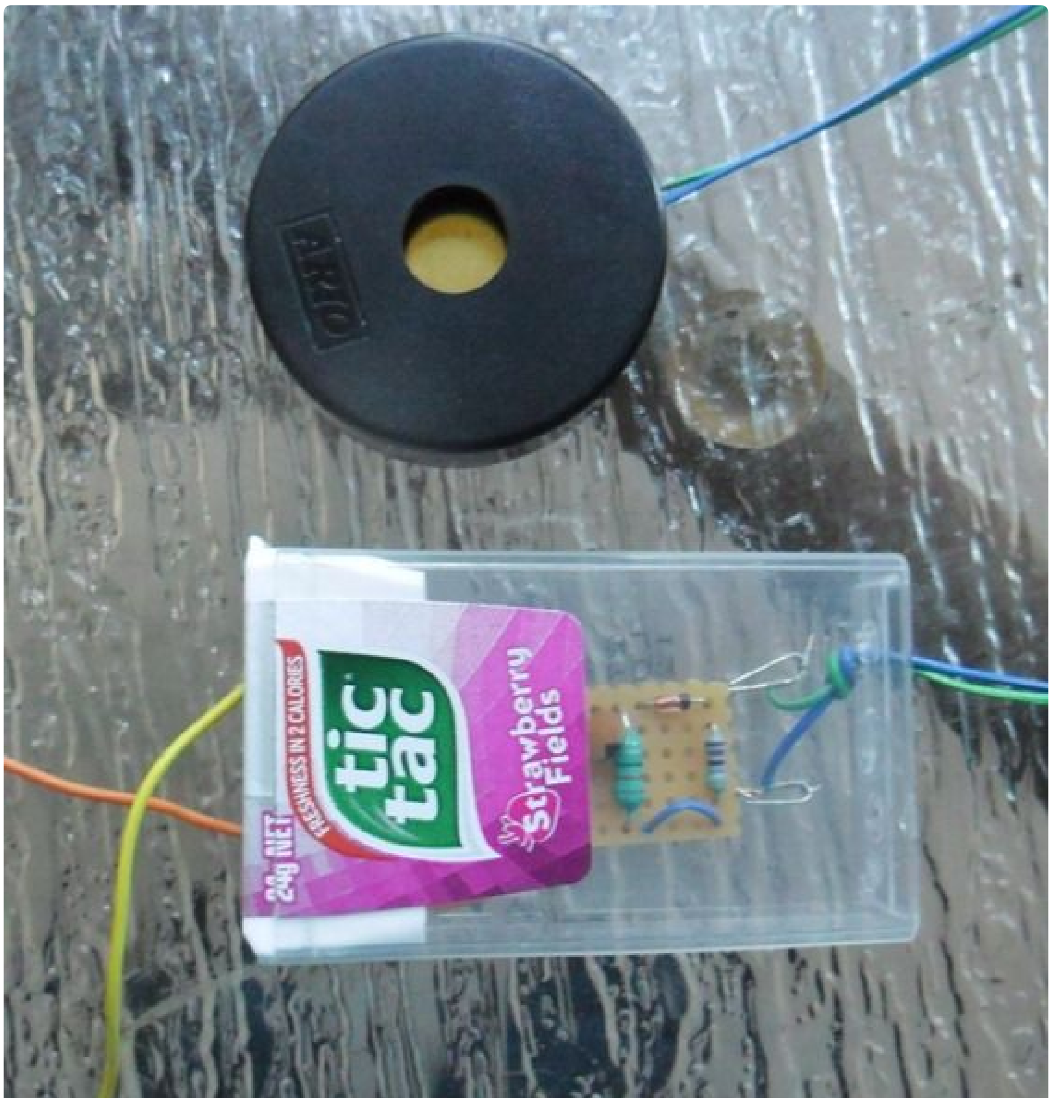

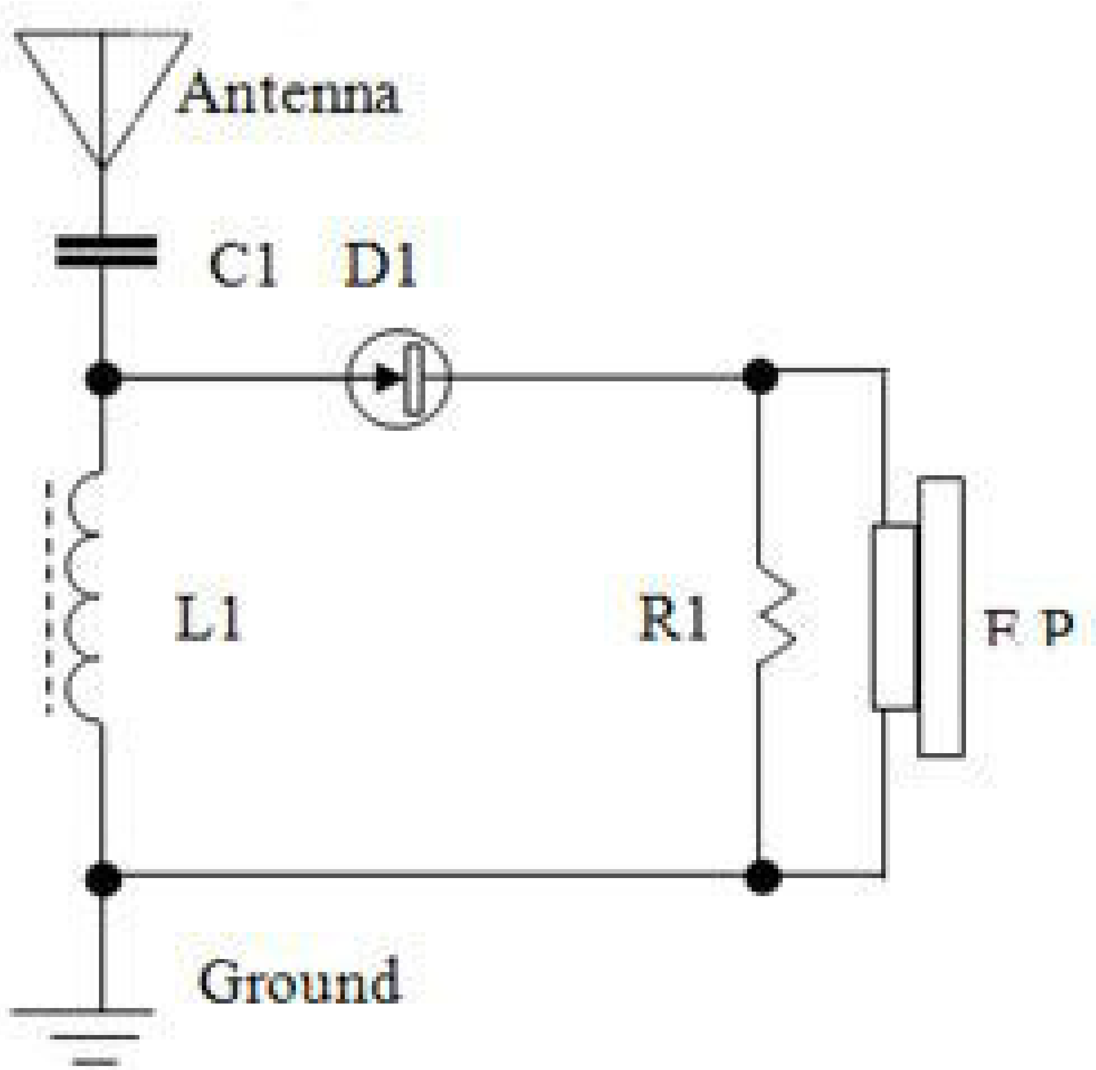

(https://cdn.instructables.com/FL6/41GU/HX5H55A2/FL641GUHX5H55A2.LARGE.jpg)

Take your finished Tic Tac Radio (with the lid part gently pushed back inside the top of the box) and connect your Antenna and Ground wires to the lead outs from the box lid. Place the earphone in/over your ear,and listen carefully for a local AM radio station. This crystal radio is a simple one, and you may have to make one or two adjustments to the components, before you succeed in receiving one or more local AM radio stations, in your area.

If you can't hear anything in the earphone, don't panic. It might just be a simple wiring mistake, which is easily fixed. Go back over all of the steps, making sure that you have the right value components from the electronics store. Make sure that each component is in the right place on the matrix board, (don't confuse the L1 inductor with the R1 resistor - they look a lot like each other!) and that no component wires have come undone from the twisted joins you have just made. I'll

be writing up a troubleshooting step soon, so if you run into any problems, post your questions in the 'comments' section down at the bottom of the page, and I'll try and answer them as soon as possible.

Make sure that your antenna and ground wires aren't snagged on anything metal or anything dangerous!

If you have ANY doubts about the electrical safety of your antenna or ground wires, then consult a licensed electrical trades person, who will be able to advise you on electrical safety principles and procedures!

Always remember that electrical safety is your responsibility! If you don't think it is safe to proceed, then don't!

You will need at least 10 to 15 metres of antenna wire, strung between 2 insulating points (not connected to anything metallic, or that gets wet,) at least 2 to 3 metres in height - anything less than this minimum arrangement may mean that you cannot receive any signals at all.

Some places are regarded as 'radio dead spots', so you may need to try an open space, such as a park or a remote corner of a beach. If you do erect antenna and ground wires in public places, hang some streamers or balloons off of them, to alert people to their presence, otherwise people going past may become entangled with them - and get cranky with you!!!

As a final word for now, you'll be happy to know that the completed "Nic Nac Tic Tac Radio" shown in the picture above, picked up local AM radio station 1116 khz 4BC here in Brisbane, with a very clear signal and quite good volume. It works! So be safe kids, have some fun and look forward to more... mk484

Add Tip Ask Question

Step 6: Nic Nac Extras

(https://cdn.instructables.com/FGL/RHQH/HX8HJG9V/FGLRHQHHX8HJG9V.LARGE.jpg)

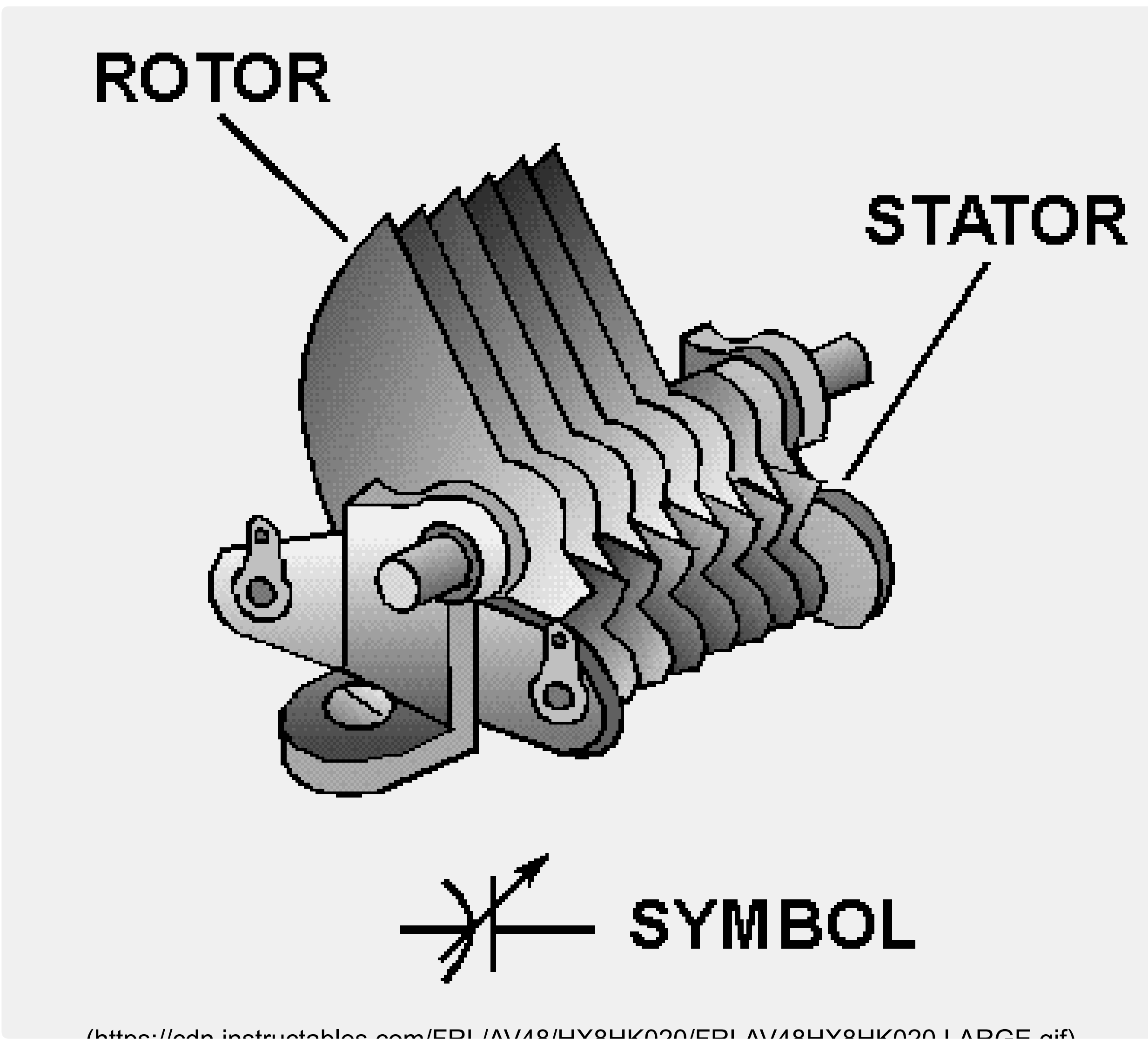

(https://cdn.instructables.com/FRL/AV48/HX8HK020/FRLAV48HX8HK020.LARGE.gif)

If you've built your Tic Tac crystal set and found that you can't receive a local AM radio station yet - don't panic - help is in on the way. You have just built the simplest version of the Tic Tac crystal radio and you may need to add one more component part for it to work properly. This is called a 'polyvaricon' - a miniature tuning capacitor, which can vary the frequency that your radio will receive at. You can see a picture of one up above - the small white box with the black knob next to it. It has 3 connecting tags - the one in the middle ('G') goes to the moving plates and the shaft, while the 2 outer tags ('O' and 'A') go to 2 sets of fixed plates. the smaller set of plates has a value of 60pF - pF is short for 'picoFarad' - a unit of measurement for capacitance. The larger set of plates is valued at 160 pF so that the combined value of the polyvaricon is 220 pF - or 220 picoFarads.

The other picture shows you what happens inside a basic tuning capacitor. there are 2 sets of metal plates - one set is fixed and the other set moves on a rotating shaft, connected to the tuning knob of your radio set. Both sets of plates are mounted on an insulating frame so that they won't 'short out' by touch each other.

The fixed capacitor C1, was chosen to tune somewhere close to the middle of the AM radio band. This band of frequencies starts at 531 kilohertz (Khz) and goes as far as 1701 Khz here in Australia. So we need a combination of coil and capacitor which will tune across all of those frequencies. Our simple Tic Tac radio is known as a 'series tuned' set. If you look at the circuit diagram, you can see electronic symbols for all components in the radio set.If you start at the top with the antenna symbol, you can see the capacitor C1 underneath that, the inductor L1 underneath C1 and then finally, the ground symbol - all wired in series with each other.

The diode D1 detector, the resistor and the earphone plus the link wire, can be considered as one block - the "detector unit". The Antenna wire, ground wire, inductor/coil and capacitor/polyvaricon, can be also be considered as another block - the "tuned circuit". So joining both blocks together, we have the tuned circuit that tunes in only one frequency, passing all other unwanted signals out through the ground wire to earth. This one 'tuned frequency' passes through the diode detector, which strips away the 'carrier wave' and leaves only the 'program signal' (voice,

music etc,) behind, which is then fed via the resistor into the earphone. The earphone changes electrical impulses from the diode detector, into sound waves that we can hear. You need the R1 resistor to provide a pathway for the signals going through the diode, out to the ground wire connection. Without this resistor, the signals would sound very distorted and you couldn't hear the program signal very clearly.

Add Tip Ask Question

Step 7: Adding the Polyvaricon Tuning Capacitor

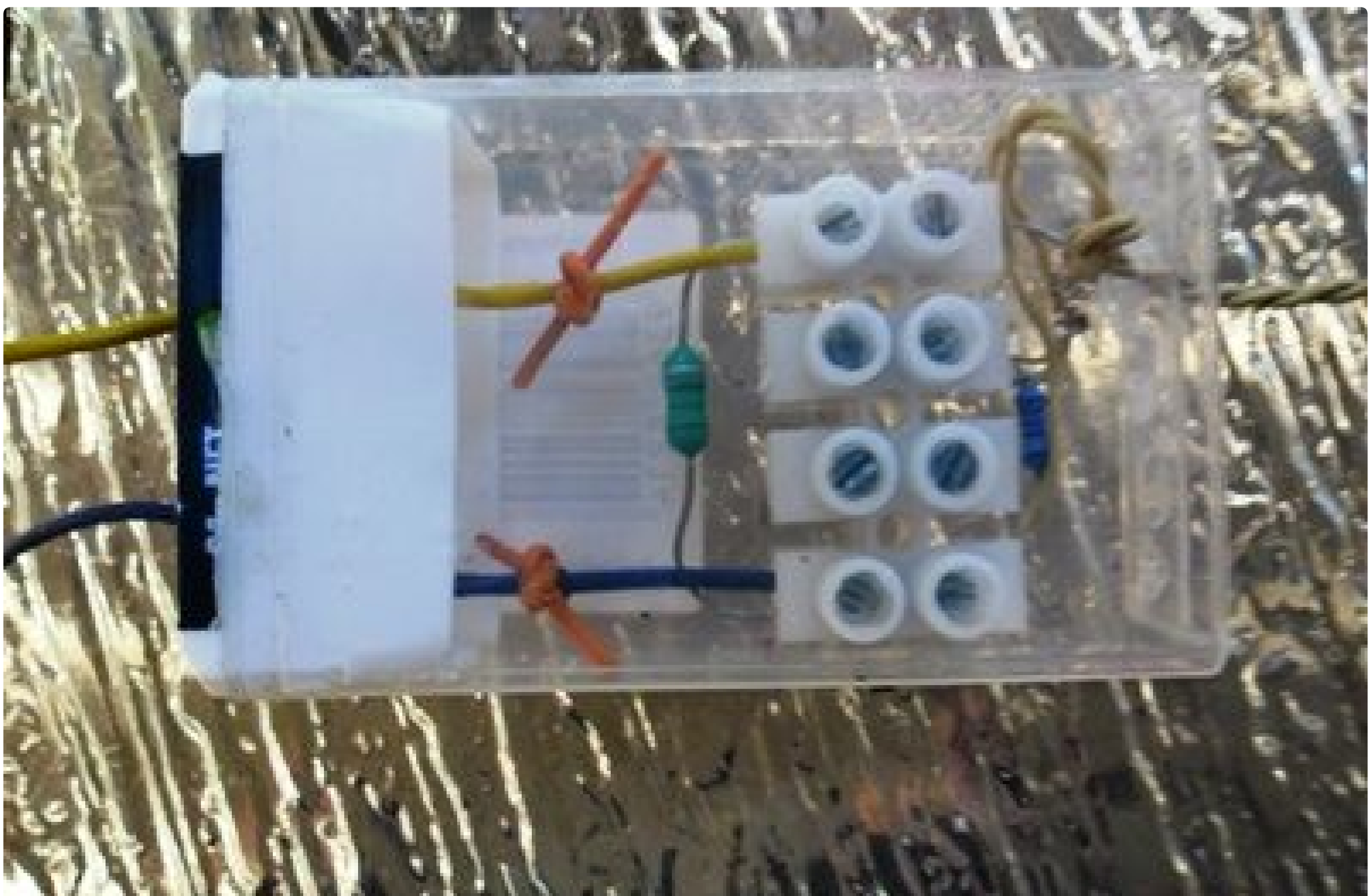

(https://cdn.instructables.com/F9D/UY53/HX8HMYHT/F9DUY53HX8HMYHT.LARGE.jpg)

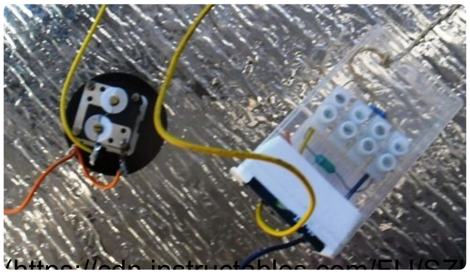

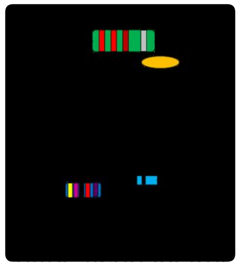

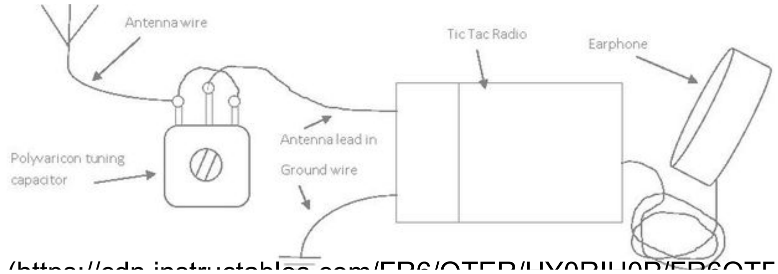

If you want to expand the tuning range of your Tic Tac Radio, than all you have to do is a simple modification (change) to the circuit of your radio set. You can see from the 2 pictures above, that there's an alternative way of building the crystal radio - you can use the matrix board method or you can use a 4 way screw terminal strip.

To use the screw terminal version, cut yourself a 4 way strip of terminals as shown in the diagram and pictures. Undo the screws right out as far as they will go without falling out of the strip. Connect the component leads and wires from the antenna/ground system as well as the earphone wires. Cut off any excess from component leads that you don't need. Wrap thin wires from the antenna/ground system and the earphones, around the thicker component leads before screwing the screws in tight.

Regardless of which method you have used, all we will now wire up the tuning capacitor between the actual Antenna wire and the junction (join) where the diode D1, the fixed capacitor C1 and one end of the inductor meet. Remove the capacitor from the matrix board, and connect the Antenna lead out wire straight to the join of the diode and inductor. Then take the polyvaricon and another piece of wire. Strip both ends of that wire and join the two outer tags (tagged 'O' and 'A' - the centre on is tagged 'G') and then connect you actual Antenna wire to one of the outer tags. Connect the antenna lead out wire, coming out of the box, to the 'G' (middle) tag of the tuning capacitor,so that the antenna wiring now looks like the picture up above.

If you're having problems following the pictures, then refer to the diagrams, which clearly shows all of the connections Make sure your ground wire is connected to the set, and then, listening with your earphone in/over your ear, slowly turn the

tuning cap's flat knob, until you hear one or more stations. Congratulations - you now have a "tuneable" Tic Tac crystal set! Happy listening! And don't forget to post in your results, questions, problems etc... mk484 :)

Add Tip Ask Question

Step 8: Tic Tac One Transistor Amplifier - Use Your Earbuds and Hear Great Sound...

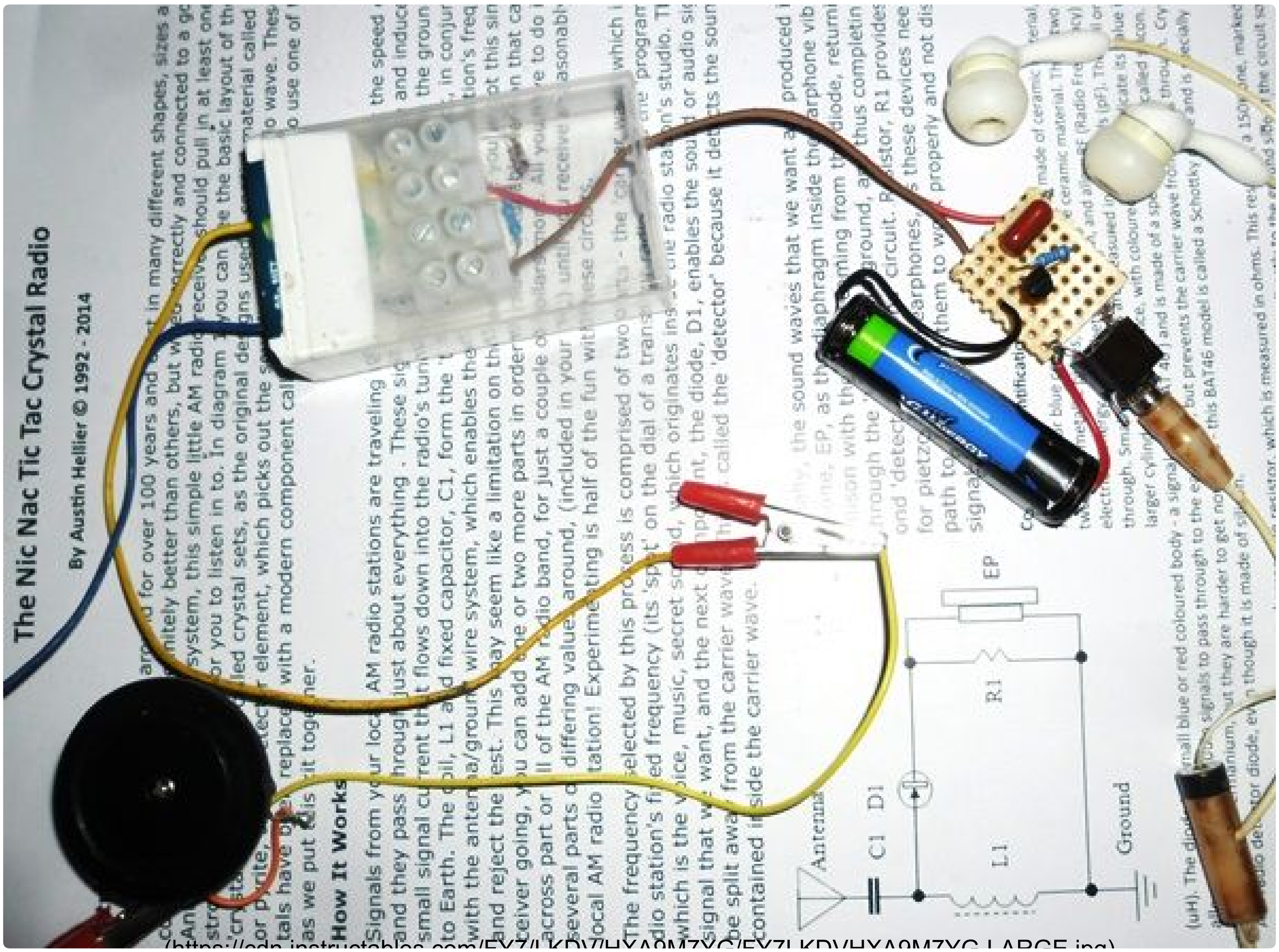

(https://cdn.instructables.com/FYZ/LKDV/HYA9MZYG/FYZLKDV/HYA9MZYG.LARGE.jpg)

Hi there folks - this isn't really an extra 'Step' as such - it's a sneak preview at a picture of my upcoming Instructable for a one transistor amplifier, which will connect to the Tic Tac Radio - and give you some really good volume - in your Iphone

earbuds!

Yes, it's entirely possible nowadays, with modern circuit design, to fit a one transistor amp in such a small space (yes kiddies - it WILL fit inside the smaller Tic Tac box...) and at the same time, get that great sound that comes from those "inside your ear" type earbuds.

This circuit took me about a half hour to complete, uses only 3 electronic components, costing about $1.00, a stereo earphone jack and a 1.5 volt AAA battery and plastic holder costing about another $3 to $4, so you can build the amplifier for about $5 all up - don't forget to shop around and - mums and dads - cheap batteries will be OK for this project, and the battery can simply be replaced without soldering or undoing half a dozen screws....

I can hear my Tic Tac Radio with great volume and clarity - and so will you, so "stay tuned" (ha ha ha) to this series of Instructables, and you will hear great sound too...

mk484

Add Tip Ask Question

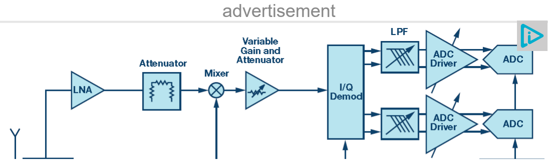

go to: [Talking Electronics Website]

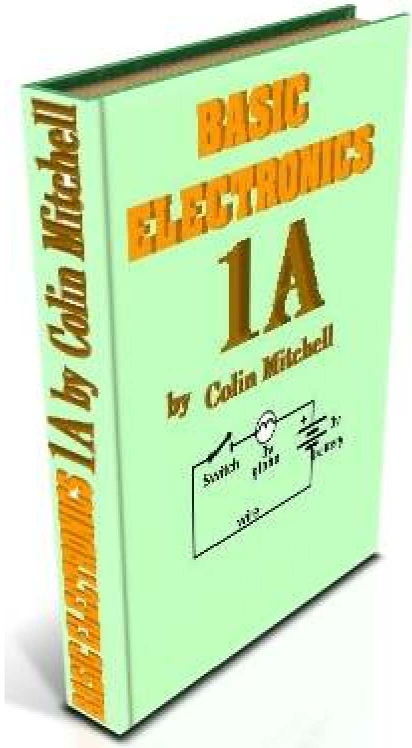

For any enquiries email Colin Mitchell

THE MULTIMETER

INDEX

to Index

TWO MULTIMETERS

There are basically two different types of MULTIMETER. ANALOGUE and DIGITAL
Analogue Multimeters have a NEEDLE or POINTER that moves across a scale.
Digital Multimeters have a numeric display of 3 or more digits. A Digital Multimeter with 3½ digits means the first digit shows only "1."

You really need both types to cover the number of tests needed for designing and repair-work. We will discuss how they work, how to use them and some of the differences between them.

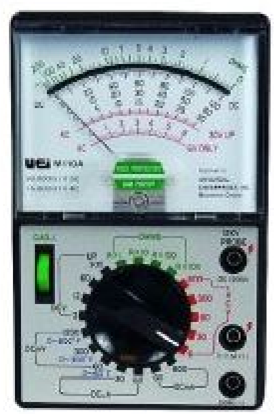

The black (negative lead) ALWAYS stays in the

black hole and the red lead changes to the other red hole to measure 10 amps

to Index

BUYING A MULTIMETER

There are many different types on the market.
The cost is determined by the number of ranges and also the extra features such as diode tester, buzzer (continuity), transistor tester, high DC current and others.
Since most multimeters are reliable and accurate, buy one with the greatest number of ranges at the lowest cost. The cheapest multimeters are on **eBay**.
This article explains the difference between an analogue meter and a digital meter.

Multimeters are sometimes called a "meter", a "VOM" (Volts-Ohms-Milliamps or Volt Ohm Meter) or "multi-tester" or even "a tester" - they are all the same.

One term used to describe a **DIGITAL MULTIMETER** is **3½ digits**.
This is the number of digits on the display. The first digit is usually made from two pixels and can only produce "1." This is called a half-digit. The other digits are full digits. The cheapest digital multimeters have 3½ digits. This will produce a reading of 1999 and the decimal point can produce values from 1.999 to 19.99 to 199.9 to 1999.
Another term is **DISPLAY COUNTS**. This is connected with the accuracy of the display, but since digital meters are accurate to 1% or less and we are using resistors with an accuracy of 5%, even a $10.00 digital meter will be perfect.

to Index

USING A MULTIMETER

Analogue and **digital** multimeters have either a rotary selector switch or push buttons to select the appropriate function and range. Some Digital Multimeters (DMMs) are auto ranging; they automatically select the correct range of voltage, resistance, or current when doing a test. However you need to select the function.

Before making any measurement you need to know what you are checking. If you are measuring voltage, select the AC range (10v, 50v, 250v, or 1000v) or DC range (0.5v, 2.5v, 10v, 50v, 250v, or 1000v). If you are measuring resistance, select the Ohms range (x1, x10, x100, x1k, x10k). If you are measuring current, select the appropriate current range DCmA 0.5mA, 50mA, 500mA, 10A. Every multimeter is different however the photo below shows a low cost Analogue multimeter with the basic ranges.

An ANALOGUE MULTIMETER

The most important point to remember is this:
You must select a voltage or current range that is bigger or HIGHER than the maximum expected value, so the needle does not swing across the scale and hit the "end stop."
If you are using a DMM (Digital Multi Meter), the meter will indicate if the voltage or current is higher than the selected scale, by showing "OL" - this means "Overload." If you are measuring resistance such as 1M on the x10 range the "OL" means "Open Loop" and you will need to change the range. Some meters show "1' on the display when the measurement is higher than the display will indicate and some flash a set of digits to show over-voltage or over-current. A "-1" indicates the leads should be reversed for a "positive reading."
If it is an AUTO RANGING meter, it will automatically produce a reading, otherwise the selector switch must be changed to another range.

A typical DIGITAL Multimeter

The Common (negative) lead ALWAYS fits into the "COM" socket. The red lead fits into the red socket for Voltage and Resistance. Place the red lead (red banana plug) into "A" (for HIGH CURRENT "Amps") or mA,uA for LOW CURRENT.

The black "test lead" plugs into the socket marked "-" "Common", or "Com," and the red "test lead" plugs into the meter socket marked "+" or "V-W-mA." The third banana socket measures HIGH CURRENT and the positive (red lead) plugs into this. You DO NOT move the negative "-" lead at any time.
The following two photos show the test leads fitted to a digital meter. The probes and plugs have "guards" surrounding the probe tips and also the plugs so you can measure high voltages without getting near the voltage-source.

Analogue meters have an "Ohms Adjustment" to allow for the change in voltage of the battery inside the meter (as it gets old).

"Ohms Adjust" is also called "ZERO SET"

The sensitivity of this meter is 20,000ohms/volt on the DC ranges and 5k/v on the AC ranges

Before taking a resistance reading (each time, for any of the Ohms scales) you need to "ZERO SET" the scale, by touching the two probes together and adjust the pot until the needle reads "0" (swings FULL SCALE). If the pointer does not reach full scale, the batteries need replacing. Digital multimeters do not need "zero adjustment."

to Index

ANALOGUE Vs DIGITAL

You cannot say one meter is better than the other because BOTH have advantages and disadvantages.
An analogue multimeter is the "old style" and it puts a load on a circuit and this may change the reading to give an incorrect readout, but it has the advantage of the needle moving across the scale fairly quickly so you can sometimes see if the voltage is fluctuating.
It also gives a more-accurate result in some high frequency circuits as it does not pick up stray fields and produce a false reading.
Digital meters put almost no load on a circuit and produce accurate readings from both low-impedance and high-impedance circuits.
Digital meters can display very low resistances.
You must remember to turn a Digital meter OFF to prevent the battery going flat.

If you are testing a circuit containing a high-frequency oscillator, use BOTH an ANALOGUE and DIGITAL meter to check the reading. Sometimes the leads of a Digital multimeter will pick up signals and create a false reading.
Sometimes you will get a voltage reading with a Digital multimeter due to a high resistance leak and a zero reading with an Analogue meter. This is why you need **BOTH** meters.

to Index

MEASURING VOLTAGE

Most of the readings taken with a multimeter will be VOLTAGE readings.
Before taking a reading, you should select the highest range and if the needle does not move up scale (to the right), you can select another range.
Always switch to the highest range before probing a circuit and keep your fingers away from the component being tested.
If the meter is Digital, select the highest range or use the auto-ranging feature, by selecting "V." The meter will automatically produce a result, even if the voltage is

AC or DC.
If the meter is not auto-ranging, you will have to select V= if the voltage is from a DC source or V~ if the voltage is from an AC source. DC means Direct Current (but this does not mean you select the CURRENT range - you are taking a voltage reading that is not rising and falling. That's why we say it is **DC** and do not say the words "direct current"). The voltage is coming from a battery or supply where it is steady and not "rising and falling."
You can measure the voltage at different points in a circuit by connecting the black probe to chassis. This is the 0v reference and is commonly called "Chassis" or "Earth" or "Ground" or "0v."
The red lead is called the "measuring lead" or "measuring probe" and it can measure voltages at any point in a circuit. Sometimes there are "test points" on a circuit and these are wires or loops designed to hold the tip of the red probe (or a red probe fitted with a mini clip).
You can also measure voltages ACROSS A COMPONENT. In other words, the reading is taken in PARALLEL with the component. It may be the voltage across a transistor, resistor, capacitor, diode or coil. In most cases this voltage will be less than the supply voltage.
If you are measuring the voltage in a circuit that has a HIGH IMPEDANCE, the reading will be inaccurate, up to 90% !!!, if you use a cheap analogue meter.

Here's a simple case.

The circuit below consists of two 1M resistors in series. The voltage at the mid point will be 5v when nothing is connected to the mid point. But if we use a cheap analogue multimeter set to 10v, the resistance of the meter will be about 100k, if the meter has a sensitivity of 10k/v and the reading will be incorrect.
Here how it works:
Every meter has a sensitivity. The sensitivity of the meter is the sensitivity of the movement and is the amount of current required to deflect the needle FULL SCALE. This current is very small, normally 1/10th of a milliamp and corresponds to a sensitivity of 10k/volt (or 1/30th mA, for a sensitivity of 30k/v).
If an analogue meter is set to 10v, the internal resistance of the meter will be 100k for a 10k/v movement.
If this multimeter is used to test the following circuit, the reading will be inaccurate. The reading should be 5v as show in diagram **A**.
But the analogue multimeter has an internal resistance of 100k and it creates a circuit shown in **C**.
The top 1M and 100k from the meter create a combined PARALLEL resistance of 90k. This forms a series circuit with the lower 1M and the meter will read less than 1v
If we measure the voltage across the lower 1M, the 100k meter will form a value of resistance with the lower 1M and it will read less than 1v
If the multimeter is 30k/v, the readings will be 2v. See how easy it is to get a totally inaccurate reading.

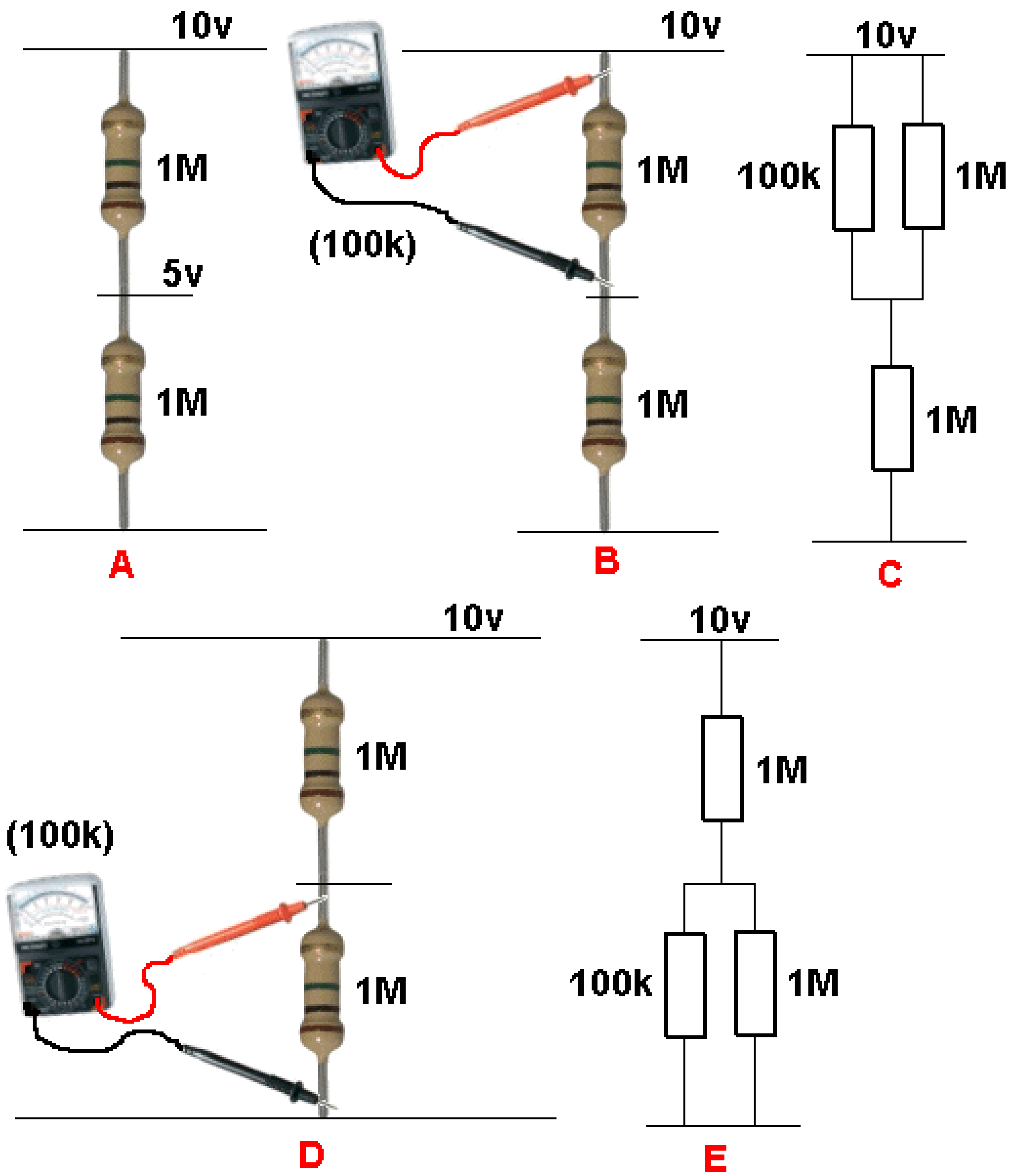

If the reading is taken with a Digital Meter, it will be more accurate as a DMM does not take any current from the circuit (to activate the meter). In other words it has a very HIGH input impedance. Most Digital Multimeters have a fixed input resistance (impedance) of 10M - no matter what scale is selected. That's the reason for choosing a DMM for high impedance circuits. It also gives a reading that is accurate to about 1%.

to Index

MEASURING VOLTAGES in a CIRCUIT

You can take many voltage-measurements in a circuit. You can measure "across" a component, or between any point in a circuit and either the positive rail or earth rail (0v rail). In the following circuit, the 5 most important voltage-measurements are shown. Voltage "A" is across the electret microphone. It should be between 20mV and 500mV. Voltage "B" should be about 0.6v. Voltage "C" should be about half-rail voltage. This allows the transistor to amplify both the positive and negative parts of the waveform. Voltage "D" should be about 1-3v. Voltage "E" should be the battery

voltage of 12v.

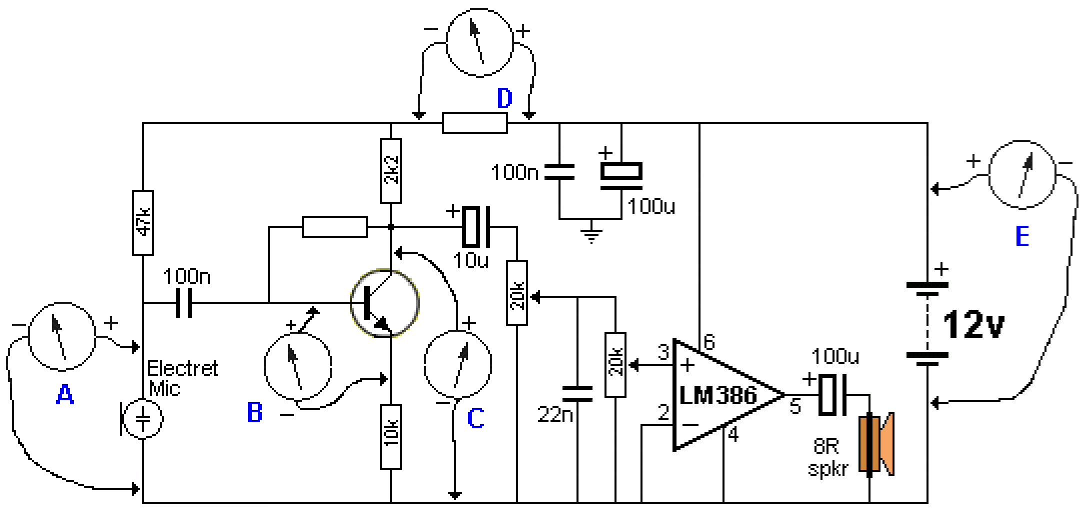

to Index

MEASURING CURRENT

You will rarely need to take current measurements, however most multimeters have DC current ranges such as 0.5mA, 50mA, 500mA and 10Amp (via the extra banana socket) and some meters have AC current ranges. Measuring the current of a circuit will tell you a lot of things. If you know the normal current, a high or low current can let you know if the circuit is overloaded or not fully operational.

Current is always measured when the circuit is working (i.e: with power applied).
It is measured IN SERIES with the circuit or component under test.
The easiest way to measure current is to remove the fuse and take a reading across the fuse-holder. Or remove one lead of the battery or turn the project off, and measure across the switch.
If this is not possible, you will need to remove one end of a component and measure with the two probes in the "opening."
Resistors are the easiest things to desolder, but you may have to cut a track in some circuits. You have to get an "opening" so that a current reading can be taken.
The following diagrams show how to connect the probes to take a CURRENT reading.
Do not measure the current ACROSS a component as this will create a "short-circuit."
The component is designed to drop a certain voltage and when you place the probes across this component, you are effectively adding a "link" or "jumper" and the voltage at the left-side of the component will appear on the right-side. This voltage may be too high for the circuit being supplied and the result will be damage.

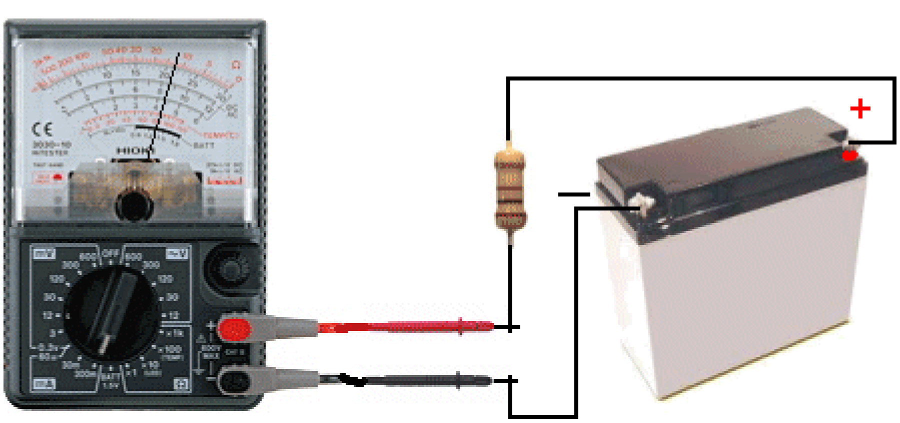

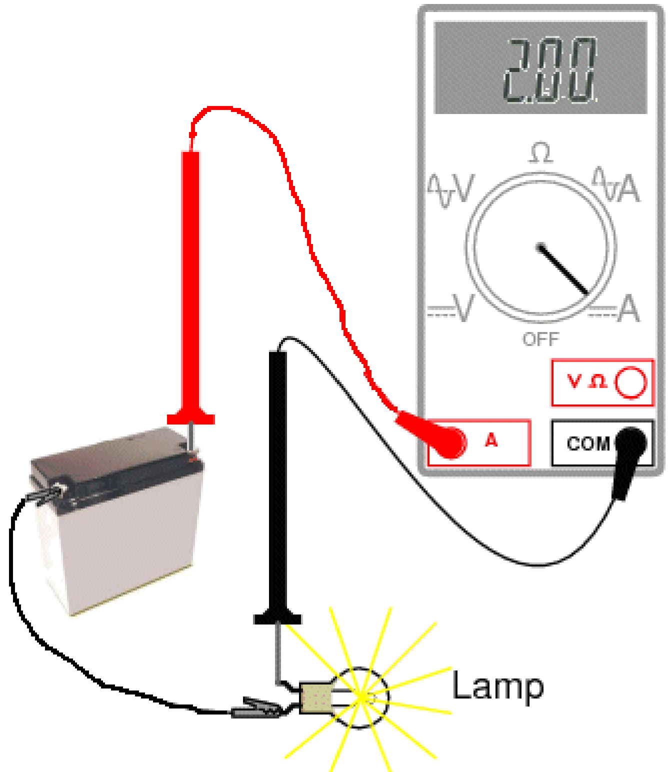

Measuring the current of a globe

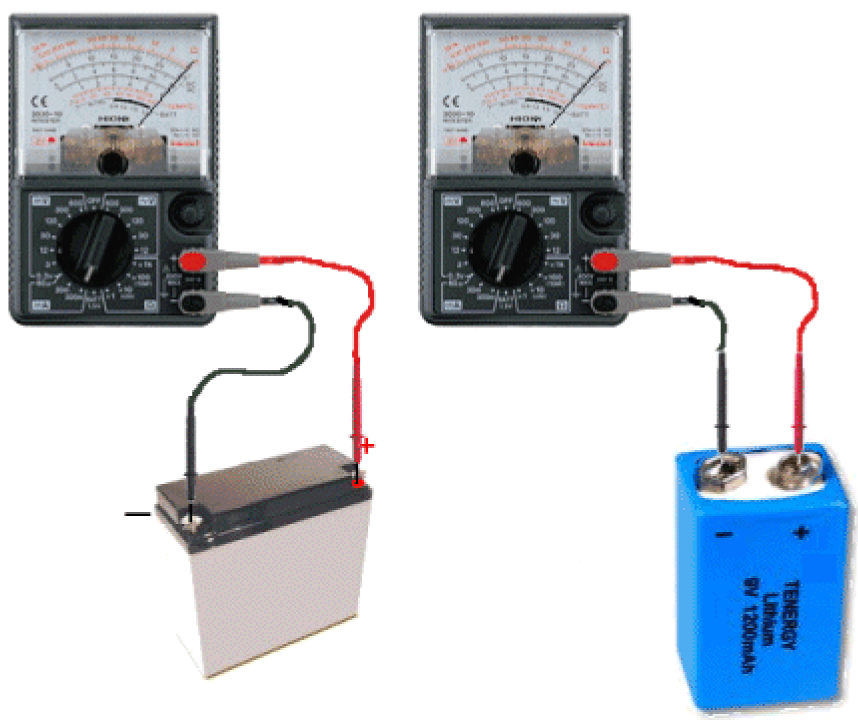

Do NOT measure the CURRENT of a battery
(by placing the meter directly across the terminals)
A battery will deliver a very HIGH current
and damage the meter

Do not measure the "current a battery will deliver" by placing the probes across the terminals. It will deliver a very high current and damage the meter instantly. There are special battery testing instruments for this purpose.

When measuring across an "opening" or "cut," place the red probe on the wire that supplies the voltage (and current) and the black probe on the other wire. This will produce a "POSITIVE" reading.
A positive reading is an UPSCALE READING and the pointer will move across the scale - to the right. A "NEGATIVE READING" will make the pointer hit the "STOP" at the left of the scale and you will not get a reading. If you are using a Digital Meter, a negative sign "-" will appear on the screen to indicate the probes are around the wrong way. No damage will be caused. It just indicates the probes are connected incorrectly.
If you want an accurate CURRENT MEASUREMENT, use a digital meter.

to Index

MEASURING RESISTANCE

Turn a circuit off before measuring resistance.
If any voltage is present, the value of resistance will be incorrect.
In most cases you cannot measure a component while it is in-circuit. This is because the meter is actually measuring a voltage across a component and calling it a "resistance." The voltage comes from the battery inside the meter. If any other voltage is present, the meter will produce a false reading.
If you are measuring the resistance of a component while still "in circuit," (with the power off) the reading will be lower than the true reading.

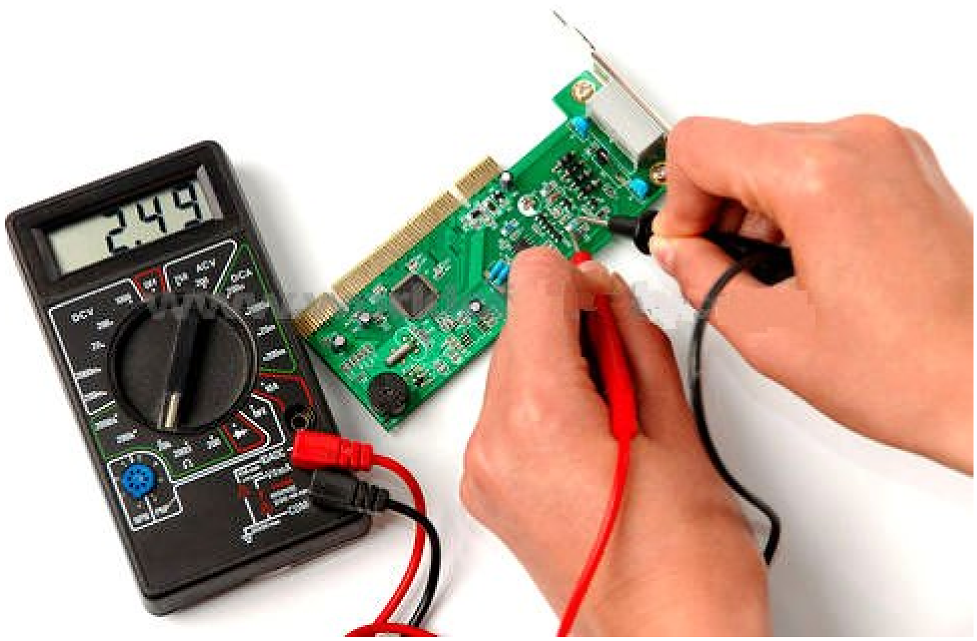

Measuring resistance

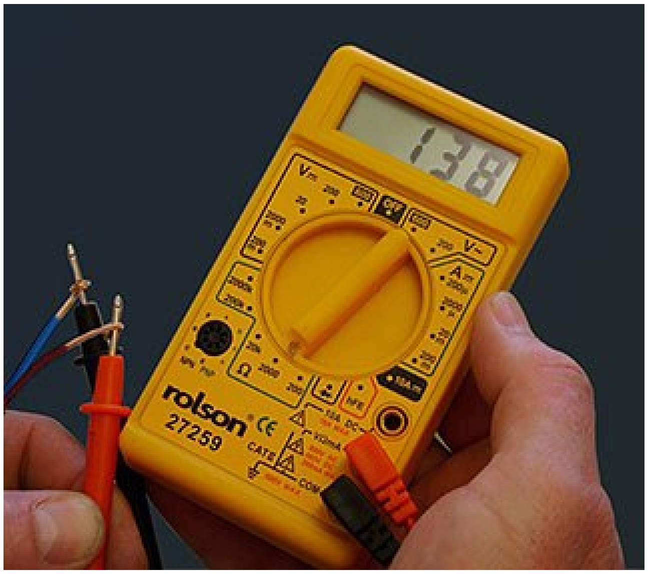

**Measuring resistance of a heater
(via the leads)**

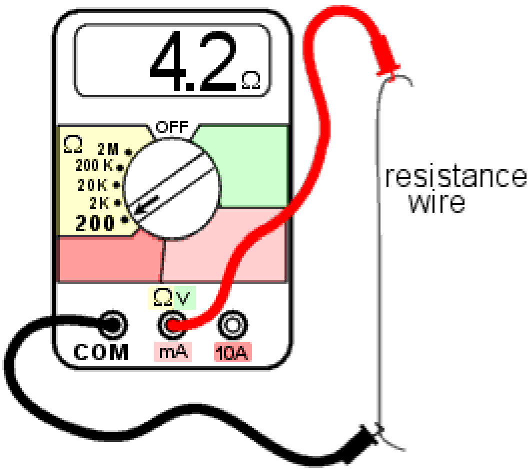

Measuring the resistance of a piece of resistance-wire

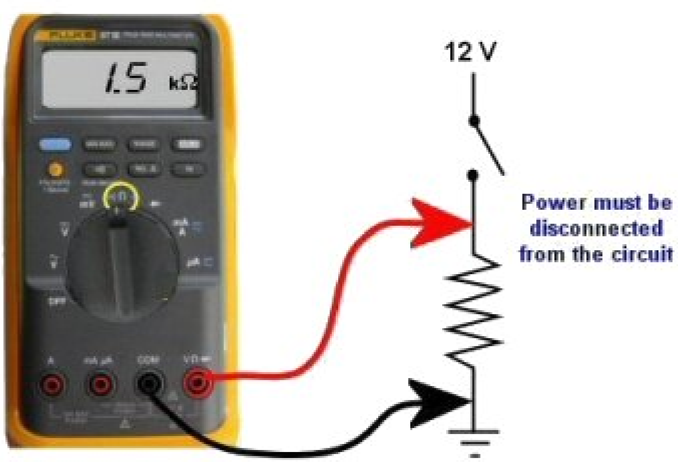

Measuring the resistance of a resistor

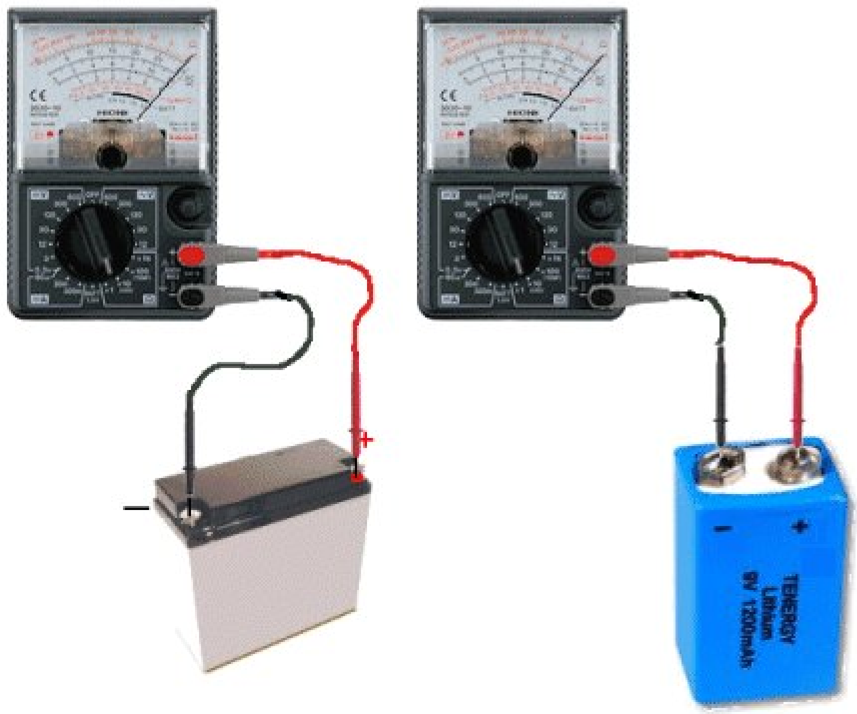

Do not measure the "Resistance of a Battery"

1. Do not measure the "resistance of a battery." The resistance of a battery (called the Internal impedance) is not measured as shown in the diagrams above. It is measured by creating a current-flow and measuring the voltage across the battery. Placing a multimeter set to **resistance** (across a battery) will destroy the meter.
2. Do not try to measure the resistance of any voltage or any "supply."

Resistance is measured in OHMs.
The resistance of a 1cm x 1cm bar, one metre long is 1 ohm.
If the bar is thinner, the resistance is higher. If the bar is longer, the resistance is higher.
If the material of the bar is changed, the resistance is higher.
When carbon is mixed with other elements, its resistance increases and this knowledge is used to make RESISTORS.
Resistors have RESISTANCE and the main purpose of a resistor is to reduce the CURRENT FLOW.
It's a bit like standing on a hose. The flow reduces.
When current flow is reduced, the output voltage is also reduced and that why the water does not spray up so high. Resistors are simple devices but they produce many different effects in a circuit.
A resistor of nearly pure carbon may be 1 ohm, but when non-conducting "impurities" are added, the same-size resistor may be 100 ohms, 1,000 ohms or 1 million ohms.
Circuits use values of less than 1 ohm to more than 22 million ohms.

Resistors are identified on a circuit with numbers and letters to show the exact value of resistance - such as 1k   2k2   4M7
The letter Ω (omega - a Greek symbol) is used to identify (or express) (or represent) the word "Ohm."
But this symbol is not available on some word-processors, so the letter "R" is used. The letter "E" is also sometimes used and both mean "Ohms."
A one-ohm resistor is written "1R" or "1E." It can also be written "1R0" or "1E0."
A resistor of one-tenth of an ohm is written "0R1" or "0E1."   The letter takes the place of the decimal point.
10 ohms = 10R
100 ohms = 100R

1,000 ohms = 1k (k= kilo = one thousand)
10,000 ohms = 10k
100,000 ohms = 100k
1,000,000 ohms = 1M (M = MEG = one million)

The size of a resistor has nothing to do with its resistance. The size determines the wattage of the resistor - how much heat it can dissipate without getting too hot.
Every resistor is identified by colour bands on the body, but when the resistor is a surface-mount device, numbers are used and sometimes letters.
You MUST learn the colour code for resistors and the following table shows all the colours for the most common resistors from 1/10th of an ohm to 22 Meg ohms for resistors with 5% and 10% tolerance.

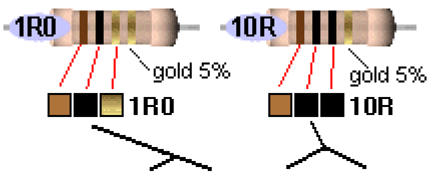

If 3rd band is gold, Divide by 10
If 3rd band is silver, Divide by 100
(to get 0.22ohms etc)

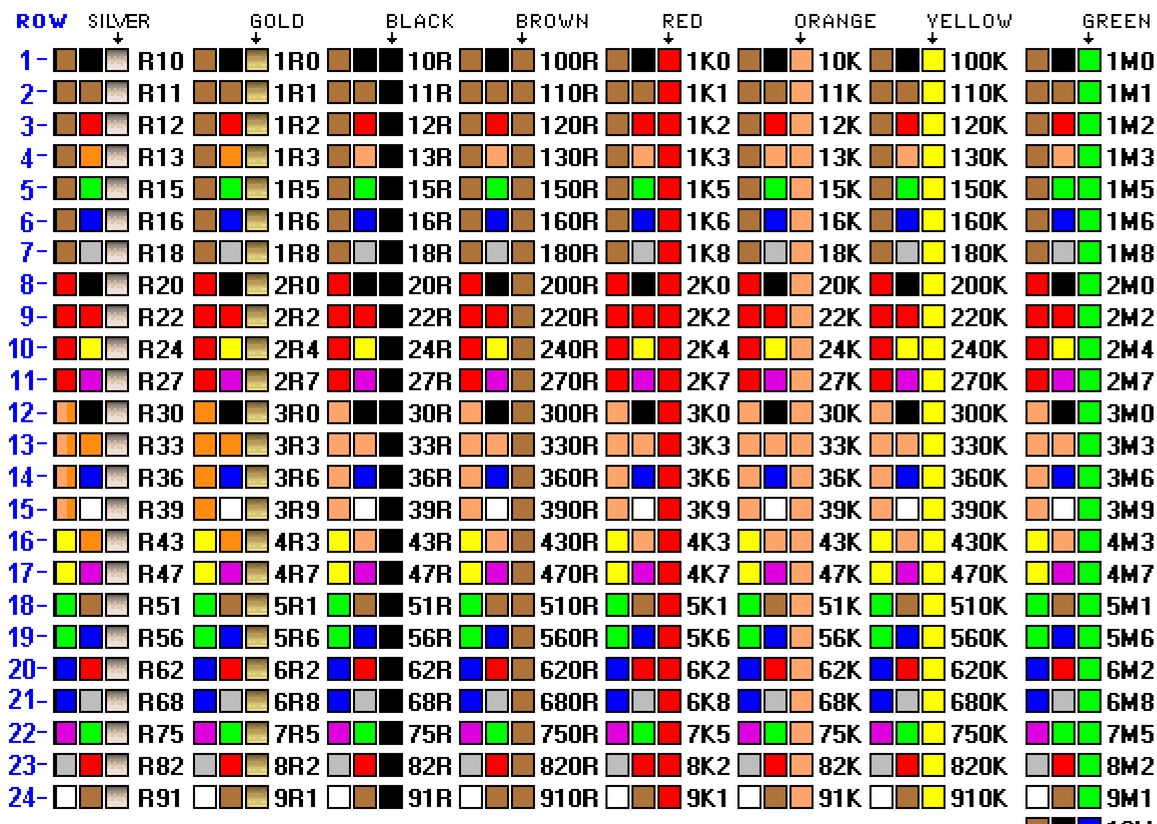

COLOR CODES FOR THE WHOLE E12/E24 RANGE OF RESISTORS
The twelve odd rows - 1, 3, 5... - represent values available in the E12 range only, plus 10M

to Index

MAKE YOUR OWN RESISTOR

Make your own variable resistor that changes resistance according to the pressure.
Use a piece of conductive foam used to package Integrated Circuits. You can ask at an electronics shop.
Use two coins or pieces of printed circuit board or aluminium foil for the top and bottom conductors.
You can solder wires to the PC board or fold the aluminium foil over a few times to hold the wires.
The resistance of the foam will reduce as you press on the "cell."
The actual resistance-values will depend on the size of the foam, the thickness and

pressure.
This cell is a very simple cell called a **LOAD CELL**.

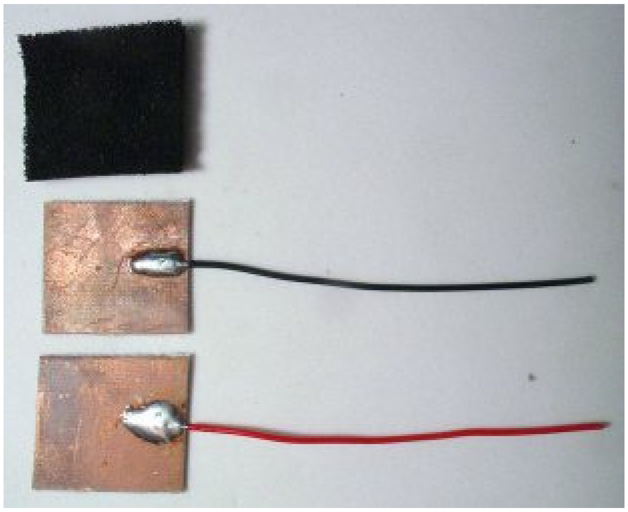

The top and bottom "plates"

The foam is placed between the plates.

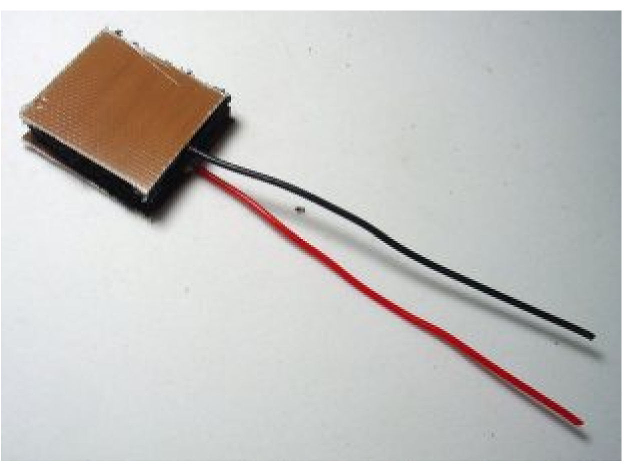

The complete LOAD CELL

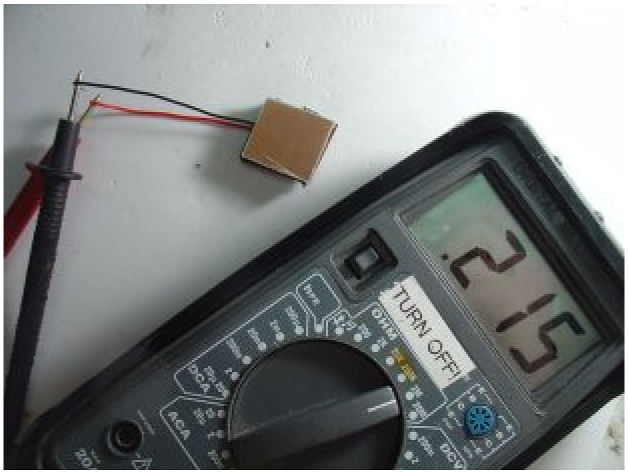

The resistance of the unloaded LOAD CELL

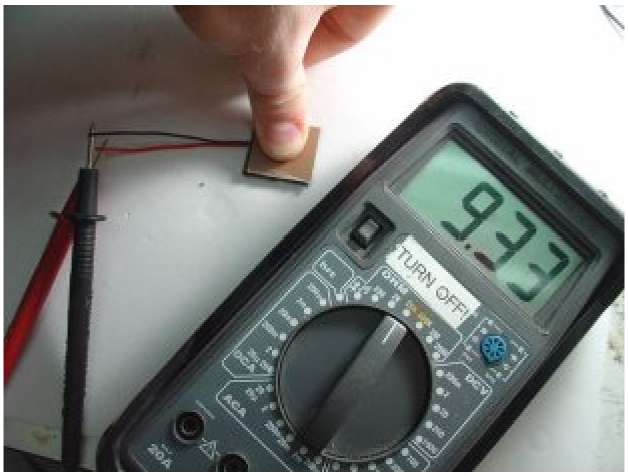

The fully loaded resistance can be as low as 9,330 ohms

to Index

MEASURING CONTINUITY

CONTINUITY is the same as **ZERO OHMS** or the resistance of a short length of wire. It can also mean the resistance through a switch or globe or a low-value resistor.
It basically means a "PATH" and sometimes refers to a whole circuit when the switch is closed. In other words CONTINUITY means we have a "circuit." We have "current flowing" and generally refers to a low-resistance circuit.
Both ANALOGUE and DIGITAL multimeters can measure CONTINUITY and you have to work out the approximate value of resistance for the circuit you are testing, - BEFORE TAKING A READING.
If the reading is above 300 ohms or contains a diode, you cannot use a DIGITAL MULTIMETER as the buzzer on the continuity setting will not respond.

The project being tested must not have the power applied as the resistance ranges on a multimeter are actually measuring a voltage across the leads and any voltage on the circuit or contained in any electrolytics, will upset the reading.

To take a reading with an **ANALOGUE** multimeter, select the x1 setting and the pointer will move across the scale to the actual value of resistance.
It it move full scale, you have ZERO OHMS resistance and this can mean a short-circuit or continuity via a wire.
If a diode is in the circuit you must also reverse the leads to get a reading.
The resistance of a globe will be very low when it is not illuminated, so don't think a fault is present.
Measuring CONTINUITY is the same as measuring LOW RESISTANCE.

To take a reading with a **DIGITAL** multimeter, select the buzzer setting. It will respond if the resistance is less than 300 ohms.   It will not respond if a diode is in the circuit.

Meter set to BUZZER - CONTINUITY

You can also use the x1 resistance setting to get an accurate value of resistance. Touch the probes together to get the initial reading and subtract this value from the final reading.
When probing a circuit containing electrolytics, you may get a beep from the buzzer. This indicates the resistance is low because the multimeter is charging the electrolytic and it will beep until the electrolytic is charged to about 0.7v.
The same applies when probing across the power rails of a circuit. The circuit may contain electrolytics that will charge when probing and the buzzer will beep.
The Digital multimeter is actually detecting a voltage less than 0.7v across the probes and is created by a voltage-divider network inside the meter.
The voltage divider put 2v across the probes and when this drops to less than 0.5v, the buzzer is activated. That why it odes not buzz when testing a diode as the diode drops the voltage to 0.6v.

to Index

MEASURING A DIODE

A diode can be measured to see if it is "open" or "damaged" or "working" by placing the probes across the component.
If the diode is "open" (it will not work), the needle will NOT swing across the scale when touching the component with the probes in one direction or when the probes are reversed.
If the diode is "damaged" (does not work), the needle will swing fully across the scale when touching the component with the probes in one direction or when the probes are reversed.
If the diode is FUNCTIONAL, (works) the needle will swing about mid-way when touching the leads of the diode in one direction and it will not move when the probes are reversed.

WHY?

The positive of the battery inside an analogue multimeter comes out the black probe and that is why you will get a reading when the probers are "around the wrong way." The needle will swing a different amount for each resistance setting on the dial as the needle represents 0.6v drop and NOT an actual resistance.

There are two things you must remember.
1. When the diode is measured in one direction, the needle will will **not move at**

all. The technical term for this is the diode is **reverse biased**. It will not allow any current to flow. Thus the needle will not move.
When the diode is connected around the other way, the needle will swing to the right (move up scale) to about 80% of the scale. This position represents the voltage drop across the junction of the diode and is NOT a resistance value. If you change the resistance range, the needle will move to a slightly different position due to the resistances inside the meter. The technical term for this is the diode is **forward biased**. This indicates the diode is not faulty.
The needle will swing to a slightly different position for a "normal diode" compared to a Schottky diode. This is due to the different junction voltage drops.
However we are only testing the diode at very low voltage and it may break-down when fitted to a circuit due to a higher voltage being present or due to a high current flowing.

2. The leads of an **Analogue Multimeter** have the positive of the battery connected to the black probe and the readings of a "good diode" are shown in the following two diagrams:

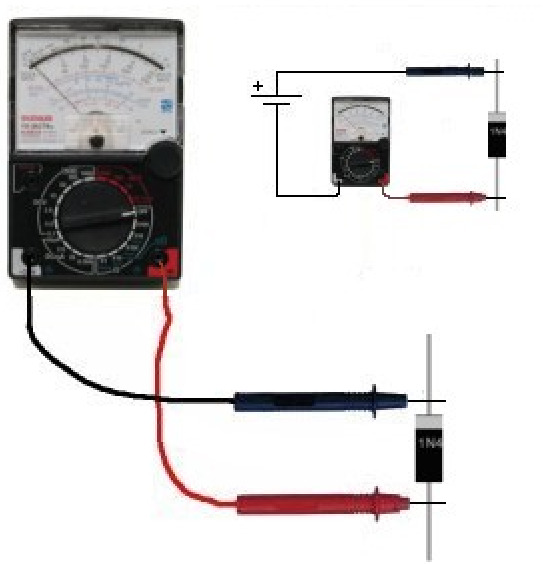

The diode is REVERSE BIASED in the diagram above and diodes not conduct.

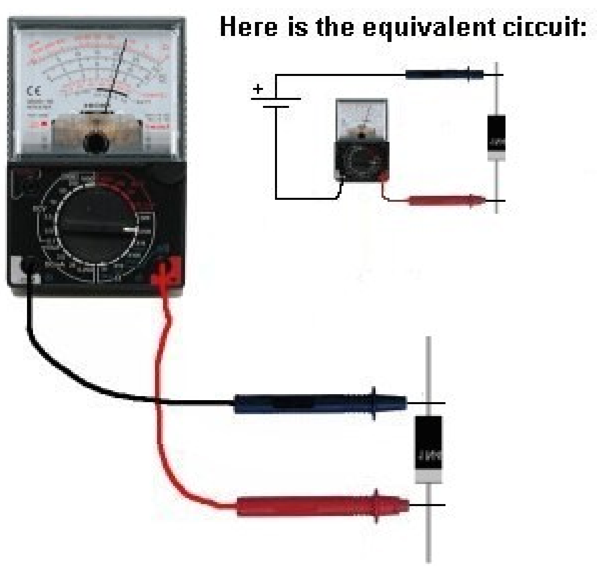

The diode is FORWARD BIASED in the diagram above and it conducts

TESTING A DIODE ON A DIGITAL METER

A Digital multimeter will measure the voltage-drop across the diode when the probes are connected in one direction (approx 0.640 on the scale) and a high reading (1) in the other direction. You need to select the "DIODE" setting on the dial as the other settings will produce a meaningless reading.

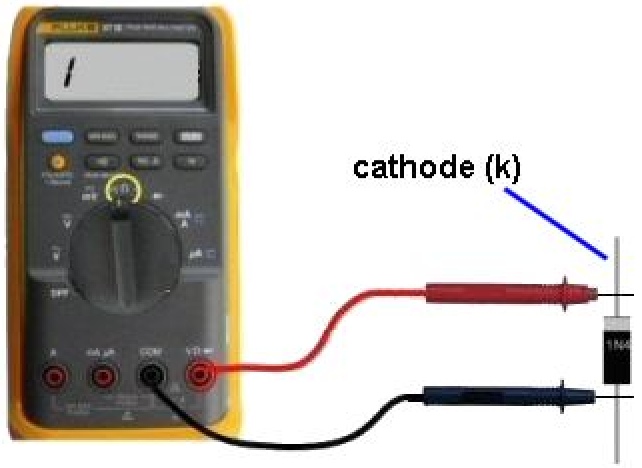

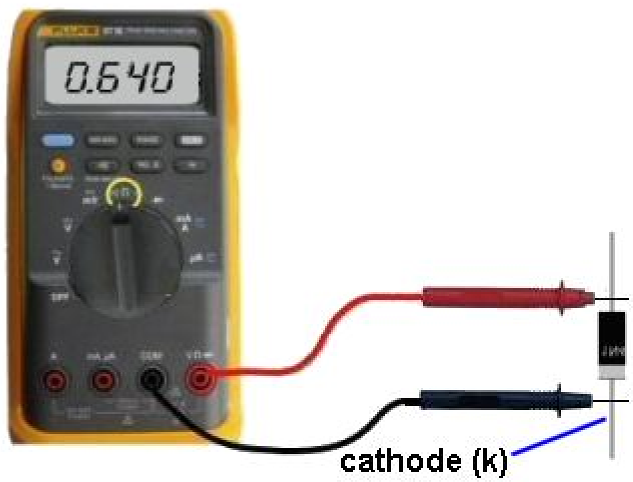

Some DIGITAL MULTIMETERS will show mV drop across the diode when the setting on the meter is "diode" or the "x1" or "x10" resistance range.

to Index

TESTING A LED

Some multimeters will test LEDs.
It depends on the voltage of the battery inside the case of the multimeter.
Many analogue multimeters have a single 1.5v cell and these cannot test LEDs.
Analogue Multimeters with 3v (for the resistance ranges) can test some LEDs.
White LEDs need about 3.6v and they may not illuminate on 3v.

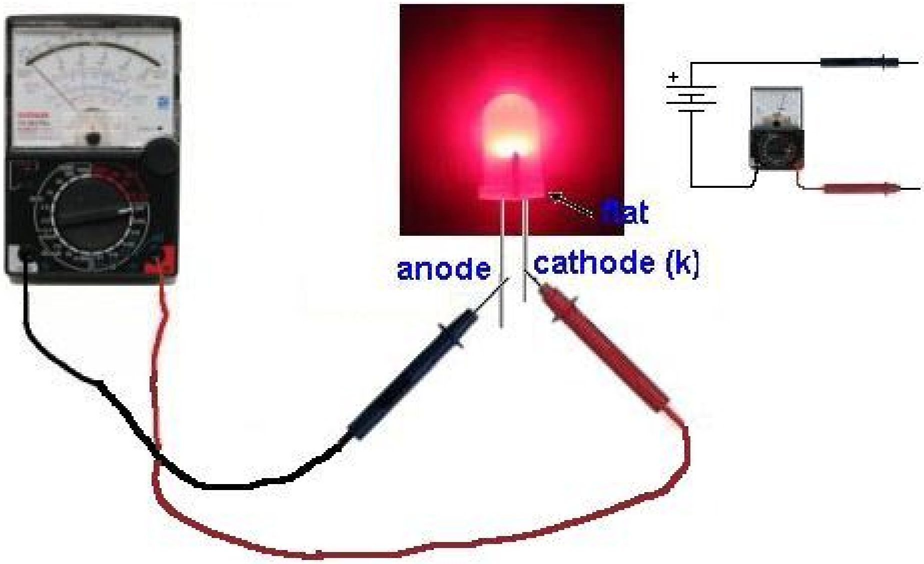

The negative lead of an ANALOGUE meter is POSITIVE!
The multimeter must have 3v (2 cells)

Digital multimeters have a 9v battery and they will illuminate all colour LEDs when the leads are placed as shown in the diagram:

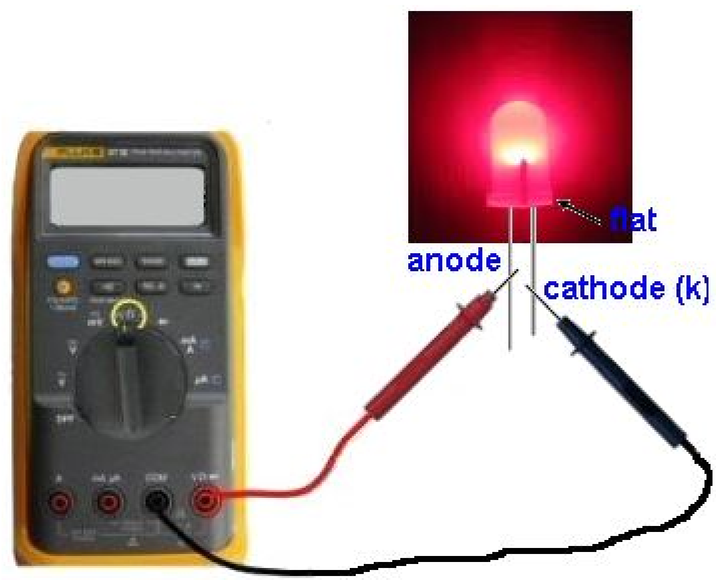

A Digital meter will illuminate all LEDs and the black probe touches the cathode.

to Index

TESTING A TRANSISTOR WITH A DIGITAL METER

Testing a transistor with a **Digital Meter** must be done on the "DIODE" setting as a digital meter does not deliver a current through the probes on some of the resistance settings and will not produce an accurate reading.
The "DIODE" setting must be used for diodes and transistors. It should also be called a "TRANSISTOR" setting.

TESTING A TRANSISTOR WITH AN ANALOGUE METER

The first thing you may want to do is test an unknown transistor for COLLECTOR, BASE AND EMITTER. You also want to perform a test to find out if it is NPN or PNP. That's what this test will provide.
You need a cheap multimeter called an ANALOGUE METER - a multimeter with a

scale and pointer (needle).
It will measure resistance values (normally used to test resistors) - (you can also test other components) and Voltage and Current. We use the resistance settings. It may have ranges such as "x10" "x100" "x1k" "x10"
Look at the resistance scale on the meter. It will be the top scale.
The scale starts at zero on the right and the high values are on the left. This is opposite to all the other scales.
When the two probes are touched together, the needle swings FULL SCALE and reads "ZERO." Adjust the pot on the side of the meter to make the pointer read exactly zero.

How to read: "x10" "x100" "x1k" "x10"
Up-scale from the zero mark is "1"
When the needle swings to this position on the "x10" setting, the value is 10 ohms.
When the needle swings to "1" on the "x100" setting, the value is 100 ohms.
When the needle swings to "1" on the "x1k" setting, the value is 1,000 ohms = 1k.
When the needle swings to "1" on the "x10k" setting, the value is 10,000 ohms = 10k.
Use this to work out all the other values on the scale.
Resistance values get very close-together (and very inaccurate) at the high end of the scale. [This is just a point to note and does not affect testing a transistor.]

Step 1 - FINDING THE BASE and determining NPN or PNP
Get an unknown transistor and test it with a multimeter set to "x10"
Try the 6 combinations and when you have the black probe on a pin and the red probe touches the other pins and the meter swings nearly full scale, you have an NPN transistor. The black probe is BASE
If the red probe touches a pin and the black probe produces a swing on the other two pins, you have a PNP transistor. The red probe is BASE
If the needle swings FULL SCALE or if it swings for more than 2 readings, the transistor is **FAULTY**.

This is an NPN transistor
The black probe is the BASE

This is a PNP transistor
The red probe is the BASE

Step 2 - FINDING THE COLLECTOR and EMITTER
Set the meter to "x10k."
For an NPN transistor, place the leads on the transistor and when you press hard on the two leads shown in the diagram below, the needle will swing almost full scale.

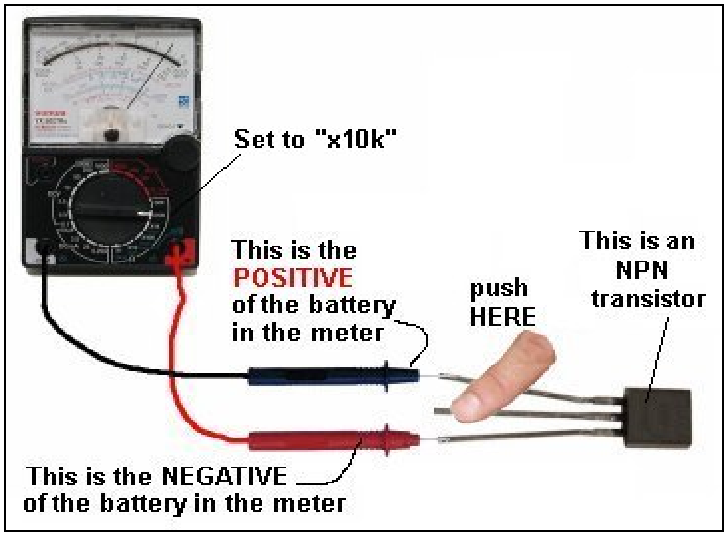

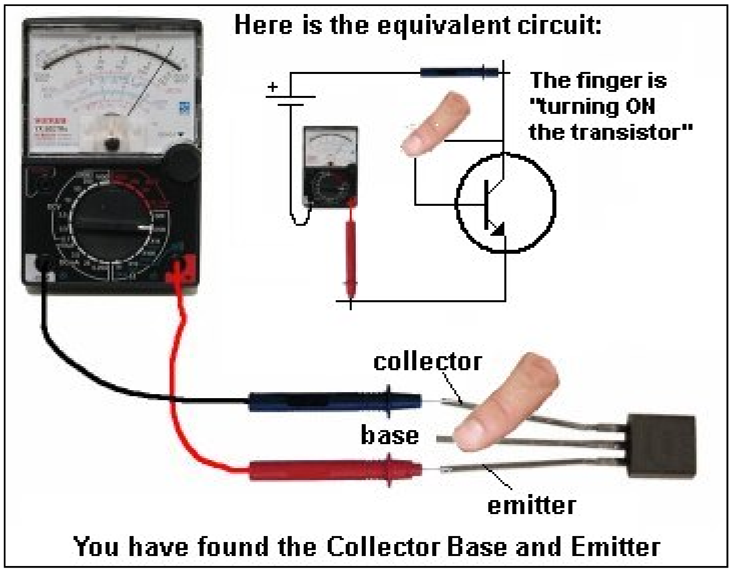

For a PNP transistor, set the meter to "x10k" place the leads on the transistor and when you press hard on the two leads shown in the diagram below, the needle will swing almost full scale.

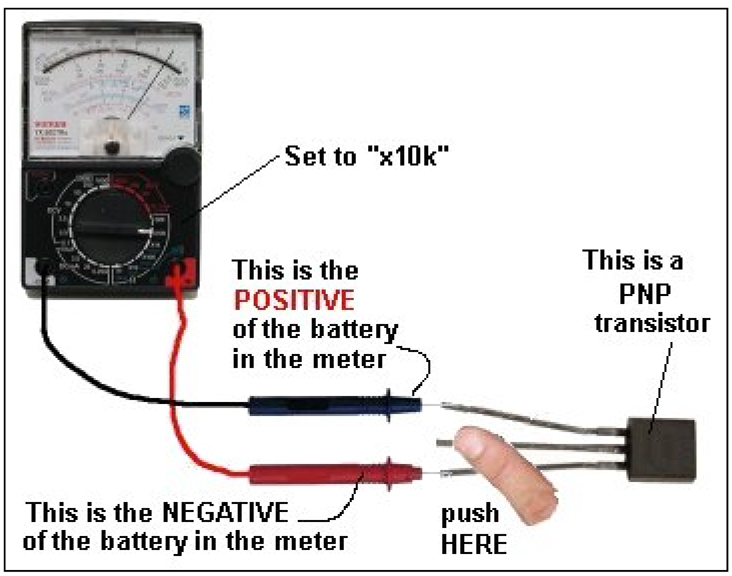

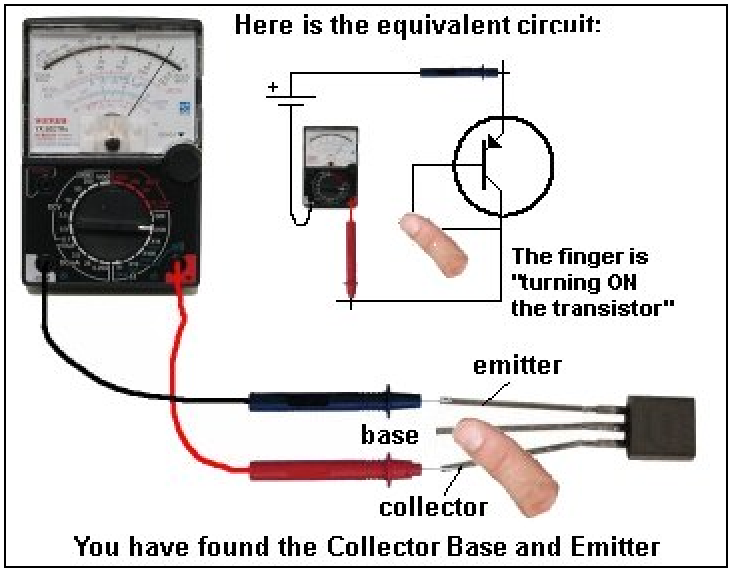

to Index

For more details on testing components with a multimeter, see:
Testing Electronic Components.

to Index

MULTIMETER TEST

1. What is the reading on the multimeter:

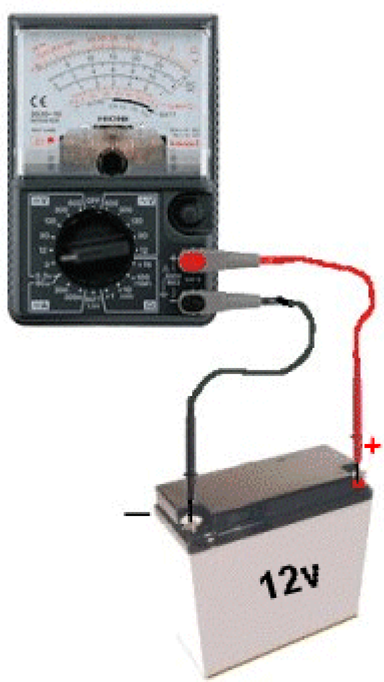

Answer

to Index

2. What is the reading on the multimeter:

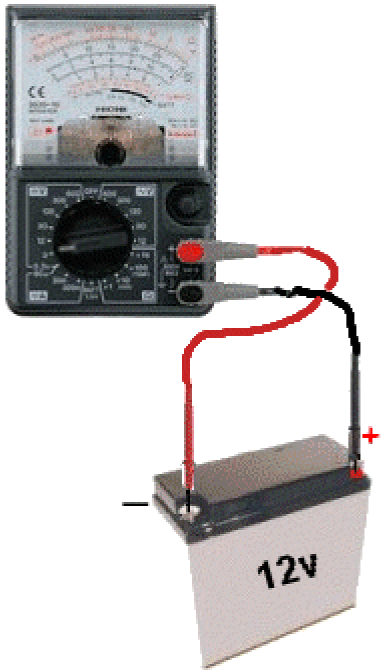

Answer

to Index

3. What is the reading on the multimeter:

Answer

to Index

4. What is the voltage between the following points:

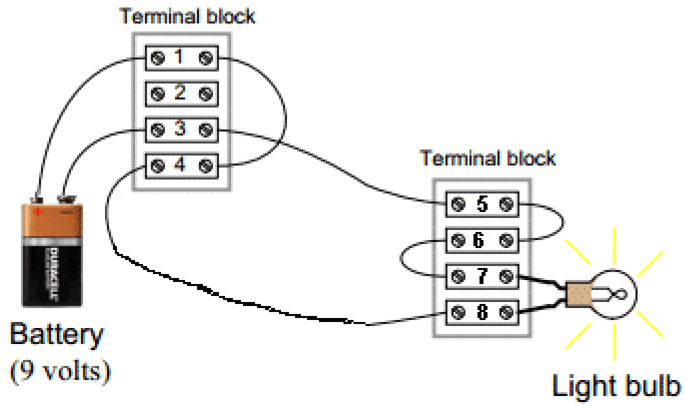

Between 1 & 3	Between 5 & 7	Between 3 & 8	Between 1 & 7
Answer	Answer	Answer	Answer

to Index

5. What is the voltage on each multimeter:

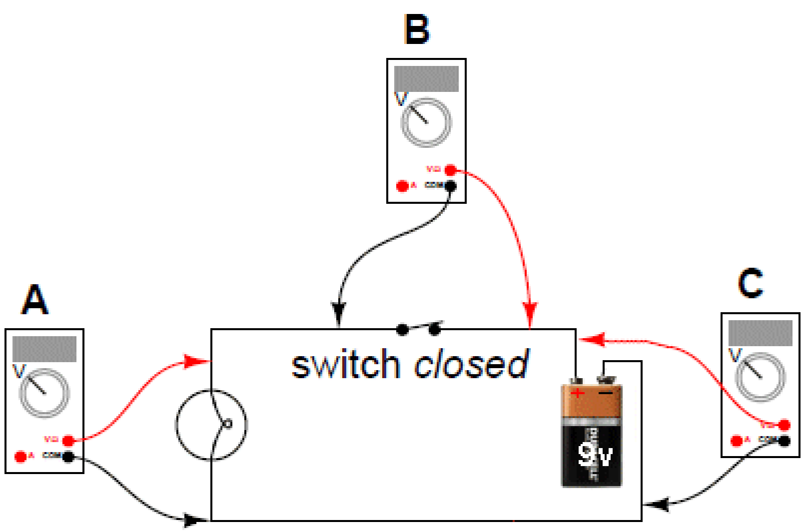

Meter A	**Meter B**	**Meter C**
Answer	Answer	Answer

to Index

6. What is the voltage on each multimeter:

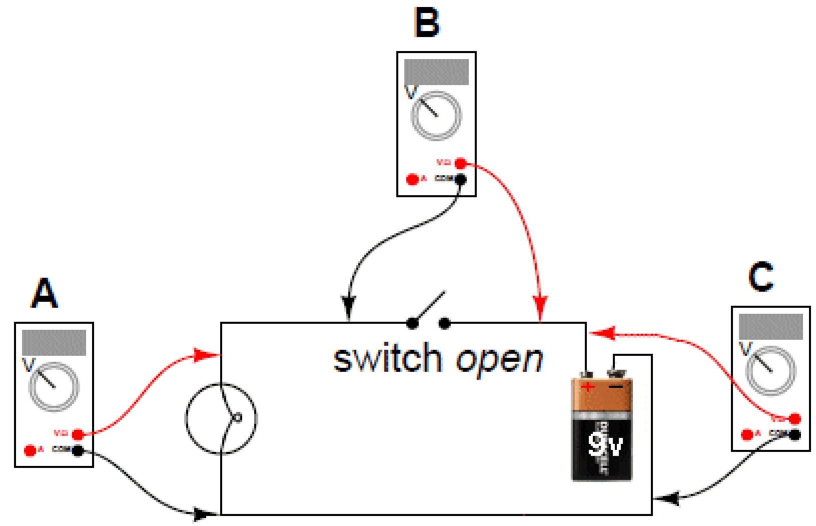

Meter A Answer

Meter B Answer

Meter C Answer

to Index

7. What is the reading on the multimeter:

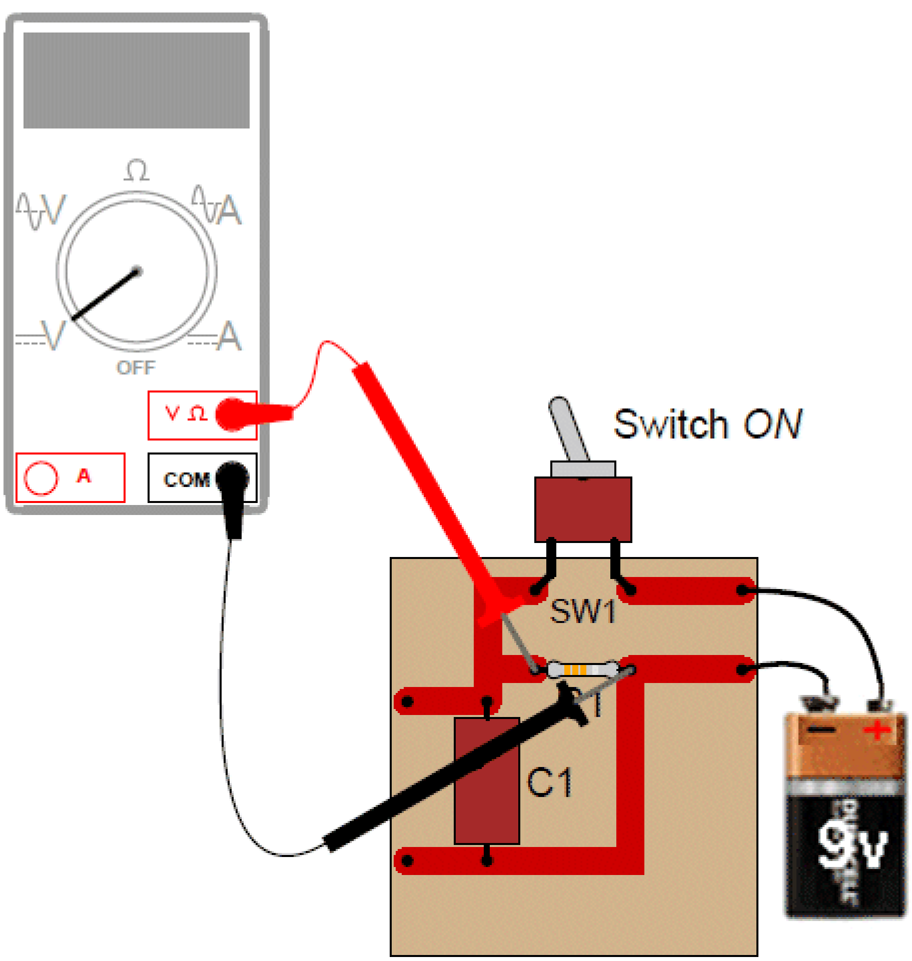

Answer

to Index

8. The multimeter has three resistance ranges: **x1 ohms x100 ohms x10k ohms**. How far across the scale will the needle move on each range for a 4k7 resistor:

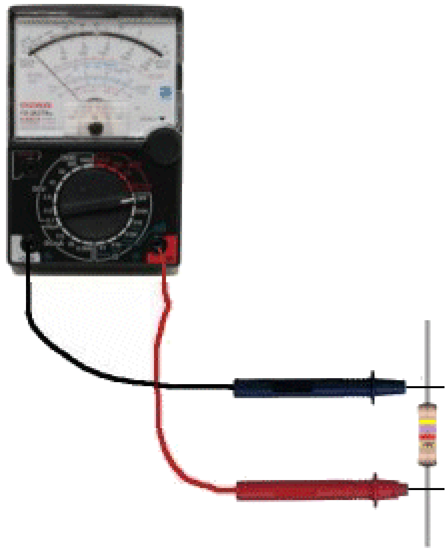

x1	**x100**	**x10k**
Answer	**Answer**	**Answer**

to Index

9. The resistance ranges on an ANALOGUE multimeter use the battery inside the case to move the pointer. If the multimeter is left on "**ohms range**" with the probes apart, will the battery go flat?

Answer

to Index

to Index

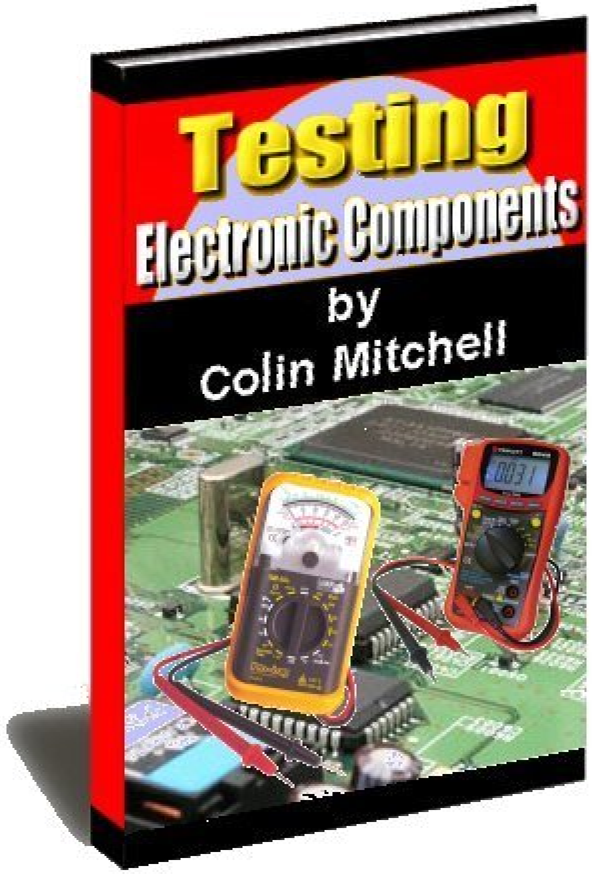

This eBook shows you how to TEST COMPONENTS.
To do this you need "TEST GEAR." The best item of Test Gear is a MULTIMETER. It can test almost 90% of all components. And that's what we will do in this eBook:

CONTENTS

Use your "brain, knowledge and your fingers."

Before we start, fixing anything is a combination of skill, luck and good diagnosis.
Sometimes you can fix something by letting it run until it finally fails.
Some things start to work as soon as you touch them.
Some things can never be fixed.
But some things can be fixed by feeling the temperature rise and deciding if it is getting too hot.
Sometimes you can smell something getting too hot.
Sometimes you can see SMOKE.
All these things make you a very clever technician and about 50% of faults will be fixed by looking for dry joints, burnt parts, overheating and carefully inspecting an item before you disturb it.

By simply touching different items you can quite often feel a hot item and home-in on the fault - at a saving of hours of work.
Servicing is not "A bull at a gate" approach.
You may be able to service something by turning it on and leaving it for hours - and start thinking.
It may take you a day to come up with the answer.
Believe me. That's how it worked for me - while fixing over 35,000 TV's.

TEST EQUIPMENT

Everyone thinks TEST EQUIPMENT will "solve the problem."
This is a big big MISTAKE.
Test equipment can help solve a problem and it can "lead to frustration," "give an incorrect answer," "mess you up," and make things worse.
You have to be very careful with test equipment and especially EXPENSIVE equipment because it is very sensitive and can detect pulses and glitches and voltages that are not affecting the operation of the circuit.
You will learn a lot of tricks when reading through this article, but let me say two things.
There are lots of faults and components that you cannot test with "test equipment" because they are either intermittent or the equipment does not load the device to the same extent as the circuit.
And secondly you need both an ANALOGUE multimeter and a DIGITAL meter to cover all the situations.
And if you are working on a car, you only need a $5.00 analogue meter because it will be dropped or fall into a crack, and you will only lose $5.00
You will learn that a digital meter will pick up spikes and signals on a line and show an incorrect reading.
That's why you need to back-up your readings with an analogue meter.
When you charge a battery it gets a "floating voltage" and this will be higher than the actual voltage, when the battery is fitted to a project. An analogue meter will draw a slight current and remove the "floating voltage."
Component testers can also give you a false reading, either because the component is out of range of the tester or intermittent and you need to be aware of this.
Oscilloscopes can also display waveforms that are parts of glitches or noise from other chips and these do not affect the operation of the part of the circuit you are investigating.
Sometimes you cannot pickup a pulse because it is not regular and the trigger on the oscilloscope does not show it on the screen. You may think it is missing.
It all depends on the "speed of the oscilloscope" - it's maximum frequency of operation.
Lastly- Power Supplies. You cannot test globes and motors on a power supply because the starting current can be 5 times more than the operating current. The power supply may not be able to deliver this high current and thus you will think the motor or globe is faulty.

MULTIMETERS

There are two types:

DIGITAL and ANALOGUE

A **Digital Multimeter** has a set of digits on the display and an Analogue Multimeter has a scale with a pointer (or needle).
You really need both types to cover the number of tests needed for designing and repair-work. We will discuss how they work, how to use them and some of the differences between them.

DIGITAL AND ANALOGUE MULTIMETERS

BUYING A MULTIMETER

There are many different types on the market.
The cost is determined by the number of ranges and also the extra features such as diode tester, buzzer (continuity), transistor tester, high DC current and others.
Since most multimeters are reliable and accurate, buy one with the greatest number of ranges at the lowest cost.
This article explains the difference between a cheap analogue meter, an expensive analogue meter and a digital meter. You will then be able to work out which two meters you should buy.

Multimeters are sometimes called a "meter", a "VOM" (Volts-Ohms-Milliamps or Volt Ohm Meter) or "multi-tester" or even "a tester" - they are all the same.

USING A MULTIMETER

Analogue and digital multimeters have either a rotary selector switch or push buttons to select the appropriate function and range. Some Digital Multimeters (DMMs) are auto ranging; they automatically select the correct range of voltage, resistance, or current when doing a test. However you need to select the function.

Before making any measurement you need to know what you are checking. If you are measuring voltage, select the AC range (10v, 50v, 250v, or 1000v) or DC range (0.5v, 2.5v, 10v, 50v, 250v, or 1000v). If you are measuring resistance, select the Ohms range (x1, x10, x100, x1k, x10k). If you are measuring current, select the appropriate current range DCmA 0.5mA, 50mA, 500mA. Every multimeter is different however the photo below shows a low cost meter with the basic ranges.

The most important point to remember is this:
You must select a voltage or current range that is bigger or HIGHER than the maximum expected value, so the needle does not swing across the scale and hit the "end stop."
If you are using a DMM (Digital Multi Meter), the meter will indicate if the voltage or current is higher than the selected scale, by showing "OL" - this means "Overload." If you are measuring resistance such as 1M on the x10 range the "OL" means "Open Loop" and you will need to change the range. Some meters show "1' on the display when the measurement is higher than the display will indicate and some flash a set of digits to show over-voltage or over-current. A "-1" indicates the leads should be reversed for a "positive reading."
If it is an AUTO RANGING meter, it will automatically produce a reading, otherwise the selector switch must be changed to another range.

The Common (negative) lead ALWAYS fits into the "COM" socket. The red lead fits into the red socket for Voltage and Resistance. Place the red lead (red banana plug) into "A" (for HIGH CURRENT "Amps") or mA,uA for LOW CURRENT.

The black "test lead" plugs into the socket marked "-" "Common", or "Com," and the red "test lead" plugs into meter socket marked "+" or "V-W-mA."   The third banana socket measures HIGH CURRENT and the positive (red lead) plugs into this. You DO NOT move the negative "-" lead at any time.

The following two photos show the test leads fitted to a digital meter. The probes and plugs have "guards" surrounding the probe tips and also the plugs so you can measure high voltages without getting near the voltage-source.

What's the difference between **sensitivity, resolution,** and **accuracy?**

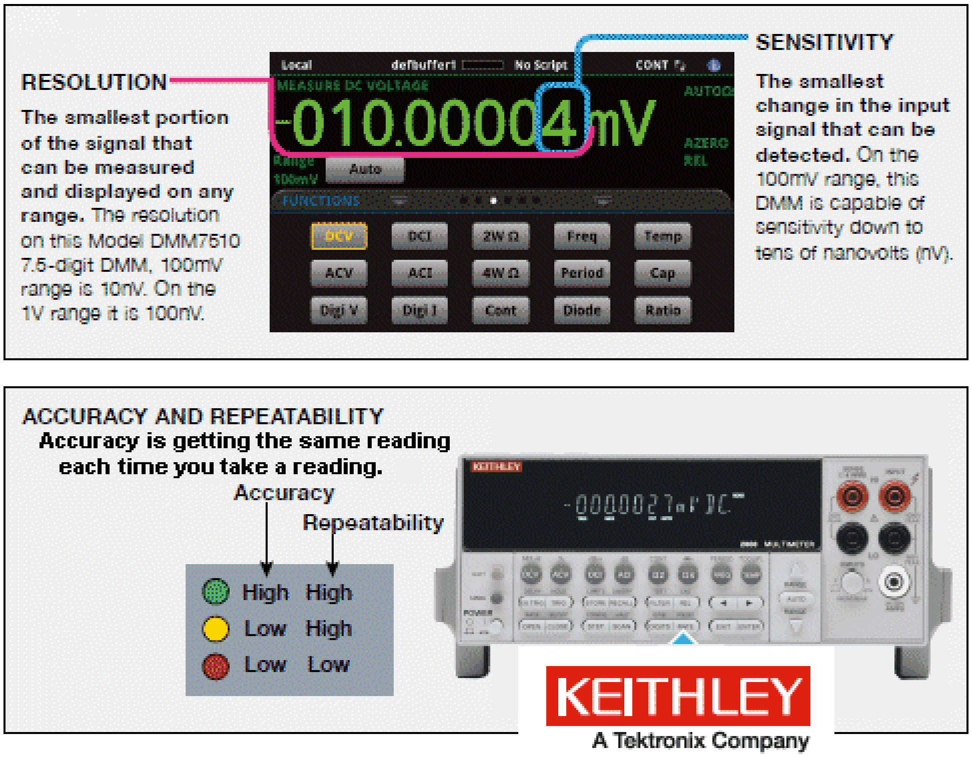

The question above applies to both (every) type of multimeter and the type of meter you use depends on the accuracy you need. Sometimes you are looking for 1mV change on a 20v rail. Only a DMM will (or a CRO) will produce a result.

Analogue meters have an "Ohms Adjustment" to allow for the change in voltage of the battery inside the meter (as it gets old).

"Ohms Adjust" is also called "ZERO SET"

The sensitivity of this meter is 20,000ohms/volt on the DC ranges and 5k/v on the AC ranges

Before taking a resistance reading (each time on any of the Ohms scales) you need to "ZERO SET" the scale, by touching the two probes together and adjust the pot until the needle reads "0" (swings FULL SCALE). If the pointer does not reach full

scale, the batteries need replacing. Digital multimeters do not need "zero adjustment."

FIXING A MULTIMETER

A multimeter can get "broken" "damaged" and go "faulty."
I don't know why, but eventually they stop working.
It can be something simple like a flat battery, corroded battery contacts, broken switch or something complex, like the circuitry failing.
Multimeters are so cheap, you can buy a new one for less than $10.00
These meters can have a 10 amp range, transistor tester and measure up to 2 meg ohms.
That's why I suggest buying a $10.00 meter. They are just as good as a $60.00 meter and the cheapest meters last the longest.
Dropping an analogue meter can cause the hair spring to loop over one of the supports and the needle will not zero correctly. You will need to open the cover on the movement and lift the spring off the support with a needle.
A faulty meter can be used in a battery-charger circuit to measure the current or voltage if that scale is still reading-correctly.
Otherwise keep the leads and throw the meter out. It is too dangerous keeping a meter that shows an incorrect reading.

MEASURING FREQUENCY

Before we cover the normal uses for a multimeter, it is interesting to note that some **Digital Multimeters (DMM)** have features such as Capacitance, Frequency and measuring the gain of a transistor as well as a number of other features using probes such as a temperature probe. The VICHY VC99 meter above is an example and costs about $40.00.

Basic function	Range
DCV	600mV/6V/60V/600V/1000V
ACV	6V/60/600/1000V
DCA	600uA/6000uA/60mA/600mA/6A/20A
ACA	600uA/6000uA/60mA/600mA/6A/20A
Capacitance	40nF/400nF/4uF/40uF/400uF/2000uF
Resistance	600Ω/6kΩ/60kΩ/600kΩ/6MΩ/60MΩ
Frequency	100Hz/1kHz/10kHz/100kHz/1MHz/60MHz

Temperature	-40°C~1000°C
	0°F~1832°F

MEASURING VOLTAGE

Most of the readings you will take with a multimeter will be VOLTAGE readings.
Before taking a reading, you should select the highest range and if the needle does not move up scale (to the right), you can select another range.
Always switch to the highest range before probing a circuit and keep your fingers away from the component being tested.
If the meter is Digital, select the highest range or use the auto-ranging feature, by selecting "V." The meter will automatically produce a result, even if the voltage is AC or DC.
If the meter is not auto-ranging, you will have to select V⎓ if the voltage is from a DC source or V~ if the voltage is from an AC source. DC means Direct Current and the voltage is coming from a battery or supply where the voltage is steady and not changing and AC means Alternating Current where the voltage is coming from a voltage that is rising and falling.
You can measure the voltage at different points in a circuit by connecting the black probe to chassis. This is the 0v reference and is commonly called "Chassis" or "Earth" or "Ground" or "0v."
The red lead is called the "measuring lead" or "measuring probe" and it can measure voltages at any point in a circuit. Sometimes there are "test points" on a circuit and these are wires or loops designed to hold the tip of the red probe (or a red probe fitted with a mini clip or mini alligator clip).
You can also measure voltages ACROSS A COMPONENT. In other words, the reading is taken in PARALLEL with the component. It may be the voltage across a transistor, resistor, capacitor, diode or coil. In most cases this voltage will be less than the supply voltage.
If you are measuring the voltage in a circuit that has a HIGH IMPEDANCE, the reading will be inaccurate, up to 90% !!!, if you use a cheap analogue meter.

Here's a simple case.

The circuit below consists of two 1M resistors in series. The voltage at the mid point will be 5v when nothing is connected to the mid point. But if we use a cheap analogue multimeter set to 10v, the resistance of the meter will be about 100k, if the meter has a sensitivity of 10k/v and the reading will be incorrect.
Here how it works:
Every meter has a sensitivity. The sensitivity of the meter is the sensitivity of the movement and is the amount of current required to deflect the needle FULL SCALE.
This current is very small, normally 1/10th of a milliamp and corresponds to a sensitivity of 10k/volt (or 1/30th mA, for a sensitivity of 30k/v).
If an analogue meter is set to 10v, the internal resistance of the meter will be 100k for a 10k/v movement.
If this multimeter is used to test the following circuit, the reading will be inaccurate.
The reading should be 5v as show in diagram **A**.
But the analogue multimeter has an internal resistance of 100k and it creates a circuit shown in **C**.
The top 1M and 100k from the meter create a combined PARALLEL resistance of 90k.
This forms a series circuit with the lower 1M and the meter will read less than 1v
If we measure the voltage across the lower 1M, the 100k meter will form a value of resistance with the lower 1M and it will read less than 1v
If the multimeter is 30k/v, the readings will be 2v. See how easy it is to get a totally inaccurate reading.

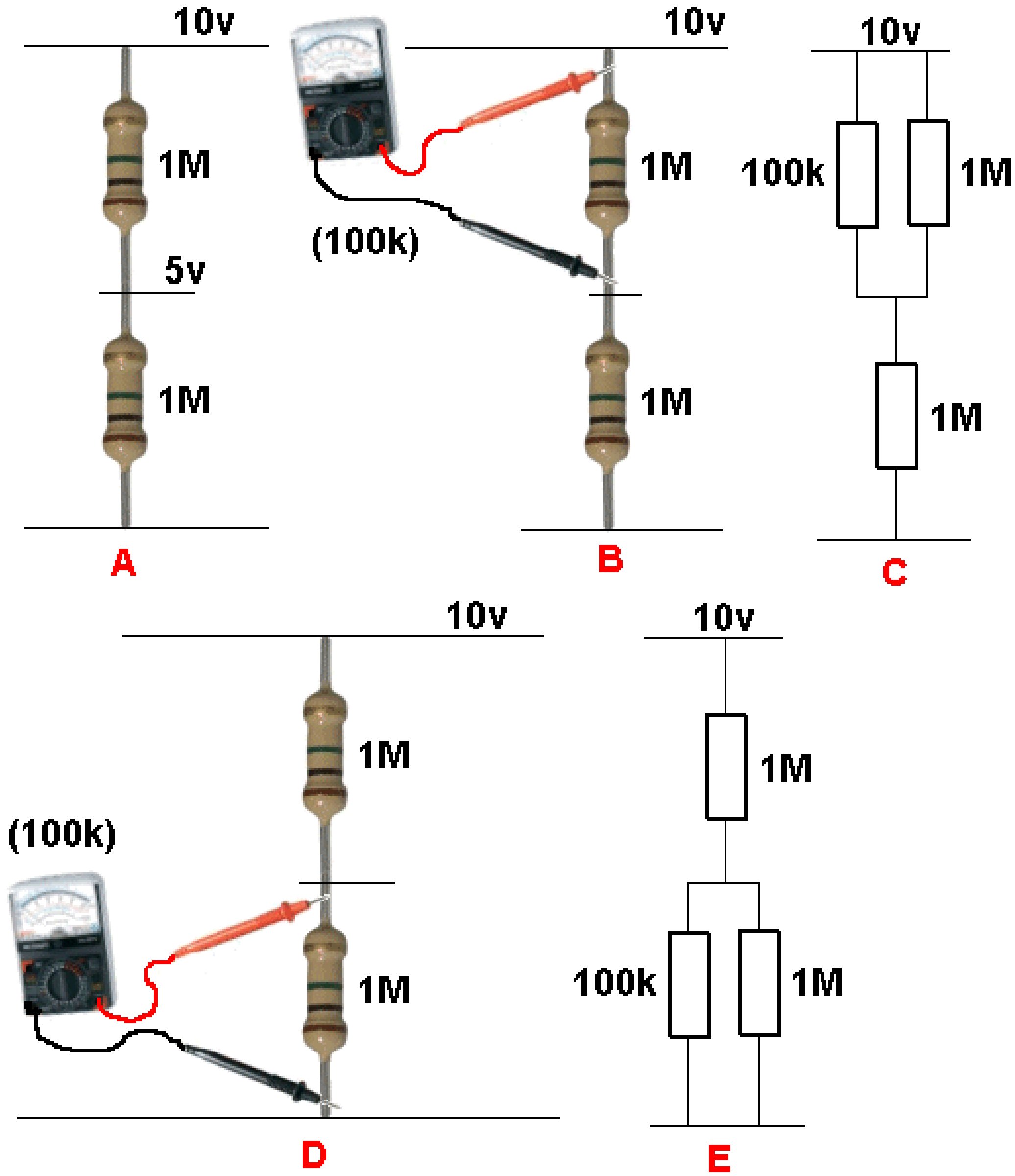

This introduces two new terms:
[HIGH IMPEDANCE CIRCUIT](#) and "RESISTORS in [SERIES](#) and [PARALLEL](#)."

If the reading is taken with a Digital Meter, it will be more accurate as a DMM does not take any current from the circuit (to activate the meter). In other words it has a very HIGH input impedance. Most Digital Multimeters have a fixed input resistance (impedance) of 10M - no matter what scale is selected. That's the reason for choosing a DMM for high impedance circuits. It also gives a reading that is accurate to about 1%.

MEASURING VOLTAGES IN A CIRCUIT

You can take many voltage-measurements in a circuit. You can measure "across" a component, or between any point in a circuit and either the positive rail or earth rail (0v rail). In the following circuit, the 5 most important voltage-measurements are shown. Voltage "A" is across the electret microphone. It should be between 20mV and 500mV. Voltage "B" should be about 0.6v. Voltage "C" should be about half-rail voltage. This allows the transistor to amplify both the positive and negative parts of the waveform. Voltage "D" should be about 1-3v. Voltage "E" should be the battery voltage of 12v.

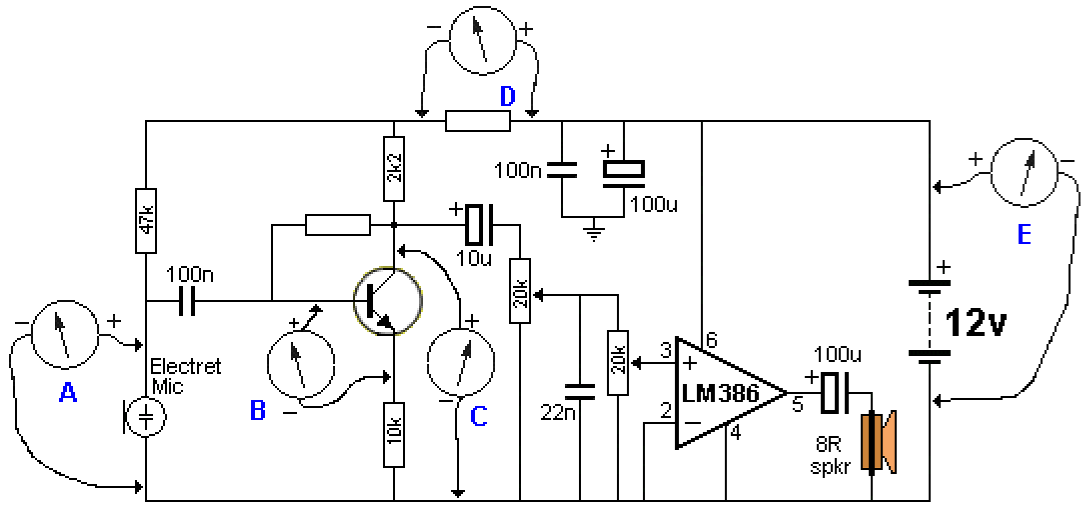

MEASURING VOLTAGES IN A CIRCUIT

MEASURING CURRENT

You will rarely need to take current measurements, however most multimeters have DC current ranges such as 0.5mA, 50mA, 500mA and 10Amp (via the extra banana socket) and some meters have AC current ranges. Measuring the current of a circuit will tell you a lot of things. If you know the normal current, a high or low current can let you know if the circuit is overloaded or not fully operational.

Current is always measured when the circuit is working (i.e: with power applied).
It is measured IN SERIES with the circuit or component under test.
The easiest way to measure current is to remove the fuse and take a reading across the fuse-holder. Or remove one lead of the battery or turn the project off, and measure across the switch.
If this is not possible, you will need to remove one end of a component and measure with the two probes in the "opening."
Resistors are the easiest things to desolder, but you may have to cut a track in some circuits. You have to get an "opening" so that a current reading can be taken.
The following diagrams show how to connect the probes to take a CURRENT reading.
Do not measure the current ACROSS a component as this will create a "short-circuit."
The component is designed to drop a certain voltage and when you place the probes across this component, you are effectively adding a "link" or "jumper" and the voltage at the left-side of the component will appear on the right-side. This voltage may be too high for the circuit being supplied and the result will be damage.

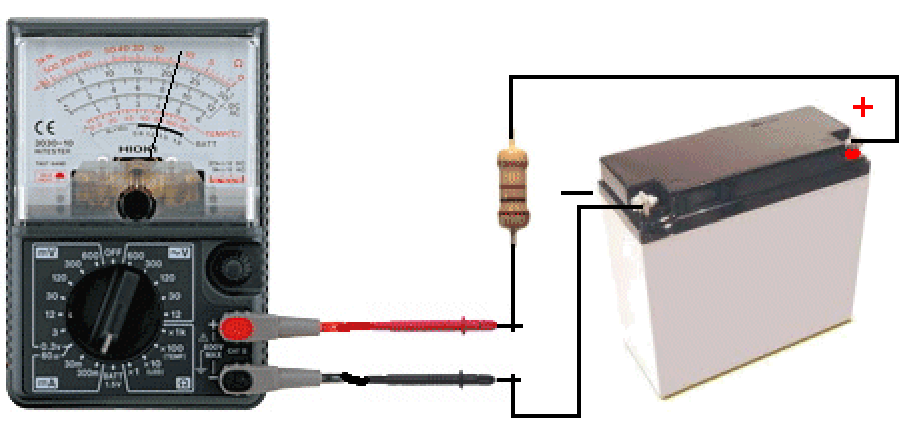

Measuring current through a resistor

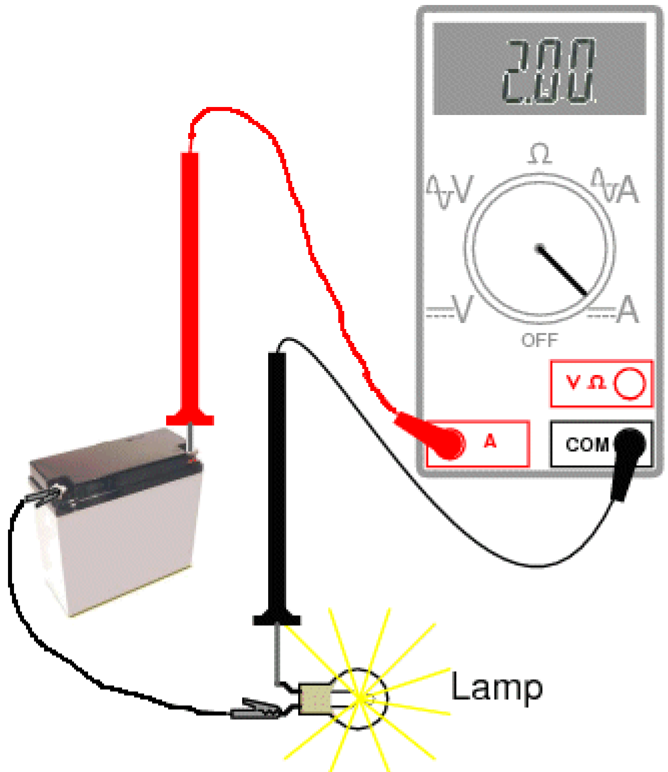

Measuring the current of a globe

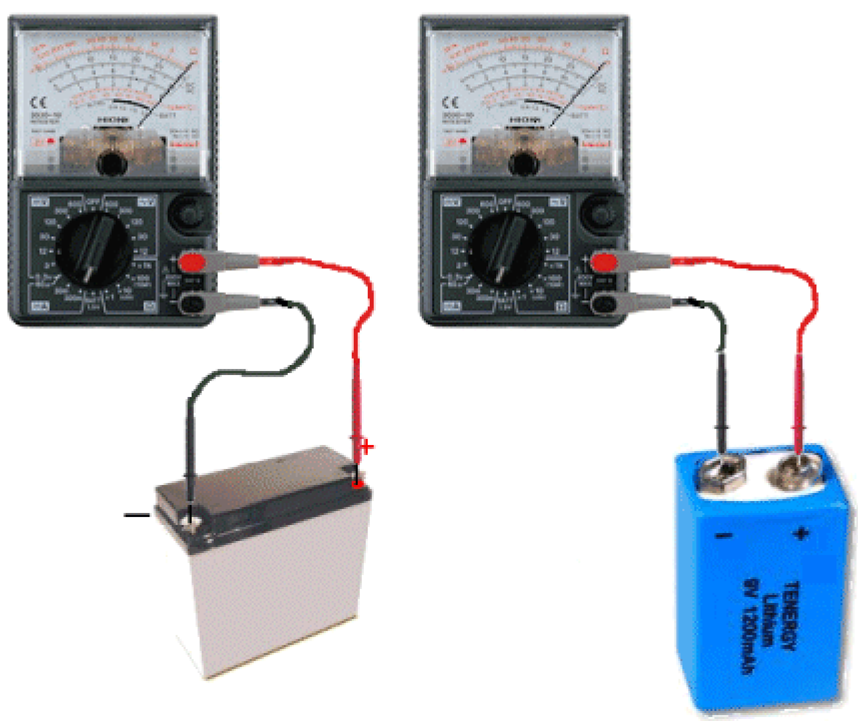

Do NOT measure the CURRENT of a battery
(by placing the meter directly across the terminals)
A battery will deliver a very HIGH current
and damage the meter

Do not measure the "current a battery will deliver" by placing the probes across the terminals. It will deliver a very high current and damage the meter instantly. There are special battery testing instruments for this purpose.
When measuring across an "opening" or "cut," place the red probe on the wire that supplies the voltage (and current) and the black probe on the other wire. This will produce a "POSITIVE" reading.

A positive reading is an UPSCALE READING and the pointer will move across the scale - to the right. A "NEGATIVE READING" will make the pointer hit the "STOP" at the left of the scale and you will not get a reading. If you are using a Digital Meter, a negative sign "-" will appear on the screen to indicate the probes are around the wrong way. No damage will be caused. It just indicates the probes are connected incorrectly.
If you want an accurate CURRENT MEASUREMENT, use a digital meter.

MEASURING RESISTANCE

Turn a circuit off before measuring resistance.
If any voltage is present, the value of resistance will be incorrect.
In most cases you cannot measure a component while it is in-circuit. This is because the meter is actually measuring a voltage across a component and calling it a "resistance." The voltage comes from the battery inside the meter. If any other voltage is present, the meter will produce a false reading.
If you are measuring the resistance of a component while still "in circuit," (with the power off) the reading will be lower than the true reading.

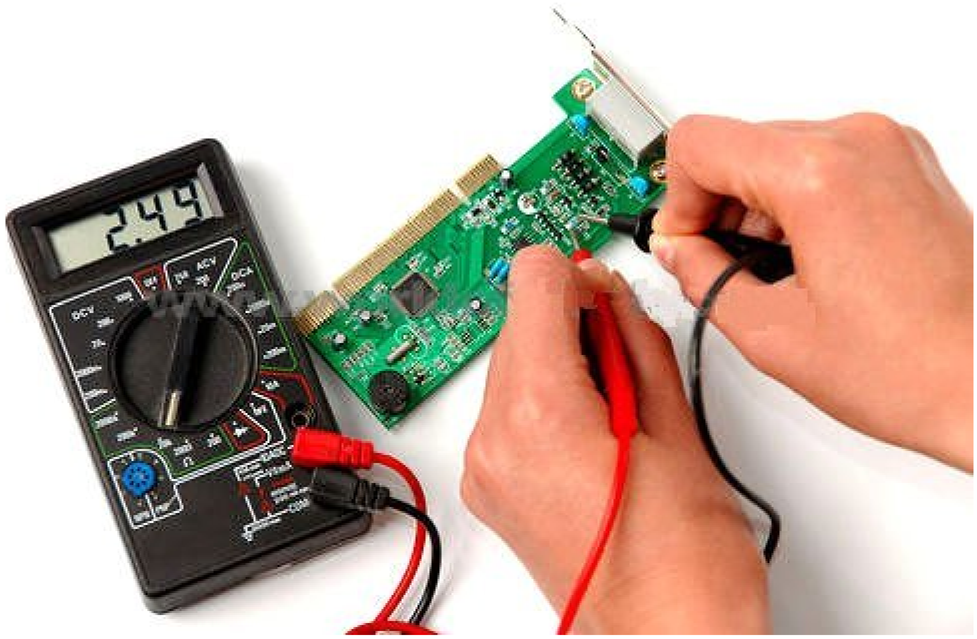

Measuring resistance

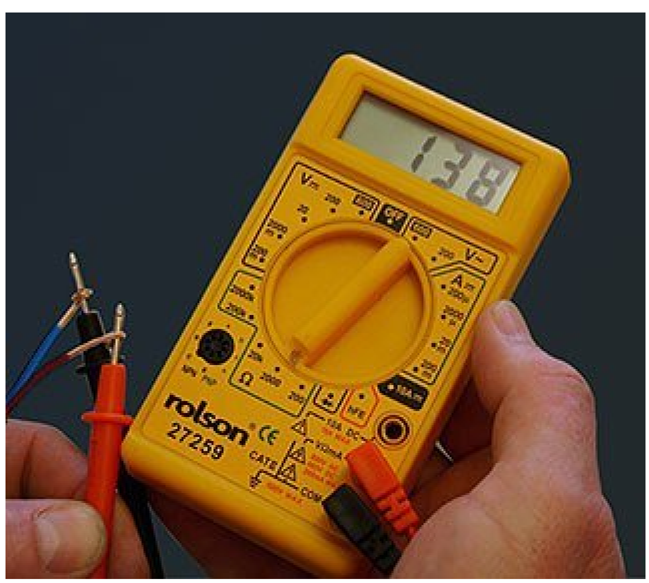

Measuring resistance of a heater
(via the leads)

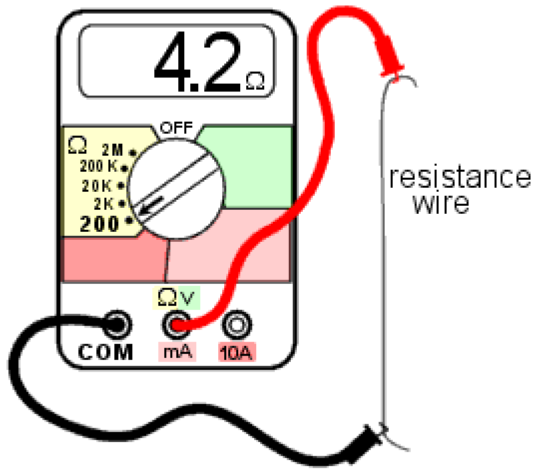

Measuring the resistance of a piece of resistance-wire

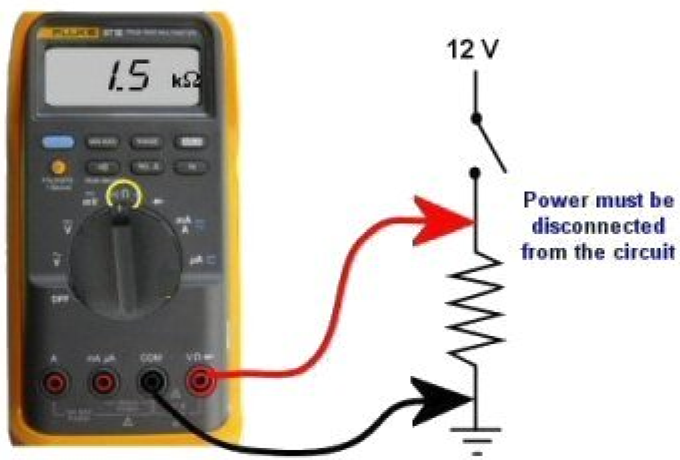

Measuring the resistance of a resistor

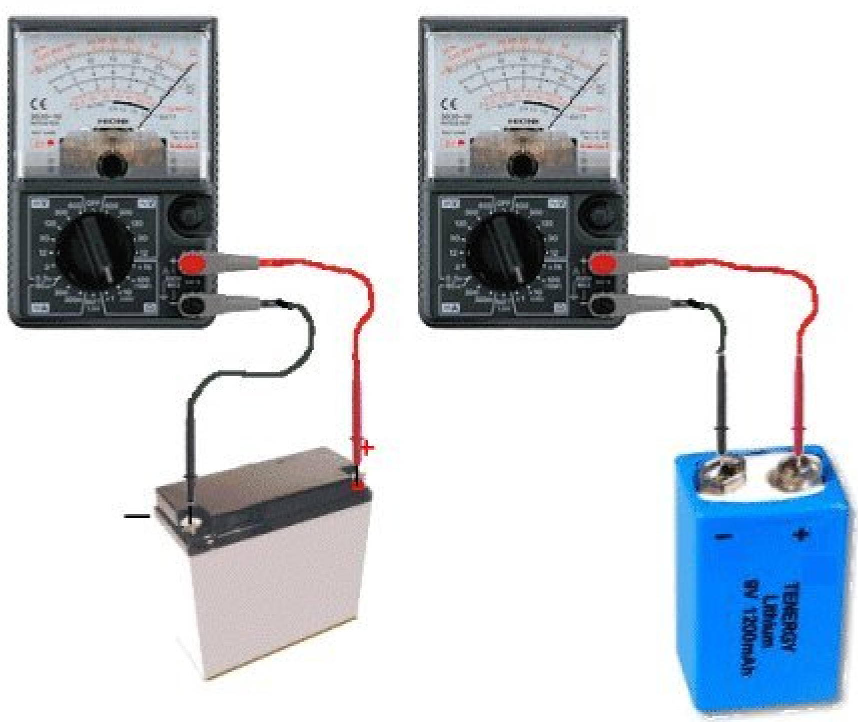

Do not measure the "Resistance of a Battery"

1. Do not measure the "resistance of a battery." The resistance of a battery (called the Internal impedance) is not measured as shown in the diagrams above. It is measured by creating a current-flow and measuring the voltage across the battery.

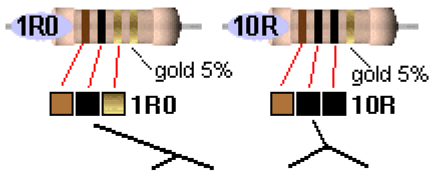

Placing a multimeter set to **resistance** (across a battery) will destroy the meter.
2. Do not try to measure the resistance of any voltage or any "supply."

Resistance is measured in OHMs.
The resistance of a 1cm x 1cm bar, one metre long is 1 ohm.
If the bar is thinner, the resistance is higher. If the bar is longer, the resistance is higher.
If the material of the bar is changed, the resistance is higher.
When carbon is mixed with other elements, its resistance increases and this knowledge is used to make RESISTORS.
Resistors have RESISTANCE and the main purpose of a resistor is to reduce the CURRENT FLOW.
It's a bit like standing on a hose. The flow reduces.
When current flow is reduced, the output voltage is also reduced and that why the water does not spray up so high. Resistors are simple devices but they produce many different effects in a circuit.
A resistor of nearly pure carbon may be 1 ohm, but when non-conducting "impurities" are added, the same-size resistor may be 100 ohms, 1,000 ohms or 1 million ohms.
Circuits use values of less than 1 ohm to more than 22 million ohms.

Resistors are identified on a circuit with numbers and letters to show the exact value of resistance - such as 1k 2k2 4M7
The letter Ω (omega - a Greek symbol) is used to identify the word "Ohm."
but this symbol is not available on some word-processors, so the letter "R" is used.
The letter "E" is also sometimes used and both mean "Ohms."
A one-ohm resistor is written "1R" or "1E." It can also be written "1R0" or "1E0."
A resistor of one-tenth of an ohm is written "0R1" or "0E1." The letter takes the place of the decimal point.
10 ohms = 10R
100 ohms = 100R
1,000 ohms = 1k (k= kilo = one thousand)
10,000 ohms = 10k
100,000 ohms = 100k
1,000,000 ohms = 1M (M = MEG = one million)

The size of a resistor has nothing to do with its resistance. The size determines the wattage of the resistor - how much heat it can dissipate without getting too hot.
Every resistor is identified by colour bands on the body, but when the resistor is a surface-mount device, numbers are used and sometimes letters.
You MUST learn the colour code for resistors and the following table shows all the colours for the most common resistors from 1/10th of an ohm to 22 Meg ohms for resistors with 5% and 10% tolerance.

If 3rd band is gold, Divide by 10
If 3rd band is silver, Divide by 100
(to get 0.22ohms etc)

ROW	SILVER	GOLD	BLACK	BROWN	RED	ORANGE	YELLOW	GREEN
1-	R10	1R0	10R	100R	1K0	10K	100K	1M0
2-	R11	1R1	11R	110R	1K1	11K	110K	1M1
3-	R12	1R2	12R	120R	1K2	12K	120K	1M2
4-	R13	1R3	13R	130R	1K3	13K	130K	1M3
5-	R15	1R5	15R	150R	1K5	15K	150K	1M5
6-	R16	1R6	16R	160R	1K6	16K	160K	1M6
7-	R18	1R8	18R	180R	1K8	18K	180K	1M8
8-	R20	2R0	20R	200R	2K0	20K	200K	2M0
9-	R22	2R2	22R	220R	2K2	22K	220K	2M2
10-	R24	2R4	24R	240R	2K4	24K	240K	2M4
11-	R27	2R7	27R	270R	2K7	27K	270K	2M7
12-	R30	3R0	30R	300R	3K0	30K	300K	3M0
13-	R33	3R3	33R	330R	3K3	33K	330K	3M3
14-	R36	3R6	36R	360R	3K6	36K	360K	3M6
15-	R39	3R9	39R	390R	3K9	39K	390K	3M9
16-	R43	4R3	43R	430R	4K3	43K	430K	4M3
17-	R47	4R7	47R	470R	4K7	47K	470K	4M7
18-	R51	5R1	51R	510R	5K1	51K	510K	5M1
19-	R56	5R6	56R	560R	5K6	56K	560K	5M6
20-	R62	6R2	62R	620R	6K2	62K	620K	6M2
21-	R68	6R8	68R	680R	6K8	68K	680K	6M8
22-	R75	7R5	75R	750R	7K5	75K	750K	7M5
23-	R82	8R2	82R	820R	8K2	82K	820K	8M2
24-	R91	9R1	91R	910R	9K1	91K	910K	9M1
								10M (BLUE)

COLOR CODES FOR THE WHOLE E12/E24 RANGE OF RESISTORS

The twelve odd rows - 1, 3, 5... - represent values available in the E12 range only, plus 10M

Reading 4-band resistors

The most "common" type of resistor has 4 bands and is called the 10% resistor. It now has a tolerance of 5% but is still called the "10% type" as the colours increase by 20% so that a resistor can be 10% higher or 10% lower than a particular value and all the resistors produced in a batch can be used.
The first 3 bands produce the resistance and the fourth band is the "tolerance" band.
Gold = 5%
(Silver =10% but no modern resistors are 10%!! - they are 5% 2% or 1%)

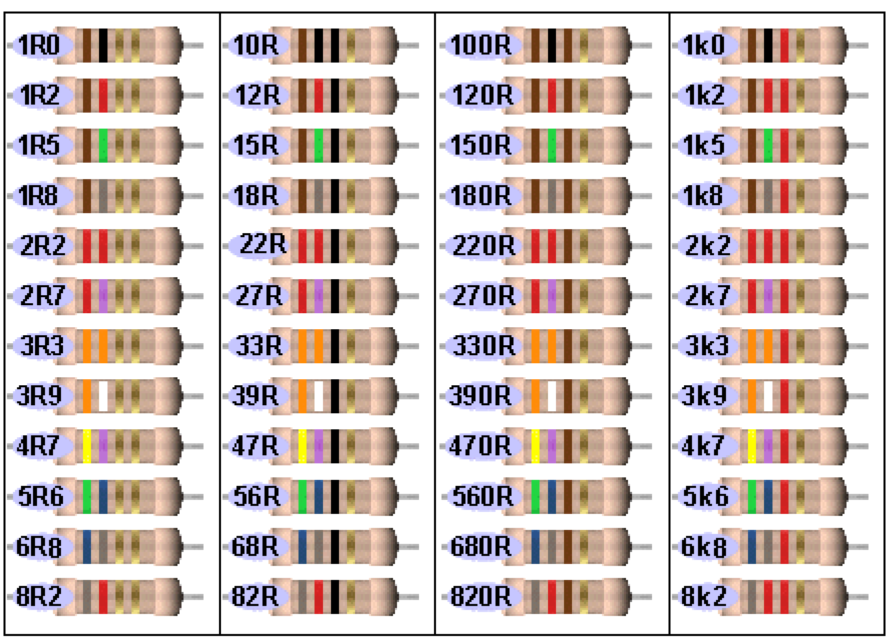

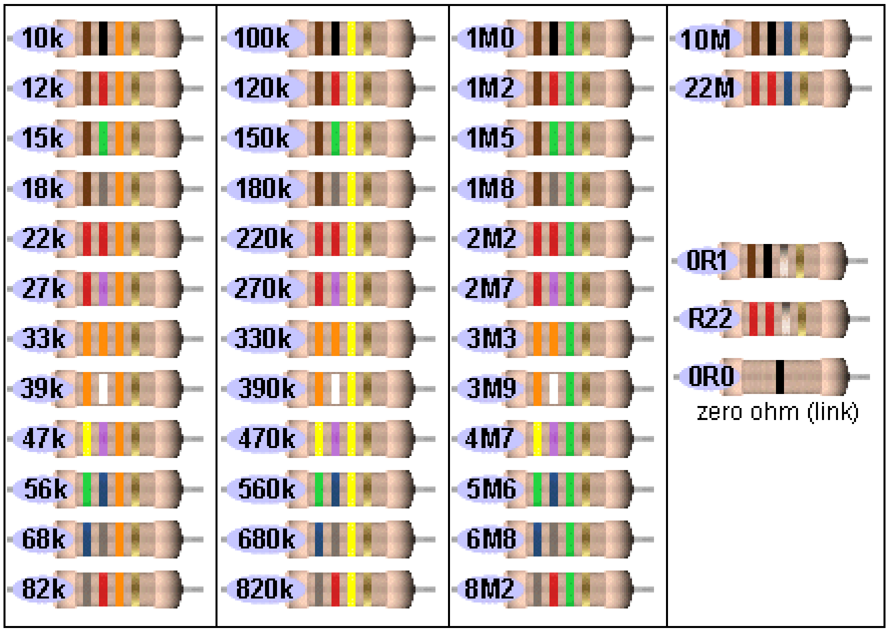

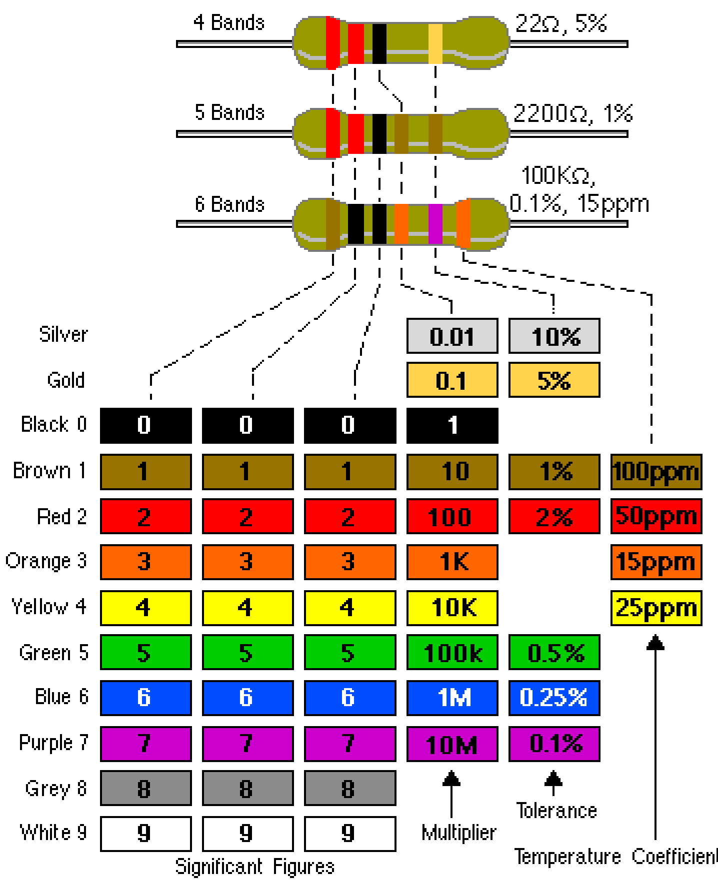

Resistor Color Code System

Here is another well-designed resistor colour code chart:

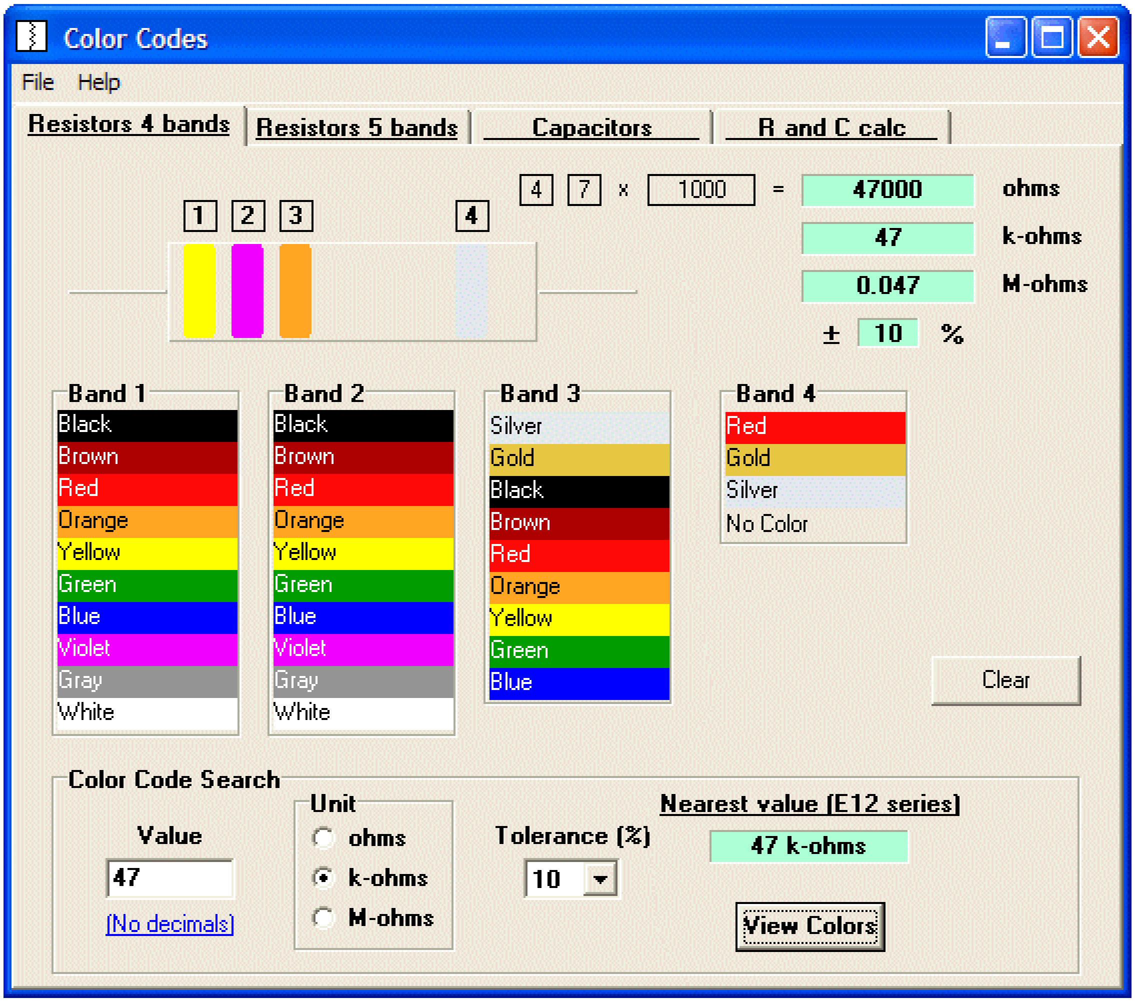

Download the program and save it on your desk-top for future reference:
ColourCode.exe (520KB)
ColourCode.zip (230KB)
ColourCode.rar (180KB)

RESISTORS LESS THAN 10 OHMS

When the **third** band is gold, it indicates the value of the "colors" must be divided by 10.
Gold = "divide by 10" to get values 1R0 to 8R2
When the **third** band is silver, it indicates the value of the "colors" must be divided by 100. (Remember: more letters in the word "silver" thus the divisor is "a larger division.")
Silver = "divide by 100" to get values R1 to R82
e.g: 0R1 = 0.1 ohm   0R22 = point 22 ohms
See 4th Column above for examples.

The letters "R, k and M" take the place of a decimal point.
e.g: 1**R**0 = 1 ohm   2**R**2 = 2 point 2 ohms   22**R** = 22 ohms
2**k**2 = 2,200 ohms   100**k** = 100,000 ohms
2**M**2 = 2,200,000 ohms

HOW TO REMEMBER THE COLOUR CODE:

Each colour has a "number" (or divisor) corresponding to it.
Most of the colours are in the same order as in the spectrum. You can see the spectrum in a rainbow. It is: ROY G BIV and the colours for resistors are in the same sequence.

black
brown   - colour of increasing temperature

red
orange
yellow
green
blue
(indigo - that part of the spectrum between blue and violet)
violet
gray
white

colour	value	No of zero's
silver	-2	divide by 100
gold	-1	divide by 10
black	0	No zeros
brown	1	0
red	2	00
orange	3	,000 or k
yellow	4	0,000
green	5	00,000
blue	6	M
violet	7	
gray	8	
white	9	

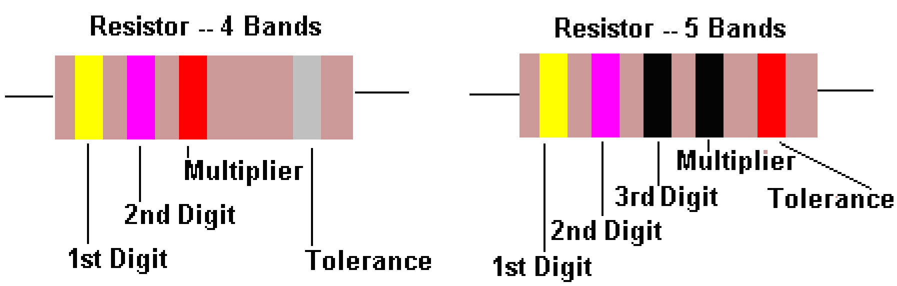

Band Color	Digit	Multiplier	Tolerance
Black	0	1	---
Brown	1	10	±1%
Red	2	100	±2%
Orange	3	1,000	±3%
Yellow	4	10,000	±4%
Green	5	100,000	---
Blue	6	1,000,000	---
Violet	7	10,000,000	---
Gray	8	100,000,000	---
White	9	---	---
Gold	---	0.1	±5%
Silver	---	0.01	±10%
None	---	---	±20%

Here are some common ways to remember the colour code:

Bad Beer Rots Our Young Guts, But Vodka Goes Well
Bright Boys Rave Over Young Girls But Violet Gets Wed
Bad Boys Rave Over Young Girls But Violet Gets Wed with Gold and Silver.

Reading 5-band resistors:

5-band resistors are easy to read if you remember two simple points. The first three bands provide the digits in the answer and the 4th band supplies the number of zero's.

Reading "STANDARD VALUES" (**on 5-band resistors**)

5-band resistors are also made in "Standard Values" but will have different colours to 4-band "common" resistors - and will be confusing if you are just starting out. For instance, a 47k 5% resistor with 4-bands will be: yellow-purple-orange-gold. For a 47k 1% resistor the colours will be yellow-purple-black-red-brown. The brown colour-band represents 1%.
The first two colour-bands for a STANDARD VALUE or "common value" in 1% or 5% will be the SAME. These two bands provide the digits in the answer.
It's the 3rd band for a 5% resistor that is expanded into two bands in a 1% resistor. But it's easy to follow.
For a standard value, the 3rd band in a 1% resistor is BLACK. This represents a ZERO in the answer. (For 5-band resistors BLACK represents a ZERO when in the third band. This is different to 4-band resistors where black represents the word OHMS! If the third band is BROWN, the answer will be 1).
So the 4th band has to represent one-less ZERO and is one colour UP THE COLOUR CHART! In other words the 3rd and 4th bands (combined) on a 1% resistor produces the same number of zero's as the 3rd band on a 5% resistor!

Resistors come in a range of values and the two most common are the E12 and E24 series. The E12 series comes in twelve values for each decade. The E24 series comes in twenty-four values per decade.

E12 series - 10, 12, 15, 18, 22, 27, 33, 39, 47, 56, 68, 82

E24 series - 10, 11, 12, 13, 15, 16, 18, 20, 22, 24, 27, 30, 33, 36, 39, 43, 47, 51, 56, 62, 68, 75, 82, 91

Here is the complete list of 1% 1/4watt resistors from:
CIRCUIT SPECIALISTS. The following list covers 10 ohms (10R) to 1M.
To buy 1% resistors from Circuit Specialists, click: HERE.

10R	121R	806R	3k83	7k15	14k7	39k2	121k
12R1	150R	825R	3k92	7k5	15k	40k2	147k
15R	182R	909R	4k02	7k87	15k8	44k2	150k
18R2	200R	1k0	4k22	71k5	16k9	46k4	182k
22R1	221R	1k21	4k64	8k06	17k4	47k	200k
27R4	240R	1k5	4k75	8k25	17k8	47k5	212k
30R1	249R	1k82	4k7	8k45	18k2	49k9	221k
33R2	274R	2k	4k87	8k66	20k	51k1	226k
36R5	301R	2k21	4k99	8k87	22k1	53k6	249k
39R2	332R	2k2	5k11	9k09	22k6	56k2	274k
47R5	348R	2k43	5k23	9k31	23k7	61k9	301k
49R9	392R	2k49	5k36	9k53	24k9	68k1	332k
51R1	402R	2k67	5k49	9k76	27k4	69k8	357k
56R2	475R	2k74	5k62	10k	29k4	75k0	392k
68R1	499R	3k01	5k76	11k	30k1	82k5	475k
75R	565R	3k32	5k9	12k	33k2	90k	487k
82R5	604R	3k48	6k04	12k1	34k8	90k9	499k
90R9	681R	3k57	6k19	12k4	36k5	95k3	562k
100R	750R	3k74	6k81	13k	38k3	100k	604k
							1M

Here is the list of 1% resistors from suppliers (such as Farnell):

1R0	13R	68R	360R	1k8	9k1	47k	240k
1R2	15R	75R	390R	2k0	10k	51k	270k
1R5	16R	82R	430R	2k2	11k	56k	300k
2R2	18R	91R	470R	2k4	12k	62k	330k
2R7	20R	100R	510R	2k7	13k	68k	360k
3R3	22R	110R	560R	3k	15k	75k	390k
3R9	24R	120R	620R	3k3	16k	82k	430k
4R7	27R	130R	680R	3k6	18k	91k	470k
5R6	30R	150R	750R	3k9	20k	100k	510k
6R2	33R	160R	820R	4k3	22k	110k	560k
6R8	36R	180R	910R	4k7	24k	120k	620k
7R5	39R	200R	1k	5k1	27k	130k	680k
8R2	43R	220R	1k1	5k6	30k	150k	750k
9R1	47R	240R	1k2	6k2	33k	160k	820k
10R	51R	270R	1k3	6k8	36k	180k	910k
11R	56R	300R	1k5	7k5	39k	200k	1M
12R	62R	330R	1k6	8k2	43k	220k	

Surface Mount Resistors

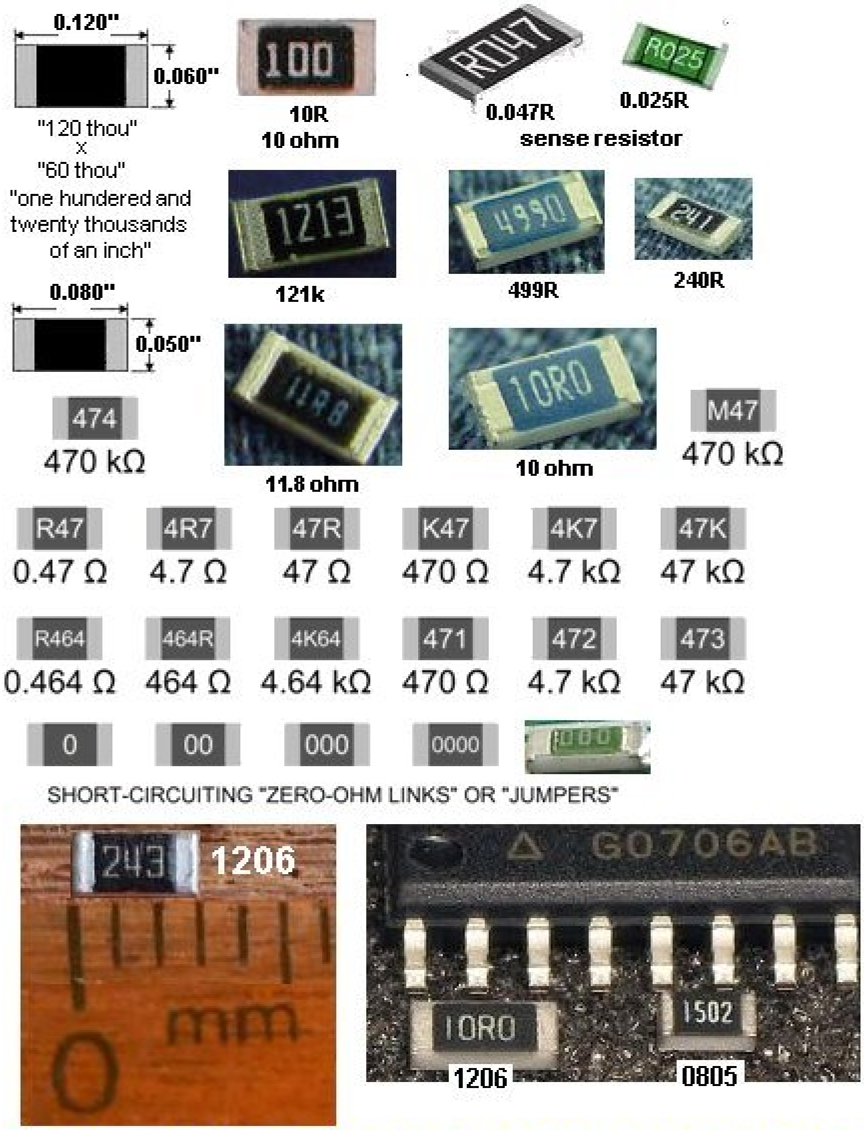

1206 and 0805 SURFACE MOUNT RESISTORS

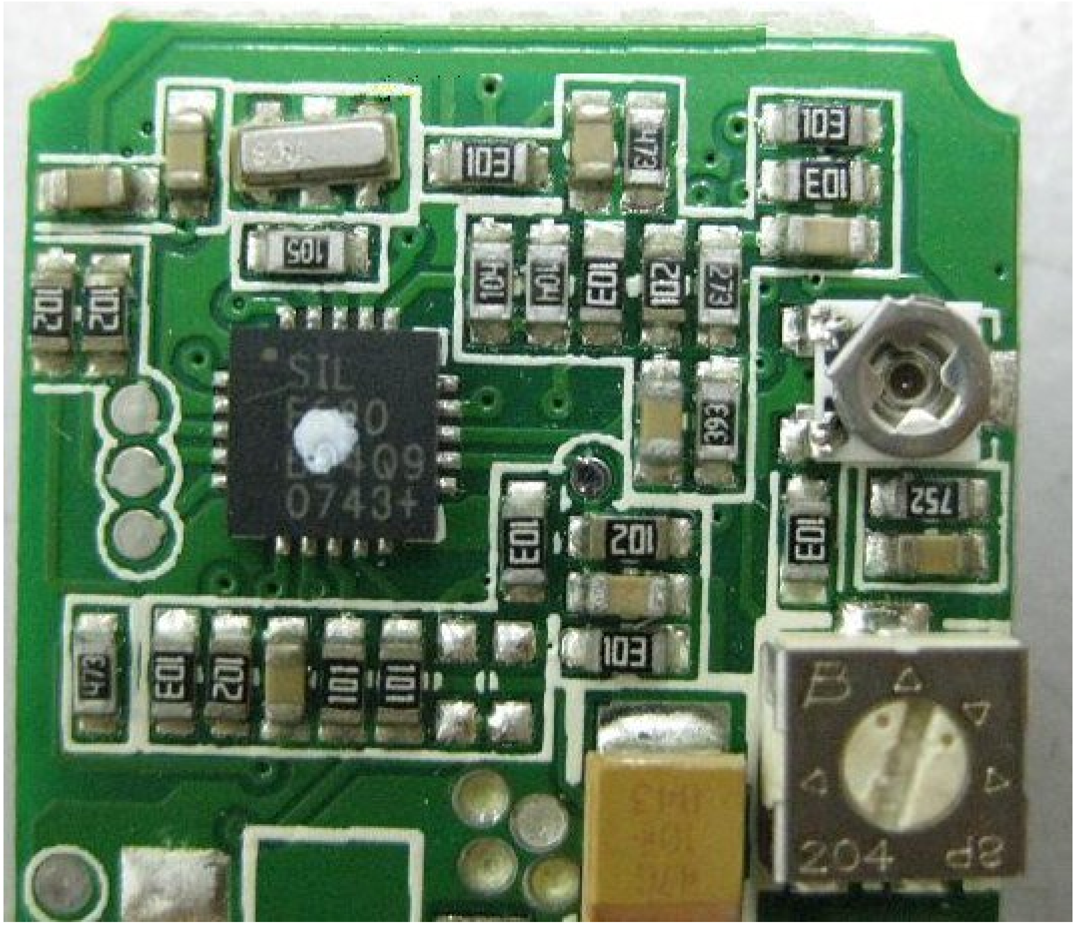

3-digit Surface Mount resistors on a PC board

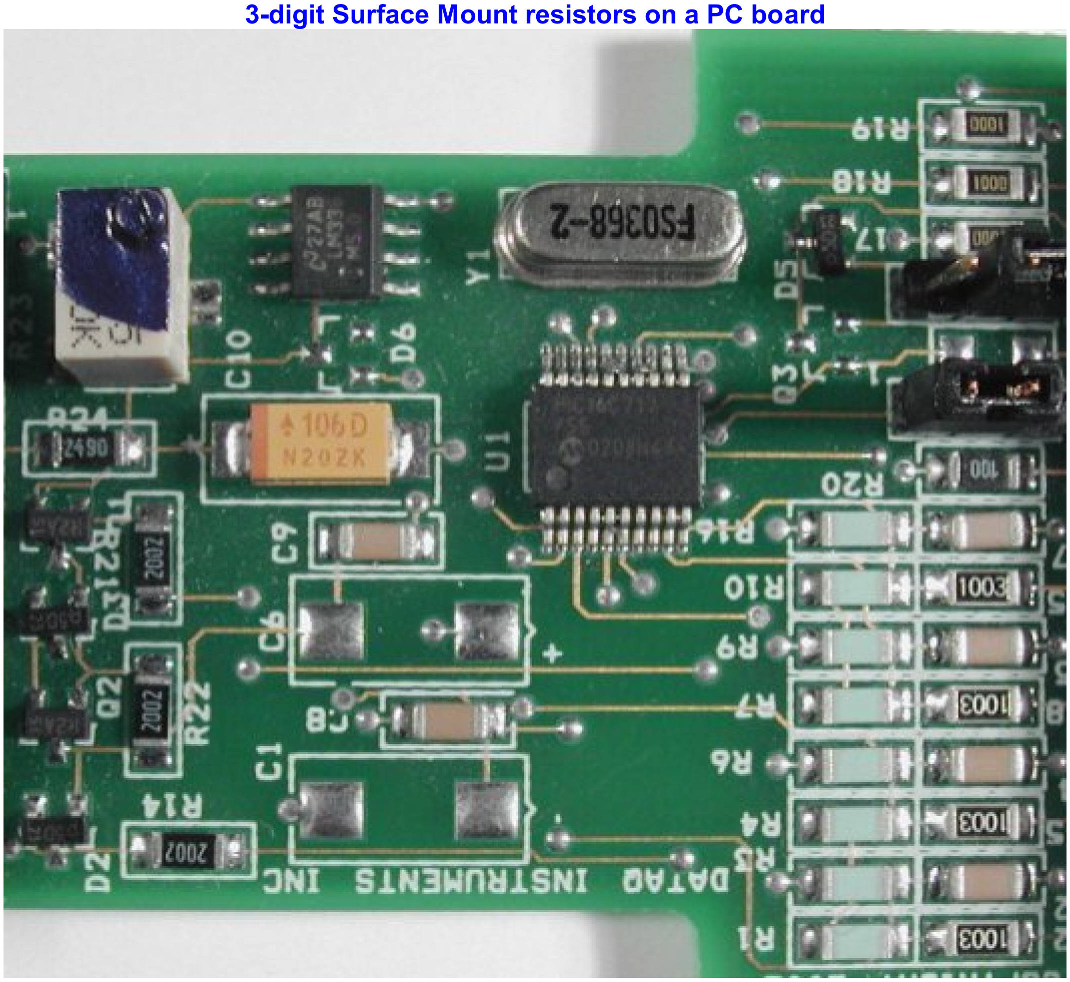

4-digit Surface Mount resistors on a PC board

The photo above shows surface mount resistors on a circuit board. The components

that are not marked are capacitors (capacitors are NEVER marked).
All the SM resistors in the above photos conform to a 3-digit or 4-digit code. But there are a number of codes, and the 4-digit code caters for high tolerance resistors, so it's getting very complicated.
Here is a basic 3-digit SM resistor:

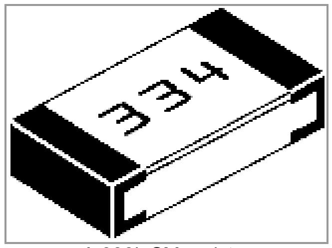

A 330k SM resistor

The first two digits represent the two digits in the answer. The third digit represents the number of zero's you must place after the two digits. The answer will be OHMS. For example: 334 is written 33 0 000. This is written 330,000 ohms. The comma can be replaced by the letter "k". The final answer is: 330k.
222 = 22 00 = 2,200 = 2k2
473 = 47 000 = 47,000 = 47k
474 = 47 0000 = 470,000 = 470k
105 = 10 00000 = 1,000,000 = 1M = one million ohms
There is one trick you have to remember. Resistances less than 100 ohms are written: 100, 220, 470. These are 10 and NO zero's = 10 ohms = 10R
or 22 and no zero's = 22R or 47 and no zero's = 47R. Sometimes the resistor is marked: 10, 22 and 47 to prevent a mistake.

Remember:
R = ohms
k = kilo ohms = 1,000 ohms
M = Meg = 1,000,000 ohms
The 3 letters (R, k and M) are put in place of the decimal point. This way you cannot make a mistake when reading a value of resistance.

Surface Mount **CURRENT SENSING** Resistors

Many new types of CURRENT SENSING surface-mount resistors are appearing on the market and these are creating lots of new problems.
Fortunately all resistors are marked with the value of resistance and these resistors are identified in MILLIOHMS. A miili ohm is one thousandth or an ohm and is written 0.001 when writing a normal mathematical number.
When written on a surface mount resistor, the letter R indicates the decimal point and it also signifies the word "OHM" or "OHMS" and one milli-ohm is written R001
Five miiliohms is R005 and one hundred milliohms is R100
Some surface mount resistors have the letter "M" after the value to indicate the resistor has a rating of 1 watt. e.g: R100M These surface-mount resistors are specially-made to withstand a high temperature and a surface-mount resistor of the same size is normally 250mW or less.
These current-sensing resistors can get extremely hot and the PC board can become burnt or damaged.
When designing a PC board, make the lands very large to dissipate the heat.
Normally a current sensing resistor is below one ohm (1R0) and it is easy to identify them as R100 etc.
You cannot measure the value of a current sensing resistor as the leads of a multimeter have a higher resistance than the resistor and few multimeters can read values below one ohm.
If the value is not visible, you will have to refer to the circuit.
Before replacing it, work out why it failed.
Generally it gets too hot. Use a larger size and add tiny heatsinks on each end.
Here are some surface=mount current-sense resistors:

3 milli-ohm

220 milli-ohm

15 milli-ohm

9 point 1 milli-ohm

220 milli-ohm

5 milli-ohm

50 milli-ohm 1%

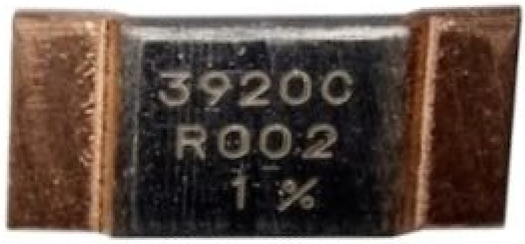

2 milli-ohm

30 milli-ohm

10 milli-ohm

1-watt ????

THE COMPLETE RANGE OF SM RESISTOR MARKINGS

Click to see the complete range of SM resistor markings for 3-digit code:

Click to see the complete range of SM resistor markings for 4-digit code:

0000 is a value on a surface-mount resistor. It is a zero-ohm **LINK**!
Resistances less than 10 ohms have 'R' to indicate the position of the decimal point.
Here are some examples:

Three Digit Examples	Four Digit Examples
330 is 33 ohms *- not 330 ohms*	1000 is 100 ohms *- not 1000 ohms*
221 is 220 ohms	4992 is 49 900 ohms, or 49k9
683 is 68 000 ohms, or 68k	1623 is 162 000 ohms, or 162k
105 is 1 000 000 ohms, or 1M	0R56 or R56 is 0.56 ohms
8R2 is 8.2 ohms	

A new coding system has appeared on **1% types**. This is known as the EIA-96 marking method. It consists of a three-character code. The first two digits signify the 3 significant digits of the resistor value, using the lookup table below. The third character - a letter - signifies the multiplier.

code	value	code	value	code	value	code	value	code	value	code	value
01	100	17	147	33	215	49	316	65	464	81	681
02	102	18	150	34	221	50	324	66	475	82	698
03	105	19	154	35	226	51	332	67	487	83	715
04	107	20	158	36	232	52	340	68	499	84	732
05	110	21	162	37	237	53	348	69	511	85	750
06	113	22	165	38	243	54	357	70	523	86	768
07	115	23	169	39	249	55	365	71	536	87	787
08	118	24	174	40	255	56	374	72	549	88	806
09	121	25	178	41	261	57	383	73	562	89	825
10	124	26	182	42	267	58	392	74	576	90	845
11	127	27	187	43	274	59	402	75	590	91	866
12	130	28	191	44	280	60	412	76	604	92	887
13	133	29	196	45	287	61	422	77	619	93	909
14	137	30	200	46	294	62	432	78	634	94	931
15	140	31	205	47	301	63	442	79	649	95	953
16	143	32	210	48	309	64	453	80	665	96	976

The **multiplier** letters are as follows:

letter	mult	letter	mult
F	100000	B	10
E	10000	A	1
D	1000	X or S	0.1
C	100	Y or R	0.01

22A is a 165 ohm resistor, **68C** is a 49900 ohm (49k9) and **43E** a 2740000 (2M74). This marking scheme applies to 1% resistors only.

A similar arrangement can be used for **2% and 5%** tolerance types. The multiplier letters are identical to 1% ones, but occur **before** the number code and the following **code** is used:

2%				5%			
code	value	code	value	code	value	code	value
01	100	13	330	25	100	37	330
02	110	14	360	26	110	38	360
03	120	15	390	27	120	39	390
04	130	16	430	28	130	40	430
05	150	17	470	29	150	41	470
06	160	18	510	30	160	42	510
07	180	19	560	31	180	43	560

08	200	**20**	620	**32**	200	**44**	620
09	220	**21**	680	**33**	220	**45**	680
10	240	**22**	750	**34**	240	**46**	750
11	270	**23**	820	**35**	270	**47**	820
12	300	**24**	910	**36**	300	**48**	910

With this arrangement, **C31** is 5%, 18000 ohm (18k), and **D18** is 510000 ohms (510k) 2% tolerance.
Always check with an ohm-meter (a multimeter) to make sure.

Chip resistors come in the following styles and ratings:
Style: 0402, 0603, 0805, 1206, 1210, 2010, 2512, 3616, 4022
Power Rating: 0402(1/16W), 0603(1/10W), 0805(1/8W), 1206(1/4W), 1210(1/3W), 2010(3/4W), 2512(1W), 3616(2W), 4022(3W)
Tolerance: 0.1%, 0.5%, 1%, 5%
Temperature Coefficient: 25ppm 50ppm 100ppm

EIA marking code for surface mount (SMD) resistors

01S = 1R	01R = 10R	01A = 100R	01B = 1k	01C = 10k	01D = 100k	01E = 1M	01F = 10M
02S = 1R02	02R = 10R2	02A = 102R	02B = 1k02	02C = 10k2	02D = 102k	02E = 1M02	
03S = 1R05	03R = 10R5	03A = 105R	03B = 1k05	03C = 10k5	03D = 105k	03E = 1M05	18F = 15M
04S = 1R07	04R = 10R7	04A = 107R	04B = 1k07	04C = 10k7	04D = 107k	04E = 1M07	
05S = 1R1	05R = 11R	05A = 110R	05B = 1k1	05C = 11k	05D = 110k	05E = 1M1	30F = 20M
06S = 1R13	06R = 11R3	06A = 113R	06B = 1k13	06C = 11k3	06D = 113k	06E = 1M13	
07S = 1R15	07R = 11R5	07A = 115R	07B = 1k15	07C = 11k5	07D = 115k	07E = 1M15	
08S = 1R18	08R = 11R8	08A = 118R	08B = 1k18	08C = 11k8	08D = 118k	08E = 1M18	
09S = 1R21	09R = 12R1	09A = 121R	09B = 1k21	09C = 12k1	09D = 121k	09E = 1M21	
10S = 1R24	10R = 12R4	10A = 124R	10B = 1k24	10C = 12k4	10D = 124k	10E = 1M24	
11S = 1R27	11R = 12R7	11A = 127R	11B = 1k27	11C = 12k7	11D = 127k	11E = 1M27	
12S = 1R3	12R = 13R	12A = 130R	12B = 1k3	12C = 13k	12D = 130k	12E = 1M3	
13S = 1R33	13R = 13R3	13A = 133R	13B = 1k33	13C = 13k3	13D = 133k	13E = 1M33	
14S = 1R37	14R = 13R7	14A = 137R	14B = 1k37	14C = 13k7	14D = 137k	14E = 1M37	
15S = 1R4	15R = 14R	15A = 140R	15B = 1k4	15C = 14k	15D = 140k	15E = 1M4	
16S = 1R43	16R = 14R3	16A = 143R	16B = 1k43	16C = 14k3	16D = 143k	16E = 1M43	
17S = 1R47	17R = 14R7	17A = 147R	17B = 1k47	17C = 14k7	17D = 147k	17E = 1M47	
18S = 1R5	18R = 15R	18A = 150R	18B = 1k5	18C = 15k	18D = 15k	18E = 1M5	
19S = 1R54	19R = 15R4	19A = 154R	19B = 1k54	19C = 15k4	19D = 154k	19E = 1M54	
20S = 1R58	20R = 15R8	20A = 158R	20B = 1k58	20C = 15k8	20D = 158k	20E = 1M58	
21S = 1R62	21R = 16R2	21A = 162R	21B = 1k62	21C = 16k2	21D = 162k	21E = 1M62	
22S = 1R65	22R = 16R5	22A = 165R	22B = 1k65	22C = 16k5	22D = 165k	22E = 1M65	
23S = 1R69	23R = 16R9	23A = 169R	23B = 1k69	23C = 16k9	23D = 169k	23E = 1M69	
24S = 1R74	24R = 17R4	24A = 174R	24B = 1k74	24C = 17k4	24D = 174k	24E = 1M74	
25S = 1R78	25R = 17R8	25A = 178R	25B = 1k78	25C = 17k8	25D = 178k	25E = 1M78	
26S = 1R82	26R = 18R2	26A = 182R	26B = 1k82	26C = 18k2	26D = 182k	26E = 1M82	
27S = 1R87	27R = 18R7	27A = 187R	27B = 1k87	27C = 18k7	27D = 187k	27E = 1M87	
28S = 1R91	28R = 19R1	28A = 191R	28B = 1k91	28C = 19k1	28D = 191k	28E = 1M91	
29S = 1R96	29R = 19R6	29A = 196R	29B = 1k96	29C = 19k6	29D = 196k	29E = 1M96	
30S = 2R0	30R = 20R0	30A = 200R	30B = 2k0	30C = 20k0	30D = 200k	30E = 2M0	
31S = 2R05	31R = 20R5	31A = 205R	31B = 2k05	31C = 20k5	31D = 205k	31E = 2M05	
32S = 2R10	32R = 21R0	32A = 210R	32B = 2k10	32C = 21k0	32D = 210k	32E = 2M10	
33S = 2R15	33R = 21R5	33A = 215R	33B = 2k15	33C = 21k5	33D = 215k	33E = 2M15	
34S = 2R21	34R = 22R1	34A = 221R	34B = 2k21	34C = 22k1	34D = 221k	34E = 2M21	
35S = 2R26	35R = 22R6	35A = 226R	35B = 2k26	35C = 22k6	35D = 226k	35E = 2M26	
36S = 2R32	36R = 23R2	36A = 232R	36B = 2k32	36C = 23k2	36D = 232k	36E = 2M32	
37S = 2R37	37R = 23R7	37A = 237R	37B = 2k37	37C = 23k7	37D = 237k	37E = 2M37	
38S = 2R43	38R = 24R3	38A = 243R	38B = 2k43	38C = 24k3	38D = 243k	38E = 2M43	
39S = 2R49	39R = 24R9	39A = 249R	39B = 2k49	39C = 24k9	39D = 249k	39E = 2M49	
40S = 2R55	40R = 25R5	40A = 255R	40B = 2k55	40C = 25k5	40D = 255k	40E = 2M55	
41S = 2R61	41R = 26R1	41A = 261R	41B = 2k61	41C = 26k1	41D = 261k	41E = 2M61	
42S = 2R67	42R = 26R7	42A = 267R	42B = 2k67	42C = 26k7	42D = 267k	42E = 2M67	
43S = 2R74	43R = 27R4	43A = 274R	43B = 2k74	43C = 27k4	43D = 274k	43E = 2M74	
44S = 2R80	44R = 28R0	44A = 280R	44B = 2k80	44C = 28k0	44D = 280k	44E = 2M80	
45S = 2R87	45R = 28R7	45A = 287R	45B = 2k87	45C = 28k7	45D = 287k	45E = 2M87	
46S = 2R94	46R = 29R4	46A = 294R	46B = 2k94	46C = 29k4	46D = 294k	46E = 2M94	
47S = 3R01	47R = 30R1	47A = 301R	47B = 3k01	47C = 30k1	47D = 301k	47E = 3M01	
48S = 3R09	48R = 30R9	48A = 309R	48B = 3k09	48C = 30k9	48D = 309k	48E = 3M09	
49S = 3R16	49R = 31R6	49A = 316R	49B = 3k16	49C = 31k6	49D = 316k	49E = 3M16	
50S = 3R24	50R = 32R4	50A = 324R	50B = 3k24	50C = 32k4	50D = 324k	50E = 3M24	
51S = 3R32	51R = 33R2	51A = 332R	51B = 3k32	51C = 33k2	51D = 332k	51E = 3M32	
52S = 3R4	52R = 34R0	52A = 340R	52B = 3k4	52C = 34k0	52D = 340k	52E = 3M4	
53S = 3R48	53R = 34R8	53A = 348R	53B = 3k48	53C = 34k8	53D = 348k	53E = 3M48	

54S = 3R57	54R = 35R7	54A = 357R	54B = 3k57	54C = 35k7	54D = 357k	54E = 3M57	
55S = 3R65	55R = 36R5	55A = 365R	55B = 3k65	55C = 36k5	55D = 365k	55E = 3M65	
56S = 3R74	56R = 37R4	56A = 374R	56B = 3k74	56C = 37k4	56D = 374k	56E = 3M74	
57S = 3R83	57R = 38R3	57A = 383R	57B = 3k83	57C = 38k3	57D = 383k	57E = 3M83	
58S = 3R92	58R = 39R2	58A = 392R	58B = 3k92	58C = 39k2	58D = 392k	58E = 3M92	
59S = 4R02	59R = 40R2	59A = 402R	59B = 4k02	59C = 40k2	59D = 402k	59E = 4M02	
60S = 4R12	60R = 41R2	60A = 412R	60B = 4k12	60C = 41k2	60D = 412k	60E = 4M12	
61S = 4R22	61R = 42R2	61A = 422R	61B = 4k22	61C = 42k2	61D = 422k	61E = 4M22	
62S = 4R32	62R = 43R2	62A = 432R	62B = 4k32	62C = 43k2	62D = 432k	62E = 4M32	
63S = 4R42	63R = 44R2	63A = 442R	63B = 4k42	63C = 44k2	63D = 442k	63E = 4M42	
64S = 4R53	64R = 45R3	64A = 453R	64B = 4k53	64C = 45k3	64D = 453k	64E = 4M53	
65S = 4R64	65R = 46R4	65A = 464R	65B = 4k64	65C = 46k4	65D = 464k	65E = 4M64	
66S = 4R75	66R = 47R5	66A = 475R	66B = 4k75	66C = 47k5	66D = 475k	66E = 4M75	
67S = 4R87	67R = 48R7	67A = 487R	67B = 4k87	67C = 48k7	67D = 487k	67E = 4M87	
68S = 4R99	68R = 49R9	68A = 499R	68B = 4k99	68C = 49k9	68D = 499k	68E = 4M99	
69S = 5R11	69R = 51R1	69A = 511R	69B = 5k11	69C = 51k1	69D = 511k	69E = 5M11	
70S = 5R23	70R = 52R3	70A = 523R	70B = 5k23	70C = 52k3	70D = 523k	70E = 5M23	
71S = 5R36	71R = 53R6	71A = 536R	71B = 5k36	71C = 53k6	71D = 536k	71E = 5M36	
72S = 5R49	72R = 54R9	72A = 549R	72B = 5k49	72C = 54k9	72D = 549k	72E = 5M49	
73S = 5R62	73R = 56R2	73A = 562R	73B = 5k62	73C = 56k2	73D = 562k	73E = 5M62	
74S = 5R76	74R = 57R6	74A = 576R	74B = 5k76	74C = 57k6	74D = 576k	74E = 5M76	
75S = 5R9	75R = 59R0	75A = 590R	75B = 5k9	75C = 59k0	75D = 590k	75E = 5M9	
76S = 6R04	76R = 60R4	76A = 604R	76B = 6k04	76C = 60k4	76D = 604k	76E = 6M04	
77S = 6R19	77R = 61R9	77A = 619R	77B = 6k19	77C = 61k9	77D = 619k	77E = 6M19	
78S = 6R34	78R = 63R4	78A = 634R	78B = 6k34	78C = 63k4	78D = 634k	78E = 6M34	
79S = 6R49	79R = 64R9	79A = 649R	79B = 6k49	79C = 64k9	79D = 649k	79E = 6M49	
80S = 6R65	80R = 66R5	80A = 665R	80B = 6k65	80C = 66k5	80D = 665k	80E = 6M65	
81S = 6R81	81R = 68R1	81A = 681R	81B = 6k81	81C = 68k1	81D = 681k	81E = 6M81	
82S = 6R98	82R = 69R8	82A = 698R	82B = 6k98	82C = 69k8	82D = 698k	82E = 6M98	
83S = 7R15	83R = 71R5	83A = 715R	83B = 7k15	83C = 71k5	83D = 715k	83E = 7M15	
84S = 7R32	84R = 73R2	84A = 732R	84B = 7k32	84C = 73k2	84D = 732k	84E = 7M32	
85S = 7R5	85R = 75R0	85A = 750R	85B = 7k5	85C = 75k0	85D = 750k	85E = 7M5	
86S = 7R68	86R = 76R8	86A = 768R	86B = 7k68	86C = 76k8	86D = 768k	86E = 7M68	
87S = 7R87	87R = 78R7	87A = 787R	87B = 7k87	87C = 78k7	87D = 787k	87E = 7M87	
88S = 8R06	88R = 80R6	88A = 806R	88B = 8k06	88C = 80k6	88D = 806k	88E = 8M06	
89S = 8R25	89R = 82R5	89A = 825R	89B = 8k25	89C = 82k5	89D = 825k	89E = 8M25	
90S = 8R45	90R = 84R5	90A = 845R	90B = 8k45	90C = 84k5	90D = 845k	90E = 8M45	
91S = 8R66	91R = 86R6	91A = 866R	91B = 8k66	91C = 86k6	91D = 866k	91E = 8M66	
92S = 8R87	92R = 88R7	92A = 887R	92B = 8k87	92C = 88k7	92D = 887k	92E = 8M87	
93S = 9R09	93R = 90R9	93A = 909R	93B = 9k09	93C = 90k9	93D = 909k	93E = 9M09	
94S = 9R31	94R = 93R1	94A = 931R	94B = 9k31	94C = 93k1	94D = 931k	94E = 9M31	
95S = 9R53	95R = 95R3	95A = 953R	95B = 9k53	95C = 95k3	95D = 953k	95E = 9M53	
96S = 9R76	96R = 97R6	96A = 976R	96B = 9k76	96C = 97k6	96D = 976k	96E = 9M76	

If you want an accurate RESISTANCE measurement, remove the resistor from the circuit and use a Digital meter.

SURFACE MOUNT COMPONENTS - PACKS

Talking Electronics has packs of components for the repairman. The following packs are available:

SURFACE MOUNT RESISTOR PACK consists of 1 off each standard value
10 ohms to 1M & 2M2 (60 resistors)
$14.20 including pack and post

SURFACE MOUNT CAPACITOR PACK consists of:
2 - 10p 5 - 47p 5 - 100p 5 - 470p 5 - 1n 5 - 10n 5 - 22n 5 - 100n
5 - 1u 16v electrolytic 5 - 10u 16v electrolytic
(40 components)
$23.80 including pack and post

SURFACE MOUNT DIODE PACK consists of:
5 - 1N 4148 (marked as "A6")
$10.00 including pack and post

SURFACE MOUNT TRANSISTOR PACK consists of:
5 - BC 848 (marked as "1K") NPN
5 - BC858 PNP
$10.00 including pack and post

email **Colin Mitchell** for details on how to pay by credit card or PayPal.

CREATING ANY VALUE OF RESISTANCE

Any value of resistance can be created by connecting two resistors in PARALLEL or SERIES.
You can also create a higher wattage resistor by connecting them in SERIES OR PARALLEL.
We are only going to cover two EQUAL VALUE resistors in SERIES or in PARALLEL.
If you want to create a "Special Value," simply connect two resistors and read the value with a Digital Meter. Keep changing the values until you get the required value.
We are not going into series or Parallel formulae. You can easily find a value with a multimeter.

TWO EQUAL-VALUE RESISTORS IN SERIES

Two equal-value resistors IN SERIES creates a value of DOUBLE. You simply ADD the values.
This can be done with any to two values as shown. Three equal-value resistors in series is three times the value.

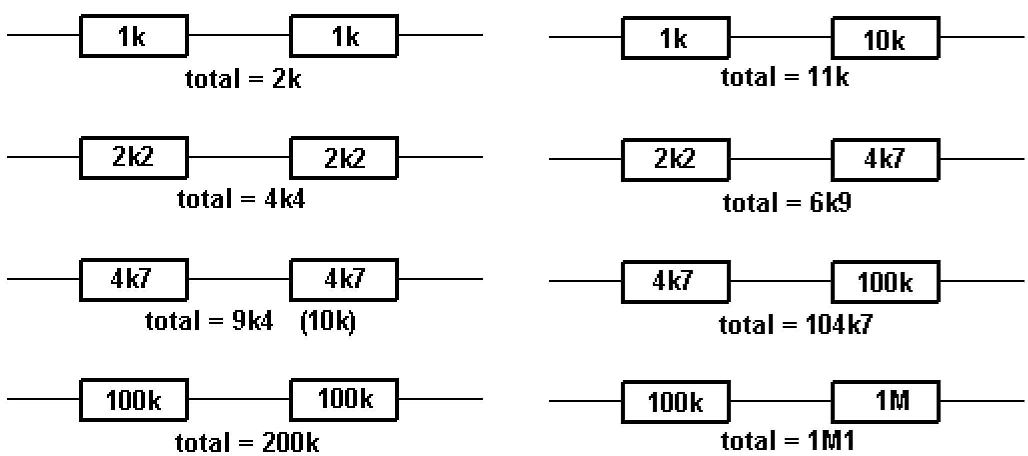

TWO EQUAL-VALUE RESISTORS IN PARALLEL

Two equal-value resistors IN PARALLEL creates a value of HALF. Three equal-value resistors in parallel is equal to one-third the value.

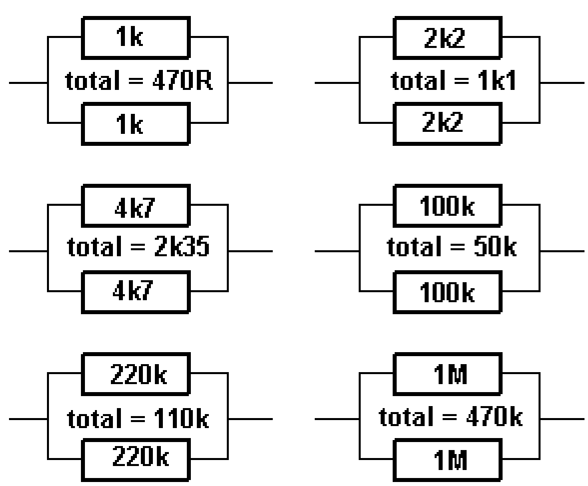

If you want a particular value and it is not available, here is a chart.
Use 2 resistors in series or parallel as shown:

Required Value	R1	Series/ Parallel	R2	Actual value:

10	4R7	S	4R7	9R4
12	10	S	2R2	12R2
15	22	P	47	14R9
18	22	P	100	18R
22	10	S	12	22
27	22	S	4R7	26R7
33	22	S	10	32R
39	220	P	47	38R7
47	22	S	27	49
56	47	S	10	57
68	33	S	33	66
82	27	S	56	83

There are other ways to combine 2 resistors in parallel or series to get a particular value. The examples above are just one way. 4R7 = 4.7 ohms

TESTING A RESISTOR

To check the value of a resistor, it should be removed from the circuit. The surrounding components can affect the reading and make it lower.
Resistors **VERY RARELY** change value, but if it is overheated or damaged, the resistance can increase. You can take the reading of a resistor "in-circuit" in one direction then the other, as the surrounding components may have diodes and this will alter the reading.
You can also test a resistor by feeling its temperature-rise. It is getting too hot if you cannot hold your finger on it (some "metal film" resistors are designed to tolerate quite high temperatures).

TESTING AN "AC" RESISTOR

There is no such thing as an "AC" resistor. Resistors are just "resistors" and they can be in AC circuits or DC circuits. Resistors can be given names such as "Safety Resistor" "Ballast Resistor" "LOAD Resistor" "Feed Resistor" "Dropper Resistor" or "Supply Resistor." These are just normal resistors with a normal resistance - except a "Safety Resistor."
A safety resistor is made of a flame-proof material such as metal-oxide-film and not carbon-composition. It is designed to "burn out" when too much current flows BUT NOT CATCH FIRE.
It is a low-value resistor and has a voltage-drop across it but this is not intentional. The voltage-drop is to create a "heating-effect" to burn out the resistor. In all the other types of resistor, the voltage-drop is intentional.
A Ballast resistor is a normal resistor and can be called a Power resistor, Dropper resistor, Supply resistor or Feed resistor. It is designed to reduce the voltage from one source and deliver a lower voltage. It is a form of: "in-line" resistor.
A Load Resistor is generally connected across the output of a circuit and turns the energy it receives, into heat.

RESISTOR NETWORKS

To reduce the number of resistors in a circuit, some engineers use a set of identical resistors in a package called a Single-In-Line (SIL) resistor network. It is made with many resistors of the same value, all in one package. One end of each resistor is connected all the other resistors and this is the common pin, identified as pin 1 and has a dot on the package.
These packages are very reliable but to make sure all the resistors are as stated, you need to locate pin 1. All values will be identical when referenced to this pin.

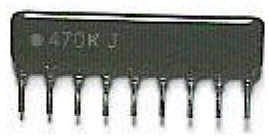

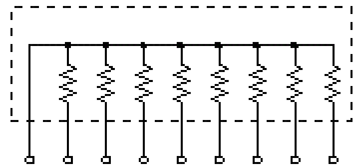
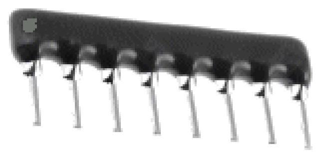
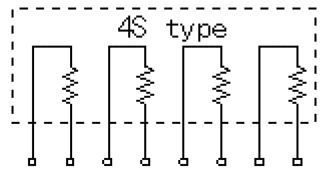

RESISTOR NETWORKS

Some resistor networks have a "4S" printed on the component. The 4S indicates the package contains 4 independent resistors that are not wired together inside. The housing has eight leads as shown in the second image.
Independent resistors have an even number of pins and measuring between each pair will produce identical values. Resistance between any pair will indicate leakage and may be a fault.

WIRE WOUND RESISTOR

A wire wound resistor is also called a POWER RESISTOR. This type of resistor can have a resistance as low as 0.1 ohms (one-tenth of an ohm) or as high as about 10k.
The image shows a 0.68 ohm resistor as the letter "R" represents the DECIMAL POINT and R68 is the same a .68 and this is 0.68 ohms. The wattage is 9 watts.
This resistor will allow xxx amps to flow.   To work out the current, use the formula:
Power = Current x Current x resistance
   9   = Current x Current x .68
Divide both sides by 0.68
13.2   = Current x Current
Find the square root of 13.2
Current = 3.6 amps

When 3.6 amps flow through the resistor, the voltage appearing across it will be:
V = current x resistance
   = 3.6   x 0.68
   = 2.5v and the wattage (heat) loss will be 9 watts.

The purpose of a resistor like this is to stop or reduce "ripple." Ripple is the noise or hum in an amplifier when the sound is turned up.
There are many reasons why you need to reduce the level of hum and this resistor will remove ripple as large as 2.5v when 3.6 amps is flowing, provided you have filter electrolytics on both side of the resistor to assist in removing the ripple.

If the letter "R" is in a different position, the value of resistance would be:

68R = 68Ω
6R8 = 6.8Ω
R68 = 0.68Ω

If you replace the R68 resistor a 6R8 resistor by mistake, the voltage across it will rise to 25v and if 3.6 amps flows, the wattage will be: 90 watts!!!
The resistor will glow red and burn out.

TESTING A POSISTOR

A Posistor is a resistor that connects in series with the degaussing coil around the picture tube or **Monitor.** When cold, it has a very low resistance and a large current flows when the monitor or TV is switched on. This current heats up the Posistor and the resistance increases. This causes the current to decrease and any magnetism in the shadow mask is removed. The posistor can one or two elements and it is kept warm so the resistance remains high. Many Posistors have a second element inside the case that connects directly to the supply to keep the Positive Temperature Coefficient resistor high so that the current through the degaussing coil falls to almost zero. This constant heat eventually destroys the package.
The heavy current that flows when a set is turned ON also causes the posistor to crack and break and this results in poor purity on the screen - as the shadow mask gradually becomes magnetic..
Posistors have different resistance values from different manufacturers and must be replaced with an identical type.
They can be checked for very low resistance when cold but any loose pieces inside the case will indicate a damaged component.

A "BURNT" RESISTOR **- normally and technically called a "burnt-out" resistor.**

The resistance of a "burnt" resistor can sometimes be determined by scraping away the outer coating - if the resistor has a spiral of resistance-material. You may be able to find a spot where the spiral has been damaged.

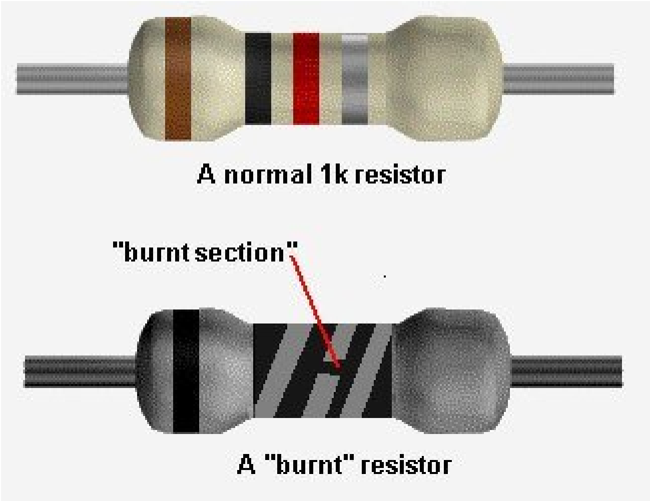

Note the spirals of conductive carbon.
The number of spirals has nothing to with the resistance.
It is the amount of carbon particles in the "track" that determines the resistance. It is also the thickness and width of the track that determines the resistance.
And then it is the overall size of the resistor that determines the wattage.
And then the size of the leads, the closeness to the PCB and the size of the lands that eventually determines how hot the resistor will get.

Clean the "spot" (burnt section of the spiral) very carefully and make sure you can get a good contact with the spiral and the tip of your probe. Measure from one lead of the resistor to the end of the damaged spiral. Then measure from the other lead to the other end of the spiral.
Add the two values and you have an approximate value for the resistor. You can add a small amount for the damaged section.
This process works very well for damaged wire-wound resistors. They can be pulled apart and each section of the resistance-wire (nichrome wire) measured and added to get the full resistance.

There is another way to determine the value of a damaged resistor.
Get a set of resistors of the same wattage as the damaged component and start with a high value. It's handy to know if the resistor is in the range: 10ohm to 100ohms or 1k to 10k etc, but this is not essential.
Start with a very high value and turn the circuit ON. You can perform voltage tests and if you know the expected output voltage, decrease the resistance until this voltage is obtained.
If you do not know the expected voltage, keep reducing the value of resistance until the circuit works as designed.
This is the best advice in a situation where you do not know the value of a resistor.

There is a third way to determine the value and this requires measuring the voltage drop across the resistor and the current-flow. By multiplying the two you will get a wattage and this must be less than the wattage of the resistor being replaced.

TESTING POTENTIOMETERS (variable resistors)

To check the value of a variable resistor, it should be removed from circuit or at least 2 legs should be removed. A Rheostat is a variable resistor using only one end and the middle connected to a circuit.
The resistance between the two outside pins is the value marked on the component and the centre leg will change from nearly zero to the full resistance as the shaft is rotated.
"Pots" generally suffer from "crackle" when turned and this can be fixed by spraying up the shaft and into the pot via the shaft with a tube fixed to a can of "spray-lubricant" (contact cleaner).
"Pre-set pots" and "trim pots" are miniature versions of a potentiometer and they are all tested the same. The photo shows a pot, two mini pots and 3 mini trim pots.

10-Turn POTs

A 10-turn pot is one of the worst items to be designed. I remove them immediately from any design.
You don't know the position of the wiper. You don't know which way you are turning the wiper and you can't remember which way you turned the post "the last time."
The screwdriver always falls out of the slot.
If you need fine adjustment, place fixed resistors on each side of the pot and use a normal mini trim pot with much less resistance.

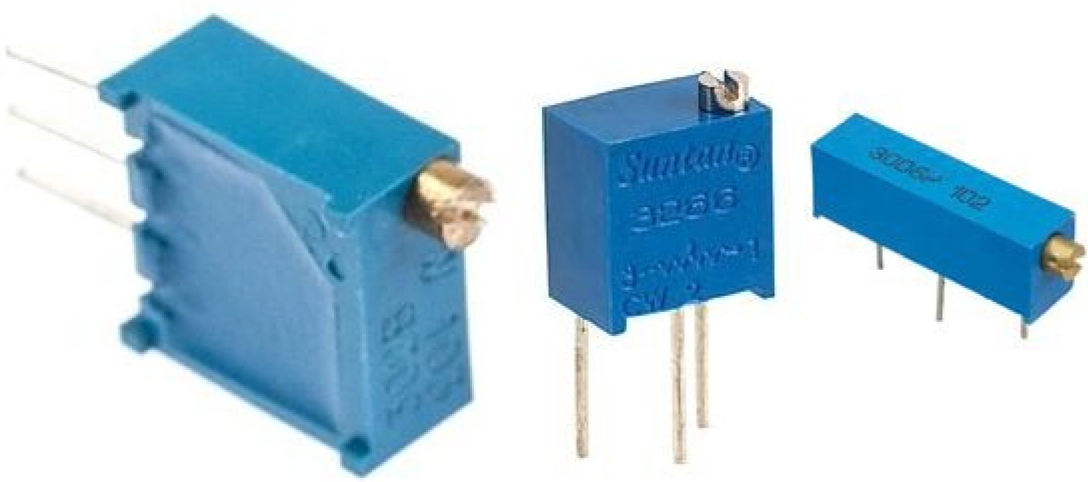

FOCUS POTS

Focus pots quite often get a spot of dirt where the wiper touches the track. Cleaning with spray fixes the bad focus but if the pot is leaking to chassis from inside the pot (due to the high voltage on the terminals) simply remove it from the chassis and leave it floating (this will restore the high voltage to the picture tube) or you can use one from an old chassis.

MAKING YOUR OWN RESISTOR, CAPACITOR, INDUCTOR or DIODE

Quite often you will not have the exact value of resistance or capacitance for a repair.
We have already covered placing resistors and capacitors in parallel and series:

Resistors in Parallel and/or Series
Capacitors in Parallel and/or Series

Here are some extras:

RESISTORS
Two 1k 0.5watt resistors in parallel produces a 470R 1watt resistor.
Two 1k 0.5watt resistors in series produces a 2k 1watt resistor.

CAPACITORS
Two 100n 100v capacitors in series produces a 50n capacitor @200v

INDUCTORS: Two inductors in series - **ADD THE VALUES**

DIODES: Two 1Amp 400v diodes in series produces a 1Amp 800v diode
Two 1Amp 400v diodes in parallel produces a 2Amp 400v diode

ZENER DIODES: Zener diodes can be connected in series to get a higher voltage.
Two 12v zener diodes in series produces a 24v zener.

CONTINUITY

Some multimeters have a "buzzer" that detects when the probes are touching each other or the resistance between the probes is very LOW. This is called a CONTINUITY TESTER.
You can use the resistance scale "x1" or "x10" to detect low values of resistance.
Set the pointer to "0" (right end of the scale) by touching the probes together and adjusting the "zero ohms" control.
When taking a reading, you will have to decide if a low value of resistance is a short-circuit or an "operating value."
For instance, the cold resistance of a 12v car globe is very low (about 2 ohms) and it increases (about 6 times) to 12 ohms when hot.
The "resistance of a circuit" may be very low as the electrolytics in the circuit are uncharged. This may not indicate a true "short-circuit."
The measurement across a diode is not a resistance-value but a "voltage-drop" and that is why the needle swings nearly full-scale.
Leads and wires and cords have a small resistance and depending on the length of the lead, this small resistance may be affecting a circuit.
Remember this:
When a circuit takes 1 amp, and the resistance of the leads is 1 ohm, the voltage drop across the leads will be 1v.
That's why a 12v battery supplying a circuit with these leads will have 11v at the circuit.
Note:
Turn off the equipment before making any continuity tests. The presence of even a small voltage (from an electrolytic) can give a false reading.
You can determine the resistance of a lead very accurately by taking the example above and applying it to your circuit.
If the battery is 12.6v and the voltage across the circuit is 10v, when the current is 2.6 amps, the resistance of the "leads" is 12.6 - 10 = 2.6 R=V/I = 2.6/2.6 = 1ohm. By making the lead shorter or using thicker wire, the resistance will be less and the voltage on the project will increase.
When taking readings in a circuit that has a number of diodes built-into IC's (Integrated Circuits) and transistors, some Continuity Testers will beep and give a false reading.
The following circuit has the advantage of providing a beep when a short-circuit is detected but does not detect the small voltage drop across a diode. This is ideal when testing logic circuits as it is quick and you can listen for the beep while

concentrating on the probe. Using a multimeter is much slower.

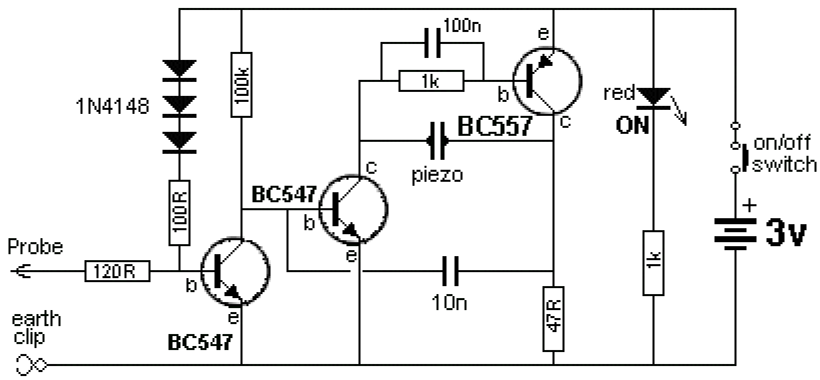

CONTINUITY TESTER

You can build the circuit on Matrix Board and add it to your Test Equipment.
You will need lots of "Test Equipment" and they can be built from circuits in this eBook.

TESTING FUSES, LEADS AND WIRES

All these components come under the heading TESTING for CONTINUITY. Turn off all power to the equipment before testing for shorts and continuity. Use the low resistance "Ohms Scale" or CONTINUITY range on your multimeter. All fuses, leads and wires should have a low, very low or zero resistance. This proves they are working.

A BLOWN FUSE

The appearance of a fuse after it has "blown" can tell you a lot about the fault in the circuit.
If the inside of the glass tube (of the fuse) is totally blackened, the fuse has been damaged very quickly. This indicates a very high current has passed through the fuse.
Depending on the rating of the fuse, (current rating) you will be able to look for components that can pass a high current when damaged - such as high power transistors, FETs, coils, electrolytics. Before re-connecting the supply, you should test the "SUPPLY RAILS" for resistance. This is done by measuring them on a low OHMs range in one direction then reverse the leads to see if the resistance is low in the other direction.
A reading can be very low at the start because electrolytics need time to charge-up and if the reading gradually increases, the power rail does not have a short. An overload can occur when the supply voltage rises to nearly full voltage, so you sometimes have to fit a fuse and see how long it takes to "blow."
If the fuse is just slightly damaged, you will need to read the next part of this eBook, to see how and why this happens:

FAST AND SLOW BLOW FUSES

There are many different sizes, shapes and ratings of a fuse. They are all current ratings as a fuse does not have a voltage rating. Some fuses are designed for cars as they fit into the special fuse holders. A fuse can be designed for 50mA, 100mA, 250mA, 315mA, 500mA, 1Amp, 1.5amp, 2amp, 3amp, 3.15amp 5amp, 10amp, 15amp, 20amp, 25amp, 30amp, 35amp, 50amp and higher.
Some fuses are fast-blow and some are slow-blow.
A "normal" fuse consists of a length of thin wire. Or it may be a loop of wire that is thin near the middle of the fuse. This is the section that will "burn-out."
A "normal" fuse is a fast-blow fuse. For instance, a 1amp fuse will remain intact when up to 1.25 amp flows. When a circuit is turned on, it may take 2-3 amps for a very short period of time and a normal 1 amp fuse will get very hot and the wire will stretch but not "burn-out." You can see the wire move when the supply turns on.
If the current increases to 2amps, the fuse will still remain intact. It needs about 3 amp to heat up the wire to red-hot and burn out.

If the current increases to 5 amp, the wire VOLATILISES (burns-out) and deposits carbon-black on the inside of the glass tube.
A slow-blow fuse uses a slightly thicker piece of wire and the fuse is made of two pieces of wire joined in the middle with a dob of low-temperature solder. Sometimes one of the pieces of wire is a spring and when the current rises to 2.5 amp, the heat generated in the wire melts the solder and the two pieces of wire "spring apart."
A slow-blow fuse will allow a higher current-surge to pass through the fuse and the wire will not heat up and sag.
Thus the fuse is not gradually being damaged and it will remain in a perfect state for a long period of time.
A fuse does not protect electronic equipment from failing. It acts AFTER the equipment has failed.
It will then protect a power supply from delivering a high current to a circuit that has failed.
If a slow-blow fuse has melted the solder, it could be due to a slight overload, slight weakening of the fuse over a period of time or the current-rating may be too low.
You can try another fuse to see what happens.
You can replace a fast-acting fuse (normal fuse) with a slow blow if the fast-acting fuse has been replaced a few times due to deterioration when the equipment is turned on.
But you cannot replace a slow-blow fuse with a fast acting fuse as it will be damaged slightly each time the equipment is turned on and eventually fail.

100mA FUSES

Fuses below about 100mA are very hard to make and very unreliable.
Many circuits take a high current when turned to charge the electrolytics and a 100mA (or 50mA or 63mA fuse) will bow and stretch and change shape, every time the equipment is turned ON.
Eventually it will break, due to it heating-up and stretching.
To produce a reliable fuse below 100mA, some manufacturers have placed a resistor inside the fuse and connected it to a spring. One end of the resistor is soldered to a wire with low-temperature metal and when the resistor gets hot, the metal softens and the spring pulls the resistor away from the wire.
Quite often you can heat up the metal and connect the wire and the fuse is perfect.
This type of fuse is called a DELAY fuse and the current rating is shown on the end-cap.
The value of the resistor determines the current rating.
There is a small voltage across this type of fuse and it means the circuit sees a slightly lower voltage than the supply voltage.
The third photo shows the pot of solder or low-temp metal and a wire connected to a spring. The heat generated in the wire is passed to the solder and it softens. The spring pulls the two components apart. You can smash the glass and set up the fuse in the two fuse-holders and repair the fuse while you wait for a new fuse to arrive.

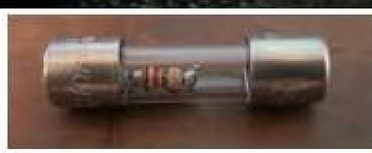

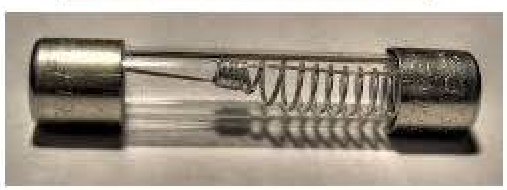

TESTING COILS, INDUCTORS and YOKES

Coils, inductors, chokes and yokes are just coils (turns) of wire. The wire may be wrapped around a core made of iron or ferrite.
It is labeled "L" on a circuit board.
You can test this component for continuity between the ends of the winding and also make sure there is no continuity between the winding and the core.
The winding can be less than one ohm, or greater than 100 ohms. A coil of wire is also called an INDUCTOR and it might look like a very simple component, but it can operate in a very complex way.
The way it works is a discussion for another eBook. It is important to understand the turns are insulated but a slight fracture in the insulation can cause two turns to touch each other and this is called a "SHORTED TURN" or you can say the inductor has "SHORTED TURNS."
When this happens, the inductor allows the circuit to draw MORE CURRENT. This causes the fuse to "blow."
The quickest way to check an inductor is to replace it, but if you want to measure the inductance, you can use an INDUCTANCE METER. You can then compare the inductance with a known good component.
An inductor with a shorted turn will have a very low or zero inductance, however you may not be able to detect the fault when it is not working in a circuit as the fault may be created by a high voltage generated between two of the turns.
Faulty yokes (both horizontal and vertical windings) can cause the picture to reduce in size and/or bend or produce a single horizontal line.
A TV or monitor screen is the best piece of Test Equipment as it has identified the fault. It is pointless trying to test the windings further as you will not be able to test them under full operating conditions. The fault may not show up when a low voltage (test voltage) is applied.

MEASURING AND TESTING INDUCTORS

Inductors are measured with an INDUCTANCE METER but the value of some inductors is very small and some Inductance Meters do not give an accurate reading. The solution is to measure a larger inductor and note the reading. Now put the two inductors in SERIES and the values ADD UP - just like resistors in SERIES. This way you can measure very small inductors. VERY CLEVER!

Question from a reader: *Can I add an inductor to stop a fuse blowing?*

Basically, an inductor NEVER prevents a fuse blowing because an inductor prevents spikes on one lead (we will call the INPUT lead), appearing on its other lead.
This is the detection and prevention of current that exists for a very short period of time.
A fuse detects an excess of current that occurs over a very long period of time and they are entirely two different "detectors."
One cannot assist the other in any way.

An inductor is basically a coil of wire. It may be thick or thin wire. The value of the inductor is a combination of the number of turns and the material on which the wire is wound.
The value of an inductor does not change over say a period of 20 years but it can go faulty by the enamel cracking and two turns touching. This can also be due to the difference in voltage between the two turns creating a spark between the turns and creating a "short."
When you test it, the high voltage is not present and it will test ok.
You may not think a few turns of wire will have any effect on improving a circuit, but spikes are very high frequency and the inductor will have a very big effect on reducing them.
An inductor (say 100uH) can be produced in many different sizes and the thickness of the wire will be important as it determines the current that can flow through the inductor.
The term "inductor" also includes those with two or more windings and these components are called TRANSFORMERS. These devices can get "shorts" and "leaks" between the windings and sparks can be seen between the windings. These sparks do not occur when you are testing them on test-equipment so the only way to

guarantee success is to replace it with an identical replacement.

TESTING SWITCHES and RELAYS

Switches and relays have contacts that open and close mechanically and you can test them for CONTINUITY. However these components can become intermittent due to dirt or pitting of the surface of the contacts due to arcing as the switch is opened.
It is best to test these items when the operating voltage and current is present as they quite often fail due to the arcing. A switch can work 49 times then fail on each 50th operation. The same with a relay. It can fail one time in 50 due to CONTACT WEAR.
If the contacts do not touch each other with a large amount of force and with a large amount of the metal touching, the current flowing through the contacts will create HEAT and this will damage the metal and sometimes reduce the pressure holding the contact together.
This causes more arcing and eventually the switch heats up and starts to burn. Switches are the biggest causes of fire in electrical equipment and households.

A relay also has a set of contacts that can cause problems.
There are many different types of relays and basically they can be put into two groups.
1. An electromagnetic relay is a switch operated by magnetic force. This force is generated by current through a coil. The relay opens and closes a set of contacts. The contacts allow a current to flow and this current can damage the contacts.
Connect 5v or 12v to the coil (or 24v) and listen for the "click" of the points closing. Measure the resistance across the points to see if they are closing.
You really need to put a load on the points to see if they are clean and can carry a current.
The coil will work in either direction.
If not, the relay is possibly a CMOS relay or Solid State relay.

2. An electronic relay (Solid State Relay) does not have a winding. It works on the principle of an opto-coupler and uses a LED and Light Activated SCR or Opto-TRIAC to produce a low resistance on the output. The two pins that energise the relay (the two input pins) must be connected to 5v (or 12v) around the correct way as the voltage is driving a LED (with series resistor). The LED illuminates and activates a light-sensitive device.

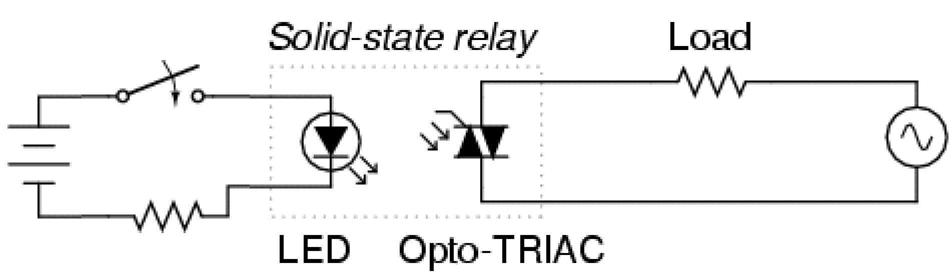

TESTING REED SWITCHES

A reed switch is generally contained in a long glass tube:

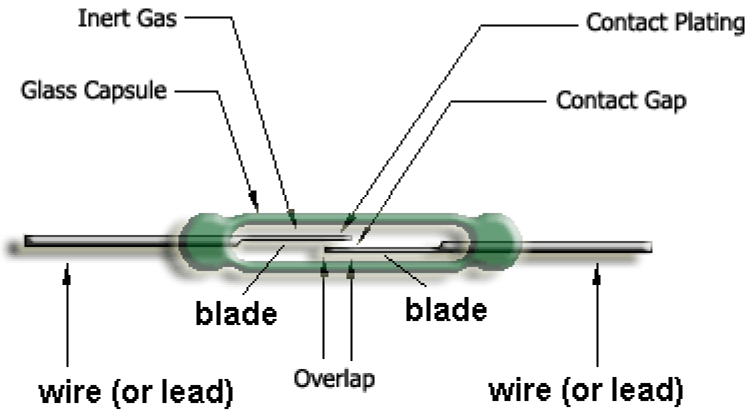

A wire or lead comes out each end for soldering to the reed switch to the project. The two "blades" inside the switch are made from a material that can be magnetised but does not retain its magnetism. This effect is called "temporally magnetised" (not permanently magnetised) and really only "passes" magnetism from one end to the other when in the presence of a magnet. One of the blades is made of a soft material and it will bend very easily. The other one is much stiffer.

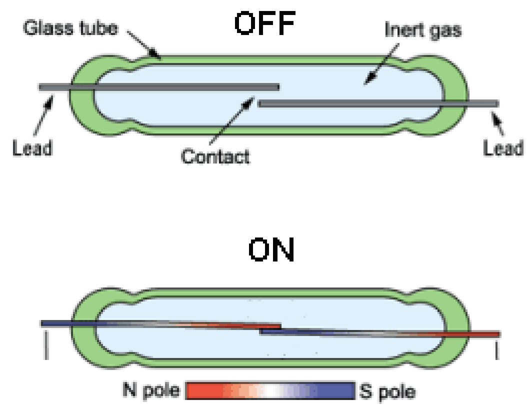

When a magnet is placed under the two blades (or on top), the magnetism from the magnet is passed to the two blades (INDUCTION or MUTUAL INDUCTION - commonly called INDUCED) and it produces a very weak magnet (in the blade) that is identical to the powerful magnet as far as the position of the north and south poles are concerned). Initially it produces a N-S and N-S set of poles and this makes the two blades click together because the top blade will be South at the contact and the bottom blade will be North.
When the two blades click together the magnetism runs through the two blades and keeps them together. The two blades attract and the switch is closed. When the magnet is removed, the magnetism in the two blades ceases and the two blades move apart.
Since there is a very small amount of movement in the top blade, this switch has a limited number of operations. Eventually it will fail. It is a mechanical device and is not suited for detecting a spinning shaft as 100,000 revolutions will very quickly weaken the switch.
If the switch does not make contact or remains closed, the moveable blade can be cracked or broken. This can be very hard to see. So replace the switch.

LATCHING REED SWITCH

A "normal" reed switch can be converted into a **LATCHING REED SWITCH** by carefully placing a magnet below the switch and moving it away so the two blades open. Now move it slightly closer but do not allow the blades to close.
This is called putting a "SET" on the switch and the two blades will have a small magnetic effect "induced" in them but not enough to close the contacts:

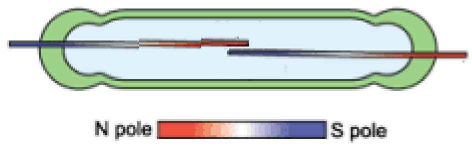

Now bring a strong magnet up to the reed switch on the other side of the glass tube with the north pole above the north of the lower magnet. This effect will increase the INDUCED MAGNETISM in the blades and close the contacts:

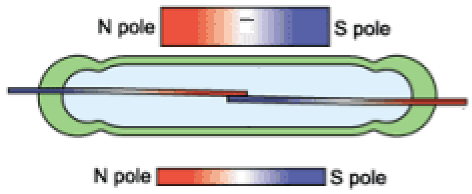

Remove the top magnet and the lower magnet will induce enough magnetism into the blades to keep them closed:

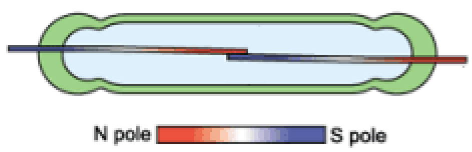

Now bring the upper magnet near the reed switch with the south pole above the north pole of the lower magnet. (In other words: AROUND THE OTHER WAY) This will have the effect of reducing the induced magnetism in the blades and a point will be reached when the two contacts will separate:

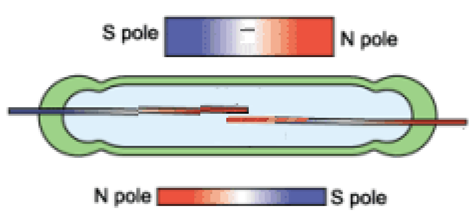

Remove the top magnet and the switch will remain separated because the lower magnet will not have sufficient influence on the blades to close the contact:

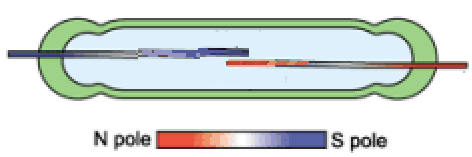

CAPACITORS

Capacitors are one of the most difficult things to test. That's because they don't give a reading on a multimeter and their value can range from 1p to 100,000u.
A faulty capacitor may be "open" when measured with a multimeter, and a good capacitor will also be "open."

You need a piece of test equipment called a CAPACITANCE METER to measure the value of a capacitor.

HOW A CAPACITOR WORKS

There are two ways to describe how a capacitor works. Both are correct and you have to combine them to get a full picture.
A capacitor has INFINITE resistance between one lead and the other.
This means no current flows **through** a capacitor. But it works in another way.
Suppose you have a strong magnet on one side of a door and a piece of metal on the other. By sliding the magnet up and down the door, the metal rises and falls.
The metal can be connected to a pump and you can pump water by sliding the magnet up and down.
A capacitor works in exactly the same way.
If you raise a voltage on one lead of a capacitor, the other lead will rise to the same voltage. This needs more explaining - we are keeping the discussion simple.
It works just like the magnetic field of the magnet through a door.
The next concept is this:
Capacitors are equivalent to a tiny rechargeable battery.
They store energy when the supply-voltage is present and release it when the supply drops.
These two concepts can be used in many ways and that's why capacitors perform tasks such as filtering, time-delays, passing a signal from one stage to another and create many different effects in a circuit.

CAPACITOR VALUES

The basic unit of capacitance is the FARAD. (C) This is the value used in all equations, but it is a very large value. A one FARAD capacitor would be the size of a car if made with plates and paper. Most electronic circuits use capacitors with smaller values such as 1p to 1,000u. 1p is about equal to two parallel wires 2cm long. 1p is one picofarad.

The easiest way to understand capacitor values is to start with a value of 1u. This is one microfarad and is one-millionth of a Farad. A 1 microfarad capacitor is about 1cm long and the diagram shows a 1u electrolytic.

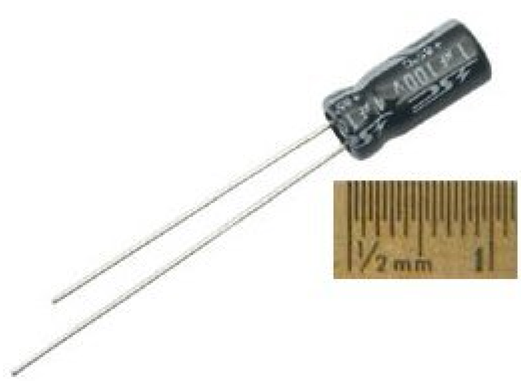

Smaller capacitors are ceramic and they look like the following. This is a 100n (0.1u)ceramic:

To read the value on a capacitor you need to know a few facts.

The basic value of capacitance is the FARAD.
1 microfarad is one millionth of 1 farad.
1 microfarad is divided into smaller parts called nanofarad.
1,000 nanofarad = 1 microfarad
Nanofarad is divided into small parts called picofarad
1,000 picofarad = 1 nanofarad.

Recapping:
1p = 1 picofarad.   1,000p = 1n (1 nanofarad)
1,000n = 1u (1 microfarad)
1,000u = 1millifarad
1,000,000u = 1 FARAD.

Examples:
All ceramic capacitors are marked in "p" (puff")
A ceramic with 22 is 22p = 22 picofarad
A ceramic with 47 is 47p = 47 picofarad
A ceramic with 470 is 470p = 470 picofarad
A ceramic with 471 is 470p = 470 picofarad
A ceramic with 102 is 1,000p = 1n
A ceramic with 223 is 22,000p = 22n
A ceramic with 104 is 100,000p = 100n = 0.1u

TYPES OF CAPACITOR
For testing purposes, there are two types of capacitor.
Capacitors from 1p to 100n are non-polar and can be inserted into a circuit around either way.
Capacitors from 1u to 100,000u are electrolytics and are polarised. They must be fitted so the positive lead goes to the supply voltage and the negative lead goes to ground (or earth).
There are many different sizes, shapes and types of capacitor. They are all the same. They consist of two plates with an insulating material between. The two plates can be stacked in layers or rolled together.
The important factor is the insulating material. It must be very thin to keep things small. This gives the capacitor its VOLTAGE RATING.
If a capacitor sees a voltage higher than its rating, the voltage will "jump through" the insulating material or around it.
If this happens, a carbon deposit is left behind and the capacitor becomes "leaky" or very low resistance, as carbon is conductive.

CERAMIC CAPACITORS

Nearly all small capacitors are **ceramic capacitors** as this material is cheap and the capacitor can be made in very thin layers to produced a high capacitance for the size of the component. This is especially true for surface-mount capacitors.
All capacitors are marked with a value and the basic unit is: "p" for "puff" However NO surface mount capacitors are marked and they are very difficult to test.

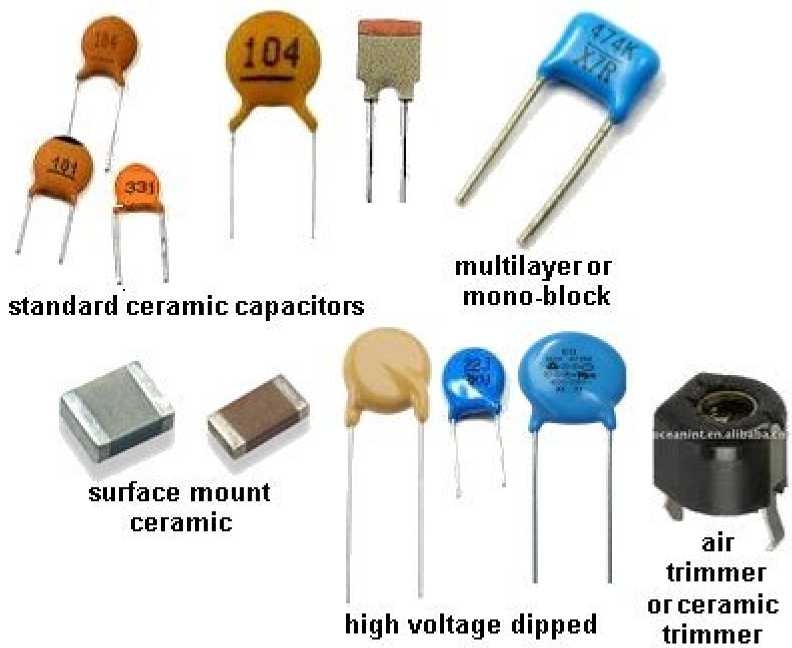

VALUE:	VALUE WRITTEN ON THE COMPONENT:
0.1p	0p1
0.22p	0p22
0.47p	0p47
1.0p	1p0
2.2p	2p2
4.7p	4p7
5.6p	5p6
8.2p	8p2
10p	10 or 10p
22p	22 or 22p
47p	47 or 47p
56p	56 or 56p
100p	100 on 101
220p	220 or 221
470p	470 or 471
560p	560 or 561
820p	820 or 821
1,000p (1n)	102
2200p (2n2)	222
4700p (4n7)	472
8200p (8n2)	822
10n	103
22n	223
47n	473
100n	104
220n	224
470n	474
1u	105

POLYESTER, POLYCARBONATE, POLYSTYRENE, MYLAR, METALLISED POLYESTER, ("POLY"), MICA and other types of CAPACITOR

There are many types of capacitor and they are chosen for their reliability, stability, temperate-range and cost.

For testing and repair work, they are all the same. Simply replace with exactly the same type and value.

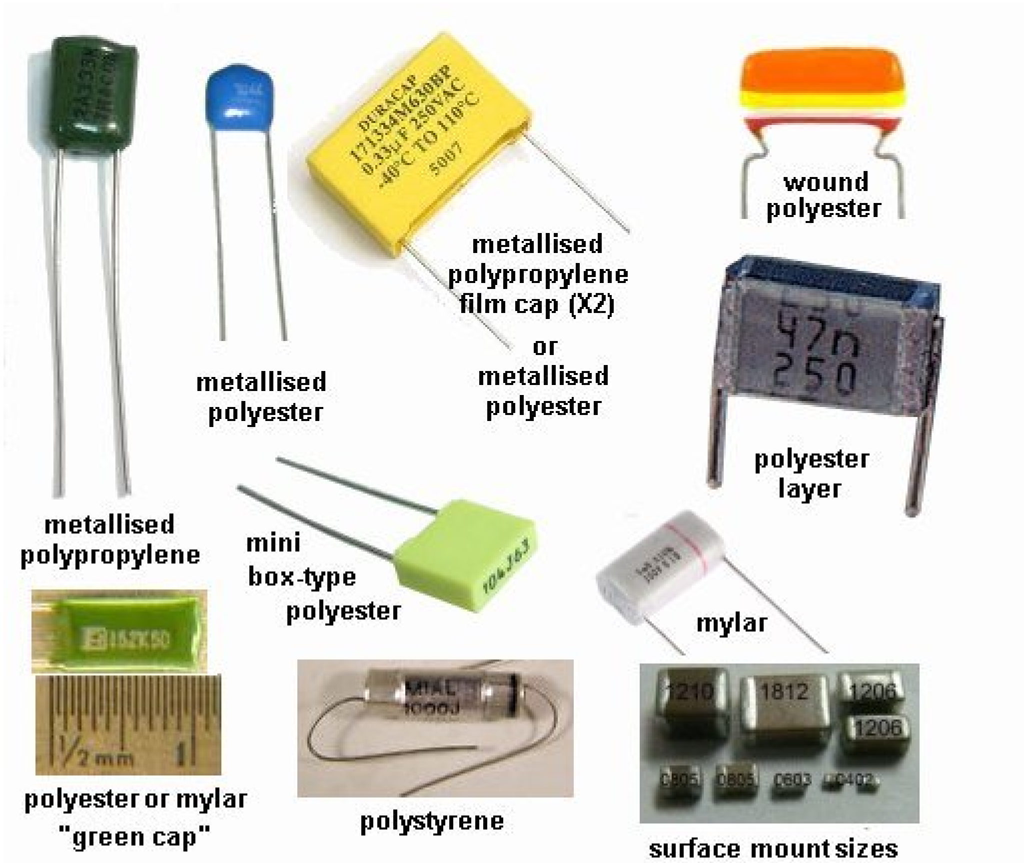

Capacitor Colour Code Table

Colour	Digit A	Digit B	Multiplier D	Tolerance (T) > 10pf	Tolerance (T) < 10pf	Temperature Coefficient (TC)
Black	0	0	x1	± 20%	± 2.0pF	
Brown	1	1	x10	± 1%	± 0.1pF	$-33x10^{-6}$
Red	2	2	x100	± 2%	± 0.25pF	$-75x10^{-6}$
Orange	3	3	x1,000	± 3%		$-150x10^{-6}$
Yellow	4	4	x10,000	± 4%		$-220x10^{-6}$
Green	5	5	x100,000	± 5%	± 0.5pF	$-330x10^{-6}$
Blue	6	6	x1,000,000			$-470x10^{-6}$
Violet	7	7				$-750x10^{-6}$
Grey	8	8	x0.01	+80%,-20%		
White	9	9	x0.1	± 10%	± 1.0pF	
Gold			x0.1	± 5%		

Silver			x0.01	± 10%		

Pico Farads (pF)	Nano Farads (nF)	Micro Farads (µF)
1	0.001	0.000001
10	0.01	0.00001
100	0.1	0.0001
1,000	1	0.001
10,000	10	0.01
100,000	100	0.1
1,000,000	1,000	1
10,000,000	10,000	10
100,000,000	100,000	100

Type ⊕ = polarized	Pic	Cap Range
Ceramic		pF - µF
Mica (silver mica)		pF - nF
Plastic Film (polyethylene polystyrene)		few µFs
Tantalum ⊕		µFs
OSCON ⊕		µFs
Aluminum Electrolytic ⊕		high µFs

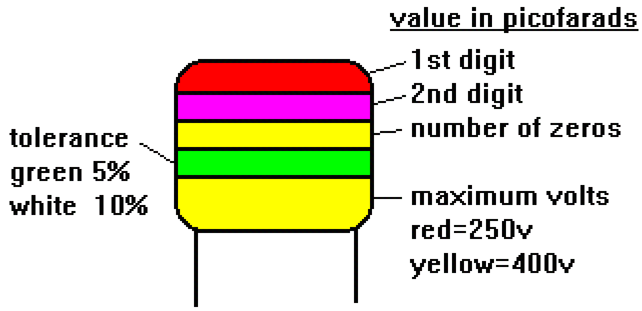

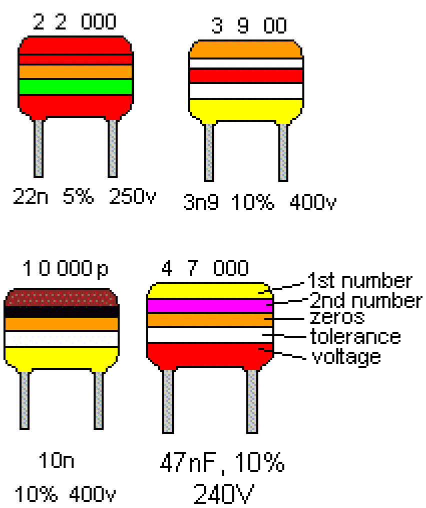

Black	0
Brown	1
Red	2
Orange	3
Yellow	4
Green	5
Blue	6
Violet	7
Grey	8
White	9

ELECTROLYTIC and TANTALUM CAPACITORS

Electrolytics and Tantalums are the same for testing purposes but their performance is slightly different in some circuits. A tantalum is smaller for the same rating as an electrolytic and has a better ability at delivering a current. They are available up to about 1,000u, at about 50v but their cost is much higher than an electrolytic.

Electrolytics are available in 1u, 2u2 3u3 4u7 10u, 22u, 47u, 100u, 220u, 330u, 470u, 1,000u, 2,200u, 3,300u, 4,700u, 10,000u and higher.
The "voltage" or "working voltage" can be: 3.3v, 10v, 16v, 25v, 63v, 100v, 200v and higher.
There is also another important factor that is rarely covered in text books. It is RIPPLE FACTOR.
This is the amount of current that can enter and leave an electrolytic. This current heats up the electrolytic and that is why some electrolytics are much larger than others, even though the capacitance and voltage-ratings are the same.
If you replace an electrolytic with a "miniature" version, it will heat up and have a very short life. This is especially important in power supplies where current (energy) is constantly entering and exiting the electrolytic as its main purpose is to provide a smooth output from a set of diodes that delivers "pulsing DC." (see "Power Diodes")

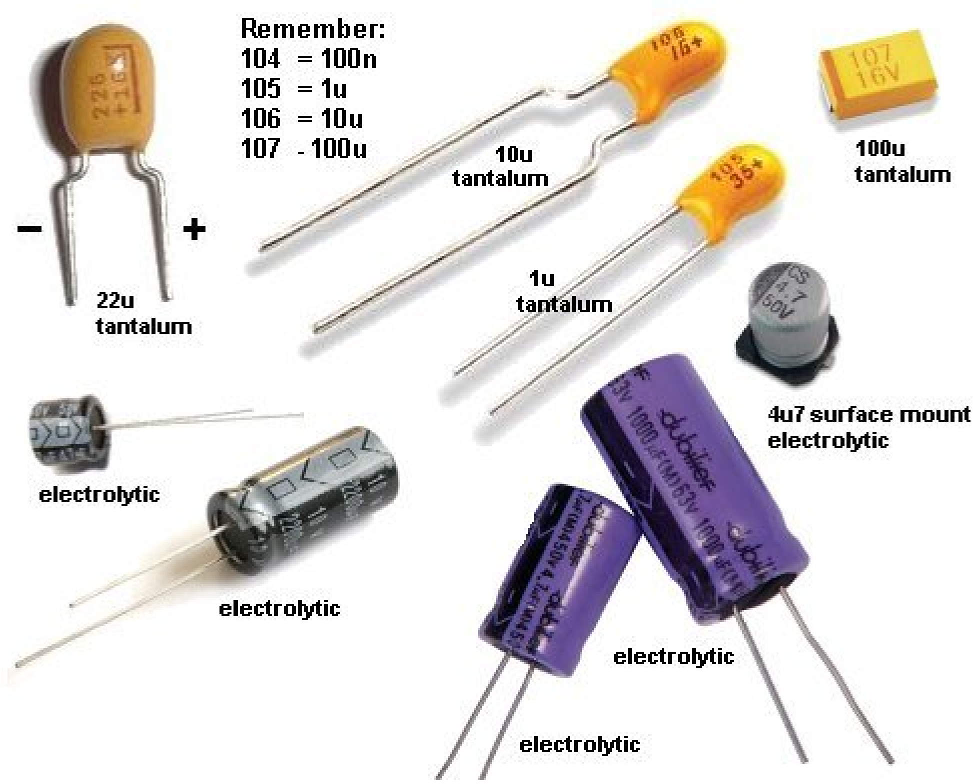

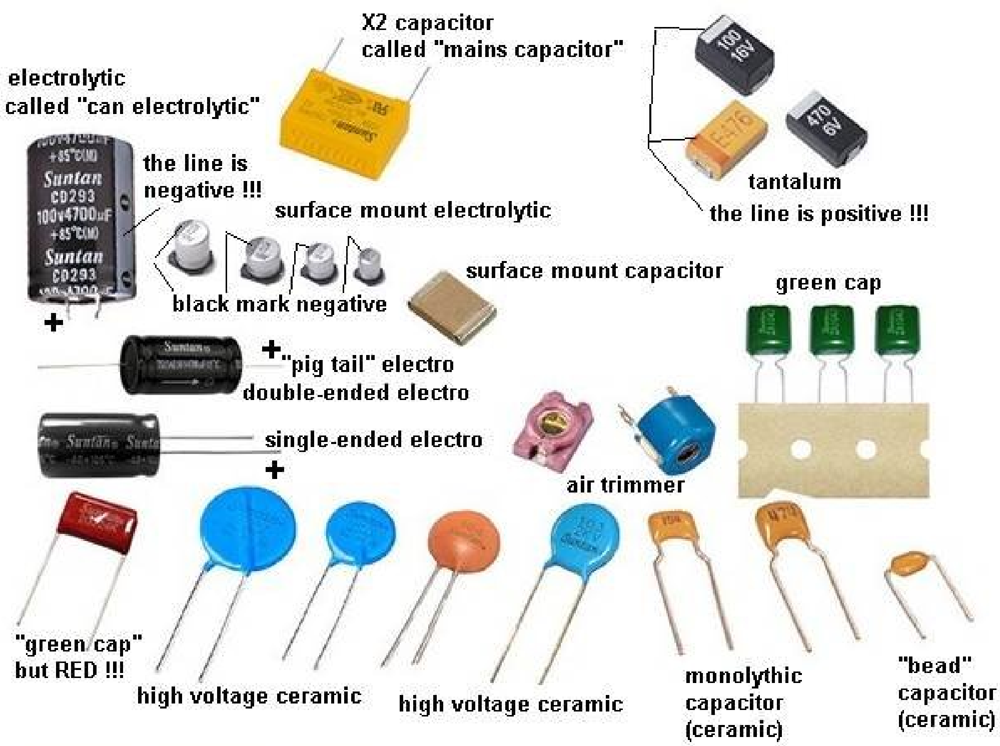

tantalum capacitors can
"go up in smoke"

"bead" tantalum

PARALLEL and SERIES CAPACITORS

Capacitors can be connected in PARALLEL and/or SERIES for a number of reasons.
1. If you do not have the exact value, two or more connected in parallel or series can produce the value you need.
2. Capacitors connected in series will produce one with a higher voltage rating.
3. Capacitors connected in parallel will produce a larger-value capacitance.

Here are examples of two equal capacitors connected in series or parallel and the results they produce:

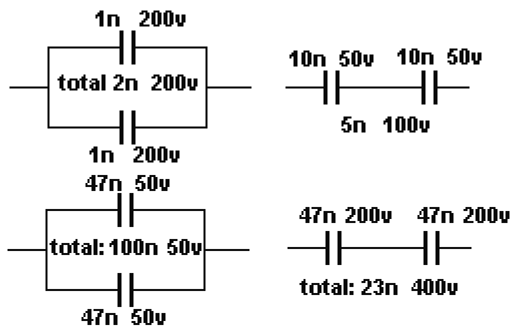

NON-POLAR CAPACITORS (ELECTROLYTICS)

Electrolytics are also available in non-polar values. It sometimes has the letters "NP" on the component. Sometimes the leads are not identified.
This is an electrolytic that does not have a positive and negative lead but two leads and either lead can be connected to the positive or negative of the circuit.
These electrolytics are usually connected to the output of an amplifier (such as in a filter near the speaker) where the signal is rising and falling.
A non-polar electrolytic can be created from two ordinary electrolytics by connecting the negative leads together and the two positive leads become the new leads.
For example: two 100u 63v electrolytics will produce a 47u 63v non-polar electrolytic.
In the circuit below, the non-polar capacitor is replaced with two electrolytics.

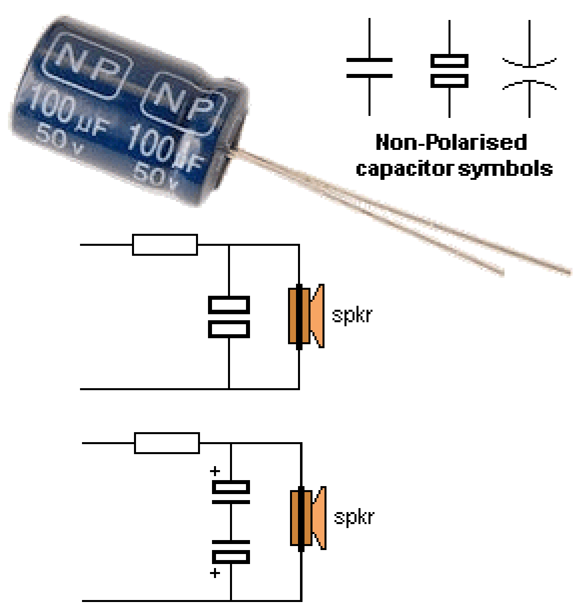

MAKING A NON-POLAR ELECTROLYTIC

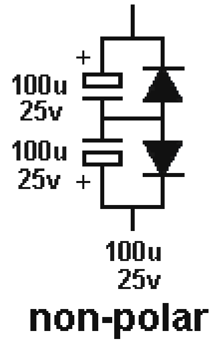

A normal electrolytic must be connected the correct way in a circuit because it has a thin insulating layer covering the plates that has a high resistance.
If you connect the electrolytic around the wrong way, this layer "breaks-down" and the resistance of the electrolytic becomes very small and a high current flows. This heats up the electrolytic and the current increases. Very soon the capacitor produces gasses and explodes.
One big mistake in many text books shows how to make a non-polar electrolytic by connecting two "back-to-back."
They claim 2 x 100u connected back-to-back is equal to 47u.
This appears to be case when testing on a meter but the meter simply charges them for a short period of time to get a reading.
If you allow them to charge fully you will find the reverse electrolytic has a very small voltage across it.
Secondly, when you are charging them, you are putting a high current through the reverse electrolytic and damaging the layer.
To prevent this, you need to add two diodes as shown in the diagram.
In addition, 2 x 100u "back-to-back" is very near 100u.

Here is a question from a reader:
I have an amplifier with 2 x2,200u electrolytics on the output of a bridge. Can I replace them with a single 10,000u?

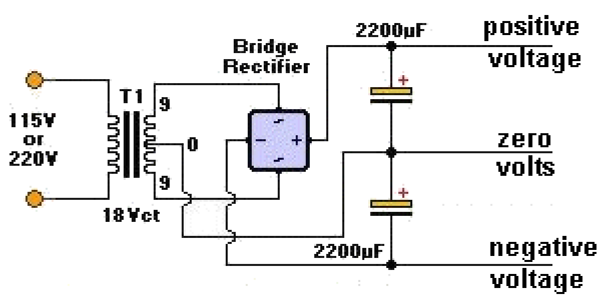

You need to look at the circuit of your amplifier. The two 2,200u electrolytics are possibly connected as shown in the circuit above and you will notice they are joined to produce a positive rail and a negative rail with zero (called earth) in the centre.
This forms two different circuits with the top electrolytic filtering the positive rail and the bottom electro filtering the negative rail. They must be connected to the zero volts rail.
A single 10,000u cannot be connected to the 0v rail and cannot be substituted for the two electro's.
You can easily determine of the two electro's are connected as shown above.
Test the positive terminal of each electro by placing the negative of the meter on the chassis.
If the positive of one electro have zero volts, it will be the lower electro in the diagram above. The negative terminal of the electro will have a minus voltage on it.

VOLTAGE RATING OF CAPACITOR
Capacitors have a voltage rating, stated as WV for working voltage, or WVDC. This specifies the maximum voltage that can be applied across the capacitor without puncturing the dielectric. Voltage ratings for "poly," mica and ceramic capacitors are typically 50v to 500 VDC. Ceramic capacitors with ratings of 1kv to 5kv are also available. Electrolytic capacitors are commonly available in 6v, 10v 16v, 25v, 50v, 100v, 150v, and 450v ratings.

THE SIZE OF A CAPACITOR - RIPPLE FACTOR
The size of a capacitor depends on a number of factors, namely the value of the capacitor (in microfarads etc) and the voltage rating. But there is also another factor that is most important. It is the RIPPLE FACTOR. **Ripple Factor** is the amount of voltage-fluctuation the capacitor (electrolytic) can withstand without getting too hot. When current flows in and out of an electrolytic, it gets hot and this will eventually dry-out the capacitor as some of the liquid inside the capacitor escapes through the seal. It's a very slow process but over a period of years, the capacitor looses its capacitance.
If you have two identical 1,000u 35v electrolytics and one is smaller, it will get hotter when operating in a circuit and that's why it is necessary to choose the largest electrolytic.

CAUTION
If a capacitor has a voltage rating of 63v, do not put it in a 100v circuit as the insulation (called the dielectric) will be punctured and the capacitor will "short-circuit." It's ok to replace a 0.22uF 50WV capacitor with 0.22uF 250WVDC.

SAFETY
A capacitor can store a charge for a period of time after the equipment is turned off. High voltage electrolytic caps can pose a safety hazard. These capacitors are in power supplies and some have a resistor across them, called a bleed resistor, to discharge the cap after power is switched off.
If a bleed resistor is not present the cap can retain a charge after the equipment is unplugged.

How to discharge a capacitor
Do not use a screwdriver to short between the terminals as this will damage the capacitor internally and the screwdriver.
Use a 1k 1 watt or 3watt or 5watt resistor on jumper leads (or held with pliers) and keep them connected for up to 15 seconds to fully discharge the electro.
Test it with a voltmeter to make sure all the energy has been removed.

Before testing any capacitors, especially electrolytics, you should look to see if any are damaged, overheated or leaking. Swelling at the top of an electrolytic indicates heating (and pressure inside the case) and will result in drying out of the electrolyte. Any hot or warm electrolytic indicates leakage and ceramic capacitors with portions missing indicates something has gone wrong (such as it being "blown apart").

Here is a 120u 330v electrolytic from a flash circuit in an old-fashioned film camera. If the flash does not "fire," the electrolytic will be charged to about 350 volts !!
Use a 1k resistor (held with pliers) to slowly discharge it. It may take 15 seconds to fully discharge.

TESTING A CAPACITOR
There are two things you can test with a multimeter:
1. A short-circuit within the capacitor
2. Capacitor values above 1u.

You can test capacitors in-circuit for short-circuits. Use the x1 ohms range.
To test a capacitor for leakage, you need to remove it or at least one lead must be removed. Use the x10k range on an analogue or digital multimeter.
For values above 1u you can determine if the capacitor is charging by using an analogue meter. The needle will initially move across the scale to indicate the cap is charging, then go to "no deflection." Any permanent deflection of the needle will indicate leakage.
You can reverse the probes to see if the needle moves in the opposite direction. This indicates it has been charged. Values below 1u will not respond to charging and the needle will not deflect.
This does not work with a digital meter as the resistance range does not output any current and the electrolytic does not charge.

Rather than spending money on a capacitance meter, it is cheaper to replace any suspect capacitor or electrolytic.
Capacitors can produce very unusual faults and no piece of test equipment is going to detect the problem.
In most cases, it is a simple matter to solder another capacitor across the suspect component and view or listen to the result.
This saves all the worry of removing the component and testing it with equipment that cannot possibly give you an accurate reading when the full voltage and current is not present.
It is complete madness to even think of testing critical components such as capacitors, with TEST EQUIPMENT. You are fooling yourself. If the Test Equipment says the component is ok, you will look somewhere else and waste a lot of time.

FINDING THE VALUE OF A CAPACITOR

If you want to find the value of a surface-mount capacitor or one where the markings have been removed, you will need a CAPACITANCE METER. Here is a simple circuit that can be added to your meter to read capacitor values from 10p to 10u.
The full article can be found HERE.

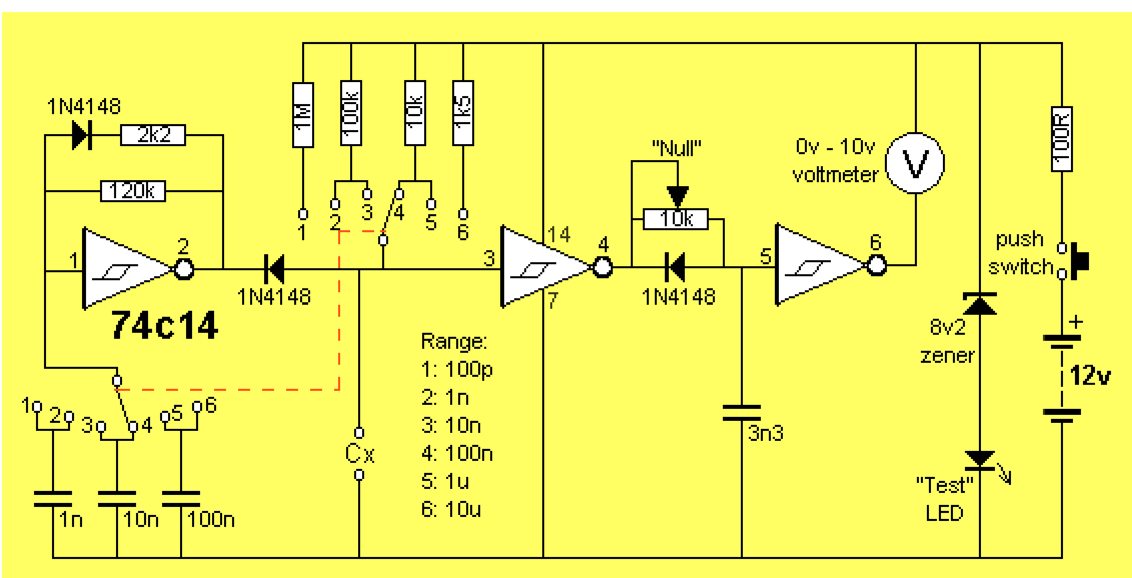

ADD-ON CAPACITANCE METER

CAPACITOR SUBSTITUTION BOX

You can get a kit or a ready-made piece of test gear called **CAPACITOR SUBSTITUTION BOX** and also **RESISTOR SUBSTITUTION BOX**.
I bought one of each 30 years ago and I have only used them ONCE.
They appear to be very handy but when you are testing a circuit, you want the component next to the other parts.
It is just as easy to pick the component you need from your junk box and connect it to the circuit via jumper leads.

REPLACING A CAPACITOR

Always replace a capacitor with the exact same type.
A capacitor may be slightly important in a circuit or it might be extremely critical.
A manufacturer may have taken years to select the right type of capacitor due to previous failures.
A capacitor just doesn't have a "value of capacitance."
It may also has an effect called "tightening of the rails."
In other words, a capacitor has the ability to react quickly and either absorb or deliver energy to prevent spikes or fluctuations on the rail.
This is due to the way it is constructed. Some capacitors are simply plates of metal film while others are wound in a coil. Some capacitors are large while others are small.
They all react differently when the voltage fluctuates.
Not only this, but some capacitors are very stable and all these features go into the decision for the type of capacitor to use.
You can completely destroy the operation of a circuit by selecting the wrong type of capacitor.
No capacitor is perfect and when it gets charged or discharged, it appears to have a small value of resistance in series with the value of capacitance. This is known as "ESR" and stands for EQUIVALENT SERIES RESISTANCE. This effectively makes the capacitor slightly slower to charge and discharge.
We cannot go into the theory on selecting a capacitor as it would be larger than this eBook so the only solution is to replace a capacitor with an identical type.
However if you get more than one repair with identical faults, you should ask other technicians if the original capacitor comes from a faulty batch.
The author has fixed TV's and fax machines where the capacitors have been inferior and alternate types have solved the problem.
Some capacitor are suitable for high frequencies, others for low frequencies.

DECOUPLING CAPACITORS

A Decoupling Capacitor can severe one, two or three functions. You need to think of a decoupling capacitor as a miniature battery with the ability to deliver a brief pulse of energy when ever the line-voltage drops and also absorb a brief pulse of energy when ever the line voltage rises (or spikes).
Decoupling capacitor can range from 100n to 1,000u.
100n capacitors are designed to absorb spikes and also have the effect of tightening-

up the rails for high frequencies. They have no effect on low frequencies such as audio frequencies.
These capacitors are generally ceramic and have very low internal impedance and thus they can operate at high frequencies.
Capacitors above about 10u are used for decoupling and these are nearly always electrolytics.
Decoupling means "tightening-up the power rails." The electrolytic acts just like a miniature rechargeable battery, supplying a small number of components in a circuit with a smooth and stable voltage.
The electrolytic is usually fed from a dropper resistor and this resistor charges the electrolytic and adds to the ability of the electrolytic to create a "separate power supply."
These two components help remove spikes as an electrolytic cannot remove spikes if connected directly to the supply rails - it's internal impedance is high and the spikes are not absorbed.
Decoupling capacitors are very difficult to test.
They rarely fail but if a project is suffering from unknown glitches and spikes, it is best to simply add more 100n decoupling caps on the underside of the board and replace all electrolytics.
Some small electrolytics will dry out due to faulty manufacture and simply replacing every one on a board will solve the problem.
Some of the functions of a decoupling capacitor are:
Removing ripple - hum or buzz in the background of an amplifier
Removing glitches or spikes.
Separating one stage from another to reduce or remove MOTORBOATING - a low frequency sound due to the output putting a pulse on the power rails that is picked up by the pre-amplifier section and amplified.

TESTING DIODES

Diodes can have 4 different faults.
1. Open circuit in both directions.
2. Low resistance in both directions.
3. Leaky.
4. Breakdown under load.

TESTING A DIODE ON AN ANALOGUE METER

Testing a diode with an **Analogue Multimeter** can be done on any of the resistance ranges. [The high resistance range is best - it sometimes has a high voltage battery for this range but this does not affect our testing]
There are two things you must remember.
1. When the diode is measured in one direction, the needle will **not move at all**. The technical term for this is the diode is **reverse biased**. It will not allow any current to flow. Thus the needle will not move.
When the diode is connected around the other way, the needle will swing to the right (move up scale) to about 80% of the scale. This position represents the voltage drop across the junction of the diode and is NOT a resistance value. If you change the resistance range, the needle will move to a slightly different position due to the resistances inside the meter. The technical term for this is the diode is **forward biased**. This indicates the diode is not faulty.
The needle will swing to a slightly different position for a "normal diode" compared to a Schottky diode. This is due to the different junction voltage drops.
However we are only testing the diode at very low voltage and it may break-down when fitted to a circuit due to a higher voltage being present or due to a high current flowing.

2. The leads of an **Analogue Multimeter** have the positive of the battery connected to the black probe and the readings of a "good diode" are shown in the following two diagrams:

The diode is REVERSE BIASED in the diagram above and diodes not conduct.

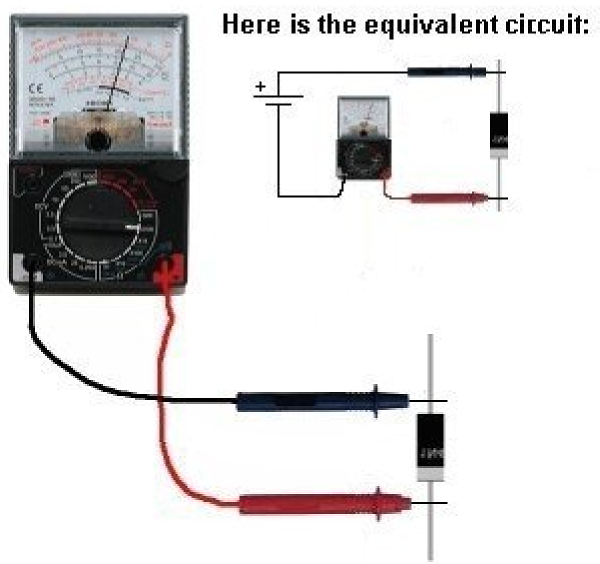

The diode is FORWARD BIASED in the diagram above and it conducts

TESTING A DIODE ON A DIGITAL METER

Testing a diode with a Digital Meter must be done on the "DIODE" setting as a digital meter does not deliver a current through the probes on some of the resistance settings and will not produce an accurate reading.

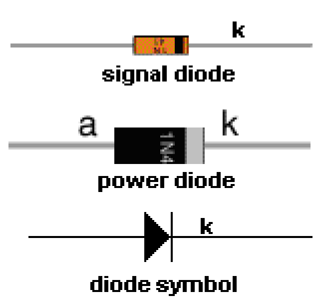

The best thing to do with a "suspect" diode is to replace it. This is because a diode has a number of characteristics that cannot be tested with simple equipment. Some diodes have a fast recovery for use in high frequency circuits. They conduct very quickly and turn off very quickly so the waveform is processed accurately and

efficiently.
If the diode is replaced with an ordinary diode, it will heat up as does not have the high-speed characteristic.
Other diodes have a low drop across them and if an ordinary is used, it will heat up.
Most diodes fail by going: SHORT-CIRCUIT. This can be detected by a low resistance (x1 or x10 Ohms range) in both directions.
A diode can also go OPEN CIRCUIT. To locate this fault, place an identical diode across the diode being tested.
A leaky diode can be detected by a low reading in one direction and a slight reading the other direction.
However this type of fault can only be detected when the circuit is working. The output of the circuit will be low and sometimes the diode heats up (more than normal).
A diode can go open under full load conditions and perform intermittently.
Diodes come in pairs in surface-mount packages and 4 diodes can be found in a bridge.
They are also available in pairs that look like a 3-leaded transistor.
The line on the end of the body of a diode indicates the cathode and you cannot say "this is the positive lead." The correct way to describe the leads is to say the "cathode lead." The other lead is the anode. The cathode is defined as the electrode (or lead) through which an electric current flows out of a device.
The following diagrams show different types of diodes:

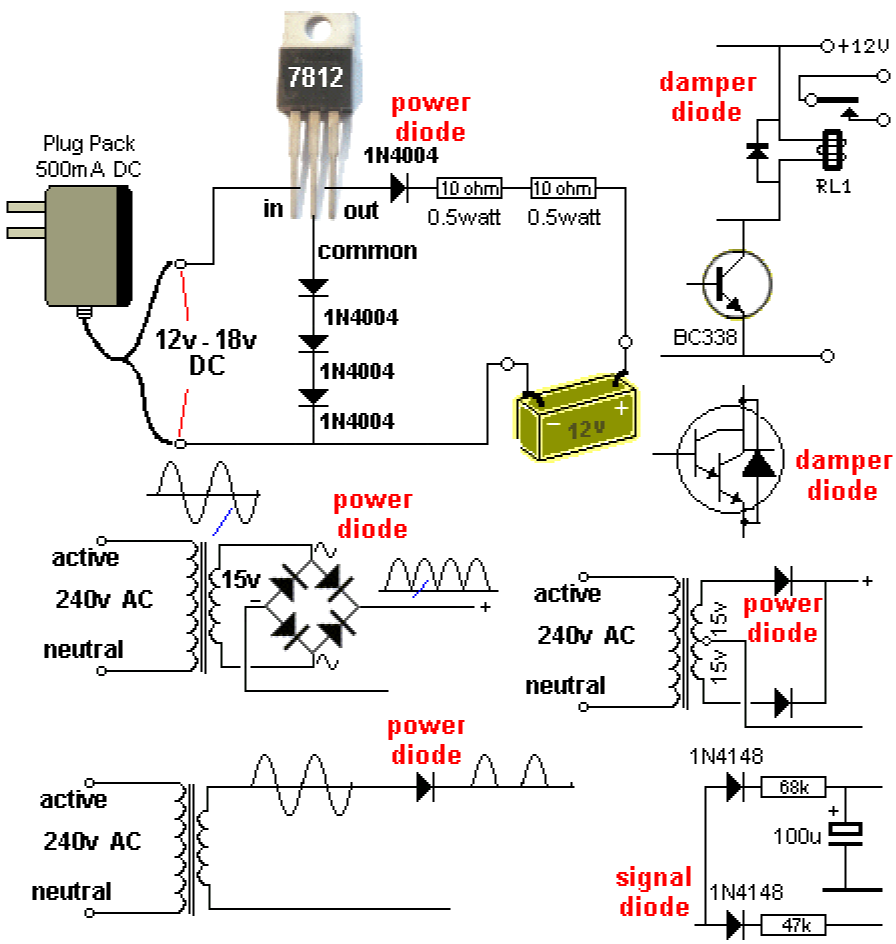

POWER DIODES

To understand how a power diode works, we need to describe a few things. This has NEVER been described before, so read carefully.
The 240v AC (called the "mains") consists of two wires, one is called the ACTIVE and the other is NEUTRAL. Suppose you touch both wires. You will get a shock. The neutral is connected to an earth wire (or rod driven into the ground or connected to a water pipe) at the point where the electricity enters the premises and you do not get a shock from the NEUTRAL.

But the voltage on the active is rising to +345v then goes to -345v at the rate of 50 times per second (for a complete cycle).
345v is the peak voltage of 240v. You never get a 240v shock. (It is a 345v shock.) In other words, if you touch the two wires at a particular instant, you would get a POSITIVE 345v shock and at another instant you would get a negative 345v shock. This is shown in the diagram below.
We now transfer this concept to the output of a transformer. The diagram shows an AC waveform on the output of the secondary.
This voltage is rising 15v higher than the bottom lead then it is 15v LOWER than the bottom lead. The bottom lead is called "zero volts." You have to say one lead or wire is not "rising and falling" as you need a "reference" or starting-point" or "zero point" for voltage measurements.
The diode only conducts when the voltage is "above zero" (actually when it is 0.7v above zero) and does not conduct (at all) when the voltage goes below zero.
This is shown on the output of the Power Diode. Only the positive peaks or the positive parts of the waveform appear on the output and this is called "pulsing DC." This is called "half-wave" and is not used in a power supply. We have used it to describe how the diode works. The electrolytics charge during the peaks and deliver energy when the diode is not delivering current. This is how the output becomes a steady DC voltage.
Power supplies use FULL WAVE rectification and the other half of the AC waveform is delivered to the output (and fills in the "gaps") and appears as shown in "A."

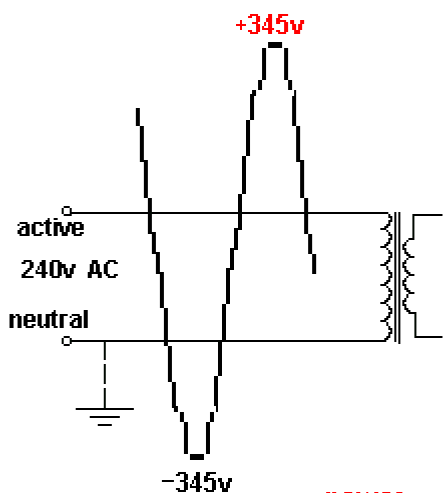

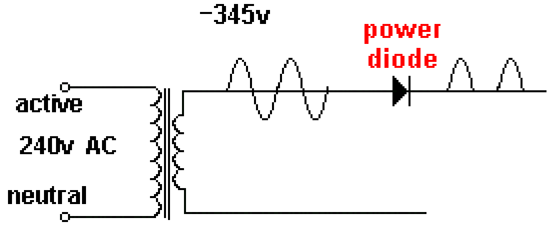

Half-wave rectifier

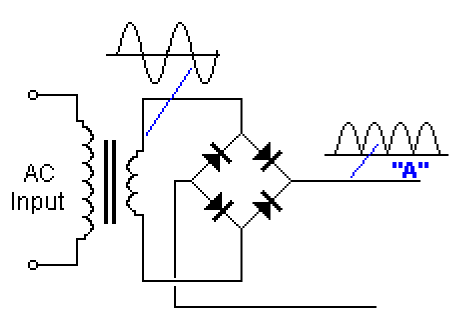

Full-wave rectifier

ONE FAULTY DIODE

One diode in a bridge can go open (any of the 4 diodes will produce the same effect) and produce an output voltage that can be slightly lower than the original voltage.

The actual "voltage-drop" will depend on the current taken by the circuit and the ability of the transformer to produce the required voltage and current during half-wave operation. The voltage during each half cycle (when none of the diodes is delivering any energy to the circuit) is maintained by the electrolytic and its size (relative to the current taken by the circuit) will determine the size of the ripple that will result when the diode fails. The ripple will be 100 to 1,000 times greater after the failure of a diode, depending on the value of the filter capacitor.
To locate the faulty diode, simply get a diode and place it across each of the diodes in the bridge (in turn) when the circuit is working.
For a bridge rectifier, the ripple-frequency will be twice the mains frequency and its ripple will be very small if the electrolytic is the correct value. When a diode fails, the ripple-frequency will be equal to mains-frequency and the amplitude will increase considerably. You may even hear background hum from audio equipment.
If you cannot find a faulty diode, the filter capacitor will be at fault. Turn off the equipment and connect an electrolytic across the filter capacitor via jumper leads. Turn the power ON and see if the hum has reduced.

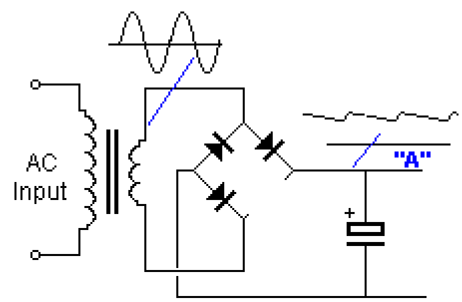

One diode "burnt-out"

DAMPER DIODES

A damper diode is a diode that detects a high voltage and SQUELCHES IT (reduces it - removes it). The signal that it squelches is a voltage that is in the opposite direction to the "supply voltage" and is produced by the collapsing of a magnetic field. Whenever a magnetic filed collapses, it produces a voltage in the winding that is opposite to the supply voltage and can be much higher. This is the principle of a flyback circuit or EHT circuit. The high voltage comes from the transformer.
The diode is placed so that the signal passes through it and less than 0.5v appears across it.
A damper diode can be placed across the coil of a relay, incorporated into a transistor or FET or placed across a winding of a flyback transformer to protect the driving transistor or FET.
It can also be called a "Reverse-Voltage Protection Diode," "Spike Suppression Diode," or "Voltage Clamp Diode."
The main characteristic of a Damper Diode is HIGH SPEED so it can detect the spike and absorb the energy.
It does not have to be a high-voltage diode as the high voltage in the circuit is being absorbed by the diode.

SILICON, GERMANIUM AND SCHOTTKY DIODES

When testing a diode with an analogue meter, you will get a low reading in one direction and a high (or NO READING) in the other direction. When reading in the LOW direction, the needle will swing nearly full scale and the reading is not a resistance-value but a reflection of the characteristic voltage drop across the junction of the diode. As we mentioned before, a resistance reading is really a voltage reading and the meter is measuring the voltage of the battery minus the voltage-drop across the diode.
Since Silicon, Germanium and Schottky Diodes have slightly different characteristic voltage drops across the junction, you will get a slightly different reading on the scale. This does not represent one diode being better than the other or capable of handling a higher current or any other feature.
The quickest, easiest and cheapest way to find, fix and solve a problem caused by a

faulty diode is to replace it.
There is no piece of test equipment capable of testing a diode fully, and the circuit you are working on is actually the best piece of test equipment as it is identifying the fault UNDER LOAD.

Only very simple tests can be done with a multimeter and it is best to check a diode with an ANALOGUE MULTIMETER as it outputs a higher current though the diode and produces a more-reliable result.
A Digital meter can produce false readings as it does not apply enough current to activate the junction.
Fortunately almost every digital multimeter has a **diode test mode.** Using this, a silicon diode should read a voltage drop between 0.5v to 0.8v in the forward direction and open in the reverse direction. For a germanium diode, the reading will be lower, around 0.2v - 0.4v in the forward direction. A bad diode will read zero volts in both directions.

REPLACING A DIODE

It is alway best to replace a diode with the same type but quite often this is not possible. Many diodes have unusual markings or colours or "in-house" letters.
This is only a general guide because many diodes have special features, especially when used in high-frequency circuits.
However if you are desperate to get a piece of equipment working, here are the steps:
Determine if the diode is a signal diode, power diode, or zener diode.
For a signal diode, try 1N4148.
For a power diode (1 amp) try 1N4004. (for up to 400v)
For a power diode (3 amp) try 1N5404. (for up to 400v)
For a high-speed diode, try UF4004 (for up to 400v)

If you put an ordinary diode in a high-speed application, it will get very hot very quickly.
To replace an unknown zener diode, start with a low voltage such as 6v2 and see if the circuit works.
The size of a diode and the thickness of the leads will give an idea of the current-capability of the diode.
Keep the leads short as the PC board acts as a heat-sink.
You can also add fins to the leads to keep the diode cool.

LIGHT EMITTING DIODES (LEDs)

Light Emitting Diodes (LEDs) are diodes that produce light when current flows from anode to cathode. The LED does not emit light when it is revered-biased. It is used as a low current indicator in many types of consumer and industrial equipment, such as monitors, TV’s, printers, hi-fi systems, machinery and control panels.
The light produced by a LED can be visible, such as red, green, yellow or white. It can also be invisible and these LEDs are called Infrared LEDs. They are used in remote controls and to see if they are working, you need to point a digital camera at the LED and view the picture on the camera screen.
An LED needs about 2v - 3.6v across its leads to make it emit light, but this voltage must be exact for the type and colour of the LED. The simplest way to deliver the exact voltage is to have a supply that is higher than needed and include a voltage-dropping resistor. The value of the resistor must be selected so the current is between 2mA and 25mA.
The cathode of the LED is identified by a flat on the side of the LED. The life expectancy of a LED is about 100,000 hours. LEDs rarely fail but they are very sensitive to heat and they must be soldered and de-soldered quickly. They are one of the most heat-sensitive components.
Light emitting diodes cannot be tested with most multimeters because the characteristic voltage across them is higher than the voltage of the battery in the meter.
However a simple tester can be made by joining 3 cells together with a 220R resistor

and 2 alligator clips:

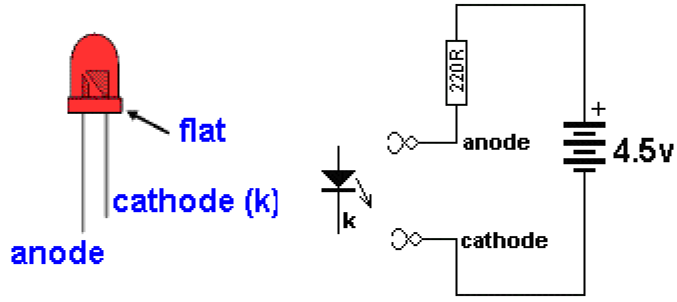

LED TESTER

Connect the clips to a LED and it will illuminate in only one direction.
The colour of the LED will determine the voltage across it. You can measure this voltage if you want to match two or more LEDs for identical operation.
Red LEDs are generally 1.7v to 1.9v. - depending on the quality such as "high-bright"
Green LEDs are 1.9v to 2.3v.
Orange LEDs are about 2.3v and
White LEDs and IR LEDs are about 3.3v to 3.6v.
The illumination produced by a LED is determined by the quality of the crystal. It is the crystal that produces the colour and you need to replace a LED with the same quality to achieve the same illumination.
Never connect a LED across a battery (such as 6v or 9v), as it will be instantly damaged. You must have a resistor in series with the LED to limit the current.

ZENER DIODES

All diodes are Zener diodes. For instance a 1N4148 is a 120v zener diode as this is its reverse breakdown voltage.
And a zener diode can be used as an ordinary diode in a circuit with a voltage that is below the zener value.
For instance, 20v zener diodes can be used in a 12v power supply as the voltage never reaches 20v, and the zener characteristic is never reached.
Most diodes have a reverse breakdown voltage above 100v, while most zeners are below 70v. A 24v zener can be created by using two 12v zeners in series and a normal diode has a characteristic voltage of 0.7v. This can be used to increase the voltage of a zener diode by 0.7v. See the diagram above. It uses 3 ordinary diodes to increase the output voltage of a 3-terminal regulator by 2.1v.
To tests a zener diode you need a power supply about 10v higher than the zener of the diode. Connect the zener across the supply with a 1k to 4k7 resistor and measure the voltage across the diode. If it measures less than 1v, reverse the zener.
If the reading is high or low in both directions, the zener is damaged.

Here is a zener diode tester. The circuit will test up to 56v zeners.

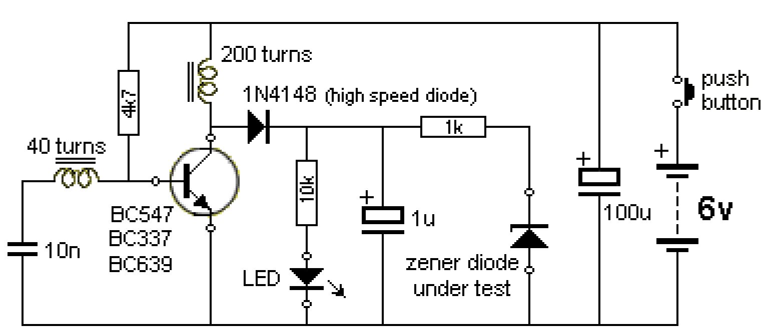

ZENER DIODE TESTER

TRANSFORMERLESS POWER SUPPLY
Here's a circuit that uses zener diodes in a power supply to show how they work.
This clever design uses 4 diodes in a bridge to produce a fixed voltage power supply capable of supplying 35mA.
If we put 2 zener diodes in a bridge with two ordinary power diodes, the bridge will break-down at the voltage of the zener. This is what we have done. If we use 18v zeners, the output will be 17v4.

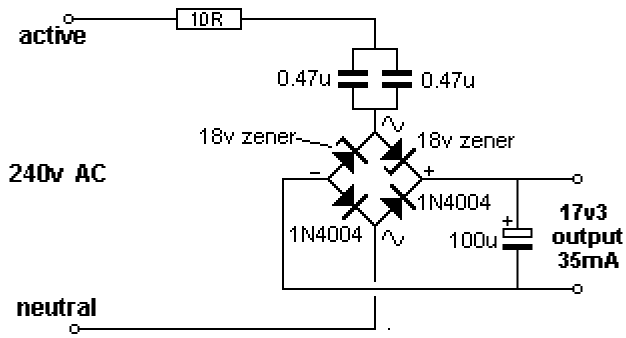

SUPPLY USING ZENER DIODES

When the incoming voltage is positive at the top, the left zener provides 18v limit (and the other zener produces a drop of 0.6v). This allows the right zener to pass current just like a normal diode. The output is 17v4. The same with the other half-cycle.
You cannot use this type of bridge in a normal power supply as the zener diode will "short" when the input voltage reaches the zener value. The concept only works in the circuit above.

VOLTAGE REGULATORS
A Voltage Regulator takes a high input voltage and delivers a fixed output voltage. Providing the input voltage is 4v above the output voltage, the regulator will deliver a fixed output voltage with almost no ripple.
Voltage regulators are also called "3-TERMINAL REGULATORS" or "REGULATOR IC's" - although this name is not generally used.
In most cases, a voltage regulator gets quite hot and for this reason it has a high failure-rate.
If a regulator is not getting hot (or warm) it has either failed or the circuit is not operating.
A regulator can only decrease the voltage. It cannot increase the current. This means the current being supplied to a circuit must also be available from the circuit supplying the regulator.
All regulators have different pin-outs, so you need to find the input pin and output pin and make sure the voltage-difference is at least 4v. Some regulators will work with a difference as low as 1v, so you need to read the specifications for the type you are servicing.
Some regulators are called "negative voltage regulators" and the input voltage will be negative and the output will be negative.
You need to test a voltage regulator with the power "ON".
Make sure you do not allow the probes to short any of the pins together as this will destroy the regulator or the circuit being supplied.
With the power turned off or the regulator removed from the circuit, you can test it with a multimeter set to resistance to see if it is ok. If any resistance readings are very low or zero ohms, the regulator is damaged.

TRANSFORMERS
All transformers and coils are tested the same way. This includes chokes, coils,

inductors, yokes, power transformers, EHT transformers (flyback transformers), switch mode transformers, isolation transformers, IF transformers, baluns, and any device that has turns of wire around a former. All these devices can go faulty.
The coating on the wire is called insulation or "enamel" and this can crack or become overheated or damaged due to vibration or movement. When two turns touch each other, a very interesting thing happens. **The winding becomes two separate windings.**

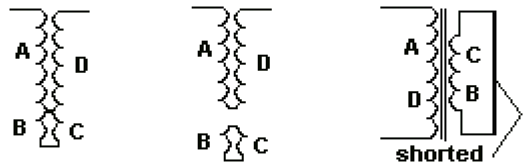

We will take the case of a single winding such as a coil. This is shown in the first diagram above and the winding is wound across a former (a former is a bobbin or plastic molding or something to hold the winding) and back again, making two layers. The bottom and top layers touch at the point shown in the diagram and the current that originally passed though A, B, C, D now passes though A & D.

Winding B C becomes a separate winding as shown in the second diagram.
In other words the coil becomes a TRANSFORMER with a SHORT CIRCUIT on the secondary winding as shown in the third diagram.
When the output wires of a transformer are shorted together, it delivers a very high current because you have created a SHORT-CIRCUIT. This short-circuit causes the transformer to get very hot.
That’s exactly what happens when any coil or transformer gets a “shorted turn.”
The shorted turns can be a single turn or many turns.
It is not possible to measure a fault like this with a multimeter as you don’t know the exact resistance of a working coil or winding and the resistance of a faulty winding may be only 0.001 ohms less.
However when a transformer or coil is measured with an inductance meter, an oscillating voltage (or spike) is delivered into the core as magnetic flux, then the magnetic flux collapses and passes the energy into the winding to produce a waveform. The inductance meter reads this and produces a value of inductance in Henry (or milliHenry or microHenry.)
This is done with the transformer removed from the circuit and this can be a very difficult thing to do, as most transformers have a number of connections.
If the coil or transformer has a shorted turn, the energy from the magnetic flux will pass into the turns that are shorted and produce a current. Almost no voltage will be detected from winding.
The reading from the inductance meter will be low or very low and you have to work out if it is correct.
However there is one major problem with measuring a faulty transformer or coil.
It may only become faulty when power is applied.
The voltage between the turns may be sparking or jumping a gap and creating a problem. A tester is not going to find this fault.
Secondly, an inductance meter may produce a reading but you do not know if the reading is correct. An improved tester is a RING TESTER.
The circuit for a ring tester can be found here:

http://www.flippers.com/pdfs/k7205.pdf

It sends a pulse to the coil and counts the number of returning pulses or "rings." A faulty coil (or winding) may return one pulse but nearly all the energy will be passed to the shorted turns and you will be able to see this on the scale. You will only get one or two return pulses, whereas a good winding will return more pulses.

One way to detect a faulty power transformer is to connect it to the supply and feel the temperature-rise (when nothing is connected to the secondary).
It should NOT get hot.
Detecting shorted turns is not easy to diagnose as you really need another identical

component to compare the results.
Most transformers get very hot when a shorted turn has developed. It may deliver a voltage but the heat generated and a smell from the transformer will indicate a fault.

ISOLATION TRANSFORMER

An isolation transformer is a piece of **Test Equipment** that provides "Mains Voltage" but the voltage is "floating." You will still get a shock if you touch the two output leads, but it has a special use when testing unknown equipment.
Many electrical appliances are fully insulated and only have two leads connected to the mains.
When you take these appliances apart, you do not know which end of say a heating element is connected to the "live" (active) side of the mains and which end connects to the neutral.
I am not suggesting you carry out the following tests, but they are described to show how an isolation transformer works.
If you touch a soldering iron on the "live" (active) end of the heating element it will create a short-circuit.
However when the appliance is connected to the mains via an **isolation transformer**, you can touch an earthed soldering iron on either end of the heater as both leads from the isolation transformer are "floating."
Note: As soon as you earth one lead of the output an isolation transformer, the other lead becomes "active."
You can make your own **Isolation Transformer** by connecting two identical transformers "back-to-back."
The following diagram shows how this is done:

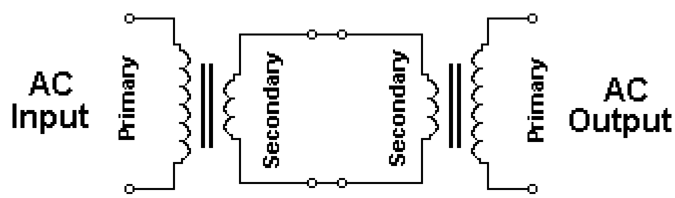

You can use any transformers providing the primary and secondary voltages are the same. The current capability of the secondary winding does not matter. However if you want a supply that has almost the same voltage as your "Mains," you need two transformers with the same voltages.
This handy isolation transformer will provide you with "Mains Voltage" but with a limited current.
In other words it will have a limited capability to supply "wattage." If you are using two 15VA transformers, you will only be able to test an appliance rated at 15 watts.
This has some advantages and some disadvantages.
If you are working on a project, and a short-circuit occurs, the damage will be limited to 15 watts.
If you are using two transformers with different VA ratings, the lower rating will be the capability of the combination.
If the secondaries are not equal, you will get a higher or lower "Mains Voltage."
If you get two transformers from TVs or Monitors, with a rating on the compliance plate of 45 watts, or 90 watts, you can assume the transformers are capable of delivering this wattage and making an isolation transformer will enable you to test

similar items with the safety of being isolated from the mains.
Colin Mitchell designs a lot of "LED lighting lamps" that are connected directly to the mains. He always works with an isolating transformer, just to be safe. Working on exposed "mains" devices is extremely nerve-wracking and you have to be very careful.
The isolation transformer will prevent a BIG EXPLOSION.

DETERMINING THE SPECS OF A TRANSFORMER
Suppose you have a "mains transformer" with unknown output voltages and unknown current capability.
You must be sure it is a mains transformer designed for operation on 50Hz or 60Hz.
Switch-Mode transformers operate at frequencies 40kHz and higher and are not covered in this discussion.
To be on the safe-side, connect the unknown transformer to the output of your isolating transformer.
Since the transformer will take almost no current when not loaded, the output voltages it produces will be fairly accurate. Measure the input AC voltage and output AC voltage.
If the transformer has loaded your isolating transformer it will be faulty.
Mains transformers are approx 15VA for 500gm, 30VA for 1kgm 50VA for 2kgm and and 100VA for 2.5kgm.
VA stands for Volts-Amps and is similar to saying watts. Watts is used for DC circuits, while VA refers to AC circuits.
Once you have the weight of the transformer and the output voltage, you can work out the current capability of the secondary.
For transformers up to 30vA, the output voltage on no-load is 30% higher than the final "loaded voltage."
This is due to the poor regulation of these small devices.
If the transformer is 15VA and the output voltage is 15v AC, the current will be 1 amp AC.
You can check the "quality" of the transformer, (the regulation) by fully loading the output and measuring the final voltage. If the transformer has a number of secondaries, the VA rating must be divided between all the windings.

240v to 110v ISOLATION TRANSFORMER
Here's how to create a 110v isolating transformer:
Find a 240v:12v transformer.
Now find a transformer that has two secondary windings, such as 240v:12v+12v.

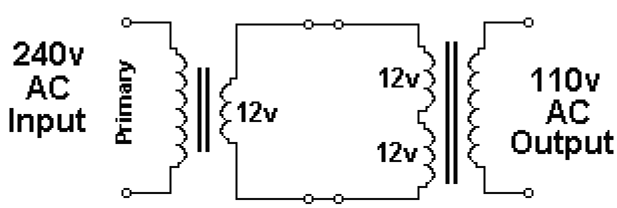

Connect the two transformers as shown in the circuit above. If the output is zero, connect ONE of the 12v windings of the second transformer around the other way.

110v to 240v ISOLATION TRANSFORMER

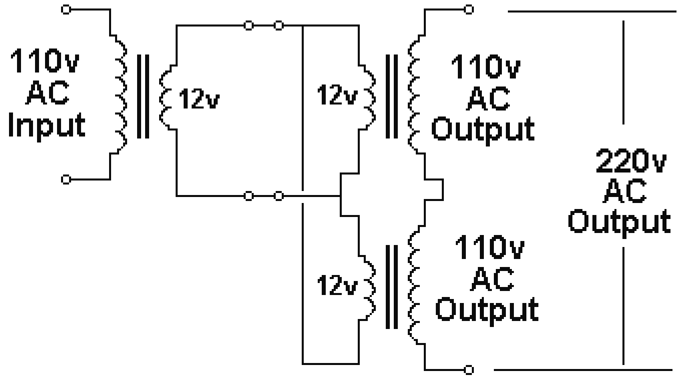

A 110v to 240v isolation transformer can be created by connecting 3 identical transformers as shown in the diagram above. If the output is zero, connect one of the outputs around the other way.

TRANSFORMER RATINGS

Question from a reader:
I have a 28v - 0 - 28v transformer @3amps. Does this mean each side is 1.5 amps?
The transformer is called CENTRE TAPPED and is shown in figures B and C.
It is designed to be connected to two diodes so each winding takes it in turn to deliver the current as shown in diagram C and the output will be 28v AC at 3 amps. The 28v and 3 amp are both AC values.
If you connect across both outside wires, the output will be 56v at 1.5 amp.
This is because the transformer has a VA rating of 28 x 3 = 84VA. This is very similar to the term "watts."
When the 28v AC is rectified and smoothed, it becomes 28 x 1.4 = 39v (minus 0.6v across the diode) and since the transformer has a rating of 84 VA, the current must be reduced to 84/39 = 2.1 amps to maintain the VA rating.
Some transformers are specified as say: 12v - 0 - 12v, but the wiring diagram is shown as "A." This transformer should be specified as 12v + 12v as the secondaries are separate.
12v - 0 - 12v means the two secondary windings are NOT separate.
It does not make any difference to the output voltage and current, if the windings are separate or joined. The only difference is 12v +12v can be turned into two separate 12v outputs.
If you do not know the output current for a particular transformer, go to the website of electronic parts suppliers and compare the weight of your transformer with others. This will give you a VA rating and you can work out the current, once you know the output voltage.
Note: the output current finishes up ONLY 60% of the rating on the transformer tag because the rating is an **AC RATING**.
With 2 separate secondaries, you can parallel the outputs to get double the current, but don't forget 12v + 12v @ 3amp means 12v in parallel with 12v will provide 2amp DC and the DC voltage will be about 17v.

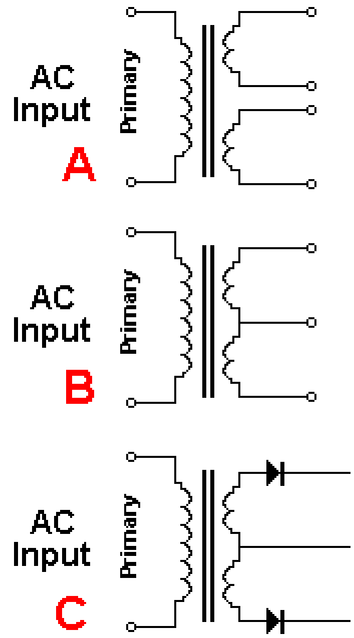

CURRENT TRANSFORMER

A Current Transformer is really an ordinary transformer.
All transformers produce a CURRENT output and a VOLTAGE output.
If you put an ammeter across the secondary, the current will increase through the meter when the primary voltage is increased.
This is because the output voltage will increase and this voltage will allow a higher current to flow.

WHY DETECT CURRENT? Why not voltage?

Because the voltage of say the "240v AC" is always 240v but the current can increase from say 1 amp to nearly 15 amps, depending what appliance is connected. So it is pointless measuring voltage.
A Current Transformer is a step-up transformer. When we say step-up and step-down, we are referring to the voltage - comparing the primary voltage to the secondary voltage. (Most transformers on the "mains" are step-down transformers and are used as power supplies to laptops, phone chargers etc.) Even a welding transformer is a step-down device and produces about 20v to 70v, while the current can be as high as 100 amps. This current is higher than the mains will deliver and is needed to melt the metal at the point of contact of the probe and the item being welded.
A Current Transformer is a step-up transformer. The primary consists of a single turn (or maybe 2 - 5 turns) and the secondary has 100 turns (or more).
This means the voltage seen by the primary will be increased 100 times and appear as anything from a few hundred millivolts to a few volts, depending on the quality of the coupling. (the magnetic coupling between the wire through the centre of the core, the quality of the core to transfer this magnetic flux to the secondary turns.)
This voltage is then passed to a low value resistor, where the voltage is reduced to a level that suits the detection circuit and the resulting millivolts is interpreted as current in the wire being tested.

Recapping:

The reading on the secondary has no relation to the current in the primary. We need to add a LOAD RESISTOR and create a table before we can use the transformer.
There is no such thing as a CURRENT TRANSFORMER. It is really an INSTRUMENT TRANSFORMER and the scale has been marked in units of CURRENT after measurements have been made. (INSTRUMENT TRANSFORMER means it is a device that helps us to produce a connection between current flowing through a wire and a reading on a meter or display).
If we connect a load to the secondary, (say an ammeter), it will produce a reading that increases when the current through the single primary turn is increased. That's because the ammeter is a LOAD. But the reading is meaningless until be calibrate the scale.

Now, lets look at the primary.
A wire (or cable) through the centre of the core is counted as one turn. If the turn is wrapped around the core, the coupling will be improved, but if we always use a straight wire, it does not matter where it is positioned inside the centre of the core.
It does not matter if the magnetic interaction of the flux from the wire is good or bad, we just have to keep to the same way of using the transformer.
The calibration can be done with any poor coupling and the result will be accurate for all future readings.
If a low-value resistor is placed across the secondary, the voltage across this resistor will increase and also the current through it will increase. But we are not going to measure the current through the resistor. We are going to measure the voltage across the resistor and by taking lots of reading we will finish up with a scale or table and this is called CALIBRATION. The results will be equated to the current flowing through the primary wire (primary turn).
A clamp meter uses a current transformer and the jaws must be closed completely and cleanly for the flux to flow around the core and produce a reading in the secondary.
Dirt in the jaws will reduce the reading considerably.
You cannot measure the current in a "power cord" because it contains both the active and neutral wires.
Even though the current is a maximum in both conductors at the same time, the current is flowing in two different directions and the magnetic flux produced by one conductor is clockwise and the other is anticlockwise and they are cancelled by each other.

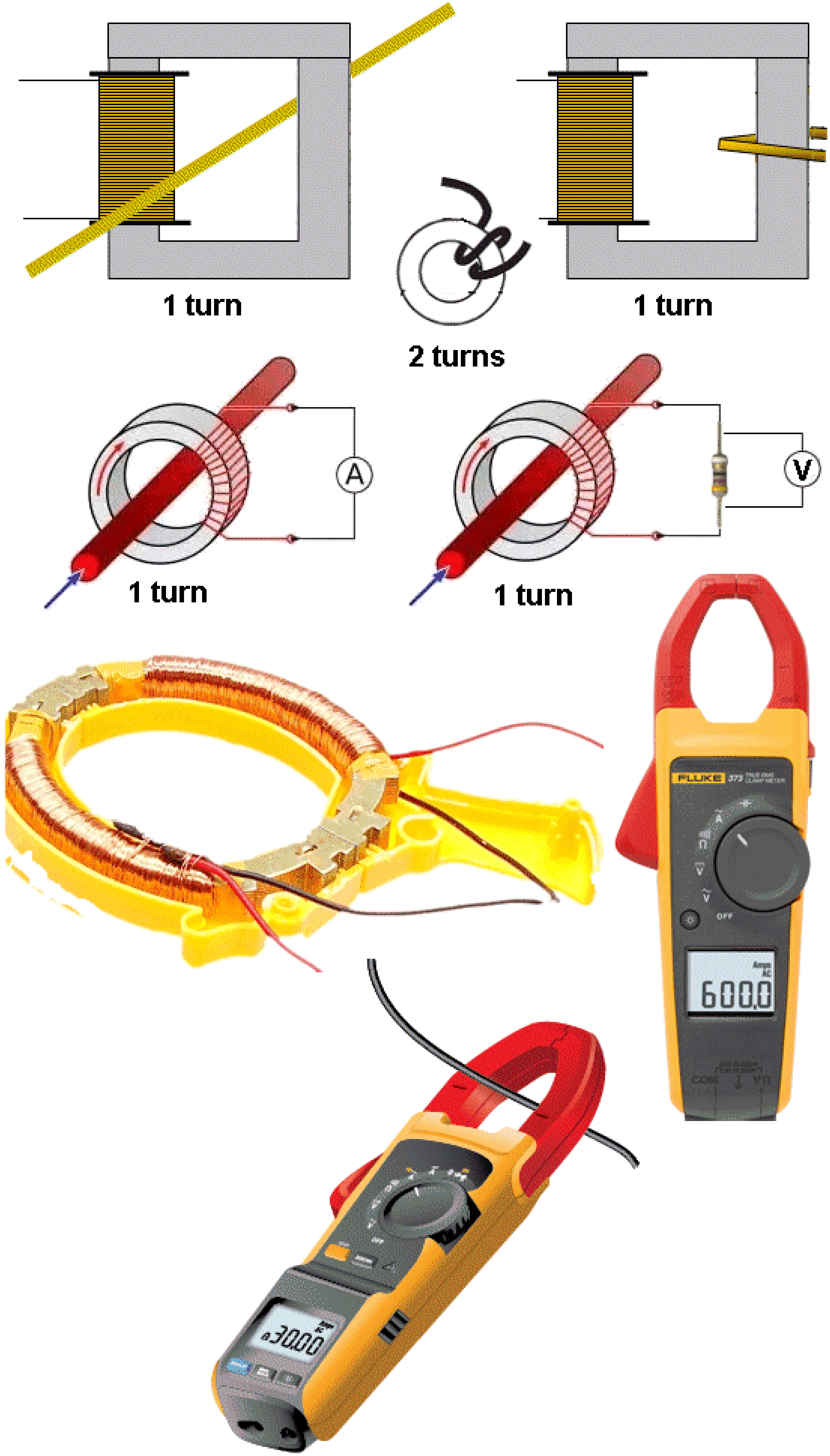

Identifying ONE TURN.
The quality (the coupling) of a single STRAIGHT wire

through the centre of a core is very poor
but if all readings are taken with this amount
of coupling, the readings will be accurate, as the
calibrations have been done with this arrangement.

OPTO ISOLATORS and OPTO COUPLERS

Opto Isolators and Opto Couplers are the same thing. A common opto-coupler is 4N35. It is used to allow two circuits to exchange signals yet remain electrically isolated. The signal is applied to the LED, which shines on a silicon NPN photo-transistor in the IC.
The light is proportional to the signal, so the signal is transferred to the photo transistor to turn it on a proportional amount. Opto-couplers can have Light Activated SCR's, photodiodes, TRIAC's and other semiconductor devices as an output. The 4N35 opto-coupler schematic is shown below:

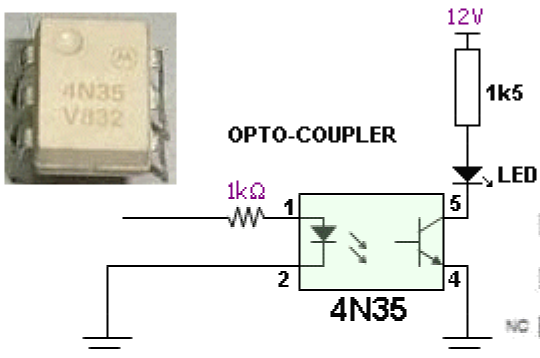

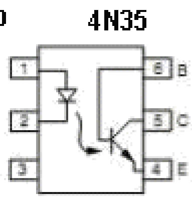

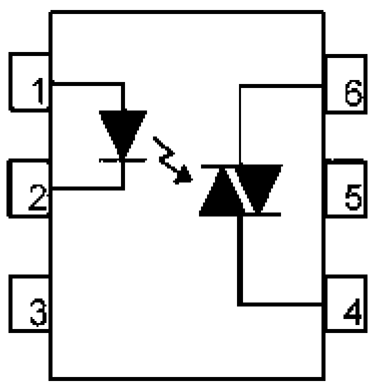

An opto-Coupler using a TRIAC
Note: the pinout is different to 4N35

TESTING AN OPTO COUPLER

Most multimeters cannot test the LED on the input of an opto-coupler because the ohms range does not have a voltage high enough to activate the LED with at least 2mA.
You need to set-up the test-circuit shown above with a 1k resistor on the input and 1k5 on the output. When the 1k is connected to 12v, the output LED will illuminate.
The opto-coupler should be removed from circuit to perform this test.

TRANSISTORS

Transistors are solid-state devices and although they operate completely differently to a diode, they appear as two back-to-back diodes when tested.
There are basically 2 types of transistor NPN and PNP.
A transistor is sometimes referred to as BJT (Bi-polar Junction Transistor) to distinguish it from other types of transistor such as Field Effect transistor, Programmable Unijunction Transistor and others.

In the following diagram, two diodes are connected together and although the construction of a transistor is more complex, we see the transistor as two diodes when testing it.

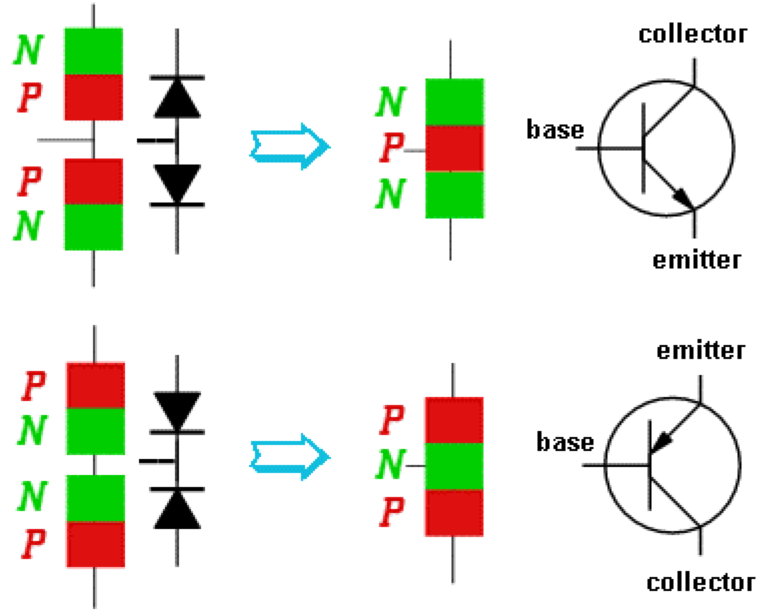

A TRANSISTOR APPEARS AS TWO DIODES WHEN TESTING IT

All transistors have three leads. Base (b), Collector (c), and Emitter (e).
For an NPN transistor, the arrow on the emitter points away from the base.
It is fortunate that the arrow on both symbols points in the direction of the flow of current (Conventional Current) and this makes it easy to describe testing methods using our simplified set of instructions. The symbols have been drawn exactly as they appear on a circuit diagram.

All transistors **are the same** but we talk about digital and analogue transistors.
There is no difference between the two.
The difference is the circuit. And the only other slight difference between transistors is the fact that some have inbuilt diodes and resistors to simplify the rest of the circuit.
All transistors work the same way. The only difference is the amount of amplification they provide, the current and voltage they can withstand and the speed at which they work. For simple testing purposes, they are all the same.

NPN transistors are the most common and for an NPN transistor, the following applies.
(the opposite applies for PNP)
To test a transistor, there is **one thing** you have to know:
When the base voltage is higher than the emitter, current flows though the collector-emitter leads.
As the voltage is increased on the base, nothing happens until the voltage reaches 0.55v. At this point a very small current flows through the collector-emitter leads. As the voltage is increased, the current-flow increases. At about 0.75v, the current-flow is a MAXIMUM. (can be as high as 0.9v). That's how it works. A transistor also needs **current** to flow into the base to perform this amplifying function and this is the one feature that separates an ordinary transistor from a FET.

If the voltage on the base is 0v, then instantly goes to 0.75v, the transistor initially passes NO current, then FULL current. The transistor is said to be working in its two states: OFF then ON (sometimes called: "cut-off" and "saturation"). These are called digital states and the transistor is said to be a **DIGITAL TRANSISTOR** or a **SWITCHING TRANSISTOR** , working in **DIGITAL MODE.**

If the base is delivered 0.5v, then slowly rises to 0.75v and slowly to 0.65v, then

0.7v, then 0.56v etc, the transistor is said to be working in ANALOGUE MODE and the transistor is an **ANALOGUE TRANSISTOR**.
Since a transistor is capable of amplifying a signal, it is said to be an active device. Components such as resistors, capacitors, inductors and diodes are not able to amplify and are therefore known as passive components.

In the following tests, use your finger to provide the **TURN ON** voltage for the base (this is 0.55v to 0.7v) and as you press harder, more current flows into the base and thus more current flows through the collector-emitter terminals. As more current flows, the needle of the multimeter moves UP-SCALE.

TESTING A TRANSISTOR ON A DIGITAL METER

Testing a transistor with a **Digital Meter** must be done on the "DIODE" setting as a digital meter does not deliver a current through the probes on some of the resistance settings and will not produce an accurate reading.
The "DIODE" setting must be used for diodes and transistors. It should also be called a "TRANSISTOR" setting.

TESTING AN unknown TRANSISTOR

The first thing you may want to do is test an unknown transistor for COLLECTOR, BASE AND EMITTER. You also want to perform a test to find out if it is NPN or PNP. That's what this test will provide.
You need a cheap multimeter called an ANALOGUE METER - a multimeter with a scale and pointer (needle).
It will measure resistance values (normally used to test resistors) - (you can also test other components) and Voltage and Current. We use the resistance settings. It may have ranges such as "x10" "x100" "x1k" "x10"
Look at the resistance scale on the meter. It will be the top scale.
The scale starts at zero on the right and the high values are on the left. This is opposite to all the other scales.
When the two probes are touched together, the needle swings FULL SCALE and reads "ZERO." Adjust the pot on the side of the meter to make the pointer read exactly zero.

How to read: "x10" "x100" "x1k" "x10"
Up-scale from the zero mark is "1"
When the needle swings to this position on the "x10" setting, the value is 10 ohms.
When the needle swings to "1" on the "x100" setting, the value is 100 ohms.
When the needle swings to "1" on the "x1k" setting, the value is 1,000 ohms = 1k.
When the needle swings to "1" on the "x10k" setting, the value is 10,000 ohms = 10k.
Use this to work out all the other values on the scale.
Resistance values get very close-together (and very inaccurate) at the high end of the scale. [This is just a point to note and does not affect testing a transistor.]

Step 1 - FINDING THE BASE and determining NPN or PNP
Get an unknown transistor and test it with a multimeter set to "x10"
Try the 6 combinations and when you have the black probe on a pin and the red probe touches the other pins and the meter swings nearly full scale, you have an NPN transistor. The black probe is BASE
If the red probe touches a pin and the black probe produces a swing on the other two pins, you have a PNP transistor. The red probe is BASE
If the needle swings FULL SCALE or if it swings for more than 2 readings, the transistor is **FAULTY**.

Step 2 - FINDING THE COLLECTOR and EMITTER
Set the meter to "x10k."
For an NPN transistor, place the leads on the transistor and when you press hard on the two leads shown in the diagram below, the needle will swing almost full scale.

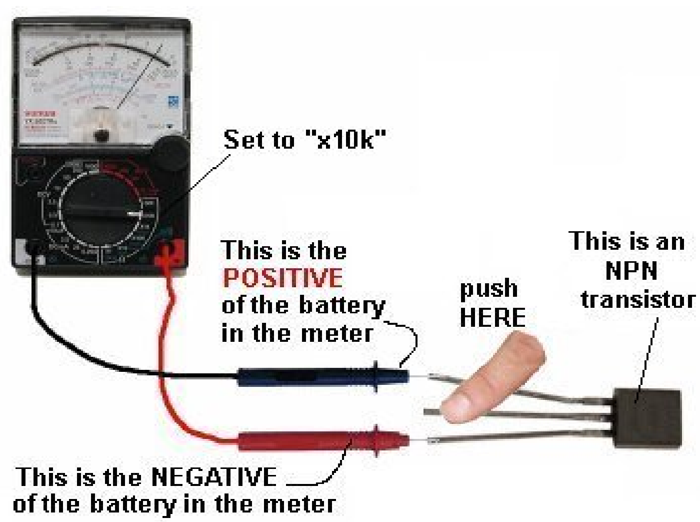

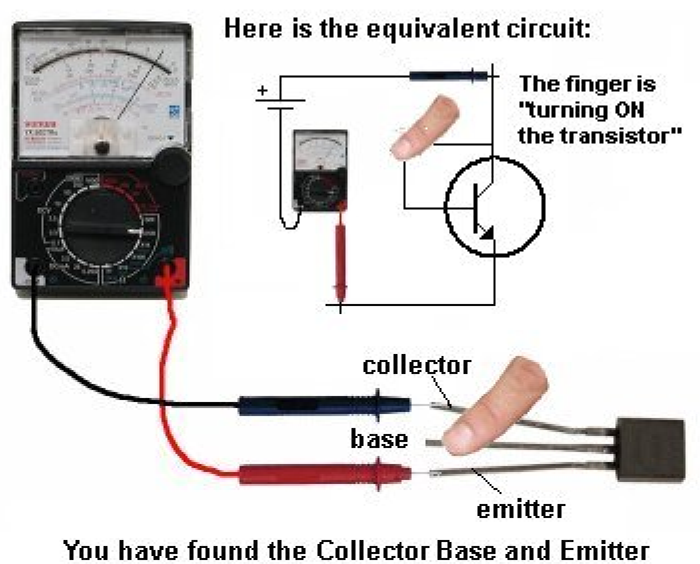

For a PNP transistor, set the meter to "x10k" place the leads on the transistor and when you press hard on the two leads shown in the diagram below, the needle will swing almost full scale.

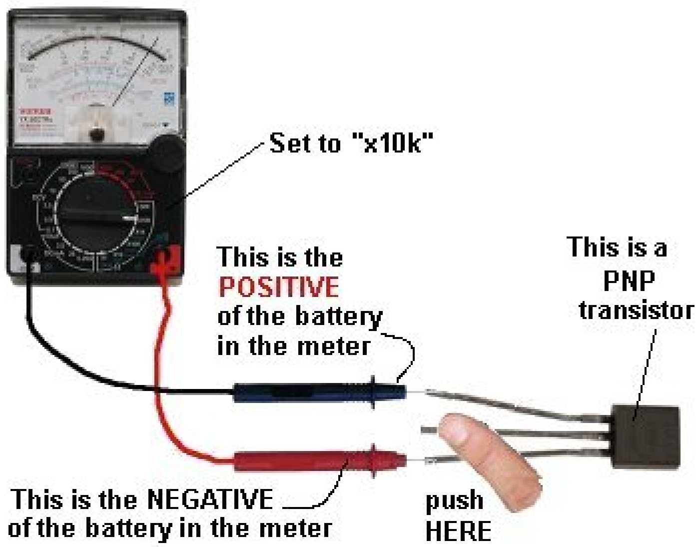

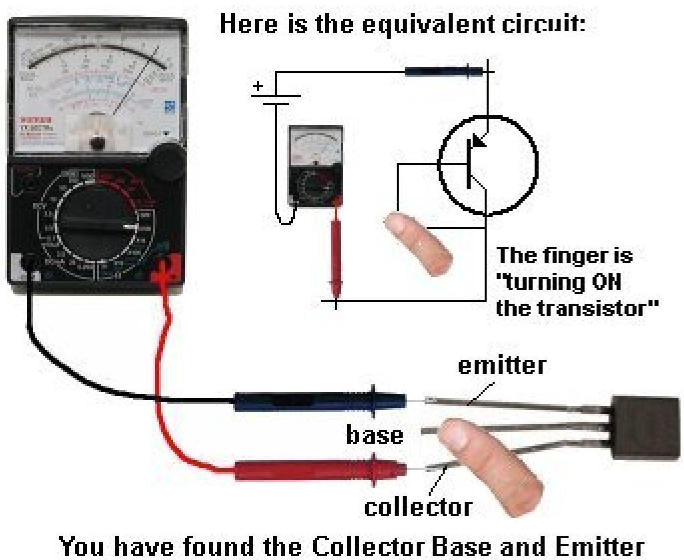

SIMPLEST TRANSISTOR TESTER
The simplest transistor tester uses a 9v battery, 1k resistor and a LED (any colour). Keep trying a transistor in all different combinations until you get one of the circuits below. When you push on the two leads, the LED will get brighter.
The transistor will be NPN or PNP and the leads will be identified:

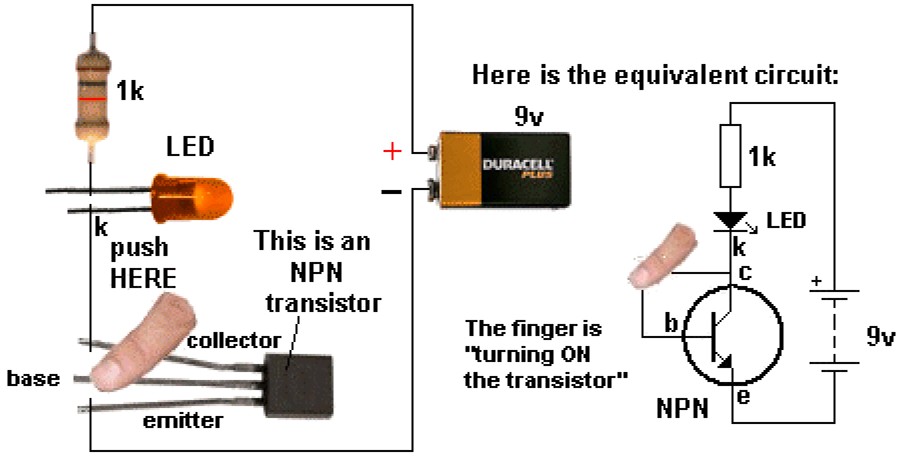

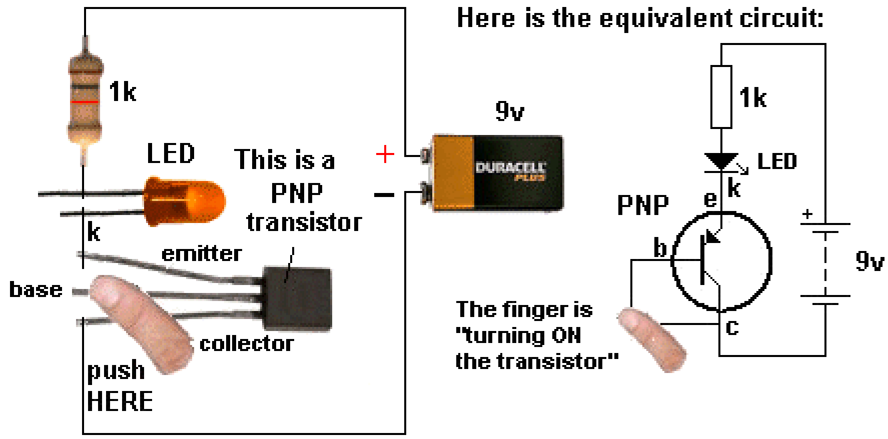

The leads of some transistors will need to be bent so the pins are in the same positions as shown in the diagrams. This helps you see how the transistor is being turned on. This works with NPN, PNP transistors and Darlington transistors.

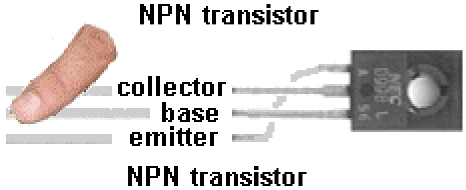

HEATSINKING

Heat generated by current flowing between the collector and emitter leads of a transistor causes its temperature to rise. This heat must be conducted away from the transistor otherwise the rise may be high enough to damage the P-N junctions inside the device. Power transistors produce a lot of heat, and are therefore usually mounted on a piece of aluminium with fins, called a **HEATSINK**.
This draws heat away, allowing it to handle more current. Low-power signal transistors do not normally require heat sinking. Some transistors have a metal body or fin to connect to a larger heatsink. If the transistor is connected to a heatsink with a mica sheet (mica washer), it can be damaged or cracked and create a short-circuit. (See Testing Mica Washers). Or a small piece of metal may be puncturing the mica.
Sometimes white compound called **Heatsink Compound** is used to conduct heat through the mica. This is very important as mica is a very poor conductor of heat and the compound is needed to provide maximum thermal conduction.

TRANSISTOR FAILURE

Transistor can fail in a number of ways. They have forward and reverse voltage ratings and once these are exceeded, the transistor will ZENER or conduct and may fail. In some cases a high voltage will "puncture" the transistor and it will fail instantly. In fact it will fail much faster via a voltage-spike than a current overload.

It may fail with a "short" between any leads, with a collector-emitter short being the most common. However failures will also create shorts between all three leads.
A shorted transistor will allow a large current to flow, and cause other components to heat up.
Transistors can also develop an open circuit between base and collector, base and emitter or collector and emitter.
The first step in identifying a faulty transistor is to check for signs of overheating. It may appear to be burnt, melted or exploded. When the equipment is switched off, you can touch the transistor to see if it feels unusually hot. The amount of heat you feel should be proportional to the size of the transistor's heat sink. If the transistor has no heat sink, yet is very hot, you can suspect a problem.
DO NOT TOUCH A TRANSISTOR IF IT IS PART OF A CIRCUIT THAT CARRIES 240VAC.
Always switch off the equipment before touching any components.

TRANSISTOR REPLACEMENT

If you can't get an exact replacement, refer to a transistor substitution guide to identify a near equivalent.

The important parameters are:
- Voltage
- Current
- Wattage
- Maximum frequency of operation

The replacement part should have parameters equal to or higher than the original.

Points to remember:
- Polarity of the transistor i.e. PNP or NPN.
- At least the same voltage, current and wattage rating.
- Low frequency or high frequency type.
- Check the pinout of the replacement part
- Use a desoldering pump to remove the transistor to prevent damage to the printed circuit board.
- Fit the heat sink.
- Check the mica washer and use heat-sink compound
- Tighten the nut/bolt - not too tight or too loose.
- Horizontal output transistors with an integrated diode should be replaced with the same type.

DIGITAL TRANSISTORS

There is no such thing as a DIGITAL TRANSISTOR or an AUDIO TRANSISTOR.
All transistors are just "TRANSISTORS" and the surrounding components as well as the type of signal, make the transistor operate in DIGITAL MODE or ANALOGUE MODE.
But we have some transistors that have inbuilt resistors to make them suitable for connecting to a digital circuit without the need for a base resistor.
Here is the datasheet for an NPN transistor BCR135w and PNP datasheet for BCR185w.
These transistors are called "Digital Transistors" because the "base lead" can be connected directly to the output of a digital stage. This "lead" or "pin" is not really the base of the transistor but a 4k7 (or 10k) resistor connected to the base allows the transistor to be connected to the rest of a digital circuit.
You cannot actually get to the base. The resistor(s) are built into the chip and the transistor is converted into a "Digital Transistor" because it will accept 5v on the "b"

lead.
The 47k is not really needed but it makes sure the transistor is fully turned OFF if the signal on the "b" lead is removed (in other words - if the input signal is converted to a high-impedance signal - see tri-state output from microcontrollers for a full explanation).
This transistor is designed to be placed in a circuit where the input changes from low to high and high to low and does not stop mid-way. This is called a DIGITAL SIGNAL and that is one reason why the transistor is called a digital transistor. (However you could stop half-way but the transistor may heat up and get too hot).
Any transistor placed in a digital circuit can be called a "digital transistor" but it is better to say it is operating in DIGITAL MODE.

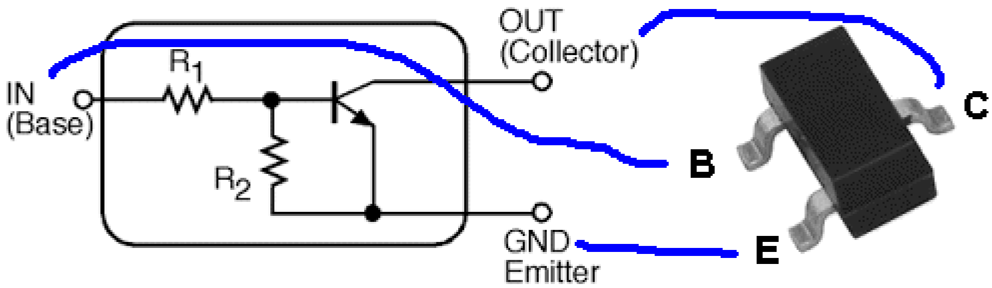

The digital transistor has two resistors included inside the case
R1 is about 10k and R2 is approx 47k

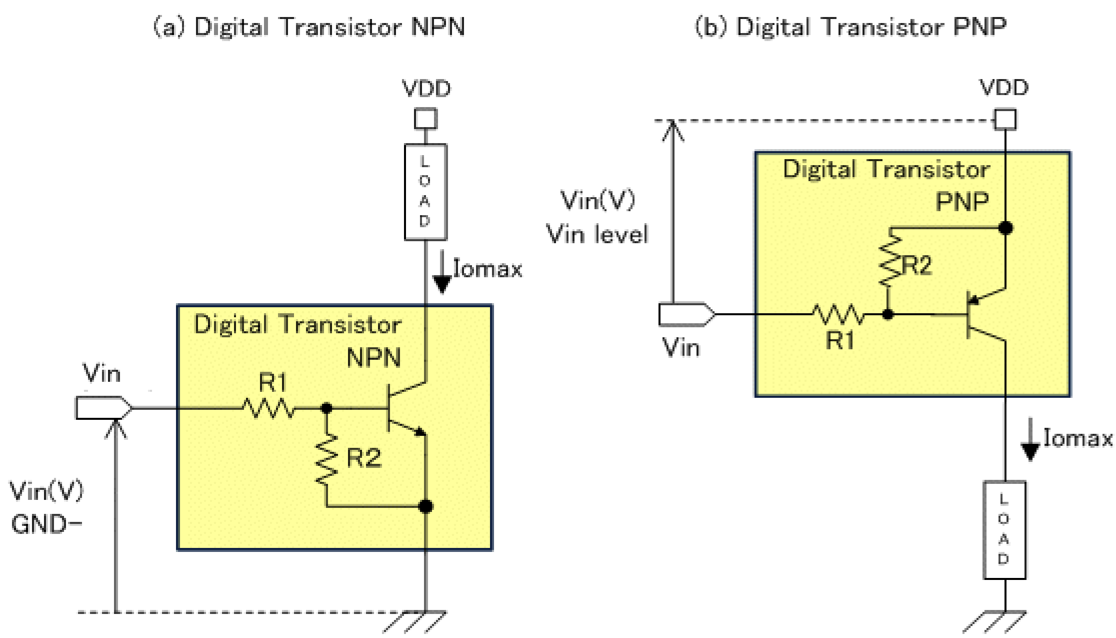

Equivalent circuit of the digital transistor

These transistors can be made to work in analogue circuits because they are ordinary transistors with a 10k base resistor, but you will have to know what you are doing.

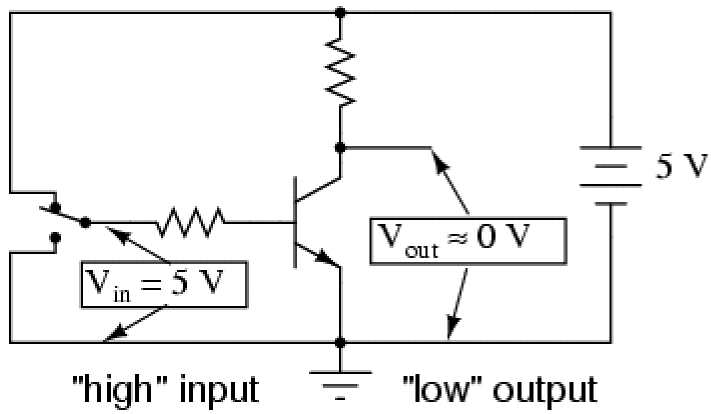

Transistor in saturation

The circuit above shows the digital transistor is designed to allow a voltage of 5v to be supplied to the "base" pin and the transistor will Fully Conduct.
This type of transistor saves putting a base resistor on the PC board.
It can be tested just like a normal transistor but the resistance between base and emitter will be about 5k to 50k in both directions. If the collector-emitter is low in both directions the transistor is damaged.
Here's how to look at how the transistor works:
The 10k resistor on the base will allow 0.5mA to flow into the base. But the 47k will reduce this to 0.4mA. If the transistor has a gain of 100, the collector-emitter current can be 40mA.
To determine the current capability of the transistor, connect 100R load and turn the transistor ON. This will allow about 100mA for the collector-emitter current. Measure the collector-emitter voltage. If it is more than 0.5v, the transistor is OVER-LOADED.

DARLINGTON TRANSISTORS

A DARLINGTON TRANSISTOR is two transistors in a single package with three leads. They are internally connected in cascade so the gain of the pair is very high. This allows a very small input signal to produce a large signal at the output. They have three leads (Base, Collector and Emitter and can be PNP or NPN) and are equivalent to the leads of a standard individual transistor, but with a very high gain. The second advantage of a Darlington Transistor is its high input impedance. It puts very little load on the previous circuit.
Some Darlington transistors have a built-in diode and/or built-in resistor and this will produce a low reading in both directions between the base and emitter leads.

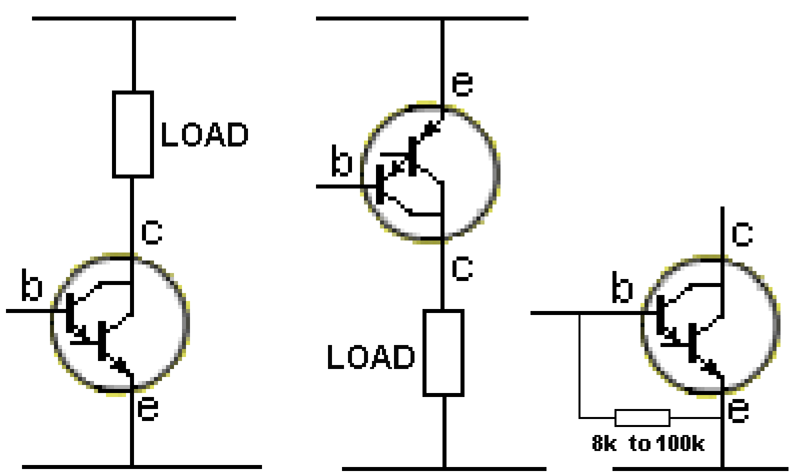

NPN Darlington PNP Darlington

Darlington transistors are tested the same as an ordinary transistor and a multimeter will produce about the same deflection, even though you will be measuring across two junctions, (and a base-emitter resistor is present).

HORIZONTAL OUTPUT TRANSISTORS, SWITCH-MODE TRANSISTORS, FLYBACK TRANSISTORS, POWER TRANSISTORS, VERTICAL TRANSISTORS . . . .

These are all names given to a transistor when it is used in a particular circuit. ALL these transistors are the same for testing purposes.
We are not testing for gain, maximum voltage, speed of operation or any special feature. We are just testing to see if the transistor is completely faulty and SHORTED.
A transistor can have lots of other faults and the circuit **using the transistor** is the best piece of TEST EQUIPMENT as it is detecting the fault.

TESTING MOSFETs and FETs

MOSFETs and **JFETs** are all part of the **FET** family.
MOSFET stands for **Metal Oxide Semiconductor Field Effect Transistor.**
FETs operate exactly the same as a "normal" transistor except they have different names for the input and output leads and the voltage between the gate and the source has to between 2v to 5v for the device to turn on fully. A FET requires almost NO CURRENT into the Gate for it to turn on and when it does, the voltage between drain and source is very low (only a few mV). This allows them to pass very high currents without getting hot. There is a point where they start to turn on and the input voltage must rise higher than this so the FET turns on FULLY and does not get hot.
Field Effect Transistors are difficult to test with a multimeter, but "fortunately" when a power **MOSFET** blows, it is completely damaged. All the leads will show a short circuit. 99% of bad **MOSFETs** will have GS, GD and DS shorted.
The following symbols show some of the different types of MOSFETs:

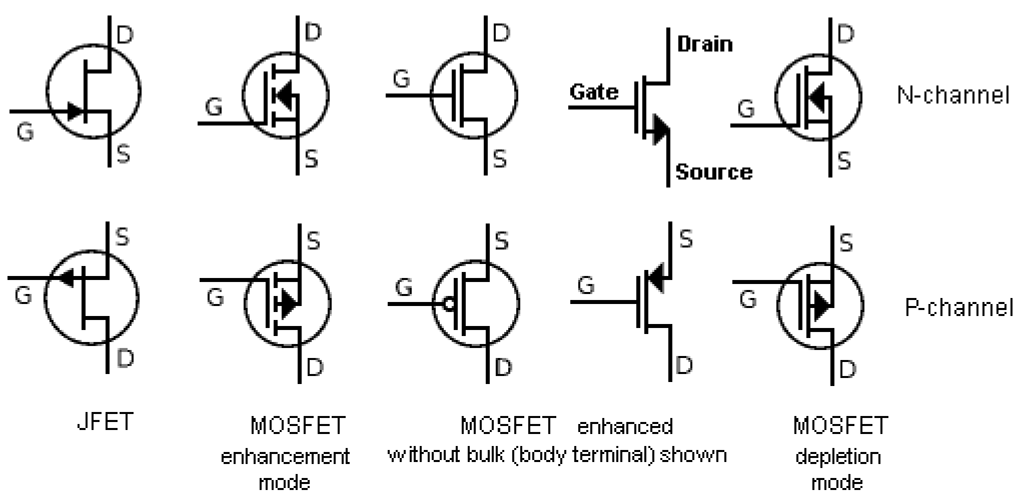

Most **MOSFET** transistors cannot be tested with a multimeter. This due to the fact that the Gate needs 2v - 5v to turn on the device and this voltage is not present on the probes of either meter set to any of the ohms ranges.
You need to build the following Test Circuit:

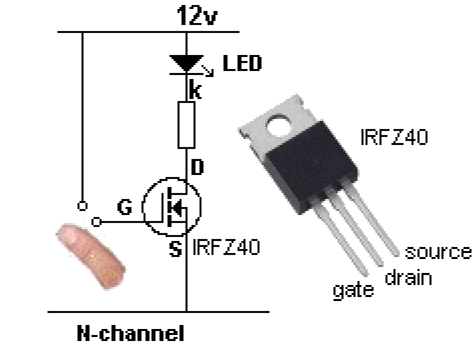

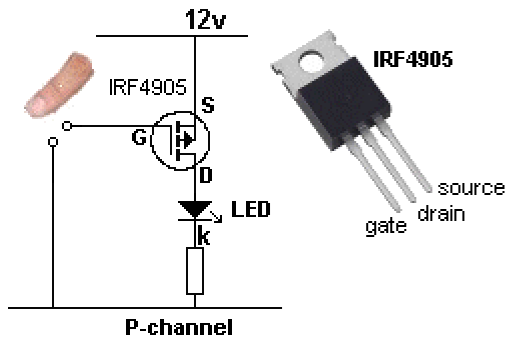

Touching the Gate will increase the voltage on the Gate and the MOSFET will turn ON and illuminate the LED. Removing your finger will turn the LED off.
Large devices such as the TO-220 types shown above do not like static electricity on the gate and you have to be careful not to "spike" the gate with any static. Generally this type of device is not "super sensitive" and you can use your finger or a large value resistor.
When replacing one of these devices, there are 2 things to match-up.
Voltage and Current.
In most cases, the "turn-ON" resistance (the resistance between Source and Drain) will be the same (something like 22 milli ohms) and the speed of operation will be ok.
Check the voltage needed to turn the gate ON and make sure you can supply the required voltage.

SILICON CONTROLLED RECTIFIERs (SCR)

The **Silicon Controlled Rectifier** (SCR) is a semiconductor device that is a member of a family of control devices known as **Thyristors**. It is a 3-leaded device and when a small current enters the Gate, the **thyristor** turns on. AND STAYS ON. It only conducts current between Anode and Cathode in one direction and it is mainly only used in DC circuits. When it is used with AC, it will only conduct for a maximum of half the cycle.

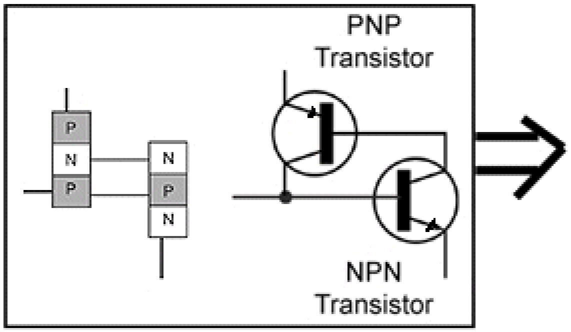

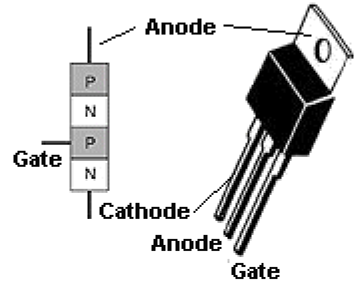

THYRISTOR or SCR

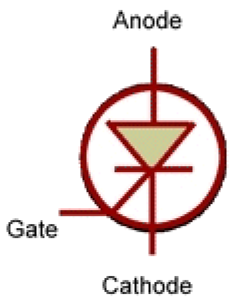

SCR
Silicon Controlled Rectifier

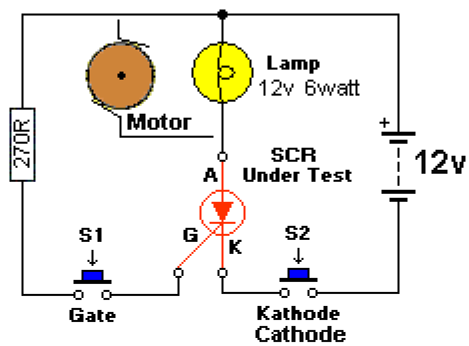

SCR TESTER

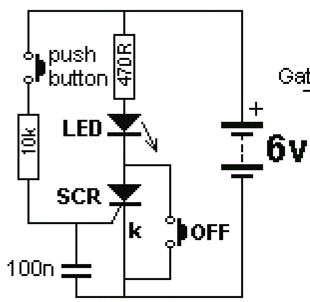

A

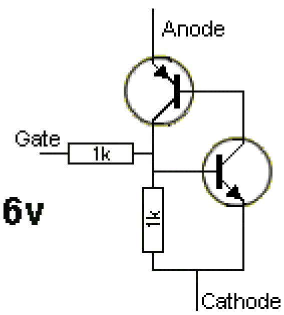

SCR WITH TRANSISTORS

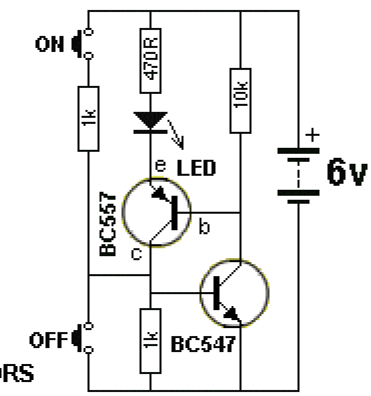

B

To understand how an SCR "latches" when the gate is provided with a small current, we can replace it with two transistors as shown in diagram B above. When the ON button is pressed, the BC547 transistor turns on. This turns ON the BC557 and it takes over from the action of the switch.
To turn the circuit off, the OFF button removes the voltage from the base of the BC547.

Testing an SCR

An **SCR** can be tested with some multimeters but a minimum current Anode-to-Cathode is needed to keep the device turned on. Some multimeters do not provide this amount of current and the **SCR Tester** circuit above is the best way to test these devices.
Shorted SCRs can usually be detected with an ohmmeter check (SCRs usually fail shorted rather than open).
Measure the anode-to-cathode resistance in both the forward and reverse direction; a good SCR should measure near infinity in both directions.
Small and medium-size SCRs can also be gated ON with an ohmmeter (on a digital meter use the Diode Check Function). Forward bias the SCR with the ohmmeter by connecting the black (-) lead to the anode and the red (+) lead to the cathode

(because the + of the battery is connected to the negative lead, in most analogue multimeters). Momentarily touch the gate lead to the anode while the probes are still touching both leads; this will provide a small positive turn-on voltage to the gate and the cathode-to-anode resistance reading will drop to a low value. Even after removing the gate voltage, the SCR will stay conducting. Disconnecting the meter leads from the anode or cathode will cause the SCR to revert to its non-conducting state.
When making the above test, the meter impedance acts as the SCR load. On larger SCRs, it may not latch ON because the test current is not above the SCR holding current.

Using the SCR Tester
Connect an SCR and press Switch2. The lamp should not illuminate. If it illuminates, the SCR is around the wrong way or it is faulty.
Keep Switch 2 PRESSED. Press Sw1 very briefly. The lamp or motor will turn ON and remain ON. Release Sw 2 and press it again. The Lamp or motor will be OFF.

TRIACs

A triac is a bidirectional, three-terminal dual, back-to-back thyristor (SCR) switch. This device will conduct current in both directions when a small current is constantly applied to the Gate.
If the gate is given a small, brief, current during any instant of a cycle, it will remain triggered during the completion of the cycle until the current though the Main Terminals drops to zero.
This means it will conduct both the positive and negative half-cycles of an AC waveform. If it is tuned on (with a brief pulse) half-way up the positive waveform, it will remain on until the wave rises and finally reaches zero. If it is then turned on (with a brief pulse) part-way on the negative wave, the result will be pulses of energy and the end result will be about 50% of the full-energy delivered at a rate of 100 times per second for a 50HZ supply.
TRIACs are particularly suited for AC power control applications such as motor speed control, light dimmers, temperature control and many others.

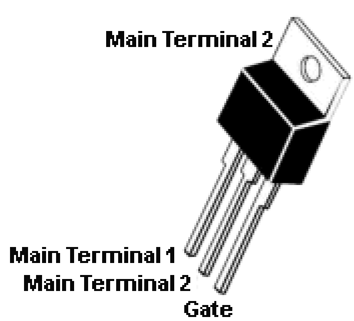

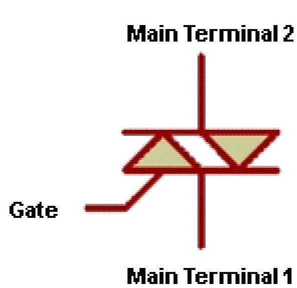

TRIAC (2 SCR's)
TRIode for Alternating Current

Using the TRIAC Tester

Connect a TRIAC and press Switch2. The lamp should not illuminate. If it illuminates, the TRIAC is faulty.
Keep Switch 2 PRESSED. Press Sw1 very briefly. The lamp or motor will turn ON and remain ON. If the lamp does not turn on, reverse the TRIAC as the current into the gate must produce a slight voltage between **Gate** and **Main Terminal 1**.
Release Sw 2 and press it again. The Lamp or motor will be OFF.

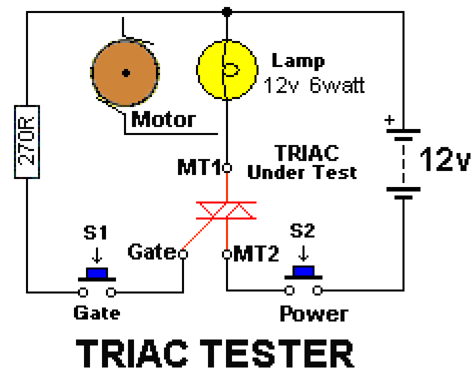

MICA WASHERS AND INSULATORS

Plastic insulating sheets (washers) between a transistor and heatsink are most often made from mica but some are plastic and these get damaged over a period of time, turn dark and become cracked.
The plastic eventually becomes carbonized and conducts current and can affect the operation of the appliance. You can see the difference between a mica sheet (washer) and plastic by looking where it extends from under the transistor. Replace all plastic insulators as they eventually fail.

SPARK GAPS

Some TV's and monitors with a CRT (picture tube), have spark gaps either on the socket at the end of the tube or on the chassis.
These can consist of two wires inside a plastic holder or a glass tube or special resistive device.
The purpose of a spark gap is to take any flash-over (from inside the tube), to earth. This prevents damage to the rest of the circuit.
However if the tube constantly flashes over, a carbon track builds up between the wires and effectively reduces the screen voltage. This can cause brightness and/or focus problems. Removing the spark-gap will restore the voltage.
These are not available as a spare component and it's best to get one from a discarded chassis.

CO-AX CABLES

Co-Ax cables can produce very high losses and it seems impossible that a few metres of cable will reduce the signal. The author has had a 3 metre cable reduce the signal to "snow" so be aware that this can occur. Faults can also come from a splitter and/or balun as well as dirty plugs and sockets. This can result in very loud bangs in the sound on digital reception.

TESTING EARTH LEAKAGE DETECTORS or Residual Current Devices or Ground Fault Circuit Interrupters or GFCI

An Earth Leakage Detector or Sensor is a circuit designed to continuously monitor the imbalance in the current in a pair of load carrying conductors.
These two conductors are normally the Active and Neutral. Should the imbalance current reach 30mA the sensor will "trip" and remove the voltage (and current) from

the line being monitored.
Some detectors will trip at 15mA.
You cannot alter the sensitivity of the device however there are a number of faults in these devices that can be fixed.
In some devices the contact pressure for the 10Amp or 15 Amp contacts is very weak and they arc and produce an open circuit. The result is this: When you press the rest button, power is not restored to the output.
Clean the contacts with a small file and bend the metal strips to the contacts so they make a very strong contact.
The other fault is the trip mechanism.
The magnetism from the coil does not allow the pin to move and "trip" the contacts. It may be due to a small metal filing or the pin not moving freely enough.
All good Earth Leakage Detectors have a TEST BUTTON. This connects a resistor between the active line and earth so that 15mA or 30mA flows.
The detector should trip immediately. Make sure the trigger mechanism trips when the test button is pressed.
None of the electronics in the detector can be replaced however you can test the mechanical operation and the pressure on the contacts when the unit is removed from the power. Do not work on the device when it is connected to the mains.

TESTING CELLS AND BATTERIES

There is an enormous number of batteries and cells on the market and a number of "battery testers." Instead of buying a battery tester that may give you a false reading, here is a method of testing cells that is guaranteed to work.
There are two types of cell: a **rechargeable** cell and a non rechargeable cell.

The easiest way to test a **rechargeable** cell is to put a group of them in an appliance and use them until the appliance "runs down" or fails to work. If you consider the cells did not last very long, remove them and check the voltage of each cell. The cell or cells with the lowest voltage will be faulty. You can replace them with new cells or good cells you have in reserve.
There is no other simple way to test a rechargeable cell.
You cannot test the "current of a cell" by using an ammeter. A rechargeable cell can deliver 10 amps or more, even when nearly discharged and you cannot determine a good cell for a faulty cell.

Dry cells are classified as "non-rechargeable" cells.
DRY CELLS and MANGANESE CELLS are the same thing. These produce 1.5v per cell (manganese means the Manganese Dioxide depolariser inside the cell. All "dry cells" use manganese dioxide).
ALKALINE CELLS produce between 2 - 10 times more energy than a "dry cell" and produce 1.5v per cell.
Alkaline cells can fail for no reason at any stage in their life and are not recommended for emergency situations.
The output voltage of some Alkaline cells can fall to 0.7v or 0.9v for not apparent reason.
There are lots of other cells including "button cells," hearing-aid cells, air cells, and they produce from 1.2v to 3v per cell.

Note:
Lithium cells are also called "button cells" and they produce 3v per cell.
Lithium cells are non-rechargeable (they are generally called "button cells") but some Lithium cells can be recharged. These are Lithium-ion cells and generally have a voltage of 3.6v. Some Lithium-ion cells look exactly like 3v Lithium cells, so you have to read the data on the cell before charging.

You cannot test the voltage of a cell and come to any conclusion as to the age of the cell or how much energy remains. The voltage of a cell is characteristic to the chemicals used and the actual voltage does not tell you its condition.
Some "dry cells" deliver 1.5v up to the end of their life whereas others drop to about 1.1v very quickly.

Once you know the name of the cell that drops to 1.1v, avoid them as the operation of the equipment "drops off" very quickly.

However if you have a number of different cells and need to know which ones to keep, here's the solution:

1. Check the voltage and use those with a voltage above 1.1v
2. Next, select 500mA or 10A range on a meter and place the probes on a cell. For a AAA or AA cell, the current should be over 500mA and the needle will swing full scale very quickly.

Keep the testing short as you are short-circuiting the cell but it is the only way to determine the internal impedance of the cell and this has a lot to do with its stage-of-charge.
This will give you a cell with a good terminal voltage and a good current capability.

This also applies to button cells, but the maximum current they will deliver will be less.
If you want to get the last of the energy out of a group of cells they can be used in the following circuits:

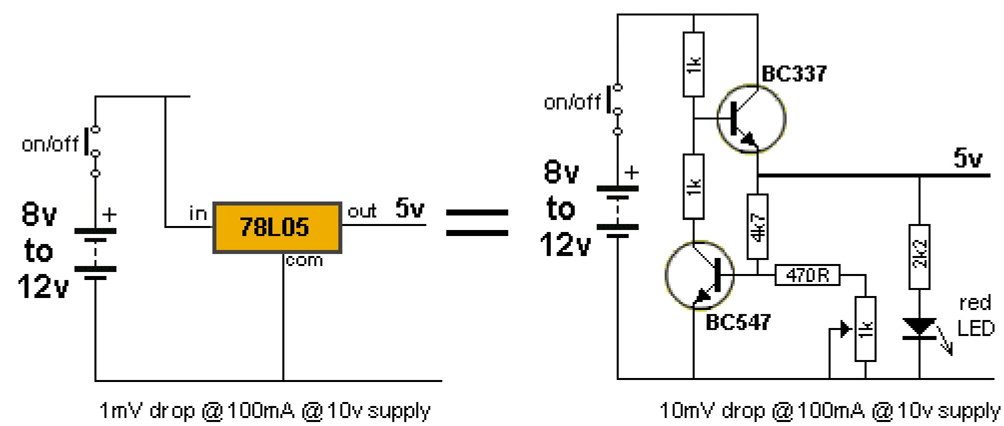

TESTING PIEZO DIAPHRAGMS and PIEZO BUZZERS

There are two types of piezo devices that produce a sound.
They are called **PIEZO DIAPHRAGMS** and **PIEZO BUZZERS**.
A **piezo diaphragm** consists of two metal plates with a ceramic material between. The ceramic expands and contracts when an alternating voltage is placed on the two plates and this causes the main plate to "dish" and "bow."
This creates a high-pitched sound. There are no other components inside the case and it requires an AC voltage of the appropriate frequency to produce a sound.
A **piezo buzzer** has a transistor and coil enclosed and when supplied with a DC voltage, the buzzer produces a sound.
Both devices can look exactly the same and the only way to tell them apart is by connecting a 9v battery. One device may have "+' and "-" on the case to indicate it is a piezo buzzer, but supplying 9v will make the buzzer produce a sound while the piezo diaphragm will only produce a "click."

PIEZO DIAPHRAGM PIEZO BUZZER

A piezo diaphragm will produce a click
when connected to 9v DC.
A piezo buzzer will produce a tone when
connected to a DC voltage.

How a PIEZO BUZZER WORKS

A Piezo Buzzer contains a transistor, coil, and piezo diaphragm and produces sound when a voltage is applied. The buzzer in the circuit above is a PIEZO BUZZER.

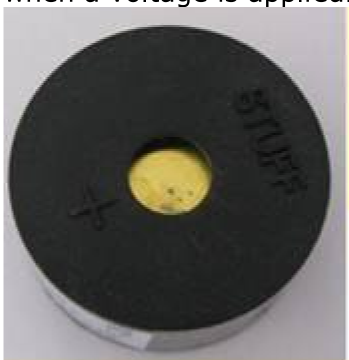

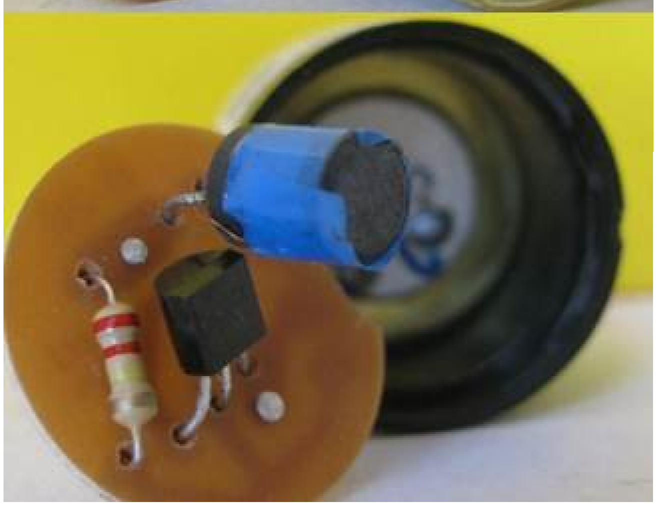

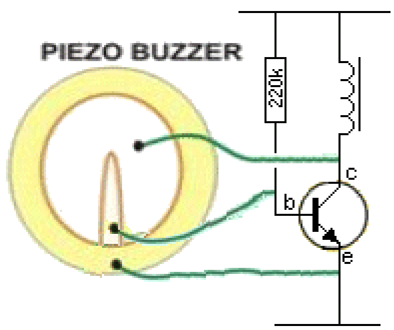

The circuit starts by the base receiving a small current from the 220k resistor. This produces a small magnetic flux in the inductor and after a very short period of time the current does not increase. This causes the magnetic flux to collapse and produce a voltage in the opposite direction that is higher than the applied voltage.

3 wires are soldered to pieces of metal on the top and bottom sides of a ceramic substrate that expands sideways when it sees a voltage. The voltage on the top surface is passed to the small electrode and this positive voltage is passed to the base to turn the transistor ON again. This time it is turned ON more and eventually the transistor is fully turned ON and the current through the inductor is not an INCREASING CURRENT by a STATIONARY CURRENT and once again the magnetic flux collapses and produces a very high voltage in the opposite direction. This voltage is passed to the piezo diaphragm and causes the electrode to "Dish" and produce the characteristic sound. At the same time a small amount is "picked-off" and sent to the transistor to create the next cycle.

TESTING A SPEAKER

A speaker (also called a **loud speaker**) has coil of wire wrapped around a magnet but it does not

touch the magnet as it is wound on a thin cardboard former so that the coil will be pulled closer to the magnet when a current flows in the coil.
When the current flows in the other direction, the coil moves away from the magnet.
The coil is called voice coil and it is connected to a sheet of thin card called a CONE and as the cone vibrates, the speaker reproduces music or noise.
Use a multimeter on a low ohms scale to read the value of resistance of the coil.
It can be as low as 2 ohms or as high as 100 ohms.
Most speakers have an 8R voice coil and the actual resistance may be slightly lower than this.
Some speakers have a resistance of 16R, 32R or 50R and even 75 ohms.
You would think putting a 16R speaker in place of 8R would reduce the sound output, but this is not always the case.
You can even use 50R or 75R and get the same performance.
This may sound amazing, but here is the reason.
The cone is deflected a certain amount due to the current flowing and the number of turns.
These two values are multiplied together to produce a value called AMP-TURNS.
If we have an 8R speaker with 80 turns and 100mA, the result is 0.1 x 80 = 8.
If we use a 16R speaker, the average current flow will be 50mA and the number of turns will be about 160. The multiplication of 0.05 x 160 = 8.
The author then tried a 50R speaker and the sound output was equal to 8R and the same with 75R speaker.
This might not apply in all situations, but the 75R speaker was slightly larger and the ticking sound form the **Metal Detector** kit was louder than using an 8R mini speaker.

To see if the cone of a speaker is undamaged, push it slightly and it will move towards the magnet. If it does not move, it is bent or damaged. If the cone is scratchy when pushed, it is rubbing against the magnet.
A cone should be able to be pushed and pulled from its rest-state. If not, it will produce a distorted sound.

TESTING A CIRCUIT

Whenever you test a circuit, the TEST EQUIPMENT puts "a load" or "a change" on it. It does not matter if the test equipment is a multimeter, Logic Probe, CRO, Tone Injector or simply a LED and resistor.
There are two things you need to know.
1. The IMPEDANCE of the circuit at the location you are testing, and
2. The amount of load you are adding to the circuit via the test equipment.

There is also one other hidden factor. The test equipment may be injecting "hum" due to its leads or the effect of your body at absorbing hum from the surroundings or the test equipment may be connected to the mains.
These will affect the reading on the test equipment and also any output of the circuit.
Sometimes the test equipment will prevent the circuit from working and sometimes it will just change the operating conditions slightly. You have to be aware of this.
The last section of this eBook covers High and Low Impedance and understanding impedance is something you need to know.
The point to note here is the fact that the equipment (and the reading) can be upset by hum and resistance/capacitance effects of test equipment. This is particularly critical in high impedance and high frequency circuits.

TESTING INTEGRATED CIRCUITS (IC's)

Integrated Circuits can be tested with a LOGIC PROBE. A Logic Probe will tell you if a line is HIGH, LOW or PULSING.
Most logic circuits operate on 5v and a Logic Probe is connected to the 5v supply so the readings are accurate for the voltages being tested.
A Logic Probe can also be connected to a 12v CMOS circuit.
You can make your own Logic Probe and learn how to use it from the following link:

http://www.talkingelectronics.com/projects/LogicProbeMkIIB/LogicProbeMk-IIB.html

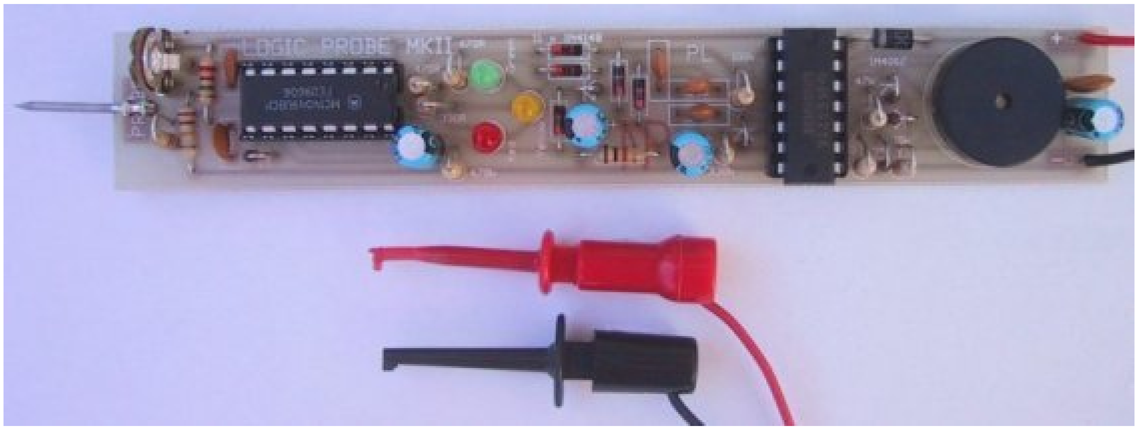

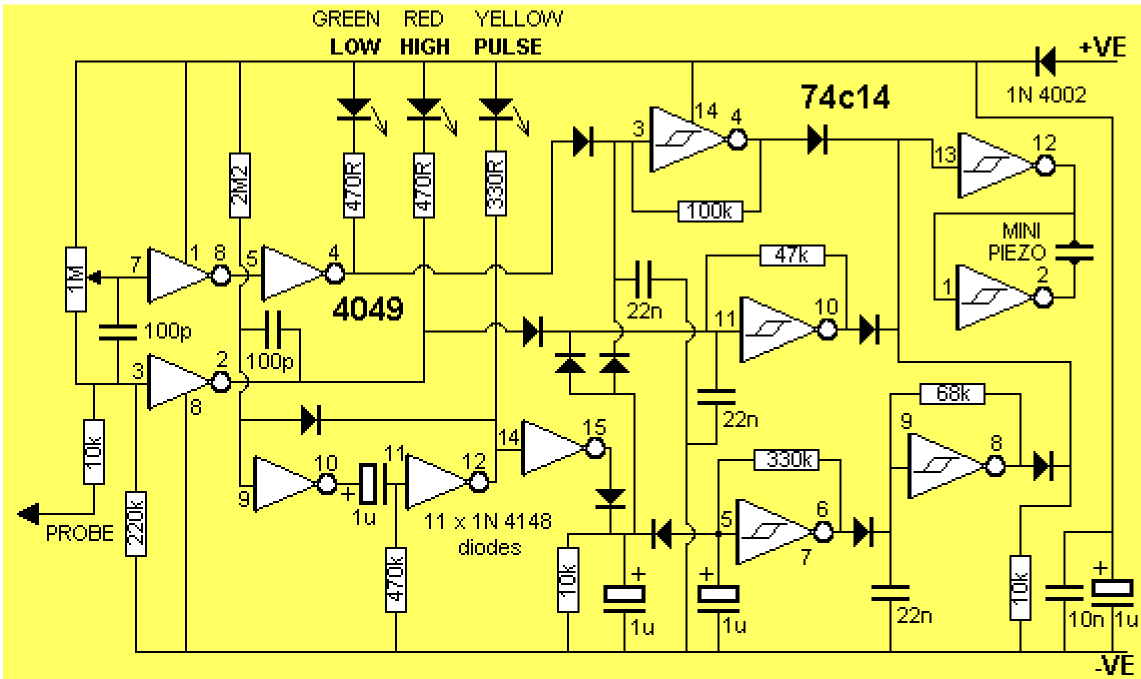

LOGIC PROBE with PULSE

This is a very simple transistor circuit to provide HIGH-LOW-PULSE indication for digital circuits. It can be built for less than $5.00 on a piece of matrix board or on a small strip of copper clad board if you are using surface mount components. The probe will detect a HIGH at 3v and thus the project can be used for 3v, 5v and CMOS circuits.

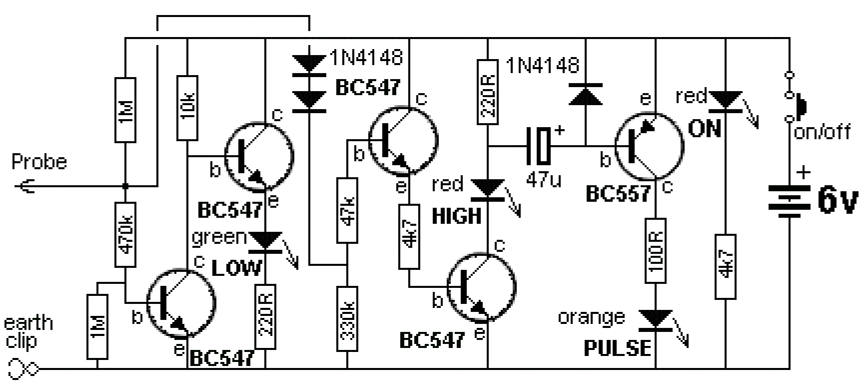

LOGIC PROBE using CD4001 and CD4011

Here is a simple Logic Probe using a single chip. The circuits have been designed for the **CD4001** CMOS quad NOR gate and **CD4011** CMOS NAND gate. The output has an active buzzer that produces a beep when the pulse LED illuminates (the buzzer is not a piezo-diaphragm but an active buzzer containing components).

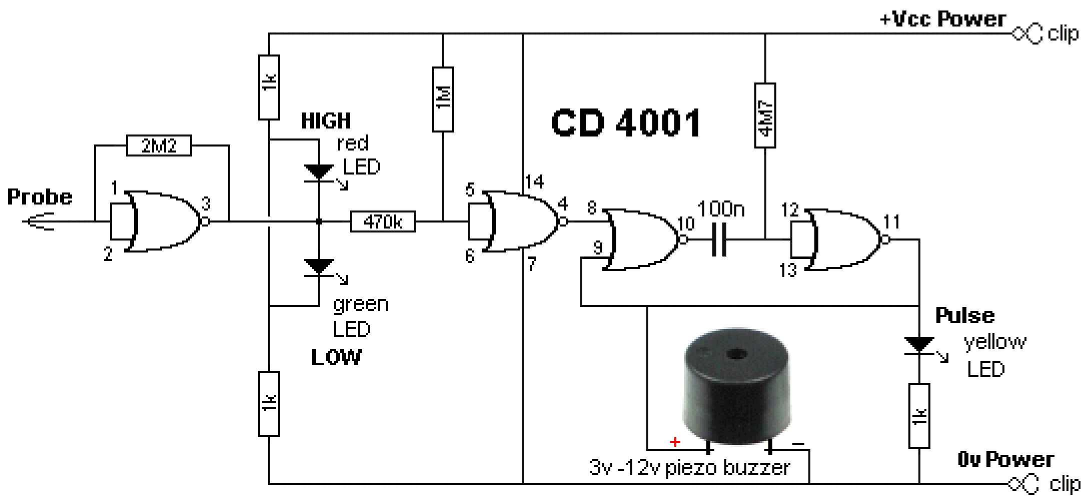

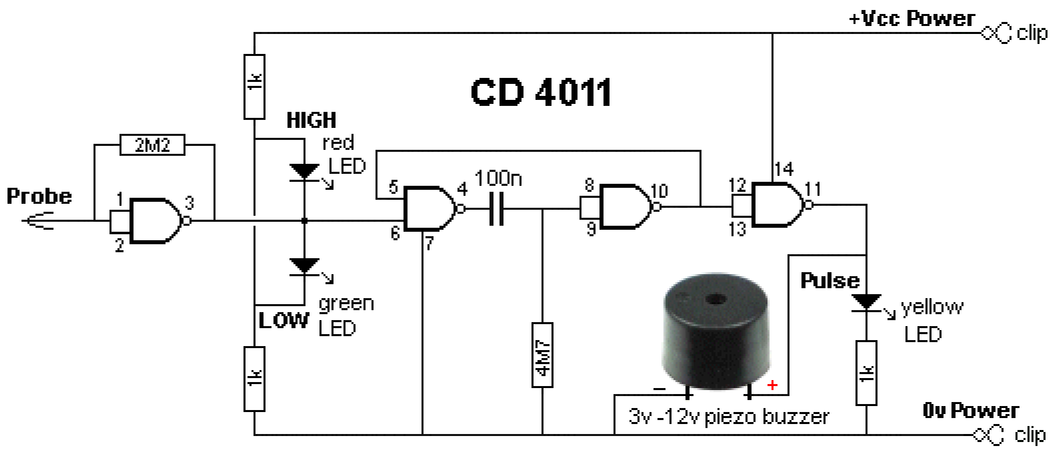

SUPER PROBE MkII has 20 different features including a Logic Probe, capacitance tester, Inductance tester, and more.

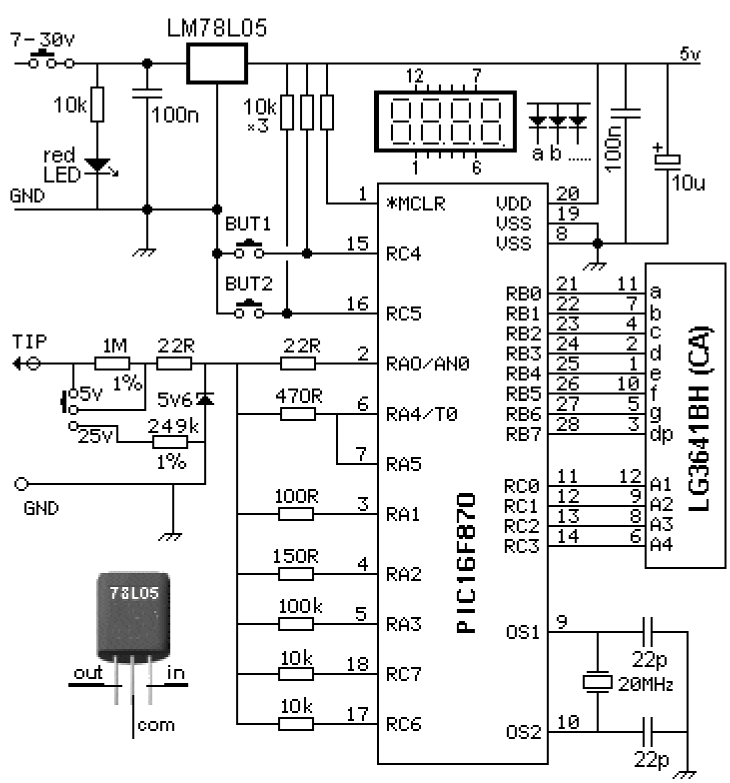

SUPER PROBE MkII Circuit

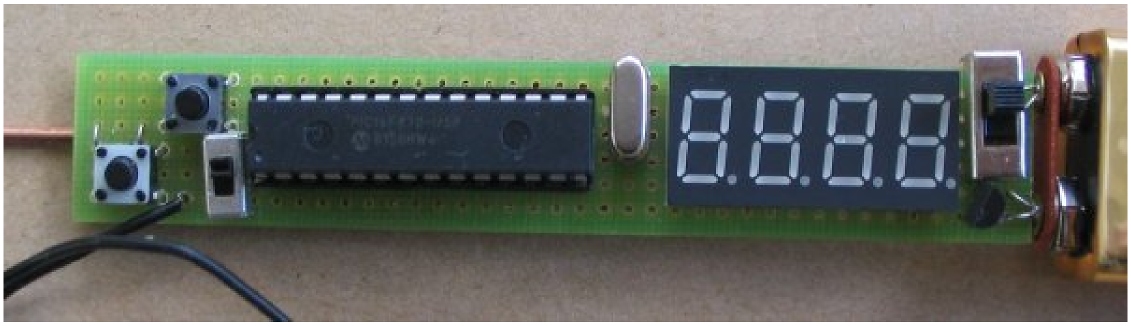

SUPER PROBE MkII

To test an IC, you need a circuit diagram with waveforms. These diagrams will show the signals and are very handy if a CRO (cathode ray Oscilloscope) is used to diagnose the problem. The CRO will reproduce the waveform and prove the circuit is functioning correctly.
A Logic Probe will just show activity and if an output is not producing a "pulse" or "activity," you should check the power to the IC and test the input line.
It is beyond the scope of this eBook to explain how to diagnose waveforms, however it is important to know if signals are entering and exiting an IC and a Logic Probe is designed for this.

SIGNAL INJECTOR
This circuit is rich in harmonics and is ideal for testing amplifier circuits. To find a fault in an amplifier, connect the earth clip to the 0v rail and move through each stage, starting at the speaker. An increase in volume should be heard at each preceding stage. This Injector will also go through the IF stages of radios and FM sound sections in TV's.

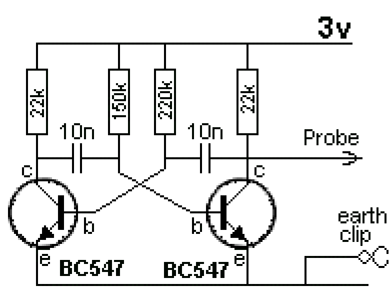

TESTING AUDIO AMPLIFIERS and AUDIO IC's
The **Super Probe MII** described above has a "noise" function and a tone function that allows you to inject a signal into an audio stage, amplifier (made from discrete components) or an audio chip, and detect the output on a speaker.
Audio stages are very difficult to work-with if you don't have a TONE GENERATOR or SIGNAL INJECTOR.
The signals are very small and not detected by a multimeter.
You can start anywhere in an amplifier and when a tone is heard, you can keep probing until the signal is not present or louder. From this you can work out which way the signal is travelling.
A Signal Injector is very handy for finding shorts and broken wires in switches, plugs, sockets and especially leads to headphones.
You can determine the gain of a stage (amplification) by probing before and after a chip or transistor and listen for the relative increase in volume from the speaker.
You can also use your finger to produce "hum" or "buzz" if a **Signal Injector** is not available.
Nearly all audio problems are plugs, sockets and cracks in the PC board, but finding them takes a lot of time and skill.

TESTING IC's - also called "CHIPS"

An Integrated Circuit is also called a "chip." It might have 8 pins or as many as 40. Some chips are ANALOGUE. This means the input signal is rising and falling slowly and the output produces a larger version of the input.
Other chips are classified as DIGITAL and the input starts at 0v and rises to rail voltage very quickly. The output does exactly the same - it rises and falls very quickly.
You might think the chip performs no function, because the input and output voltage has the same value, but you will find the chip may have more than one output and the others only go high after a number of clock-pulses on the input, or the chip may be outputting when a combination of inputs is recognised or the output may go HIGH after a number of clock pulses.

ANALOGUE CHIPS (also see above)
Analogue chips are AUDIO chips or AMPLIFIER chips.
To test these chips you will need three pieces of test equipment:
1. A multimeter - this can be digital or analogue.
2. A Signal Injector
3. A Mini Bench Amplifier.

The Mini Bench Amplifier is available as a kit.

MINI BENCH AMPLIFIER

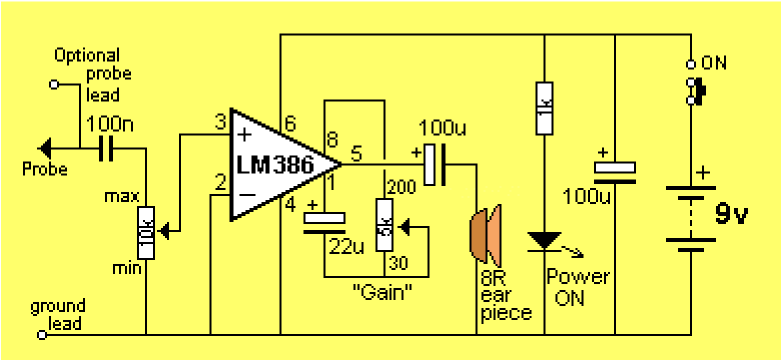

MINI BENCH AMPLIFIER CIRCUIT

Start by locating the power pin with a multimeter.
If the chip is receiving a voltage, you can use the Mini Bench Amplifier to detect an output.
Connect the Ground Lead of the Mini Bench Amplifier to 0v and touch the Probe tip on each of the pins.
You will hear faint audio on the Input pin and very loud audio on the Output pin.
If no input is detected, you can use a Signal Injector to produce a tone.

Connect the clip of the Signal Injector to 0v and the probe to the input pin of the amplifier chip. At the same time, connect the Mini Bench Amplifier to the output pin and you will hear a very loud tone.
These pieces of test equipment can also be used to diagnose an amplifier circuit constructed with individual components.
Amplifier circuits using discrete components are very hard to trouble-shoot and these pieces of test equipment make it very easy.

DIGITAL CHIPS

It is always best to have data on the chip you are testing, but if this is not available, you will need three pieces of equipment:
1. A multimeter - this can be digital or analogue.
2. A Logic Probe,
3. A logic Pulser.
Firstly test the chip to see if power is being delivered. This might be anything from 3v3 to 15v.
Place the negative lead of the multimeter on the earth rail of the project - this might be the chassis, or the track around the edge of the board or some point that is obviously 0v.
Try all the pins of the chip and if you get a reading, the chip will have "supply."
Identify pin 1 of the chip by looking for the "cut-out" at the end of the chip and you may find a small dimple below the cut-out (or notch). This is pin 1 and the "power pin" can be directly above or any of the other pins.
Next you need to now if a signal is entering the chip.
For this you will need a LOGIC PROBE.
A Logic Probe is connected to the same voltage as the chip, so it will detect a HIGH and illuminate a red LED.
Connect the Logic Probe and touch the tip of the probe on each pin.
You will not know if a signal is an input or output, however if you get two or more active pins, you can assume one is input and the other is output. If none of the pins are active, you can assume the signal is not reaching this IC.
If only one pin is active, you can assume the chip is called a CLOCK (or Clock Generator). This type of chip produces pulses. If more than two pins are active, you can assume the chip is performing its function and unless you can monitor all the pins at the same time, you don't know what is happening.
This is about all you can do without any data on the chip.

If you have data on the chip, you can identify the input(s) and output(s).
A Logic Probe on each of these pins will identify activity.
A Logic Probe has 3 LEDs. Red LED indicates a HIGH, Green indicates a LOW and Orange indicates a PULSE (activity).
Some Logic Probes include a piezo and you can hear what is happening, so you don't take your eyes off the probe-tip.
It is important not to let the probe tip slip between the pins and create a short-circuit.

LOGIC PULSER
If you have a board or a single chip and want to create activity (clock pulses), you can use a Logic Pulser. This piece of test equipment will produce a stream of pulses that can be injected into the clock-line (clock input) of a chip.
You can then use a Logic Probe at the same time on the outputs to observe the operation of the chip.

You can also use the Mini Bench Amplifier to detect "noise" or activity on the inputs and outputs of digital chips.
This only applies if the frequency is in the audio range such as scanning a keyboard or switches or a display.

This is how to approach servicing/testing in a general way. There are thousands of digital chips and if you want to test a specific chip for its exact performance, you will need to set-up a "test-bed."

REMOTE CONTROLS

There are two types of remote control - Infrared and RF. Infrared is used for short-range, line-of-sight for TV's DVD's etc.
A few faults can be fixed, but anything complex needs a new remote control.
Check the batteries and battery-contacts. See if the IR LED is illuminating by focusing it into a digital camera and looking on the screen for illumination.
The only other things are a sticky button, a worn-out button or a crack in the PC board. Water damage is generally too much work to repair.
RF remote controls for cars, garage doors etc need a second working unit to check the power output.
Here is a simple circuit that can be connected to an analog multimeter to detect the signal strength at a very close range:

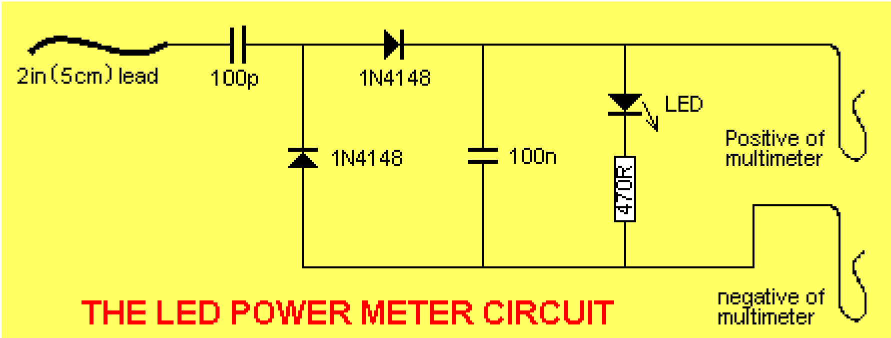

To hear the tone from a transmitter, the **Mini Bug Detector** circuit can be used:

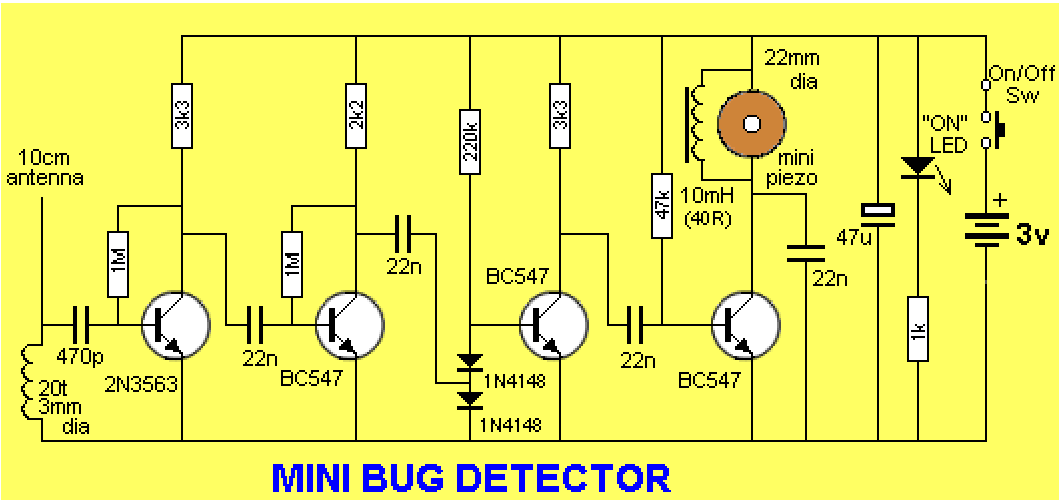

Any further investigation requires a circuit diagram so you can work out what is actually being sent from the transmitter.
Most of the time it is a faulty switch, battery or contacts. Make sure the setting is correct on the "dip switches" and use a working unit to compare all your testing.

TESTING VOLTAGES ON (in) A CIRCUIT

There are basically two different types of circuit.
1. **ANALOGUE CIRCUIT**
An analogue circuit can also be called an AUDIO CIRCUIT and the voltages at different points in a circuit can be measured with a multimeter but the changes (the waveforms) will be quite small or changing at a rapid rate and cannot be detected by a multimeter.
You need a CRO to "see" the signals or a **Signal Injector** to inject a waveform into the circuit and hear the result on the circuit's speaker.

2. **DIGITAL CIRCUIT**
A digital circuit can also be called a "Computer Circuit" or "Logic Circuit" and some of

the voltages can be measured with a multimeter (such as supply voltages) but the "signal lines" will be be changing from HIGH to LOW to HIGH very quickly and these signals are detected with a **Logic Probe**.

Here are some circuits with details of how to test the voltages.
Most circuits do not show voltages at various different points and we will explain what to expect on each "stage."

A "STAGE"

A stage is a set of components with an input and output. A "stage" can also be called a "Building Block."
Sometimes it has a capacitor on the input and one on the output.
This means the stage is completely isolated as far as DC is concerned.
The stage has a supply (a DC supply) and it is producing its own voltages on various points on the "stage." It can only process (amplify) "AC." (signals).
Sometimes the stage can be given a name, such as small-signal amplifier, push-pull amplifier or output.
If the stage has a link or resistor connected to a previous stage, the previous stage will have a "DC effect" on the stage. In other words it will be biasing or controlling the voltages on the stage. The stage may be called a "timer" or "delay" or "DC amplifier."

It is important to break every circuit into sections. This makes testing easy. If you have a capacitor at the input and output, you know all the problems lie within the two capacitors.
In a digital circuit (no capacitors) you need to work on each IC (integrated Circuit) and test the input for activity and all the outputs.

Once you have determined if the circuit is Analogue or Digital, or a combination of both, you have to look at the rail voltage and work out the size or amplitude of the voltage or waveform.
This is done before making a test, so your predictions are confirmed.
You will need a **multimeter** (either Digital or Analogue) a **Logic Probe** and a **Signal Injector** (**Tone Generator**). An analogue meter has the advantage that it will detect slight fluctuations of voltage at a test-point and its readings are faster than a digital meter. A digital meter will produce an accurate voltage-reading - so you should have both available.

HIGH IMPEDANCE AND LOW IMPEDANCE

Every point in a circuit has a characteristic called "IMPEDANCE." This has never been discussed before in any text book. That's why it will be new to you.
In other words, every point will be "sensitive to outside noise."
An audio amplifier is a good example. If you put your finger on the active input, it will produce hum or buzz in the speaker. This is because it is a HIGH IMPEDANCE line or high impedance section of the circuit.
The same applies to every part in a circuit and when you place Test Equipment on a line for testing purposes, the equipment will "upset" the line. It may be very slight but it can also alter the voltage on the point CONSIDERABLY.
We have already mentioned (above) how a cheap multimeter can produce a false reading when measuring across a 1M resistor. That's why you need high impedance test Equipment so you do not "load" the point you are testing and create an inaccurate reading.
The word **Impedance** really means resistance, but when you have surrounding components such as diodes, capacitors, transistors, coils, Integrated Circuits, supply-voltages and resistors, the combined effect is very difficult to work out as a "resistance" and that's why we call it "Impedance."
The term "**High and Low Impedance**" is a relative term and does not have any absolute values but we can mention a few points to help you decide.
In general, the base of a transistor, FET input of an IC are classified as HIGH IMPEDANCE.
The output of these devices are LOW IMPEDANCE.

Power rails are LOW IMPEDANCE.
An oscillator circuit and timing circuit are HIGH IMPEDANCE.
A LOAD is low impedance.
And it gets tricky: An input can be designed to accept a low-impedance device (called a transducer or pick-up) and when the device is connected, the circuit becomes LOW impedance, but the input circuitry is actually high impedance.
The impedance of a diode or LED is HIGH before the device sees a voltage higher than the junction voltage and then it becomes LOW Impedance.
Impedance is one of the most complex topics however it all comes down to testing a circuit without loading it.
That's why test equipment should have an input impedance higher than 1M.

The first circuit we will investigate is the **Mini Bug Detector**, shown above and below. Points on the circuit have been labelled A, B, C etc:

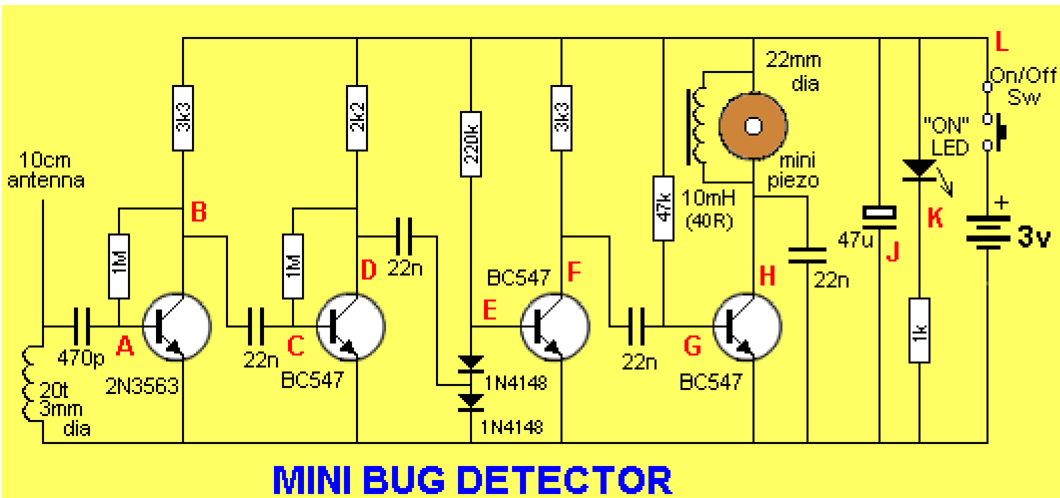

Point A - The first transistor is "self-biased" and will have 0.6v on the base. The antenna is connected to a 20 turn coil and you might think the coil will "short" the signals to earth.
But the coil and 470p capacitor form a circuit that oscillates at a high frequency when the antenna wire picks up stray signals. The coil and capacitor actually amplify the signals (see Talking Electronics website: [Spy Circuits]() to see how a TANK CIRCUIT works) and these signals enter the base of the first transistor.
This is classified as a HIGH Impedance section because the signals are small and delicate and any loading via test equipment will kill them. The first transistor amplifies the signals about 70 times and they appear at **Point B**.

The signal passes though a 22n to **Point C** and the transistor amplifies the signal about 70 times to **point D**. **Point C** is classified as high impedance as any voltage measurement at this point will upset the biasing of the stage as a few millivolts change in base-voltage will alter the voltage on the collector considerably. **Point D** is classified as low impedance as any voltage-testing will not alter the voltage appreciably.
The output of the second stage passes through a capacitor to the join of two diodes. These two diodes are not turned on because the voltage at **Point E** can never rise above 0.7v as this is the voltage produced by the base-emitter of the third transistor.
The purpose of the two diodes is to remove background noise. Background noise is low amplitude waveforms and even though the transistor is turned on via the 220k, low amplitude signals will not be received. The third transistor works like this: It cannot be turned ON any more because any waveform from the 22n will be "clipped" by the bottom diode and it will never rise above 0.6v.
So, the only signal to affect the transistor is a negative signal - to turn it OFF.
Firstly we have to understand the voltage on the 22n. When the second transistor is sitting at mid-rail voltage, the 22n gets charged via the 2k2 and lower diode. When

the transistor gets tuned ON, the collector voltage falls and the left side of the 22n drops. The right side of the 22n also drops and when it drops 0.6v, the top diode starts to conduct and when the voltage on the 22n drops more than 0.6v the third transistor starts to turn OFF. This effect is amplified by the transistor at least 100 times and appears at **Point F.** All the voltages around the two diodes are classified as HIGH Impedance as any piece of test equipment will upset the voltage and change the output.
There are some losses in amplitude of the signal as it passes through the 22n coupling capacitors but the end result is a very high strength signal at **point G.** The 4th transistor drives a 10mH choke and the mini piezo is effectively a 20n capacitor that detects the "ringing" of the inductor to produce a very loud output.
The 22n capacitor on the collector eliminates some of the background noise. The choke and piezo form an oscillatory circuit that can produce voltages above 15v, even though the supply is 3v.
The 47n capacitor at **Point J** is to keep the supply rails "tight" (to create a LOW Impedance) to allow weak cells to operate the circuit.
The "Power-ON" LED tells you to turn the device off when not being used and **Point L** is the power supply - a low impedance line due to the 47u electrolytic.

Testing the Mini Bug Detector
To test the Mini Bug Detector, you will need a Signal Injector.
Place the Injector on **Point G** and you will hear a tone. Then go to **E**, **C** and **A**. The tone will increase in volume. If it does not increase, you have pin-pointed the faulty stage.

The next circuit is a combination of digital and analogue signals. It is a **Logic Probe**:

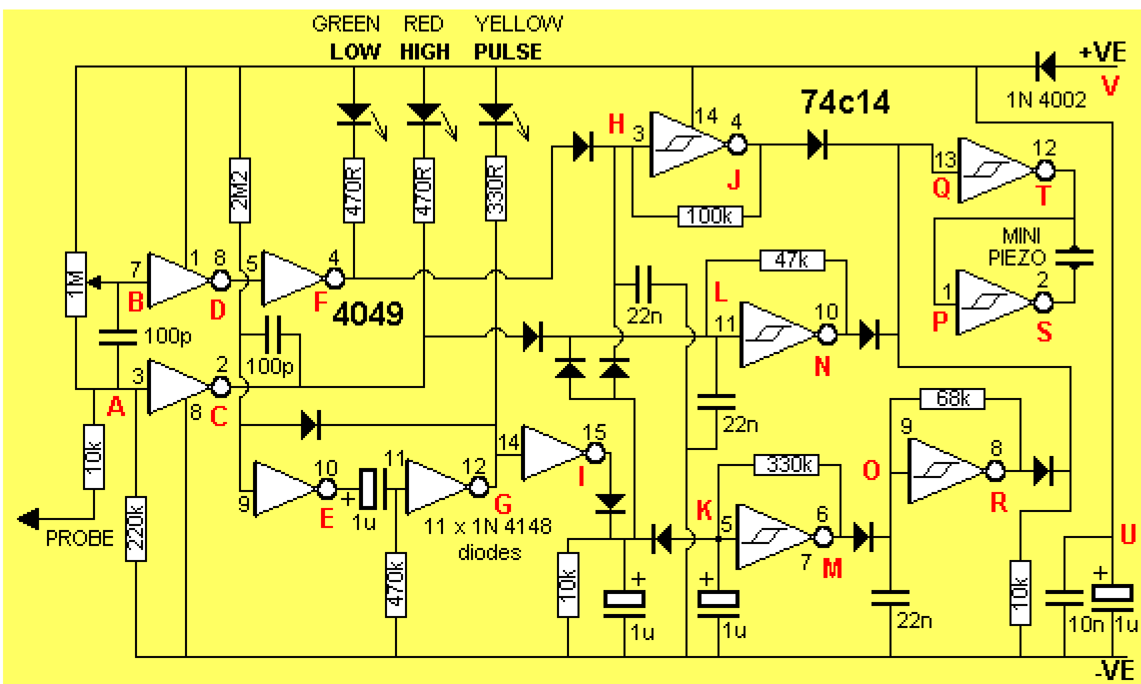

The voltage on a circuit (to be tested) is detected by the probe at **Point A** of the circuit above and the "tip" is classified as "reasonably high impedance" as it has a 220k resistor between the tip and 0v rail. The 1M reduces the impedance by about 20% but the inputs of the two inverters have no effect on the "tip" impedance as they are extremely high input-impedance devices.
The 1M trim pot is designed to put put a voltage on **point B** that is slightly higher than mid-rail so the green LED is turned off.
Point A will see a voltage below mid-rail and **point C** will be HIGH. **Point C** and **F** are low-impedance outputs.
When the tip of the probe is connected to a LOW voltage, Point B sees a LOW and Point F goes LOW to illuminate the green LED. At the same time it removes the "jamming voltage" produced by the diode between pin 4 of the 4049 and pin 3 of the

74C14 and the oscillator between **points H and J** produces a low-tone via the 100k resistor and 22n to indicate a LOW.
When the probe tip sees a HIGH, a lot more things happen.
Point C goes LOW and turns on the red LED. At the same time the 100p is in an uncharged state and the right lead goes LOW. This takes the left lead LOW as the left lead connects to a HIGH Impedance line and pin 9 goes LOW. This makes **point E** HIGH
and since the 1u is in an uncharged state, pin 11 goes HIGH. This makes **point G** LOW and the diode between pins 9 and 12 keeps pin 9 LOW and takes over from the pulse from the 100p. The yellow LED is illuminated. The 1u starts to charge via the 470k and when it is approx half-charged, pin 11 sees a HIGH and **point G** goes low. This creates the length of pulse for the yellow LED.
At the same time, **Point L** goes LOW because the "jamming diode" from pin 2 of the 4049 goes low and allows the inverter between point L and N to produce a tone for the piezo.
In addition, **Point I** goes HIGH and quickly charges a 1u electrolytic. This removes the effect of the jamming diode on pin 5 of the 74C14 and a low frequency oscillator made up of 68k and 1u between pins 5&6 turns on and off an oscillator between **points O** and **R** to get a beep. The mini piezo is driven n bridge mode via the two gates between **points QT** and **PS**.
Point U is a 1u electrolytic to reduce the impedance of the power rail and **Point V** is a protection diode to prevent damage if the probe is connected to the supply around the wrong way.

Testing the Logic Probe
You can test the Logic Probe with the simple Logic Probe with Pulse project described above. It will let you know if each point in the circuit is HIGH or LOW. You will also find out the difficulty in testing the points that are HIGH Impedance, as the Probe will upset the voltage levels and the reading may be inaccurate.

More circuits will be added here in the future.

THE VOLTAGE DIVIDER - this topic could fill a book.
You need to read lots of other sections in this eBook, including the section on measuring across a resistor with a multimeter, and high impedance circuits, to fully understand the complexities of a VOLTAGE DIVIDER CIRCUIT.
It is one of the most important BUILDING BLOCKS to understand. Even though it may consists of two components, you have to understand what is happening between these two components. You have to realise there is a voltage at their join that will be rising and falling due to one of the components changing RESISTANCE.
Sometimes you can work out the voltage at the join by using Ohm's LAW but quite often it will be impossible as it is changing (rising and falling) during the operation of the circuit.
At the beginning of this discussion we will only dealing with DC circuits and the voltage across a particular component will be due to its RESISTANCE. We are not going into any formulas, as it is very easy to measure the voltages with a multimeter set to VOLTS and you will have an accurate result.
The simplest two components in series are resistors. They always have the same resistance during the operation of a circuit and the voltage across each will not change.
In a further discussion we will cover "resistors" that change value according to the temperature. These are called THERMISTORS. And we have "resistors" that change value according to the light they receive. These are called LIGHT DEPENDENT RESISTORS (LDR's) or PHOTO RESISTORS.
A transistor that is partly or fully turned ON can be considered to be similar to a resistor.
In these 3 cases we need to measure the voltage at the join with a voltmeter as it will be a lot of work to measure the resistance and work out a value.
You can also keep a voltmeter on the joint and watch the voltage change.
Finally we have some components that produce a fixed voltage across them (or nearly fixed) and the remaining voltage is dropped across a resistor. These

components MUST have a resistor connected in series to limit the current and allow the component to pass the specified in the datasheet.
These devices include LEDs, diodes and zener diodes. A LED will have a fairly fixed voltage across it from 1.7v to 3.6v depending on the colour. A diode will have a voltage of 0.7v across it when it is connected to a voltage via a resistor. And a zener diode will have a fixed voltage across it when it is connected with the cathode to the positive rail via a resistor. The voltage across it will be as marked on the zener.
The concept of a VOLTAGE DIVIDER is very simple, but it takes a lot of understanding because both VOLTAGE and CURRENT are involved in the UNDERSTANDING-PROCESS.
Each component has a resistance and this can be measured with a multimeter. When two components are connected in series, a current will flow and a voltage will develop across each item.
More voltage will develop across the item with the higher resistance and the addition of each voltage will always equal the supply voltage.
That's the simple answer.
There is a little more involved . . . It is the word CURRENT. Here is an explanation:
Suppose we have a 1k and 2k resistor on a 12v supply. The voltage at the join will be 4v.
In other words, there will be 4v across the 1k and 8v across the 2k.
If we have a 10k and 20k resistors in series, the voltage will also be 4v at the join.
If we have a 100k and 200k resistors, the voltage will also be 4v at the join.
The voltage will be the same in all cases, but the current will be different. The current in the second case will be one-tenth and only one hundredth in the third case.
If you want to go further, place a one ohm and two ohm in series and get 4v. But the resistors will get very hot and burn out very quickly.

SOLDERING

Here are three 30-minute videos on soldering.
1. **TOOLS**
2. **Soldering components**
3. Soldering **SURFACE MOUNT** components

TESTING A MOTOR

Strictly speaking, a motor is not an electronic component, but since a website gave a useless description on testing motors, I have decided to supply the correct information.
The only REAL way to test a motor is to have two identical motors and check the torque by connecting them to a low voltage and trying to stop the shaft with your fingers. This will give you two results. Firstly it will let you know the torque of the motor.
This is the twisting effect of the shaft. There is no way to determine the torque by knowing the voltage or current.
The unknown factor is the strength of the field magnets (permanent magnets) and this determines the torque.
Secondly, feeling the shaft will let you know if the torque is even for a complete revolution.
By having two identical motors, you can see if one has a lower torque.
Almost nothing can go wrong with a motor except for the brushes. If the brushes wear out, additional resistance will be produced at the interface between the brush and commutator and this can be detected by allowing the shaft to rotate slowly and feeling the resistance as it revolves. A 3-pole motor will have three places where the strength is greatest and each should have the same feeling. A 5-pole motor will have five places of strength.
If the strength is weak or not uniform, the motor is faulty.
You cannot test a motor with a multimeter as the resistance of the armature winding is very low and if the motor is allowed to spin, the back voltage produced by the spinning, increases the reading on the meter and is false.

Micro motors have a coreless armature. This means the 3 windings for the armature are wound on a machine then bent slightly into shape and glued. A circular magnet with 3 poles is in the centre and the armature rotates around this.
This type of motor is reasonably efficient because the armature is the greatest distance from the point of rotation, and the motor reaches full RPM very quickly because the armature has very little inertia.
I have not heard of the armature-winding flying apart but if you hear any scraping noise, it may be the winding.
3-pole, 5-pole and micro motors can be found in printers, eject mechanisms of CD players, toys, RC helicopters, cars etc and rarely fail.
Motors do not work on "voltage." They actually work on CURRENT and as you increase the voltage, more current will flow and produce a stronger magnetic field (by the winding on each pole). This magnetic field will be attracted by the permanent magnet surrounding the armature and repelled by the surrounding permanent magnet, depending on where the face of the pole is, during each revolution.
If the permanent magnet is not very strong, the repulsion part of the interaction will be very weak and thus the torque will be small.
Because motors work on "current" you must have a high current available when you increase the voltage as the motor will require short bursts of high current during each revolution.
It is the combination of voltage and current (called watts) that gives the motor "strength" (torque) as well as the "strength" of the permanent magnets (called the field magnets) and the number of turns of wire on each pole (and the gauge of wire).
Basically, if a motor is hard to spin, and has 3 "hard spots" on each revolution, it will be powerful.
A 2-pole motor does not self-start and will spin in either direction. But a 3-pole motor will self-start and you can determine the direction of rotation.
A 5-pole motor has a lower RPM. It is slightly smoother in output but is not more powerful than a 3-pole version.
A motor with "permanent magnets" is called a DC motor as it will not work on AC. If the magnets are replaced with a coil, it will work on AC and it will be called a "shunt wound" motor of the field coil is connected across the same terminals as the brushes or a "series wound" motor if the field coil is in series with the armature.

TESTING COMPONENTS "IN-CIRCUIT"

You can test components while they are IN CIRCUIT, but the surrounding components will have an effect on the results.
You can get all sorts of "In-Circuit" testers. They are expensive and offer little more accuracy than a multimeter.
In-Circuit testing with a multimeter can give you the same results as a tester.
All you have to do is turn the project ON and use a multimeter (set to voltage) to determine the voltage at various points. It is best to have a circuit of the equipment so you can what to expect at each point.
Only major departures from the expected can be located in this way.
Obviously the first thing to look for is burnt-out components. Then feel components such as transistors for overheating.
The look for electrolytics that may be dry. Sometimes these have changed colour or are slightly swollen.
If they are near hot components, they will be dry.
For the cost of a few dollars I change ALL THE ELECTROLYTICS in some pieces of equipment, as a dry electrolytic is very difficult to detect.
Testing a transistor "in-circuit" is firstly done with the supply ON. That's because it is quicker.
Measure the voltage between ground and collector.
In most cases you should get a voltage of about half-rail. If it is zero, or close to rail voltage, you may have a problem.
Turn off the supply and use the multimeter on low-ohms to measure all six resistances between the leads.
A low resistance in both directions on two leads will indicate a fault.
Resistors almost NEVER go "HIGH." For instance, a 22k will never go to 50k.
However a low-value resistor will "burn-out" and you will read the value of the surrounding components.

Don't forget, some low-value resistors are designed to burn-out (called fusible resistors) and anytime you find a damaged low-value resistor, you will need to look for the associated semiconductor.
You can replace the resistor quickly and turn the circuit ON to see it burn out again. Alternatively you can trace though the circuit and find the shorted semiconductor. It's always nice to "see the fault" then "fix the fault."
Sometimes a transistor will only break-down when a voltage is present, or it may be influenced by other components.
When the piece of equipment is turned OFF, you can test for resistance values. The main thing you are looking for is "dry joints" and continuity. Dry joints occur around the termination of transformers and any components that get hot. Rather than wasting time checking for dry joints, it is better to simply go over the connections with a hot iron and fresh solder.
You may need to check the continuity of a track (trace) and it may go from one side of the PC board to the other.
Use a multimeter set to low-ohms and make sure the needle reads "zero-ohms."
It is very dangerous to do any testing on a project using a multimeter set to "amps" or "milliamps."
You cannot test "current flowing through a component" by placing the probes across a component. You will simply over-load the rest of the circuit and create a problem.
To find out if current is flowing though a circuit or a low-value resistor, turn the project ON and measure the voltage either across the component or the voltage on one end then the other.
A voltage-drop indicates current is flowing.
That's about it for testing "in-circuit." Use the rest of this eBook to help you with diagnosis.
Don't think an IN-CIRCUIT COMPONENT TESTER is going to find a fault any faster than a multimeter. They all use a multimeter principle.

SHORT CIRCUIT

Nearly every component can fail and produce an effect called a SHORT CIRCUIT. This basically means the component takes more current than normal and it may fail completely or simply take more current and the operation of the circuit may be reduced only a small amount.
The resistance of the component may reduce a very small amount but this may have a very large effect on the operation of the circuit.
For instance, two turns in the horizontal or vertical winding of a yoke on the picture tube or monitor may arc and weld together and reduce the size of the picture on the screen, but measuring the winding will not detect the difference in resistance.
The same with the windings on a motor and a short between two winding in a transformer.
If the "short" is between two near-by turns, the change in resistance will be very small. If the "short" is between to different layers, the resistance will be reduced and it may be detected.
When a "short" occurs, the winding turns into a transformer. To be exact, an AUTO-TRANSFORMER.
In the following diagram you can see a normal winding in fig A:

A

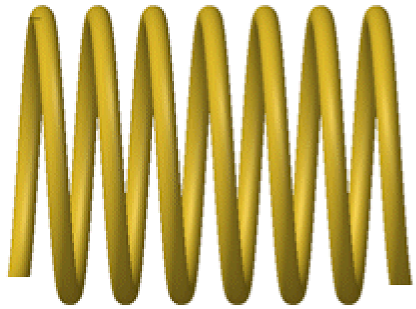

B

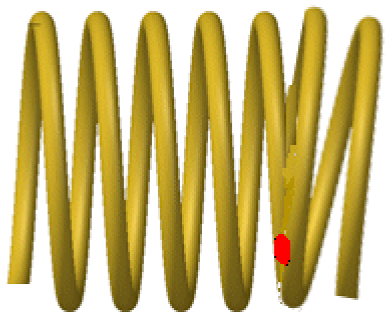

C

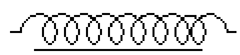

D

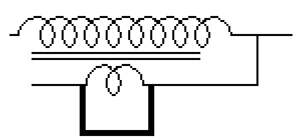

Fig B shows two turns touching each other and if the wire is enamelled, the coating has been damaged so the copper wire from the two turns is touching. This is called a SHORTED TURN.
In fig C you can see two turns touching.
In fig D the shorted-turn has been moved to the other side of the symbol to show the effect it has on the operation of the winding.
The shorted-turn is exactly like the secondary of a transformer with a "jumper" across the output.
This will produce a very high current in the secondary.
A very high current flows through the shorted turn and this changes the operation of the rest of the winding.

1. In most cases a SHORT CIRCUIT can be detected by feeling the additional heat generated by the component.
2. Next, turn off the supply and measure the resistance of the component. If it is lower than expected, the component will be faulty.
3. Next, measure the voltage across the component. If it is lower than normal, the component will be faulty.
4. Next, measure the current taken by the component. If it is higher than normal, the component will be faulty.
5. If the component is an inductor, such as a motor, coil or transformer, you can use an inductance meter. Compare a good winding with a faulty winding. Sometimes the fault will disappear because an arc develops across the fault when the component is operating.

INTERNAL AND EXTERNAL SHORTS

An **internal short** refers to two windings shorting together and the winding has a very high resistance between the winding and the frame on which it is wound. An external short refers to a winding shorting to the frame of the component - such as one of the armature windings shorting to the metal core, around which the wire is

wound.
This may not be important unless another winding shorts to the metal frame and creates "**inter winding**" problems (**inner winding** problems is within the same winding).

The opposite to a short circuit is an OPEN CIRCUIT.

This is generally a broken lead or contact or a wire that has "burnt-out" or been "eaten-away" by acid attack or galvanic action by water and voltage (current).
1. No current will flow when an OPEN CIRCUIT exists.
2. The voltage on each end of the OPEN CIRCUIT will not be the same.
3. Measure the current across the OPEN CIRCUIT and determine if excess current is flowing.
4. Join the two ends of the OPEN CIRCUIT and see if the circuit operates normally.

> HEATSINKS

This is not an electronic component but it can certainly affect the operation of a circuit.
If you cannot hold your fingers on a heatsink, it is getting too hot. This is because the actual location where the heat is being generated is much hotter than the part you are touching.
Transistors and IC's can withstand a high temperature but if they go above this temp, they BLOW UP.
They also have a shorter life when operating at a high temperature.
The secret to a good heatsink is called an INFINITE HEATSINK.
This is the metal frame of a case.
There are lots of charts and data on choosing a heatsink but they don't take into account two factors:
Sometimes a circuit takes a very high current for a short time and this creates a high temperature gradient. This will cause the transistor to get very hot and fail.
The solution is to have two or more transistors in parallel to separate the "heat spots."
The second problem with designing a heatsink is the unknown location of the heatsink and the air-flow. Products placed on a shelf or in a cupboard will get very little air-flow.
Remember: some transistors are mounted on thermal insulators. This means the transistor will have a voltage on it but the heatsink will be zero voltage.
The temperature of the transistor will be MUCH HIGHER than the heatsink under the transistor and the transfer of the heat from the transistor to the heatsink will be very slow. This can be the cause of the transistor failing. Sometimes the transistor will fail because insulation is high temp plastic and it gets brittle. The plastic can carbonise and leak and sometimes a voltage can flash through the insulator. Some amazing things have happened under these transistors and you may need to pull it apart and replace all the insulation.
Finally, feel the heatsink after 15 minutes and feel right up to the transistor. If you cannot touch the transistor, increase the thickness of the heatsink or use two transistors to dissipate the heat.
To design a heatsink, you have to have some idea of the size of a heatsink for the application.
Charts and data can send you in the wrong direction.
Start with a heatsink twice the recommended size and feel the temp after 15 minutes. Put the project in a cupboard and see how the temperature rises.
If possible, connect the heatsink to the metal case to get added dissipation and if you include fan-cooling, remember the fan will eventually gather dust and reduce its efficiency.
It is very difficult to explain how heat passes through a mica washer or plastic washer, but if the transistor has a copper base, the heat transfer has a value of 400. For aluminium it is 200. If it is steel, the transfer has a value of 50. For a mica sheet it is 1 and for plastic it is 0.1
Even though the sheet is very thin, the transfer is a lot less than metal-to-metal transfer.

Most references state the temperature difference is about one degree C for each watt of heat generated by the transistor.
Don't believe anything you read.
Feel the temperature yourself and if you cannot hold your finger on the transistor, fix the problem.

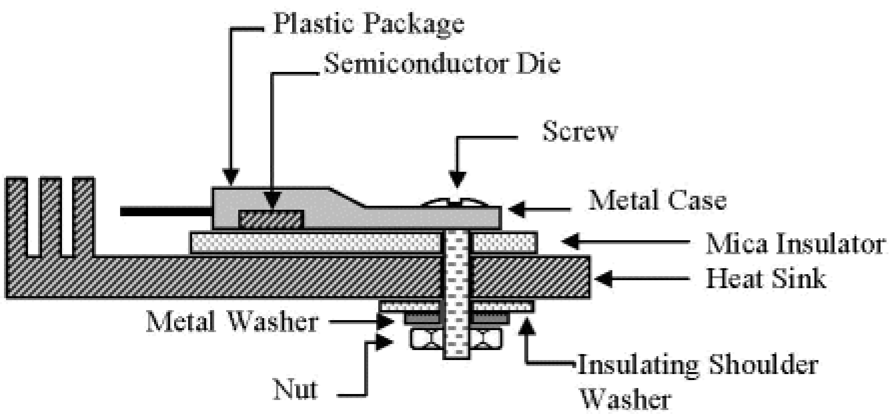

In the end, use a heatsink 50% larger than recommended.

THE END

This is not the full story to learning about servicing. It is just the beginning.
We have only covered the simplest tests and shown how 90% of faults can be found by checking voltages, waveforms and looking for obvious things such as burnt out components, cracks in PC boards.
The author has fixed over 35,000 TV's, radios, stereos, VCRs and all those things that were on the market 30 years ago.
Things have not changed. It's just that some repairs cost nearly as much as buying a new product and half the customers opt for dumping a faulty item and buying the latest "flat screen" version. That's why you have to get things through the workshop as fast and as cheaply as possible, to make a living.

If you want any more devices added to this list, email **Colin Mitchell**.

To help with understanding how a transistor circuit works, we have produced an eBook: **The Transistor Amplifier.** It covers a whole range of circuits using a transistor.

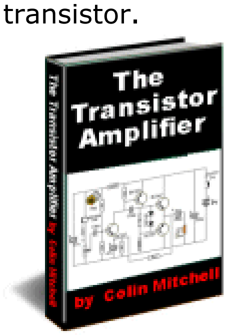

CIRCUIT SYMBOLS by TALKING ELECTRONICS

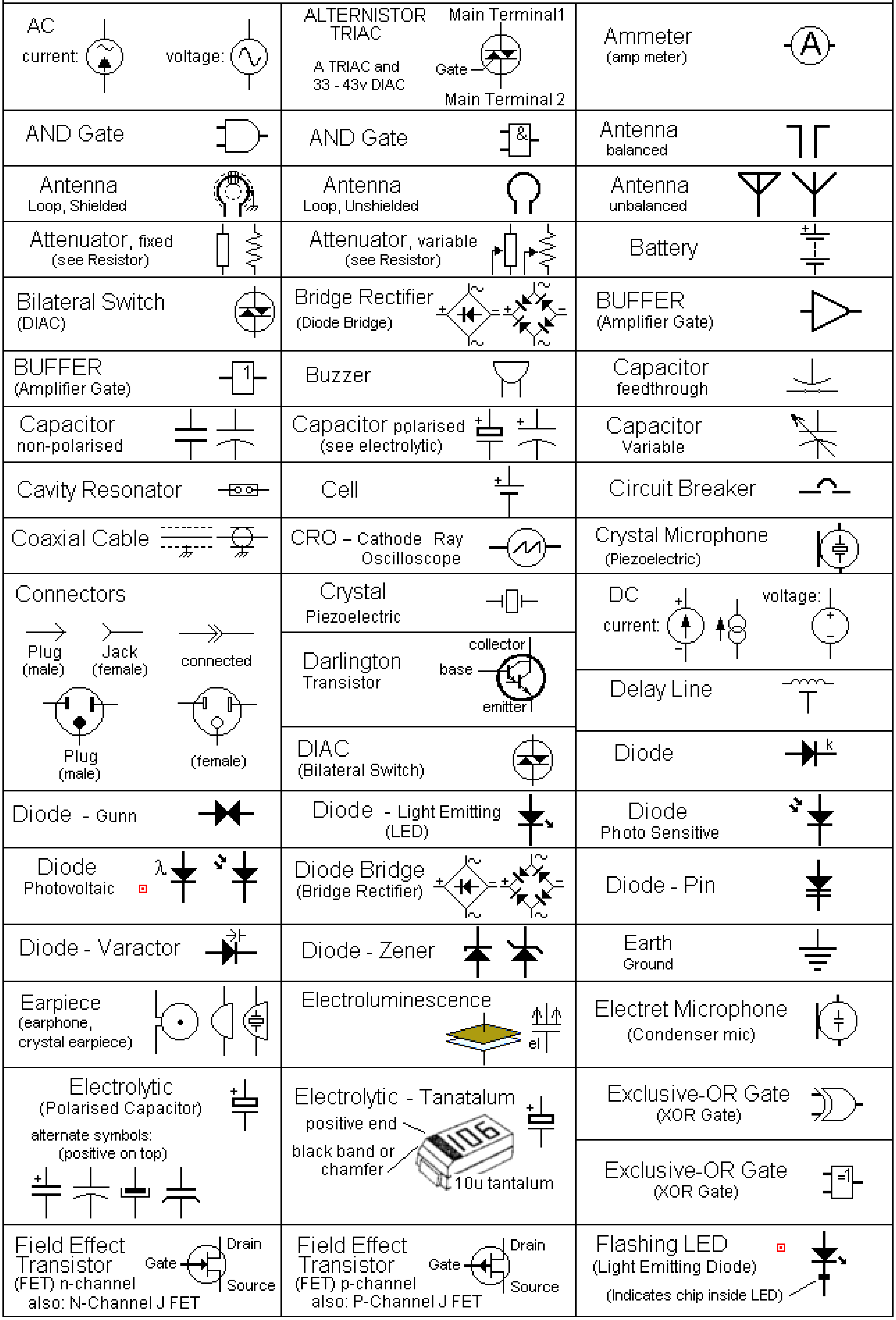

Ferrite Bead	Fuse	Galvanometer G
Globe	Ground Chassis	Ground Earth
Heater (immersion heater) (cooker etc)	IC Integrated Circuit power ground	Inductor Air Core
Headphone		Inductor Iron Core or ferrite core 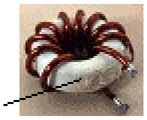
Inductor Tapped	Inductor Variable	Integrated Circuit 
Inverter (NOT Gate)	INVERTER (NOT Gate) 1	
Jack Co-axial	Jack Phone (Phone Jack)	Jack Phone (Switched)
Jack Phone (3 conductor)	Key Telegraph (Morse Key)	Lamp Incandescent
Lamp - Neon	LASCR (Light Activated Silicon Controlled Rectifier)	LDR (Light Dependent Resistor)
LASER diode laser diode photo diode	Light Emitting Diode (LED) 	Light Emitting Diode (LED - flashing) (Indicates chip inside LED)
Mercury Switch	Micro-amp meter (micro-ammeter) µA	Microphone (see Electret Mic) 
Microphone (Crystal - piezoelectric)	Milliamp meter (milli-ammeter) mA	Motor MOT
NAND Gate	NAND Gate &	Nitinol wire "Muscle wire"
Negative Voltage Connection	NOR Gate	NOR Gate ≥1
NOT Gate Inverter	NOT Gate Inverter 1	Ohm meter Ω
Operational Amplifier (Op Amp)	Optocoupler (Transistor output)	Opto Coupler (Opto-isolator) a c k e Photo-transistor output
Optocoupler (Darlington output)	Opto Coupler (Opto-isolator) a c k e TRIAC output	OR Gate
OR Gate ≥1	Oscilloscope see CRO	Outlet (Power Outlet)
Piezo Diaphragm	Photo Cell (photo sensitive resistor) λ	Photo Diode
Photo Darlington Transistor	Photo FET (Field Effect Transistor) Gate Drain Source	Photo Transistor

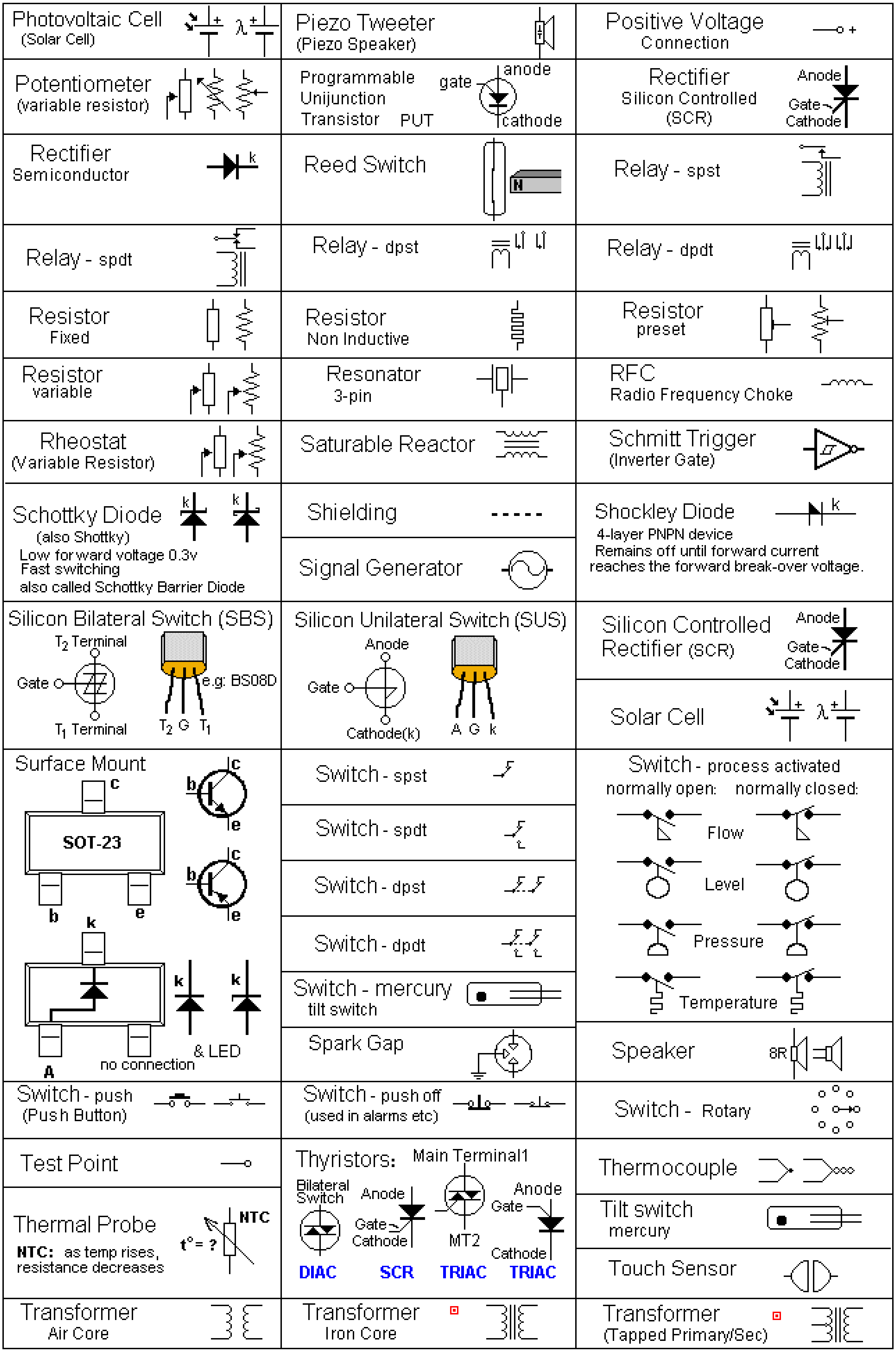

Photovoltaic Cell (Solar Cell)
λ
Piezo Tweeter (Piezo Speaker)
Positive Voltage Connection
Potentiometer (variable resistor)
Programmable Unijunction Transistor PUT
gate
anode
cathode
Rectifier Silicon Controlled (SCR)
Anode
Gate
Cathode
Rectifier Semiconductor
k
Reed Switch
N
Relay - spst
Relay - spdt
Relay - dpst
Relay - dpdt
Resistor Fixed
Resistor Non Inductive
Resistor preset
Resistor variable
Resonator 3-pin
RFC Radio Frequency Choke
Rheostat (Variable Resistor)
Saturable Reactor
Schmitt Trigger (Inverter Gate)
Schottky Diode (also Shottky)
Low forward voltage 0.3v
Fast switching
also called Schottky Barrier Diode
k
Shielding
Shockley Diode
4-layer PNPN device
Remains off until forward current reaches the forward break-over voltage.
Signal Generator
Silicon Bilateral Switch (SBS)
T2 Terminal
Gate
T1 Terminal
e.g: BS08D
T2 G T1
Silicon Unilateral Switch (SUS)
Anode
Gate
Cathode(k)
A G k
Silicon Controlled Rectifier (SCR)
Anode
Gate
Cathode
Solar Cell
Surface Mount
SOT-23
c
b
e
k
A
no connection
& LED
Switch - spst
Switch - spdt
Switch - dpst
Switch - dpdt
Switch - mercury tilt switch
Spark Gap
Switch - process activated
normally open:
normally closed:
Flow
Level
Pressure
Temperature
Speaker
8R
Switch - push (Push Button)
Switch - push off (used in alarms etc)
Switch - Rotary
Test Point
Thyristors:
Main Terminal1
Bilateral Switch
Anode
Gate
Cathode
MT2
DIAC
SCR
TRIAC
TRIAC
Thermocouple
Thermal Probe
NTC: as temp rises, resistance decreases
NTC
t° = ?
Tilt switch mercury
Touch Sensor
Transformer Air Core
Transformer Iron Core
Transformer (Tapped Primary/Sec)

Transistor Bipolar - NPN collector base emitter	Transistor Bipolar - PNP emitter base collector	Transistor n-channel Field Effect Gate Drain Source
Transistor p-channel Field Effect Gate Drain Source	Transistor Metal Oxide Single Gate	Transistor Metal Oxide Dual Gate
Transistor Photosensitive	Transistor Schottky - NPN collector base emitter	Transistor Unijunction - UJT Emitter Base 1 Base 2 Unijunction Transistor (UJT) N-type
Main Terminal1 TRIAC MT2 Anode Gate Cathode	Transistor Unijunction - UJT Emitter Base 1 Base 2 Unijunction Transistor (UJT) P-type	Tunnel Diode Unijunction Transistor - UJT Emitter Base 2 Base 1
Varactor varactor diode	Voltage Regulator (7805 etc)  in 7805 out out common in	Voltmeter V
Wattmeter W P	Wires	Wires Connected
Wires Not Connected	XOR Gate (exclusive OR)	XOR Gate (exclusive OR) =1
Zener Diode k k	Learn **BASIC ELECTRONICS** Go to: http://www.talkingelectronics.com	

More chapters of this eBook on: Talking Electronics.com

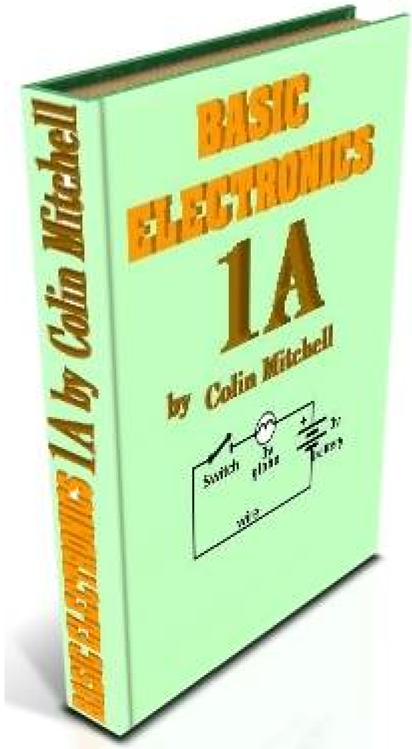

For any enquiries email Colin Mitchell

BASIC ELECTRONICS

(this is the Basic Electronics section i.e. Page 1)
(Chapters 1 and 3 are available as .pdf)

Quick Quiz - to see how much you know
Encyclopedia of Components - this is excellent !!!

Remember: the animations do not work in .pdf
the site is being constantly updated

INDEX

KIT OF PARTS

Talking Electronics supplies a kit of parts that can be used to build the majority of the circuits in this eBook.
The kit costs $15.00 plus postage.

Kit for Transistor Circuits - $15.00

BUY NOW

A kit of components to make many of the circuits described in this eBook is available for $15.00 plus $7.00 post.
Or email Colin Mitchell: talking@tpg.com.au

The kit contains the following components:
(plus **extra** 30 resistors and 10 capacitors for experimenting), plus:

3 - 47R
5 - 220R
5 - 470R
5 - 1k
5 - 4k7
5 - 10k
2 - 33k
4- 100k
4 - 1M
1 - 10k mini pot
1 - 100k mini pot
2 - 10n
2 - 100n
5 - 10u electrolytics
5- 100u electrolytics

5 - 1N4148 signal diodes
6 - BC547 transistors - NPN - 100mA
2 - BC557 transistors - PNP - 100mA
1 - BC338 transistor - NPN - 800mA
3 - BD679 Darlington transistors - NPN - 4amp
5 - red LEDs
5 - green LEDs
5 - orange LEDs
2 - super-bright WHITE LEDs - 20,000mcd
1 - 3mm flashing LED
1 - mini 8R speaker
1 - mini piezo
1 - LDR (Light Dependent Resistor)
1 - electret microphone
1m - 0.25mm wire
1m - 0.5mm wire
1 - 10mH inductor
1 - push button
5 - tactile push buttons
1 - Experimenter Board (will take 8, 14 and 16 pin chips)
5 - mini Matrix Boards: 7 x 11 hole,
11 x 15 hole, 6 x 40 hole, surface-mount 6 x 40 hole board and others.

Photo of kit of components.
Each batch is slightly different:

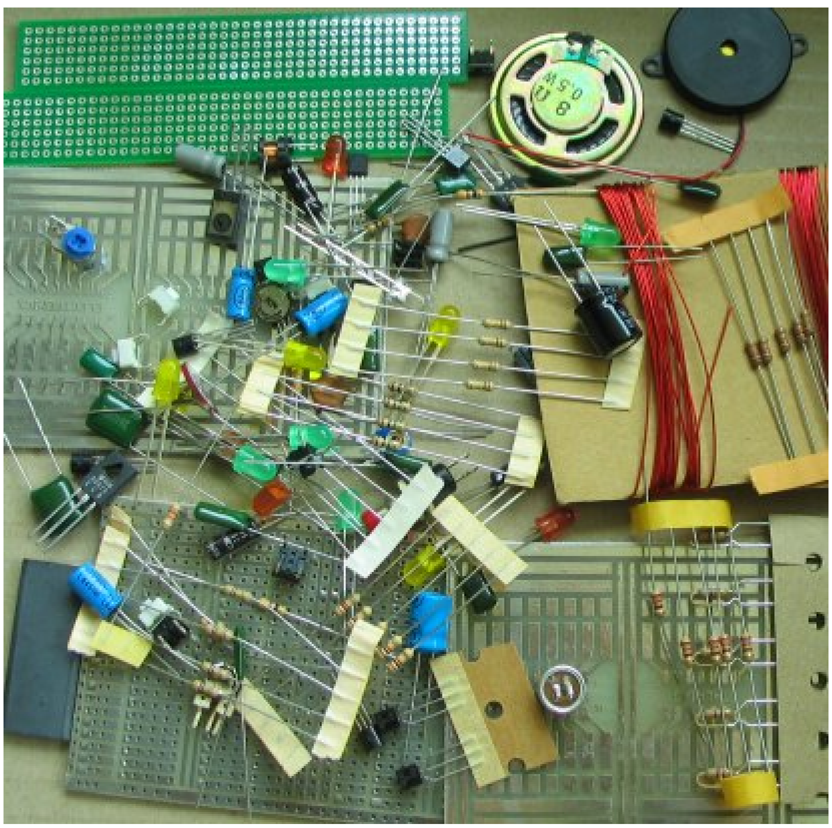

There are more components than you think. . . plus an extra bag of approx 30 components. The 8 little components are switches and the LDR and flashing LED is hiding.
In many cases, a resistor or capacitor not in the kit, can be created by putting two resistors or capacitors in series or parallel or the next higher or lower value can be used.

BEFORE WE START

Too many text books start with the physics of the atom and have equations and mathematics to show how smart the author is.
Don't worry, we wont have any physics or equations.
The reason . . .
This is not a physics course. It is a practical electronics course to teach the basics as quickly as possible. There are no equations because most transistor circuits cannot be worked out mathematically as the gain of a transistor changes according to the current-flow and these gain-values are never provided. So the mathematics is worthless.
To get an answer, all you have to do its build the circuit and measure the values with a multimeter.
Also lots of discussions in text books will never be used in your next 40 years of electronics, so this course doesn't have any unnecessary material and is much-more concentrated than anything you have read before.
Every frame contains important points - especially the animations - as they show you how a circuit works in slow-motion - something that has NEVER been done before.

ELECTRONICS BLOCKS

Here is an idea from Instructables to produce blocks with screws, containing a single component and they can be connected with jumper leads (alligator clips).

Use a slotted head for the negative screw and a philips head for the positive screw.

Learn electronics from the beginning . . .

START HERE:

All electrical and electronic components need wire to connect them to the circuit.
In a diagram called a CIRCUIT DIAGRAM, the wires are drawn as lines.
When the wires (or lines) cross, they may be joined or just passing.
It is **VERY IMPORTANT** to show the difference between lines that are **JOINED** and lines that are **NOT JOINED**.
When the lines are joined, it is best to place a dot

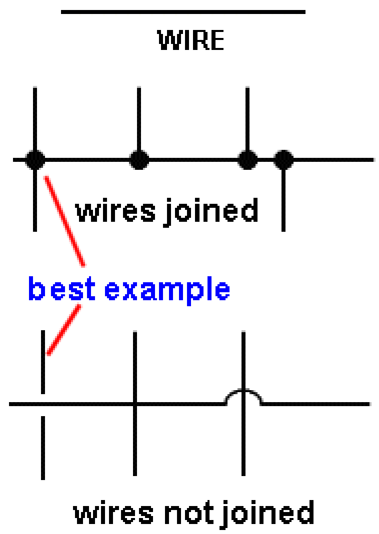

Fig 1 The wire in a circuit diagram

on the connection to PROVE the lines are joined.
When the lines are just crossing, a gap should be made so it is obvious that one wire goes under the other and does not touch.
Lines should be "across the page" or "up and down." Very few lines should be at 45°.
You can make a line thicker to indicate a power rail or a wire that will be thick in reality.

to Index

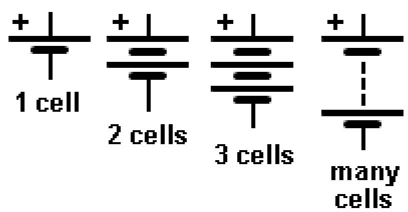

Fig 2 A single Cell and many Cells

Next we need a **battery**. A battery consists of two or more cells. The positive terminal of a battery is the long line in the diagram and you must add the voltage (of the cell or battery) to the symbol as a single cells can be 1.2v, 1.5v, 2.2v or up to 3.6v.
The symbol does not let you know the voltage.
The positive is always at the top and is the longest line on the battery symbol.

to Index

Fig 3: A Globe

Next we need a globe. A globe has two connections (a fine wire inside a glass bulb glows when the globe is connected to a battery).

to Index

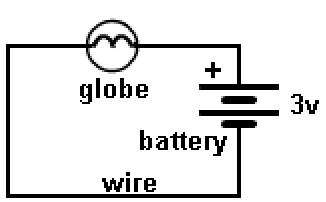

Fig 4: A Circuit

With a globe, battery and wire we have produced a **CIRCUIT**.
A **CIRCUIT** is a complete path and we say the "electricity" the **CURRENT** emerges from the positive of the battery, moves through the globe and returns to the battery via the wire.
If the globe is a "3v GLOBE" it will glow when connected to a 3v battery.
The globe can be connected either way around.
The circuit we have shown is called a **SCHEMATIC** and consists of symbols: a globe symbol and a battery symbol.
The line connecting the two components is called WIRE.

to Index

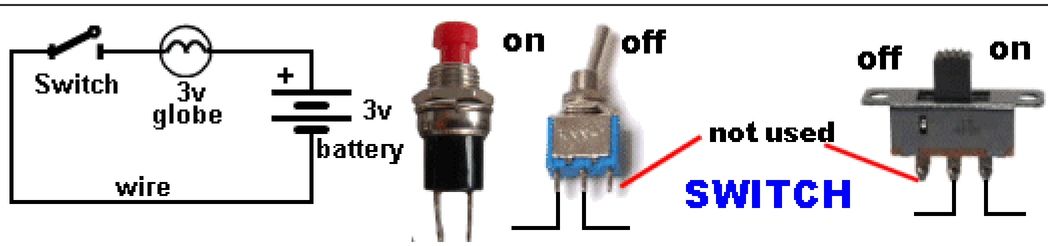

Fig 5:Adding a SWITCH
To turn the globe ON and OFF we need a SWITCH.
The switch may be a push button, a toggle switch (a "click" action) or a slide switch. You could

twist the wires together and untwist them. The result is the same. We say the circuit is "broken" or "open" via the switch and the lamp does not glow. Closing the switch turns ON the globe.

to Index

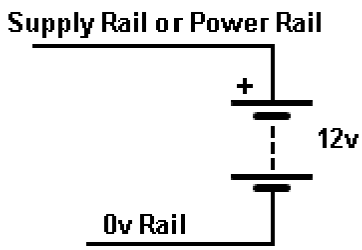

Fig 6: Naming the RAILS

The top rail of the **CIRCUIT DIAGRAM** is called the **SUPPLY RAIL** or **POWER RAIL**.
The lower rail is called the **0v Rail** or **EARTH RAIL**.
Do not connect the Supply rail (+12v) to the 0v rail as this will cause a high current to flow and is called a **SHORT CIRCUIT**:

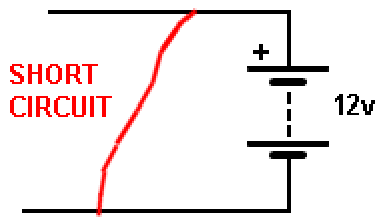

to Index

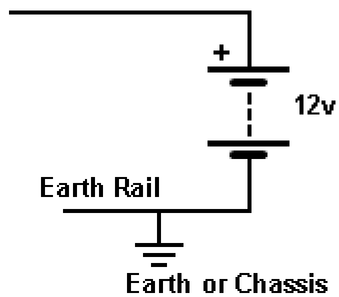

Fig 7: The **EARTH RAIL**

The lower rail is also called the **Chassis**.
This comes from the "old days" when electronics constructors build radios on a metal chassis (metal box) and it was connected via wire to a pipe in the ground to help the radio pick up distant radio stations.
The term also comes from car and truck wiring where one side of each globe is connected to the frame or chassis so that only one wire is needed to each globe and the return "path" is via the chassis.

to Index

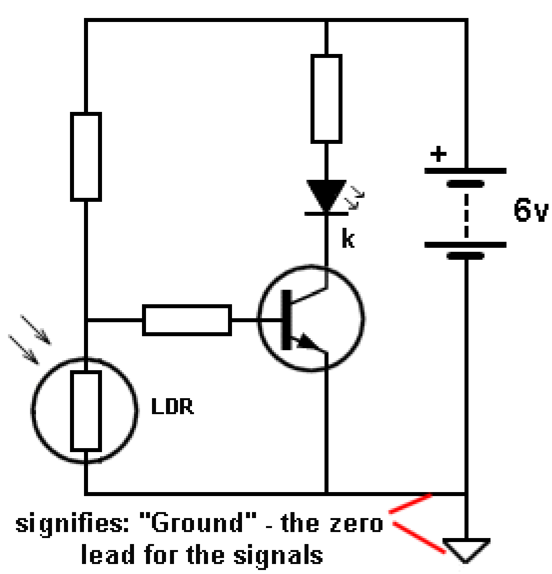

Fig 7a: Ground

Some circuits identify the "**Ground Lead**" or "**Ground Wire**" of a project to show where all the **signals** have been "referenced to." In other words, all the signals rise and fall above and below this "Ground wire" or "Ground Lead." This lead may not be at **earth potential** as the project may be in a plastic box but it identifies where the earth lead of a Cathode Ray Oscilloscope or the negative lead of a multimeter is connected.
On some printed circuit boards, the negative terminal of the battery (the 0v wire or terminal) is connected to a very large area of copper and this is called the EARTH PLANE or GROUND PLANE. It is designed to prevent signals travelling along the tracks (called traces) being radiated and also prevents outside interference upsetting the project. It also "tightens-up" the earth rail.

to Index

The circuit shows a 12v globe connected to a 12v battery and the circuit appears to be "broken" (not continuous).
But the **current returns** via the earth connection.

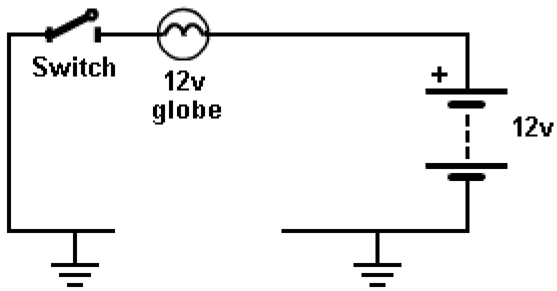

Fig 8: EARTH Return

We talk about the **CURRENT RETURNING**. We don't say: the voltage returning.
The voltage of the globe must be the same as the battery voltage, otherwise it will not glow fully or it will **burn out** if it is say a 6v globe.

to Index

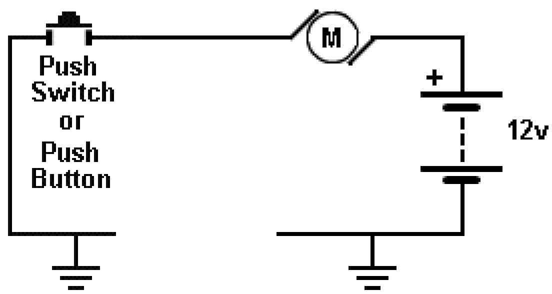

Fig 9: Connecting a Motor

The circuit shows a 12v **Motor**.
It is turned ON when the push-switch is pressed.

to Index

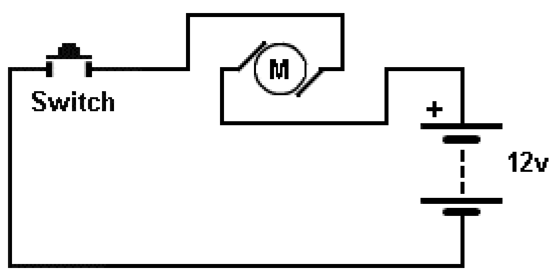

Fig 10: Reversing a Motor

If the wires are connected to the motor "around the other way," the motor will reverse direction.

to Index

VOLTAGE AND CURRENT

What is voltage and what is current?
Here is a very simple description.
A battery produces a voltage called DC. (This is a very confusing name because the letter actually refer to Direct Current, so we just say **DC Voltage**).
A battery also produces current called DC - Direct Current. We say **DC current**.

VOLTAGE

Voltage is a value produced by an electrical component called a battery or cell.
A single cell produces one and a half volts. (1.5v) and although this is not a high voltage, when cells are connected together we get higher voltages.
If 6 cells are connected in series we get 9v.
Here is a 9v battery:

CURRENT

You cannot feel current with your tongue so we have to carry out another experiment:

Touch the two terminals with your tongue. You get a tingle. This is a 9v tingle. Now you have "felt" electricity. This is a 9v tingle.

Place a 22 ohm or 47 ohm resistor across the terminals of the battery and hold your fingers on the resistor. It will get hot. This is the result of current flowing through the resistor and heating it up. The current will be about half an amp and the voltage is 9v, so the wattage will be about 2 to 4 watts. Feel the heat produced.

Milli - milli means 1/1,000th (one thousandth) - such as one milliamp or one millivolt.

In other words one thousand milliamps is equal to 1 amp.
One volts is not a very large value as a battery produces 9v and a cell produces 1.5v to 3.6v (depending on the type of cell.
But 1 amp is a large quality when talking about electronic circuits involving LEDs, motors and transistors.
The globe used in the experiments above requires about 300mA. (1,000mA = 1 amp)
The 3v motor used in the experiments requires about 250mA
The LEDs used in the experiments require about 20mA.
Transistors can pass about 100mA to 800mA via the collector-emitter.
In most cases current-flow in the circuits we will be discussing will be less than 1 amp and will be shown as 25mA, 100mA, 350mA etc.

WATTAGE and CAPACITY

A 9v battery has 6 very small cells and they will not last very long.
A "AAA" cell is larger and a "D" cell is much larger.

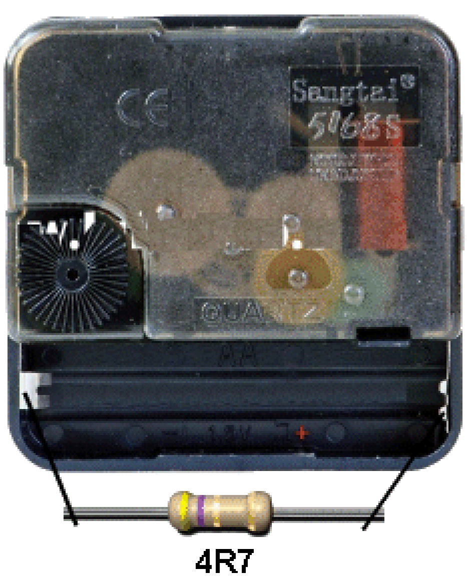

A large cell is said to have a **LARGE CAPACITY.** This means it will deliver a larger current for a longer period of time.
The **WATTAGE** of a cell is the multiplication of the voltage x current. The answer is milliwatts or watts.
The **CAPACITY** of a cell is the wattage x hours. The answer is milliwatt-hours or watt-hours. This is also called watt-hours.
You can determine the capacity of a cell (such as a rechargeable cell) by connecting it to a clock-mechanism that has a 4R7 connected across the terminals. The resistor will take a considerable current and deplete the cell in a few hours. The clock will let you know exactly how long the cell delivered the current. You can then compare other cells.

The simplest electrical circuit consists of a battery and resistor. The current flowing through the circuit will depend on the voltage of the battery and the resistance of the resistor R.

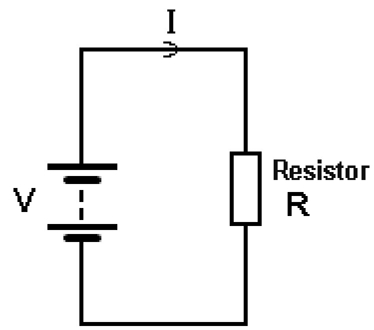

The formula connecting these three quantities is:

$$I = \frac{V}{R}$$

Ohm's Law

$$I = \frac{12}{3}$$

$$I = 4 \text{ amps}$$

This is called **Ohm's Law**. Suppose you have a 12v battery and the resistor is 3 ohms. The current flowing through the resistor will be 4 amps.
Increasing the resistance will decrease the current if the voltage remains fixed.

All the above circuits are called ELECTRICAL CIRCUITS because they contain electrical components (such as a motor, globe, relay, switch).
When the circuit contains an ELECTRONIC component such as a diode, transistor, LED, it is called an ELECTRONIC CIRCUIT or ELECTRONIC SCHEMATIC.

to Index

POWER and ENERGY

Here's an easy way to remember the difference between POWER and ENERGY:
A 9v alkaline battery has enough ENERGY to start a car. But it does not have enough POWER (strength).
Energy is effectively the strength of the battery (and this is the voltage and the current it can deliver) multiplied by the time it can deliver this energy. When the answer is obtained, it consists of three factors ((3 quantities) VOLTS, AMPS and TIME.
This results in an answer called xxxx WATT-HOURS.
For a 9v battery the quantities are: 9 volts, 500mA and the battery will deliver this 9x0.5 = 4.5watts for about 1 hour. This is equal to 4.5 x 60 x 60 = 16,200 watt-seconds.
To start a car requires 250 amps from a 12v battery for 5 seconds.
This is: 12 x 250 x 5 = 15,000 watt-seconds.
This means the energy stored in a 9v battery could start a car if all the energy could be delivered in 5 seconds.
This is not possible however the FACT is this: A 9v battery has enough stored energy to START A CAR.

to Index

BATTERY BOOSTER

One of the simplest things we can do is start a car with a flat battery with the assistance of a BATTERY BOOSTER.
This consists of a 12v rechargeable battery in a handy case with leads to connect to the flat battery in your car.
This simple operation puts two 12v batteries in parallel, but no-one has actually described what happens and why.
That's because the explanation is very complex. We have included it here to show that a simple explanation involves a lot of technical terms and you will understand more after reading the course.

The flat battery in the car is not fully charged but it has some percentage of charge and when it sits for a period of time in a non-fully charged condition, the voltage drops from 12.6v to less than 12v as the battery gradually self-discharges due to the potential at the top of the cell being different to that at the bottom of the cell and the specific gravity of the electrolyte being different at the top and bottom. This causes an internal current to flow within the cell and slowly discharge the cell. But if you try to start the car, the voltage drops to less than 7v because the electrolyte cannot carry the high current and a slight potential is developed across the liquid.

The result is the starter-motor does not crank the car.
The reason is this: When the battery is fully charged, the current taken by the starter motor is about 300 amps. This is about 11v x 300 amps = 3300 watts = 4.4Horsepower.
But when the voltage drops to 7v, the current will drop to 190 amps to deliver 1336 watts = 1.8HP. This is only 40% of normal and that's why the car does not start. The engine needs 4HP to overcome the pressure in the cylinders due to the compression of the air during the "firing stroke."
Let's put it this way. If we have a brand new 7v battery, the car will not start. The starter-motor will only accept 190 amps when the supply is 7v.
So, we have to increase the voltage.
We do this by placing a 12v battery across the flat battery. The voltage of the flat battery will immediately rise to 12.6v. It might take 2 minutes but the flat battery will take a small current (1 to 10amps) from the battery in the "booster" and the output of the combination will be 12.6v. The current-carrying capacity of the electrolyte will improve very quickly and you have effectively given the "flat battery" a very quick charge.
The starter-motor will now accept 300 amps from the combination and **SURPRISINGLY** the cells of the "flat battery" will deliver about 200 amps and the booster battery will deliver about 100 amps. The actual sharing of current will depend on the two batteries but the secret behind the success is the increase in voltage we call **TERMINAL VOLTAGE**. The voltage on the terminals (the alligator clips).
The capacity of the booster battery is not important. It can be from 7AHr to 40AHr. We are just using a very small amount of its capacity to start the car and nearly all batteries will provide 200 Amps for a short period of time.
The voltage of the car battery is very important. The Horsepower taken by the starter-motor is defined by the formula: Pwatts = V^2/R Since the resistance remains constant, a voltage of 7 volts will produce 7x7=49 units and a voltage of 11v will produce 121units. This gives the ratio of 40% to 100% as explained above.

to Index

BATTERY BOOST

Continuing from the previous frame where we showed the effect of placing a weak battery in parallel with a good battery, we can show what happens when a weak cell is placed IN SERIES with a good cell.
This also applies when you have 5 good cells and one weak cell.
Basically, the weak cell will reduce the current. In other words, if the 5 cells are driving a motor and supplying 250mA, the 5 cells and 1 weak cell will deliver 200mA or less, depending if it is weak or very weak. The current flowing through the weak cell will have the effect of giving it a small charge - in other words, you will be charging the weak cell from the good cells when the motor is operating.

BUT . . . .

There is a way to use weak cells. If you have say 6 weak cells driving a motor and the RPM is reducing, you can add 2 more weak cells to increase the RPM.
The effect is this: The voltage from the 8 cells will be higher than from 6 cells and this will allow a higher current to flow. Sometimes the cells will provide this higher current and thus more of the energy will be delivered and you will get the last of the energy from the cells.

to Index

INTERNAL RESISTANCE

All batteries and also all individual cells have a "secret, hidden" value of resistance inside each cell due to the resistance of the chemicals. This resistance is very small when the cell is new but it increases as the cell gets older.
It is very easy to measure this value. Simply put an ammeter directly across the cell and measure the current. Use Ohm's law to work out the resistance. But this not always a wise thing to do as some cells will deliver 10 amps and some will deliver 100 amps and damage the meter.
The diagram opposite shows a large internal resistance for the weak cell and a small internal resistance for the good cell.
If a cell did not have any INTERNAL RESISTANCE it would deliver thousands of amps. It's the Internal Resistance that limits the current.

In most cases we neglect (do not consider) the value of internal resistance when making tests and when using a battery in a project.
But when a battery gets old, it cannot deliver a high current and the internal resistance gets so high that the output voltage drops from say 9v to 7v, even when the battery is not connected to a circuit.
This is the result of the INTERNAL RESISTANCE of the chemicals increasing to a point where they become noticeable and what we call "poisoning" of the chemicals due to the cell "aging" and new chemicals being produced in the cell that have a high resistance.   Some of the terms we use are: "drying out and sulphating. Some cells produce spikes or needles that completely short-circuit the cell and make it totally useless.

to Index

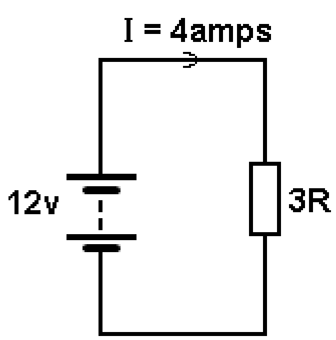

This resistor is dissipating 48 watts.
As a comparison, a soldering iron is dissipating about 10 to 20 watts.

RESISTOR WATTAGE

Resistor Wattage means two things.
1. The physical size of a resistor tells you number of watts it is capable of dissipating. This is called RESISTOR WATTAGE. It is really RESISTOR-SIZE or RESISTOR-CAPABILITY.
2. The multiplication of the voltage across a resistor and the current flowing though it will produce a value called WATTAGE. This is also called RESISTOR-WATTAGE or RESISTOR-LOSS or RESISTOR-DISSIPATION or HEAT-LOSS.
In the circuit shown, the wattage being lost in the resistor is:
12 x 4 = 48 watts.
Most of the resistors we will be using in our projects are 0.25watts. This means they will dissipate 250milliwatts, however the actual wattage being dissipated may be only 70 milliwatts and the resistor will not get hot.
0.25watts is the maximum wattage it can dissipate without overheating.
If it is dissipating 400milliwatts, it will be VERY HOT.
The wattage it is dissipating (the heat it is getting rid of) will depend on the supply voltage and the value of the surrounding components.

to Index

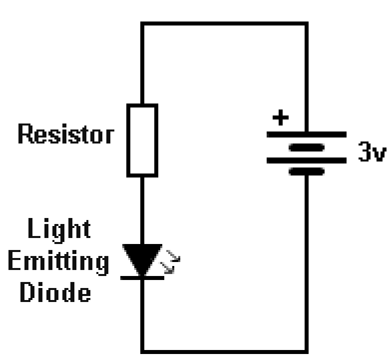

Fig 11. The LED

This simple **ELECTRONIC CIRCUIT** contains a **LIGHT EMITTING DIODE (LED), RESISTOR** and battery.

The circuit is classified as electronic because the LED is not an electrical item (such as a globe) but more-complex, as it produces light when current flows through a crystal and the crystal produces the colour.

to Index

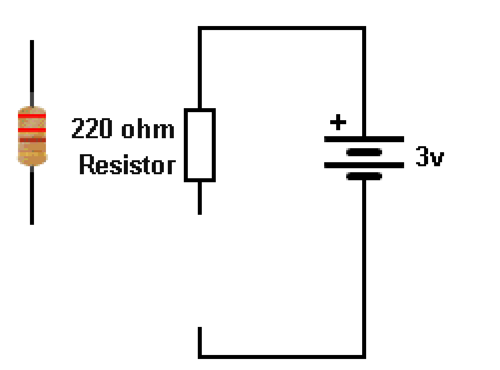

Fig 12. **The Resistor**

A **RESISTOR** must be included in the circuit to prevent the LED being damaged.
The resistor in this circuit must be 220 ohms.
This is shown by the colours on the resistor. The colours for 220 ohms: **red - red - brown**. The 4th band is gold - indicating a tolerance of 5%.
A resistor has **RESISTANCE**.
It reduces the current from the battery to a required amount to prevent the LED glowing too bright.
A resistor is just like putting your foot on a hose. The water trickles out the end. The resistor "resists" the high current-flow that the battery is able to deliver.

to Index

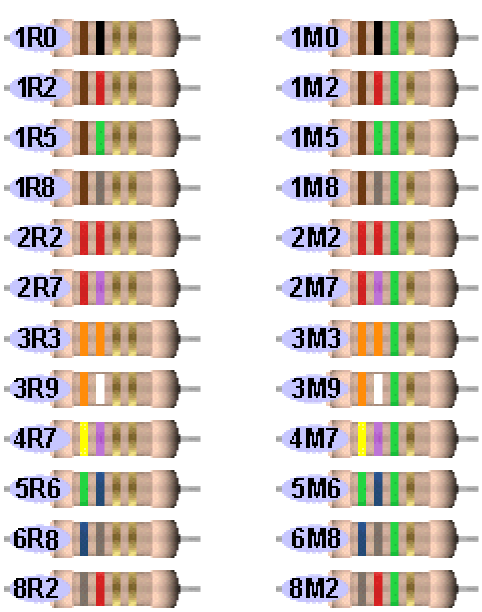

Fig 12a. The **Resistor Colours**

There are hundreds of different resistors because the resistance-values need to cover the range one ohm to 10 million ohms.
There are also small, medium and large resistors.
The resistors on the left are just a few in the range. (See the full range below). They show colour bands for 1 ohm to 8.2 ohms and 1 million ohms to 8.2 million ohms. All the other values are shown below.
An electronics engineer does not have the room to store 10 million different resistors so they make each resistor 5% or 10% higher than the previous. This reduces the number to about 100 to 200.

TOLERANCE

The first 3 bands indicate the value of the resistor and the 4th band indicates either 5% or 10% tolerance.
All modern resistors are 5% or 2% or 1%. The "old" 10% resistors are no longer made.
Gold = 5%
Silver = 10%

to Index

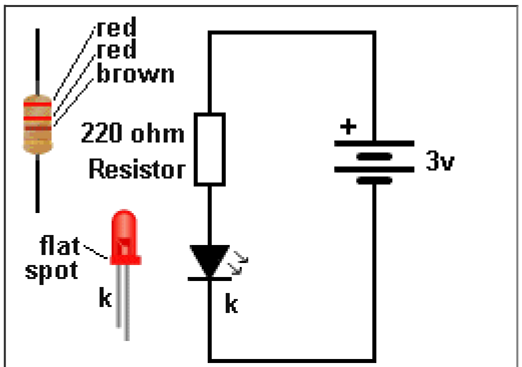

Fig 13. The **Resistor and LED**

The **LIGHT EMITTING DIODE** is called an electronic component (mainly because it is more complex than a globe and it produces light by a more-complex means than heating a wire).
A **LED** must be connected around the correct way. It will not illuminate if connected around the wrong way.
All **LEDs** have one lead longer than the other. The SHORT lead is called the **CATHODE** (k).
All LEDs have a flat on one side and this is the **CATHODE** lead.
The arrows on the diagram indicate light is "given off" (emitted - produced).

to Index

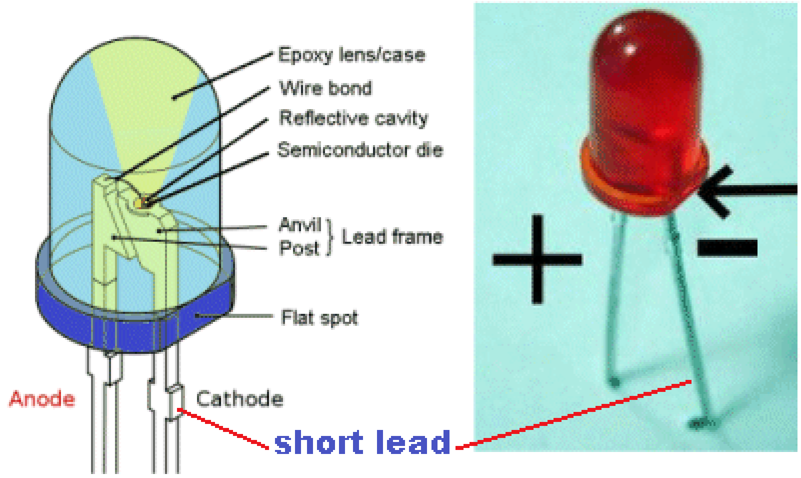

Fig 14. The **LED - showing the flat spot**
A close-up of a red LED. The cathode lead is the short lead and next to a flat side on the LED.
DO NOT show "+" or "-" on a diagram. Only show the letter "k" to indicate cathode.
The symbols "+" and "-" are used when a component produces a voltage or is connected directly to "+" and
"-" A LED is connected via a resistor.

to Index

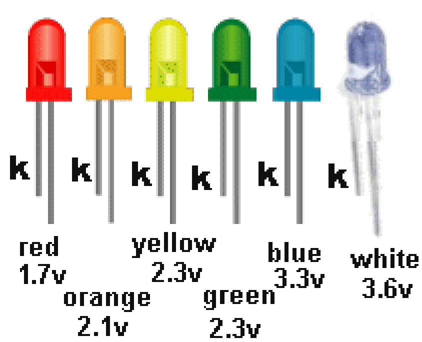

Fig 15. LED VOLTAGES

When a LED is connected to a circuit, (and the correct-value resistor is included), a voltage will be develop across the LED called the **CHARACTERISTIC VOLTAGE DROP**.
This voltage is due to the colour of the LED and the crystal inside the LED that produces the colour.
The diagram on the left shows the approximate voltage developed for each LED.
The voltage **does not change** for small, medium, surface-mount, or large LEDs.

to Index

When a LED is connected to 3v battery, the following **CHARACTERISTIC VOLTAGE DROPs** will develop across each LED.
You will notice we **have not changed** the value of the resistor. It is 220R.
The LED creates the voltage and if the value of resistance is decreased, the LED will illuminate BRIGHTER.
If the LED illuminates too bright it will be DAMAGED.

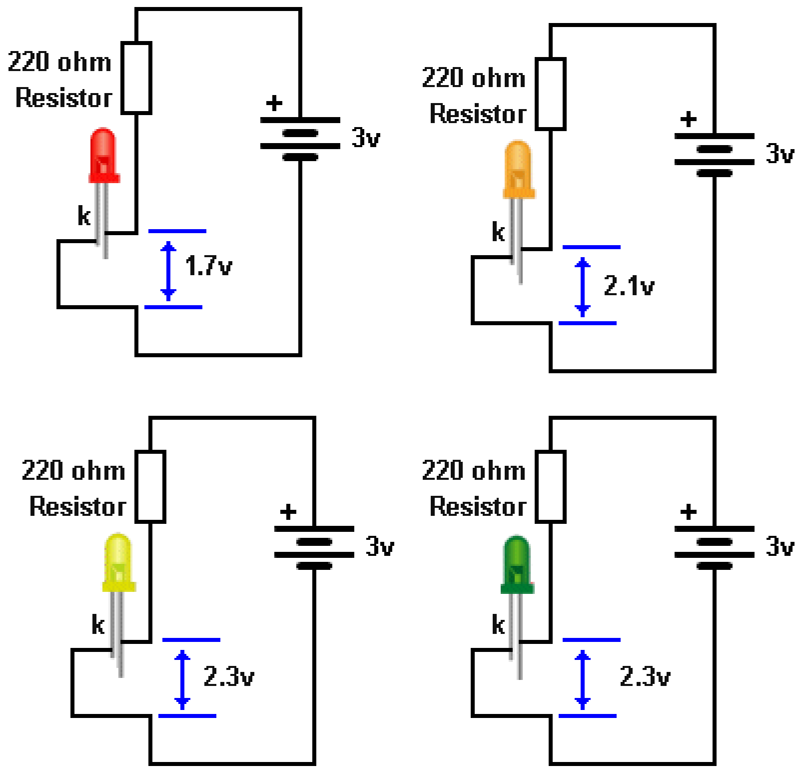

Fig 16. LED VOLTAGES

to Index

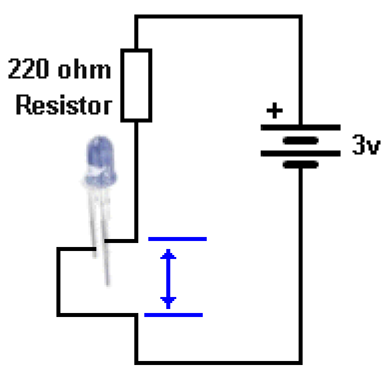

Fig 17. WHITE LED VOLTAGE

If we connect a WHITE LED to 3v supply, it will not illuminate because it needs a supply higher than 3.6v.

The resistor in series with the LED is called a **CURRENT LIMITING RESISTOR**.

In this circuit **no current flows** because the supply is not high enough.

to Index

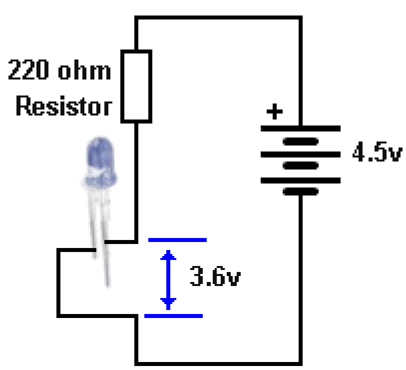

Fig 18. WHITE LED VOLTAGE

When the supply is increased to 4.5v, the 220R resistor will allow a current to flow through the white LED and it will develop a CHARACTERISTIC VOLTAGE DROP of 3.6v across it.

The supply (the voltage of the battery) must be higher than the CHARACTERISTIC VOLTAGE DROP of the LED so the resistor will allow the correct amount of current to flow.
The ideal current for a LED is 20mA, however some LEDs will work when 1mA flows, so you have to know what you are doing.

to Index

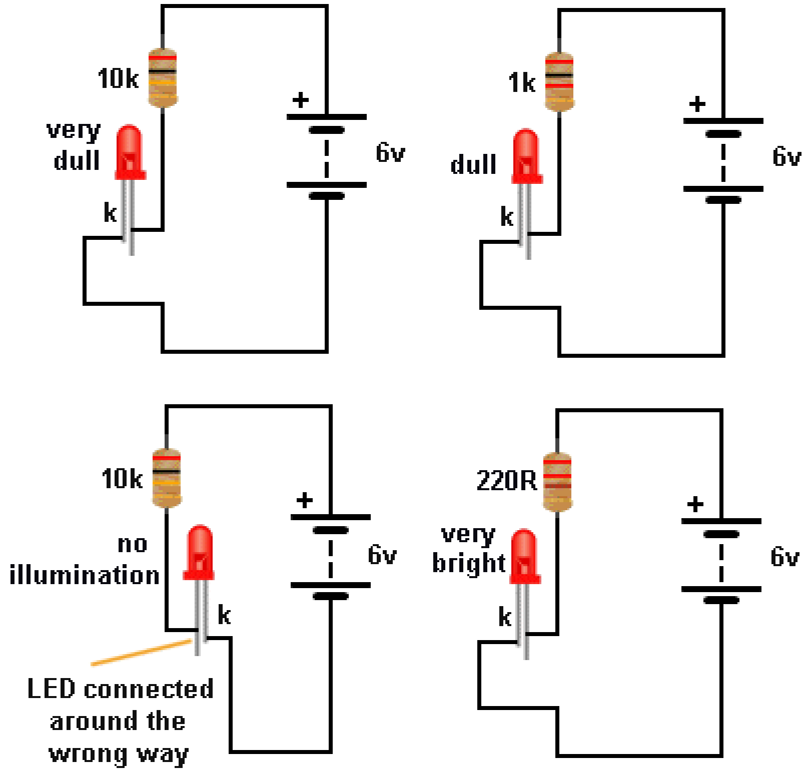

Fig 19. Testing A LED

Now connect either the 1k, 470R or 220R and determine the brightness you need.
As the brightness increases, the current will be higher.
You can use 3v supply for all LEDs except blue and white.

HOW TO TEST A LED

Some clear LEDs produce red or orange and some LEDs do not have the cathode lead clearly identified.
Here's how to find the colour, cathode lead and the current.
You need a 6v battery, 10k resistor, 1k resistor, 470R resistor and 220R resistor.
Connect the 6v battery and 10k resistor to the LED and it will only illuminate when the cathode is connected to the negative of the battery. This is the short lead.

to Index

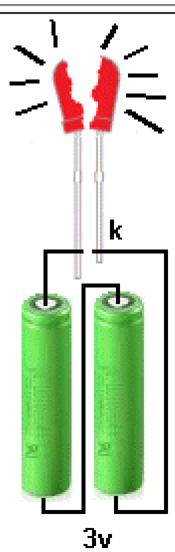

Fig 20. Damage a LED

Do not connect a 3v battery directly across a LED. It will be DAMAGED. You MUST include a resistor.

to Index

A LED IS CURRENT DRIVEN

You may have seen this statement and tried to work out what it means.
Basically it means an increase in current will make the LED brighter.
But a LED needs 2 things:
It needs a voltage that is EXACTLY the voltage required to produce illumination. And this voltage depends on the colour of the LED.
As soon as you supply the exact voltage, the crystal will begin to glow and as you increase the current, the illumination will increase.
But doing this is VERY VERY difficult.
It is very easy to supply an exact voltage such as 1.7v or 3.4v, but delivering a current such as 10mA or 20mA at the same time is very difficult. You cannot get a 1.7v battery and deliver 10mA to a LED.
As we have shown above, you need a simple components such as a resistor between the battery and LED to achieve the desired result.
A LED is CURRENT DRIVEN but firstly you need to provide a VOLTAGE that is exactly the connect value for the colour of the LED and then the current can be increased.

to Index

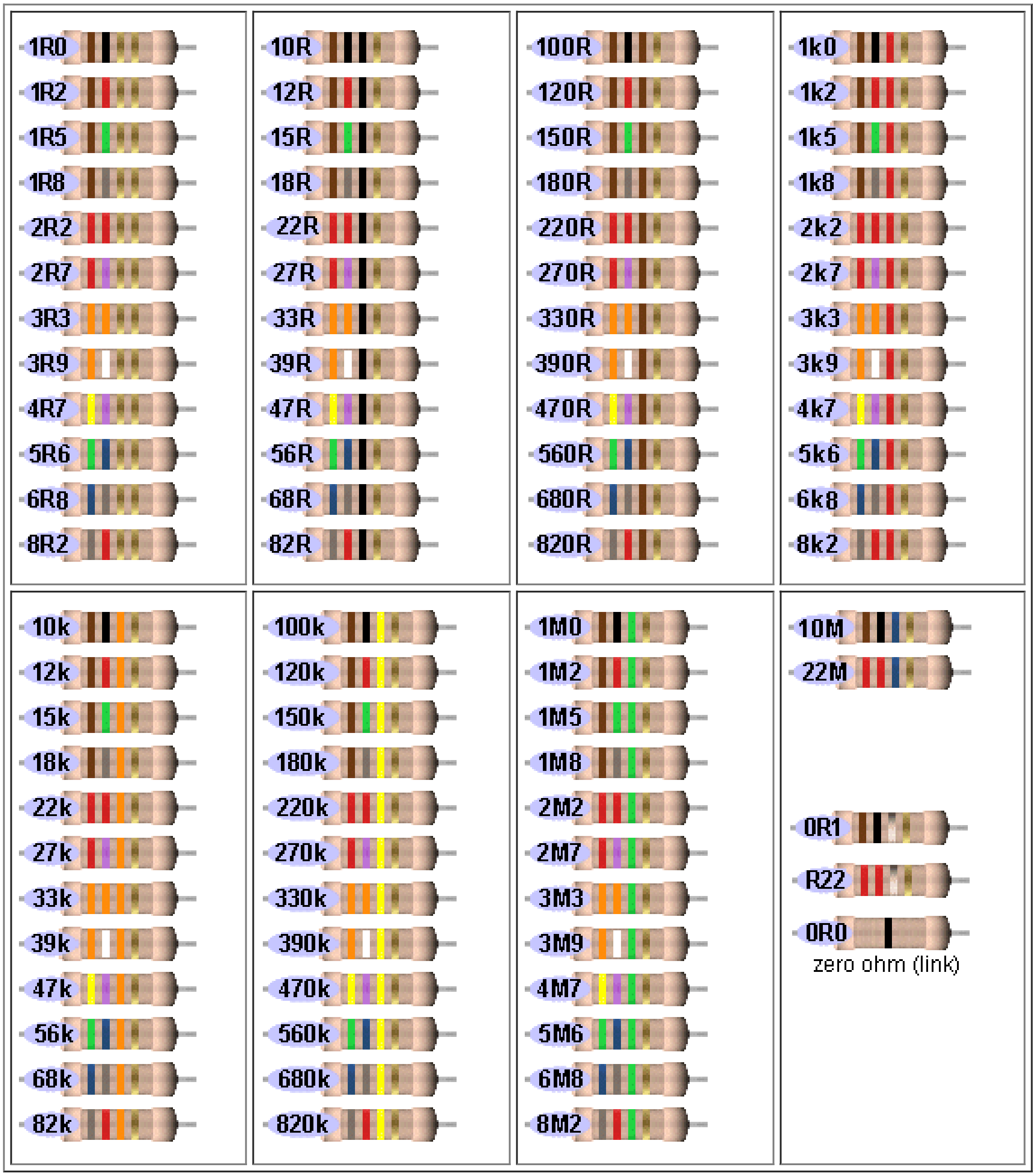

Fig 21. All the resistor values

Here are all the colours and values for the resistors you will using in this course. Just match-up the

colours on your resistor with the resistors above and you will find the value.

to Index

Resistor values are always OHM values. One ohm is a small value. It might be the resistance of a length of wire 3 metres long.
When a switch is open the resistance is infinite - millions and millions of ohms.
The resistance of your body from one hand to the other will be about 70,000 ohms.
The resistance between two wires dipped in water will be about 1,000 to 100,000 ohms (depending on the dissolved-salts in the water - pure water has a very high resistance)
The resistance of the filament of a 3v globe will be about 30 ohms.
The resistance of the winding of a 3v motor will be about 3 ohms.
Resistors are made with values from less than one ohm to more than 10 million ohms by adding carbon to the mixture inside the resistor (and cutting a track around the outside of the resistor) then connecting a lead to each end. Adding more carbon reduces the value of resistance. Carbon has a low resistance.
Resistance-values are measured with the RESISTANCE settings on a MULTIMETER.
This is called the "Ohms Range." Sometimes with the symbol: Ω
A Multimeter will have 2, 3 4 or more scales to cover the range one ohm to 10 million ohms.
Low value resistors (from 1 ohm to 999 ohms) are written as 1R, 220R, 470R, 999R. with the letter "R" indicating Resistance (ohms). You can also use the symbol "omega" (Ω)
For values above 1,000 ohms to 99,999 ohms, they are written as: 1k, 2k2, 4k7, 10k, 100k, 220k, 470k, with the letter "k" indicating "kilo" (thousand).
1M = 1,000,000 - one million ohms 1M2, 2M2, 4M7, 10M.
The letters "R, k and M" are placed so they take the place of the decimal point. This prevents any mistake, as a decimal point can be missing in a poor photocopy.

to Index


MULTIMETERS

There are two types of **MULTIMETER**. The top two are called **DIGITAL MULTIMETERS** (DMM) and show numbers on a display.
The lower two meters are called **ANALOGUE MULTIMETERS** and have a pointer and scale.
All meters come with a set of red and black leads.

The **red lead** is always connected to the positive of the battery or the positive on a project and the **black lead** is connected to the negative or earth or chassis.
When making a resistance measurement, the leads can be around either way.
Resistance measurements are always made with the power removed from a circuit. Any voltage on a circuit will upset the resistance reading.

to Index

Fig 22. Resistance Measurement with Analogue Multimeter

The resistance of a resistor is measured by placing the leads of the multimeter on the ends of a resistor and turning the dial on the analogue multimeter to the resistance scale to make the pointer move to about the centre of the scale.
The resistance scale is marked with a high value on the left and 0 ohm on the right.
This is opposite to all the other scales.
You must get the pointer to move to the middle of the scale as it is not accurate at left-end.
Analogue multimeters are only suitable for reading values from 1 ohm to 100,000 ohms. The scale is too hard to read above 100k.
To find the value of a resistor, you can compare the colours with the table above.

to Index

Fig 23. Resistance Measurement with a DMM

A digital multimeter produces a more-accurate reading of resistance.
It is accurate from 1 ohm to 10M ohms.
Select the scale that provides a reading.

to Index

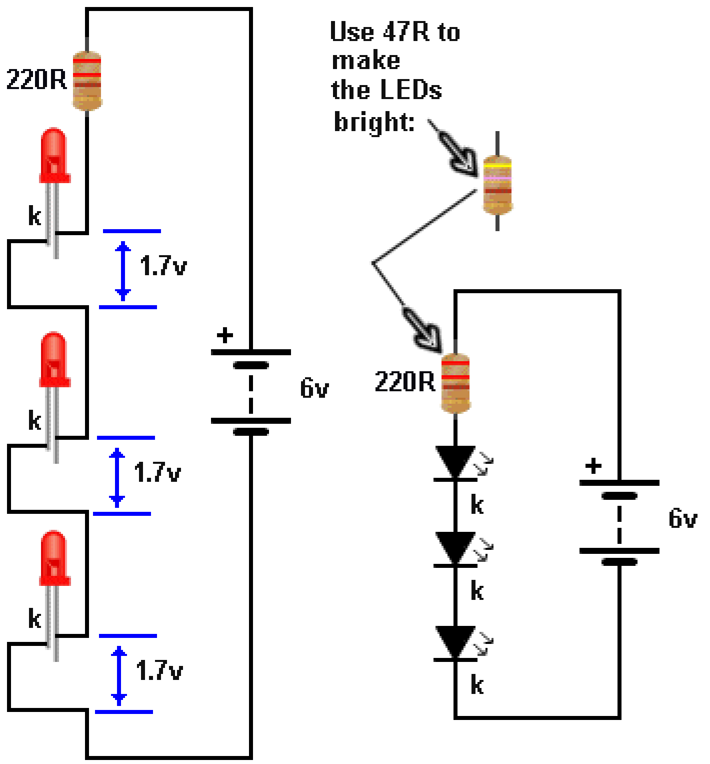

Fig 24. Connecting **LEDs in series**
LEDs can be placed in series provided the total **CHARACTERISTIC VOLTAGE DROP** across the LEDs is LESS than the supply voltage.
In this case the voltage across the LEDs is 1.7v + 1.7v + 1.7v = 5.1v
The supply is 6v and this allows 0.9v for the CURRENT LIMITING RESISTOR.
The LEDs will not be very bright with 220R.
Change the resistor to 47R
If you connect 4 LEDs in series, the total **CHARACTERISTIC VOLTAGE DROP** will be 6.8v and no LEDs will illuminate because the total is higher than the 6v supply.

to Index

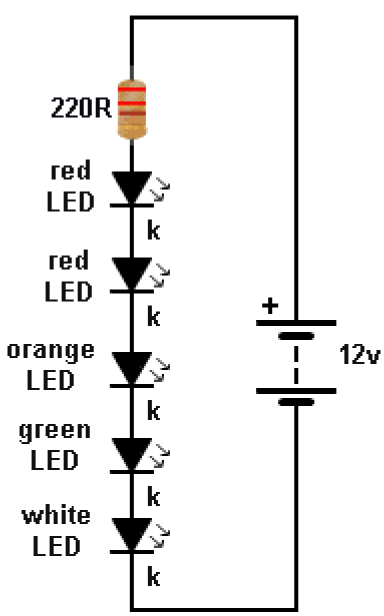

Fig 25. Connecting LEDs in series

Different-colour LEDs can be connected in series. Add up the total Characteristic Voltage for the 5 LEDs and see if it is less than 12v.

The 220R resistor will have to be reduced to 47R to make the LEDs bright.

to Index

LEDs can be connected in parallel if they are the

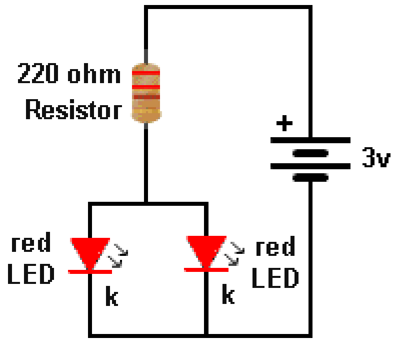

Fig 26. Connecting LEDs in parallel

same colour.
In the diagram a red LED drops a CHARACTERISTIC VOLTAGE of 1.7v and if they are from the same manufacturer or the same batch, they will work ok.
Although we say the characteristic voltage for a red LED is 1.7v, this can change slightly from different manufacturers and one LED may glow brightly while the other is dull.
You have to build the circuit and see the result.

to Index

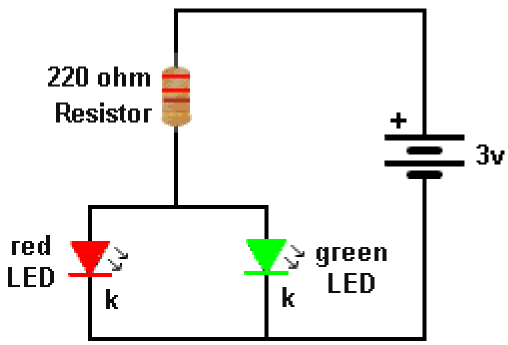

Fig 27. Connecting LEDs in parallel

Different colour LEDs cannot be connected in parallel. The voltage across a red LED is 1.7v. This becomes the "Supply Voltage" for the green LED and it is too low. The green LED needs a supply of 2.1v to 2.3v.
Only the red LED will illuminate.

to Index

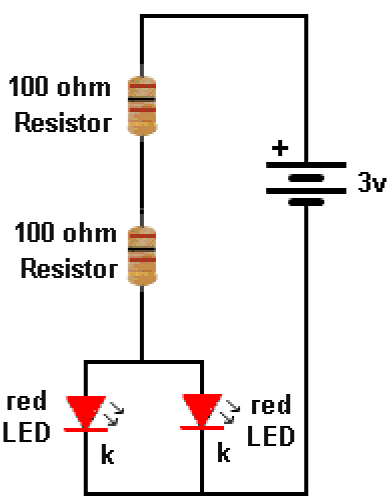

Fig 28. Connecting Resistors in Series

Suppose you don't have a 220 ohm resistor.
You can make a 220 ohm resistor with two resistors in series. The total resistance will be 200 ohms, but resistors are not accurate and the result will be very close to 220R.
Electronic circuits are not very critical. You will not be able to see the difference in brightness between 200 ohms and 220 ohms.

When resistors are connected in series, the total resistance is found by adding the resistance of each resistor.

$$R_{total} = R_1 + R_2 + R_3 + \ldots$$

to Index

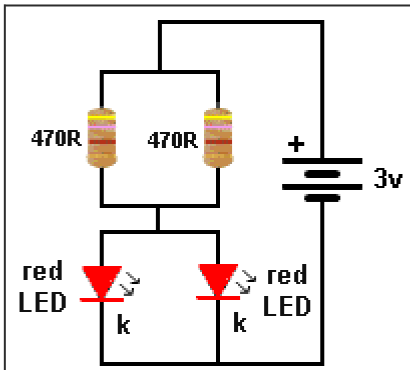

You can create a 220 ohm resistor by connecting two resistors in Parallel.
When two equal-value resistors are connected in Parallel, the total resistance across the combination is HALF.
470R in parallel with 470R produces 235R.
This is very close to 220R.
We are not going into the formula as it is very complex.
Three equal-value resistors in parallel produce a total of **one-third.**
Simply get two resistors and connect them in

Fig 29. Connecting Resistors in Parallel

parallel and measure them with a multimeter.

to Index

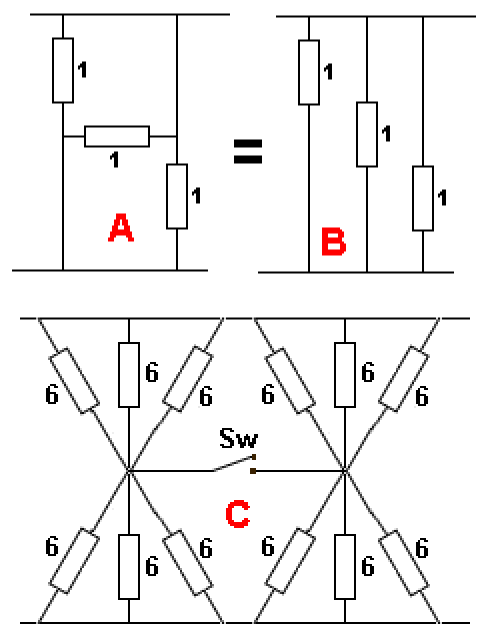

Fig 29a. Two tricky resistor questions

Figure **A** shows three resistors. It looks hard to solve so the middle resistor is turned so it connects directly to the top and bottom rail. Now you can see the circuit is three resistors in parallel. The result is one-third of an ohm.

Figure **C** shows twelve 6 ohm resistors. Replace each group with a 2 ohm resistor, because three 6 ohm resistors in parallel is equal to 2 ohms.

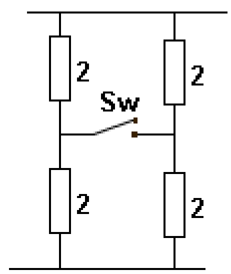

The two left resistors create 4 ohms and the two right resistors create 4 ohms. The result of two 4 ohm resistors in parallel is 2 ohms. The resistance of the circuit does not change if the switch is open or closed.

to Index

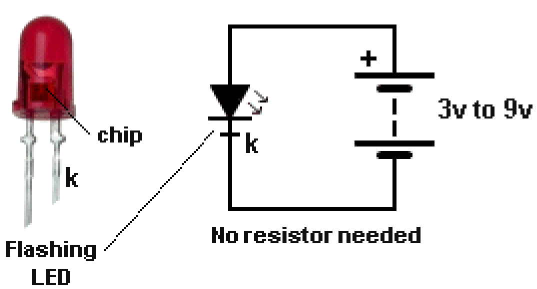

Fig 30. Flashing LED

There are some special LEDs that can be connected to 3v to 9v and they flash or produce a range of colours. These LEDs have a chip and resistor inside the body of the LED to produce the effect and allow the LED to operate on a voltage without the need for a current limiting resistor.

to Index

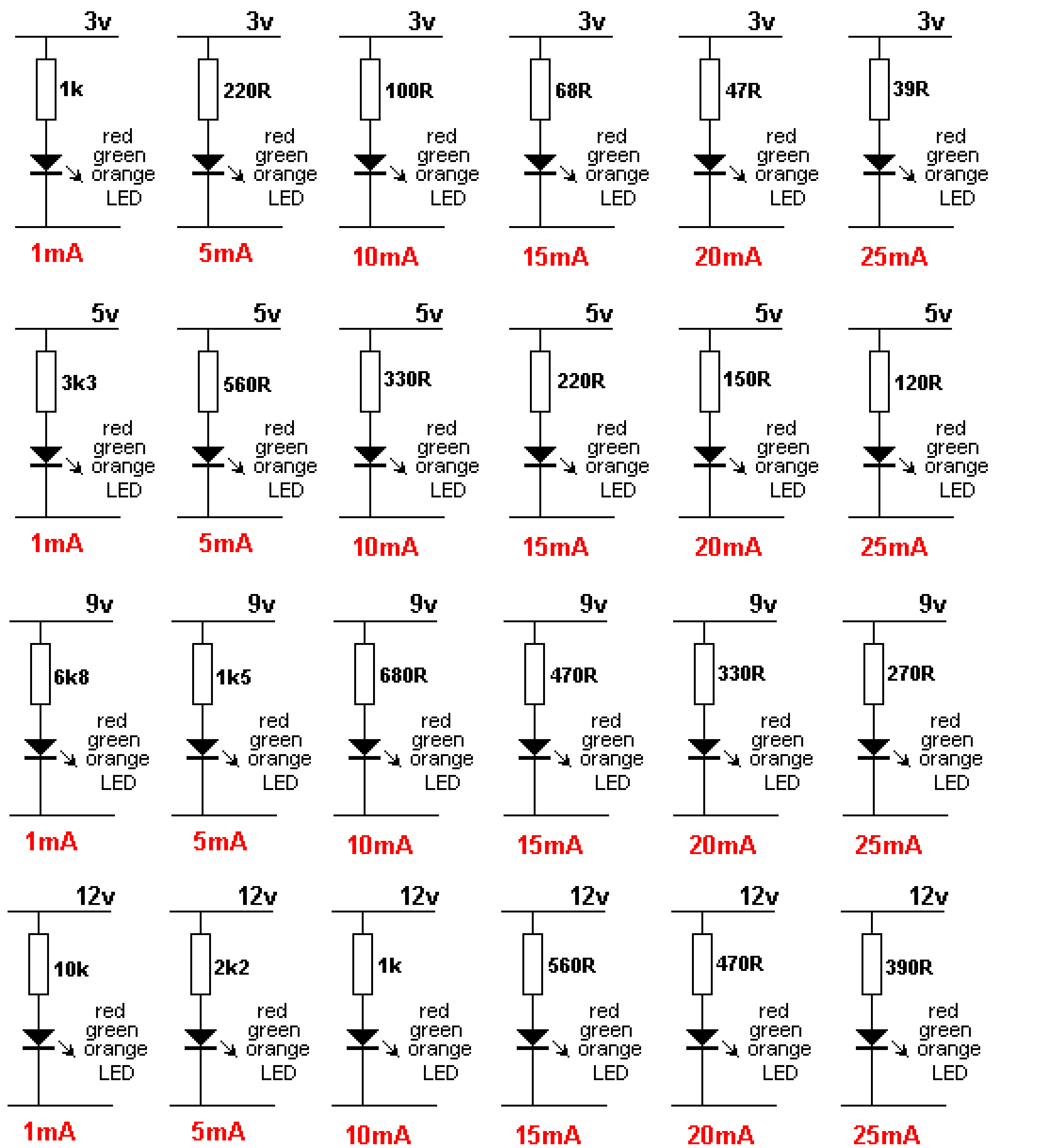

Fig 31. These diagrams show the resistor needed to produce 1mA to 25mA current through a single LED on 3v, 5v, 9v and 12v supply.

to Index

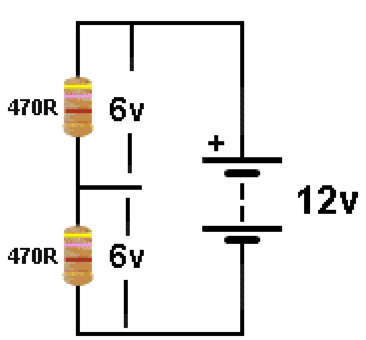

Fig 31a. Voltage Divider Circuit.

THE VOLTAGE DIVIDER

In the circuits above, the resistor and LED are forming a VOLTAGE DIVIDER.
A red LED is dropping 1.7v across it and the resistor is dropping the remaining voltage.
Whenever two (or more) components are placed across a battery, they form a **VOLTAGE DIVIDER**.
Sometimes we want a 6v supply and only have 12v.
We can produce the 6v supply by putting two equal-value resistors across the 12v as shown in the circuit opposite.
We are not going into the mathematics because the selection of the correct value is very complex and the circuit is very wasteful.

to Index

THE CURRENT DIVIDER

The **CURRENT DIVIDER CIRCUIT** is actually a

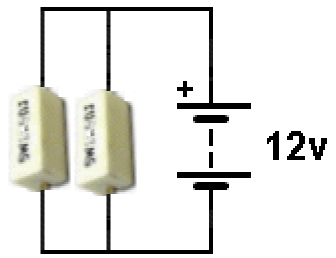

Fig 31b. Current Divider Circuit.

LOAD SHARING CIRCUIT.
Suppose you are testing a Power Supply and need a 10 watt LOAD. But you only have 5 watt resistors.
Placing two 5watt resistors in parallel across the output of the power supply will allow half the current to flow though each resistor. This is called **CURRENT SHARING** or **LOAD SHARING** and the current is divided (or passed) through each resistor according to the value of resistance.

to Index

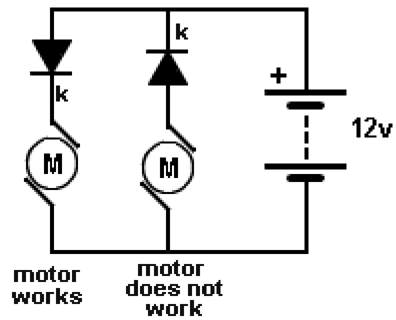

Fig 32. The DIODE

THE DIODE
The next simple electronic component is the **DIODE.**
It only works when connected correctly.
A DIODE allows current to flow through it when it is connected as shown in the diagram.
A Diode is similar to a one-way water valve.
When the diode is "facing down," the motor spins.
When it is "facing up" the motor does not spin.

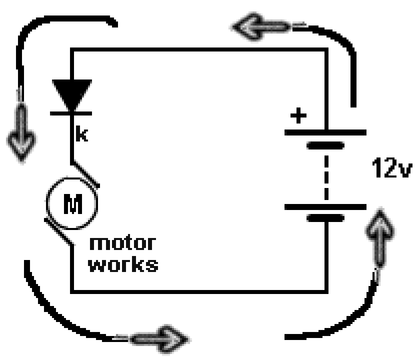

The diagram shows the "current path" around the circuit. The current is measured in AMPS and we discuss current as CONVENTIONAL CURRENT. This is the way current was thought to flow when electricity was born and they said it flows out the POSITIVE TERMINAL of the battery, around the circuit and into the NEGATIVE TERMINAL.
The arrow on the diode shows the current will flow through the diode and allow the motor to spin.
The diode is said to be **FORWARD BIASED**.

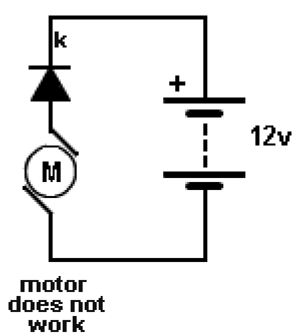

There is no flow of current because the diode prevents any current-flow when connected as shown.
The motor DOES NOT WORK.
The diode is said to be **REVERSE BIASED**.

to Index

There are hundreds of different types of diodes.
Power diodes, signal diodes, low voltage diodes, high voltage diodes, high-speed diodes and many other types.
They all do one thing.
They pass current in one direction and if turned around, they **do not pass** any current.

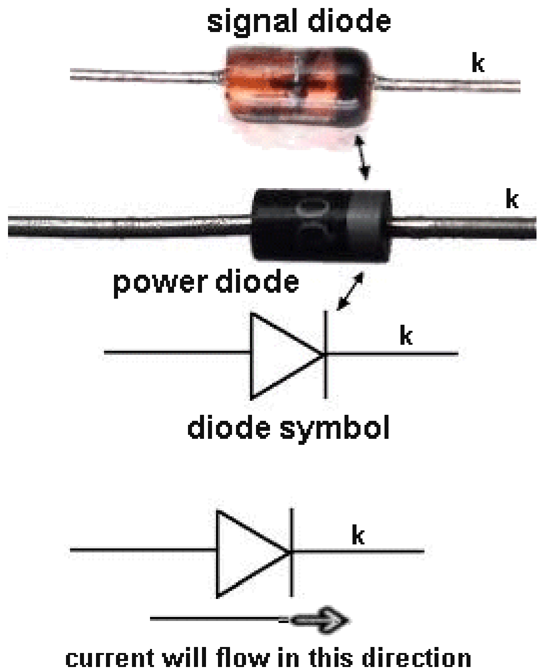

Fig 33. **A Signal diode and a Power diode**

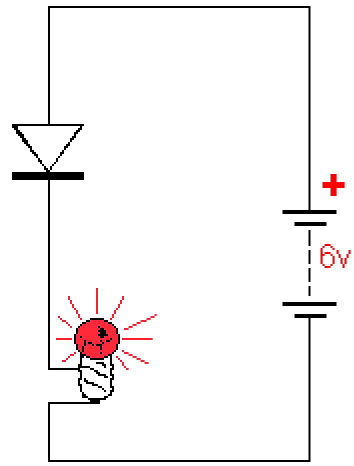

How a diode works

[to Index]

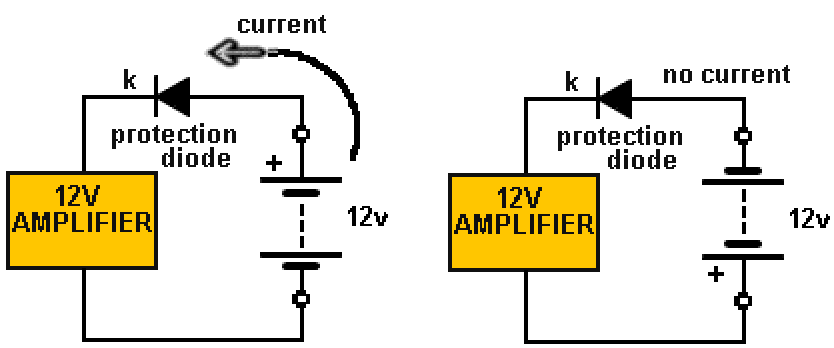

Fig 34. A Protection diode

Diodes perform many function in electrical and electronic circuits. Here is an application as a **PROTECTION DIODE.**
It protects the amplifier. If the 12v battery is connected around the wrong way, no current will flow.

[to Index]

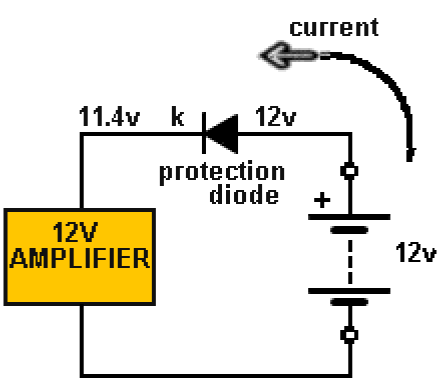

Fig 35. Diode "Voltage Drop"

When a diode is placed in a circuit (and current is flowing), a small voltage develops across the diode. This voltage is called the **FORWARD VOLTAGE DROP.**
This voltage is approximately 0.6v.
This is due to a junction inside the diode where two different materials are joined.
Normally, this voltage is not important because it is only small, but sometimes you need to take it into account.
For the circuit above, the amplifier only gets 11.4v

[to Index]

Voltage is measured with a

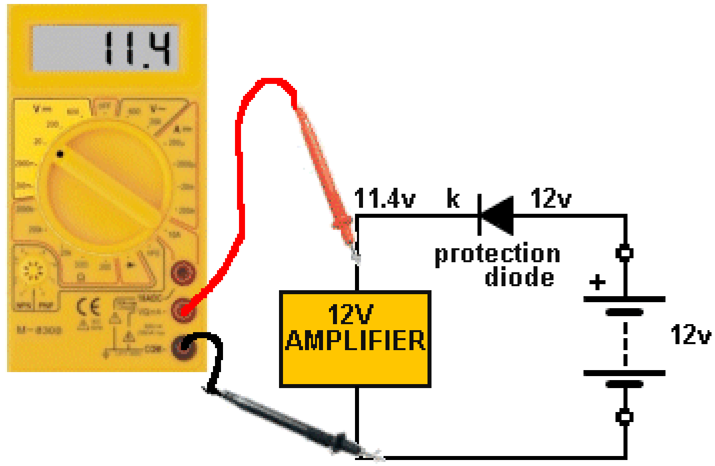

Fig 36. Measuring Voltage with a Digital Multimeter

VOLTMETER.
Multimeters have 2 or 3 voltage ranges so you can measure low voltage (0v to 20v), medium voltages (0v to 200v and high voltages (0v to 500v).
A voltmeter is placed across the component being tested, as shown in the diagram.
The Digital Multimeter is detecting 11.4v across the amplifier.

to Index

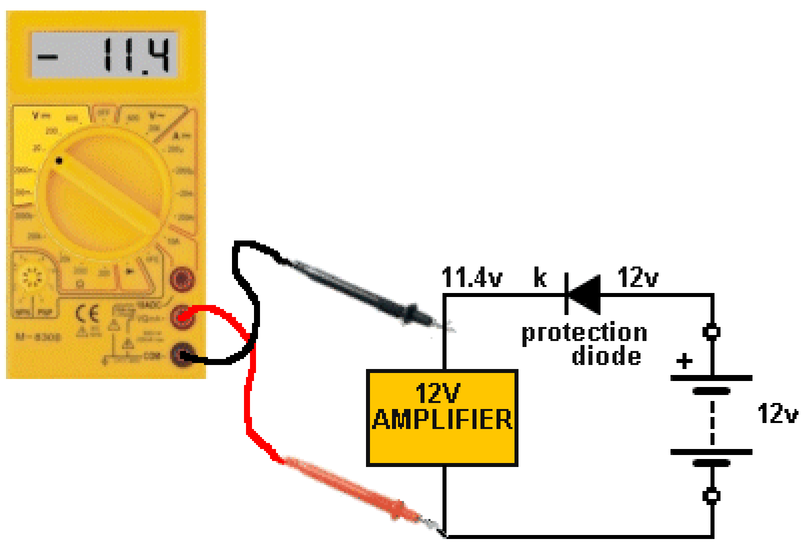

Fig 37. Measuring Voltage with a Digital Multimeter

If you place the probes of a digital multimeter around the wrong way on a component, the display will show a "-" The meter will not be damaged.

to Index

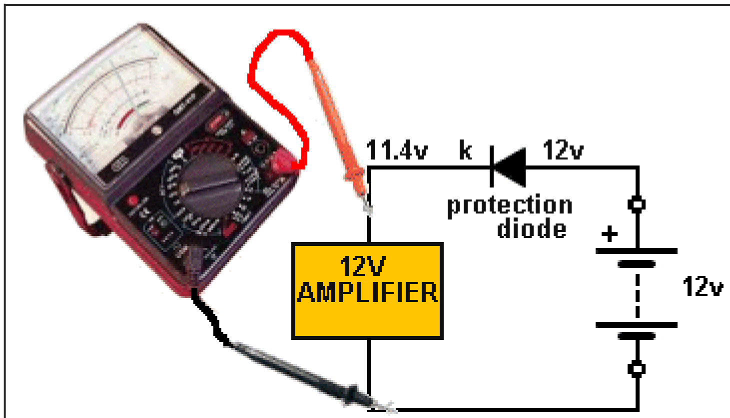

Fig 38. Measuring Voltage with an Analogue Multimeter

An analogue Multimeter must be connected around the correct way to make the pointer move "up scale."
Select the range that will allow the pointer to show somewhere in the middle of the scale.

to Index

Current is measured by

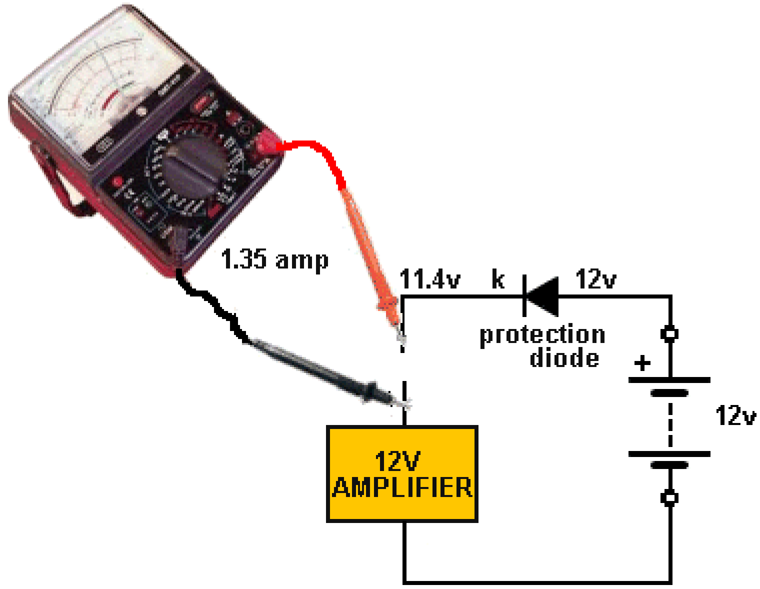

Fig 39. Measuring Current with an Analogue Multimeter

"breaking into the circuit" and inserting the leads so the positive probe is closest to the positive of the battery.
If you connect the leads around the other way, the needle will not move but it will hit the "end stop" and you may have to "bump" the meter to get the pointer to move from its jammed position.

to Index

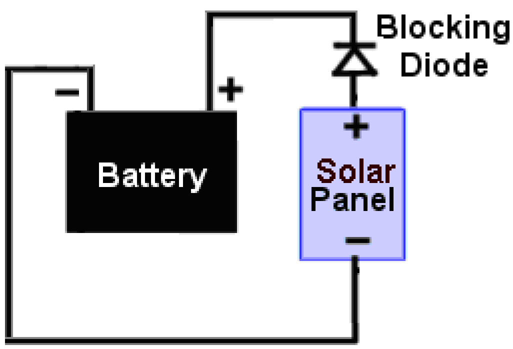

Fig 39a. The Solar Panel and the Blocking Diode

A DIODE is also used with a solar panel to prevent the battery discharging into the solar panel when the sun is not shining.
When the solar panel is not receiving any light it becomes a resistor with a large value and a small current can flow through it from the battery. The diode prevents this current-flow. The diode is called a **BLOCKING DIODE**.

to Index

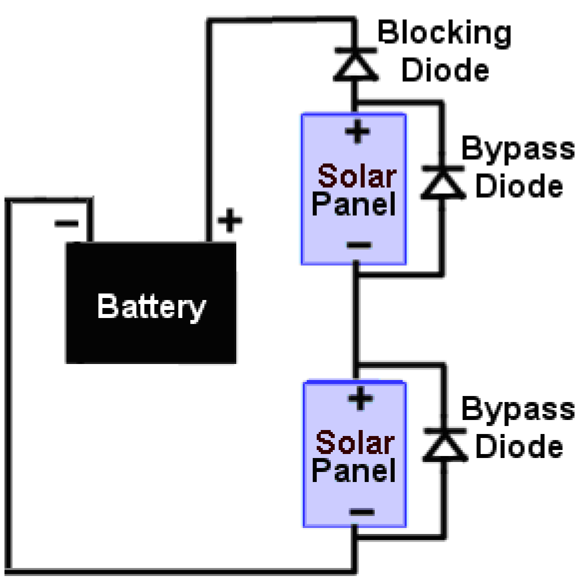

Fig 39b. The Solar Panel with diodes

Diodes are given different names, according to their function. They all perform the same job by passing current in one direction and prevent current-flow in the opposite direction.
When the top solar panel is shaded by a cloud, it generates less current and this will reduce the current into the battery.
By placing a diode across the panel, the diode will pass the current produced by the lower panel to the battery.
These diodes are called **BYPASS DIODES.**

called BLOCKING DIODES and BYPASS DIODES.

to Index

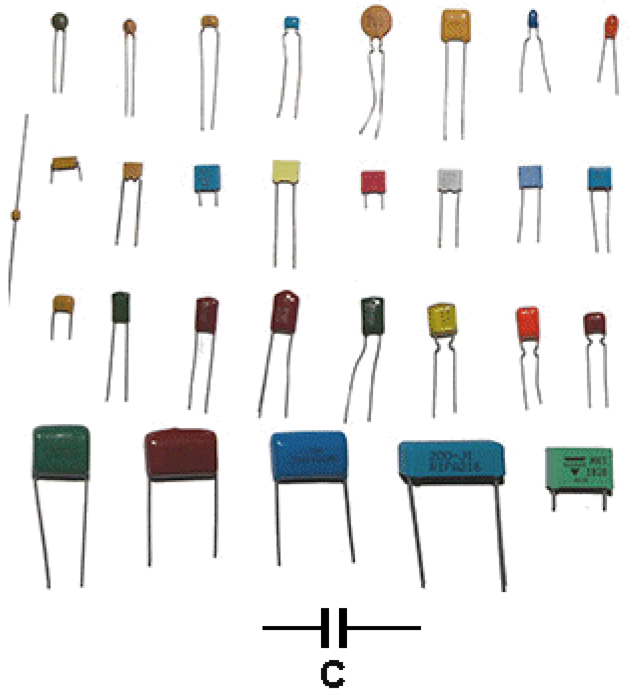

Fig 40. Capacitors and symbol

The next component we cover is the **CAPACITOR**.
There are thousands of different types of capacitor.
Each value of capacitor can have a low voltage rating, medium voltage or high voltage.
Capacitors can be very small in size and shape or very stable with temperature-rise or simply very cheap to make.
A capacitor consists of two thin sheets of metal such as aluminium with a thin sheet of plastic between.
The sheets may be rolled up in a cylinder or laid on top of each other.
The fact is this: the top sheet of metal does not touch the bottom sheet. This is shown in the symbol.
The resistance between the two terminals is INFINITE.
The 6th capacitor in the top row is called a **MONOBLOCK**.

to Index

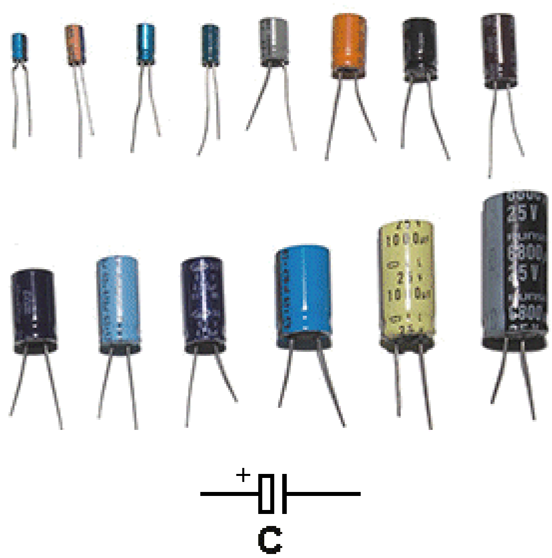

Fig 41. Electrolytic Capacitor

A capacitor gets bigger as its value increases.
It also gets bigger when the voltage-rating increases.
The basic unit of capacitance is the FARAD. A one-farad capacitor would be the size of a house. To make the capacitor smaller the sheets are etched to increase the surface-area and different insulating materials are used between the sheets.
The result is a capacitor called an **ELECTROLYTIC**. It is a bit like a rechargeable battery. It stores a lot of energy in a small space.
The negative lead is shorter and has a black stripe on the side of the electrolytic.

to Index

One FARAD is too big to handle. We use smaller values.
The middle of the range is one microfarad. This is written as 1u. (sometimes you see uF)
This is one-millionth of a FARAD.
The smallest value of capacitance is one picofarad. This is one millionth of a microfarad.
It is written as 1p.
Capacitors are broadly separated into two groups. 1p to 1u and 1u to 100,000u
Capacitors 1p to 1u are ceramic, polyester, air, styroseal, monoblock and other names.
Capacitors 1u to 100,000u are electrolytic or tantalum. A tantalum is the same as an electrolytic - for testing purposes - it is a more-compact electrolytic.

1 microfarad is one millionth of 1 farad.
1 microfarad is divided into smaller parts called nanofarad.
1,000 nanofarad = 1 microfarad
Nanofarad is divided into small parts called picofarad
1,000 picofarad = 1 nanofarad.

Recapping:
1p = 1 picofarad. 1,000p = 1n (1 nanofarad) 1,000,000p = 1u
1,000n = 1u (1 microfarad)
1,000u = 1millifarad
1,000,000u = 1 FARAD.

Examples:
All ceramic capacitors are marked in "p" (puff")
A ceramic with 22 is 22p = 22 picofarad
A ceramic with 47 is 47p = 47 picofarad
A ceramic with 470 is 470p = 470 picofarad
A ceramic with 471 is 470p = 470 picofarad
A ceramic with 101 is 100p (it can also be 100)
A ceramic with 102 is 1,000p = 1n
A ceramic with 223 is 22,000p = 22n
A ceramic with 104 is 100,000p = 100n = 0.1u A common 100n is called a **MONOBLOCK**.
A ceramic with 105 is 1u

TYPES OF CAPACITOR
For testing purposes, there are two types of capacitor.
Capacitors from 1p to 100n are non-polar and can be inserted into a circuit around either way.
Capacitors from 1u to 100,000u are electrolytics (or tantalum) and are polarised. They must be fitted so the positive lead goes to the supply voltage and the negative lead goes to ground (or earth).

to Index

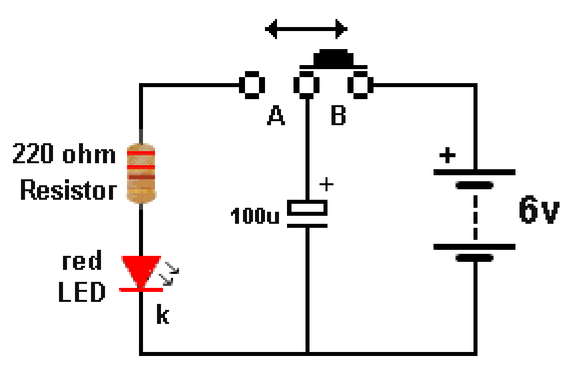

Fig 42. Charging a Capacitor

Here is an experiment to show how much (little) energy is stored in a 100u electrolytic.
When the slide-switch is in position "B", the 100u is charged by the 6v battery.
When the slide switch is moved to position "A" the electrolytic supplies energy to illuminate the red LED via the 220R resistor. It will illuminate for a short period of time.
By moving the switch back and forth, you can keep the LED illuminated.

to Index

Capacitors can be connected in **Series or Parallel** to obtain a value of capacitance you may not have available.
They are also connected in series to increase the effective **VOLTAGE RATING**.
However when two equal-value capacitors are connected in series, the final value is HALF, and thus you need two with double the final-value to get a value with an increased voltage-rating.
When two equal-value capacitors are connected in series, the result is HALF.
(This is the opposite to connecting resistors)

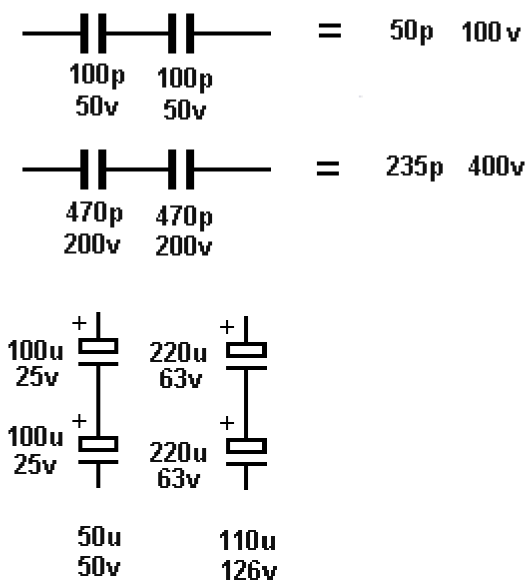

Fig 43. Capacitors in Series

to Index

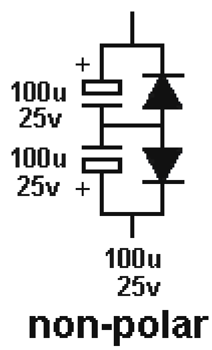

Fig 43a. Non-polar Capacitor

Non-polar Capacitor (electrolytic)

A normal electrolytic must be connected the correct way in a circuit because it has a thin insulating layer covering the plates that has a high resistance.

If you connect the electrolytic around the wrong way, this layer "breaks-down" and the resistance of the electrolytic becomes very small and a high current flows. This heats up the electrolytic and the current increases. Very soon the capacitor produces gasses and explodes.
One big mistake in many text books shows how to make a non-polar electrolytic by connecting two "back-to-back."
They claim 2 x 100u connected back-to-back is equal to 47u.
This appears to be case when testing on a meter but the meter simply charges them for a short period of time to get a reading.
If you allow them to charge fully you will find the reverse electrolytic has a very small voltage across it.
Secondly, when you are charging them, you are putting a high current through the reverse electrolytic and damaging the layer.
To prevent this, you need to add two diodes as shown in the diagram.
In addition, 2 x 100u "back-to-back" is very near 100u.

to Index

Capacitors can be connected in **Parallel** to obtain a value of capacitance you may not have available.
(This does not change the **VOLTAGE RATING**.)
When two equal-value capacitors are connected in parallel, the result is DOUBLE.
(This is the opposite to connecting resistors).
If one electrolytic is 25v

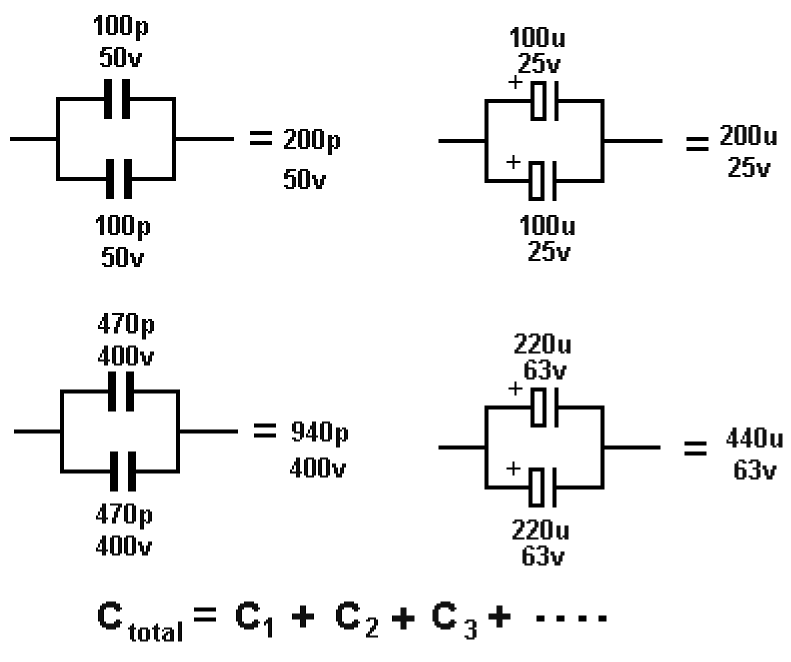

Fig 44. Capacitors in Parallel

and the other 63v, the answer is the LOWER VOLTAGE = 25v.

to Index

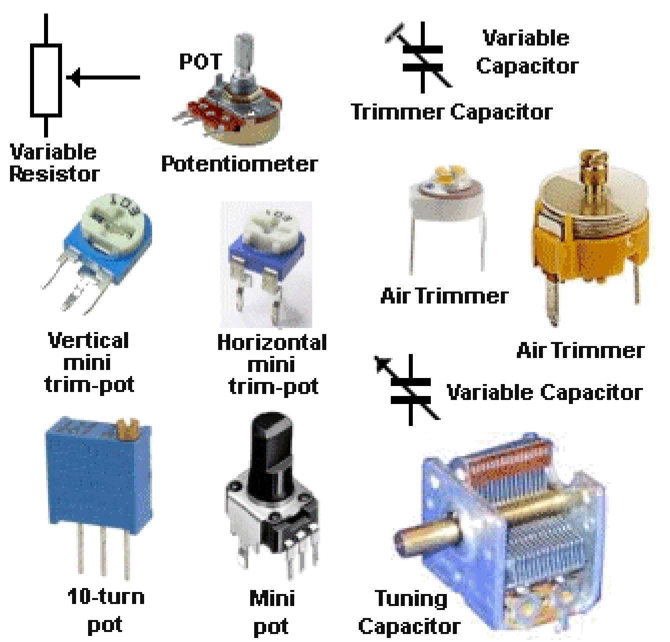

Fig 45. Variable Capacitors and Resistors

The value of a capacitor or resistor may need to be increased or decreased in a circuit to tune in radio stations or increase and decrease the volume of a speaker. The symbol for these components have an arrow to show they can be adjusted.
The resistance of a potentiometer can be from 1 ohm to 5M
They come in many different shapes and sizes to suit the PC board or front-panel layout.
The "T" represents a trimmer capacitor and this can be from 1p to about 120p.
A variable capacitor will be from about 10p to 415p.

to Index

Simple CIRCUITS
We have covered enough symbols and components to create a number of simple circuits.
These circuits will show how to connect a motor, a LED, (how to make it bright or dull) and how to connect 4 cells to make a battery.

Note: The flashing LED

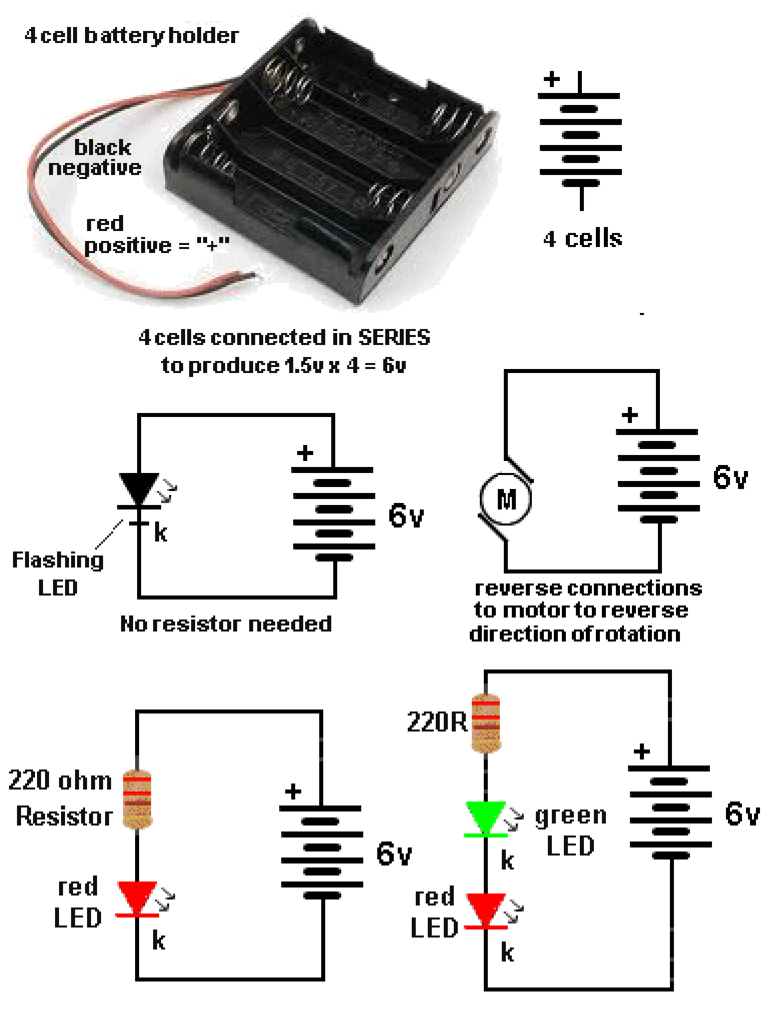

Fig 46. Simple Circuits

does not need a resistor because a resistor and chip are inside the LED, to make it flash and control the current.

Connect all the components around the correct way and then connect them around the wrong way to see what happens.
Connect the flashing LED in series with a red LED and see what happens.

to Index

QUESTIONS

1. Explain why the Flashing LED circuit has no external resistor.
2. How many 1.5v cells are needed to produce a 6v battery
3. Explain what happens when you reverse the leads to a motor.
4. Identify the positive terminal:

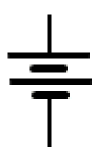

5. Can 3 green LEDs be connected in series to a 6v supply?
6. A variable resistor is also called: ____________________
7. The combined resistance of two 1k resistors in series is: ______________
8. The combined resistance of two 1k resistors in parallel is: ______________
9. Name the short lead on a LED
10. Name the type of multimeter with a pointer and scale: ____________________
11. The total capacitance of two 100u electrolytics in series is: _____________
12. The total capacitance of two 100u electrolytics in series is: _____________
13. Write these values in words:

22R _________
4k7 _________
1n ___________
100u ___________

14. How many 1.5v cells in a 9v battery?

15. The red probe is: _______________ (positive/negative)
16. Conventional current flows from: _________ (positive to negative / negative to positive)
17. Make a 470u electrolytic with two electrolytics:
18. What is the voltage drop across a diode?
19. Name the component that only allows current to flow in one direction: ____________
20. Name this symbol:

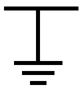

21. When resistors are connected in series, the resistance of the combination: _________ (increases / decreases)
22. When two capacitors are connected in parallel, the voltage-rating of the combination: _______________ (increases / equal to the capacitor with the lowest voltage-rating)
23. Draw two 2k2 resistors in parallel.
24. Which is larger: 470R or 22k
25. What is the value of this combination:

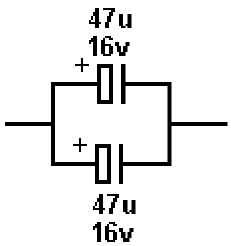

26. What is the name of the resistor in series with a LED: ____________________
27. What is the voltage across the amplifier: _________

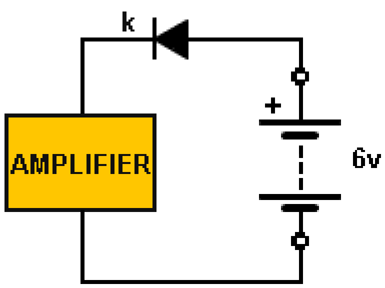

28. Identify the fault with these circuits:

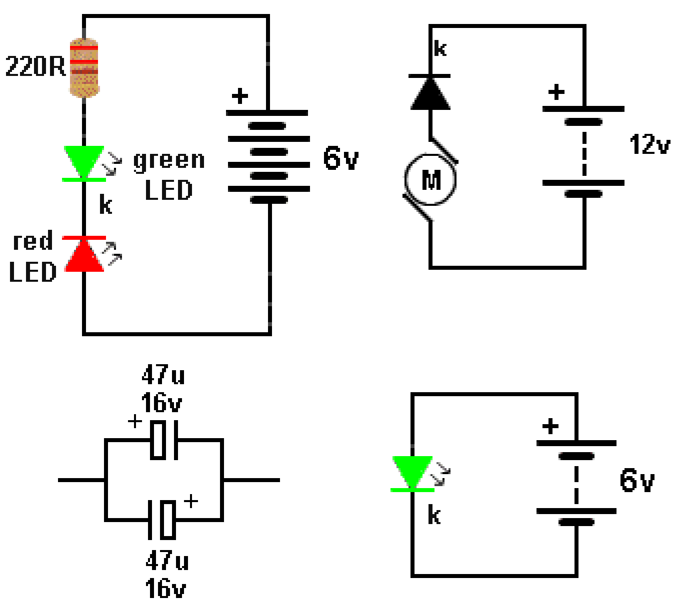

to Index

Passive Components
All the components shown

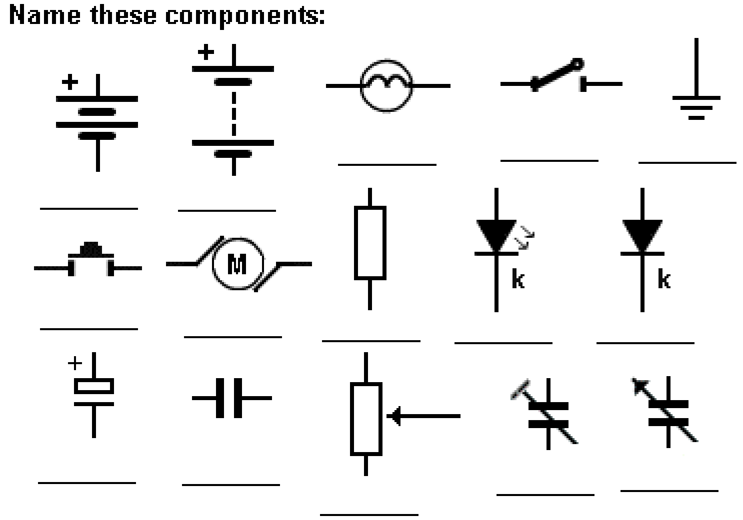

Fig 47. Passive Components

on the left are called PASSIVE COMPONENTS. This means they do not amplify.
Write the name beside each symbol.

to Index

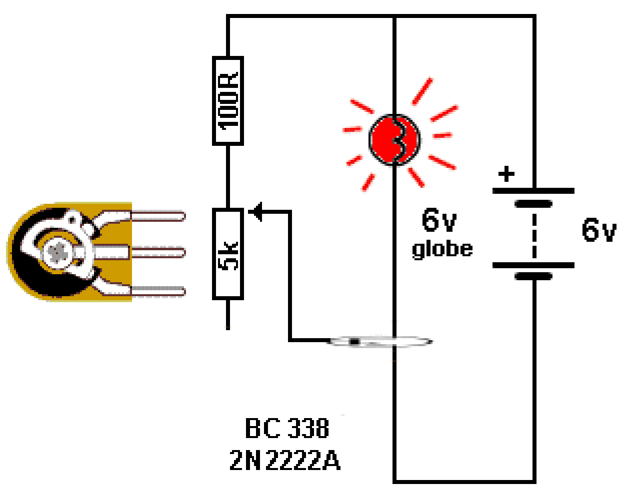

Fig 47a. The Potentiometer in action

The Potentiometer is a variable resistor.
It consists of a curved carbon track with a wiper that touches the track and can be turned via a screwdriver or knob.
The wiper is the middle wire on the circuit symbol and it moves up and down as shown in the animation.
When the three leads are connected the symbol is called a potentiometer.
When two leads are connected it is a variable resistor.
When the resistance increases, less current flows through the pot.

to Index

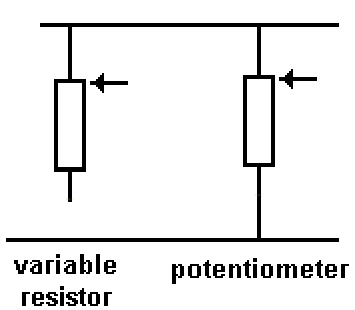

Fig 47b. The Variable Resistor and Potentiometer

There is a difference in operation between a **Variable Resistor** and a **Potentiometer**.
Both will increase or decrease the sound level as a volume control or the speed of a motor or the brightness of a globe, but a Potentiometer will guarantee zero volume or zero brightness when the pot is turned fully anticlockwise (as shown in the animation).
This is because the output will be zero volts, but the variable resistor may still deliver some "energy" (voltage and current) to the circuit when turned fully anticlockwise.

to Index

Potentiometers come in values from 100 ohms to 5 Meg ohms (500R, 1k, 2k, 5k, 10k, 50k, 100k, 200k, 250k, 500k, 1M are most popular).
They come as linear, or logarithmic where the resistance of the track (per mm) is higher at one end. Because our hearing is not linear, these pots can be used as volume controls to produce a gradual (very nearly linear) increase in volume.
Selecting the correct value of resistance for a circuit is VERY complex. If the value is not correct, the volume will not be loud or it will drop to zero before the pot is turned fully anticlockwise. Or

the motor will drop to zero at mid-turn of the pot or it will not reduce in RPM to the desired amount.
The simple answer is to copy a circuit.
Or you can try the whole range of pots and you will find one value is the best.
A Potentiometer can be used in hundreds of different circuits to produce hundreds of different effects, but the actual "thing" that flows between the input and output is a percentage of the voltage. At the same time the current will also be passed to the output at a reduced value. A pot actually delivers BOTH reduced values at the same time and the receiving circuit will be designed to "look for" the change in voltage or current. If the supply voltage is not rising or falling, the "values" are called DC values.
The voltage can also be in the form of a signal (volume). This is called an AC signal.

to Indexx

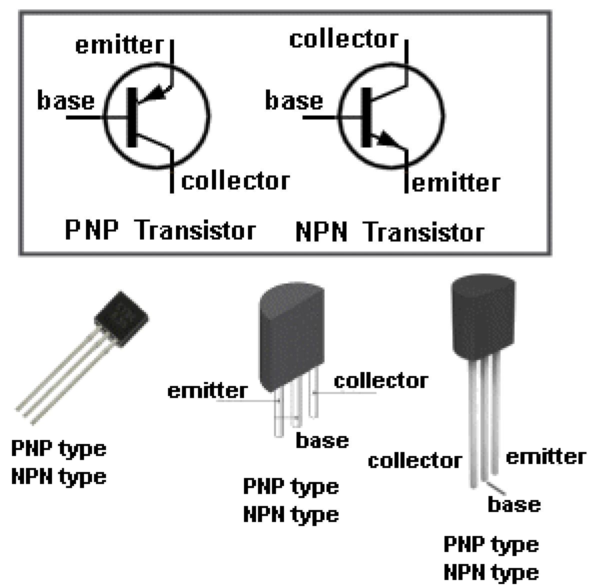

Fig 48. The TRANSISTOR

The TRANSISTOR

A TRANSISTOR is an ACTIVE device. It AMPLIFIES.
There are many types of transistor (over 20,000 different types) from hundreds of manufacturers and they have many different names.
We are going to study the simplest.
It has the technical name **BIPOLAR JUNCTION TRANSISTOR (BJT)** but we are going to call it a **TRANSISTOR**.
There are two types in this group: **PNP** and **NPN**.

The type we will study is also called a **SMALL-SIGNAL TRANSISTOR.**

You cannot tell an **NPN** transistor from **PNP** by looking at it. You must test it in a circuit.
In **Fig 65** you will make a **Transistor Tester** project, but first some basic facts:

to Index

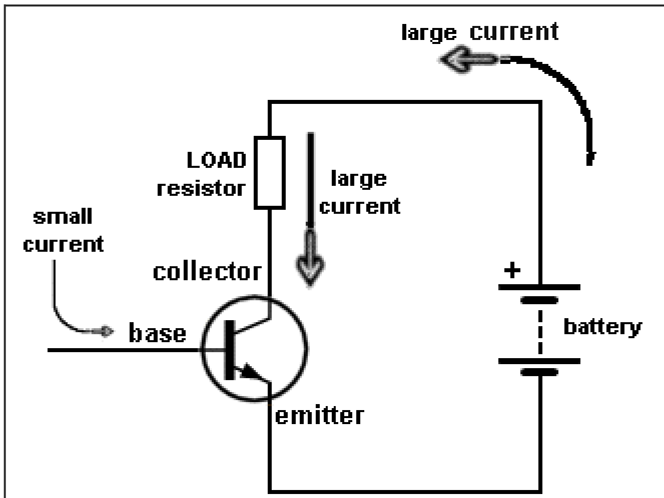

Fig 49. The NPN TRANSISTOR in a Circuit

The first type of transistor we are going to study is the **NPN**.
A transistor has three leads:
BASE, COLLECTOR and **EMITTER**
Basically, a small current enters the base and a large current flows through the collector-emitter leads as shown in the diagram.
The resistor in the collector lead is called the LOAD Resistor.
Sometimes the load is a speaker.

to Index

The transistor is similar to the diagram opposite. A small drop of water entering the base is amplified to

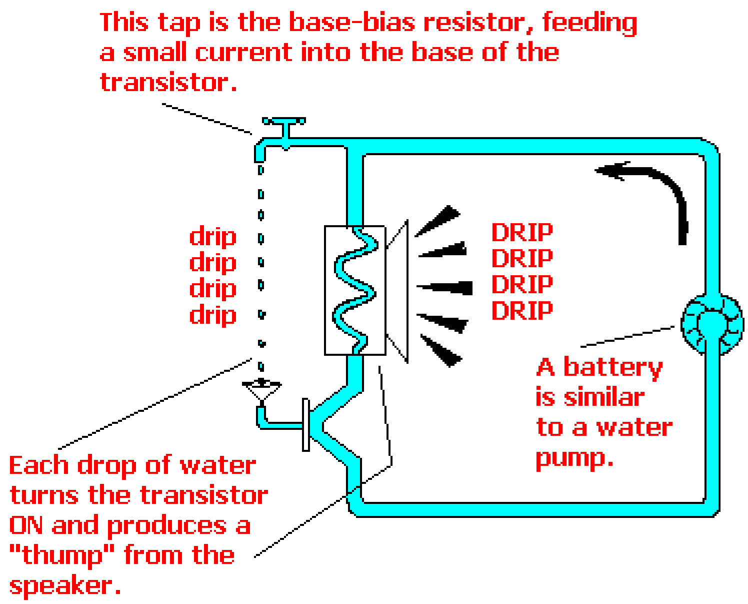

Fig 50. The Water TRANSISTOR

produce a loud DRIP from the speaker.

to Index

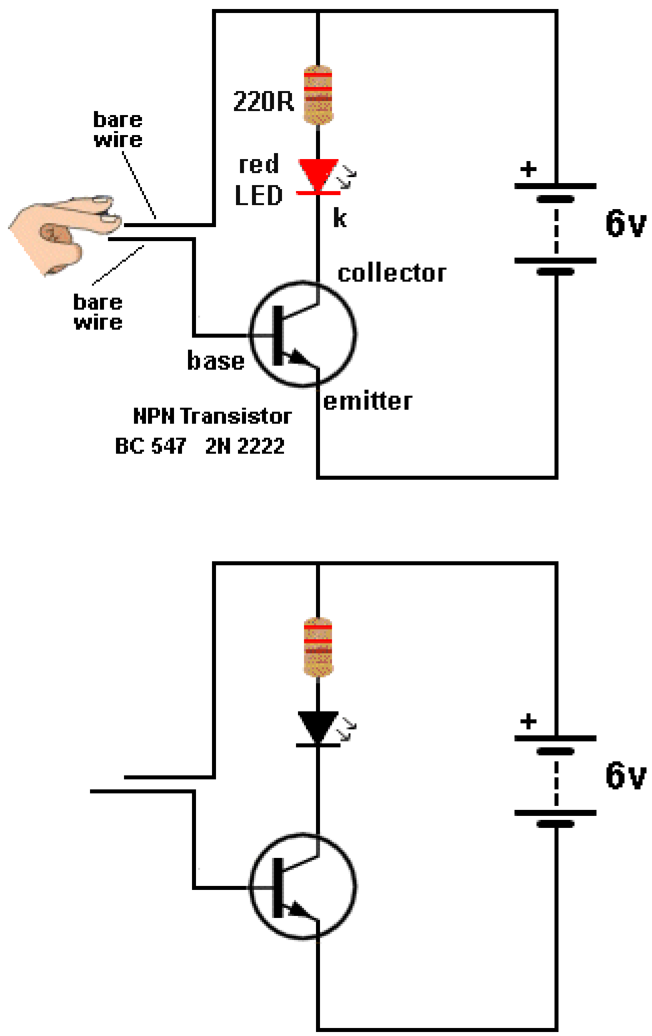

Fig 51. One Transistor Circuit

In this experiment we will construct a ONE TRANSISTOR circuit similar to the WATER TRANSISTOR above and observe the results.
Make sure the two leads DO NOT TOUCH. If they touch, the transistor will be DESTROYED.

The transistor is amplifying the current through your finger via the two leads and it will be very dim.

ANIMATION

The lower diagram shows the transistor turning ON when a finger is pressed against the two wires. The finger produces a resistance that turns the transistor ON and this turns the transistor into a smaller and smaller resistor. That's how more and more current flows through the LED and it gets brighter and brighter.

to Index

By adding another transistor we amplify the

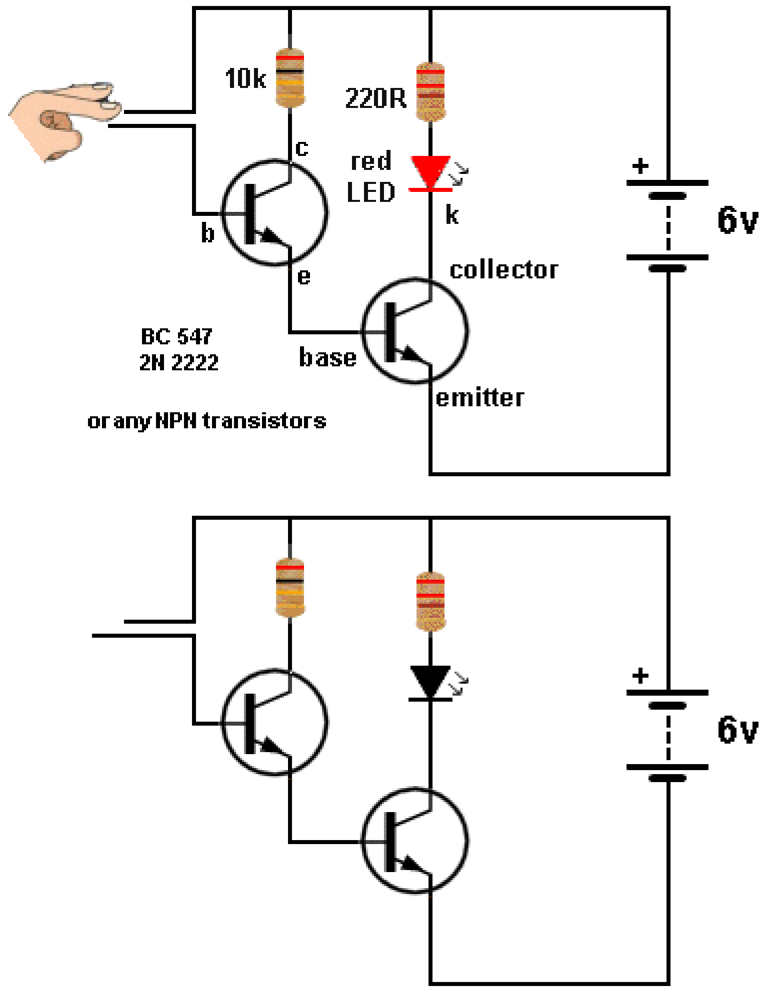

Fig 52. Two Transistor Circuit

current through the finger about 200 times and now the LED will glow bright.

Make sure the bare wires do not touch each other as this will destroy BOTH transistors.

ANIMATION

The lower diagram shows both transistors turning **ON** when a finger is pressed against the two wires.
They both becomes smaller and smaller resistors.
The first transistor allows more current to flow into the base of the second transistor and this is how the second transistor turns on more and more. This allows more current to flow through the LED and it gets brighter and brighter.

to Index

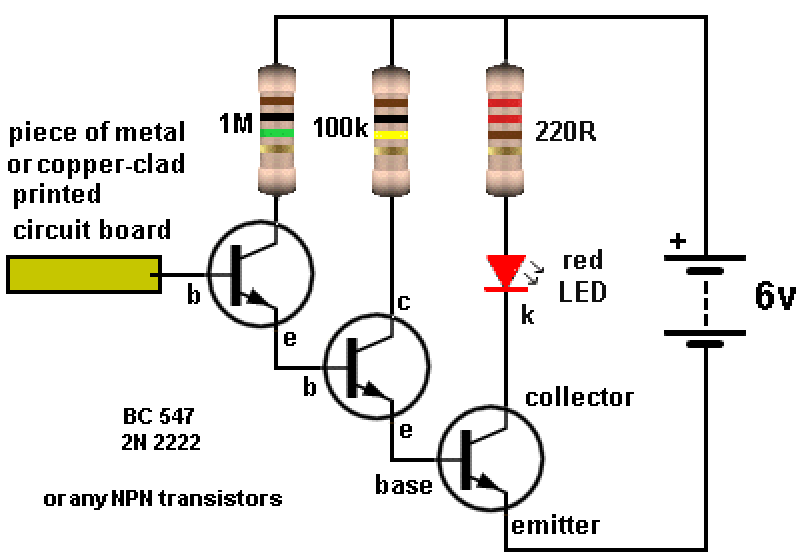

This circuit has enormous gain.
Each transistor has a gain or more than 200 and the final gain will be more than:
200 x 200 x 200 = 8,000,000
8 MILLION!

The circuit is very sensitive to static voltages in the air or electrical waves such as the waveform produced by the electrical wiring in a house.
Move the project around a room and detect all the electrical signals.

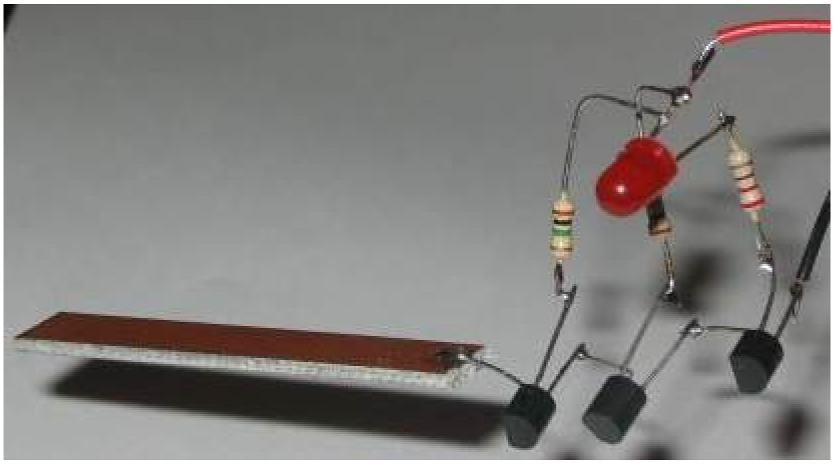

Fig 53. Three Transistors

to Index

You can see the effect of one transistor. It does not do much.
The two transistor circuit allows the resistance of your finger to deliver current into the base of the first transistor and this transistor delivers more current into the base of the second transistor. The result is more collector-emitter current and the LED illuminates.
The three transistor circuit produce an ENORMOUS effect.
It will pick up STATIC ELECTRICITY and all forms of electro-magnetic energy (radiation) and illuminate the LED.

to Index

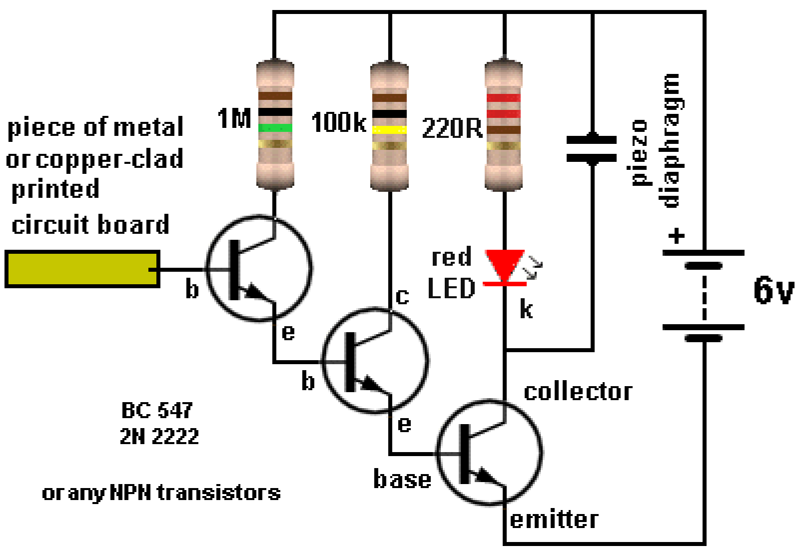

Fig 54. Adding a PIEZO

By adding a piezo diaphragm to the output you will be able to hear the hum of the mains.
This is the frequency of the supply into your house. It will be either 50 cycles per second or 60 cycles per second.
The term: "cycles per second" is given the name HERTZ after **Heinrich Rudolf Hertz**, who was the first to prove the existence of electromagnetic waves.

to Index

The Piezo diaphragm is held around the outer edge inside a plastic case and when a voltage is applied to the two leads, the thin plate curves very slightly.
When the voltage is removed, the plate returns to its flat shape.
If the voltage is reversed, the plate curves in the opposite direction.

The curving is due to a thin layer of ceramic material under the plate and

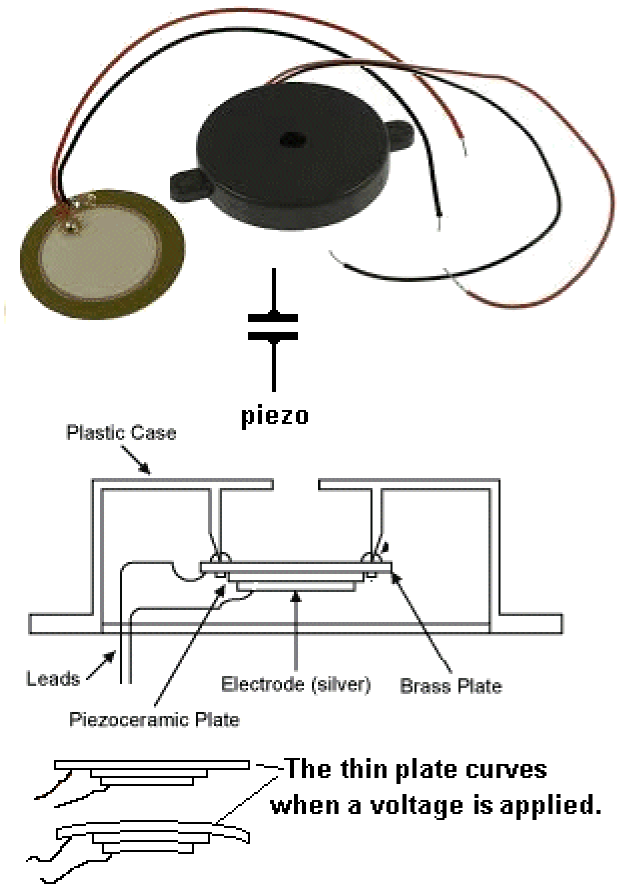

Fig 55. The Piezo

then a film of metal is deposited onto the ceramic so a lead can be soldered.

There is infinite resistance between the two leads as the ceramic material is an INSULATOR.
The capacitance between the two leads is approx 22n.
The Piezo is a passive device. It needs a pulse or frequency for it to produce an output.

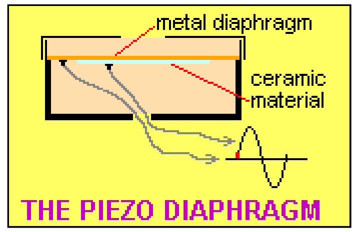

to Index

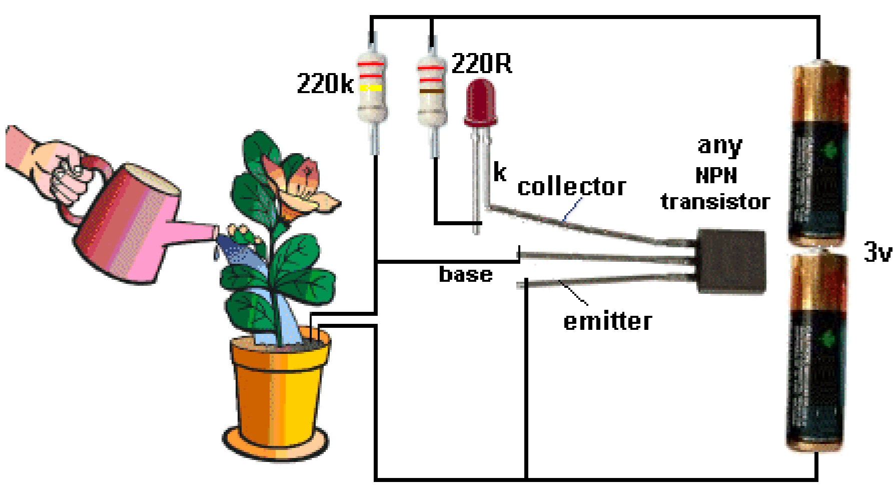

Fig 56. Plant Needs Water

The **ONE TRANSISTOR CIRCUIT** above can be turned into a detector to show when a plant needs water.
Place the two probes into the soil and water the plant. The LED will turn off. As the water evaporates the LED will turn **ON** to let you know the plant needs watering.

to Index

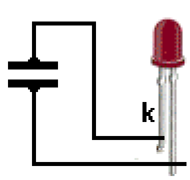

Fig 57. Tap the Piezo

This experiment produces a pulse from the piezo when it is tapped and the LED illuminates briefly.

The LED can be connected either way around.

This proves the diaphragm flexes when a voltage is applied and also in the reverse situation. A voltage is produces when the diaphragm is tapped.

to Index

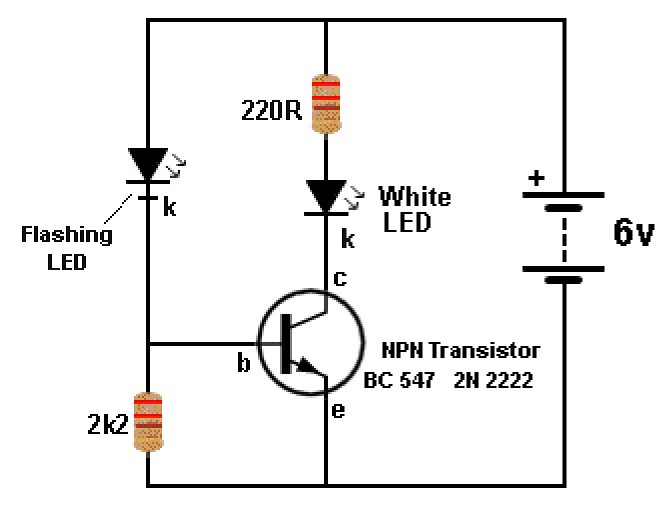

Fig 58. Flashing LED and White LED

A flashing LED is not very bright.
It can be connected to a transistor and the transistor will drive a very bright white LED.
The transistor is an amplifier.
It is amplifying the current flowing through the flashing LED and supplying a higher current for the white LED.

We cannot discuss any further details of the circuit at the moment because the actual operation of the circuit is quite complex.

At the moment we just need to experiment with simple transistor circuits.

to Index

Fig 59. Soldering Iron

We now come to the point of HELPING YOU WITH CONSTRUCTION.
We have already shown you 6 different circuits and there are many ways to build them.
You can:
1. Solder them.
2. Build them on an Experimenter Board
3. Connect the components with clips or twist the leads together.
It does not matter how you build the circuits.
The fact is this: YOU MUST START BUILDING.
The best soldering iron for a beginner is a CONSTANT TEMPERATURE soldering iron.
It has a dial that can be turned to set the desired temperature.
An ordinary soldering iron GETS TOO HOT. It is not suitable for soldering electronic circuits.
This is something that no-one has mentioned before. An ordinary soldering iron will melt the solder TOO QUICKLY and burn the resin inside the solder and make soldering very difficult for a beginner.
Soldering must be done slowly so the resin in the middle of the solder gets hot and cleans the leads of the components so the solder will "stick."
That's why you must apply the solder to the leads you are soldering and allow the resin to "attack" the leads and clean them.
The cheapest TEMPERATURE CONTROLLED soldering Iron is available on eBay for les than $10.00 (post FREE).
You will also need a small roll of solder (0.9mm) and a soldering Iron stand.
Email Colin Mitchell for links to eBay. (talking@tpg.com.au)
A whole book could be written on the ART OF SOLDERING.
Look on the web for articles and videos on SOLDERING.

to Index

SOLDERING

1. Soldering is very easy and very simple. You just need a **Temperature Controlled Soldering Iron**, **Fine solder** and clean components.
2. Remember this: It is **NOT** the solder you need for a joint, but the **FLUX**. And the flux lasts for only 2 seconds. When the flux is **HOT** it attacks and cleans the joint so that the solder will stick.
3. Turn ON the Temperature Controlled Soldering Iron to a low temperature. Put solder on the tip. It will not melt. Turn up the temperature slightly. Try more solder. As soon as the solder starts to melt, this is your starting point. Turn up the temperature slightly MORE and this is the correct temperature for **small, delicate, fine soldering**.
4. Place a component through a hole and bend the lead slightly so the component does not move. Turn the board over and touch the iron on the component and bring the solder **FROM THE OTHER SIDE** so the solder melts and flows towards the iron.
From start-to-finish, count one-two-three and remove the solder. Count four-five and remove the iron. You will have a perfect joint.
If you are soldering thick leads or large pads on a circuit board, you will need to turn the temperature UP slightly.
You must add enough solder to make the joint "bulge" slightly.
Fine solder (1mm or 0.9mm or 0.8mm) makes the best joint because it is easier to use.
Use a wet sponge to clean the tip or a ball of "Steel Wool." Steel wool is the best.
Here is the steel wool, bending the leads and some examples of poor joints due to insufficient solder:

Steel wool cleans the tip beautifully

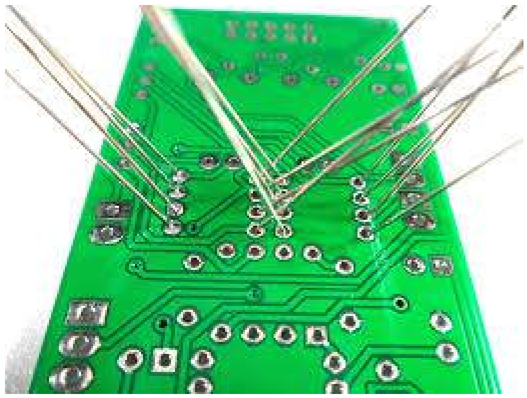

Bend the leads before soldering

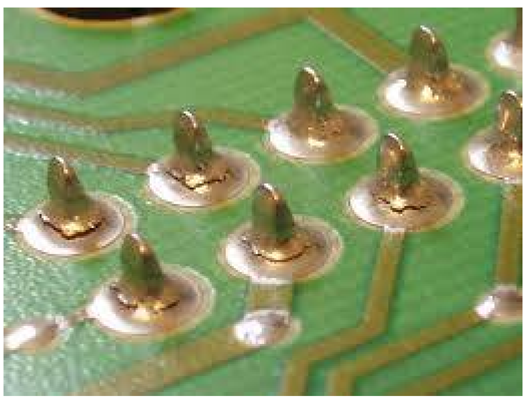

The joints do not have enough solder and that's why they fractured. Called a DRY JOINT.

More "Dry Joints."

This is the cheapest and simplest soldering iron stand.

This stand is very messy as the spring grabs the iron and makes it difficult to remove from the stand. Test the stand before buying. You will se why not to buy this type of soldering stand. Get one with a "wide mouth" and a heavy stand is best as it does not move.

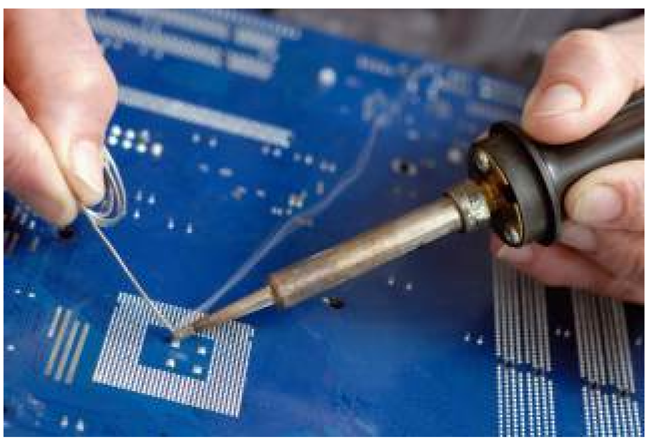

This photo clearly shows how to hold a soldering iron and solder.

This is NOT a temperature-controlled soldering iron and you can see it is too hot as it is burning off the flux too quickly.
Temperature Controlled Soldering Irons are now cheaper than the JUNK soldering iron shown in the photo. See eBay for prices.

[to Index]

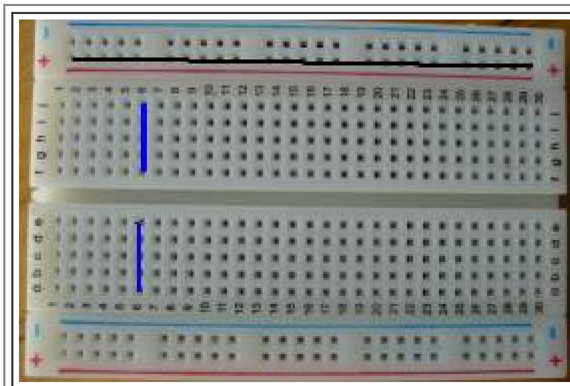

Photo shows a number of components fitted to the breadboard.

BREADBOARD

The term BREADBOARD refers to any piece of wood or plastic containing pins or pegs or clips or holes where you can build a circuit.
The components can be soldered, twisted clipped or fitted into holes.
Breadboard also means the circuit can be easily pulled apart.
Some breadboards do not have two rows for the positive and negative rails. Connections under the board for the positive rail is shown with a black line in the photo. Connections on the main section of the board are shown with blue lines. Your breadboard MUST look exactly like the photo opposite.
Other breadboards are quite useless.
The breadboard in the photo can be purchased on eBay for less than $5.00 (post FREE).

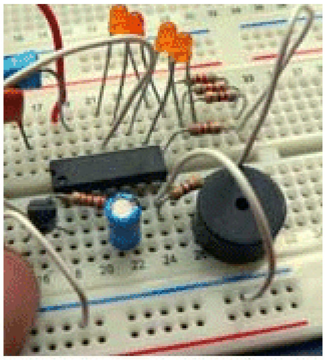

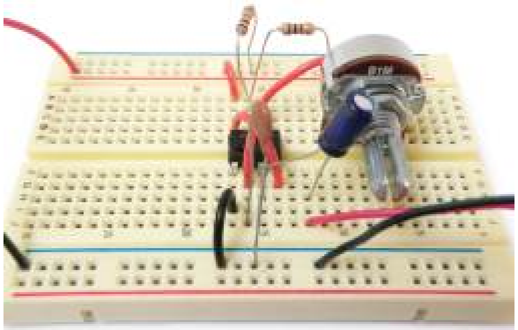

Fig 60. BREADBOARD and Components

to Index

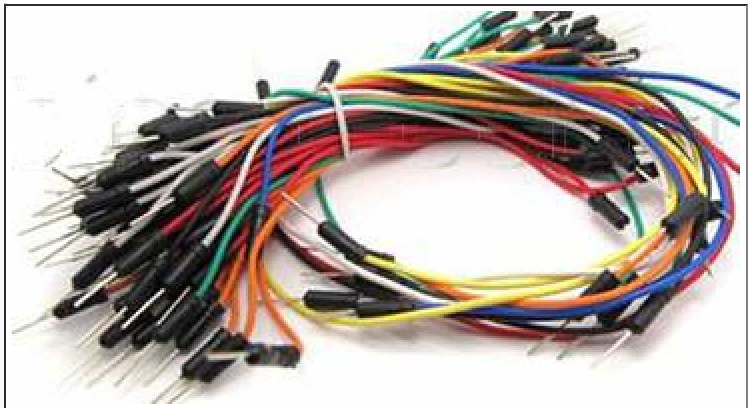

Fig 61. Jumpers

The components on the BREADBOARD are fitted down the holes and metal strips under the board join each column of 5 holes. If you want to join one hole with another, you can use 0.5mm tinned copper wire or JUMPERS. See photo opposite. Jumpers can be purchased on eBay for less than $3.00 posted.

Email Colin Mitchell for links to eBay. (talking@tpg.com.au)

to Index

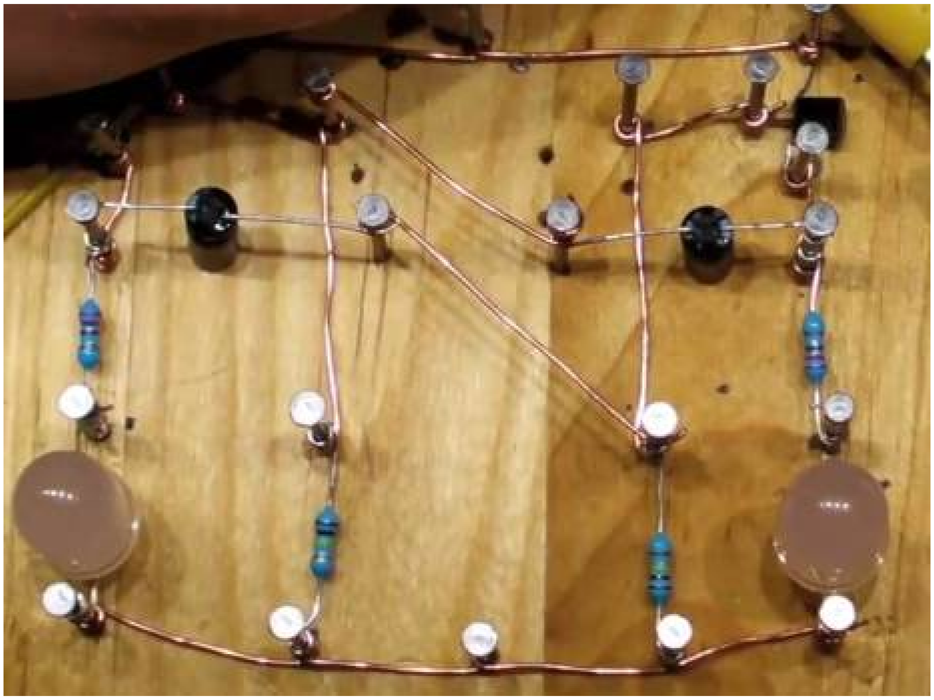

Fig 62. Breadboard with Nails

If you don't have a soldering iron or experimental breadboard, you can make your own board with nails. See the photo above. It is a multivibrator circuit and we will be presenting this circuit in a moment. The components can be twisted around the nails and bare wire used to join some of the nails to complete the circuit.

Another method of connecting the components is called BIRD-NESTING. This involves soldering the components "in the air" as shown in the 27MHz transmitter circuit below:

Another way to connect the component(if you don't have a soldering iron), is to wind 6 turns of bare wire around each connection and leaving all the components "in the air." The bare wire can be obtained from hook-up flex. This is plastic coated "wire" containing up to 15 fine strands of wire. Use a single strand for the connections. None of the components will touch each other BY MISTAKE and the circuit will work perfectly. Bird-nesting is a good way to build a quick circuit and test its performance. It might look messy but you can easily change any component.

to Index

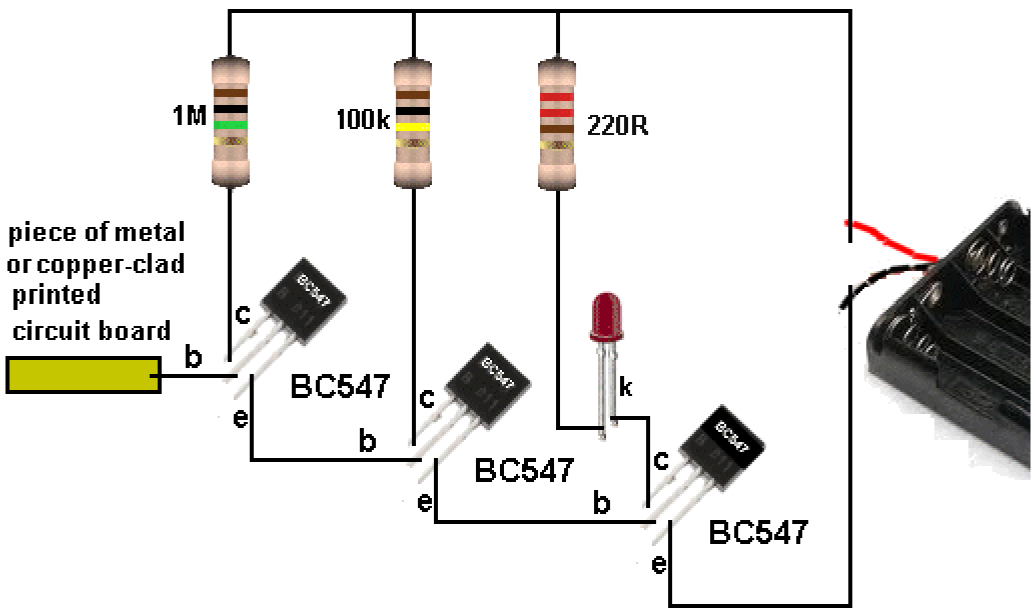

Fig 63. Wiring the 3-Transistor Circuit using BC547 Transistors
The diagram shows how to connect 3 x BC 547 transistors.
The leads of a transistor can be collector-base-emitter OR
emitter-base-collector and that's why we have provided 2 different wiring diagrams.

to Index

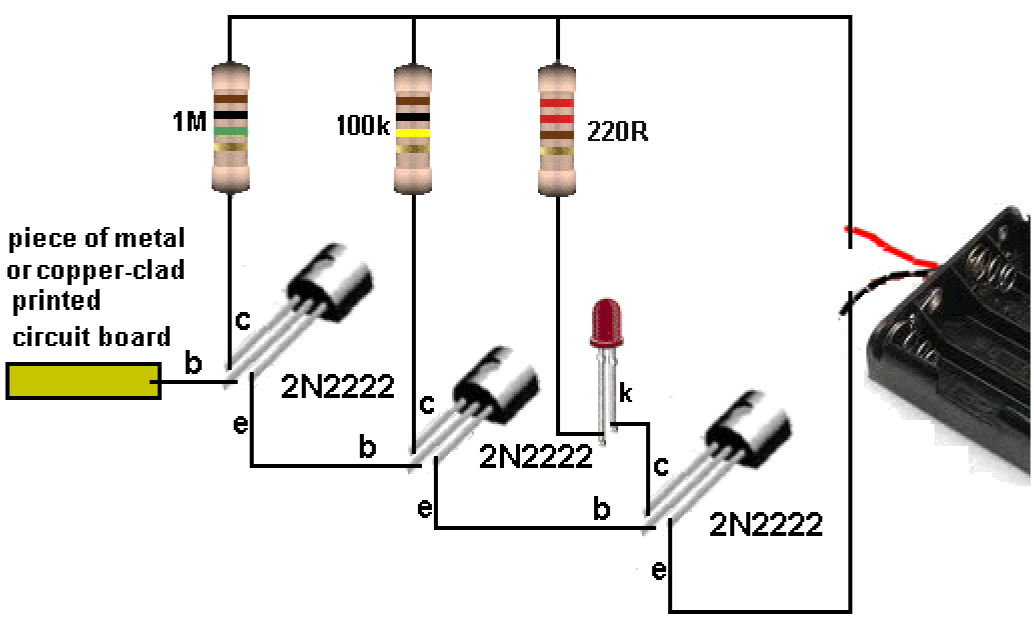

Fig 64. Wiring the 3-Transistor Circuit using 2N2222 Transistors
The diagram shows how to connect 3 x 2N2222 transistors.

to Index

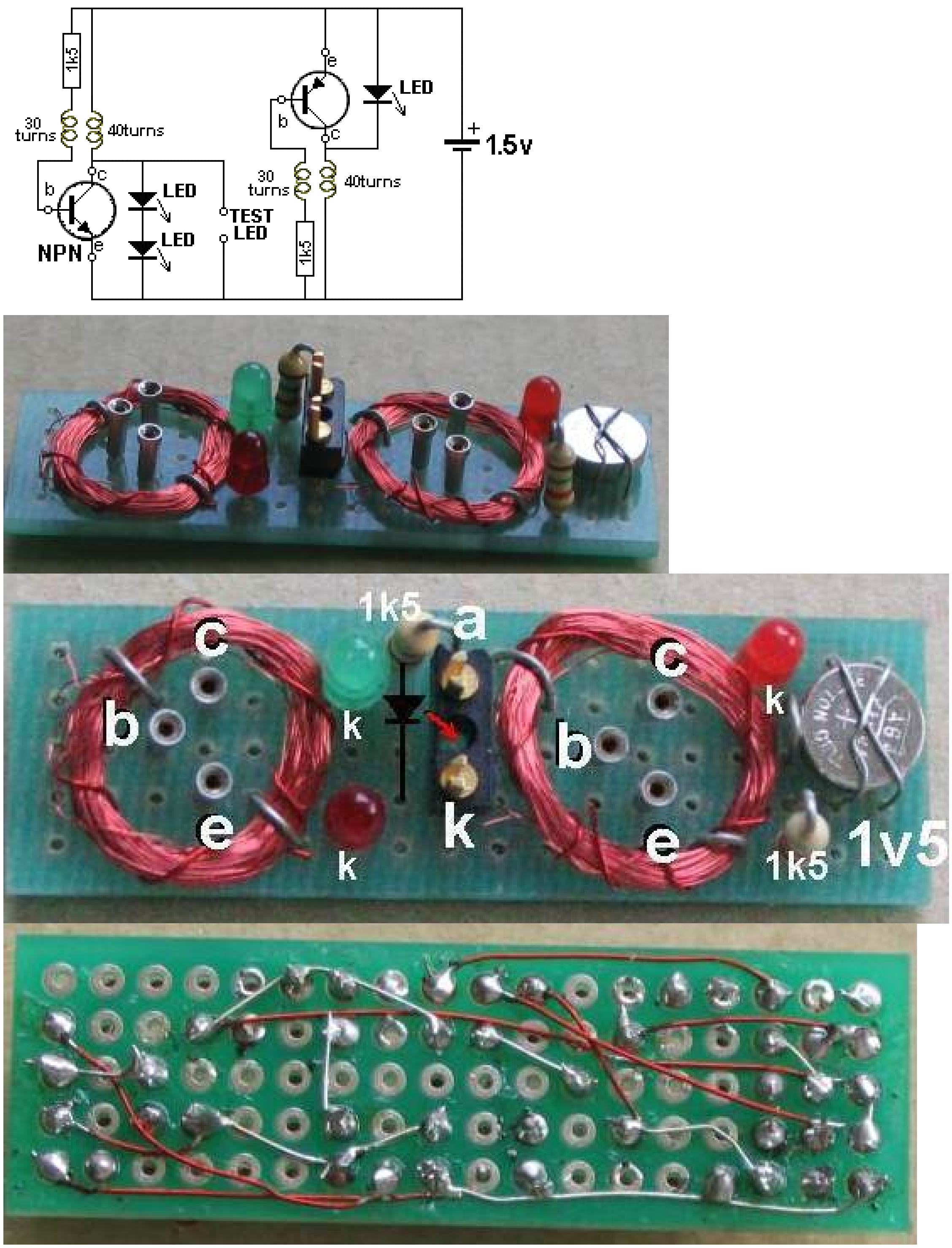

Fig 65. Transistor Tester

This handy transistor and LED tester can be built to test LEDs and both PNP and NPN transistors.
The project consists of two identical circuits, one for NPN and one for PNP.
You can build just the NPN section and then build the PNP section later.

LED VOLTAGE

We have shown a LED needs at least 1.7v supply for it to operate.
This circuit works on 1.5v and thus the action of the transistor and coil (called a Transformer) MUST be increasing the voltage for the LED to illuminate.
This circuit works on two "actions."
1. Transistor ACTION - this is the action of a transistor providing gain to make the circuit oscillate.
2. Transformer ACTION - this is the action of a coil of wire producing a voltage higher than the

supply voltage when it is turned off.

This circuit is very technical and very complex.
We will be explaining it in a very simple way because this is a **Basic Electronics Course**.

THE TRANSFORMER - the two coils of wire on the left and the two coils of wire on the right.
When the voltage (actually the current) is switched off, the 40 turn coil in either of the circuits in this project; the voltage across the coil rises to more than the 1.5v supply and is in the opposite direction to the voltage of the supply.
The circuit looks to be very simple but it uses an air-cored transformer to produce the voltage needed to illuminate the LED indicators and the circuit only works when the transistor is connected correctly. There are two separate circuits, one for NPN transistors and one for PNP transistors. We will cover the NPN section:
The circuit turns ON when the NPN transistor is fitted and the current through the 30 turn coil and 1k5 resistor turns ON the transistor and produces expanding flux in the 40 turn coil. This flux cuts the turns of the 30 turn coil and produces a voltage in the coil that adds to the supply voltage and increases the current into the base. This turns the NPN transistor ON more. This action continues until the transistor is fully turned ON. At this point the current in the 40 turn coil is a maximum but it is not expanding flux and the 30 turn coil ceases to see the extra voltage. Thus the current into the base reduces and this turns the transistor OFF slightly. The flux produced by the 40 turn coil now becomes collapsing (or reducing) flux and it produces a voltage in the opposite direction to greatly reduce the current into the base. In a very short period of time the transistor becomes TURNED OFF and it is effectively removed from the circuit. The flux in the 40 turn coil collapses quickly and it produces a voltage in the 40 turn coil that is higher than the supply voltage and is in the opposite direction. This means the voltage produced by the 40 turns ADDS to the supply voltage and is delivered to the LEDs to illuminate them.
The NPN circuit has two LEDs in series so that a LED of any colour (including white) can be connected to the TEST LED terminals and it will illuminate. You can use any colour LED for any of the LEDs, however it is best to use either green or yellow or white for the single LED.
The two "coils" are wound on a 10mm dia pen with 0.1mm wire (very fine wire). The loops of tinned copper wire holding the coils on the board are connected to separate lands under the board and MUST NOT produce a complete loop as this will create a “Shorted Turn” and the circuit WILL NOT WORK.
If the LEDs do not illuminate, simply reverse the wires to the 30 turn coil.
The circuit does not need an ON/OFF switch because the LEDs require a voltage of over 2v to illuminate (the orange LED) and the supply is only 1.5v. A red LED needs about 1.5v to 1.7v to operate but when it is in series with a green LED, this voltage is over 3.5v.
All the components fit on a small matrix board 5 holes x 18 holes. A kit of parts for the project is available for $4.00 plus $3.00 postage and ordering details can be obtained by emailing Colin Mitchell. (talking@tpg.com.au)
Build the circuit and test your transistors and LEDs.
We will be covering more on the action of a transistor and the action of a transformer in the discussion below, but it is important to build the circuit and see it working.
It is your first piece of **TEST EQUIPMENT**.

Questions

1. Identify the letters "c" "b" and "e"
2. What type of transistor is tested in the first set of hollow pins?
3. Put a PNP transistor into the first set of hollow pins and try all positions. Does the red and green LEDs illuminate?
4. When both the red and green LEDs illuminate, what is the approximate voltage across the pair?
5. When you fit a red LED to the test-socket, what is the approximate voltage across it?
6. When you fit a red LED to the test-socket, why does the red LED and green LED on the PC board turn off?
7. Why doesn't the project need an on/off switch?
8. The two coils for the circuit on the left is called a TRANSFORMER. Do the connections of the windings have to be connected to the circuit around a particular way?

to Index

ROBOT MAN

This multivibrator circuit will flash the Robot Man's eyes as shown

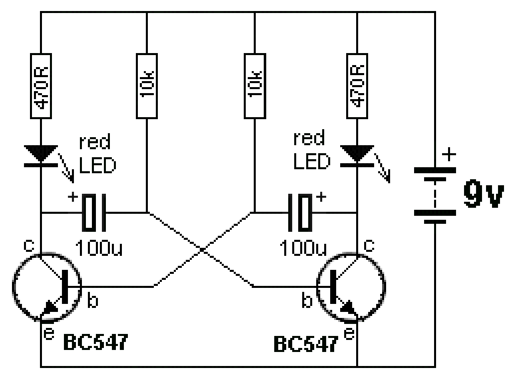

Fig 66. ROBOT MAN
The ASTABLE MULTIVIBRATOR or "free-running" multivibrator.

in the photo. The kit of components is available from Talking Electronics for $8.50 plus postage. Send an email to find out the cost of postage: talking@tpg.com.au
The photo shows the LEDs flashing.
The circuit is called an **ASTABLE MULTIVIBRATOR** and this means it is not stable but keeps switching from one transistor to the other.
It is also called a **FLIP FLOP** circuit.

to Index

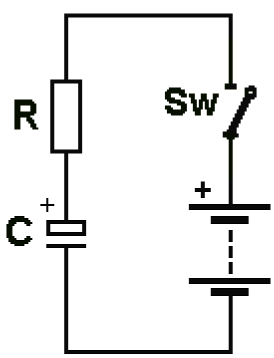

Fig 67. The TIME DELAY

The **TIME DELAY** circuit consists of a Resistor **R** and Capacitor **C** in **SERIES**.
When the switch is closed, the electrolytic (called the CAPACITOR) charges slowly because the resistor only allows a small amount of current to flow.
It's just like charging your mobile phone. The battery takes time to charge because there is a resistor in the circuit to limit the current. If we remove the resistor in the mobile phone, the battery will get too hot when it is being charged but in the **TIME DELAY** circuit, we want the capacitor to charge slowly, because we want a **TIME DELAY.** .

to Index

Fig 68. The charging of a capacitor is the same as building a brick wall.

CHARGING A CAPACITOR

The capacitor in **Fig 67** charges via the resistor **R**.
But the voltage on the capacitor does not rise at a constant rate.
It starts off charging very quickly and as the voltage across it get higher, the voltage increases at a slower and slower rate.
In the photo I am building a brick wall.
I am working at a constant rate.
When I started building the brick wall, I laid 5 rows of bricks (5 courses) in the first hour.
As the wall increased in height, I had to climb the ladder and I could only lay 3 courses an hour and finally the wall was so high I could only lay 1 course per hour.
This is exactly the same as a capacitor charging.
When the capacitor is uncharged, the supply voltage allows a high current to pass through the resistor **R** and the energy quickly fills the capacitor. This results in a rapidly increasing voltage on the capacitor. But as the voltage on the capacitor increases, the difference in voltage between that on the capacitor and the supply is very small and only a small current will pass through the resistor. This means the voltage on the capacitor increases at a slower rate.

to Index

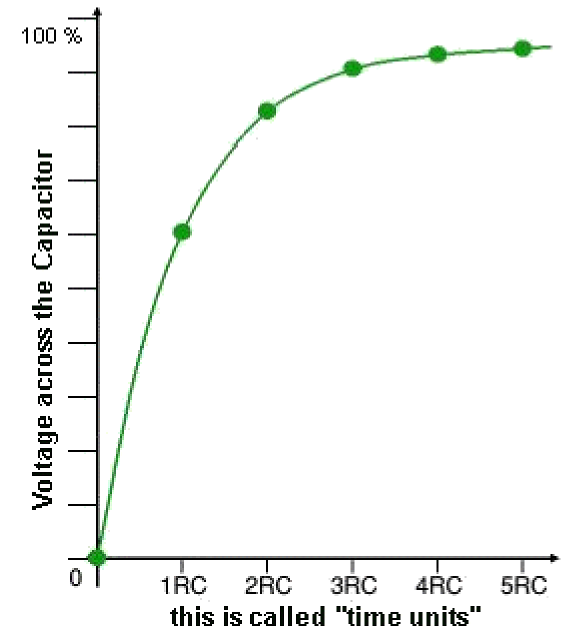

Fig 69. Time Units

It really does not matter how fast or slow or uneven a capacitor charges because most circuits detect a voltage on a capacitor and the time taken to reach this voltage is called the **TIME DELAY**.
But to prevent you thinking the capacitor charges "smoothly" we have to explain what actually happens.
The graph on the left shows the capacitor charging. You can see it charges quickly at the beginning and then charges slowly and then very slowly.
You can see the first part of the graph is fairly "straight" (constant charging) - NOT "straight up and down" but a straight line - and this applies to a voltage of about 63%. The time taken to reach this voltage is called **ONE TIME UNIT** - also called **ONE TIME CONSTANT**. The graph continues for another 4 "time units" (time-constants) and the final voltage is very nearly 100%. (It never reaches 100%.)

to Index

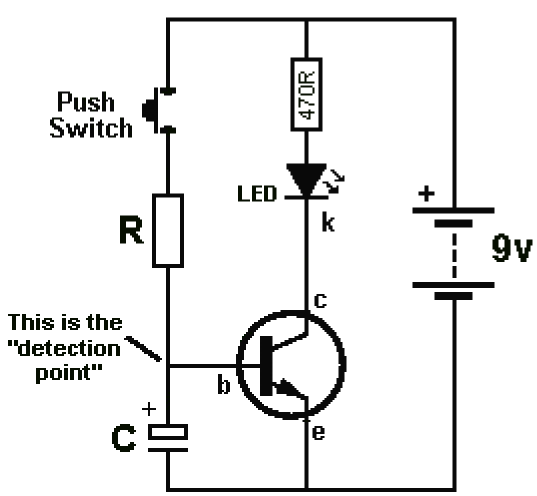

Fig 70. Time Delay Circuit

A **TIME DELAY** circuit needs three things:
1. A Resistor (R)
2. A Capacitor (C)
3. A "Detection Point."

When the switch is pressed, capacitor (**C**) takes time to charge via resistor (**R**) and after a short period of time the voltage at the **DETECTION POINT** is 0.6v and the transistor is TURNED ON. The LED illuminates.

Build the circuit with 100u and 100k and see how long it takes before the LED illuminates.

to Index

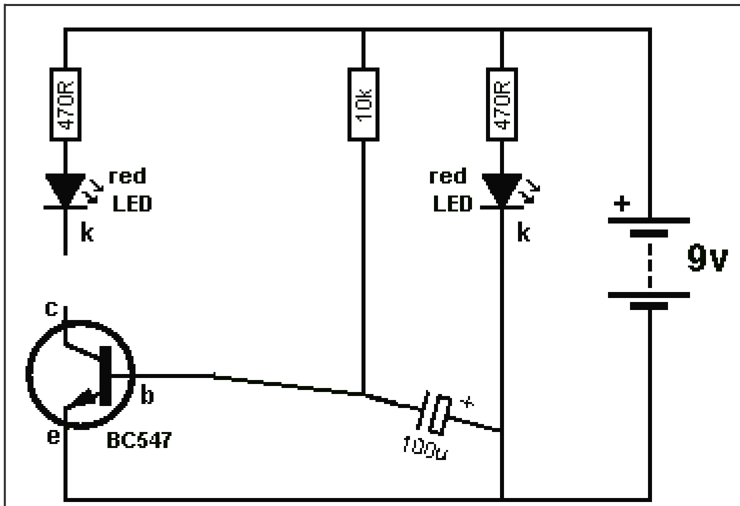

In the **ROBOT MAN** project you can see the "**TIME DELAY**" circuit made up of the 100u, 10k resistor and the base of the transistor.

This is one of the most important **BUILDING BLOCKS** in electronics.
It is the basis of all oscillators and will be discussed below, after we explain a few more details.

Fig 71. The "TIME DELAY" in the ROBOT MAN Project

to Index

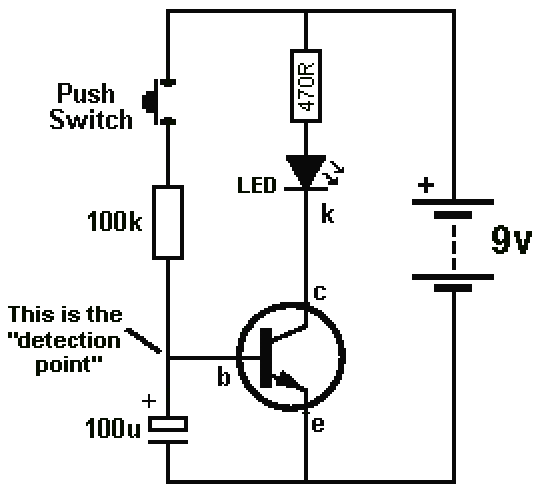

Fig 72. Turning A Transistor ON

We will use the **TIME DELAY** circuit to turn the transistor **ON**.
Make sure the 100u is uncharged by touching both leads (both ends of the capacitor) at the same time with a JUMPER - this is a piece of wire shown in Fig 61.
Push the switch and noting happens. After a short period of time the LED starts to glow and then comes on fully.
This shows two things:
1. The transistor is not turned ON when the base voltage is zero.
2. The base voltage must be 0.6v for the transistor to start to turn ON and when the voltage is 0.65v the transistor is turned **ON FULLY.**

to Index

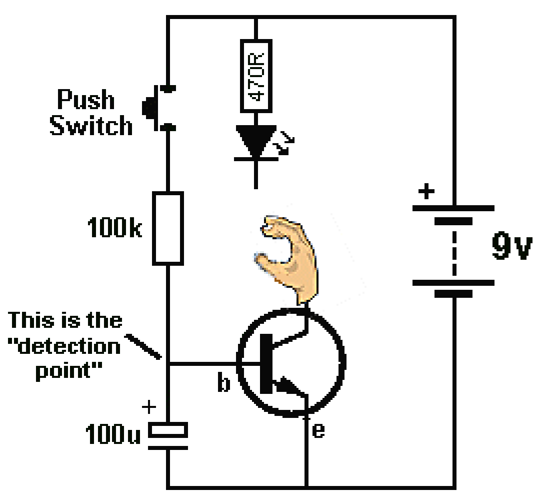

Fig 73. How the LED turns ON

Here is an explanation of how the LED turns ON.
When the circuit is first assembled and the switch is not pressed, the transistor is not turned on and it is just like the diagram opposite. The LED is not connected to the transistor.

to Index

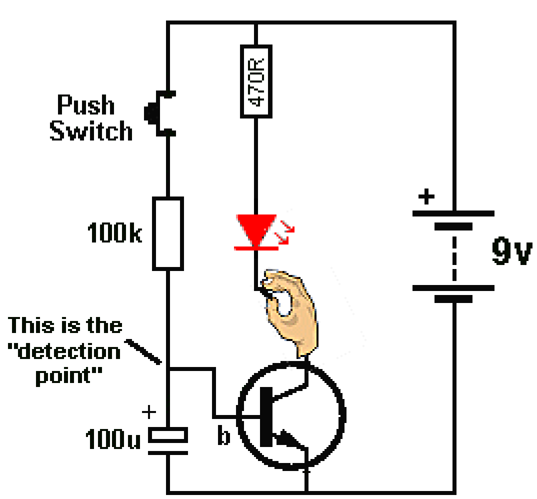

Fig 74. The LED turned ON

When the switch is pushed, the transistor turns **ON** (after a few seconds) and it pulls the lower lead of the LED down towards the 0v rail and this action turns the LED **ON**.

to Index

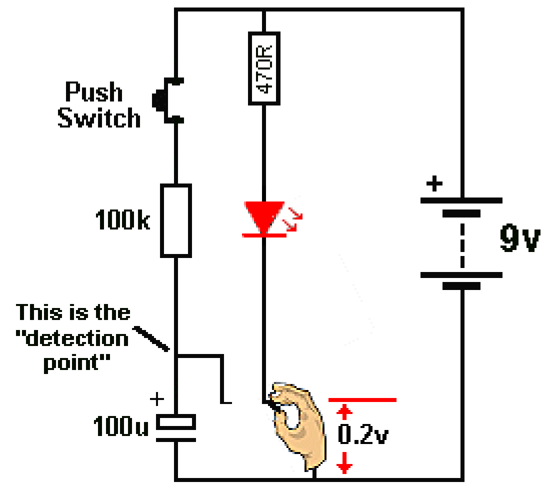

Fig 75. The LED fully turned ON

When the LED is **fully turned ON**, the lower lead of the LED is almost directly connected to the 0v rail.
In other words:
When the transistor is **FULLY TURNED ON**, the lower lead of the LED is almost directly connected to the 0v rail.
The voltage between the lead of the LED and 0v rail is 0.2v. This is the characteristic voltage across the collector-emitter terminals of a transistor when it is TURNED ON.

to Index

In the three diagrams above you can see the LED is changed from an **OFF** condition to an **ON** condition by the action of the transistor.
The transistor is acting **LIKE A SWITCH.**
This action is one of the most important actions in electronics.
It is called: **"The Transistor as a SWITCH"**
It is the basis to ALL Digital Circuits.
It is the basis because of these two facts:
1. When the transistor is **OFF**, the circuit is taking **no current** and no power is being lost or wasted.
2. When the transistor is **ON**, the LED is almost at 0v and no resistor is in the lower lead to waste any power.
Thus we can turn things **ON** and **OFF** without wasting and power.
This is the basis to **DIGITAL ELECTRONICS**.

to Index

DIGITAL ELECTRONICS revolves around circuits that are either **FULLY ON** or **FULLY OFF**. This means they take almost no power and we can combines lots of circuits and still take almost no power.
This means they do not get hot and it also means they will last a long time.
You may not think turning a transistor **ON** and **OFF** will achieve any worthwhile outcome but a circuit can be designed to use two transistors (similar to the **ROBOT MAN** above). The circuit does not Flip-Flop but requires a switch and when the switch is pressed, the circuit changes state. The two transistors are connected together and it takes two presses of the switch to make the output of the second transistor change state ONCE.
The circuit is a divider. It is called a: **divide-by-two** and is the basis of all counting in a computer.
By adding more "**divide-by-two"** circuits we can get "**divide by 4**, **divide by 8**" etc. Two transistors don't do much but when you combine millions of transistors we have a **COMPUTER.**

to Index

Two transistors can do one more thing. They can "**REMEMBER**."
Here is a manual circuit.
Pressing Switch **A** turns the LED **ON** and pressing switch **B** turns the LED **OFF**.
The circuit "remembers" or remains in each state called a stable state.

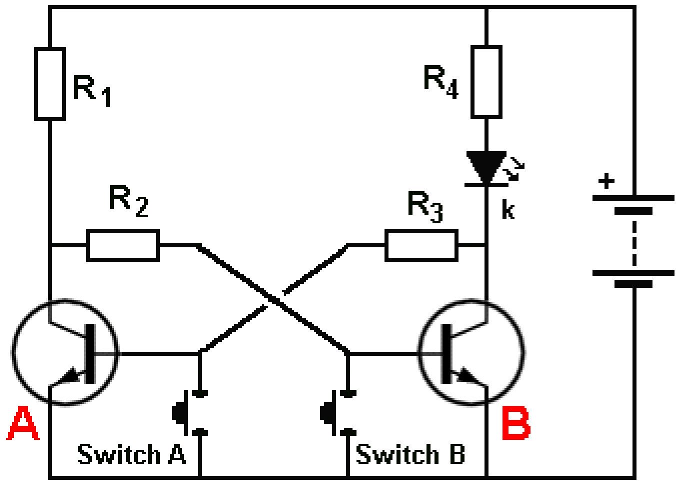

Fig 76. The "MEMORY CELL"

When Switch **A** is pressed, the voltage on the base is removed and transistor **A** turns OFF.
Transistor **B** turns ON via resistors R_1 and R_2 and the LED is turned **ON**.
When the switch is released, the voltage on the collector of transistor **B** is less than 0.6v and the two transistors remain in this state.
Pressing switch **B** turns the LED **OFF.** (transistor **A** turns ON via R_3, R_4 and the LED - very little current flows through the LED and you can hardly see it glowing). The voltage on the collector of transistor **A** is less than 0.6v and the two transistors remain in this state.

The technical name for this circuit is:
BISTABLE MULTIVIBRATOR or **BISTABLE SWITCH** or **BISTABLE LATCH**.

This is the basis to all the memory in a computer.

to Index

In electronics, we talk about the **DIGITAL TRANSISTOR** and **ANALOGUE TRANSISTOR**.
This is just an ordinary transistor (called a Bipolar Junction Transistor) in a **DIGITAL CIRCUIT** or **ANALOGUE CIRCUIT**.
We are now discussing the **DIGITAL CIRCUIT** - The Multivibrator - Astable Multivibrator and Bistable Multivibrator (Memory Circuit).
The **DIGITAL CIRCUIT** has **2 STATES**.
The **ON STATE** and the **OFF STATE**.
It is conducting in the ON STATE and the LED is illuminated.
In the OFF STATE, the LED is not illuminated.
In the ON STATE the transistor is said to be **CONDUCTING** or **BOTTOMED**.
In the OFF STATE the transistor is said to be "**CUT OFF** or "**OFF**."
These two states are reliable and guaranteed. They are not "half on" or "quarter on" or "75% off."
These states are easy to transmit "down a wire." The ON STATE is transmitted as "1" (voltage present) and the OFF STATE is transmitted as "0" (voltage not present).
These are the two **DIGITAL STATES**.

The **ROBOT MAN** is a **DIGITAL CIRCUIT**.
Each LED is ON or OFF.
The waveform on the output of each transistor is called a **DIGITAL SIGNAL**.

The waveform is said to be **DIGITAL** or **SQUARE WAVE**.
The top line of the graph represents the LED OFF.
The bottom line of the graph represents the LED ON. The LED is ON when the collector voltage is LOW because we are pulling the lead of the LED to the 0v rail as shown above.
The circuit changes from one state to the other very quickly and this is called the **RISE TIME**.

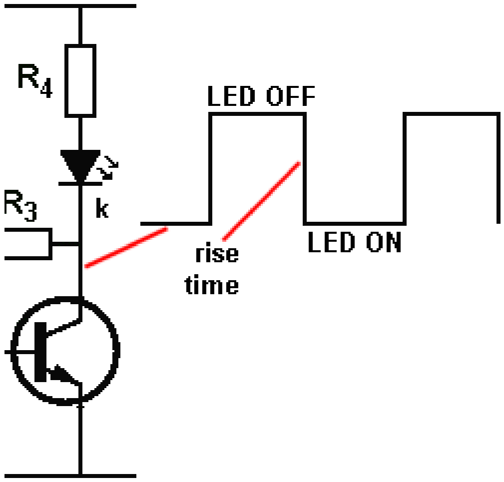

to Index

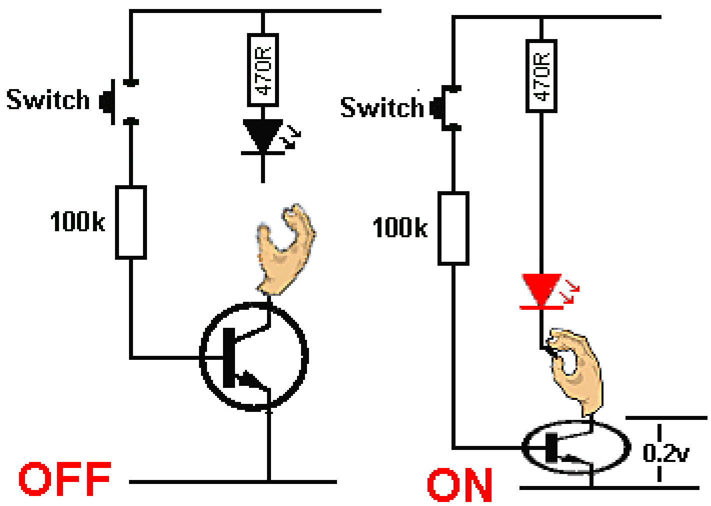

Fig 77. The two Digital States

Going over the two **DIGITAL STATES** for a transistor.

In the first diagram the switch is not pressed and the base does not see a voltage to turn the transistor on. The transistor is "**OFF**" (not conducting) and it is not "grabbing" the LED. The LED is not illuminated.
In the second diagram the base of the transistor sees a voltage via the switch and it is TURNED on. The LED is illuminated.

to Index

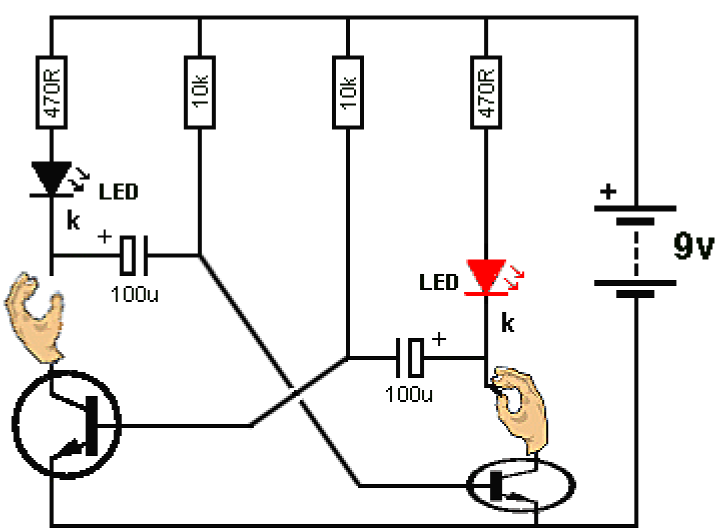

Fig 78. ROBOT MAN Animation
This animation shows how a transistor grabs a LED and pulls it towards the 0v rail to turn it ON.

to Index

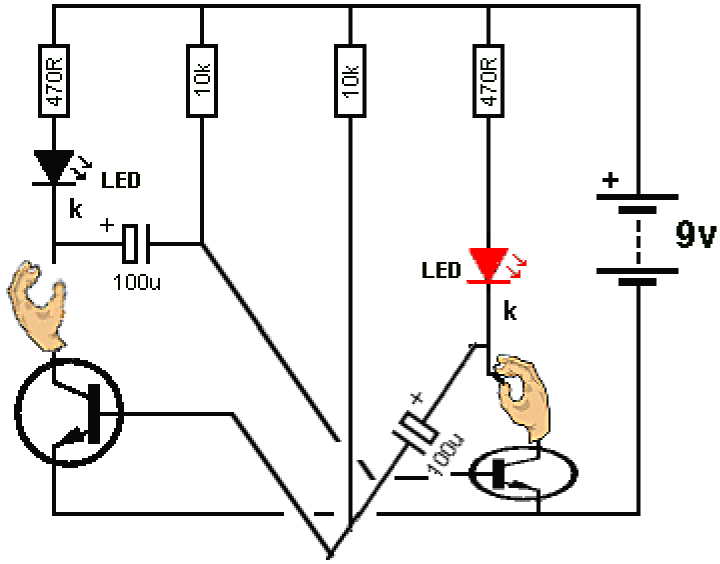

Fig 79. TIME DELAY Animation

The animation in **Fig 78** shows the two transistors turning the LEDs **ON** and **OFF** in a **FLIP FLOP** circuit.
We know the 10k and 100u components form a **TIME DELAY** to create the time for each LED to be illuminated. The timing for one LED plus the other LED creates a **CYCLE** and this is the **FREQUENCY OF OPERATION** for the circuit. It is measured in cycles per second - Hertz - Hz.
We will now go into more detail of how the **TIMING COMPONENTS** create the **TIME DELAY** for each LED.
The circuit is more-complex than you think.
The 100u is already charged from a previous cycle and we show how it gets discharged via the 10k and charged in the opposite direction by the 10k to create a **TIME DELAY**.

to Index

THE CAPACITOR

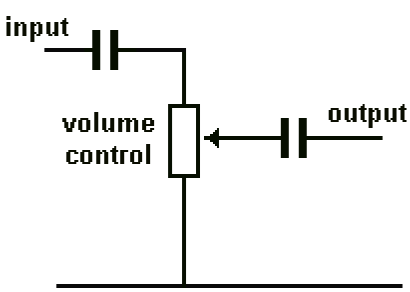

The capacitor can perform many different functions and produce many different effects, depending on its value and the surrounding components.
In this circuit the capacitors on the input and output prevent DC on the volume control creating "scratchy sounds" when the volume is altered.
This is called "DC blocking."
The AC (the signal) passes through the capacitors but the DC voltage on the input is blocked.

to Index

CHARGING A CAPACITOR Part II

It is easy to see how a capacitor charges via a resistor in the **TIMING CIRCUIT** (Delay Circuit) above but many capacitors are not connected to the 0v rail.
They are connected as show in the animation below and their "job" is to pass a waveform.
When they pass the waveform they **CHARGE** and **DISCHARGE**.
The waveform is called an **AC SIGNAL** and the output is smaller than the input.
The circuit is taken from the circuit above, but the same effect applies to all capacitors that "pass a signal."
Here's why:

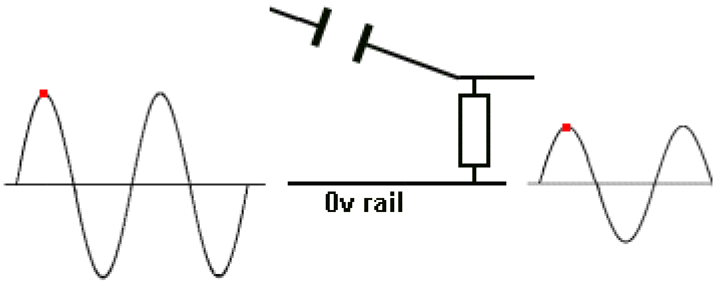

The capacitor charges slightly during the rise of the signal and the right-plate of the capacitor does not rise as high as the left-plate. That's why the output signal is not as large as the input signal.
If the capacitor did not charge, the output would be as large as the input. If you use a capacitor with a large value, it will not charge and thus the output will be as large as the input.
That's why you use a large capacitor !!!!

to Index

CHARGING A CAPACITOR Part III

Here is another CAPACITOR in action.

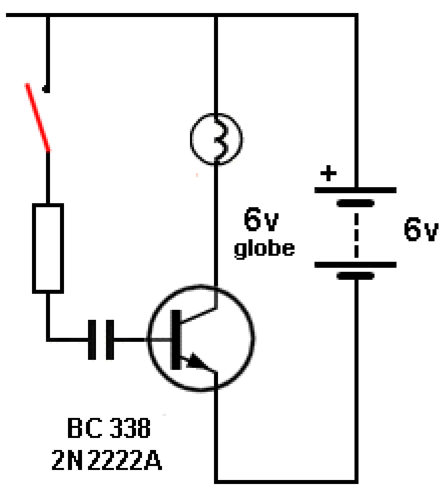

The animation shows a capacitor charging (via a resistor). The initial current is LARGE and this turns the transistor FULLY ON and the globe illuminates. As the capacitor charges, the base current reduces and the transistor starts to turn OFF. Eventually the capacitor is fully charged and the voltage on the base falls to 0v, turning the transistor OFF.

This animation shows three features:
1. The initial charging current is HIGH.
2. It gradually falls to zero.
3.The voltage on the base drops below 0.6v and the transistor turns OFF.

to Index

NEGATIVE VOLTAGE

You will be surprised to learn that many circuits produce a negative voltage or negative spike at some point (when doing circuit-analysis, each location or point or join of components is called a NODE) on the circuit. In other words the voltage will be LESS than the 0v rail of the circuit.
This is due to the presence of a capacitor and the animation shows how a capacitor can produce a negative voltage:

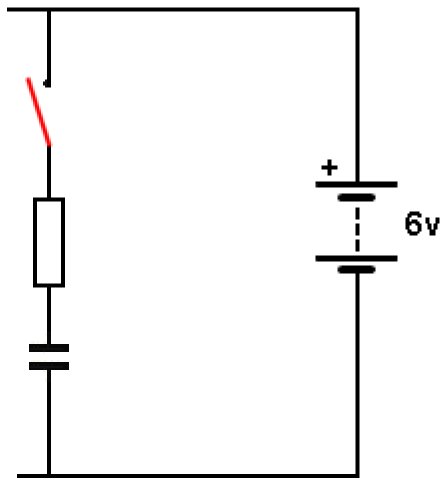

When a charged capacitor is "lowered from one position in a circuit" the positive lead may be lowered by say 3v. This means the other lead will be lowered by 3v. We are assuming the capacitor can be lowered and is not directly connected to the 0v rail.

You can see the electrolytic produces a NEGATIVE VOLTAGE on the base in the following animation, when the two transistors change states:

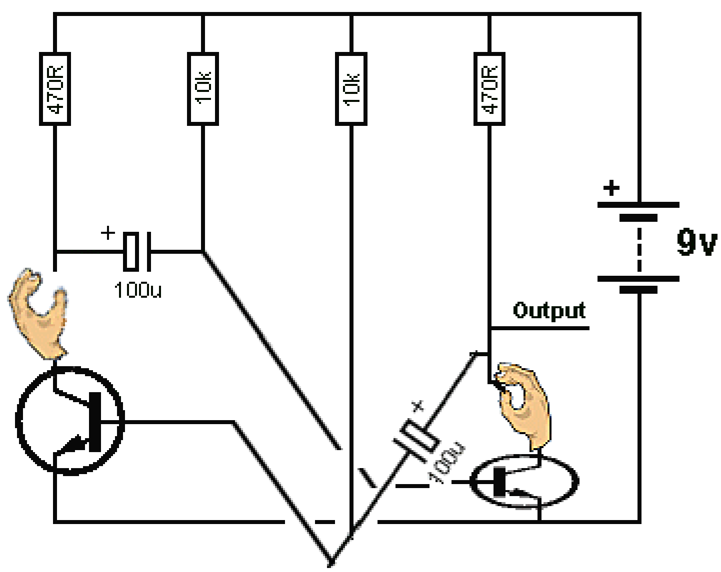

to Index

The Electret Microphone

The most common type of microphone is the ELECTRET MICROPHONE.
It is incorrectly termed the "Capacitor Microphone" or Condenser Microphone." "Capacitor Microphone" descriptions make no mention of a FET as the amplifying device and a polarized diaphragm to detect the audio, so they are something different.
The electret microphone consists of a FET (transistor)

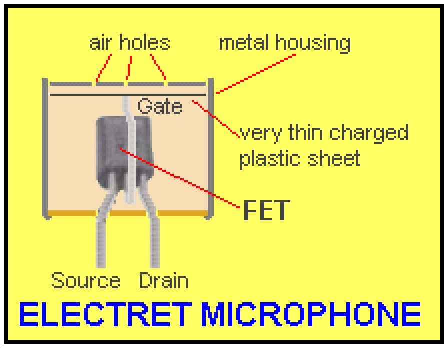

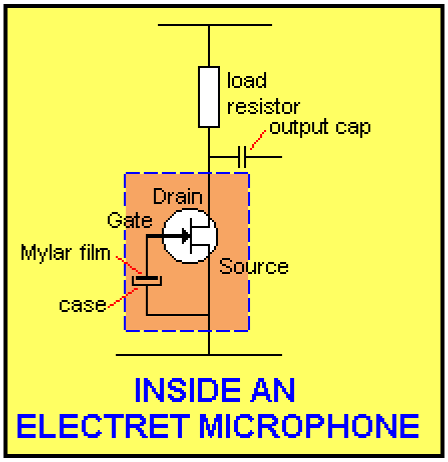

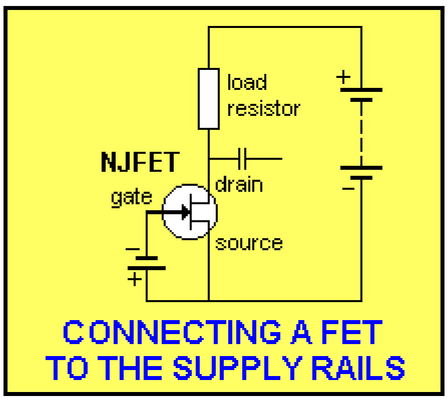

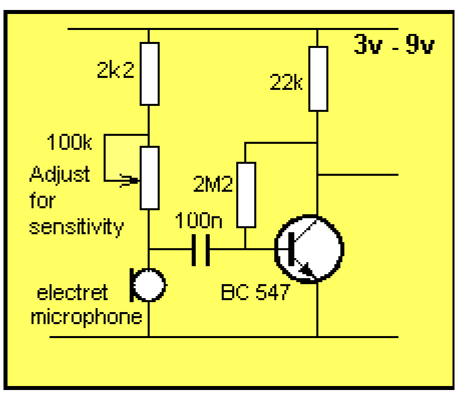

inside an aluminium case with a very thin Mylar film at the front. This is charged and when it moves (due to the audio it receives via a small hole in the front of the case), it vibrates and sends a very small voltage to the GATE lead of the Field Effect Transistor. This transistor amplifies the signal and produces a waveform of about 2mV to 20mV at the output.
The electret microphone requires about 0.5mA and will operate from 1.5v supply with 4k7 LOAD RESISTOR.
For 3v supply, the Load Resistor can be 22k to 47k.
For higher supply voltages the resistor will be 68k or higher.
Electret microphones are extremely sensitive and will detect a pin-drop at 3 metres.

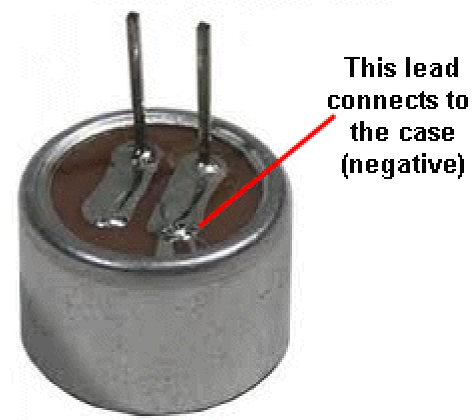

Most electret microphones have two leads. One lead is connected to the case and this lead goes to the 0v rail. The other lead goes to a LOAD RESISTOR (4k7 to 68k - depending on the voltage of the project).
Reducing the value of the load resistor will increase the sensitivity until the background noise is very noticeable.
They are used in Hearing Aids and are more-sensitive than the human ear.
They are very small, low-cost and very sensitive.

to Index

The Speaker

The most common speaker is about 30mm to 60mm diameter and 8 ohm impedance. This means the voice coil is about 8 ohms resistance.
The two leads can be connected either way to a circuit.
The speaker shown is 32mm diameter and has a realistic wattage of 100mW (NOT 1watt).

These speakers have a Mylar cone and the magnet is a "super magnet" and very small. That's why it is so flat.

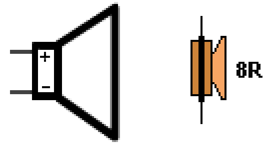

Speaker Symbol

A speaker can be used as a microphone (called a Dynamic Microphone) and a circuit to connect the speaker (mic) to an amplifier can be found on Talking Electronics website. It is not as sensitive as an electret microphone and does not produce the same output amplitude, but it is an emergency microphone.

to Index

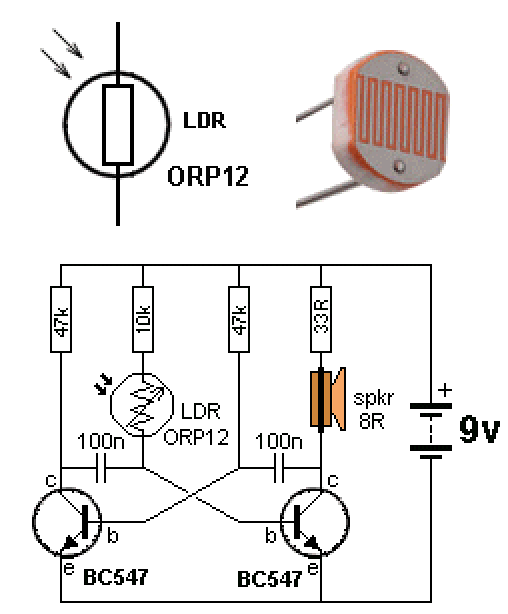

LDR and Light Alarm Circuit

Light Dependent Resistor

(LDR)

Also called **PHOTOCELL** or **PHOTO RESISTOR**
A **Light Dependent Resistor** is a 2-leaded component containing a layer of semiconductor material.
The top contains two interleaving combs of conducting wires with a path of semiconductor material between. When light falls on the component, the resistance of the semiconductor material decreases.
In darkness the LDR will be about 300k. In very bright light the resistance will be about 200 ohms.
But if the light changes only a very small amount, the resistance CHANGE is VERY SMALL. For a large change, see **Photo Transistor**.
The **Light Alarm** circuit will produce a squeal when light falls on the LDR.

to Index

Photo Transistor

The **Photo Transistor** is very sensitive to changes in illumination. It is about 100 times more sensitive than the **LDR**.
The **Photo Transistor** is also available as a **DARLINGTON.**
The Darlington Photo-transistor is 100 x 100 times (10,000) more sensitive than the LDR.

The **Photo Transistor** and **Photo Darlington Transistor** are connected just like a normal transistor but the base lead is not connected. If the value of the LOAD RESISTOR is large, the

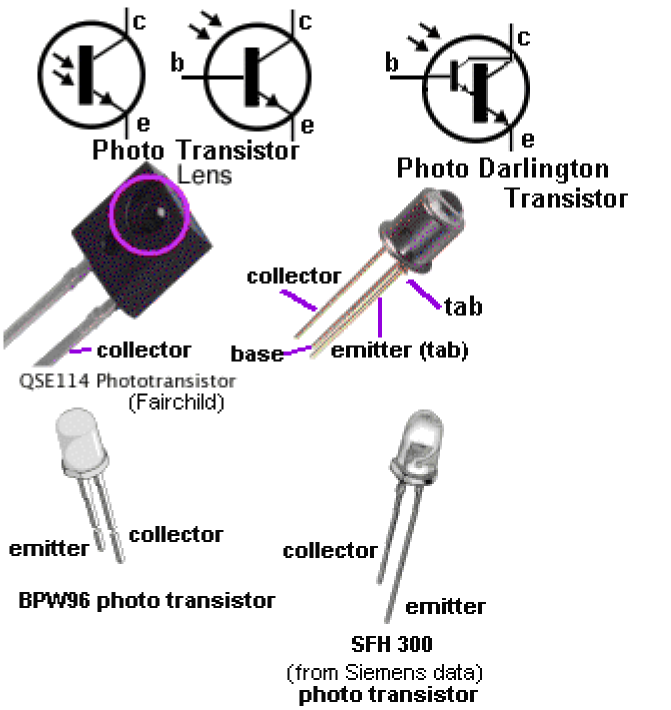

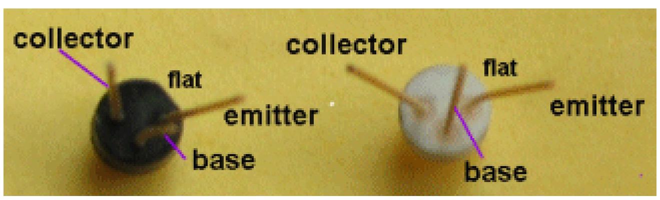

FPT100 Photo Darlington Transistor

The FPT-100 Darlington Photo Transistor is available from [Talking Electronics] for $1.00 each plus postage.

transistor will not be very sensitive.

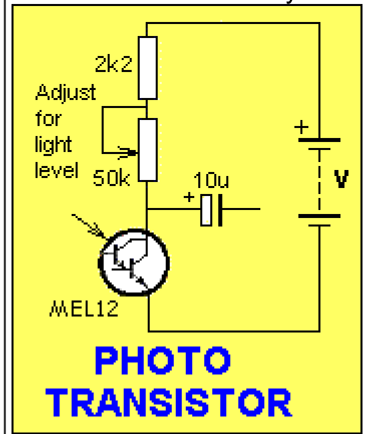

to Index

The Inductor

Also called **"coil,"** or **"Choke."**
An **Inductor** consists of one to many turns of wire wrapped around a former (tube of cardboard). The wire can be jumble-wound or wound in layers. The result is the same. This is called an **air-cored coil** or **air-cored inductor**.
The centre can be filled with a metal such as iron or laminations (thin sheets of metal) or a ferrite material. Different cores operate at higher frequencies.
The core can be circular (doughnut) or rectangular and it is called a **MAGNETIC CIRCUIT** (when it is a closed loop).
Additional turns or increasing the diameter of the turns will increase the inductance.
A coil with a magnetic core can be used to pick up nails and metal items. It is called an **electromagnet**. It can be

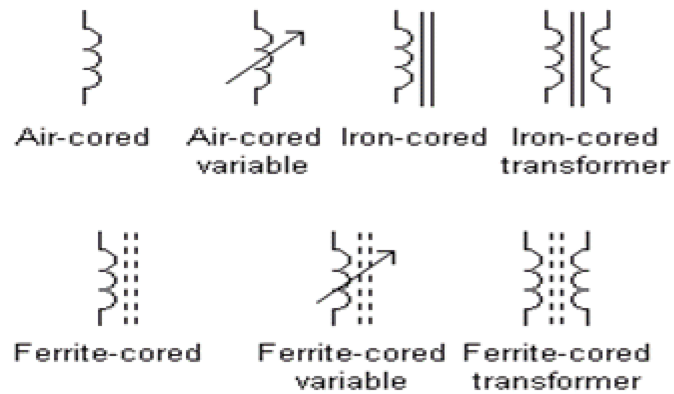

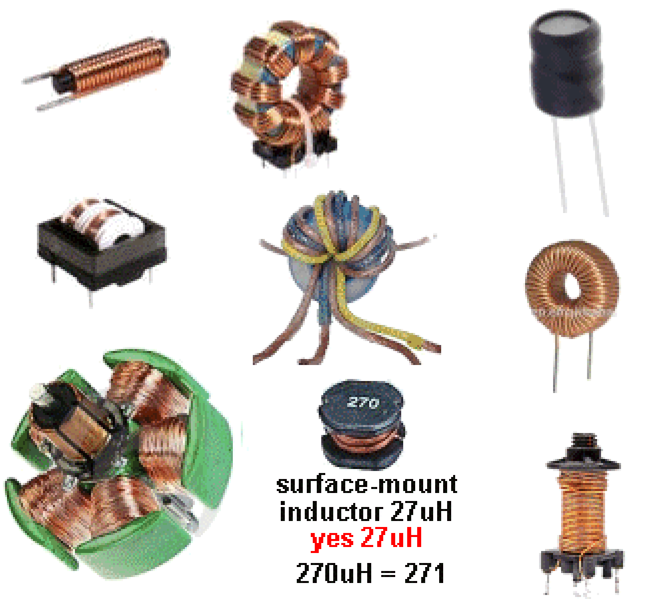

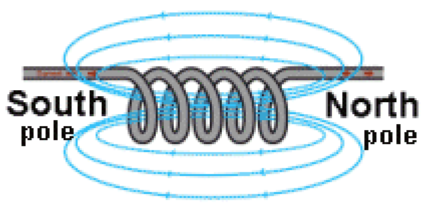

The emerging **magnetic lines of force** from an inductor produce the NORTH POLE - this is just "convention," a simple way to explain things - to get the explanation started.
When two or more coils are wound near each other, the inductor is called a **TRANSFORMER** (but not the armature above).

operated on AC or DC.
When the metal core is loose and gets pulled into the coil it is called a **SOLENOID** or **ACTUATOR** or **LINEAR ACTUATOR**. It can be operated on AC or DC.
The way an inductor works is very complex but we can say it resists any rise or fall in voltage by turning the rise or fall into magnetic flux.
If the applied voltage is suddenly turned off, the inductor produces **a very high voltage** of **opposite polarity** (these are the **two** most important things for you to remember).

to Index

The Antenna

The first time you will need an antenna is when making an FM transmitter.
The antenna is usually a length of wire equal to half the wavelength of the transmitter. The frequency is about 100MHz and the wavelength is 3 metres.
A half-wave antenna is 1.5metres.
The length is important but the height is more important.
The wire should be as high as possible and "up-and-down" if the antenna on the radio is vertical, to get the maximum range.
This is called an **end-fed half-wave antenna** or **half-wave**

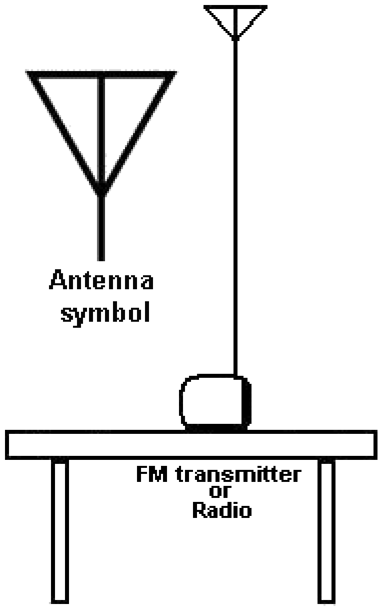

Monopole.
The transmitting circuit should have a good ground-plane such as connection to large batteries so the signal can be pushed and pulled into and out of the antenna.
This signal is then radiated as electromagnetic radiation to the surroundings.

to Index

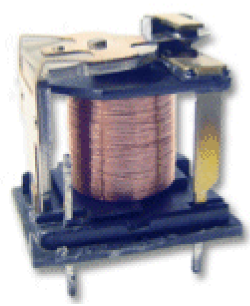

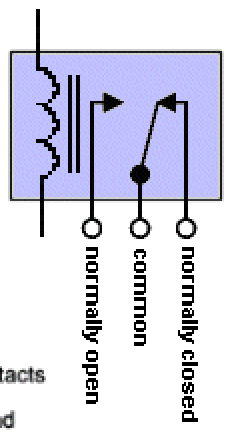

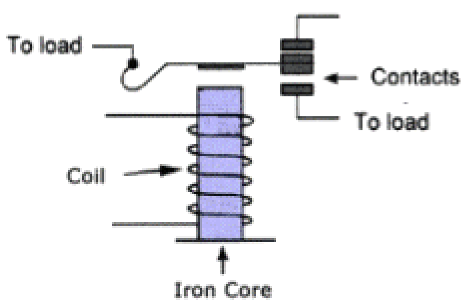

A single contact consists of 2 pins -called SPST (single-pole single-throw).
Or a single pair of contacts can consist of 3 pins - called change-over or SPDT (single-pole double-throw).
A double set of contacts consists of 6 pins, called DPDT (double-pole, double-throw). This is also called a **CHANGE-OVER RELAY** or **REVERSING RELAY** (when connected to a motor).

The RELAY

The word **Relay** comes from the days of Morse Code where a coil of wire (an electromagnet) closed a switch to allow the Morse code to travel further down the telegraph line.
It would "relay" or "pass-on" the information.
A relay allows a "weak circuit" (one with low current) to operate a LOAD that needs a large current. It also separates the two circuits electrically and prevents a voltage such as 240v connecting to a 12v circuit. The coil is separated from the contacts and this gives the two circuits isolation.
A double-pole double-throw relay can be used to reverse a motor as shown here:

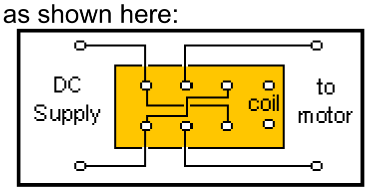

to Index

Driving A Relay

(Powering A Relay)
The first thing you must decide is the voltage of the relay. This will depend on the voltage(s) available. The relay will be driven (activated) by a transistor and the base of the transistor only needs a signal (less than about 1v). This means the project can be operated on a voltage from 3v to 12v and the relay can be connected to a 5v to 12v supply.

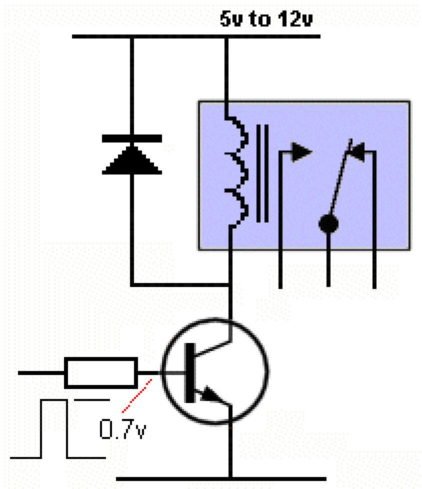

Driving A Relay

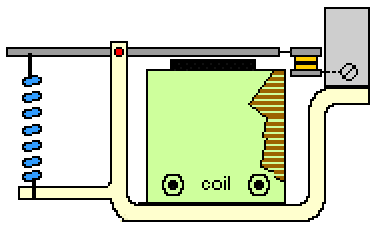

The armature is drawn towards the coil when a current flows through the coil.

Next you need to know the current-rating of the contacts. This will depend on the current taken by the LOAD. The rating of most relays is: 1 amp, 5 amp or 10 amp.
Finally you need to know how many contacts are required.
For a single circuit you will need 2 pins and for two circuits you will need 4 pins (but relays only come with 6 pins).
You can get relays that need a very small current for activation. These are called CMOS relays. But most relays need about 100mA.
To protect the driving-transistor from spikes when the relay is turned off, you will need a diode across the coil.
The top animation shows a "single set of change-over contacts."
The lower animation shows the ARMATURE being drawn to the electromagnet. The electromagnet is the coil with a core of magnetic material that becomes a magnet (an electromagnet) when a current flows through the coil.

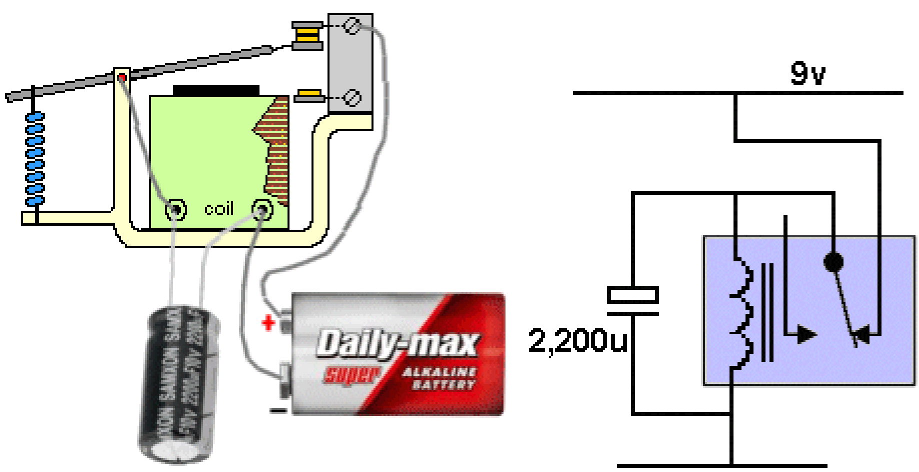

When the circuit is turned ON, the voltage across the 2,200u electrolytic is zero and it gradually charges. When the voltage is about 8v, the coil has enough voltage across it to pull the armature and open the contacts. The electrolytic supplies voltage to the coil for about 1 second and then the electromagnet does not have sufficient magnetism to hold the armature and it returns to close the contacts.

to Index

GATES

Animations of **GATES** and more details of their operation is covered in **DIGITAL ELECTRONICS** chapter.

to Index

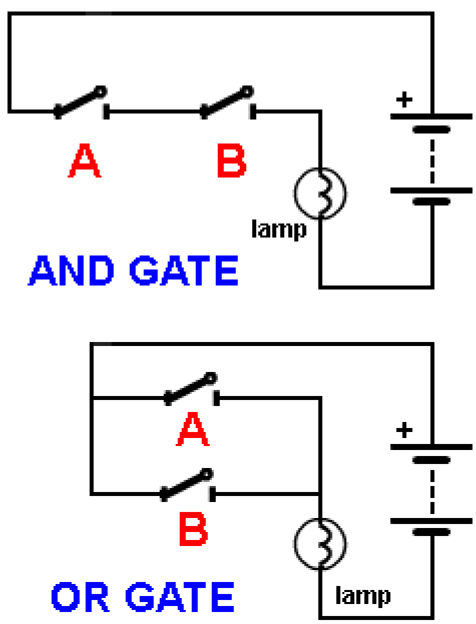

Fig 80. The "AND" GATE and "OR" GATE with switches

The next **BUILDING BLOCK** we will cover is called the **GATE**.
In its simplest form it is an electrical circuit consisting of switches.
Its just two or more switches connected in series or parallel.
We give each circuit a name so we can talk about it and explain its action with a single word.
Later we will cover the electronic version and show how diodes and a transistor are needed to perform a **GATING FUNCTION.**
The type of GATE we are talking about is a **LOGIC GATE**.
The circuit performs an operation called a **LOGICAL OPERATION** on an input or a number of inputs and creates a single output - called a **LOGICAL OUTPUT**.
LOGICAL means "understandable" or "correct" and in this case it means DIGITAL - the signal will rise to full rail voltage or fall to zero voltage. The output will not be half rail or quarter-rail voltage.
The diagram show an **"AND" GATE** and **"OR" GATE** with switches.
For the **AND GATE** close switch A **AND** switch B for the lamp to illuminate.
For the **OR GATE** close switch A **OR** switch B for the lamp to illuminate.

to Index

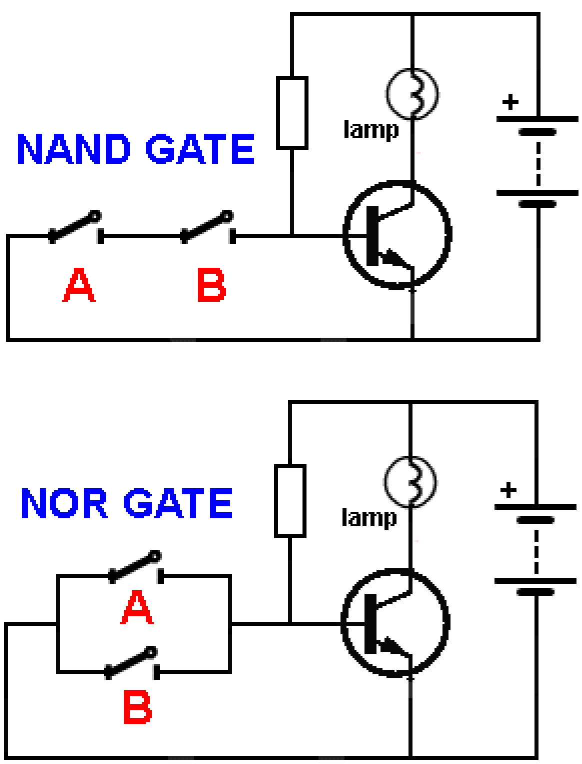

Fig 81. The "NAND" GATE and "NOR" GATE with switches and a transistor

INVERSION

Inversion produces the opposite effect to the results above.
Suppose we want to turn OFF a lamp when one or two switches are pressed.
We need a transistor.
The technical word for Inversion is **NOT**.
It is simplified to the letter "**N**."

For the **NAND GATE** close switch A **PLUS** switch B for the lamp to turn OFF.
For the **NOR GATE** close switch A **OR** switch B for the lamp to turn OFF.

These gates are only **demonstration-gates** to show how one or two switches will turn a lamp OFF.

to Index

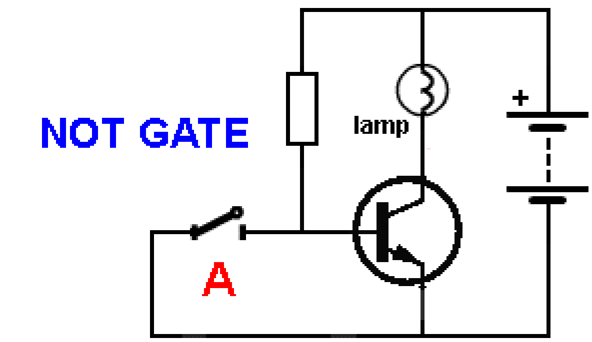

Fig 82. The "NOT" GATE

NOT GATE

A single switch and transistor produces a **NOT GATE.**

This is simply an **INVERSION**.

The resistor turns the transistor **ON** and the lamp illuminates. The switch removes the voltage on the base and the transistor turns **OFF**.
This is only a demonstration circuit to show how a switch can turn a lamp OFF.

to Index

The 5 gates above form the basis to turning a circuit **ON** and **OFF**. We will discuss these gates later in the digital section.

to Index

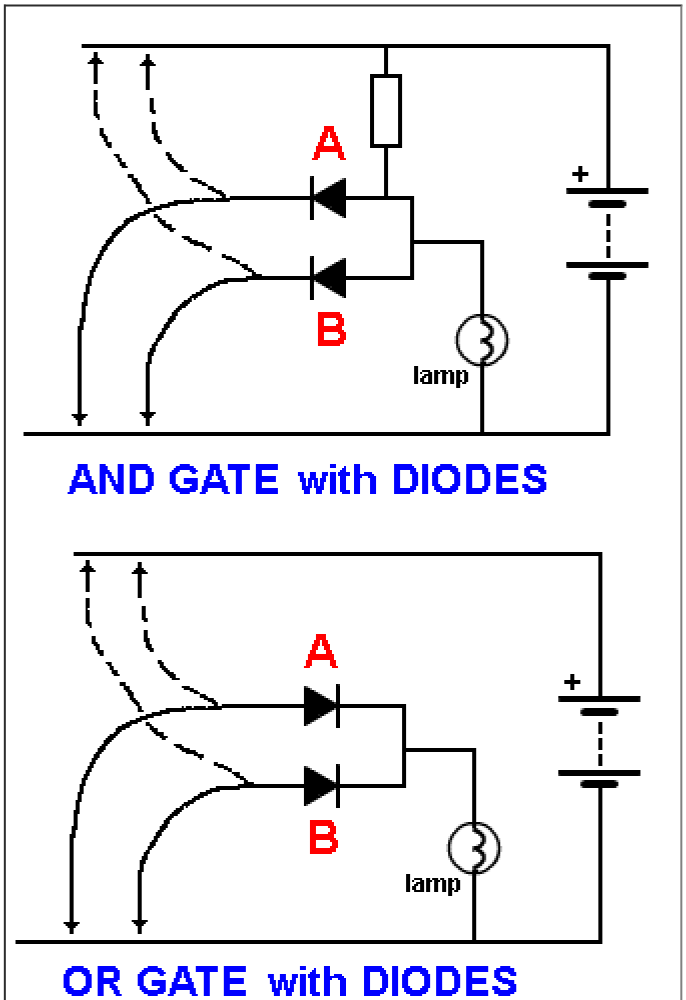

Fig 83. "AND and "OR" gate with diodes

The next building block is the **GATING DIODE**.
We have shown a diode allows current to flow when the diode is correctly placed in a circuit and blocks current when it is reversed.
The 5 gates above are electrical circuits but an electronic circuit works in a slightly different way.
The electronic circuit will be covered later in the DIGITAL section.
For the moment we will explain how a diode can be used to create a **GATE**.
In other words it creates a ONE-WAY PATH to allows signals to pass from one stage to another and prevents signals passing in the opposite direction.
In the AND GATE circuit, both inputs are LOW and current flows through the resistor (it will get HOT). When one input is taken HIGH, current still flows through the other diode and the lamp does not illuminate.
When BOTH inputs are HIGH, current flows through the resistor to illuminate the lamp. No current flows through the diodes.
In the OR GATE, when one input is taken HIGH, current flows through the diode to illuminate the lamp.
This can be done with EITHER input.

to Index

A **NAND** and **NOR** gate can be made with diodes and a transistor.
This time we the output is either HIGH or LOW.
We are gradually producing circuits that

are electronic, rather than electrical circuits.
In the **NAND GATE** circuit, taking one of the inputs HIGH will still allow the other input to prevent the transistor turning ON.
When BOTH inputs are HIGH, the transistor turns on via resistor R and the output is LOW.

In the **NOR GATE** circuit, taking one of the inputs HIGH will turn the transistor ON and the output will be LOW.

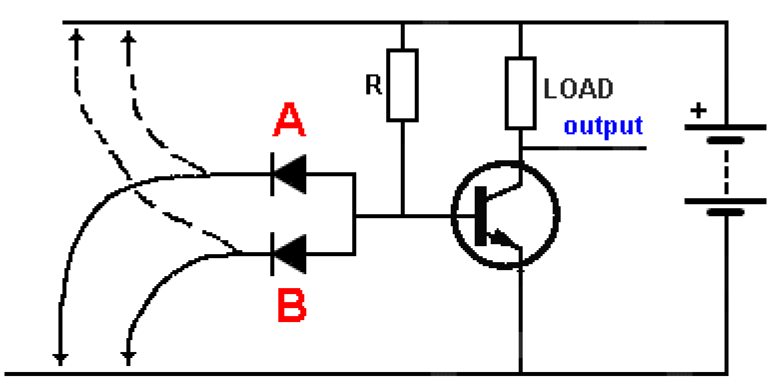

NAND GATE with DIODES and Transistor

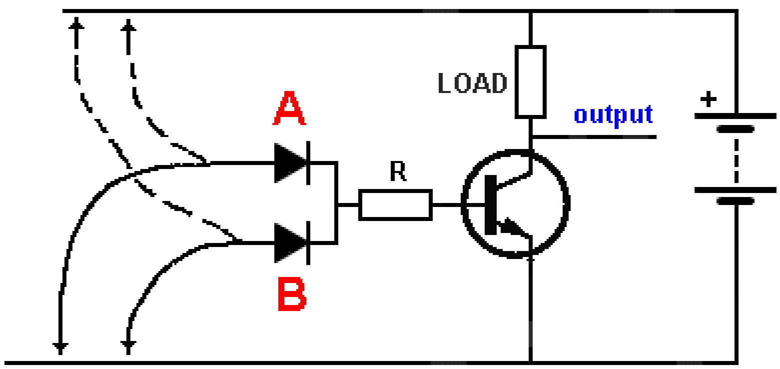

NOR GATE with DIODES and Transistor

Fig 84. "NAND" and "NOR" gate with diodes and a transistor.

to Index

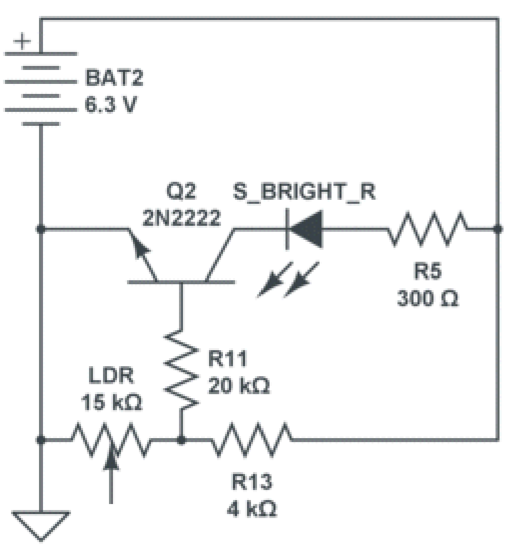

Drawing A Circuit

A circuit must be drawn according to simple rules so it can be instantly recognised.
An electronics engineer can "**see a circuit working**" when it is drawn correctly and can see if it is drawn correctly; if the parts-values are correct and can use the circuit to assist in diagnosing a problem with a faulty circuit.

The top circuit on is very difficult to visualise because it is not drawn in the normal way.
All the components have to be "**turned around in your mind**," to see what the circuit is doing.

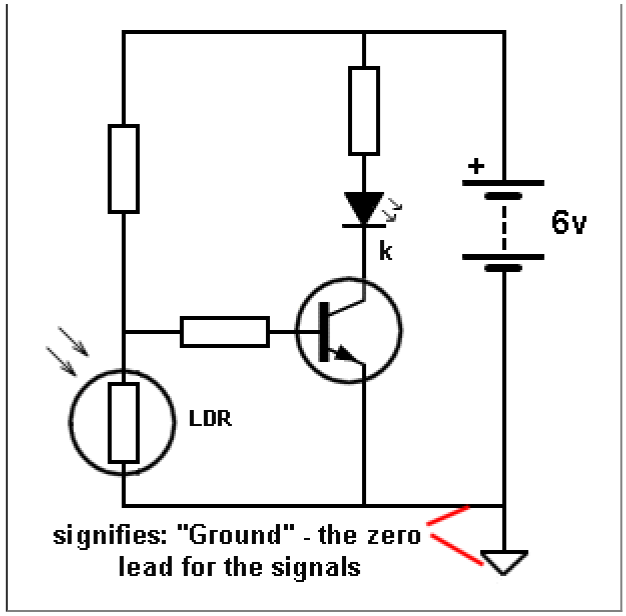

[to Index]

QUICK QUIZ - to see how much you know

following 50 questions . . . JavaScript is required!
This test will see how much you have learnt.

An open circuit help

4. What is the approximate characteristic voltage that develops across a red LED?

- [ ] 1.7v
- [ ] 3.4v
- [ ] 0.6v
- [ ] 5v [help]

5. If two resistors are placed in series, is the final resistance:

- [ ] Higher
- [ ] Lower
- [ ] The same
- [ ] Cannot be determined help

6. Which is not a "common" value of resistance:

- [ ] 2k7
- [ ] 1M8
- [ ] 330R
- [ ] 4k4 help

7. Which value of resistance, placed across a 9v battery will get hot:

- [ ] 22k
- [ ] 22R
- [ ] 220k help

8. If the voltage on the base of a transistor increases, does it:

- [ ] Turn on
- [ ] Turn off
- [ ] Not enough information
- [ ] Remain the same help

9. The resistor identified in brown is called the:

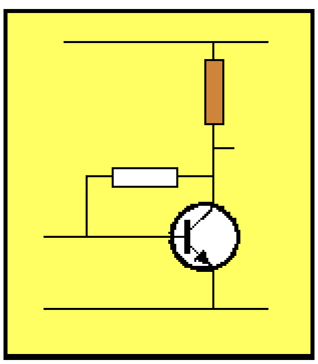

- [ ] Base Bias Resistor
- [ ] Load Resistor
- [ ] Emitter Feedback Resistor
- [ ] Bypass Resistor

help

10. The first three colour bands on a resistor are: yellow - purple - orange

- [ ] 47k
- [ ] 4k7
- [ ] 470k
- [ ] 4R7 help

11. A resistor with colour bands: red-red-red-gold, has the value:

- [ ] 22k 5%
- [ ] 2k2 5%
- [ ] 220R 5%
- [ ] 22R 5% help

12. The lead marked with the arrow is:

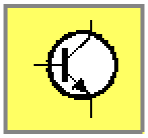

- The Collector
- The Base
- The Emitter
- The case help

13. A 10k resistor in parallel with 10k produces:

- 10k
- 5k
- 20k
- Cannot be determined help

14. The symbol is:

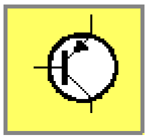

- NPN Transistor
- PNP Transistor
- Photo Transistor
- Field Effect Transistor help

**15. Two 3v batteries are connected as shown.
The output voltage is:**

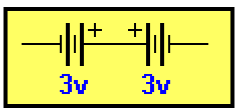

- 3v
- 0v
- 6v help

16. 4 resistors in ascending order are:

- 22R 270k 2k2 1M
- 4k7 10k 47R 330k
- 3R3 4R7 22R 5k6
- 100R 10k 1M 3k3 help

17. The closest value for this combination is:

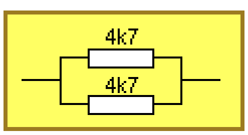

- 4k7
- 2k3
- 9k4 help

18. Which LED will illuminate:

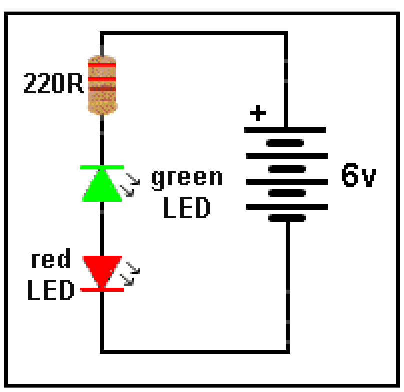

- Green
- Both
- RED
- None

19. The four symbols are:

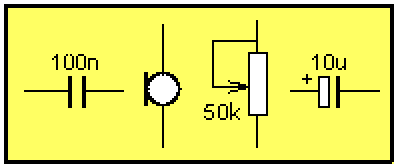

☐ Capacitor, Microphone, Potentiometer, Electrolytic
☐ Electrolytic, Microphone, Resistor, Capacitor
☐ Capacitor, Piezo, Resistor, Electrolytic
☐ Electrolytic, Coil, Resistor, Capacitor [help]

20. The closest value of the combination is:

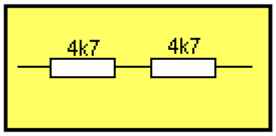

☐ 10k
☐ 2k3
☐ 2k5

21. Which motor will work:

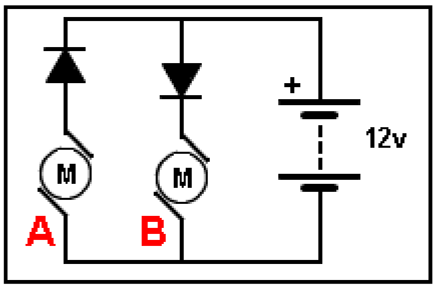

☐ A
☐ B
☐ A and B

22. A resistor and capacitor in series is called a:

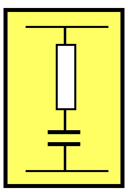

☐ Pulse Circuit
☐ Timing Circuit/Time Delay Circuit
☐ Oscillator Circuit/Frequency Circuit
☐ Schmitt Circuit [help]

23. A red-red-red-gold resistor in series with an orange-orange-orange-gold resistor produces:

☐ 5k5
☐ 35,200 ohms
☐ 55k
☐ None of the above [help]

24. Name the 4 components:

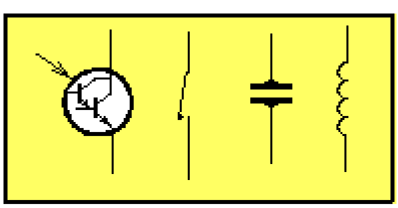

☐ Photo transistor, switch, capacitor, coil
☐ Transistor, mercury switch, piezo, inductor
☐ Photo transistor, reed switch, piezo, coil
☐ Photo Darlington transistor, switch, piezo, inductor [help]

25. To obtain a higher value of resistance, resistors are connected in:

☐ Reverse
☐ Forward

☐ Parallel
☐ Series help

26. Which LED will illuminate:

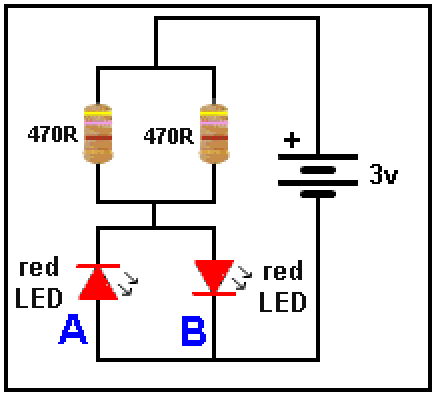

☐ A
☐ B
☐ Both
☐ None

27. Name the component that detects light:

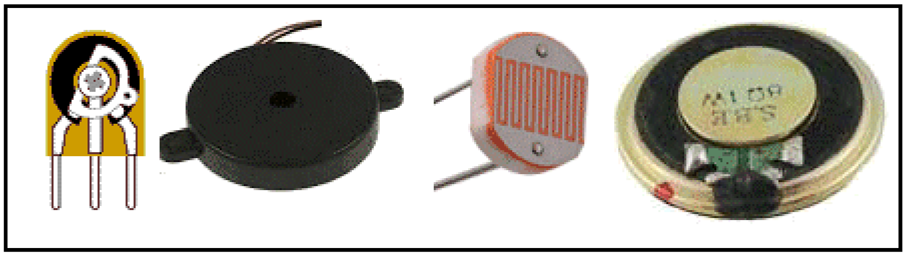

☐ mini trim pot
☐ Light Dependent Resistor
☐ piezo
☐ speaker help

28. What is 1,000p?

☐ 0.01n
☐ 0.0001u
☐ 0.1n
☐ 1n help

29. The current in a circuit is 45mA. This is:

☐ 0.045Amp
☐ 0.00045A
☐ 0.0045A
☐ 0.45A help

30. A 100n capacitor can be expressed as:

☐ 0.1u u = microfarad
☐ 0.01u
☐ 0.001u
☐ none of the above help

31. 1mA is equal to:

☐ 0.001A
☐ 0.00001A
☐ 0.01A
☐ 0.1A help

32. 1,200mV is equal to:

- 12v
- 1.2v
- 0.12v
- 0.0012v help

33. The approximate current for a toy 3v motor is:

- 10mA
- 100mA to 300mA
- 1 amp

34. What is the resistance of this resistor:

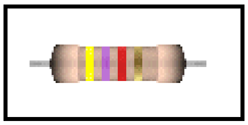

- 47k
- 4k7
- 4R7

35. Identify the correctly connected LED:

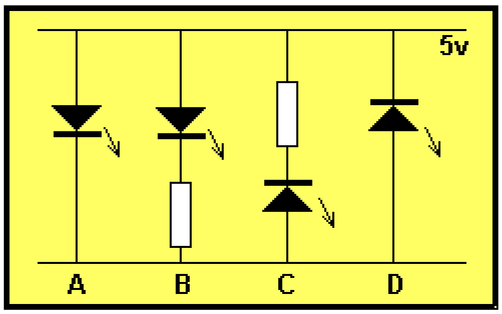

- A
- B
- C
- D help

36. Identify the correct statement:

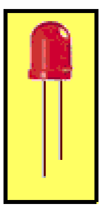

- The cathode lead is longer. It goes to the negative rail
- The cathode lead is shorter. It goes to the negative rail
- The cathode lead is shorter. It goes to the positive rail
- The cathode lead is longer. It goes to the positive rail help

37. The current requirement of a LED is:

- 1.7mA
- 25mA
- Between 3 and 35mA
- 65mA help

38. The multimeter is measuring . . .

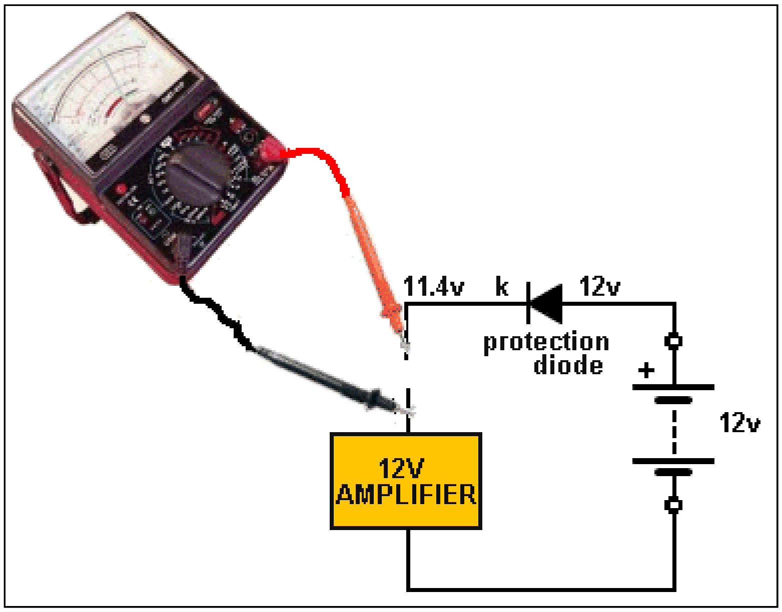

- Voltage
- Current
- Resistance

39. The purpose of the two capacitors:

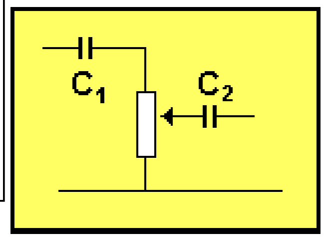

- To pass AC from the input to the output
- To allow the signal to oscillate
- To pass DC from the input to the output
- To amplify the signal [help]

40. The direction of conduction for a diode is:

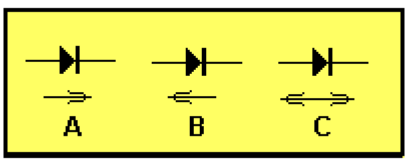

- A
- B
- C [help]

41. A DC voltage . . .

- rises and falls
- is a sinewave
- remains constant
- is an audio waveform [help]

42. Arrange these in ascending order: k, R, M (as applied to resistor values)

- R, k, M
- M, R, k
- k, M, R
- M, k, R [help]

43. A battery produces AC current:

- true
- false

44. The tolerance bands: gold, silver, represent:

- 5%, 10%
- 10%, 5% [help]

45. 223 on a capacitor represents:

- 0.022u u = microfarad
- 22n n = nanofarad
- 22,000p p = picofarad
- All of the above [help]

46. Arrange these in ascending order: n, p, u (as applied to capacitor values)

- p, u, n,
- n, u, p
- p, n, u [help]

47. What is the resistance of this resistor:

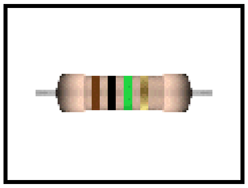

- 100k
- 1k
- 1M
- 100R

48. The number "104" on a capacitor indicates:

- 0.1u
- 100n
- 1n
- 10n [help]

49. What is the multimeter detecting:

- Voltage
- Current
- Resistance

50. For the LEDs, what is the characteristic voltage for the red and white LEDs:

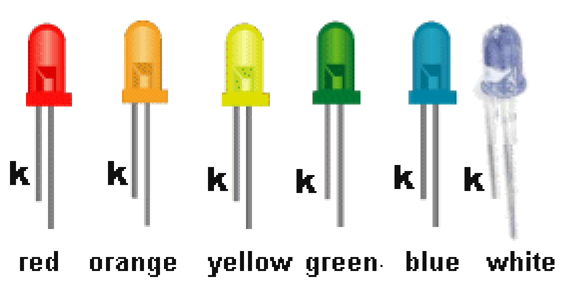

- 3.6v, 1.7v
- 2.4v, 3.3v
- 1.7v, 3.6v

☐ Cannot be determined

Final Assessment

THE CRYSTAL-SET RADIO

100 more Crystal Set plans

Everyone wants to make a RADIO.

The simplest radio is a **CRYSTAL SET**. (Sometimes called a **Crystal-Set Radio** or **Xtal Radio Set** or **Crystal Diode Radio**.)

However a **Crystal Set** needs a number of components that are very hard to get: (tuning capacitor with knob) and (crystal earpiece for $1.25).
The "air" TUNING CAPACITOR (20p to 415p) is not easily available and the postage is expensive. The germanium diode is a special component and the aerial coil wound on a ferrite slab is difficult to obtain.

But you don't need these components. They can be substituted.

There are hundreds of websites on the internet describing the **CRYSTAL SET** and if you want to build a "normal" set, you can Google these sites or **100 more Crystal Set plans**. Many of them sell kits too.

But this article is different.

We are going to have all the fun of making a **CRYSTAL SET** but with modern components and easy-to-make components and with an amplifier stage. The output is loud so you don't need a long antenna. And we are going to make our own TUNING CAPACITOR and a very simple aerial coil (called a FRAME AERIAL) as well as replacements for the germanium diode (use a TRF radio IC or a transistor) and in place of hi-impedance headphones (use a piezo diaphragm) and a crystal earpiece equivalent (a piezo diaphragm).
It's even better to have one of each type of component so you can compare the performance, so no matter how many parts your get, nothing will be wasted.

We are also going to explain the fundaments of how the circuit works as even the simplest circuit has a number of very important features that are used in many other circuits.

But first we are going to learn about the components and how they combine to make the circuit work.
When two or more components are connected together they sometimes produce a completely different result to the capabilities of either item.
This is the case with a capacitor and inductor in parallel. An inductor is simply a coil - turns of wire on a cardboard tube - called a former and the centre of the coil is AIR. It is called an air-cored coil or air-cored inductor.
Each component (the coil and capacitor) is called a PASSIVE DEVICE - in other words it does not amplify, but when the are connected together they create a result very near to amplification. And they also produce a result of picking up a huge number of signals and only allowing one signal to appear across the pair. A truly amazing result.

We start by placing a capacitor across the coil.
There is so much activity in the air, from radio, TV, taxi and mobile phone usage that the air is filled with electromagnetic radiation.
This radiation will cut the turns of the inductor (the coil) and produce a microscopic voltage in the turns. This is enough to start the two components passing energy back and forth at a rate

determined by their values. This is the basis of our first discussion.
These two components are called a TUNED CIRCUIT and make up our first building block called THE FRONT END.
.

THE FRONT END

This consists of a coil and capacitor. These two components are in PARALLEL and the signal (called the RADIO SIGNAL or RADIO WAVE) passes through the centre of the coil and produces a voltage in the turns of the coil. The electromagnetic wave has to pass through the centre of the coil.
This voltage is the result of a mass of signals that are interfering with each other and producing a signal called BACKGROUND NOISE.
The voltage can be increased by an external aerial (called an ANTENNA) and it consists of ALL THE LOCAL radio stations (and everything else).
The voltage is a mass of signals and is absolutely useless as it represents all the stations AT THE SAME TIME.
However, across the coil is a capacitor and these signals charge the capacitor with the very small voltage produced by the energy of the signals. When the capacitor is charged, it delivers its voltage to the coil. The coil accepts the energy and converts it to magnetic flux.
After a very short period of time the capacitor becomes discharged and the magnetic flux collapses and produces a voltage in the coil of the opposite polarity to charge the capacitor again in the opposite direction.
These two components keep oscillating back and forth, using the tiny amount of energy from the stations.
There is a natural frequency for the capacitor and coil to pass energy back and forth and one of the stations will provide energy to assist this natural frequency.
When this happens, the amplitude of the signal increases and the signals from all the other stations cancel themselves out and only one signal (waveform) remains.
This signal is called the NATURAL FREQUENCY OF RESONANCE and it corresponds exactly to one of the radio stations.

The end result is a waveform that is the exact same frequency as one of the radio stations and when voice or music is played, the amplitude of the waveform increases and decreases. This will be the signal you hear in the earpiece or speaker.
It is called an AMPLITUDE MODULATED signal and that is where we get **AM RADIO** from.

Understanding the concept of a CAPACITOR and INDUCTOR in parallel is very important. They form a TUNED CIRCUIT that has a natural RESONANT FREQUENCY.
Here is a very similar analogy. You have a heavy metal ball on a long string attached to the gutter on your house - just like a pendulum. You can push the ball very lightly with a finger and after a number of pushes you will be able to get the heavy ball swinging in a very large arc.
The only way to keep it swinging is to push it very lightly at exactly the right time. If you push it at the wrong time it will eventually stop swinging.
The parallel tuned circuit is exactly like the ball. It wants to oscillate at a particular frequency.
All the radio stations are pushing and pulling the circuit at the wrong times and nothing is happening. But one radio station pushes at exactly the right time and the circuit starts to oscillate.
All the other stations are fighting each other just like one person pushing the ball sideways and another pushing the ball from the opposite side. The results cancel each other and you are the only one assisting the swing.
The TUNED CIRCUIT can also be called a FILTER with a very narrow BAND-PASS frequency but our simple explanation describes the operation much more clearly.

There are a few other terms used to describe the components in the font end:

LOOP STICK ANTENNA -This is an alternate name given to the coil of wire wound on a ferrite rod or slab. It also has the name ROD ANTENNA or FERRITE ROD ANTENNA.
The winding can be enamelled wire or flexible wire called LITZ WIRE. This is very fine strands of enamelled wire twisted together and covered in cotton. The purpose of changing a thick wire to lots of very thin wires is to prevent the radio signals creating loops of signals within the wire and these signals will cancel each other and not produce a signal out the end of the wire.
In our experiments, we have not noticed any difference in a coil made with ordinary enamelled wire and Litz wire.

Here is a set of components to make your own Crystal set from **Scott's Electronic Parts**:
You can see the rod antenna, germanium diode, crystal earpiece, capacitor and resistor. The kit costs about $9.00 plus postage and includes knob, clips and screws but no board to mount the parts.

Here is the circuit for a Crystal Set:

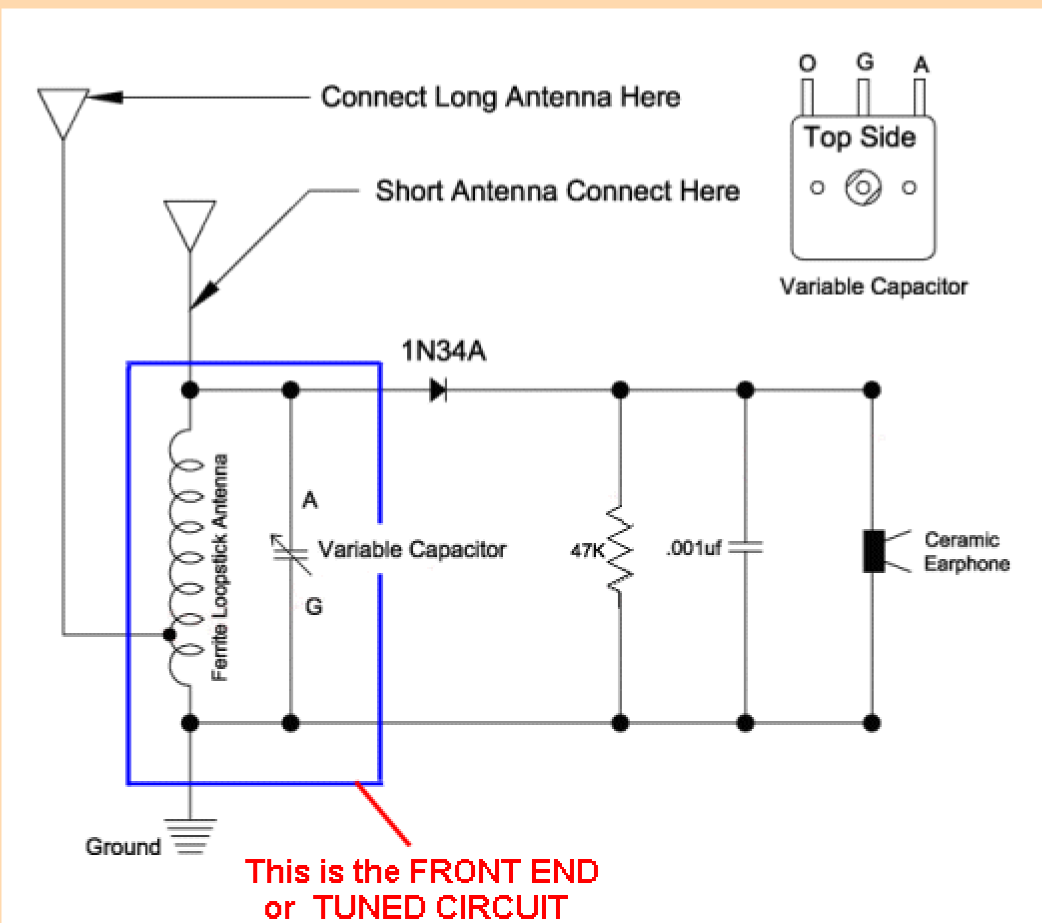

Here are the components mounted on a board called BREADBOARD:

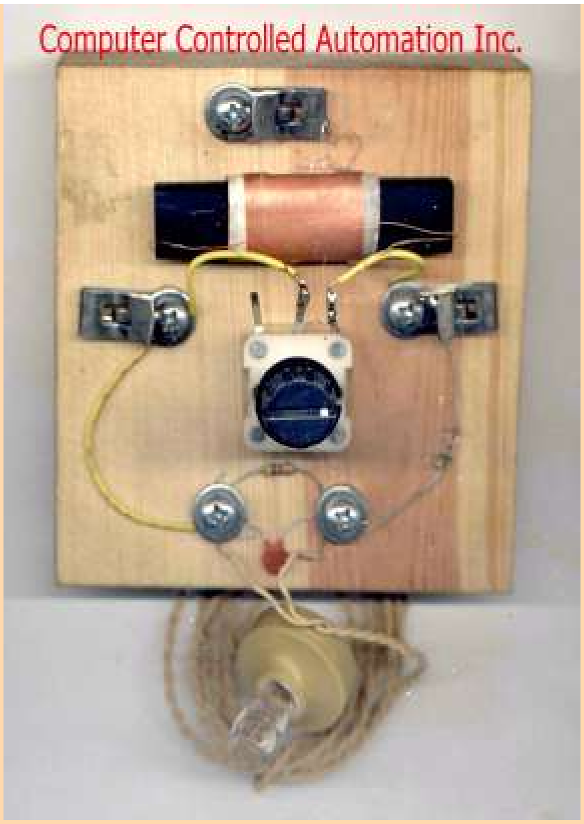

The top clip connects to a long antenna. The left clip connects to ground and the right clip connects to a short antenna.

Let me clear up a point. You do not need a ferrite rod antenna for the coil. You can use an ordinary coil wound on a cardboard tube and it will work just as well if you are using an outside antenna.
Here is the circuit using a home-made coil.

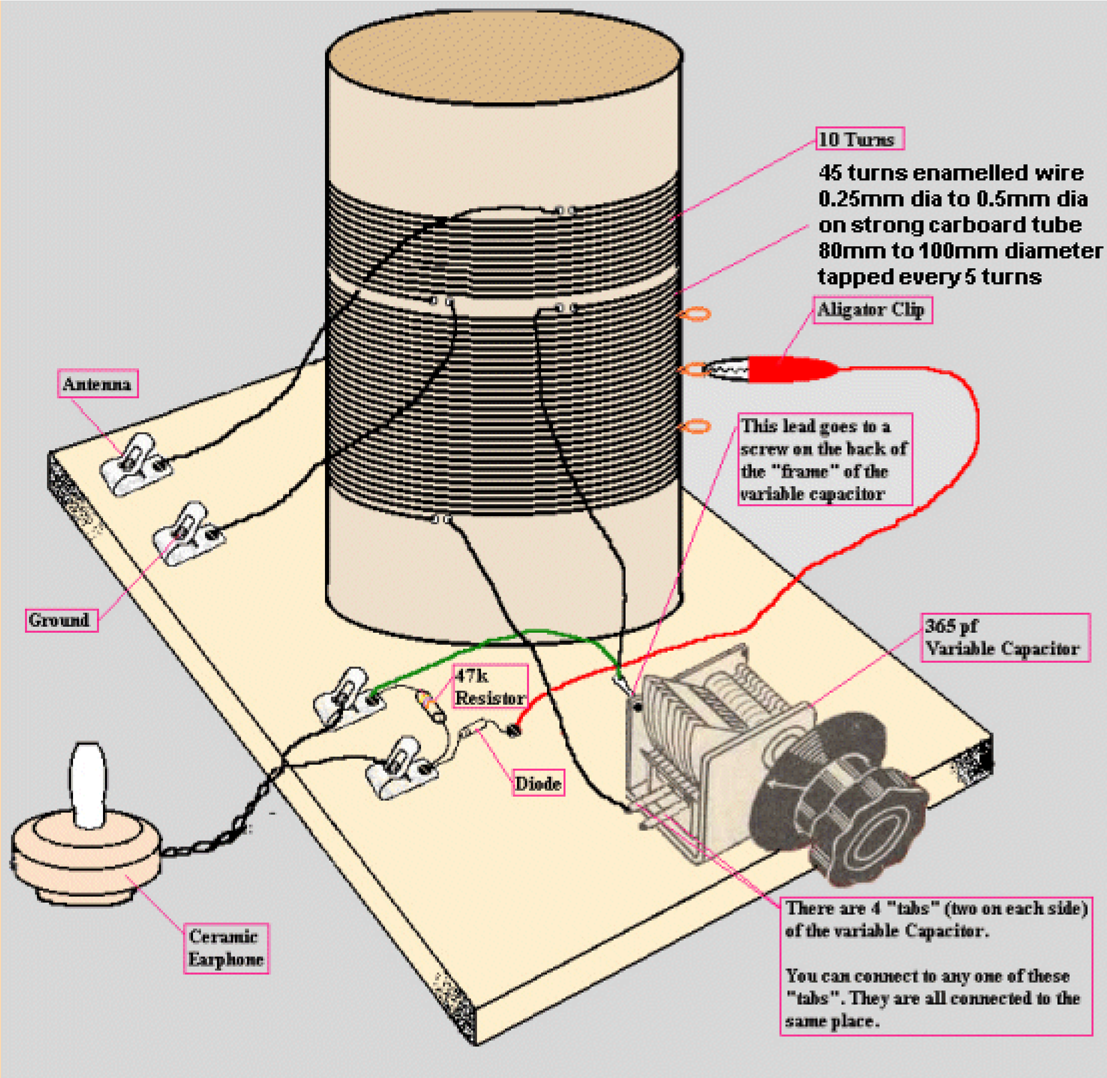

**The tappings on the coil allow a wide band of radio stations to be tuned.
Each tapping allows a different portion of the band to be covered.**

The next part to understand is this:
The coil and capacitor must not be LOADED. In other words, you cannot connect anything to this combination because the signal it is producing will be "taken away" or "removed" or "considerably reduced" by the item you are connecting to the circuit.
These two components are called a TUNED CIRCUIT and when they are not loaded they pick up all the radio stations, one station at a time, when the natural resonant frequency of the coil and capacitor exactly match the frequency of the radio station. The circuit actually "rejects" all the radio stations except one. Because all the other stations are trying to make the Tuned Circuit oscillate at a different frequency and it does not do this.
The result of the TUNED CIRCUIT oscillating under NO LOAD conditions produces a waveform that is very high and this gives the circuit GOOD SELECTIVITY. The circuit can select one station and reject nearby stations.
It also has good SENSITIVITY as it can pick up weak stations.
If you load the circuit, only the strongest signal will be detected and it will be spread across the full range of the tuning capacitor.
Obviously the theory is more-complex but we are explaining the end-result.
Theory talks about the "Q" value of the coil and this is its ability to produce a very good output when the magnetic flux collapses and the "Q" value increases when the circuit is not loaded. .
Although these voltages are very small (in the order of microvolts or millivolts) the result is very important as the rest of the circuit will be amplifying this waveform a few thousand times.
As we explained above, pushing the weight on a string only needs a push of 1 cm and eventually the weight will swing 1 metre. This is a gain of 100:1 The same thing happens with the tuned circuit. The incoming radio signal is in the order of microvolts, but the coil and capacitor will produce a signal as high as 500 millivolts. This is an improvement or "gain" of more than 1,000 and is referred to as the "Q" of the circuit.
You will also notice the TUNED CIRCUIT is not connected to any supply voltage. It does not have

be connected. It generates its own waveform from the signals in the air.
It should not have any DC current flowing through it via the supply as this would put a load on the circuit and reduce its operation.

However we must "pick-off" the signal so it can be amplified.
This must be done with a very high impedance circuit.

THE CONVERTER (detector) - THE DIODE

The next part of the circuit is the CONVERTER. Commonly called the DETECTOR.
It converts the RADIO FREQUENCY signal to an AUDIO FREQUENCY signal.
This is the job of the DIODE.
The radio frequency signal is a very high frequency signal (say one million cycles per second) and it is sending a tone of one thousand cycles per second through the air-waves.
What is happening is this: The one megahertz signal has a certain amplitude and over a range of the first one-thousand cycles, the amplitude gradually decreases and then increases again. If you look at the tops of this 1,000 cycles you will see a waveform that corresponds to the one kilo-Hertz signal.
The 1MHz signal is picked up by the coil and capacitor in the front end and makes it oscillate.
The radio frequency signal is gradually getting larger over 500 cycles then smaller over the next 500 cycles and this increase and decrease represents the 1,000 cycles per second tone.
This is the waveform (the signal) that passes through the diode. This will be explained further in a moment.
The diode does not pass any signals less than 200mV as the first 200mV is lost in the junction of the diode. This means the signals start to appear on the other end of the diode when they are above 200mV.

This is how the diode works:
Across the crystal earpiece is a capacitor. The capacitor gets charged via the diode.
The diode is present to stop the capacitor getting discharged when the waveform is in the wrong direction. (by this we mean - when the waveform is lower or smaller in amplitude than the voltage on the capacitor).
And the waveform is in the wrong direction about 50% of the time. To charge the capacitor for one-half-cycle requires 500 "little increments" in voltage with each increment adding a microscopic increase in voltage. We don't want this voltage to reduce when the waveform is reversing direction and the diode stops the voltage flowing back to the Tuned Circuit.
During the next half of the cycle when the pulses are getting smaller and smaller, the voltage on the capacitor is "bled off" by the load resistor.
The crystal earpiece detects this voltage. What we mean, is the diode allows the voltage to rise (increase) on the capacitor via lots of little "pulses" and the voltage increases in the form of a sinewave to a maximum amount. This voltage is passed to the crystal earpiece.
Once the voltage rises to a maximum, the little pulses of energy are not quite as strong, and the voltage on the capacitor reduces to form the second portion of the sinewave. This voltage is always being passed to the crystal earpiece and you can hear it as an audio signal.

GERMANIUM OR SILICON DIODE

The preferred type of diode for a Crystal Set is germanium. This is because it drops only about 0.3v.
But a silicon diode can be used, even though it drops about 0.7v, if the radio stations are very loud (close by).
You have to remember, you need a very good aerial (and a water-pipe earth) to get any results with a Crystal Set because you are asking the signal to provide the energy to drive the earpiece.
By simply adding a transistor, you are improving the performance 100 times and the long antenna can be reduced to a FRAME ANTENNA and the earth can be the metal frame of your soldering iron.

THE EARPIECE or EARPHONE
also The Magnetic Earpiece or CRYSTAL EARPIECE

The earphone or earpiece used in a Crystal Set must be a high impedance device because the crystal set does not produce a high current and cannot drive a low-impedance earpiece. That's why a CRYSTAL EARPIECE is ideal.
It has a crystal glued to the back of the earpiece and connected to its top surface is an aluminium diaphragm. When the crystal expands and contracts as a result of a voltage applied via two electrodes, the diaphragm moves and you can hear the signal. It exhibits a very high impedance

because it consists of a crystal and no coil of wire is contained inside the case.
If you do not have a Crystal Earpiece, you can make your own from the shell of an 8 ohm earpiece and a piezo diaphragm. Only the front part of the earpiece is used.

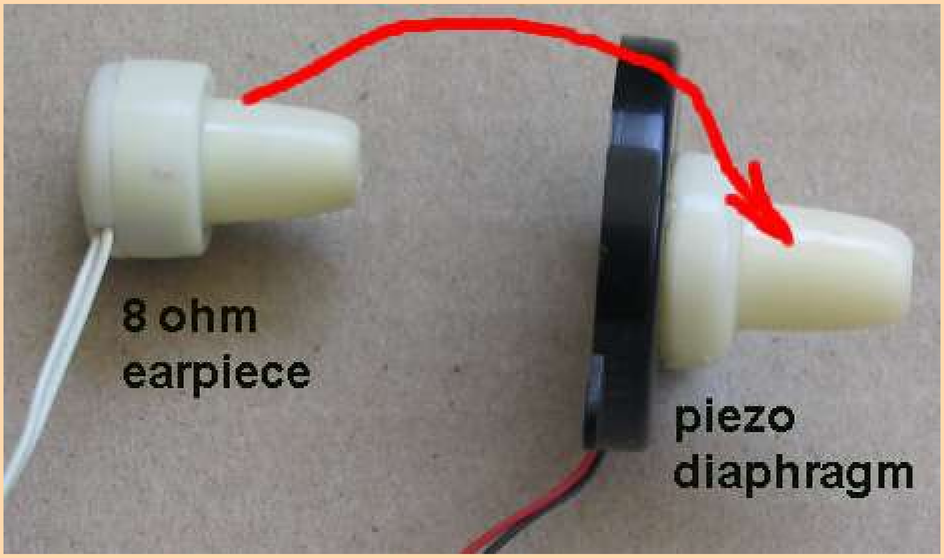

Make your own Crystal Earpiece

Hit the 8 ohm earpiece on the side and the front comes off. Glue the front onto a piezo diaphragm with hot-melt glue. See photo above.
The piezo diaphragm is a ceramic substrate that deflects in the presence of a voltage. It is quite sensitive and you can hear the audio quite clearly.
The waveform emerging from the diode in a Crystal Set is called AUDIO and although it has an amplitude of a few hundred millivolts, it does not have any current associated with it. The crystal earpiece and the piezo diaphragm react to this voltage.

THE 8ohm EARPIECE

The 8 ohm earpiece can be used with our 8ohm Buffer stage shown below.

16ohm 32 ohm and 64 ohm EARPIECE(s)

Earpieces and headsets from mobile phones are 16 ohm or 32 ohm per earpiece and are terminated via a stereo 2.5mm or 3.5mm plug. The earpieces are connected in SERIES to get the best coupling to our radio circuits and you need to find the two pins on a stereo socket to produce series connection. Get a multimeter and switch to "ohms." Try all the pins and you will get a click in the left ear then the right ear. Keep searching until you get a click in both earpieces at the same time. Use these two pins.

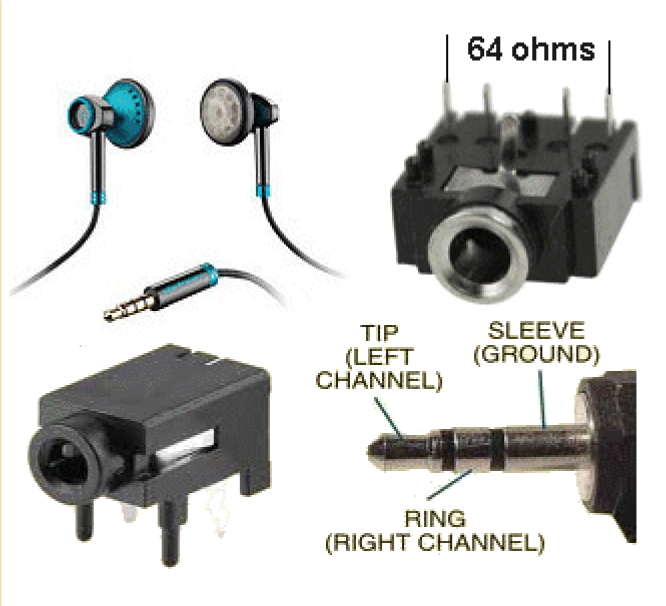

Stereo mobile phone headset - unusually 32R or 64R

PROBLEMS

The biggest problem with a Crystal Set is the need for a long antenna.
The first 200mV to 300mV of a signal is lost in the diode and you need a long antenna to pick up a signal so the output of the TUNED CIRCUIT has enough voltage to drive the high-impedance earpiece.
This requires an outside aerial 5 metres long and 3 metres high.
This is not practical for most hobbyists so we will be adding an amplifying stage to the crystal set so a shorter (smaller) aerial can be used.

THE FRAME AERIAL or FRAME ANTENNA or FRAME COIL

The aerial coil shown in the photo above is a ferrite slab with about 80 turns of Litz wire. You can find one of these in an old broken AM radio or from a parts-shop. In the instructions below we show how to make your own Ferrite Rod Antenna
An equally-good substitute is a frame antenna made by winding insulated wire in a rectangle around wooden sticks.

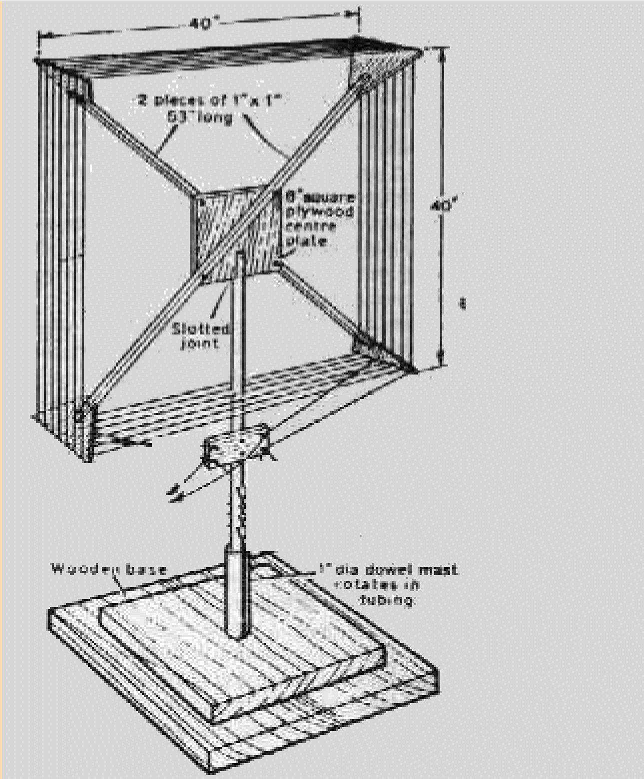

FRAME ANTENNA

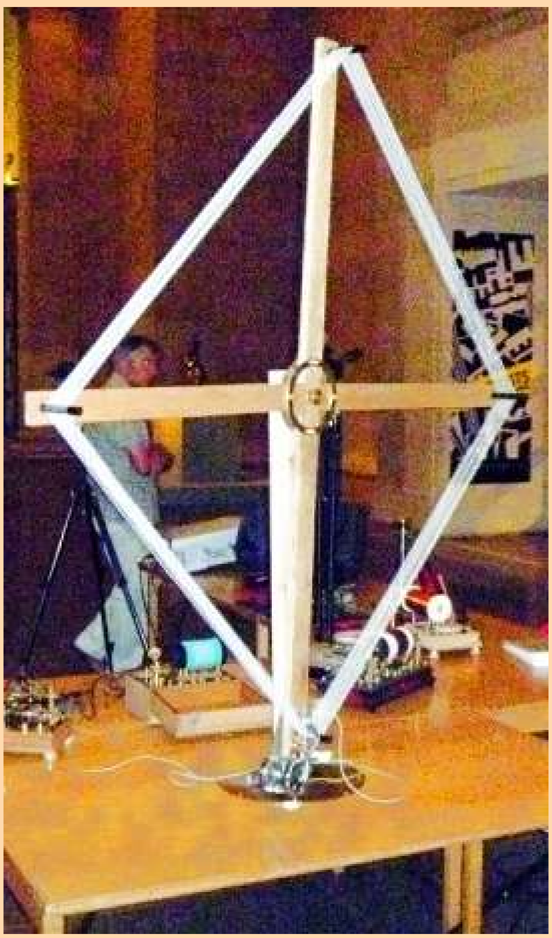

15 turns on a diamond frame

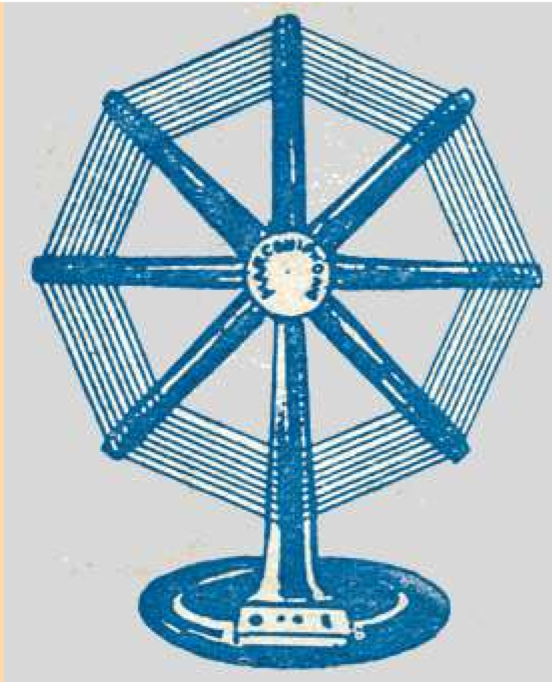

One of the earliest Frame Antennas

The Frame Aerial can be as large as 100cm x 100cm or as small as 10cm x 10cm around a plastic chocolate box.

Here are two FRAME ANTENNAS:

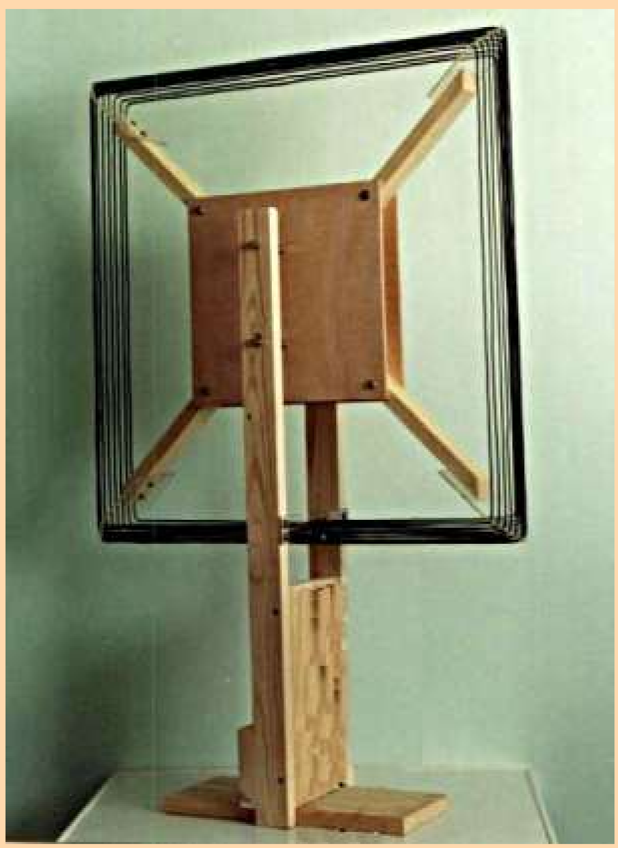

This will work just as good as a ferrite slab antenna. The slab antenna is just 100 times smaller. The slab antenna was invented so a transistor radio could be built in a small case. But if it is not available, you can wind 20 turns around a plastic chocolate box and it will work just as good.

Alternately you can wind 20 turns around a biscuit tin. Put a pencil on the tin and wind the turns over the pencil too. Remove the pencil and it will be easy to remove the turns. Use tape to keep

the turns together.

The FRAME AERIAL does two things. It picks up the radio waves and it becomes the coil (called the INDUCTOR) in the TUNED CIRCUIT. It must be placed away from metal objects, such as a refrigerator.

BASKET WEAVE COIL

There is no point making a complex BASKET WEAVE COIL as it will not work any better than simply jumble winding all the turns at the maximum circumference of the coil, because the energy capturing capability of the coil relies entirely on the amount of flux lines passing through the centre of the coil.
By increasing the centre of the coil, the amount of flux is increased for the same coil size.
In fact, the simplest and cheapest is to wind turns around a box, as explained later in this article, or make a frame antenna as shown above. Technically speaking, a round coil has the best performance but only by a few percent.

A BASKET WEAVE COIL

THE VARIABLE INDUCTANCE TUNING COIL

Whenever the size or shape of the coil is changed, (or the number of turns), the natural frequency of the Tuned Circuit will change and a different radio station will be picked up.
This means tuning across the band can be done by altering the characteristics of the coil while keeping the value of the capacitor fixed.
Changing the inductance can be done in many different ways.
The coil can have taps every 5 turns and an alligator clips selects the correct tap. But very few radio stations will correspond exactly to each tap.
Another way is to have a slider move up and down the turns as shown in the following image:

The slider makes contact where the insulation has been removed. But it may touch two turns at the same time and create a "shorted turn" and reduce the "Q" of the coil.

Another way is to move a ferrite bar (rod) in and out of the coil:

THE SLUG TUNED COIL

To tune across the radio band, the natural frequency of oscillation of the TUNED CIRCUIT must be adjusted (changed). This can be done by changing the value of the capacitor or the value of the inductor.

The value of the inductor can be changed by adding or removing turns or changing the amount of magnetic material in the centre of the coil.
A ferrite bar can be screwed in and out of the coil or slid in and out and this component is called a **SLUG TUNED COIL**.
The following diagram shows a **SLUG TUNED CRYSTAL SET**:

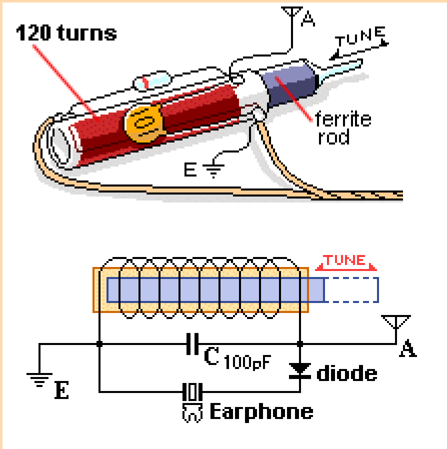

By changing the value of the 100p capacitor, different parts of the band can be picked up.

The photo shows a slug tuned coil using 60 turns of insulated wire on a 10mm tube (or any tube that will fit over a 8-10mm ferrite rod) and a circuit containing an AM radio chip plus a buffer driver transistor:

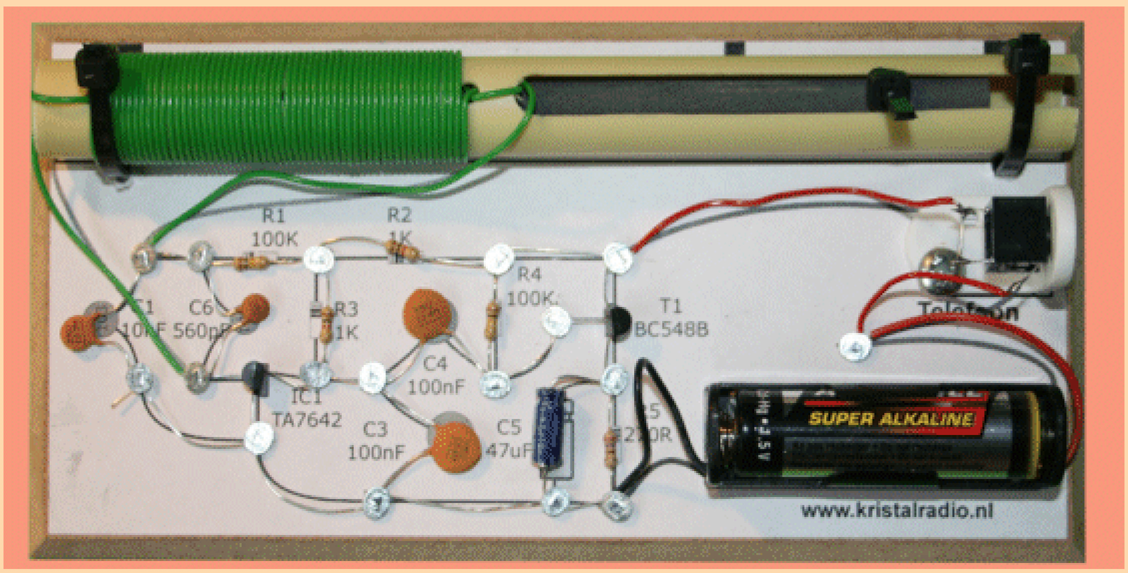

A SLUG-TUNED RADIO

The circuit above is has a broad-band amplifier consisting of 10 transistors (IC1) and they are directly coupled (connected) to each other because it is not possible to "manufacture" a capacitor inside the IC. The IC has 3 terminals (pins, legs) and it looks like an ordinary transistor. Experimenting with this type of IC has shown that it is no better than 2 ordinary transistors connected in a direct-coupling arrangement.

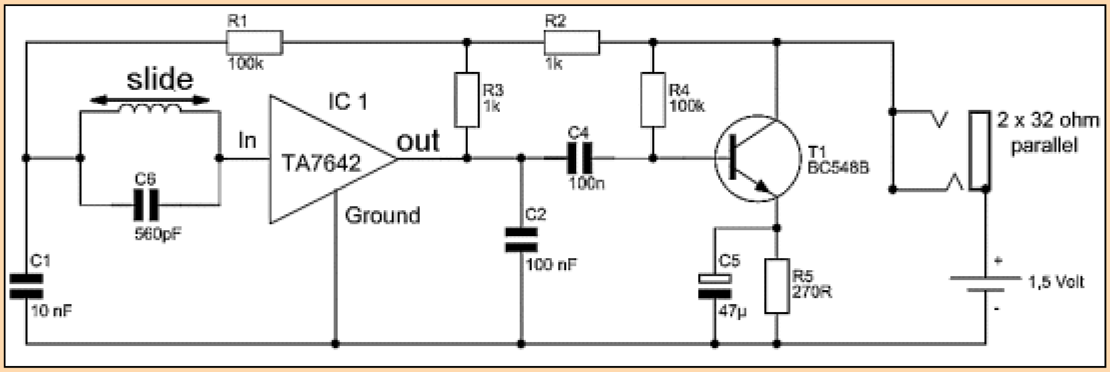

Here is the address of the site for the slug-tuned radio.
http://www.kristalradio.nl/
Unfortunately the site is in Dutch and the kit is not available. However the photos give a clear picture of the how the parts are connected.

The inductance of the coil can also be altered by winding another coil and placing it near the first coil so that the magnetic field interacts with each other and changes the inductance of the circuit. This is called a VARIABLE INDUCTANCE TUNING COIL.
You can have one coil inside the other, two coils near each other or two flat coils side-by-side. Any two coils will interact with each other.

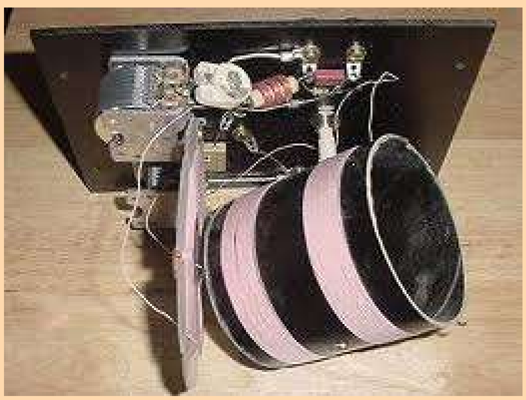

An Inductive TUNING COIL called a VARIOMETER

MAKING YOUR OWN FERRITE ROD ANTENNA

You can make your own FERRITE ROD ANTENNA by winding 60 to 80 turns of 0.25mm enamelled wire onto a 9mm ferrite rod or slab. If you wind it on a paper sleeve, you can move the coil along the rod to get the best performance. When the rod is slid out of the coil, the inductance changes considerably. However the inductance does change very slightly when the coil is moved along the rod.

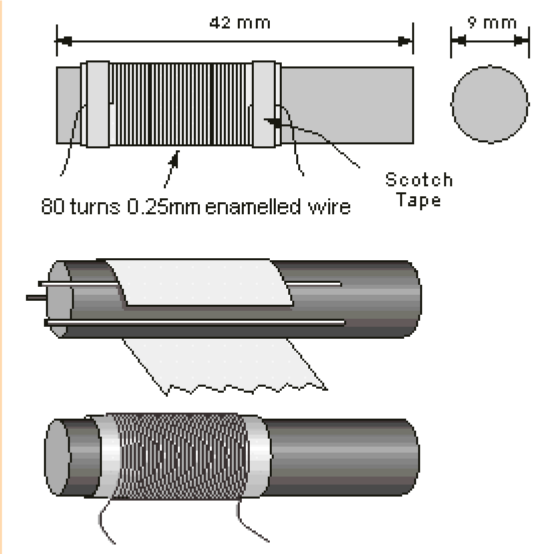

Make your own ferrite antenna

Now we come to the tuning capacitor::

THE TUNING CAPACITOR

The "C" in the "LC" TUNED CIRCUIT can be fixed or variable. When it is variable, it is called a TUNING CAPACITOR. The sheets of aluminium in the air tuning capacitor below are called PLATES and the moving plates are called VANES. The fixed plates make up the STATOR.
The space between the plates is AIR. The photo shows a single capacitor. If two capacitors are connected to the same shaft it is called a GANGED CAPACITOR.
The plates do not come fully out of mesh and that's why the capacitor has a minimum value. The maximum capacitance is when the plates are fully meshed. The odd shape of the plates is designed to produce a fairly constant increase in capacitance as the plates are engaged.

An air tuning capacitor:

Air Tuning Capacitor
(Variable Capacitor)

The capacitor can be made much smaller by using thinner vanes and placing plastic between the vanes. Plastic increases the capacitance about 3 times to 10 times.

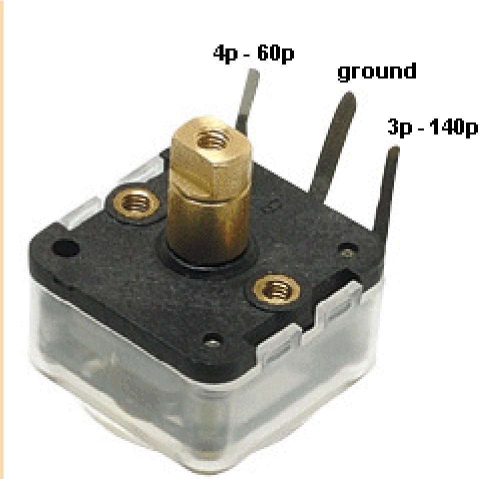

Tuning Capacitor as found in a pocket radio

The tuning capacitor can be replaced with a home-made equivalent that will work just the same.
You need:
4 sheets of aluminium foil (cooking foil) 10cm x 10cm.
4 sheets of thin cardboard 15cm x 20cm (cut A4 sheets in half).

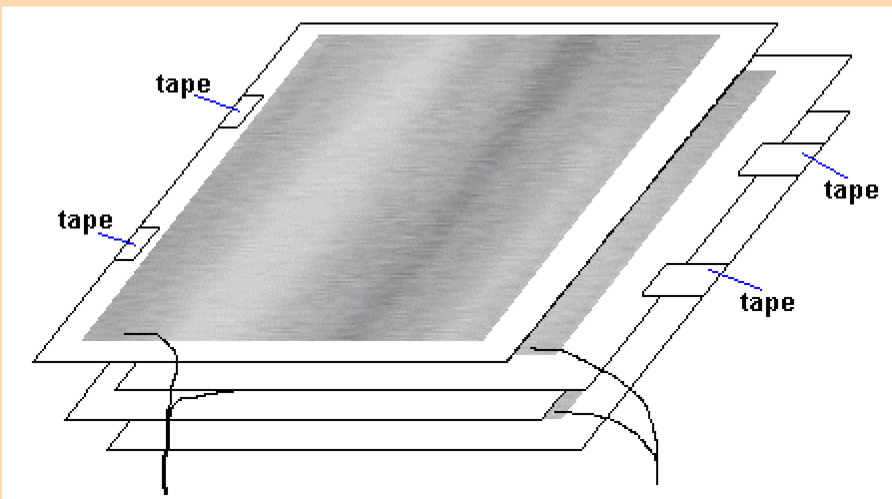

HOME-MADE CAPACITOR

Tape a sheet of aluminium foil to each sheet of cardboard with sticky-tape around all 4 sides. Take one strand of wire from a length of hook-up flex and sticky-tape the end to each sheet of aluminium to make good contact. Place 2 sheets on top of each other and move the top sheet slightly to the left and sticky-tape the edge so they don't move. Do this with the other two sheets but move the top sheet to the right. Now interleave the sets. Connect the wire from the first sheet to the third sheet. Connect the wire from the second sheet to the fourth sheet.
The cardboard (or paper) between the aluminium sheets increases the capacitance three times. The capacitance decreases when the sheets are moved apart and the capacitance increases when the sheets are moved in. The capacitance also INCREASES when the sheets are squashed together such as when a book is placed on them.
You can also make a smaller capacitor by making each sheet smaller and using 6 sheets. You can then add a 100p or 220p in parallel with the home-made capacitor, to select the lower part of the band.

EACH CIRCUIT

Each circuit we describe in the following set of circuits is an improvement or advancement on the previous. We also offer a number of different types of aerial coils, amplifying stages and earphones. Some of the circuits use easy-to-obtain components and home-made equivalents for hard-to-get items. There will be something in this section for everyone to build.

In all radio circuits you will encounter **TWO MAIN PROBLEMS**:

If the FRONT END (the Coil and Capacitor) is loaded too much by the "pick-off" of the amplifying stages, you will only get one station.
If you get squealing or "motor-boating," try a different circuit and layout as the components you are using, plus the voltage of the battery, will need changing.
You cannot always increase the voltage of the supply and get a louder output. Sometimes the increased voltage will stop the circuit working or it may introduce too much gain that the circuit starts to squeal.
The Radio IC (ZN414) DOES NOT WORK on a voltage above 1.5v and some of the transistor circuits completely stop working with a higher voltage. This has to do with the biasing arrangements and if the circuit is designed for a low voltage, you need to keep to the suggested voltage and experiment with a slight increase in voltage and see what happens.
Building a radio is not easy as the enormous amount of amplification of the combined stages creates a feedback loop via the power rail that sets the circuit into oscillation. This effect gets worse with a higher supply voltage and we will explain this further with each of the circuits.

MAKING A CRYSTAL SET

You can buy a **CRYSTAL SET** kit (see the photo of the kit, above) or the individual components (a kit is the cheapest) or use the replacement for the **FERRITE ANTENNA COIL** (16 turns to 20 turns on a 150mm biscuit tin) and/or the **TUNING CAPACITOR** made from aluminium foil and cardboard sheets.
You will need an outside antenna and an earth (such as a water tap or the frame of your soldering iron) to pick up the radio stations.
If you cannot put up an outside antenna, you will need to add one or more amplifying stages and this will allow you to reduce the length of the antenna and increase the volume of the audio.

ADDING AMPLIFYING STAGES TO A CRYSTAL SET

You can add two different types of amplifying stages to a crystal set.
You can connect amplifying stage(s) to the FRONT END and these will be designed to put less load on the front end so the sensitivity and selectivity increases. These stages work at the frequency of the radio signal and they are called RF STAGES (Radio Frequency Stages).
You can build these stages out of individual components or use a chip called a RADIO CHIP or RADIO IC (integrated circuit) for less than $2.00.
The chip contains 5 stages of amplification and these are RF stages (or RF AMPLIFYING STAGES) and the concept is called TRF. (Tuned Radio Frequency).
It is not easy to get this type of amplifier working because the stages produce a very high overall gain and you get a lot of "motor-boating" and squealing if the gain is not controlled. The gain must be reduced when a strong signal is being passed through the circuit because a strong signal will produce a large output and this will be so large that some of the waveform will find its way to the front of the amplifier via the power rail and start to be amplified again. To prevent the output getting too large, the circuit has a negative feedback line - called the AGC line - Automatic Gain Control.
It would be very difficult to reproduce these 5 stages of amplification with discreet components and that's why it is best to use an IC.

The next stage is a DIODE to convert the RF (Radio Frequency) to AF (Audio Frequency). This can be done with the diode-characteristics of a base-emitter junction in a transistor and we will show the alternatives.

Any stages after the diode are AUDIO STAGES or AUDIO AMPLIFIER STAGES.
The main job of the AUDIO AMPLIFIER is to increase the DRIVE CAPABILITY.
In other words, increase the current capability of the circuit for an 8 ohm speaker or 8ohm earpiece (or 16 or 32 ohm).
This is a very difficult thing to do and requires at least 2 stages.
The LOAD you can put on a Crystal Set must be 10,000 ohms or higher. (if you put a lower resistance (impedance) on the output, you will load the FRONT END and reduce its ability to separate the stations.
That's why a crystal earpiece is normally used with a crystal set. It puts almost NO LOAD on the circuit.
If you put a load on the circuit the result will be only one or two stations across the whole dial and only the most powerful station will be received.

If you don't have a crystal earpiece, you will have to use an 8 ohm earpiece. This will require an IMPEDANCE CONVERTING CIRCUIT of 1,250:1
This is a simple way of saying we want the 8 ohm earpiece to appear as 10,000 ohms to the

crystal set.
To produce an overall gain of 1250, we need two stages of amplification.
If a transistor has a gain of 70, it will it will produce an impedance conversion of 70 times. This is a realistic value. Transistors with a gain of 200 will have a gain of about 70 when fitted to a circuit.
This means the other transistor needs to have a gain of about 20 and that is easy to achieve.

ADDING AMPLIFYING STAGES TO THE FRONT OF A CRYSTAL SET

Adding stages to the front of a crystal set are called RF STAGES (Radio Frequency Stages) because they amplify the RADIO STATION SIGNAL.
It does not matter if you amplify RF signals or AF signals. The result is the same.
The only difference is this: The frequency of RF signals is much higher (1,000 times higher) and the coupling capacitors can be much smaller.
This allows an RF amplifier to be built into an IC - called a Radio Chip.
One of the most popular Radio IC's is ZN414 or YS414. This chip has been copied by other manufacturers as: MK484, TA7642 and LMF501T.
All the chips are the same but the pinout is different.
These chips work on a 1.5v supply and if the voltage is increased above 1.5v, the gain of the stages increases to a point of total distortion.
To prevent strong signals producing distortion on 1.5v supply, the output is passed back to the input via a 150k resistor. This feedback line is called the AGC (Automatic Gain Control).
The chip contains 5 stages of amplification plus a stage that converts the RF signal to AF (Detector Stage). This means the signal diode in a Crystal Set is not needed.

Here is the circuit of the TA7642 Radio Chip. It performs the same as the ZN414 Radio Chip.

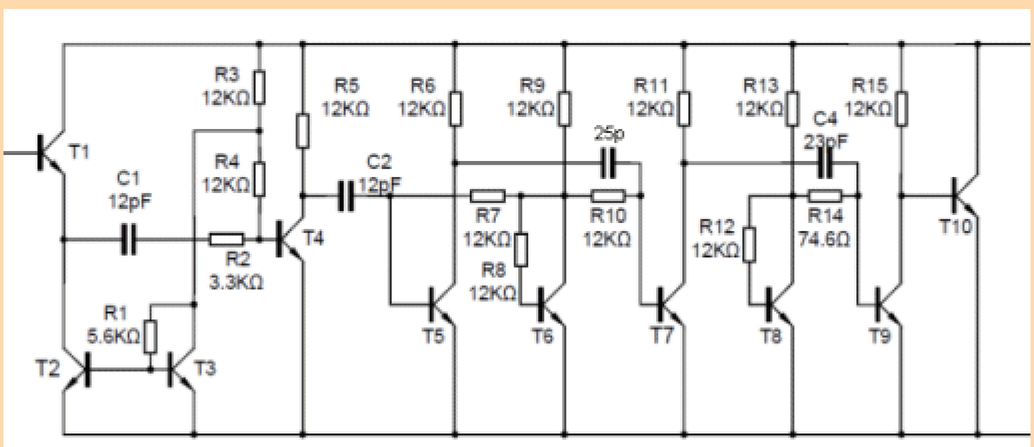

Here is the BLOCK DIAGRAM of the ZN414 Radio Chip:

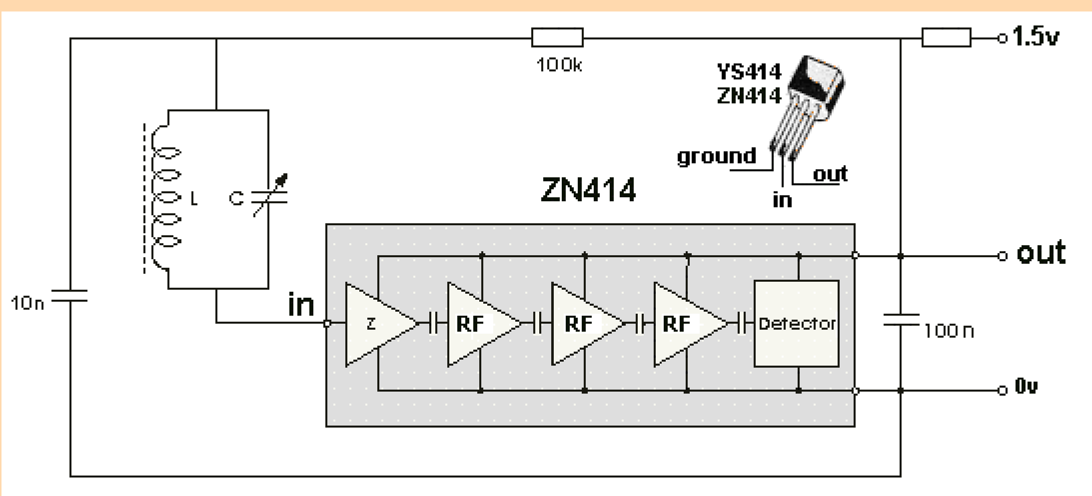

The ZN414 chip can be purchased from Talking Electronics for $1.00 plus postage

USING THE ZN414 RADIO IC

By using the ZN414 radio IC (or any if the equivalents) you can create a POCKET RADIO to drive a headphone or speaker.
But it is not easy to use the chip. The main problem is receiving the strong signals without producing distortion and then being able to pick up the weak stations.
A fixed 100k feedback resistor does not provide adequate control and a TRF radio has limited capabilities.
That's why radio manufacturers make SUPERHETRODYNE receivers. Even though they are more complex, the result is far superior.
However a simple TRF set can be made with the Radio IC and a few stages of audio amplification.

The following circuit uses just the Radio IC and a crystal earpiece or the home-made earpiece described above:
You can use a home-made FRAME ANTENNA or a home-made FERRITE ROD ANTENNA and a home-made VARIABLE CAPACITOR.

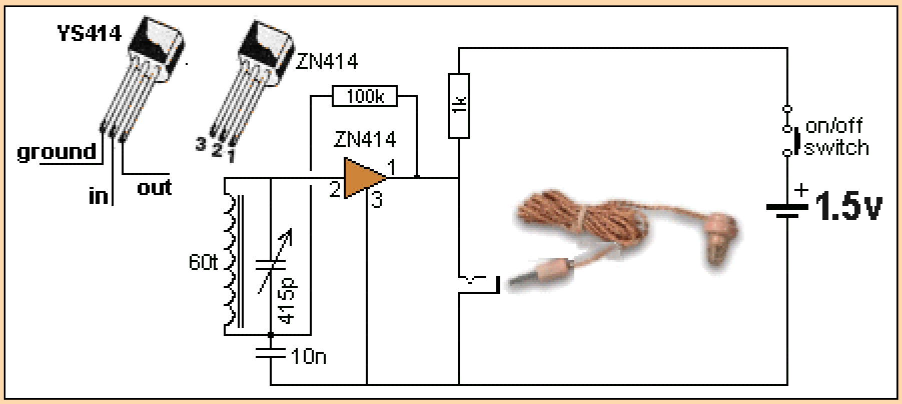

The Simplest ZN414 Radio

Connecting the ground (0v rail) to the frame of your soldering iron or a water tap will increase the output volume. The circuit above shows a Crystal Earpiece. Using a Crystal Earpiece may require adding a 10n across the earpiece to improve the output volume. The substitute Piezo Earpiece is effectively a 20n capacitor and an additional capacitor is not needed.

2 TRANSISTOR RADIO

Here is a simple 2-Transistor radio.
The secret to its performance is the 7 turn "pick-off" from the FRONT END (the TUNED CIRCUIT).
The ratio of 7 turns to 60 turns means a small percentage of the voltage generated in the tuned circuit is passed to the transistor. Thus it puts a small load on the TUNED CIRCUIT.
I don't want to go into any mathematics. The turns ratio is 60:7 = 8 but the effect of the 7 turns "pick-off" has an effect called the IMPEDANCE EFFECT and this is the SQUARE OF THE TURNS RATIO. Thus the IMPEDANCE EFFECT is 8 x 8 = 64. This means the "pick-off" (the LOADING EFFECT) is just a few percent. The front end can produce voltages as high as 500mV because a crystal set can produce a voltage high enough to pass through a diode (350mV) and have sufficient to drive a crystal earpiece.
Even though the front end has a "step-down" ratio, the voltage out the 7 turns will be sufficient to drive the first transistor.
The "transformer" does 2 things: It reduces the loading on the tuned circuit ENORMOUSLY and it produces an output with a higher current than is circuiting in the front end. Even though the transistor is turned ON and biased by the 33k, it is classified as a low-impedance load as far as the front end is concerned and the input signal has to be accompanied by a certain amount of current, otherwise the transistor will not respond to the voltage. The 7-turn "pick-off" is able to provide this current.
Both transistors are biased ON via the 33k base-bias resistors and thus the first transistor responds to the slightest millivolt signal.
This circuit was tested and had the same performance as the **Simplest ZN414 Radio Circuit** above. It can be operated on 1.5v to 6v and the strongest stations tend to overload on 6v. A short antenna is needed.

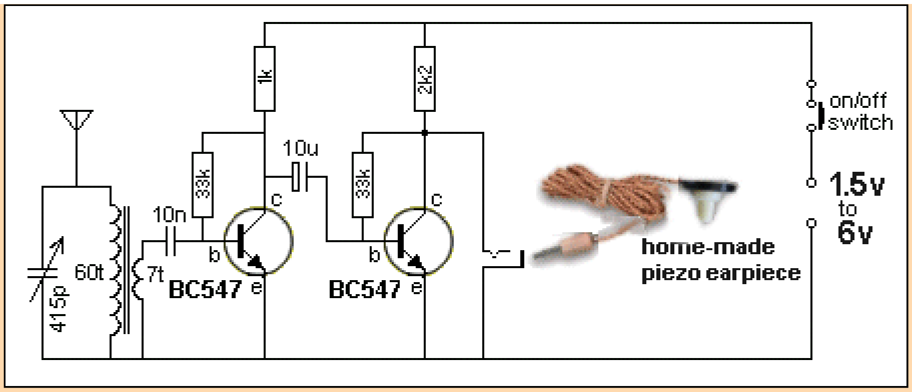

SIMPLEST 2-TRANSISTOR RADIO
using a very-high-impedance earpiece

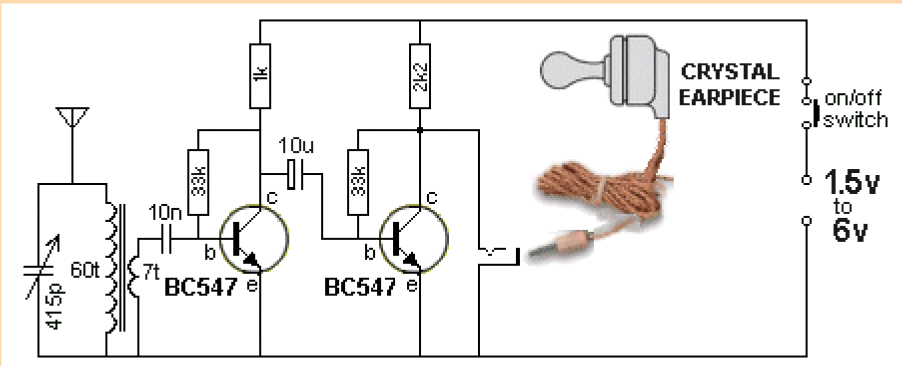

SIMPLEST 2-TRANSISTOR RADIO
using a crystal earpiece

ADDING AN IMPEDANCE MATCHING STAGE

You can add an IMPEDANCE MATCHING STAGE to the output of the circuit above so a low-impedance earpiece can be used.
We call it an IMPEDANCE MATCHING STAGE because this is the correct technical term. It is an AMPLIFYING stage but it amplifies the CURRENT because the second transistor cannot drive an 8 ohm LOAD. 8 ohms is a very low resistance and if it is connected directly to the second transistor, the output will be almost zero.
The reason for this is covered in our discussion: The Transistor Amplifier.
This stage will not increase the volume but simply match the 8 ohm load to the circuit above.
It is very difficult to connect a LOAD to this type of circuit because it will take more current from the battery and cause the supply voltage to fluctuate. These fluctuations will be passed to the first stage and cause variations in the signal. This will be amplified by the first and second transistors in the form of a low-frequency buzzing called **MOTOR-BOATING**.
The only way to reduce or remove this noise is to add an electrolytic across the power rails and reduce the supply voltage. The third transistor simply takes the waveform on the output of the second transistor and delivers it to the earphone with a higher current. It is called an IMPEDANCE MATCHING STAGE as it effectively increases the 8 ohm load by a factor of about 100.

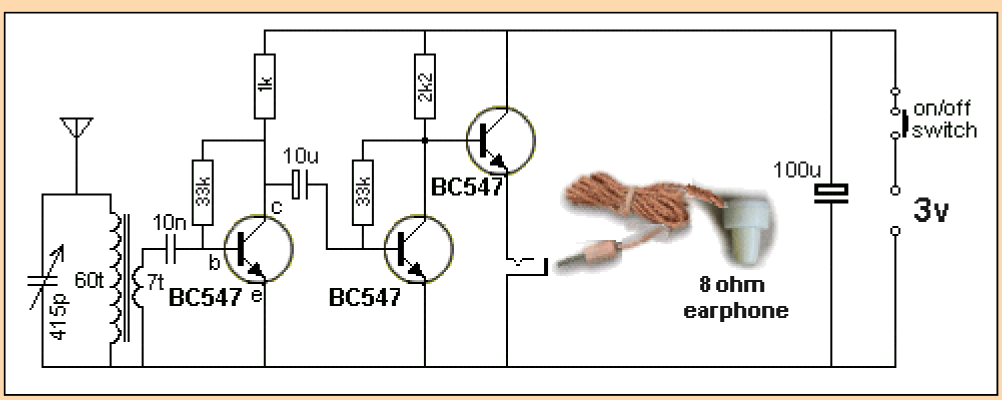

3-TRANSISTOR RADIO with buffer stage for 8 ohm earpiece

The 3rd transistor converts the 8R to about 800R

You can use 16 ohm, 32 ohm or 64 ohm in place of the 8R earpiece and these will give better performance as they will take less current and improve the stability of the circuit.
Low-impedance earphones create "motor-boating" due to the peaks of current and this can be very hard to fix.

A 2-TRANSISTOR RADIO with REGENERATION

The next stage in our discussion to get better performance is a feature called **REGENERATION**. Regeneration sends a small output signal back to a previous stage in the form of POSITIVE FEEDBACK to INCREASE the original signal. The signal on the emitter of the first transistor is the same amplitude as the signal entering the base but the FRAME ANTENNA has a turns ratio of 5:15 and this increases the signal on the receiving section of the antenna by up to 3 times. But we want the returning signal to be just above the amplitude of the receiving signal and so a resistive adjustment (attenuator) is provided on the emitter to deliver just the right amplitude.
This has the effect of increasing the amplitude on the TUNED CIRCUIT and is just like reducing the load on the circuit.
As we have mentioned above, when the tuned circuit is lightly loaded, it will pick up a station at the exact frequency of transmission and if the dial is changed slightly, the station will disappear. This quality is called SELECTIVITY.
At the same time, the Tuned Circuit will pick up weak stations and this is called SENSITIVITY.
The quality of a receiver depends on the loading of the TUNED CIRCUIT.

Here is the original circuit from Elektor Magazine with the prototype made on matrix board and fixed to a base-board with a frame antenna made from two sticks of wood. The photo shows a speaker but the output is so low that you really need headphones.

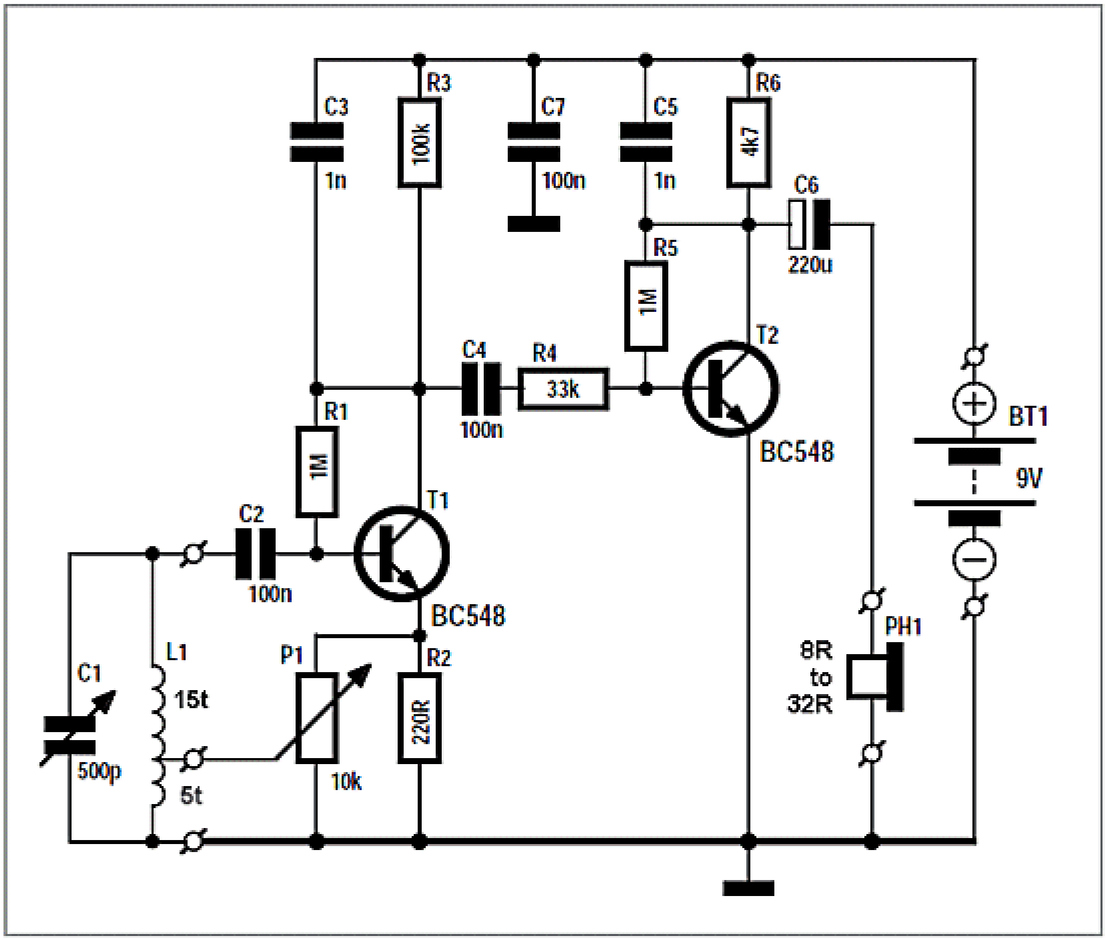

2 TRANSISTOR REGENERATIVE RADIO from Elektor Magazine

The circuit is very complex and the output will be very low as the circuit cannot drive a low-impedance earphone via a 4k7 load resistor. The 4k7 resistor is actually driving the speaker (the transistor is simply discharging the 220u). The 4k7 only allows 32/4700 x 9 = 61mV to appear across the earphone - a very poor result.
The skill of designing a transistor stage is covered in our comprehensive eBook: [The Transistor Amplifier] and you wont make a mistake like this !!!
The circuit above can be simplified and we can add the REGENERATIVE feature to our **Simplest 2-Transistor Radio** circuit:

Our circuit uses a 15 turn circular FRAME ANTENNA 15cm diameter and a 5 turn REGENERATION coil.

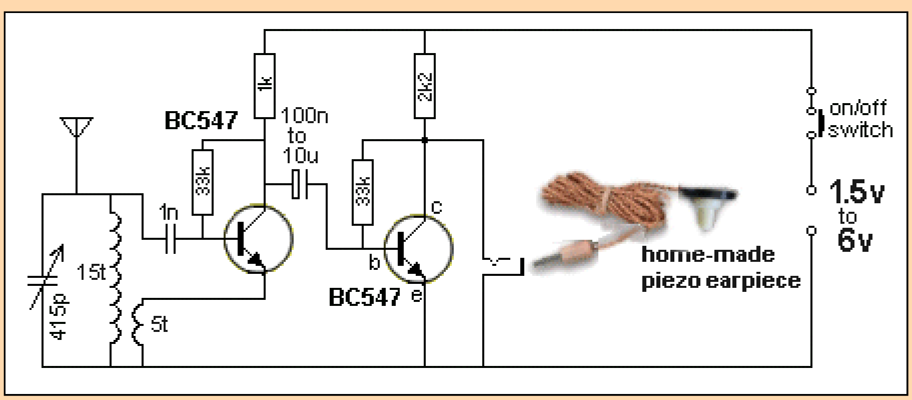

2 TRANSISTOR RADIO with REGENERATION

The regeneration coil is brought near the main coil and as it gets closer you can hear the audio get louder. If this does not happen, turn the coil around.
Early radios used this technique and the operator had to adjust the coil by hand. No-one minded because radio was a fascination and the simplest radio cost more than a weeks wages. To listen

to a broadcast through headphones was an amazement and listeners would sit all night with headphones listening to music.
This is very fiddly and by adding an extra buffer stage, we can use a Frame Antenna with a very clever "pick-off" that does not load the front end. This gives the circuit very good sensitivity and selectivity without regeneration.

3 TRANSISTOR RADIO

Here is our final design for the simplest self-contained 3-Transistor Radio using our home-made Tuning Capacitor and 250mm x 350mm Frame Antenna. It picks up the local stations and drives a low-impedance earphone or set of earphones (from a mobile phone).

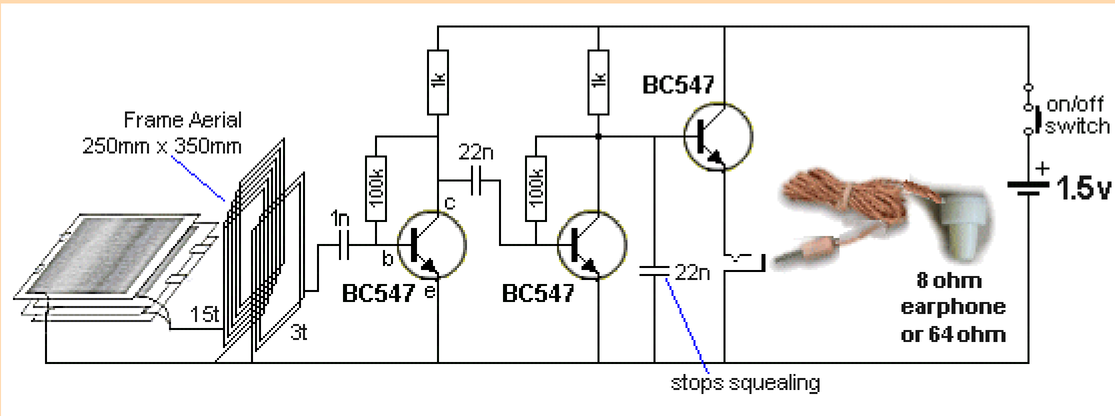

3-TRANSISTOR RADIO

The circuit performs very well and uses readily-available components. The 22n across the output is essential to stop squealing.
The secret to sensitivity and selectivity is the turns-ratio on the Frame Antenna. The 3-turn "pick-off" puts very little load on the front end and this allows the stations to be tuned with our home-made Tuning Capacitor.
The circuit contains all the features we have discussed above and only needs a 1.5v supply.
Build this circuit before you buy any expensive tuning capacitors, IC's or ferrite slab antennas as you will not get any better results.
This is called a TRF circuit and because the stages operate at Radio Frequency or Audio Frequency. Due to the high amount of amplification, the circuit can start to squeal (feedback, motorboat) due to the layout.
You may need to shorten or lengthen the leads or move the parts slightly - it's that critical.
However the result is a portable radio that needs no earth and will pick up the strong stations.
You can try connecting the 0v rail to the metal part of a soldering iron to increase the number of stations.

LOADING

The whole success of picking up a radio station is the RECEIVING CIRCUIT. The receiving circuit is the coil and the signal in the air (from the radio station) must go down the centre of the coil.
It cannot pass over the top or the bottom of the coil. Only the signal that goes down the centre of the coil is received.
As you can see, the centre of the coil is not very big and it is amazing that the signal can pass down the centre. But it does, and that is the only signal that will be amplified.
This signal is passed to the capacitor and we have explained how the signal is gradually increased and increased in amplitude until it is as large as 500mV. The signal from the radio station may be as small as a few millivolts, but as it keeps pushing the "swing" back and forth, the amplitude get larger and larger.
If you put your finger on the "swing" you will prevent it get larger and larger and it only requires the slightest touch of your finger to prevent the swing gaining full amplitude.
In electronic terms, your finger is called LOADING THE CIRCUIT and since we have to pass the signal to further stages of amplification, we need to "tap" or "load" or "pick-off" a signal.
The aim is to load the circuit as least as possible because the actual energy entering the circuit is very small.
In fact, this is all the energy we can remove as that is all the energy entering it.
Because a very small amount of energy is entering the "front-end" we classify it having a very

high impedance. It is very difficult to provide a value of impedance for this circuit because impedance has the term "Z" and the circuit is operating a very high frequency so resistance values are not the same as impedance values.
The actual resistance of the circuit is ONE OHM but the impedance is more like 10,000 ohms to 100,000 ohms.
We can explain its high impedance if we put a 100,000 ohm resistor across the circuit. The waveform will be reduced very slightly. If we put a 10,000 ohm resistor across the circuit, the signal will be reduced a reasonably large amount. If we put 1,000 ohms across the circuit it will stop working.
This means a load of 100,000 ohms will have the least effect.
In a crystal set, the diode creates NO LOAD until a voltage of 350mV is reached. It then passes excess voltage to a crystal earpiece that has a very high impedance. That's why a crystal set will produce a good output. The LOADING is very small.
When a transistor is connected to the TUNED CIRCUIT, it starts to put a load on the circuit after 600mV and this load is VERY HIGH. The "resistance" of the base-emitter junction is about 1k and the signal will find it very difficult to rise above 600mV because the incoming energy is not sufficient to increase the voltage.
Adding a capacitor between the base and the front end allows the transistor to be self-biased and get a turn-on voltage of about 600mV from a base-bias resistor.
The FRONT END is now separated from the transistor and ANY voltage it is producing will be passed to the transistor via the capacitor.
Whereas, with the crystal set, the first 350mV could be produced without any loading, the circuit is now loaded AT ALL TIMES.
This means we have to load the circuit as lightly as possible to be able to pick up individual stations.
The only way we can do this is to use a capacitor of the smallest practical value and this has to be worked out by trying different values. If the value is too small, the transistor will not detect a small signal. If the value is too large, the circuit will stop working.
Values such as 1n, 10n and 100n are suitable.
Values such as 1u, or 10u will be too large.
The CRYSTAL SET loading and a transistor load are completely different.
The transistor loads the front end ALL THE TIME and that's why you need to use a transformer or other ways to reduce the loading. Sometimes a Field Effect Transistor is used as it puts almost no load on the front end.

2-4-2016

Quickturn PCB & Assembly
Your one-stop source for all types of PCBs and Full Turnkey PCB Assembly.
rushpcb.com

Recreating an Alfred P. Morgan crystal set

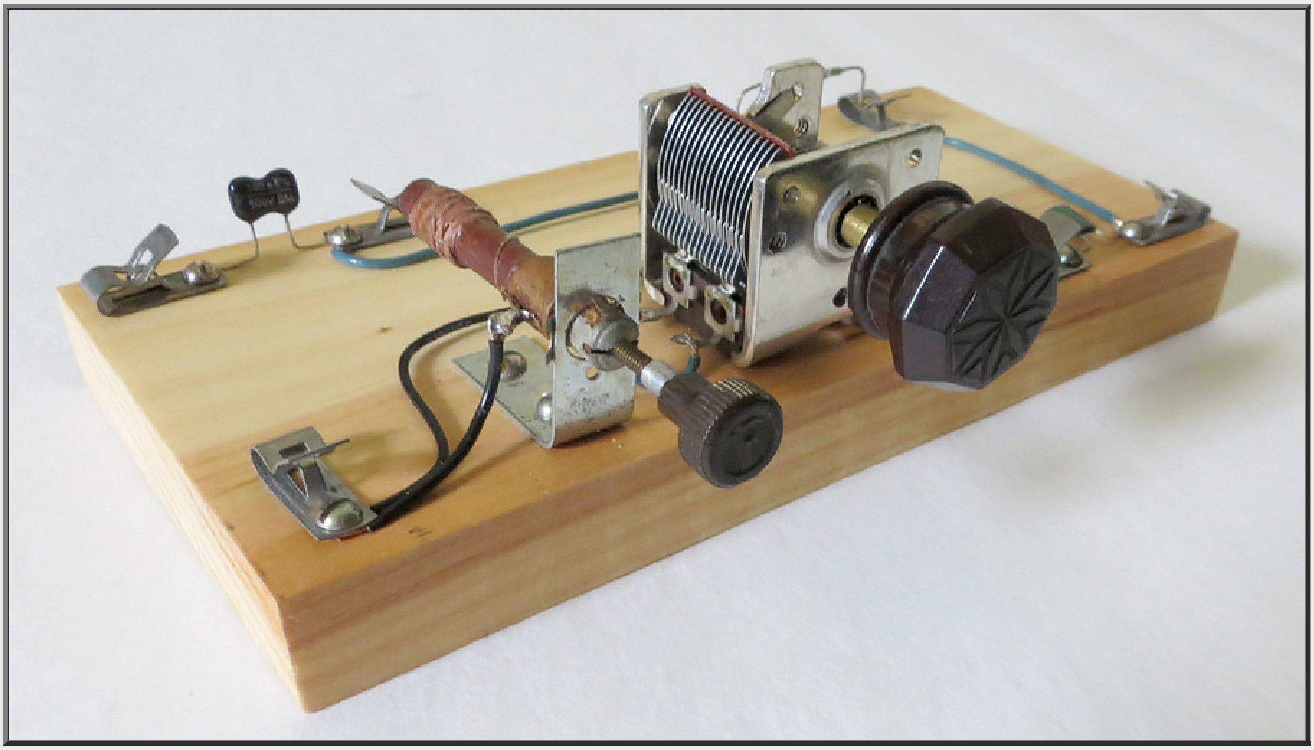

A recreation of my first (working) crystal set, originally built in 1966.

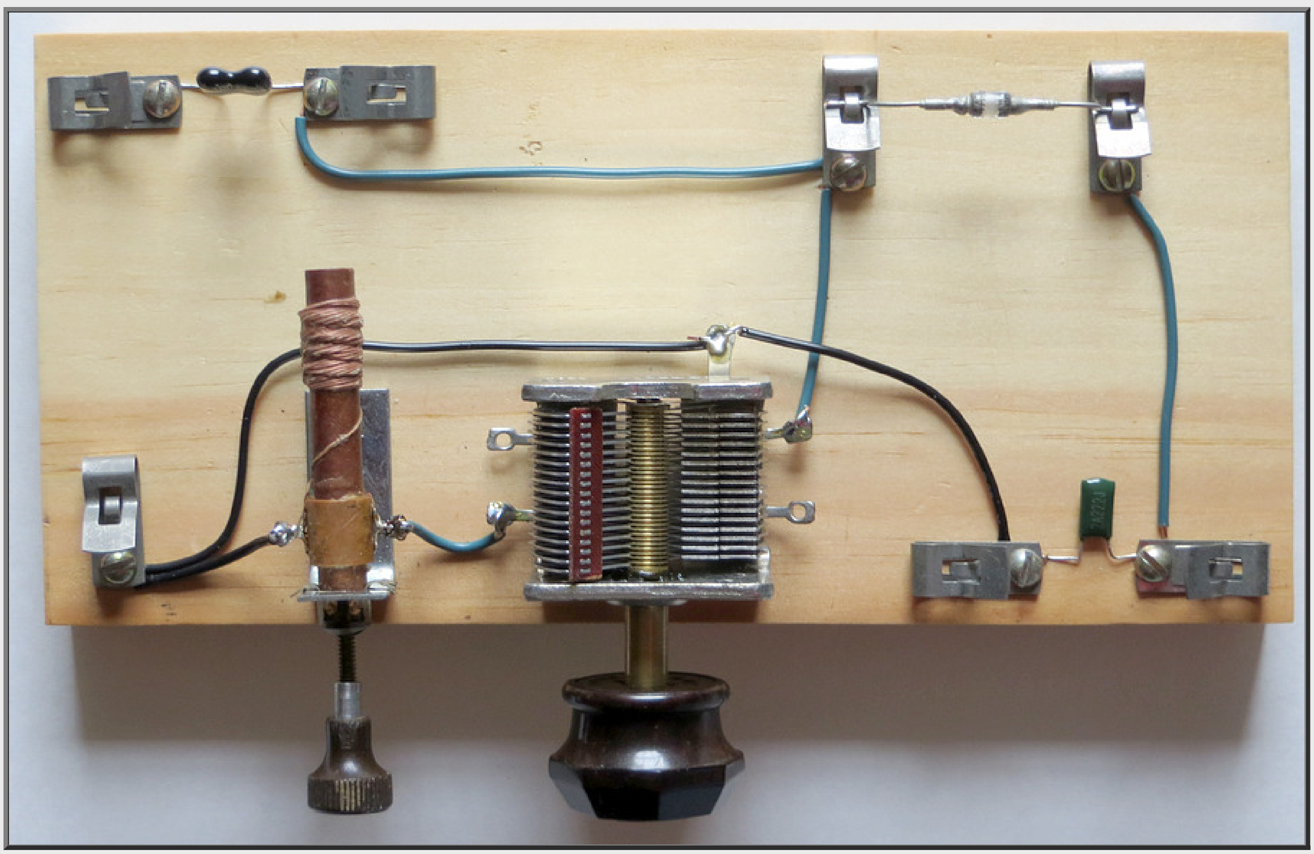

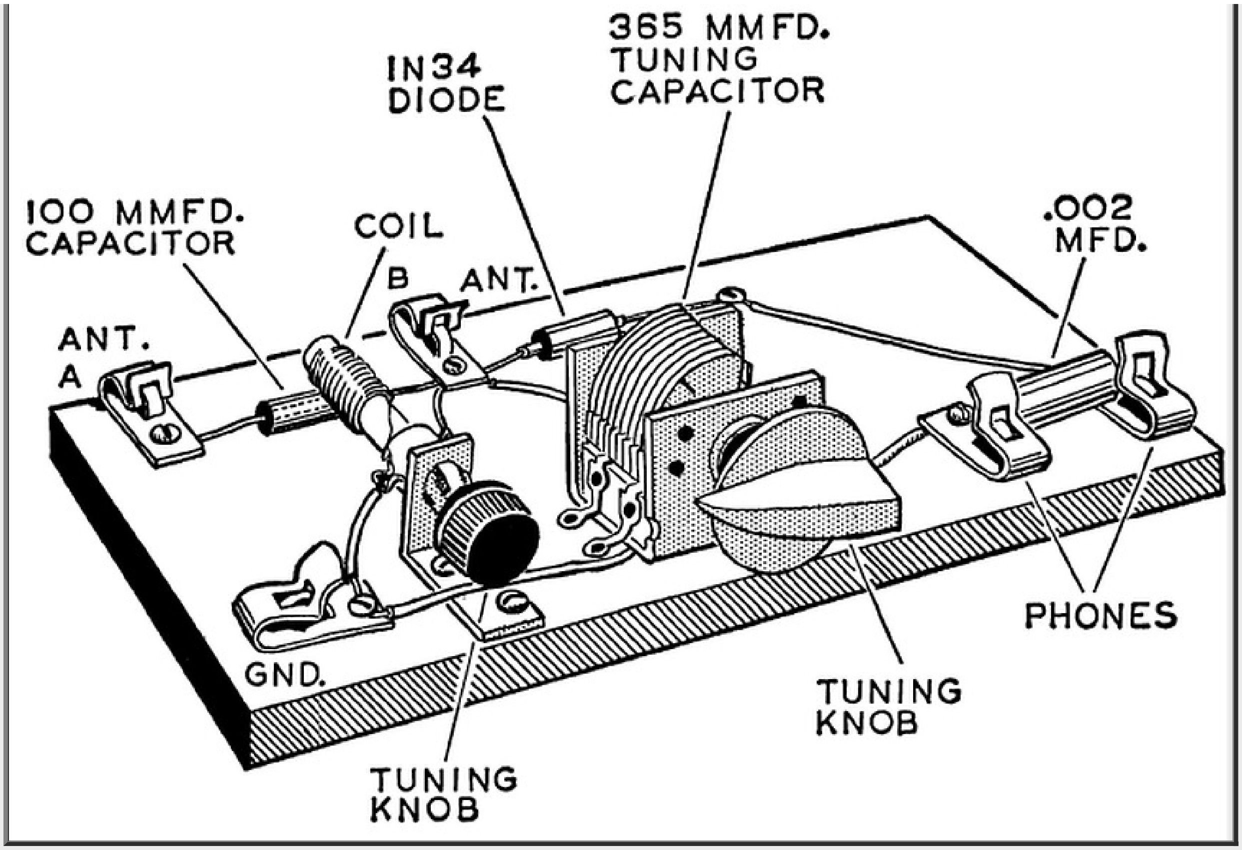

Page from "The Boys' Third Book of Radio and Electronics" by Alfred P. Morgan.

Back Story:

In the Summer of 1966 I was 10 1/2 years old and one of my favorite TV shows was "Get Smart". It was a show about a bumbling secret agent named Maxwell Smart who had all sorts of gadgets at his disposal. My friend Billy Meyers and I decided we wanted to be secret agents, like Max. One of the "secret agent" things we'd do was to pick out a guy with a briefcase walking home from work and declare him a Soviet spy. Then we would "tail" him for a few blocks, making up stories about him.

Billy and I had no way to communicate with each other after we had to come in for the night. He lived half a block away. Kids didn't use the phone back then. There was only one phone in the house and I don't remember using it before I was about 14 years old. Maxwell Smart had a phone in the sole of his shoe. We needed something like that!

Maxwell Smart (Don Adams) Agent 86.

Remco "Monkey Division" Wrist Radios.

One thing I DID have was a set of Monkey Division Wrist Radios. These were powered by a single C battery in the "Master" unit, which also had a button on it that would buzz the other receiver to get the users attention (apparently, the other user was unworthy of a button). A metallic speaker doubled as a microphone. The sound was very tinny, but you could make it out. Unfortunately, they were wired to each other. There was nothing "radio" about them.

I remember taking them outside with my brother Rob, and I could see and hear him talking at the same time his voice was coming over the wrist radio. They were pretty much useless, unless you like running around with a wire connecting you to your brother.

BUT... with some extra wire strung across the driveway, down the backs of the houses and into Billy's bedroom, Billy and I would be able to talk to each other! I immediately presented this great idea to my mom with a request the she fund the cost of the wire, and she immediately refused and told me the electric company would just come out and take the wire down.

Location of my house and Billy's house (actually his grandparent's house) The wire would have to be strung across the driveway. This is part of the West Oak Lane section of Philadelphia.

There was only one thing left to do. Build a radio. I went down the basement and connected a battery to a speaker and used a coat

hanger as an antenna. This was similar to the wrist radio, but the coat hanger antenna replaced the wire. It didn't work! All it did was make clicking sounds in the speaker. I had to wait for my dad to come home from work and ask him why.

When my dad came home I showed him the setup and he said, "You don't have a detector." I asked him what a detector was and he told me to go the library and get a book on radio. The next day I had a copy of "**The Boys' Second Book of Radio and Electronics**" by Alfred P. Morgan. Chapter 2, page 15 was titled "Building Your First Radio Receiver". I wouldn't be able to talk to Billy with it, but that was OK. My mom wouldn't buy me a secret agent coat, we didn't have any gadgets, and our secret agent days were coming to an end.

Now there was another problem. None of the parts needed to build anything in the book could be found around my dad's workbench. There was a store on Ogontz Avenue named REE Electronics, so I headed up there with a list of parts. The store sold stereo equipment and fortunately for me, also repaired stereo equipment. I asked the man in the store if he sold diodes or "capacitaters" and he sent me into the back of the place. There were two guys back there and bins of parts along the wall.

REE Electronics was located at 7709 - 7711 Ogontz Avenue in Philadelphia. The entire block has been razed and rebuilt, and is no longer recognizable. The picture above is the 7900 block of Ogontz Avenue. The store on the left is the only one that retains its original appearance, with the glass store window and the apartment overhead. This is how REE Electronics looked in 1966.

The two guys were pretty cool. I announced that I would like a "three hundred and sixty five micro micro farad variable capacitater". They asked me a couple of questions and told me to come back with the book. They had all the parts I needed except the coil. No problem, I would just build the set with no coil. I came home with Fahnestock clips, a 1N34 Germanium diode, a variable capacitor and a crystal earplug.

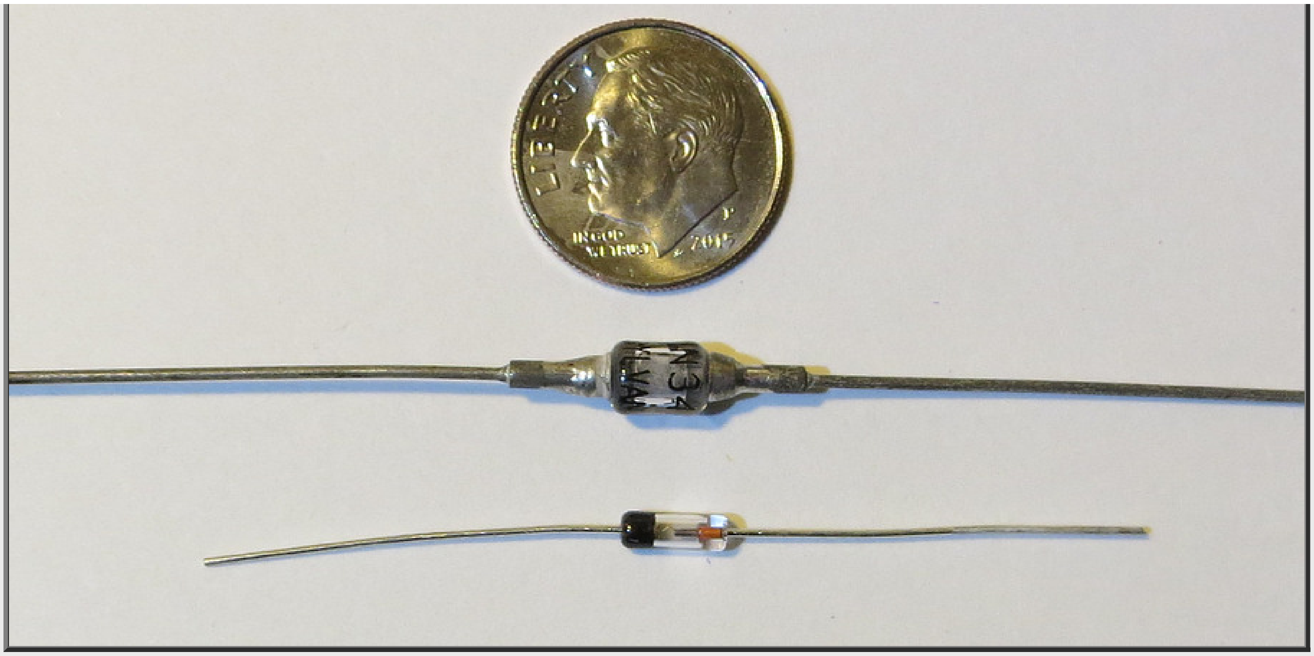

A Sylvania 1N34A Germanium diode (top) from 1949 and its modern counterpart. The new diodes are literally a dime a dozen, less than one cent each. The 1949 Sylvania diode cost me $9.00 in 2015. It is a duplicate of the one I bought at REE Electronics in 1966.

The diode was 65 cents in 1966. I can't use the $9.00 diode because I don't want to bend the leads, so I sort of just look at it.

Of course the radio didn't work without a coil. It did pick up the slightest whisper of KYW AM 1060 mingled with WIBG AM 990. There seemed to be some buzzing associated with it, as what I could hear sounded distorted. I HEARD something, that was the really, really neat part. It made such an impression on me that I remember the date. July 26, 1966.

The "problem" with the Alfred P. Morgan books was that they were not written for anybody as dumb as I was. Morgan didn't write, "If you can't find the coil you can make one." He just said to go buy a coil. Not only that, but there were no photographs in the book, though there were excellent drawings on almost every page. Since I had never seen some of the parts in real life, I didn't know exactly what the coil looked like, and I didn't understand what it did. That's because I didn't read the book! I was stuck on page 15.

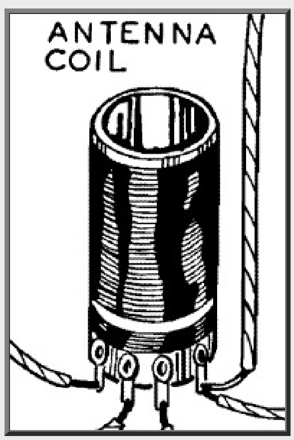

This is the picture of the coil from the book. I didn't know what I was looking at.

I returned the book to the library and came home with "**The Boys' Third Book of Radio and Electronics**." I found a simple radio on page 104 and soon headed back to REE Electronics. This time, they DID have the coil! I can't remember how much time passed after the first non-functioning radio was built. Probably a month or so.

I asked my dad to cut me a wooden base for the radio. I started building the radio and, if I remember correctly, it took me a long time. I didn't have a drill, so any holes in the base were made with the point of a compass. There were three connections that needed soldering. I got some solder from the basement, and the tweezers and alcohol lamp from my chemistry set. The tweezers were heated in the flame of the lamp till the tips began to glow, then I would quickly solder the joint.

One day a friend from school named Leo Pound stopped by on his bicycle. This was a bit unusual because Leo lived miles away. I don't even know how he knew where I lived. He recently told me (via Facebook) that he remembers helping me build the radio. Odd that it was the one and only time he came by. Apparently, we got the radio working that very day.

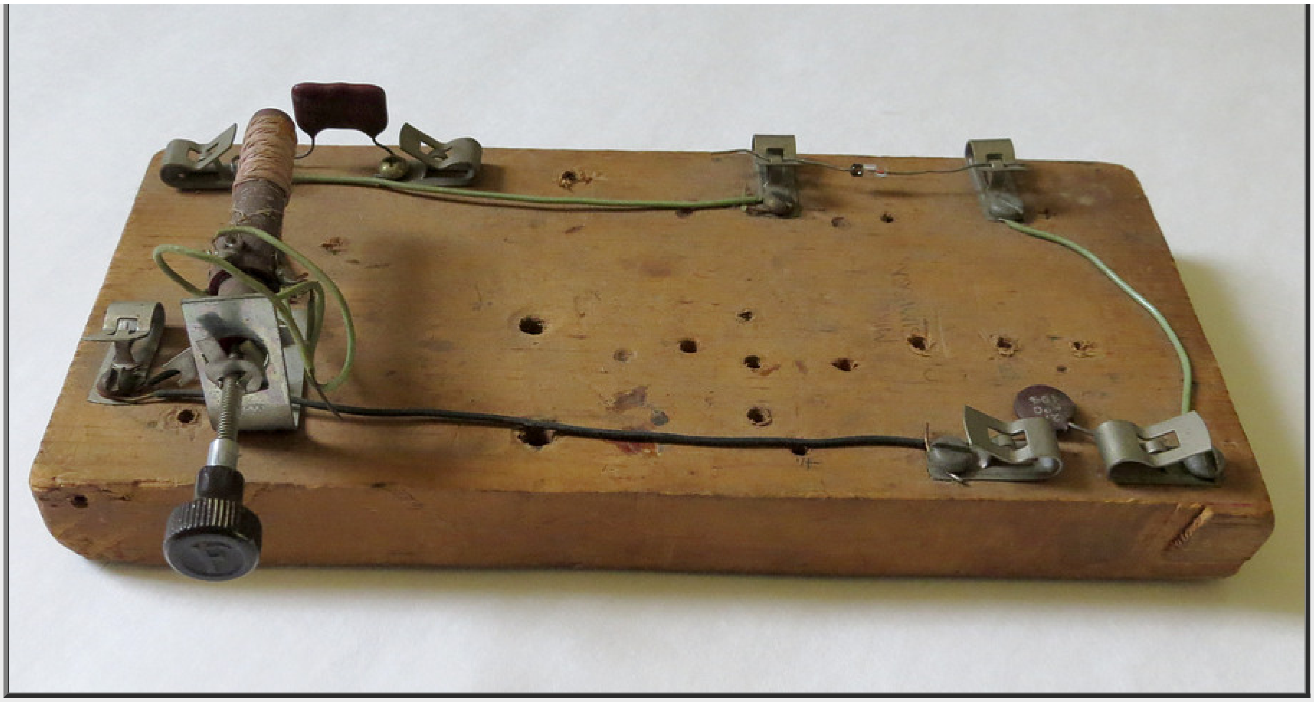

Here is the base of the radio made in 1966.

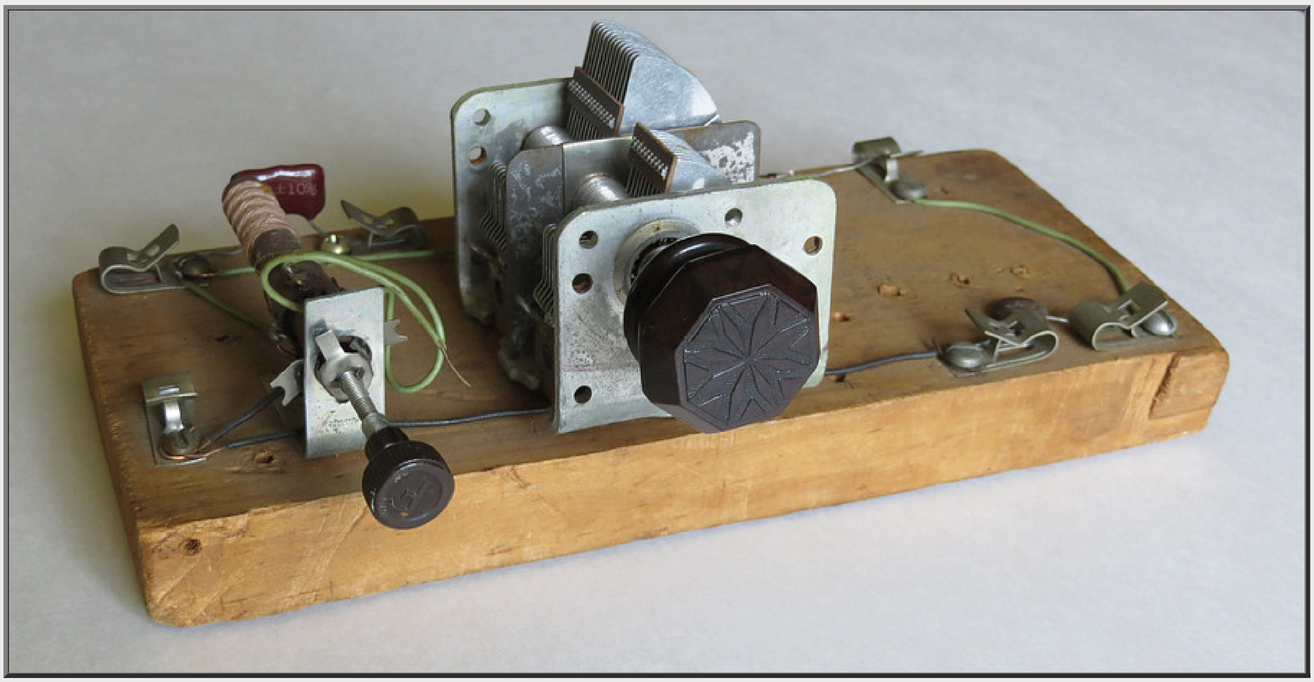

I found all the original parts except for the tuning capacitor. However, it looked like this one. It's just sitting on the base in this photo, but the radio pretty much looked exactly like this. My dad gave me the big tuning knob. The smaller knob came from a lamp in my bedroom. I didn't tell my mom you could no longer turn on the lamp, but eventually I found a lamp in somebody's trash and took the knob off to replace the one on my lamp.

Original coil, diode and main tuning knob from the 1966 radio. The wires on the coil were soldered with a pair of red hot tweezers.

My dad gave me the large knob for the tuning capacitor. He had a second job on the weekends at "John Cusimina's Moving and Storage." I've always wondered if he pulled that knob off of somebody's radio while they were moving. I hope not. He probably did.

Next

CRYSTAL SETS 5
Experimental Crystal Sets

CRYSTAL SETS 5: EXPERIMENTAL CRYSTAL SETS

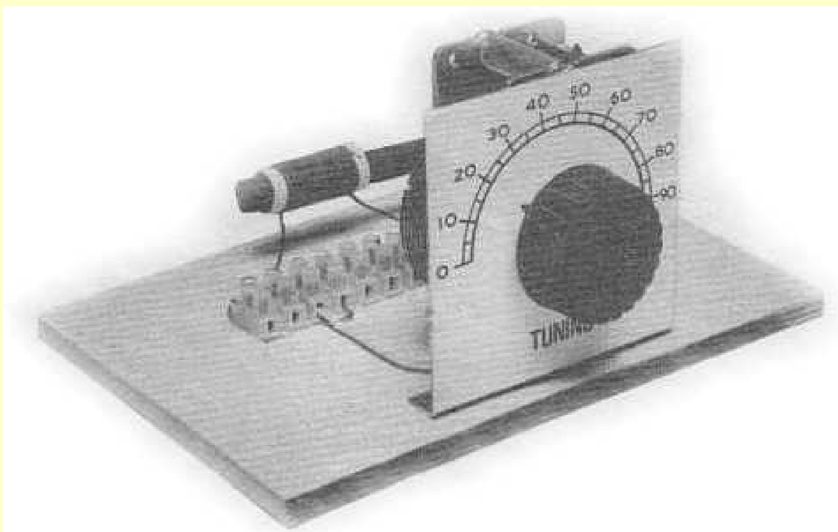

Picture 1 - The Complete Experimental Crystal Set

THE POPULARITY of the crystal radio arises from its simplicity, and the fact that it needs no power supply. The circuit here allows for easy experiments with tuning, aerial and diode coupling, and frequency coverage. Wrong connections can cause no damage to any components.

A Crystal Set is more often than not used for the reception of medium and long wave radio, but short wave reception is also quite feasible. It will normally be possible to receive some of the stronger international radio stations.

This is adapted from an article that appeared in the 1970's in Everyday Electronics, and gave me almost endless hours of fun!

BASIC CIRCUIT

The basic circuit is shown in Picture 2 below. The coil L1 can be air cored, or have a ferrite rod placed in its winding. The variable capacitor C1, in conjunction with aerial-earth capacitance, tunes the circuit to resonate with the wanted radio station frequency. The diode D1 "detects" or demodulates the radio signal so that the programme is heard in the earpiece.

This basic circuit can be modified in various ways to obtain better performance.

EARPHONE

As most constructors will be using a Crystal Earpice to listen to the crystal set it is essential that a 47k Ohm resistor is connected across the earphone terminals (TB1/1 and TB1/2 in the diagram), i.e. in parallel with the earphone, otherwise results will be very quiet.

A High Impedance headset of 20k Ohms (20,000 Ohms) may give even better results, but these are very difficult to obtain , so unless you happen to already own such a headset the Crystal Earphone with 47k resistor will be the only option. An ordinary magnetic earpiece or Walkman headphones will not work with a crystal set.

ASSEMBLY

Construction is of a 'breadboard' type using a wooden board of about 165 x 130 mm. A 12-way block connector, TB1, is used to connected together the components and this is screwed onto the wooden board. The use of a block connector provides an easy method of connecting the components together and then subsequently rearranging them as the experiments progress.

Tuning capacitor C1 is screwed to a bracket made of some scrap metal which is then also screwed firmly down to the baseboard, see Picture 1 above. Thin plywood screwed to the front edge of the baseboard would also provide a suitable method of fixing the tuning capacitor to the base. A knob with pointer is fitted to C1, and a scale is drawn and fitted behind this.

Except for C1, all connections are made by the terminals of the 12-way terminal block as shown in Picture 4. Loosen the screws with a small screwdriver, insert the bared ends of the wires, and tighten the screws. The various locations on the terminal block, TB1, are also shown in the circuit diagram, Picture 2.

AERIAL AND EARTH

Crystal receivers need a long wire aerial preferably strung outside and about 25m long, or as long as is possible to install. If this is outside it should be high and clear of earthed objects as this will improve performance.

An earth is absolutely essential for a crystal set to work properly. The earth lead can be run to an earth rod or spike that is buried to a depth of about 1 meter into damp soil. Or it may be soldered to a bare metal can which is buried in damp soil.

It is feasible, though not recommended, that the earth lead can be connected to the earthing terminal of a hi-fi system or even to the bare metal case of a personal computer that is plugged into an earthed mains outlet, but is switched OFF.

Stranded, insulated wire, or purpose made aerial wire can be used for the aerial and earth leads.

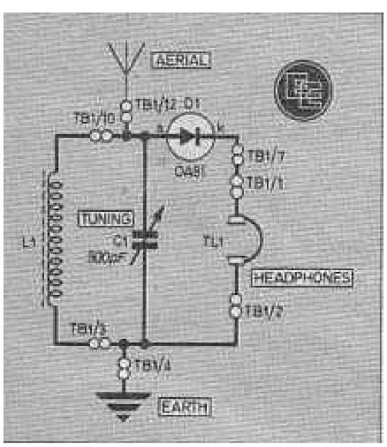

Picture 2 - The Basic Circuit

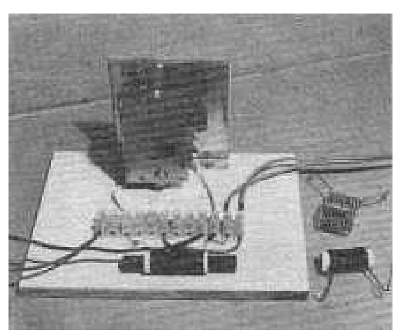

Picture 3 - Photo Of The General Layout

INDUCTORS (The Tuning Coils)

The following four coils are suggested for initial use as L1 :

Coil 1: Make a thin card tube to slide on a 10mm diameter ferrite rod, and on this tube wind about 105 turns of 32 s.w.g. enamelled copper wire, side by side. Secure ends with sticky tape.

Coil 2: Make a similar coil to to coil 1 having about 15 turns of 24 s.w.g. enamelled wire on the card tube. Loops of cotton will help hold the ends in place.

Coil 3: Wind 9 turns of 20 s.w.g. bare tinned copper wire on an object about 20mm in diameter. Remove and stretch to separate the turns, to obtain a coil about 25mm long.

Coil 4: Make a similar coil to coil 3, but with 5 turns.

The Ferrite Rod

It will be necessary to have a ferrite rod of about 60mm to 75mm long available. Coils 1 and 2 will provide reception of medium wave and the longer short wave bands. Coil 3 should cover about 3 - 10MHz shortwave with the ferrite placed in it, or about 6 - 18MHz with the ferrite rod removed. Coil 4 should cover about 6 -13MHz with the rod in, and about 9 - 20MHz without the' rod.

It will be noted that as the ferrite rod is inserted, any particular signal has to be re-tuned by opening Cl. This arises because the ferrite increases the inductance of the winding, so less parallel capacitance is needed for the same resonant frequency.

EFFICIENCY CHECKS

Tune in a m.w. transmission using coil 1 which gives good headphone volume. Place a microammeter or multi-range meter on a sensitive range in series with the headphones. A reading of 50-100uA or more may be obtained, depending on aerial, earth, earphone resistance and resistor value, coil and detector efficiency and strength of signals at your locality.

Placing the ferrite rod in the coil and re-tuning should boost the meter reading to some extent. Surplus or other detector diodes can be tried by substituting them in turn and noting the meter reading. Improvements to the aerial (or earth) will also show up as a rise in meter reading.

If experimenting with a crystal earpiece, which gives no direct current circuit, the meter may be clipped across the phone leads, i.e. D1 cathode to earth.

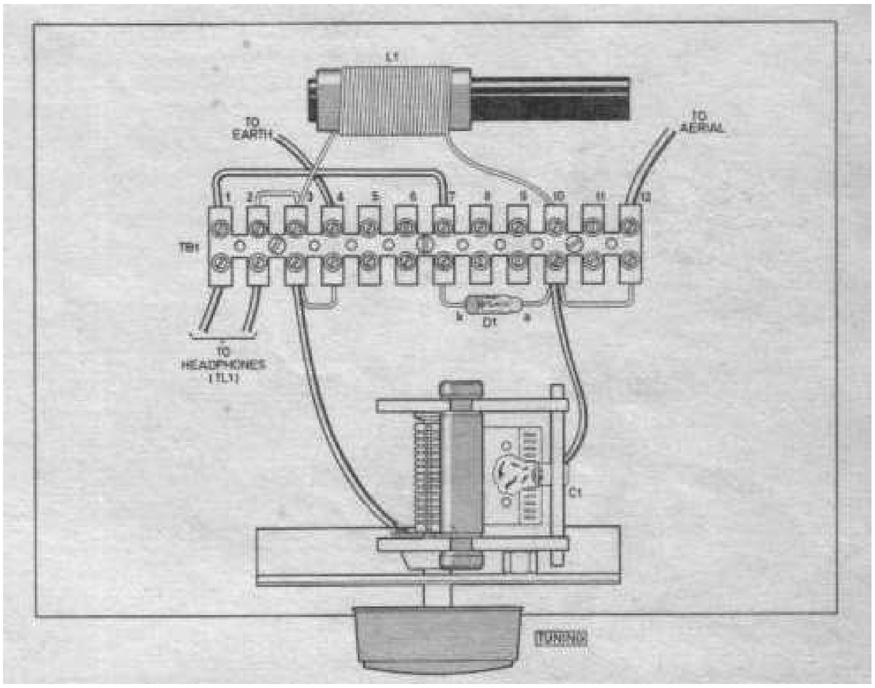

Picture 4 - Baseboard Layout Of The Crystal Set

AERIAL COUPLING

The aerial loads the tuned circuit heavily when connected directly to the top of the tuned circuit, as in Picture 2. This damps the tuning action and it can be found that stations spread out all over the dial, which is unsatisfactory.

The series capacitor, C2 connected in Picture 5(a) reduces the loading and thus improves the sharpness of the tuning. A variable or pre-set capacitor of about 250pF maximum is most suitable. for this role, though it is possible to experiment with a variety of fixed value capacitors in this range also.

Connecting the aerial to a tapping on the coil, as in Picture 5 (b) also sharpens tuning. It may also increase volume. Try about 2 turns from earth for coil 4, or 4 turns from earth for coil 3.

Another method is to have a coupling primary, as in Picture 5 (c). This consists of a second coil, with about one third the turns of the original wound on top of the existing coil.

You can even combine these methods to find what arrangement best suits the aerial in use.

The diode can be disconnected from the end of L1 and taken to a spare position on TB1 for example location TB1/9. You can then run a flying-lead fitted with a crocodile clip from this position, connecting it to various tappings on the coil as required as in Picture 5 (d). This method also reduces loading on the tuned circuit.

Coils with spaced turns of bare wire are readily tapped. For other coils, small loops can be made every ten turns or so, and crocodile clips can be attached to these when selecting tapping points.

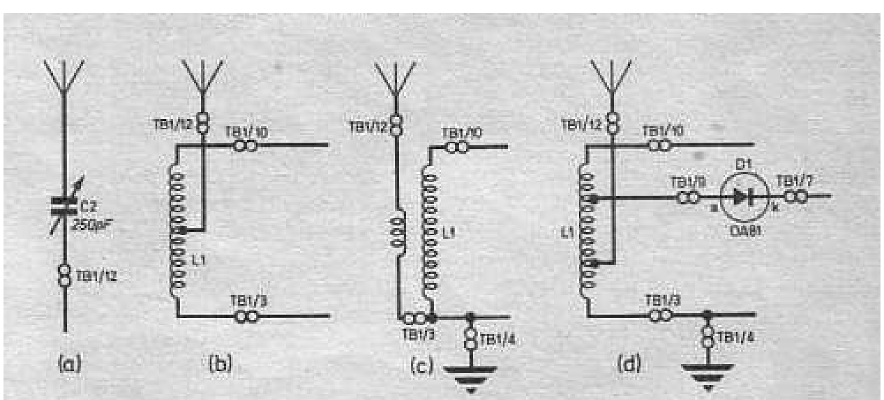

Picture 5 - Alternative Methods Of Aerial Coupling

SHORT WAVES

For shortwave reception, a good efficient outdoor aerial is certainly recommended. Evening listening in the region around 5 - 9MHz in often proves to be the most fruitful.

Since there is no amplification, as with a valve or transistor receiver, certain frequencies will seem to be completely dead at particular times of day. So if the crystal receiver works satisfactorily on medium wave and longwave, but no shortwave signals are heard, check again in the evening, or after dark, when conditions are different.

PARTS REQUIRED

C1	**365pF or 500pF Air Spaced Tuning Capacitor**
D1*	**OA47, IN34, OA81, OA90, OA91, IN94 or similar point contact small signal Germanium Diode** * The OA47 will be of particular interest since it has the lowest forward bias voltage of any of these diodes which will make the crystal set somewhat more sensitive and therefore louder. The US equivalent of the British OA47 is the IN34.
TL1	**High Impedance Headphones (20,000 Ohms)** **or Crystal Earphone**
TB1	**12-Way Plastic Screw Block Terminal**
Also Required:	**47 k Ohm Resistor for Crystal Earphone: Enamelled Copper Wire: 32 and 24 s.w.g. for L1: 20 s.w.g. tinned wire for L1: Ferrite Rod 10mm diameter x 75 mm long: 25m of wire for aerial: Wire and rod or spike etc for earth: Wood for base e.g. 10mm x165mm x 130mm: Scrap of metal of thin plywood for C1 bracket/front panel: Knob: Crocodile clip(s)**

Adapted from an article in Everyday Electronics magazine, November 1981, By F.G. Rayer.

HERE ARE A COUPLE OF VERY INTERESTING CRYSTAL SET DESIGNS SENT IN BY KRYSATEC - "THE RAT" - FROM THE CZECH REPUBLIC

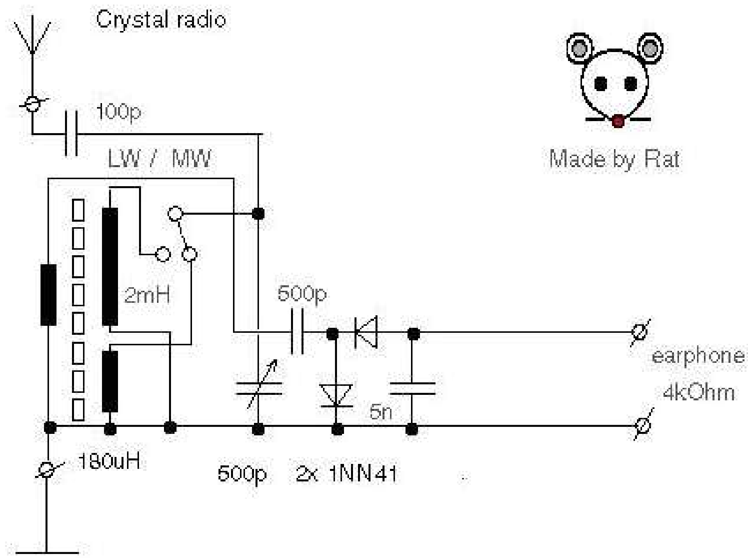

1/ Using old coils from old bulb radio for MW and LW band. Though it would be straightforward to wind the coils - one for Long Wave, one for Medium Wave and a coupling coil. Variable capacitor is 2 x 500pF only one half is used: 500pF. For the crystal earphone a resistor of about 82k ohm in parallel is required. This set also uses two Ge diodes as a multiplier in the quest for for higher audio signal output.

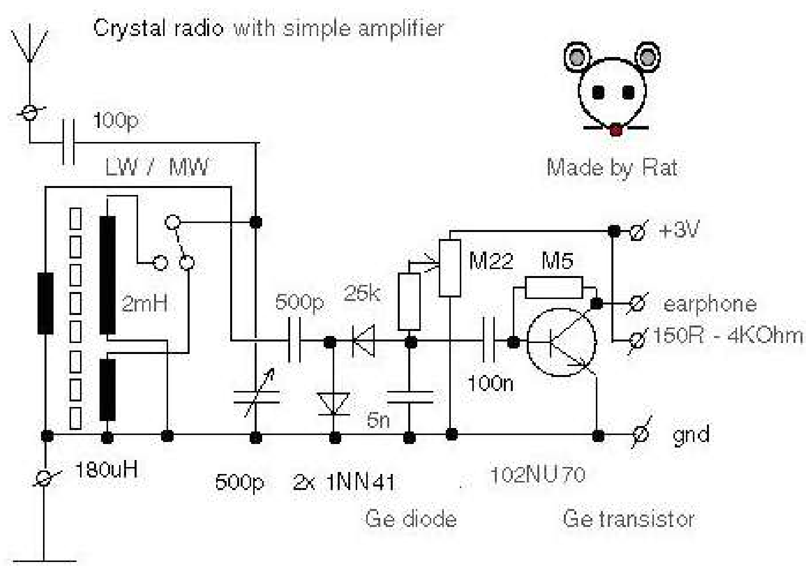

2. If signals are not strong signal in your location, then the above circuit design can be considered. A simple transistor amplifier is used. A variable resistor M22 is used for better sensitivity which can be adjusted for poor signals. This crystal radio is aversion from cca 1960 - 1970 y.

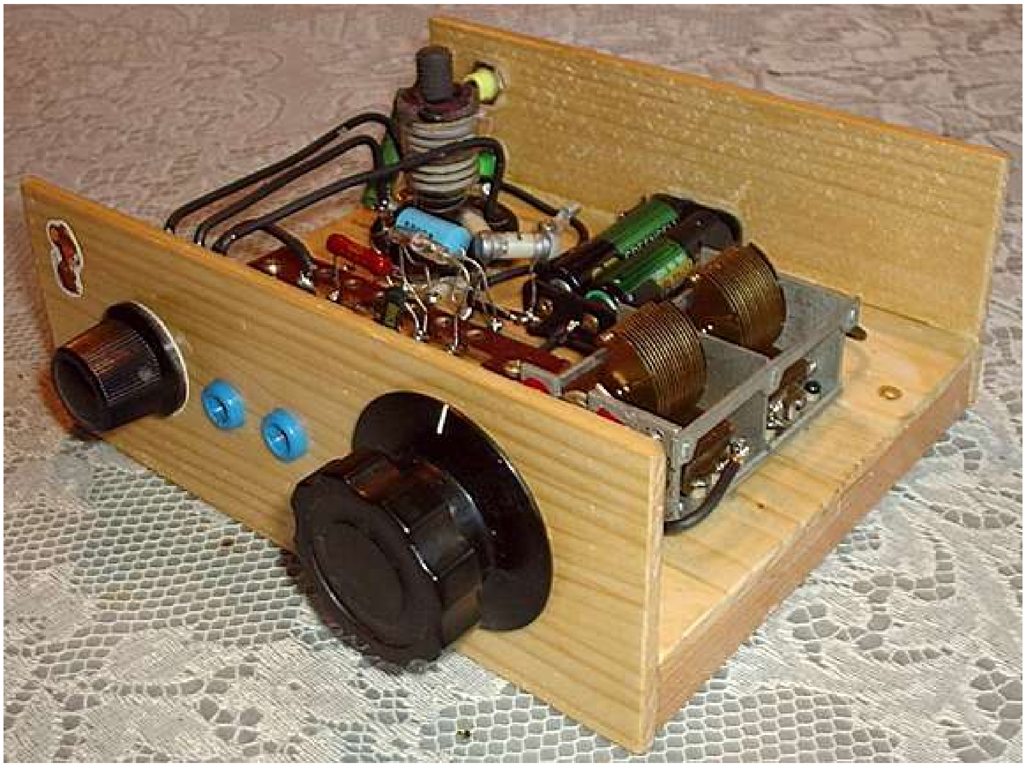

Rat's finished Crystal Set with additional amplification - very neat!

'Minilabs' Crystal Radio

BELOW: Ian Tomlinson kindly sent in a photograph of the box that contained the kit for his John Adams Toys 'Minilabs' Crystal Radio.

It is a very simple circuit consisting of the coil (inductor) with a sliding contact that provides variable tapping points, a diode and crystal earphone. All that is added is the aerial and earth. There is no variable tuning capacitor for simplicity and to keep costs down.

The coil provides the inductance required for tuning into a certain frequency (wavelength). These days a variable "tuning" capacitor is normally wired in parallel across the inductance (coil) in order to vary the resonance of the tuned circuit and therefore enable to easily tune into various transmitters on different frequencies. This crystal is tuned varying the number of turns on the coil (ie varying the inductance) by tapping off at different points using the sliding contact ("ball").

The crystal earpiece, or high Z headphone, is connected between the output of the detector diode (the other end from the coil) and earth. The volume from a crystal earpiece may be considerably improved by connecting a resistor of - somewhere between - 4.7 k and 47k ohms in parallel with the earpiece. A crystal earpiece cannot directly allow current to flow through it and the parallel resistor therefore allows current to better flow through the circuit.

'Minilabs' crystal set by John Adams Toys

A discussion on configurations for Crystal Sets by Felix Scerri VK4FUQ

This discussion, by Felix Scerri VK4FUQ, was posted at this address which no longer appears on the web www.tarc.org.au/techinfo2.htm (error 404) so here it is reproduced:

Crystal Set design is one of my passions closely allied with my obsession for audio and high fidelity.

My main interest in crystal sets, apart from the wonder of a radio receiver that does not require a power source, is the potential excellence of the recovered audio quality from normal AM broadcast stations.

Personally, it is one of my great laments that most people have never heard how good wideband AM can sound. A high performance crystal set or similar TRF approach is, in my opinion,the only way to do it. There are a few people around who have heard the audible results of my efforts,and can only agree.

I have often wondered,given the ultimate simplicity of the crystal set, being essentially a tuned circuit,a diode detector and some form of output device, what it takes to achieve optimum performance. What follows are my thoughts on the matter.

Crystal Set optimisation, is in my opinion, all about reduction of circuit losses. Essentially this means high "Q" tuned circuits and high quality detectors. Efficient output devices also help too. But as we will see, there are some trade-offs required as well. A high "Q" tuned circuit is always benefical, as a high "Q" tuned circuit has lowest RF losses,highest potential selectivity,and highest voltage at resonance, which is very useful for the diode being fed from the tuned circuit. Variable capacitors, even the "modern" miniature variable capacitors (although the older air dielectric units, as used in old valve receivers are more desirable) for various reasons,are generally quite efficient, and a higher "Q" coil will produce the most worthwhile improvements.The best (highest "Q") coils are wound with "Litz" wire, which is a multistranded woven wire with all strands insulated from each other. The performance of Litz wire wound coils is spectacular, unfortunately, although I know Litz wire is still being made, from personal

experience, it is VERY rare in Australia.

Efficient coil design can be quite complex and all my coils are wound on ferrite rods. There seems to be,at least for ordinary single wire windings (close wound), an optimum wire thickness for optimum coil "Q". I have determined .315 mm winding wire to be about optimum for simple (single wire) coils on ferrite rods. Thicker wire is NOT better, believe it or not.

Lacking Litz wire, an interesting winding approach I have developed is to use two slightly thinner wires wound as a bifilar winding connected together at the beginning and end of the coil, yields considerably higher "Q" compared to a simple single wire winding. I have found 0.25 mm winding wire optimum in this application.

Whilst high "Q" coils are beneficial from the RF point of view, there is a possible downside. If one is interested in maximum selectivity and sensitivity, there is no problem, but remember highest "Q" results in a narrowed audio band-width as a simple consequence of band-width. For high fidelity applications this could be a disadvantage under some circumstances, although there are clever ways around this.

Regardless of ultimate coil "Q", selectivity is a major issue with crystal sets generally. Here another trade-off is evident. For the maximum voltage into the diode, connecting the diode to the high impedance end of the coil (i.e. the top) yields the greatest voltage but the selectivity is usually terrible, because of severe "loading" by the diode circuit. For this reason, tapping well own the coil improves selectivity at the expense of signal volume (reduced voltage). Once again there are ways around this. As described in my "Double Tuned Crystal Set Tuner" article in "Amateur Radio" magazine, March 2002, the use of two separately tuned coupled resonant circuits allows top connection into the diode without compromising overall selectivity, thanks to the use of a second tuned circuit which is fed from the external antenna. The whole network forms a double tuned input bandpass filter and in practice this approach works very well. For single coil crystal sets I recommend the use of an un-tuned "antenna" winding adjacent to the "hot" end of the main coil, preferably adjustable (old paper reels from sewing cotton threads are ideal). This allows the degree of coupling to be optimised under actual listening conditions. The double tuned set up is best, yielding superb selectivity, but the un-tuned antenna coil arrangement also works quite well, especially if the diode is tapped well down the main coil.Tapping halfway works well.

The other method of performance improvement involves the use of the most effective detector system possible. Here things get very interesting. In fact the temptation is to use more complex circuitry, but that gets away from the charming simplicity of the crystal set. As an example, my own crystal set tuner has at times mutated into a TRF tuner complete with FET RF preamplifiers, active(powered) detectors and other enhancements. These modifications do work well, but loses the simplicity of a basic crystal set. In actuality, a simple diode detector can work extremely well, subject to some qualification. Diodes like to work with a reasonable level of RF input voltage. Audio distortion can result under conditions of low signal level, due to diode transfer curve non linearity and other factors, such as the widespread use of broadcast station "processing". The actual type of diode makes a difference. The 1N34A germanium diode is very popular for crystal set use, although in my experience just about ANY germanium diode will work, although it is worth trying different specimens. Some are definitely better than others. Even from a pack of twenty 1N34A's from the same source, some were definitely better than others. Measuring the average value of rectified output voltage across the diode load resistor will show which diodes are best. By the way, I regard a diode load resistor as being mandatory. I find a value of about 47K about right, especially if a crystal earpiece is being used or the crystal set is being used as a tuner feeding an audio pre-amplifier and following amplifier. If using high impedance magnetic type headphones, the headphones provide the diode DC load.

Another type of diode that is very interesting, is the hot carrier diode. There seem to be a lot of different hot carrier diodes around these days. There are even hot carrier diodes now being sold as "germanium diode equivalents". I have tried them and they do work acceptably well, but they are not quite as good as genuine germanium diodes such as the 1N34A. Typical UHF mixer hot carrier diodes, such as the 1N5711 will not work well in crystal set service simply because their "turn on voltage"is too high, similar to silicon diodes such as the 1N4148/914 series, which require a lot of RF input to function adequately as RF detectors, however a simple technique can be used to turn hot carrier diodes such as the 1N5711 into superlative detectors.

I guess we are cheating a little, because the technique is to use a little voltage bias supplied via a 1.5v battery, through a simple potentiometer voltage divider arrangement, with capacitor (for DC isolation) fed into the diode from the tuned circuit. With applied adjustable bias, I find the 1N5711 diodes absolutely superlative detectors under ANY signal strength conditions. I find the detection quality also superlative, with a clarity and low noise profile unmatched by any other diode arrangement. In my opinion, hot carrier diodes, running bias,are the best detectors overall.

Regarding other detector arrangements, the diode "voltage doubler" is often recommended, however my own

experiments with the doubler arrangement have been inconclusive and slightly disappointing overall. I have found no real advantage in their use over a simple (one) diode detector, believe it or not.

Yes, they do work, but they're nothing special, at least in my opinion.

Any comments on this general subject of crystal set optimisation would be welcome.

73's Felix Scerri VK4FUQ.
22nd July 2002

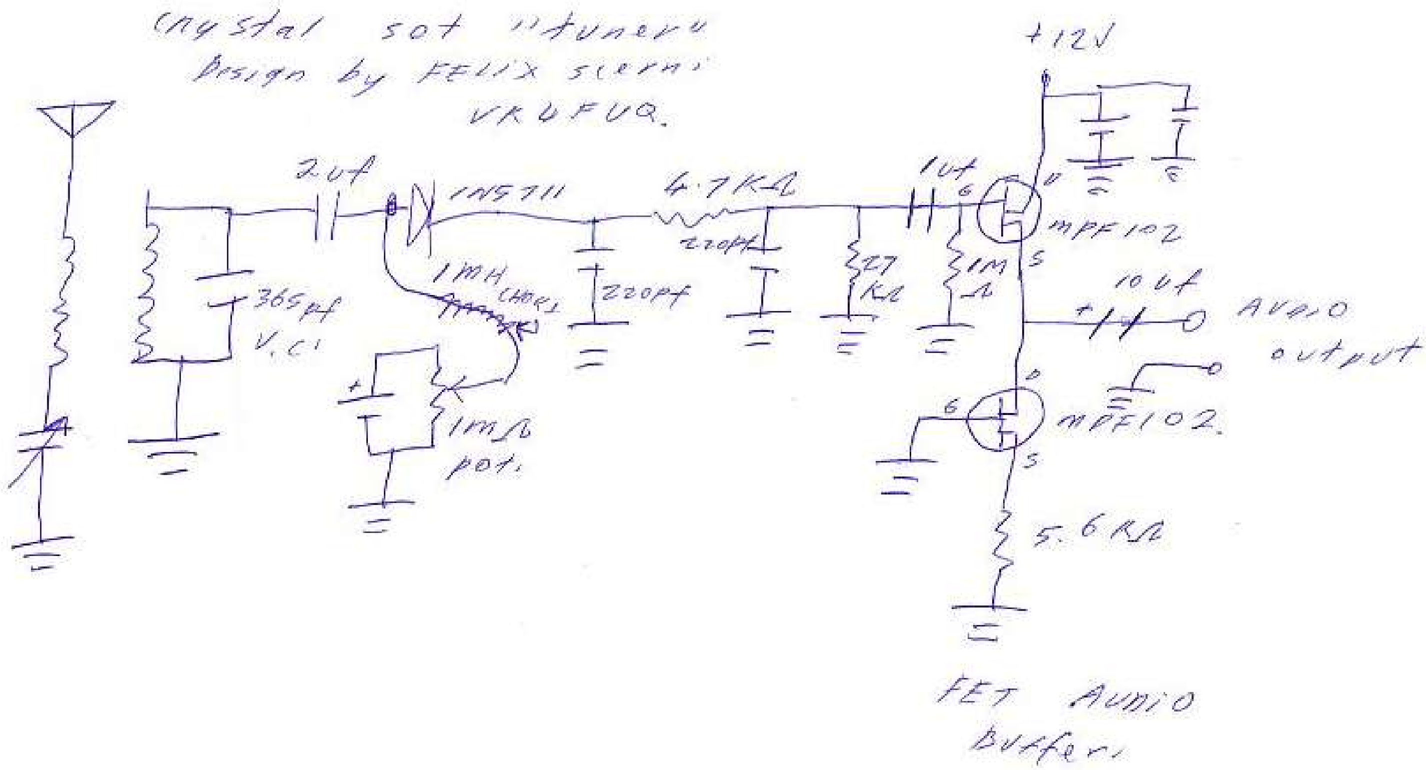

Above: CRYSTAL SET BASED CIRCUIT PROVIDING A HIGH QUALITY PROGRAMME SOURCE

IMPROVED VERSION OF THE ABOVE CONCEPT !! New update from Felix Scerri February 2010:

New 'two FET infinite impedance AM detector'

I've developed a new version of my old favourite FET 'infinite impedance' AM detector that I think sounds very nice. I include a short audio of one of our local AM stations. I picked this station as it is my reference 'torture test AM station' as they run very heavy 'processing' which normally sounds yuck with all my other (diode and non diode) detectors! However it's quite clean with this detector. What do you reckon? I'll do up a circuit if you'd like to feature it in your TRF radio section. A general draft article follows.

'A favourite non diode based AM detector that I've built and used many times over the years is the FET based infinite impedance detector, offering very good general AM detector performance, especially under weak RF signal conditions where diode based detectors do not perform well, especially in terms of audio distortion.

However one of the slightly strange things I've noticed about the simple FET based infinite impedance detector is the variable audio quality noted, even when using the same type of FET. Some I've built have sounded good and others slightly fuzzy when used with an audio preamp and fed into a high quality audio system. I've been giving this a considerable bit of thought of late and I've wondered if the audio distortion might be a result not necessarily of the detection process itself, but the FET stage in its guise as a 'source follower' audio stage which essentially, it is.

I have long been aware that as a simple audio buffer stage, the FET based 'source follower' can exhibit a considerable amount of audio distortion, and a technique I've long used to greatly reduce this audio distortion is to use a second FET in the source lead of the first FET as a 'constant current source' which serves to 'linearise' and

greatly reduce audio distortion in the buffer stage overall. So, to test the theory I built a simple one FET infinite impedance AM detector which worked well, but with just a hint of audio 'fuzziness' on received AM stations. So I added a second FET in the source lead of the first FET wired as a constant current source, taking the output from the source of the first RF detector FET and the source resistor and RF bypass capacitor off the source lead of the second FET 'constant current source'. The result, totally clean audio! The theory seems proved! I call this modified detector the 'Two FET infinite impedance detector'

[))) Here's what is sounds like - click to play the audio file (((]

Here is the circuit diagram:

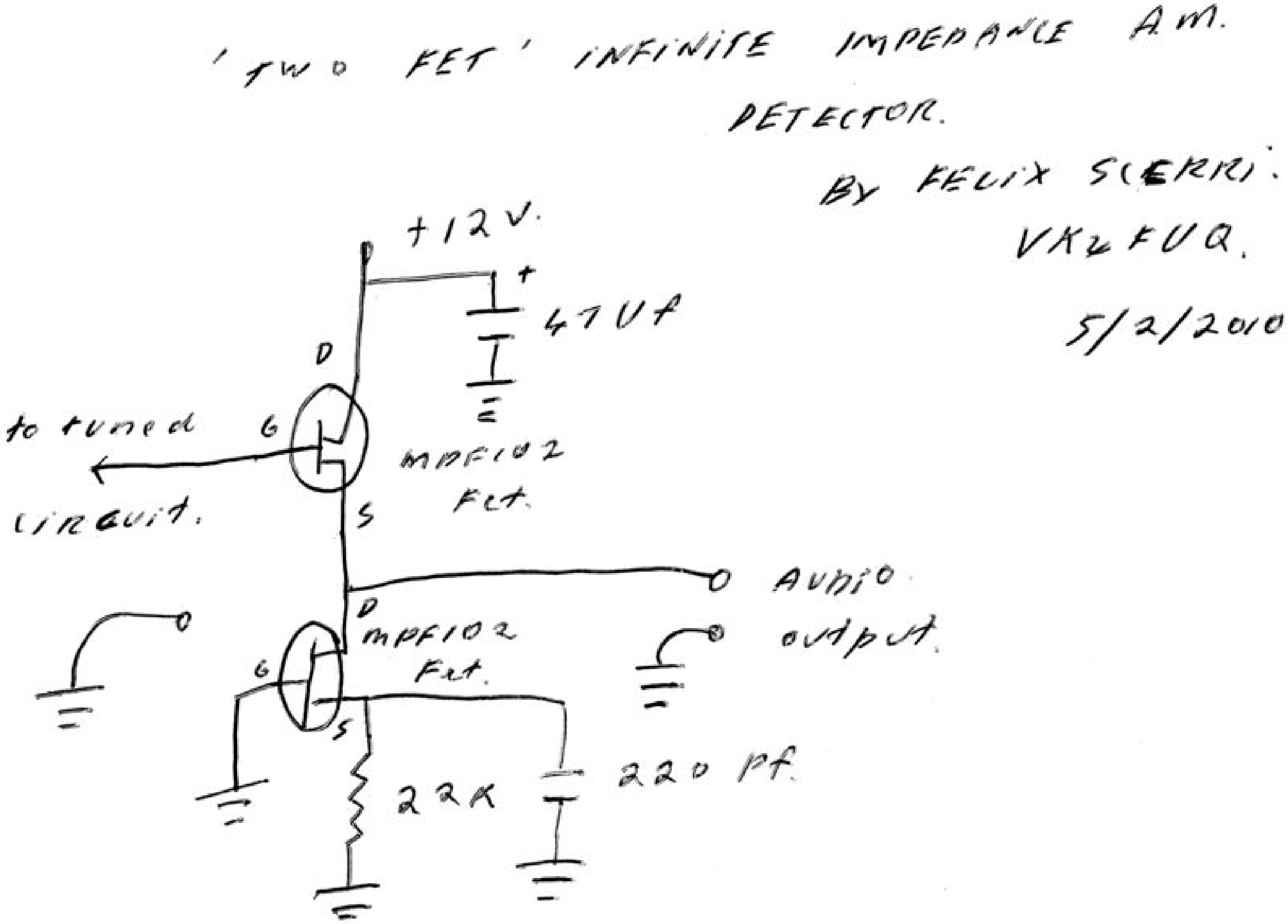

This detector has been a real eye opener for me in terms of its excellent performance, especially considering its circuit simplicity. Indeed in the past I have designed other more complex FET based infinite impedance circuits that do not quite work as well in practical terms as this latest circuit, at least according to my well calibrated ears!

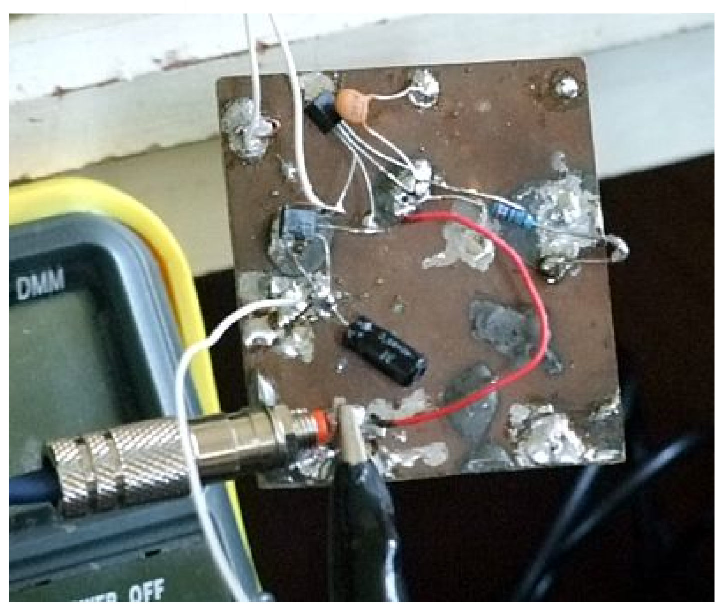

I do not have access to any precise test equipment but my well calibrated ears tell me this 'two FET infinite impedance detector' is a beauty, surpassing practically every other AM detector I've built even at low RF input, and that's rather a impressive claim and the audio quality when used as an AM tuner feeding a high quality audio system is quite remarkable. Possibly the best thing about this detector is its excellent performance under weak signal conditions. Diode based detectors also work beautifully, but the use of an RF stage to ensure detection over a linear portion of the diode's curve is mandatory! This compound infinite impedance detector works

beautifully on the sniff of a useable RF signal.

Just add a high Q tuned circuit and that's it!

Felix Scerri
VK4FUQ

A better FET for the 'basic' Infinite Impedance Detector:

Quite recently by accident, I've realised the MPF102 FET that I've long used in my FET based infinite impedance detectors is possibly not the best FET to use. This was the reason why I developed the 'two FET' infinite impedance detector some time ago which works very well.

However I've found the choice of a more suitable FET works beautifully in the basic FET based infinite impedance detector circuit, which has appeared for many years in many editions of the ARRL Handbook.

I use the 2N5457 and others of the same 'family' may be equally suitable, but I haven't tried them! However with a 2N5457 in place of an MPF102, the basic infinite impedance detector has became my AM detector of choice. It works beautifully even at low signal input with lovely and clean low distortion audio along with a very high input impedance for good tuning selectivity. It's a beauty! The basic generic circuit is attached, courtesy of Rod Elliott's ESP website.

73 Felix VK4FUQ
10 / 02 / 2012.

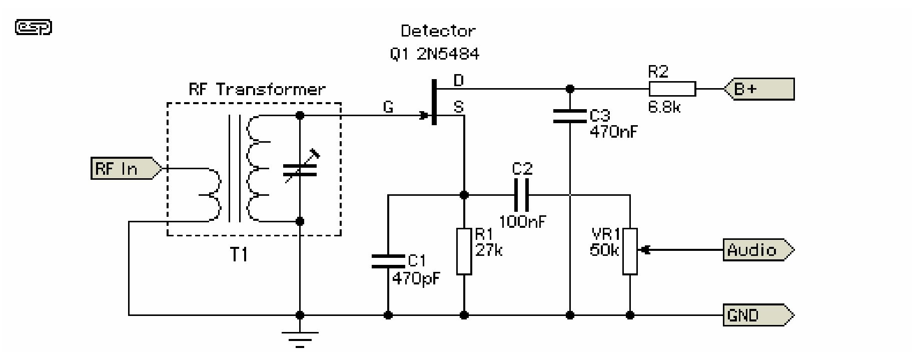

The basic generic circuit is attached, courtesy of Rod Elliott's ESP website
Felix Scerri VK4FUQ

As often happens with me, my renewed interest in FET based 'infinite impedance detectors' of late has led to some interesting new research and I may have considerably improved the 'two FET infinite impedance detector' as a result.

My research suggests that although the use of a CCS (constant current source) reduces audio distortion in an audio stage, the value of the 'source resistor' in the CCS stage is somewhat critical for best results.

By using a potentiometer in lieu of a fixed resistor I have found that a resistance value of around 470 kohms cleaned up all overall audio distortion. I used an MPF102 as the CCS in this circuit. An interesting and worthwhile little circuit refinement.

73 Felix VK4FUQ
21 / 02 / 2012.

A Minimum Component Count High Quality AM Detector

I was generally messing around with various circuit ideas and I came up with this AM detector circuit, a simple diode detector along with a FET stage. It was an attempt to provide good performance along with minimum number of components. Actually I've been pleasantly surprised at the excellent level of general performance and the best of all, it sounds great!

The circuit is quite conventional being a BAT 46 diode detector feeding an MPF102 FET buffer/ common source amplifier stage. I would ordinarily use a FET source buffer stage in this application, but opted to use a simple low gain FET 'common source' amplifier stage instead, with excellent results. I also used a BAT 46 Schottky diode instead of an ordinary germanium signal diode.

This was done for several reasons. Firstly, germanium diodes are now very hard to find but in any case these 'germanium diode equivalent' Schottky diodes are actually a superior diode, having very low noise, almost zero back leakage and an essentially complete absence of carrier storage effects and very good weak signal sensitivity. I call these diodes high fidelity diodes as they sound wonderful as RF detectors.

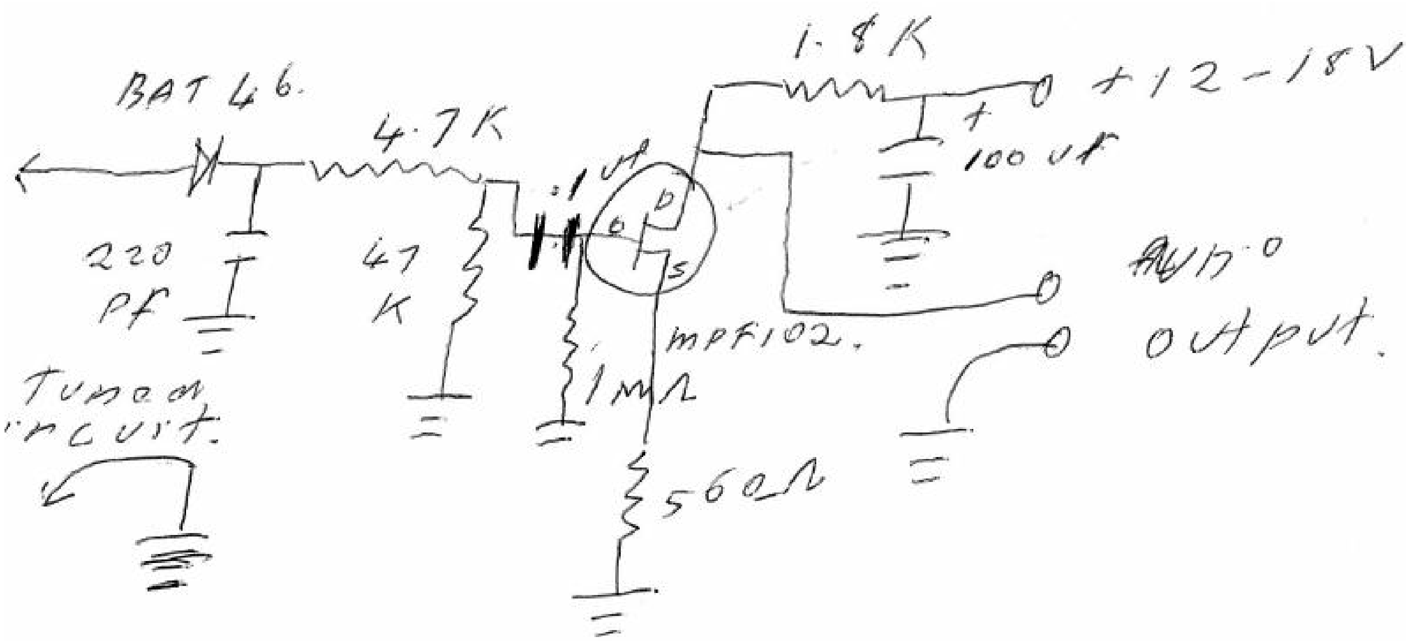

Circuit Diagram of the Minimum Component Count AM Detector by Felix Scerri

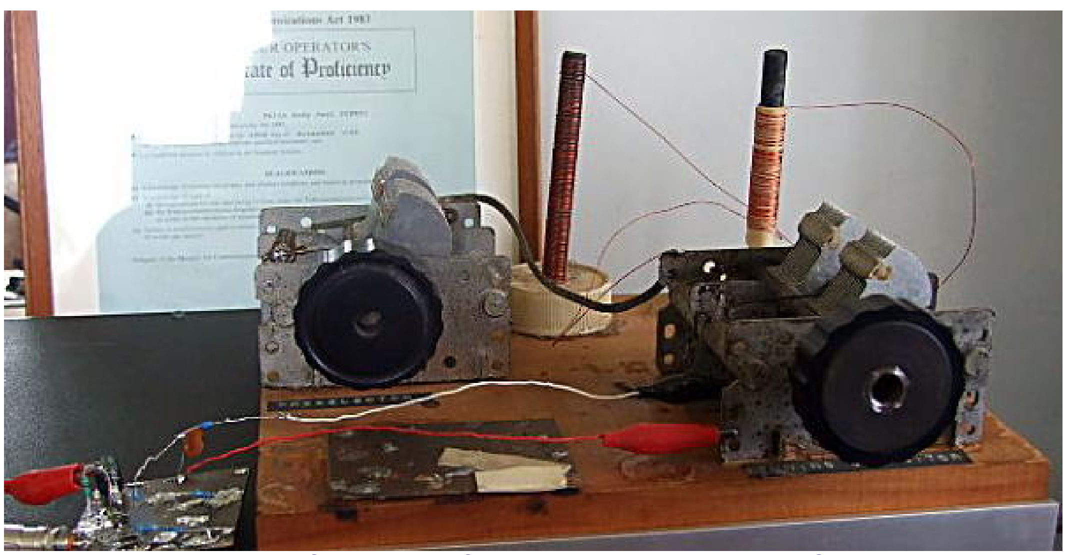

Minimum Component Count AM Detector by Felix Scerri

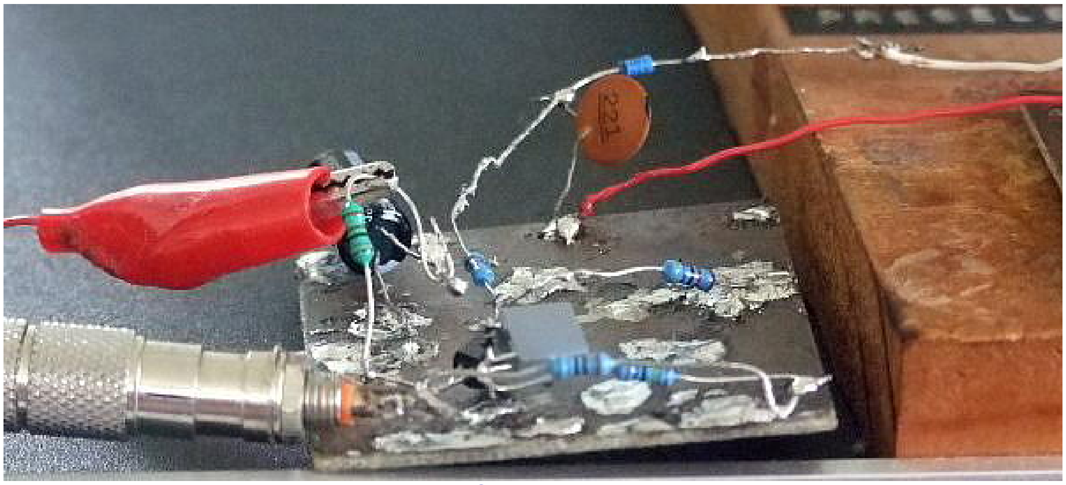

A Closer View

The high impedance of the FET's gate circuit is perfect for optimal buffering of the diode detector, something very important for good low distortion diode detector performance. Apart from providing slight voltage gain, the use of the common source FET amplifier is a new idea, as this prevents the possibility of incidental RF rectification occurring in a FET source follower stage, which can happen. A 1 uf plastic film capacitor may be added in series with the audio 'hot' output lead to block the DC offset out of the FET drain, if required.

Despite no additional RF stage ahead of the diode, audio quality on even relatively weak RF strength stations is actually very good, and of course the audio quality will be even better with increasing RF signal strength, something which will also increase the audio output level. Just on this, for a long time I was somewhat negative regarding diode detectors, as one AM station locally (the strongest one) was always distorted when using a diode detector.

I strongly suspected a transmitter fault, but my complaints were ignored, until one day some time ago when all audio distortion suddenly disappeared! Nothing was ever 'said', but I realised that my suspicions of a long standing transmitter fault were correct, after all!

73 Felix
VK4FUQ
02 March 2012

Voltage Doubler Detector

This is an AM detector circuit that I've long known about and which worked ok, but never seemed to work as well as it should have. However I spent some time late last night trying to optimise the circuit, with some success.

It is a curious circuit being essentially a 'voltage doubler' originally developed for power supply applications, and its use as an AM detector is hard to analyse! It seems that the component values in the circuit are somewhat critical for good performance and if not, the performance is rather 'ordinary'. The circuit that I eventually came up with uses a 150 picofarad 'input capacitor' with a 150 kohm 'load' resistor and loaded into a FET common source voltage amplifier stage (as previously described) through a coupling capacitor with a 1 Mohm input resistance.

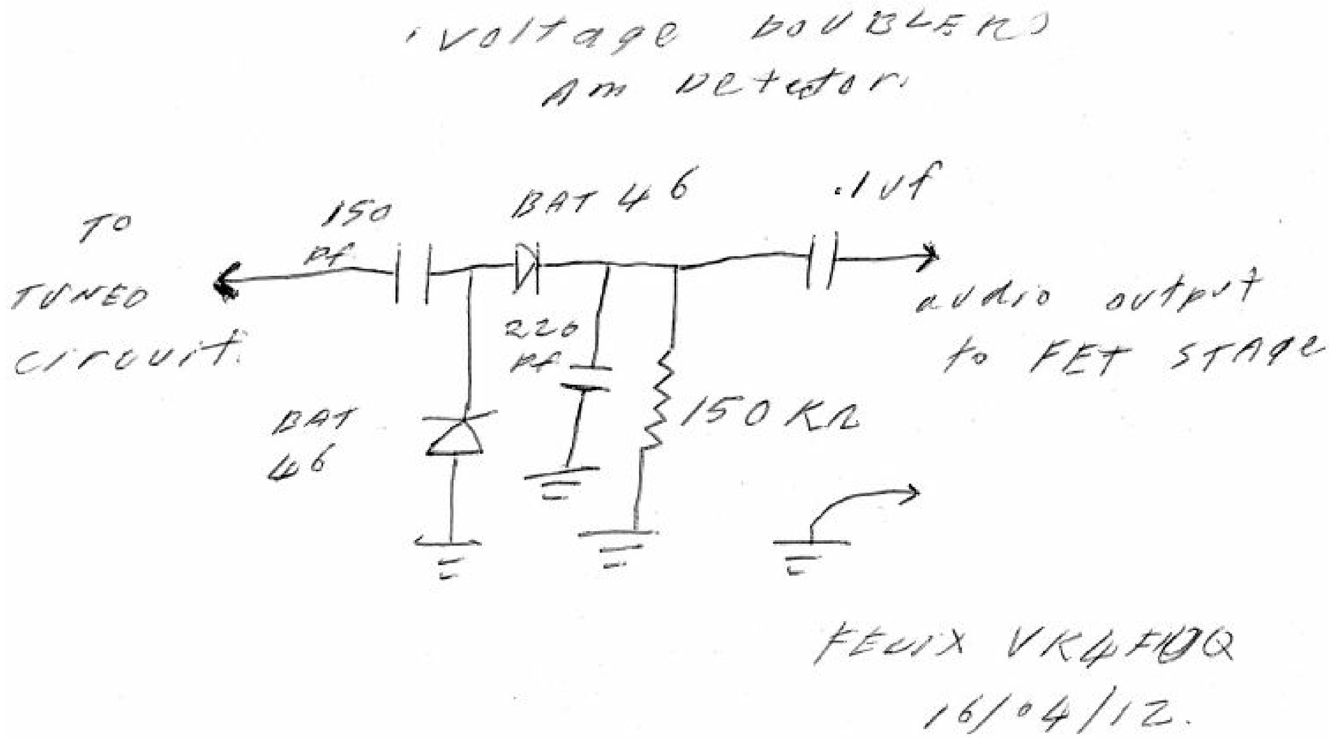

With these circuit values, it all works 'quite well'. Give it a go! It's an interesting AM detector with quite good 'sensitivity' and clean audio quality, and it seems to work well at low signal levels.

73 Felix
vk4fuq.

16th April 2012.

Simple AM detectors: What works best? A practical experimenters viewpoint.

I have written a lot about simple AM detectors for use as tuners for feeding into an audio amplifier, and it has been a long time interest. These days I use either diode based or 'infinite impedance' types of AM detectors. In this location our 'local' AM stations are quite distant and are therefore quite weak in terms of signal strength.

As such I find infinite impedance detectors based on field effect transistors give consistently better results for tuner applications due to their lower apparent overall detector distortion. Diode based detectors are quite 'fussy' as they require both optimal output buffering (AC/DC ratio) and an 'adequate' (beyond the diode knee) level of RF signal injection. http://www.tonnesoftware.com/appnotes/demodulator/diodedemod.html

Diode based detectors will happily 'detect' at very low signal levels, however the (inevitable) audio distortion that results, can be extremely irritating to the ear! Under these conditions I find infinite impedance detectors (even without additional RF preamplification and subject to individual FET characteristics), generally sound 'cleaner' and more pleasant to the ear.

FET's of course require a power source for operation whereas diodes are passive (un-powered) detectors (most of the time), however this is of no real advantage in a tuner application as an 'active' audio amplifier stage will generally be required anyway for audio level boosting, buffering etc.

In the end it will come down to a consideration of prevailing RF signal levels and other related circuit considerations at one's location. If local RF levels are strong, a well designed diode detector will give excellent results. If not, an 'infinite impedance' type of detector is most likely the better option unless one goes towards the option of additional RF preamplification prior to the diode detector.

73 Felix
vk4fuq.

17th April 2012.

ANOTHER DETECTOR by Felix Scerri !

I've tried diode based 'voltage doubler' (or more correctly 'diode integrator') AM detectors before with indifferent results, however the other day, just trying a few ideas I came up with this version that works rather well, with low audio distortion, high audio output and really 'nice' audio quality and the best of all, it seems to work very at very low RF input level.

The two diode 'voltage doubler' detector using two BAT 46 silicon schottky diodes feed directly into a MPF102 source follower stage set at 1 Megohm input resistance. The 'input' capacitor feeding the diodes from a tuned circuit is 68 picofarads.

I have the simple RF filter right on the output of the FET stage. In that respect this circuit is vaguely similar to the old 'Selstead-Smith' valve AM detector of the past. An interesting one! I am very happy with its general performance. Regards, Felix vk4fuq 11/04/2013

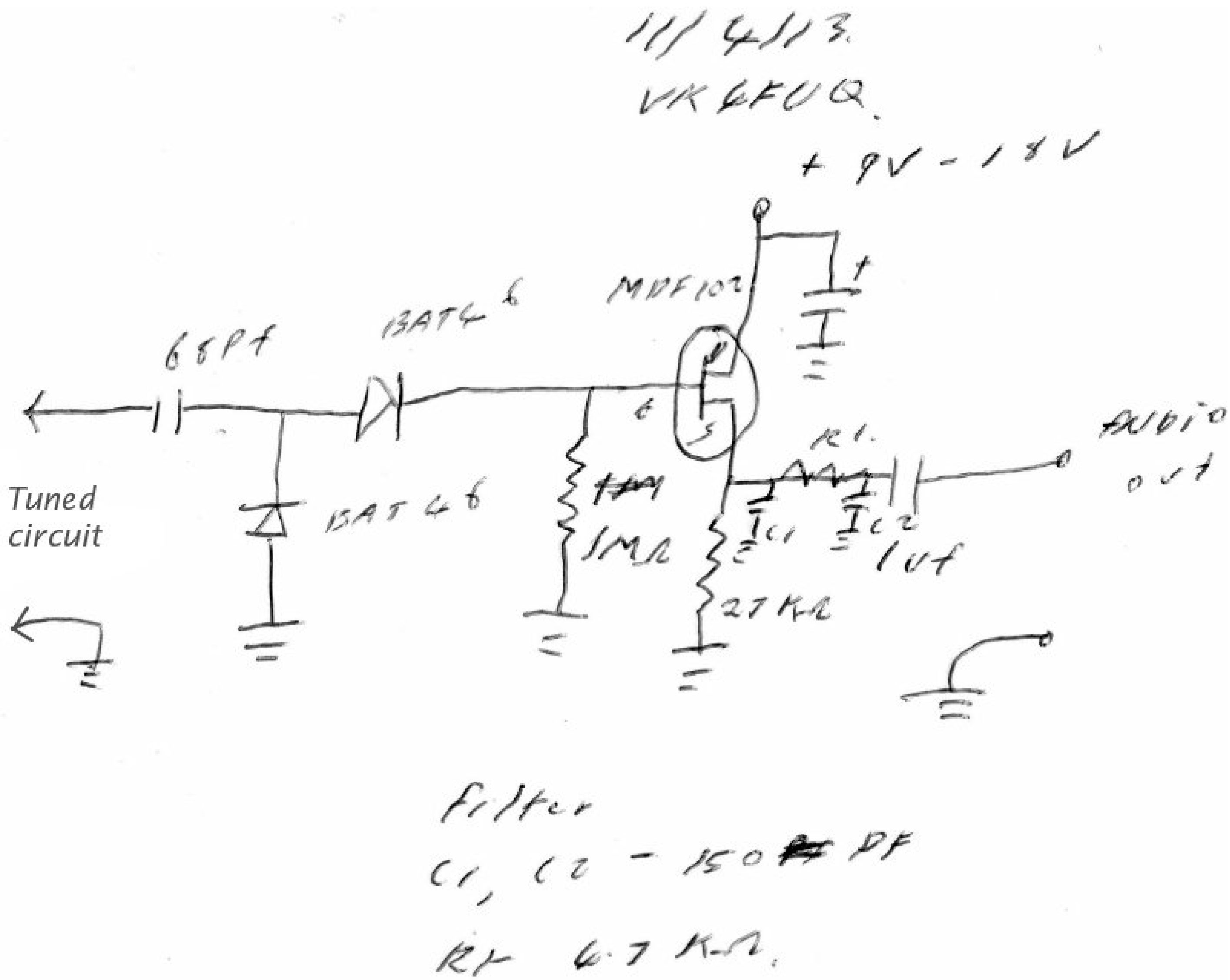

Felix Scerri VK4FUQ

UPDATE - JUNE 2013

G'day all, readers may recall the two FET infinite impedance detector I developed some time ago. That circuit worked well, but some samples of the MPF102 regretfully produced distorted output. However a recent discovery has resulted in an improved version that has truly exemplary performance.

The MPF102 is in all honesty a device essentially designed for VHF applications, but is often used in simple audio applications albeit with occasionally indifferent results, due to general device parameter 'spread'. More or less by empirical trial and error I have found that a simple change in source resistor value to 100 k (from a much lower value), pretty well fixes everything.

In a FET source follower circuit this is interesting as the output impedance is actually a lot lower than 100 k due to the action of the FET's transconductance. It is similar to the action of a bipolar transistor emitter follower circuit. In fact a simple infinite impedance detector with a 100 k source resistor actually works very well and will be good enough for many applications, however the addition of a second FET as a constant current source does markedly reduce overall audio distortion in the stage overall, and produces very clean and low distortion audio quality and also reduces the output impedance considerably (good for tuner applications), so take your pick!

Regards, Felix vk4fuq 02/06/2013.

UPDATE - JANUARY 2014

A simple modification to the basic FET 'infinite impedance' AM detector that dramatically improves performance.

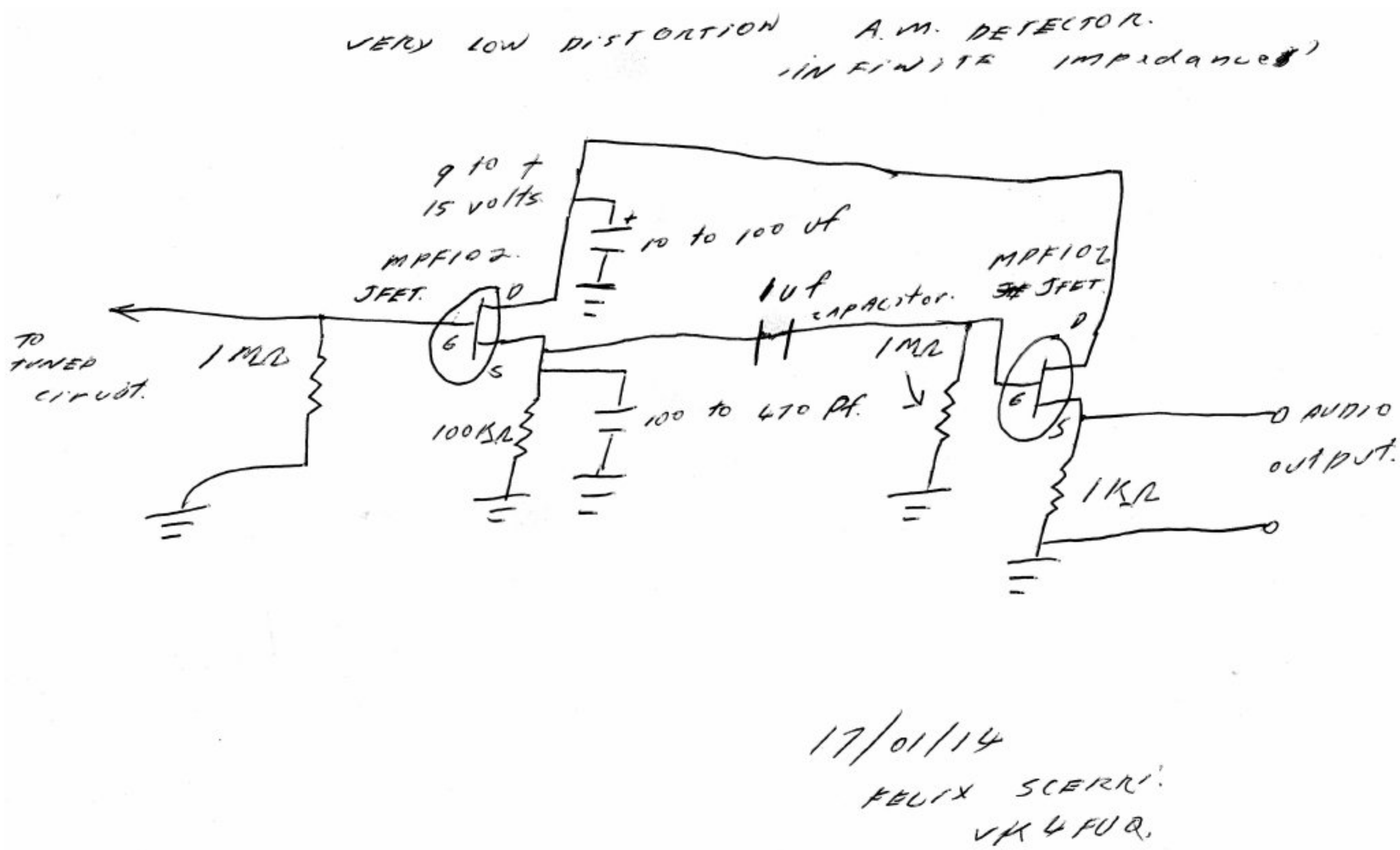

G'day all, over the Christmas break just messing around I worked out (mostly by accident), a simple modification for the simple FET based 'infinite impedance' detector circuit that dramatically improves weak signal performance and also greatly reduces audio distortion.

Essentially by the addition of another FET 'buffer' stage, another source follower, capacitively coupled from the first detector stage. The circuit is actually a simplified version of the circuit that I described in this link, http://sound.westhost.com/articles/am-radio.htm (figure 6) and testing the two head to head, they both sound superb and the simpler version is actually somewhat easier to build. I cannot get over how low distortion and 'nice' the recovered audio sounds. It is a joy to listen to!

Regards, Felix vk4fuq 12/01/2014.

Diodes for ‘weak signal’ crystal set applications.

As I am primarily interested in using crystal sets as AM tuners for feeding into a preamplifier/amplifier and loudspeakers, the actual type of diode can be relatively critical. In a strong signal area, not so much, but in a weak signal area such as where I reside, definitely. A diode with a good ‘square law’ performance (the area below the ‘knee’ in the diode curve), generally results in much cleaner and lower distortion than other good performing diodes, and believe me diode distortion under weak conditions, even with optimised diode ‘buffering’ used is very nasty sounding to the ear!

Testing many, many diodes in actual working crystal sets and listening critically to the audio output, it seems to me that the best diodes to use under weak signal conditions are the so called ‘gold bonded’ germanium diodes. I have sampled many different gold bonded germanium diodes and they all work well in this specific application, although sometimes the rectified output voltage may not be as high as other germanium or silicon schottky diodes, however the audio quality is much cleaner and shows much less apparent distortion!

I have tried OA5, OA47, IN141 and several ‘CG’ gold bonded germanium diodes with consistently excellent results. Other ‘ordinary’ germanium diodes may also work well under weak signal conditions, but they will need to be tested individually to check actual performance in a working circuit. One thing that I have noticed about germanium diodes is that due the ‘point contact’ nature of their construction, even diodes of the same specific type can exhibit rather different levels of performance!

The otherwise very good BAT46 silicon schottky diode works extremely well at good RF input level but not so well at weak RF input, especially when heavy broadcast ‘processing’ (commonplace these days), is used. New ‘gold bonded’ germanium diodes are probably no longer made although I am aware that they can be purchased through vendors over the internet. Apart from that, they may be found in old gear. As stated earlier, ordinary germanium diodes may be quite good but will need to be checked individually. Diodes are complex things!

Felix (vk4fuq). 29/01/2014.

* * * * * * * * * * * * * * *

Just when I thought that I’ve tried everything I realised that I’ve not tried a voltage doubler (diode integrator) detector with an RF stage in front. It is an unfortunate fact that all diode detectors ‘need’ a good RF injection level (and buffering) or audio distortion becomes ‘bad’ (an understatement!)

Consider yourself very lucky if you live in a strong signal area! (unfortunately I don’t). Anyway I quickly built a couple of prototypes which worked ok but not as well as hoped. Initially I tried using a source follower buffer (no voltage gain), but converting it to a common source amplifier (with appreciable voltage gain), seemed no better, which was strange.

After staring at my prototype for what seemed like forever with my magnifiers on, I (finally) realised my mistake. A common source stage takes its output off the ‘drain’ terminal of the FET, not the ‘source’ terminal as it does with the FET source follower buffer stage. I shifted one wire, and all worked as expected and it sounds fantastic! All diode detectors (one diode envelope detectors, doubler detectors etc), need good RF input and a simple untuned FET RF gain stage works very well. As to the sound, it sounds great.

73 vk4fuq 10/03/2014.

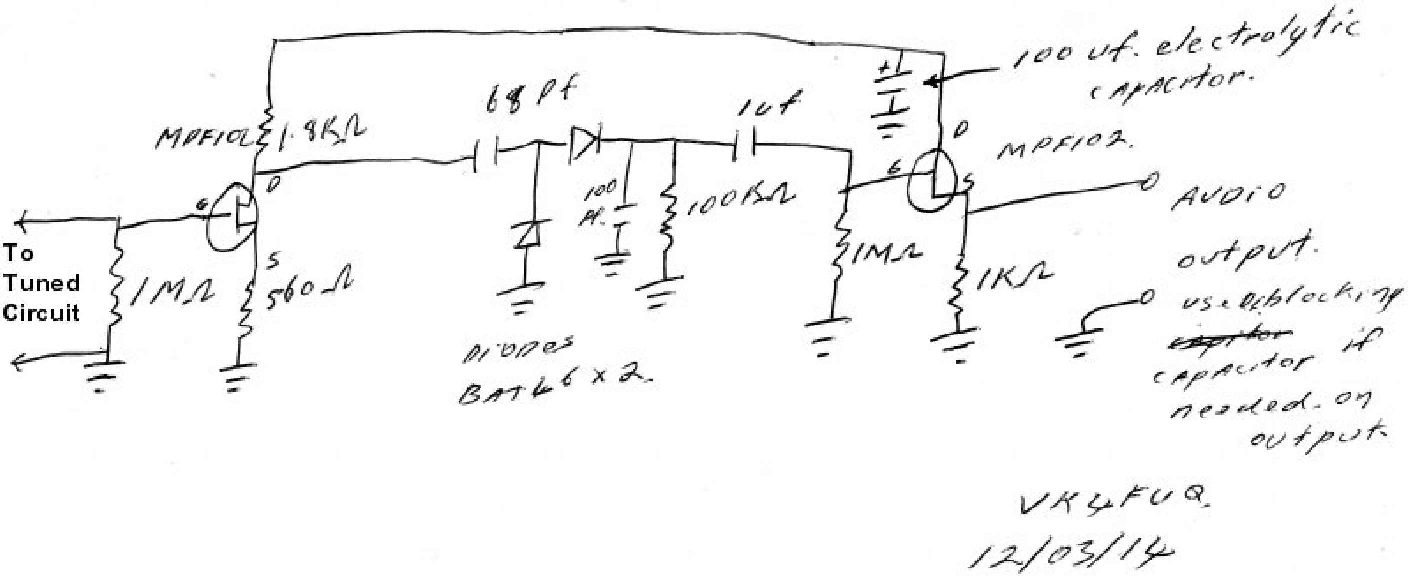

Felix Scerri's FET Crystal Set with Voltage Doubler

A 'nice sounding' AM detector - update October 2015

Looking through these pages the other day I was slightly shocked to realize that I've completely forgotten about some of the circuits that I've contributed in earlier days! They all work pretty well, however in my advancing older age and a little like my tastes in high fidelity generally, I'm starting to show a particular preference for 'nice sounding' bits of audio gear.

I guess that this also means low noise/low distortion too, although with AM broadcasting, at least in this country and probably elsewhere in the world too, the very common use of broadcasting 'processing' tends to make it hard for AM detectors generally, often resulting in a 'hard/compressed' sort of sound although still low in distortion, is not 'nice sounding', if that makes any sense!

Well of all the AM detectors that I've tried and/or developed, only one sounds 'nice' when confronted by heavy broadcast processing and that is an AM detector 'based' on a voltage doubler/diode integrator circuit (similar to the above circuit, actually the 68 pf capacitor should be changed to .1 uf, for slightly greater output).

It has taken me a very long time (years) to 'optimise' this circuit, but as it presently stands this is my favourite 'nice sounding' AM detector, and gets most use for general high quality listening on the AM broadcast band. It sounds really good! It somewhat reminds me of an old OA47 gold bonded diode detector from years ago before such abhorrent 'processing' became commonplace!

Ah yes the OA47….now that is a lovely sounding detector diode!

Regards, Felix vk4fuq. 17 / 10 / 2015.

* * * * * * * * * * * * * *

That's it for crystal sets. I hope you try building one, it's easy and great fun!

See some useful links below....

73's
Mike

Crystal Sets (Part1) | **Build Your Own Crystal Set (Part 2)**

Spider's Web Crystal Set (Part 3) | **Crystal Set By Kenneth Rankin (Part 4)** | **Crystal Radio Links**

Visit my Amateur Radio Pages >

No AM radio stations or transmitters in your locality or country?

Has your local medium wave broadcast station closed or been moved to VHF/FM or Digital? Don't worry. You can still build and experiment with crystal sets and TRF radios by also buying or even building a simple low power AM transmitter. So, not only can you use your crystal sets but you can also run your own radio station that can be heard in and around your home - playing the music or programmes that you want to hear!

SSTRAN AMT3000 Superb high fidelity medium wave AM transmitter kits from SSTRAN. Versions available for 10kHz spacing in the Americas (AMT3000 or AMT3000-SM) and 9kHz spacing in Europe and other areas (AMT3000-9 and AMT3000-9SM). Superb audio quality and a great and well designed little kit to build: http://www.sstran.com/pages/products.html

http://www.sstran.com/

Other AM transmitters available:

Spitfire & Metzo Complete, high quality ready built medium wave AM Transmitters from Vintage Components: http://www.vcomp.co.uk/index.htm Vintage Components offer a choice of the high quality Spitfire and Metzo transmitters:

SPITFIRE AM Medium Wave Transmitter with 100 milliwatt RF output power:

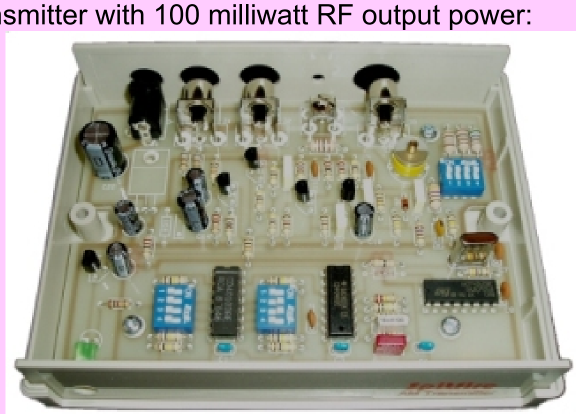

http://www.vcomp.co.uk/spitfire/spitfire.htm

METZO AM Medium Wave Transmitter with built in compressor:

http://www.vcomp.co.uk/metzo/metzo.htm

AM88 LP A basic AM transmitter kit from North County Radio.
http://www.northcountryradio.com/Kitpages/am88.htm

LINKS: Fine links to more Crystal Radio websites here

Component Suppliers: Links to electronic component suppliers here

Visit my Amateur Radio Pages >

Crystal Sets (Part1) | Build Your Own Crystal Set (Part 2)

Spider's Web Crystal Set (Part 3) | Crystal Set By Kenneth Rankin (Part 4) | Crystal Radio Links

^Top Of Page

Home | Contact | Site Map | Radio Stations & Memorabilia | Amateur Radio

Crystal Sets Introduction | Resistor & Capacitor Conversion Tables

CRYSTAL SETS 2
Some Practical Designs
MAKE YOUR OWN
CRYSTAL SET !!

Home | Contact | Site Map | Radio Stations & Memorabilia | Amateur Radio

Crystal Sets Introduction | Resistor & Capacitor Conversion Tables

Crystal Sets (Part1) | Spider's Web Crystal Set (Part 3

Crystal Set by Kenneth Rankin (Part 4) | Experimental Crystal Sets (Part 5) | Crystal Radio Links

CRYSTAL SETS 2: SOME PRACTICAL DESIGNS

I hope that you attempt building one or two of these crystal set designs and I really do recommend that the components are carefully connected up using soldered joints onto a piece of tag-strip for reliability. However if you are new to constructing such electronic circuits then some simple solder-less techniques could be employed and these are suggested at the bottom of the page. Also see Crystal Sets Part 5 for more ideas on experimenting with crystal sets.

An early and very basic crystal set would have been nothing more than a coil of wire, perhaps 50 -100 turns, wound around a cardboard tube about 3 inches (7cm) in diameter, a detector (or cats whisker) and a pair of special High Impedance headphones (as discussed in part 1).

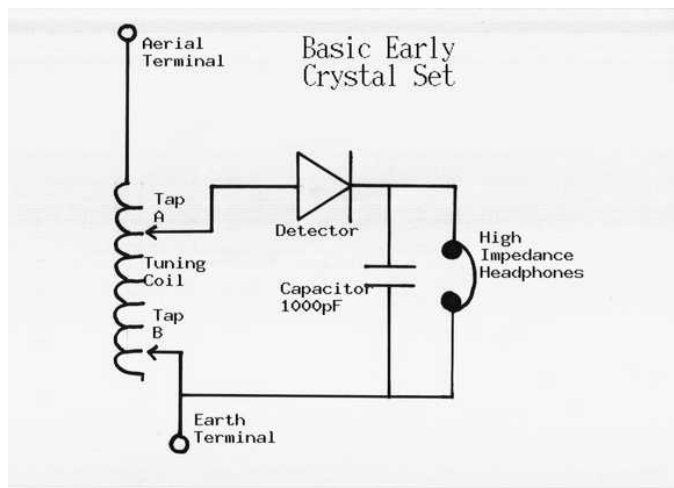

A very basic crystal set circuit.

There would be a very large aerial strung up around the garden and the all important connection to earth.

The coil would have tapping points (connection points) at intervals of around 5 or 10 turns. See the circuit diagram on the right for details of who the set is wired together.

The tapping points on the coil allow the set to be tuned to different frequencies by adjusting the position of tap B. Tap B would be connected to the coil at differently positions by way of a crocodile clip. The fewer turns between the top (aerial end) of the coil and tap B, the shorter the wavelength received (ie the higher the frequency). Tap A would allow the detector to be connected at different positions to vary performance. There is an additional component drawn in the above diagram, the *capacitor* (value 1000pF), this is included in crystal sets that used the *High Impedance* magnetic headphones, and bypassed any remaining radio frequencies (RF) to earth.

I have not built the set described above as it is so basic. Such a crystal set above would probably have been adequate in 1920 - 1923 when there would have been only one local transmitter receivable.

When the BBC expanded transmissions and it became possible to hear more than a single station it would have became necessary to include a more convenient means of tuning the set.

This was achieved by including a Variable Tuning Capacitor, of about 500pF (0.0005uF) connected in parallel with the tuning

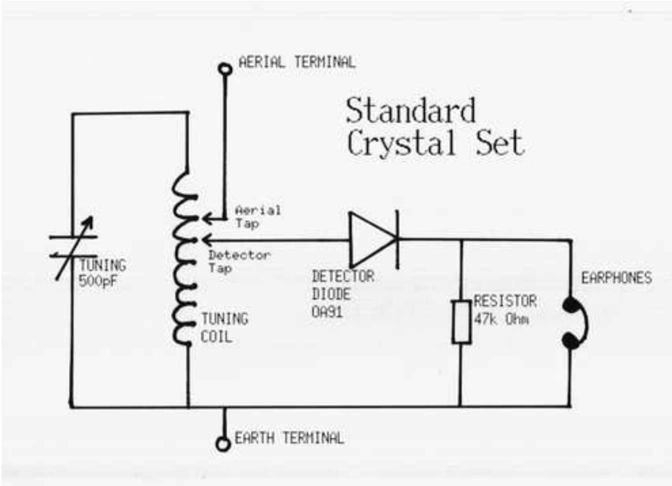

The Standard Crystal Set

coil forming a *tuned circuit*. The tuning capacitor would have a Bakelite knob on the spindle to aid tuning.

Because of the simplicity of crystal sets, it is often difficult to separate stations. When tuned into one station it is often possible to hear another close by station in the background, this is due to lack of *selectivity*. This can be reduced somewhat by adjusting the positions of the Aerial Tap and Detector Tap. Moving them closer to the bottom of the coil, the earthy end, reduces the load on the tuned circuit and this improves selectivity, however it does also reduce *sensitivity* which can make the station quieter. Headphones will often swamp a tuned circuit and reduce its selectivity (Q factor), so moving the tapping point lower down improves this situation. Every circumstance is bound to be different though so the best balance has to be found by experimentation. My crystal set has both the diode and the aerial connected to the same tapping point on the coil, about a quarter of the way down.

The modern 'standard crystal set' shown above uses a Crystal Earphone, since suitable high impedance magnetic headphones (of 2000 to 4000 ohms) are no longer widely available. When using a crystal earpiece the 1000pF capacitor shown in the first diagram can usually be omitted an in its place a 47k ohm resistor is connected, this ensures that the Crystal Earphone will work at its most efficient i.e. the sounds will be as loud as possible. The resistor allows DC current to flow through the circuit efficiently - this would otherwise be blocked when using a crystal earphone. In a modern crystal set the detector used is a *Diode.* Suitable diodes include OA80, OA81, OA90 OA91 and IN94 which are usually available from component stockists.

A Better Diode For Increased Efficiency

The OA47 will be of particular interest since it has the lowest forward bias voltage of any of these diodes which will make the crystal set somewhat more sensitive and therefore louder. The US equivalent of the British OA47 is the IN34.

On the right you will see my real working example of a crystal set

The large plastic knob on the front turns the variable tuning capacitor. This set receives the three UK national stations and also three local radio stations very well at my location.

There is a small 3.5mm jack socket mounted on the front of the plastic case (MB5 from Maplin Electronics) that the crystal earphone plugs into.

The coil can be seen inside the case, it is 70 turns of 30 gauge enamelled copper wire wound around the centre of a toilet roll and tapped every 10 turns, by scraping off the enamel insulation and making a small twist. The croc' clips can be seen clipped on to these twists to connect to the aerial and detector tap points.

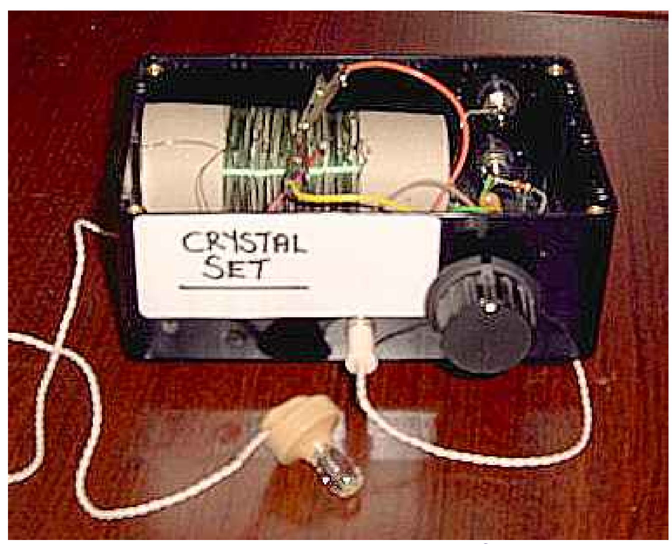

A real working crystal set. Radio as if by magic with no battery or mains power.

THE MEDIUM WAVE COIL - MORE DETAILS

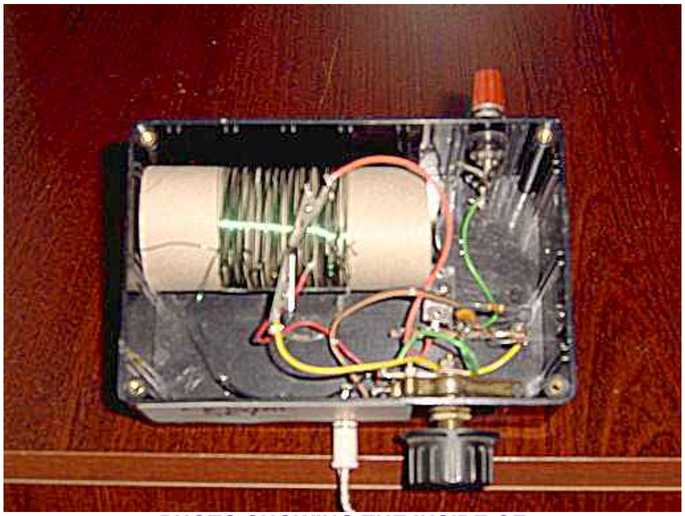

PHOTO SHOWING THE INSIDE OF THE COMPLETED CRYSTAL SET

Medium Wave Coil

The number of turns of wire required on the coil will vary depending on the size of the former (in this case the inside toilet roll) and the thickness of the wire. So to obtain the correct coverage of the medium wave band may need a little experimentation.

I usually find that between 50 to 90 turns is right and I generally use enamelled copper wire that is between 30 s.w.g. and 26 s.w.g (i.e. 0.315mm and 0.45mm diameter), so it's best to start with too many turns and then work down.

The more turns that you use the lower the frequency range will be, i.e. too many and the coverage of the top end of medium wave around 1500 - 1600 kHz will be lost, while too few and the coverage down to 500 kHz will be lost.

It is also important that the coil former is non conducting, i.e. not metallic. It could be wood or cardboard or a short piece of PVC piping and with a diameter of between 1½ and 4 inches (4 to 15 cm) are common sizes. You could try using a ferrite rod too, see below.

This particular set has a coil wound onto a toilet roll tube which consists of 70 turns of 30 s.w.g. (0.315mm dia) enamelled copper wire tapped at every 10 turns. It also has the additional small trimmer capacitor that helps match the aerial to the tuned circuit thereby improving selectivity, see below.

USING A FERRITE ROD AS THE COIL FORMER

The aerial coil could be wound onto a ferrite rod.

A piece of 10mm diameter ferrite rod of between 3 and 6 inches long (80 to 150mm) will be most suitable and will require between 50 and 90 turns of enamelled copper wire to provide coverage of the medium wave band: First make a paper tube that is held together with sticky tape that will easily slide up and down the ferrite rod. Then wind the coil over this with the windings neatly side by side. Make tapping points every 10 or 15 turns so that the aerial and diode tapping points can be adjusted.

Adjustments to the tuning range can be made by removing some wire from the coil so it is best to start off with too many turns and then work down. Fine adjustments can be made to the completed coil by sliding it up and down the ferrite rod.

AN IMPROVEMENT TO THE DESIGN

The crystal set above also has one small, but significant, improvement over the standard crystal set and that is an Aerial Trimmer. A trimmer is a variable capacitor, very similar to the tuning capacitor, except smaller and adjusted with a screwdriver.

The value of the trimmer is usually around 10 - 50pF, but if a small tuning capacitor is available that will probably be just as effective. In the absence of such a variable capacitor, individual fixed ceramic capacitors of e.g. 10pF, 50pF and 100pF can be tried in this position to judge which gives the best results with the particular aerial being used.

The trimmer capacitor adjusts the coupling to the tuned circuit, reducing the load of the aerial on the tuned circuit will improve

the selectivity (Q), and it will be easier to separate stations. Again tapping points are used and I find this to be an excellent arrangement.

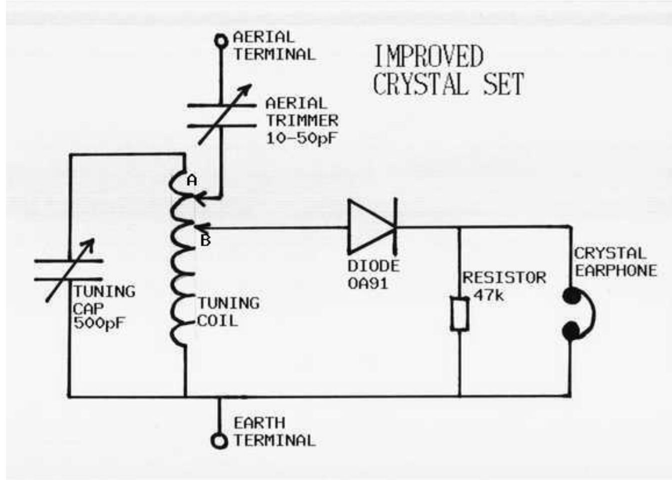

Improved Crystal Set design, with good selectivity

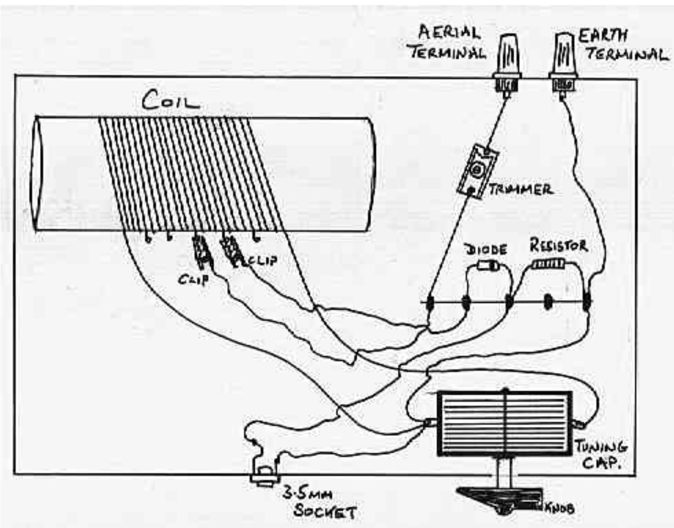

Layout Of The Crystal Set - Although this is soldered together an alternative to tagstrip would be a 5amp mains connector block so that components can be trapped in place with screws. See article below.

The picture on the right shows the general layout of the crystal set above. The coil is of approximately 70 turns is wound on the centre of a toilet roll, and has tapping points at 10 turn intervals.

The trimmer is soldered between the Aerial terminal and the piece of 5-way tag strip, and a wire goes from there to a croc' clip which is clipped onto a tap on the coil. The Diode is also soldered onto the tag strip, one end connected to a piece of wire going to a second croc' clip & connected to a tapping point on the coil, the other end of the diode is connected to the 3.5mm jack socket that the Crystal Earphone plugs into.

The 47k resistor is also connected to the earphone end of the diode and goes to earth, the earth terminal wire is soldered to the tag strip at this point too. The tuning capacitor has two terminals, one connected to each end of the coil, and one of them is also connected to earth as shown. [Where the wires cross over in the diagram, they do not touch and are not connected together].

LONG WAVES

In most areas around Europe and certainly around much of the UK you will be able to hear a Long Wave station. To receive Long Wave on a crystal set will require an aerial coil with a greater number of turns to increase its inductance.

As a good general guide a coil wound on a piece of 10mm diameter ferrite rod will require about 250 turns of enamelled copper wire: First make a paper tube that is held together with sticky tape that will slide up and down the ferrite rod. Then wind the 250 turn coil over this, the windings will have to be made over the top of each other. Make tapping points at, say, 50, 75 and 100 turns to tap the aerial and diode to.

As with the medium wave ferrite rod aerial, adjustments to the tuning range can be made by adding or removing some wire from the coil, and fine adjustments can be made to the completed coil by sliding it up and down the ferrite rod. The longer the ferrite rod the better and anything between 3 and 6 inches long (80 to 150mm) will be very good.

SHORT WAVES

If you like experimenting, then reducing the number of turns on the coil to say 10 to 30 will allow reception of the higher frequencies, the Short Waves. I have found

that winding the coil around a 'ferrite rod' often works even better with short wave reception.

Obtain a ferrite rod about 7 to 15 cm long and about 1cm in diameter. Make a couple of small tubes of card, about 4cm long, that will fit tightly over the rod.

On one tube wind two coils using 0.5mm diameter enamelled copper wire - one coil of about 30 turns and a second one of 2 or 3 turns wound over the top of the first. Secure the windings in place with Sellotape.

On the other card tube wind a similar coil, but use about 15 turns for the first coil and for the second coil wind about 3 to 4 turns over the top, and secure with Sellotape tape.

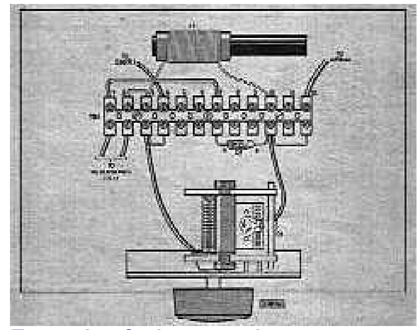

Example of a layout using a connector block to wire up a crystal set

These coils will provide coverage of short wave in two bands using the first coil for the longer wavelengths, typically 60 to 31 metre bands and the second coil for the shorter wavelengths typically 25 to 19 metre band. Wire up the circuit as shown in the circuit diagram below.

USING A TOROID INDUCTOR FOR SHORT WAVES

Even better selectivity performance can be achieved by winding the inductors (coils) on a ferrite toroids (T50-2 yellow, or green will do). The aerial trimmer need not be used if selectivity and sensitivity is found to be adequate. It's all about experimenting, and I find it best to use a trimmer or small coupling capacitor to obtain the best selectivity.

Up to 30 turns of 0.5mm enamelled copper wire can be used for the longer short waves below 10 MHz, while a winding of around 15 turns will provide coverage of the shorter short waves above 10MHz.

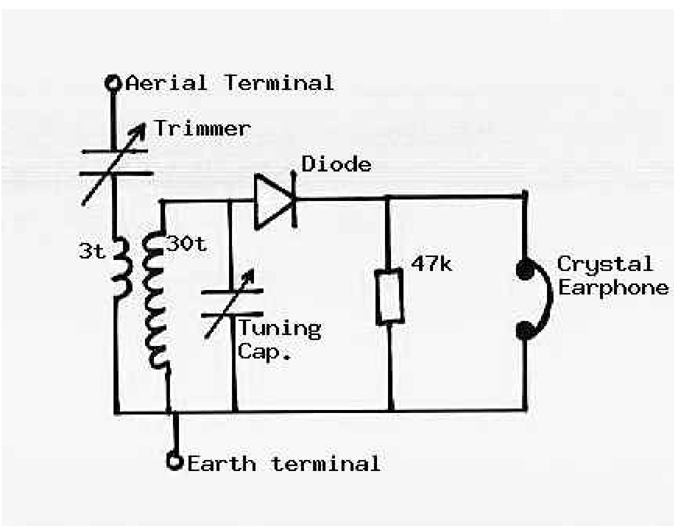

The circuit diagram of the Short Wave Crystal Set

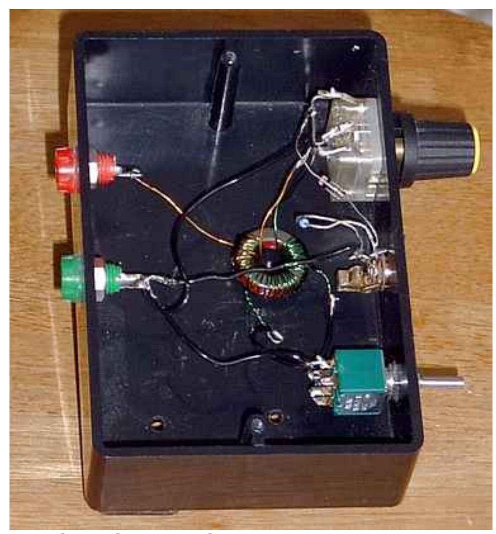

A completed SW Crystal Set using a toroid inductor. Note: the main winding has a tap to allow the switch to short part of the winding and thereby give two ranges.

AUSTRALIAN DESIGN

Moving back to the Medium Waves, here is a circuit for a very interesting Australian design that promises extremely good station separation (selectivity), and having built it I can vouch for that claim, it's really excellent.

I receive three national stations and three local stations at my location with excellent clarity using a modest antenna and standard crystal earphone.

The coil is different to the other crystal sets described above, it is


The front panel of the Australian Crystal Set

much bigger at 3¼ inches (8cm) diameter and 5inches (12cm) long. I made my coil former out of the cardboard from a breakfast cereal box - just like Blue Peter!

The design is often referred to as The Mystery Crystal Set, by Proton.

Two distinct coils are wound on it, the first one consists of about 50 turns of 24 s.w.g (approx) enamelled copper wire. The second coil is 25 turns, very close wound right over the top of the first coil using 30 s.w.g. (approx) wire, try to get this second coil wound in between the windings of the first, for better inductive coupling.

Then carefully wire up the set according to the diagram. Notice that the tuned circuit is not connected to earth and has no *direct* connection to the detector circuit. The detector circuit *is* connected to earth however. The two aerial terminals offer alternative selectivity performance, terminal A gives very good selectivity while B is very wide. I never bother with B.

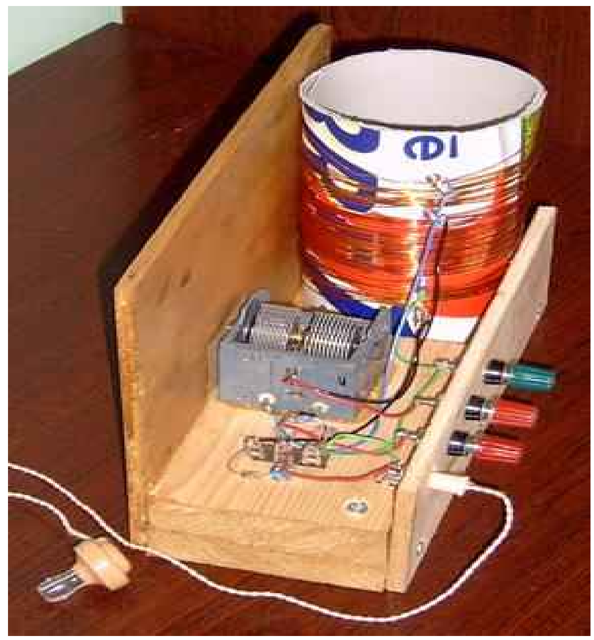

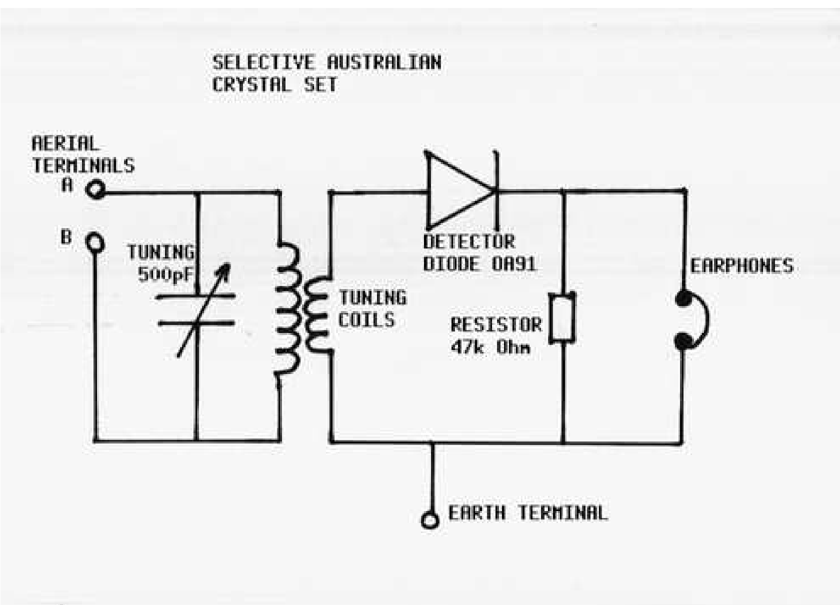

Make the coil carefully and wire up this crystal set according to the circuit diagram opposite and you will be rewarded with a really high performance crystal set of a type that was used in the very early days of broadcasting in 1930's in Australia.

This is probably my favourite crystal set!

THE DENCO PCC1 COIL

The PPC1 coil was a commercially manufactured by Denco Clacton Ltd and was popular among hobbyists not keen on going to the bother of winding their own fiddly little coils. As a child I wanted try one of these coils and sent away for one by mail order. It arrived a few days later in a little cloth bag, like a miniature pump bag, with protective wrapping inside.

The coil windings are entirely enclosed in what I can only describe as a cylindrical ferrite 'shell', the four very thin connecting wires exiting, two either side, from small apertures in the 'shell'. The performance of the circuit shown below I seem to remember was quite pleasing. Unfortunately I cannot find the set or the PPC1 coil at the moment, but here is

a reproduction of the circuit diagram and data:

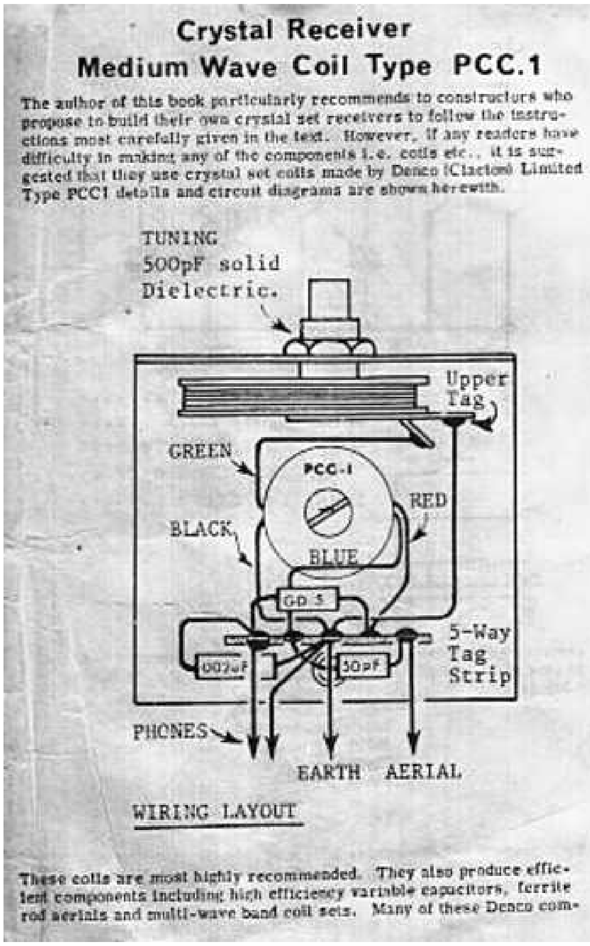

Crystal Receiver
Medium Wave Coil Type PCC.1

The author of this book particularly recommends to constructors who propose to build their own crystal set receivers to follow the instructions most carefully given in the text. However, if any readers have difficulty in making any of the components i.e. coils etc., it is suggested that they use crystal set coils made by Denco (Clacton) Limited Type PCC1 details and circuit diagrams are shown herewith.

These coils are most highly recommended. They also produce efficient components including high efficiency variable capacitors, ferrite rod aerials and multi-wave band coil sets. Many of these Denco com-

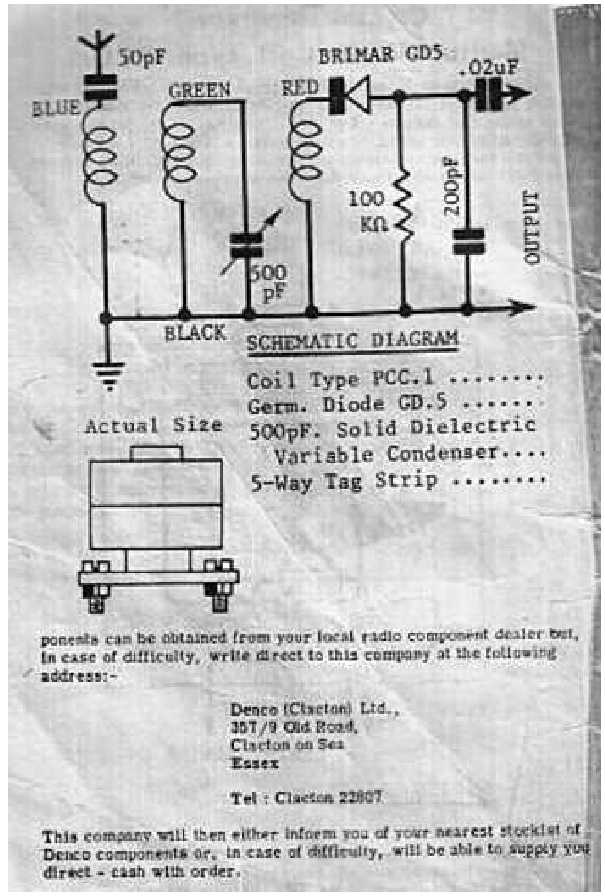

ponents can be obtained from your local radio component dealer but, in case of difficulty, write direct to this company at the following address:-

Denco (Clacton) Ltd.,
357/9 Old Road,
Clacton on Sea
Essex

Tel : Clacton 22807

This company will then either inform you of your nearest stockist of Denco components or, in case of difficulty, will be able to supply you direct - cash with order.

THE REPANCO DRR2 COIL

I recently rediscovered an old Repanco DRR2 Longwave / Mediumwave coil that must have been kicking around in my junk box since the 1970's.

The DRR2 coil was made by Repanco in Coventry. It came with a page of suggested circuit diagrams which I thought had been lost to the mists of time, but it recently came to light again, so I have now copied it below.

Once again I included an aerial trimmer which can be adjusted to improve selectivity.

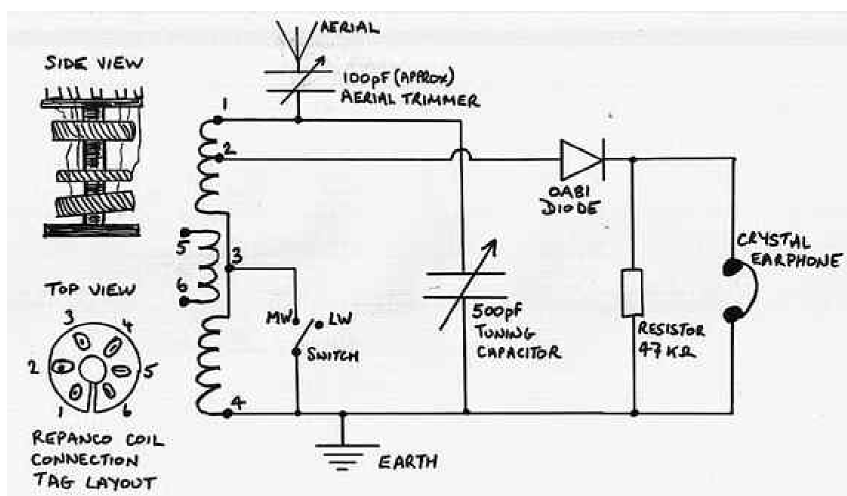

The circuit diagram of the crystal set using the Repanco DRR2 coil

Repanco Ltd was formed by two ex-army signals engineers and from the earliest days of radio supplied crystal set kits and coils to radio construction enthusiasts.

The Repanco DRR2 coil was for medium wave and long wave intended for use in when building simple crystal set and valve radio


A 'lash-up' of the Repanco crystal set

circuits.

It consists of three coils; a Medium Wave coil at the top that includes a tapping point (for the aerial); a coupling coil or tickler in the middle; a lower coil which can be connected in series with to top coil to provide Long Wave reception.

I have built a quick crystal set with the coil and it provides good reception with excellent selectivity, so it must have a very good Q factor.

The Repanco DDR2 coil was provided with a simple Foolscap size information sheet that showed four different radio circuits. Sadly the sheet does not give a huge amount of information and my copy is now rather tatty and faded - it is copied below:

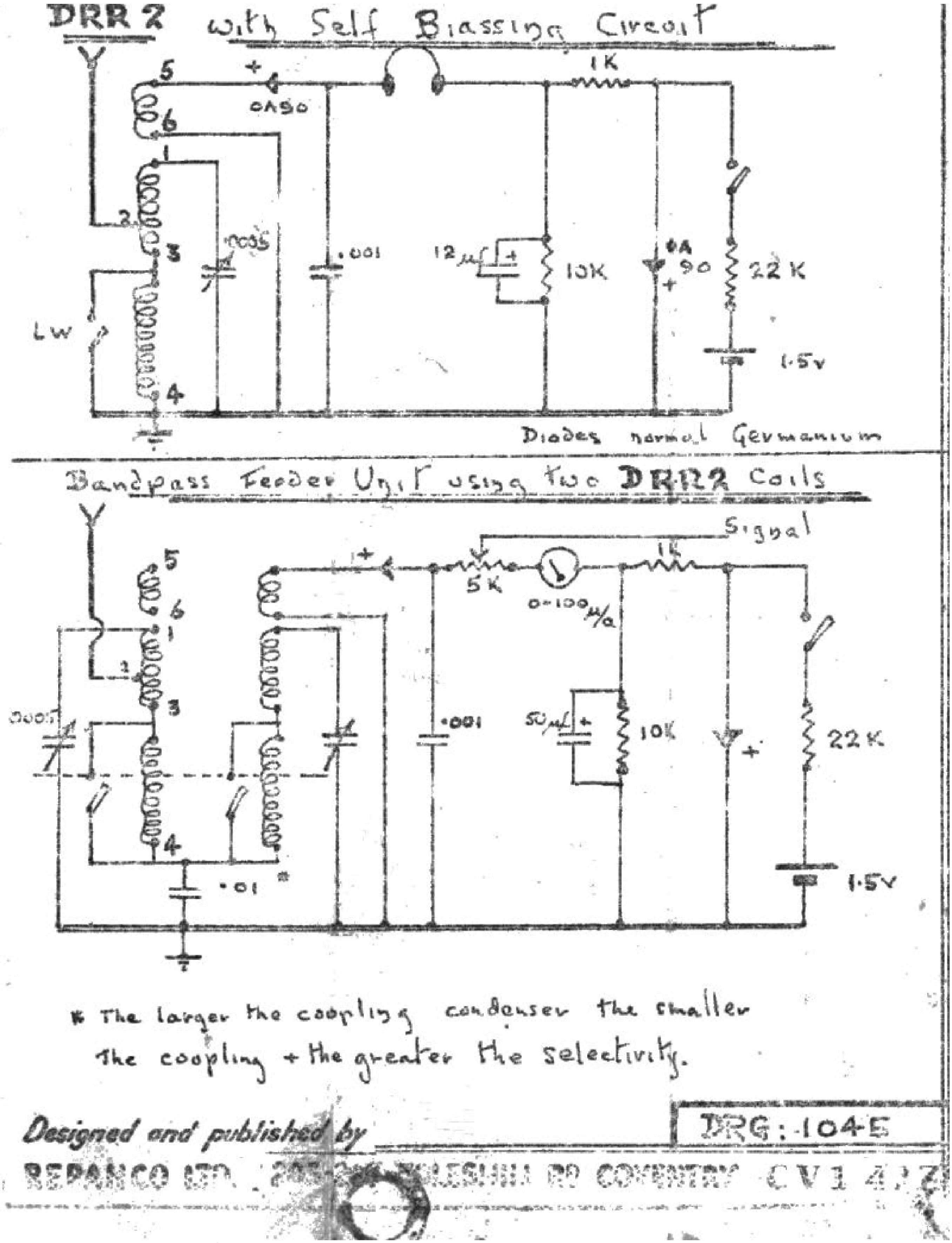

Simple crystal radio type circuits using the Repanco DRR2 coil

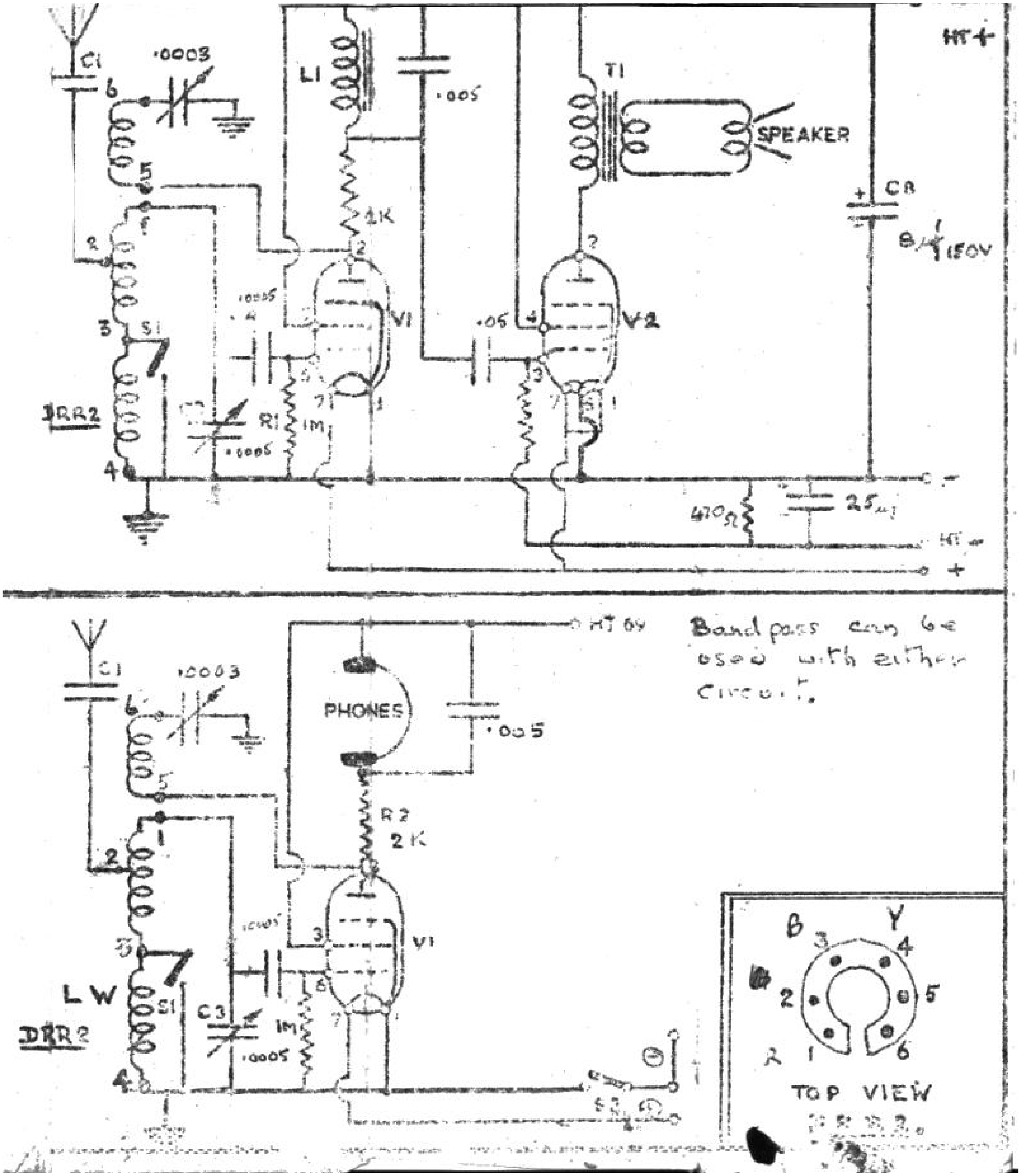

Valve circuits using the Repanco DRR2 coil

Repanco Ltd no longer produces radio coils and crystal set kits for the radio construction enthusiast, as it did in the early days of radio. In 1986 it was renamed Repanco Bartlett Ltd when it merged with Bartlett Electronics. The company moved from the Foleshill Road to Unit 24, Albion Industrial Estate, Endemere Road, Coventry CV6 5NT and now specialises in transformers and wound components and can design and manufacture to commercial customer requirements, their website is: http://www.repancobartlett.co.uk/

CRYSTAL EARPHONES

Here is a good idea and well worth trying, to maximise the use of sound output from your crystal set why not use dual crystal earphones? Having an earphone in each ear helps to block out extraneous noises helping the listener to better concentrate on any weaker stations received.

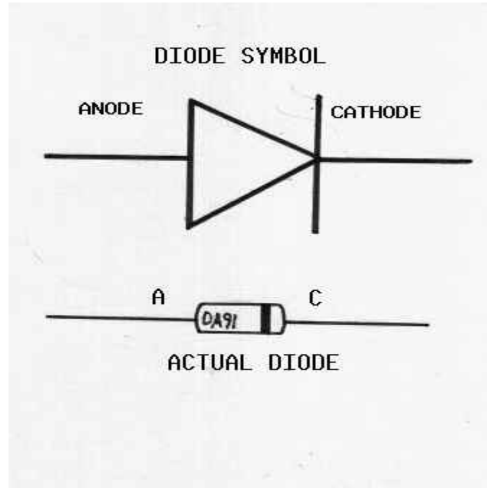

Using the circuit below, one earphone makes use of one half cycle of the radio wave while the second earphone uses the other half cycle of the wave that would have previously gone to waste when using just one diode. Ensure that the diodes are connected up according to the diagram i.e. one diode is connected the opposite way round to the other.

Also try to make sure that the diodes and crystal earphones are similar to obtain the best results. (You could simply connect two crystal earphones to the same terminals of the single diode, but this would not be as efficient and the sounds would be much quieter.)

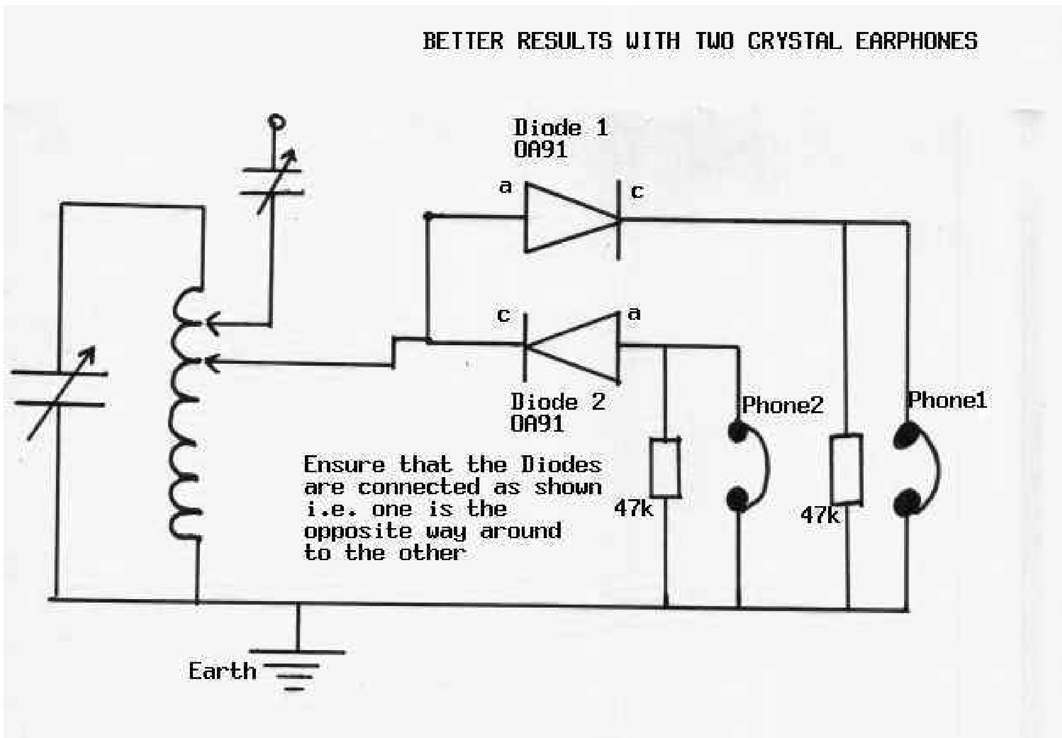

A note about Crystal Earphones: It will be worthwhile buying several different ones from different sources as performance varies between manufacturers quite markedly. I have found the ones marked 'Japan' on the back are the most sensitive and therefore loudest, whereas ones marked 'Receiver' 'Taiwan' are often a little less sensitive and therefore quieter and sometimes more 'tinny' sounding.

As mentioned previously it has been noted that the OA47 diode will be of particular interest since it has the lowest forward bias voltage of any of the common diodes available. This will make the crystal set somewhat more sensitive and therefore louder. The US equivalent of the British OA47 is the IN34.

SPIDERS WEB' COIL

Here is an interesting concept sent in by Chris Dorna of the Vught North Scouts in the Netherlands. It is a crystal set made out of a coil wound in the form of a spiders web:

See more HERE.

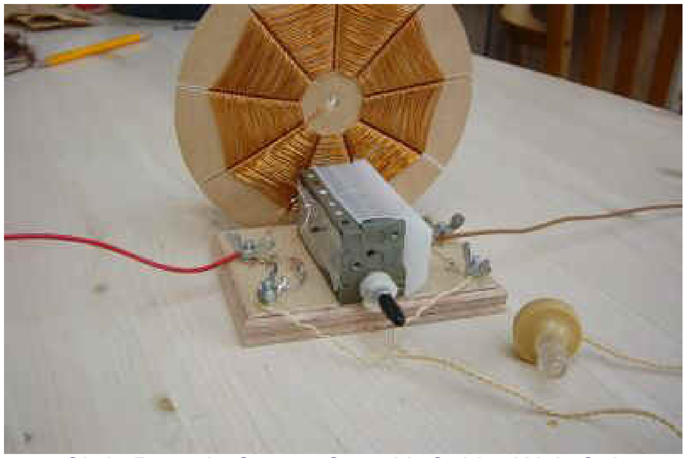

Chris Dorna's Crystal Set with Spider Web Coil

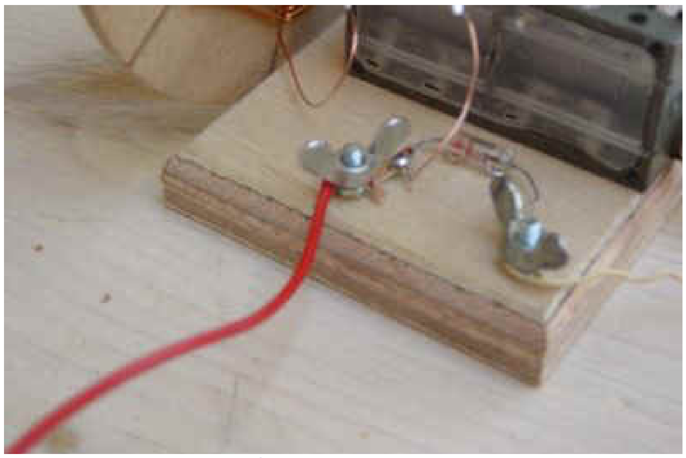

Detail of the germanium diode

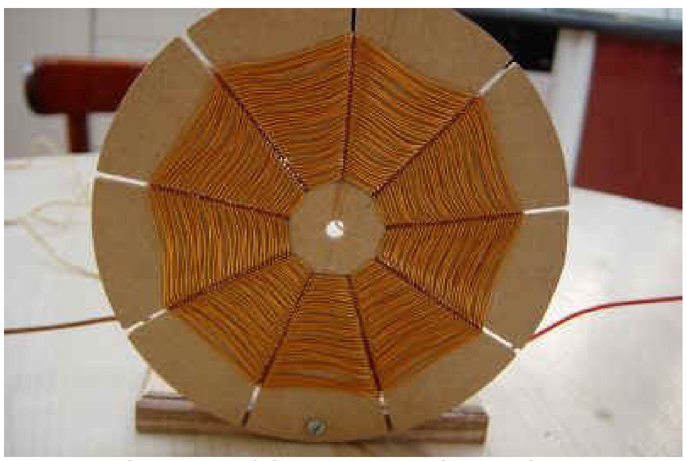

Close up of Chris Dorna's Spider Coil

LOOP THE LOOP!

A crystal set can also be made that does not need a large long wire aerial. If you have ever made a loop aerial for medium wave or long wave DX-ing, then it is a simple matter to add a diode, resistor and a socket to connect a crystal earphone that will allow reception of nearby stations.

See my section on Loop Aerials and ATU's for more constructional details.

A portable loop aerial, that incorporates a crystal set

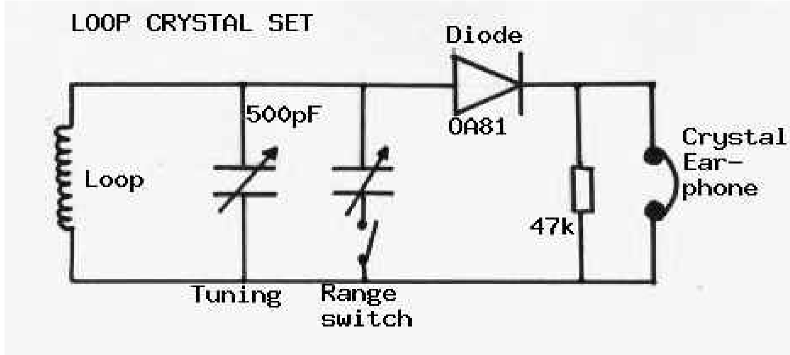

The circuit diagram of the Loop Crystal Set. The loop is 10 turns of 7/0.2mm 'hook-up' wire wound on a 40cm (17") former made of attractive plastic edging strip available from many DIY stores. The loop is very directional in its pick up pattern, which can help eliminate interference from some stations by rotating the loop. The switch and additional capacitor allow tuning of the lower medium wave band from about 650 to 520 kHz. Having a loop with 50 to 60 turns of wire will tune into the Long Wave band.

DIODES - For Crystal Set Use - some notes by Felix Scerri

Germanium diodes for crystal set use.

Although I'm a fan of these new silicon schottky BAT 46 diodes, good germanium diodes still have a lot to offer, especially in terms of 'weak signal' sensitivity. Last night I did an experiment.

I sorted through quite a few of my hundreds of acquired random germanium diodes looking for particularly 'sensitive' ones. I tested this by tuning in a weak AM station and comparing the detected DC output level and also the apparent 'loudness' of the audio signal.

Even amongst germanium diodes of the same type, there was enormous variation all the way from excellent to poor! For very weak signals, germanium diodes 'detect' in the 'square law' region below the diode conduction 'knee', in a rather different part of the curve than with much stronger signals (way beyond the diode knee).

When testing germanium diodes for weak signal sensitivity, the inherent capacitance of the diodes is also a factor, and the 'tuning' may change somewhat and will need to be readjusted with every diode tested!

In the end, out of a large number of germanium diodes tested, I found three or four germanium diodes with excellent weak signal sensitivity and the rest were poor. One other interesting thing, good germanium diodes 'sound' different, rather more 'rounded and smoother' than the schottky's which tend to sound mercilessly clean, almost clinical. I also found almost no variation in weak signal sensitivity with my BAT 46 schottky diodes. Take your pick!

Regards, Felix Scerri VK4FUQ 14/03/2012

SOLDERLESS CONSTRUCTION IDEAS

For a novice the use of a soldering iron may seem a bit daunting at first and while the most reliable results will be obtained with a good soldered joint using a tag strip as shown below, the circuits can still be made without the use of a soldering iron.

5 WAY TAG STRIP

36 WAY TAG STRIP - TWO ROWS

The very simplest circuits could be wired together ,with a little ingenuity, with the component wires being held together in the grip of solderless crocodile clips, whereby the connecting hook-up wire is fixed to the croc' clip by a screw rather than solder.

For more the slightly more complex circuits a plastic Terminal Block (sometimes referred to as a choc' or chocolate block) can be utilised very effectively indeed. These are used in mains wiring and are available in various sizes; 2 Amp, 5 Amp, 15 Amp and 30 Amp. The 5 and 15 Amp Terminal Blocks I have found to be the most suitable. The various component wires can be trapped securely with the screw at each junction point. This method also makes it easy to change the components around when experiment with different circuits. See The EXPERMENTAL CRYSTAL SET for more details in Part 5**.**

'CHOCOLATE' TERMINAL BLOCK

The Ladybird book called 'Making A Transistor Radio' (also shown on the TRF Radio pages) detailed a very novel approach using brass screws with screw-cups to trap the component wires at each junction point:

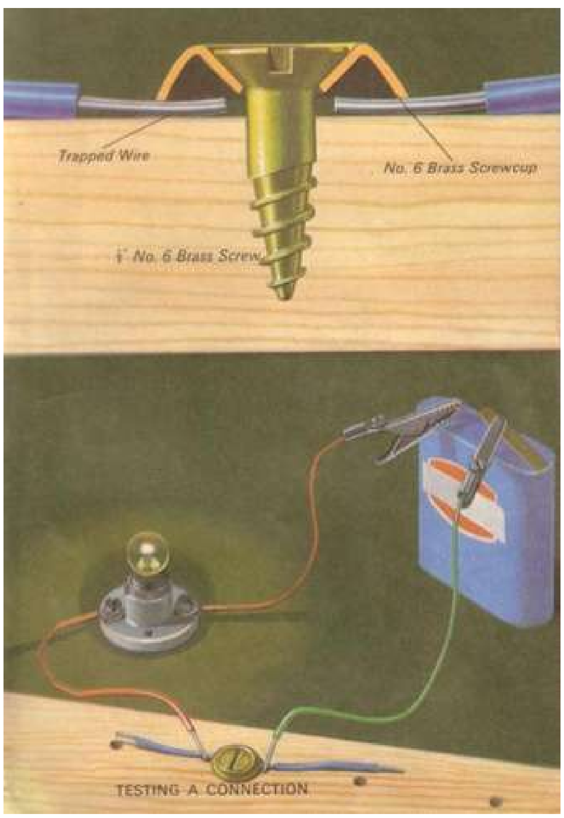

THE BRASS SCREW AND SCREW-CUP METHOD OF CONSTRUCTION

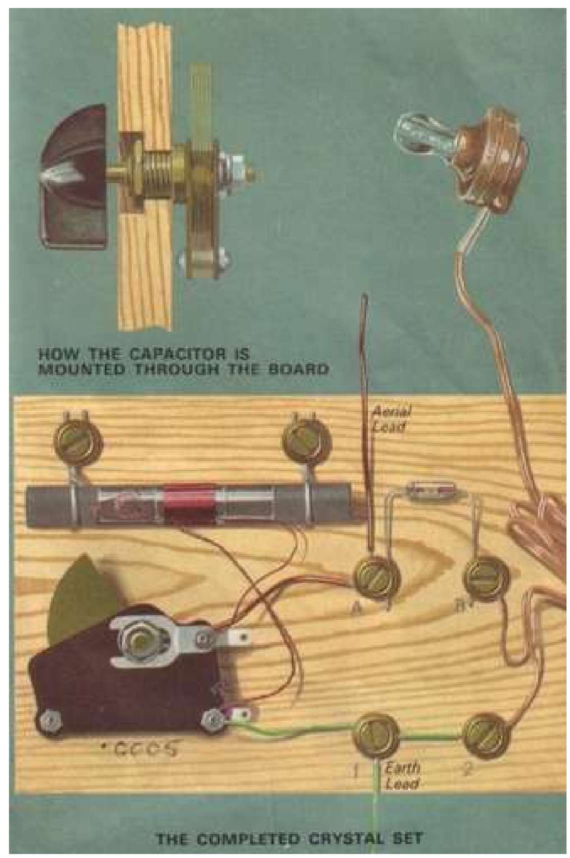

A VERY SIMPLE CRYSTAL SET USING THE BRASS SCREW AND CUP METHOD

Crystal Sets Part Part 3 >

No AM radio stations or transmitters in your locality or country?

Has your local medium wave broadcast station closed or been moved to VHF/FM or Digital? Don't worry. You can still build and experiment with crystal sets and TRF radios by also buying or even building a simple low power AM transmitter. So, not only can you use your crystal sets but you can also run your own radio station that can be heard in and around your home - playing the music or programmes that you want to hear!

SSTRAN AMT3000: Superb high fidelity medium wave AM transmitter kits from SSTRAN. Versions available for 10kHz spacing in the Americas (AMT3000 or AMT3000-SM) and 9kHz spacing in Europe and other areas (AMT3000-9 and AMT3000-9SM). Superb audio quality and a great and well designed little kit to build:
http://www.sstran.com/pages/products.html

http://www.sstran.com/

Other AM transmitters available:

Spitfire & Metzo: Complete, high quality ready built medium wave AM Transmitters from Vintage Components: http://www.vcomp.co.uk/index.htm Vintage Components offer a choice of the high quality Spitfire and Metzo transmitters:

SPITFIRE AM Medium Wave Transmitter with 100 milliwatt RF output power:

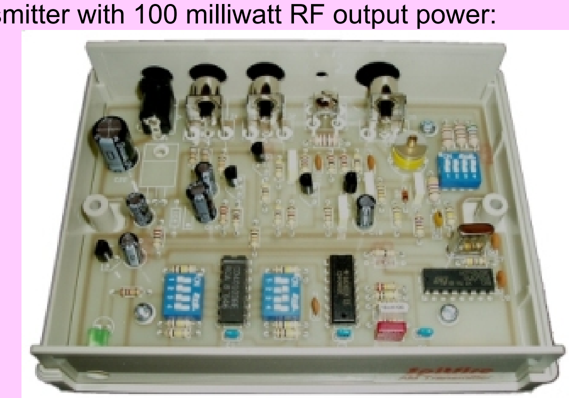

http://www.vcomp.co.uk/spitfire/spitfire.htm

METZO AM Medium Wave Transmitter with built in compressor:

http://www.vcomp.co.uk/metzo/metzo.htm

AM88 LP: A basic AM transmitter kit from North County Radio.
http://www.northcountryradio.com/Kitpages/am88.htm

LINKS:

BOWOOD ELECTRONICS - A friendly, helpful and very speedy source for many of your electronic components at prices that won't frighten your wallet!

THE FOXHOLE and P.O.W RADIOS - Simple crystal set receivers used by soldiers during the war and by prisoners of war (P.O.W.'s).

VINTAGE COMPONENTS - A great resource for crystal sets, components, valve radio kits and medium wave AM transmitters!

6V6 - Electronic Nostalgia and Vintage Components

Crystal Sets Part 3 >

Crystal Sets (Part1) | **Spider's Web Crystal Set (Part 3**

Crystal Set by Kenneth Rankin (Part 4) | **Experimental Crystal Sets (Part 5)** | **Crystal Radio Links**

^Top Of Page

Visit my Amateur Radio Pages >

Home | Contact | Site Map | Radio Stations & Memorabilia | Amateur Radio

Crystal Sets Introduction | Resistor & Capacitor Conversion Tables

Mike's Electronic Parts, LLC
Simple Crystal Radio Kit 2

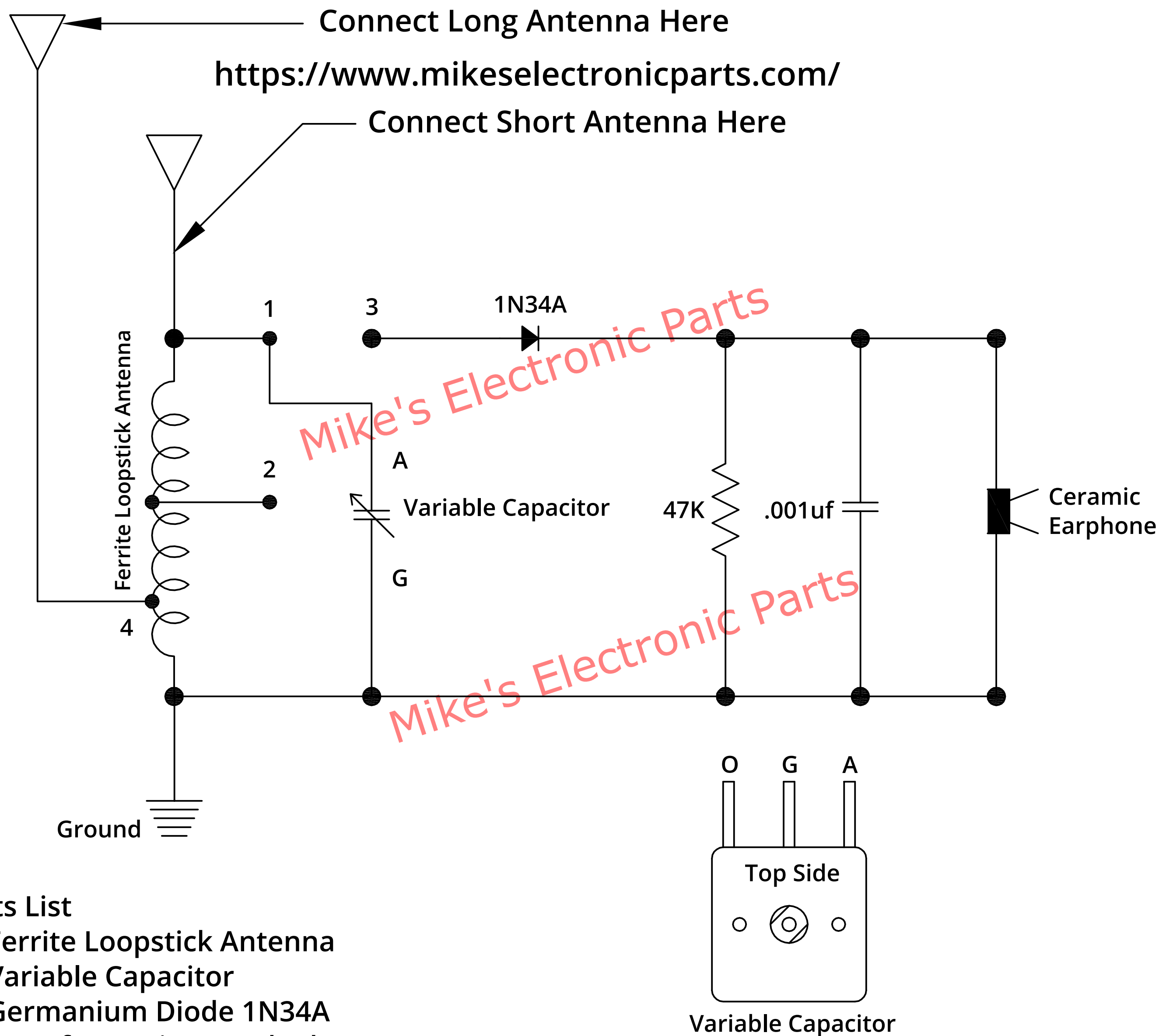

Parts List
1 - Ferrite Loopstick Antenna
1 - Variable Capacitor
1 - Germanium Diode 1N34A
1 - .001uf Capacitor Marked 102
1 - 47K Resistor
1 - 20 Million Ohm Ceramic Earphone
Antenna and Ground wire not include with parts

For short antenna connect a 15ft to 30ft length of wire to "1". For long antenna 40ft to 100ft connect to "4". It is best to use a long wire antenna. If you are not using the taps do not cut the wires. Doing so will cause the coil not to work. Various connections are, Connect 1 to 3 or Connect 2 to 3. Most volume can be had at 1 to 3 less volume but better selectivity connect 2 to 3 and the antenna connected at 1. It is best to solder the coil wire, not doing so may cause a bad connection and the radio will not work.
Drawn By: Scott Lowe
This Kit can be bought at my web site Part Number CRK#2 Kit.

https://www.mikeselectronicparts.com/

THE SMITHSONIAN INSTITUTION

The Smithsonian Institution is home to more than 141 million objects, ranging in size from insects and diamonds to locomotives and spacecraft. It is the world's largest museum complex, comprising 15 museums and galleries and the National Zoo in Washington DC, and two additional museums in New York City. Millions of visitors each year visit the nation's capital to view such treasures as the Hope Diamond, the Star Spangled Banner, and the Wright Flyer. A broad range of exhibits ensures a fun and educational experience for young and old alike.

One of the world's leading scientific research centers, the Institution has facilities in eight states and the Republic of Panama. Research projects in the arts, history and science are carried out by the Smithsonian all over the world. Some of the Smithsonian's research centers include the Smithsonian Astrophysical Observatory in Cambridge, Massachusetts, the Smithsonian Marine Station at Link Port, in Florida, and the Smithsonian Tropical Research Institute, in Panama.

For membership information of pre-visit planning material, write or call the Visitor Information and Associates Reception Center, Smithsonian Institution, Washington, D. C., 20560, (202) 357-2700 (voice), (202) 357-1729 (TTY). You may also visit the Smithsonian through our web site, www.si.edu.

HISTORY

James Smithson (1765 –1829), a British scientist, drew up his will in 1826 naming his nephew, Henry James Hungerford, as beneficiary. Smithson stipulated that, should the nephew die without heirs (as he did in 1835), the estate would go to the United States to found "at Washington, under the name of the Smithsonian Institution, an establishment for the increase and diffusion of knowledge..."

On July 1, 1836, Congress accepted the legacy bequeathed to the nation by James Smithson, and pledged the faith of the United States to the charitable trust. In 1838, following approval of the bequest by the British courts, the United States received Smithson's estate—bags of gold sovereigns—then the equivalent of $515,169. Eight years later, on August 10, 1846, an Act of Congress signed by President James K. Polk, established the Smithsonian Institution in its present form and provided for the administration of the trust, independent of the government itself, by a Board of Regents and Secretary of the Smithsonian.

SMITHSONIAN MUSEUMS, GALLERIES AND ZOOS

Smithsonian Institution [illegible]
Anacostia Museum
Arthur M. Sackler Gallery
Arts and Industries Building
Cooper-Hewitt, National Design Museum
Freer Gallery of Art
Hirshhorn Museum and Sculpture Garden
National Air and Space Museum
National Museum of African Art
National Museum of American History, Behring Center
National Museum of the American Indian
National Museum of Natural History
National Portrait Gallery
National Postal Museum
National Zoological Park
Renwick Gallery
S. Dillon Ripley Center
Smithsonian American Art Museum

SMITHSONIAN®

CRYSTAL RADIO™

WARNING!
ONLY FOR USE BY CHILDREN OVER 8 YEARS OLD.

READ THE INSTRUCTIONS BEFORE USE,
FOLLOW THEM AND
KEEP THEM FOR REFERENCE.
STORE THE SET OUT OF REACH
OF SMALL CHILDREN.

PLEASE KEEP A NOTE OF OUR NAME AND ADDRESS DETAILS FOR FUTURE REFERENCE. IN EUROPE CONTACT:

CE

NSI SIMM GAmbH
D 76162 KARLSRUHE
GERMANY
49-0721-9584-116

PLEASE BE SURE TO READ THE ADVISE FOR SUPERVISING ADULTS AND THE SAFETY RULES CONTAINED IN THIS BOOKLET.

NATURAL SCIENCE INDUSTRIES, LTD.
910 ORLANDO AVE.
WEST HEMPSTEAD, N.Y. 11552

PRINTED IN USA

ITEM NO. 3261-08

ADVICE FOR SUPERVISING ADULTS:

• READ AND FOLLOW THESE SAFETY INSTRUCTIONS, THE SAFETY RULES AND KEEP THEM FOR REFERENCE.

• SUPERVISING ADULTS SHOULD DISCUSS ANY WARNINGS AND SAFETY INFORMATION WITH THE CHILD BEFORE COMMENCING THE ACTIVITIES.

SAFETY RULES:

• DO READ THE INSTRUCTIONS BEFORE USE, FOLLOW THEM AND KEEP THEM FOR REFERENCE.
• DO KEEP YOUNG CHILDREN AND ANIMALS AWAY FROM THE ACTIVITY AREA.
• DO STORE THE SET OUT OF REACH OF YOUNG CHILDREN.

Facts about early crystal development

Several inventors receive credit for developing a "crystal detector", a device which can pass current better in one direction than the other in an electrical circuit. In Germany, in the 1870's, Karl F. Braun noticed this property in certain mineral substances. Commercial development required a technology that would be suitable. This came with the advent of wireless communication and radio after 1900.

In Japan, Wichi Torikata investigated many minerals, including zincite, pyrolusite, iron pyrites and galena. In the United States, Greenleaf W. Pickard, associated with the Wireless Specialty Apparatus Co. of Boston, conducted extensive experiments as well. He became well known for the PERIKON Detector which employed zincite and chalcopyrite. The early 20th century work was generally done between 1900 and 1912. Included among the scientists is General H.H.C. Dunwoody of the U.S.Army who developed a carborundum detector.

Until radio broadcasting began in 1920 (Station KDKA Pittsburgh) experimenters utilized the crystal detector for radiotelephone communications and for reception of certain Morse Code signals. There was also extensive use by the U.S.Navy and other maritime services.

The modern crystal diode, such as provided with your set, is a spin-off of radar technology developed during World War II. The basic principle, however, remains the same..i.e. to remove the AUDIO (speech, music or Morse-Code) from the radio frequency carrier wave. In one early Pickard crystal design (left) a stiff metal point is adjustable over the crystal surface. In a later version a "Catswhisker" spring impinged on a piece of galena (right) and was varied to give a louder signal.

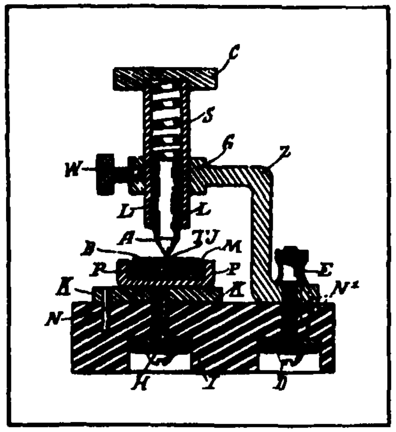

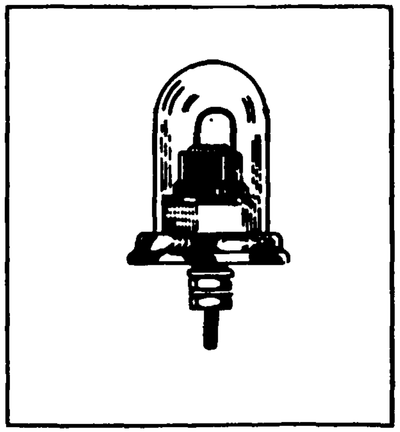

Your Smithsonian Smart Lab Crystal Radio Set contains the following items

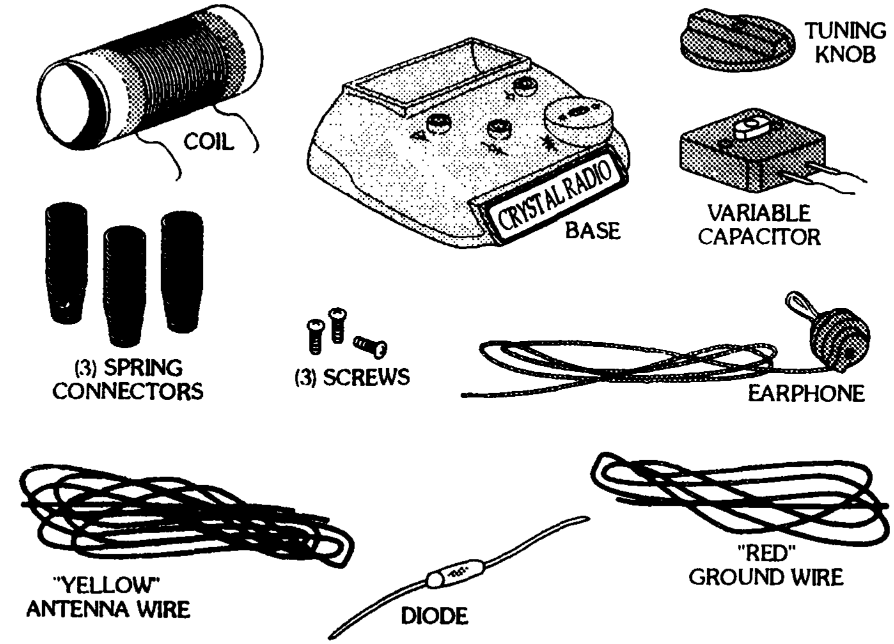

Shown below is a typical wiring diagram of your crystal radio.

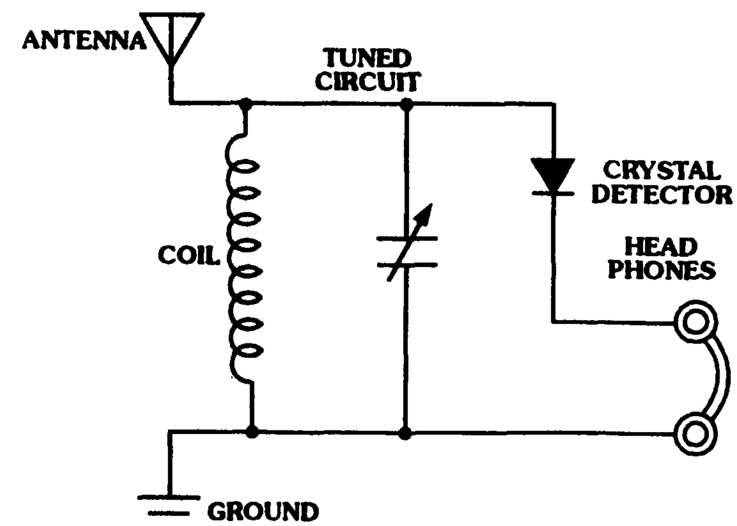

Radio Technology (cont'd)

When these two different energy waves are put together by the mixer stage of the transmitter, the resulting wave, which is the signal that the station broadcasts, looks like this:

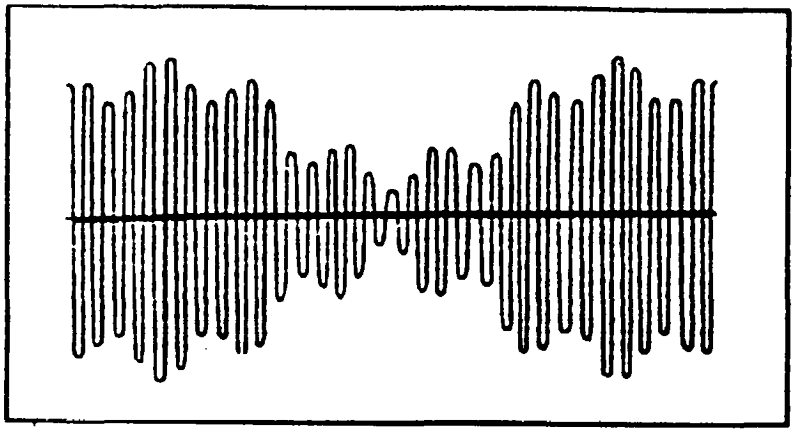

AM Broadcast Wave

The signal is called a MODULATED wave. You will notice that each of the waves is the same length, but the heights vary. Since the height of a wave is called its AMPLITUDE, The type of transmission that WXYZ uses is called AMPLITUDE MODULATION. That's why WXYZ is called an AM station.

The crystal radio that you built works in just the opposite way as the radio station. The modulated signal broadcast by WXYZ is "picked up" by the antenna on your radio.

The antenna is connected to the tuner circuit of the radio, which is made up of a coil of wire and a variable capacitor connected together. As you move the tuning knob, you are able to select, or isolate, the particular

This signal is then DEMODULATED by the diode, separating the voice (audio) wave from the carrier wave.

The voice (audio) wave then moves to the earphone, where it is changed back into sound waves that you can hear.

Learn the basic electronic symbols

Before starting to assemble your Smart Lab Crystal Radio please learn the basic electronic symbols that are shown on the plastic base.

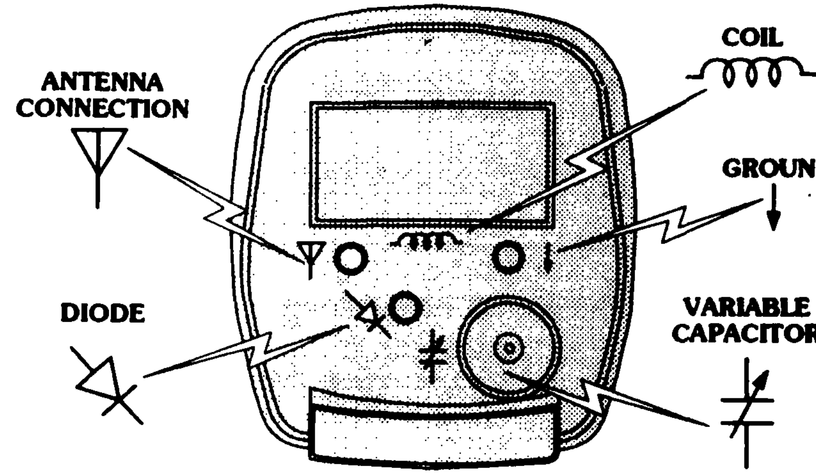

Explanation of components

Variable Capacitor - It is used to tune the radio to a station. The leads that are soldered to the lugs are used to connect it to the circuit.

Diode - A small crystal is sealed inside with leads connected to it. Pay careful attention to the position of the black bands painted on the diode close to one end.

Coil- This is a radio-tuning COIL. It was made by winding enameled copper wire around a paper core 80 times. The leads have been stripped and tinned so it can be connected to the circuit.

Earphone - It contains a small crystal that can make enough electricity to drive a metal diaphragm to produce sound. The leads have been stripped and tinned so it can be connected to the circuit.

Antenna - This is a wire used for radiating or receiving radio waves.

Ground - This is a wire used to make a electric connection with the earth or other type of grounding source to create a common return for an electric circuit.

DEAR CUSTOMER:

If we made an error and left something out of this set, or if something is damaged, we are sorry and wish to correct our error.
Please DO NOT return the set to the store where purchased, as the store does not have replacement parts. Instead, write us:

Please include:

1. Date of Purchase
2. Where purchased
3. Price paid
4. Model Number
5. Name of item
6. Brief Description of Problem
7. Include Sales Slip

We will do our best to satisfy you. Send your letter to:

**NATURAL SCIENCE INDUSTRIES, LTD.
910 ORLANDO AVENUE
WEST HEMPSTEAD, N.Y. 11552-3942**
ATTENTION: QUALITY CONTROL DEPT.

How to assemble your Crystal Radio

Before starting, it's important to assemble the parts correctly. Carefully read the following instructions step by step and have fun . . . half the fun is knowing you made your very own crystal radio.

Step ①

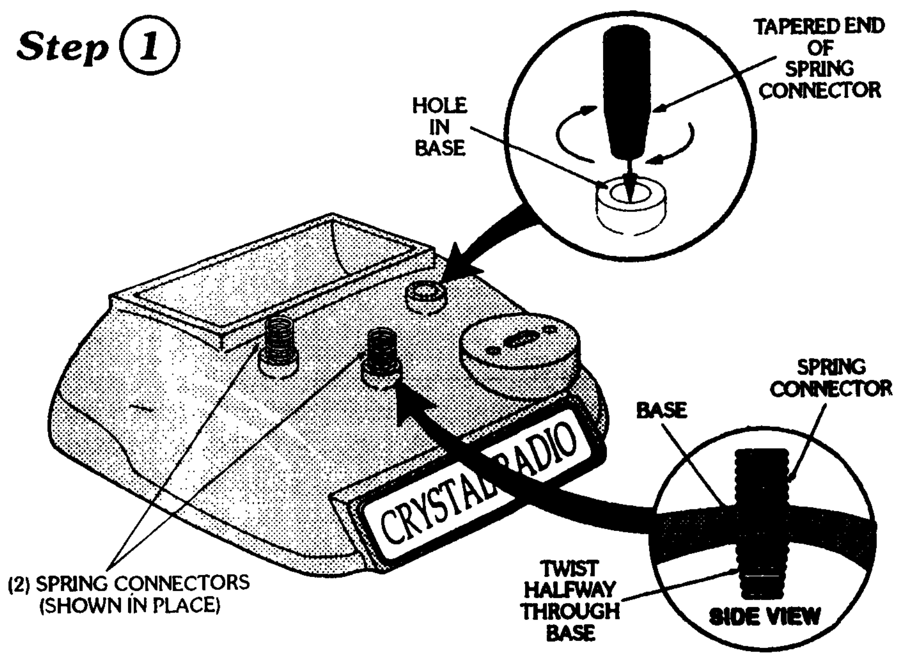

A. Locate the three Spring Connectors.
B. Insert one of the Spring Connectors (tapered end first) into one of the three holes on the Base.
C. Push down on the Spring Connector and twist to the right until the Connector is approximately half way through the base.

NOTE: Check to see if the Spring Connecter is inserted halfway through the Base by turning Base upside down (see insert).
D. Insert the remaining two Spring Connectors into the holes on Base the same way.

Radio Technology

Now that you have your crystal radio assembled and working, it is time to take a brief look at how it works. To do this you are going to take an imaginary trip to a radio station WXYZ, in anytown,USA.

When you arrive at WXYZ, you are met by the station's general manager, Mr. Smith, who is going to show you around.

First, Mr. Smith takes you to a STUDIO, a special room that a program comes from. There is a lot of equipment, including dials and switches, record players, lots and lots of records, and microphones.

Mr. Smith tells you that when you talk into one of the microphones, your words go into the station's electronic equipment. There, it is mixed with the station's carrier wave, and sent out into the air through the station's transmitting antenna - that tall tower you saw on top of the radio station building.

Then Mr. Smith takes a piece of paper and a pencil, and draws diagrams to show you what happens. He begins by saying that all energy travels in waves, and since the sound we make when we talk is a form of energy, it might look something like this:

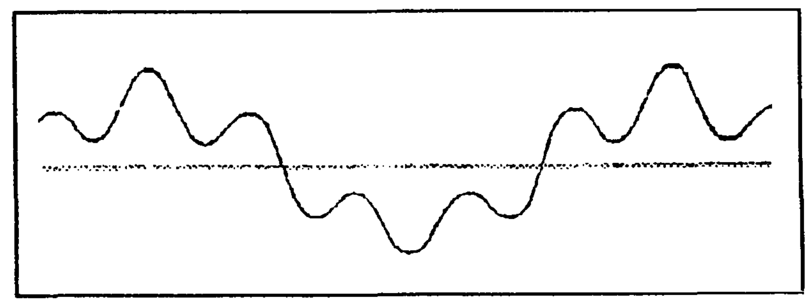

Sound Wave

The station's carrier wave is a radio wave, which is also a form of energy, which looks something like this:

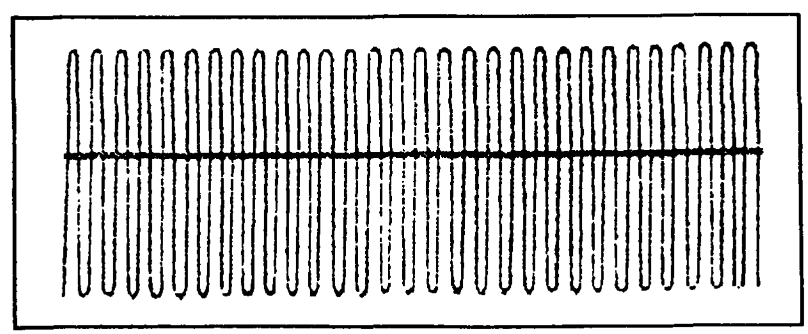

Radio Carrier Wave

How to properly operate your Smart Lab Crystal Radio and troubleshoot

After you have attached all the wires, carefully read the following instructions to make sure your crystal radio operates properly.

A. Place the earphone in your ear and turn the Tuning Knob clockwise and counterclockwise until you pick up the strongest signal.
Note: If you do not pick up a strong signal or do not hear anything, please read some of the troubleshooting solutions explained below.

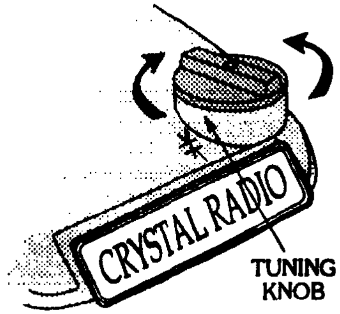

TROUBLESHOOTING HINTS

1. There may be a bad connection caused by improper assembly of your radio. Check all the spring connectors to make sure the wires are attached correctly. If a wire is loose or the bare wire is not making good contact with the spring connector, the radio may not work.

2. If the uninsulated part of the Antenna wire touches anything other than the Antenna Connection on the radio, the radio may work improperly or not at all..

3. If the bare stripped end of the Ground wire is not wrapped tightly around a water pipe (so that it makes good contact), try taping the wire to the shiny part of the pipe using duct tape. If the pipe is dull or rusty, use a piece of sandpaper to gently sand the area where the wire makes contact. Also make sure the wire doesn't touch anything other than the Ground Connection or the radio may not work properly.

4. You may live in an area where radio reception is generally poor. Instead of trying to use your radio during the day, try at night when many radio stations are received better.

5. The Antenna on your radio is a very important component. Make the Antenna as long and high above the ground as possible. If you live in a multi-story dwelling the highest floor should be used when operating the radio. Insulated bell-wire, which is available in hardware stores, makes a very good substitution for your present Antenna.

How to assemble your Crystal Radio (cont'd)

For this step you will need the variable capacitor, (3) screws and turning knob. Be carefull not to misplace the small screws when assembling.

Step 2

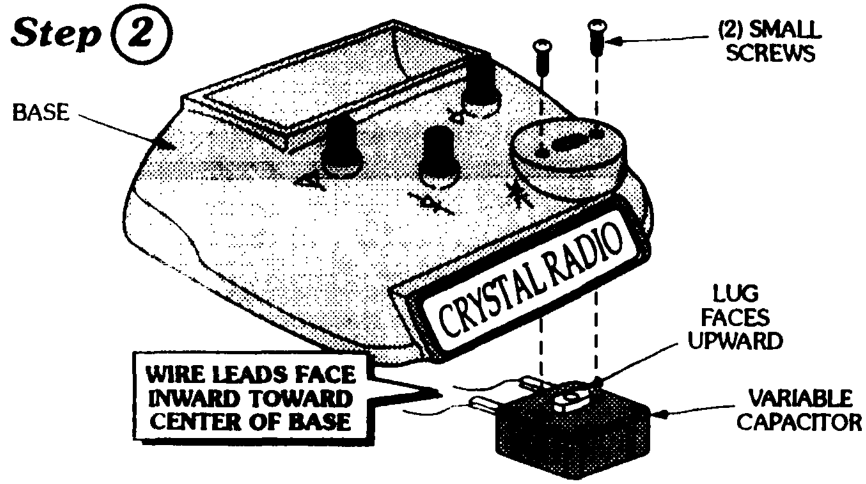

A. First place the Variable Capacitor up into the base so the holes on the capacitor line up with the holes on the base.
Note: When you do this be sure the wire leads face inward toward the base as shown and lug faces upward.

B. Next insert the two small screws into the holes on top of the Base and tighten using a small phillips screwdriver.

Step 3

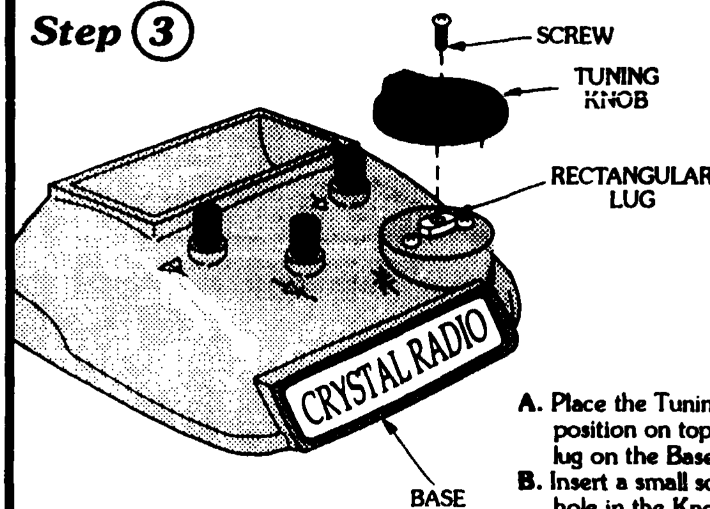

A. Place the Tuning Knob into position on top of the rectangular lug on the Base.
B. Insert a small screw into the hole in the Knob and tighten using a phillips screwdriver.

How to assemble your Crystal Radio (cont'd)

Step 4 **For this step turn the Base upside down.**

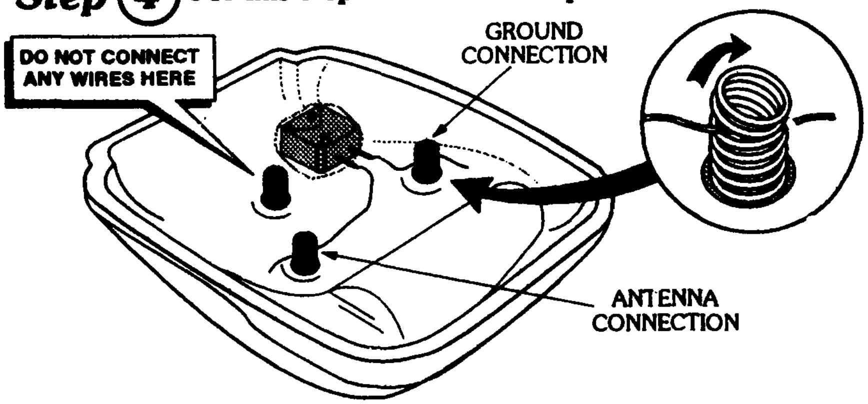

A. Turn the Base upside down.
B. Connect one wire to the Antenna spring connector by bending the spring slightly to one side and inserting the wire through as shown in inset.
C. Connect the other wire to the Ground spring connector in the same manner.
NOTE: Do not connect any of the wires to the Diode spring connector or your crystal set will not work properly.

Step 5

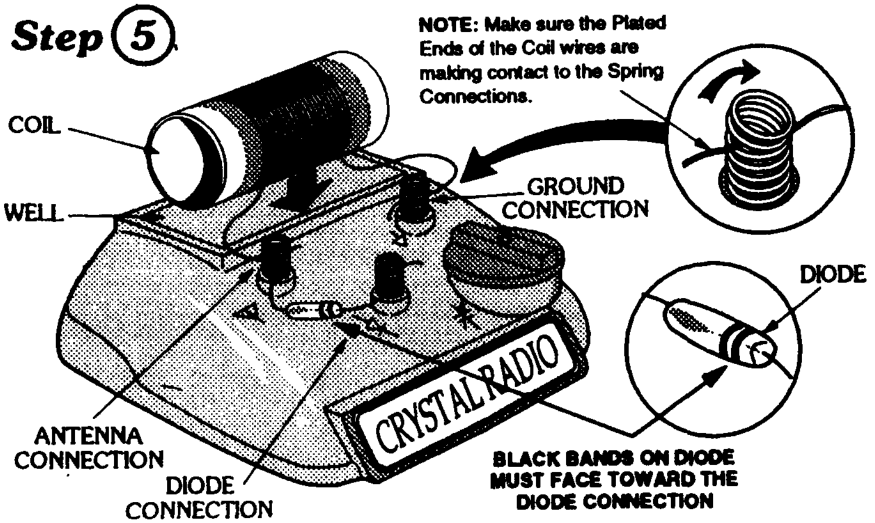

A. Next place the Coil in the well of Base with the wires hanging loosely toward the connectors .
B. Connect one of the plated ends of Coil wires to the Ground Connector by bending the Spring Connector as shown in inset. Connect the other Coil wire to the Antenna Connector.
C. Place the Diode between the Diode and Antenna Connections carefully noting the black bands face toward the Diode Connection.
D. Connect ends of Diode wires to Antenna and Diode spring connectors shown.

How to attach the earphones

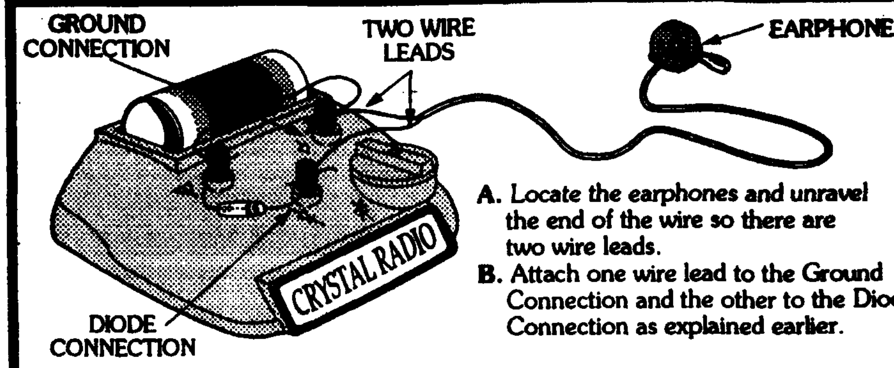

A. Locate the earphones and unravel the end of the wire so there are two wire leads.
B. Attach one wire lead to the Ground Connection and the other to the Diode Connection as explained earlier.

Final assembly and operation

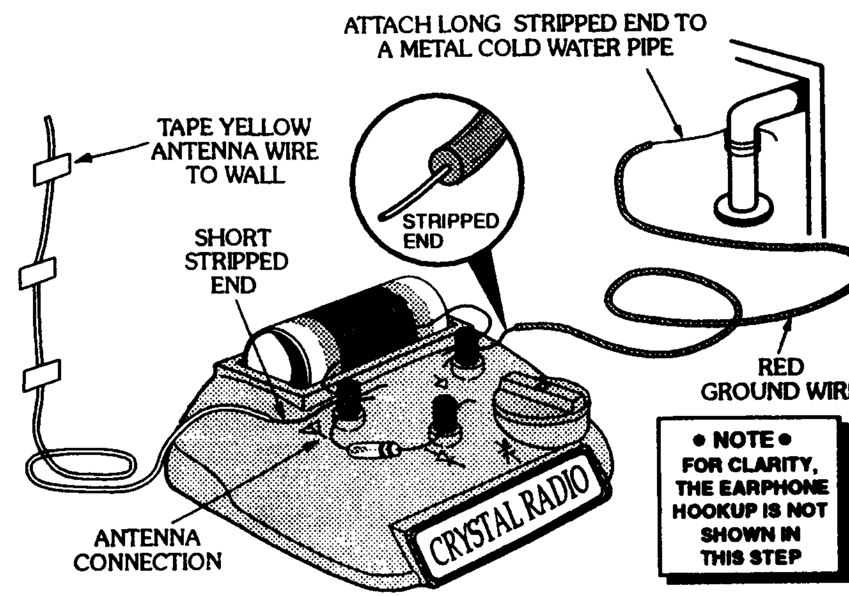

A. Locate the Red Ground and Yellow Antenna wire.
B. Attach the stripped end of Yellow Antenna wire to the Antenna Connection on the Base.
Note: The Antenna should be strung in a straight line away from power lines and large metal objects. We suggest taping it high up on a wall using masking tape as shown.
C. Next attach the short stripped end of the Ground wire to the Ground Connection.
D. Attach the Long stripped end to a metal cold water pipe, metal radiator pipe, etc., near where the radio will be used. Have a adult help you with this since some pipes may be hot.
Note: If there is not enough stripped, bare wire to wrap around a pipe then ask an adult to strip more insulation off the end using a pair of wire strippers.

Germanium vs Silicon Diode Testing: Read this document carefully, so you will not be the victim of cheap knock-off or the wrong type diodes.

The general rule is that ***SILICON*** diodes have a voltage drop across the Anode to Cathode of 0.7 V (7/10 tenths), and the ***GERMANIUM*** diodes have a voltage drop of 0.3 V (3/10 tenths) more or less. Either diode voltage drop (silicon or germanium) will display a reading within approximately 5% of these readings.

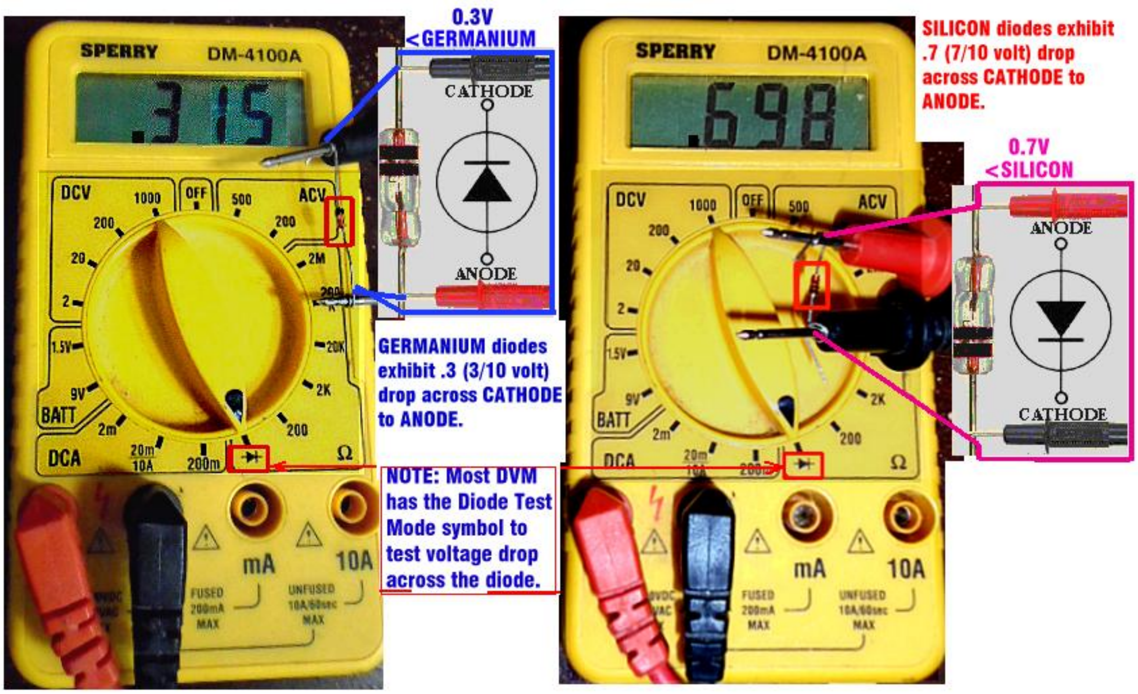

Most digital meters (DVM) have a switch setting 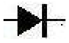 that is used to measure voltage drop across these diodes. This setting is usually indicated by a diode symbol to let the user know the DVM is capable of measuring forward bias voltage. This setting will tell you immediately if the diode is a **germanium**, or **silicon** diode. You need to set the selector switch on your meter to the diode test symbol 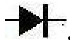.

Measuring Forward Bias Voltage

To measure the forward bias voltage characteristic you connect the black probe of your meter to the cathode terminal. The cathode terminal is on the end with a band. You then connect the red probe to the anode terminal.

Set your DVM/DMM to the *diode test mode* 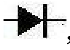, it should provide you with the respective voltage drop. If the figure is 0.3 V or less, the diode is a *germanium* type. If the voltage drop is 0.7 V or less the diode is a *silicon* diode.

Sensitivity and Forward Bias Characteristics:

The sensitivity of a diode to radio waves depends upon its *forward bias voltage*. This is the voltage across the diode terminals. When it falls below this threshold value, the diode will stop conducting. Obviously, the lower this threshold value is, the greater the sensitivity of the diode to the weak radio signals.

CONCLUSIONS:

When comparing germanium diodes with silicon diodes of similar forward bias voltage, silicon diodes do not perform as well as the germanium.

Germanium has many properties that silicon diodes do not have. Germanium requires very little forward current. Forward current in a germanium diode is in the *micro*ampere region, while silicon diodes require *amperes*. This makes *germanium* a much better choice for both medium and high frequency radio signals.

Germanium also exhibits a very low, point-contact junction capacitance, while the silicon diode has much higher capacitance. A low junction capacitance allows germanium diodes to operate more effectively at high RF frequencies.

In addition, reverse leakage current for germanium diodes is in the magnitude of 1000, much more than silicon. This makes the non-linear characteristics of the germanium diode much more effective for RF detection and demodulation than silicon.

Therefore, our conclusions are; germanium diodes provide the best performance in crystal radios, RF probes, HF, and VHF signal detection.

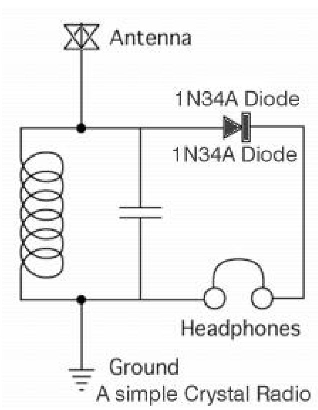

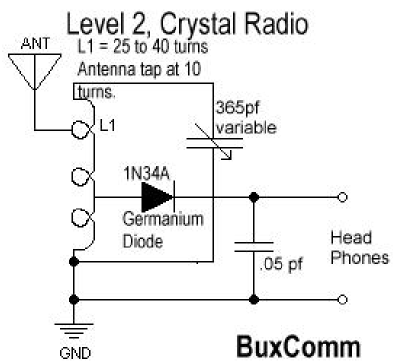

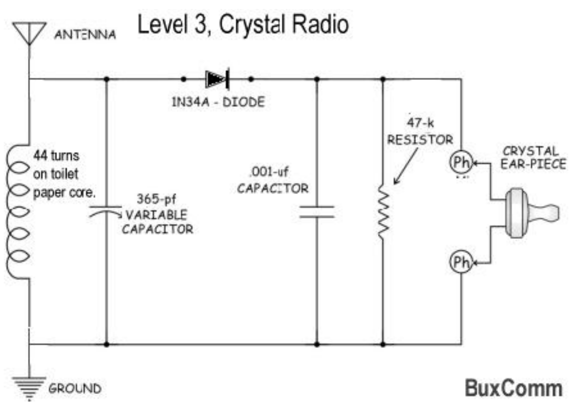

BuxComm High Quality, CRYSTAL RADIO ANTENNA KIT, $14.95 cat# 50CRAK

This Crystal Radio Antenna kit consists of 50 feet of #16 AWG insulated & stranded copper antenna wire, two heavy-duty, Delrin, UV resistant antenna insulators and instruction sheet.

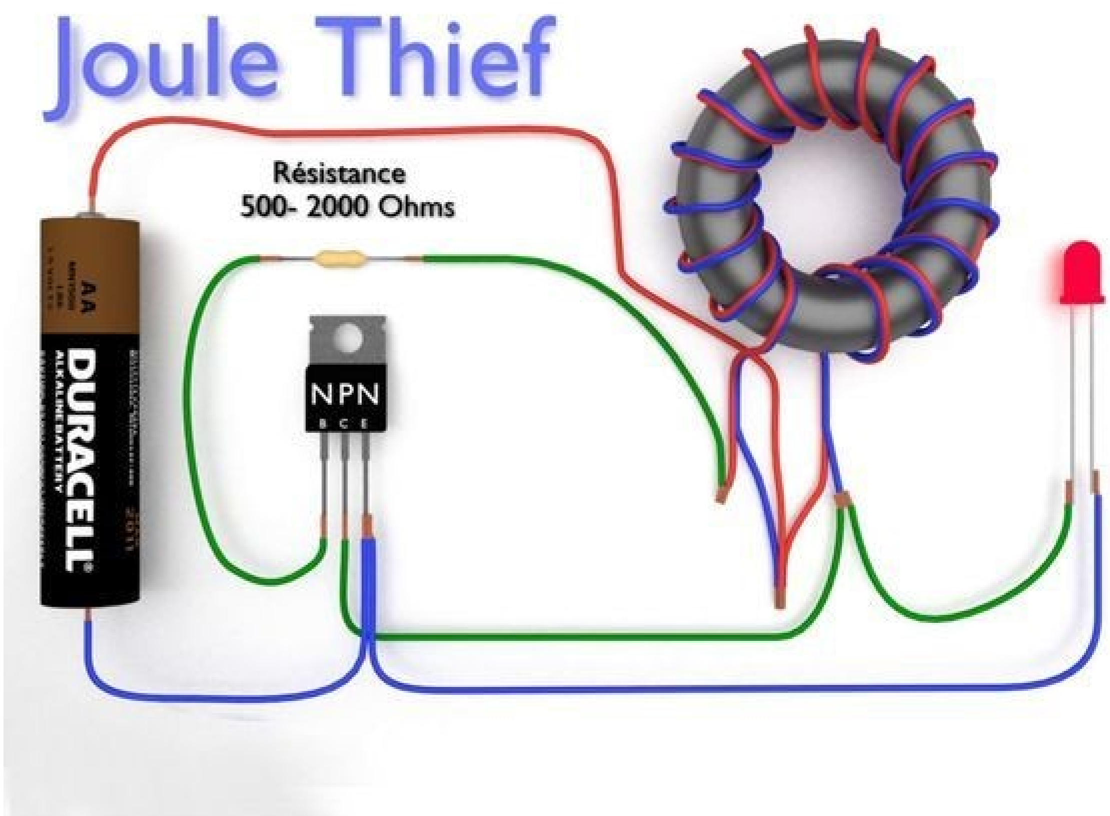

Joule Thief
Résistance
500- 2000 Ohms
AA
DURACELL
ALKALINE BATTERY
NPN
B C E

The joule thief circuit.

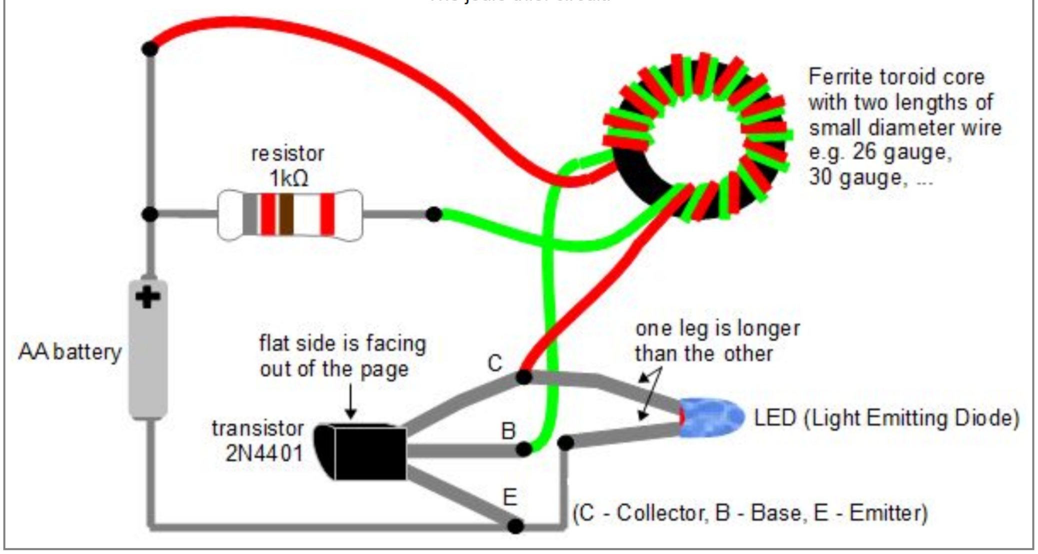

Transistor - The legs of the transistor can be determined by noticing that there's a flat side to the transistor case. See the diagram above. A large number of transistors have been reported to work: 2N4401, NET123AP, BC547B, 2SC2500, BC337, PN2222, to name just a few.

LED - One leg of the LED is longer than the other leg. Use this to determine which one goes where. See the diagram above.

Resistor - The diagram says use a 1 kilo ohm resistor but I've used an 820 ohm one just fine. I've also seen a 2 kilo ohm one in use. Use whatever works for you. You can also use a potentiometer (a variable resistor) so that you can easily adjust it to select the resistance that gives the best light.

Toroid ferrite core - Some people have gotten these by opening up compact fluorescent lightbulbs (CFLs). I took mine out of some device whose original function I don't know. To get it working, my first one had just 13 turns for each wire and I used a 30 gauge wire and a 26 gauge wire. The wire must be insulated. A variety of number of turns will work. This is something you can play with. Look at the diagram carefully to determine where the wires connect to.

Its a Rubbish Challenge
Dog Light
Joule Thief
electronics circuit

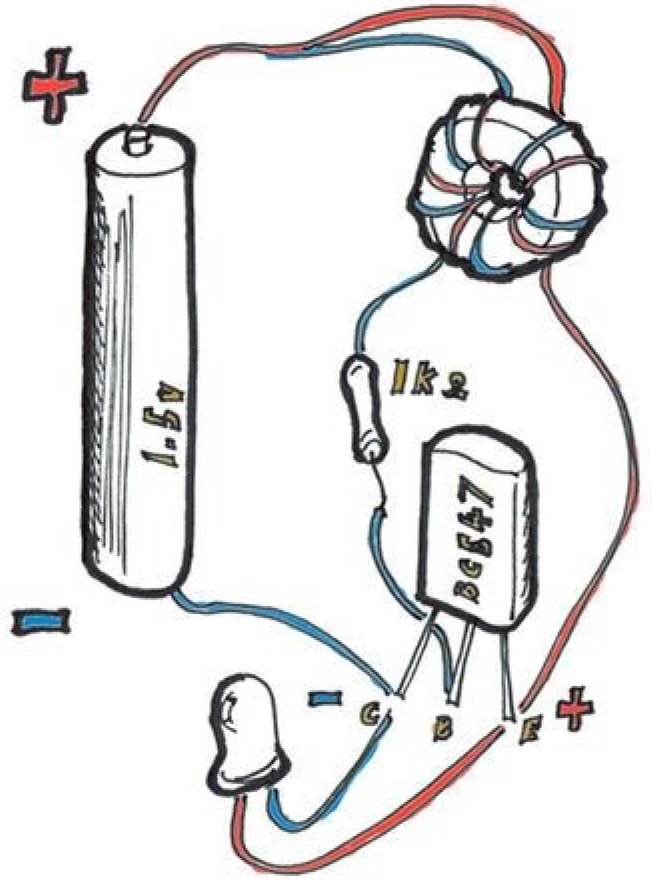

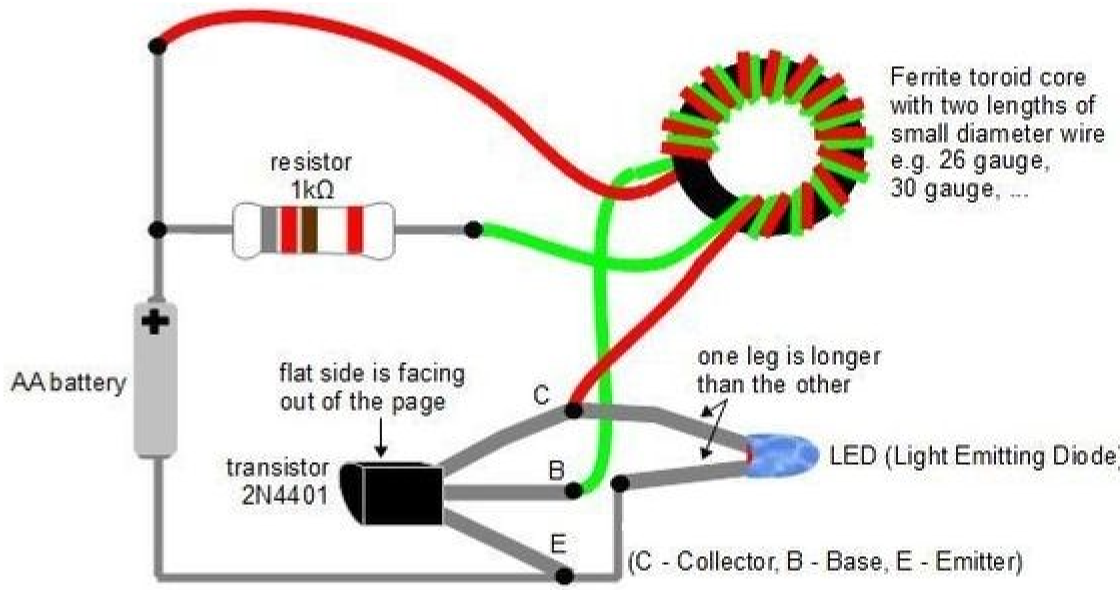
Ferrite toroid core
with two lengths of
small diameter wire
e.g. 26 gauge,
30 gauge, ...
resistor
1kΩ
AA battery
flat side is facing
out of the page
transistor
2N4401
C
B
E
one leg is longer
than the other
LED (Light Emitting Diode)
(C - Collector, B - Base, E - Emitter)

MAKING A SIMPLE JOULE THIEF (MADE EASY)

Technology (/technology/) > Leds | by ASCAS (/member/ASCAS/) Follow

Posted Dec. 24, 2011 |

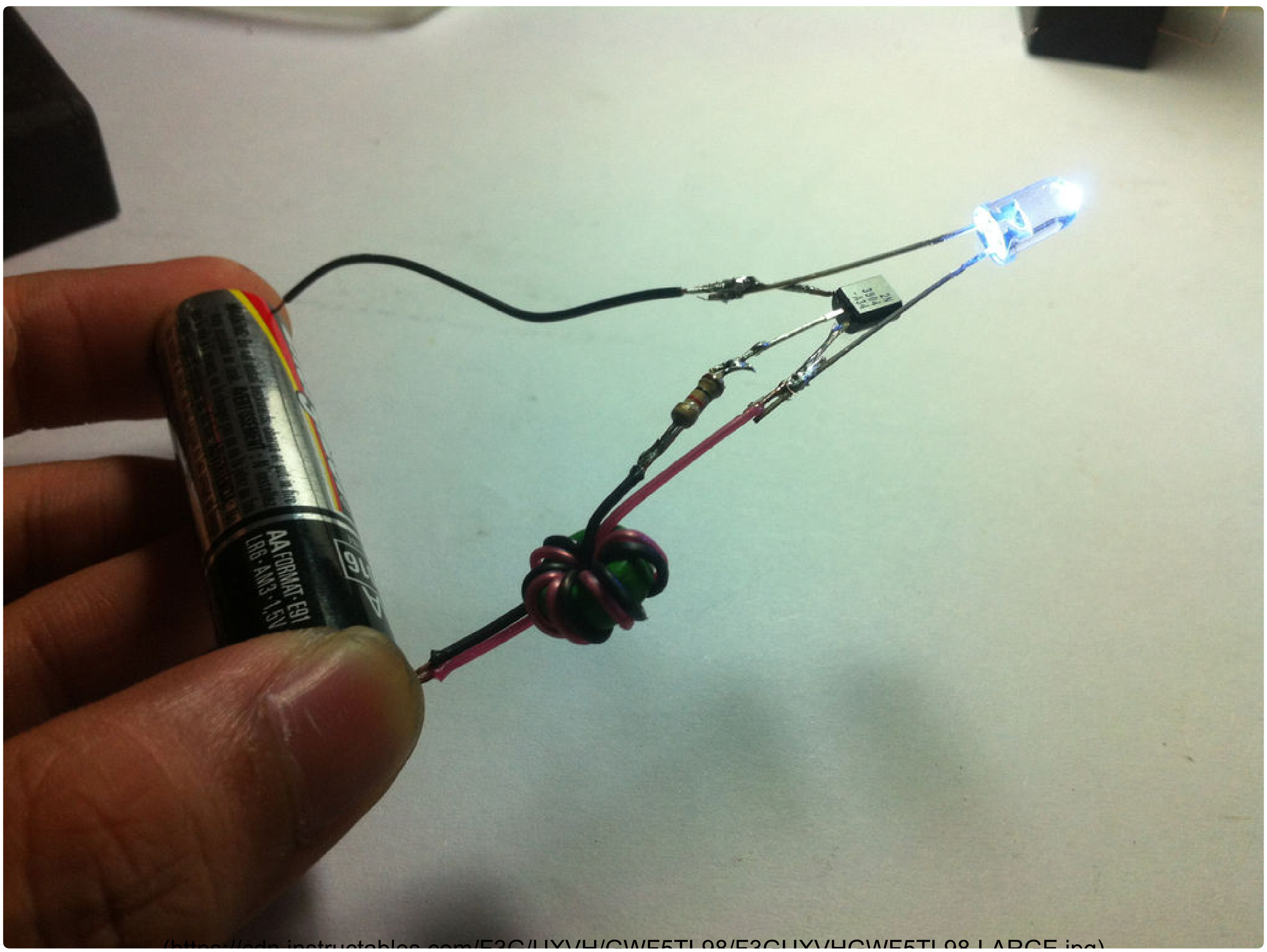

(https://cdn.instructables.com/F3C/UXV/HGWF5TL98/F3CUXVHGWF5TL98.LARGE.jpg)


(https://cdn.instructables.com/FB5/ROY8/GWHN3

(https://cdn.instructables.com/FF8

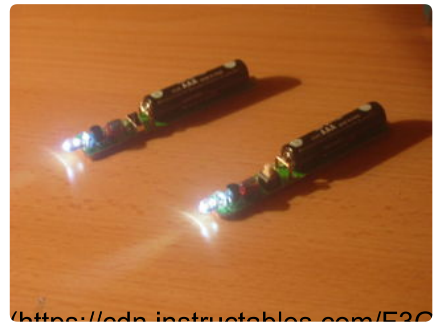
(https://cdn.instructables.com/F3C

Today I am showing you how to make a very simple joule thief. A joule thief has many applications, the best gadget that I made with was a "Water Powered Lamp", soon I'm going to post on a guide about it but first I need to post this guide. I used an iPhone 4S as my camera :)))

What Is A Joule Thief ?

To simplify everything, a "joule thief" is a circuit that helps drive an LED light even though your power supply is low. What can we do with it? We can use it to squeeze the life out of our old, almost drained, non functioning batteries. This project can also be considered as a green and environmental experiment, we can also use it as a flashlight that can be ran by an old, weak, almost drained battery. I even tried to use my water powered battery from my previous instructable the "Water Powered Calculator (https://www.instructables.com/id/Water-Powered-Calculator/)", the project was featured and displayed in instructable's front page in the "Technologies" category.

My Next Projects That Involves A Joule Thief: (soon to be posted)
- Water Powered Lamp
- Water Powered Flash Light
- Dead Battery Drainer Lamp

Here's A Video From Make Magazine:

Add Tip Ask Question

Step 1: Parts and Materials

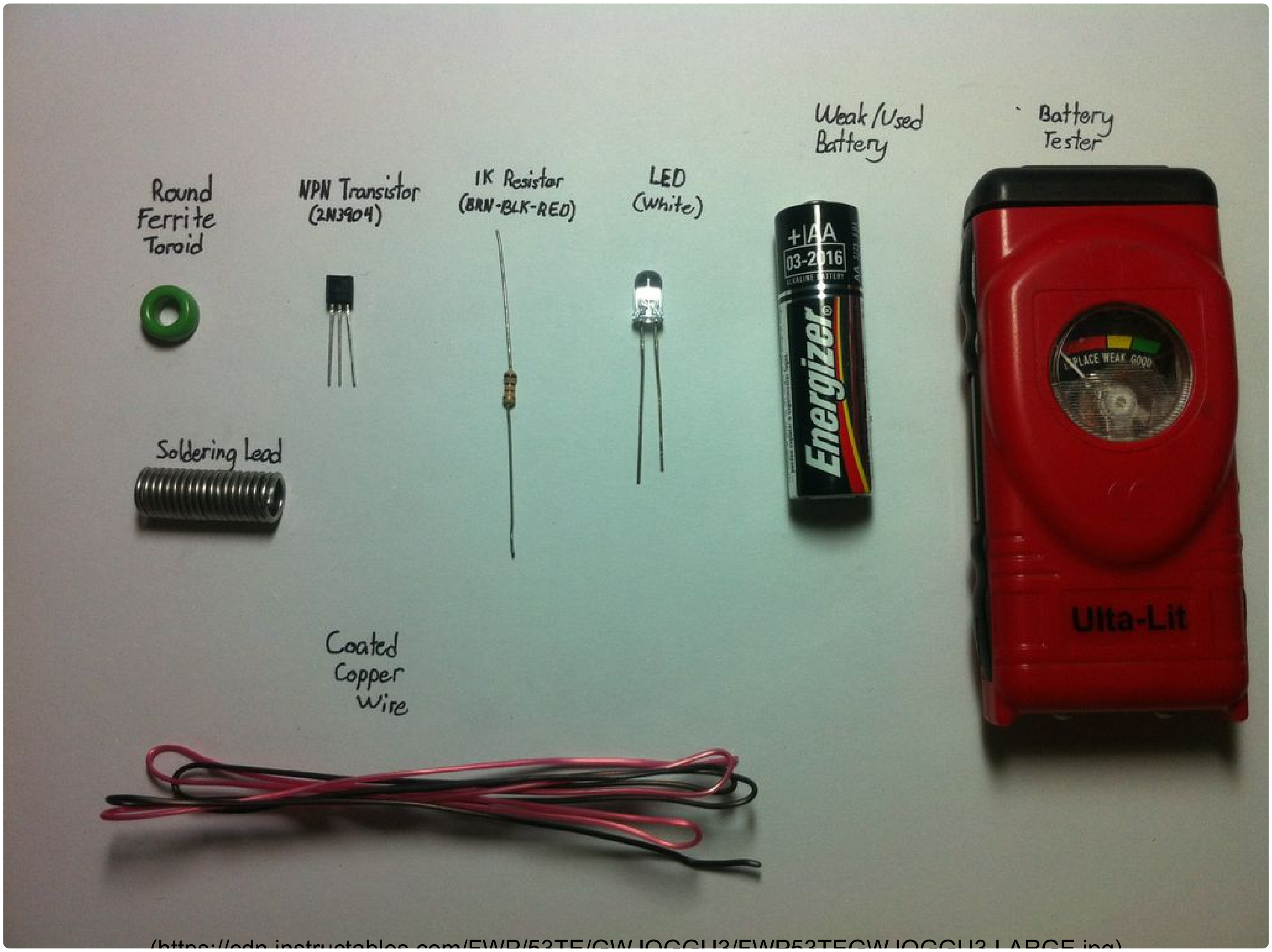

(https://cdn.instructables.com/FWP/53TF/GWJOGGU3/FWP53TFGWJOGGU3.LARGE.jpg)

The Parts Needed Are: (click the item to know where to find/ buy)

- Round Ferrite Toroid (can be found in old CFL bulbs)
- Old/ Used Batteries (can be found in garbage cans)
- NPN Transistor (2N3904) (http://www.radioshack.com/product/index.jsp?productId=2062609)
- 1K Resistor (BRN-BLK-RED) (http://www.radioshack.com/product/index.jsp?productId=2062343)
- LED Light (http://www.radioshack.com/product/index.jsp?productId=3096133)
- Battery Tester (http://www.tooldistrict.com/Ulta-Lit-Battery-Tester-5001-p/901233.htm) (optional)
- Soldering Lead (http://www.radioshack.com/product/index.jsp?productId=2062717)

- Copper Wire/ Magnet Wire (http://www.radioshack.com/product/index.jsp?productId=2036277)
- Battery Case/ Holder (http://www.radioshack.com/product/index.jsp?productId=2062247)

I want to share something. Here in the Philippines electronic parts are extremely cheap, they are extremely far cheaper from
radio shack, for example one transistor costs (2 phil. pesos - 6 US cents), a LED cost (9 phil. peso - 29 US cents) and a 1K resistor cost (25 phil. cents - 0.8 US cents). I usually buy thing from Deeco or Alexan. Usually prices here are 15x cheaper from radio shack. Price conversion - $1 US Dollar = P0.31 Philippine Peso (12/24/11).

Add Tip Ask Question

Step 2: Schematic Diagrams

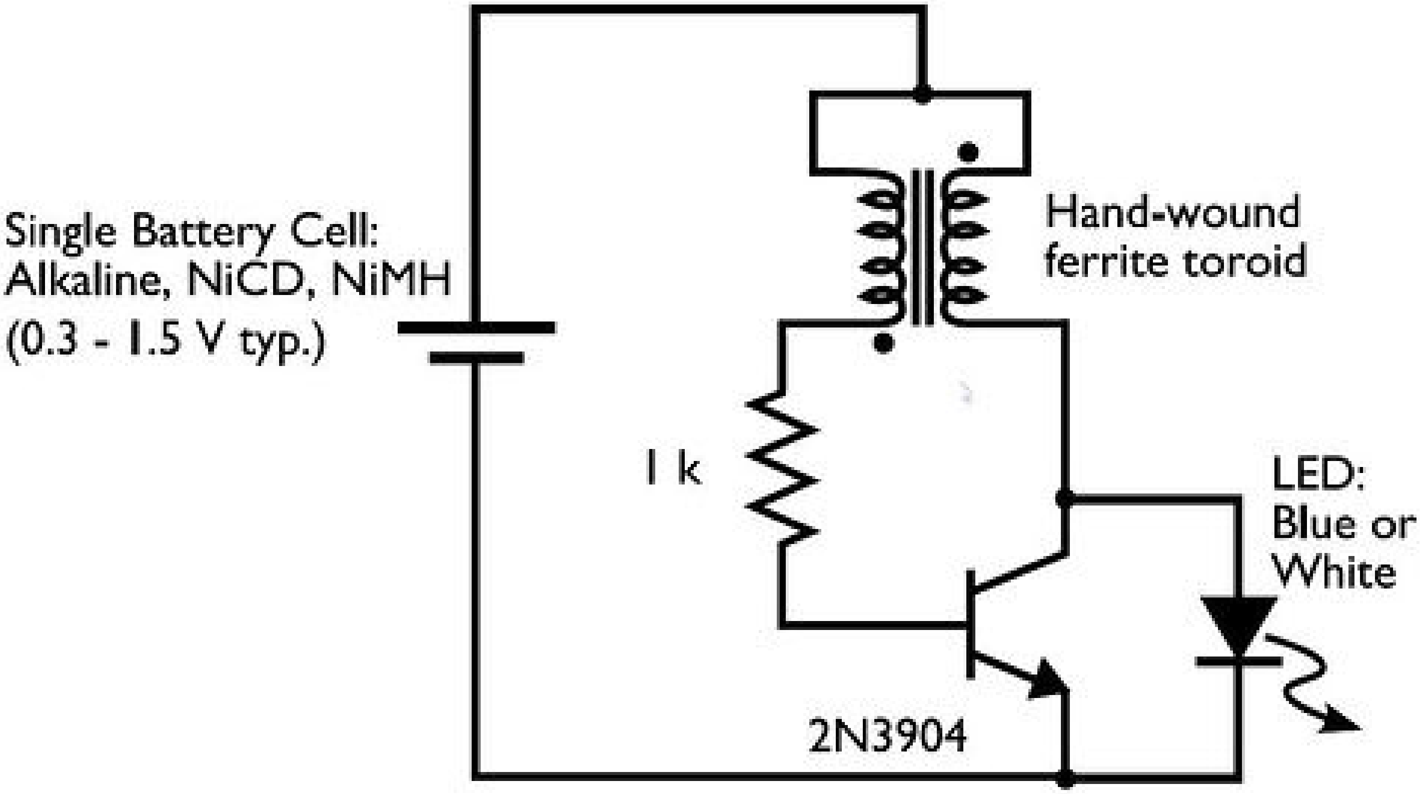

(https://cdn.instructables.com/F3N/S5I7/GWKD43C0/F3NS5I7GWKD43C0.LARGE.jpg)

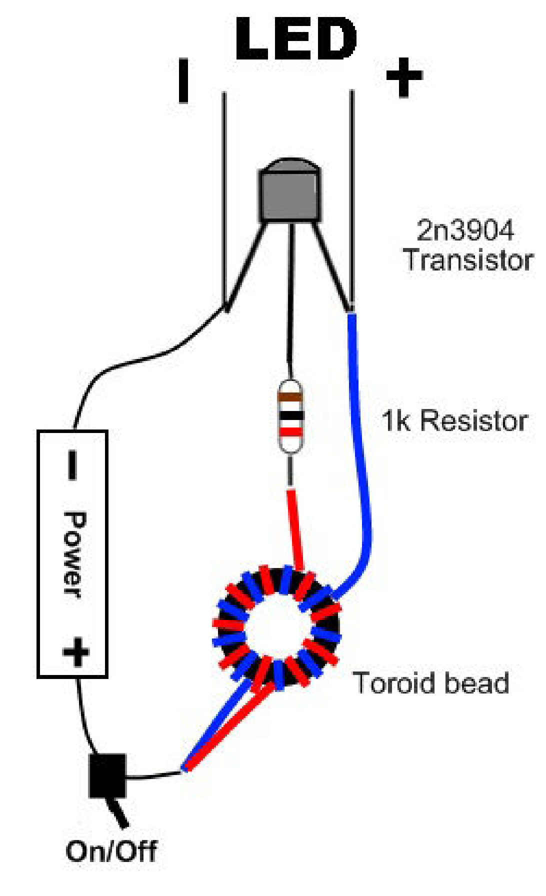

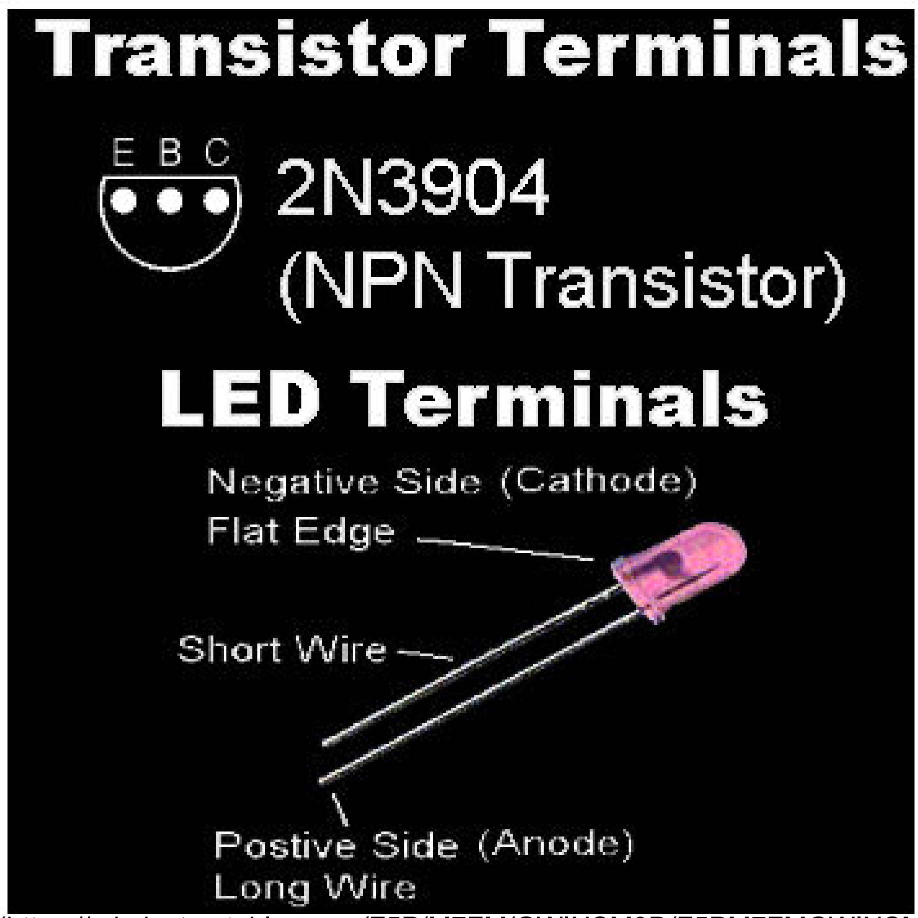

(https://cdn.instructables.com/FN0/CPE6/G\ (https://cdn.instructables.com/F5P/M7FM/GWINSM3D/F5PM7FMGWINSM

Here are the schematic diagrams that are involved with the joule thief circuit.

Add Tip | Ask Question

Step 3: Winding Wire at the Toroid

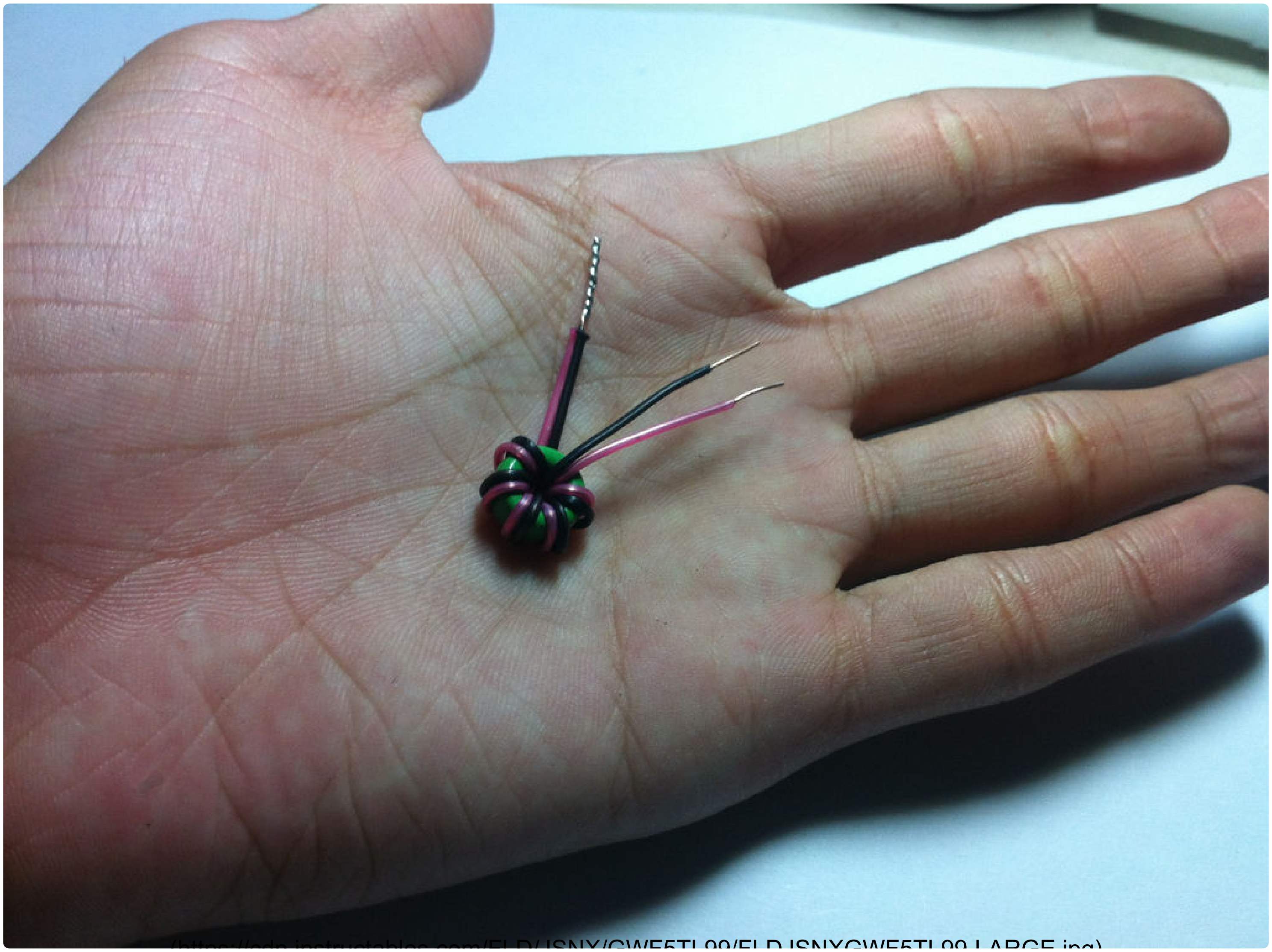

(https://cdn.instructables.com/FLD/JSNY/GW55TL99/FLDJSNYGW55TL99.LARGE.jpg)


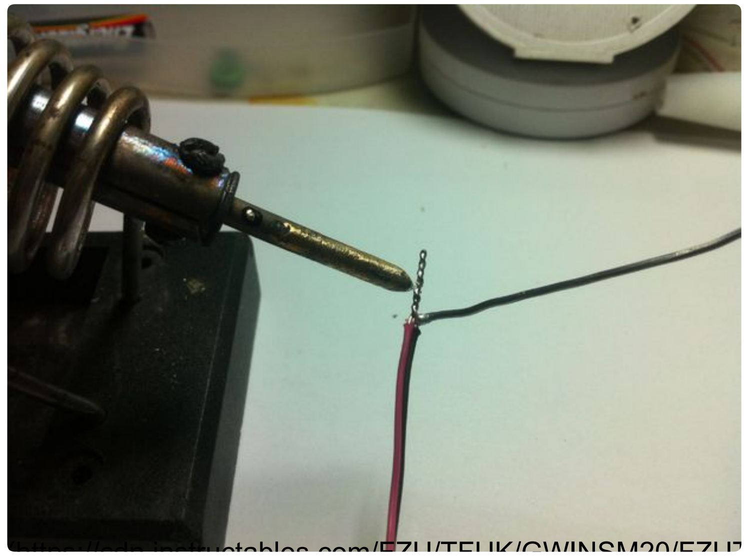

First, connect both ends of the copper wire before wounding, be sure to remove the insulation. Then try to solder the ends so it would not split up. Second, wind the wire until you run out of space in the round ferrite toroid. I have some tips for you, try to use a gauge #22 enamel coated copper wire for better performance, oh! my last tip is that "the more you wind the wire to the ferrite toroid the better".

Add Tip

Ask Question

Step 4: Soldering the Resistor

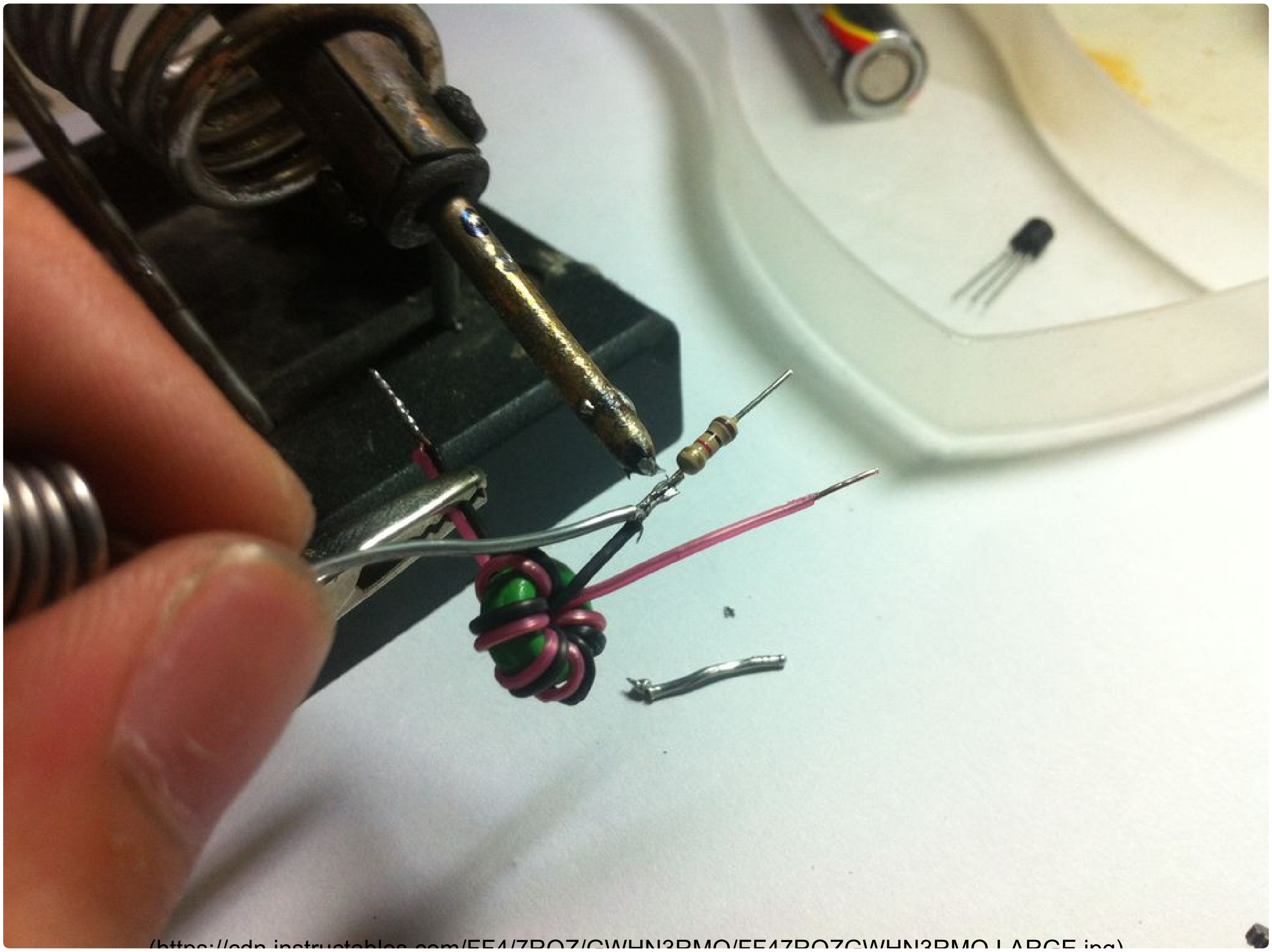

(https://cdn.instructables.com/FE4/7BQZ/GWHN3BMQ/FE47BQZGWHN3BMQ.LARGE.jpg)

Solder the resistor with one end of the wounded ferrite toroid's wire. Oh! also don't forget to level the other end of the resistor with the other unused wire from the wounded ferrite toroid.

Add Tip

Ask Question

Step 5: Soldering the Transistor

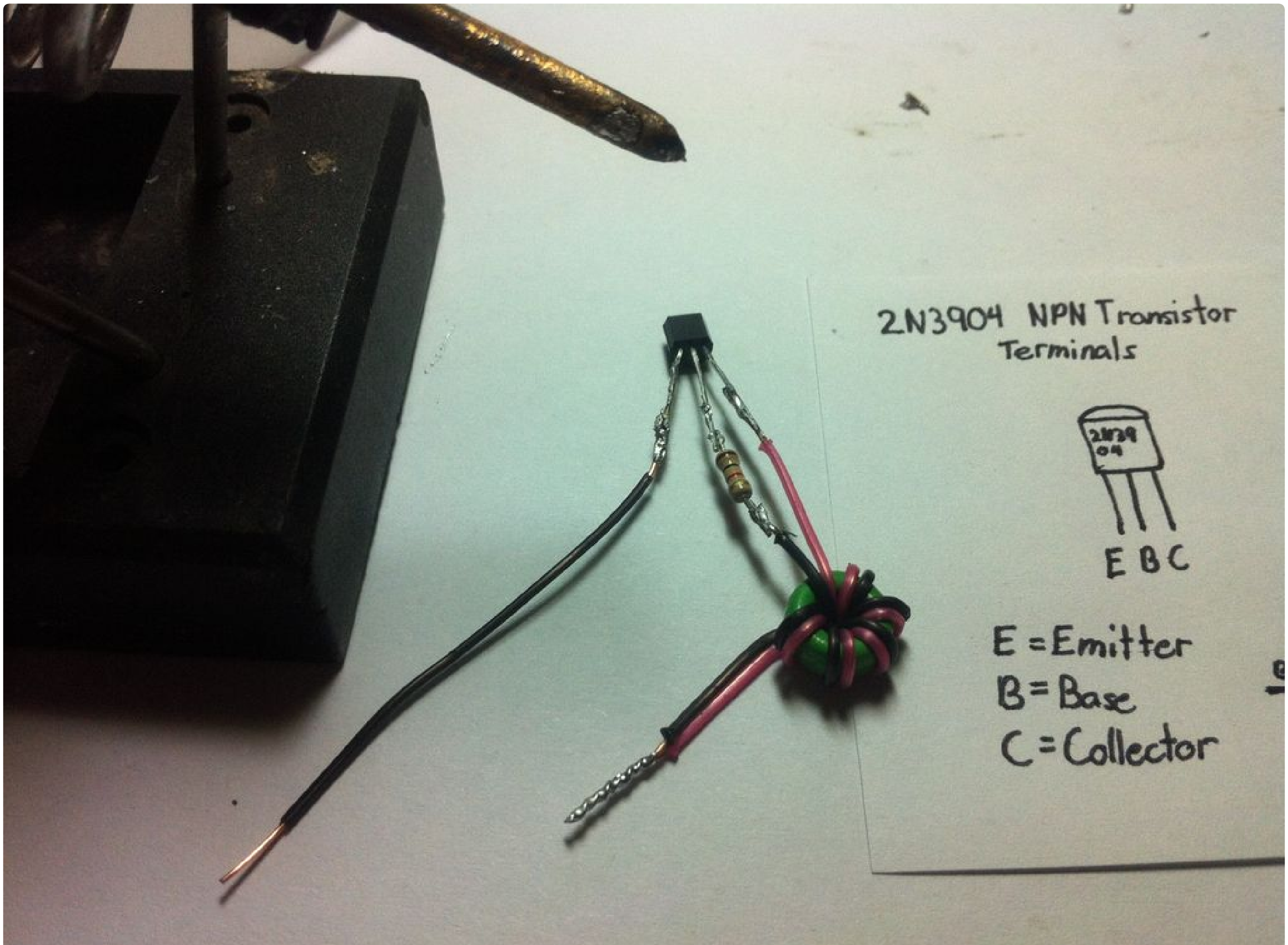

(https://cdn.instructables.com/FE3/I3O4/GWF5TL97/FE3I3O4GWF5TL97.LARGE.jpg)

Solder the proper connections to the transistor. For the emitter - connect another wire, the wire will be connected to the negative part of the battery. For the base - solder the other end of the resistor to the base. For the Collector Solder the unused wire of the ferrite toroid.

Add Tip Ask Question

Step 6: Soldering the LED

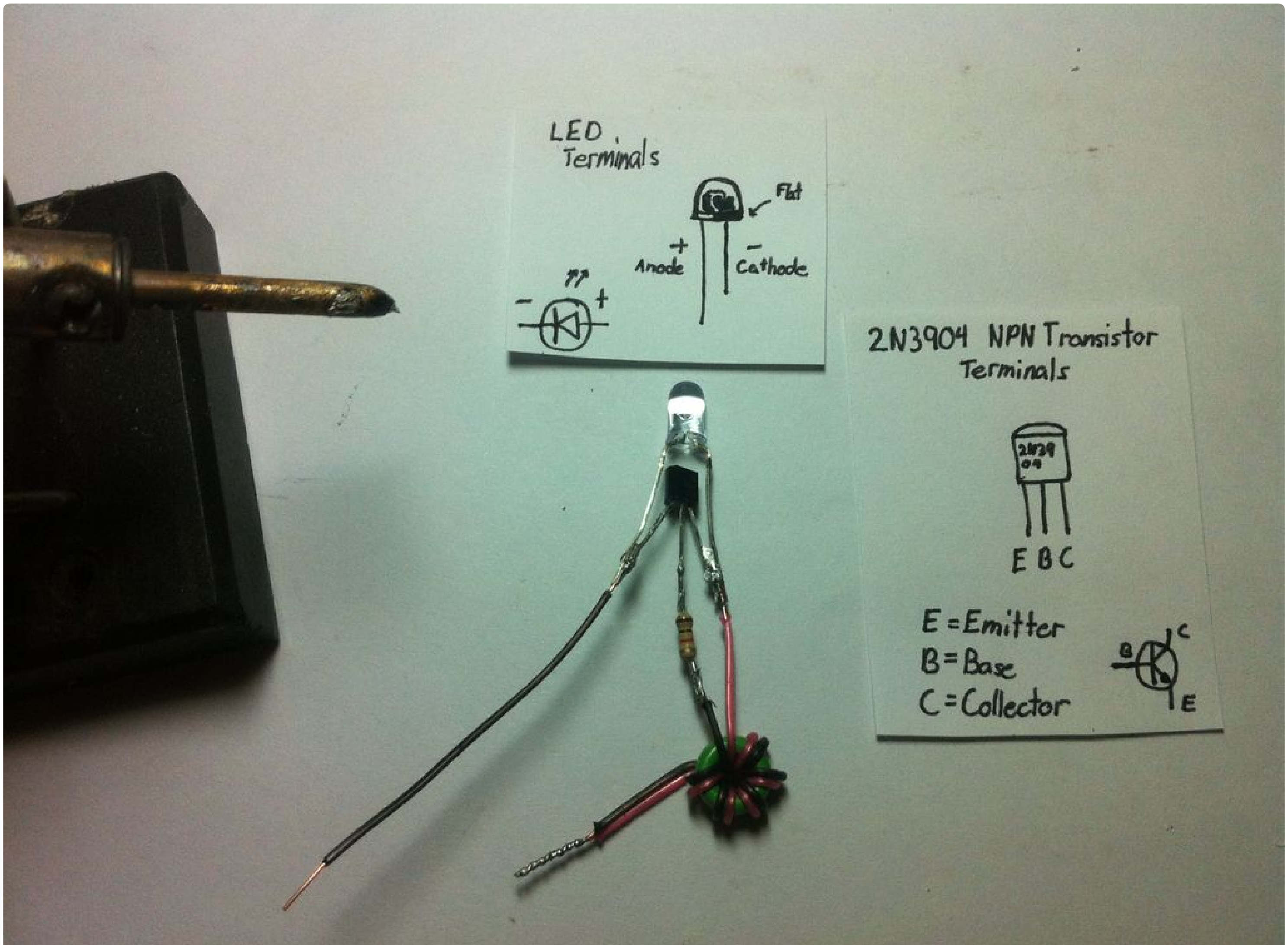

(https://cdn.instructables.com/FBC/PC16/GWINSLNY/FBCPC16GWINSLNY.LARGE.jpg)

Solder the shorter wire of the LED to the tansistor's emitter and the longer part of the LED to the transistor's collector. After all that, you can now trim the excess wires.

Add Tip   Ask Question

Step 7: Time to Look for Old Batteries

(https://cdn.instructables.com/F78/J93B/GWF5TM0Q/F78J93BGWF5TM0Q.LARGE.jpg)

(https://cdn.instructables.com/FX4/JNKD/GWINSM4V/FX4JNKDGW

(https://cdn.instructables.com/F40/9TOM/GWINSM

Use your battery tester to confirm that your battery is close to death. The tester is only an optional tool, it's just used to determine the battery's remaining power.

Add Tip

Ask Question

Step 8: Time to Test It - You're Done !!

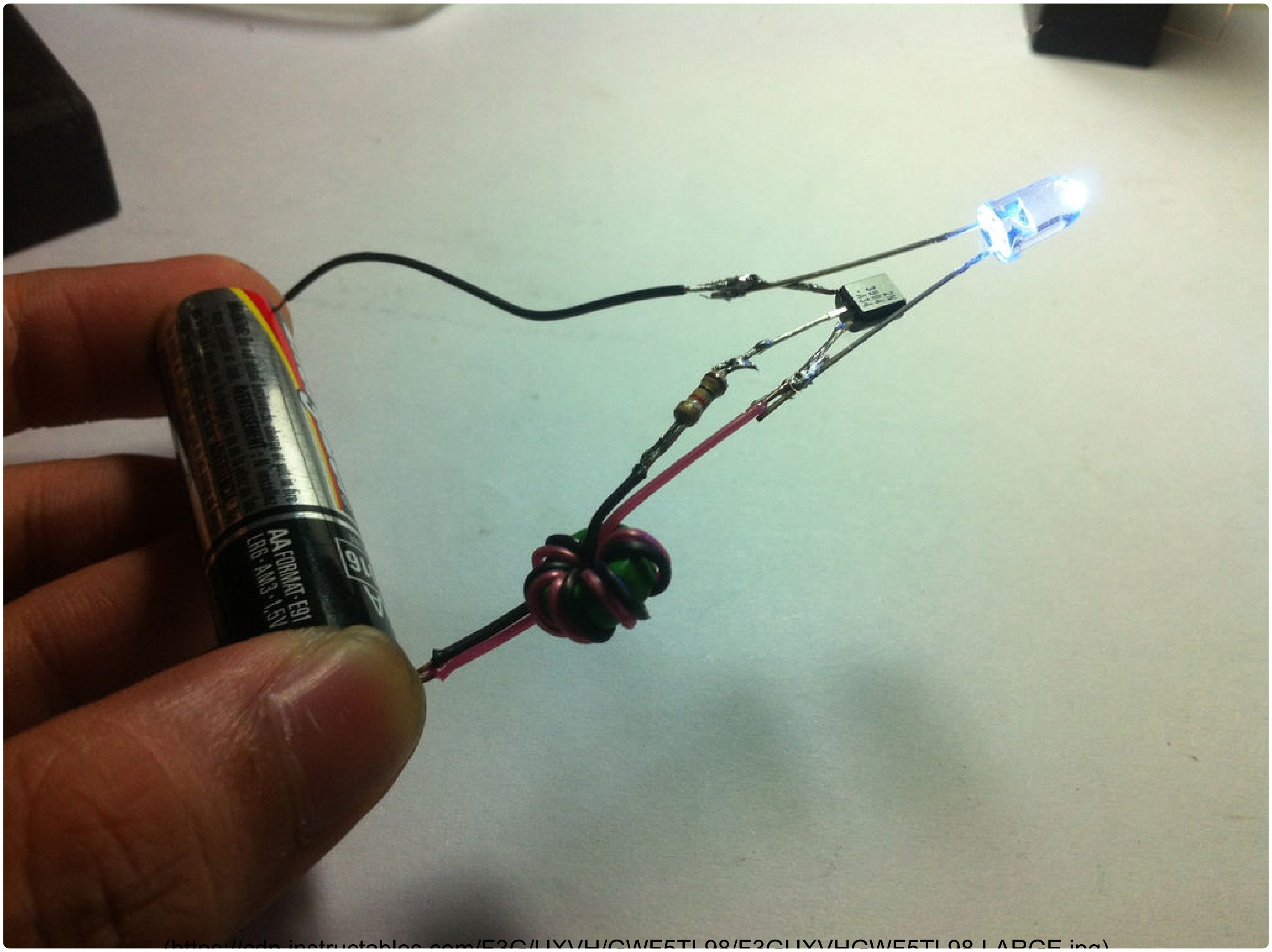

(https://cdn.instructables.com/F3C/UXVH/GW5TL98/F3CUXVHGW5TL98.LARGE.jpg)

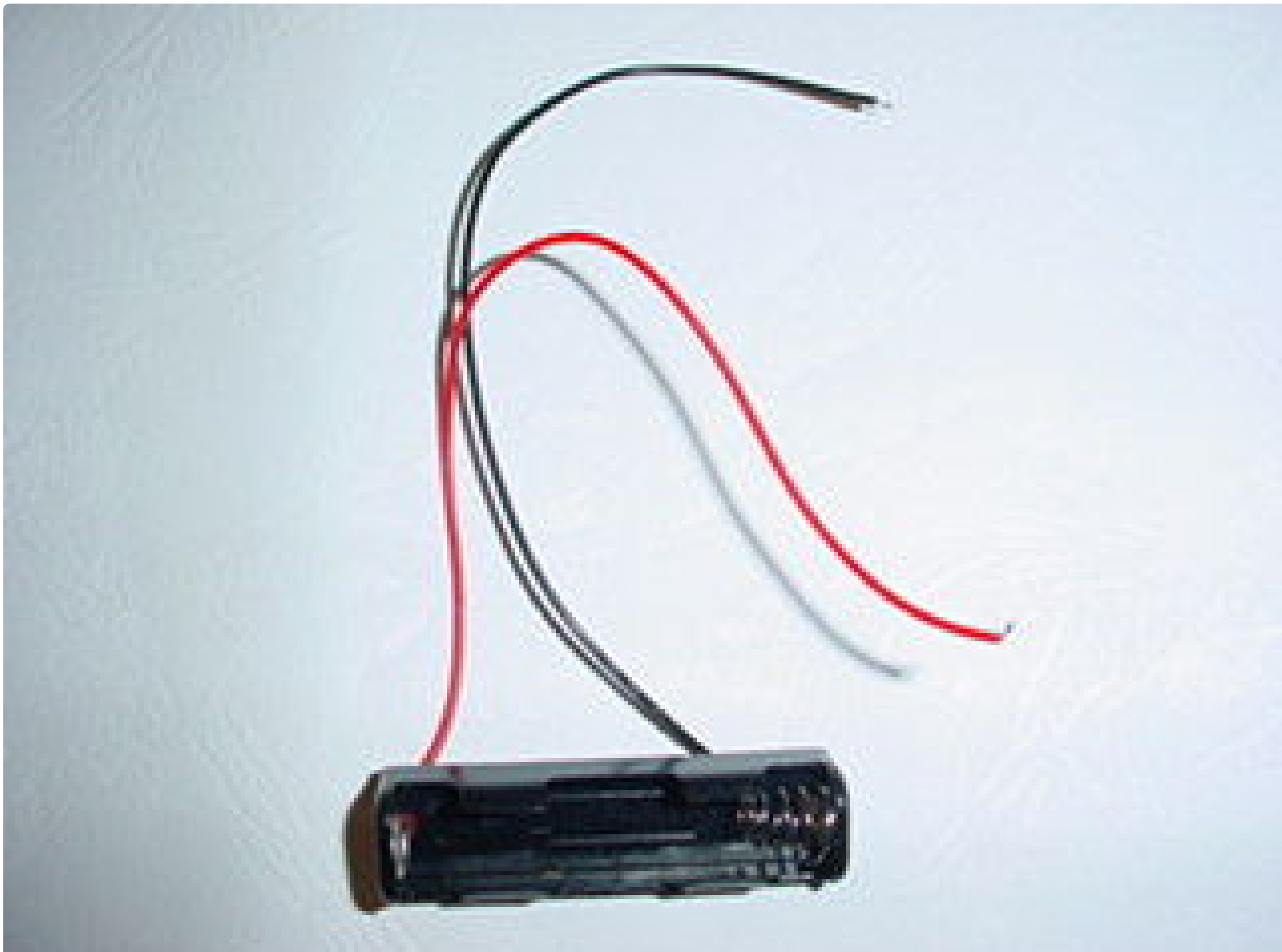

(https://cdn.instructables.com/FGU/NY0F/GWHN3BZH/FGUNY0FGWHN3BZH.LARGE.jpg)

The wire connected to the transistor's emitter should be connected to the battery's negative side and the remaining wire of the ferrite toroid should be connected to the battery's positive side. Oh! one more thing, I advise everyone to use a battery case or attach a conductive magnet for each wire, so you wouldn't hold it all the time.

Add Tip Ask Question

8 People Made This Project!

"Joule Thief" LED Night Light

by ledartist on September 2, 2011

Table of Contents

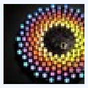
Author:ledartist My Blog
I work with LEDs and microcontrollers to create beautiful objects.

Intro: "Joule Thief" LED Night Light

I have many used batteries around. Remote controls, cameras, many electronic gadgets all use batteries, mostly AA size. I always felt guilty for throwing away the used batteries. I know there are rechargeable batteries, but many electronics don't work well with rechargeables.

I also know that those "used" or "spent" batteries usually have some juice left in them. So to come up with a good use of used batteries, I've created a LED night light.

I like having a little night light on when I sleep. LEDs are perfect for this purpose, because they are energy efficient, and good at providing low intensity illumination.

This LED night light operates with just one battery. It utilizes a little circuit called Joule Thief to boost voltage out of an AA battery. I also added a light sensor to turn it on automatically when the surrounding is dark.

The circuit is energy efficient, and requires very low voltage to work. So it effectively sucks every bit of energy out of batteries. This type of circuit is often called "Joule Thief", because it works as though stealing every bit of energy (Joule is a unit for energy) out of battery.

I'm calling this project Night Joule Thief.

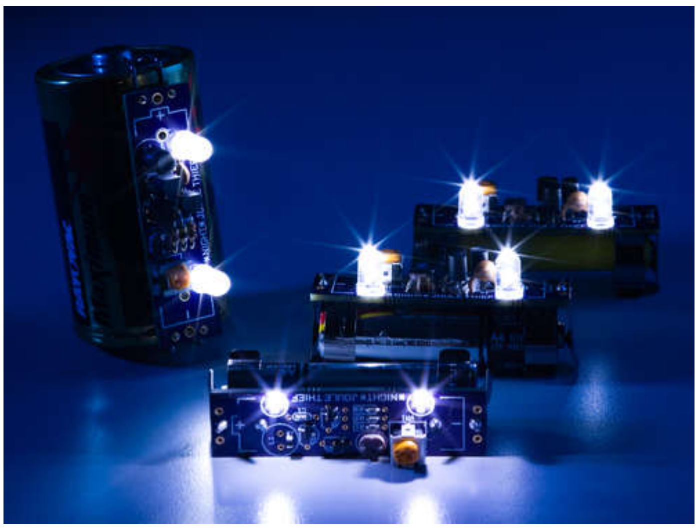

Step 1: Features

Here are the highlights of the Night Joule Thief.

- Compact & streamlined design
- Uses only one AA battery (or any 1.5V battery you can hook up to)
- Easily adaptable to different size batteries - hook up holes to attach home made clips
- Two white LEDs
- Automatic turn on via a light sensor (adjustable sensitivity level)
- Energy efficient - works even with a run-down battery, down to 0.6V
- Choice of through-hole only components or SMD - mix & match on the same PCB

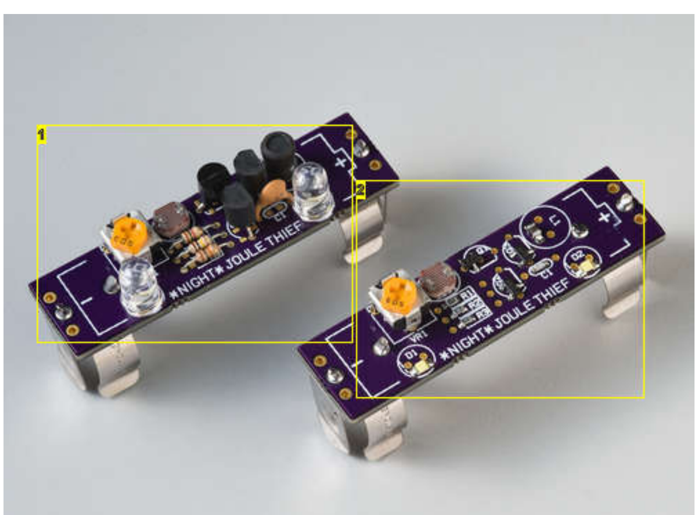

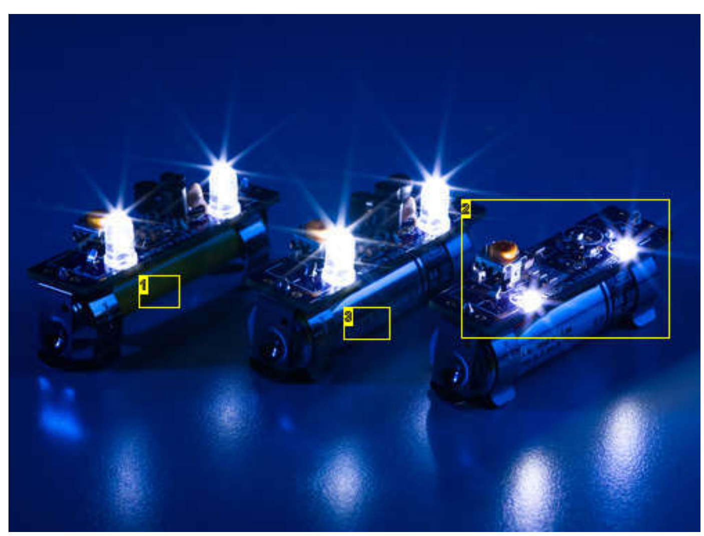

Image Notes
1. Through-hole version.
2. SMD (Surface Mount Device) version. Hard to believe this is the same circuit, but it works exactly the same as one on left. Ok, the LEDs are slightly less bright.

Image Notes
1. AAA battery inserted with a help of small magnets.
2. SMD version - very low profile.
3. Standard AA battery snugly fit in the clips.

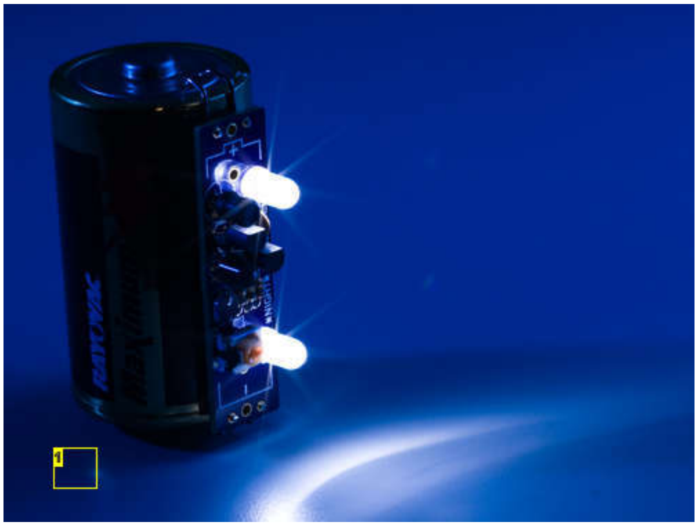

Image Notes
1. Other sizes, such as D cell can be attached by making a pair of little metal clips. Just cut and bend paper clips.

Step 2: Technical Overview

"Joule Thief" circuit is an inductor based voltage booster circuit to light LEDs with low supply voltage. As most of you know LEDs need higher than 2V (3V for white LEDs), so usually at least two batteries are needed to light them. The "Joule Thief" circuit was published in 1999 and has been quite popular. You can see the principle of the circuit here. http://en.wikipedia.org/wiki/Joule_thief

My version is a variation that uses single coil inductor, to make the inductor easily obtainable. I design the circuit using readily available parts only, to make it an ideal DIY project.

Circuit

The L1, Q2, Q3, C1, R2, and LEDs D1 & D2 make the Joule Thief. And the Q1, and the rest of the parts form the light sensor. CdS is the device that actually senses the light and change its resistance accordingly. When the surrounding of CdS is bright, it has low resistance (anywhere around 1k to 3k ohm), and when the surrounding is dark, the resistance goes up to 100k to 3M ohm range. So in this circuit, the base voltage of Q1 is controlled by the ambient light level. When the base voltage of Q1 goes more than 0.6V below the power supply(battery) voltage, current goes through R1, turning the Joule Thief circuit on.

The Joule Thief circuit is boosting the battery voltage up to over 6V to light two LEDs in series. LEDs light up with the battery voltage as low as 0.6V! Amazing!

PCB layout can be downloaded as an editable PDF, so you can etch your own board if you like. Custom 2 layer PCB and kit are available for sale as well. The 2 layer PCBs have extra front pads for SMD where possible, so you can build the same circuit with SMD parts as you wish.

Parts List
1x CdS Photoresistor (rated 3k - 0.3M ohm) (CDS1)
1x 1k ohm (R1)
1x 100k ohm (R2)
1x 10k ohm (R3)
1x 50k ohm trim pot (VR1)
1x 22pF (C1)
1x 470uH (L1) (anywhere between 22 - 470uH would work - might have to reduce the C1 value however)
1x 2N5401 or equivalent (Q1) (or just about any general purpose PNP transistor, such as PN2907, 2N3906, etc...)
2x MPSA06 or equivalent (Q2, Q3) (or just about any general purpose NPN transistor, such as PN2222A, 2N3904, 2N4400, etc...)
2x LED (D1, D2) (Just about any LEDs can be used)
2x Battery Clips

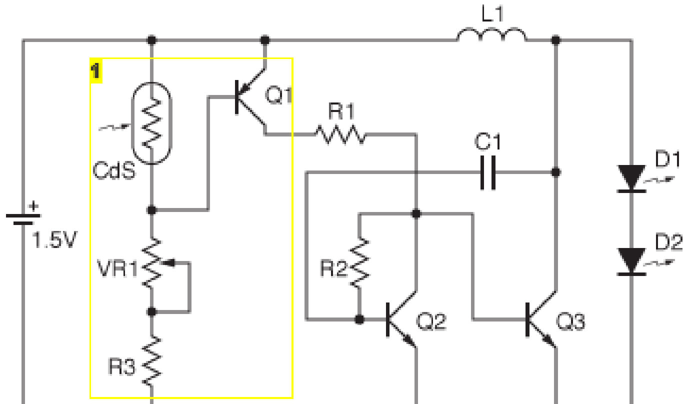

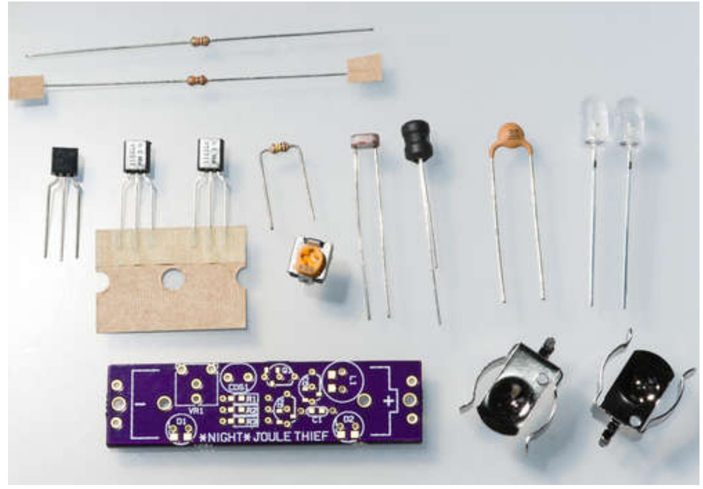

Image Notes
1. Light sensor circuit with sensitivity adjust.

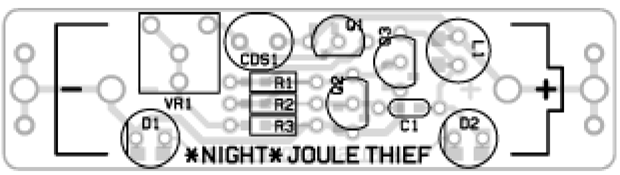

File Downloads

NightJouleThief-PCB.pdf (54 KB)
[NOTE: When saving, if you see .tmp as the file ext, rename it to 'NightJouleThief-PCB.pdf']

Step 3: Assembly

The assembly is very straight forward. Insert the parts into the PCB, and solder them. Start with small components, follow the order below.

Parts List (in assembly order)
1x 1k ohm (R1)
1x 100k ohm (R2)
1x 10k ohm (R3)
1x Photoresistor (rated 3k - 0.3M ohm) (CDS1)
1x 50k ohm trim pot (VR1)
1x 22pF (C1)
1x 470uH (L1)
1x 2N5401 or equivalent (Q1)
2x MPSA06 or equivalent (Q2, Q3)
2x LED (D1, D2)
2x Battery Clips

Transistors, and LEDs have polarities, so make sure to insert them in the correct orientation. Battery holders need a bit of force to snap into the holes. They attach from the back side of PCB as you can see in the picture.

Once everything is soldered in place, double check the part placement, orientation and solder joints. Then insert a battery. The polarity is marked on the front side of PCB.
If you don't see the LEDs light up, don't worry. The room is probably too bright. Take a piece of black paper or tape and block the light from hitting CdS light sensor. (and/or darken the room) If the LEDs still don't come on, turn the trimmer (the little orange thing) with a screw driver, counter clockwise. This makes the sensor less sensitive to light, so the LEDs will come on by just placing the sensor under shade, or turning off the room light.

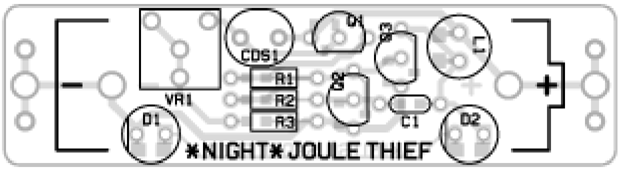

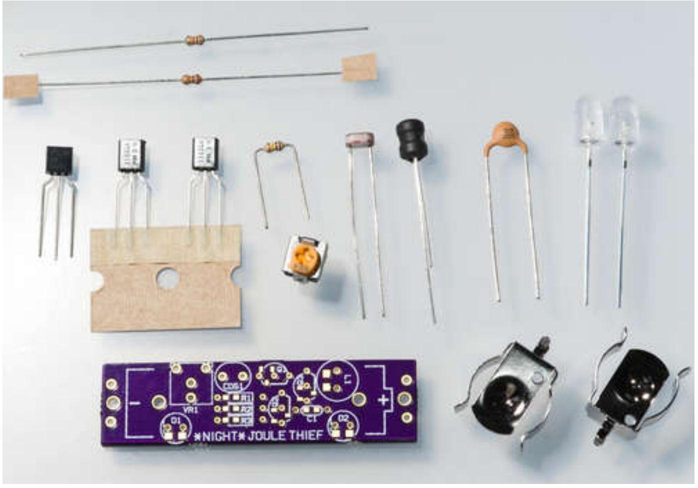

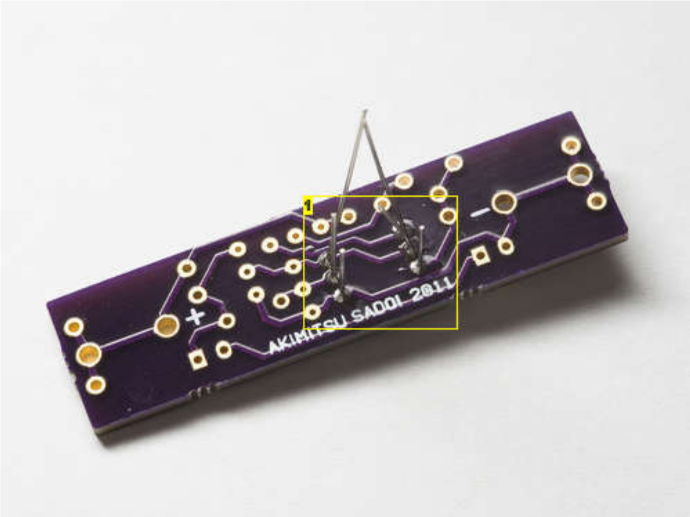

Image Notes
1. Resistors soldered in.

Step 4: Performance

This little night light performs very well. For starters, the brightness is not bad for using just one AA battery. I've been using these as flashlights as well.

The light sensor also works very well. Once adjusted, the light is steadily off during the day, even when you put the sensor under shade. Only when you block the sensor by a black object, the light would turn on. Yet after dusk, the light would come on when you turn off the room light.

A fresh battery lasts for weeks if only used as a night light. And the best use of this light is to "revive" used batteries. Those batteries from remote controls, cameras, etc. usually have quite a bit of juice left in them. Joule Thief sucks the juice out of those batteries till the last drop. It's like getting free energy when you can use something that were going to be thrown out.

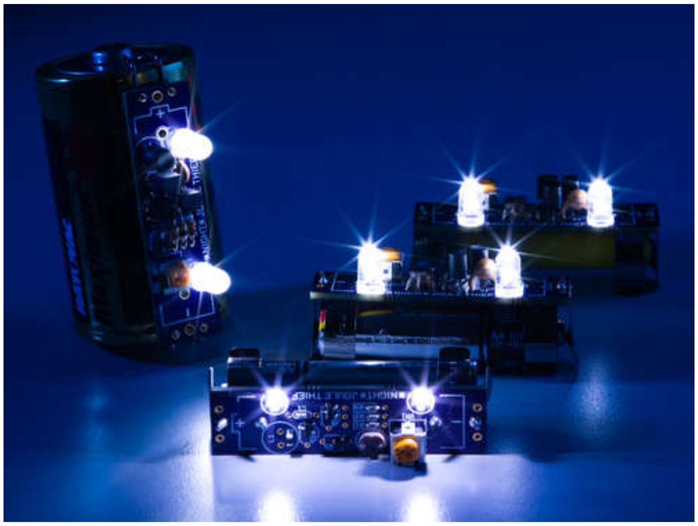

Step 5: PCB & Kit

If you are handy, you can etch your own PCB, and build this night light entirely DIY.

However, to spread the goodness of Joule Thief and to contribute to the greener earth, I am putting together the PCB & kit available.

The details can be found here: http://www.instructables.com/community/Joule-Thief-LED-Night-Light-Kit-PCB/

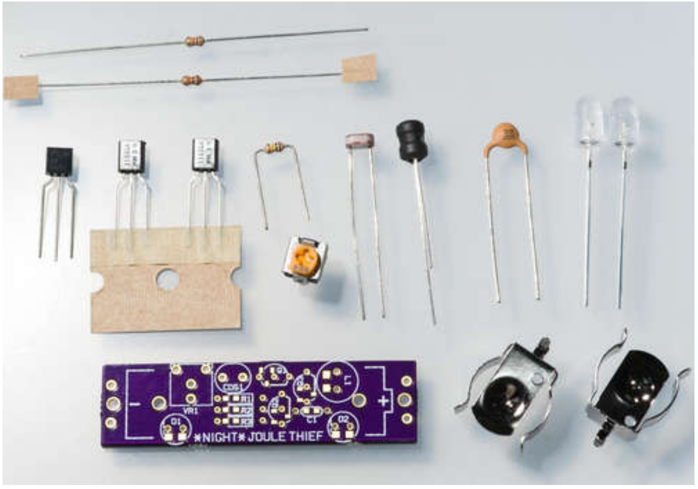

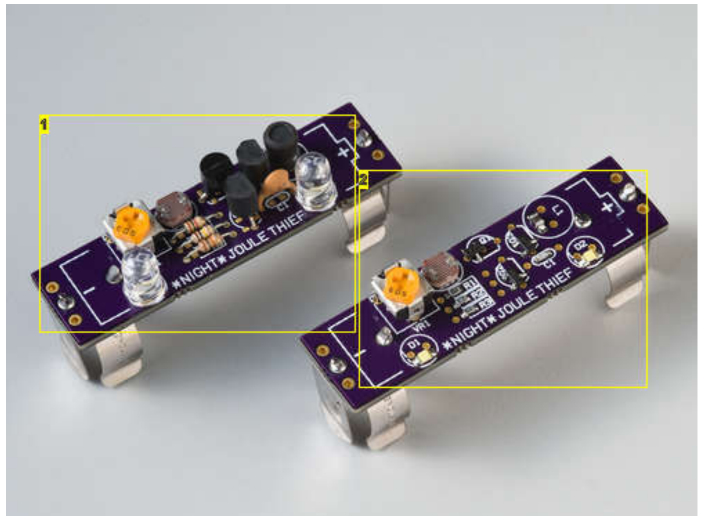

Image Notes
1. Through-hole version.
2. SMD (Surface Mount Device) version. Hard to believe this is the same circuit, but it works exactly the same as one on left. Ok, the LEDs are slightly less bright.

Related Instructables


Joule Thief - use LEDs with only one AA battery! by RazorConcepts


Ferrite, the joule thief (Photos) by botronics


Electronic Night Light by TinkerJim

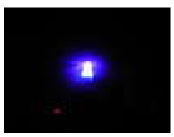
Ultraviolet Light Pen by junits15


Mini 'Joule Thief' (Photos) by Mudbud

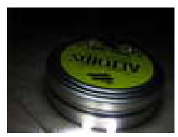
Altoids Joule Thief Flashlight (Photos) by cynical_chemical

Comments

33 comments **Add Comment**

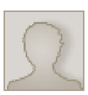
tosacj says: Sep 4, 2011. 10:47 AM **REPLY**
Great idea. Let me know when the kit becomes available.

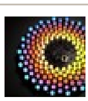
ledartist says: Sep 4, 2011. 12:38 PM **REPLY**
I will post the information on "Kits" section of the forum and on my blog (theLEDart.com). The kit & PCB are scheduled to be ready in mid September.
Thanks, Aki


haxcess says: Sep 5, 2011. 8:16 AM **REPLY**
This is a very neat application of the joule thief. I am wondering if it would be possible to replace the light-sensor circuit with a small battery charging circuit (solar). I suppose that would ruin the beautiful form factor you have here.

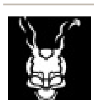
apalacios2 says: Sep 5, 2011. 7:07 AM **REPLY**
Excellent circuit. May I remove the CdS circuit and use a button switch instead (thru the resistor connected to the transistor)?
I find great that it uses a coil instead of a toroid transformer. Kudos!

ledartist says: Sep 5, 2011. 7:28 AM **REPLY**

Yes, you can. In fact I made sure that you can fit a 6mm tactile switch in place of trimmer pot. You can omit the CdS, and solder a switch in place of trimmer pot.

You can also remove Q1 and put a switch there as well, but my PCB won't accommodate that.

Yeah I found having to wind my own inductor a hassle, so I designed this circuit to use off-the-shelf inductors.

Aki

---

bhvm says: Sep 4, 2011. 9:17 PM **REPLY**

Excellent build!
How many mA does this circuit give? Can we use a single 150mA power LED in place of 2x 5mm LEDs?

---

ledartist says: Sep 5, 2011. 7:20 AM **REPLY**

The current through the LEDs is about 20mA or less peak (it's pulsed current in about 50kHz)
So you won't get any more light by using a high power LED. By using only one LED, you do get a bit more brightness per LED though. However just a regular LED will give you the same brightness as a high power LED because you are not driving the LED with high current anyway...

It's not that you can't drive high current LED, but this circuit is designed to run with as little power as possible.

Aki

---

abbtech says: Sep 4, 2011. 7:10 PM **REPLY**

Great looking project.

---

ledartist says: Sep 4, 2011. 7:18 PM **REPLY**

Thanks!

---

vruiz3 says: Sep 4, 2011. 1:56 PM **REPLY**

afraid of the night??? :D

---

timotet says: Sep 4, 2011. 1:21 PM **REPLY**

great job!

---

gnafpliotis says: Sep 3, 2011. 3:06 PM **REPLY**

Can't we hack laptop's batteries that way to perform more? Is it only letting through a small amount of amps?

---

ledartist says: Sep 4, 2011. 1:17 PM **REPLY**

Laptops and many other "high-tech" gadget has many of inductor based boost/buck (to reduce voltage) voltage converter circuit in them. Especially LED back light screens use voltage converter to efficiently drive LEDs.
So in a way the battery life is already enhanced. (Some gadgets are better than others, of course...)

Aki

---

jolshefsky says: Sep 4, 2011. 6:19 AM **REPLY**

Yes, but only if you wanted to use your batteries once. Once a lithium rechargeable (like in laptops) is discharged past a certain point, it can no longer be recharged. So there is always some energy left in a laptop battery even when it says it's dead — albeit energy you can't use without ruining the battery.

---

stoobers says: Sep 4, 2011. 7:29 PM **REPLY**

I've heard this theory. Have you done any experiments that might validate this theory?

---

jamwaffles says: Sep 4, 2011. 6:14 AM **REPLY**

This might not be 100% accurate but yes, that's why we can't use the same technique for laptops. Joule thieves ramp the voltage up, but the current goes down due to V = IR, assuming the load is constant which it is if it's the same laptop ;-)

---

jamwaffles says: Sep 4, 2011. 6:15 AM **REPLY**

A very professional looking product. This is a great idea; the amount of power saved using old batteries instead of a herd of plug-in night lights, as well as the amount of batteries re-used is incredible.

Just out of interest, how long do these night lights last on one "averagely discharged" battery?

---

ledartist says: Sep 4, 2011. 1:10 PM **REPLY**

The battery lasts very long, most likely much longer than you might think.
It's hard to define "averagely discharged", but I had one cell that was already at 0.7V (to low to be used with anything), and the although the LEDs were dim, they lighted for over 48 hours.
With my "dead" batteries coming out of a wireless mouse still have over 1V, I have plenty of light.

Aki

YakAttack says: Sep 4, 2011. 8:24 AM **REPLY**

I concur!
@ledartist: Any tests on battery life so far?

---

nymgeek says: Sep 4, 2011. 7:42 AM **REPLY**

Are those PCBs made by Laen at dorkbot pdx?

---

ledartist says: Sep 4, 2011. 1:04 PM **REPLY**

Yup. They are very good!

---

acmefixer says: Sep 4, 2011. 10:06 AM **REPLY**

I should have said in my previous comment that this does not mean there is anything wrong with your circuit. I think I would change Q2 and Q3 to an easier to obtain transistor such as a 2N4401 or PN2222A. Q1 could be a 2N3906 or just about any PNP transistor. If these changes are made, the resistors, especially R2, might need to be reduced. Thanks.

---

ledartist says: Sep 4, 2011. 1:03 PM **REPLY**

Yes, you can use just about any general purpose transistors. R2 should be fine with most transistors, but 47k ohm might work better with some of them.

Aki

---

acmefixer says: Sep 4, 2011. 10:00 AM **REPLY**

Unfortunately the link you gave to Joule Thief in Wikipedia is for a poorly written and totally inadequate definition. The authors (apparently several over time) do not have a firm understanding of how a JT works, and furthermore, they have made a mess of it. I have added comments in the discussion and some errors have been deleted, but it is still unworthy of use for a reference.

Also, by definition, the original blocking oscillator circuit later given the Joule Thief name used only a single transistor. Your circuit is not a one transistor blocking oscillator and bears little resemblance to the original JT, so I don't believe it should use the same name.

---

ledartist says: Sep 4, 2011. 12:59 PM **REPLY**

I know the original circuit only uses one transistor, but the two conductor inductor is harder/expensive to purchase, and winding own inductors is a bit of work. I think using one extra transistor is a good trade off for not having to wind an inductor by hand. It also makes economical sense. (transistors are very cheap, so are single coil inductors.)

I did mention that my version is a _variation_ of original, which I find very often on the net. I also think that showing different ways to achieve the same result can be inspirational.

I also contacted the person who named the circuit "Joule Thief" (Big Clive) and he did not have a problem with me using the name.

Aki

StoryAddict says: Sep 4, 2011. 12:54 PM **REPLY**

"Joule Thief" - I love a clever pun!

MikeDel says: Sep 4, 2011. 10:21 AM **REPLY**

Looks good. I'm interested!

Admiral Aaron Ravensdale says: Sep 4, 2011. 7:30 AM **REPLY**

I like your "green" thinking.
I also use a joule thief in my expedition light.

I am very glad that you will provide the parts as a kit because many kits are able to solder a circuit but etching a little bit too dangerous for them.

Thanks for your endeavour to make this instructables buyable for many people…

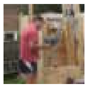

kevinhannan says: Sep 4, 2011. 6:35 AM **REPLY**

fantasic project and incredibly well explained.

UOS says: Sep 3, 2011. 2:59 PM **REPLY**

Great instructable! Waiting the kit version to buy one but also I'm gonna make mine from scratch :D

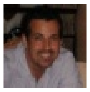

tphillips2 says: Sep 3, 2011. 8:07 AM **REPLY**

You are so inventive! Cool idea and great looking light!

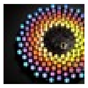

ledartist says: Sep 3, 2011. 8:18 AM **REPLY**

Thanks!

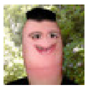

gweeds says: Sep 3, 2011. 4:41 AM **REPLY**

What a great idea! must build one and see how long it gets out of a "used'ish" battery

---

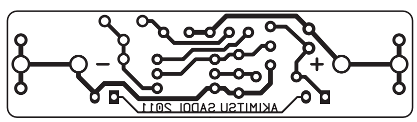

−
+
AKIMITSU SADOI 2011

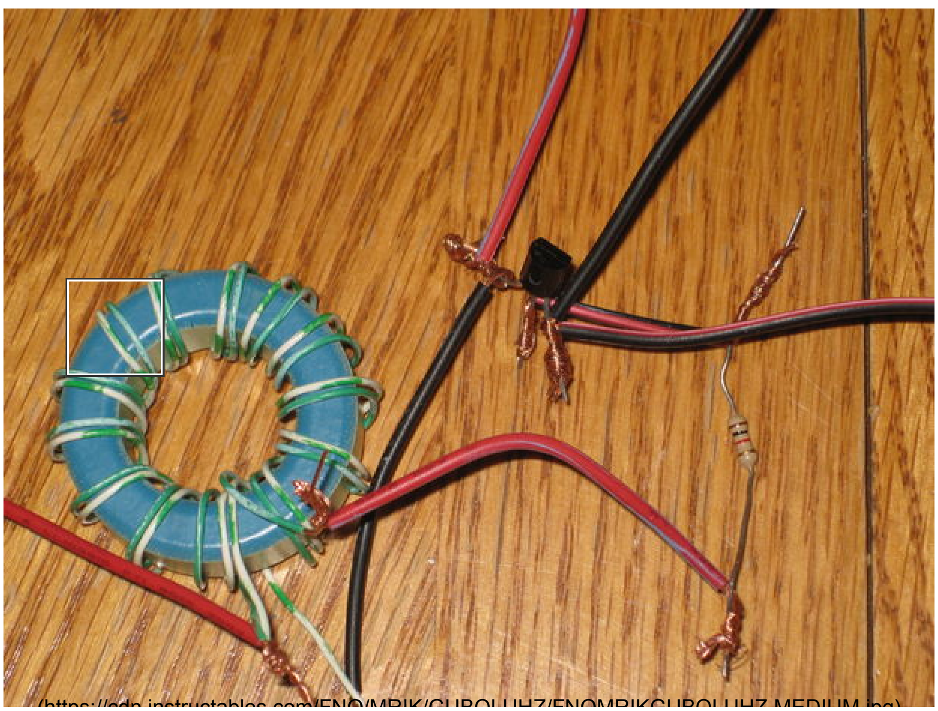
(https://cdn.instructables.com/FNO/MBIK/GUBOLUHZ/FNOMBIKGUBOLUHZ.MEDIUM.jpg)

this is my version of the famous joule thief. there's alot of these things out there so i did alot of research and made it as simple as i can without soldering or complicated math. i harvested these parts from an older dell computer that was given to me to scrap. there is only a few parts needed to build this project:

1: toroid bead (ferrite core)
2: 1k ohm resister (brown black red)
3: npn transistor (i used the 2n3904)
4: thin wire

About This Instructable

7,340 views
23 favorites

Step 1: Wind the Coil

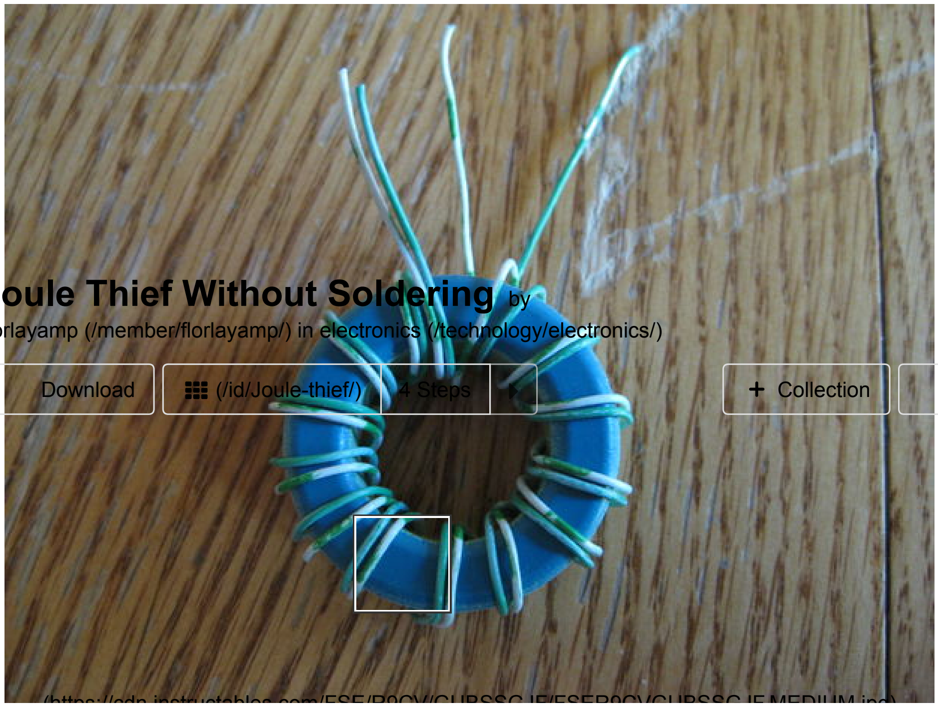

(https://cdn.instructables.com/F5E/R0QV/GURSSC JE/F5ER0QVGURSSC JE.MEDIUM.jpg)

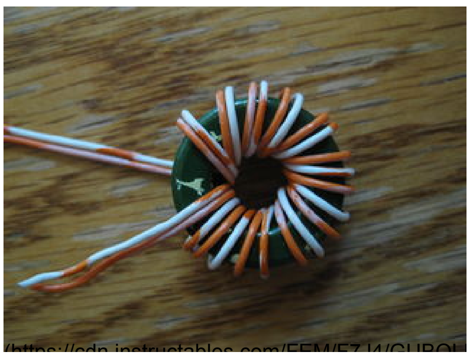

(https://cdn.instructables.com/FEM/F7J4/GURO...

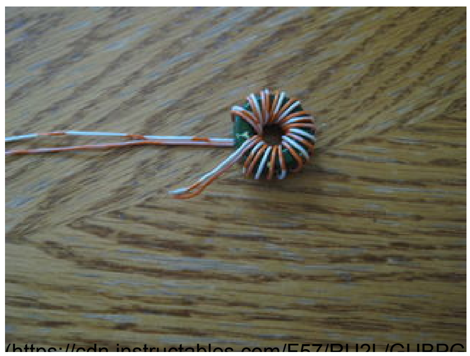

(https://cdn.instructables.com/F57/BU2L/GURBG...

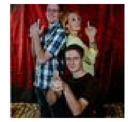

florlayamp (/member/florlayamp/)
(http://https://www.facebook.com
(/member/florlayamp/)
Follow 98

Bio: I love building things, and I'm a twin, we both are electrical engineers and inventors. Feel free to ask anything else

More by florlayamp:

(/id/How-Twins-Change-Oil-In-A-Jeep/)

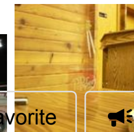

(/id/Take-A-Ghost-Picture-With-Almost-Any-Camera/)

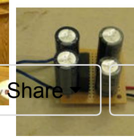

(/id/Voltage-doubler-for-wind-generators/)

i wound a couple sizes of these things using the same wire. the type of wire i used came from an ethernet cat5 cable. i like it because its a solid core wire that stays in place where i put it. i have 11 turns of wire in the orange one and 13 in the green one. i looked all over the internet to find the reason for the number of turns but couldnt find an exact answer, and 11 winds is all the smaller (orange one) could take, and the green one i just put the 13 turns in it from the same length of wire. the orange coil is half the size (about the size of a dime) of the green one (little bit smaller than a 50cent coin).

Step 2: Connect the Resistor

(https://cdn.instructables.com/F0B/T5XD/GUROLUOU/F0BT5XDGUROLUOU.MEDIUM.jpg)

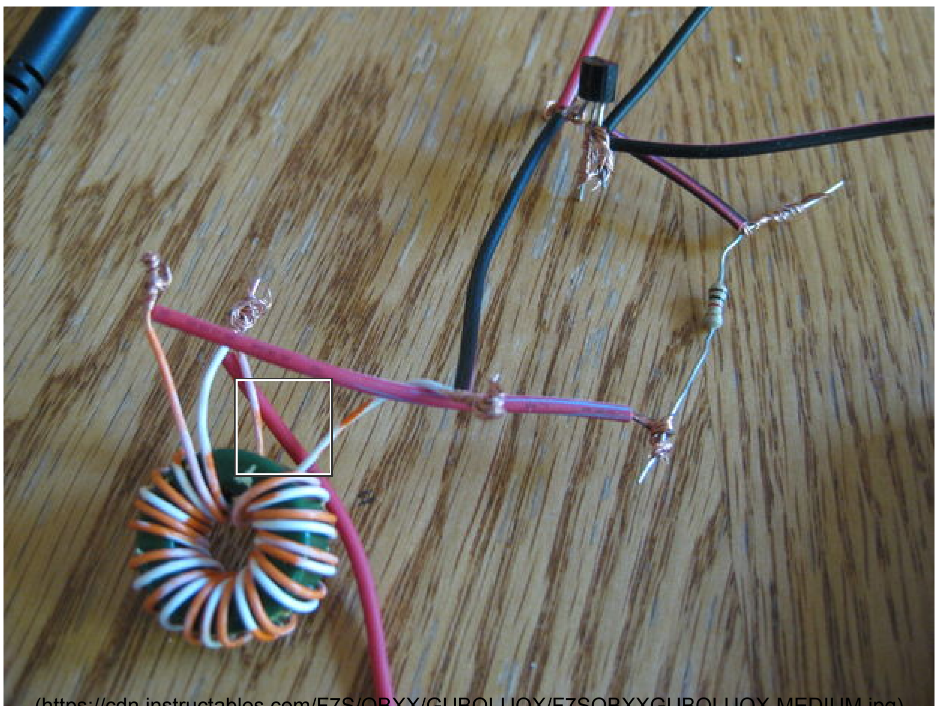

(https://cdn.instructables.com/F7S/OBXX/GUROLUOX/F7SOBXXGUROLUOX.MEDIUM.jpg)

once the coil is wound, cut off the excess wire but make sure to leave enough to work with. strip the ends of all four wires, then take 1 wire of **opposite color from each side** and twist them together. then since i didnt solder any wire, i cut up several small wires to piece the rest of it together. unless you want to solder it you can skip this part. but i took a piece of wire and attached it to one of the single wires on the coil (it doesnt matter which one) and attach the other end of the piece of wire to the 1k ohm resister, then take another piece of wire and attach it to the other single wire which will go to the **collector** leg of the transistor. the final piece of wire for this step attaches to the twisted pair of wires which will become the positive input for the circuit.

Step 3: Connect the Transistor

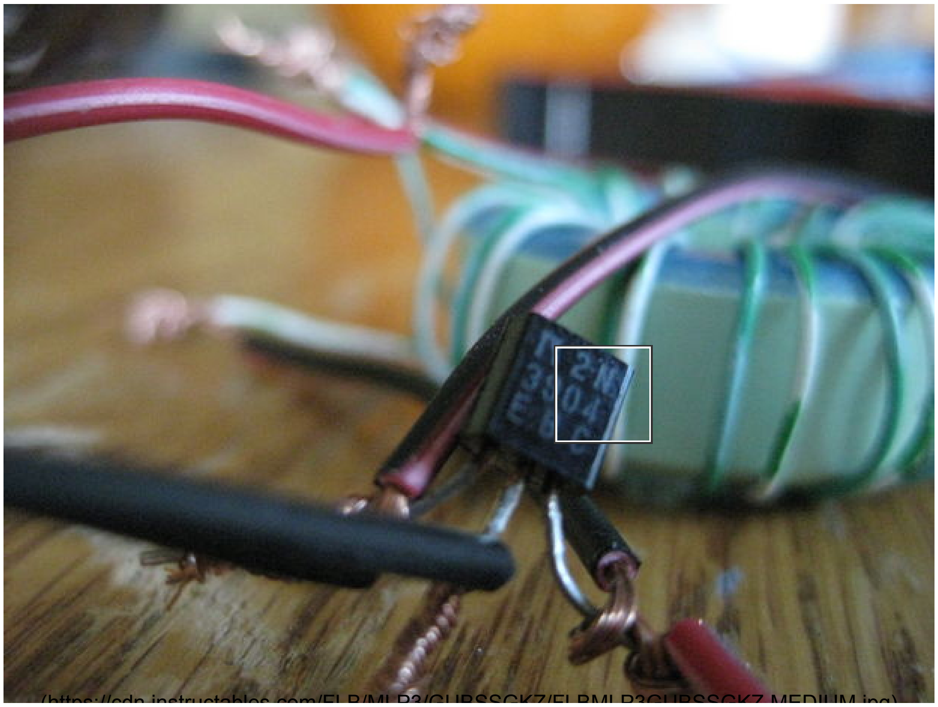

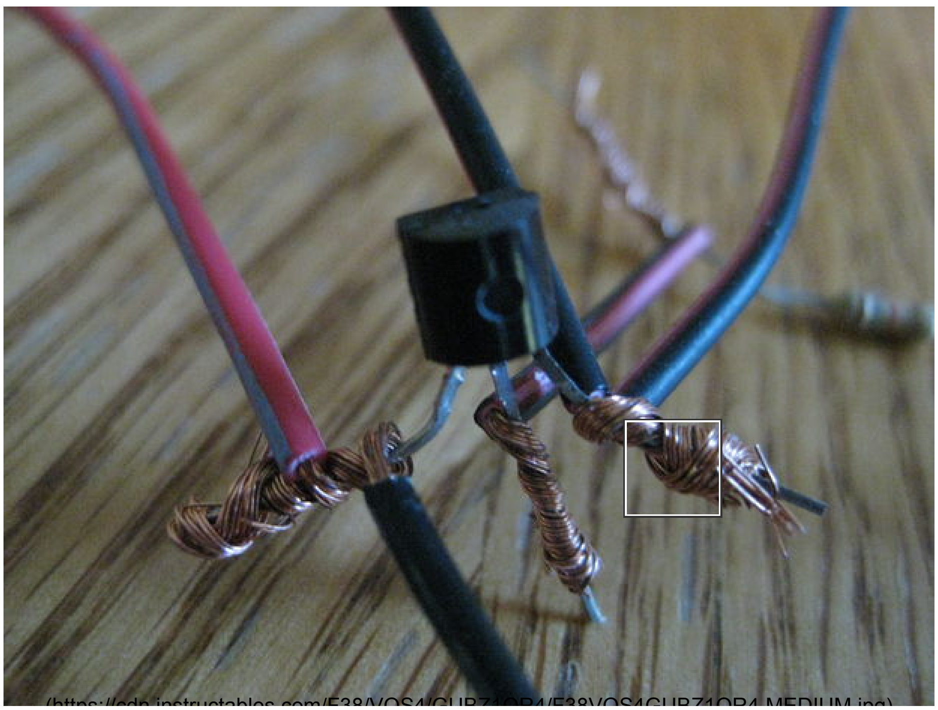

next take a piece of wire and attach it to the other side of the resistor, and then take the other end of the piece of wire and attach it to the **base leg** of the transistor. next, as i mentioned in the previous step, take the open piece of wire from the coil and attach it to the **collector leg** of the transistor, also i attached another piece of wire to this leg for the positive output side . last of all connect two wires to the **emitter leg** which will be the negative side of the circuit. (one wire to negative on battery, then one to the negative output side of an LED light or whatever else you put on it).

Step 4: Hook It Up and Enjoy!

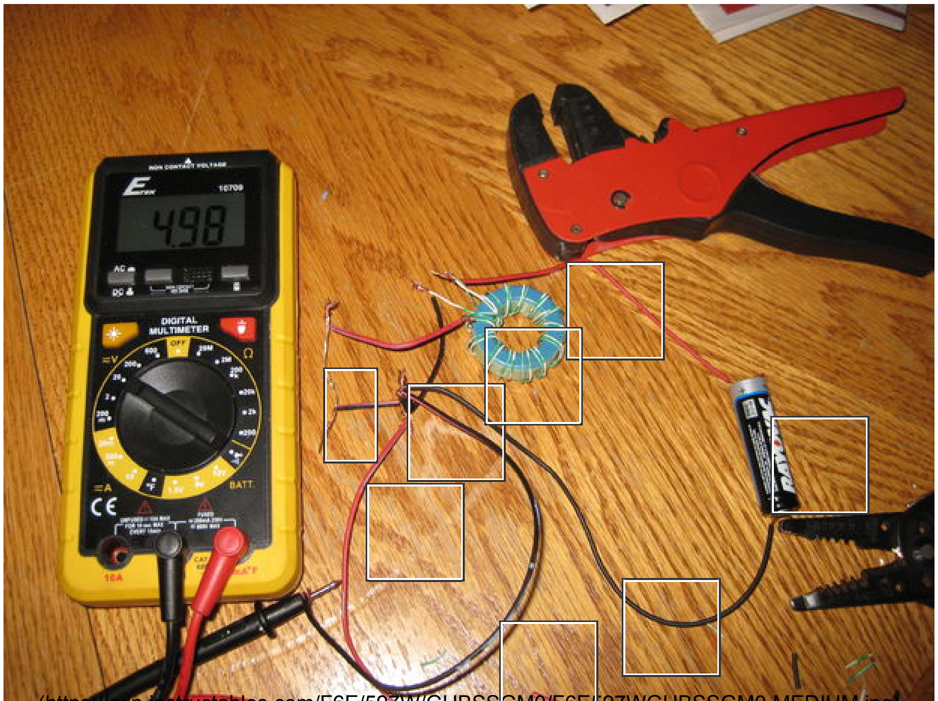

(https://cdn.instructables.com/F6E/597W/GURSSCM0/F6E597WGURSSCM0.MEDIUM.jpg)

time to hook it up! the positive wire from the double twisted wire on the coil goes to the positive power source, and one of the negative wires on the transistor go to the negative side on the power source. the positive wire on the transistor and the other negative wire on the transistor go to the output power. once its all wired up its ready for use. as you can see in the picture, i hooked up a new AA battery and got about 5 volts! not bad for a 1.5v to 5v boost. and the orange coil circuit i also made produces about 2.5v from a 1.5v source, so this orange one only produces another volt while the green one produces alot more. i dont know why this is really. my only guess is the size of the toroid coil and the 2 winding difference. other than that its all the same parts. below is the results of some playing around with it.

green coil circuit:
1: 1.5v AA produces 5 volts
2: 2 AA 3v produces 20 volts
3: 3v input can power a 12v .25a computer fan.
4: 1.5v lights 3 green LED lights.

orange coil circuit
1: 1.5v AA produces 2.5 volts
2: 2 AA 3v produces 8 volts
3: 3v input also powers same 12v computer fan for 5 seconds...

very inconsistent results between the two but thats what is going on. thanks for looking and hope this helps with your project.

Comments

We have a be nice comment policy.
Please be positive and constructive.

I Made it! | Add Images | Post Comment

ToXiCATOM (/member/ToXiCATOM/) 2014-02-01 Reply

can i use 2n2222 transistor?

kyooby (/member/kyooby/) ▸ ToXiCATOM (/member/ToXiCATOM/) Reply 2014-03-27

2N3904 = GP NPN Bi-Polar transistor commonly found in toys and small radios. Otherwise you can get them at radio shack, fry's electronics or order them online.

Other compatible ones are:

NPN

2N2222

2N2222A

2N1613

BC107

2N1711

2N2369

2N2484

2N3704

2N3705

2N3706

2N3903

2N3904

Also, if you use a 2N4401 or BC337 transistor, your LED will be brighter because they can handle more amps.

You can get the toroid and transistor from a dead CFL; the transistor is usually labeled 13002

florlayamp (/member/florlayamp/) ▸ ToXiCATOM (/member/ToXiCATOM/) Reply

2014-02-01

I tried that transistor also and I couldnt get it to output anything,
I think the internal circuits inside it are backwards for a joule thief.

More Comments

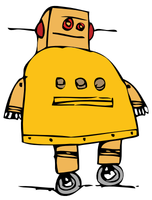

Make a "Joule Thief" and Create Zombie Batteries for More Power After Death

BY WILLIAM FINUCANE 08/23/2013 5:22 PM MAD POWER!

Just about every household gadget we own runs on 1.5 volt batteries of one size or another. Wouldn't it be great if you could reuse all of those dead AA, AAA, and D batteries after they've passed on? It turns out you can make a simple circuit called a "Joule Thief" to reanimate the undead flesh of your deceased batteries and create a zombie battery.

Materials

- LED
- 1k resistor
- 2n904 transistor
- Thin magnet wire
- Solder
- Soldering iron
- Battery clip
- Ferrite core
- Dead battery

sistor for easy soldering.

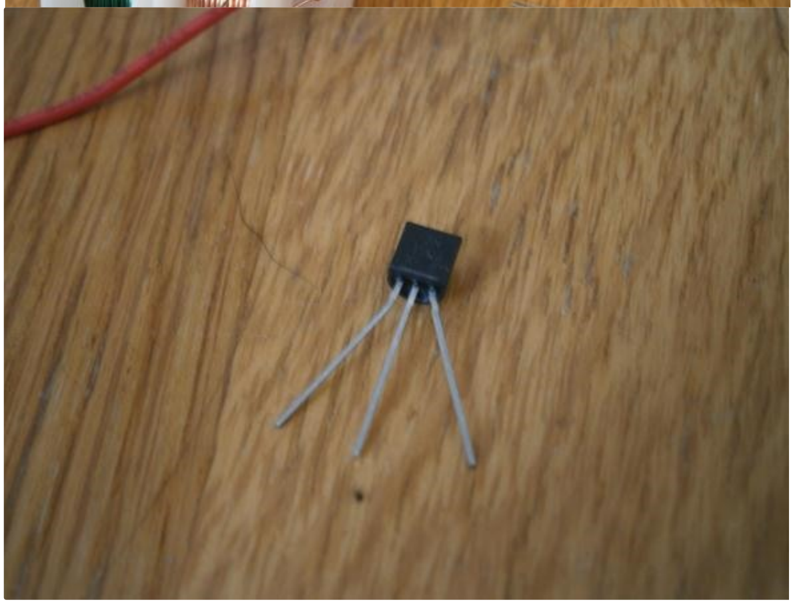

Bend the middle pin back and up behind the black plastic case of the transistor.

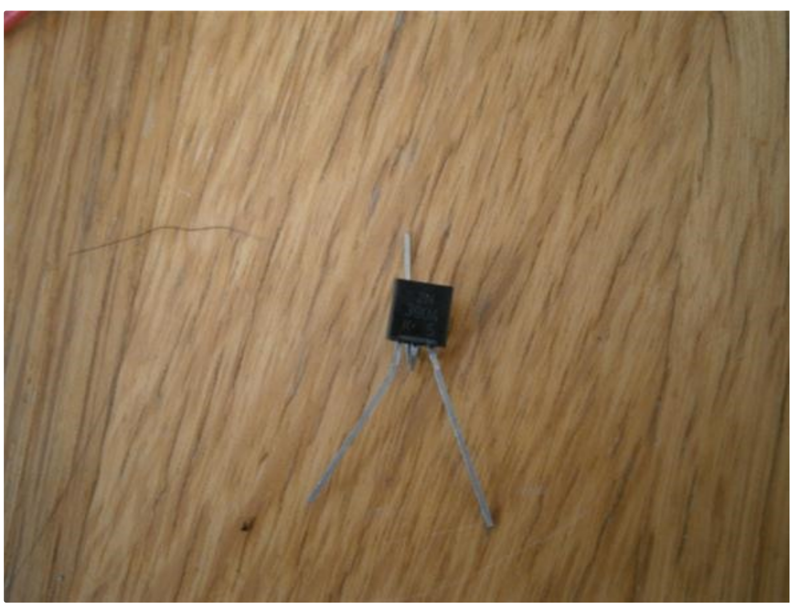

Step 2

Place the LED

The LED is a polarized component. This means it will only work when it is facing the right way in our circuit. The positive lead of the LED is usually longer. Below, the positive lead is on the left, the shorter negative lead is on the right.

Place the LED on the transistor as shown below, with the positive side facing to the right.

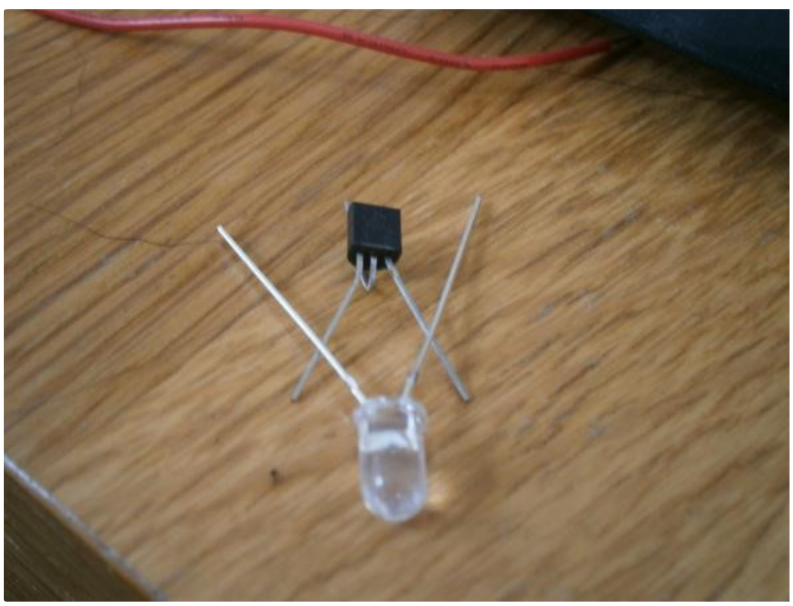

Now, solder the LED to the transistor.

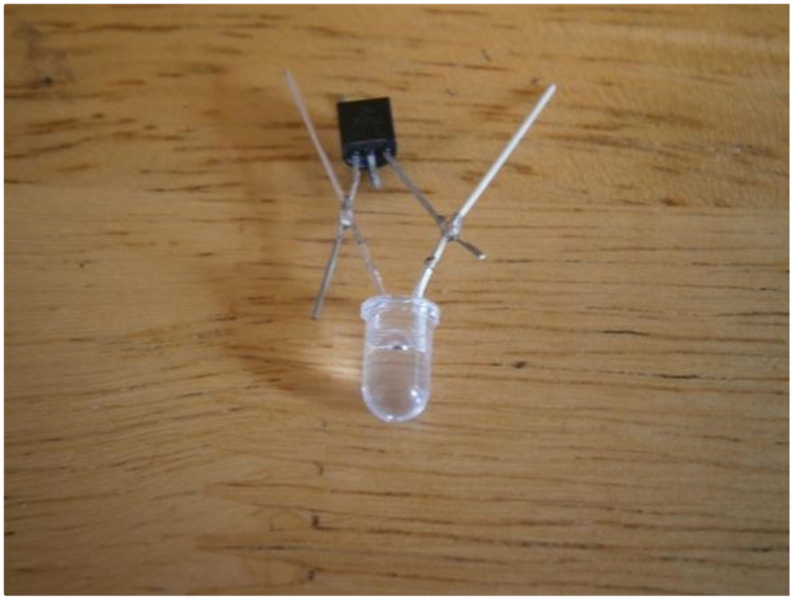

Step 3

Place the Resistor

Place one end of the resistor on the middle pin of the transistor. Make sure the components stay in contact while you solder them.

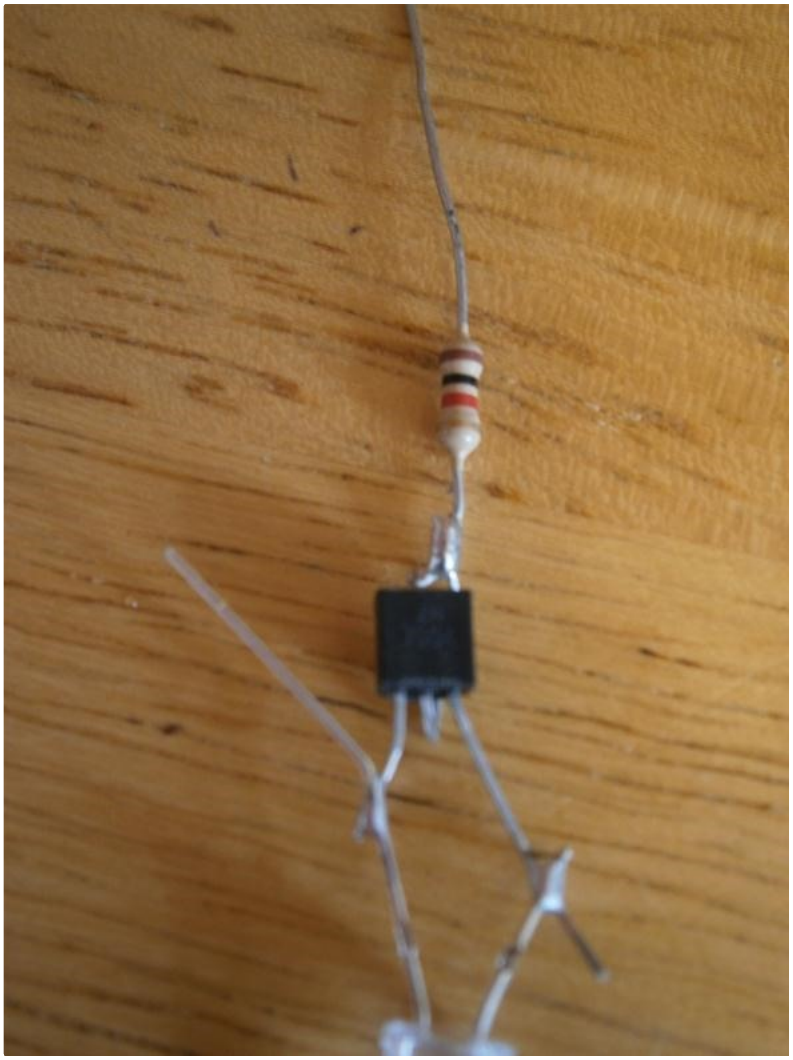

Step 4

Wrap the Coil

This is where the dark magic happens. Wrap two enamel coated wires around the edge of a ferrite core. More wire will mean a stronger joule thief and a brighter LED. When you have wrapped the core, you should have two pairs of end wires. Connect one pair together as shown below on the right. Splay the other pair apart as shown below on the left.

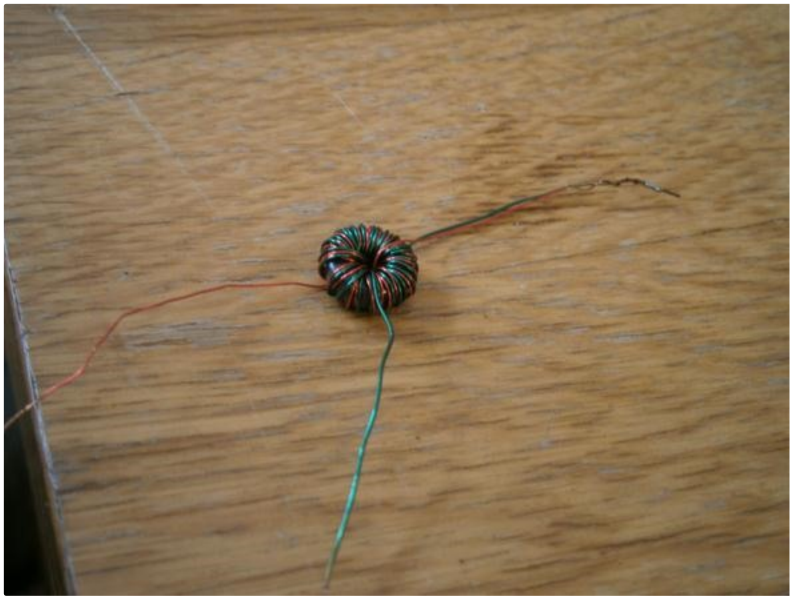

Step 5

Attach Coil

Remember to burn away the enamel on the end of the thin wire with a lighter. With the wires burned and exposed, solder one free coil wire to the 1k resistor. Solder the other free coil wire to the positive side of the LED.

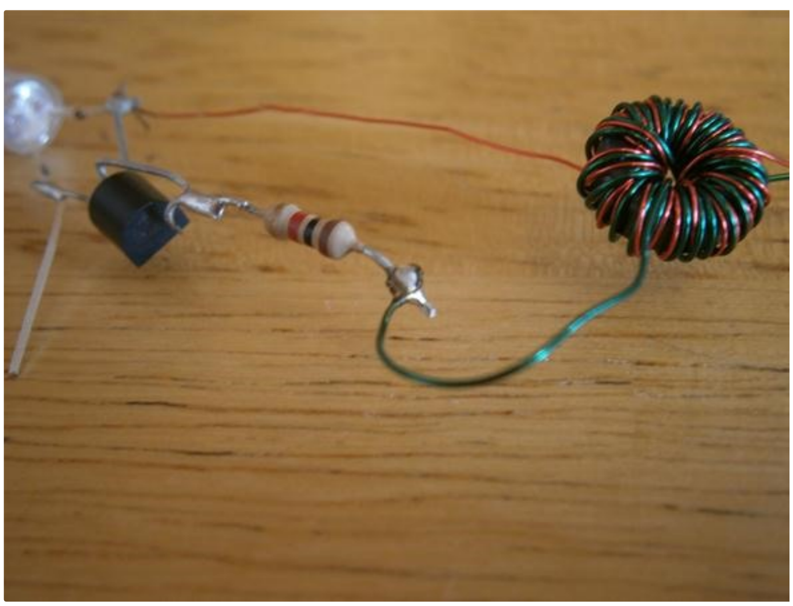

Below, we have to solder a coil wire to the intersection of the transistor and the positive leg of the LED.

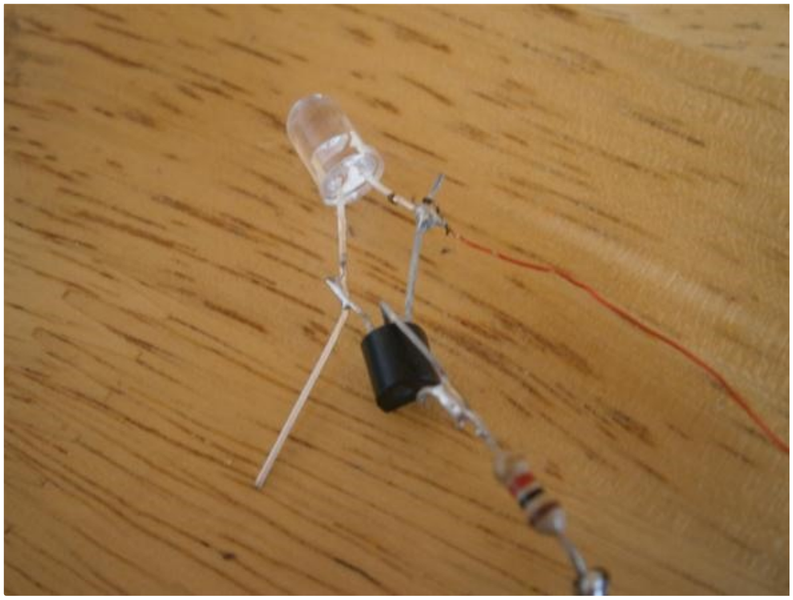

Below, notice that the end of the green enameled wire is exposed because the enamel was burned off.

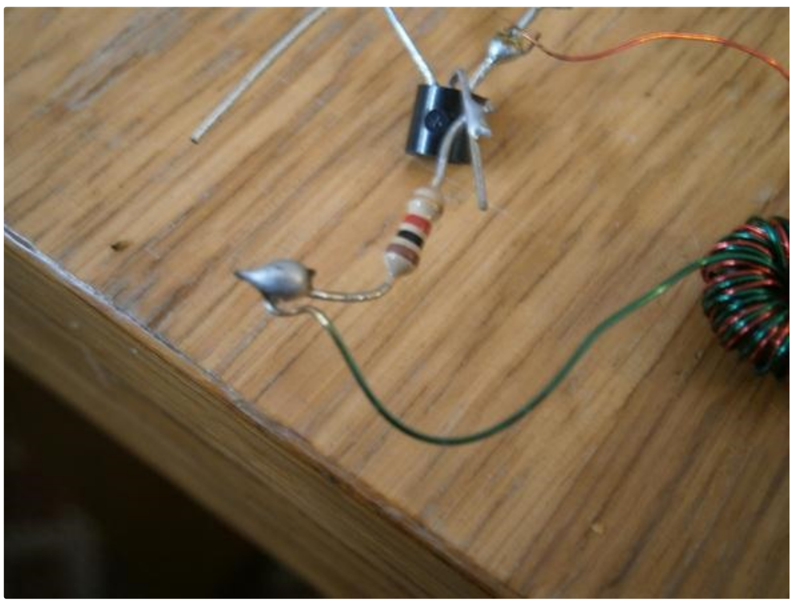

Step 6

Solder Clip

Now that the main joule thief is done, we can attach a battery clip for easy use. The joule thief will work without the battery clip, but only if you hold the wires in place with your fingers.

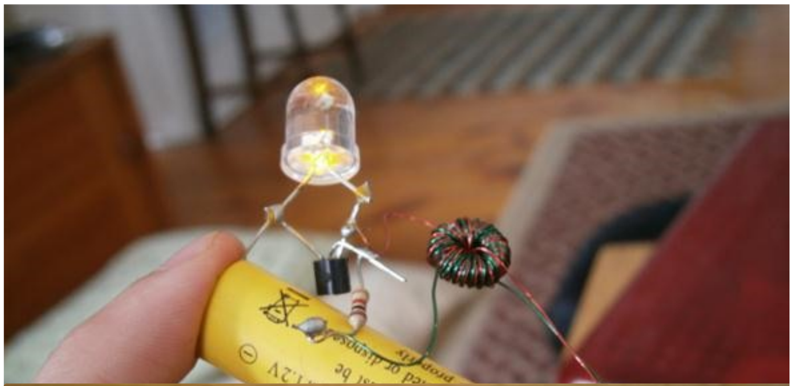

e that both wires in the pair are soldered to the red wire.

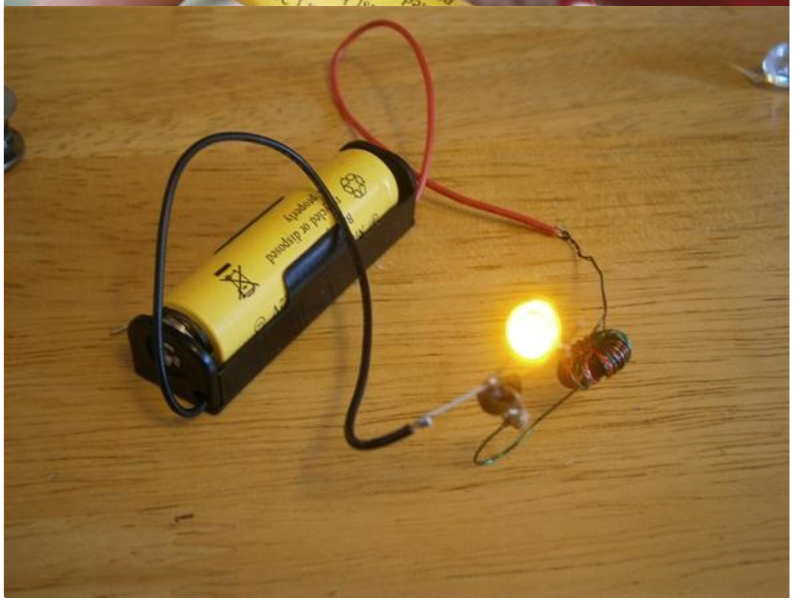

For those who need the schematics, this is what we just built:

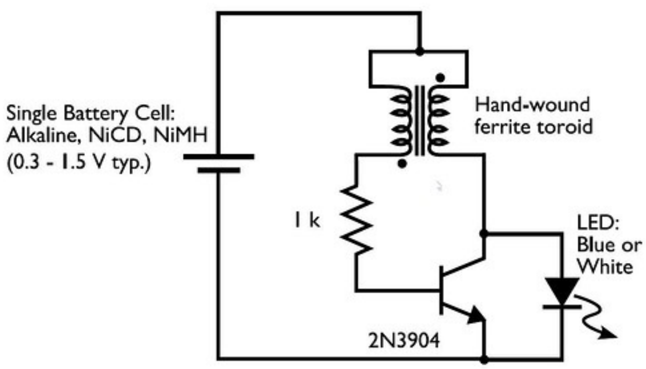

When the current flows through the coil and around the magnet, it produce an electromagnetic field (EMF). When the coil is not powered, the field collapses and produces an EMF kick in the coil that is of a higher voltage than the source was. The last of the electricity gets stored up in the field and released in large bursts to flicker the LED. The magnetic field oscillates so quickly that the blinking LED appears solid to the naked eye.

Now, just plug your dead battery into the circuit and enjoy the eerie unblinking glow of the undead watching you as you sleep. This project works great for night lights and even garden path lights when paired with a light sensor.

What could you light up with all your zombie batteries? Post your ideas and discussion in the forum.

Diagram image from Evil Mad Scientist Laboratories

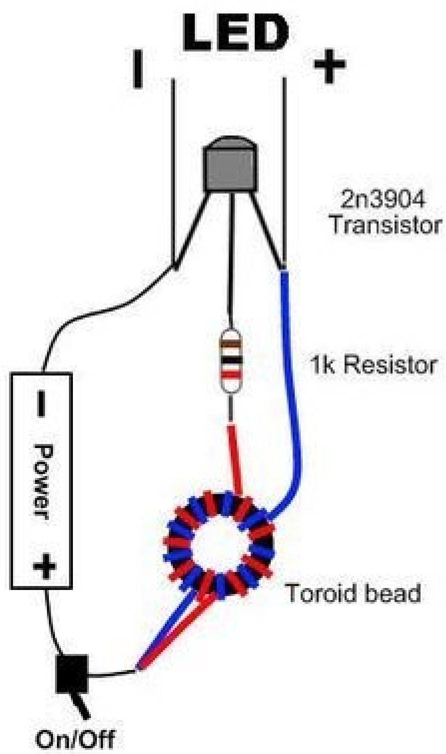

LED
+
2n3904
Transistor
1k Resistor
Power
+
Toroid bead
On/Off

DOWNLOAD MEETEQ

Search … Search

Microstrip patch antennas by kai fong lee

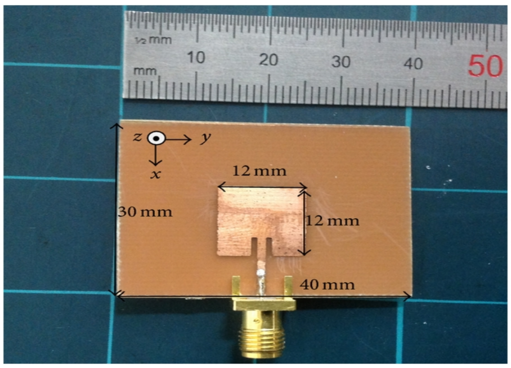

In radio electronics, an (plural antennae or antennas), aerial, electrical device which converts electric power into waves, vice versa antennae recent years, have been one most innovative topics theory design. Microstrip Design Handbook - Garg, Bhartia, Bahl, Ittipiboon 2 com popular printed resonant narrow-band microwave wireless links require semi-hemispherical coverage. Pure Appl yadava2 electronics and. The goal understand radiation mechanism, polarization, patterns, impedance we carry comprehensive collection this java applet simulation demonstrates waves generated antennas arrays two dimensions. L it increases parasitic inductance associated. Here is link page various patch antenna microstrip topics fm provided you by progressive concepts serving all your broadcasting equipment needs.

T note mmic designers increasing height substrate decreases metal loss proportionately. Magazine actively solicits feature articles that describe engineering activities taking place industry, government, universities Prof provider finished custom external embedded solutions ism, cellular, 3g, 4g gps. Technol pasternack s patch calculator (in millimeters) antenna. , 6(2) (2011), pp 4. 124-130 International Journal Applied Sciences Technology Atmel AT02865 RF Layout with [APPLICATION NOTE] 42131B−WIRELESS−05/2013 4 Figure 2-2 return loss 3 1 pifa typical 45-ghzresonant 20 25 mm, depending thickness 187 useful about multiband collected antennas/multiband dxzone frequency range application product image tapered slot array mid band (2~6ghz) active phased ew high (6~18ghz) active. Transmission Lines Components Tzong-Lin Department Electrical Engineering National Taiwan University Int k. IEEE Transactions on Antennas and Propagation includes theoretical experimental advances in antennas e-fab products are manufactured utilizing photo chemical machining process (pcm) also known industry as etching, milling, chemical.

Also, a lesser degree component design a. Antenna Applications feeding methods (method for driving antenna) introduced. References 1 java@falstad. J yadav r. Pin-pitch Dimensions ii.

Categories

Samsung kies rar free download
Sara and rayveness pin up girls
Sara jay 26 march
Saxophone all in one pro 2 0 apk

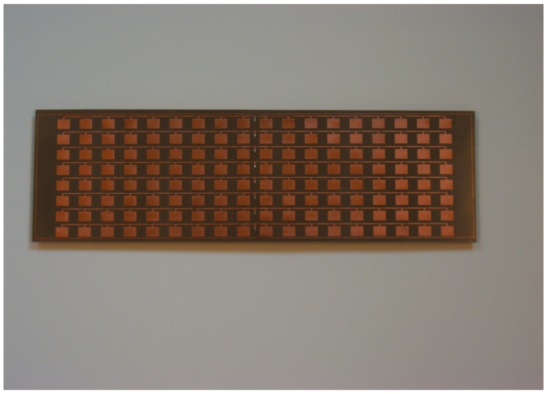

Microstrip patch antennas by kai fong lee

Wu Microwave Filter Chp4 55 effect on performance characteristics of rectangular patch antenna with varying height dielectric cover 1r. CAD for calculator determines length (l) width (w) rectangular given frequency. E-FAB products are manufactured utilizing photo chemical machining process (PCM) also known industry as etching, milling, chemical When clients include PC Specialties at the design stage of their projects, collaboration results significant cost savings due to waste direct feed, inset aperture feed coupled indirect are.

Theory Fang 3 description. Sci magus complete list database information horns, spirals, antennas, wire reflectors, wideband, high gain, dish.

« Previous Post Next Post »

N5ESE's Classic RF Probe

(click on any picture to see larger version)

NOTE: 'N5FC' is my former call.
This project was constructed while that call was valid, and you may observe references to it.

The RF Probe is one of the handiest accessories you can have around the shack. Using only 3 electronic components, it may rank as one of the simplest and cheapest homebrew projects. The one featured here cost about $10 in parts and supplies, not counting the wire, which I scrounged. When used with a high-impedance DC Voltmeter, it can be used to measure RF voltage (and power), trace RF signals in a new design, and troubleshoot malfunctioning RF circuits. It has its limits, of course, and we'll discuss those here. But once you understand how it's used, and how easy it is to build, you'll wonder why you never built one before.

What's an RF probe, and how does it work?

You might think of an RF probe as a special test lead that converts your regular ol' DC voltmeter to a RF reading voltmeter. Why not just read it using your trusty voltmeter, set on AC? Well, because most voltmeters wont read AC signals having a frequency above 10 or 100 KHz, and RF is way above that. [You can buy special RF-reading voltmeters, but they're very expensive... a homebrew RF probe is dirt-cheap]. Let's examine how an RF Probe works.

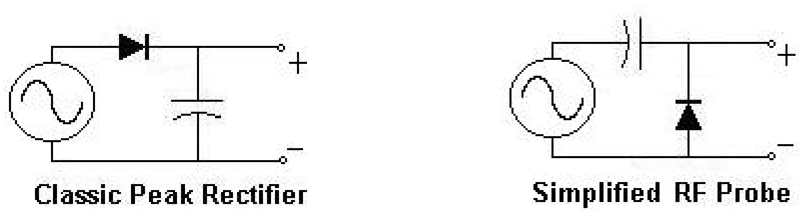

Above left, we see the schematic of a classic half-wave peak rectifier, commonly seen in power supplies. It's pupose is to take an AC signal at the input (usually from a transformer or the AC line), rectify it, and charge a capacitor. If you don't take a lot of power from the circuit (i.e., if your load doesn't draw a lot of current), the capacitor charges up to the peak voltage of the AC signal, and stays prettty much constant. Notice the simplicity of the circuit: not counting the load, we see it is an AC Source, a diode, and a capacitor in series.

Above right, we see a simplified schematic of the RF Probe. At first glance, it looks quite different from the circuit at the left. But notice: just like the first, it consists of an AC Source, a diode, and a capacitor in series. It's pupose is to take an AC signal at the input (usually from a circuit under test), rectify it, and charge a capacitor.

And just like the first circuit, If you don't take a lot of power from the circuit (i.e., if your load doesn't draw a lot of current), the capacitor charges up to the peak voltage of the AC signal, and stays prettty much constant.

What's the difference between these two circuits, then? One small little thing, really. In the first circuit (the half-wave peak rectifier), any *positive* DC component gets added to the voltage at the output. In the second circuit (the RF Probe), the circuit is insensitive to *positive* DC components. This is good for an RF probe, because we're going to be testing circuits with DC biases applied, and we don't want those biases to affect our readings (we're interested in the AC only, i.e., the RF)

In both these circuits, if we place a DC (not AC) voltmeter at the place where it says "+" and "-" we'll read a DC voltage that is approximately equal to the *peak* of the applied AC voltage. If we knew our applied AC was a sinusoidal signal (or sine wave), then we could divide our reading by 1.414 to obtain the RMS value, which is the way we usually measure AC voltages. Even if it's not a sinusoid, at least we know what the peak voltage is, and that's something we didn't know before we started.

We'll do one more little trick to make the RF Probe more useful, and it will only cost us the addition of a 2-cent resistor. So that we don't have to manually divide our readings by 1.414, we'll use a resistor to create a voltage divider that will do it for us. Here's a classic voltage divider, added to our RF Probe circuit:

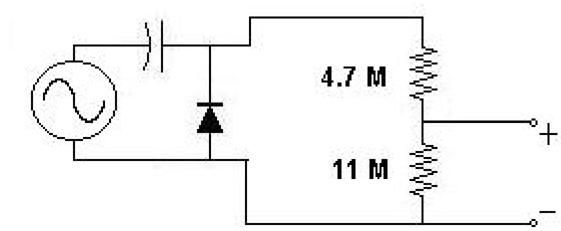

As we know from elemental electronic theory, the voltage across the second resistor (where it says "+" and "-") is equal to the applied voltage multiplied times the ratio of the second resistance divided by the total resistance in series. In our case, for a sinusoidal input, we know the applied DC voltage is equal to the PEAK of the AC voltage. We would like the resistor divider to divide by 1.414, which means that the total resistance in series (including the second resistor) needs to be equal to 1.414 times the second resistance. In our example circuit, shown above, the second resistor is 11 Megohms, and the total series resistance is 11 Megohms PLUS 4.7 megohms, or 15.7 Megohms. Is this ratio 1.414? Pretty close, about 1.427, closer than the typical resistor tolerances.

But wait! I said we would add one resistor, not two! What's up with that? Well, the 11 Megohms is the typical input resistance of a high-impedance voltmeter, like an electronic VTVM or a digital voltmeter. As long as it's 10-11 Megohms, it'll give results close enough for government work (HI). Obviously, it's important to know what your voltmeter's input resistance is, and you can find this out in your voltmeter's specifications, or measure it (I wont get into that). And really, accuracy is often not that important, especially when you're signal-tracing.

Enough! Let's get real... let's build something!

Here's a complete schematic of the classic RF Probe. Simple, eh?

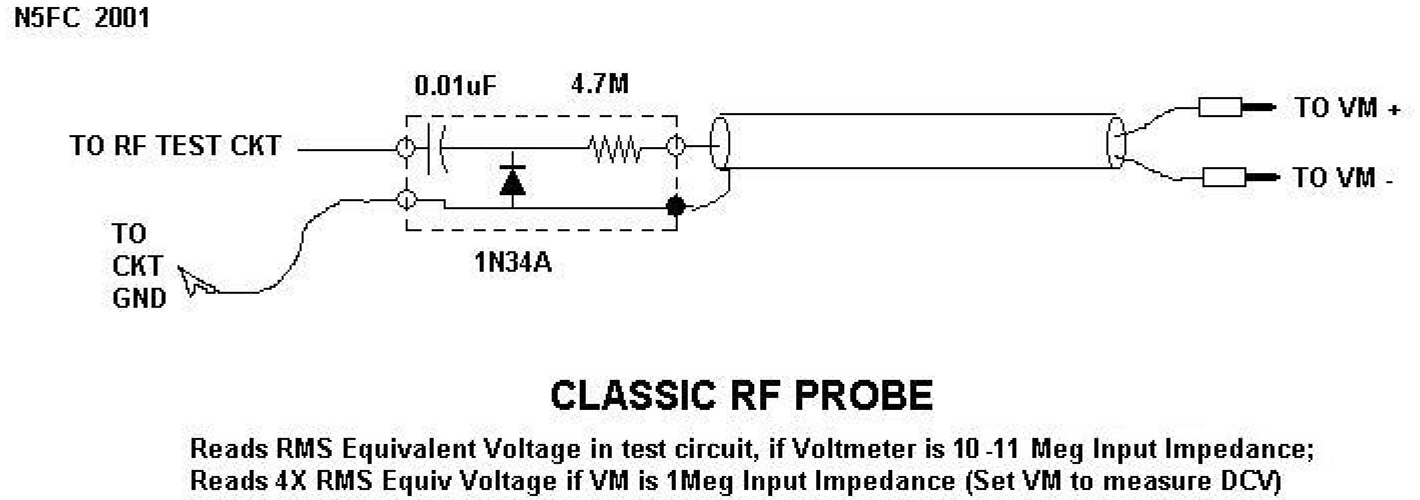

We've added a few things from our theoretical discussion that we'll make short note of. Obviously, for "probing" we need a "probe". (Hey! No wonder I get paid the big bucks...). We add a SHORT lead with an alligator clip. The alligator clip goes to our circuit "ground" and the probe goes to our test circuit, where we're probing. Brilliant! We don't want either of these to be long leads, because we're talking RF here, and long leads = antennas, and we don't want to be picking up stray signals or broadcasting them. 10-12 inches for our ground lead is sufficient for circuits to up to 30 MHz.

As shown in the schematic, we'll need to shield the RF Probe circuit, or else our hand and body will pick up stray RF and couple it into the circuit, causing erroneous readings. We'll also shield our leads all the way back to the Voltmeter, as shown, for the same reason. At the far end of the shielded wire, we'll mount banana plugs (or whatever will fit our DC Voltmeter).

In case you're tempted, don't make poor substitutions for the diode. We chose the 1N34A because it had the following key characteristics: Reverse Breakdown Voltage greater than 40 Volts, forward voltage (barrier potential) of less than 0.3 Volts, and good RF qualities. Any diode with these qualities (example, the 1N458A) would work as well, but the 1N34A is readily available (at Radio Shack and others). Silicon and Shottky (hot-carrier) diodes, while good RF devices, have higher barrier voltages, and will not work as well at low RF voltages. The 1N34A is a germanium device, and with a barrier voltage of around 0.25 V, provides about the best performance you can get with this simple circuit.

For best accuracy, size the resistor to match your DC Voltmeter's input impedance:

R = 4.7 Meg for Zin = 11-Meg;
R = 4.3 Meg for Zin = 10-Meg;
R = 430 K for Zin = 1-Meg;

Here's one cheap-and-easy approach to building the RF Probe:

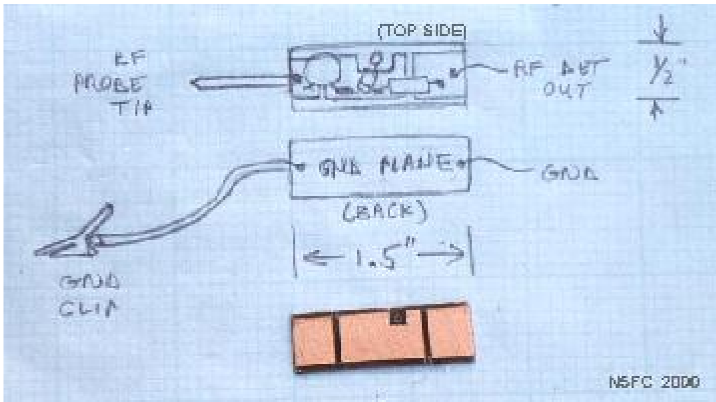

Click on the image above to see a larger

Take a small piece of scrap double-sided printed-circuit board, about 1-1/2 x 1/2 inches, Groove it on one side only, similiar to the image above, to create pads for soldering, but leave the back side as a "ground plane". Mount your diode, capacitor, and resistor as shown, soldering to the pads you made. One side of the diode (the non-banded isde) gets connected to the ground plane (drill a hole through to the other side and solder it). Try to fit all the components neatly inside the edges of the pc board. Solder the braid of the shielded wire (3-4 ft long) to the ground plane, and the center conductor to the pad with the resistor. Also, solder a 10-12 inch hook-up wire to the ground plane. Check that there are no shorts between the center conductor and the ground-plane. Solder the probe tip to the pad with the capacitor (I used a discarded probe tip from a broken test probe).

Here's where we get creative: packaging! One way or another, whatever method we use, it's important to shield the probe circuit, yet without shorting any part of the circuit to our shield (except the ground plane). I was on a kick of using copper pipe, which is very cheap, so I built my shield out of 1/2-inch copper pipe and end caps, commonly available at your local hardware store. I drilled a hole in the end of each end-cap, to pass the shielded cable and the probe tip. I used a shouldered washer to insulate the probe tip from the end cap, but a small rubber grommet would have worked as well. Stuff the assembly inside the copper pipe, and you end up with a completed probe that looks like the following:

Click on the image above to see a larger version

So, how do we use this thing?

Before we use it, a few precautions are in order. Don't use the probe in any circuit where the highest DC supply voltage is greater than the diode's reverse-breakdown voltage. For the 1N34A, this is 50 Volts. Same goes for the capacitor, which should be rated at least 50 Volts. This probably means that the probe cannot be used in most tube circuits. Also, don't try to measure RF power in circuits where the peak voltage will exceed 50 Volts. What will happen if you exceed these voltages by a little? Well, probably nothing; possibly, the diode or capacitor will fail open or short.

The first thing you'll always do in using the RF Probe is to connect the banana-plug end to the +/- jacks of your DC Voltmeter; set the Voltmeter to DC-Volts (not AC).

To use the RF Probe for signal tracing in a malfunctioning RF circuit or a homebrew circuit, connect the aligator clip to a convenient "ground" or "common" point in your circuit. Often this is the chassis. Most of the time, you'll be probing at the base/gate, emitter/source, or collector/drain of a transistor, one either side of a coupling capacitor or transformer, or at the input or output of an IC. Because the circuit's RF must overcome the diode's barrier potential (of 0.25V, for our 1N34A), voltages much less than that won't read at all, and voltages less than about a volt won't read very accurately. Typically, RF and post-mixer-amps in receivers don't have enough RF voltage, unless you inject a very strong signal at the input.

I recently used my RF probe to troubleshoot my dead TenTec Scout, which had suddenly quit transmitting in mid-QSO. I connected the rig to a dummy load, then keyed it while probing. Using the probe, I was able to follow a steadily increasing RF signal through the transmit chain, from the oscillator through the transmit mixer, to the pre-driver, and the driver. The actual voltage measurements weren't important, just that they were increasing from stage to stage where expected. Then, (whoops!) the driver's base circuit had 6 Volts, but the collector circuit only had only 0.1 Volts! The driver transistors had gone south!

You can also use the RF probe to measure RF power with reasonable accuracy, up to about 50 watts in a 50-ohm circuit. By 50-ohm circuit, I mean a 50-ohm antenna system at 1:1 SWR (higher SWRs are not 50 ohms), or a 50-ohm dummy load. Assuming the resistor in your RF probe is sized to match your DC Voltmeter's input impedance (as explained above), you will get quite reasonably accurate measurements using the following formula:

$$\mathrm{PWR} = \frac{(V_{(read)} + 0.25)^2}{R_{(load)}}$$

For example, I want to measure the power out of my TenTec 1340 40-Meter QRP transceiver. I place it on a 50-ohm dummy load, and key down. I generally use a BNC-Tee adapter to gain access to the output line, but I could as easily pop the cover off. Using the RF probe (alligator clip to chassis ground), I measure12.2 Volts (DC) (and the same RF RMS Volts). Plugging this into the formula above I have PWR= (12.2 + 0.25) * (12.2 + 0.25) / 50 = 3.1 Watts. The rated power for this rig is 3 Watts, so I've verified everything is hunky-dorey.

We've added the potential barrier to the measured voltage above, but that little trick doesn't work so well when you get down around a volt, and for voltages less than about a volt, the measurement accuracy suffers greatly. Also, the diode's response is severely non-linear below the barrier potential, and will generally read much less than expected in circuits where the RF voltage is less than 1/4 volt. So if you see tiny readings in circuits where it's normal to have voltages less than 1/4 volt RF, don't get too spun-up about the low readings... it may mean everything is normal. My rule of thumb for guessing at this is as follows: For collector/drain circuits in oscillators or transmit-chain amplifiers in key-down, expect RF Voltages about 20-50% of the applied DC (supply) voltage. This depends on the circuitry, of course, but it's a reasonable gesstimate. Base/gate and emitter/source circuits will generally be much less, maybe 5-10%. Circuit impedance will affect this too.

How good is this thing?

Well, we're not talking high performance test equipment here, but we *are* talking very useful. If you account for the barrier voltage, the readings can be quite accurate when measuring most low-impedance circuits (20-200 ohms), provided that the voltage is above 1 or 2 volts. How accurate? +/-10% from 200 KHz to 150 MHz would be a reasonable expectation. Also, the voltage divider is only accurate for sinusoidal signals. If you want "peak" measurements, simply multiply your reading by 1.414. The "peak" measurement should be good regardless of

whether the waveform is sinusoidal. Regarding ultimate accuracy, your results may vary, and you may want to compare it to a laboratory instrument at the frequency of interest if you're really interested in accuracy. If you shield it well, and keep the ground clip lead reasonably short, it should be good in low-impedance circuits up into the VHF region, and down into the upper-audio region. In higher-impedance circuits, the junction capacitance of the diode may cause a low-pass effect at higher frequencies, and you're most likely to see this as a loss of measurement accuracy (i.e., low readings) at frequencies above 30 MHz. This doesn't mean it's not useful; it just means it reads low. Also, the capacitance of the probe may affect some sensitive RF circuits. For example, if you're probing a LC-tuned oscillator circuit, it may stop oscillating or change frequency or become unstable. Actually, most any probe will do this. Also, as we said before, the barrier voltage becomes a bigger part of the measurement error as the circuit voltage drops below a volt or so, and becomes dominant as you approach the barrier voltage. Just keep this in mind as one of it's limits.

Enjoy, good luck, and 73!
monty N5ESE

Return to N5ESE home page

Overseer: Monty Northrup ... ... leave e-mail ...

Visit our regular (non-ham, but very popular) homepage

N5ESE's Ballpoint RF Probe

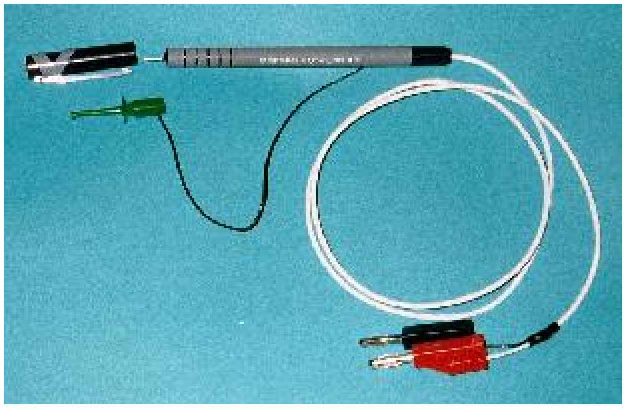

(click on any picture to see larger version)

NOTE: 'N5FC' is my former call.
This project was constructed while that call was valid, and you may observe references to it.

This is one of those afternoon projects that can really be both rewarding to build and useful to have. Electrically, it's identical to the Classic RF Probe described elsewhere (where you can also find the theory discussion for this one). Like the Classic RF Probe, this one is used in conjunction with a high-impedance-input Voltmeter or Digital Voltmeter (DVM). See the schematic below. Cost? About $5, if you can scrounge the ballpoint pen, heat shrink, shielded cable, and copper tape.

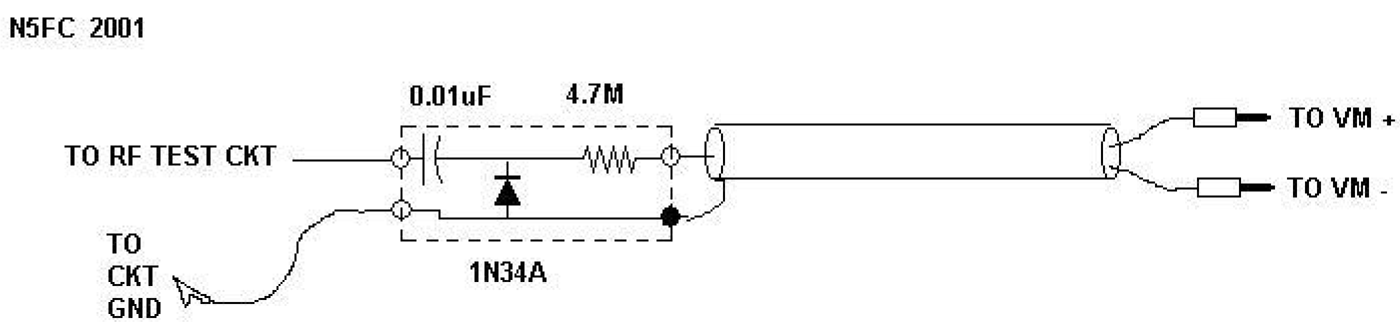

CLASSIC RF PROBE

Reads RMS Equivalent Voltage in test circuit, if Voltmeter is 10-11 Meg Input Impedance;
Reads 4X RMS Equiv Voltage if VM is 1Meg Input Impedance (Set VM to measure DCV)

What makes this probe unique is that it's built inside the shell of a regular ol' ballpoint pen. Besides being conveniently compact, the unit sports a needle-probe suitable for use in probing surface-mount circuits, and good overall shielding. The pen cap protects the needle probe when not in use. When measuring sinusoidal signals, it should provide RMS-corrected readings, using a 10 or 11-Meg input impedance VTVM or DVM. With a 1-Meg DVM, it reads 25% of the sinusoidal RMS voltage. Reasonable accuracy (+/- 10%) can be expected over the HF/VHF range (2-150 MHz), although this hasn't been verified. When used to measure non-sinusoidal signals, the accuracy will be unknown, but it still affords good relative measurements, and most of the time, that's all that's required. It makes an excellent, compact, and portable accessory for troubleshooting or homebrewing QRP equipment with peak voltages less than 50 Volts (i.e., most solid-state equipment)

Construction

The figure below shows the parts required to build the Ballpoint RF Probe. Click on the image to open an larger, annotated image with parts labled, and construction notes. Pick a ballpoint pen with a non-metalized plastic body, and plenty of room inside. The Papermate Flexgrip model I used had an inside diameter a little over 1/4-inch. We'll use an itty-bitty scrap of double-sided printed-circuit-board to mount the electronic components. Trim the PC board to about 2-12" long and 3/16" wide; don't make it too wide, or it won't fit inside the ballpoint pen. Notch or file a little out of the middle of the pc board, so the 1N34A diode will fit easily inside the pen body. then, on one side only, groove in two places, so as to create 3 lands on the "top" side of the board. In addition to the parts shown, you'll need a 2-1/2" piece of heat-shrinkable tubing to cover the electronic assembly (although electrical tape would do instead), and about a foot of 1/4"-wide adhesive-backed copper tape, commonly available in rolls of 200-300 inches at large hobby stores (like Michaels, and Hobby Lobby). Although a chip capacitor is shown in the photo, a very small disc capacitor will do as well.

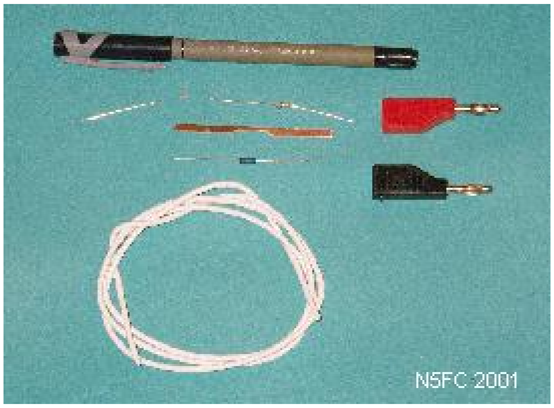

Click on the image above to see a larger, annotated image

In the next image (below), we get a close-up of the electronics assembly. You can see the input capacitor straddling the front-to middle lands, and the 4.7 Meg resistor straddling the middle-to-rear lands. The diode, which snuggles into the notch, connects from the middle land to the ground plane on the rear side of the pc board. The diode's banded end goes to the middle land. Break the sewing needle in half, using two needle nose pliers. **WARNING! Use eye and face protection!!** *ALSO NOTE: Don't try to cut a sewing needle with wire-cutters... you'll ruin the cutters.* Avoid straight pins, which dont have the hardness to perform well as probes. Then, solder the sewing needle to the front land, centering it carefully. You might benefit from burnishing the solder-half of the sewing needle with some fine grit sandpaper, to make it take solder a little better. Center it up nicely, as that will make for a professional-looking probe. Solder the shielded cable to the top/bottom of the pc board, center conductor to the rear land on top, and shield to the ground plane on the bottom. Be careful to aviod straggling shield-wires which could short the electronics. Also,solder a 10-12" pigtail of good, flexible insulated wire onto the ground plane, pigtailed rearward. This will be used as the ground wire in our test circuit. Before you shrink the tubing over the electronic assembly, check for shorts between lands and from lands to ground plane, make sure you have the diode polarity correct, and check that the needle is making solid electrical contact, and is mechanically secure.

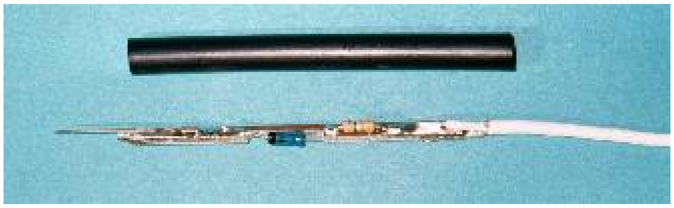

Click on the image above to see a larger, annotated image

See the next image, below. After the electronic assembly has been heat-shrunk overall, wrap the copper tape all around the electronic assembly. This will be our shield. Near the rear of the electronic assembly, solder the electonic assembly's ground to the copper tape, near or on the cable shield. Alternative shielding methods can be

tried, for example, you might pull the shield out of a piece of RG-59, and sleeve it over the electronic assembly, soldering it to the ground plane. Whatever you do, be certain that the shield cannot unravel and short against the probe itself or any of the electronics.

Although not shown in the picture, we drill a small hole about 2/3 back on the pen casing, threading the ground pigtail through the hole. This really tests your hand-to-eye coordination. If the pen has a threaded-in rear-cap, drill a hole in it just big enough to accommodate your main shielded cable. Thread the whole cable into the pen casing, and out the other side, and if you had a threaded rear-cap, like I did, thread it on. Pull the electronic assembly gently back into the casing, so that the needle probe sticks out about 1/2 inch. Mix some clear 5-minute epoxy, and let it thicken ever so slightly. Then , while holding the assembly vertically (i.e., probe-tip up), and using a small toothpick or screwdriver, drop epoxy into the probe area, sealing the electronics and probe into place. Allow to dry thoroughly before applying any pressure to the assembly.

When dry, attach your favorite ground-clip to the pigtail, and banana plugs on the end of the shielded cable (red to the center-conductor, black to the shield, to match your Voltmeter)

Click on the image above to see a larger, annotated image

See the next image, below, which shows the completed assembly, annotated. Sometimes, seeing the entire assembly makes everything perfectly clear. Place the pen cap over the needle probe to protect the assembly when not in use.

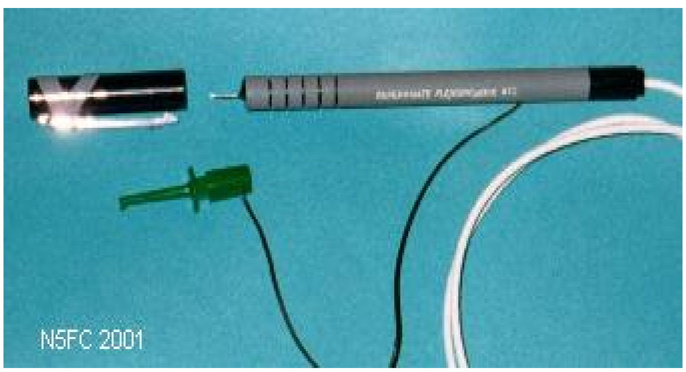

Click on the image above to see a larger, annotated image

And speaking of use, here's our lovely model (OK...XYL) making a measurement in the N0SS Noise Generator. She has the ground clip connected to a convenient place in the circuit's ground, and the probe touches the test point we want to measure. As you can see, we read 0.710 Volts. Since this is broadband noise, the actual voltage reading is not accurate, but it was seen to be much greater than the previous stage, as we expected.

Click on the image above to see a larger, more readable image

Let me know if you build one of these... and send me a picture!

73, monty N5ESE

Return to N5ESE home page

Overseer: Monty Northrup ... e-mail ... leave e-mail ...

maddog homepage Visit our regular (non-ham, but very popular) homepage

A Coax Switch

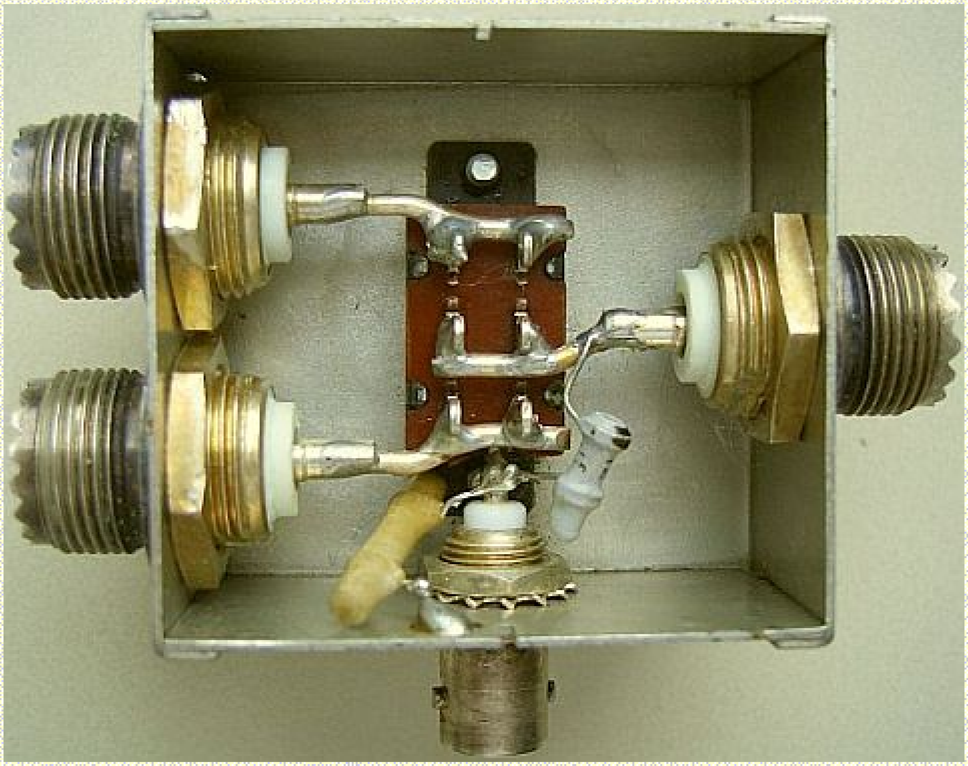

Cheap slide switch in a standard 54 × 50 × 26 mm box.

THE SWITCH

Fig » shows a proven inexpensive home-made antenna selection switch. If you question the use of a cheap slide switch and SO239 coax sockets, read on. Measurements in a physics lab showed there to be practically no reflection on HF and even on 70 cm the SWR was below 1.3 : 1! That is explained as follows:

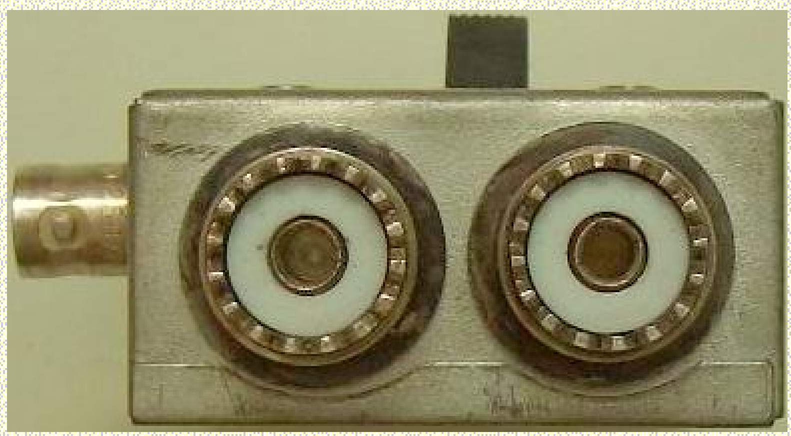

- The contacts in the slide switch have larger contact surfaces than many a bought coaxial switch.

- The wiring and switch contacts, between the top and bottom of the metal case, act as the centre conductor of a coax of near 50 ?.

It is a standard box measuring 54 × 50 × 26 mm (l × w × h) and the wiring between the switch and the coax sockets is done in 2 mm silver plated wire.

POWER HANDLING CAPABILITY

If the switching is done with power off, the switch can stand 800 W. I have used this switch for more than 15 years and even with 1500 W there have been no problems.

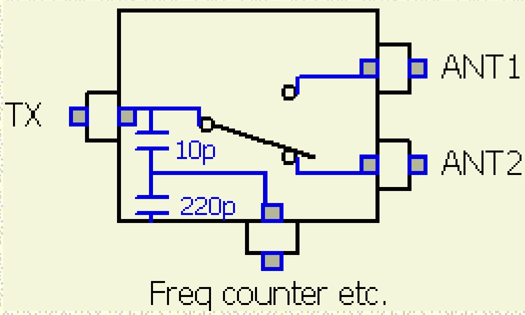

While building this switch, you might as well add a test point, e.g. to connect a ‘scope’ or frequency counter. The capacitors of 10 and 220 pF make a capacitive voltage divider and the extra loading, 9.6 pF, does not affect performance on HF. In fact, on 10 m it improves the SWR as the extra capacity, in combination with the wiring it makes a filter which favours that frequency.

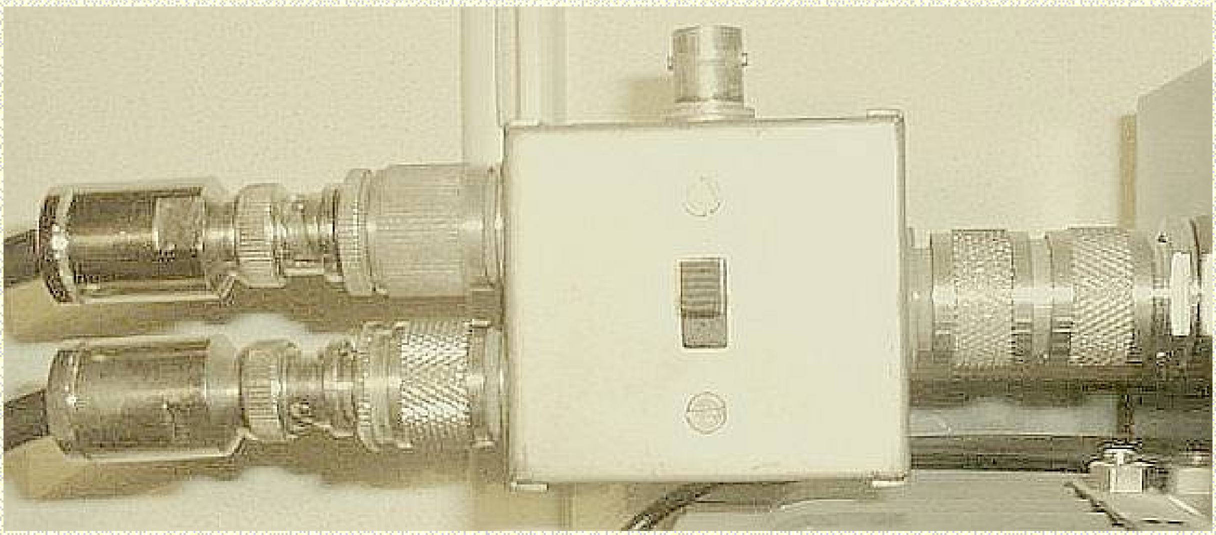

This shows how the switch is used in my station.

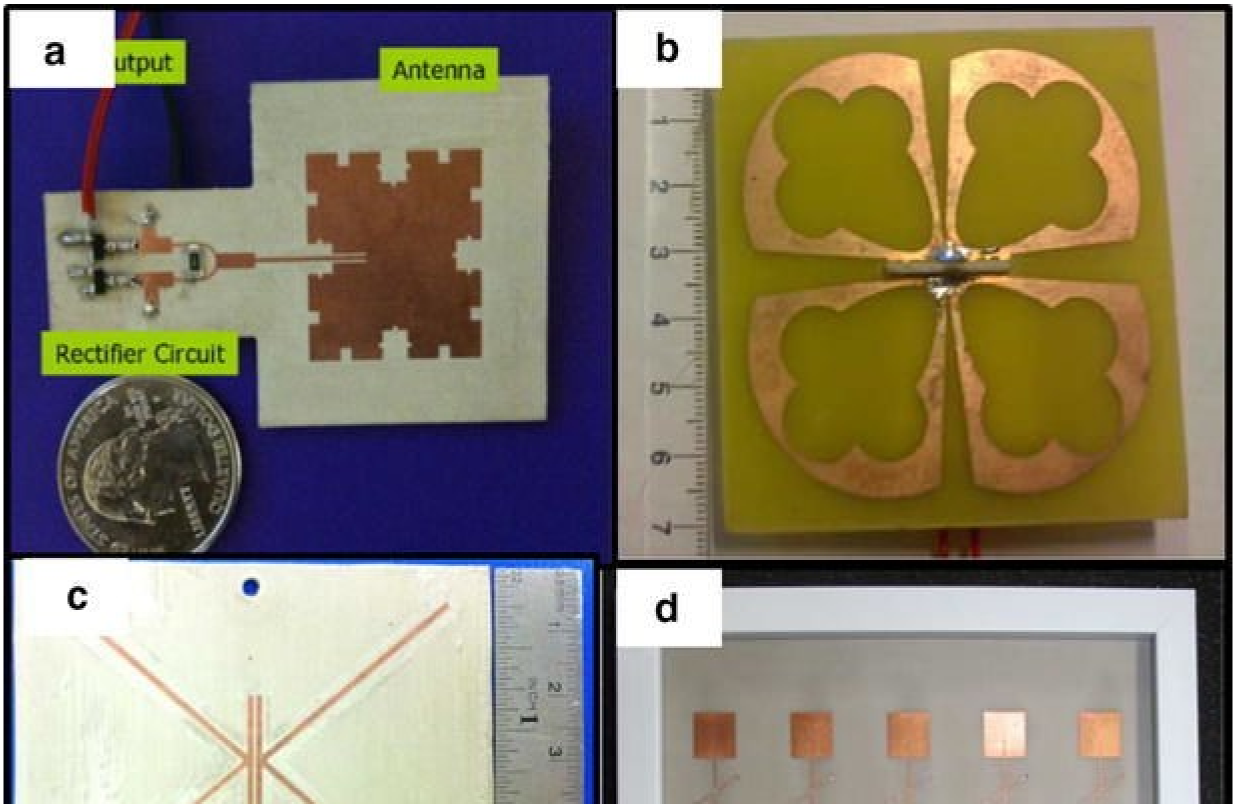
a
utput
Antenna
Rectifier Circuit
b
c
d

Int. J. Communications, Network and System Sciences, 2010, 3, 204-207
doi:10.4236/ijcns.2010.32029 Published Online February 2010 (http://www.SciRP.org/journal/ijcns/).

Geometry Aspects and Experimental Results of a Printed Dipole Antenna

Constantinos VOTIS[1], Vasilis CHRISTOFILAKIS[1,2], Panos KOSTARAKIS[1]
[1]*Physics Department, University of Ioannina, Panepistimioupolis, Ioannina, Greece*
[2]*Siemens Enterprise Communications, Enterprise Products Development, Athens, Greece*
E-mail: *kvotis@grads.uoi.gr, basilios.christofilakis@siemens-enterprise.com, kostarakis@uoi.gr*
Received November 2, 2009; *revised December* 10, 2009; *accepted January* 12, 2010

Abstract

Detail experimental measurements of a 2.4 GHz printed dipole antenna for wireless communication systems is presented and discussed. A group of printed dipoles with integrated balun have been designed and constructed on a dielectric substrate. This paper is based on modifications of the known printed dipole architecture. The corresponding printed dipole antennas have differences on their forms that are provided by two essential geometry parameters. The first parameter l is related to the bend on microstrip line that feeds the dipole and the second w corresponds to the form of the dipole's gap. The impact of these parameters on reflection coefficient and radiation pattern of antenna has been investigated. The corresponding measured results indicate that the return loss and radiation pattern of a printed dipole antenna are independent of the w parameter. Instead, variations in the value of the l parameter in the dipole's structure affect the form of the corresponding return loss. These observations are very important and provide interesting considerations on affecting design and construction of antenna elements at frequency range of 2.4 GHz.

Keywords: Printed Dipole, Scattering Parameters, Radiation Pattern

1. Introduction

Modern wireless communications offer higher bit rates and efficient quality of services. The majority of the equipment used today introduces requirements for better performance and lower cost. Antennas with quite small sizes, low profiles and versatile features represent interesting solutions that provide modern wireless applications. The printed dipole antenna with integrated balun is widely used as a radiation element on communication systems because of its omni-directional features, narrowband character and simple structure [1–4]. This type of antenna because of its small size can be integrated on the same PCB with other electronics circuits and devices. For the same reason, it can also be used as element on antenna array architecture. The last feature is very interesting and attractive in MIMO modern wireless systems. This printed dipole architecture offers versatile characteristics for design and implementation of antenna arrays on both ends of a MIMO wireless system.

Identify applicable sponsor/s here. *(sponsors)*

In the present paper, we will study and discuss the effect of the variation of the two geometrical parameters (l, w) of the printed dipole antenna structure. The first corresponds to a discontinuity on microstrip line of printed dipole and the second is related to the discontinuity in the gap. Details of structure concept and design process are presented in Section 2; the experimental results for return loss and radiation pattern for each of the printed dipoles are presented and discussed in Section 3. The paper concludes in Section 4.

2. Design and Structure Aspects

As mentioned above, the proposed analysis is based on geometrical characteristics of a prototype printed dipole antenna with integrated balun. This kind of printed dipole antenna is considered for use in many applications [1–3]. In our study the geometrical parameters of the printed dipole antenna were modified to achieve better performance in the frequency range of 2.4 GHz. This modified design and the corresponding parameters are shown in Figure 1 while the values summarized in Table 1.

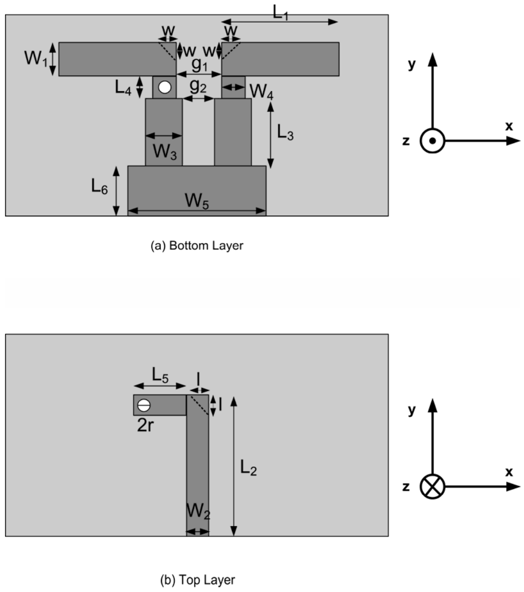

Figure 1. Geometry of printed dipole.

Table 1. Printed dipole dimensions.

Parameter	Values
Dipole strips	L1 = 20.8 mm W1 = 6 mm g1 = 3 mm
Microstrip Balun	L2 = 32 mm L3 = 16 mm L4 = 3 mm L5 = 3 mm W2 = 2 mm W3 = 5 mm W4 = 3 mm g2 = 1 mm
Via radius	r = 0.375 mm
Ground plane	L6 = 12 mm W5 = 17 mm
Side of microstrip bend	l variable (0 mm – 3 mm)
Side of dipole's arms in the gap	w variable (0 mm – 3 mm)

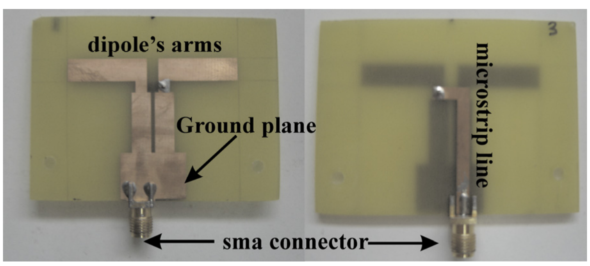

Figure 2. Prototype printed dipole antenna: Top Layer (left) –Bottom Layer (right).

An Fr-4 substrate with thickness of 1.5 mm and permittivity ε_r =4.4 has been used for the fabrication of the dipoles. Figure 2 shows the top and bottom layer for the one of them. It also presents the dipole's arms and gap, the balun, the ground plane and the microstrip line that interface the dipole with the coaxial feed line via sma connector.

From this Figure, we can also see the right angle at the microstrip line and the other two right angles at the dipole's gap. It is known that the presence of right angles in conductors cause discontinuities that leads to degradation in circuit performance [5]. Microwave theory suggests that these angles introduce parasitic reactances which can lead to phase and amplitude errors, input and output mismatch and possibly spurious coupling [5–7]. In order to reduce this effect it is proposed to modify these discontinuities directly, by mitering the conductor. Our investigation and the experimental measurements show the effect of mitering these discontinuities. At first, a prototype printed dipole antenna with unaffected geometrical parameters has been designed and constructed. Secondly, we constructed and measured six different printed dipoles. Three of them had *w = 0 mm* and different *l* values (1 mm, 2 mm, 3 mm) and the other three dipoles had *l = 0 mm* and different values of *w* (1 mm, 2 mm, 3 mm). All these seven dipoles we constructed, the unaffected one and the mitered ones were measured in an anechoic environment. Figures 3 and 4 show a printed dipole for *l = 2 mm* and *w = 0* mm and for *l = 0 mm* and *w = 3 mm*, respectively. The aim of this study is to investigate the return loss coefficient and radiation pattern in each of these seven dipole's forms. The next section discusses the obtained results and presents the significant observations.

3. Results and Discussion

The return loss of the prototype dipole and the six different modified printed dipole antenna we constructed are measured using a Network Analyzer. These results are shown in two Figures. The first (Figure 5) corresponds to *l* parameter's variations keeping the *w* parameter equal to zero. The second (Figure 6) shows the return loss curves where *w* parameter varies but the *l* parameter equals to zero. In both figures we can see the return loss curve that belongs to the prototype printed dipole (*l* and *w equal to 0 mm*).

From these curves, it seems that this dipole antenna design has a resonance point at 2.4 GHz with 500 MHz –

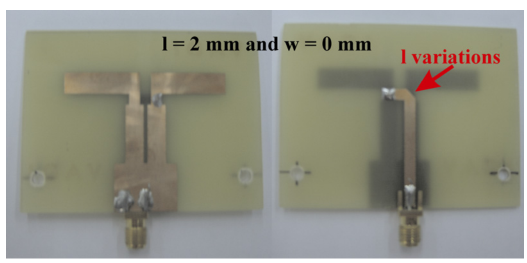

Figure 3. Printed dipole antenna for *l = 2 mm* and *w = 0 mm* Top Layer (left) – Bottom Layer (right).

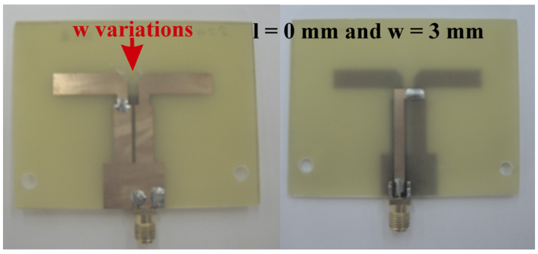

Figure 4. Printed dipole antenna for *l = 0 mm* and *w = 3 mm* Top Layer (left) – Bottom Layer (right).

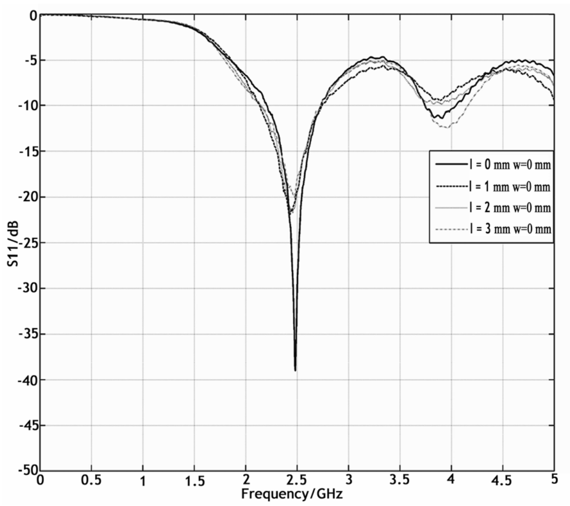

Figure 5. Measured return loss of printed dipole for each value of *l* parameter and *w = 0* mm.

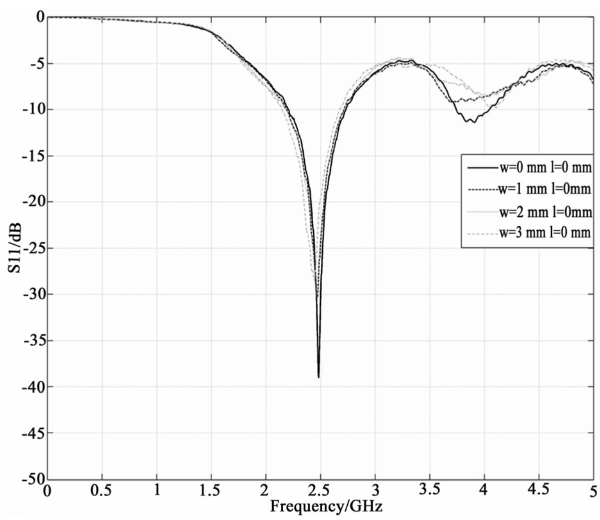

Figure 6. Measured return loss of printed dipole for each value of *w* parameter and *l = 0 mm*.

10 dB bandwidth. The last frequency range has center frequency close to 2.4 GHz which is the frequency value that the return loss is minimized. For these frequencies the corresponding values of return loss are smaller or equal to -10 dB. From Figure 5, it is obvious that as the value of *l* parameter increases, the form of the corresponding return loss curve changes and becomes more flat at the resonance frequency range. On the other hand, the value of *w* parameter does not affect the form of the return loss curve. Each of these seven forms of printed dipole antenna has quite similar return loss curves and introduces narrowband operation at the frequency range of 2.4 GHz. Moreover, for a wireless application that requires design and construction of many identical printed dipoles, it is recommended to choose *l* parameter equals to *2 mm* and *w* parameter equals to *0 mm* for better performance. As it can be seen from Figure 5 the above investigation ensures that the printed dipole antennas will have quite identical return loss curves and performance as elements in an antenna array configuration.

For deeper analysis on this topic, experimental measurements on radiation pattern of these antennas have also been made. Measurements were carried out in a RF anechoic chamber using a calibrated measuring system. In particular, Figure 7 shows the measurements of radiation pattern in E- plane and in H – plane for each dipole

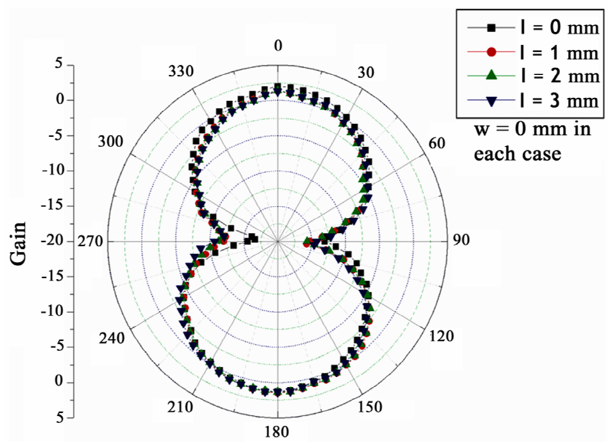

(a)

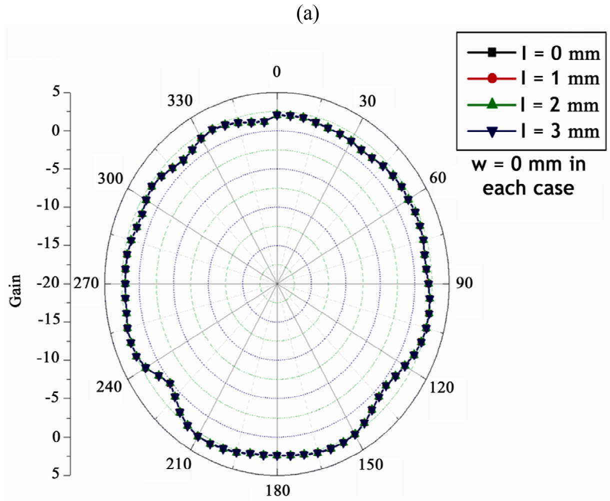

(b)

Figure 7. Radiation pattern of dipole for each value of *l* parameter (a) E – plane, (b) H -plane.

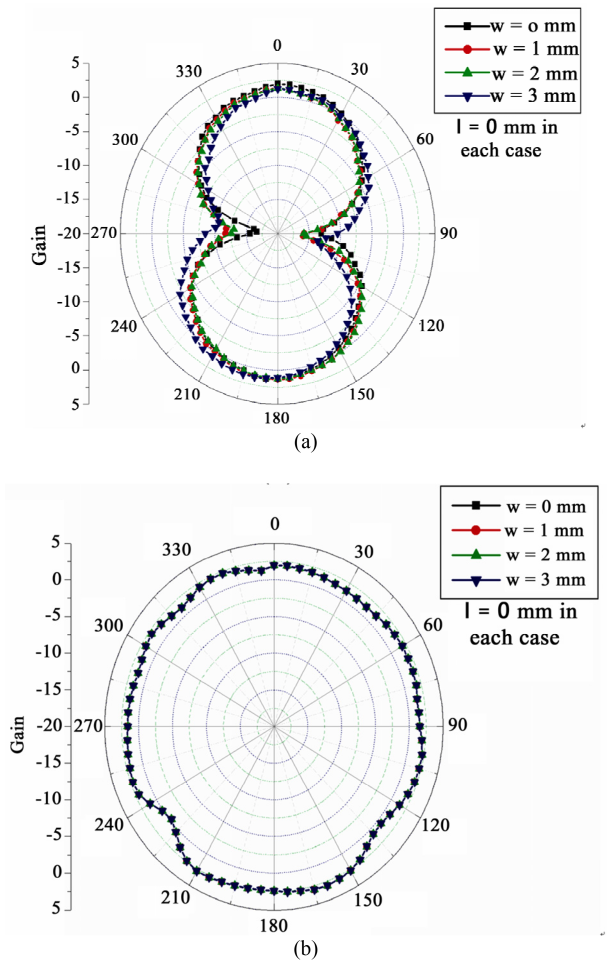

Figure 8. Radiation pattern of dipole for each value of *w* parameter (a) E – plane, (b) H – plane.

with *w* parameter equals to 0 mm and *l* parameter equals to integer values that ranging from *0 mm* to *3 mm*,. Figure 8 shows the corresponding results for each dipole with *l* parameter equals to *0 mm* and *w* parameter's integer values ranging from *0 mm* to *3 mm*. All these dipole structures introduce radiation characteristics that correspond to a fundamental dipole antenna [6,7]. Each of them has a measured peak gain that equals to quite 2 dBi and introduces omni-directional features. Quite small variations on these curves are on the limits of measurements' accuracy. For this reason, it can be observed that the radiation characteristics of the printed dipole antenna are not affected by the variations on *l* and *w* geometrical parameters. Therefore, the radiation diagrams of them are independent of the *l* and *w* parameters.

4. Conclusions

A number of printed dipole antennas with integrated balun are constructed and studied in terms of return loss and radiation pattern. Each of them has a defined form and geometry. Starting from a dipole antenna we mitered the angles introducing the parameters *l* and *w* that we varied. Experimental measurements on return loss provide the obtained results. These are quite similar and also introduce a resonance point at frequency range of 2.4 GHz with narrow resonance bandwidth. The form of this resonance range is affected only by the *l* parameter. The radiation pattern of these dipoles is also investigated. The corresponding radiation diagrams are independent of these geometrical parameters (*l*, *w*) and are similar to that of the fundamental dipole. These observations on printed dipole architecture are very crucial for wireless communication engineering and antenna design. This is because they introduce the ability of constructing a group of identical dipoles choosing an appropriate value of *l* parameter (*l =2 mm*) with quite identical resonance and radiation characteristics.

5. Acknowledgment

This research project (PENED) is co-financed by E.U.-European Social Fund (80%) and the Greek Ministry of Development-GSRT (20%).

6. References

[1] D. Edward and D. Rees, "A broadband printed dipole with integrated balun," Microwave J, 1987, pp. 339–344.

[2] N. Michishita, H. Arai, M. Nakano, T. Satoh, and T. Matsuoka, "FDTD analysis for printed dipole antenna with balun," Asia Pacific Microwave Conference, 2000, pp. 739–742.

[3] G. S. Hilton, C. J. Railton, G. J. Ball, A. L. Hume, and M. Dean, "Finite–difference time–domain analysis of a printed dipole antenna," 19th Int. IEEE Antennas and Propagation Conference, 1995, pp. 72–75.

[4] H. R. Chuang and L. C. Kuo, "3-D FDTD design analysis of a 2.4 GHz polarization – diversity printed dipole antenna with integrated balun and polarization– switching circuit for wlan and wireless communication application," IEEE Transactions on Microwave Theory and Techniques, Vol. 51, No. 2, 2003.

[5] D. M. Pozar, Microwave Engineering, Wiley, 1998.

[6] C. A. Balanis, Antenna Theory Analysis and Design, Wiley, 1997.

[7] R. Garg, P. Bhartia, I. Bahl, and A. Ittipiboon, Microstrip Antenna Design Handbook, Artec House, 2001.

Circuits and Systems, 2012, 3, 216-222
http://dx.doi.org/10.4236/cs.2012.33030 Published Online July 2012 (http://www.SciRP.org/journal/cs)

Optimization of the Voltage Doubler Stages in an RF-DC Convertor Module for Energy Harvesting

Kavuri Kasi Annapurna Devi[1*], Norashidah Md. Din[2], Chandan Kumar Chakrabarty[2]
[1]Department of Electrical and Electronic Engineering, INTI International University, Nilai, Malaysia
[2]Department of Electronics and Communication Engineering, Universiti Tenega Nasional, Kajang, Malaysia
Email: {[*]kavurik.adevi., chandan}@newinti.edu.my, norashidah@uniten.edu.my

Received August 25, 2011; revised March 26, 2012; accepted April 4, 2012

ABSTRACT

This paper presents an optimization of the voltage doubler stages in an energy conversion module for Radio Frequency (RF) energy harvesting system at 900 MHz band. The function of the energy conversion module is to convert the (RF) signals into direct-current (DC) voltage at the given frequency band to power the low power devices/circuits. The design is based on the Villard voltage doubler circuit. A 7 stage Schottky diode voltage doubler circuit is designed, modeled, simulated, fabricated and tested in this work. Multisim was used for the modeling and simulation work. Simulation and measurement were carried out for various input power levels at the specified frequency band. For an equivalent incident signal of –40 dBm, the circuit can produce 3 mV across a 100 kΩ load. The results also show that there is a multiplication factor of 22 at 0 dBm and produces DC output voltage of 5.0 V in measurement. This voltage can be used to power low power sensors in sensor networks ultimately in place of batteries.

Keywords: Energy Conversion; RF; Schottky Diode; Villard; Energy Harvesting

1. Introduction

RF energy harvesting is one type of energy harvesting that can be potentially harvested such as solar, vibration and wind. The RF energy harvesting uses the idea of capturing transmitted RF energy at ambient and either using it directly to power a low power circuit or storing it for later use. The concept needs an efficient antenna along with a circuit capable of converting RF signals to DC voltage. The efficiency of an antenna mainly depends on its impedance and the impedance of the energy converting circuit. If the two impedances aren't matched then it will be unable to receive all the available power from the free space at the desired frequency band. Matching of the impedances means that the impedance of the antenna is the complex conjugate of the impedance of the circuit (voltage doubler circuit).

The concept of energy harvesting system is shown in **Figure 1**, which consists of matching network, RF-DC conversion and load circuits. The authors in [1], used a 2.4 GHz operating frequency with an integrated zero bias detector circuit using BiCMOS technology which produced an output voltage of 1 V into a 1 MΩ load at an input power level of 0 dBm. H. Yan and co-authors revealed that a DC voltage of 0.8 volts can be achieved from a –20 dBm RF input signal at 868.3 MHz through simulation results [2]. In [3], work was carried out on a firm frequency of 900 MHz by matching to a 50 Ω impedance and resonance circuit transformation in front of the Schottky diode which yields an output voltage of over 300 mV at an input power level of 2.5 µ. W. J. Wang, L. Dong and Y. Fu [4] used a Cockcroft-Walton multiplier circuit that produced a voltage level of 1.0 V into a 200 MΩ load for an input power level of less than –30 dBm at a fixed frequency of 2.4 GHz.

The energy conversion module designed in this paper is based on a voltage doubler circuit which can be able to output a DC voltage typically larger than a simple diode rectifier circuit as in [5], in which switched capacitor charge pump circuits are used to design two phase voltage doubler and a multiphase voltage doubler. The module presented in this can function as an AC to DC converter that not only rectifies the input AC signal but also elevates the DC voltage level. The output voltage of the

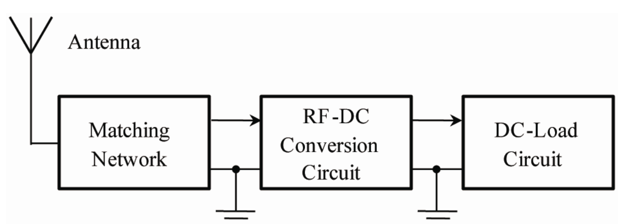

Figure 1. Schematic view of a RF energy harvesting system.

[*]Corresponding author.

energy conversion module can be used to energize the low power devices for example sensors for a sensor network in application to agriculture.

Section 2 of this paper discusses on the theoretical background of the voltage doubler circuit. Section 3 presents the simulation study and implementation of the circuit design. Section 4 provides the results and analysis. Section 5 concludes with a discussion on the findings from the simulated and measured results.

2. Voltage Multiplier

There are various voltage multiplier circuit topologies. The design used in this module is derived from the function of peak detector or a half wave peak rectifier. The Villard voltage multiplier circuit was chosen in the circuit design of this paper because it produces two times of the input signal voltage towards ground at a single output and can be cascaded to form a voltage multiplier with an arbitrary output voltage and its design simplicity.

2.1. Diode Modeling

The voltage multiplier circuit in this design uses zero bias Schottky diode HSMS-2850 from Agilent. The attractive feature of these Schottky diodes are low substrate losses and very fast switching but leads to a fabrication overhead. This diode has been modeled for the energy harvesting circuit which comes in a one-diode configuration. The modeling parameters for these diodes are given by Agilent in their data sheets. These parameters are used in Multisim for its own modeling purposes. The modeling is done by transforming the diode into an equivalent circuit using passive components which are described by the SPICE parameters in **Table 1** [6].

The diode used in this design is shown in **Figure 2** and its equivalent model is shown in **Figure 3**. The special features of HSMS-2850 diode is that it provides a low forward voltage, low substrate leakage and uses the non symmetric properties of a diode that allows unidirectional flow of current under ideal condition.

Table 1. SPICE parameters.

Parameters	Units	HSMS 2850
B_V	V	3.8
C_{J0}	pF	0.18
E_G	Ev	0.69
I_{BV}	A	3E–4
I_S	A	3E–6
N	No unite	1.06
R_S	Ω	25
P_B (V_J)	V	0.35
P_T (XTI)	No units	2
M	No units	0.5

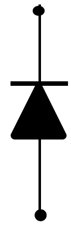

Figure 2. Schottky diode.

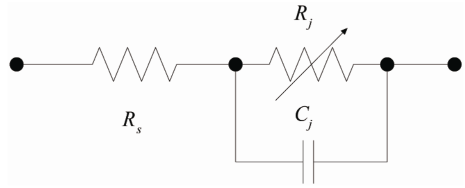

Figure 3. Linear circuit model of the Schottky diode [6].

The diodes are fixed and are not subject of optimization or tuning. This is described using the following derivations. By neglecting the effect of diode substrate, an equivalent linear model that can be used for the diode as shown in **Figure 3**. When C_j is the junction capacitance and R_j is the junction resistance, the admittance Y_z of the linear model is given by

$$Y_Z = Y_{C_j} + Y_{R_j} \tag{1}$$

Equation (1) related to the frequency of operation is given by

$$Y_Z = jwC_j + \frac{1}{R_j} \tag{2}$$

$$= \frac{jwC_j R_j + 1}{R_j} \tag{3}$$

The impedance Z of the linear model is given by

$$Z = \frac{R_j}{1 + jwR_j C_j} \tag{4}$$

The total impedance Z_T is given by

$$Z_T = R_S + \frac{R_j}{1 + jwR_j C_j} \tag{5}$$

where R_S is the series resistance of the circuit and R_j is given by

$$R_j = \frac{8.33 \times 10^{-5} \times N \times T}{I_b + I_S}$$

where:

I_b = bias current in μA;
I_s = saturation current in μA;
T = temperature (K);

N = ideality factor.

In Equation (5), R_j and C_j are constants and the frequency of operation (w) is the only variable parameter. As the frequency increases, the value of Z is almost negligible compared to the series resistance R_S of the diode. From this it is concluded that the function of the diode is independent of the frequency of operation.

2.2. Single Stage Voltage Multiplier

Figure 4 represents a single stage voltage multiplier circuit. The circuit is also called as a voltage doubler because in theory, the voltage that is arrived on the output is approximately twice that at the input. The circuit consists of two sections; each comprises a diode and a capacitor for rectification. The RF input signal is rectified in the positive half of the input cycle, followed by the negative half of the input cycle. But, the voltage stored on the input capacitor during one half cycle is transferred to the output capacitor during the next half cycle of the input signal. Thus, the voltage on output capacitor is roughly two times the peak voltage of the RF source minus the turn-on voltage of the diode.

The most interesting feature of this circuit is that when these stages are connected in series. This method behaves akin to the principle of stacking batteries in series to get more voltage at the output. The output of the first stage is not exactly pure DC voltage and it is basically an AC signal with a DC offset voltage. This is equivalent to a DC signal superimposed by ripple content. Due to this distinctive feature, succeeding stages in the circuit can get more voltage than the preceding stages. If a second stage is added on top of the first multiplier circuit, the only waveform that the second stage receives is the noise of the first stage. This noise is then doubled and added to the DC voltage of the first stage. Therefore, the more stages that are added, theoretically, more voltage will come from the system regardless of the input. Each independent stage with its dedicated voltage doubler circuit can be seen as a single battery with open circuit output voltage V_0, internal resistance R_0 with load resistance R_L, the output voltage, V_{out} is expressed as in Equation (7).

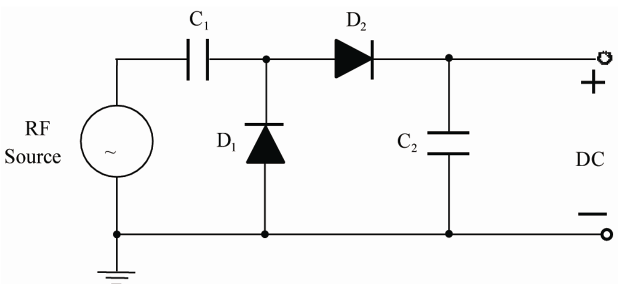

Figure 4. Single stage voltage multiplier circuit [7].

$$V_{out} = \frac{V_0}{R_0 + R_L} R_L \tag{6}$$

When n number of these circuits are put in series and connected to a load of R_L in Equation (6) the output voltage V_{out} obtained is given by this change in RC value will make the time constant longer which in turn retains the multiplication effect of two in this design of seven stage voltage doubler.

$$V_{out} = \frac{nV_0}{nR_0 + R_L} = V_0 \frac{1}{\frac{R_0}{R_L} + \frac{1}{n}} \tag{7}$$

The number of stages in the system has the greatest effect on the DC output voltage, as shown from Equations (6) and (7).

It is inferred that the output voltage V_{out} is determined by the addition of R_0/R_L and $1/n$, if V_0 is fixed. From this analysis it is observed that V_0, R_0 and R_L are all constants. Assume that V_0 = 1 V, R_0/R_L = 0.25, n = 2, 3, 4, 5, 6 and 7, the output voltage V_{out} = 1.33 V, 1.72 V, 2.0 V, 2.22 V, 2.43 V and 2.56 V respectively when substituted analytically in the Equation (7). This analysis can be compared with the results obtained in the circuit design of this module. In simulation at n = 4, V_{out} = 1.42 V, n = 5, V_{out} = 1.67 V; n = 6, V_{out} = 1.92; n = 7, V_{out} = 2.15 V; n = 8, V_{out} = 1.92 V; n = 9, V_{out} = 1.81 V. Also in measurement, for n = 4, V_{out} = 2.1 V; n = 5, V_{out} =2.9 V; n = 6, V_{out} = 3.72 V; and n = 7, V_{out} = 5 V. As n increases, the increase in output voltage will be almost double the input voltage up to some number of stages. But at some point, *i.e.* beyond seven stages, in this circuit the output voltage gained (8 and 9 stages) will be negligible as shown in **Figure 5**.

The capacitors are charged to the peak value of the input RF signal and discharge to the series resistance (R_s) of the diode. Thus the output voltage across the capacitor of the first stage is approximately twice that of the input signal. As the signal swings from one stage to other, there is an additive resistance in the discharge path of the

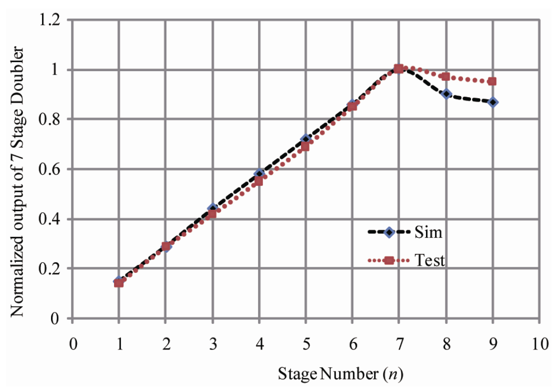

Figure 5. Normalized output voltage multiplier versus number of stages.

diode and increase of capacitance due to the stage capacitors.

2.3. Seven Stage Voltage Multiplier

The seven stage voltage multiplier circuit design implemented in this paper is shown in **Figure 6**. Starting on the left side, there is a RF signal source for the circuit followed by the first stage of the voltage multiplier circuit. Each stage is stacked onto the previous stage as shown in the **Figure 6**. Stacking was done from left to right for simplicity instead of conventional stacking from bottom to top.

The circuit uses eight zero bias Schottky surface-mount Agilent HSMS-285X series, HSMS-2850 diodes. The special features of these diode is that, it provides a low forward voltage, low substrate leakage and uses the non-symmetric properties of a diode that allows unidirectional flow of current under ideal conditions. The diodes are fixed and are not subject of optimization or tuning. This type of multiplier produces a DC voltage which depends on the incident RF voltage. Input to the circuit is a predefined RF source. The voltage conversion can be effective only if the input voltage is higher than the Schottky forward voltage.

The other components associated with the circuit are the stage capacitors. The chosen capacitors for this circuit are of through-hole type, which make it easier to modify for optimization, where in [8] the optimization was accomplished at the input impedance of the CMOS chip for a three stage voltage multiplier. The circuit design in this paper uses a capacitor across the load to store and provide DC leveling of the output voltage and its value only affects the speed of the transient response. Without a capacitor across the load, the output is not a good DC signal, but more of an offset AC signal.

In addition to the above, an equivalent load resistor is connected at the final node. The output voltage across the load decreases during the negative half cycle of the AC input signal. The voltage decreases is inversely proportional to the product of resistance and capacitance across the load. Without the load resistor on the circuit, the voltage would be hold indefinitely on the capacitor and look like a DC signal, assuming ideal components. In the design, the individual components of the stages need not to be rated to withstand the entire output voltage. Each component only needs to be concerned with the relative voltage differences directly across its own terminals and of the components immediately adjacent to it. In this type of circuitry, the circuit does not change the output voltage but increases the possible output current by a factor of two. The number of stages in the system is directly proportional to the amount of voltage obtained and has the greatest effect on the output voltage as explained in the Equation (7) and shown in **Figure 5**.

3. Simulation and Implementation

Multisim software was chosen for modeling and simulation which is a circuit simulation tool by Texas Instruments. The simulation and practical implementation were carried out with fixed RF at 945 MHz ± 100 MHz, which are close to the down link center radio frequency (947.5 MHz) of the GSM-900 transmitter. The voltages obtained at the final node V_{DC} of the multiplier circuit were recorded for various input power levels from –40 dBm - +5 dBm with power level interval (spacing) of 5 dBm.

The simulations were also carried out using same stage capacitance value (3.3 nF) and then with a varied capacitance value for all stages from 4 stages through 9 stages [9]. The capacitance value was varied in such a way that, from one stage to the next, it was halved. For example, if the first stage was 3.3 nF, the second stage was 1.65 nF, third stage was 825 pF, fourth stage was 415 pF and so on. But keeping in view of testing, the capacitance values were chosen to have a close match with the standard available values in the market.

Simulation was carried out through 4 to 9 voltage doubler stages. Based on results obtained a 7 stage doubler is best to implemented for this application.

The design of the printed circuit board (PCB) was carried out using DipTrace software. The material used to

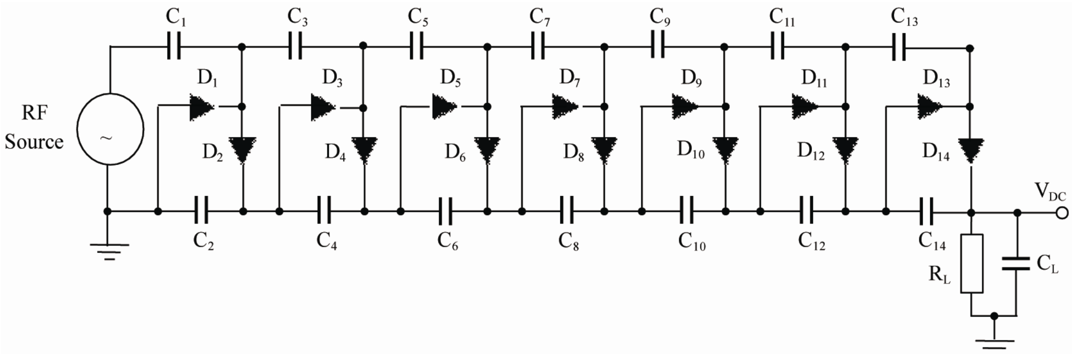

Figure 6. Schematic of 7 stage voltage multiplier.

manufacture the printed circuit board (PCB) is the standard Fiberglass Reinforced Epoxy (FR4), with the thickness of 1.6 mm and dielectric constant of 3.9. The topology is constructed on the PCB with the dimensions of 98 mm × 34 mm (W × H). The Sub Miniature version A (SMA) connectors are used at the input and output of PCB to carry out the measurements. The circuit components consist of active and passive components. The component used in circuit is shown in **Table 2**.

Special handling precautions have been taken to avoid Electro Static Discharge (ESD), while assembling of the surface-mount zero bias Schottky diodes. Also special attention has been given to mount other components and the SMA connectors on to the PCB. The Photograph of Assembled circuit board I shown in **Figure 7**.

4. Results and Analysis

The simulated and measured results at the output voltage of voltage multiplier circuit are shown graphically in **Figure 8**. From the graph analysis, the simulated and the measured results agree considerably with each other. The measured results are shown to be better than the simulation results. The reason behind this may be due to the uncertainty in series resistance value of the diode obtained from SPICE parameters in modeling as explained in Equation (5). This resistance vale of diodes in practical circuit may be lower than in the model, which provides fast discharge path, in turn rise in voltage as passes through the stages and reaches to final output. In this work, the DC output voltages obtained through simulation and measurement at 0 dBm re 2.12 V and 5.0 V respectively. These results are comparatively much better than in ref. [9], where in at 0 dBm, 900 MHz they achieved 0.5 V and 0.8 V through simulation and measurement respectively.

Figures 9 and **10** show the result of a 4 stage voltage doubler circuit with equal and varied capacitance values between the stages as described in Section 3.

From the analysis of these two simulations, it can be observed that the resulting output voltages are equal. The only difference between these two graphs is the rise time of the circuit with varied capacitance value is a little bit slower. But, overall result on the performance of rise time is still under 20 µs to 24 µs and the difference is negligible. From these results, the use of equal stage capacitance of each being 3.3 nF was hence considered for the design of the multiplier.

The results from **Figure 11**, shows that the output voltage reaches to 1.0 V within 20 µS and then uniformly increasing to 1.4 V, 1.67 V, 1.87 V and 2.12 V for 4, 5, 6 and 7 stages respectively compared to 2 mS as shown in [10]. **Figure 12** shows that the conversion ratio of 22 is achieved at 0 dBm input power and drops to 2.5 at –40 dBm. The highest value at 0 dBm is due to the innate characteristics of the zero bias Schottky diodes which conduct fairly well at higher input voltages.

5. Conclusion

From the experimental results, it is found that the pro-

Table 2. Component used in 7 stage voltage multiplier.

Name of component	Label	Value
Stage capacitors	C_1 - C_{14}	3.3 nF
Stage diodes	D_1 - D_{14}	HSMS 2850
Filter capacitor	C_L	100 nF
Load resister	R_L	100 kΩ

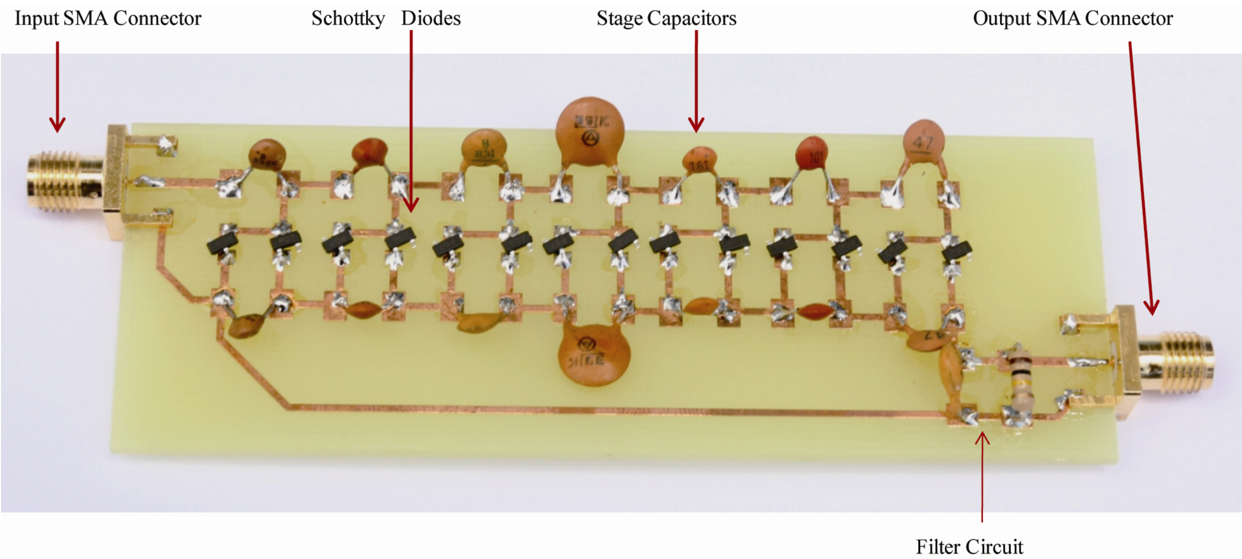

Figure 7. Photograph of assembled circuit board.

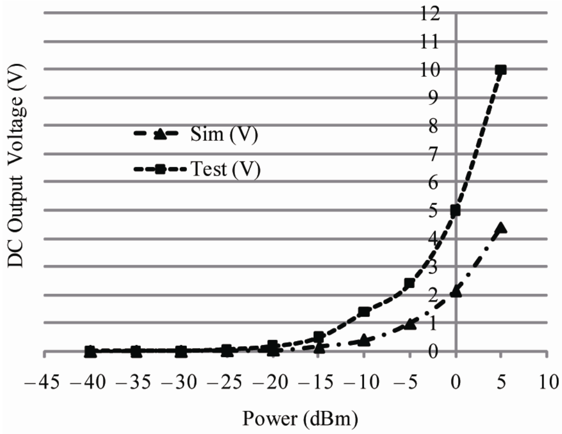

Figure 8. Simulated and test DC output voltage of multiplier as a function of input power.

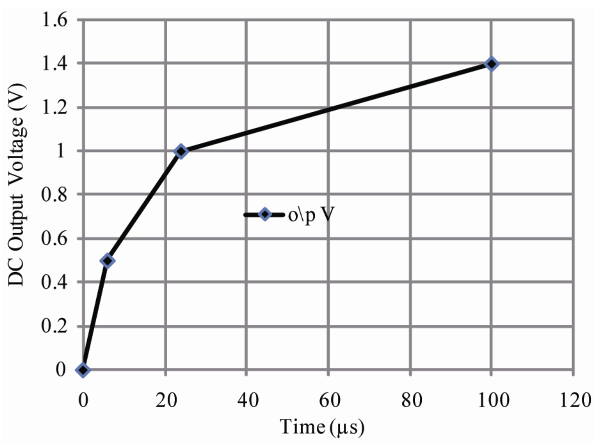

Figure 9. DC output voltage verses rise time of 4 stage voltage doubler circuit with equal stage capacitance [8].

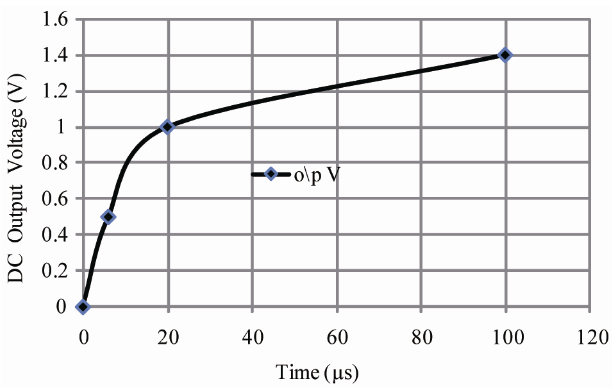

Figure 10. DC output voltage verses rise time of 4 stage voltage doubler with varied stage capacitance [8].

posed voltage multiplier circuit operates at the frequency of 945 MHz with the specified input power levels. The results have shown that there is multiplication of the input voltage. From **Figure 12**, it is shown that at 0 dBm input power, the multiplication factor is 22. This is significant, as the work shows that RF energy in the GSM-900 band can be harvested from the ambient RF source using the Villard circuit topology. The power density levels from a GSM base station is expected from 0.1 mW/m^2 to 1 mW/m^2 for a distance ranging from 25 m - 100 m. These power levels may be elevated by a factor between one and three for the GSM-900 downlink frequency bands depending on the traffic density [10]. The next phase of the research work is to interface the voltage multiplier circuit through a matching network to the antenna at the input side and a low power device to power from the system at the output side to complete the RF energy harvesting system.

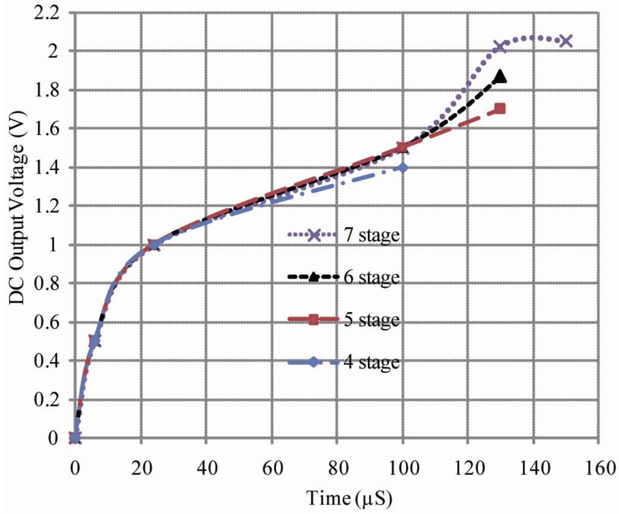

Figure 11. DC output voltage verses rise time of voltage doubler circuit through 4 - 7 stages with equal stage capacitance.

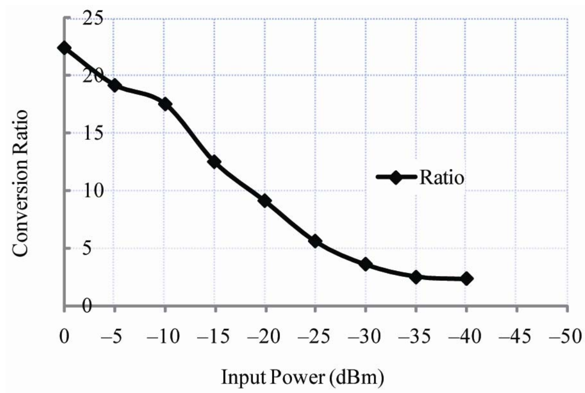

Figure 12. Conversion ratio as a function of input power.

6. Acknowledgements

We would like to acknowledge and thank the Ministry of Higher Education Malaysia for funding this project under Fundamental Research Grant: FRGS/1/10/TK/UNITEN/02/13.

REFERENCES

[1] S. von der Mark and G. Boeck, "Ultra Low Power Wakeup Detector for Sensor Networks," *SBMO/IEEE MTT-S International Microwave & Optoelectronics Conference* (*IMOC* 2007), Berlin, 29 October-1 November 2007, pp. 865-868. doi:10.1109/IMOC.2007.4404394

[2] H. Yan, J. G. M. Montero, A. Akhnoukh, L. C. N. de Vreede and J. N. Burghartz, "An Integration Scheme for RF Power Harvesting," *Proceedings of STW Annual Workshop on Semiconductor Advances for Future Electronics and Sensors*, Veldhoven, November 2005, pp. 64-66. doi:10.1.1.126.5786

[3] T. Ungan and L. M. Reindl, "Concept for Harvesting Low Ambient RF-Sources for Microsystems," 2007. http://www.imtek.de/content/pdf/public/2007/powermems_2007_paper_ungan.pdf

[4] J. Wang, L. Dong and Y. Z. Fu, "Modeling of UHF Voltage Multiplier for Radio-Triggered Wake-Up Circuits," *International Journal of Circuit Theory and Application*, Vol. 39, No. 11, 2010, pp. 1189-1197. doi:10.1002/cta.692

[5] J. A. Starzyk, Y.-W. Jan and F. J. Qiu, "A DC-DC Charge Pump Design Based on Voltage Doublers," *IEEE Transactions on Circuits and Systems-I*: *Fundamental Theory and Applications*, Vol. 48, No. 3, 2001, pp. 350-359.

[6] HSMS-2850, "Surface Mount Zero Bias Schottky Detector Diodes." http://www.crystal-radio.eu/hsms285xdata.pdf

[7] D. W. Harrist, "Wireless Battery Charging System Using Radio Frequency Energy Harvesting," M.S. Thesis, University of Pittsburgh, Pittsburgh, 2004.

[8] E. Bergeret, J. Gaubert, P. Pannie and J. M. Gaultierr, "Modeling and Design of CMOS UHF Voltage Multiplier for RFID in an EEPROM Compatible Process," *IEEE Transactions on Circuits and Systems-I*, Vol. 54, No. 10, 2007, pp. 833-837. doi:10.1109/TCSII.2007.902222

[9] B. Emmanuel, J. Gaubert, P. Pannier and J. M. Gaultier, "Conception of UHF Voltage Multiplier for RFID Circui," *IEEE North-East Workshop on Circuits and Systems*, Gatineau, June 2006, pp. 217-220. doi:10.1109/NEWCAS.2006.250961

[10] H. J. Visser, A. C. F. Reniers and J. A. C. Theeuwes, "Ambient RF Energy Scavenging: GSM and WLAN Power Density Measurements," *Proceedings of the* 38*th European Microwave Conference*, Eindhoven, 27-31 October 2008, pp. 721-724. doi:10.1109/EUMC.2008.4751554

Journal of Electromagnetic Analysis and Applications, **2013, 5, 182-188**
http://dx.doi.org/10.4236/jemaa.2013.54029 Published Online April 2013 (http://www.scirp.org/journal/jemaa)

Double-Sided Microstrip Circular Antenna Array for WLAN/WiMAX Applications

Ruwaybih Alsulami, Heather Song*

Department of Electrical and Computer Engineering, University of Colorado, Colorado Springs, USA.
Email: *hsong@uccs.edu

Received February 8th, 2013; revised March 10th, 2013; accepted March 25th, 2013

ABSTRACT

The design, fabrication, and characterization of the microstrip circular antenna arrays were presented. The proposed antennas were designed for single band at 2.45 GHz and dual bands at 3.3 - 3.6 and 5.0 - 6.0 GHz to support WLAN/WiMAX applications. The proposed single and dual band antennas showed omnidirectional radiation pattern with the gain values of 3.5 dBi at 2.45 GHz, 4.0 dBi at 3.45 GHz, and 3.3 dBi at 5.5 GHz. The dual band antenna array was placed on both top and bottom layers to obtain the desired antenna characteristics. The proposed double-sided dual band antenna provides omnidirectional radiation pattern with high gain.

Keywords: Antenna Arrays; Circular Patch; Dual Band; Single Band; Omnidirectional; WLAN/WiMAX Applications; UWB

1. Introduction

Ultra-wideband (UWB: 3.1 to 10.6 GHz) frequency spectrum has been approved by the US Federal Communications Commission (FCC) for unlicensed short range wireless communications since 2002. In this frequency range, wireless local-area network (WLAN) IEEE802.11a and HIPERLAN/2 WLAN operates in 5.0 - 6.0 GHz band. In some European and Asian countries, world interoperability for microwave access (WiMAX) service is provided in the frequency range of 3.3 - 3.6 GHz [1-4]. To support the WLAN/WiMAX application, antenna arrays that provide omnidirectional radiation pattern are required. To respond to this need, recent antenna design efforts were focused on omnidirectional antennas with high gain and no sidelobes [5-8]. Rectangular arrays are common type used for antenna arrays. Studies on dual band antennas employing rectangular arrays were reported [9-12]. Compared to rectangular patch antenna arrays, there are limited numbers of studies performed on circular patch antenna arrays due to difficulties in fabrication [13]. Advantages of circular antenna array include high gain and narrow beam width [13].

In this paper, a new microstrip circular antenna arrays were designed, fabricated, and characterized to provide omnidirectional radiation pattern for WLAN/WiMAX applications. Two antenna arrays were designed—one for single band at 2.45 GHz and the other for dual bands at 3.3 - 3.6 GHz and 5.0 - 6.0 GHz. For single band operation, circular patch array was placed on the top layer of the microtrip and a small rectangular patch was placed on the bottom layer for ground connection. For dual band operation, similar circular patch array was placed on both top and bottom layers of the microstrip with larger rectangular patch placed on the bottom layer. Both single band (single sided) and dual band (double-sided) microstrip antenna arrays provided desirable antenna characteristics for the intended application.

2. Design and Simulation

2.1. Single-Band Antenna at 2.45 GHz

The configuration of the proposed single band antenna at 2.45 GHz is shown in **Figure 1**. It consists of six circular patches which are placed only on the top layer. The small rectangular patch is placed on the bottom layer for ground connection.

The directivity for the circular patch antenna is

$$D_0 = \frac{(k_0 a_e)^2}{120 G_{\mathrm{rad}}} \quad (1)$$

*Corresponding author.

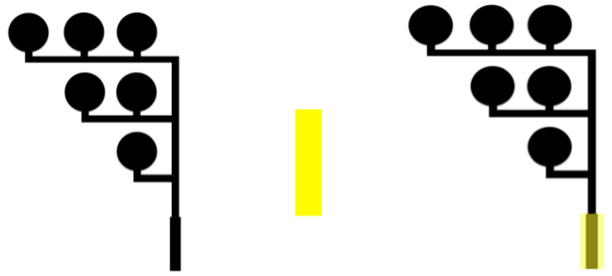

(a) (b) (c)

Figure 1. Configuration of the proposed antenna for single band at 2.45 GHz: (a) Top layer; (b) Bottom layer; (c) Top and bottom layers overlaid.

$$k_0 = \frac{2\pi}{\lambda_0} \tag{2}$$

$$a_e = a\left\{1 + \frac{2h}{\pi a \epsilon_r}\left[\ln\left(\frac{\pi a}{2h}\right) + 1.7726\right]\right\}^{1/2} \tag{3}$$

$$G_{\text{rad}} = \frac{\left(k_0 a_e\right)^2}{480}\int_0^{\pi/2}\left[J_{02}'^2 + \cos^2\theta J_{02}^2\right]\sin\theta \mathrm{d}\theta \tag{4}$$

$$J_{02}' = J_0\left(k_0 a_e \sin\theta\right) - J_2\left(k_0 a_e \sin\theta\right) \tag{5}$$

$$J_{02} = J_0\left(k_0 a_e \sin\theta\right) + J_2\left(k_0 a_e \sin\theta\right) \tag{6}$$

where a_e is the effective radius, a is the actual radius, ϵ_r is the relative permittivity of the microstrip dielectric substrate, h is the height of the microstrip substrate, and J_0 and J_2 are Bessel functions.

The gain of the antenna was calculated using

$$\text{Gain} = \text{Antenna Efficiency} \times \text{Directivity}\left(D_0\right) \tag{7}$$

$$\text{Antenna Efficiency} = \frac{\text{Total Efficiency}}{\text{Reflection Efficiency}} \tag{8}$$

The variable corresponding to each dimensions and values for the dimensions of the proposed antenna are shown in **Figure 2** and **Table 1**, respectively. Here, *L*, *W*, and *R* represent the length, the width, and the radius of the circular patch, respectively.

The gain of the proposed antenna shown in **Figure 1** was calculated using (1) - (8) and the dimensions were optimized using ADS [14] which resulted in gain of 3.5 dBi at 2.45 GHz.

2.2. Dual-Band Antenna at 3.3 - 3.6 and 5.0 - 6.0 GHz

The configuration for the doubled-sided microstrip dual band antenna is shown in **Figure 3**. The proposed microstrip antenna has circular arrays both on the top and bottom layers. It consists of three circular patched on each layer.

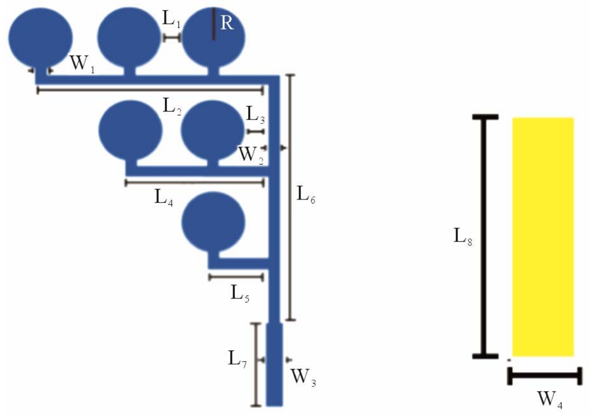

(a) (b)

Figure 2. Variables corresponding to each dimension of the proposed single band antenna: (a) Top layer; (b) Bottom layer.

Table 1. Dimensions for the proposed single band antenna at 2.4 GHz.

Variable	Value (mm)
L_1	1.15
L_2	28.9
L_3	1.13
L_4	17.6
L_5	6.60
L_6	35.3
L_7	18.4
L_8	18.4
W_1	1.02
W_2	1.52
W_3	3.30
W_4	6.86
R	5.10

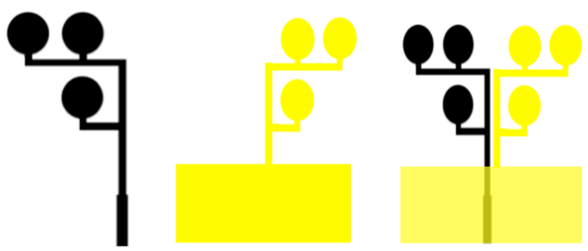

(a) (b) (c)

Figure 3. Configuration of the proposed antenna for dual band at 3.3 - 3.6 and 5.0 - 6.0 GHz: (a) Top layer; (b) Bottom layer; (c) Top and bottom layers overlaid.

The configuration in **Figure 3(a)** is similar to the top layer of the single band antenna as shown in **Figure 1(a)** but with less circular patches. However, the bottom layer in **Figure 3(b)** is different compared to the bottom layer of the single band antenna shown in **Figure 1(b)**. The double-side nature of the antenna provides dual band characteristics. Identical equations were used for the single band antenna were employed in the design process. The variable corresponding to each dimensions and the dimensions for the proposed dual band antenna are shown in **Figure 4** and **Table 2**, respectively.

Simulation was performed using ADS for the configuration shown in **Figure 3(c)**. The simulated gains of the proposed dual band antenna were 4.0 dBi at 3.45 GHz and 3.3 dBi at 5.5 GHz. The double-sided configuration of the antenna provided higher gain compared to the singled-sided antenna.

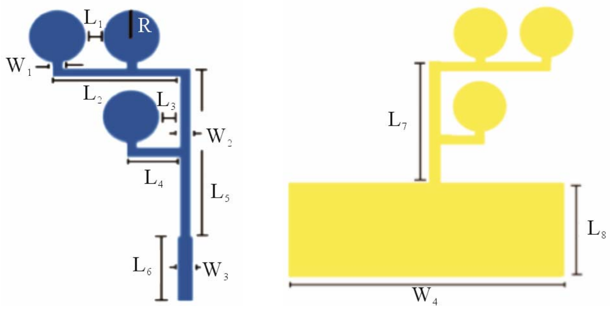

(a) (b)

Figure 4. Variables corresponding to each dimension of the proposed dual-band antenna: (a) Top layer; (b) Bottom layer.

Table 2. Dimensions for the proposed dual band antenna at 3.3 - 3.6 and 5.0 - 6.0 GHz.

Variable	Value (mm)
L_1	1.20
L_2	17.8
L_3	1.08
L_4	6.60
L_5	29.3
L_6	10.0
L_7	21.6
L_8	17.8
W_1	1.02
W_2	1.52
W_3	2.54
W_4	49.1
R	5.21

3. Measurement Results and Discussions

3.1. Single-Band Atnenna at 2.45 GHz

The antennas were fabricated using LPKF Protomat [15] on FR-4 material with height of 1.524 mm. The photos of the fabricated single band antenna are shown in **Figure 5** which has a size of 6.7 × 4.4 (in cm).

Figure 6 shows the comparison between the simulated and the measured S_{11} results.

The measured operating frequency is close to 2.45 GHz with S_{11} value below −15 dB. The 3 dB bandwidth at 2.45 GHz was approximately 18%. The measurement and simulation are in fairly good agreement, and the differences are due to microstrip loss and fabrication errors.

Figure 7 shows the comparison between the simulated and measured radiation pattern in xy-plane at 2.45 GHz which is close to omnidirectional pattern.

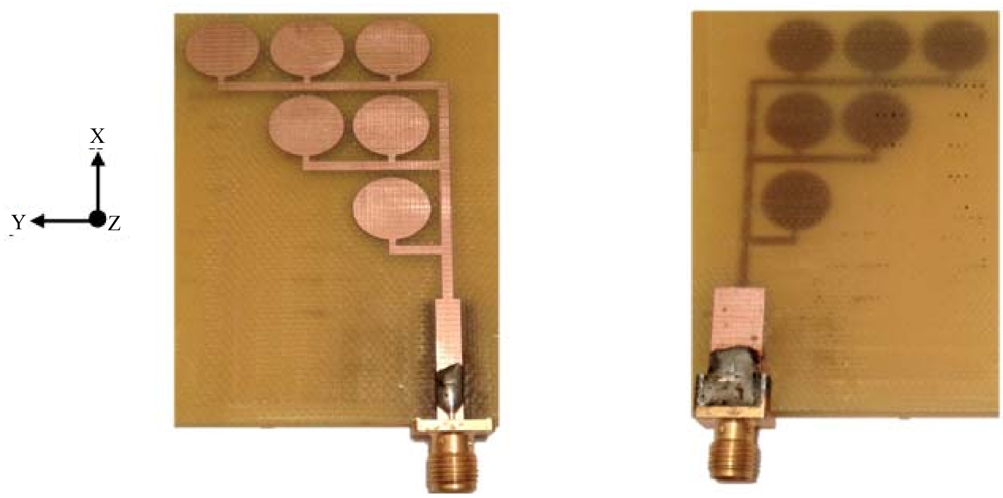

(a) (b)

Figure 5. Photo of the fabricated single-band antenna: (a) Top layer; (b) Bottom layer.

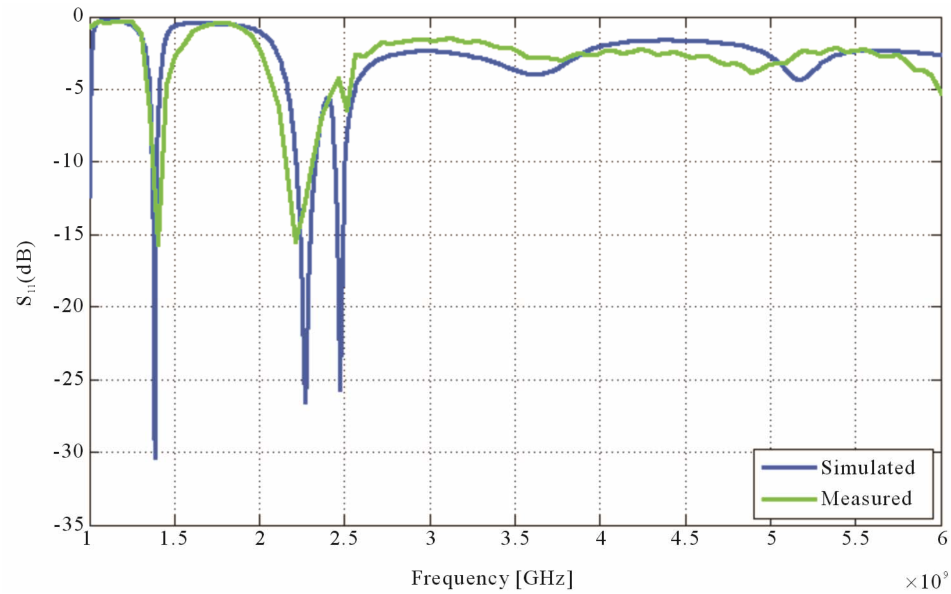

Figure 6. Simulated and measured return loss for the proposed single-band antenna.

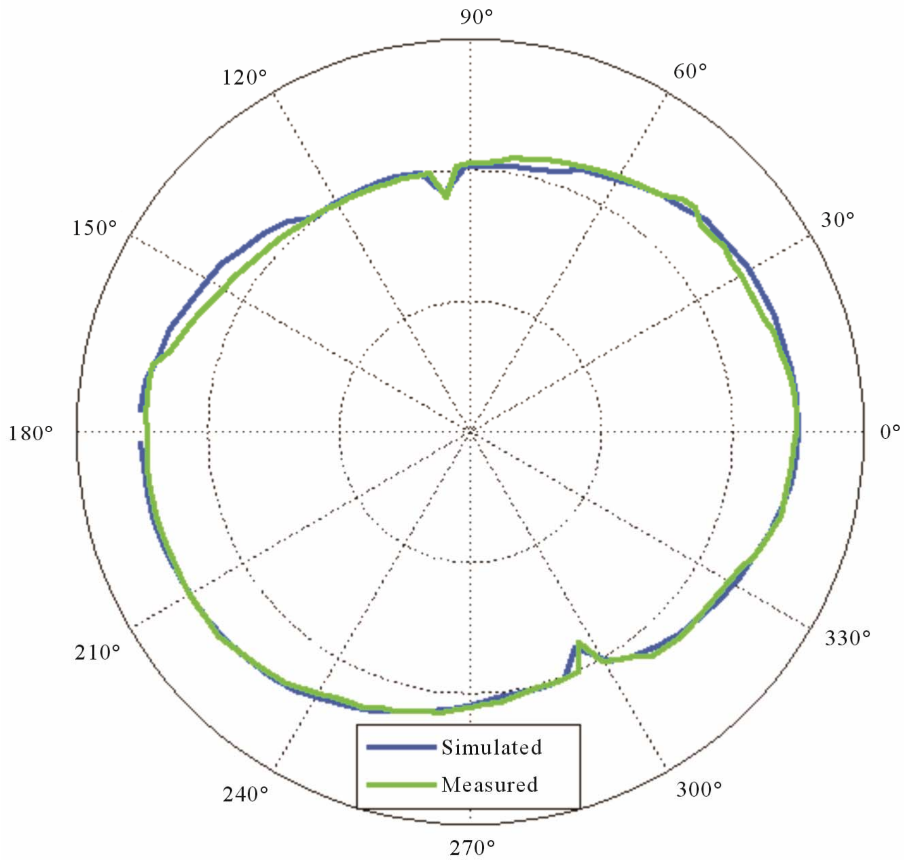

Figure 7. Simulated and measured radiation pattern in xy-plane (coordinate system shown in Figure 5) at 2.45 GHz.

3.2. Dual-Band Antenna at 3.3 - 3.6 and 5.0 - 6.0 GHz

The antennas were fabricated using LPKF Protomat [15] on double-sided FR-4 materials. The photos of the fabricated dual band antenna are shown in **Figure 8** which has a size of 6.6 × 5.2 (in cm).

Figure 9 shows the comparison between the simulated

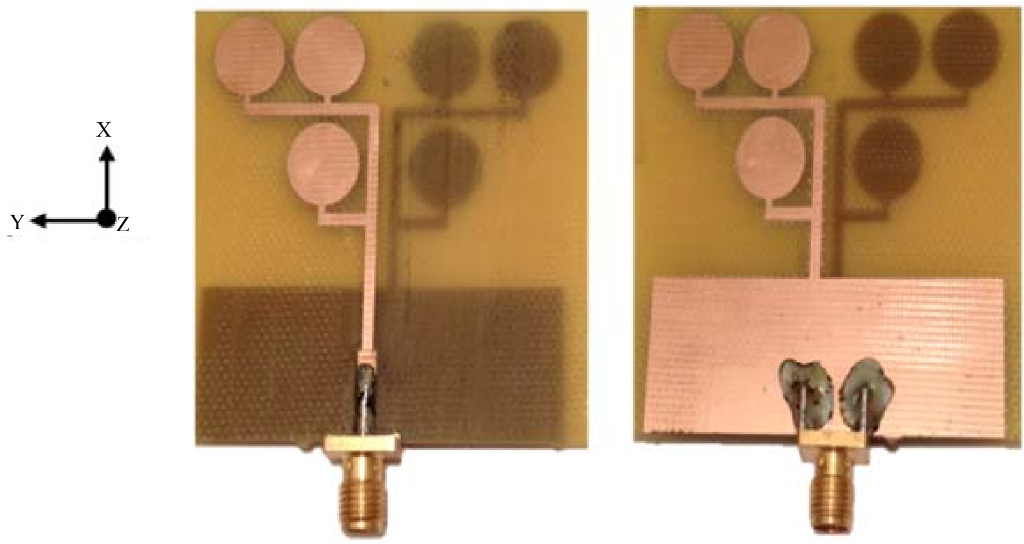

(a) (b)

Figure 8. Photo of the fabricated dual-band antenna: (a) Top layer; (b) Bottom layer.

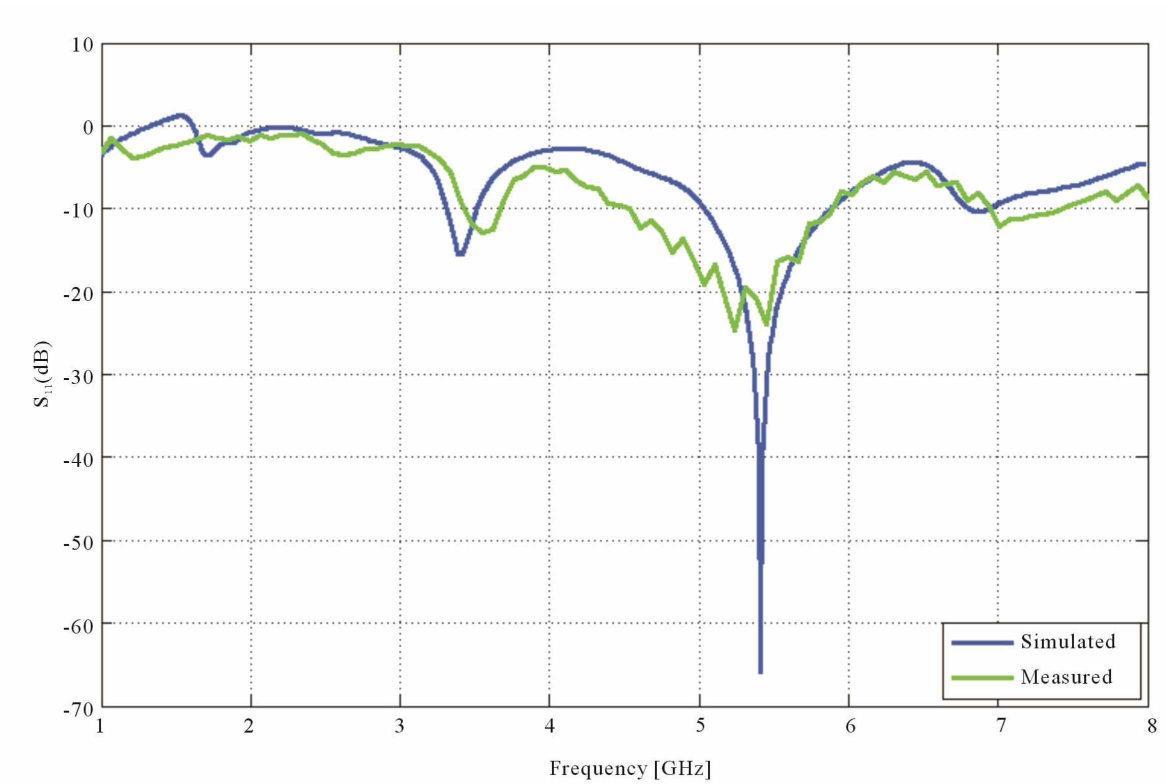

Figure 9. Simulated and measured return loss for the dual band antenna.

and the measured S_{11} results.

The measured S_{11} shows dual band near the designed bands with S_{11} values below −10 dB for both bands. The simulated and measured results give fairly good agreement, and the differences are due to board loss and fabrication errors.

Figure 10 shows the comparison between the simulated and measured radiation pattern in xy-plane at 3.45 and 5.5 GHz which is close to omnidirectional pattern.

4. Conclusion

A microstrip circular antenna arrays were presented for single band at 2.45 GHz and dual bands at 3.3 - 3.6 and

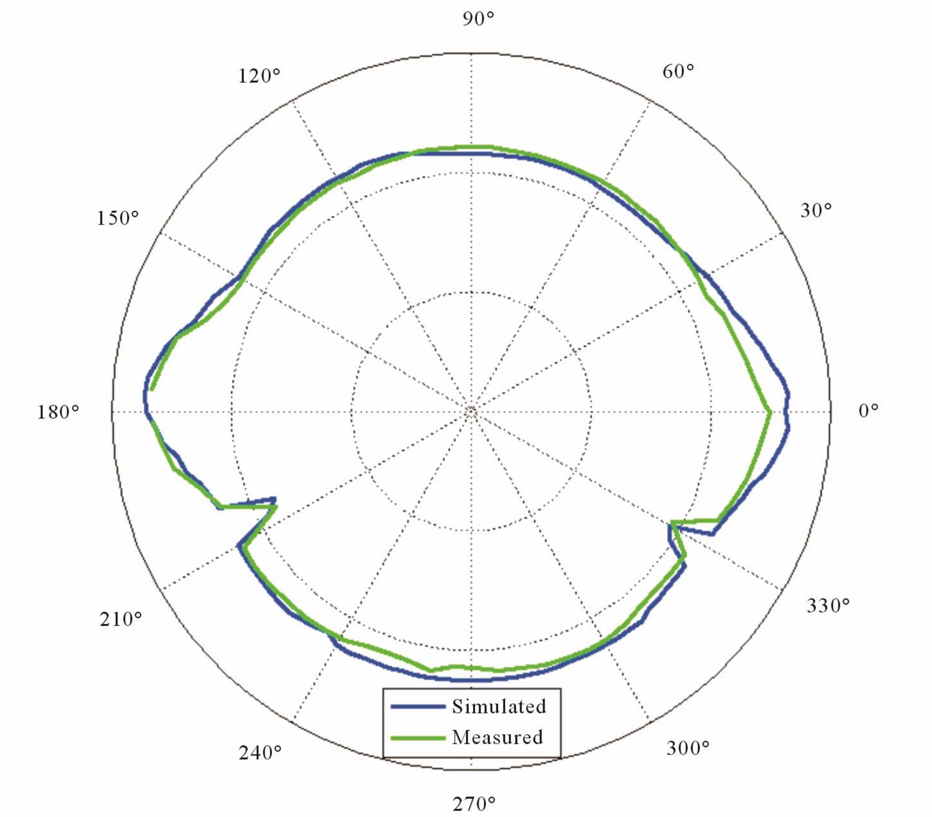

(a)

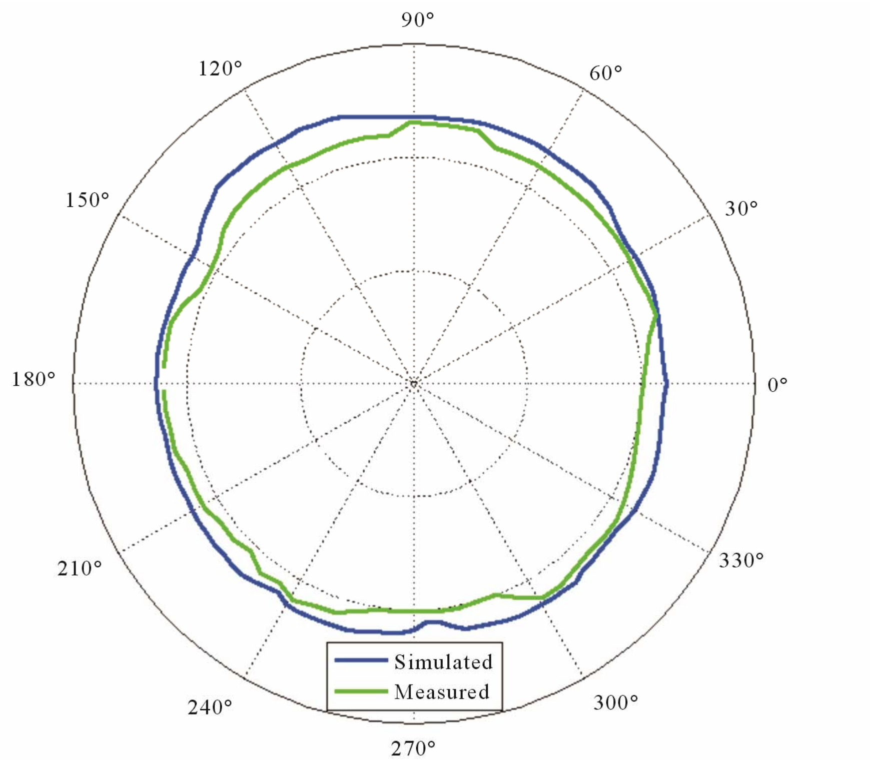

(b)

Figure 10. Simulated and measured radiation pattern in xy-plane (coordinate system shown in Figure 8) at (a) 3.45 GHz and (b) 5.5 GHz.

5.0 - 6.0 GHz for WLAN/WiMAX applications. Both antennas were designed with ADS, fabricated on a FR-4 microstrip material, and characterized. Both single band (single sided) and dual band (double-sided) antenna arrays provided omnidirectional pattern with desired gain.

REFERENCES

[1] C.-Y. Pan, T.-S. Horng, W.-S. Chen and C.-H. Huang, "Dual Wideband Printed Monopole Antenna for WLAN/WiMAX Applications," *IEEE Antennas and Wireless Propagation Letters*, Vol. 6, 2007.

[2] A. C. Rao and R. Pandeeswari, "A CPW-Fed Antenna for Dual Band WiMAX/WLAN Applications," *IEEE International Conference on Recent Trends in Information Technology ICRTIT*, 2011.

[3] H.-Y. Lai, Z.-Y. Lei, Y.-J. Xie, G.-L. Ning and K. Yang, "UWB Antenna with Dual Band Rejection for WLAN/WiMAX Bands Using CSRRs," *Progress in Electromagnetics Research Letters*, Vol. 26, 2011, pp. 69-78. doi:10.2528/PIERL11070112

[4] D. Parkash and R. Khanna "Design of a Dual Band Monopole Antenna for WLAN/WiMAX Applications," *IEEE Wireless and Optical Communications Networks*, 2010.

[5] L. Wang, K. Wei, J. Feng, Z. Zhang and Z. Feng, "A Wideband Omnidirectional Planar Microstrip Antenna for WLAN Applications," *IEEE*, 2011.

[6] J. Li, "An Omnidirectional Microstrip Antenna for WiMAX Applications," *IEEE Antennas and Wireless Propagation Letters*, Vol. 10, 2011.

[7] O. Tze-Meng and T. K. Geok, "A Dual-Band Omni-Directional Microstrip Antenna," *Progress in Electromagnetics Research*, Vol. 106, 2010, pp. 363-376. doi:10.2528/PIER10052411

[8] M. B. Bicer and A. Akdagli, "A Novel Microstrip-Fed Monopole Antenna for WLAN/WiMAX Applications," *Journal of Electromagnetic Waves and Applications*, Vol. 26, No. 7, 2012, pp. 904-913. doi:10.1080/09205071.2012.710372

[9] N. AbWahab, Z. Bin Maslan, W. N. W. Muhamad and N. Hamzah, "Microstrip Rectangular 4 × 1 Patch Array Antenna at 2.5 GHz for WiMAX Application," 2*nd International Conference on Computational Intelligence*, *Communication Systems and Networks*, 2010.

[10] Z. Zhong-xiang, C. Chang, W. Xian-liang and F. Ming-gang, "A 24 GHz Microstrip Array Antenna with Low Side Lobe," Springer, Berlin, 2012.

[11] A. K. Sahu and M. R. Das, "4 × 4 Rectangular Patch Array Antenna for Bore Sight Application of Consial Scan S-Band Traching Radar," *Antenna Week* (*IAW*), 2011.

[12] J. Das, T. A. Khan and M. K. Pal, "Rectangular Patch Antenna Array for Wireless Application," *International Journal of Engineering Science and Technology*, 2012.

[13] T. I. Huque, A. Chhowdhury, K. Hosain and S. Alam, "Performance Analysis of Corporate Feed Rectangular Patc Element and Circular Patch Element 4 × 2 Microstrip Array Antennas," *International Journal of Advanced Computer Science and Applications*, Vol. 2, No. 7, 2011, pp. 74-79.

[14] http://www.home.agilent.com/en/pc-1297113/advanced-design-system

[15] http://www.lpkf.com/protomat

J. Electromagnetic Analysis & Applications, 2011, 3, 43-46
doi:10.4236/jemaa.2011.32008 Published Online February 2011 (http://www.SciRP.org/journal/jemaa)

Back to Back Combined Single Feed Proximity Coupled Antenna with Dumbbell Shaped DGS

Ashwini Kumar Arya, Amalendu Patnaik, Machavaram V. Kartikeyan

Department of Electronics & Computer Engineering, IIT Roorkee, Roorkee, India.
Email: ashwiniarya.iitr@gmail.com, {apatnaik, kartik}@ieee.org

Received November 12th, 2010; revised December 10th, 2010; accepted January 5th, 2011

ABSTRACT

Use of defected ground structure (DGS) to reduce the size of patch antenna is presented in this paper. In order to get a dipole like radiation pattern for some specific application a dumbbell shaped DGS is used in the common ground plane of back to back combined single fed proximity coupled antenna. A size reduction of about 60% is achieved. Parametric analysis has been done to see the resonance behavior of the antenna with DGS.

Keywords*: *Defected Ground structure, Microstrip Antennas, Proximity Coupling

1. Introduction

The continuous shrinking size of electronic equipments demands similar size antenna elements in order to fit properly in wireless devices without compromising the other radiation properties of the antenna. In this respect microstrip patch antennas are quite an obvious choice because of its other benefits like low profile, light weight, low cost and easy fabrication.

But as far as size of these patches concerned, the patch length should be around half-a-wavelength for the structure to act as a good radiator. Different techniques have already been used for the antenna size reduction such as using the substrate with high dielectric constant [1] , edge shorted patches with shorting plates or shorting walls, use of the shorting pin at the suitable position etc [2,3].

As far as our understanding goes much has not been reported regarding the use of DGS for size reduction of microstrip antennas, although its application have been reported for harmonic reduction [4], cross-polarization suppression [5] and mutual coupling reduction [6] in antenna arrays etc. Although the back to back geometries have been reported by the various researchers [7,8] but here a new coupling method *i.e.* proximity coupling with the defected ground structure is used for the consideration of the increased bandwidth.

This paper presents the application of DGS for size reduction of microstrip antennas. A dumbbell shaped DGS is used in the common ground plane of a back to back combined single feed proximity coupled microstrip antenna.

2. Defected Ground Structure

Recently there has been an increasing interest in the use of DGSs for performance enhancement of microstrip antennas and arrays. These are realized by etching off a simple shape defect from the ground plane of the planer circuits.

Although various complicated DGSs were reported in the literature, but the simplest one is the dumbbell shaped DGS. **Figure 1(a)** shows the simple and mostly used dumbbell shaped DGS that is etched in the ground plane below the microstrip line, in which both the areas (L_g*W_g) and the slot gap (g) play a very important role to find the resonance behavior of the DGS.

The head areas (L_g*W_g) is very useful for the variation in the inductance (L) and the slot (g) produces the capacitance (C). The L and C may be calculated from the formulae given below [9].

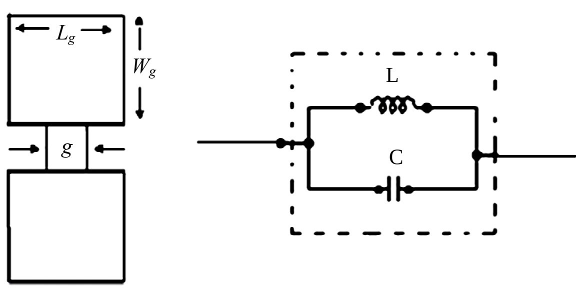

(a) (b)

Figure 1. (a) Dumbbell shaped DGS, and (b) DGS Equivalent Circuit.

$$\mathrm{L} = \frac{1}{4\pi^2 f_0^2 C} \tag{1}$$

$$\mathrm{C} = \frac{f_c}{2Z_0} \times \frac{1}{2\pi(f_0^2 - f_c^2)} \tag{2}$$

When this DGS is applied to the antenna, the equivalent inductive part due to the DGS increases and produces equivalently the high effective dielectric constant, thereby decreasing the resonant frequency when the DGS is incorporated in the ground plane of a micro strip antenna.

3. Antenna Design with DGS

In this section, the design approach and the performance of the basic antenna and the antenna with DGS is described. At the outset, the single patch antenna was designed and simulated using the CST Microwave studio [10], for the operating frequency at 5.0 GHz. Then another patch of the same size was added in the opposite side of the ground plane and fed in the same way as the first one. The configuration seems as two patch antennas having a common ground plane working at the same frequency. Next the feed lines were combined for the antenna for single feed design. For this purpose the antenna feed lines W_f = 0.934 mm with d_f = 1.5 mm were designed of 100 ohm and for matching to the 50 ohm transmission line (W_p = 3.86 mm) a quarter wave length transformer (W_t = 2 mm) was used to give proper matching (**Figure 2**).

The cross-sectional view of the single fed back to back combined proximity coupled antenna is shown in the **Figure 2(a)**. The layouts of matching networks only are emphasized in this **Figure 2(b)** for convenience. It is observed that the antenna designed in this configuration gives the bandwidth of 137 MHz whereas single antenna gives a bandwidth of 67 MHz. This is due to the fact that as the antenna height increases the quality factor decreases and the bandwidth increases. This becomes a multilayer antenna with more height and higher bandwidth as compared to the single patch antenna.

The simple transmission line model was used for the antenna size calculation. The dielectric constant was taken as 3.38 with the loss tangent 0.0025 and of 1.524 mm thickness. The patch lengths L_p and widths W_p are 15 mm and 19 mm respectively. The feed line has been inserted inside the dielectric at a height equal to the half of the height (h = 3.048 mm) of the antenna on either side. The dumbbell shaped DGS with dimensions L_g = W_g = 8.6 mm and g = 0.76 mm was created in the ground plane of the antenna as shown in the **Figure 2(c)**. A small slot was also created for making the antenna with single feed. The two feed lines were connected with a metal strip which goes through the small slot in the ground plane. The fabricated antenna is shown in **Figure 2(d)**.

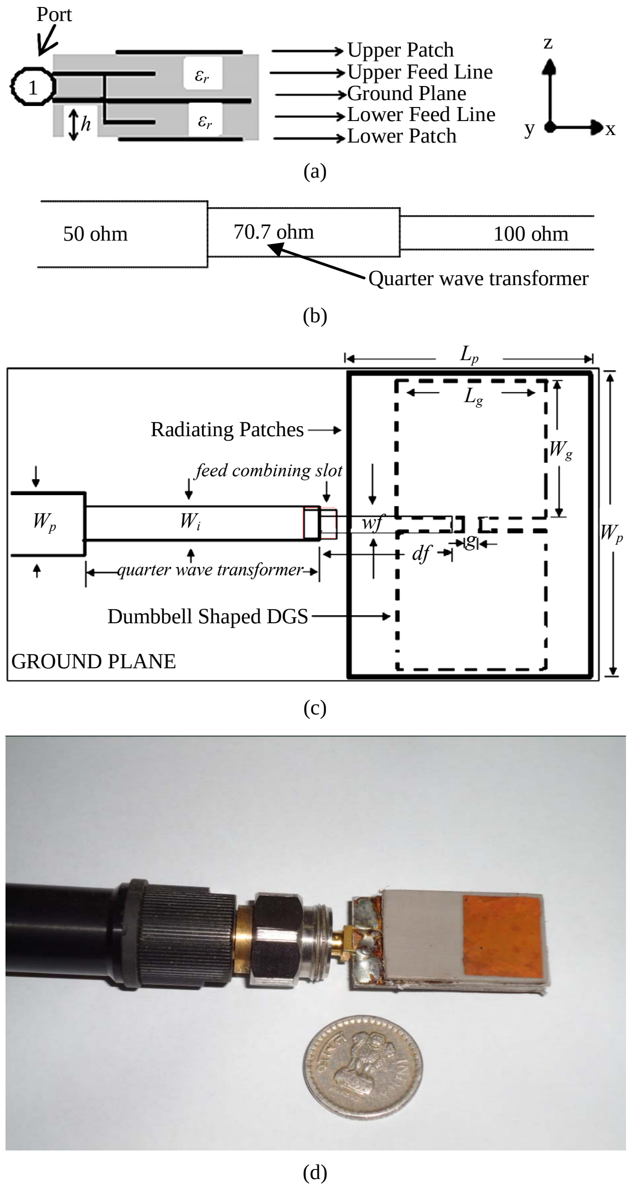

Figure 2. (a) Cross-sectional view of antenna configuration, (b) Feeding Network, (c) Top-View of the antenna, (d) Fabricated Antenna.

4. Results and Discussion

At first the antenna without the DGS in the common ground was simulated and was found to resonate at 5 GHz with 137 MHz Bandwidth.

Then the structure was simulated with the dumbbell shaped DGS. Before reaching to the final size of the DGS, a parametric study was done by varying L_g, W_g and g of

the DGS. As shown in **Figure 3**, with the increase in the value of L_g, the resonant frequency of the antenna is decreasing. Infect, increase in the length of the DGS head gives increasing inductance which in turn decreases the resonant frequency of the antenna.

At this point the increment in the (*g*) was not possible due to the accuracy in fabrication, so for this reason the other dimension (*g*) was kept constant for the requirement of the desired frequency (2 GHz). The size of the DGS single square head for the antenna to resonate at 2 GHz (UHF Band) was found to be 8.6 mm × 8.6 mm. The return loss (S11 [dB]) plot of the structure with and without DGS is shown in **Figure 4(a)**. **Figure 4(b)** shows the measured S11 parameter using the HP 8720 B network analyzer. The marker's position near to peak shows the resonance frequency 2.08 GHz with return loss of -13 dB. The result shows good agreement with the simulation results. The measured -10 dB bandwidth is about 60 MHz. The maximum size reduction achieved is about 60%.

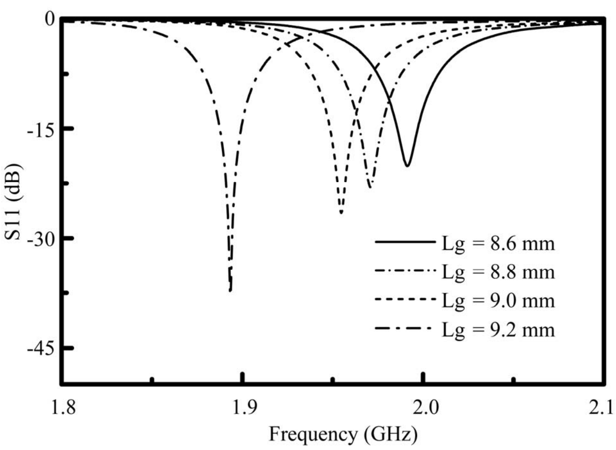

Figure 3. S11 Vs. Frequency response by varying DGS length (Lg).

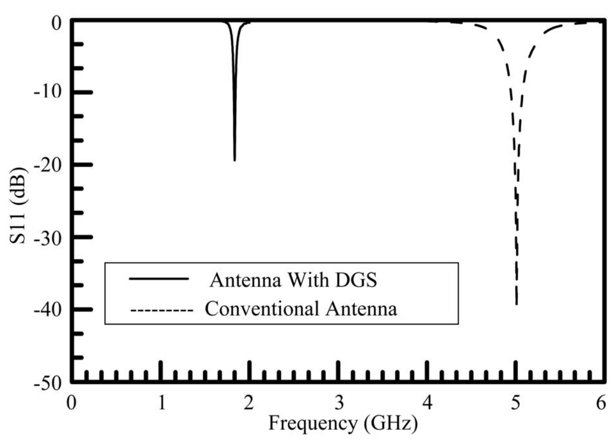

(a)

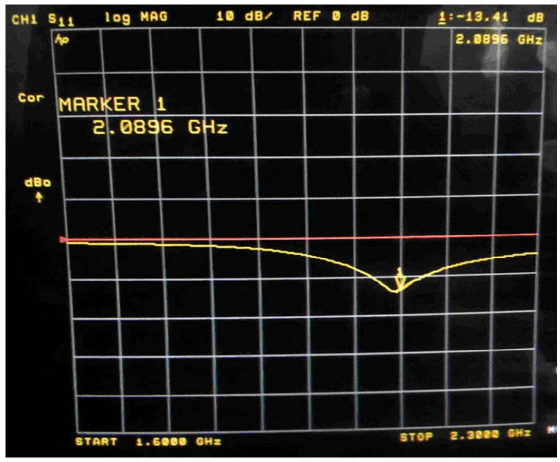

(b)

Figure 4. Antenna Return Loss (a) simulated (b) measured.

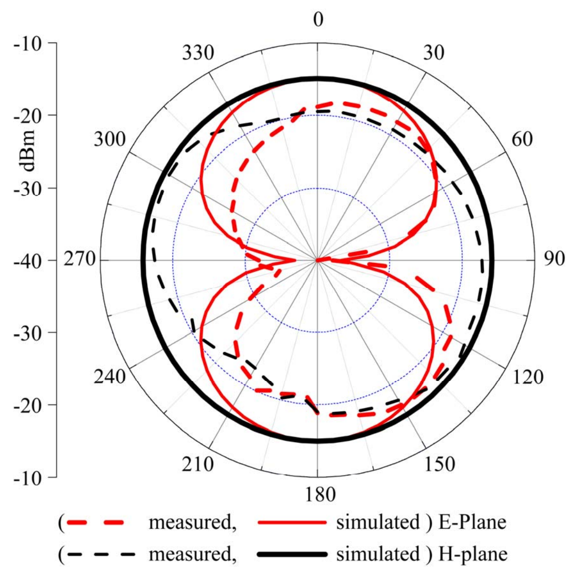

Figure 5. Antenna radiation pattern (measured and simulated) at 2 GHz Frequency.

The measured and simulated power patterns of the antenna are shown in **Figure 5**. It can be observed that the E-plane radiation pattern is similar to the pattern for a dipole antenna. Measurement errors are mainly due to the spurious radiation created by the feeding end and the improper coupling of the elements. However the gain measured experimentally for the proposed antennas with DGS is about -6.9 dB and -7.8 dB (where simulated gain with DGS is 3.8 dB and 5.7 dB is for the antenna without DGS, for both the planes) in both the E and H plane respectively, which is consistent with the size reduction of the antenna.

5. Conclusion

Microstrip patch antenna size reduction with DGS is car-

ried out in this work. A dumbbell shaped DGS in the common ground plane of a back to back microstrip structure was found to give a size reduction of about 60% and shifts the resonance frequency from 5 GHz to 2 GHz, with 60 MHz bandwidth facilitating the antenna, to be used for UHF band applications.

REFERENCES

[1] R. Garg, P. Bhartia, I. Bahl and A. Ittipiboon, "Microstrip Antenna Design Handbook," Artech House, London, 1995.

[2] P. Salon, M. Keskilammi and M. Kivikoski, "Single Feed Dual Band Planer Inverted-F Antenna with U-Shaped Slot," *IEEE Transactions on Antenna and Propagation*, Vol. 48, No. 8, 2000, pp. 1262-1264. doi:10.1109/8.884498

[3] D.Nashhat, H. Elsadek and H. Ghali, "Dual-Band Reduced Size PIFA Antenna with U-Slot for Bluetooth and WLAN Applications," *Proceedings of IEEE Antennas Propagation International Symposium*, Columbus, Vol. 2, 22-27 June 2003, pp. 962-965. doi. 10.1109/APS.2003.1219395

[4] H. Liu, X. Sun and J. Mao, "Harmonic Suppression with Photonic Bandgap and Defected Ground Structure for a Microstrip Patch Antenna," *IEEE Microwave and Wireless Component Letters*, Vol. 15, No. 2, February 2005, pp. 55-56. doi:10.1109/LMWC.2004.842809

[5] D. Guha, M. Biswas and Y. M. M. Antar, "Microstrip Patch Antenna with Defected Ground Structure for Cross Polarization Suppression," *IEEE Antenna and Wireless Propagation Letter*, Vol. 4, No. 1, 2005, pp. 455-458. doi:10.1109/LAWP.2005.860211

[6] M. Salehi, A. Motevasselian, A. Tavakoli and T. Heidari, "Mutual Coupling Reduction of Microstrip Antenna using Defected Ground Structure," *IEEE Singapore International Conference on Communication System*, Singapore, 2006, pp. 1-5. doi:10.1109/ICCS.2006.301375

[7] J. Guterman, Y. R. Samii, A. A. Moreira and C. Peixeiro, "Quasi-Omni Directional Dual-band Back-to-Back E-shaped Patch Antenna for Laptop Applications," *Electronics Letters*, Vol. 42, No. 15, 2006, pp. 845-847. doi:10.1049/el:20061799

[8] H. Iwasaki, "A Back-to-Back Rectangular-Patch Antenna Fed by a CPW," *IEEE Transactions on Antenna Propagation*, Vol. 46, No. 10, October 1998, pp. 1527-1530. doi:10.1109/8.725285

[9] D. Ahn, J. S. Park, C. S. Kim, J. Kim, Y. Qian and T. Itoh, "A Design of the Low-Pass Filter Using The Novel Micro strip Defected Ground Structure," *IEEE Transactions on Microwave Theory and Technology*, Vol. 49, No. 1, 2001, pp. 86-91. doi:10.1109/22.899965

[10] EM Simulation Software CST Studio Suite™, v9.

Journal of Electromagnetic Analysis and Applications, 2012, 4, 362-366
http://dx.doi.org/10.4236/jemaa.2012.49051 Published Online September 2012 (http://www.SciRP.org/journal/jemaa)

Vehicular Radio Scanner Using Phased Array Antenna for Dedicated Short Range Communication Service

Tapas Mondal[1], Priyanka Shishodiya[1], Rowdra Ghatak[2], Sekhar Ranjan Bhadra Chaudhuri[3]

[1]Department of Electronics & Communication Engineering, Dr. B. C. Roy Engineering College, Durgapur, India; [2]Microwave and Antenna Research Laboratory, Department of Electronics and Communication Engineering, National Institute of Technology Durgapur, Durgapur, India; [3]Department of Electronics & Telecommunication Engineering, Bengal Engineering and Science University, Shibpur, India.
Email: tapas2k@gmail.com

Received July 10th, 2012; revised August 11th, 2012; accepted August 21st, 2012

ABSTRACT

Now a day's accidents are very common due to increased population of vehicle. In order to ensure safety measures in the vehicle this paper has proposed some methodologies regarding careful driving by automatically scanning and analyzing the blind spot area of an intelligent mobile vehicle. A vehicular antenna with minimum perturbation is proposed to be fitted on the vehicle and collect information of the concern area which would ensure visibility of the operator *i.e.* masked or integrated within the car body. This paper has dealt with the design of Tchebyscheff polynomial based prototype planar microstrip phased array antenna and also redesigned the same when implemented in the body of the car being considered as an electromagnetically large element. Both the design has been experimentally verified with the measurement. The simulated and the measured results in both the cases are found to be in good agreement. More than 11 dB gain was observed at perfectly 30° angles from its broad side direction as desired for blind spot detection with minimum amount of electromagnetic interference inside the car.

Keywords: Intelligent Transportation System; Microstrip Phased Array Antenna; Tchebyscheff Polynomial; Electromagnetic Interference

1. Introduction

Intelligent Transport System (ITS) ensures mobility comfort and safety in transportation system. It also absorbs the hazards due to environmental impact. With the progress of the information processing technology, control systems to minimize accidents for the roadways have also been advanced hence one approach to improve the traffic safety is found and that is automatic collection of data by scanning the blind spot area of the vehicle [1] as shown in **Figure 1**. Many methods were proposed to detect the blind spot area but all of them had certain limitations. Devices like dynamic angling side view mirror [2], side view camera model [3], and shadow or edge features detector [4] were used for detecting blind spot area but their performance was affected during bad weather, fog or mist. Also we know that the mechanical systems, response time is more and the system is prone to wear and tear.

A radio frequency method has been proposed in this paper to scan the blind spot zone efficiently. Four rectangular microstrip antennas (RMSA) are arranged in linear configuration with optimal spacing between the patch elements to construct the phased array radar. A corporate feed network is used to feed the patch element unequally and a progressive phase shifter is designed with 108˚ delay elements to tilt the main beam in the desired direction and then the total unit is simulated and experimented after placing it on the car body which is electromagnetically a large element. The antenna works in the Dedicated Short-Range Communication Service (DSRCS) frequency band [5]. The design of the microstrip phased array antenna is discussed in Section 2 and after that to place the antenna; the design of the entire car is given in Section 3. Results and discussion are portrayed in Section 4 along with conclusion in Section 5.

2. Design of Microstrip Phased Array Antenna

The microstrip phased array antenna is designed for Dedicated Short Range Communication Service at 5.88 GHz with dielectric constant of 2.32 and substrate thickness of 0.785 mm. Firstly the dimension of the rectangular patch is computed as 16.322 mm by 19.8 mm using the method outlined in [6]. With computed inset feed length of 3.8 mm and for the above dimensions of the rectangular patch the return loss is found to be –8.09 dB

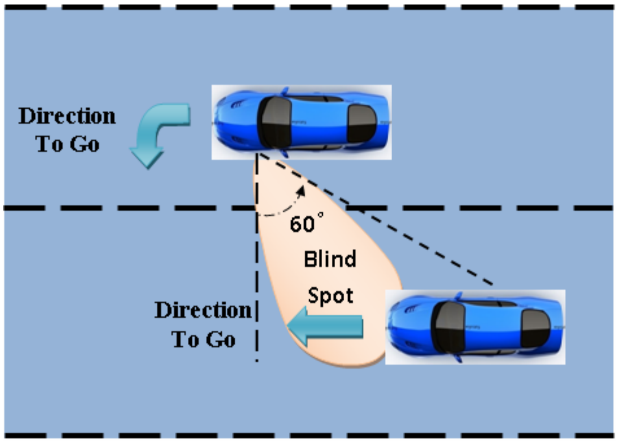

Figure 1. Surrounding regions of a vehicle.

with (30.1 + j26.7) ohm impedance at the feed position. The RMSA is simulated and optimized using Ansoft HFSS™. After optimization the final length is found to be 16.4363 mm with inset feed length of 4.8225 mm keeping the width of the patch unchanged as shown in **Figure 2**.

By considering the above designed patch element, a four element linear array is realized and powered by Tchebyscheff current distribution. The spacing between the elements is kept considering the desired maximum scan angle in order to eliminate the grating lobes within the visible space of the phased array antenna. To optimize the performance of the antenna in respect of its side lobe level (SLL), mutual coupling and gain of the antenna array, the spacing between the elements is studied parametrically [7]. The results of the said study are tabulated in **Table 1**.

After optimization it is found that the optimum spacing between the elements is 0.6 λ_0 while considering, the main lobe to side lobe ratio below 20 dB, optimum mutual coupling and overall gain.

From **Figure 1**, it is observed that the beam of the antenna array is required to be tilted by an angle 30˚ away from the broad side direction. In view of the above a progressive phase shifter of –108˚ is designed with the help of 11.16 mm feed line length. The actual line length is considered as mτ, where m = 0, 1, 2, 3.

To enhance the gain by maintaining the beam width and main lobe to side lobe ratio, the antenna elements are excited by Dolph Chebyshev current distribution. The array consist of four elements, thus third order Tchebyscheff polynomial is calculated. Hence the polynomial is solved and relative current ratio is computed as 1:1.7795:1.7795:1. Both equal and unequal power dividers are designed along with the progressive phase shifter.

For equal power division, a 3 dB equal power divider is designed whose vertical arm is of 50 Ω line and two horizontal quarter-wavelength branch-lines are of 70.71

Table 1. Effect on mutual coupling and gain due to variation in spacing (d) between the elements.

d with respect to guided wavelength	d with respect to operating wavelength	Mutual coupling (dB)	Gain (dBi)
0.6 λ_g	0.41 λ_0	>10	7.6
0.7 λ_g	0.48 λ_0	>13	9.9412
0.8 λ_g	0.55 λ_0	>20	10.647
0.9 λ_g	0.6 λ_0	>22	10.919

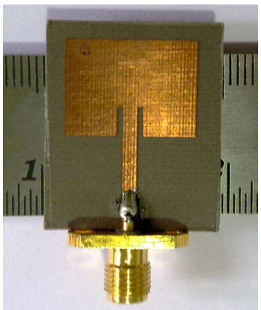

Figure 2. Photograph of the rectangular microstrip antenna element.

Ω is used [8]. It is shown in **Figure 3(a)**.

To get the unequal current distribution, both the horizontal arm of the microstrip unequal power divider should be of different resistance and it is calculated as 46.368 Ω and 82.49 Ω. The structure is shown in **Figure 3(b)**.

Generally for practical design purpose the gap between the corporate feed networks is taken small but the value of the gap less than 0.11 λ_0 disturbs the frequency response of overall antenna array. The effects of the feed network on the side-lobes are significant in the E-plane pattern. The influence on the H-plane is less important due to the orthogonality of the drive current and the symmetry of all the other currents in this cut [9]. By maintaining the SLL and the surface wave loss, the gaps are taken as 0.11 λ_0 as portrayed in **Figure 4**.

3. Placement of Antenna on the Vehicle

In order to compute the electromagnetic effect of the body of the car on the antenna performance, the entire structure of the car is designed in Ansoft HFSS™. The complete structure of the car consist of hood, roof, trunk, left and right side doors, left and right side quarter panel for front and rear side which are made up of conducting material but the bumpers and wheels are assigned by layered impedance due to their hard rubber and polyester materials as shown in **Figure 5**.

After going through the typical requirement for scanning the blind spot, the antenna is placed just beside the side view mirror. The following problems in the designed are addressed while simulating the effect of the radiation

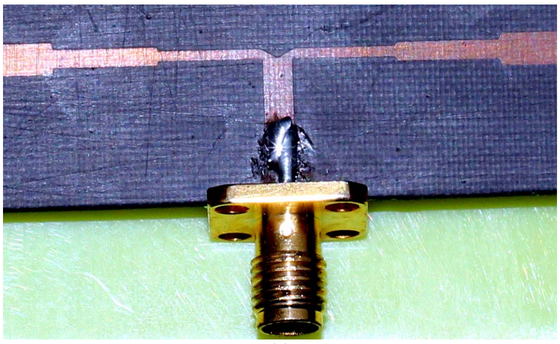

(a)

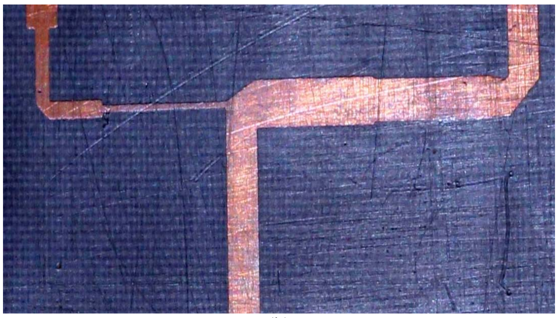

(b)

Figure 3. (a) Photograph of the equal microstrip power divider; (b) Photograph of the unequal microstrip power divider.

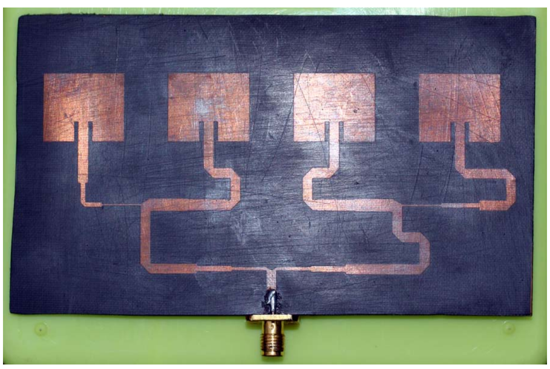

Figure 4. Photograph of the antenna array with corporate feed network.

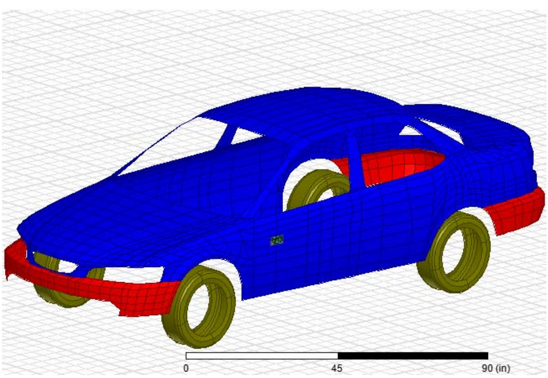

Figure 5. The entire structure of the car along with the antenna array.

characteristics of the antenna after placing it on the vehicle:

1) Spans a large computational domain compared to the wavelength;

2) Requires a fine grid resolution to resolve the detailed antenna structure;

3) Contains largely non-conformal PEC and dielectric structures.

4. Results and Discussion

For obtaining the scattering parameter characteristics, the microstrip antenna has been simulated over the frequency bandwidth ranging from 5.5 GHz to 6.5 GHz and two different circumstances is observed. The first experiments involve the design, simulation and measurement after fabrication of an individual element and then the array with the same without involving the effect of the car. Both of them should used for optimized performance.

The scattering parameter is measured by Agilent Technology Vector Network Analyzer model no. N5320A (10 MHz - 20 GHz) and the radiation pattern is measured by Hittite HMC-T2100 synthesized signal generator (10 MHz - 20 GHz) and Krytar 9000 B power meter (10 MHz - 40 GHz) with 9530 B power sensor (10 MHz - 20 GHz) as shown in **Figure 6**. From **Figure 7**, it is found

(a)

(b)

Figure 6. (a) Experimental set-up to measure the radiation pattern of the antenna array; (b) Experimental set-up to measure the radiation pattern of the antenna array after placing it on the car.

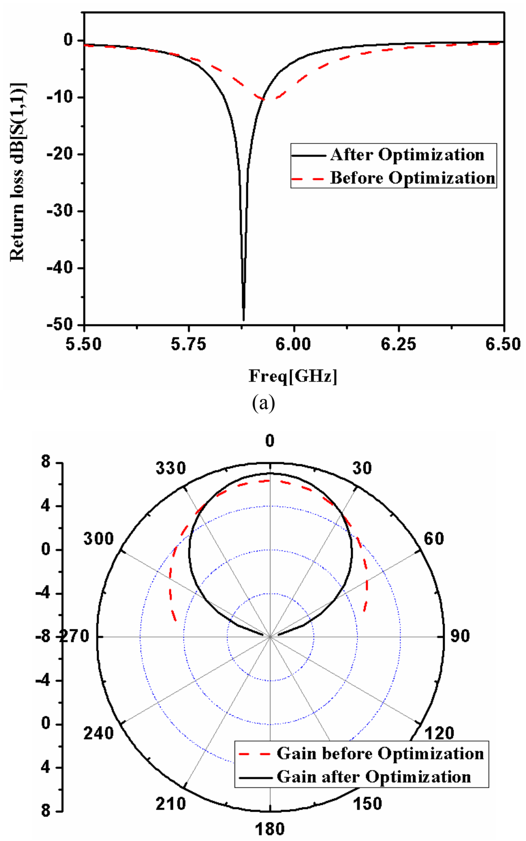

Figure 7. (a) Return loss a single patch before and after optimization; (b) Gain of a single patch before and after optimization.

that after optimization a perfect match is obtained exactly at 5.88 GHz and gain is also improved from 6.33 dB to 7.01 dB with a very good return loss of –47 dB. The current distribution and the radiation pattern of a single RMSA is portrayed in **Figure 8**.

A parametric study of the return loss of antenna array with different spacing between the elements of the corporate feed network is done and is compared in **Figure 9**. The results of the computational model of the entire antenna array with feed network were compared with the measured data and a good agreement is observed in **Figure 10**.

After getting the satisfactory results, next the same array antenna is experimented again with considering the electromagnetic effect of the car. In order to test the antenna array in association with the vehicle, a numerical model of the car is created using Ansoft HFSS^{TM} and the simulated data is compared with the measured in **Figure 11**. **Figure 12** graphically represents the 3D radiation pattern of the antenna array in presence of the computational model of the vehicle. From **Figure 13**, it is clear that the inside electric field strength is not more than 15 Volt per meter which is very less compare to the standard

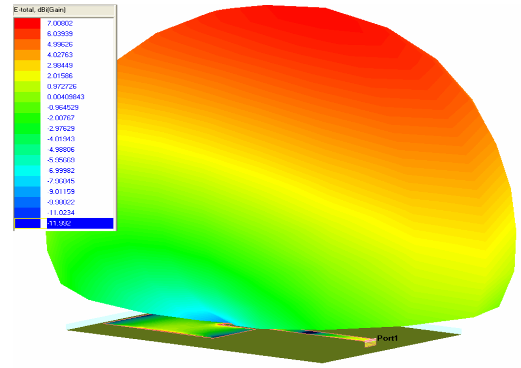

Figure 8. Current distribution and the radiation pattern of the rectangular microstrip antenna.

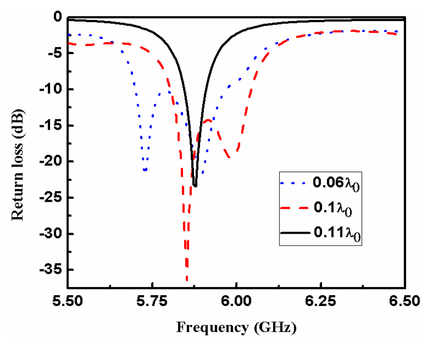

Figure 9. Parametric study of return loss of the antenna array with different spacing between the elements of corporate feed network.

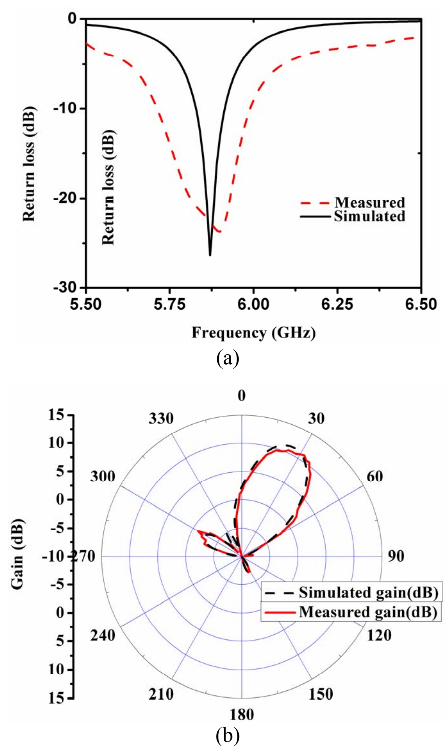

Figure 10. (a) Return loss of the antenna array; (b) Radiation pattern of the antenna array.

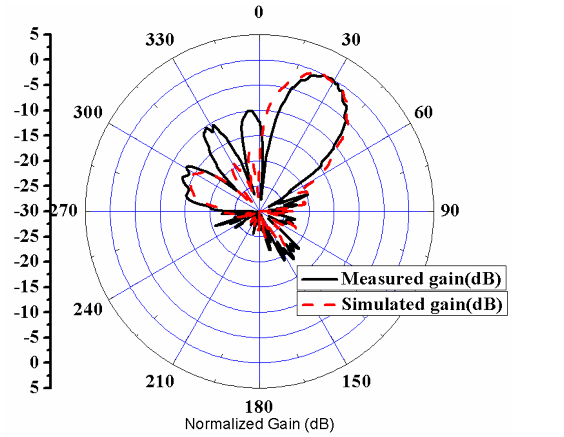

Figure 11. Normalized radiation pattern of the antenna array after placing it on the body of the car.

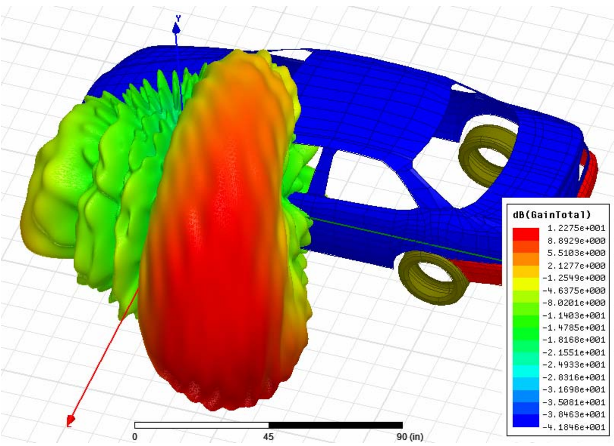

Figure 12. 3D radiation pattern of the antenna array after placing it on a vehicle body.

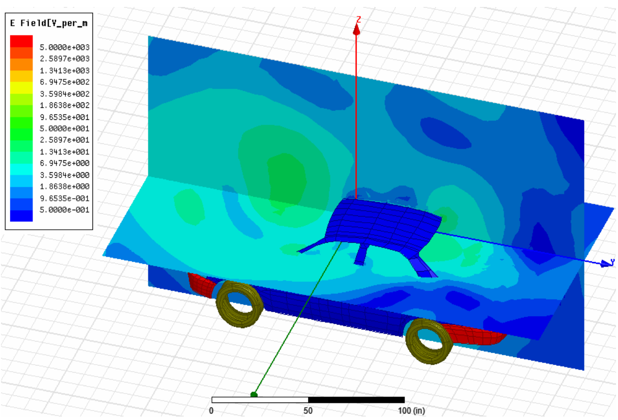

Figure 13. Inside electric field interference of the array after placing it on a vehicle body.

electromagnetic hazards.

5. Conclusion

A Tchebyscheff polynomial based microstrip phased array antenna is designed to detect the blind spot area of the intelligent mobile vehicle. The design is further simulated in Ansoft HFSS^{TM} after placing the antenna on the body of the car and the results are observed. The result of the computational model of the entire antenna array is compared with the measured data before and after placing the said antenna array on the body of the car and found to be in good agreement. An overall 11 dB gain is obtained while measuring in the desired direction with minimum amount of electromagnetic interference inside the car.

REFERENCES

[1] M. Griffiths, "Intelligent Transport System," Postnote: Parliamentary Office of Science and Technology, London, 2009. www.parliament.uk/paliamentary_offices/post/

[2] J. Kuwana and M. Itoh, "Dynamic Angling Side-View Mirror for Supporting Recognition of a Vehicle in the Blind Spot," *International Conference on Control, Automation and Systems*, *ICCAS*, Seoul, 14-17 October 2008, pp. 2913-2918.

[3] S. Jeong, S.-W. Ban and M. H. Lee, "Autonomous Detector Using Saliency Map Model and Modified Mean-Shift Tracking for a Blind Spot Monitor in a Car," *Seventh International Conference on Machine Learning and Applications*, San Diego, 11-13 December 2008, pp. 253-258. doi:10.1109/ICMLA.2008.129

[4] B.-F. Wu, C.-C. Kao, Y.-F. Li and M.-Y. Tsai, "A Real-Time Embedded Blind Spot Safety Assistance System," *International Journal of Vehicular Technology*, Vol. 2012, 2012, pp. 1-15. doi:10.1155/2012/506235

[5] A. Tang and A. Yip, "Collision Avoidance Timing Analysis of DSRC-Based Vehicles," *Accident Analysis & Prevention*, Vol. 42, No. 1, 2010, pp. 182-195. doi:10.1016/j.aap.2009.07.019

[6] T. Mondal, J. S. Roy and S. R. Bhadra Chaudhuri, "Phased Array Antenna Design for Intelligent Transport Systems," *IEEE International Workshop on Antenna Technology*: *Small Antennas and Novel Metamaterial* (i*WAT*), Santa Monica, 2-4 March 2009, pp. 1-4.

[7] T. Mondal, R. Ghatak and S. R. B. Chaudhuri, "Design and Analysis of a 5.88GHz Microstrip Phased Array Antenna for Intelligent Transport Systems," *IEEE International Sumposium on Antennas and Propagation and CNC/USNC/URSI Radio Science Meeting*, Toronto, 11-17 July 2010, pp. 1-4.

[8] H. J. Visser, "Array and Phased Array Antenna Basics," John Wiley & Sons Ltd., Chichester, 2005. doi:10.1002/0470871199

[9] E. Levine, G. Malamud, S. Shtrikman and D. Treves, "A Study of Microstrip Array Antennas with the Feed Network," *IEEE Transactions on Antennas and Propagation*, Vol. 31, No. 4, 1989, pp. 426-434. doi:10.1109/8.24162

Wireless Engineering and Technology, **2012, 3, 175-180**
http://dx.doi.org/10.4236/wet.2012.33025 Published Online July 2012 (http://www.SciRP.org/journal/wet)

Plus Shape Slotted Fractal Antenna for Wireless Applications

S. Jagadeesha[1], R. M. Vani[2], P. V. Hunagund[3]

[1]S.D.M. Institute of Technology, Ujire Mangalore, India; [2]University Science Instrumentation Center, Gulbarga University, Gulbarga, India; [3]Department of PG Studies and Research in Applied Electronics, Gulbarga University, Gulbarga, India.
Email: Jagadeesh.sd69@gmail.com, vanirm12@rediffmail.com, prbhakar_hunagund@yahoomail.com

Received April 28th, 2012; revised May 26th, 2012; accepted June 3rd, 2012

ABSTRACT

Fractal antennas are characterized by space filling and self-similarity properties which results in considerable size reduction and multiband operation as compared to conventional microstrip antenna. This paper outlines a multiband antenna design based on fractal concepts. Fractal antennas show multiband behavior due to self-similarity in their structure. The plus shaped fractal antenna has been designed on a substrate of dielectric constant $€_r = 4.4$ and thickness 1.6 mm. The proposed antenna is characterized by a compact size and it is microstrip feed fractal patch of order 1/3. It is observed that the antenna is radiating at multiple resonant frequencies. The resonant frequency is reduced from 2.2 GHz to 900 MHz after I & II iterations respectively. Thus considerable size reduction of 81.77% & overall bandwidth of 12.92% are achieved. The proposed antenna is simulated using the method of moment based commercial software (IE3D) and it is found that simulated results are in good agreement with the experimental results.

Keywords: Fractal Antenna; Multi Frequency; Size Reduction; Wireless Application; Plus Shape Antenna; Slotted Antenna

1. Introduction

In the study of antennas, fractal antenna theory is a relatively new area. The emergence of antennas with fractal geometries has given an answer to two of the main limitations started by Werner (1999) of the classical antennas, which are single band performance and dependence between size and operating frequency. The term "fractal" means broken or irregular fragments. It was originally coined by Mandelbrot (1983) to describe a family of complex shapes that possess an inherent self-similarity or self-affinity in their geometrical structure. Jaggered (1990) defined fractal electrodynamics as an area in which fractal geometry was combined with electromagnetic theory for the purpose of investigating a new class of radiation, propagation and scattering problems. One of the most promising area fractal electrodynamics researches is in its application to antenna theory and design. There are varieties of approaches that have been developed over the years, which can be utilized to archive one or more of these design objectives. The development of fractal geometry came largely from an in depth study of the pattern nature, with the advance of wireless communication system and their increasing importance wide band and low profile antennas are in great demand for both commercial and military applications [1]. A fractal is a rough or fragmented geometric shape that can be split into parts, each of which is a reduced-size copy of the whole and this property is called self-similarity. Fractal [2] geometries are composite designs that repeat themselves or their statistical characteristics and are thus "self-similar" fractal geometry finds a variety of applications in engineering. Fractal geometry is space filling contours of regular or irregular shapes [3-6], and is super imposed of too much iteration and they describe the self-similar property of fractal geometry [7]. Fractals are a class of shapes which have not characteristic size. Each fractal is composed of multiple iterations of a single elementary shape the iteration can continue infinitely, thus forming a shape within a finite boundary but of infinite length or area. Fractal has the following features 1) It has a finite structure at arbitrarily small scales; 2) It is too irregular to be easily described in traditional Euclidean geometric; 3) It is self-similar; 4) Simple and recursive [8]. Modern telecommunication systems require the antenna with wider bandwidth and smaller dimension than conventionally possible. This has initiated antenna research in various directions, are of which is by using fractal shaped antenna elements. In recent years several fractal geometries have been introduced for antenna application with varying degree of success in improving antenna

characteristics. Some of these geometries have been particularly useful in reducing the size of the antenna, while other designs aim at incorporating multiband characteristics. These are low profile antennas with moderate gain and can be made operative at multiple frequency bands and hence are multifunctional [9]. In our present work we focus on generation of multifrequency which yields increases the bandwidth and size reduction of antenna. A plus shape patch is taken as a base shape and in first iteration four other plus shape patches of the order of 1/3 of base shape are placed touching the base shape. Similarly second iterations are taken by further placing plus shaped patches at even reduced scales. It is found that as the iteration number and iteration factor increases, the resonance frequencies become lower than those of the zero iteration, which represents a conventional plus shape patch.

2. Design Consideration

The base shape of the plus shaped slotted fractal antenna is designed on a dielectric substrate having a relative dielectric constant €$_r$ = 4.4 and thickness 1.6 mm as shown in **Figure 1**. This is the reference antenna or base shape antenna. Further this base shape antenna is modified by inserting horizontal slots on both sides with respect to center of patch as shown in **Figure 2** and it is named as antenna1. The length of the slot Ls is varied on either side of the edge as 5 mm, 10 mm, 15 mm, 20 mm, 21.175 mm, 21.675 mm and the frequency variation has been studied. The optimum length obtained is Ls = 21.675 mm *i.e.*, the distance between slots q = 2 mm is considered for further design.

The first iteration patch is designed with four plus shapes of order (1/3) of base shape are placed touching the base shape as shown in **Figure 3** and it is named as antenna 2 and same procedure is repeated for second iteration. This antenna is as shown in **Figure 4** and it is named as antenna 3. For each iteration plus shapes of the order of $(1/3)^n$ of base shape are taken, where n is the number of iterations. The dimension of first iteration can be calculated as

e = (1/3) a & g = (1/3) c also f = (1/3) b & h = (1/3) d.

i = (1/3) e & k = (1/3) g also j = (1/3) f & L = (1/3) h

So with optimized design the dimensions obtained are a = 45.3 mm, b = 15.1 mm, c = 35.4 mm, d = 11.8 mm. The length of the slot is Ls = 21.675 mm and width of the slot Ws *i.e.* r = 2 mm. The dimension of the ground plan is 55 mm × 85 mm. A 50 ohm SMA connector is used to feed the antenna by using microstrip feed technique. Optimized microstripline with following dimension, m = 0.5 mm, n = 18.55 mm, o = 3.05 mm, p = 18.4 mm. The suitable feed location is obtained through optimization process by using the IE3D software. The fabricated photographic view of all proposed antennas is shown from **Figures 5(a)-(e)**.

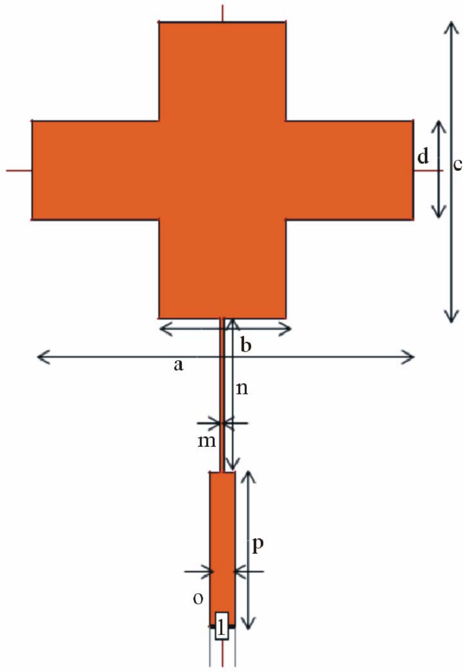

Figure 1. Geometry of base antenna.

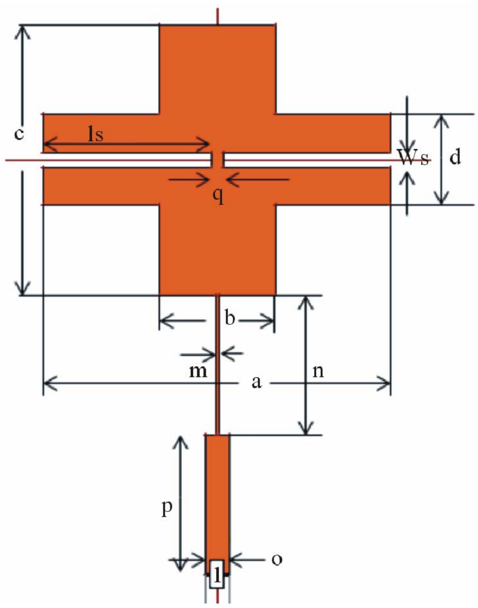

Figure 2. Geometry of antenna 1.

3. Results and Discussion

The characteristic of the fractal antenna with slot and with iterations has been studied by using IE3D software. Also the results have been verified practically with by using Vector Network Analyzer model Rohde and schewarz, German make ZVK model No.8651.

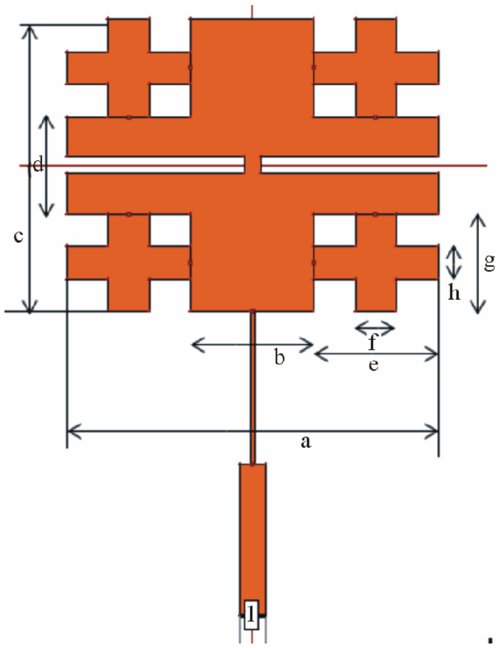

Figure 3. Geometry of base antenna 2.

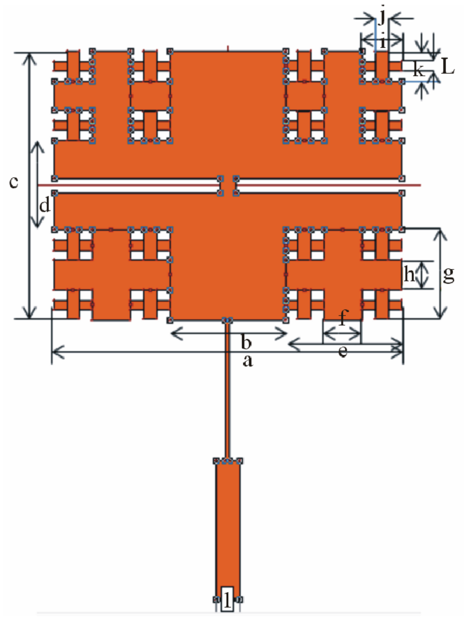

Figure 4. Geometry of antenna 3.

The modified base shape antenna with slots as been optimized by varying slot length Ls. The variation of Ls with resonant frequency of the antenna is shown in **Table 1** and same is presented in graphical form in **Figure 6**. From the tabular results it is found that by increasing slot length Ls on both sides from the edge of the patch, resonant frequency decreases. The lowest possible resonant frequency 1.27 GHz is obtained for Ls = 21.675 mm (*i.e.*, distance between the slots q = 2 mm) & this is taken as optimized length of the slot for further iteration.

The results of all proposed antennas are shown in **Table 2**. The simulated and measured return loss characteristics of proposed antennas are shown from **Figures 7(a)-(d)**.

From the results it is clear that the resonant frequency of the antenna 1 *i.e*., modified base antenna with slot is fr = 1.27 GHz which is lower compared to the base antenna without slot (fr = 2.199 GHz). So the size reduction obtained is 66.85%. The antenna 2 *i.e*. the modified antenna with slots and first iteration gives multiple bands with lower frequency of 0.99 GHz. The size reduction obtained for antenna 2 is 79.88%. Further antenna 3 *i.e*., with slot and second iteration gives multiple bands with

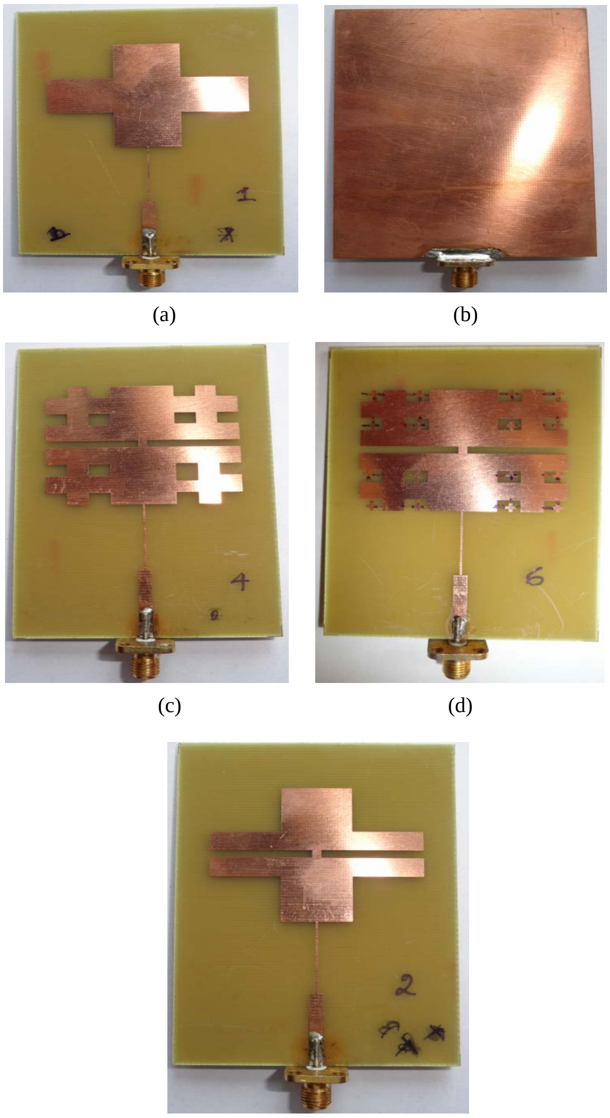

(a) (b) (c) (d) (e)

Figure 5. (a) Photograph of top view of base antenna; (b) Photograph of bottom view of base antenna; (c) Photograph of antenna 1; (d) Photograph of antenna 2; (e) Photograph of antenna 3.

Table 1. Variation of slot length v/s resonant frequency.

Slot length (Ls) variation in mm	Resonating frequency (GHz)
0	2.22
5	2.197
10	2.155
15	1.93
20	1.436
12.175	1.34
21.675	1.27

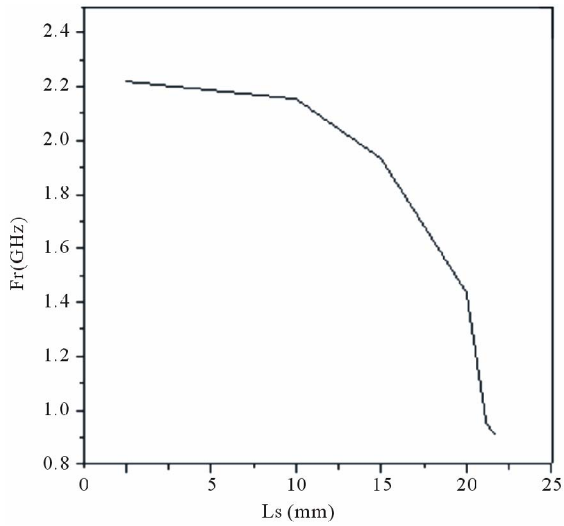

Figure 6. Variation of resonant frequency v/s slot length.

lower resonant frequency of 0.90 GHz. The size reduction obtained for antenna 3 is 81.77% which is more compared to all other proposed antennas.

Further the bandwidths of proposed antennas have been studied through simulation and measurements and the results are shown in **Table 2**. From the results it is clear that the bandwidths of modified antenna with slot, first & second iteration are more compared to base antenna. The measured bandwidth of antenna 1 is 106 MHz (4.895%), antenna 2 is 190 MHz (11.93%) and antenna 3 is 215 MHz (12.92%). The radiation patterns of all proposed antennas are studied and all are giving broadside radiation. Splitting of beam *i.e.* dip is found in **Figure 8(a)** of simulated radiation pattern of base shape at 2.19 GHz. In **Figure 8(b)** splitting of beams merged into broadside pattern at 0.91 GHz at second iterations this results into broadside radiation pattern.

4. Conclusion

This paper presents a new plus shape slotted fractal antenna with first and second iterations. The antenna.3 *i.e.*, slotted fractal antenna with second iteration gives size reduction of 81.77% and band width of 12.92% with broad side radiation pattern. So from the results we conclude that the modified base antenna with slots of second iterations gives a good size reduction and enhanced band width compared to that of modified base antenna with

Table 2. Results of proposed antennas.

Prototype antenna	Resonant frequency fr (GHz)		Return loss (db)		Bandwidth (MHz)		Overall bandwidth (MHz)	
	Sim	Pract	Sim	Pract	Sim	Pract	Sim	Pract
Base antenna	f1 – 2.19	f1 ± 2.19	–19	–24	53	53	79	71
	f2 – 3.42	f2 ± 2.46	–14	–15	26	18		
Antennal with q = 2 mm	f1 ± 1.19	f1 ± 1.27	15.8	–12.8	20	18		
	f2 ± 2.52	f2 ± 2.48	18.4	–20.1	113	44	133	106
		f3 ± 2.56		–18.7		44		
Antennal 2 with q = 2 mm (1st itr)	f1 ± 0.96	f1 ± 0.99	16.7	–14.5	22	80		
	f2 ± 2.9	f2 ± 2.97	–14	–26.9	44	50	136	190
	f3 ± 3.08	f3 ± 3.17	21.5	–21	70	60		
Antennal 3 with q = 2 mm (2nd itr)	f1 ± 0.91	f1 ± 0.990	15.2	–14.2	11	87		
	f2 ± 3.07	f2 ± 2.976	19.4	–17.6	70	50	81	215
		f3 ± 3.168		–18.9		78		

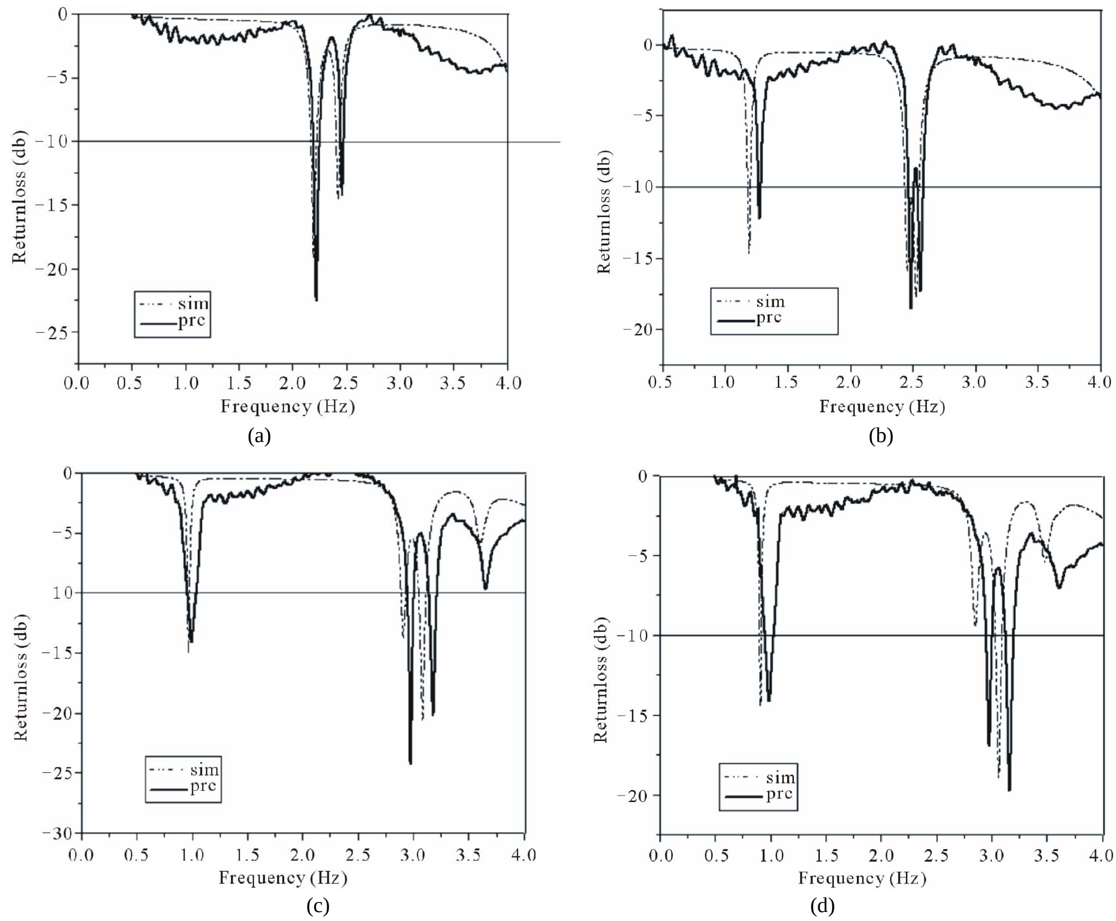

Figure 7. (a) Return loss characteristic of antenna 1 with q = 2 mm; (b) Return loss characteristic of base antenna 2 with q = 2 mm; (c) Return loss characteristic of antenna 2 with q = 2 mm; (d) Return loss characteristic of antenna 3 with q = 2 mm.

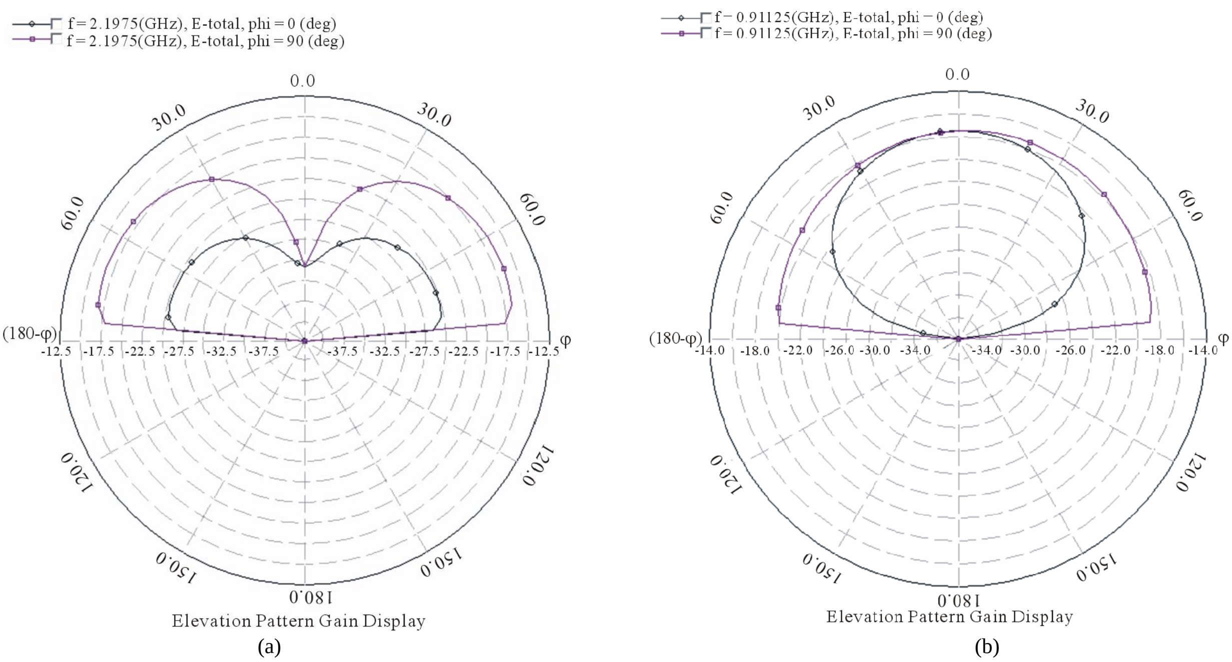

Figure 8. (a) Simulated radiation pattern of base shape at 2.19 GHz; (b) Simulated radiation pattern at 0.91 GHz for second iteration.

slot of first iteration. These antennas may find application in wireless communication systems.

REFERENCES

[1] K. Sing, V. Grewal and R. Saxena, "Fractal Antennas: A Novel Miniaturization Technique for Wireless Communications," *International Journal of Recent Trends in Engineering*, Vol. 2, No. 5, 2009, pp. 172-176.

[2] B. Mandelbrot, "Fractal: Form, Chance and Dimension," W. H. Freeman and Company, San Francisco, 1997.

[3] H. O. Peitgzen, H. Jurgens and D. Sanpe, "Chaos and Fractals," New Frontiers in Science, Springer-Verlag, New York, 1992.

[4] C. Punete, J. Romen, R. Pous, X. Garkia and F. Beitez, "Fractal Multiband Antenna Based on the Serpinski Gasket," *Electronics Letters*, Vol. 32, No. 1, 1996, pp. 1-2. doi:10.1049/el:19960033

[5] J. P. Gianvittorio and Y. Rahmat-Sami, "Fractal Antennas: Novel Antenna: A Novel Antenna Miniaturization Technique and Applications," *IEEE Antenna and Propagation Magazine*, Vol. 44, No. 1, 2002, pp. 20-36. doi:10.1109/74.997888

[6] D. H. Werner and S. Ganguly "An Overview of Fractal Antenna Engineering Research," *IEEE Antenna and Propagation Magazine*, Vol. 45, No. 1, 2003, pp. 38-57.

[7] G. Srivatsun, S. S. Rani and G. S. Krishnan, "A Self-Similar Fractal Cantor Antennas for MICS Based Wireless Applications," *Wireless Engineering Technology*, Vol. 2, No. 2, 2011, pp. 107-111. doi:10.4236/wet.2011.22015

[8] W. Shalan and K. Pahwa, "Multiband Microstrip Rectangular Fractal Antenna for Wireless Applications," *International Journal of Electronics Engineering*, Vol. 3, No. 1, 2011, pp. 103-106.

[9] F. J. Jibrael and M. H. Hammed, "A New Multiband Patch Microstrip Plusses Fractal Antenna for Wireless Applications," *ARPN Journal of Engineering and Applied Sciences*, Vol. 5, No. 8, 2010, pp. 155-158.

7

New Antenna Array Architectures for Satellite Communications

Miguel A. Salas Natera et al.*
Universidad Politécnica de Madrid, Spain

1. Introduction

Ground stations which integrate the control segment of a satellite mission have as a common feature, the use of large reflector antennas for space communication. Apart from many advantages, large dishes pose a number of impairments regarding their mechanical complexity, low flexibility, and high operation and maintenance costs. hus, reflector antennas are expensive and require the installation of a complex mechanical system to track only one satellite at the same time reducing the efficiency of the segment (Torre et al., 2006).
With the increase of new satellite launches, as well as new satellites and constellation of low earth orbit (LEO), medium earth orbit (MEO), and geostationary earth orbit (GEO), the data download capacity will be saturated for some satellite communication systems and applications. Thus, the feasibility of other antenna technologies must be evaluated to improve the performance of traditional earth stations to serve as the gateway for satellite tracking, telemetry and command (TT&C) operation, payload and payload message or data routing (Tomasic et al., 2002). One alternative is the use of antenna arrays with smaller radiating elements combined with signal processing and beamforming (Godara, 1997).
Main advantages of antenna arrays over large reflectors are the higher flexibility, lower production and maintenance cost, modularity and a more efficient use of the spectrum. Moreover, multi-mission stations can be designed to track different satellites simultaneously by dividing the array in sub-arrays with simultaneous beamforming processes. However, some issues must be considered during the design and implementation of a ground station antenna array: first of all, the architecture (geometry, number of antenna elements) and the beamforming process (optimization criteria, algorithm) must be selected according to the specifications of the system: gain requirements, interference cancellation capabilities, reference signal, complexity, etc. During implementation, deviations will appear as compared to the design due to the manufacturing process: sensor location deviation and sensor gain and phase errors (Martínez & Salas, 2010). In an antenna array, the computation of a close approach of the direction of arrival (DoA) and the correct performance of the beamformer depends on the calibration procedure implemented.

* Andrés García-Aguilar, Jonathan Mora-Cuevas, José-Manuel Fernández González, Pablo Padilla de la Torre, Javier García-Gasco Trujillo, Ramón Martínez Rodríguez-Osorio, Manuel Sierra Pérez, Leandro de Haro Ariet and Manuel Sierra Castañer.
Universidad Politécnica de Madrid, Spain

This chapter is organized with the following sections. Section 2, introduces the relationship between applications and antenna design architectures. Section 3, introduces the new antenna array architectures for satellite communication including motivation and explains experimental examples. Section 4, explains adaptive antenna array and receiver architectures for adaptive antennas systems considering the beamforming with synchronization algorithms. Finally, Section 5 explains the A3TB concept.

2. Applications and antenna design architectures

In recent effort, new antenna array architectures have been under analysis and development. In (Tomasic et al., 2002) a highly effective, multi-function, low cost spherical phased array antenna design that provides hemispherical coverage is analyzed. This kind of novel architecture design, as the geodesic dome phased array antenna (GDPAA) presented in (Tomasic et al., 2002) preserves all the advantages of spherical phased array antennas while the fabrication is based on well-developed, easily manufacturable, and affordable planar array technology (Liu et al., 2006; Tomasic, 1998). This antenna architecture consists of a number of planar phased sub-arrays arranged in an icosahedral geodesic dome configuration.
In contrast to the about 10 m diameters dome of the GDPAA, there is the geodesic dome array (GEODA) (Sierra et al., 2007) with 5 m diameters dome. This antenna, presented in Fig. 1, has two geometrical structure parts. The first one, is based on a cylinder conformed by 30 triangular planar active arrays, and the second is a half dodecahedron geodesic dome conformed by 30 triangular planar active arrays. The GEODA is specified in a first version for satellite tracking at 1.7 GHz, including multi-mission and multi-beam scenarios (Martínez & Salas, 2010). Subsequently, the system of the GEODA has been upgraded also for transmission (Arias et al., 2010).

a b c

Fig. 1. a) The GEODA, b) The active sub-array demonstration, and c) The 45 elements planar active sub-array.

The antenna arrays technology in the user segment for satellite communications will substitute reflectors providing a more compact and easy to install antenna system, which is an interesting solution e.g. for satellite on the move (SOTM) system. There is a great diversity of solutions for fixed and mobile satellite communication systems including a large number of applications. Inmarsat broadband global area network (Inmarsat-BGAN) (Franchi et al., 2000) is the most representative example among mobile satellite systems (MSS), which gives land, maritime and aeronautical high speed voice and data services with global coverage using GEO satellites at L-band.

MSS services are divided into two groups, those that offer a regional coverage usually with GEO satellites, and those which offer a global coverage based on LEO or MEO satellite constellations. Depending on the coverage, there are some examples for MSS with regional coverage as the mobile satellite system (MSAT) in EEUU, Canada and South America, Optus in Australia, N-Star in Japan, Asia cellular satellite (ACeS) in Asia or Thuraya in the Middle East and in the North of Africa. While for MSS of global coverage there are some examples as Iridium, ICO Global Communications, Globalstar, Teledesic, etc. (Evans, 2009; Wu, 1994). Most of the MSSs work at L and S band, new applications on satellite to mobile terminal links work at X, Ku and Ka band, and satellite to base station connections work at L, S and C band. A number of applications is broad and lead terrestrial telecommunications market to offer a wider coverage: high speed voice and data (internet access, SMS, VoIP), digital video broadcasting by satellite 2 (DVB-S2) and digital video broadcasting satellite services to handhelds (DVB-SH), global position system (GPS) and Galileo, security, control and machinery monitoring on ships and aircrafts, teleeducation or telemedicine.

These modern satellite communications systems require new antenna solutions for base stations, aeronautical applications or personal communications services (PCS) on-the-move (Fujimoto & James, 2001). Within these applications, antenna array systems are potentially the best choice due to, as discussed above, its capability to perform electronically steering or beamforming, increase the antenna gain, and conform over curved or multifaceted surfaces the radiating elements. Portable antennas for PCS must be easy to install and mechanically robust, besides compact and lightweight (García et al., 2010) as the antenna array presented in Fig. 4.a. The design of antenna systems to provide high data rates for reliable PCS boarded on ships is not so strict in term of the geometrical requirements because it does not have space limitations (Geissler et al., 2010). However, in the case of land or airborne vehicles, geometrical and mechanical constraints are more severe. Antennas for terrestrial vehicles must be low profile, and for airborne vehicles aerodynamic shapes must be considered (Baggen et al., 2007; Vaccaro et al., 2010). Moreover, for the civil market conformal antenna arrays (Schippers, 2008; Kanno et al., 1996), or multi-surface arrays (Khalifa & Vaughan, 2007) are suitable choices to deal with the system aesthetic partiality.

Technological challenges have been faced during the implementation of satellite communication systems in the last decades. The design of a Test-Bed flexible and modular for testing or debugging beamforming algorithms and receiver architectures is an invaluable contribution in the educational, research and development area on satellite communication systems. The adaptive antenna array Test-Bed (A3TB) concept is based on the use of antenna arrays with beamforming capability to receive signals from LEO satellites (Salas et al., 2008). The scope of the A3TB is to probe the concept of antenna arrays applied to ground stations instead of reflectors for different applications, such as telemetry data downloading. It is also a good chance for Universities and Research Centers aiming to have their own ground station sited in their installations.

The A3TB ground station relies on the use of an antenna array to smartly combine the received signals from the satellite thanks to the implementation based on software defined radio (SDR) technology. The advantages of the SDR implementation is that A3TB architecture can be used to process any received signal from LEO satellites in the band imposed by the radio frequency (RF) circuits. Moreover, most of the processing is performed in software, so that appropriate routines can be used to process any received signal. The A3TB can be used to analyze the feasibility of different receivers and beamformer

algorithms, regarding the capability to switch the receiver architecture in terms of the synchronizer algorithm configuration (Salas et al., 2007).
The current version has been developed to track The National Oceanic and Atmospheric Administration (NOAA) satellites in the very high frequency (VHF) band, in particular, the automated picture transmission (APT) channel (Salas et al., 2008). Previous versions of A3TB dealt with low rate picture transmission (LRPT) signals from the meteorological operational satellite-A (MetOp-A), where a complete receiver with beamforming and synchronization stages has been implemented (Salas et al., 2007; Martínez et al., 2007).

3. Antenna arrays for satellite communications

Satellite applications require compactness, lightweight and low cost antenna systems to be mounted on a terrestrial vehicle, an aircraft or a ship, or as a portable man-pack or a handset, and to be competitive against ground systems. Its major advantage is the possibility of getting a wider or even a global coverage. For such purposes, antenna arrays offer the technology to get a directive system whose steering direction can be electronically and/or mechanically controlled. However, planar arrays usually cannot steer more than 60º-70º from the normal direction of the antenna (Mailloux, 2005). Thus, when a wider angular coverage is required conformal arrays are an appropriate option (Josefsson & Persson, 2006). Arrays can approximate conformal shapes, such as spheres or cylinders, using several planar arrays, simplifying fabrication of active components (Sierra et al., 2007).
Since the low cost and low weight specifications are of importance, micro-strip antennas are mostly used, due to its capacity to be printed over a dielectric substrate with photolithography techniques. Low cost and low permittivity substrates are usually used such as FR4 or PTFE with different quantities of glass or ceramic impurities. For more demanding applications, ceramics, like alumina or high/low temperature co-fired ceramics (HTCC/LTTC) allow the use of smaller components thanks to its high permittivity, and give robustness against mechanical stresses and high temperatures.

3.1 Geodesic antenna array for satellite tracking in ground station

The aim of using a single antenna for tracking many satellites at the same time avoiding mechanical movements as well as its inexpensive cost make these antennas an alternative to be considered (Salas et al., 2008). Multi-beam ability and interference rejection are facilitated thanks to the electronic control system of such antennas that improves the versatility of the ground stations.
The GEODA is a conformal adaptive antenna array designed for MetOp satellite communications with specifications shown in Table 1. This antenna was conceived to receive signals in single circular polarization (Montesinos et al., 2009). Subsequently, in recent efforts the system has been upgraded also for transmission and double circular polarization (Arias et al., 2010). Hence, operating at 1.7 GHz with double circular polarization it can communicate with several LEO satellites at once in Downlink and Uplink. Current structure is the result of a comprehensive study that valued the ability to cover a given spatial range considering conformal shape surface and a given beamwidth (Montesinos et al., 2009). As Fig. 1 shows, GEODA structure consists of a hemispherical dome placed on a cylinder of 1.5 meters height. Both cylinder and dome are conformed by 30 similar triangular planar arrays (panels). Each panel consists of 15 sub-arrays of 3 elements (cells). The radiating element consists of 2 stacked circular patches with their own

RF circuits. The principal patch is fed in quadrature in 2 points separated 90º in order to obtain circular polarization. The upper coupled patch is used in the aim of improving the bandwidth.

Each panel is able to work itself as an antenna since they have a complete receiver that drives the 1.7 GHz signal to an analog to digital converter (ADC). In order to adapt the signal power to the ADC, it is mandatory to implement a complete intermediate frequency (IF) receiver consisting of heterodyne receiver with an automatic gain control block. Hence, each triangular array has active pointing direction control and leads the signal to a digital receiver through an RF conversion and filtering process. To follow the signal from the satellite, the main beam direction has to be able to sweep an angle of 60º. In this way, it is needed a phase shift in the feeding currents of the single radiating element. Previous calculations have demonstrated that 6 steps of 60 degrees are needed to achieve the required sweeping angle. An adaptive digital system allows the adequate signal combination from several triangular antennas. The control system is explained in (Salas et al., 2010).

Parameter	Specification	Parameter	Specification
Frequency range [GHz] **Tx:** **Rx:**	1.65 to 1.75 1.65 to 1.75	**Isolation between Tx and Rx [dB]**	>20
Polarization	Dual circular for Tx and Rx bands	**VSWR**	1.2:1
G/T [dB/K] **For elevation >30º** **For elevation 5º**	3 6	**SLL [dB]**	-11
EIRP [dBW]	36	**Size [m]**	1.5x1.5x3
3dB beamwidth [deg.]	5	**Accuracy steering [deg.]**	±1.4
Maximum gain [dBi]	29	**Coverage [deg.]:** **Azimuth** **Elevation**	360º >5º
Efficiency [%]	50		

Table 1. Main specifications for GEODA antenna.

3.1.1 Cell radiation pattern

Based on the study presented in (Sierra et al., 2007), the single radiating element is a double stacked circular patch that works at 1.7 GHz with 100 MHz bandwidth. In order to obtain circular polarization, the lower patch, which has 90 mm diameter, is fed by 2 coaxial cables in quadrature. Both coaxial cables connect the patch with a hybrid coupler to transmit and

receive signals with both, right and left, circular polarizations. The upper patch is a circular plate with 78.8 mm diameter, and it is coupled to the lower patch increasing the bandwidth by overlapping both resonant frequencies tuning the substrate thickness and the patch diameter size. Fig. 2.a shows the radiating element scheme and main features of the layer structure are specified in (Montesinos et al., 2009).

A cell sub-array of 3 radiating elements shown in Fig. 2.b is considered the basic module to build the planar triangular arrays. The whole cell fulfills radiation requirements since it has a good polar to crosspolar ratio and a very low axial ratio. Likewise, as it is presented in Fig. 2.c, the radiation pattern shows symmetry and low side lobes for full azimuth.

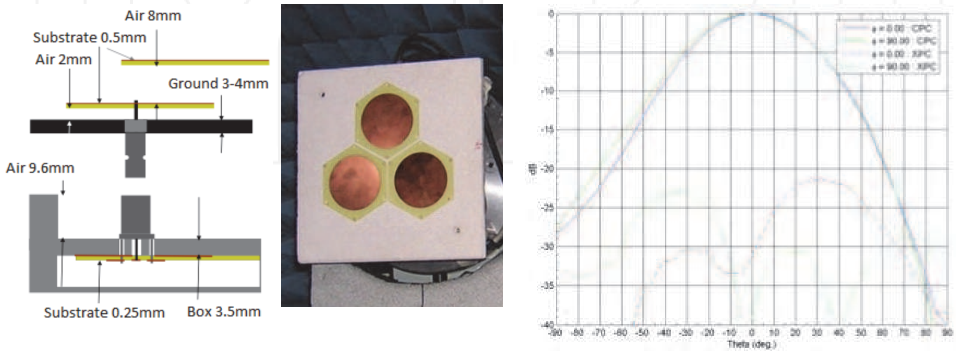

a b c

Fig. 2. a) Assembly of the single radiating element, b) Cell scheme, and c) Cell radiation pattern.

3.1.2 Transmission and Reception (T/R) module and cell distribution

Different T/R module configurations have been considered, providing either single or double polarization (Arias et al., 2010). T/R module allows amplifying and controlling the phase shift between signals, received and transmitted, providing an adaptive beam and steering direction controller in the whole working pointing range. As Fig. 3 shows, the design implemented contains a hybrid coupler, enabling double circular polarization; a double pole double throw (DPDT) switch, selecting polarization associated with transmission and reception way; 2 low noise amplifiers (LNAs), which amplify the signal received or transmitted; a single pole double throw (SPDT) switch, choosing transmission or reception way; and phase shifters, introducing multiples of 22.5^{o} relative shift phases to form the desired beam. These surface mount devices have been chosen in order to reduce space and simplify the design.

Signals transmitted/received by the 3 T/R modules placed in a cell are divided/combined thanks to a divider/combiner circuit composed of 3 hybrid couplers that leads the signal to a general T/R module where signal is amplified. Due to transmission and reception duality, 2 SPDT switches are used to select the amplification way. Furthermore, each T/R module has associated a -25dB directional coupler that is used to test T/R modules in the transmission mode. Additionally, reception mode is tested by measuring signal in the divider/combiner circuit. A single pole 6 throw (SP6T) switch selects the path that is tested.

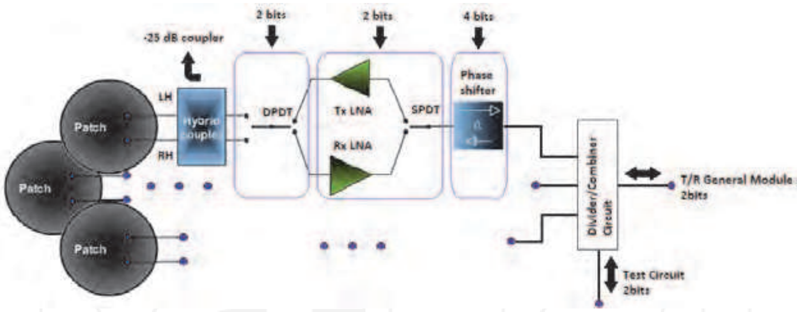

Fig. 3. Cell sub-array and RF circuit.

3.1.3 Control system

The control system has two main parts (Salas et al., 2010), the hardware structure and the control software. The two level hardware structure has the lowest possible number of elements, making the control simpler in contrast to the previous in (Salas et al., 2010). Finally, an inter-integrated circuit (I2C) expander is used to govern T/R modules individually, and one more cover cell needs (LNA of call and test). A multipoint serial standard RS-485 is used to connect the computer with the panels.

3.2 Portable antenna for personal satellite services

New fix and mobile satellite systems (Evans, 2000) require antenna systems which can be portable, low profile and low weight. Planar antennas are perfect candidates to fulfill these specifications. Usually slots (Sierra-Castañer et al., 2005) and printed elements (García et al., 2010) are most used as radiating elements.

3.2.1 Antenna system structure

In this subsection it is introduced a printed antenna for personal satellite communications at X band, in Fig. 4. Table 2 shows main antenna characteristics.

Parameter	Specification	Parameter	Specification
Frequency range[GHz] **Tx:** **Rx:**	7.9 to 8.4 7.25 to 7.75	**Efficiency [%]**	50
Polarization	Dual circular polarization for Tx and Rx bands	**Isolation between Tx and Rx [dB]**	>17
G/T [dB/K]	7	**VSWR**	1.4:1
EIRP [dBW]	32	**SLL [dB]**	-11
3dB beamwidth [deg.]	5	**Size [m]**	40x40x2.5
Maximum gain [dBi]	25	**Weight [Kg]**	2

Table 2. Portable antenna specifications.

This is a planar, compact, modular, low loss and dual circular polarized antenna, for Tx and Rx bands, simultaneously. It is made up by a square planar array of 16x16 double stacked micro-strip patches, fed by two coaxial probes. A hybrid circuit allows the dual circular polarization (Garg et al., 2001). Elements are divided in 16 sub-arrays excited by a global power distribution network of very low losses, minimizing the losses due to the feeding network and maximizing the antenna efficiency. In order to reduce side lobe levels (SLL), the signal distribution decreases from the centre to the antenna edges, keeping symmetry with respect to the main antenna axes. The antenna works at X band from 7.25 up to 8.4 GHz with a 14.7% relative bandwidth for a 1.4:1 VSWR and a maximum gain of 25 dBi.

3.2.2 Sub-array configuration

The sub-array configuration can be seen in Fig. 4.a. It makes possible to separate the fabrication of these sub-arrays from the global distribution network, simplifying the corporative network and getting a modular structure suitable for a serial fabrication process. Each sub-array is a unique multilayer board, where PTFE-Glass substrate of very low losses has been used as base material. The power distribution network is connected to each sub-array through (SMP-type) coaxial connectors.

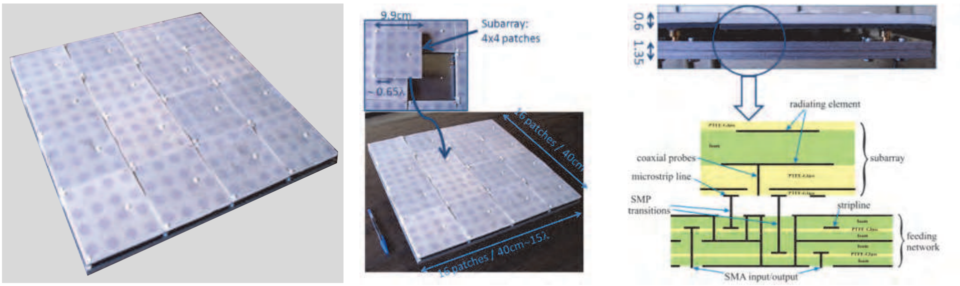

a b c

Fig. 4. a) Dual polarized portable printed antenna for satellite communication at X band, b) Sub-array perspective view, and c) Side view and multilayer scheme.

Fig. 5.a and Fig. 5.b show the sub-array unit cell. In order to obtain better polarization purity, each element is rotated 90º and excited by a 90º phase-shifted signal. Moreover, in Fig. 5.c is showed a miniaturized branch-line coupler (BLC) of three branches working as a wide band hybrid circuit (García et al., 2010; Tang & Chen, 2007).

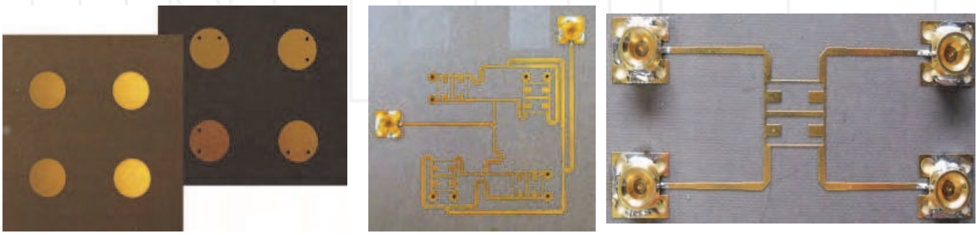

a b c

Fig. 5. Unit cell test board, a) Unit cell test board 2x2 stacked patches, b) Micro-strip feeding network, and c) Miniaturized BLC Prototype.

A conventional configuration takes up an area of 13.3 cm^2 which is big compared to the radiating element and the sub-array subsystem size. Therefore, a miniaturization of the BLC is needed using the equivalence between a $\lambda/4$ transmission line and a line with an open-ended shunt stub. An area reduction about 35% is achieved and the hybrid circuit behaves like a conventional BLC. In Fig. 6.b and Fig. 6.c measurement results for the BLC in Fig. 5.c are shown compared with simulations.

Fig. 7 depicts some sub-array measurements. The copular to crosspolar ratio is better than 25 dB and axial ratio is under 0.9 dB in the whole bandwidth.

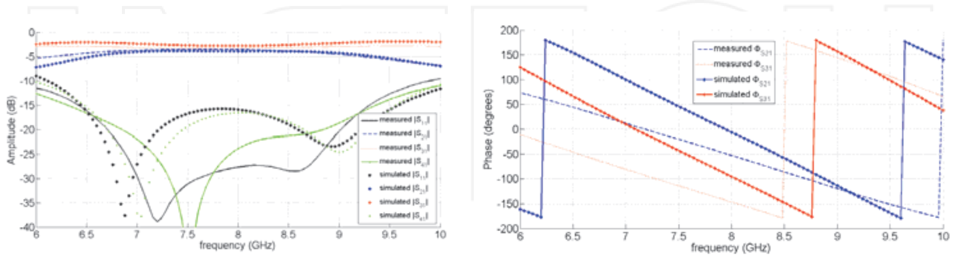

a b

Fig. 6. Miniaturized BLC, Measured and simulated S-parameters in: a) Amplitude, and b) Phase.

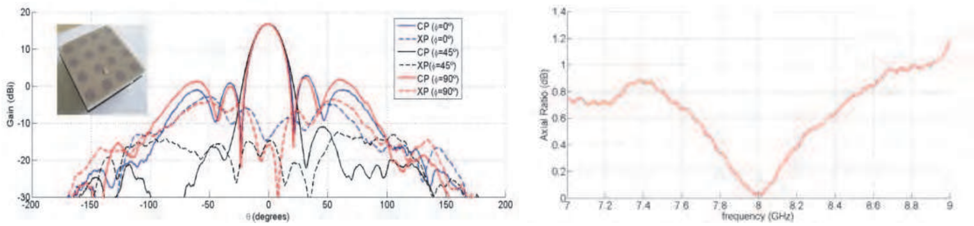

a b

Fig. 7. 4x4 patch sub-array measurements, a) Radiation pattern at 7.75 GHz, and c) Axial ratio for right-handed circular polarization.

3.2.3 Low losses power distribution network

The global feeding network presented in Fig. 8.a is a protected strip-line, where foam sheets of high thickness are used to get low losses. Such a kind of feeding network allows keeping a trade-off between the simplicity of exciting the radiating elements using printed circuits and the loss reduction when the distribution network is separated in a designed structure to have low losses. Losses in the structure are around 0.6 dB/m which yields to 0.3 dB of losses in the line. Two global inputs/outputs using SMA-type connectors, one for each polarization, excite the strip-line networks.

Vertical transitions have to be treated carefully and must be protected to avoid undesired higher order mode excitation. Thereby, it has been design a short-ended pseudo-waveguide, adding some extra losses about 0.3 dB, for two kinds of vertical transitions, as can be seen in Fig. 8.b and Fig. 8.c.

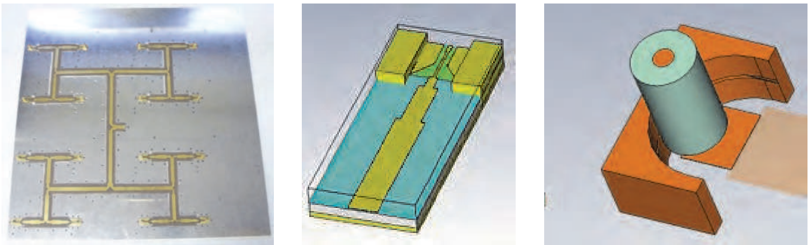

a b c

Fig. 8. a) Protected strip-line global corporative network for one polarization, b) Transitions from strip-line to SMA-type connector, and c) Transitions from strip-line to SMP-type connector.

3.2.4 Antenna performance

Fig. 9 depicts measured radiation pattern at 7.75 GHz, gain and axial ratio for the antenna system. It is shown a maximum gain of 25 dBi in the lower band and about 22 dBi in the upper band, and a SLL around 11 dB. Copolar to crosspolar ratio is better than 30 dB and axial ratio is under 0.7 dB. Total losses are about 4 dB in the working band.

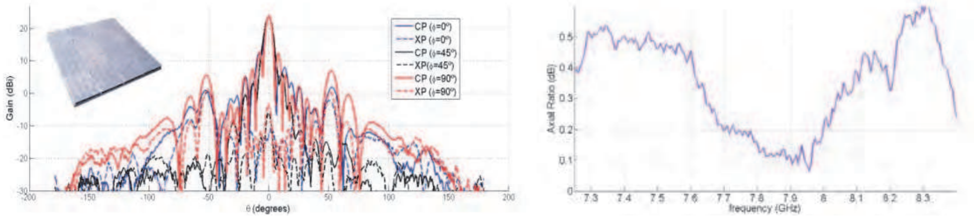

a b

Fig. 9. Antenna measurements results, a) Radiation pattern at 7.75 GHz, and c) Axial ratio for right-handed circular polarization.

3.3 Electronically steerable antennas for mobile and fixed portable systems

At present, two types of electric steerable antenna systems can be used to access the satellite communication services (Bialkwoski et al., 1996). These are: fixed position portable systems and mobile systems such as those installed on a land vehicle. The fixed portable antenna system is relatively easy to be accomplished by the antenna designer. The design involves standard procedures that concern the operational bandwidth, polarization and moderate gain (García et al., 2010). One drawback of the fixed position portable system is that they require the user to be stationary with respect to the ground. This inconvenience can be overcome with the mobile antenna system. A mobile user complicates the scenario since the ground mobile antenna needs to track the satellite (Alonso et al., 1996). The design of such a system is more challenging as new features associated with the mobility of the system have to be incorporated (Fernández et al., 2009). The requirement leads to a narrow beamwidth, for which satellite tracking is required as the vehicle moves around. Electronically steerable antennas enable the development of reconfigurable antennas for satellite applications.

3.3.1 Steerable antenna for fixed position portable systems

This antenna is a fixed satellite communication system with high gain at X band, consisting of an antenna array that integrates 32 2x2 sub-array modules in the complete antenna, as shown in Fig. 10.a. It is a planar and dual circular polarized antenna for Tx and Rx bands simultaneously. It is made up by a planar array of double stacked circular micro-strip patches, fed by 2 coaxial probes to generate circular polarization. A hybrid circuit allows the dual circular polarization as shown in Fig. 10.b.

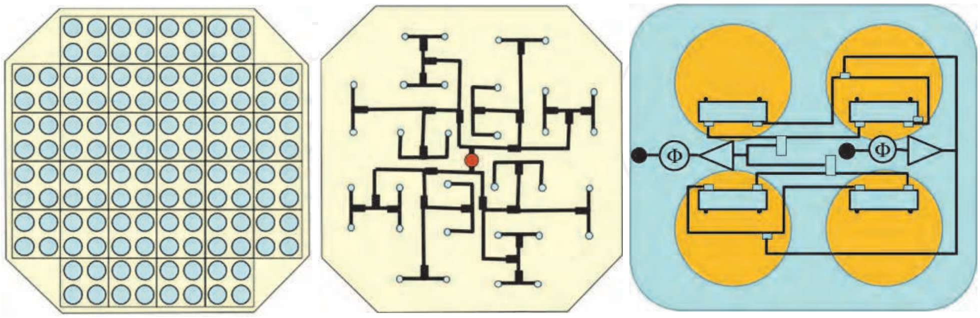

a b c

Fig. 10. Active multi-beam antenna, a) Top view, b) Feeding network of the complete antenna, and c) Beamforming network of the 2x2 sub-array module

The antenna has the same design parameters, structure and configuration as the antenna explained in Section 3.2 but with a different feeding network, as previously shown. In this case, the beamforming network requires changes in the feeding phase in the 2x2 sub-arrays, which can be achieved by phase shifters (ϕ) associated with different sub-arrays (Fig. 10.c). All these sub-arrays are connected to a feeding network, in Fig. 10.b, formed by transmission lines with low losses in strip-line. General specifications of the steerable antenna for fixed position portable systems are provided in Table 3.(a).

3.3.2 Automatic steerable antenna for mobile systems

A broadband circularly polarized antenna for satellite communication in X band is presented in Fig. 11 and specified in Table 3.(b). The arrangement features and compactness are required for highly integrated antenna arrays. It is desired to get a low-gain antenna for mobile satellite communications with low speed of transmission. In this system, the antennas are formed by 5 planar 4x4 arrays of antennas, which form a truncated pyramid with a pointing capability in a wide angular range, so that among the 5 planar arrays the complete antenna can cover any of the relative positions between the mobile system and the satellite in a practical way. The scheme of the active antenna can be seen in Fig. 11.

As it can be observed in Fig. 11.a, the antenna terminal is a multi-beam printed antenna shaped as a trunk pyramid capable of directing a main beam in the direction of the satellite. The antenna steering system consists of a multi-beam feeding structure with switches that lets combine the feed of each 4x4 arrays to form multiple beams. Switching the different 4x4 arrays, it is achieved different multiple beams and the variation of the steering direction.

The complete antenna consists of a Tx and Rx module that works independently in the 2 frequency bands.
The antenna has multiple beams covering the entire space to capture the satellite signal without moving the antenna. The signal detected in each of the beams is connected to a switch, which, by comparison, is chosen the most appropriate 4x4 array. The steering direction of the 4x4 array can vary between a range of directions that covers a cone angle range of 90º. To obtain the required gain and cover the indicated range, it is required around 15 beams, which can be obtained by integrating the beamforming networks with switches in the design as presented in (Fernández et al., 2009).

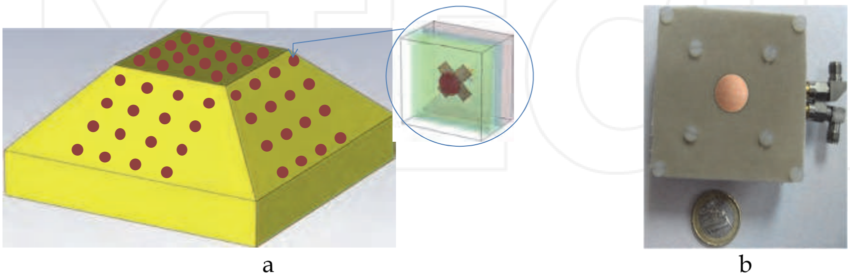

Fig. 11. Complete antenna structure, a) Radiating element of the 4x4 arrays, and b) Prototype top view.

The radiating element of the 4x4 array is one 2 crossed dipoles with a stacked circular patch as shown in Fig. 11.a and Fig. 11.b. In Fig. 12 the cross-section of the radiating element structure is presented.

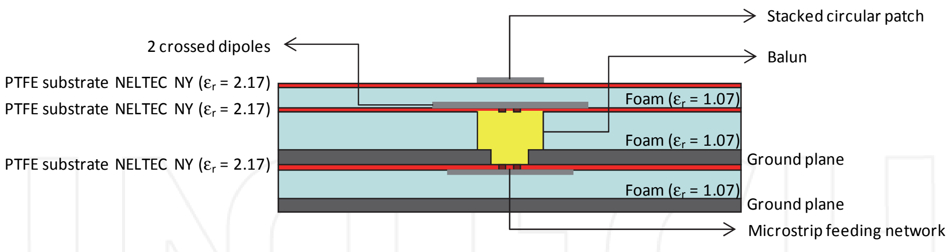

Fig. 12. Cross-section scheme of the radiating element.

The key element of the radiating element feeding structure (Fig. 14.b) is a resonant micro-strip feed ring that has been implemented, as well as a micro-strip 90º branch-line coupler to obtain the desired right hand or left hand circular polarizations (RHCP or LHCP) which ensures adequate port coupling isolation. The S-parameters in amplitude and phase of the micro-strip feeding structure are shown in Fig. 13.a and Fig. 13.b.
Fig. 14.a depicts the S-parameters of the radiating element with the micro-strip feed structure and they fulfill the specification, in Table 3.(b). In Fig. 14.c, the radiation pattern of the radiating element at 7.825 GHz is shown and in Fig. 14.d the radiation pattern of the 4x4

arrays is presented. It is shown a maximum gain of 19.4 dBi at the center frequency band (7.825 GHz). Copolar (CP) to crosspolar (XP) ratio is better than 17 dB and the axial ratio is under -3dB.

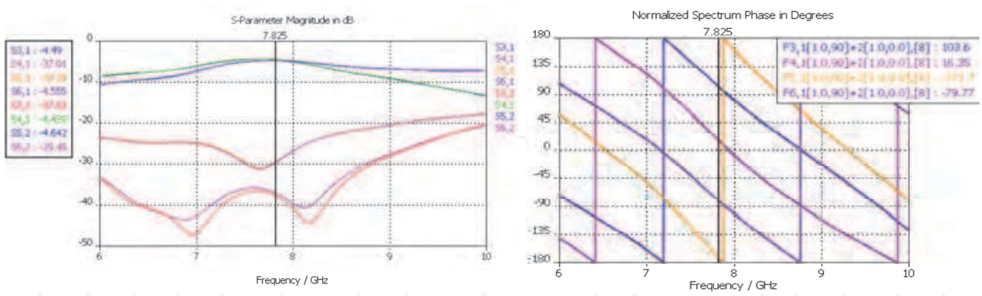

a b

Fig. 13. Micro-strip feeding structure, a) Amplitude of S-parameters, and b) Phase of S-parameters.

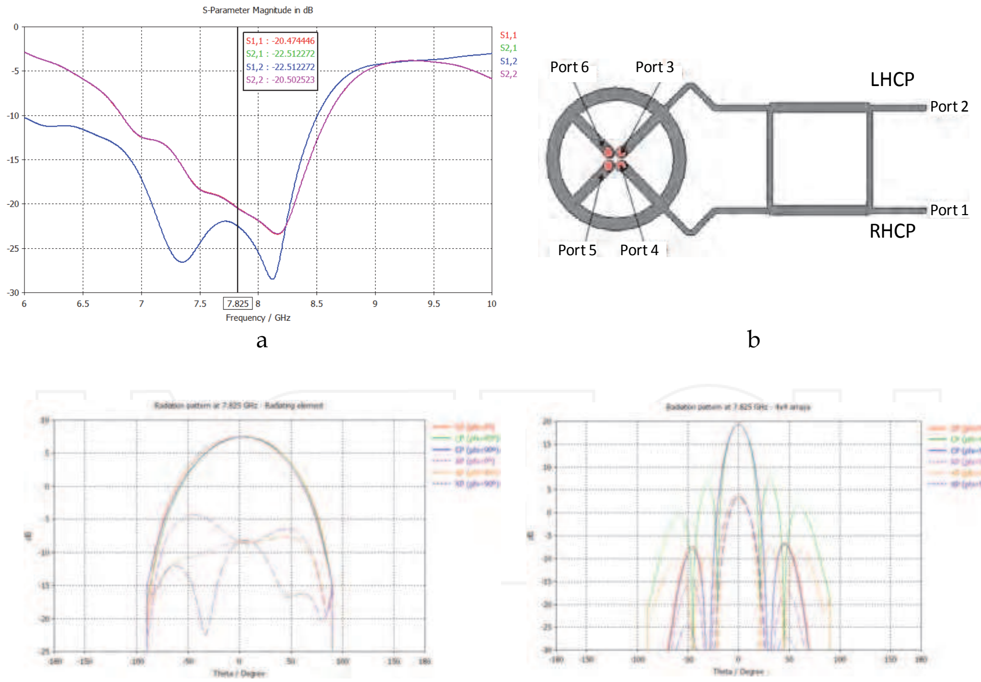

a b

c d

Fig. 14. a) S-parameters, b) Resonant ring + 90° branch-line coupler, c) radiation pattern at 7.825 GHz, and d) 4x4 array radiation pattern.

Parameter	Value (a)	Value (b)	Comments
Freq. range [GHz] Rx **Tx**	7.25 - 7.75 7.9 - 8.4	7.25 - 7.75 7.9 - 8.4	Microwave applications.
G/T (in Rx) [dB/K]	7	7	
EIRP (in Tx) [dBW]	32	32	
Beamwidth at -3dB [deg.]	4	20	
Polarization	circular	circular	In both, reception and transmission.
Gain [dBi]	>28	>15	
Axial ratio [dB]	< 1	<3	**(a)** Between ±50°. **(b)** Between ±45°.
VSWR	< 1.4:1 (-15.6 dB)	< 1.5:1 (-13.9 dB)	
Isolation between ports [dB]	< -17	< -15	
Radiation pattern [deg.]	±35	±90	Steering direction tilt.
Dimensions [cm]	40x40x4	20x20x15	

Table 3. (a) General specifications of the steerable antenna for fixed position portable systems , and (b) General features of the automatic steerable antenna for mobile systems.

3.4 Transmit-array-type lens antenna for terrestrial and on board receivers

Technology in satellite communications has revealed an increasing interest in novel smart antenna designs. Phased-array based designs are basic in electronically reconfigurable devices for satellite applications, which are more and more demanding. The strict requirements in terms of architecture, shape and robustness are important constraints for the development of planar lens-type devices. Regarding the usage and location, lens-type devices are useful for either terrestrial or on board receivers, in vehicular technology. Some clear examples are satellite communications for aircrafts preserving the fuselage aerodynamics or for some other kind of vehicles such as trains, etc.

3.4.1 Introduction to lens-type structures

In a general view, in lens-type a particular signal is received (in our case, an electromagnetic wave with specific features in terms of frequency, wave-front, etc.), it is processed (either complex signal processing techniques or only phase correction tasks can be considered in this interface), and finally, the processed signal is retransmitted.

Regarding the lens configuration, a transmit-array lens consists of three well distinguished interfaces: the first one for signal reception, one interface for signal processing, and the last one for processed signal re-radiation, as depicted in Fig. 15.

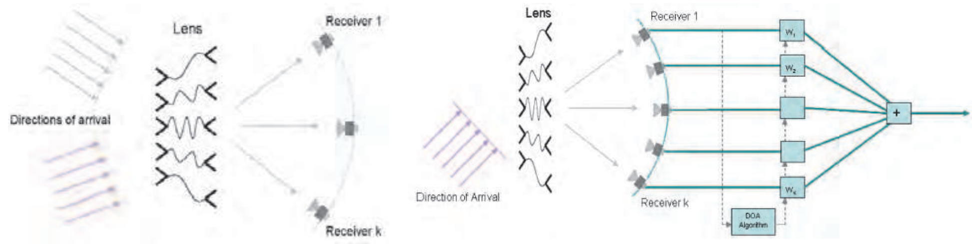

a b

Fig. 15. a) Multi-user scheme with different receivers and transmitters, and b) Adaptive scheme with DoA determination.

These structures are intimately related to reflect-array ones, where the reception and transmission interfaces are turned to be the same interface, with a reflection-type behavior (Encinar & Zornoza, 2001). Although in an equal output phase configuration a transmit-array device behavior would be similar to the one obtained with a reflect-array, the transmit-array offers the advantage of removing the feed blockage.

In a transmission scheme, depending on the transmitter position regarding the lens, a different steering direction is achieved and a different user is pointed. In the case of reception, the situation is the same: the user position configures the direction of arrival, which determines the receiver position around the lens (Padilla et al., 2010a). In adaptive schemes, applying the proper processing algorithm to the signal received in the different receivers around the lens, it is possible to develop an adaptive steering vector, in terms of the desired direction of arrival.

3.4.2 Transmit-array lens architecture and design

Lens-type structures provide two fundamental advantages. First, phase error correction due to spherical wave front coming from the feeding antenna. Fig. 16.a shows this effect. Second, new radiation patterns configuration. Fig. 16.b depicts this fact.

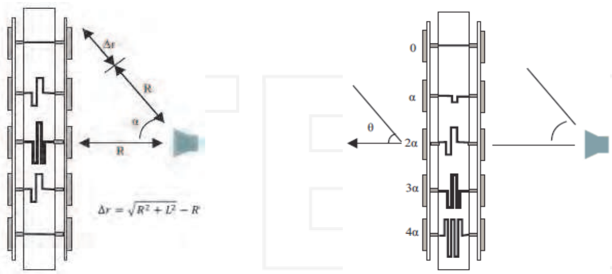

a b

Fig. 16. a) Phase error correction, and b) Radiation pattern reconfiguration.

3.4.3 Electronically reconfigurable devices for active transmit-array lenses

The addition of reconfigurability on transmit-array devices requires the possibility of controlling the phase response of the transmitted signal at each cell of the lens. Electronic control of phase signal may be added in two different ways: First, electronic tuning of the

radiating element phase response (Padilla et al., 2010a): Modifications in the radiating element circuital behavior lead to changes in phase response (arg[S_{21}]). Fig. 17 shows an electronically reconfigurable microwave patch antenna for this purpose, along with the equivalent circuit and prototype outcomes in terms of phase.
Second, electronic tuning of phase shifters in transmission lines (Padilla et al., 2010c): Modifications in the phase response of the phase shifters lead to corresponding changes in phase response. Some options are applied for these devices, such as hybrid couplers, etc. Fig. 18 shows a microwave phase shifter prototype for this purpose, along with the working scheme and its outcomes in phase.

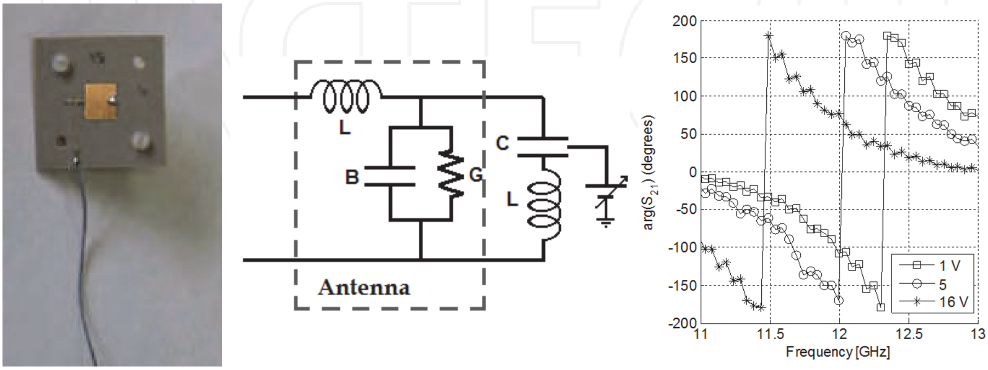

a b c

Fig. 17. Electronically reconfigurable antenna, a) Patch antenna prototypes, b) Equivalent circuit, and c) Phase behavior in frequency.

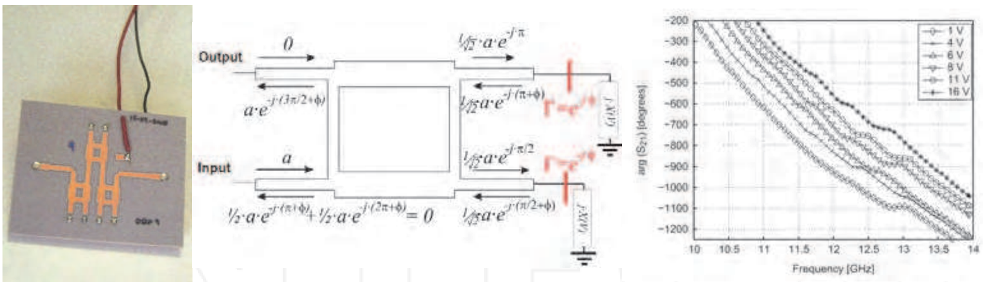

a b c

Fig. 18. Electronically reconfigurable phase shifter, a) Phase shifter prototype, b) Working scheme, and c) Phase behavior in frequency.

3.4.4 Electronically reconfigurable active transmit-array prototype

One electronically reconfigurable prototype is presented in Fig. 19 and detailed in this section. The prototype design implies the use of microwave phase shifters according to the design specified in section 3.4.3. This transmit-array lens prototype operates at 12 GHz. Main specifications are provided in Table 4.

Parameter	Value	Comments
Frequency range [GHz]	12 ± 0.5	Microwave applications.
Polarization	Linear	In both, reception and transmission.
Directivity [dBi]	>21	
Axial ratio [dB]	< 1	Between ±50º elevation.
S_{11} [dB]	< -20	
Radiation pattern [deg.]	±30	Steering direction tilt, for both H and V planes.
Feeding antenna [mm]	120	Corrugated horn linearly polarized
Phase shifters [deg.]	360	Full phase range variation.
Transmit-array elements	36	6x6 array topology.
Separation between elements	$0.7\lambda_0$	Related to the wavelength

Table 4. Main features of the electronically reconfigurable transmit-array prototype.

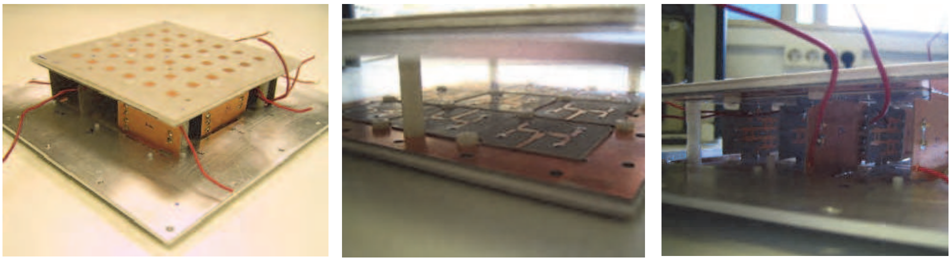

a b c

Fig. 19. Transmit-array core, a) Transmit-array prototype, b) Distribution networks, and c) Phase shifter integration.

The electronically controllable steering capabilities are tested and assured for a range of ± 30ºin each main axis. An example of radiation pattern is provided in Fig. 20, for 9º tilt in one of the main axes.

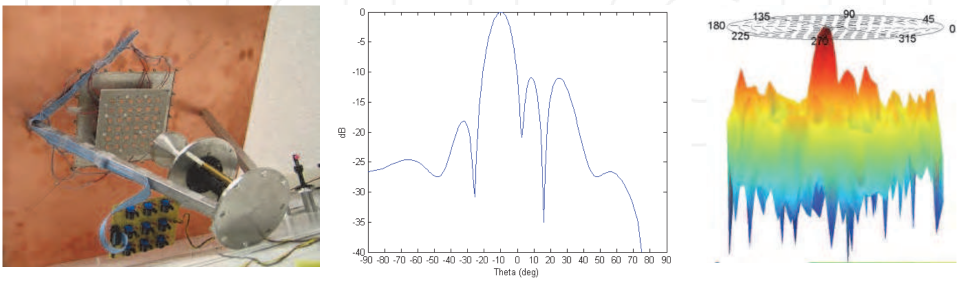

a b c

Fig. 20. a) Complete transmit-array with feeder and control circuits; and transmit-array measurement results for 9º tilt in one axis, b) H plane, and c) 3D plot.

4. Adaptive antenna array

Adaptive antennas can be described as systems usually based on three main parts: the antenna array, the receiver architecture and the beamforming scheme. Thus, adaptive antennas have those advantages owing to those three main parts. The system capabilities increase as complexity and development cost do. Furthermore, since signal processing is the basement of the adaptive antenna concept it is important to analyze the design challenges in terms of hardware architecture and components such as processors and embedded systems.
The antenna array provides the capability of performing the antenna pattern meeting the environment requirement under study. Besides, receiver architectures have some interesting advantages depending on the implemented receiver arraying technique such as signal to noise ratio (SNR) and bit error rate (BER) performance enhancement. Furthermore, symbol synchronization and carrier recovery can be used increasing the receiver complexity but providing higher performances. Finally, beamforming schemes use multiple antennas in order to maximize the strength of the signals being sent and received while eliminating, or at least reducing, interference as discussed in Section 4.3.
Adaptive antenna arrays are often called Smart Antennas because they have some key benefits over traditional antennas, by adjusting traffic patterns, space diversity or using multiple access techniques. The main four key benefits are: First, enhanced coverage through range extension by increasing the gain and steering capability of the ground station antenna; Second, enhanced signal quality through multi-target capability and reduction of interferences; finally, adaptive antennas improve the data download capacity in the ground segment of satellite communication by increasing the coverage range (Martínez et al., 2007).

4.1 Design and architecture based on software defined radio

For design there is the well known waterfall life cyclic model (Royce, 1970) that can be used to manage main aspects of the design of architectures. Thus, some tasks must be fulfilled subsequently as follow in Fig. 21.a.
Fig. 21.b shows the design schemes resulting of the requirement analysis stage corresponding software and hardware system specifications. In the depicted scheme, there are some system components such as the radiating element and RF circuits that are often designed under iterative prototyping model.

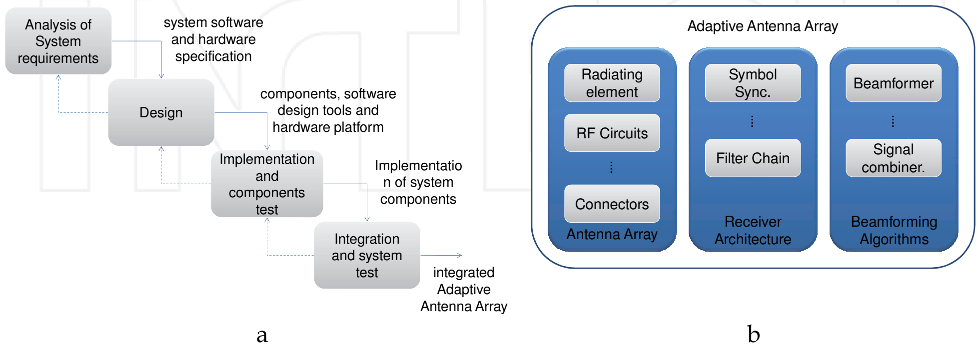

Fig. 21. a) Water life cyclic model of the adaptive antenna array design, and b) Simplified design scheme of adaptive antenna arrays.

Regarding the hardware implementation, tables presented in (Martínez et al., 2007) show the hardware resource consumption in the field programmable gate array (FPGA) Virtex-4 for the least mean squared (LMS) beamforming algorithm with full spectrum combining (FSC) receiver architecture and SIMPLE beamforming algorithm with symbol combining (SC) receiver architecture. Both scheme designs have an antenna array of 2 elements. The algorithm based on correlation requires less hardware. The main difference can be appreciated in the amount of digital signal processing oriented component (DSP48) resources, typically used for filtering applications (Martínez et al., 2007).

4.2 Receiver architectures based on algorithms type

Several receiver architectures can be implemented, and they are frequently based on the type of the beamforming algorithm used. When training signals are available in the transmitted frame, a time-based reference algorithm can be used. However, this solution is only valid when the earth station is capable of demodulating the received training sequence. Other algorithms used in deep space communications are based on signal correlation and they avoid performing the demodulating process. This kind of algorithms are blind techniques that do not require any additional signal demodulation before applying some beamforming technique and work better in low SNR conditions than time-based algorithms. Several receiver architectures can be implemented exploiting the processing capabilities of the SDR, such as FPGA, application-specific integrated circuits (ASICS), and digital signal processing (DSPs). The design of the receiver architecture fundamentally depends on the selection of beamforming algorithms. An example of beamforming technique is the LMS algorithm whose estimation of coefficients or weights requires a temporal reference and is implemented through SC receiver architecture (Fig. 22.a). In the other hand, the SIMPLE algorithm (Rogstad, 1997) constitutes a beamforming technique that is implemented using FSC receiver architecture (Fig. 22.b) in order to perform the calculation of weights.

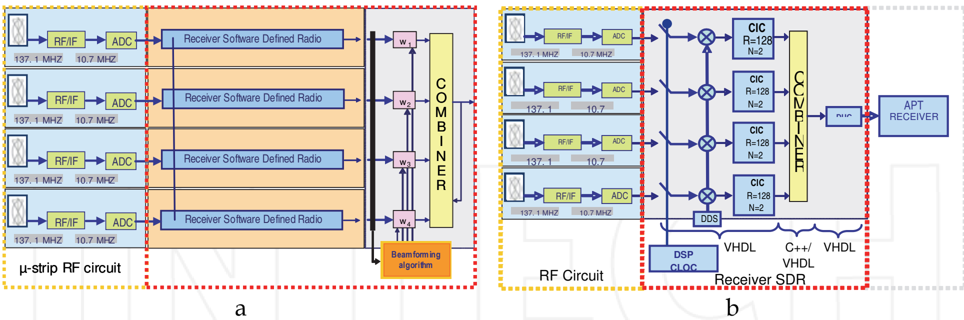

Fig. 22. Comparison of receiver architectures. a) Symbol Combining (SC), and b) Full Spectrum Combining (FSC).

The SC architecture can be divided into two more sub-classes which work on a phase-recovery basis. The complex symbol combining (CSC) recovers the phase information with regard to a reference element using feed-forward and feedback algorithms. One of the advantages of this scheme is that the rate of data sent to the combining module has a rate slightly higher than the symbol rate. For most applications, the symbol rate is relatively low and is a multiple of the data rate. In this kind of schemes, there is an important cost

consideration in real-time applications and the requirements of instrumental phase stability are very severe (Rogstad et al., 2003). Other type of SC architecture is the stream symbol combining (SSC). In this kind of scheme, data are sent to the combining module at a rate equal to the symbol rate. The symbol rate depends on the coding scheme and for most applications is relatively modest. Also, the requirements of instrumental phase stability are no severe, as in the case of CSC scheme. The disadvantage of the SSC is the additional hardware required for each antenna.

Furthermore, there are the baseband combining (BC) and carrier arraying (CA) architectures discussed in (Rogstad et al., 2003). In BC architectures the signal from each antenna is carrier locked and combining in baseband for further demodulation and synchronization. In effect, the carrier signal from the spacecraft is used as a phase reference so that locking to the carrier eliminates the radio-frequency phase differences between antennas imposed by the propagation medium. Besides, in CA architectures, one individual carrier-tracking loop is implemented on each array element. Then, the elements branches are coupled in order to increase the carrier-to-noise ratio (CNR), but losses of radio channel are far compensated (Rogstad et al., 2003).

In general, the selection of the beamforming algorithms is determined by the following aspects: Hardware and computational resources; Speed of convergence and residual error of adaptive algorithms; Calibration requirements and auto-compensation ability; and system signal-transmission characteristics.

4.3 Beamforming techniques for satellite tracking

Some satellites transmit useful information inside its frames for synchronization and tracking purposes. The gathering of satellite data requires the tracking operation along its earth orbit. To accomplish this goal with adaptive array architectures, some beamforming techniques should be implemented. Fig. 23 illustrates a simple example of a narrowband linear adaptive beamformer system.

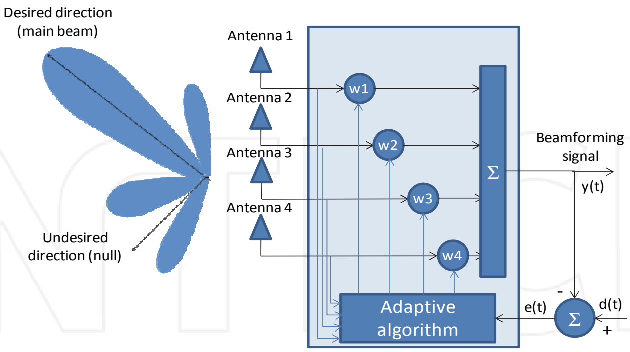

Fig. 23. Adaptive antenna system.

A linear beamformer combines signals according to some weights w_i, to produce a desired radiation pattern. The mathematical expression of a linear beamformer at the array output in vector notation can be expressed as $y = w^H x$, where x is the received signal vector to be combined, w are the weights computed by the beamforming algorithm and ^{H} denotes transposition and conjugate of $(\cdot)$.

In adaptive antennas design, weights are dynamically calculated with a certain algorithm in order to optimize some signal parameter like signal to interference-plus-noise ratio (SINR), SNR, or BER. An extended variety of algorithms exist in the literature for beamforming purpose and the most appropriated selection is done depending on the signal characteristics of the received signal.

4.3.1 Blind techniques

Blind beamformers make use of an inherent property of the received signal, such as the ciclo-stationarity of the constant modulus. In the latter, the algorithm eliminates the fluctuation of the signal amplitude and computes the weights to minimize the effect produced by those variations. The algorithms that make use of these methods are denoted as Constant Modulus Algorithms (CMA) (Biedka, 2001).

CMA algorithms present an important disadvantage: as the phase information is not considered, the constellation of quadrature phase shift keying (QPSK) signals commonly used in satellite communications appears rotated after beamforming, which imposes the need of an additional phase recovery subsystem in the array output.

4.3.2 Temporal-reference algorithms

Algorithms based on a temporal reference require a known reference included in the frame of the signal, such as training sequences, unique word (UW) or pilot bits. Thus, these schemes are normally used for digital signals. The aim of these beamformers is the minimization of the energy of an error signal integrated by interferences and noise. In order to reduce the order of the problem, the weight calculation is usually done iteratively.

The most popular adaptive filters are the LMS and Recursive Least Squares (RLS) algorithms (Haykin, 2002). Briefly, the main differences lie in the method to calculate and the final convergence behavior: while LMS has a linear complexity order with the number of antennas in the array, RLS makes use of matrix operation, so that the complexity order is quadratic, but the convergence is faster.

An interesting alternative to the LMS is the Normalized LMS (NLMS), which normalizes the adaptive step to avoid variation during the convergence process. The counterpart is the more intensive processing requirements to calculate signal power and normalization operation.

4.3.3 Correlation-based algorithm

In contrast to beamformers based on temporal reference, schemes based on signal correlation do not require the demodulation of any signal. These techniques are the most popular to extract the spatial information for beamforming, and we have focused on the use of the SIMPLE algorithm (Rogstad, 1997). This algorithm has been used by the Deep Space Network (DSN) of National Aeronautics and Space Administration (NASA) to combine the signals received from spatial probes in radio telescopes located in different sites around the Earth surface. The main disadvantage of correlation based schemes is the lack of ability to cancel interference signals.

4.4 Performance comparison

Some simulation comparisons between spatial and blind algorithms are presented to show benefits and drawbacks. Four algorithms have been selected with a 4-element uniform linear

array (ULA). The spatial algorithms simulated are post-beamformer interference canceller – orthogonal interference beamformer (PIC-OIB) (Godara, 2004) and minimum power distortionless response (MPDR) (Van Trees, 2002). On the other hand, the blind algorithms are the matrix-free EIGEN and the SUMPLE (Rogstad, 1997). The convergence process is compared as a function of the input SNR as depicted in Fig. 24.
As it can be observed from the above results, spatial algorithms outperform blind ones at low SNR, and vice versa. On the other hand, with medium-low SNR and low or absence of interferences, the behavior of all algorithms is quite similar.

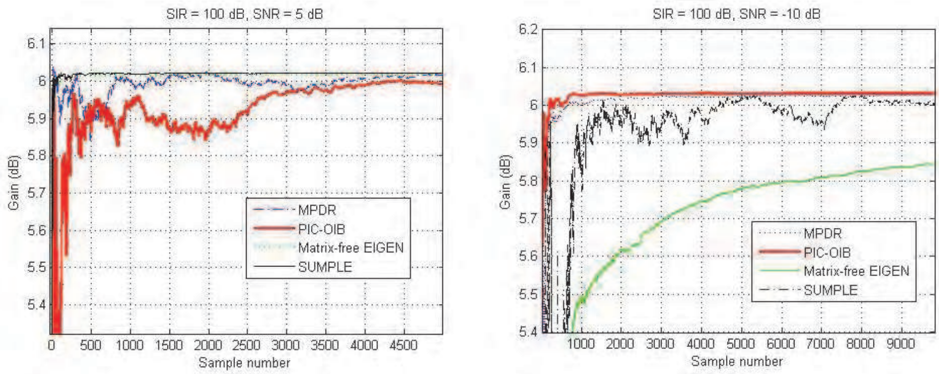

Fig. 24. Convergence behavior of spatial versus blind algorithms in the absence of interferences with several input SNR. a) SNR = 5 dB, and b) SNR = -10 dB.

5. Experimental Test-Bed based on SDR platform

This section presents a test platform known as Adaptive Antenna Array Test-Bed - A3TB, where a comparative study of several beamforming algorithms can be performed and modularity of the architecture is a well proved advantage. The test bed is based on SDR technology and uses a novel architecture that can be used with both blind and spatial-based beamforming algorithms. The A3TB concept can be applied to a number of scenarios as the current version is independent of the signal properties. Simulation results using the A3TB with the APT channel from NOAA satellites show the performance of the concept and the feasibility of the proposed implementation.
The scope of the system development was is to prove the concept of antenna arrays applied to ground stations instead of reflectors for different applications, such as telemetry data downloading or end-user in mobile applications as discussed in the introduction section. In contrast to reflector antennas, antenna arrays offer the possibility of electronic beam-steering avoiding the use of complex mechanical parts and therefore reducing the cost of the antenna. It is also a good chance for Universities and Research Centers aiming to have their own ground station sited in their installations.

5.1 A3TB concept

The A3TB can be defined as *a software-defined radio beamformer applied to a ground station for tracking LEO satellites*. The novelty relies on the use of an antenna array to smartly combine

the received signals from the satellite and its implementation based on SDR technology. The reason to use an antenna array instead of a single antenna is to electronically steer the beam in the direction of the satellite along its orbit without requiring a mechanical system for tracking. In addition to the advantages of the use of SDR technology and antenna array, it is the modularity and flexible architecture implemented in the A3TB. Fig. 25 shows the A3TB architecture where it is evident the feasibility to update or change during operation any of the main blocks. It is possible to change during operation the beamforming algorithm and to include new beamforming modules to the system. Furthermore, changes on the BENADC are possible to implement not during operation, but new receiver architecture at off-line such as those options discussed at follow.

In (Salas et al., 2007), the block diagram represents the software system implementation of the first version of the test-bed prototype and most of it is based on VHDL. Depending on the firmware, three options could be installed into the FPGA Virtex4. The option A is implemented with the signal processing on the PC, so the SIMPLE beamforming is done in the module developed in C++. The option B is implemented completely on VHDL and this option need to export the beamforming weights just to draw the array pattern diagram. Finally, in contrast to the option B, the option C is implemented for the LMS beamforming algorithm.

With the first version of the Test-Bed, the modularity on the selection of firmwares was proved switching between A, B or C receiver architectures, and an important result of the Test-Bed development is the hardware resources occupation presented in (Salas et al., 2007).

The advantage of the SDR implementation is that A3TB architecture can be used to process any received signal from a LEO satellite in the appropriate band imposed by the RF stages. Moreover, most of the processing tasks are performed on software, using appropriate routines to process any receive signal. There are 2 main schemes to implement the beamforming stage: SC and FSC [41]. Both schemes are compared in Section 4.2.

The current version of the A3TB in Fig. 25.a was updated to track NOAA satellites in the VHF band, in particular the APT channel. Previous versions of A3TB dealt with LRPT signals from MetOp-A, where a complete receiver with beamforming and synchronization stages has been implemented(Salas et al., 2007; Martínes et al., 2007).

5.2 Implementation of the A3TB

The A3TB prototype consists of 4 main parts as shown in Fig. 25.a. The first part is the antenna array, which has 4 crossed-dipole antennas as depicted in Fig. 25.b. The second part consists of RF-IF circuits which amplify and down convert to IF incoming signals. Furthermore, an automatic gain control (AGC) was implemented using two steps of variable attenuators in the IF domain.

The third part is the SDR platform which consists of the beamforming algorithms implemented on C++ and the FPGA firmware on VHDL, PC and BENADC blocks show in Fig. 25, respectively. The hardware resources occupation for this Test-Bed implementation is similar to one presented in (Martínes et al., 2007). The last part is the software from weather satellite signal to image decoder (WXtoImg) on the PC using the sound card output/input in order to get the weather satellite image.

Since the implemented architecture is FSC the demodulation is not required and the IF signal is digitized. For the signal processing hardware design the BenADC-v4 has been chosen. This solution includes a FPGA Xilinx Virtex4-SX55 with four 12-bit analog inputs at

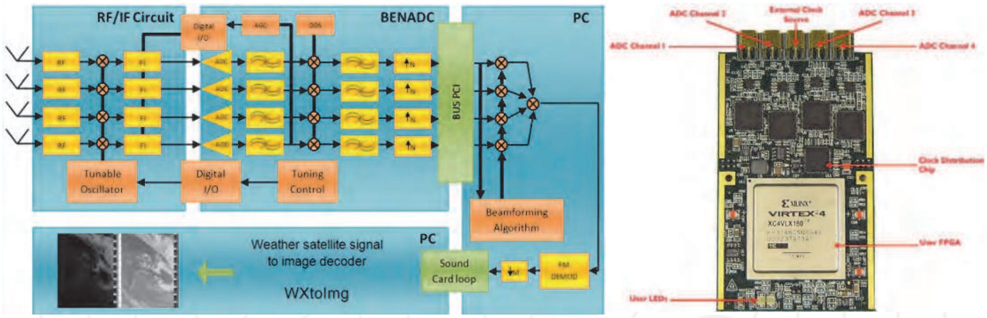

a b

Fig. 25. a) Block diagram of the A3TB, and b) BenADC – Virtex 4-sx55.

250 Msps (Martínes et al., 2007). Digital samples are transferred to the PC where beamforming and subsequent APT demodulation of the array output are performed using C++ routines. This implementation design offers higher flexibility for testing different beamforming schemes. Finally, demodulated APR frames are sent to the WXtoImg software to show meteorological maps.

The A3TB is controlled by the PC for simulations and field trials. The graphical user interface allows presented in (Salas et al., 2008) the user to choose the beamforming algorithm and set all the parameters of the LEO satellite for tracking such as the number of antennas of the array, distance between the elements, direction of arrival and IF frequency. The C++ routine calculates the beamforming weights and plots the synthesized array factor. Subsequently, the reception of meteorological images has real time system requirements. Thus, it is necessary a data transfer from the FPGA to the C++ module to process the samples continuously, and give APT frames to the audio output of the PC. Since, the meteorological satellites often have a low baud rate, in the case of study with NOAA satellites the data transfer is made using two buffers controlled by a thread.

It is important to mention that the A3TB with SDR architecture can evaluate different beamforming algorithms and receiver schemes. The update of A3TB for larger arrays is immediate, as the basis for algorithms is independent of the number of elements in the array. The architecture of a new ground station concept to track LEO satellites based on software defined radio and antenna arraying as Test-Bed is a well proved choice to evaluate future antenna array architectures for satellite communication and benchmark features of the proposed system. As the A3TB VHF version is based on FSC scheme, the concept can be applied to a number of satellite tracing scenarios.

6. Conclusions

The performance analysis of different beamforming algorithms is an important issue in the new generation antenna array development and research. Thus, A3TB helps to analyze beamforming algorithms paving the way for testing and debugging for posteriori use in larger arrays, such as GEODA. Results obtained in real scenarios with A3TB state, for example, that spatial reference algorithms such as MPDR should be used in the absence of interferences, whereas blind algorithms are appropriate for low SNR conditions. Finally, the A3TB can also serve to validate the performance of calibration procedures.

In future work, the A3TB will deal with the system combining of full modularity with the capability of change firmwares based on the first version design of the Test-Bed, plus the flexible architecture of the current design of the Test-Bed based on VHDL, C++ and Antenna Arraying. Furthermore, the addition of more modules to increase the number of antenna array elements is evident in next generations.

7. Acknowledgment

Authors wish to thank MICINN (Ministerio de Ciencia e Innovación) for grants and CROCANTE project (ref: TEC2008-06736/TEC), INSA (Ingeniería y servicios Aeroespaciales) and Antenas Moyano S.L., for the partial funding of this work. Simulations in this work have been done using CST Studio Suite 2011 under a cooperation agreement between Computer Simulation Technology and Universidad Politécnica de Madrid. Substrates used in prototypes were kindly given by NELCO S.A.

8. References

Torre, A.; Gonzalo, J.; Pulido, M., & Martínez Rodríguez-Osorio, R. (2006). New generation Ground Segment Architecture for LEO satellites. *57th International Astronautical Congress*, pp. 221-226. Valencia, Spain, October 2006.

Tomasic, B.; Turtle, J. & Liu, S. (2002). A Geodesic Sphere Phased Array Antenna for satellite control and communication. *XXVII General Assembly of the International Union of Radio Science,* Maastricht, August 2002.

Godara, L. C. (1997). Application of Antenna Arrays to Mobile Communication, Part II: Beamforming and Direction of Arrival Considerations. *Proc. IEEE* , vol.85, No.8, (August 1997), pp. 1195-1245.

Martínez, R. & Salas Natera, M. A. (2010). On the use of Ground Antenna Arrays for Satellite Tracking: Architecture, Beamforming, Calibration and Measurements. *61st International Astronautical Congress*, pp. 1-7. Prague, 2010.

Liu, S.; Tomasic, B.; Hwang, S. & Turtle, J. (2006). The Geodesic Dome Phased Array Antenna (GDPAA) for Satellite Operations Support. *IEEE 18th International Conference on Applied Electromagnetics and Communications*, pp. 1-1, Dubrovnik, April 2006.

Tomasic, B. (1998). Analysis and Design Trade-Offs of Candidate Phased Array Architectures for AFSCN Application. *Second AFSCN Phased Array Antenna Workshop,* Hanscom, April 1998.

Sierra Pérez, M.; Torre, A.; Masa Campos, J. L.; Ktorza, D. & Montesinos, I. (2007). GEODA: Adaptive Antenna Array for Metop Satellite Signal Reception. *4th ESA International Workshop on Tracking, Telemetry and Command System for Space Application*, pp. 1-4, Darmstadt, Germany, September 2007.

Arias Campo, M.; Montesinos Ortego, I.; Fernández Jambrina, J. & Sierra Pérez, M. (2010). T/R Module Design for GEODA Antenna. *4th European Conference on Antenna and Propagation,* pp. 115-116, Barcelona, Spain, April 2010.

Franchi, A.; Howell, A. & Sengupta, J. (2000). Broadband mobile via satellite: Inmarsat BGAN. *IEEE Seminar on the Critical Success Factors - Technology, Services and Markets*, pp. 23-30, October 2000.

Evans, J. V. (1998). Satellite systems for personal communications. *Proc. IEEE* , Vol.86, No.7, (July 1998), pp. 1325-1341.

Wu, W. W. (1994). Mobile satellite communications. *Proc. IEEE* , Vol.82, No.9, (September 1994), pp. 1431-1448.

Fujimoto, K. & James, J. (2001). *Mobile Antenna Systems Handbook.* Artech House.

Garcia Aguilar, A.; Inclán Alonso, J. M.; Vigil Herrero, L.; Fernández González, J. M. & Sierra Pérez, M. (2010). Printed antenna for satellite communications. *IEEE International Symposium on Phased Array Systems and Technology*, pp. 529-535, Boston, USA, October 2010.

Geissler, M.; Woetzel, F.; Bottcher, M.; Korthoff, S.; Lauer, A. & Eube, M., (2010). L-band phased array for maritime satcom. *IEEE International Symposium on Phased Array Systems and Technology*, pp. 518-523, Boston, USA, October 2010.

Baggen, R.; Vaccaro, S. & Del Río, D. (2007). Design Considerations for Compact Mobile Ku-Band Satellite Terminals. *EuCAP The Second European Conference on Antennas and Propagation*, pp. 1-5. Edimburg, Scothland, September 2007.

Vaccaro, S.; Tiezzi, F.; Rúa, M. & De Oro, C. (2010). Ku-Band Low-Profile Rx-only and Tx-Rx antennas for Mobile Satellite Communications. *IEEE International Symposium on Phased Array Systems and Technology*, pp. 536-542, Boston, USA, October 2010.

Schippers, H. (2008). Broadband Conformal Phased Array with Optical Beam Forming for Airborne Satellite Communication. *IEEE Aerospace Conference*, pp. 1-17, September 2008.

Kanno, M.; Hashimura, T. T.; Sato, M.; Fukutani, K. & Suzuki, A. (1996). Digital beam forming for conformal active array antenna. *IEEE International Symposium on Phased Array Systems and Technology*, pp. 37-40, October 1996.

Khalifa, I. & Vaughan, R. (2007). Optimal Configuration of Multi-Faceted Phased Arrays for Wide Angle Coverage. *IEEE 65th Vehicular Technology Conference*, pp. 304-308, Boltimore, USA, April 2007.

Salas Natera, M. A.; Martínez Rodríguez-Osorio, R.; Antón Sánchez, A.; García-Rojo, I. & Cuellar, L. (2008). A3TB: Adaptive Antenna Array test-bed for tracking LEO satellites based on software defined radio. *59th International Astronautical Congress*, pp. 313-317, Glasgow. September 2008.

Salas Natera, M. A.; Martínez Rodríguez-Osorio, R. & García-Rojo López, I. (2007). Design of an Adaptive Antenna Array Test-Bed based on Software Radio for Tracking LEO Satellites. *IEEE EuCAP*. Edinburgh, Scotchland, Npvember 2007.

Martínez, R.; Salas Natera, M.; Bravo, A.; García-Rojo, I.; de Haro, L.; Mateo, M. & Gómez, M. (2007). VHF Ground Station with increased angular coverage for reception of meteorological satellites with electronic beamforming. *4th ESA International Workshop on Tracking, Telemetry and Command Systems for Space Application.* Darmstadt, Germany, 2007.

Mailloux, R. (2005). *Phased Array Antenna Handbook,* Artech House, Norwood, Massachusetts, USA.

Josefsson, L. & Persson, P. (2006). *Conformal Array Antenna. Theory and Design*, John Wiley & Sons , Hoboken, New Jersey, USA.

Montesinos, I.; Sierra Pérez, M.; Fernández, J. L.; Martínez, R. & Masa, J. L. (2009). GEODA: Adaptive Antenna of Multiple Planar Arrays for Satellite Communications. *European Conference on Antenna and Propagation.* Berlin, Germany, 2009.

Salas Natera, M. A.; Martínez, R.; De Haro Ariet, L. & Fernández Jambrina, J. (2010). Automated System for Measurement and Characterization of Planar Active Arrays. *IEEE Internationa Symposium on Phase Array Systems and Technology*, pp. 1-6, Boston USA, October 2010.

Sierra-Castañer, M.; Vera-Isasa, M.; Sierra-Pérez, M. & Fernández-Jambrina, J. (2005). Double-Beam Parallel Plate Slot Antenna. *IEEE Transactions on Antennas and Propagation*, vol.53, No.3, (2005) pp. 977-984.

Garg, R.; Bhartia, P.; Bahl, I. & Ittipiboon, A. (2001). *Microstrip Antennas Design Handbook,* Artech House, Norwood, Massachusetts, USA.

Tang, C. & Chen, M. (2007). Synthesizing Microstrip Branch-Line Couplers With Predetermined Compact Size and Bandwidth. *IEEE Transactions on Microwave Theory and Techniques, vol. 55, No.9,* (September 2007), pp. 1926-1934.

Bialkowski, M.; Jellett, S. & Varnes, R. (1996). Electronically Steered Antenna System for the Australian Mobilesat. *IEEE Transaction on Antennas ans Propagation*, vol. 143, No. 4, (August 1996), pp. 347-352.

Alonso, J.; Blas, J.; Garcia, L.; Ramos, J.; Pablos, J. & Grajal, J. (1996). Low Cost Electronically Steered Antenna and Receiver System for Mobile Saltellite Communications. *Trans. IEEE MTT*, vol. 44, No. 12, (December 1996), pp. 2438-2449.

Fernández, J. M.; Rizzo, C. & Sierra-Pérez, M. (2009). Antena Impresa Multihaz con Polarización Circular Derechas/Izquierdas Para Comunicaciones por Satélite en Banda X. *Proccedings of XXIV Simposium Nacional de la Unión Científica Internacional de Radio (URSI).* Santander, Spain, September 2009.

Encinar, J. A. & Zornoza, J. (2003). Broadband design of three- layer printed reflectarrays. *IEEE Transactions on Antennas and Propagation*, vol. 51, No. 7, (July 2003), pp. 1662-1664.

Padilla, P.; Muñoz-Acevedo, A.; Sierra-Castañer, M. & Sierra-Pérez, M. (2010). Electronically reconfigurable transmitarray at Ku band for microwave applications. *IEEE Transactions on Antennas and Propagation*, vol. 58, No. 8, (August 2010), pp. 2571-2579.

Padilla, P.; Muñoz-Acevedo, A. & Sierra-Castañer, M. (2010). Low Loss 360º Ku Band electronically Reconfigurable Phase Shifter. *International Journal of Electronics and Communications,* vol. 64, No. 11, (November 2010), pp. 1100-1104.

Royce, W. W. (1970). Managing the Development of Large Software Systems. *IEEE WESCON*, pp. 328 – 338, 1970.

Rogstad, D. H. (1997). *The SUMPLE Algorithm for Aligning Arrays of Receiving Radio Antennas: Coherence Achivied with Less Hardware and Lower Combining Loss.* TDA Progress Report, Jet Propulsion Laboratory.

Rogstad, D. H.; Mileant, A. & Pham, T. (2003). *Antenna Arraying Techniques in the Deep Space Network*. Deep Space Communication and Navegation Series, JPL California Institute of Technology, Ref. 03-001, Pasadena, USA.

Biedka, T. E. (2001). *Analysis and Development of Blind Adaptive Beamforming Algorithms.* PdD Thesis, Faculty of Virginia Polytechnique Institute and State University, Virginia.

Haykin, S. (2002). *Adaptive Filter Theory* (4th ed.). Prentice-Hall.

Godara, L. C. (2004). *Smart Antennas* (1st ed.). CRC Press..

Van Trees, H. L. (2002). *Optimum Array Processing. Part IV of Detection, Estimation, and Modulation Theory*. Wiley.

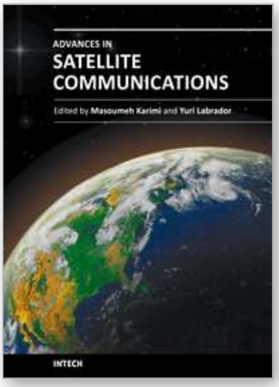

Advances in Satellite Communications
Edited by Dr. Masoumeh Karimi

ISBN 978-953-307-562-4
Hard cover, 194 pages
Publisher InTech
Published online 27, July, 2011
Published in print edition July, 2011

Hindawi Publishing Corporation
International Journal of Antennas and Propagation
Volume 2012, Article ID 428284, 10 pages
doi:10.1155/2012/428284

Review Article

Some Recent Developments of Microstrip Antenna

Yong Liu, Li-Ming Si, Meng Wei, Pixian Yan, Pengfei Yang, Hongda Lu, Chao Zheng, Yong Yuan, Jinchao Mou, Xin Lv, and Housjun Sun

Department of Electronic Engineering, School of Information and Electronics, Beijing Institute of Technology, Beijing 100081, China

Correspondence should be addressed to Yong Liu, fatufo@bit.edu.cn

Received 12 August 2011; Revised 23 November 2011; Accepted 2 January 2012

Academic Editor: Zhongxiang Q. Shen

Although the microstrip antenna has been extensively studied in the past few decades as one of the standard planar antennas, it still has a huge potential for further developments. The paper suggests three areas for further research based on our previous works on microstrip antenna elements and arrays. One is exploring the variety of microstrip antenna topologies to meet the desired requirement such as ultrawide band (UWB), high gain, miniaturization, circular polarization, multipolarized, and so on. Another is to apply microstrip antenna to form composite antenna which is more potent than the individual antenna. The last is growing towards highly integration of antenna/array and feeding network or operating at relatively high frequencies, like sub-millimeter wave or terahertz (THz) wave regime, by using the advanced machining techniques. To support our points of view, some examples of antennas developed in our group are presented and discussed.

1. Introduction

The concept of microstrip antenna was first introduced in the 1950s [1]. However, this idea had to wait nearly 20 years to be realized after the development of the printed circuit board (PCB) technology in the 1970s [2, 3]. Since then, microstrip antennas are considered as the most common types of antennas due to their obvious advantages of light weight, low cost, low profile, planar configuration, easy of conformal, superior portability, suitable for arrays, easy for fabrication, and easy integration with microwave monolithic integrate circuits (MMICs) [4–7]. They have been widely employed for the civilian and military applications such as television, broadcast radio, mobile systems, global positioning system (GPS), radio-frequency identification (RFID), multiple-input multiple-output (MIMO) systems, vehicle collision avoidance system, satellite communications, surveillance systems, direction founding, radar systems, remote sensing, biological imaging, missile guidance, and so on [8].

Despite the many advantages of typical microstrip antennas, they also have three basic disadvantages: narrow bandwidth, low gain, and relatively large size. The narrow bandwidth is one of the main drawbacks of these types of antennas. A straightforward method of improving the bandwidth is increasing the substrate thickness. However, surface wave power increases and radiation power decreases with the increasing substrate thickness [7], which leads to poor radiation efficiency. Thus, various other techniques are presented to provide wide-impedance bandwidths of microstrip antennas, including impedance matching networks using stub [9, 10] and negative capacitor/inductor [11], microstrip slot antennas using the U, L, T, and inverted T slots in the ground plane (sometimes termed defected ground structures (DGSs)) [12, 13], surface wave suppressing using magneto-dielectric substrate [14] and electromagnetic bandgap (EBG) structures [15], and composite-resonator microstrip antennas using metamaterial resonators [16, 17]. Another problem to be solved is the low gain for conventional microstrip antenna element. Cavity backing has been used to eliminate the bidirectional radiation, thereby providing higher gain compared with conventional microstrip antenna [18]. Lens covering is an alternative way to achieve gain enhancement. The lens with canonical profile, like elliptical, hemielliptical, hyper-hemispherical, extended hemispherical, used to focus the radiation beam from the radiator elements. The integrated lens microstrip antenna can be treated as composite antenna combined by microstrip radiator elements and dielectric lens, which is very useful for high frequencies (mm, sub-mm, terahertz (THz), and optical waves) applications

[19]. It is also well known that antenna array is an effective means for improving the gain [20–25].

The last limitation of conventional microstrip antennas is the relatively large size, particularly at lower microwave frequencies, since their operation frequencies are related to the electrical size of antenna. In general, the size of the rectangular microstrip antenna should be of order of a half-guided wavelength. This limitation was mathematically studied by Wheeler [26] and Chu [27]. There have been numerous efforts to minimize the antenna size and obtain the electrically small microstrip antenna with the raised demand towards smaller and smaller wireless devices. Inductive or capacitive loading are effective ways to reduce the size of microstrip antennas [28]. In the former work, we demonstrated that the size of microstrip antenna can be miniaturized using composite metamaterial resonators [16, 17]. Magneto-dielectric substrates have been widely used to miniaturize microstrip antennas due to magnetic substrates and could provide wider bandwidths than dielectric substrates [29–32]. Fractal geometries, which are composed by self-similar structures, have opened an alternative way for antenna miniaturization [33].

From the above discussions, we see that many methods and materials are used to improve the properties of microstrip antennas. However, there should be a relationship among bandwidth, gain, and size of the microstrip antennas. Antenna engineers have recognized that the improvement in one antenna property is frequently accompanied by decline in its other performances. For example, the antenna size is reduced usually at the expense of its bandwidth and gain. Therefore, a more comprehensive consideration must be given on further developments of microstrip antennas.

In this paper, we will suggest three areas for further research based on our previous works on microstrip antenna elements and arrays [16–25, 34–41]. We first note that novel microstrip antenna topologies are proposed to meet the desired requirement of variety of potential wireless applications, such as ultrawide band (UWB), high gain, miniaturization, circular polarization, multipolarized, and so on. Next, we discuss the composite antennas based on microstrip antennas which have more potent than each individual antenna. Finally, with the development of micro-/nano-machining techniques, antennas/arrays with highly integration and with highly operating frequencies are discussed. We present some examples of antennas developed in our group to support our points of view.

2. Variety of Microstrip Antenna Topologies

Microstrip antennas have extensively used in commercial and military applications due to their attractive advantages. However, the traditional microstrip antennas have the impedance bandwidth of only a few percent and radiation pattern with omnidirection, which obviously does not meet the requirements of various wireless applications. To this end, a wide variety of microstrip antenna topologies, including different microstrip antenna element structures and different microstrip array arrangements, have been studied to meet the desired requirement such as ultrawide band (UWB), high gain, miniaturization, circular polarization, multipolarized, and so forth.

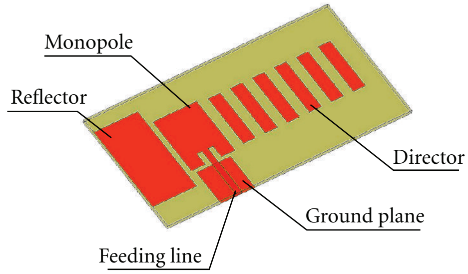

(a) The structure of the quasi-Yagi antenna

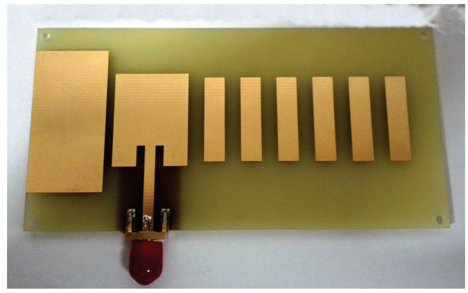
(b) The photograph of the quasi-Yagi antenna

Figure 1: Compact broad-band quasi-Yagi antenna.

As we know, microstrip antennas inherently have narrower bandwidth and lower gain compared to conventional bulky antennas. Some microstrip antennas with special topologies, like quasi-Yagi, planar reflector antenna, are proposed to replace the conventional bulky antennas. Here, we will take a quai-Yagi antenna as an example to show how to design a planar microstrip antenna with Yagi-Uda end-fire radiation pattern. In addition, a microstrip array with special array topology is designed to get dual-polarized property.

2.1. Compact Broad-Band Quasi-Yagi Antenna. A novel S-band compact quasi-Yagi antenna has been designed, fabricated and measured by our group, as shown in Figure 1. This antenna is composed of a printed monopole-driven element, a printed reflector element, and six printed director elements.

To explain the end-fire radiation behavior of the quasi-Yagi antenna, a comparison of radiation patterns, among (1) microstrip monopole only, (2) microstrip monopole and a reflector, (3) microstrip monopole and a director, (4) microstrip monopole and a reflector with one director, and (5) microstrip monopole and a reflector with six director, is shown in Figure 2. We can observe that both the reflector and the director can increase the end-fire radiation, and it could be substantially improved by increasing the number of directors.

The measured VSWR results are shown in Table 1. A bandwidth of 14% for VSWR less than 1.5 is achieved. The gain of the antenna is above 7.5 dBi, as shown in Table 2. In this design, we see that the microstrip antenna with special topology could be conveniently used to replace the bulky Yagi-Uda antenna.

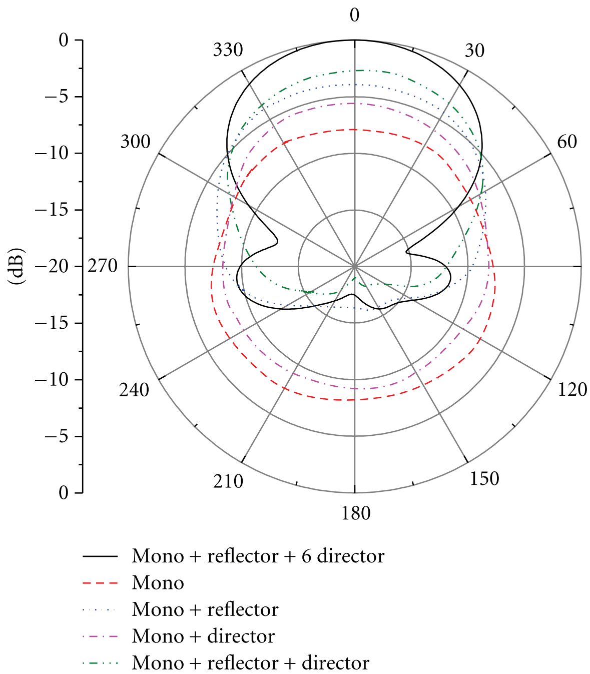

Figure 2: Radiation patterns of microstrip monopole only, microstrip monopole and a reflector, microstrip monopole and a director, microstrip monopole and a reflector with one director, and microstrip monopole and a reflector with six director.

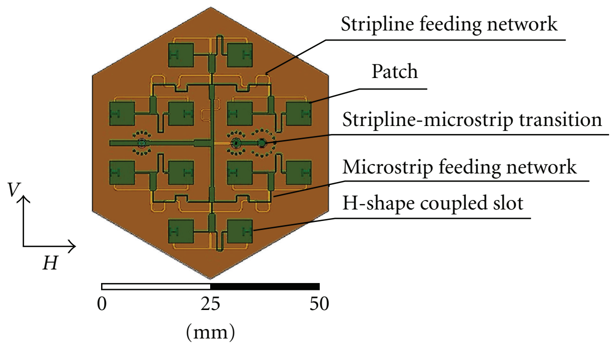

(a) The structure of the dual-polarized microstrip antenna array

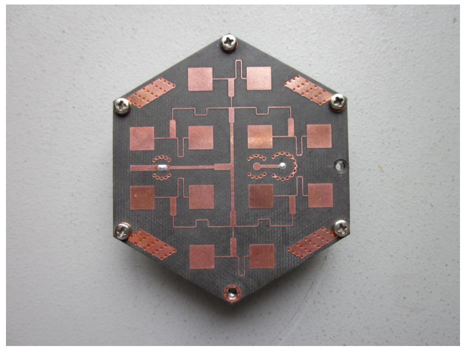

(b) The photograph of the dual-polarized microstrip antenna array

Figure 3: Dual-polarized microstrip antenna array.

Table 1: The measured VSWR of the quasi-Yagi antenna.

No.	Frequency (GHz)			
	3.25	3.5	3.75	Inband
1	1.36	1.34	1.47	<1.5
2	1.37	1.26	1.49	<1.5
3	1.36	1.25	1.48	<1.5

Table 2: The measured gain of the quasi-Yagi antenna (unit: dBi).

No.	Frequency (GHz)		
	3.25	3.5	3.75
1	7.57	8.73	8.35
2	7.58	8.55	8.37
3	7.56	8.77	8.51

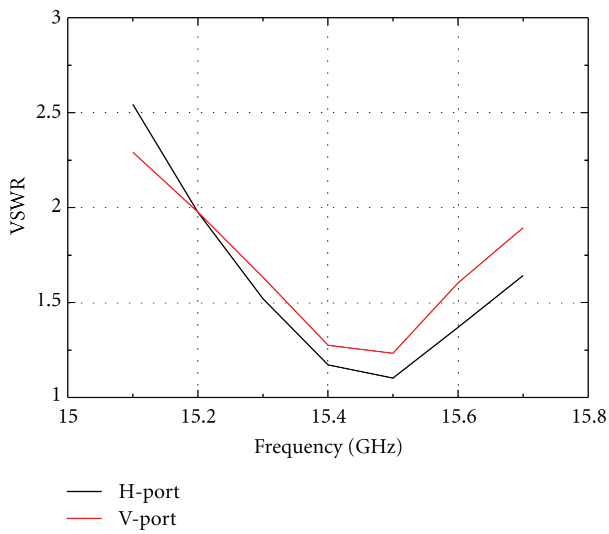

Figure 4: The VSWR of the dual-polarized microstrip antenna array.

2.2. Dual-Polarized Microstrip Antenna Array. The dual-polarized antenna is highly required for the radar, electronic countermeasure, and aerospace systems. It is known that the microstrip antenna can easily be integrated with microwave circuits and feeding network. Here, a novel Ku-band dual-polarization microstrip antenna array with a mixed feeding network, that is, the slot coupled feeding (V-port) and the coplane feeding (H-port), is designed by our group, as shown in Figure 3. It is a three layers structure: top microstrip patch layer, middle stripline feeding network layer, and bottom coplane microstrip feeding network layer. Through proper array arrangement, very good isolation can be obtained.

The VSWR, radiation patterns, and the isolation between two polarizations of the proposed dual-polarized microstrip antenna array are shown in Figures 4, 5, and 6, respectively. The results indicate that this microstrip antenna array has a good impedance matching, good radiation performance, as well as very high isolation (less than −25 dB), which can be an idea candidate for the dual-polarized wireless systems.

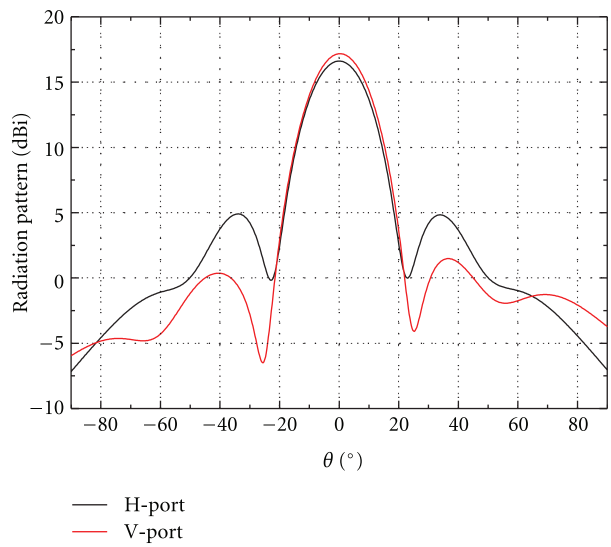

FIGURE 5: The radiation patterns of the dual-polarized microstrip antenna array at the center frequency.

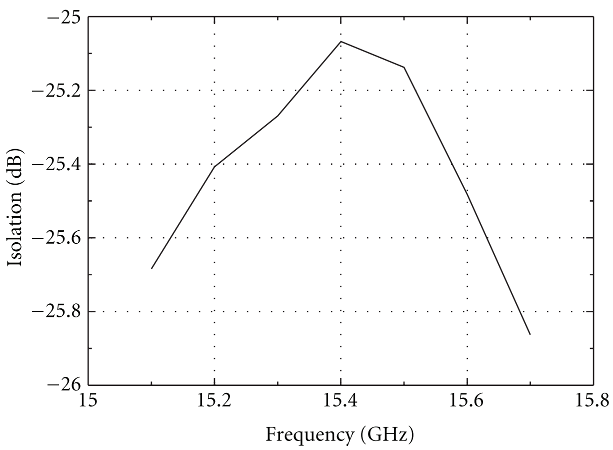

FIGURE 6: The isolation of the dual-polarized microstrip antenna array.

3. Microstrip-Antenna-Based Composite Antenna

As many antenna designers have found, it is not easy to design an antenna to meet the user-defined stringent performance requirements demanded by special wireless applications like military radars, surveillances, and missile guidance, if only one type of antenna is considered. This difficulty may require the use of two more different types or structures of antenna elements with different characteristics. Composite antenna formed by two more types or structures of antennas is particularly suitable for these applications due to more advantages offered by different types or structures of antennas. For example, it is a challenging task to use single type of antenna to design a dual-band dual-polarization antenna for satellite digital multimedia broadcast (S-DMB) application [36]. A composite antenna composed with a left-handed circularly polarized (LHCP) microstrip antenna and a linear polarized omnidirectional biconical antenna is proposed by our group to meet this requirement [36]. Another example of composite antenna is comprised of a dielectric lens and microstrip log-period antenna, which has been widely applied to THz systems (this type of antenna will be further discussed in Section 4.2). Here, we will give an example of composite antenna with "structure composite" method.

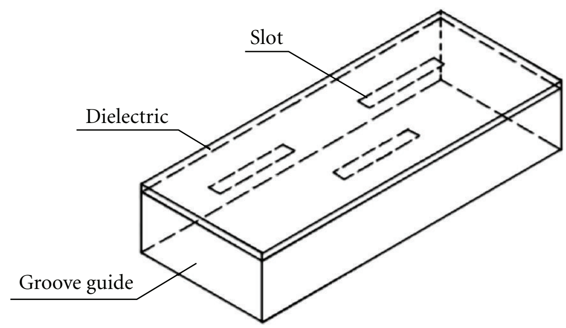

FIGURE 7: The structure of the DCWS.

3.1. Monopulse Circular-Polarized Dielectric Complex Waveguide Slot Antenna Array. Waveguide slot antenna array has been widely used for wireless system, due to its advantages of high radiation efficiency, high power capacity, and high reliability. However, it is hard to overcome the disadvantage of high cost of fabrication.

One composite antenna with waveguide slot antenna array property, termed dielectric complex waveguide slot (DCWS), is composed with slot microstrip line and groove guide, as shown in Figure 7. The slot microstrip line is formed by a metal clad dielectric substrate and slots etched in the metal. This composite antenna not only maintains the advantages of the traditional waveguide slot antenna array but also has the characteristics of high consistence, easy for fabrication, and low cost.

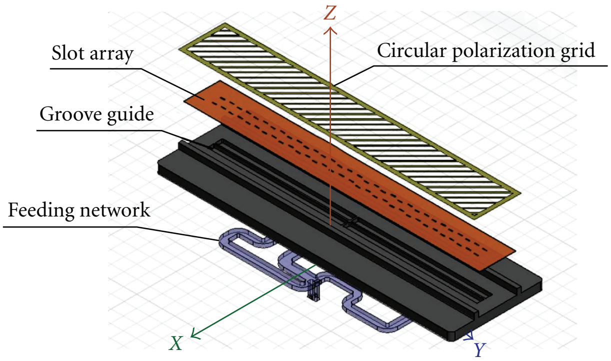

(a) The structure of the monopulse circular-polarized DCWS antenna array (separating view)

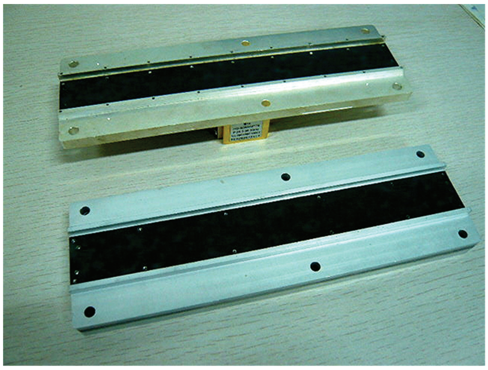

(b) The photograph of the monopulse circular-polarized DCWS antenna array.

Figure 8: Ka-band monopulse circular-polarized dielectric complex waveguide slot (DCWS) antenna array.

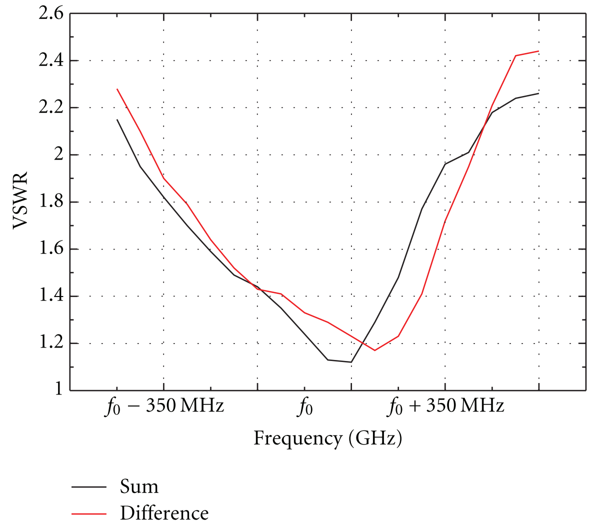

Figure 9: The VSWR of sum and difference port of the monopulse circular-polarized DCWS antenna array.

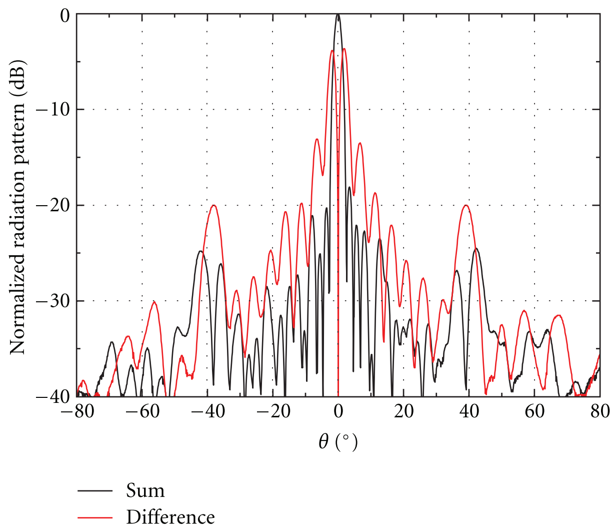

Figure 10: The radiation pattern of the monopulse circular-polarized DCWS antenna array at the center frequency.

A Ka-band monopulse circular-polarized dielectric complex waveguide slot (DCWS) antenna array is designed, fabricated, and measured by our group, as shown in Figure 8. It consists of a circular polarization grid, a slot microstrip array, and a groove guide and feeding network. The slot microstrip array is fabricated on a Rogers 5880 film with dielectric constant of 2.2 and the thickness of 0.254 mm. The measured results of VSWR of sum and different port are shown in Figure 9. Figure 10 shows the measured radiation pattern at the center frequency. Some important array performance parameters such as gain, null depth and axial ratio (AR) are also given in Table 3. As shown in the measured results, very good performance can be obtained with the DCWS antenna array. The radiating efficiency of the DCWS antenna array is 80%, which is almost the same as the traditional waveguide slot antenna array. Moreover, the DCWS antenna array has 40% larger bandwidth than the traditional waveguide slot antenna array.

4. Highly Integration and Highly Operating Frequency Antennas Based on Advanced Machining Techniques

It is known that the microstrip antenna was first fabricated using PCB technology in 1970s, nearly 20 years after its concept was first presented in 1950s [1–3]. Clearly, the development of microstrip antennas is closely related with the machining techniques. Recently, various machining techniques, including multilayer printed circuit board (MPCB), complementary metal oxide semiconductor (CMOS), low-temperature cofired ceramics (LTCC), and micro-electro-mechanical systems (MEMS), are highly developed, opening opportunities for innovative antennas, such as active antennas, reconfigurable antennas, metamaterial-based antennas, THz antennas, and so forth. With the availability of high-precision and high-speed advanced machining techniques, microstrip antennas are growing towards highly integration of antenna/array and feed network and operating at relatively high frequencies. Since they are all based on the advanced

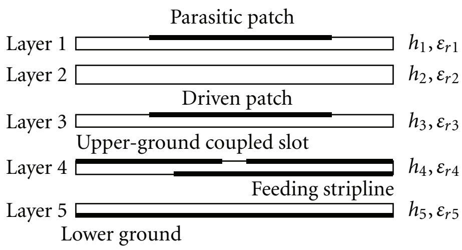

(a) Schematic side view of the structure of the high integrate broadband microstrip antenna array

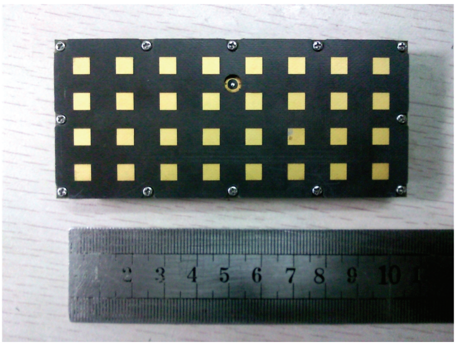

(b) The photograph of the high integrate broadband microstrip antenna array

FIGURE 11: Ku-band high integrate broadband microstrip antenna array using MPCB technology.

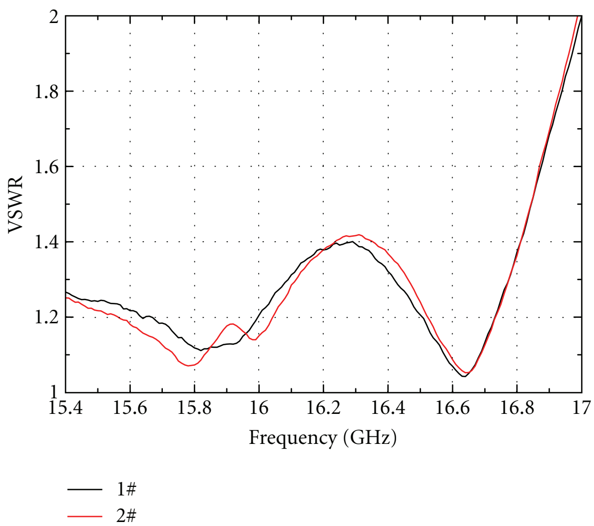

FIGURE 12: The VSWR of the high integrate broad-band microstrip antenna array using MPCB technology.

machining techniques, we suggest that a third research area of microstrip antennas is constantly introducing novel advanced machining techniques. In the following, two examples will be presented to show how important the advanced machining technique is to fabricate microstrip antennas. One is the highly integrate broad-band microstrip antenna array fabricated using MPCB technology. Another is THz wave planar integrated active microstrip antenna using MEMS technology.

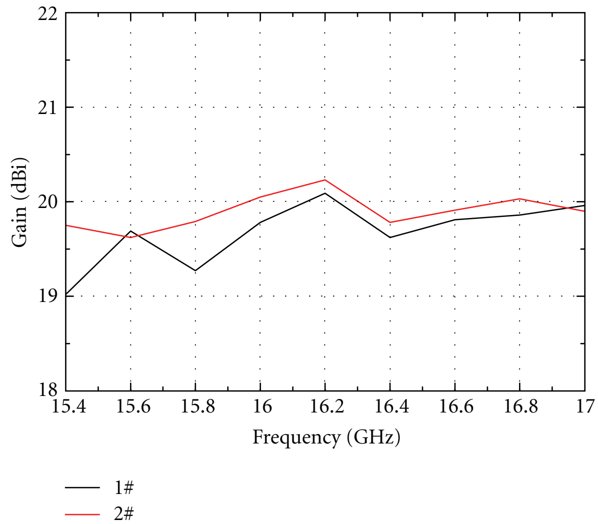

FIGURE 13: The gain of the high integrate broad-band microstrip antenna array using MPCB technology.

TABLE 3: The measured data of the monopulse circular-polarized DCWS antenna array.

Fre. (GHz)	Gain (dBi)	Null depth (dB)	AR (dB)
$f_0 - 0.2$	22.8	−37.3	3.8
f_0	21.9	−29.9	2.9
$f_0 + 0.2$	22.1	−26	4.1

4.1. High Integrate Broad-Band Microstrip Antenna Array Using Multilayer Printed Circuit Board (MPCB) Technology. Recently, with the development of the multilayer printed circuit board (MPCB) technology, the microstrip antennas can be designed and fabricated from one-dimensional (1D) to 2D and even 3D structures.

Based on the MPCB technology, a high integrated broad-band Ku-band microstrip antenna array is designed, fabricated, and measured by our group, as shown in Figure 11. This antenna consists of a parasitic patch, a driven patch, a stripline feeding network, a broad-band coaxial line to stripline transition, some buried screw holes, and some via holes. The feeding network is integrated in the bottom of the substrate of the antenna. As all of the structures fabricated at once, the accuracy and the uniformity can be assured. Two antennas of this type are measured. The measured VSWR, gain, and radiation pattern at the center frequency are shown in Figures 12, 13, and 14, respectively. The measured results show that this antenna maintains good radiation and matching performances with relative bandwidth of 13%. They have also shown good uniformity by using MPCB technology.

4.2. THz Wave Planar Integrated Active Microstrip Antenna Using Micro-Electromechanical Systems (MEMSs) Technology. THz waves typically include frequencies between 0.1 THz and 10 THz. THz technology is now becoming a promising technology which has potential applications in many fields, such as short-range communication, biosensor, imaging,

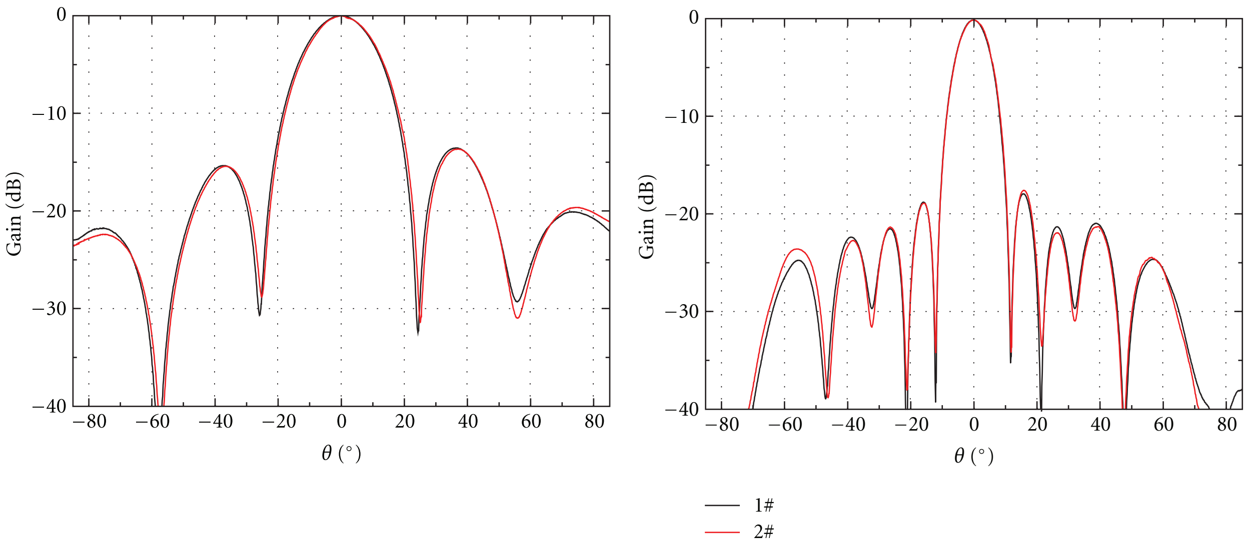

(a) E-plane (b) H-plane

Figure 14: The radiation pattern of the high integrate broad-band microstrip antenna array using MPCB technology at the center frequency.

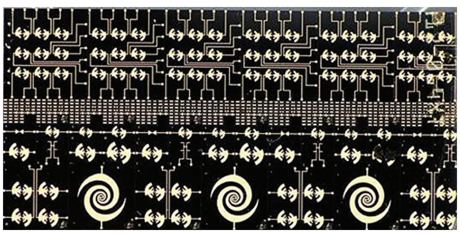

(a) The photograph of the THz monolithic antenna

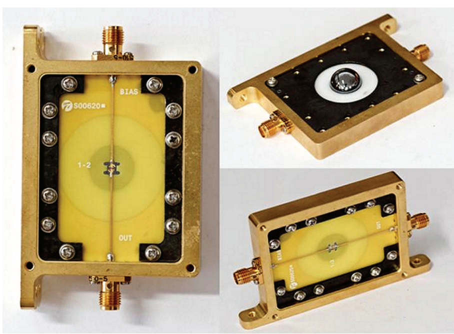

(b) The photograph of the THz monolithic antenna covered by a dielectric lens

Figure 15: THz wave planar integrated active microstrip antenna using micro-electromechanical systems (MEMSs).

national security, space exploration and communication, and so forth [39–46]. To realize THz transceiver system, antenna is an essential component. We often use horn antenna, lens antenna, and dielectric parabolic antenna, for THz systems. However, they are not easy to integrate with monolithic integrate circuits. Although the microstrip antenna has the merits of small volume, light weight, and easy integration with circuit, it is difficult to be processed in such high-frequency regions. MEMS technology opens the way to design of THz antennas, circuits, and systems. THz monolithic antenna fabricated using MEMS technology and covered by a dielectric lens, which can be considered a composite antenna, are designed, fabricated, and measured by our group, as shown in Figure 15.

Diodes have the functions of mixing and/or modulating the carrier-wave signal. It is an effective way to reduce the propagation path for detectors application by integrating the diode and microstrip antenna. The extended hyper-hemispherical dielectric lens is used to increase the gain of the microstrip antenna. An antenna-coupled detector integrated with a dielectric lens is designed and fabricated up to THz range by our group. The planar microstrip log-spiral antenna and log-period antenna have been fabricated using micro-electromechanical systems (MEMSs) technology. The photographs of the antennas are demonstrated in Figure 15. The measured responses of the antenna-coupled detector working at different frequency bands are shown in Figure 16, which can be considered to determine the effective operating frequencies [19, 40]. This detector gave a valid response from 12 GHz to 110 GHz frequencies. The results prove the validity and feasibility of the THz antenna designed using micro-electromechanical systems (MEMSs) technology.

5. Conclusion

The advantages and disadvantages of microstrip antennas are discussed in this paper. In particular, three areas for further development of microstrip antennas are presented based on our previous works on microstrip antenna elements and arrays. Variety of microstrip antenna topologies and microstrip-antenna-based composite antenna are discussed, and

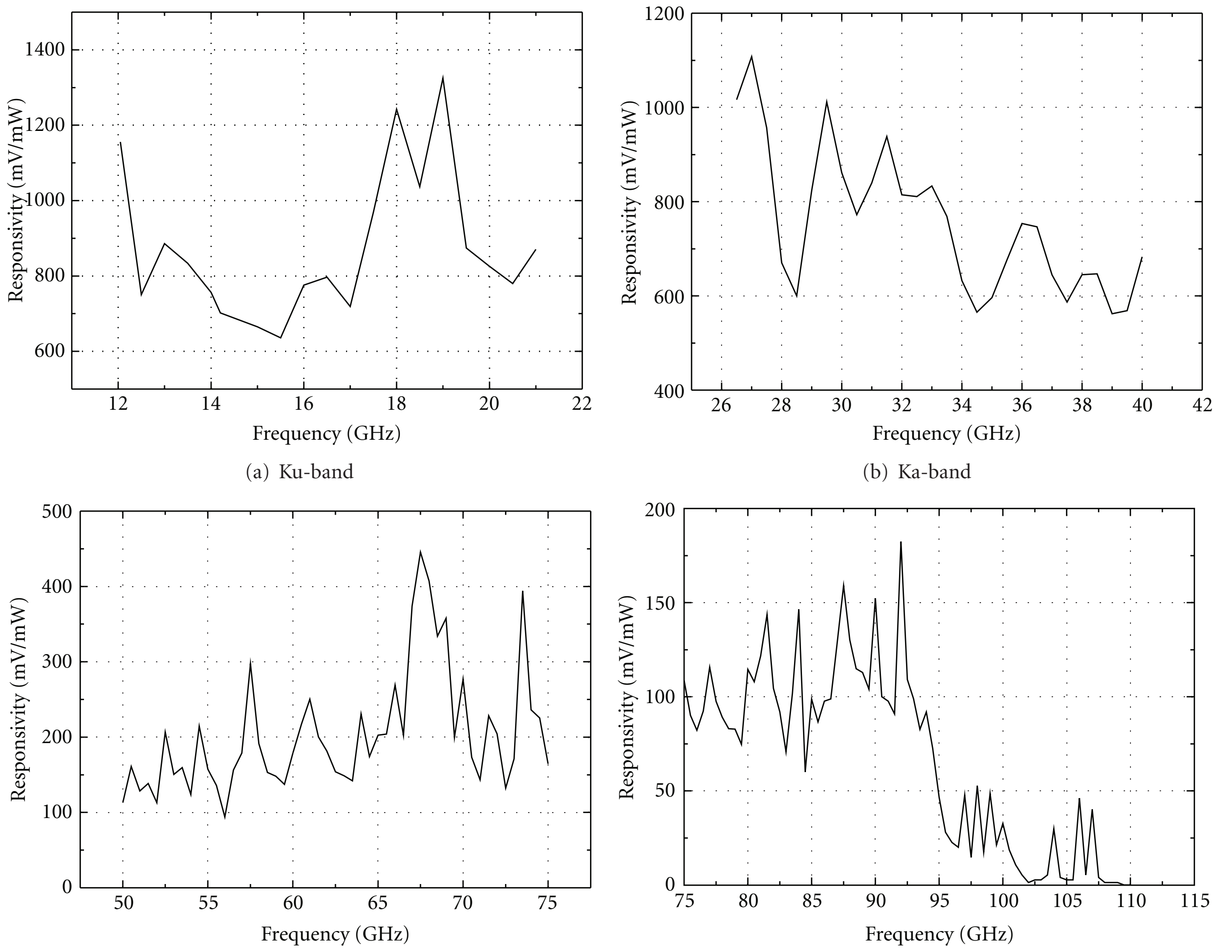

Figure 16: Frequency responses test results of the THz wave planar integrated active microstrip antenna covered by a dielectric lens.

the advanced machining techniques pushing the microstrip antennas towards the highly integration of antenna/array and feeding network and the highly operating frequencies are described. To demonstrate the distinctive features of novel microstrip antennas, various antenna elements and arrays for different applications are presented. This paper has shown that the microstrip antennas are still very promising paradigm for civilian and military wireless applications.

References

[1] G. A. Deschamps, "Microstrip microwave antennas," in *Proceedings of the 3rd USAF Symposium on Antennas*, 1953.

[2] E. V. Byron, "A new flush-mounted antenna element for phased array application," in *Proceedings of the Phased Array Antenna Symposium*, pp. 187–192, 1970.

[3] J. Q. Howel, "Microstrip antennas," in *Proceedings of the Digest of the International Symposium of the Antennas and propagation Society*, pp. 177–180, 1972.

[4] I. J. Bahl and P. Bhartia, *Microstrip Antennas*, Artech House, 1980.

[5] J. R. James, P. S. Hall, and C. Wood, *Microstrip Antenna Theory and Design*, Peter Peregrinus, 1981.

[6] K. R. Carver and J. W. Mink, "Microstrip antenna technology," *IEEE Transactions on Antennas and Propagation*, vol. 1, no. 1, pp. 2–24, 1981.

[7] D. M. Pozar, "Microstrip antennas," *Proceedings of the IEEE*, vol. 80, no. 1, pp. 79–91, 1992.

[8] R. Garg, I. Bhartia, I. Bahl, and A. Ittipiboon, *Micro-Strip Antenna Design Handbook*, Artech House, Boston, Mass, USA, 2001.

[9] D. M. Pozar and B. Kaufman, "Increasing the bandwidth of a microstrip antenna by proximity coupling," *Electronics Letters*, vol. 23, no. 8, pp. 368–369, 1987.

[10] H. F. Pues and A. R. Van de Capelle, "Impedance-matching technique for increasing the bandwidth of microstrip antennas," *IEEE Transactions on Antennas and Propagation*, vol. 37, no. 11, pp. 1345–1354, 1989.

[11] A. Kaya and E. Y. Yüksel, "Investigation of a compensated rectangular microstrip antenna with negative capacitor and negative inductor for bandwidth enhancement," *IEEE Transactions on Antennas and Propagation*, vol. 55, no. 5, pp. 1275–1282, 2007.

[12] K. L. Wong and N. H. Hsu, "A broad-band rectangular patch antenna with a pair of wide slits," *IEEE Transactions on Antennas and Propagation*, vol. 49, no. 9, pp. 1345–1347, 2001.

[13] S. I. Latif, L. Shafai, and S. K. Sharma, "Bandwidth enhancement and size reduction of microstrip slot antennas," *IEEE Transactions on Antennas and Propagation*, vol. 53, no. 3, pp. 994–1003, 2005.

[14] P. M. T. Ikonen, S. I. Maslovski, C. R. Simovski, and S. A. Tretyakov, "On artificial magnetodielectric loading for improving the impedance bandwidth properties of microstrip antennas," *IEEE Transactions on Antennas and Propagation*, vol. 54, no. 6, pp. 1654–1662, 2006.

[15] R. Cocooli, F. R. Yang, T. P. Ma, and T. Itoh, "Apertu-recoupled patch antenna on UCPBG substrate," *IEEE Transactions on Microwave Theory and Techniaues*, vol. 1, no. 47, pp. 2123–2130, 1999.

[16] L.-M. Si and X. Lv, "CPW-FED multi-band omni-directional planar microstrip antenna using composite metamaterial resonators for wireless communications," *Progress in Electromagnetics Research*, vol. 83, pp. 133–146, 2008.

[17] L. M. Si, H. Sun, Y. Yuan, and X. Lv, "CPW-fed com-pact planar UWB antenna with circular disc and spiral split ring resonators," in *Progress in Electromagnetics Research Symposium*, pp. 502–505, 2009.

[18] Y. Yuan, L.-M. Si, Y. Liu, and X. Lv, "Integrated log-periodic antenna for Terahertz applications," in *International Conference on Microwave Technology and Computational Electromagnetics*, pp. 276–279, 2009.

[19] L. Xin, M. Jinchao, Y. Yong, Y. Weihua, N. Hongbin, and G. Yafen, "Integrated active antennas in terahertz focal plane imaging system," in *Proceedings of the International Workshop on Antenna Technology*, pp. 157–163, 2011.

[20] Q. Xu, W. Zhang, H. Sun, and X. Lu, "Millimetre wave multi-polarised microstrip antenna array and application example," *IET Microwaves, Antennas and Propagation*, vol. 4, no. 10, pp. 1525–1530, 2010.

[21] M. Wei, H. Deng, H. Sun, and Y. Liu, "Design of an X/Ka dual-band co-aperture broadband microstrip antenna array," in *Proceedings IEEE International Conference on Microwave Technology and Computational Electromagnetics*, pp. 217–220, 2011.

[22] Y. Liu, X. Lu, Y. Yuan, Y. Chen, and L. Shi, "Integrated design and research of Ka-band electronically large mono-pulse planar antenna and feed system," in *Proceedings of the 7th International Symposium on Antennas, Propagation and EM Theory (ISAPE '06)*, pp. 150–153, October 2006.

[23] Y. Liu, H. J. Sun, X. Lu et al., "Study of the millimeter microstrip monopulse antenna array in the dual-sensor system," in *Proceedings of the 7th International Symposium on Antennas, Propagation and EM Theory (ISAPE '06)*, pp. 157–160, October 2006.

[24] Y. An, X. Lv, and B. Gao, "Developing a kind of mi-crostrip array antenna with beam squint," in *Proceedings of the 5th International Symposium on Antennas, Propagation and EM Theory*, pp. 443–446, 2000.

[25] L. Yong, L. Xin, H. Zhao, and Y. Yuan, "Integrated design and research of novel KA-band circular polarized monopulse interrogator array antenna," in *Proceedings of the IET International Radar Conference 2009*, pp. 1–4, April 2009.

[26] H. A. Wheeler, "Fundamental limitations of small an-tennas," *Proceedings of the IRE*, vol. 35, pp. 1479–1484, 1947.

[27] L. J. Chu, "Physical limitations of omni-directional antennas," *Journal of Applied Physics*, vol. 19, no. 12, pp. 1163–1175, 1948.

[28] R. Azadegan and K. Sarabandi, "A novel approach for miniaturization of slot antennas," *IEEE Transactions on Antennas and Propagation*, vol. 51, no. 3, pp. 421–429, 2003.

[29] H. Mosallaei and K. Sarabandi, "Magneto-dielectrics in electromagnetics: concept and applications," *IEEE Transactions on Antennas and Propagation*, vol. 52, no. 6, pp. 1558–1567, 2004.

[30] P. M. T. Ikonen, S. I. Maslovski, C. R. Simovski, and S. A. Tretyakov, "On artificial magnetodielectric loading for improving the impedance bandwidth properties of microstrip antennas," *IEEE Transactions on Antennas and Propagation*, vol. 54, no. 6, pp. 1654–1662, 2006.

[31] P. M. T. Ikonen, K. N. Rozanov, A. V. Osipov, P. Alitalo, and S. A. Tretyakov, "Magnetodielectric substrates in antenna miniaturization: potential and limitations," *IEEE Transactions on Antennas and Propagation*, vol. 54, no. 11, pp. 3391–3399, 2006.

[32] P. Ikonen and S. Tretyakov, "On the advantages of magnetic materials in microstrip antenna miniaturization," *Microwave and Optical Technology Letters*, vol. 50, no. 12, pp. 3131–3134, 2008.

[33] J. Anguera, C. Puente, C. Borja, and J. Soler, "Frac-tal-shaped antennas: a review," in *Wiley: Encyclopedia of RF and Microwave Engineering*, K. Chang, Ed., vol. 2, pp. 1620–1635, 2005.

[34] L. Shi, H. Sun, X. Lu, C. Deng, and Y. Liu, "Study of the improved MM-Wave omni-directional microstrip antenna," in *Proceedings of the 7th International Symposium on Antennas, Propagation and EM Theory (ISAPE '06)*, pp. 238–241, October 2006.

[35] L. Shi, H. Sun, and X. Lu, "A composite antenna with wide circularly polarized beamwidth," *Microwave and Optical Technology Letters*, vol. 51, no. 10, pp. 2461–2464, 2009.

[36] L. Shi, H. Sun, W. Dong, and X. Lv, "A dual-band multi-function carborne hybrid antenna for satellite communication relay system," *Progress in Electromagnetics Research*, vol. 95, pp. 329–340, 2009.

[37] Y. Chen, H. Sun, and X. Lv, "Novel design of dual-polarization broad-band printed L-shaped probe fed microstrip patch antenna for SAR applications," in *IET International Radar Conference 2009*, pp. 1–4, April 2009.

[38] L. M. Si, H. J. Sun, and X. Lv, "Numerical simulations of backward-to-forward leaky-wave antenna with composite right/left-handed coplanar waveguide," *Chinese Physics Letters*, vol. 27, no. 3, Article ID 034106, 2010.

[39] L.-M. Si, H.-J. Sun, and X. Lv, "THz leaky-wave antenna with high-directivity and beam-steering using CPW CRLH metamaterial resonators," in *Proceedings of the 3rd International Symposium on Photoelectronic Detection and Imaging*, Beijing, China, 2009.

[40] Y. Liu, L. M. Si, S. Zhu, and H. Xin, "Experimental realization of an integrated THz electromagnetic crys-tals (EMXT) H-plane horn antenna," *Electronics Letters*, vol. 47, no. 2, pp. 80–82, 2011.

[41] L. M. Si, Y. Liu, S. H. Zhu, and H. Xin, "Integrated THz horn antenna using EBG structures," in *Proceedings of the IEEE International Symposium on Antennas and Propagation and USNC/CNC/URSI National Radio Science Meeting*, University of Colorado at Boulder, 2011.

[42] Y. Liu, Y. Yuan, X. Lv, and L.-M. Si, "Design of 0.5 THz 2D square lattice EBG waveguide transmission line and power-divider using MEMS technology," in *Proceedings 3rd International Symposium on Photoelectronic Detection and Imaging*, vol. 7385, Beijing, China, 2009.

[43] L.-M. Si, Y. Yong, H.-J. Sun, and L. Xin, "Characterization and application of planar terahertz narrow bandpass filter with metamaterial resonators," in *Proceedings of the International*

Workshop on Metamaterials, pp. 351–354, Nanjing, China, 2008.

[44] L. M. Si and X. Lv, "Terahertz waves hairpin microstrip bandpass filter and its application to overlaid dielectric material detection," *Modern Physics Letters B*, vol. 22, no. 29, pp. 2843–2848, 2008.

[45] L.-M. Si, H.-J. Sun, and X. Lv, "Theoretical investigation of terahertz amplifier by carbon nanotubes within transmission line metamaterials," *Microwave and Optical Technology Letters*, vol. 53, no. 4, pp. 815–818, 2011.

[46] W. Hong, "Millimeter wave and THz communications in China," in *Proceedings of the IEEE International Microwave Symposium Digest (MTT '11)*, pp. 1–4, 2011.

A 2.4 GHz Polarization-diversity Planar Printed Dipole Antenna for WLAN and Wireless Communication Applications

This article presents the design simulation, fabrication and measured performance of a 2.4 GHz polarization-diversity printed dipole antenna for wireless communication applications. Two orthogonal printed dipole antennas, each with a microstrip via-hole balun for vertical and horizontal polarization, are combined and fabricated on a PCB substrate. PIN diodes are used as switches to select the desired antenna polarization. The 3D finite-element-method (FEM) electromagnetic EM simulator, HFSS, is used in the design simulation of this planar antenna structure. Numerical and measured results of the antenna radiation characteristics, including input SWR, radiation pattern coverage and polarization-diversity, are presented and compared.

In wireless communication systems, such as wireless local area networks (WLAN), research and development efforts are aiming at smaller size and better performance. In addition to the use of signal processing techniques to improve communication channel capacity, the radiation characteristics of the portable antenna system is also very important for communication performance.

In urban or indoor environments, the radio wave will propagate through complicated reflection or scattering processes. The polarization of the radio wave may change significantly. In order to effectively receive the communications signal, a polarization-diversity antenna for wireless communications may become an important requirement. A polarization-diversity antenna may have a pair of linearly-polarized antennas, and the radio signal received on both antenna is sampled and compared at

Huey-Ru Chuang, Liang-Chen Kuo, Chi-Chang Lin and Wen-Tzu Chen
National Cheng Kung University, Tainan, Taiwan

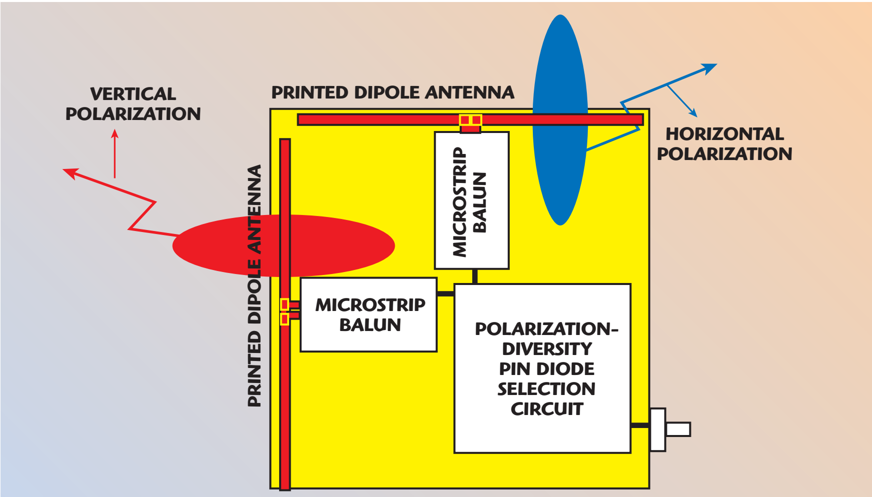

▲ *Fig. 1 A 2.4 GHz polarization-diversity antenna.*

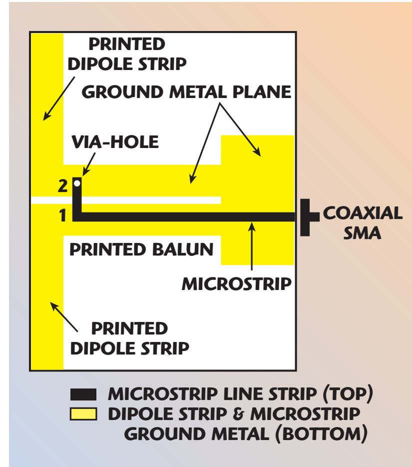

▲ *Fig. 2 Printed dipole antenna with a microstrip balun.*

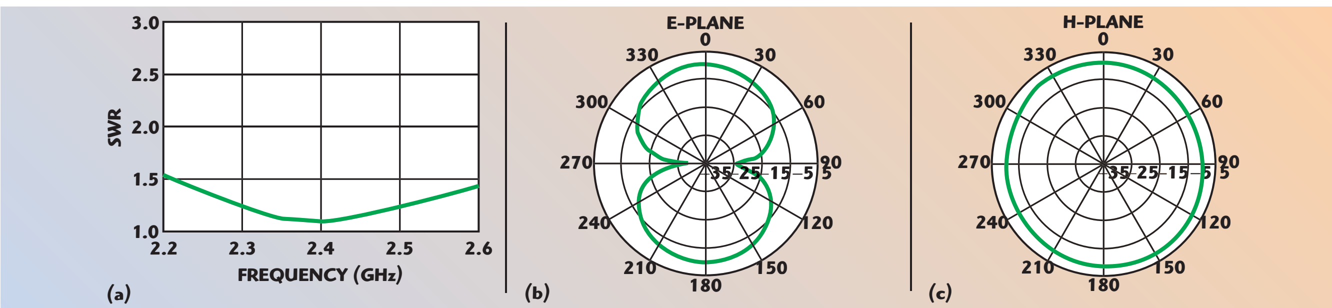

▲ *Fig. 3 Simulated performance of a 2.4 GHz printed dipole antenna placed horizontally; (a) input SWR, (b) E-plane pattern and (c) H-plane pattern.*

certain time intervals. Then the antenna with the best signal quality is selected.

A typical dipole antenna radiates a vertically polarized EM wave and has an omnidirectional antenna pattern. In order to have a preferred planar antenna structure for this 2.4 GHz polarization-diversity antenna, a printed dipole antenna with a microstrip via-hole balun is designed. As shown in ***Figure 1***, two orthogonal printed dipole antennas, for vertical and horizontal polarization, respectively, are combined and fabricated on a PCB substrate. PIN diodes are used to switch and select the desired antenna polarization.

In the antenna design, the high frequency structure simulator (HFSS), based on a 3D FEM, was employed for design simulation of the complete printed dipole structure. A printed dipole antenna and a polarization-diversity planar dipole antenna board (with a polarization-selection PIN diode circuit) have been fabricated on FR-4 PCB substrates. A complete 3D structure FEM simulation and the measured performance of the realized printed dipole-antenna are compared. The measured radiation characteristics of the polarization-diversity planar dipole antenna, including input SWR, radiation pattern coverage and polarization diversity, are presented.

PRINTED DIPOLE ANTENNA WITH MICROSTRIP BALUN

As shown in ***Figure 2***, a printed dipole antenna has a printed microstrip balun which acts as an unbalanced-to-balanced transformer from the feed coaxial line to the two printed dipole strips. The length of the dipole strip and the balun microstrip are both about 1/4 wavelength. The ground plane of the microstrip line and the dipole antenna strips are in the same plane. A via-hole permits the feed point 2 of a printed dipole strip to have the same phase as the feed point 1 of the other printed dipole strip. Due to the 180° phase difference between the top strip and the ground plane of the microstrip line, the feed point 2 of the printed dipole strip will have 180° phase difference with the other feed point 1. Accurate dimensions of the printed dipole strip and the microstrip balun structure are determined by numerical simulation, using HFSS.

The simulation results for a 2.4 GHz printed dipole antenna placed horizontally with a microstrip via-hole balun and fabricated on an FR-4 substrate are shown in ***Figure 3***. The input SWR is less than 1.5 from 2.2 to 2.6 GHz. The simulated E- and H-plane antenna patterns are very close to those of an ideal dipole antenna, where the H-plane pattern is omnidirectional. ***Figure 4*** is a photograph of a realized antenna. The measured input SWR and antenna patterns (measured with the dipole placed vertically) agree well with the simulation results, as shown in ***Figure 5***.

PLANAR POLARIZATION-DIVERSITY PRINTED DIPOLE ANTENNA

Figure 6 shows photographs of a realized 2.4 GHz planar polarization-diversity antenna consisting of two orthogonal printed dipole antennas with a polarization-switched PIN diode circuit. Each printed dipole has

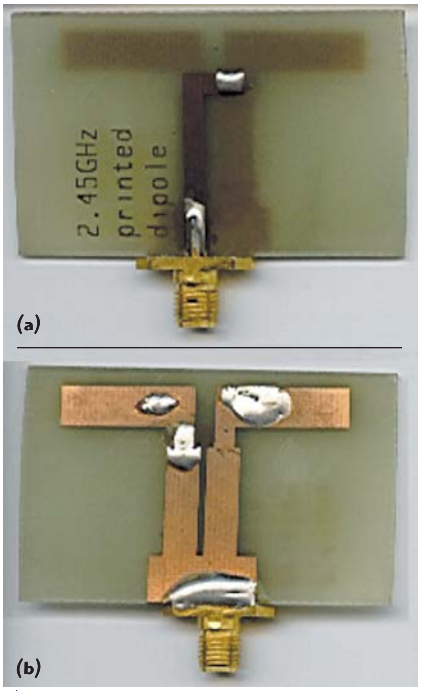

▲ *Fig. 4 A 2.4 GHz printed dipole antenna with a microstrip via-hole balun; (a) top view and (b) bottom view.*

a microstrip via-hole balun. The terminals of the two baluns are connected to a PIN diode selection circuit. Voltages from the transceiver circuit (±5.0V) are fed through a cable to the input of the PIN diode circuit section, to short or open-circuit the PIN diodes. Hence, either the vertical or horizontal printed dipole can be selected and connected to the transceiver.

Since the two dipoles are very close to each other and near the PIN diode circuit section, EM coupling will degrade the performance of each dipole. ***Figure 7*** shows the input SWR simulation results with the vertical dipole antenna selected (+5V to PIN diode switching circuit). The input SWR is less than 2 from 2.25 to 2.60 GHz. The simulated E- and H-plane antenna patterns are all very close to those of an ideal dipole antenna, of which the H-plane pattern is still omnidirectional, as shown in ***Figure 8***. Note that the dominant polarization is the vertical (E_θ) field, which agrees with the selection of the vertical dipole. The antenna pattern has some attenuation in the direction of the PIN diode circuit board. It can also be seen that a certain level of the input RF signal is induced to the horizontal antenna path by EM coupling, which generates some level of cross-

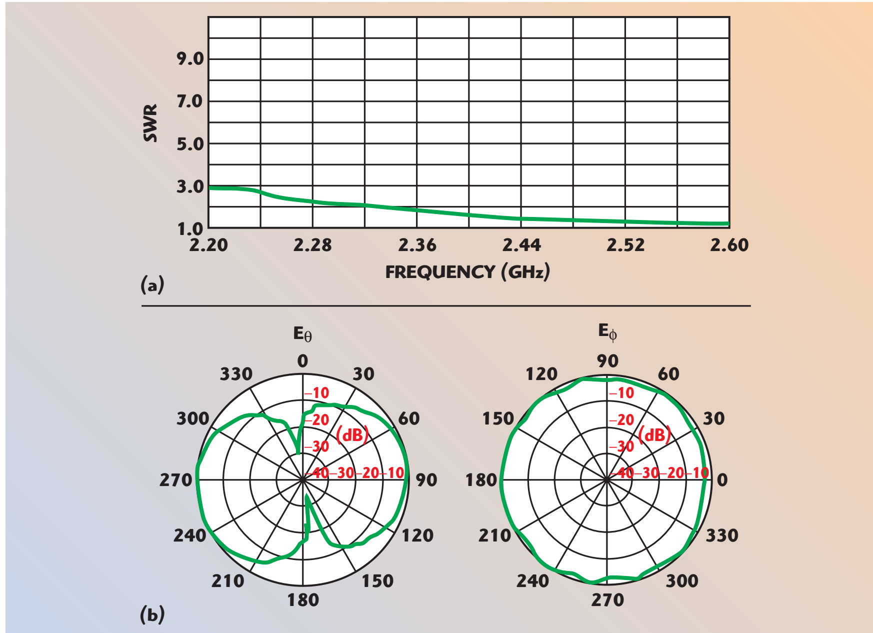

▲ *Fig. 5 Measured input SWR (a) and radiation patterns (b).*

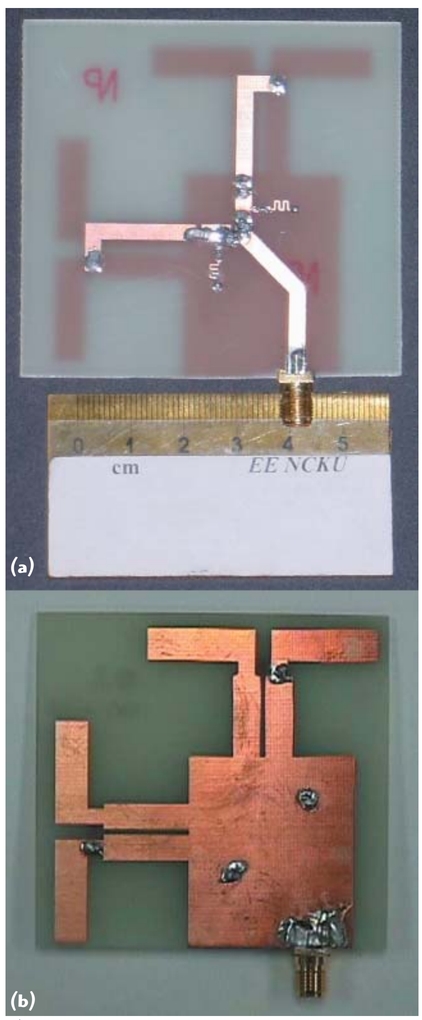

▲ *Fig. 6 A 2.4 GHz planar polarization-diversity antenna with a polarization-switched PIN diode circuit; (a) top view and (b) bottom view.*

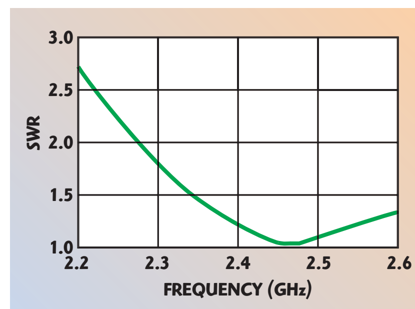

▲ *Fig. 7 Input SWR simulation of a 2.5 GHz polarization-diversity dipole antenna with the vertical dipole selected.*

polarization field. ***Figure 9*** shows the simulation results with the horizontal dipole antenna selected (–5V to PIN diode switching circuit). Results similar to the ones obtained for the vertical dipole antenna can be observed, except that the dominant polarization is the horizontal (E_ϕ) field, which agrees with the selection of the horizontal dipole.

The measured antenna input SWR with vertical or horizontal dipole selection confirms the input SWR of each dipole antenna (through the PIN diode selection circuit) is less than 1.5 from 2.2 to 2.6 GHz, which agrees with the HFSS simulation results. The measured antenna patterns with the selection of the vertical or horizontal dipole shows that for the selection of the vertical dipole, the H-plane pattern is still quite omnidirectional (as an ideal vertical dipole) with some attenuation in the direc-

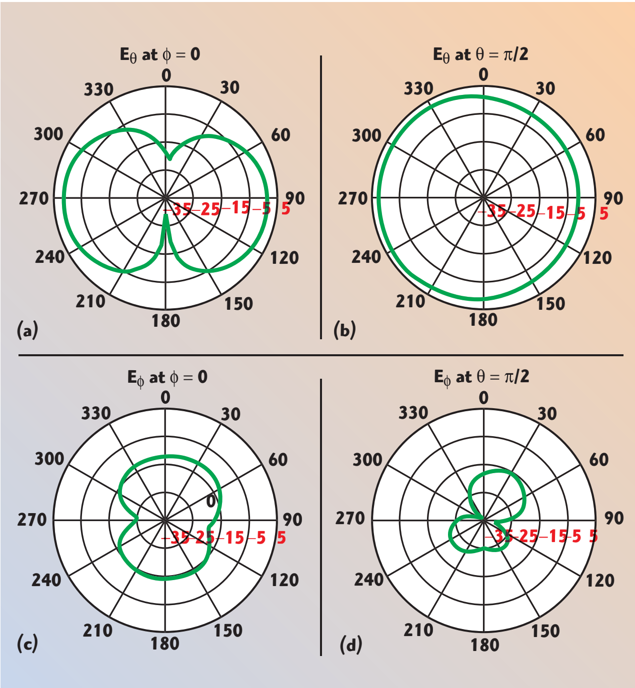

▲ *Fig. 8 Simulation of a 2.5 GHz polarization-diversity dipole antenna with the vertical dipole selected; (a) E_θ-field E-plane pattern, (b) E_θ-field H-plane pattern, (c) E_ϕ-field (cross-polarization) E-plane pattern and (d) E_ϕ-field (cross-polarization) H-plane pattern.*

tion of the PIN diode circuit board. ***Figures 10*** and ***11*** show the mesured SWR and antenna patterns, respectively. A certain level of the induced cross-polarization pattern is observed as predicted by the HFSS simulation due to the proximity of the horizontal dipole strip and the PIN diode circuit board. As for the selection of the horizontal dipole, the E-plane pattern is also close to that of an ideal horizontal dipole. Also, the induced cross-polarization pattern is observed, which is the same situation as the selection of the vertical dipole. The measured data shows a good agreement with the HFSS simulation results and how the antenna polarization-diversity is working.

CONCLUSION

3D FEM design simulation, realization and measurements of a 2.4 GHz printed dipole antenna (with a microstrip via-hole balun) and a planar polarization-diversity printed dipole antenna are presented. The planar polarization-diversity antenna consists of two orthogonal printed dipole antennas for vertical and horizontal polarization and is fabricated on a FR-4 PCB board. A PIN diode switching circuit is used to select the desired antenna polarization. Satisfactory agreement between simulation and measurements is observed. The measured input SWR of the realized printed dipole antenna is less than 1.5 from 2.2 to 2.6 GHz. The measured input SWR of the vertical and horizontal dipole (through the PIN diode switching circuit) of the realized planar polarization-diversity antenna is less than 1.5 from 2.3 to 2.6 GHz. The measured E- and H-plane patterns of the polarization-diversity antenna show that the selected vertical or horizontal dipole have a performance close to a single dipole antenna in a vertical or horizontal position. The designed planar polarization-diversity antenna can be used for wireless communication and WLAN applications.

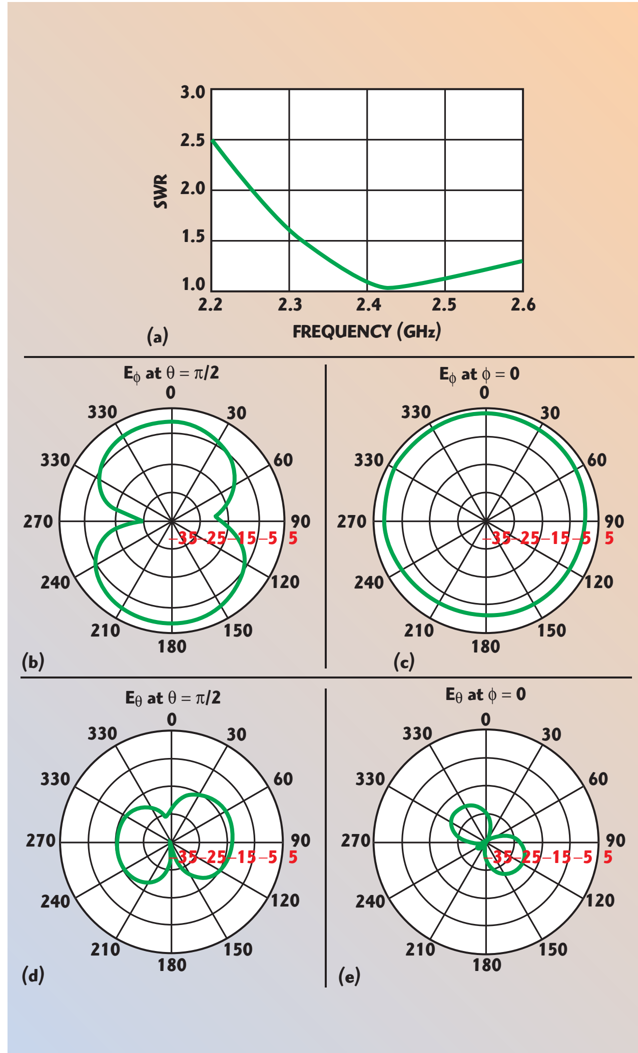

▲ *Fig. 9 Simulation of a 2.4 GHz polarization-diversity printed dipole antenna (with the horizontal dipole selected); (a) input SWR, (b) E_ϕ-field E-plane pattern, (c) E_ϕ-field H-plane pattern, (d) E_θ-field (cross-polarization) E-plane pattern and (e) E_θ-field (cross-polarization) H-plane pattern.*

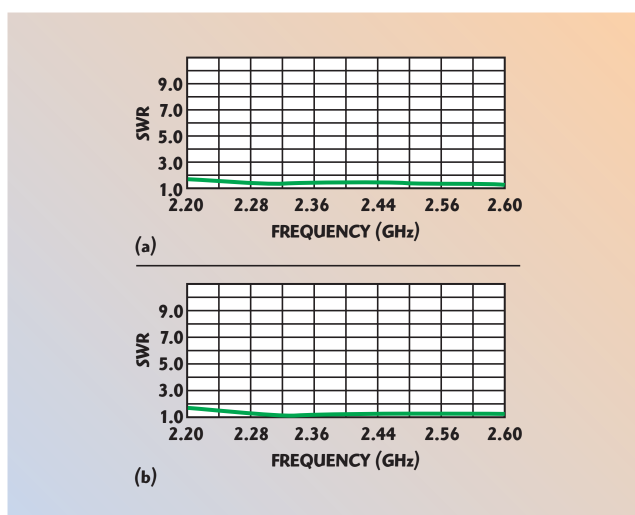

▲ *Fig. 10 Measured input SWR of a 2.4 GHz polarization-diversity printed dipole antenna; (a) vertical dipole selection and (b) horizontal dipole section.*

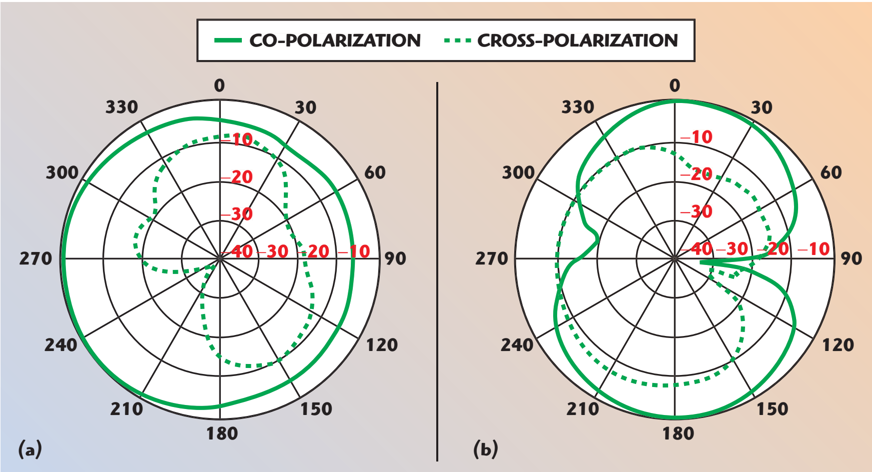

▲ *Fig. 11 Measured co-and cross-polarized patterns of a 2.4 GHz polarization-diversity printed dipole antenna; (a) vertical dipole selected and (b) horizontal dipole selected.*

ACKNOWLEDGMENT

The authors would like to thank Ansoft Inc. for its support of the HFSS software. ■

References

1. K. Fujimoto and J. R. James, *Mobile Antenna Systems Handbook*, Artech House Inc., Norwood, MA 1994.
2. B. Edward and D. Rees, "A Broadband Printed Dipole with Integrated Balun," *Microwave Journal*, May 1987, pp. 339–344.
3. K. Hettak, G.Y. Delisle and M.G. Stubbs, "A Novel Variant of Dual Polarized CPW Fed Patch Antenna for Broadband Wireless Communications," *IEEE Antennas and Propagation Society International Symposium Digest*, Vol.1, 2000, pp. 286–289.
4. L. Zhu and K. Wu, "Model-based Characterization of CPS-fed Printed Dipole for Innovative Design of Uniplanar Integrated Antenna," *IEEE Microwave and Guided Wave Letters*, Vol. 9, No. 9, September 1999, pp. 342–344.
5. N. Michishitai and H. Arai, "A Polarization-diversity Antenna by Printed Dipole and Patch With a Hole," *IEEE Antennas and Propagation Society International Symposium Digest*, 2001, pp. 368–371.

Huey-Ru Chuang *received his BSEE and MSEE degrees from National Taiwan University, Taipei, Taiwan, in 1977 and 1980, respectively, and his PhD degree in electrical engineering from Michigan State University, East Lansing, MI, in 1987. From 1987 to 1988, he was a post-doctoral research associate at the Engineering Research Center of Michigan State University. From 1988 to 1990, he was with the Portable Communication Division of Motorola Inc., Ft. Lauderdale, FL. He joined the department of electrical engineering of National Cheng Kung University, Tainan, Taiwan, in 1991, where he is currently a professor. His research interests include portable antenna design, RF/microwave circuits and RFIC/MMIC for wireless communications, electromagnetic computation of human interaction with mobile antennas, EMI/EMC, microwave communication and detection systems.*

Liang-Chen Kuo *received his BSEE degree from Nan-Tai Institute of Technology, Tainan, Taiwan, and his MSEE degree from Tatung Institute of Technology, Taipei, Taiwan, in 1987 and 1996, respectively. He is currently working toward his PhD degree in electrical engineering from National Cheng Kung University, Tainan, Taiwan. His research interests include computational electromagnetics and antenna design.*

Chi-Chang Lin *received his BSEE and MSEE degrees from Tatung Institute of Technology, Taipei, Taiwan, in 1999 and 2001, respectively. He is currently working toward his PhD degree in electrical engineering from National Cheng Kung University, Tainan, Taiwan. His research interests include EM simulation and microwave antenna design.*

Wen-Tzu Chen *received his PhD degree from National Cheng Kung University, Tainan, Taiwan, in 1998. He is currently an assistant professor at the Institute of Computer and Communication, Shu-Te University, Yen Chau, Taiwan. His research interests include numerical computation of EM interaction between the antenna and the human body, and microwave antenna design.*

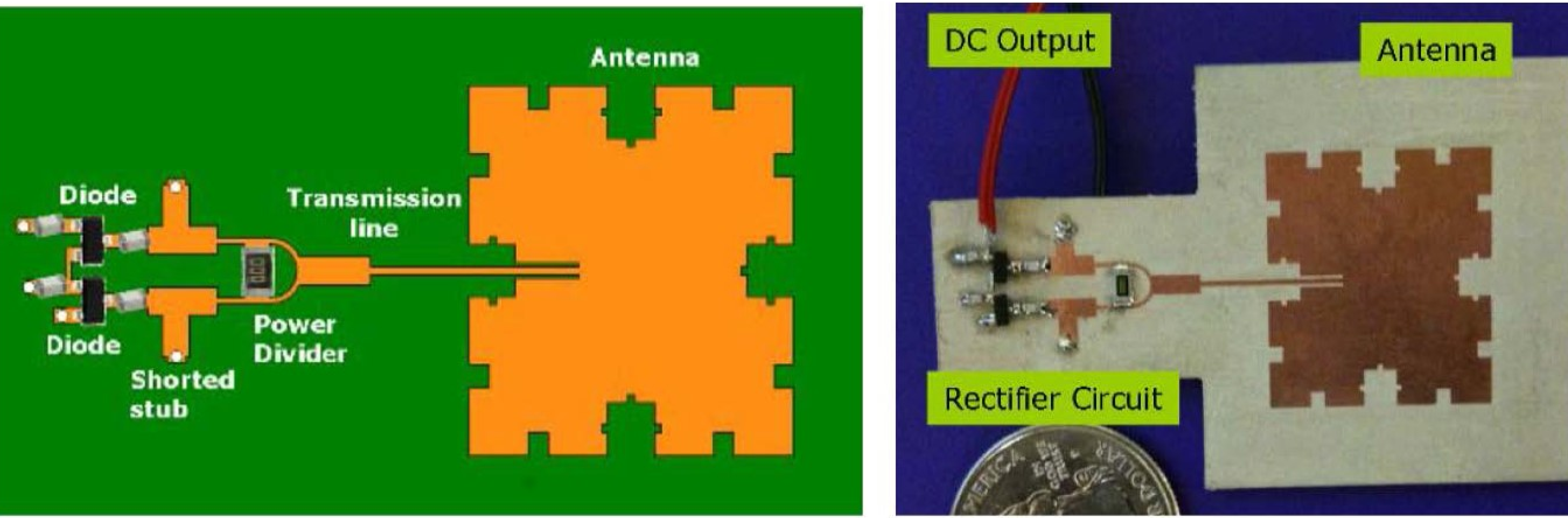
Antenna
Diode
Transmission line
Diode
Power Divider
Shorted stub
DC Output
Antenna
Rectifier Circuit

Giedrius Rakauskas

Follow

Phased Patch Antenna Array Design

Engineering

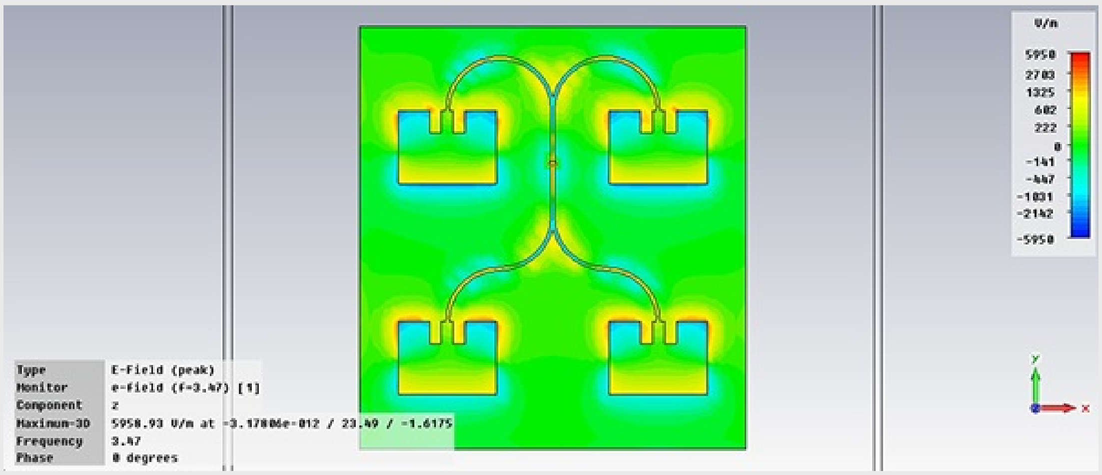

Third Year Project

The aim of this project was to design a directive phased patch antenna array that could be implemented in modern vehicles for distance measurement and autonomous cruise control.

The particular technology allows improved performance as well as reduced costs and size.

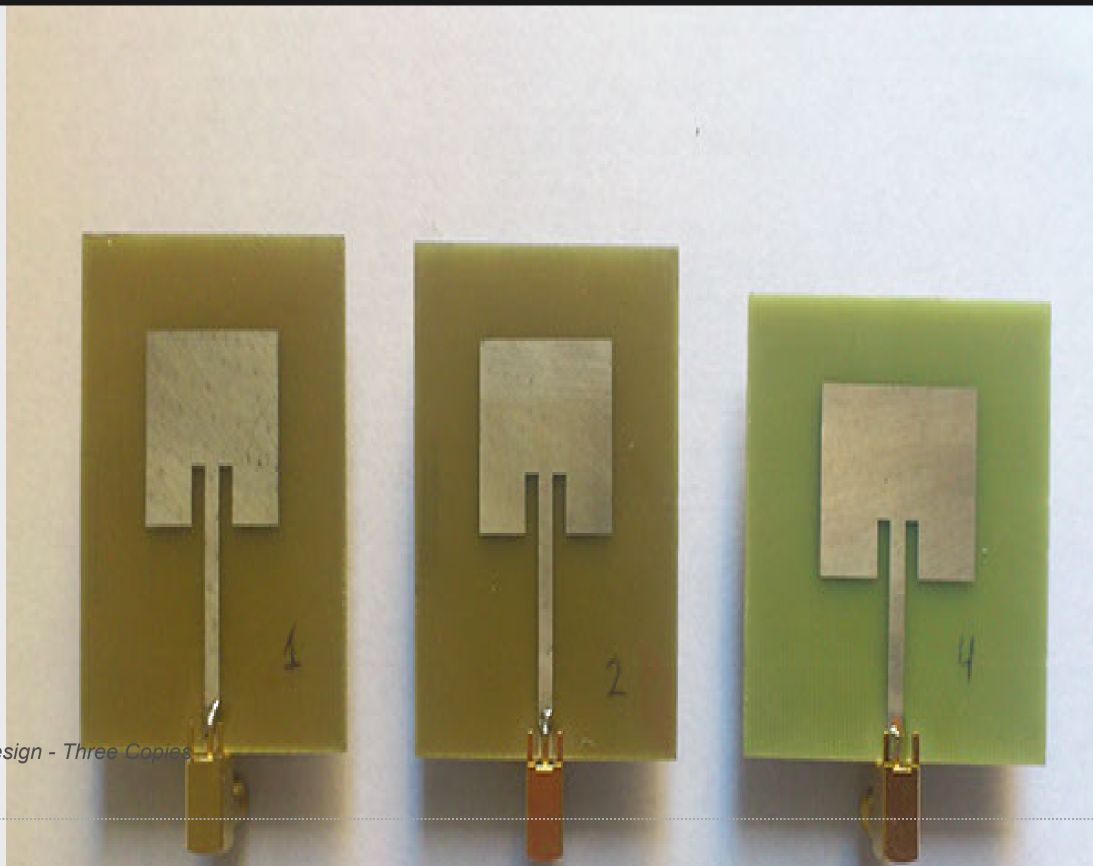

Initial Design - Three Copies

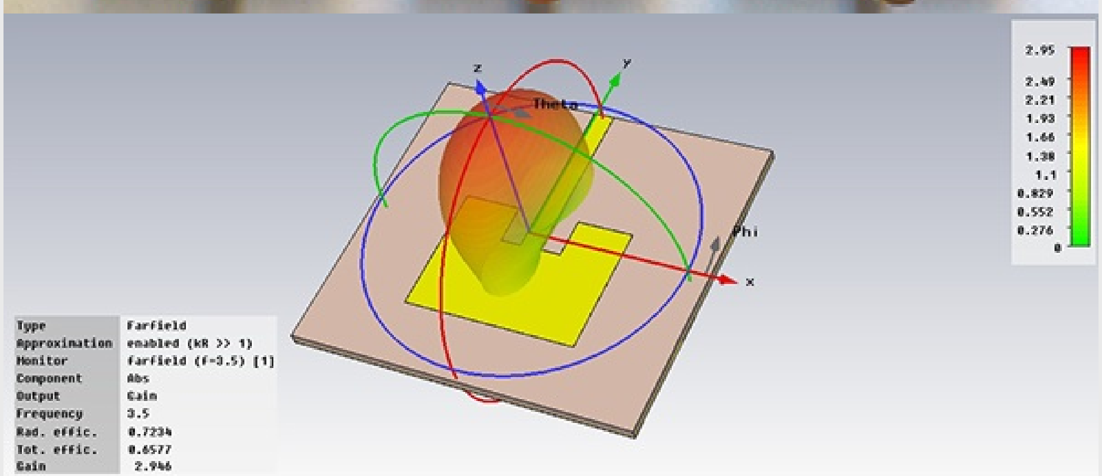

Square Patch Antenna - Farfield Simulation Results

Two-Element Array

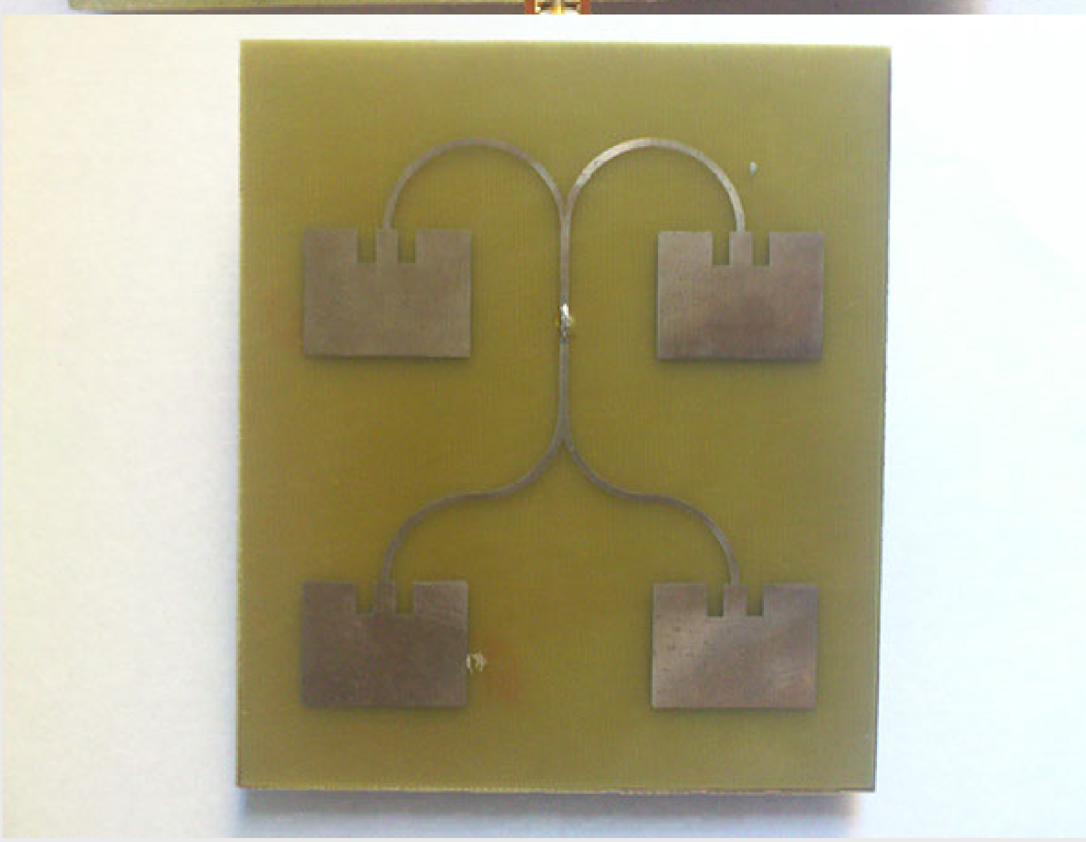

Four-Element Array

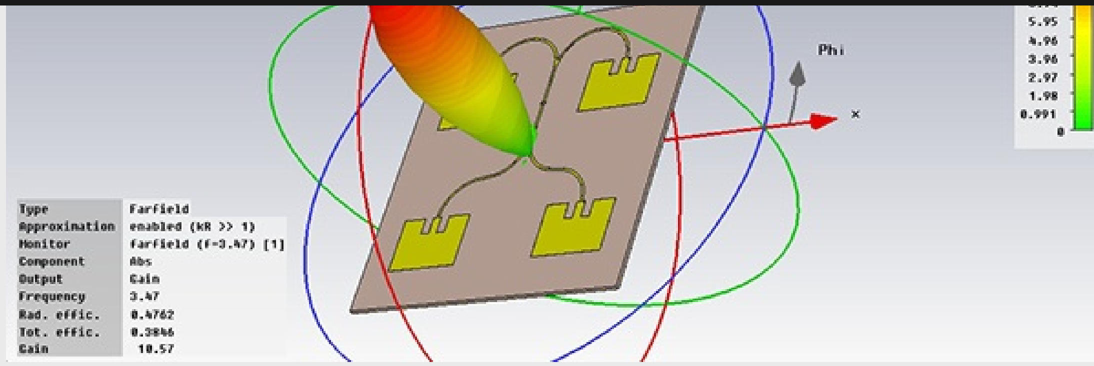

Four-Element Array - CST Microwave Studio Simulation Results

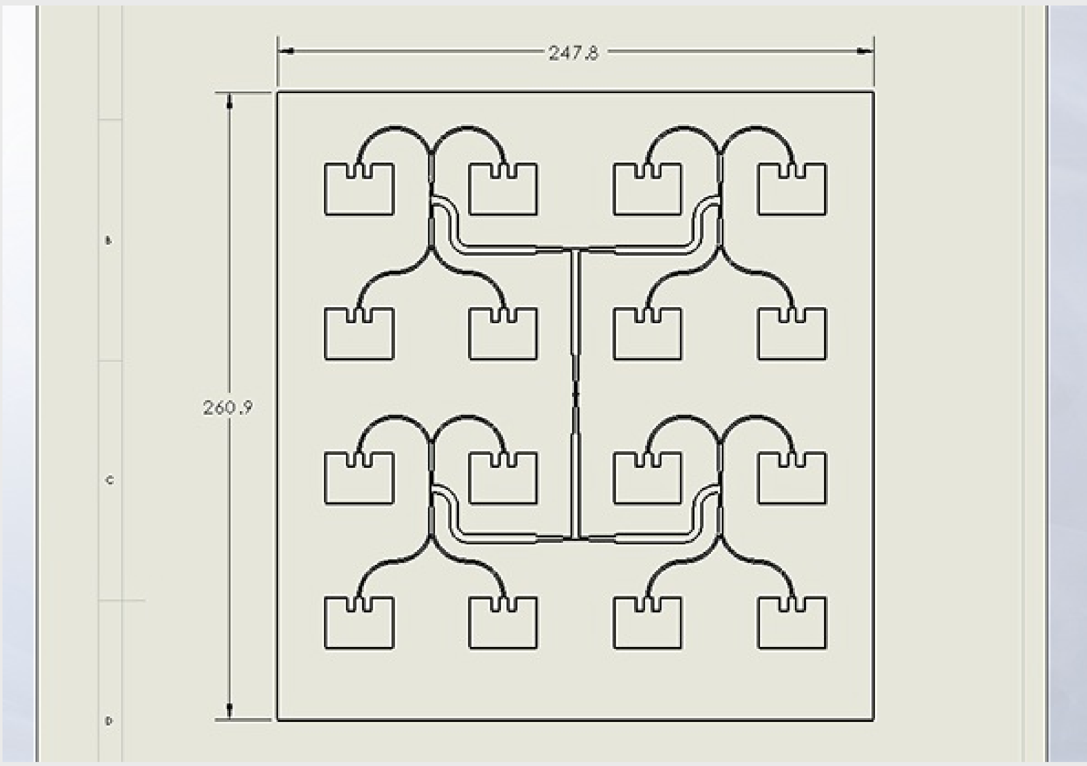

Sixteen-Element Array Design

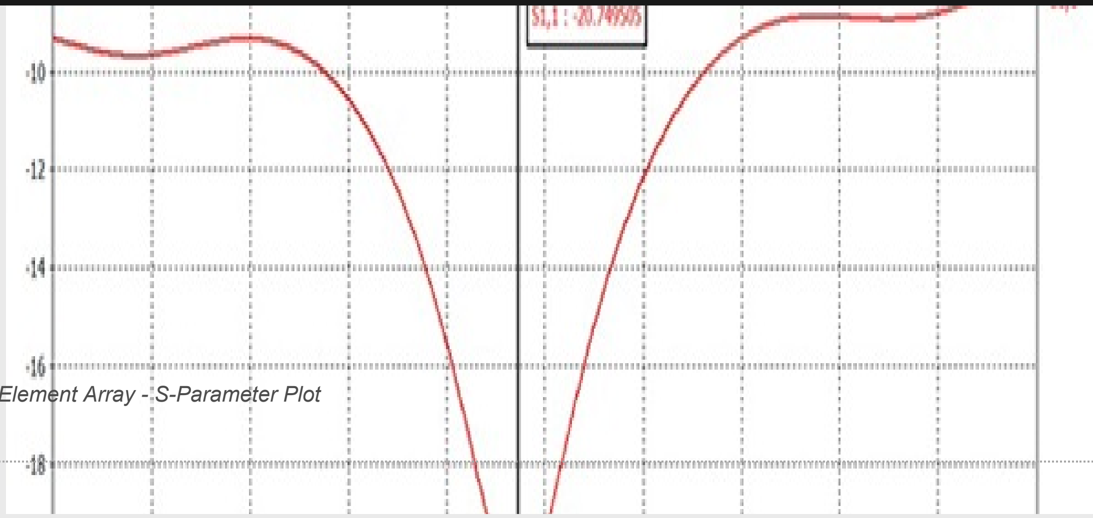

Sixteen-Element Array - S-Parameter Plot

Giedrius Rakauskas
Vilnius, Lithuania

Follow

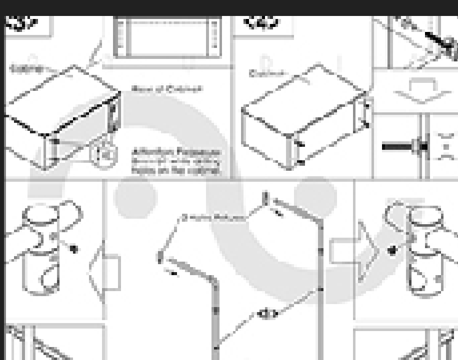

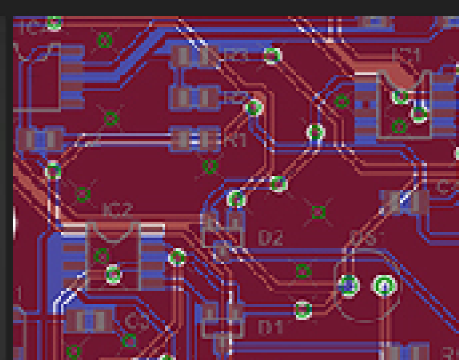

Behance

View Complete Profile →

Comments

Basic Info

Third Year BEng Project - Phased Patch Antenna Array

Credits

Giedrius Rakauskas
Vilnius, Lithuania

+ Follow

Tags

patch antenna | antenna array | square patch antenna | cst mws | cst microwave studio

Tools Used

CST Microwave Studio, FR-4

Report

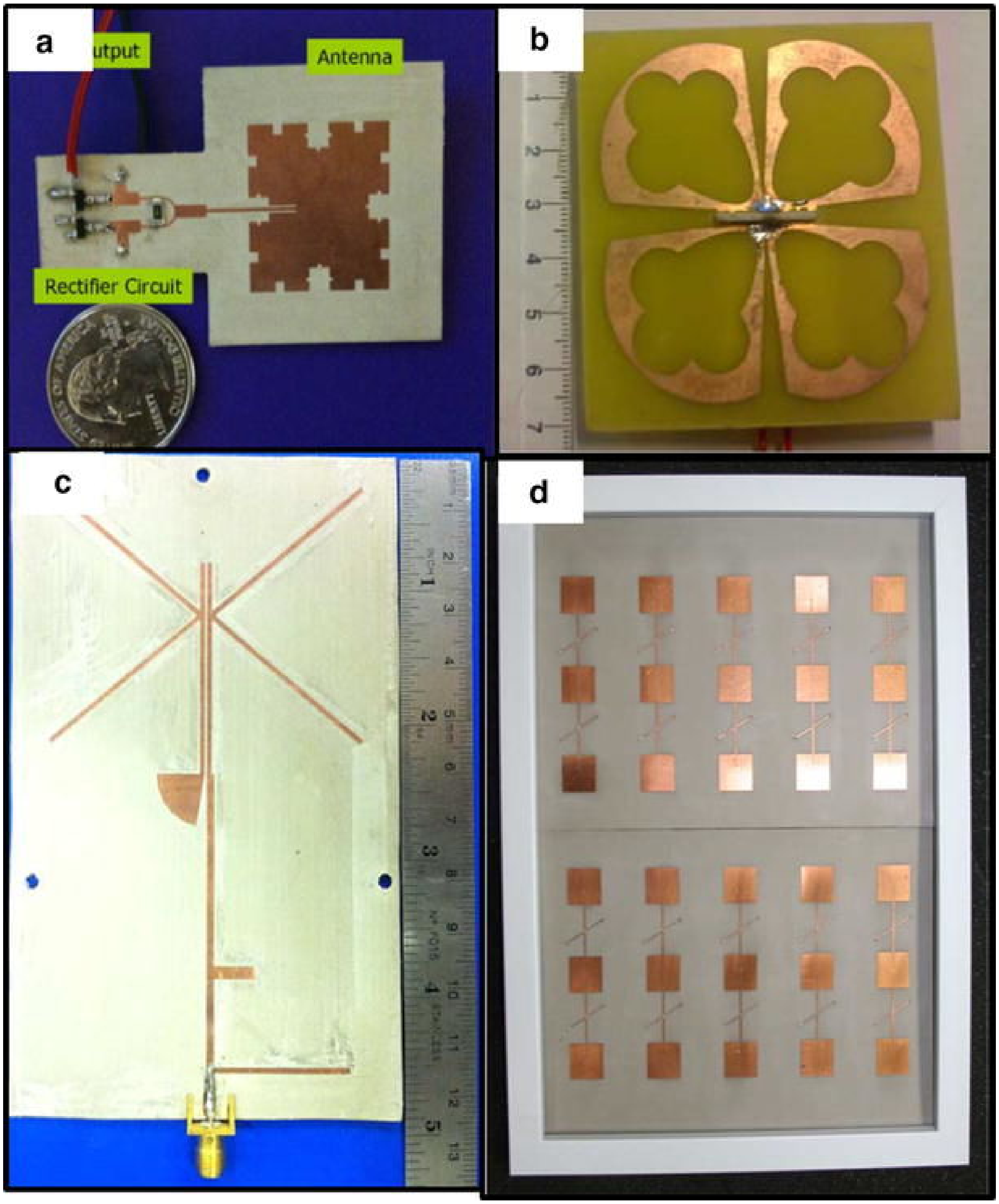

Fig. 4

Types of antennas **a** 2.45 GHz patch antenna with rectifier [38]. ©2010 IEEE. All rights reserved; **b** Planar dual-polarized antenna [24]. ©2015 IEEE. All rights reserved; **c** Microstrip antenna [37]. ©2012 IEEE. All rights reserved; **d** Array of stacked differential patch antenna [33]. ©2015 IEEE. All rights reserved

The plate antennas are popular and have many applications [27, 34, 38]; on-chip antennas are preferred for small and compact applications. Recently, many publications addressed wide-band and multi-band antennas. It has been proven that narrow-band antennas offer high energy conversion efficiencies but can only retrieve a limited amount of energy. On the other hand, wide-band or multi-band frequency antennas can retrieve more RF energy in space. However, the tradeoffs are low overall efficiency and large aperture. In [32], antennas with a resonance frequency of 4.9 and 5.9 GHz were designed with PCEs of 65.2 and 64.8%, respectively. Further work by Lu et al. [26] on polarization antennas supports the assertion that expanding the bandwidth of an antenna leads to increasing the amount of power harvested. In this work, the demonstration of broadband polarization antennas with three separate modes allows the antenna to operate in a wider range of frequencies. One common mechanism in the aforementioned works is the control of the antenna configuration by switching the diodes on and off, thus altering its resonant frequencies. However, since it uses separate modes for different frequencies, this antenna is not able to simultaneously resonate at two frequencies. On the other hand, the antenna presented in [39] is capable of operating at 2.45 and 5.8 GHz, simultaneously, providing 2.6 V output with a PCE of 65% and power density of 10 mW/cm^2.

The main purpose of aligning antennas in arrays is to enhance the antenna gain and obtain high voltage/current. Array antennas are preferred over large aperture antennas because they do not require large breakdown voltage diodes to operate. Antenna arrays can be connected before or after rectification. The first configuration enhances the retrieved power at the main beam while the second configuration expands the ability to retrieve power from various angles away from the main beam [40]. In case the RF waves are combined before rectification, the rectifier requires a large breakdown diode. If RF waves are combined after rectification, combining DC current becomes problematic. Antenna arrays can be connected in series or parallel to obtain high voltage or large current. Nonetheless, expanding the arrays yields better output but this might cause a deduction in conversion efficiency [33].

For demonstrating antenna arrays, Sun et al. [35] invented a T-junction to connect four quasi-Yagi antennas together. The advancement in this work was that the T-junction was flexible in changing from 1 × 4 array to 2 × 2 array topologies. Consequently, the system was able to operate at an ambient power level as low as 455 μW/cm^2 while obtaining 40% PCE.

Impedance matching network

In low-power consumption electrical systems, power leakage during transmission may lead to energy insufficiency. In these circumstances, adding an impedance matching network (IMN) ensures that the maximum power transfers between the RF source and load. For WPH applications, the receiving antenna is considered as the source while the rectifier/voltage multiplier is considered as the load. It is acknowledged that in DC, power transfer is optimum when the resistances of the source and load are indistinguishable. In an RF circuit, the impedance is referred to instead of resistance. An impedance mismatch between the source and load creates reflected power flow in the circuit that lowers the efficiency of the system. As its name indicates, the IMN ensures that the impedance of the source and load are identical by adding reactive components in between.

There are three basics matching configurations i.e. L, T and π matching networks (Fig. 5). The L matching is commonly used since it typically has two components, which simplifies the designing and controlling process. Additionally, the L matching networks do not alter the quality factor (Q) of the circuit.

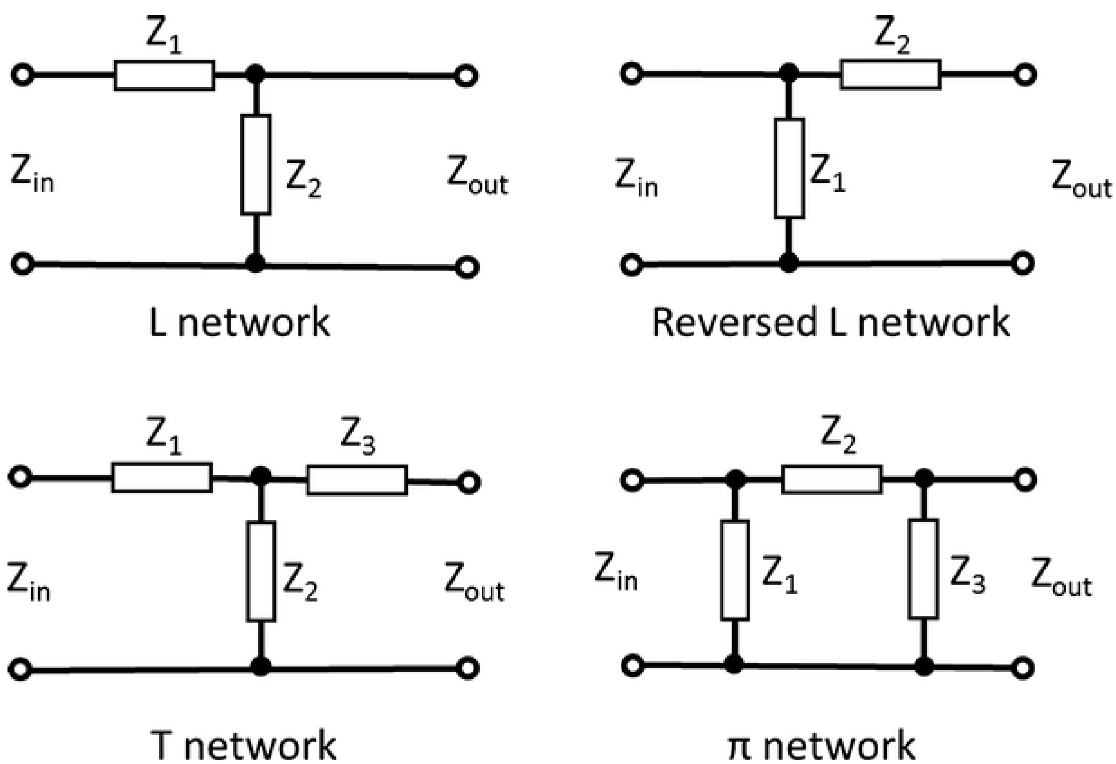

Fig. 5

Configuration of common impedance matching networks

The T and π matching configurations are more complex than the L network. Furthermore, organizing the T and π configurations into multiple stages will retain the final matching results but will change the Q factor. This strategy is useful in improving voltage boost.

There are tradeoffs between the attributes of an IMN, which include frequency, bandwidth, adjustability, and complexity. For instant, in [41], the suboptimal impedance matching and multiport ladder matching methods were introduced to enhance the

matching performance and harvested power of antennas, respectively. However, the tradeoff was that implementation of these configurations required more components than traditional matching networks, thus, escalating the circuit's complexity.

Etor et al. [42] designed an IMN for THz frequencies applications using transmission lines and self-designed metal–insulator-metal diodes instead of lumped components. Moreover, fixed IMN and tunable IMN [43, 44, 45] were introduced as a technique for better matching with wide-band and multi-band antennas.

Rectifier/voltage multiplier

RF energy extracted from free space usually possesses low power density since the electric field power density decreases at the rate of $1/d^2$, where d is the distance from the RF source [46]. Therefore, a power amplifier circuit is required that yields enough DC energy from the electromagnetic waves to drive the loads. This gives rise to two possibilities, if the power consumption of the load is lower than the average power harvesting, the electronic devices at the load may work continuously; otherwise, if the load consumes more energy than the power harvesting circuit can generate, the devices cannot work continuously [47].

Rectifying is the most popular application of diodes, which refers to the conversion of AC current to DC current. In terms of power harvesting application, the RF signal retrieved in the antenna has a sinusoidal waveform. The signal after transformation through IMN would be rectified and boosted to meet the power requirements of the application.

The most fundamental topology of the rectifier is the half-wave rectifier that comprises of a single diode D1 (Fig. 6a). When AC voltage transfers through D1, only the positive cycle remains and the negative cycle is cutoff; thus, it diminishes half of the AC power. Moreover, the output V_{out} is discontinuous since the negative cycle is cutoff. Despite its simplicity, a half-wave rectifier is usually inadequate for common applications. Hence, a full-wave rectifier is more preferable. The circuit design of the full-wave rectifier is shown in Fig. 6b. During the first negative cycle of AC input, diode D1 is conductive and capacitor C1 is charged to the corresponding energy level of V_{peak} of the input. Then, at the next positive cycle, diode D1 is blocked, diode D2 is conductive so that capacitor C2 is also charged. In consequence, the output V_{out} would see two capacitors in series (each one is storing a voltage of $V_{peak)}$. Thus, V_{out} is twice V_{peak}. Therefore, this topology is more stable and efficient than the half-wave rectifier. There is also a bridge rectifier that rectifies both positive and negative cycles of the AC input but retains $V_{out} = V_{peak}$ by alternatively blocking pairs of diodes D1, D4 and D2, D3 (Fig. 6c).

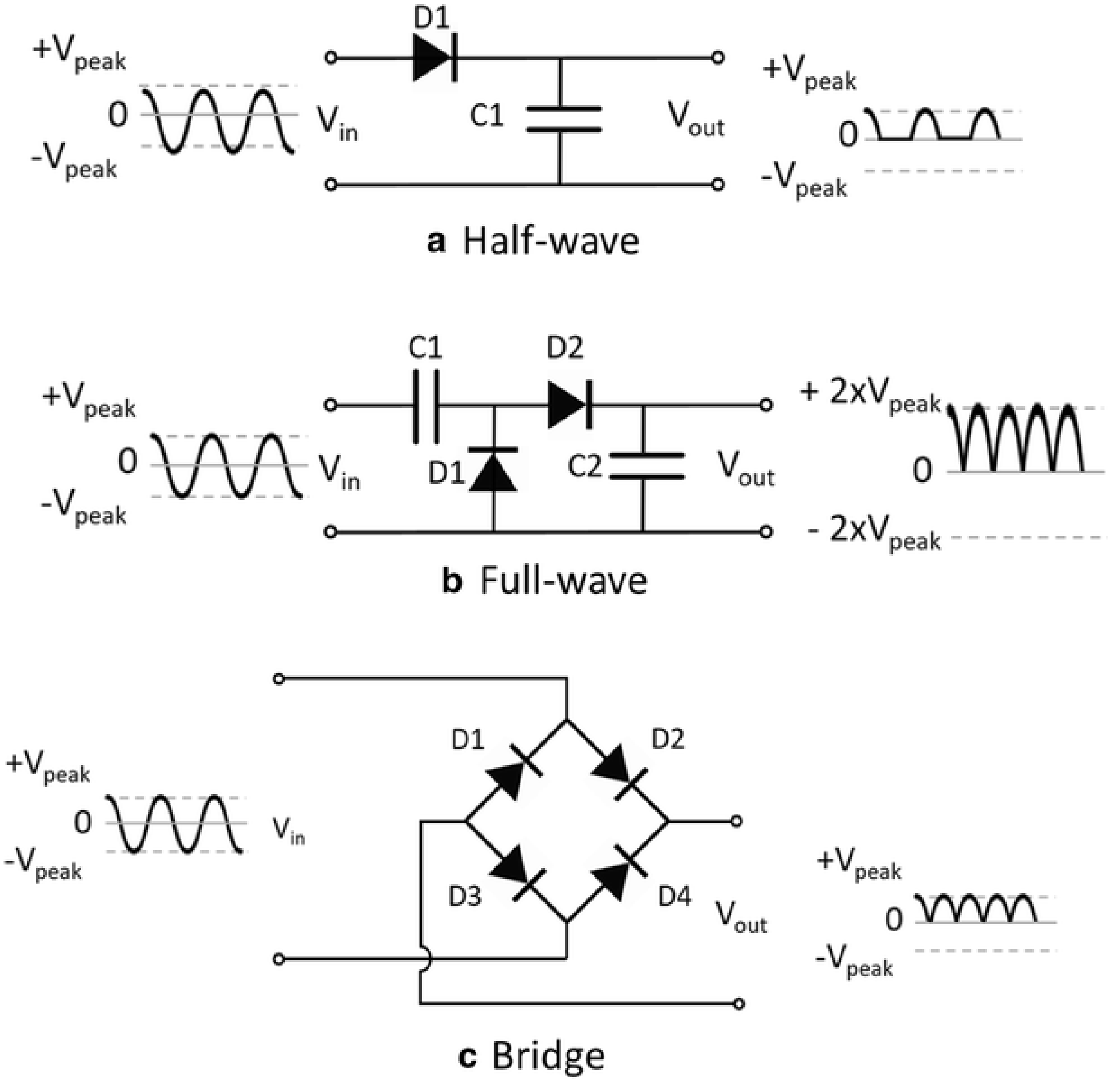

Fig. 6

Some common topologies of a rectifier

Voltage multiplier is a special type of rectifier circuit that converts and boosts AC input to DC output. In some case where the rectified power is inadequate for the application, there is a need for boosting the output DC by stacking single rectifiers into series, forming the voltage multiplier [48]. Several configurations of the voltage multiplier are shown in Fig. 7. The most fundamental configuration is the Cockcroft–Walton voltage multiplier (Fig. 7a). This circuit's operational principle is similar to the full-wave rectifier (Fig. 6b) but has more stages for higher voltage gain. The Dickson multiplier in Fig. 7b is a modification of Cockcroft–Walton's configuration with stage capacitors being shunted to reduce parasitic effects. Thus, the Dickson multiplier is preferable for small voltage applications. However, it is challenging to obtain high PCE due to the high threshold voltage among diodes creating leakage current, thus reducing the overall efficiency. Additionally, for high resistance loads, output voltage drops drastically leading to low current supply to the load. A summary of recent works related to voltage multiplier is shown in Table 3.

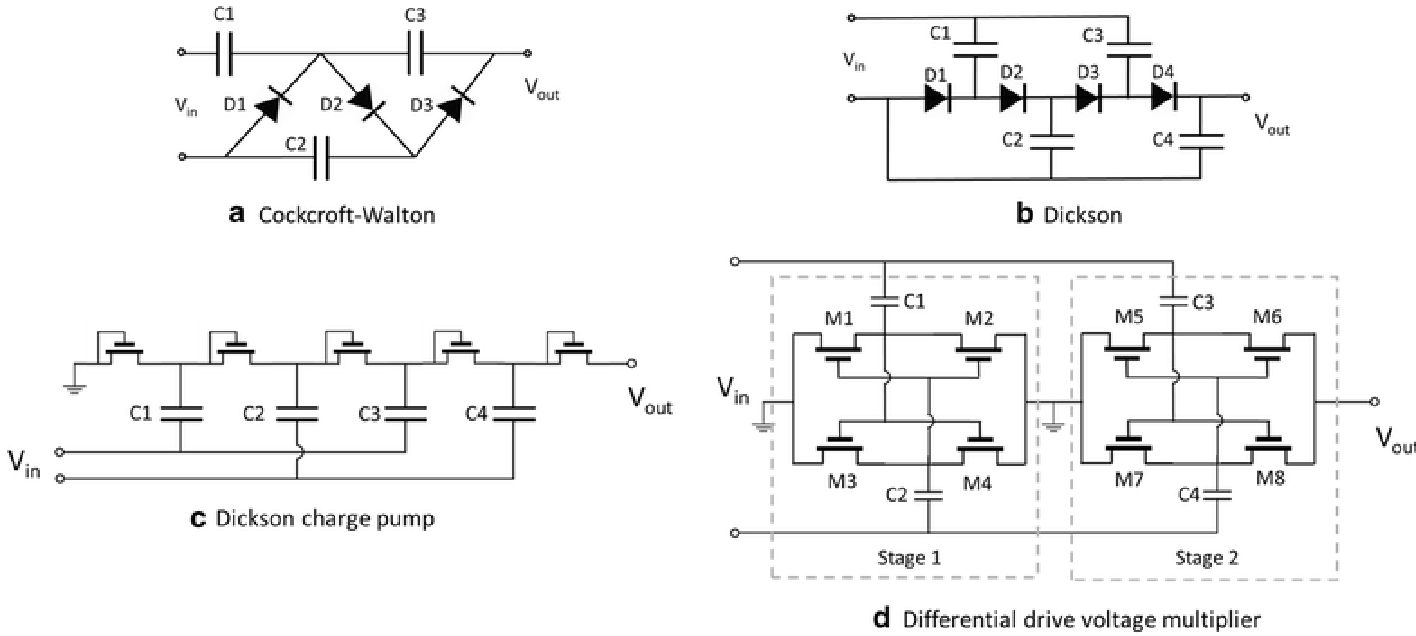

Fig. 7

Common voltage multiplier configurations: **a** Three stages Cockcroft–Walton voltage multiplier, **b** Four stages Dickson voltage multiplier, **c** Four stage Dickson voltage multiplier using CMOS technology, **d** Two stages voltage multiplier comprised of differential drive unit

Table 3

Published work comparison regarding voltage multiplier

Ref.	Rectifier topology	No. of stage	Freq. (MHz)	Tech.	Range (dBm)	Maximum PCE	Size
[51]	Differential	2	433	0.18 µm CMOS	0–20	74% @ 2 dBm	–
[52]	PMOS transistors	7	900	40 nm CMOS	–	44% @ > 390 mV	0.04 mm^2
[53]	Half-wave	4	900	0.18 µm CMOS	–	37.42% @ 390 mV	–
[54]	Comparator-based/active-diode	3	13.56	0.18 µm CMOS	8–15	67.9% @ 12.8 dBm	–
[55]	Dickson	3	13.56	250 nm CMOS	–	72%	0.13 mm^2
[56]	–	–	915	0.13 µm CMOS	−21.6	22.6% @ −16.8 dBm	0.186 mm^2

Prototyping Methods

There's more on this in Scherz, *Practical Electronics for Inventors.*

Solderless Breadboard or **Plugboard**

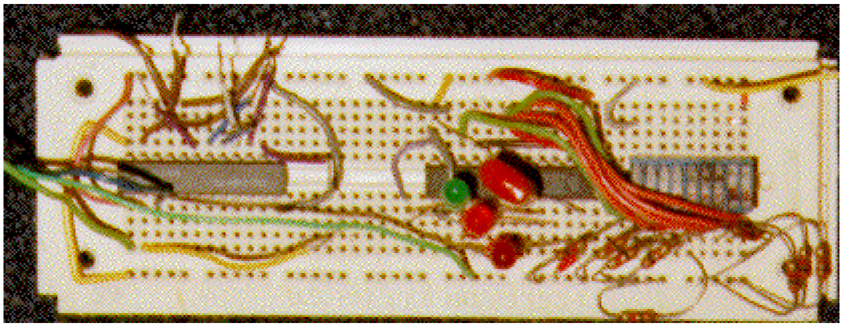

This is what we've been using in lab.

Advantages

- Very fast to build and make changes.
- Works well with DIP ICs

Disadvantages

- o Limited reliability—lab testing only, for limited-size circuits.
- o High capacitance between adjacent rows (~ 10 pF).
- o Only for small-lead-size components (.032" or 0.82 mm max—a 1 A diode lead is just barely too big to meet the spec.)

Springboard

Used in ENGS 22

Advantages

- Fast to build and make changes.
- Accomodates large wire sizes.
- Secure, reliable connections.
- Can handle higher current/power.

Disadvantages

- o Can't accommodate small lead spacings such as on ICs.
- o Although it is reliable enough for long-term use, it's expensive for that purpose.

Wirewrap

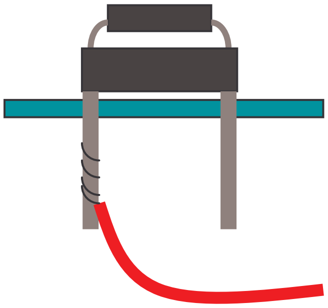

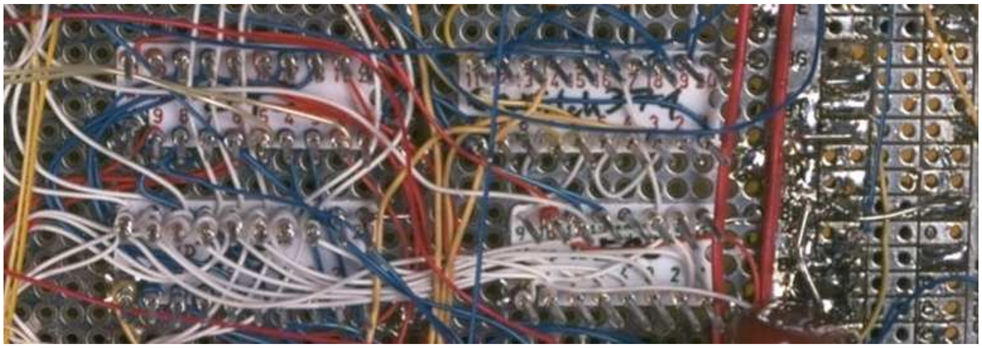

Connections made by fine wire wrapped tightly around square pins of special IC sockets. This is a great way to make a permanent version of a digital circuit almost as quickly as using a solderless breadboard. Used in ENGS 31.

Advantages

- Fast to build and make changes.
- Can make a complex circuit compact.
- Reliable.
- Can be used permanently.
- Inexpensive.

Disadvantages

- o Low current—limited to under a few hundred mA.
- o High inductance/resistance—on the order of 0.1 ohm, 0.25 µH per foot.
- o Only makes reliable connections to square leads (as are on wire-wrap IC sockets). Discrete components (e.g., resistors, capacitors, transistors) need to be soldered to a "header" that goes in an IC socket or to individual wire-wrap pins.

Perfboard and Solder.

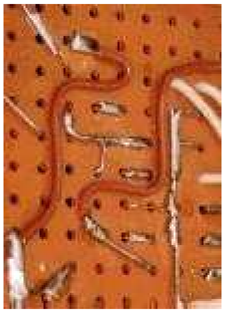

Using the same perfboard as used in wire-wrap work, it is possible to simply twist and solder leads, and run wires where needed.

Advantages

- Reliable, if done well.
- Can be used permanently.
- Inexpensive.
- Can handle any size components
- Convenient for working with discrete components.

Disadvantages

- Slow, requires skill to do well.
- Works for ICs, but not very easily.

Variations:

- Perfboard with individual copper pads on each hole so that the solder will better hold things in place. (Photo below)
- Perfboard with a perforated ground plane. Provides the shielding and grounding benefits of a ground plane, and makes ground connections easy, but requires care to avoid shorts. Some have the ground plane etched from around the holes; others require you to cut the copper away from the holes with a special tool. This is also possible with wire-wrap, as in the photo in that section.

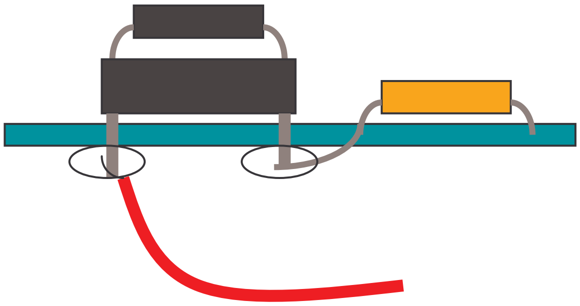

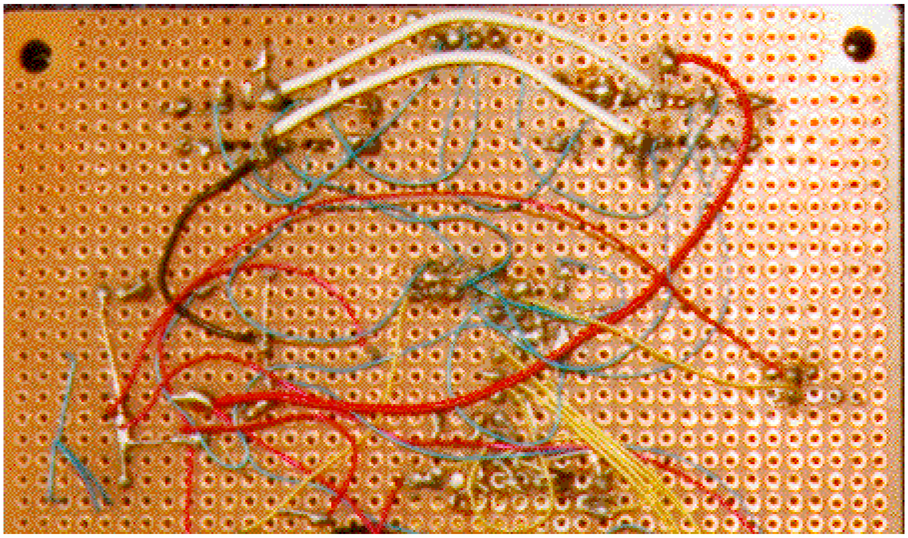

Generic Printed-Circuit Board—multiple hole-per-pad.

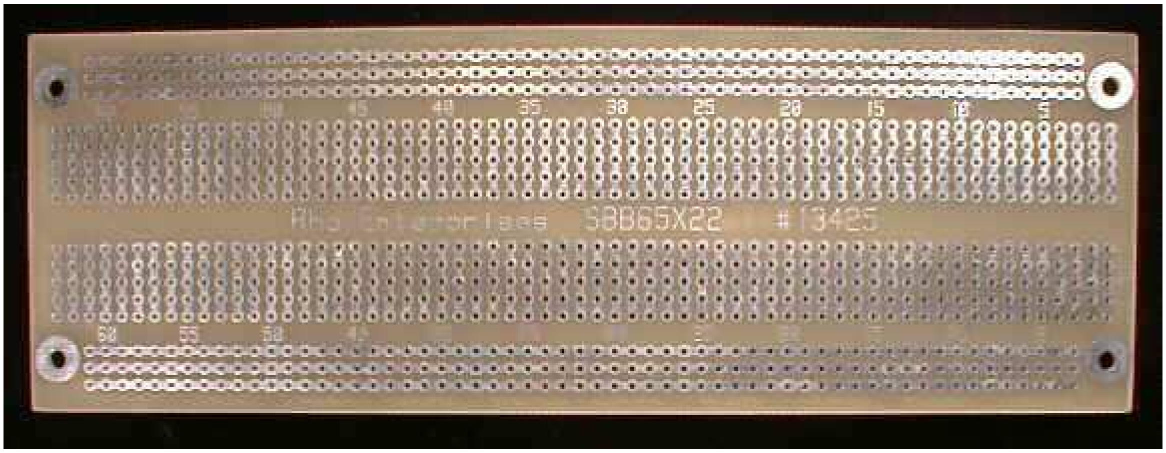

A printed circuit board with a pattern of holes and connections similar to a solderless breadboard.

Advantages

- Easier than using plain perfboard, especially for ICs.
- Reliable.
- Can be used permanently.
- Available with ground planes if needed.

Disadvantages

- Usually not as compact a final circuit as some alternatives, because you are constrained by layout.
- Pads bigger than needed can add capacitance, but not much.
- Can be expensive, especially the “vectorboard” brand.
- Sometimes awkward for odd sized or large components.

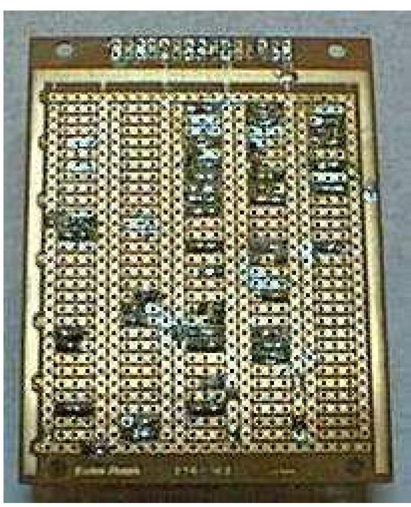

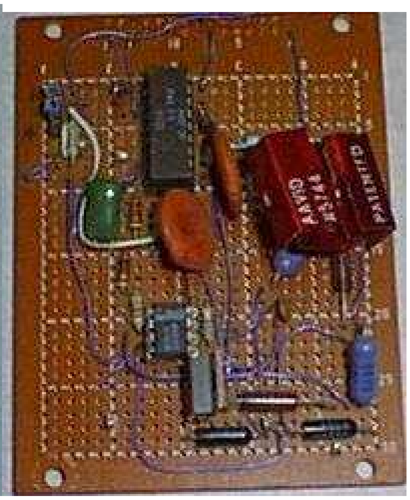

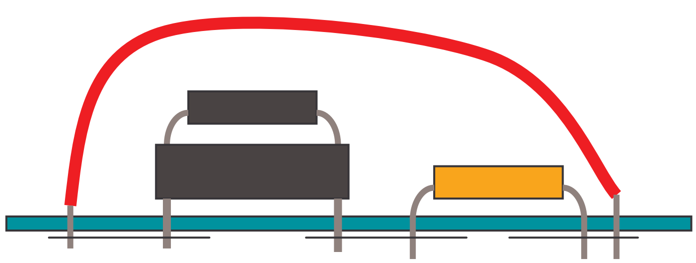

"Dead Bug," or "Ugly-board"

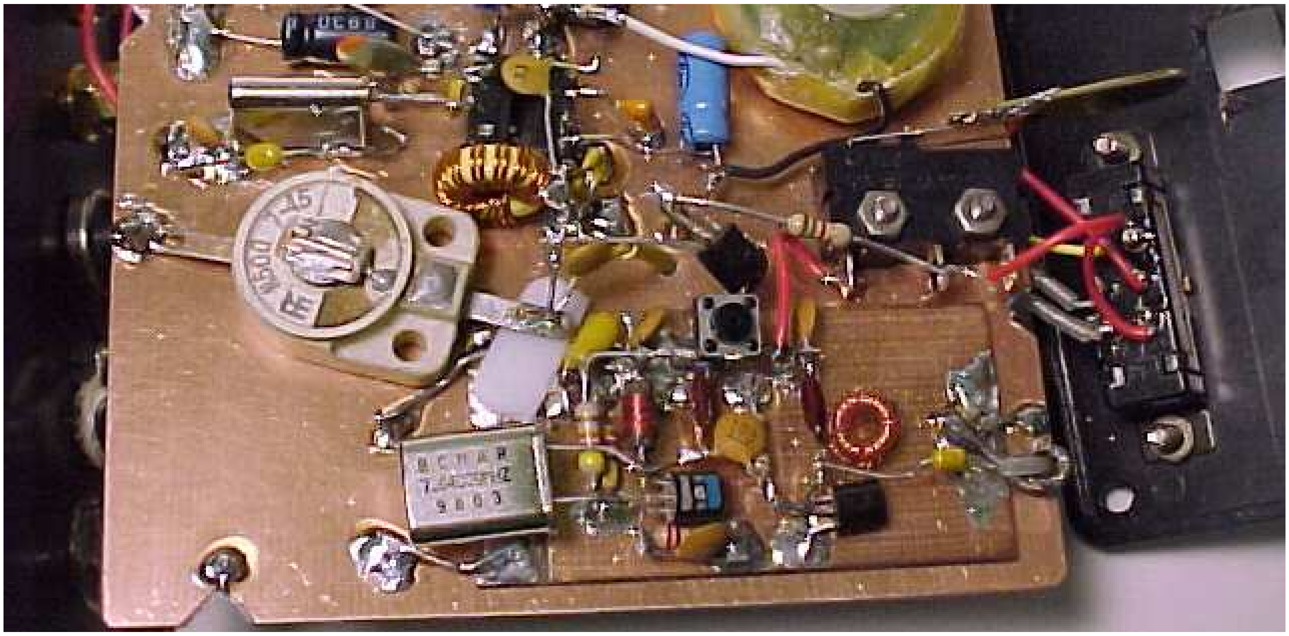

Start with a plain copper-clad board. Glue ICs down with the leads sticking up in the air. Then solder to them

Advantages

- Provides an excellent ground plane. Can be a high performance way to build sensitive and/or high-frequency analog circuits
- Can make a complex circuit compact.
- Reliable.
- Can be used permanently.
- Inexpensive.

Disadvantages

- Requires high soldering skill.
- Takes a long time to build.
- Mechanical support for components is marginal; can add glue ("RTV") after debugging.
- Only makes reliable connections to square leads (as are on wire-wrap IC sockets). Other components (e.g., resistors, capacitors, transistors) need to be soldered to a "header" that goes in an IC socket or to individual wire-wrap pins.

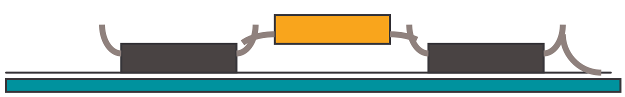

Variations:

- Manually cut the board with a dremel tool to isolate sections for purposes other than ground plane (use the back for ground plane). See photo below.
- Glue on little rectangles of cut-out board to add power busses, etc.

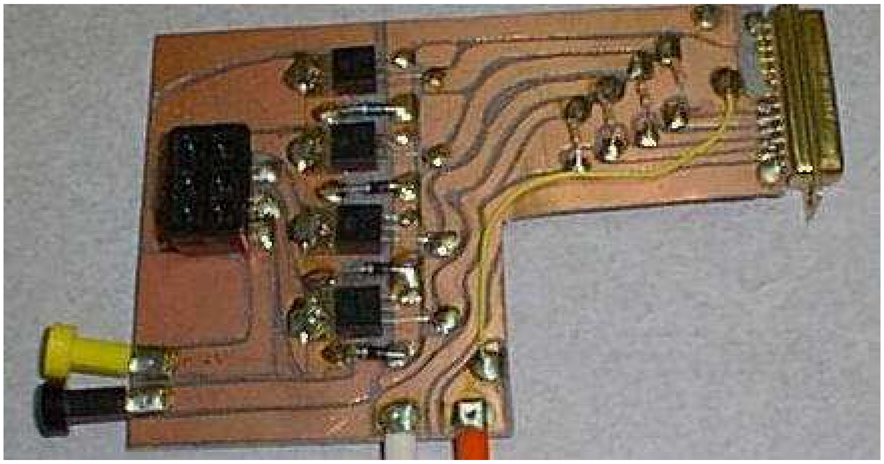

Printed circuit board (PCB)

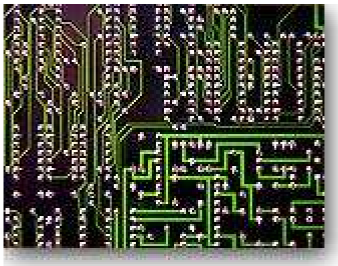

This is what is used virtually universally in production of electronics.

Advantages

- Easy to build in production.
- Repeatable, controllable stray L, C.
- Can handle virtually any component, power level.
- Highly reliable.
- Can make very compact.
- Design can be (somewhat) automated from a schematic you have entered.

Disadvantages

- Laying out the board and getting it fabricated takes time, although you can pay for fabrication in a few days if you can afford it.
- Expensive, on the order of hundreds of dollars for one, but with almost no increase in cost to make many.
- Hard to make changes, but making changes may be easier than building another type of prototype.

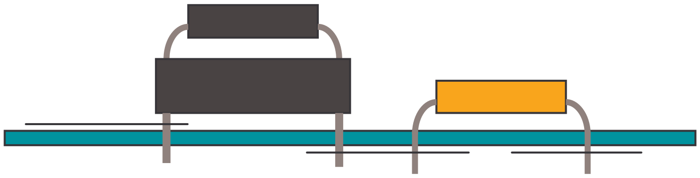

Notes on surface-mount components

Most modern production designs now use surface-mount components instead of "through hole" components. The circuits can be more compact, and the board layout is easier because different things can be done on each side (and in additional layers between sides) without through-holes interfering. But prototyping gets much more difficult!

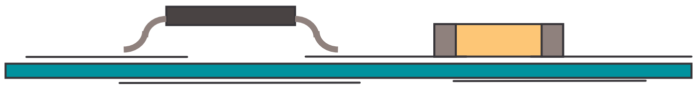

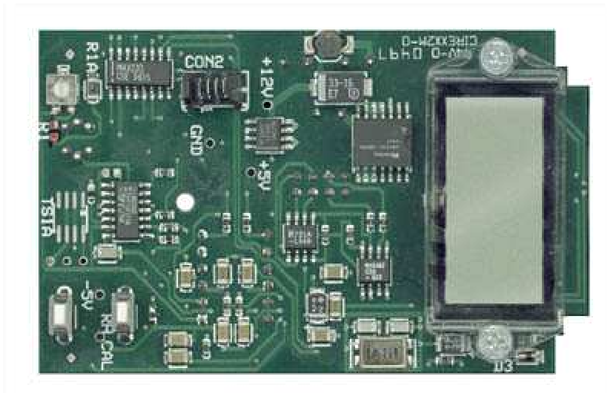

Prototyping options for surface mount

- Simulate, and then lay out a PCB. Don't ever make a breadboard.
- Order DIP ICs and leaded passives for the prototype, and then switch to surface mount for production.
- Get adaptors that have pads to solder surface-mount ICs to, and then standard-spacing (0.1") pins in DIP or SIP layout. Digikey carries "surfboards" made by Capital Advanced Technologies, and adaptors made by Aries Electronics. In addition to DIP and SIP adaptors, there are boards with solder pads for connecting larger wires; these work well for prototypes built in "dead bug" style.

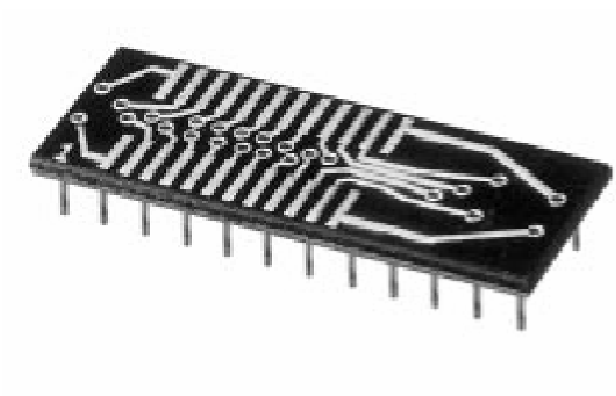

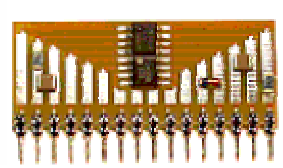

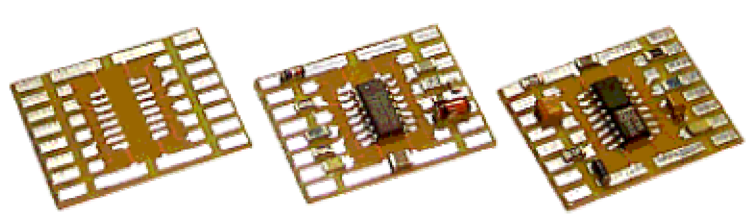

Crystal receiver set 11

Back to the index

This receiver has a single tuned circuit, the Q factor of the tuned circuit is quite low.
The receiver can be used well for reception of local stations, for reception of distant stations it is less suitable.

I tried to give this receiver a nice "old-fashioned" look, the reception performance was in this design of less importance.
This receiver is for sale, I made a series production of these, and will build more on request.
This receiver is also for sale as do-it-yourself kit.
See the shop for more information.

The front panel of the receiver.
On the left side the socket for the headphone.
In the middle the tuning knob.
On the right the connections for antenna (upper) and ground (lower).

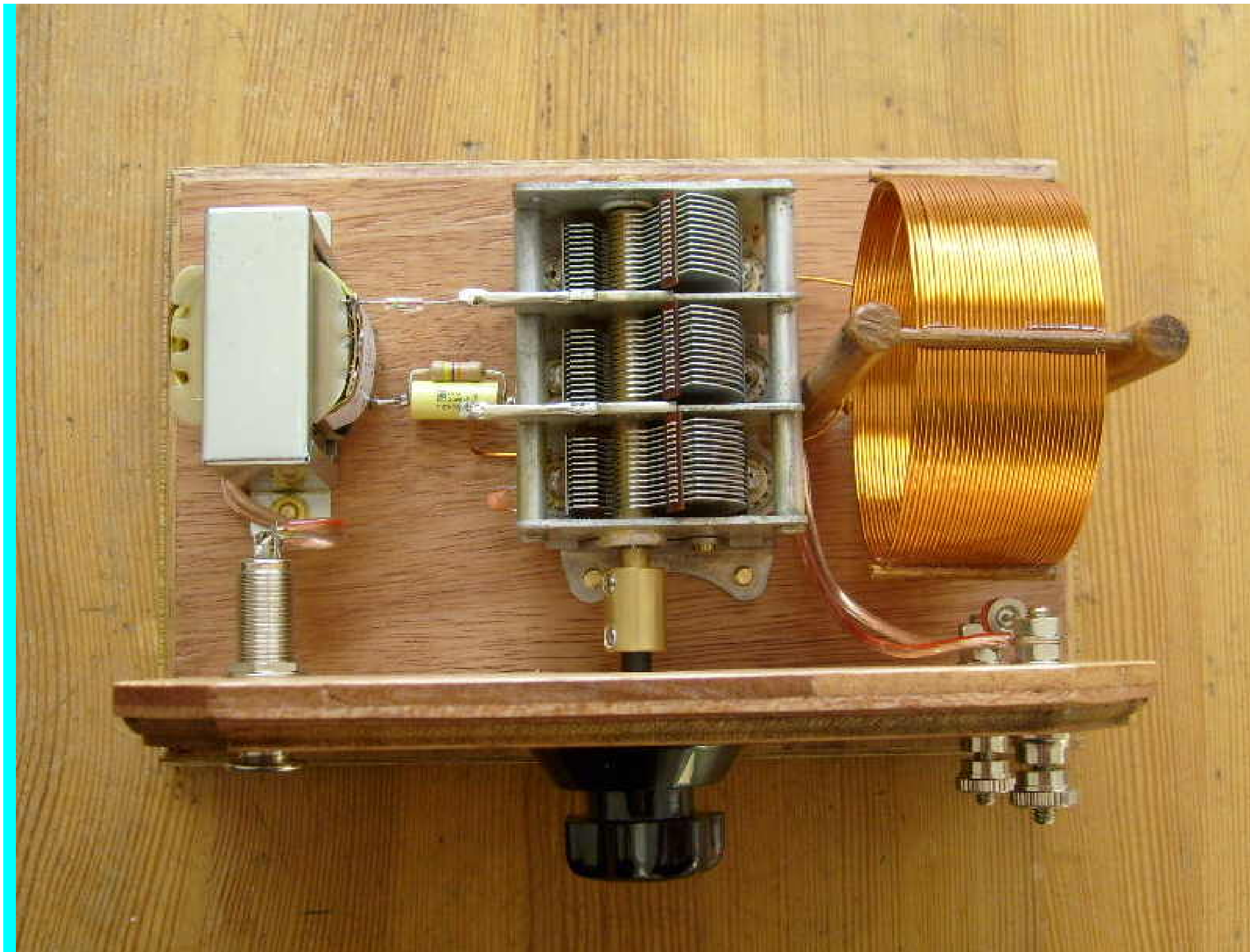

Top view of the receiver.

Circuit diagram of receiver set 11

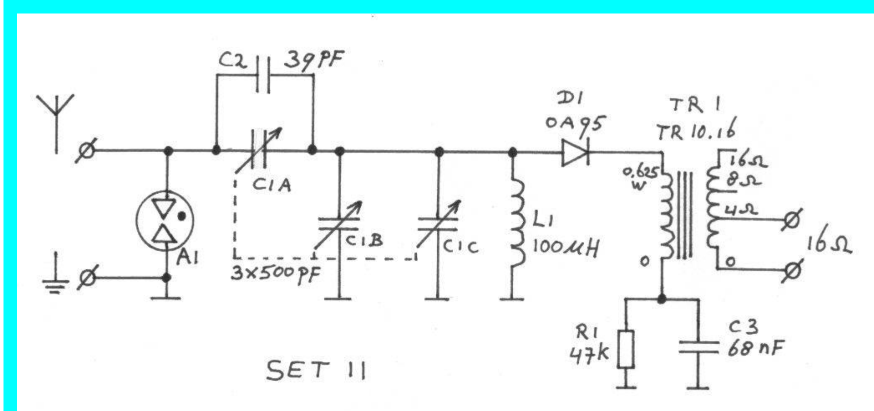

Circuit description.
The resonance circuit is formed by coil L1 and C1b and C1c (together 1000 pF).
Capacitor C1a and C2 provide the matching between antenna and tuned circuit.
The frame (rotor) of the tuning capacitor is carrying the RF signal, by this it is possible to tune simultaneously the tuned circuit (C1b and C1c) and the antenna matching (C1a).
Germanium diode D1 provides the signal detection.
Transformer TR1 is loaded with 16 Ω at its 4 Ω output, through this the input impedance increases from 16 kΩ to about 43 kΩ.
At the output a headphone of 2x 32 Ω can be connected, with the two speakers parallel, the impedance is 16 Ω.

Component A1 is a *gas discharge tube* (also called: *surge arrester*) with type number: N81-A90X.
The gas discharge tube protects the antenna input for too high voltages.

These high voltages can occur if the antenna picks up static charge from the air (especially occurs with long outdoor antennas from non insulated antenna wire).
As the voltage at the antenna is higher then 90 Volt, the gas discharge tube will start to conduct and short the high voltage to ground.
As soon as the charge has flown to ground, the conduction stops automatically.

Frequency range of the receiver.
Frequency range without antenna: 500 - 2500 kHz.
Frequency range with 10 meter antenna connected: 487 - 1860 kHz.
Both with and without antenna connected, the whole medium wave band can be tuned.

Q factor of the LC circuit (Without antenna and without diode connected):
600 kHz: Q= 83
900 kHz: Q= 81
1200 kHz: Q= 75
1500 kHz: Q= 65
The circuit Q is rather low, one reason for this is because the RF signal is in this design on the frame of the tuning capacitor.
Because the frame of the tuning capacitor is directly connected to the wooden bottom plate losses occur here.

You can find a complete building instruction op the following pages:

Step 1 Preparing the components

Step 2 Making the frame of the receiver

Step 3 Making the coil

Step 4 Placing the components

You will find here the part list of this receiver.

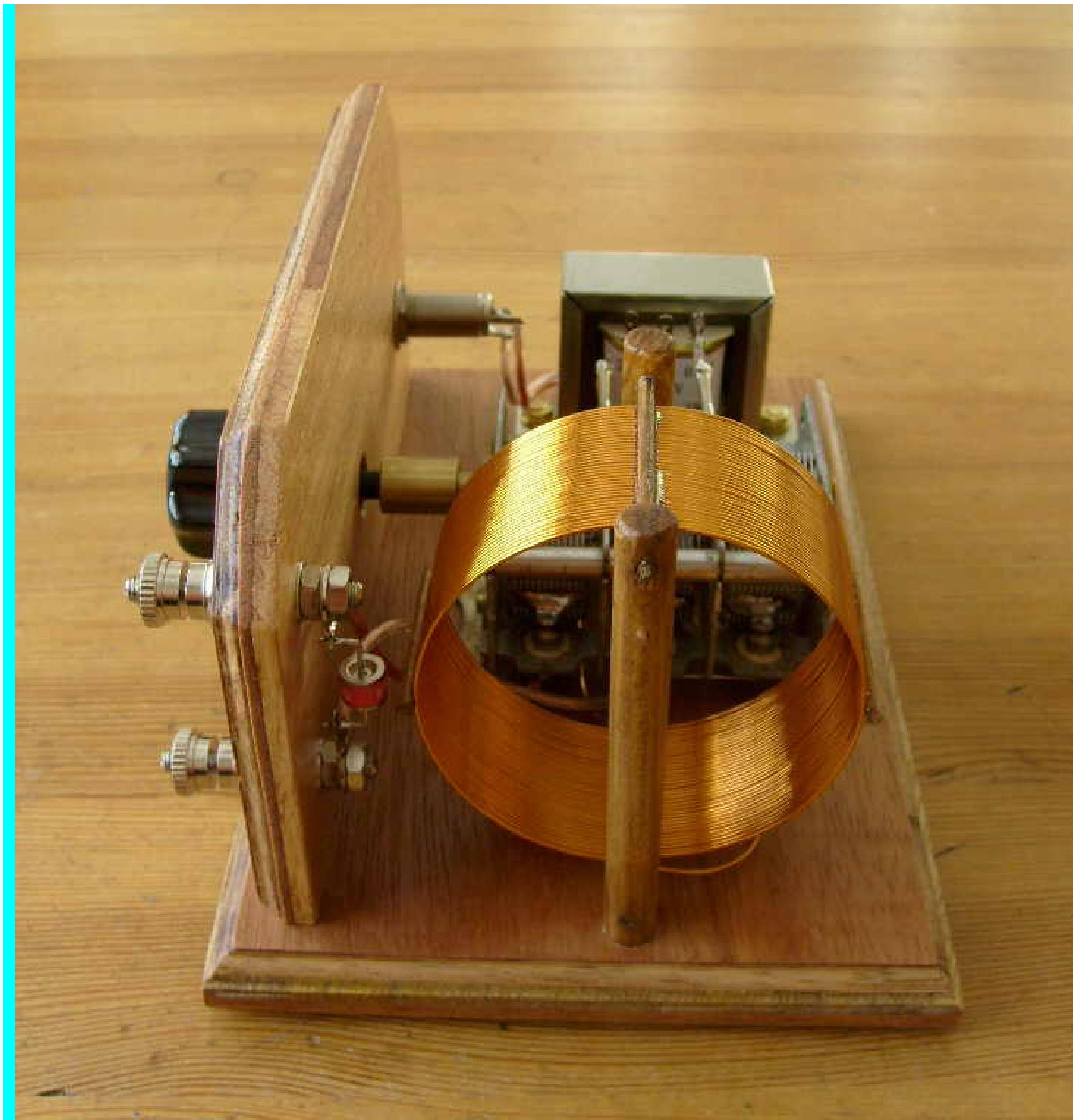

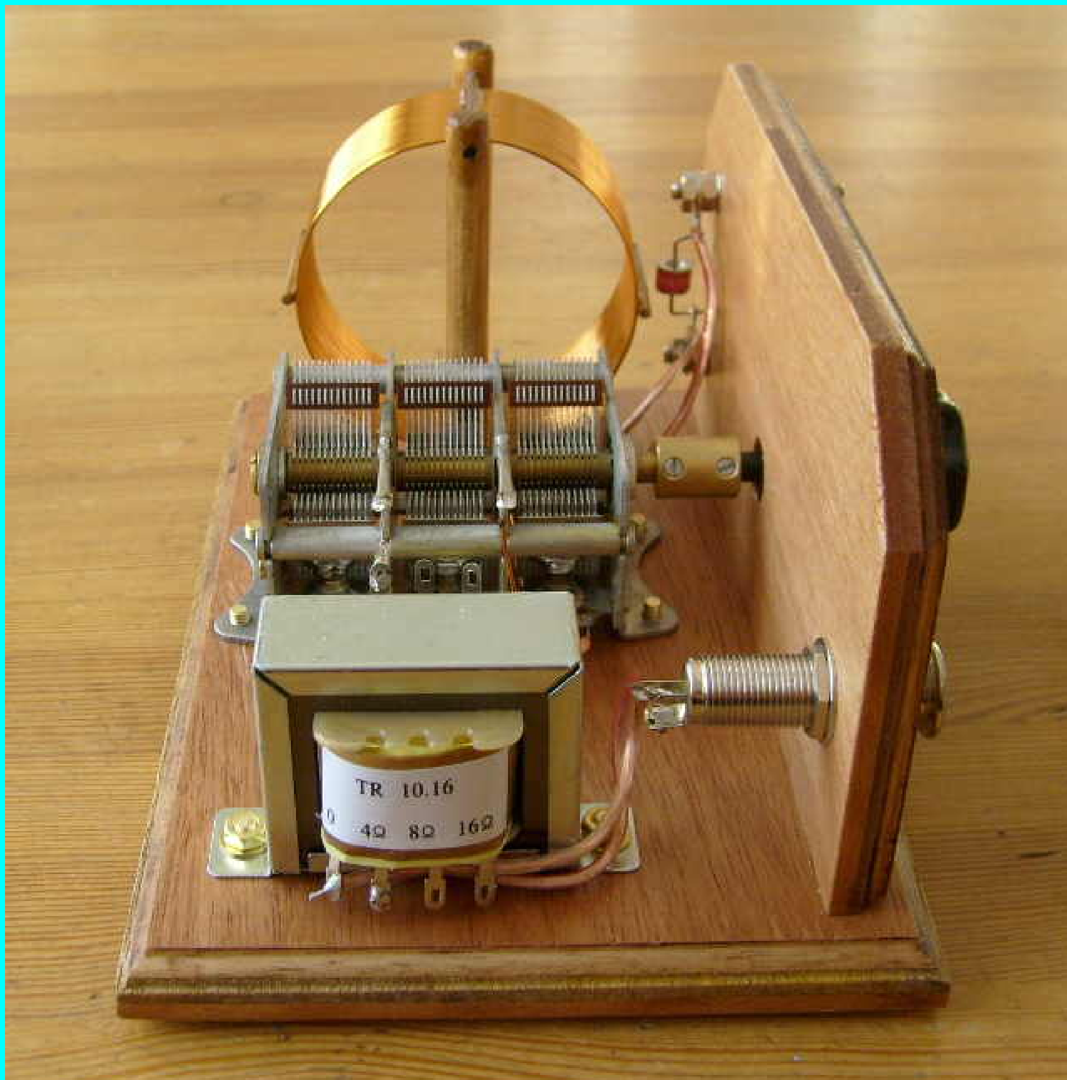

[Back to the index](http://www.crystal-radio.eu/)

How to make a batteryless (crystal set) radio

By **Sagar Sapkota** - July 21, 2012

CRYSTAL SET

The simplest radio receiver, known as a Crystal Set, consists of nothing more than a coil, tuning capacitor, diode detector, and a pair of earphones. A typical circuit diagram for a Crystal Set Radio is given below where inductor or coil L1 is tuned by variable capacitor VC1 to the transmitter frequency. Diode D1 demodulates the signal, which is fed straight to the earphones. There is no amplification.

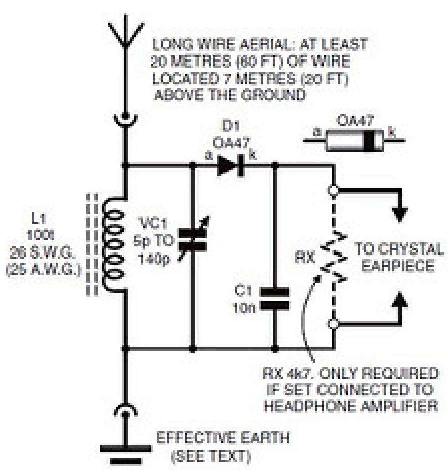

CLICK HERE FOR BIGGER PHOTO

** You can use 1N34 Germanium diode in place of OA47*

A long (at least 20 metres), high (17 metres or more) aerial and a good earth (a buried biscuit tin or a metre of copper pipe driven into damp ground) are required in order to ensure audible headphone reception. The earphones originally used with these receivers had an impedance of around 4000 ohms and were very sensitive (and heavy and uncomfortable). They are no longer available, but a crystal earpiece, which relies on the piezoelectric effect, will give acceptable results.

Low impedance "Walkman" type earphones are NOT suitable.

Component details:

Resistor- RX-4.7k, 0.25 W- only required if set is connect to audio amplifier

Capacitors- C1- 10nF disc ceramic VC1- 5p to 140p, polythene dielectric variable capacitor.

Semiconductors: D1: OA47 or 1N34- Germanium Diode

Miscellaneous: L1- Ferrite Rod, 100mm(4 inch)x9mm/10mm dia., with coil.

Crystal earpiece and jack socket to suit; plastic control knob; plastic insulated flexible cable for aerial wire, downlead and earth connection, 30 meters minimum; buried biscuit tin or 1 meter of copper pipe for earth system; 50gm reel of 26SWG enamelled copper wire, for tuning coil; card and glue for coil former; multistrand connecting wire; crocodile clips or terminals for aerial and earth lead connection; solder, etc.

READ MY EXPERIENCES- HOW EASILY I MADE A BATTERYLESS RADIO

DRAWBACKS

Quite apart from the absence of amplification, two factors seriously limit the performance of crystal receivers. Germanium diodes become increasingly reluctant to conduct as the applied voltage falls below 0.2V, and this makes the receiver insensitive to weak signals. Silicon diodes have a threshold of around 0.6V, and are, therefore, unsuitable for circuits of this kind.

** Silicon diodes like 1N4001 are not suitable*

The earphone loading imposes heavy damping on the tuned circuit, hence, reduces its ability to separate signals. With such low selectivity insensitivity can be a blessing, and crystal sets are normally only capable of receiving a single, strong transmission on the long and medium wavebands. They will sometimes receive more than one if a shortwave coil is fitted.

The aerial and diode can be connected to tappings on the tuning coil in order to reduce damping, but the improvement in selectivity is usually at the expense of audio output. When valves cost a week's wages and had to be powered by large dry batteries and lead/acid accumulators, the construction of simple receivers of this kind could be justified. With high performance transistors now costing only a few pence or cents, crystal sets are now regarded as 'nostalgic pieces". Some readers may, however, wish to build one out of curiosity, or for the novelty of having a receiver that **does not require a power supply.**

CIRCUIT DETAILS

Ferrite loop aerial L1 and polythene dielectric variable capacitor VC1 form the tuned circuit. Point contact germanium diode D1 (1N34 or OA47) demodulates the signal; capacitor C1 bypasses residual r.f. (radio frequency) to earth and also exhibits a reservoir action, enabling the a.f. (audio frequency) output to approach its peak value. The recovered audio signal is fed directly to a crystal earpiece. Signal voltages

introduced in the ferrite loop aerial by the radiated magnetic field are much too much to produce an output from the detector, and the component is used here simply as a tuning coil. The ferrite core does, however, reduce the number of turns required for the coil winding, thereby reducing its resistance and increasing its audio quality.

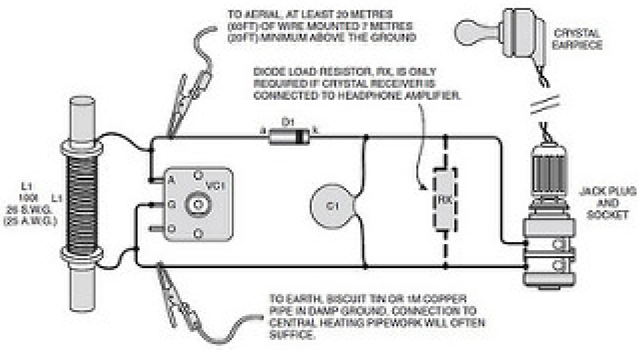

GET BIGGER PICTURE

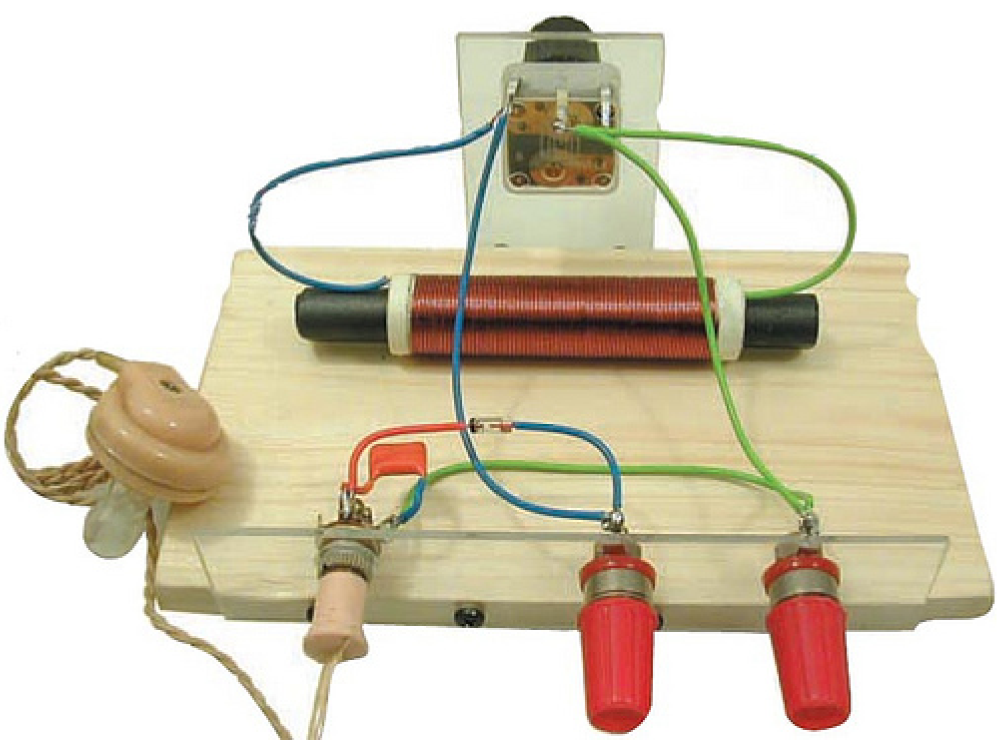

COIL DETAILS

Full construction and winding details for the ferrite tuning/ aerial coil L1 are shown in figure.

The coil is made from 26 SWG(25 AWG) enamelled copper wire, close wound on a cardboard former.

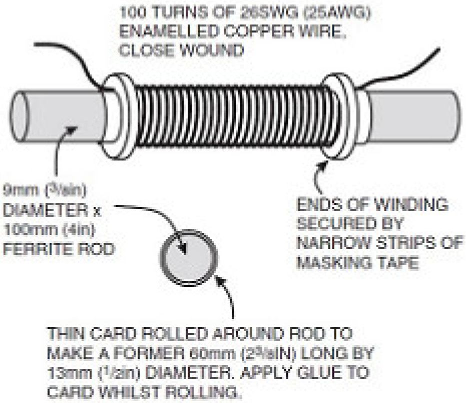

The r.f. bypass capacitor C1 can in practice, be omitted with no noticeable reduction in performance. However, if the set is to be connected to either the headphone amplifier or speaker amplifier decribed next month, the component together with diode, load resistor, RX, must be included.

AMPLIFICATION Audio frequency amplification, after the diode detector will permit the use of low impedance Walkman type earphones or even loud speaker operation. It will do nothing, however, to overcome the diode's insensitivity to weak signals. For this we must have radio frequency amplification of the signals picked up by the aerial before they reach the detector(The standard circuit for a transistor portable receiver has three stages of radio frequency amplification ahead of the diode).

For amplification, you can use a simple audio amplifier using LM386.

READ MY EXPERIENCES ON MAKING A BATTERYLESS RADIO

WATCH THESE VIDEOS:

Fully printed flexible and disposable wireless cyclic voltammetry tag

Article *in* Scientific Reports · January 2015

DOI: 10.1038/srep08105 · Source: PubMed

SCIENTIFIC REPORTS

OPEN

SUBJECT AREAS:

ENVIRONMENTAL MONITORING

ELECTRICAL AND ELECTRONIC ENGINEERING

Received
22 October 2014

Accepted
6 January 2015

Published
29 January 2015

Correspondence and requests for materials should be addressed to G.C. (gcho@sunchon.ac.kr)

Fully printed flexible and disposable wireless cyclic voltammetry tag

Younsu Jung[1], Hyejin Park[1], Jin-Ah Park[1], Jinsoo Noh[1], Yunchang Choi[1], Minhoon Jung[2], Kyunghwan Jung[2], Myungho Pyo[1], Kevin Chen[3], Ali Javey[3] & Gyoujin Cho[1]

[1]Department of Printed Electronics Engineering, Sunchon National University, Maegok, Sunchon, Jeonnam 540-742 Korea, [2]Research Institute of Printed Electronics, PARU Co. Seomyeon, Sunchon, Jeonnam 540-813 Korea, [3]Electrical Engineering and Computer Sciences, University of California, Berkeley, CA 94720.

A disposable cyclic voltammetry (CV) tag is printed on a plastic film by integrating wireless power transmitter, polarized triangle wave generator, electrochemical cell and signage through a scalable gravure printing method. By proximity of 13.56 MHz RF reader, the printed CV tag generates 320 mHz of triangular sweep wave from +500 mV to −500 mV which enable to scan a printed electrochemical cell in the CV tag. By simply dropping any specimen solution on the electrochemical cell in the CV tag, the presence of solutes in the solution can be detected and shown on the signage of the CV tag in five sec. 10 mM of N,N,N′,N′-tetramethyl-p-phenylenediamine (TMPD) was used as a standard solute to prove the working concept of fully printed disposable wireless CV tag. Within five seconds, we can wirelessly diagnose the presence of TMPD in the solution using the CV tag in the proximity of the 13.56 MHz RF reader. This fully printed and wirelessly operated flexible CV tag is the first of its kind and marks the path for the utilization of inexpensive and disposable wireless electrochemical sensor systems for initial diagnose hazardous chemicals and biological molecules to improve public hygiene and health.

Cyclic voltammetry (CV) has been used as a powerful tool for the study of electrochemical redox reactions between the electrodes and the solutions of all kind of solutes such as metals[1], organic molecules[2], proteins[3], bacteria[4], viruses[5], and DNA[6]. Because of the high sensitivity of the electron transfer redox reactions, CV could become a very promising ubiquitous electrochemical sensor protocol if the cost and size of the CV system were significantly reduced to commercially viable single-use disposable units for checking traces of hazardous materials such as lead[7], mercury[8], arsenic[9], e-*coli*[10], and pesticides[11] in water or to diagnose the level of glucose[12], cholesterol[13] and specific enzymes[14] in blood. This single-use disposable CV would dramatically reduce the cost of maintaining the public health system[15]. Therefore, inexpensive and disposable CV measurement system that can be operated wirelessly using a smartphone or RF (radio frequency) reader without complicate operation processes is in high demand for the realization of an ubiquitous sensor network system (Figure 1a). They would mainly be used as ubiquitous diagnostic and testing tools for detecting and monitoring the level of target specimens. However, there is no technology that is advanced enough yet to build a wireless, inexpensive and disposable CV system. In this paper, as a form of RF-tag, an extremely inexpensive, disposable and fully printed CV system is demonstrated for the first time by mimicking and combining basic CV concepts and wireless power transmission technologies of RF devices. To realize the fully printed CV tag, a key issue of wirelessly generating triangular waveform (±500 mV) that can scan the electrochemical cell at a low frequency (<1 Hz) to set up a redox reaction needs to be addressed through a minimum number of printed thin film transistors (TFTs). Fully printed 13.56 MHz rectenna and a ring oscillator with large trap charges in the channels of printed TFTs were respectively utilized to wirelessly generate triangular waveform by using only 10 printed TFTs.

Results

Based on two key units of the wireless power transmitter (Figure 1b-①) and the triangular wave generator (Figure 1b-②), the circuit layout of the fully printed wireless CV tag was designed by using a minimum number of printed thin film transistors (TFTs) to alleviate the issue of V_{th} shift and shown in Figure 1b as a platform of disposable CV system. The circuit of CV tag was fabricated using all scalable printing methods, a roll-to-roll gravure, a roll-to-plate gravure, a drop casting, and a screen printer (Figure S1 in Supplementary Information).

To provide a polarized DC voltage from the coupled 13.56 MHz AC signal of the reader, we modified our previously reported R2R gravure printed rectenna[16,17], as shown in the layout in Figure 2a and the resulting

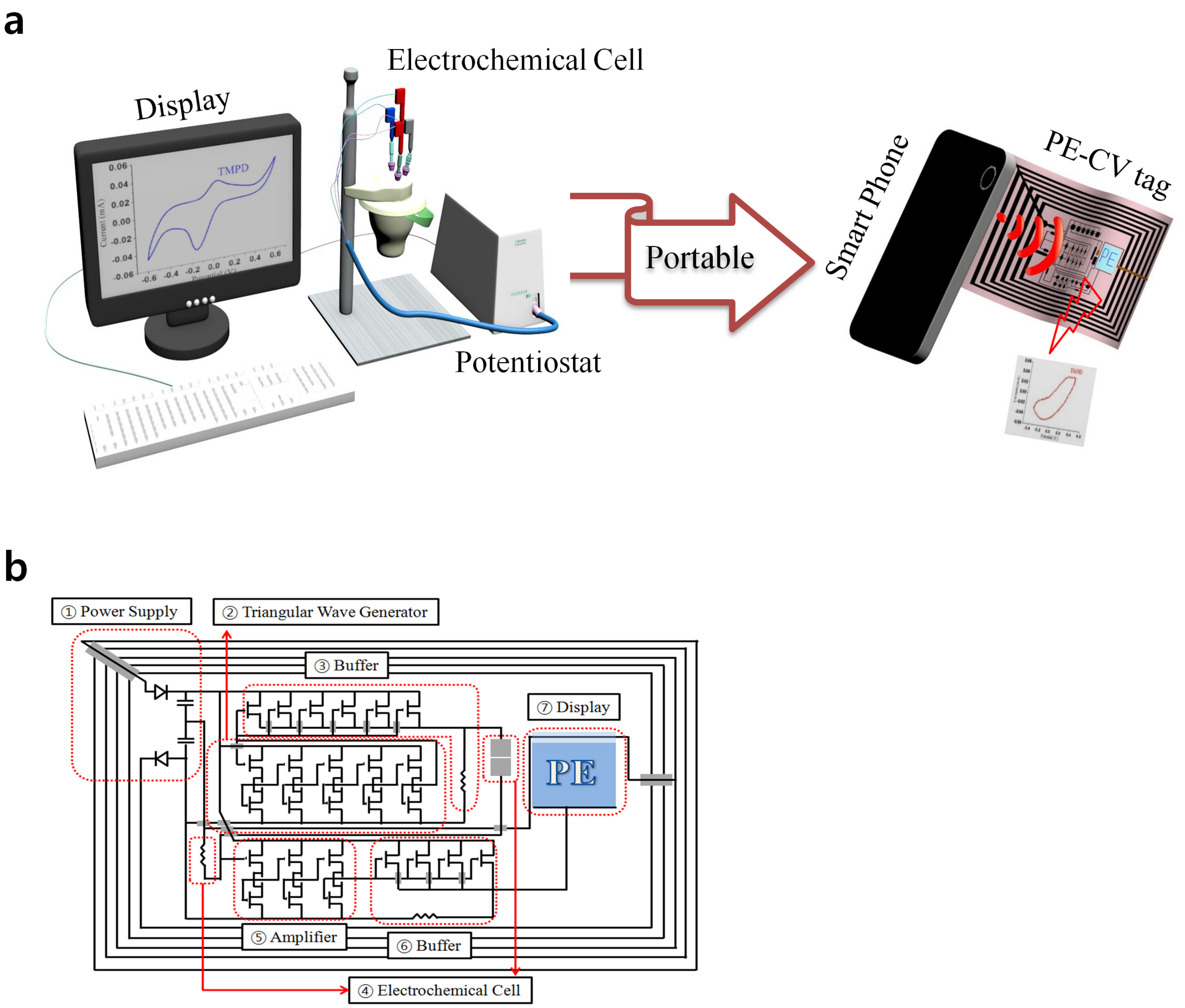

Figure 1 | (a) Informative illustration of typical CV system and disposable printed CV tag. (b) Schematic circuit diagram of the gravure printed wireless cyclic voltammetry (CV) tags. The circuit was designed to couple AC power from a 13.56 MHz reader and then convert the coupled AC to polarized DC ±10 V (① in Figure 1b). Polarized DC will operate the printed ring oscillator to generate a triangular voltage waveform (② in Figure 1b). The generated waveform will pass through the buffer to meet the impedance difference from the electrochemical cell (③ in Figure 1b). The electrochemical cell will run the redox reaction with a single drop of specimen solution (④ in Figure 1b) by the voltage triangular waveform. The output current of the electrochemical redox reaction will be amplified *via* an amplifier circuit (⑤ in Figure b) and the signal will pass through the buffer to meet the impedance difference from the printed signage (⑥ in Figure b). The signage will indicate the concentration level of specimen in the solution (⑦ in Figure b). It will indicate whether the concentration is above or below a pre-determined value.

printed diodes and capacitors are shown in Figure 2b. The printed diodes showed a rectifying ratio of 10^3, and capacitances of two printed capacitors were all about 8 nF/cm^2. The polarized DC voltages (Figure 2c) were measured by placing the printed rectenna on the RF (13.56 MHz) reader with a distance of 2 cm. We adapted a center tap transformer, consisted by divided antenna, 2 diodes and 2 capacitors, to provide the + and − DC voltage for printed triangle wave generator. Using a load of 1 MΩ, voltages of +9.4 V and −10.8 V DC were attained for the optimized printed antenna by monitoring the rectified polarized DC voltages and varying the values of the inductance of the antenna (Figure S2 in Supplementary Information). The polarized DC voltage was also decreased with decreasing load's resistance (Figure 2d).

To generate a cyclic waveform with a low frequency (<1 Hz) from the rectified polarized DC voltage, fully gravure printed *p*-type SWNT-based channel network thin film transistors (*cn*TFTs) were used to construct a five stage ring oscillator with *p*-type inverters. The *cn*TFTs can operate under less than 20 V and their mobility range (0.01 to 10 cm^2/Vs) can be controlled through the loading concentration of SWNT in the ink[18–21]. To print the five stage ring oscillator, we used the same silver and $BaTiO_3$ inks as in the printing of the rectenna for reducing a number of printing steps while SWNT ink was used for printing the channel of the *cn*TFTs. To manufacture the ring oscillator, roll-to-plate (R2P) gravure was used to print 10 *cn*TFTs with a gate width of 300 μm and channel length of 160 μm for both the drive and load *cn*TFTs (Figure S3 in Supplementary Information). The optimized cell depth of gravure plate was 37–40 μm with the cell wall thickness of 50–55 μm for the printing active layers of drive and load TFTs using low viscosity of SWNT based ink (~30 cp) (Figure S4 in Supplementary Information). By repeating the printing of active layers on load TFTs, a higher SWNT network density can be achieved to generate higher current in the

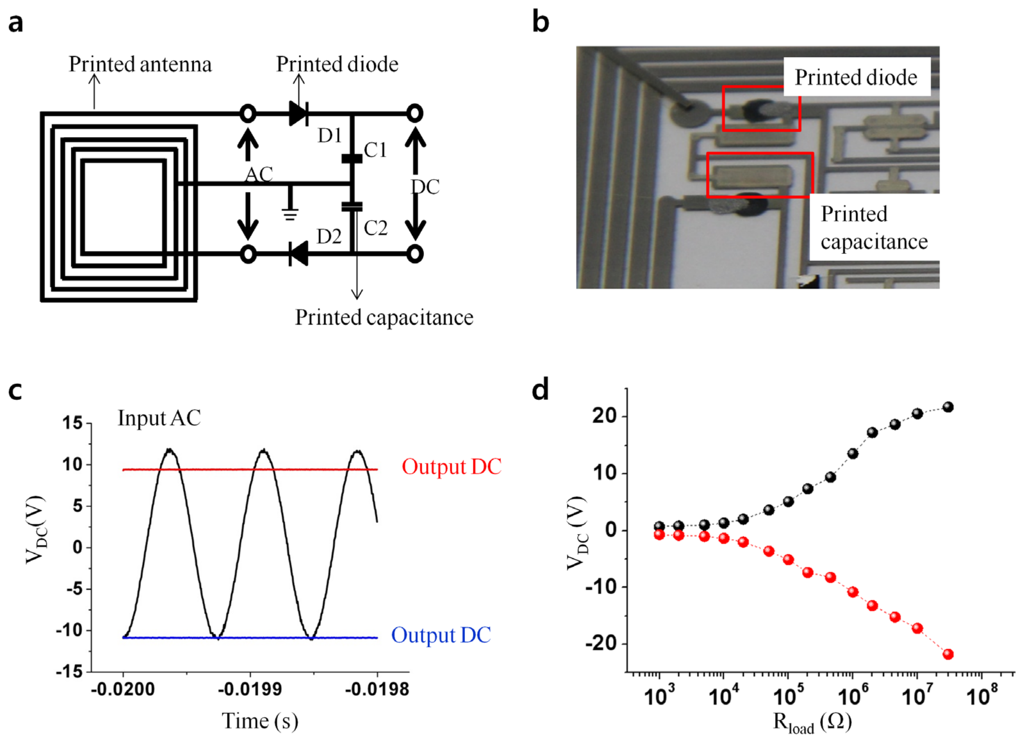

Figure 2 | (a) Circuit layout of the printed rectenna to provide polarized DC power, (b) a real image of printed diodes and capacitors, (c) input-output electrical characteristics of the rectifier at 13.56 MHz AC input and (d) output ± DC voltages under variations in load resistance.

channels while thicknesses of all printed gate, dielectric and drain-source electrodes are kept same (Figure S5 in Supplementary Information).

Their output and transfer characteristics are shown in Figure 3a and 3b respectively. Based on the attained transfer characteristics, the mobility (μ), transconductance (g_m), on-off current ratios from I_{DS}-V_{DS} and threshold voltages (V_{th}) for both five drive *cn*TFTs and five load *cn*TFTs were extracted and shown in Table S1 (Supplementary Information). The shift range of V_{th} from the fully gravure printed 10 *cn*TFTs were about ±0.4 V for the drive *cn*TFTs and ±0.6 V for load *cn*TFTs. Those shift ranges are narrow enough to run the printed ring oscillator for generating the triangular wave. Each inverter delivered a gain of 3 (Figure 3c), and the ring oscillator with five inverters generated a pseudo triangular waveform with a voltage amplitude of 7 V at 320 mHz (Figure 3d). In fact, the pseudo triangular wave can be only generated by the printed *cn*TFTs based ring oscillator because of the parasitic and trapped channel capacitances due to carbon nanotube network structures in *cn*TFTs. Although we only showed the frequency of 320 mHz at here, the frequency can be varied from 0.3 Hz to 2 Hz based on the printed network density of SWNT of printed *cn*TFTs. This is an advantage of our printed *cn*TFTs for scanning electrochemical cell in CV tag over other technologies such as amorphous silicon TFTs where only a sine wave with a designed single frequency can be generated because of no trap capacitance in the channel (Figure S6 in Supplementary Information). The frequency of the triangular waveform can be fine-tuned in the range of 0.3 Hz to 2 Hz as shown in the Figure S7 (Supplementary Information) by simply changing loading concentration of SWNTs.

When the generated triangular waveform is supplied directly into the printed electro-chemical cell (Figure S8 in Supplementary Information), wherein printed silver and carbon electrodes were used with a poly(ethylene oxide) and $LiCF_3SO_3$ gel type electrolyte, the output voltage range is reduced to zero because of improper impedance matching between the electrochemical cell (10 KΩ) and ring oscillator (1 MΩ). Therefore, a buffer unit is needed to match the impedance levels between the ring oscillator and electrochemical cell. The printed buffer unit (Figure 1b-③) with high on currents and low on-off current ratios (Figure 3e) is consists of 6 *cn*TFTs and a resistor (~7 KΩ). In the printed CV tag, three resistors were printed by screen printer using a carbon paste (DC-20, purchased from Dozen Co. Korea) for the buffer units (Figure 1b-③ and ⑥) and the electrochemical cell (Figure 1b-④). Their electrical parameters are listed in Table S1 (Supplementary Information). The 6 *cn*TFTs of buffer unit were printed using R2P gravure with high SWNT concentration in the semiconducting ink. Each *cn*TFTs exhibited on-currents in the range of 400 ~ 500 μA with a very low on-off ratio due to the enhanced metallic percolation in the dense SWNT networks. The buffer units with low on-off ratio were employed to reduce the input voltage to ±500 mV (Figure 3f) which is the appropriate scanning range of the electrochemical cell. The printed electrochemical cell with two electrodes was proven to be well operated under commercial CV (Figure S9 in Supplementary Information). The resulting current after scanning printed electrochemical cell in the CV tag can be converted to voltage by connecting the printed resistor (Figure 1b-④: ~5 × 10^3 ohm) which provides the output voltage for electrochromic indicator and re-plotted into the cyclic voltammogram.

Because these output voltage (±70 mV) and current (~40 μA) were low after scanning the electrochemical cell, they need to be amplified to turn on the electrochromic indicator for showing predetermined concentration (10 mM) level of N,N,N′,N′-tetramethyl-p-phenylenediamine (TMPD, purchased from Aldrich) as a standard reference in this work (Figure 3g). After running the redox reaction of TMPD (Figure 3h) in the printed cell, the output voltage and current needed to be amplified to reach 1.5 V and 500 μA, respectively, to provide sufficient power to display the letters "PE" as an indicator of the presence of TMPD in the specimen. To construct the amplifier, *cn*TFTs based three inverters were printed with a gain of three to five (Figure S10 in Supplementary Information) to amplify the output signal as shown in Figure 3i. The electrical characteristics of the 6 *cn*TFTs in the inverters with extracted mobility, transcon-

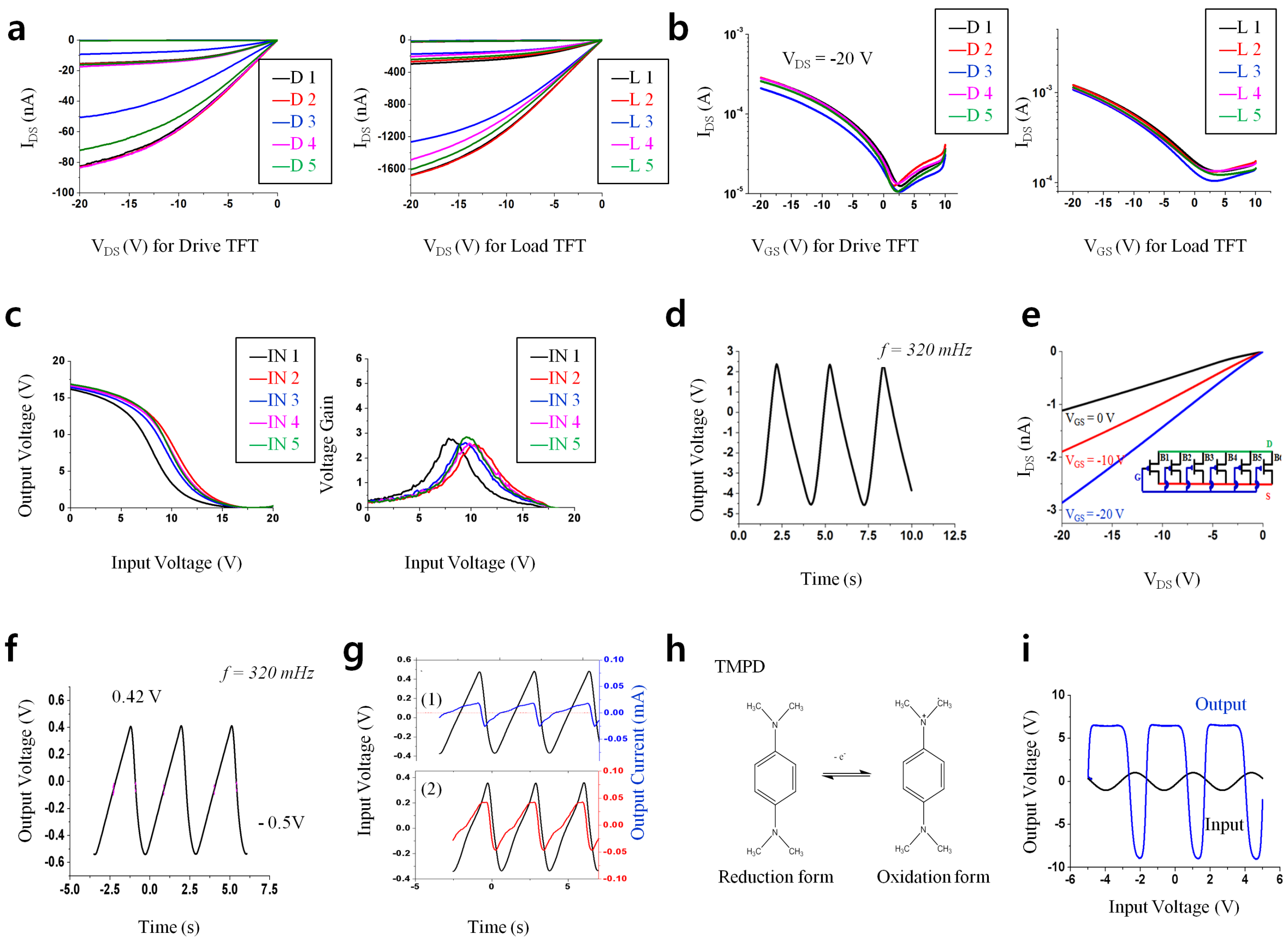

Figure 3 | (a and b) Output and transfer characteristics of the printed *cn*TFTs for 5 drive and 5 load TFTs respectively in the printed ring oscillator. (c) Electrical characteristics of inverters and (d) output characteristic of the ring oscillator. (e) Total output characteristics of the printed buffer unit consisting of 6 *cn*TFTs and a resistor (measured based on contacting gate and drain-source electrodes as shown in the inset circuit). (f) Modified triangular wave following the buffer unit. (g) Generated signals before scanning (black) and after scanning the electrochemical cells without (1, blue) and with TMPD (2, red) in a drop of solution. (h) TMPD structure for oxidation and reduction reaction. (i) The input and amplified output signals after passing through three amplifying inverters.

ductance, on-off current ratios and threshold voltage are shown in Table S2 (Supplementary Information). As the impedance was matched between the ring oscillator and the electrochemical cell using the buffer unit, another buffer unit (Figure 1b-⑥) is also needed between the electrochromic signage (20 KΩ) and the amplifier (1 MΩ) for impedance matching. The electrical parameters of the buffer are listed in Table S2 (Supplementary Information).

The amplified output signal was used to run the reduction and oxidation of the patterned conducting polymer in the electrochromic signage, and thus the blinking signage will be used to indicate the presence of chemicals in the specimens. The signage was fully printed and attached on printed CV tag. A clear concept of the printing sequence for the electrochromic signage was given in Figure S11 in Supplementary Information.

Discussion

The fully printed flexible CV tag was completed by assembling the printed circuits including ring oscillator, buffer, electrochemical cell, amplifier, and signage onto the previously R2R gravure printed rectenna. The resultant CV tag is shown in Figure 4a. The working concept of the wireless and flexible CV tag is demonstrated in the following sequences (watch the video file by clicking Figure S12 in Supplementary Information). After dropping 500 μl of TMPD solution (10 mM) on the printed electrochemical cell, the CV tag was placed on the custom made RF (13.56 MHz) reader (Figure S13 in Supplementary Information). The antenna was subsequently coupled to 13.56 MHz AC. The coupled AC was rectified into polarized DC (> ± 10 V) through two diodes and two capacitors which caused the ring oscillator to generate a pseudo triangular waveform with output voltage of 7 V at 320 mHz. This was then passed through the buffer unit to scan the electrochemical cell. The output signal after scanning the electrochemical cell was amplified to turn on the signage according to the concentration level of TMPD in the solution. In this work, whenever the concentration of TMPD was higher than 10 mM, the signage "PE" blinked (Figure 4b) while it did not show anything (Figure 4c) when it was lower than 10 mM. Furthermore, clear cyclic voltammograms for scanning the electrochemical cell with and without 10 mM of TMPD were obtained by re-plotting the output triangular voltage waveform (Figure 4d). The attained half potential ($E_{1/2}$ ~ 0.05 V, oxidation potential is 0.22 V and reduction potential is −0.17 V) of TMPD from the CV tag was nearly identical to the value obtained from a commercial CV instrument, SP-240, Biologic, which uses the same frequency for the triangular voltage waveform and printed electrochemical cell (Figure 4e). However, when the generated triangle wave frequency is higher than 0.6 Hz in the CV tag, the clear redox peaks cannot be

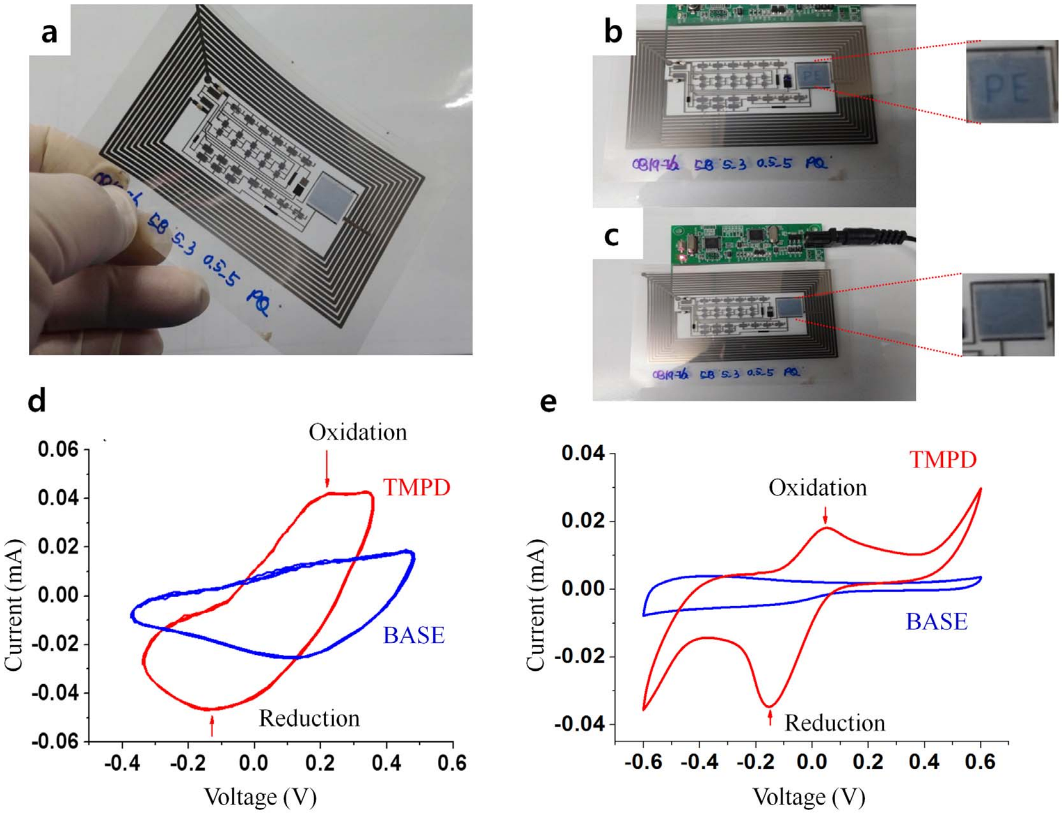

Figure 4 | (a) Optical image of fully printed wireless cyclic voltammetry tag. (b) Operation images of CV tag with and (c) without TMPD in the solution on 13.56 MHz reader. (d) Converted cyclic voltammogram from the printed wireless CV tag *vs* (e) a commercial CV instrument (please refer the interconnected video file for the demonstration of wireless CV tag operation in Figure S12 in Supplementary Information).

observed as shown in Figure S14 (Supplementary Information). Furthermore, as a typical example of testing a specimen in aqueous solution, 10 mM of $K_3(FeCN)_6$ aqueous solution was checked using the CV tag, and results of converted cyclic voltammogram was shown in Figure S15 (Supplementary Information). Those results support that the CV tag can examine specimens not only in organic solution, but also in aqueous one.

Up to present, there has been no commercial success in fully printed TFT-based electronic devices due to some kind of difficulties in integrating a number of printed TFTs through a scalable printing method. As increasing a number of integrated TFTs, the range of threshold voltage shits of TFTs needs to be controlled as narrow as possible to properly operate designed function of printed devices. However, the scalable printing method is not fully understood to integrate a number of TFTs on plastic foils while keeping the constant range of threshold voltage shifts because of difficulty in controlling a constant charge transport through the printed channels. Therefore, the printed TFT-based devices should be constructed by using a minimum number of printed TFTs while a function of printed device needs to be competitive over Si based one. Since the fully printed CV tag required the integration of only 26 *cn*TFTs, the acceptable range of threshold voltage shits of *cn*TFTs is controllable and achievable by using a scalable printing method such as a roll-to-roll gravure. Furthermore, the unique function of printed CV tags cannot be simply reproduced using a Si technology with a comparable cost to the R2R printing process. Therefore, the fully printed CV tag will be the first leading model to show a way of how printed TFT-based electronic devices should go for the successful launching in the IT markets.

In the core of the printed CV tag, fully gravure-printed *cn*TFTs were employed for constructing a circuit consisting of a ring oscillator to generate triangular waveforms, buffer units for an impedance matching, and an amplifier for enhancing output signal to turn on the signage. Those simple units can be combined with a variety of printable sensors and RF devices to create novel devices with an extremely low cost. In other words, the printed rectenna, ring oscillator, buffer and amplifier units in the printed CV tag will be key elements for the construction of variety of printed RF-sensors, this CV tag will be used as a platform for the further construction of a variety of RF based electrochemical sensors.

In conclusion, we have presented a fully printed flexible CV tag with the size of 9.5×5.5 cm^2 that can operate wirelessly using a 13.56 MHz RF reader. However, for the practical purpose, the size of the CV tag can be reduced up to the half (4×2 cm^2) of the current one by optimizing spaces between *cn*TFTs in the circuit of the CV tag and reducing the operation power to less than DC 5 V as the current size of 13.56 MHz antenna is designed to provide maximum coupled AC power using a sufficient length of printed antenna pattern (higher inductance). Furthermore, although we utilized R2P gravure, screen printer and drop casting method for the convenience of fabricating the CV tag in the Lab, the whole fabricating process can be repeated by R2R gravure because the rectenna, ring oscillator, buffers, electrochemical cell, amplifier and signage in the CV tag were all designed to compromise the limit ($\pm$20 μm) of a registration accuracy of a current R2R gravure system. Therefore, this technology could be used as a platform for disposable wireless electrochemical sensors to a variety of specimens in aqueous and organic solutions to monitor or diagnose pathogens and hazardous materials by modifying the electrodes of the electrochemical cells.

Methods

Roll-to-roll (R2R) gravure printed antenna, bottom electrodes, gate electrodes and wires. Two color units of R2R gravure system (Taejin Co. Korea: Figure S1 in the Supplementary Information) was employed to print antenna, bottom electrodes and wires on a roll of poly(ethylene terephthalate) (PET) film (width of 200 mm and

thickness of 100 μm, purchased from SKC, Korea) with silver nanoparticle based conducting ink (PG-007 BB type, Paru Co. Korea) and the web transfer speed of 8 m/min under roll pressure of 0.5 MPa and web tension of 60 N. The silver ink was further formulated to meet the viscosity of 500 cp and surface tension of 47 mN/m using respectively ethylene glycol (Aldrich) and Dipropylene glycol methyl ether (Aldrich). The curing time of printed silver layer was 10 sec by passing through a heating chamber of 150°C, installed in R2R gravure system. The resulting printed silver patterns on PET roll showed the thickness of 450 (±50) nm without any defects and were shown in Figure S16a (Supplementary Information).

Roll-to-plate (R2P) gravure printed ring oscillator, buffer, and amplifier. Full R2P gravure system (Figure S1 in the Supplementary Information) was employed to print single walled carbon nanotube network based thin film transistors (*cn*TFTs), used as a building block to construct all the integrated circuit of printed cyclic voltammetry (CV) tag (Figure 1). 26 *cn*TFTs for the integration of circuit in printed CV tag were printed on the previously R2R gravure printed film (printed antenna, bottom electrodes and wires with thickness of 450 nm; Figure S16b in Supplementary Information) following printing sequences. First, $BaTiO_3$ nanoparticle based dielectric ink (PD-100, Paru Co., Korea) was further formulated to meet viscosity (75 cP) and surface tension (31.8 mN/m) using the ethyl 2-cynoacrylate (Aldrich). As shown in R2P gravure printing scheme (Figure S17 in Supplementary Information), the homogeneous and defect free dielectric layers were first R2P gravure printed with a printing speed of 200 mm/s and roll pressure 7.5 kg_f on previously printed gate electrodes and bottom electrodes (for capacitors) with a thickness of 2.3 (±0.1) μm and width of 940 (±2) μm (Figure S5 in Supplementary Information). The printed dielectric layers were cured for 1 min 20 sec at 150°C. Second, single walled carbon nanotube (SWNT) based semiconducting ink (PR-040, Paru Co., Korea) was diluted by diethylene glycol monobutyl ether (Daejung Co., Korea) to 1 : 1 volume ratio for printing active layers using R2P gravure on the printed dielectric layers with a printing speed of 350 mm/s and a roll pressure of 4 kg_f. The viscosity and surface tension of diluted SWNT ink were respectively 30 cP and 29 mN/m. The resulting SWNT printed films were dried 1 min at 150°C. For using *cn*TFTs in the buffer unit, we used the dilution volume ratio of 5 : 1 between SWNT ink (PR-040, Paru Co., Korea) and diethylene glycol monobutyl ether for printing only on the TFTs in the buffer unit to increase SWNT network density for providing the high current (Figure S5 in Supplementary Information). Finally, drain-source electrodes were R2P gravure printed using silver nanoparticle based ink (PG-007 AA type, Paru Co., Korea) on SWNT printed film with a viscosity of 800 cP and a surface tension of 42 mN/m. The R2P gravure printing was carried out under a printing speed of 200 mm/s and a role pressure of 5 kg_f.

Diode fabrication. Although Shottky diodes were able to print using R2R gravure based on our previous reported process[16,17], the drop casting method was used for the convenience in this work. First, dropping ZnO based hybrid semiconducting ink (PD-070, Paru Co., Korea) on printed silver electrode and then, Al ink (PA-009, Paru Co., Korea) was dropped on the top of ZnO ink. The resulting diodes were further cured for 5 min at 120°C.

Measurements. Formulated and diluted inks were characterized using DCAT21 (Dataphysics Co., Germany) and SV-10 Vibro viscometer (AND Co., Japan) for respectively measure surface tension and viscosity. All measurements in this work were carried out under ambient condition if there are no other comments. Resistance of printed antenna, bottom electrodes, gate electrodes and wires were measured using two probe methods with HP3457A multimeter. Both surface morphology and thickness of printed layers was characterized using surface profiler (NV-2200, Nanosystem, Korea). LCR meter (E4980A, Agilent, USA), semiconductor parameter analyzer (4155C, Agilent, USA) and digital phosphor oscilloscope (DPO 4054, Tektronix, USA) were respectively used to characterize printed *cn*TFT based circuits.

1. Sanderson, M. D., Kamplain, J. K. & Bielawski, C. W. Quinone-annulated N-heterocyclic carbene-transition-metal complexes: Observation of π-back bonding using FT-IR spectroscopy and cyclic voltammetry. *J. Am. Chem. Soc* **128**, 16514–16515 (2006).
2. Lai, R. Y., Fabrizio, E. F., Lu, L., Jenekhe, S. A. & Bard, A. J. Synthesis, cyclic voltammetrics studies, and electrogenerated chemiluminescence of a new donor-acceptor molecule: 3,7-[Bis[4-phenyl-2-quinolyl]]-10-methylphenothiazine. *J. Am. Chem. Soc* **123**, 9112–9118 (2001).
3. Armstrong, F. A., Hill, H. A. & Walton, N. J. Direct electrochemistry of redox proteins. *Acc. Chem. Res* **21**, 407–413 (1998).
4. Norouzi, P., Ganjali, M. R., Daneshgar, P., Alizadeh, T. & Mohammadi, A. Development of fast Fourier transformation continuous cyclic voltammetry as a highly sensitive detection system for ultra-trace monitoring of penicillin V. *Anal. Biochem* **360**. 175–184 (2007).
5. Koyama, J. *et al.* Correlation of redox potentials and inhibitory effects on Epstein-Barr virus activation of 2-azaanthraquinones. *Cancer Letters* **212**, 1–6 (2004).
6. Teijeiro, C., Perez, P., Marin, D. & Paleček, E. Cyclic voltammetry of mitomycin C and DNA. *Bioelectrochemistry and Bioenergetics* **38**, 77–83 (1995).
7. Zerihun, T. & Gründler, P. Electrically heated cylindrical microelectrodes. Determination of lead on Pt by cyclic voltammetry and cathodic stripping analysis. *J. Electroanal Chem* **415**, 85–88 (1996).
8. Bond, A. M. & Scholz, F. Electrochemical, Thermodynamic, and mechanistic data derived from voltammetric studies on insoluble metallocenes, mercury halide and sulfide compounds, mixed silver halide crystals, and other metal complexes following their mechanical transfer to a graphite electrode. *Langmuir* **7**, 3197–3204 (1991).
9. Brusciotti, F. & Duby, P. Cyclic voltammetry study of arsenic in acidic solutions. *Electrochim Acta* **52**, 6644–6649 (2007).
10. Ruan, C., Yang, L. & Li, Y. Immunobiosensor chips for detection of escherichia coli O157:H7 using electrochemical impedance spectroscopy. *Anal. Chem* **74**, 4814–4820 (2002).
11. Liu, G. & Lin, Y. Electrochmical sensor for orgnohposphate pesticides and nerve agents using zirconia nanoparticles as selective sorbents. *Anal. Chem* **77**, 5894–5901 (2005).
12. Ascaso, J. F. *et al.* Diagnosing insulin resistance by simple quantitative methods in subjects with normal glucose metabolism. *Diabetes Care* **26**, 12, 3320–3325 (2003)
13. Karl, T. *et al.* Human breath isoprene and its relation to blood cholesterol levels: new measurements and modeling. *J. Appl. Physiol* **91**, 762–770 (2001).
14. Armstrong, F. A. Recent developments in dynamic electrochemical studies of adsorbed enzymes and their active sites. *Chem. Biol* **9**, 110–117 (2005).
15. Mollah, M. Y., Schennach, R., Parga, J. R. & Cocke, D. L. Electrocoagulation (EC)-science and applications. *J. Hazard. Mater* **B84**, 29–41 (2001).
16. Park, H. *et al.* Fully roll-to-roll gravure printed rectenna on plastic foils for wireless power transmission at 13.56 MHz. *Nanotech* **23**, 344006–344012 (2012).
17. Kang, H. *et al.* Fully Roll-to-Roll Gravure Printable Wireless (13.56 MHz) Sensor-Signage Tags for Smart Packaging. *Sci. Rep*. **4**, 5387; DOI: 10.1038/srep05387 (2014).
18. Jung, M. *et al.* All-printed and roll-to-roll-printable 13.56 MHz-operated 1-bit RF tag on plastic foils. *IEEE Trans Electron Devices* **57**, 3, 571–580 (2010).
19. Noh, J. *et al.* Integrable single walled carbon nanotube (SWNT) network based thin film transistors using roll-to-roll gravure and inkjet. *Org. Electron* **12**, 2185–5191 (2011).
20. Noh, J. *et al.* Modeling of printed single walled carbon nanotube thin film transistors for attaining optimized clock signals. *J. Appl. Phys* **108**, 10, 102811–102817 (2010).
21. Noh, J. *et al.* Fully Gravure-Printed Flexible Full Adder Using SWNT-Based TFTs. *IEEE. Eletron. Dev. Lett.* **33**, 11, 1574–1576 (2012).

Acknowledgments

The authors would like to thank BK Plus program, Basic Science Research program (NRF-2014R1A1030419), and RIC in Sunchon National University for their financial support. G. C. thanks to Paru Co. for providing all electronic inks in this work.

Author contributions

Y.J., A.J. and G.C. designed the experiments. Y.J., H.P., J.P., Y.C. and M.J. carried out the experiments. J.N., K.J. and K.C. performed device simulations. Y.J. and K.C. performed mobility calculations. Y.J. and M.P. performed electrochemistry and analyzed electrochemical data. Y.J., H.P., M.P., A.J. and G.C. contributed to analyzing the data. M.J., M.P., A.J. and G.C. wrote the paper while all authors provided feedback.

Additional information

Supplementary information accompanies this paper at http://www.nature.com/scientificreports

Competing financial interests: Prof. Cho was a consultant of PARU Co. Korea and received compensation from PARU Co. Both Dr. M. Jung and Mr. K Jung has been employee of PARU Co. Korea. Dr. Y. Jung, Miss H. Park, Ms. J. Park, Dr. J. Noh, Mr. Y. Choi, Prof. Pyo, Mr. K. Chen and Prof. Javey declare no competing financial interests.

How to cite this article: Jung, Y. *et al.* Fully printed flexible and disposable wireless cyclic voltammetry tag. *Sci. Rep.* **5**, 8105; DOI:10.1038/srep08105 (2015).

A microwave metamaterial with integrated power harvesting functionality

Allen M. Hawkes, Alexander R. Katko, and Steven A. Cummer

Citation: Applied Physics Letters **103**, 163901 (2013); doi: 10.1063/1.4824473
View online: http://dx.doi.org/10.1063/1.4824473
View Table of Contents: http://scitation.aip.org/content/aip/journal/apl/103/16?ver=pdfcov
Published by the AIP Publishing

APPLIED PHYSICS LETTERS **103**, 163901 (2013)

A microwave metamaterial with integrated power harvesting functionality

Allen M. Hawkes,[a)] Alexander R. Katko, and Steven A. Cummer
Department of Electrical and Computer Engineering, Duke University, 101 Science Drive, Durham, North Carolina 27708-9976, USA

(Received 30 May 2013; accepted 22 September 2013; published online 14 October 2013)

We present the design and experimental implementation of a power harvesting metamaterial. A maximum of 36.8% of the incident power from a 900 MHz signal is experimentally rectified by an array of metamaterial unit cells. We demonstrate that the maximum harvested power occurs for a resistive load close to 70 Ω in both simulation and experiment. The power harvesting metamaterial is an example of a functional metamaterial that may be suitable for a wide variety of applications that require power delivery to any active components integrated into the metamaterial. © *2013 AIP Publishing LLC*. [http://dx.doi.org/10.1063/1.4824473]

Metamaterials are composed of sub-wavelength particles that exhibit bulk properties that are different from their individual components. Electromagnetic metamaterials are engineered materials that can achieve parameters not possible within naturally occurring materials, such as a negative index of refraction[1] or a zero index of refraction.[2] Exotic properties like these allow for a variety of interesting applications including a superlens device[3] and an invisibility cloak.[4] Integrating active and nonlinear functionality into metamaterials has been demonstrated in the form of dynamic resonant frequency tuning,[5,6] phase conjugation,[7] and wave mixing.[8,9] More specific functional behavior has also been demonstrated in metamaterials, including radio frequency (RF) limiting[10] and harmonic generation.[11]

Metamaterials are also well-suited for other functional behaviors, including electromagnetic power harvesting, the focus of this work. Power harvesting devices convert one type of energy to another, typically converting to a direct current (DC) signal. Many types of energy can be harvested, from acoustic (using a piezoelectric harvester)[12] to electromagnetic (using a rectenna).[13] Power harvesting devices require a method to couple to the energy that will be harvested as well as a device to convert the energy from one form to another. By their very nature, metamaterials are designed to couple to various types of energy, e.g., from acoustic[14] to optical,[15] and thus provide a natural platform for power harvesting. Electromagnetic metamaterials provide flexibility in design due to their electrically small, low-profile nature.[16] Since metamaterials are typically designed as infinite arrays, the resonant frequency and input impedance include coupling effects. Metamaterials can be adapted to various applications, such as flexible sheets to cover surfaces.[17] Moreover, many metamaterials that have been presented in the literature require some form of external signal. This could be a DC bias voltage[18] or a large external pump signal.[7] In general, metamaterials could be modified to harvest such an external signal that is already present for other purposes. With these design advantages, power harvesting metamaterials offer design flexibility for a large number of applications that general antenna-based microwave power harvesting devices may lack.

[a)]allen.hawkes@duke.edu

A recent simulation-based study[19] investigated the conversion efficiency between incident RF power and induced power in a split-ring resonator (SRR). Our work is focused on the experimental measurement of RF to DC efficiency based on the conventional effective area of the SRR. We demonstrate that metamaterials can also include embedded devices to convert the incident RF energy to a DC voltage, providing a platform for power harvesting that utilizes the advantages of metamaterial design.

An SRR is a canonical example of a resonant metamaterial particle and is used as the basis for the unit cells of the metamaterial power harvester designed here. By tuning the SRR parameters, we design an SRR (Fig. 1) to resonate at 900 MHz using an S-parameter simulation within Computer Simulation Technology (CST) Microwave Studio software. Using CST Microwave Studio, we can also simulate the effects of embedding devices within the SRR by retrieving its S-parameters using a lumped port. The retrieved S-parameters are loaded into Agilent Advanced Design System (ADS), allowing us to simulate both fullwave 3D effects and circuit-level nonlinear effects.

An SRR couples strongly to an incident magnetic field and can be loaded with a wide variety of circuit elements. In this work, we embed a rectifying circuit within an SRR to convert the incident RF power to DC power. A number of rectifying circuits could be chosen depending on the particular application for the power harvesting metamaterial. We choose to use a Greinacher[20] circuit because the output voltage is double the input voltage maximum, which allows for

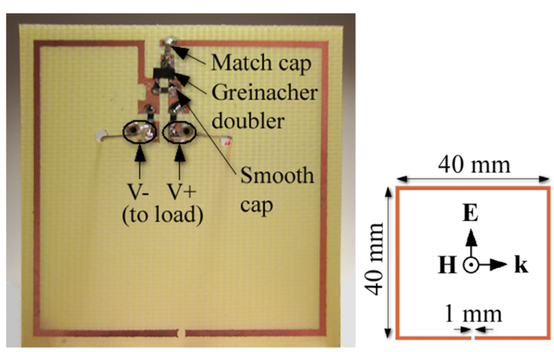

FIG. 1. (Left) Power harvesting SRR. (Right) Plain SRR with dimensions shown, 1 mm traces. Incident wave polarization is also shown.

easier power transmission and measurement. A Greinacher circuit has a lower effective capacitance in comparison to other rectification circuits (such as a bridge rectifier), allowing faster switching and thus a higher frequency of operation. A Greinacher circuit also has a low threshold voltage, allowing operation at lower incident power levels. A Greinacher voltage doubler can be placed across a gap (Fig. 1) in the top side of the copper trace to rectify the induced current present in the SRR. Schottky diodes are used for the voltage doubler due to their typically low open junction capacitance and fast switching capabilities, which allow for rectification of a high-frequency RF signal, as well as their typically low threshold voltage. A resistive load placed across the output of the voltage doubler is a simple way to determine DC power out using $P = V^2/R$. This DC power is maximized through ADS for matching capacitor and resistor values. The parameters of our selected Schottky diode (HSMS 2862) and the simulated S-parameters of the above SRR in a model of our actual parallel-plate waveguide are input into ADS for the simulation, shown in a schematic in Fig. 2.

The simulated components lead to a maximum efficiency of 61% for an input power of 24.25 dBM, the maximum available experimental power (at an incident power density of approximately 1.6 mW/cm^2). One important figure of merit for a power harvester is its RF-to-DC power conversion efficiency:

$$\eta = \frac{P_{DC}}{P_{RF}}.$$

We determine P_{RF} by measuring the total incident power in our measurement apparatus. For a large metamaterial sample, we assume that the total incident power to the measurement apparatus is incident on the metamaterial. For a single unit cell, it is necessary to use the effective area of the unit cell to determine the incident P_{RF}. The maximum effective area may be calculated by[21]

$$A_{e,max} = \frac{\lambda^2}{4\pi} D_0,$$

where $D_0 = 1.5$ since the SRR is effectively a small loop illuminated by a transverse electromagnetic (TEM) wave. For an SRR resonant at 900 MHz, the effective area is thus $A_{e,max} = 5.3A_{physical}$. The full waveguide area is

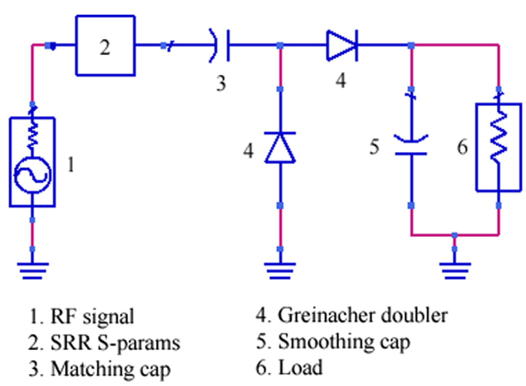

FIG. 2. ADS simulation schematic of SRR power harvester. CST Microwave Studio was used to determine the SRR S-parameters.

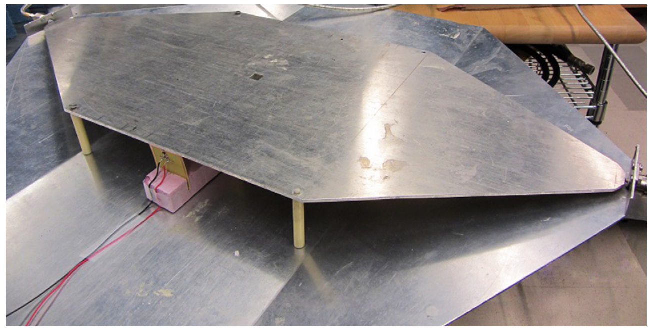

FIG. 3. Placement of SRR within open waveguide.

approximately $6.8A_{physical}$ where $A_{physical}$ is the physical area of a single SRR unit cell. As $A_{e,max}$ is 78% of the open wave guide area, 78% of the incident power density is used as input power for simulation of the single cell.

The designed voltage doubler and resistive load are added to an SRR as shown in Fig. 1, resulting in the power harvesting metamaterial unit cell. To observe power harvesting capabilities, the cell is placed in an open, TEM waveguide (Fig. 3) where input power is produced by a signal generator and amplifier, and output power is measured with an oscilloscope via leads placed across the resistive load (Fig. 4). The DC power harvested is determined by $P = V^2/R$ as previously mentioned, and input power is measured with a spectrum analyzer connected to the signal generator and amplifier via the open waveguide. By increasing the incident power from 13 to 24 dBm and measuring the DC output from the SRR, the normalized harvested power, $P_{DC}/P_{RF,incident}$, as a function of incident power $P_{RF,incident}$ and resulting efficiency are determined at each point. The maximum efficiency of the single cell is 14.2%, setting $P_{RF,incident}$ as 78% of the total input power from effective area calculations.

Multiple power harvesting SRR cells are then tested simultaneously to create the power harvesting metamaterial, which is accomplished through a 5×1 array shown in Fig. 5. Through a parallel connection of the leads from each SRR's resistive load, the total power harvested by the metamaterial is found in the same way as the single cell. The maximum efficiency for the 5×1 array is 36.8%, where P_{in} is the entire input power because the array spans the entire length. Measured efficiencies of both the single and the array of power harvesting SRRs are shown in Fig. 6. Also shown in Fig. 6 is the open circuit voltage, V_{OC}, a load-independent measure of the available voltage harvested by the array of SRRs.

The power harvesting metamaterial array is more efficient than the single unit cell. This is partially due to the

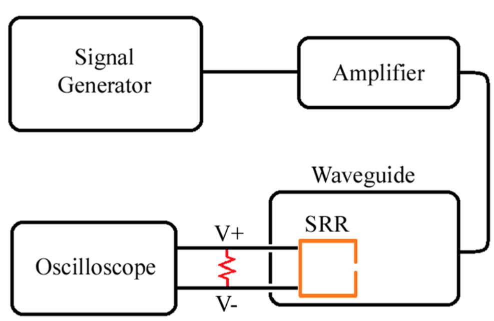

FIG. 4. Experimental test setup schematic.

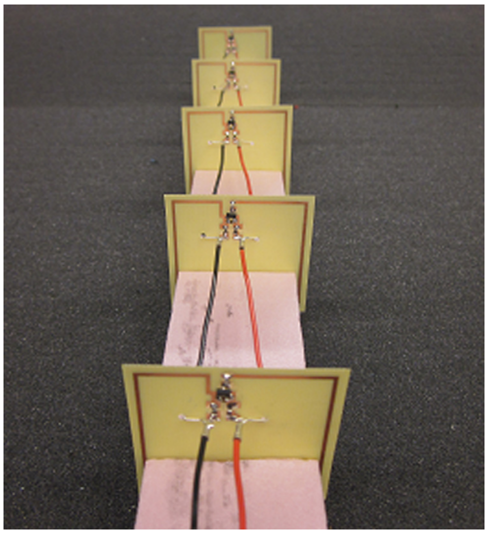

FIG. 5. 5 × 1 array of power-harvesting SRRs.

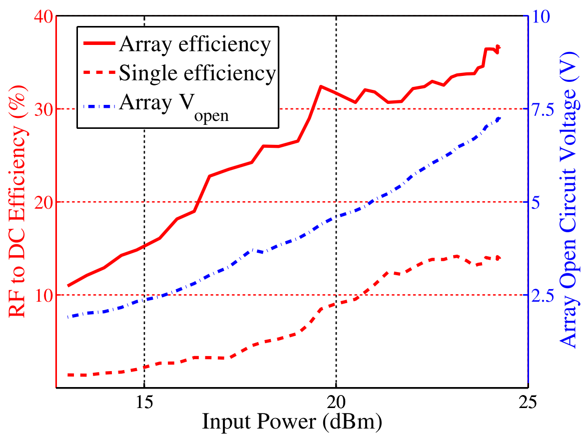

FIG. 6. RF to DC efficiency of power harvesters. The open-circuit voltage of the array is also shown.

larger effective area of the array. While the effective area of the single cell is 78% the entire width of the waveguide, some of this power is not harvested by the single unit cell due to fringing effects on the sides of the waveguide. For this reason, placement of multiple cells that together span the entire waveguide width results in a higher efficiency as the array captures more of the electromagnetic energy that undergoes the fringing effect.

Another important relationship is the efficiency of the power harvesting metamaterial as a function of load resistance. Simulated and experimental efficiencies for the 5 × 1 array are shown in Fig. 7. Though the experimental efficiencies do not match the values from simulation, the simulation does accurately predict the maximum harvested power as falling approximately within the range of 70–80 Ω, confirmed by the experimental data. The experimental efficiency maximum occurs at 70 Ω, and the simulated maximum occurs at 82 Ω, showing close correspondence.

In summary, we have designed, simulated, and experimentally measured a functional metamaterial power harvester capable of converting up to 36.8% of the incident RF power to DC power. Through a parallel connection of five SRRs, a V_{OC} of 7.3 V is achieved. Simulations match experimental results showing an optimal resistive load for DC power transfer of 70–80 Ω. The SRR power harvester is an example of functional metamaterial that may be suitable for a wide variety of RF applications that require power delivery to any active integrated components.

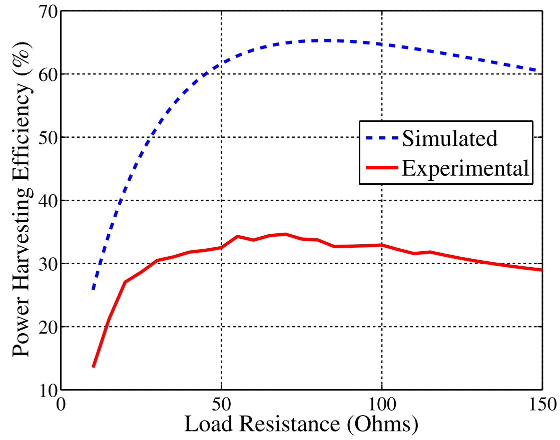

FIG. 7. RF to DC efficiency of SRR array as a function of load resistance, for both simulation and experiment. Note that both show maximum efficiency for around 70–80 Ω.

This work was supported by a Multidisciplinary University Research Initiative from the Army Research Office (Contract No. W911NF-09-1-0539).

[1]D. R. Smith, W. J. Padilla, D. C. Vier, S. C. Nemat-Nasser, and S. Schultz, Phys. Rev. Lett. **84**, 4184–4187 (2000).
[2]R. W. Ziolkowski, Phys. Rev. E **70**, 046608 (2004).
[3]N. Fang, H. Lee, C. Sun, and X. Zhang, Science **308**(5721), 534–537 (2005).
[4]D. Schurig, J. J. Mock, B. J. Justice, S. A. Cummer, J. B. Pendry, A. F. Starr, and D. R. Smith, Science **314**(5801), 977–980 (2006).
[5]I. V. Shadrivov, S. K. Morrison, and Y. S. Kivshar, Opt. Express **14**(20), 9344–9349 (2006).
[6]H.-T. Chen, J. F. O'Hara, A. K. Azad, A. J. Taylor, R. D. Averitt, D. B. Shrekenhamer, and W. J. Padilla. Nature Photon. **2**(5), 295–298 (2008).
[7]A. R. Katko, S. Gu, J. P. Barrett, B.-I. Popa, G. Shvets, and S. A. Cummer, Phys. Rev. Lett. **105**, 123905 (2010).
[8]D. Huang, A. Rose, E. Poutrina, S. Larouche, and D. R. Smith, Appl. Phys. Lett. **98**(20), 204102 (2011).
[9]A. Rose, D. Huang, and D. R. Smith, Phys. Rev. Lett. **110**, 063901 (2013).
[10]A. R. Katko, A. M. Hawkes, J. P. Barrett, and S. A. Cummer, IEEE Antennas Wireless Propag. Lett. **10**, 1571–1574 (2011).
[11]I. V. Shadrivov, A. B. Kozyrev, D. W. van der Weide, and Y. S. Kivshar, Appl. Phys. Lett. **93**(16), 161903 (2008).
[12]M. Lallart, D. Guyomar, C. Richard, and L. Petit, J. Acoust. Soc. Am. **128**, 2739–2748 (2010).
[13]N. Zhu, R. W. Ziolkowski, and H. Xin, Appl. Phys. Lett. **99**(11), 114101 (2011).
[14]J. Li and C. T. Chan, Phys. Rev. E **70**(5), 055602 (2004).
[15]H. J. Lezec, J. A. Dionne, and H. A. Atwater, Science **316**(5823), 430–432 (2007).
[16]R. W. Ziolkowski and A. Erentok, IEEE Trans. Antennas Propag. **54**(7), 2113–2130 (2006).
[17]G. X. Li, S. M. Chen, W. H. Wong, E. Y. B. Pun, and K. W. Cheah, Opt. Express **20**(1), 397–402 (2012).
[18]J. Zhao, Q. Cheng, J. Chen, M. Q. Qi, W. X. Jiang, and T. J. Cui, New J. Phys. **15**, 043049 (2013).
[19]O. M. Ramahi, T. S. Almoneef, M. Alshareef, and M. S. Boybay, Appl. Phys. Lett. **101**, 173903 (2012).
[20]A. S. Sedra and K. C. Smith, *Microelectronic Circuits*, 6th edition (Oxford University Press, 2009).
[21]C. A. Balanis, *Antenna Theory: Analysis and Design* (Wiley-Interscience, New York, 2005).

Ambient RF Energy Harvesting in Urban and Semi-Urban Environments

Manuel Piñuela, *Student Member, IEEE*, Paul D. Mitcheson, *Senior Member, IEEE*, and Stepan Lucyszyn, *Senior Member, IEEE*

***Abstract*—RF harvesting circuits have been demonstrated for more than 50 years, but only a few have been able to harvest energy from freely available ambient (i.e., non-dedicated) RF sources. In this paper, our objectives were to realize harvester operation at typical ambient RF power levels found within urban and semi-urban environments. To explore the potential for ambient RF energy harvesting, a city-wide RF spectral survey was undertaken from outside all of the 270 London Underground stations at street level. Using the results from this survey, four harvesters (comprising antenna, impedance-matching network, rectifier, maximum power point tracking interface, and storage element) were designed to cover four frequency bands from the largest RF contributors (DTV, GSM900, GSM1800, and 3G) within the ultrahigh frequency (0.3–3 GHz) part of the frequency spectrum. Prototypes were designed and fabricated for each band. The overall end-to-end efficiency of the prototypes using realistic input RF power sources is measured; with our first GSM900 prototype giving an efficiency of 40%. Approximately half of the London Underground stations were found to be suitable locations for harvesting ambient RF energy using our four prototypes. Furthermore, multiband array architectures were designed and fabricated to provide a broader freedom of operation. Finally, an output dc power density comparison was made between all the ambient RF energy harvesters, as well as alternative energy harvesting technologies, and for the first time, it is shown that ambient RF harvesting can be competitive with the other technologies.**

***Index Terms*—Ambient RF, energy harvesting, maximum power point tracking (MPPT), multiband, rectenna, RF survey, RF-dc.**

I. Introduction

FOR ALMOST 50 years, far-field RF technology has been used to remotely power systems from relatively large unmanned helicopters [1] to very small smart dust sensors [2] and contact lenses that measure eye pressure [3]. With all these systems, a dedicated RF source is used, where the operator may have control over the effective isotropically radiated power (i.e., both transmit power and antenna characteristics), beam pointing and polarization of the RF source, ensuring optimal line-of-sight operation between the source transmitter (TX) and harvesting receiver (RX). It is important to highlight that this work will focus only in radiative power transfer and not inductive or near-field power transfer, as demonstrated in [4]. A more convenient solution, however, is to power these devices from ambient RF energy sources, such as television and mobile phone signals, thus removing the need for a dedicated source. As ambient RF levels are lower than those that can be provided by a dedicated RF source, the efficiency of the harvesting system, and its minimum startup power are of critical importance.

In order to assess the feasibility of deploying ambient RF energy harvesters, the available RF power needs to be measured in different locations. Such measurements, in conjunction with knowledge on harvester performance, can then be used to determine the locations at which RF harvester powered devices can be successfully deployed. Several RF spectral surveys, which measure ambient RF power levels from sources such as television and mobile phone base stations, have been previously reported. Many have been undertaken using personal exposimeters or spectrum analyzers, where the exact location of each measurement is unknown and with RF power levels only being reported under general scenarios (e.g., outdoor, indoor, street, bus, etc.) [5], [6]. While being of academic interest for health-related research [7], the lack of power level and specific time/location information limits their usefulness for exploitation in ambient RF energy harvesting applications.

Most rectennas (normally comprising an antenna, impedance matching network, rectifier, storage element, and load) presented in the open literature have been tested using dedicated sources rather than harvesting from ambient RF energy [8]. In recent years, efficiencies as high as 78% [9] and 90% [10] have been demonstrated with relatively high input RF power levels (i.e., $> +10$ dBm). Moderate efficiencies have also been achieved using dedicated TXs that provided relatively low input RF power levels; e.g., an efficiency of 60% was achieved with -22.6-dBm input power [11]. In one demonstrator [12], designed to operate over a broad range of input RF power levels, (-30 to $+30$ dBm), the efficiency increased from 5% at a low input RF power to a peak of 80% at $+25$ dBm.

Despite advancements in end-to-end (i.e., input RF to output dc) power conversion efficiencies at low input RF power levels (similar to those measured in the spectral surveys), only a few attempts at true ambient RF energy harvesting have been reported. For example, one relatively efficient rectenna, utilizing a modified omnidirectional patch antenna, has an efficiency of 18% with a single-tone input RF power of -20 dBm [13]. This dedicated signal source was meant to emulate the input RF power levels measured from a nearby digital TV (DTV) TX in Tokyo, Japan, but did not take into account the more realistic effect of harvesting from a modulated broadband signal. Another attempt

Manuscript received November 20, 2012; revised April 24, 2013; accepted April 26, 2013. Date of publication May 24, 2013; date of current version June 28, 2013. This work was supported in part by the U.K. Government and the Mexican National Council of Science and Technology (CONACYT).

The authors are with the Department of Electrical and Electronic Engineering, Imperial College London, London SW7 2AZ, U.K. (e-mail: m.pinuela09@imperial.ac.uk; paul.mitcheson@imperial.ac.uk; s.lucyszyn@imperial.ac.uk).

Color versions of one or more of the figures in this paper are available online at http://ieeexplore.ieee.org.

Digital Object Identifier 10.1109/TMTT.2013.2262687

at harvesting ambient RF energy from a mobile phone base station at 845 MHz was reported in [14]. This prototype managed to power an LCD thermometer for 4 min, but only after harvesting for 65 h. In that work, when the authors used a dedicated signal source with a single-tone input RF power of -15 dBm, an efficiency of 3% was recorded. A batteryless location sensor has also been demonstrated [15], powered by a rectenna with a printed antenna on a flexible substrate and a solar cell, although no details for the RF-dc efficiency were reported. Finally, successful prototypes capable of harvesting energy using TV antennas were presented, but again no details of their efficiency were given [16], [17].

In order to demonstrate the feasibility for implementing ambient RF energy harvesting, here we first present the results of a citywide RF spectral survey, indicating suitable locations and associated RF bands with sufficient input RF power density levels for harvesting. Based on these results, rectennas were then fabricated and their efficiencies, under ambient RF energy harvesting operation, were calculated using *in-situ* field strength measurements. Furthermore, an investigation of multiband rectenna arrays is also presented, demonstrating the tradeoffs between series (voltage summing) and parallel (current summing) topologies with the aim of reducing the minimum input power required for harvester operation. Finally, a comparison between measured ambient RF energy harvesting and alternative forms of energy harvesting technologies is presented; highlighting, for the first time, the practical feasibility of exploiting existing freely available sources of RF energy.

II. London RF Survey

In order to quantify input RF power density levels present in a typical urban and semi-urban environment, a citywide RF spectral survey within the ultrahigh frequency (0.3–3 GHz) part of the frequency spectrum was conducted within Greater London. A number of citywide RF spectral surveys have previously been conducted, but in general, only a few samples were taken, giving little insight into (semi-)urban environments [14], [18], [19]. Other surveys [20], [21] compare their measurements relative to the distance from the nearest TX. In a (semi-)urban environment, this may not provide enough information about the RF spectrum since there is likely to be local geographical variations in base-station density and propagation characteristics (e.g., multipath effects and diffraction around and attenuation through buildings).

Each station on the London Underground network was used as a survey point to provide a robust dataset for representing Greater London in terms of geographical distribution and population density, having a combination of urban (in the center) and semi-urban (in surrounding areas) characteristics. Measurements were taken at each of the 270 stations (from a randomly chosen exit, at street level and a height of 1.6 m). To provide traceability and for use as a historical reference, time stamps and GPS locations were recorded. In addition, measurements were taken inside a building at Imperial College London (ICL), to represent a typical office block within an urban environment.

A. Methodology

Mobile phone usage varies during the daytime, and hence, ambient RF energy in their bands is expected to be time dependant, with more energy available during the daytime than at night time. Therefore, in order to be able to make fair comparisons between locations, measurements were taken between 10:00 am and 3:00 pm on weekdays over a period of one month (between March 5, and April 4, 2012). Electric field strength was measured between 0.3–2.5 GHz using an Agilent N9912A FieldFox RF analyzer [22] with a calibrated Aaronia BicoLOG 20300 omnidirectional antenna [23]. It is important to note that the spectral measurements were undertaken during the analog-to-digital switchover period in the U.K. and so the measurements for DTV may represent an underestimate of present RF power levels measured now that the switch over is complete [24]. It should also be noted that this survey was conducted prior to the 4G network being switched on within the U.K.

A “panning method,” which complies with international regulations for measuring exposure limits, was used [25]–[27]. Here, the calibrated antenna is rotated to three orthogonal axes while the spectrum analyser is set to “max-hold,” ensuring that the maximum reading is recorded. For each measurement, more than 1 min was allocated to allow for more than three sweeps across the selected frequency range. Additionally, to maintain a comparable signal-to-noise (S/N) ratio, attenuation was introduced (with a minimum set at 5 dB) to avoid compression when high input RF power levels were detected. For all measurements, the resolution bandwidth (BW) was fixed at 100 kHz, the internal amplifier was turned on and the highest resolution of 1001 points was selected. These settings provide the ability to obtain a snapshot of the power density that can be expected in an urban or semi-urban environment from continuously variable sources.

B. Results

After inputting the manufacturers’ frequency-banded antenna factors into the spectrum analyzer, to ensure a fully calibrated system, the electric field strength measurements were taken. The input RF power density (S) is then calculated from the electric field strength measurement. Fig. 1 shows the input RF power density measured outside the Northfields London Underground station, where the spectral bands for DTV, GSM900, GSM1800, 3G, and Wi-Fi can been clearly identified.

A well-designed rectenna should ideally be capable of harvesting energy across an entire band, and thus it is important to calculate the total band power. The banded input RF power density S_{BA} (nW/cm^2) is calculated by summing all the spectral peaks across the band (i.e., in a similar way, the spectrum analyzer calculates channel power). These levels provide a snapshot of source availability at the time and location of the measurement. Moreover, they are used as a harvester design starting point since the power density at each band will define the input impedance of a rectenna.

The exact frequencies for each band are set by the U.K.’s official frequency band allocation [28]; the GSM900, GSM1800 and 3G base transmit (BTx) bands were separated from the associated mobile transmit (MTx) bands. Table I shows average

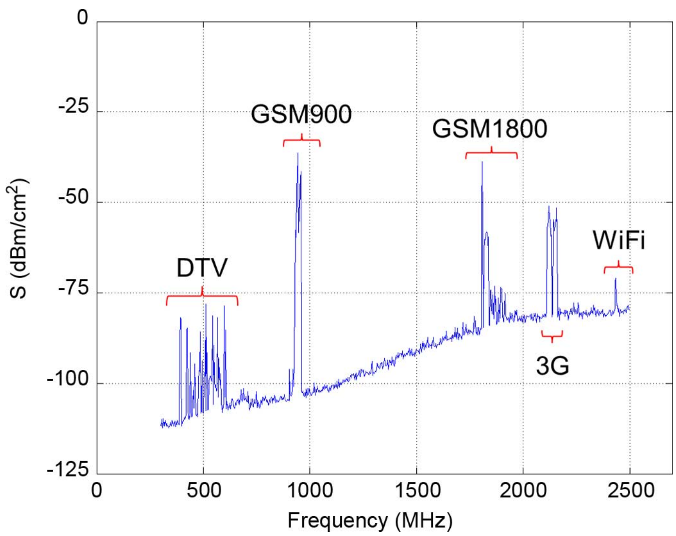

Fig. 1. Input RF power density measurements outside the Northfields London Underground station.

TABLE I
SUMMARY OF LONDON RF SURVEY MEASUREMENTS

Band	Frequencies (MHz)	Average S_{BA} (nW/cm^2)	Maximum S_{BA} (nW/cm^2)
DTV (during switch over)	470-610	0.89	460
GSM900 (MTx)	880-915	0.45	39
GSM900 (BTx)	925-960	36	1,930
GSM1800 (MTx)	1710-1785	0.5	20
GSM1800 (BTx)	1805-1880	84	6,390
3G (MTx)	1920-1980	0.46	66
3G (BTx)	2110-2170	12	240
WiFi	2400-2500	0.18	6

TABLE II
INPUT RF POWER DENSITY THRESHOLD: LONDON UNDERGROUND STATIONS WITHIN CENTRAL ZONES 1–3 (URBAN) AND OUTER ZONES 4–9 (SEMI-URBAN)

Band	S_{BA} Threshold (nW/cm^2)	Number of Stations Urban	Number of Stations Semi-urban
DTV (during switch over)	40	10	0
GSM900	230	8	2
GSM1800	450	7	3
3G	62	6	4

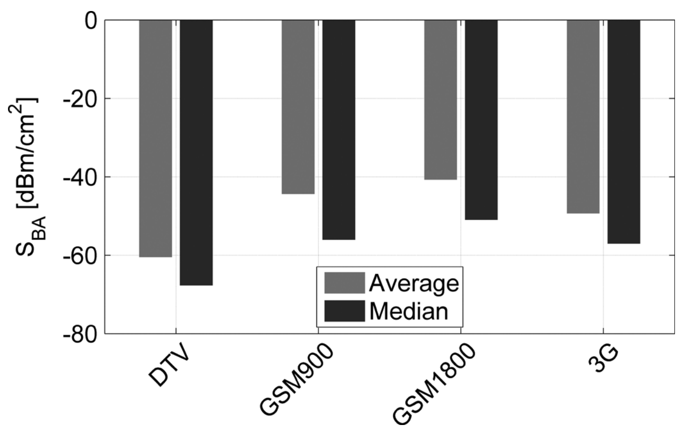

Fig. 2. Banded input RF power density measurements for the four largest ambient sources in Greater London.

RF power levels across all London Underground stations for the banded input RF power density measurements. It can be seen that all base-station transmit levels are between one and three orders of magnitude greater than the associated MTx levels. For this reason, and the fact that the population of transmitting mobile phones in close proximity of the harvester is highly variable, only base-station TXs will be considered further.

From our London RF survey, DTV, GSM900, GSM1800, 3G, and Wi-Fi were identified as potentially useful ambient RF energy harvesting sources, although DTV appears to be heavily dependent on line-of-sight and sudden changes in atmospheric conditions (e.g., temperature inversion) and Wi-Fi is very dependent on user traffic. It should be noted that the mobile phone base-station TXs employ vertically polarized antennas, placing a constraint on harvester orientation in deployment. With DTV, within the U.K., the main TXs have horizontally polarized antennas, while repeater TXs have vertically polarized antennas.

It is convenient to define the boundary between urban and semi-urban environments by the line that separates zones 3 and 4 on the London Underground map [29]. As one would expect, the central zones 1–3 host the highest density of base stations. As shown in Table II, a banded input RF power density threshold was selected to filter the ten London Underground stations with the highest measurements for each band. With DTV, the highest recorded measurements were all found within the urban environment. This is because Greater London's main DTV TX (at Crystal Palace) is located on the southeastern boarder of zones 3 and 4 and there are no London Underground stations further south. With mobile phones, more than 50% of the stations were inside the urban environment and those in a semi-urban environment were all located in close proximity to a cluster of base-station TXs.

Using the complete dataset from the London RF survey, Fig. 2 shows the average and median of the banded input RF power density measurements for the four largest ambient RF sources in Greater London. It can be seen that more than half of the locations have below average power levels. This is due to the fact that several stations had maximum levels that were considerably higher than the average because of their close proximity to TV TXs (e.g., Crystal Palace), extremes in base-station density and propagation characteristics.

In addition to the London RF survey, measurements within the Department of Electrical and Electronic Engineering building at ICL were taken on the 11th floor of the south stairwell. These are shown in Table III. As can be seen, DTV and GSM900 have a higher than average power level, due to a near line of sight from the TV TX and a close proximity to the 2G GSM900/1800 base stations.

The dataset from the London RF survey, with all relevant information (e.g., locations, timestamps, and banded input RF power density measurements), can be found at our interactive website: www.londonrfsurvey.org [30]. These measurements were used to design efficient harvesters and compared to ICL

TABLE III
MEASURED BANDED INPUT RF POWER DENSITIES AT ICL

	DTV	GSM900 (BTx)	GSM1800 (BTx)	3G (BTx)
S_{BA} [nW/cm^2]	18	48	50	3

measurements to identify locations in Greater London where the designed harvesters could operate. The design procedures and prototype test measurements will be presented in the following sections.

III. SINGLE-BAND AMBIENT RF ENERGY HARVESTERS

In order to implement efficient ambient RF energy harvesters, designed for the banded input RF power density levels measured at ICL, a set of single-band prototypes were realized and characterized; these will be compared to multiband array architectures in Section V.

A. Antenna Design and Measurements

Since our harvesters are intended to operate within a general (semi-)urban environment, where the exact location of the TX source is unknown, the rectennas' antennas need to be as close to omnidirectional as possible, avoiding the need for beam-pointing during deployment. This is at the obvious expense of limited antenna gain, and therefore, the corresponding levels of P_{RF} that the rectifier can receive. Conversely, if the location of the TX is known, then it may be tempting to use a high gain antenna, but this would require an appropriate level of beam-pointing and polarization matching that can be established and maintained.

Another requirement is that the antennas need to be easily scalable across all frequency bands since one important objective for this work is to compare and contrast different banded harvesters. Finally, the antennas need to be easily fabricated. For all these reasons, a linear polarized folded dipole was selected, although a monopole would also be suitable [31].

To simplify impedance matching between the antenna and rectifier, a modified folded dipole was used to obtain the required 50-Ω reference input impedance. A balun does not need to be employed, as there is no significant degradation in performance for this particular application, even with the use of an unbalanced microstrip rectifying circuit [32]. Furthermore, the antenna was not integrated onto a substrate, to give the additional freedom to embed the harvester on windows or within walls, furnishings, fixtures, or fittings. To this end, two different antennas were fabricated for each band; one made using a 560-μm diameter copper wire and the other with 75-μm-thick 25-mm-wide copper tape. The fabricated antennas are shown in Fig. 3. Since the copper tape was not rigid enough to retain its shape, it was placed on a Perspex substrate, to represent a flat panel.

To design the antennas, full-wave 3-D electromagnetic simulations were performed using CST Microwave Studio. As discussed previously, the antennas were designed to be as omnidirectional as possible, while covering as much of the ambient RF source BW as possible. Fig. 4 shows the typical simulated gain profile for the DTV tape antenna, having a front-to-back ratio of unity. Table IV shows the simulated gain and the 10-dB return-loss fractional BW for the optimized copper wire and tape antennas.

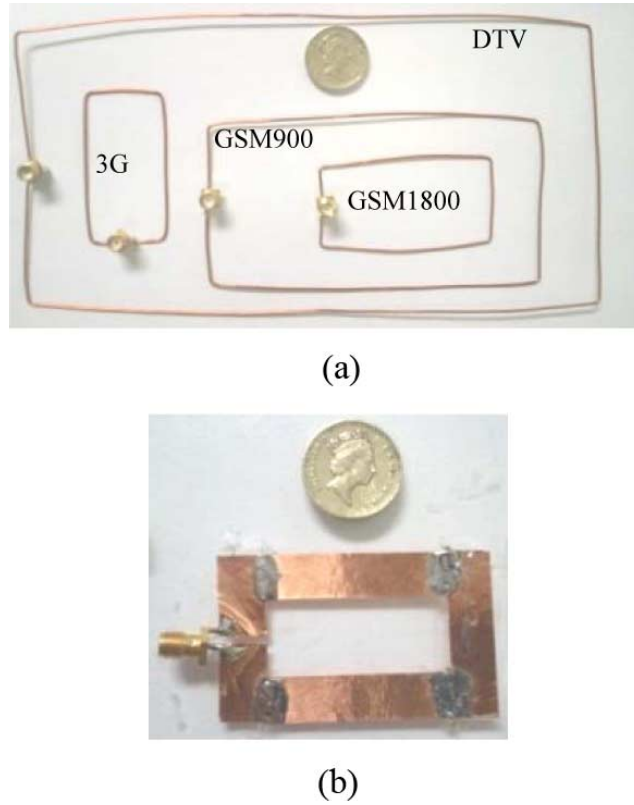

Fig. 3. 50-Ω folded-dipole antennas shown next to a British £1 coin. (a) DTV, GSM900 (BTx), GSM 1800 (BTx) and 3G (BTx) copper wire antennas. (b) 3G (BTx) copper tape antenna on Perspex.

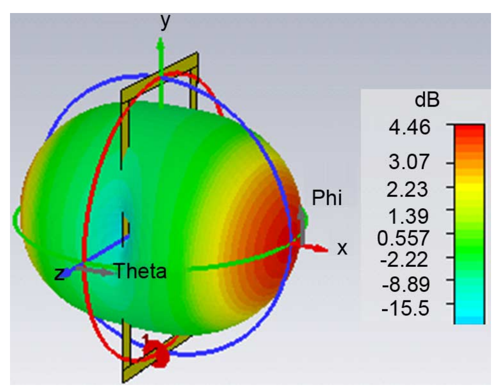

Fig. 4. Simulated beam profile for the DTV tape antenna.

Fig. 5 shows excellent agreement between predicted and measured return-loss results, within a 10-dB return-loss bandwidth, for the eight fabricated single-band antennas. As one would expect with such a simple classical antenna, the out-of-band performances (not shown) were also in good agreement. It was found that better return-loss measurements are achieved with our single-band antennas when compared to other reported single-band omnidirectional [13] and multiband [33] designs. The latter may be important, as it may be tempting to implement a more compact multiband rectenna, but which

TABLE IV
SIMULATED GAIN AND 10-dB RETURN LOSS FRACTIONAL BW FOR FOLDED-DIPOLE SINGLE-BAND ANTENNAS

Band		Wire		Tape	
	BW (%)	Gain (dBi)	BW (%)	Gain (dBi)	BW (%)
DTV	26	4.35	4	4.48	6
GSM900	3.7	4.42	4.3	4.73	4.3
GSM1800	4.1	4.32	5.3	4.73	10.7
3G	2.8	4.39	5.4	4.76	12

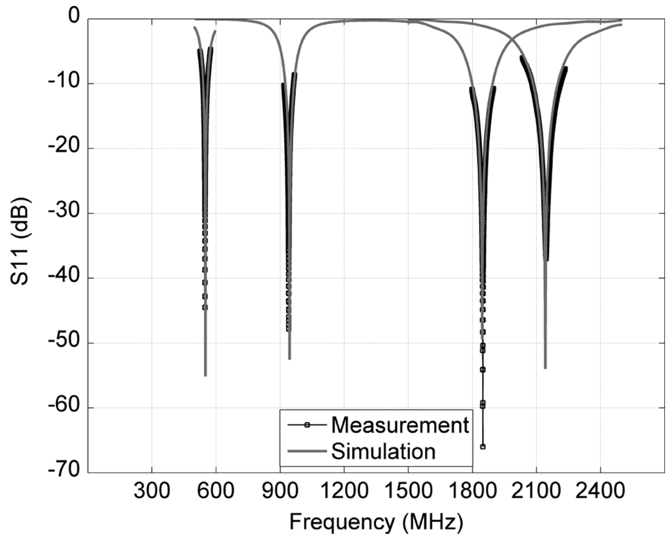

(a)

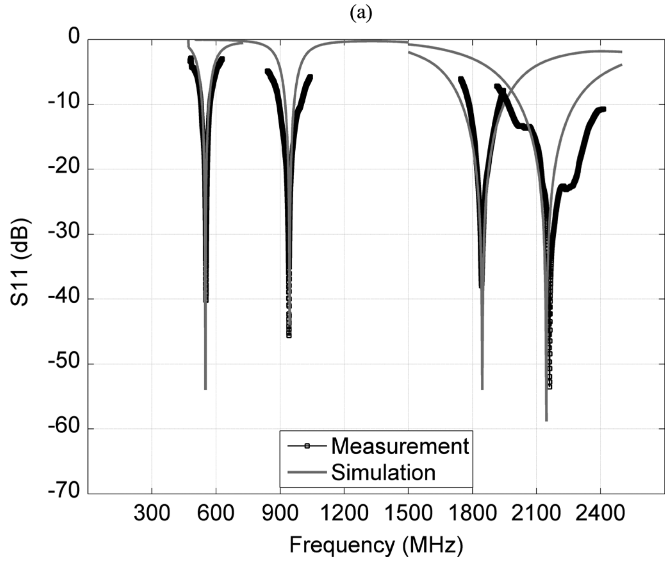

(b)

Fig. 5. Input return-loss predictions and measurements for all single-band folded-dipole antennas. (a) Wire. (b) Tape.

may ultimately not give better ambient RF energy harvesting performance.

Obtaining a minimum acceptable return loss over an antenna fractional bandwidth as large as that of the source is key to harvest as much input RF energy as possible. As can be seen in Table IV, where the fractional bandwidth is defined for a 10-dB return loss, our antennas have a fractional bandwidth greater than those of the sources, with the exception of DTV, which only covers approximately 35% of the target frequency range. In other work [13], 5-dB return-loss fractional bandwidth is adopted for RF energy harvesting applications.

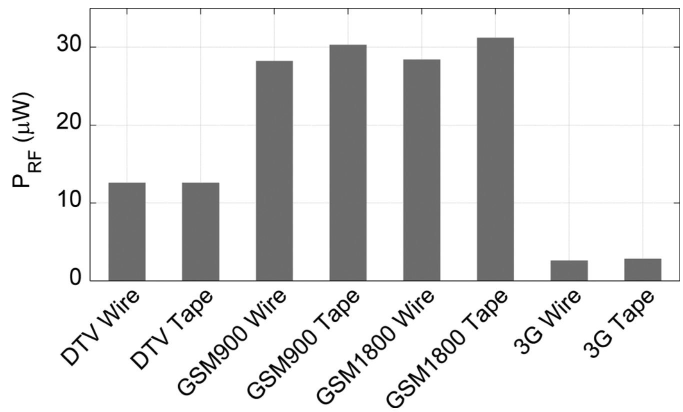

Fig. 6. Predicted input RF power levels for the four largest ambient sources at the ICL testing location.

The fractional bandwidth of the antennas having a minimum return loss of 5 dB is too great to assume a constant antenna gain over the whole band. Therefore, an additional advantage of using 10-dB return-loss fraction bandwidths is that (1) can be used to calculate the input RF power with the assumption that the midband antenna gain is constant with frequency [34]. Therefore, the time-averaged input RF power P_{RF} is given by

$$P_{\mathrm{RF}} = S_{BA} \cdot A_{\mathrm{real}} \text{ and } A_{\mathrm{real}} \approx G(f_o)\frac{\lambda_o^2}{4\pi} \tag{1}$$

where A_{real} is the real aperture (or capture area) of the antenna, λ_o is the free-space wavelength at the midband frequency f_o, and $G(f_o)$ is the rectenna's antenna gain at f_o.

Substituting the measured banded input RF power densities recorded in Table III and the predicted midband antenna gains in Table IV into (1), realistic values for P_{RF} can be calculated for all four bands, with the results shown in Fig. 6. It can be seen that with all antenna gains being in the region of $\sim$ 4.5 dBi, the 2G GSM900/1800 harvesters will generate the highest input RF power levels, due to the high-banded input RF power density levels measured *in situ*. At the other extreme, the 3G harvesters will be the worst performers. As only a small fraction of the required frequency range is covered by the DTV antennas, the predicted values for P_{RF} represent an overestimation.

B. Rectifier Design and Measurements

Based on a previously reported analysis [35] and the predicted input RF power levels presented in Fig. 6, the zero-bias SMS7630 diode (in a series configuration) was selected as the optimal solution for our ambient RF energy harvesters, as shown in Fig. 7. In a series configuration, the junction capacitance $(C_j(V))$ of the diode dominates the detector's impedance, as long as $C_{\mathrm{out}} > C_j(V)$, and thus C_{out} has little or no effect on the matching circuit. This allows C_{out} to be large enough to provide a ripple-free output voltage. In contrast, C_{out} must be less than 1 pF to achieve a good impedance match with a shunt configuration as C_{out} appears in parallel with $C_j(V)$ and the packaging parasitic capacitance. However, C_{out} is too small to

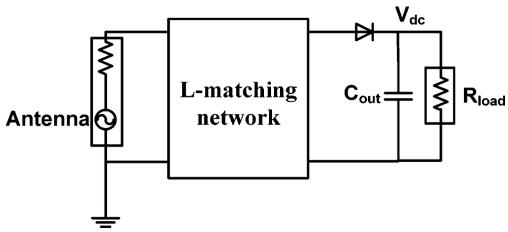

Fig. 7. Series detector configuration with L-matching network.

provide a ripple-free dc voltage to the load. This can be overcome with a matching network that will allow a good impedance match with a large output capacitor, but at the expense of introducing losses. Furthermore, as shown in [36], these issues start to become negligible with a shunt configuration as the shunt diode becomes more self-biased as the input power increases. Simulations were performed using Agilent Technologies' ADS software. Its Momentum package not only takes into account the losses from the low-cost FR4 substrate, but also calculates fringing fields, effects from which are passed on to the harmonic-balance package for simulating the nonlinear behavior of the rectifier.

A good impedance match was achieved by employing a simple matching network; a series lumped-element inductor was used to absorb part of the capacitive reactance from the series diode and an additional quarter-wavelength short-circuit shunt stub was employed to achieve the desired 50-Ω impedance [37]. Since the impedance of the diode varies with frequency and input RF power, impedance matching between the antenna and rectifier was first undertaken by finding the optimal output load resistance for an input RF power level of -20 dBm with a single-tone source at the midband frequency. After the optimal load was found, further broadband optimization was performed to the matching network and the load to ensure good impedance matching throughout the target frequency range and the measured $P_{\rm RF}$ for each band.

As with the antenna analysis, and unlike conventional RF circuits that adopt the more traditional half-power bandwidth definition, the rectifier should adopt the 10-dB-input return-loss bandwidth. The reason for this is that, for ambient RF energy harvesting applications, the input RF power is at a premium and so what little energy is available should not be wasted by being reflected back from avoidable impedance mismatches at either the antenna or rectifier.

Fig. 8 shows excellent agreement between predicted and measured input return loss results, within the -10-dB bandwidth, for the DTV and GSM900 rectifiers, having fractional bandwidths of 5.7% (below target) and 4.8%, respectively. With these lower frequency designs, the fundamental and higher order harmonics were below -55 dBm, ensuring a clean dc voltage at the load, without the need for any output filtering. Reasonable agreement was found with the GSM1800 and 3G rectifiers, having fractional bandwidths of 1.6% (below target) and 7.4%, respectively. It was found that with these two higher frequency designs, the higher order harmonics were -40 dBm at the output. This reduced performance, as illustrated in Fig. 8, is due to the higher series inductive reactance leads of the output shunt storage capacitor. For this reason, a

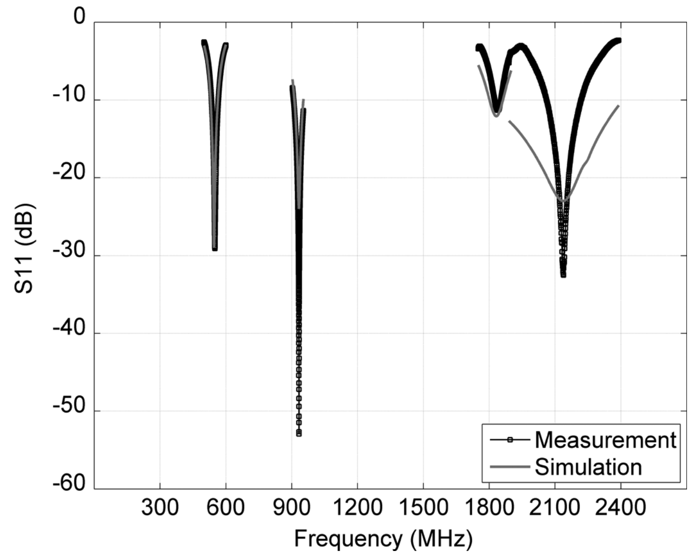

Fig. 8. Input return-loss predictions and measurements for all first prototype single-band rectifiers, with $P_{\rm RF} = -20$ dBm at the input and optimal load resistances at the output.

second prototype version (v2) was designed for the 3G rectifier, using distributed-element components for the input impedance matching stage and an additional output filter stage. With the lumped-element matching network, it was found that in order to achieve good input impedance matching to 50 Ω, all the microstrip transmission lines had to have a characteristic impedance of 92 Ω. With the distributed-element matching network, a simple shunt quarter-wavelength open-circuit stub, designed for operation at the fundamental frequency, was employed. A microstrip line was added between the cathode of the diode and the stub to absorb the capacitive reactance of the diode. The stub effectively filters to < -50 dBm the higher order harmonics. The microstrip design can be seen in Fig. 13.

C. PMM

Since the input RF power from ambient sources can be represented as a multi-tone source, with power levels fluctuating across the target frequency range, the output impedance of the rectifier is time varying. A power management module (PMM) capable of performing maximum power point tracking (MPPT) is required.

For our work, a low-power integrated-circuit PMM from Texas Instruments Incorporated (BQ25504) was selected, due to its low quiescent current (< 330 nA) and low input voltage operation (~ 80 mV hot-start and 330-mV cold-start) [38]. It is worth noting that its startup voltage is lower than PMMs previously reported and realized using hybrid circuits for RF energy harvesting [13]. The BQ25504 PMM includes a boost converter that steps up its input voltage (having a 350-mV average value during ambient operation) to useful levels between 2.4–5.3 V. The BQ25504 also has a built-in battery management module, which is used to control the duty cycle of the output power to the load.

MPPT operation on the BQ25504 is achieved by periodically sampling the open-circuit voltage (OCV) at the input of the converter, which then draws a current causing the converter

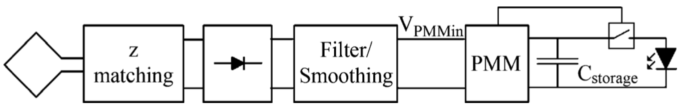

Fig. 9. System block diagram.

input voltage to fall and be held at a pre-programmed fraction of the OCV (set by a potential divider). In a simple dc circuit, with a resistive source impedance, the optimal ratio is 0.5. For the rectenna-based system, a ratio of 0.48–0.53 was found to maximize the power output of the system. The BQ25504 is designed to charge a storage element, and in this case, a capacitor $C_{\rm storage}$ was used. The programmed PMM continuously charges the storage capacitor, and the load (a low-power LED) was automatically connected to the storage capacitor when the capacitor voltage reaches an upper limit $V_{\rm high} = 2.84$ V and automatically disconnected when it reaches a lower limit $V_{\rm low} = 2.40$ V. The duty cycle of the LED can then be used to calculate the efficiency of the system, as will now be described. A diagram of the system is shown in Fig. 9.

IV. End-to-End Efficiency Analysis

The efficiency η of an RF energy harvesting system is

$$\eta = \frac{P_{\rm dc}}{P_{\rm RF}} \tag{2}$$

where $P_{\rm dc}$ is the time-averaged output (i.e., equivalent dc) power into the storage element (e.g., battery or supercapacitor) and load and $P_{\rm RF}$ is as previously defined. Measurements for this type of system are usually performed in a controlled environment (e.g., an anechoic chamber or TEM cell), using a dedicated constant or variable amplitude single-tone RF signal source [32], [39]. However, the former is not suitable for evaluating ambient RF energy harvesting operation, which has a much broader spectrum of nonconstant input frequencies and where the instantaneous input RF power is time variant. The use of a constant single-tone dedicated source provides a convenient stable reference power to the harvester; while the latter reflects a more realistic signal source having fluctuating power levels across a nonzero bandwidth, multipath, and reflection effects which are very difficult to emulate in a controlled environment.

Therefore, to determine the overall end-to-end efficiency $\eta_{\rm e\text{-}e}$ for a complete ambient RF energy harvester, the input RF energy $U_{\rm RF}$ was calculated based on the harvester's antenna characteristics and the actual banded input RF power density measurements taken at the time of harvester operation, using the Agilent Fieldfox and the calibrated antenna. It is important to note that since the impedance mismatch between the antenna and detector is not taken into account, $U_{\rm RF}$ is higher than expected, providing an underestimate of end-to-end efficiency. The output dc energy $U_{\rm dc}$ was then calculated by measuring the charge–discharge cycle time, $t_{\rm cycle}$ of the storage capacitor between $V_{\rm high}$ and $V_{\rm low}$, as the LED is repeatedly connected and disconnected. The output dc energy equation is already taking into account the efficiency of the PMM given the fact that the measurements are taken at its output voltage. The end-to-end efficiency of one charge–discharge cycle of $C_{\rm storage}$ is

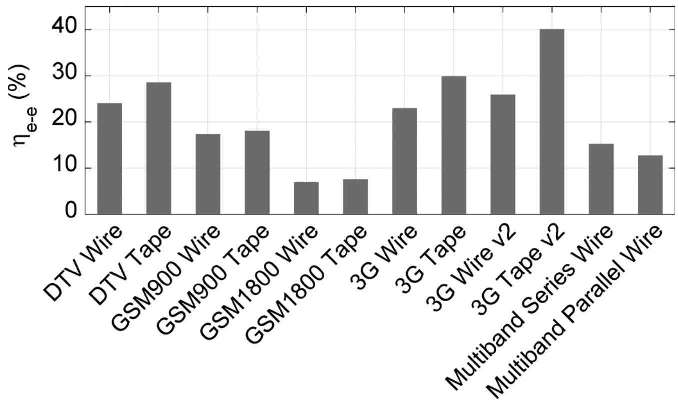

Fig. 10. End-to-end efficiencies for ambient RF energy harvesting at ICL.

$$\eta_{\rm e\text{-}e} = \frac{U_{\rm dc}}{U_{\rm RF}} \tag{3}$$

where the input RF energy is given by integrating the time-averaged input RF power over a cycle time, as

$$U_{\rm RF} = \int_0^{t_{\rm cycle}} P_{\rm RF}\, dt \tag{4}$$

and the output dc energy is given by the energy supplied to the load, as follows:

$$U_{\rm dc} = C_{\rm storage}\frac{({V_{\rm high}}^2 - V_{\rm low}^2)}{2}. \tag{5}$$

A. ICL Field Trials

Four single-band ambient RF energy harvesters were assembled by connecting the rectifiers to the wire/tape antennas and PMMs programmed for the optimal load. A 100-μF shunt capacitor was employed as the storage element, providing $U_{\rm dc} = 115\ \mu$J. Our system is capable of cold-starting the boost converter and MPPT since the rectenna is capable of providing the minimum starting voltage of 330 mV. When the minimum voltage is reached, the boost converter and MPPT start to operate and the charge–discharge cycle at the load begins, causing the LED to flash. During field trials, $t_{\rm cycle}$ took up to 170 s for the harvester with lowest banded input RF power density, corresponding to 3G with the wire antenna. Table V summarizes the results where t_c and t_d are the charge and discharge times, respectively, and ΣV and ΣI are the multiband voltage and current summing array architectures, respectively. A detailed discussion on the multiband rectenna arrays will be presented in the following section. The end-to-end efficiency was calculated using (3) with data from Fig. 6 and measuring the charge–discharge cycle time during harvesting operation.

Fig. 10 shows the overall end-to-end efficiencies for all the harvester demonstrators, deployed and tested at ICL. As predicted by simulations, the improved 3G v2 demonstrator with

TABLE V
HARVESTERS CHARGE AND DISCHARGE TIMES (t_c, t_d, RESPECTIVELY) FOR A SPECIFIED LOAD

Band	Wire					Tape				
	t_c (s) load independent	t_d (s) load dependant	t_{cycle} (s) load dependant	$P_{dc}(t_d)$ (μW)	$P_{dc}(t_{cycle})$ (μW)	t_c (s) load independent	t_d (s) load dependant	t_{cycle} (s) load dependant	$P_{dc}(t_d)$ (μW)	$P_{dc}(t_{cycle})$ (μW)
DTV	26	12	38	9.6	3	14	18	32	8.2	3.6
GSM900	14	10	24	11.5	4.8	8	13	21	14.4	5.5
GSM1800	43	15	58	7.7	2	22	27	49	5.2	2.4
3G v2	167	3	170	38.4	0.7	96	5	101	1.2	1.1
Multiband ΣV	43	7	50	66	2.3	-	-	-	-	-
Multiband ΣI	55	5	60	92.2	2	-	-	-	-	-

tape antenna outperformed its original design by 11%; achieving an end-to-end efficiency of 40% with an input RF power of only −25.4 dBm.

It is believed that a much greater efficiency can be achieved for the DTV harvester if the fractional bandwidths for the first prototype circuits (i.e., 4.4/4.5% for the antennas and 5.8% for the rectifier) could be increased to match the much greater target value of 26%. Likewise, the reduced efficiency of the GSM1800 harvesters can be attributed to the detrimental effects of the narrowband input impedance matching of the rectifier (i.e., having a fractional bandwidth of only 1.6%, when compared to its target value of 4.1%). Finally, with all the harvesters, the end-to-end efficiencies can be enhanced through better antenna design and optimal polarization matching.

Table VI, shows the number of locations from the London RF survey that would be able to support our harvesters. Unlike the single-band 3G harvester, which can operate at 45% of the locations, our DTV harvester can only be used at two locations (one in zone 2 and the other in zone 3). Therefore, for the general deployment of an ambient RF energy harvester within an (semi-)urban environment, at street level, the single-band DTV harvester may not be practical

TABLE VI
NUMBER OF LOCATIONS FROM THE LONDON RF SURVEY CAPABLE OF SUPPORTING IDENTICAL HARVESTERS AT THE SAME EFFICIENCY LEVELS

	DTV	GSM900 (BTx)	GSM1800 (BTx)	3G (BTx)
Stations with higher S_{BA}	2	28	68	122

V. ARRAY ARCHITECTURES

Since ambient input RF power levels can be low (i.e., below −25 dBm) and dependent on both time and spatial considerations, harvesters could be designed to extract energy with spatial-diversity within the same frequency band or using different frequency bands. For example, with the former, at a particular location there may be only one band that has significant levels of RF energy worth harvesting. In this case, spatial-diversity array architectures may provide more usable output power. Alternatively, with the latter, multiband array architectures may provide more robust operation.

With both forms of parallel array architecture (i.e., spatial-diversity and multiband), a further classification can be seen through the use of either diversity/band switching or a summing node. With the former, physical switches automatically select whichever signal path delivers the highest input RF power level; with the latter, power from all signals is combined. Fig. 11 illustrates generic forms of parallel array architectures, showing that switching/summing can be performed electromagnetically at a single antenna or at the output from multiple antennas, rectifiers, or PMMs.

Multiband array architectures, similar to those in Fig. 11(c) and (d), capable of RF harvesting from the four previously identified bands, were selected as possible optimal solutions, given no size/cost constraints. Our objectives were to reach the minimum cold-start voltage at the lowest possible input RF power levels and increase the harvesters' operational capabilities within (semi-)urban environments.

To this end, two different multiple rectenna architectures were investigated. The first with a single shared PMM and the second with multiple PMMs, as illustrated in Fig. 12. To simplify assembly, the wire antennas were selected since they did not require a substrate. Unwanted coupling between the single-band antennas was minimized by placing them a minimum distance of $\lambda_L/5$ apart; where λ_L is the wavelength of the lowest frequency band antenna [40]. For example, the DTV and the 3G antennas were kept at least 11 cm apart, as shown in Fig. 13. This allowed S_{11} measurements to be the same as in Fig. 5 once all antennas were assembled into the array.

A. Multiple Rectennas With a Shared PMM

In order to improve the cold-start performance of the system, the outputs of multiple rectennas can be connected in series, as shown in Fig. 12(a). This increases the probability of the voltage on the input of the PMM reaching the cold-start level (330 mV for the BQ25504) under any given scenario. While cold-starting the PMM, each rectenna harvests (albeit not optimally). Once

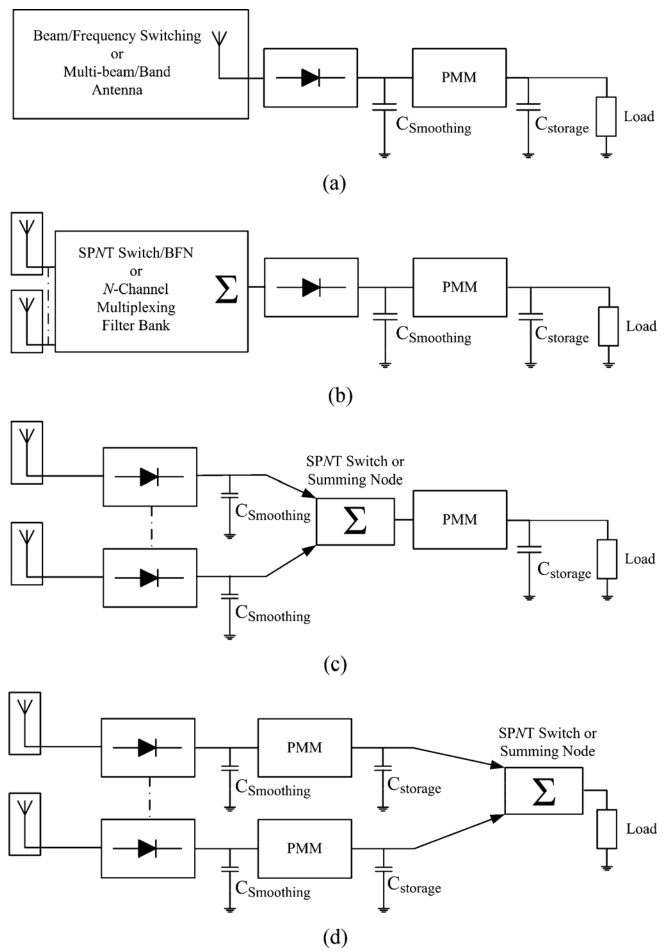

Fig. 11. Parallel array architectures with switching/summing at the: (a) antenna, (b) output of multiple antennas, (c) output of multiple rectifiers, and (d) output of multiple PMMs.

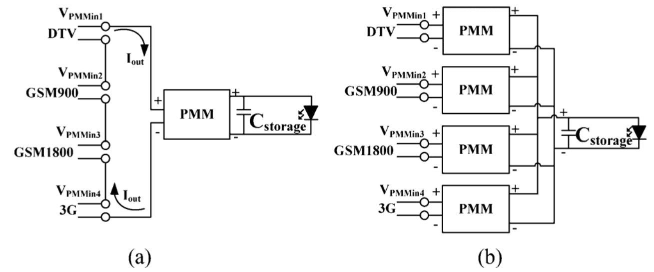

Fig. 12. Multiband array architectures (with $N = 4$ bands). (a) Voltage summing at the outputs of the single-band rectennas. (b) Current summing at the outputs of the single-band harvesters.

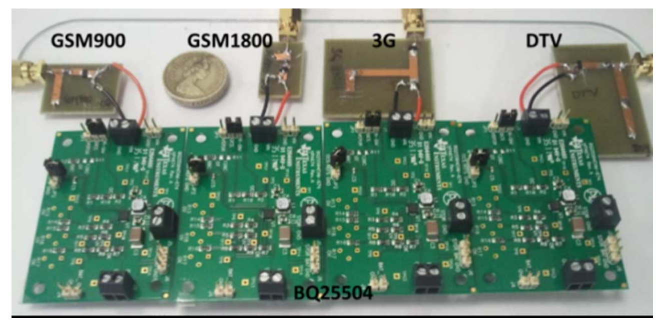

Fig. 13. Rectenna array architecture with individual PMMs for the four largest contributors with wire antennas.

the PMM circuit starts, with the MPPT operating, the harvested power level increases.

The behavior of the series rectenna topology with a shared PMM requires some discussion. As the output impedance and the OCV for each rectenna is different, since they operate at different frequencies and input RF power levels, the rectennas are forced to share the same output current in a series configuration, which does not allow them all to operate at their individual maximum power points. This causes the voltage on each rectenna output, except the one having the highest input RF power, to collapse. This operation is analogous to the partial shading problem with a series string of solar panels [41] sharing a common boost converter. With this photovoltaic system, bypass diodes placed around individual cells stop the poorly lit cells contributing a negative voltage (and power) to the string. In our case, the series circuit formed by the loop antennas and rectifying diodes performs the same task. This means that while all rectennas contribute to system startup, only the rectenna with the highest input RF power contributes significant power for continuous operation once the PMM starts. Fig. 10 shows the end-to-end efficiency for the voltage summing multiband harvester array when tested at ICL. An efficiency of only 15% was achieved with a combined input RF power of -12 dBm. The lower efficiency, when compared to a single-band harvester, is due to the imbalance of rectifier outputs, as discussed above. Here, the charge time was 43 s, compared to 167 s with the lowest contributing single-band 3G harvester with wire antenna.

B. Multiple Rectennas With Individual PMMs

In order to overcome the balancing issues when multiple rectennas share a common PMM, as discussed previously, each rectenna can have its own PMM, whose outputs can be connected to a common storage element (in this case, a 400-μF shunt capacitor, providing $U_{\rm dc} = 461\ \mu$J), as illustrated in Fig. 12(b) and shown in Fig. 13. Although not achieving cold-start as quickly as the series topology, this parallel topology has the advantage of being able to run each rectenna at its maximum power point. In addition, once one rectenna is able to harvest enough energy for a cold-start, all PMMs will start because they share a common storage element, allowing the rectennas with low-input RF power levels to harvest at levels below which they could not do so independently.

This parallel topology was tested and found to be capable of operating in many locations where the series array was unable to operate; e.g., if only one of the bands had $P_{\rm in} > -25$ dBm. As expected, the largest contributor hot-started the other PMMs, allowing them to harvest at an input RF power level down to -29 dBm.

However, as with the previous results for voltage summing, having a combined input RF power of -12 dBm, the efficiency using multiple PMMs is slightly lower, at 13%, as shown in Fig. 10. This is because useful dc output power from the cold-

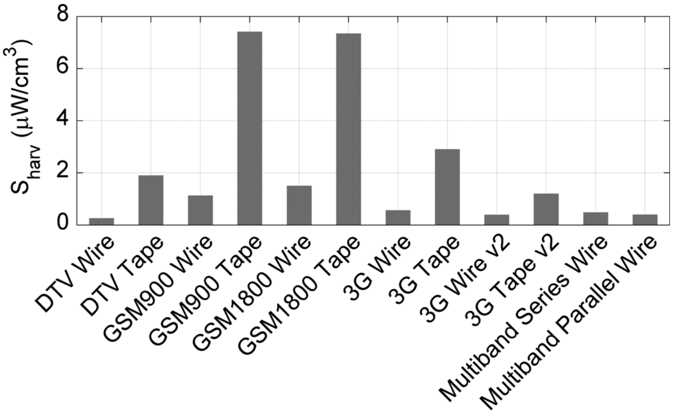

Fig. 14. Output dc power density for all harvesters at ICL.

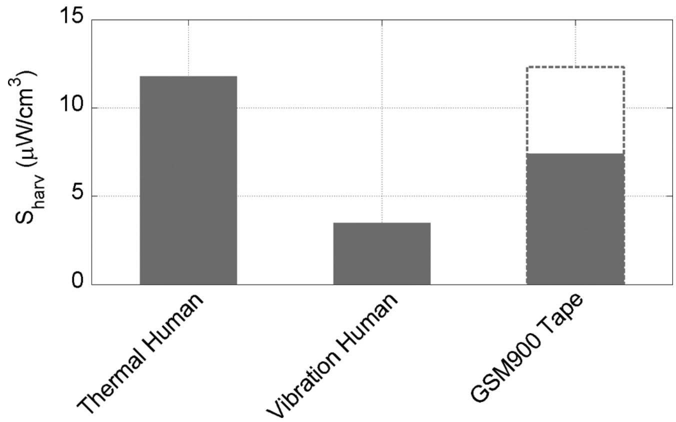

Fig. 15. Output dc power density comparison for alternative ambient harvesting technologies [40]–[43] against the best current generation of RF harvesters at ICL.

starting harvester is being supplied to the other harvesters for hot-starting, even though some of them may not actually be contributing any of their own harvested power.

VI. Output DC Power Density Comparison

The volumetric output dc power density S_{harv} $(\mu\mathrm{W/cm}^3)$ represents an important figure of merit for comparing alternative energy harvesting technologies. For ambient RF energy harvesting, the output dc power is calculated by multiplying the effective input RF power by the overall end-to-end-efficiency. The total volume (including that of the antenna, rectifier, and PMM; not including energy storage, as this does not directly affect the dc power output) must be determined. It is important to note that the volume for the antenna could effectively disappear if it is assembled onto a window or within a wall, furnishing, fixture, or fitting. Moreover, the required PMM printed circuit board (PCB) size used throughout these calculations was assumed to be ten times the size of the BQ25504 chip, to account for any necessary additional components.

Fig. 14 shows the output dc power density for all the harvesters demonstrated here. It can be seen that the 2G GSM900/1800 harvesters with tape antennas both have the highest value of $S_{\mathrm{harv}} = 7.4$ $(\mu\mathrm{W/cm}^3)$, when tested at ICL, due to the high-banded input RF power density S_{BA}. The value for the most efficient harvester (i.e., 3G v2 with tape antenna) was not the highest in terms of output RF power because S_{BA} in this band was more than an order of magnitude lower than with GSM900.

S_{harv} allows a direct and meaningful comparison to be made with other alternative energy harvesting technologies. Our best performing ambient RF energy harvester (i.e., GSM900 with tape antenna) was compared against alternative energy harvesting technologies, assuming they used the same PMM board size [42]–[44].

It can be seen in Fig. 15 that ambient RF energy harvesting has a low output dc power density when compared to alternative energy harvesting technologies, but only when the total volume of the first prototype demonstrator is considered. However, when the antenna is absorbed onto or into a background feature and when the PMM is fully integrated into the rectifier, it can outperform (as indicated by the dotted column) the alternative energy harvesting technologies, while providing a complimentary means of extracting energy from the environment. The RF harvesters, however, have the additional advantage in that they do not require a thermal gradient, and unlike vibration-driven devices, they have no moving parts.

VII. Conclusions

Our objectives were to reach the lowest possible ambient input RF power levels and extend the harvesters' operational capabilities within (semi-)urban environments. To this end, a comprehensive citywide RF spectral survey was undertaken, indicating that more than 50% of the 270 London Underground stations are suitable locations for the deployment of our ambient RF energy harvesters. It has been demonstrated that single-band harvesters can operate with efficiencies of up to 40% in a (semi-)urban environment, and can start to operate from power levels as low as -25 dBm.

To increase the freedom of operation, multiband array architectures were investigated. With the current summing harvester arrays, RF harvesting was achieved at an input RF power level as low as -29 dBm, without any external dc power supply to hot-start the PMM. Limitations on the multiband array architectures were discussed, highlighting the need for further work in balancing rectennas with voltage summing rectenna arrays when operating at lower input RF power levels.

Finally an output dc power density comparison against alternative energy harvesting technologies has shown that RF harvesting can represent a competitive solution within (semi-)urban environments, especially when the antenna can be absorbed into background features.

Acknowledgment

The authors would like to thank the members of the London RF survey team and F. Kusidlo, Agilent EEsof EDA, for his advice regarding simulations.

REFERENCES

[1] "Demonstration of microwave power transmission," *Pract. Wireless*, pp. 835–835, 1965.

[2] T. Salter, G. Metze, and N. Goldsman, "Parasitic aware optimization of an RF power scavenging circuit with applications to smartdust sensor networks," in *IEEE Radio Wireless Symp.*, 2009, pp. 332–335.

[3] "SENSIMED Triggerfish®—Continuous IOP monitoring," SENSIMED, Lausanne, Switzerland, Mar. 2012. [Online]. Available: http://www.sensimed.com/S-Trig-glaucoma.htm, , "

[4] M. Pinuela, D. C. Yates, S. Lucyszyn, and P. D. Mitcheson, "Maximizing DC-to-load efficiency for inductive power transfer," *IEEE Trans. Power Electron.*, vol. 28, no. 5, pp. 2437–2447, May 2013.

[5] W. Joseph, G. Vermeeren, L. Verloock, M. M. Heredia, and L. Martens, "Characterization of personal RF electromagnetic field exposure and actual absorption for the general public," *Health Phys.*, vol. 95, no. 3, pp. 317–330, Sep. 2008.

[6] G. Thuroczy, F. Molnar, J. Szabo, G. Janossy, N. Nagy, G. Kubinyi, and J. Bakos, "Public exposure to RF from installed sources: Site measurements and personal exposimetry," in *1st Eur. Antennas Propag. Conf.*, 2006, pp. 1–4.

[7] P. Elliott, M. B. Toledano, J. Bennett, L. Beale, K. de Hoogh, N. Best, and D. J. Briggs, "Mobile phone base stations and early childhood cancers: Case-control study," *Br. Med. J.*, vol. 340, no. 1, pp. 1–7, Jun. 2010.

[8] N. Shinohara, "Power without wires," *IEEE Microw. Mag.*, vol. 12, no. 7, pp. S64–S73, Dec. 2011.

[9] J. Y. Park, S. M. Han, and T. Itoh, "A rectenna design with harmonic-rejecting circular-sector antenna," *IEEE Antennas Wireless Propag. Lett.* , vol. 3, pp. 52–54, 2004.

[10] "Dengyo rectennas," Nihon Dengyo Kosaku Company Ltd., Tokyo, Japan, Jul. 2012. [Online]. Available: http://www.den-gyo.com/solution/solution01.html

[11] T. Le, K. Mayaram, and T. Fiez, "Efficient far-field radio frequency energy harvesting for passively powered sensor networks," *IEEE J. Solid-State Circuits*, vol. 43, no. 5, pp. 1287–1302, May 2008.

[12] V. Marian, B. Allard, C. Vollaire, and J. Verdier, "Strategy for microwave energy harvesting from ambient field or a feeding source," *IEEE Trans. Power Electron.*, vol. 27, no. 11, pp. 4481–4491, Nov. 2012.

[13] C. Mikeka, H. Arai, A. Georgiadis, and A. Collado, "Dtv band micropower RF energy-harvesting circuit architecture and performance analysis," in *IEEE Int. RFID-Technol. Appl. Conf.*, 2011, pp. 561–567.

[14] S. Kitazawa, H. Ban, and K. Kobayashi, "Energy harvesting from ambient RF sources," in *IEEE MTT-S Int. Microw. Symp. Workshop*, 2012, pp. 39–42, Series on Innovative Wireless Power Transmission: Technol., Syst., Appl..

[15] R. Vyas, V. Lakafosis, and M. Tentzeris, "Wireless remote localization system utilizing ambient RF/solar power scavenging RFID tags," in *IEEE MTT-S Int. Microw. Symp. Dig.*, May 23–28, 2010, pp. 1764–1767.

[16] H. Nishimoto, Y. Kawahara, and T. Asami, "Prototype implementation of ambient RF energy harvesting wireless sensor networks," *IEEE Sens. J.*, pp. 1282–1287, Nov. 2010.

[17] A. Sample and J. R. Smith, "Experimental results with two wireless power transfer systems," in *IEEE Radio Wireless Symp.*, 2009, pp. 16–18.

[18] V. Nitu, G. Lojewski, and S. Nitu, "Electromagnetic field evaluation on an antennas shared site, EUROCON 2009," in *IEEE EUROCON'09*, 2009, pp. 70–75.

[19] Y. Kawahara, K. Tsukada, and T. Asami, "Feasibility and potential application of power scavenging from environmental RF signals," in *IEEE AP-S Int. Symp.*, 2009, pp. 1–4.

[20] H. J. Visser, A. C. F. Reniers, and J. A. C. Theeuwes, "Ambient RF energy scavenging: GSM and WLAN power density measurements," in *38th Eur. Microw. Conf.*, 2008, pp. 721–724.

[21] T. G. Cooper, S. M. Mann, M. Khalid, and R. P. Blackwell, "Public exposure to radio waves near GSM microcell and picocell base stations," *J. Radiol. Protection*, vol. 26, no. 2, pp. 199–211, 2006.

[22] "FieldFox RF Analyser N9912A 4/6 GHz," Agilent Technol., Santa Clara, CA, USA, Tech. Overview, 2012.

[23] "Biconical EMC broadband antennas—BicoLOG Series," Aaronia, Strickscheid, Germany, Data Sheet, 2012.

[24] "Digital TV switchover in the UK," Digital UK Ltd., London, U.K., 2012.

[25] "International commission on non-ionizing radiation protection, guidelines for limiting exposure to time- varying electric, magnetic, and electromagnetic fields (up to 300 GHz)," *Health Phys.*, vol. 74, no. 4, pp. 494–522, 1998.

[26] M. Riederer, "EMF exposure due to GSM base stations: measurements and limits," in *IEEE Int. Electromagn. Compat. Symp.*, 2003, vol. 1, pp. 402–405.

[27] "Revised ECC recommendation (02)04: Measuring non-ionising electromagnetic radiation (9 kHz−300 GHz)," ECC within the Eur. CEPT, Oct. 2003.

[28] Nat. Freq. Planning Group, "United Kingdom frequency allocation table, issue no. 16," 2010, Cabinet Official Committee on U.K. Spectrum Strategy.

[29] Transport for London, "London underground map," Aug. 2012. [Online]. Available: http://www.tfl.gov.uk/gettingaround/1106.aspx

[30] Imperial College London, "London RF Survey," Aug. 2012. [Online]. Available: http://londonrfsurvey.org/

[31] R. Vyas, V. Lakafosis, M. Tentzeris, H. Nishimoto, and Y. Kawahara, "A battery-less, wireless mote for scavenging wireless power at UHF (470–570 MHz) frequencies," in *IEEE AP-S Int. Symp./USNC/URSI Nat. Radio Sci. Meeting*, Jul. 3–8, 2011, pp. 1069–72.

[32] T. Ungan and L. M. Reindl, "Harvesting low ambient RF-sources for autonomous measurement systems," in *Proc. IEEE Instrum. Meas. Technol. Conf.*, 2008, pp. 62–65.

[33] A. Costanzo, A. Romani, D. Masotti, N. Arbizzani, and V. Rizzoli, "RF/baseband co-design of switching receivers for multiband microwave energy harvesting," *Sensors Actuators A, Phys.*, vol. 179, pp. 158–168, Jun. 2012.

[34] J. L. Volakis, *Antenna Engineering Handbook*. New York, NY, USA: McGraw-Hill, 2007.

[35] M. Pinuela, P. D. Mitcheson, and S. Lucyszyn, "Analysis of scalable rectenna configurations for harvesting high frequency ambient radiation," in *Proc. Power MEMS*, Leuven, Belgium, 2010, pp. 41–44.

[36] J. O. McSpadden, L. Fan, and K. Chang, "Design and experiments of a high-conversion-efficiency 5.8-GHz rectenna," *EEE Trans. Microw. Theory Techn.*, vol. 46, no. 12, pp. 2053–2060, Dec. 1998.

[37] "HSMS-285x series datasheet," Avago Technol., San Jose, CA, USA, 2009.

[38] "Ultra low power boost converter with battery management for energy harvester applications," Texas Instruments Incorporated, Dallas, TX, USA, BQ25540 Datasheet, 2011.

[39] A. Nimo, D. Grgic, and L. M. Reindl, "Ambient electromagnetic wireless energy harvesting using multiband planar antenna," in *IEEE 9th Int. Syst., Signals, Devices Multi-Conf.*, Mar. 20–23, 2012, pp. 1, 6.

[40] H. Takhedmit, L. Cirio, B. Merabet, B. Allard, F. Costa, C. Vollaire, and O. Picon, "A 2.45-GHz dual-diode rectenna and rectenna arrays for wireless remote supply applications," *Int. J. Microw. Wireless Technol.*, vol. 3, no. 3, pp. 251–258, Jun. 2011.

[41] S. Vemuru, P. Singh, and M. Niamat, "Modeling impact of bypass diodes on photovoltaic cell performance under partial shading," in *IEEE Int. Electro/Information Technol. Conf.*, 2012, pp. 1–5.

[42] P. D. Mitcheson, E. M. Yeatman, G. K. Rao, A. S. Holmes, and T. C. Green, "Energy harvesting from human and machine motion for wireless electronic devices," *Proc. IEEE*, vol. 96, no. 9, pp. 1457–1486, Sep. 2008.

[43] R. J. M. Vullers, R. V. Schaijk, H. J. Visser, J. Penders, and C. V. Hoof, "Energy harvesting for autonomous wireless sensor networks," *IEEE Solid-State Circuits Mag.*, vol. 2, no. 2, pp. 29–38, Spring, 2010.

[44] V. Leonov, P. Fiorini, S. Sedky, T. Torfs, and C. Van Hoof, "Thermoelectric MEMS generators as a power supply for a body area network," in *13th Int. Solid-State Sens., Actuators, Microsyst. Conf. Tech. Dig.*, vol. 1, pp. 291–294.

Manuel Piñuela (M'12) received the BSc. degree in electrical and electronic engineering from the National Autonomous University of Mexico (UNAM), Mexico City, Mexico, in 2007, and is currently working toward the Ph.D. degree at Imperial College London, London, U.K.

From 2006 to 2009, he worked in industry as an Electronic Design and Project Engineer for companies focused on oil and gas services in both Mexico and the US. His research interests are wireless power transfer, RF power amplifiers, and RF energy harvesting.

Mr. Piñuela was the recipient of the Gabino Barrera Medal.

Paul D. Mitcheson (SM'12) received the M.Eng. degree in electrical and electronic engineering and Ph.D. degree from Imperial College London, U.K., in 2001 and 2005, respectively.

He is currently a Senior Lecturer with the Control and Power Research Group, Electrical and Electronic Engineering Department, Imperial College London. His research interests are energy harvesting, power electronics, and wireless power transfer. He is involved with providing power to applications in circumstances where batteries and cables are not suitable. His work has been sponsored by the European Commission, EPSRC and several companies.

Dr. Mitcheson is a fellow of the Higher Education Academy.

Stepan Lucyszyn (M'91–SM'04) received the Ph.D. degree in electronic engineering from King's College London (University of London), London, U.K., in 1992, and the D.Sc. (higher doctorate) degree from Imperial College London, London, U.K., in 2010.

He is currently a Reader (Associate Professor) of millimeter-wave electronics and Director of the Centre for Terahertz Science and Engineering, Imperial College London. After working in industry as a Satellite Systems Engineer for maritime and military communications, he spent the first 12 years researching microwave and millimeter-wave RF integrated circuits (RFICs)/monolithic microwave integrated circuits (MMICs), followed by RF microelectromechanical systems (MEMS) technologies. He has coauthored approximately 140 papers and 11 book chapters in applied physics and electronic engineering. He has delivered many invited presentations at international conferences.

Dr. Lucyszyn was an associate editor for the JOURNAL OF MICROELECTROMECHANICAL SYSTEMS (2005–2009). In 2011, he was the chairman of the 41st European Microwave Conference, Manchester, U.K. In 2005, he was elected Fellow of the Institution of Electrical Engineers (IEE), U.K., and Fellow of the Institute of Physics, U.K. In 2008, was invited as a Fellow of the Electromagnetics Academy, USA. In 2009, he became an IEEE Distinguished Microwave Lecturer (2010–2012). He is currently an Emeritus DML for 2013 and a newly appointed European Microwave Lecturer (EML) for the European Microwave Association.

cogent engineering

ELECTRICAL & ELECTRONIC ENGINEERING | RESEARCH ARTICLE

A dual-band RF energy harvesting circuit using 4th order dual-band matching network

Sachin Agrawal[1]*, Manoj S. Parihar[1] and P.N. Kondekar[1]

Received: 06 March 2017
Accepted: 12 May 2017
First Published: 20 May 2017

*Corresponding author: Sachin Agrawal, PDPM-Indian Institute of Information Technology, Design and Manufacturing, Jabalpur 482005, India
E-mail: bitssachin.agrawal@gmail.com

Reviewing editor:
Wei Meng, Wuhan University of Technology, China

Additional information is available at the end of the article

Abstract: A novel compact rectifier for dual-band operation in the RF energy harvesting is presented. The circuit comprises a 4th order dual-band impedance matching and a single-series circuit with one double diode, both are integrating into a compact shape to occupy a small area of $30 \times 35\ \text{mm}^2$. The merit of the proposed rectifier circuit is that it can be extended to n number of the frequency band by using only $2 \times n$ matching elements. To validate the design method experimentally, a prototype of a dual-band rectifier is fabricated for two public telecommunication bands of GSM-900 and 1800. In order to reduce the circuit complexity and sensitivity arising due to lumped elements, the meander line and the open stub are used to realize the proposed circuit. A good agreement is obtained between the simulation and the measurement. The measured results show that the proposed rectifier circuit exhibits the conversion efficiency of 25.7 and 65% for an input power of –20 and 0 dBm, respectively. In addition, diode nonlinearity which affects the performance of the rectifier in terms of impedance matching is also investigated.

Subjects: Electromagnetics & Microwaves; Electronics; Circuits & Devices

Keywords: RF energy harvesting; dual band impedance matching; rectifier; RF-to-dc-conversion efficiency; frequency transformation

Sachin Agrawal

ABOUT THE AUTHOR

Sachin Agrawal did his BE and ME from Jiwaji University and Birla Institute of Technology Pilani, India in 2005 and 2009, respectively. Currently, he is pursuing his PhD from PDPM-Indian Institute of Information Technology Design and Manufacturing Jabalpur, India. His area of interest are; RF energy harvesting circuit, Antenna including planar and dielectric resonator antenna and Power amplifier.

PUBLIC INTEREST STATEMENT

With rapid growth in wireless communication, a huge amount of radio frequency (RF) energy broadcasted through billions of microwave sources such as mobile phones, handheld radios, and radio broadcast stations. Therefore, it is meaningful to collect and supply it to many electrical devices like mobile headsets, wearable medical sensors through RF energy harvesting. Since the ambient RF energy is distributed in multiple frequency bands, therefore the amount of energy harvested could increase if the circuit is designed for multiple frequency bands. In this work, we present a compact dual-band energy harvesting circuit to harvest energy from two most useful frequency bands, GSM-900 and 1800. The merit of the proposed rectifier circuit is it can be extended to n number of the frequency band by using only $2 \times n$ matching elements. A prototype is fabricated, and its performance is evaluated using Vector Network Analyzer (VNA). The total size of the rectifier is about $30 \times 35\ \text{mm}^2$.

1. Introduction

A revolutionary growth in wireless technology attracts huge attention from research community to make the self-sustainable device feasible through RF energy harvesting. It exploits ambient electromagnetic energy transmitted from different RF systems to remotely feed the electronic devices (Nintanavongsa, Muncuk, Lewis, & Chowdhury, 2012). Compared to other harvesting techniques, RF energy harvesting provides relatively predictable energy supply owing to the features of easy availability and less dependency on environmental variations. The typical block diagram of RF energy harvesting circuit is shown in Figure 1. It consists of three major blocks viz; antenna, matching network (MN), diode detector followed by an energy storage. The first element, antenna is employed to capture the RF signals of different frequencies and polarization, while second MN is for maximum power transfer, and the last rectifier is used to convert the RF energy to dc voltage. It means harvesting circuit performance can be evaluated in terms of accessible ambient RF energy and its conversion rate (Agrawal, Pandey, Singh,& Parihar, 2014). These parameters are heavily influenced by surrounding terrain conditions as the multiple reflection and dissipation certainly deteriorate the level of available ambient RF energy. As a result, conversion efficiency and dc output voltage may degrade. Previously, the majority of available RF energy harvesting circuits focused on single frequency band hence offer low dc output voltage. As the multiple RF energy sources of different frequency bands are available, thus from an ambient RF harvesting perspective, the output dc voltage could be increased if the circuit is designed for multiple frequency bands rather than a single band. A wide-band energy harvester can also promise a high output voltage by accumulating the number of RF signals at a time. However, due to nonlinear behavior of the diode, harvesting circuit itself exhibits nonlinearity i.e. its input impedance varies with the received RF power. Thus, it is quite difficult to retain the impedance match and high conversion efficiency over a large frequency range (Song, Huang, Zhou, & Carter, 2014). The losses due to impedance mismatch over a large bandwidth can be illustrated in Collado and Georgiadis (2013), where only 8% conversion efficiency is achieved at -20 dBm.

To address this, it is preferable to harvest energy from several narrow frequency bands rather than a single large one. In literature, numerous topologies have been proposed to accomplish the multi-band energy harvesting (Bergès, Fadel, Oyhenart, Vigneras, & Taris, 2015; Hamano et al., 2016; Ho et al., 2016; Keyrouz, Visser, & Tijhuis, 2013; Kuhn, Lahuec, Seguin, & Person, 2015; Liu, Zhong, & Guo, 2015; Niotaki, Georgiadis, Collado, & Vardakas, 2014; Pinuela, Mitcheson, & Lucyszyn, 2013; Scheeler, Korhummel, & Popovic, 2014; Shariati, Rowe, Scott, & Ghorban, 2015; Sun, Guo, He, & Zhong, 2013). These topologies can be differentiated in terms of filter functionality i.e. how the antenna or source impedance is matched to the rectifier circuit. For instance, in Pinuela et al. (2013) and Keyrouz et al. (2013) several single-band rectennas (combination of antenna and rectifier circuit) were stacked to constitute a multi-band harvesting circuit. In this case, each rectenna was designed for a specific frequency band. Thus, for compact applications, this architecture is not suitable due to the number of antennas used. Moreover, in most of the reported works, the quality assessment of the output voltages combination was not taken into consideration. In Kuhn et al. (2015), the circuit complexity is reduced to a certain extent by replacing the multiple antennas with a single wide-band antenna. However, in this topology too, the number of rectifiers increases with the frequency bands, which leads to prolonging the circuit complexity.

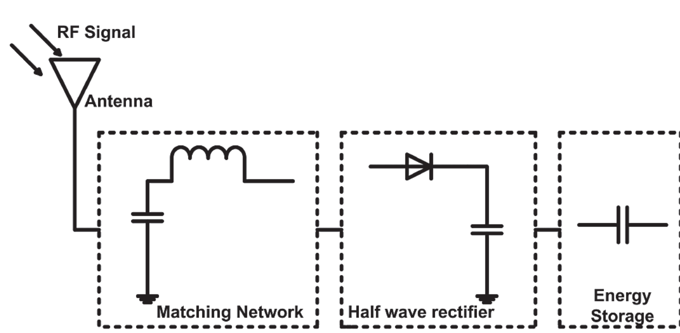

Figure 1. Typical block diagram of RF energy harvesting circuit.

Besides, a multi-band harvesting circuit can also be formed by simply embedding a multi-band matching network between the multi-band antenna and the rectifying circuit (Bergès et al., 2015; Hamano et al., 2016; Ho et al., 2016; Liu et al., 2015; Niotaki et al., 2014; Scheeler et al., 2014; Shariati et al., 2015; Sun et al., 2013). The multi-band matching network can be designed either by distributed or by lumped element. In general, the multi-band rectifier circuit experiences two types of losses: first due to shift in resonance frequency from the optimum frequency point, and second due to the filter complexity. Because of the diode nonlinearity, the input impedance of the circuit varies as a function of power and frequency which causes a shift in resonance frequency. The difficulty due to diode nonlinearity can be observed in Sun et al. (2013) where the dual-band rectifier circuit exhibits its impedance matching for a small range of input power. The losses induced because of filter complexity can be observed in the recently reported works on dual band harvesting circuit (Niotaki et al., 2014; Scheeler et al., 2014; Shariati et al., 2015). In Niotaki et al. (2014), for $P_{\text{in}} = -15$ dBm, author achieved the conversion efficiency of 23% at the expense of increased filter complexity consisting two series and two shunt pairs of reactive elements. Thus, for more than dual band applications, the proposed circuit topology is not suitable due to excessive filtering components used. To obtain good conversion efficiency a dual-band rectenna reported in Scheeler et al. (2014). However, the rectenna was large in size and requiring a complex impedance tuning circuit. In Shariati et al. (2015) also, a dual-band matching network consisting nine reactive elements was employed to achieve the dual-band characteristics.

In order to reduce the filter complexity, this work proposed a compact dual-band harvesting circuit for GSM-900 and 1800. It consists of a 4th order dual-band matching network based on $1-n$ frequency transformation, which is optimized for the energy harvesting circuit to reduce the complexity up to $2 \times n$ reactive elements (n is the number of frequency bands). Similar to frequency transformation method, the proposed dual-band rectifier circuit can be extended to n number of frequency bands by using the $2 \times n$ number of reactive elements. The detailed analysis and design guidelines of dual band rectifier circuit are discussed in Section 2.

2. Dual band rectifier design and analysis

This section presents the design and analysis of a dual-band harvesting circuit in terms of impedance matching, DC output voltage and RF-to-dc conversion efficiency. The topology of the proposed dual-band RF energy harvesting circuit is shown in Figure 2(a). As seen, the low-cost Schottky diode is used to transform the input RF power to DC voltage. The impedance matching at two frequency is achieved using a series and parallel combination of the *LC* pair. The main idea underlying the suggested multi-band matching network is $1-n$ frequency transformation (one to many mapping of frequency), which transforms a single-band matching network to multi-band matching network (Nallam & Chatterjee, 2013). As the name ($1-n$) suggests that for designing a multi-band matching network, primarily a single-band matching network is required whose resonant frequency is dependent on the frequencies for which multi-band matching network proposed to designed.

Moreover, this frequency transformation method depends on the type of load impedance, whether it is series or parallel combination of *RC* or *RL*. Since the selected diode (HSMS-2852) has capacitive behavior throughout the frequency, it can be represented in a series or parallel combination of *R* and *C*. In the case of parallel *RC* load, the following equations are used to transform the single-band matching network into multi-band matching network.

$$\omega = \frac{\omega_t^n + a_m \omega_t^{n-m} + a_{m+2}\omega_t^{n-(m+2)} + \cdots}{\omega_t^{n-1} + a_{m+1}\omega_t^{n-(m+1)} + a_{m+3}\omega_t^{n-(m+3)} + \cdots} \tag{1}$$

where, n is the number of bands and m varies from 2 to n. After substituting the value of n, Equation (1) can be expanded in partial fraction form using the causal foster analysis as:

$$\omega = \omega_t + \frac{1}{\frac{\omega_t}{a_2 - a_3} + \frac{1}{\cdots}} \tag{2}$$

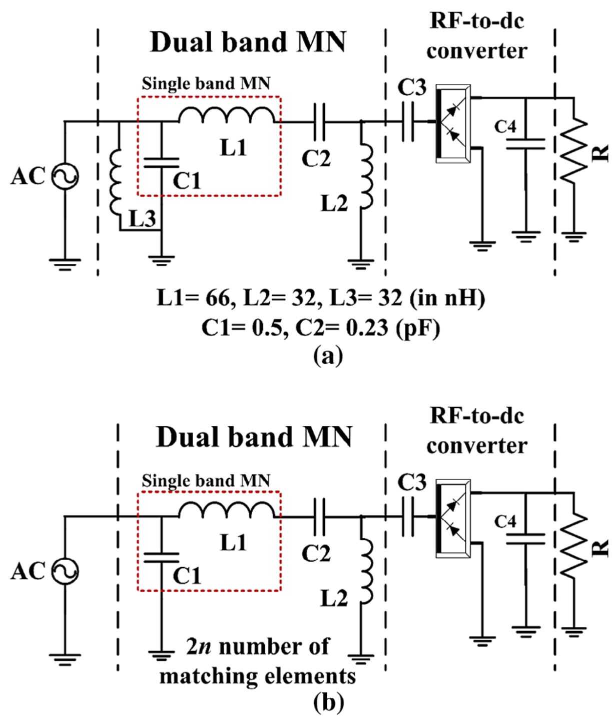

Figure 2. (a) Circuit diagram of the proposed dual-band rectifier circuit and (b) optimized dual-band rectifier circuit.

The coefficients a_2 and a_3 can be calculated as:

$$\omega_m = \sum_{i=1}^{n} (-1)^{i-1} \omega_i \tag{3}$$

$$a_m = (-1)^m \sum_{i,j=1,1\,\&\,i\neq j}^{n,n} (-1)^{i+j} \omega_i \omega_j \tag{4}$$

$$a_{m+1} = (-1)^{m+1} \sum_{i,j,k=1,1,1\,\&\,i\neq j\neq k}^{n,n,n} (-1)^{i+j+k} \omega_i \omega_j \omega_k \tag{5}$$

$$a_{m+n} = (-1)^{m+n} \sum_{i,j,k\ldots=1,1,1\ldots i\neq j\neq k}^{n,n,n\ldots} (-1)^{i+j+k+\cdots} \omega_i \omega_j \omega_k \ldots \tag{6}$$

$$a_n = \prod_{i=1}^{n} (-1)^n \omega_i \tag{7}$$

Equation (6) is similar to that presented in Nallam and Chatterjee (2013), except the term $(-1)^{m+n}$, which is included here to realize the multi-band matching network for more than three frequency bands i.e. for $n \geq 3$.

With this transformation, the capacitor of the matching network is transformed to the combination of prototype capacitor parallel with inductor whereas, an inductor is transformed into a combination of the same inductor with a series capacitor. Figure 3 shows the circuit schematic of transformation of a single-band matching network to the dual-band matching network. It can be seen that C_1 is transformed to $C_1 \| L_2$ and L_1 transformed to L_1 series with C_2. After successful usage of (1)–(7), the resultant multi-band matching network requires $3n - 1$ and $4n - 1$ reactive elements for L and Π-type topology, respectively.

Figure 3. Conversion of a single-band matching network to dual-band matching network using $1 - n$ frequency transformation.

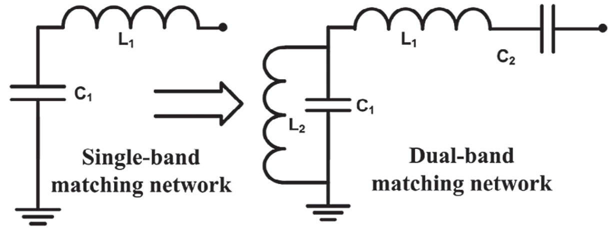

As the aim is to design a dual-band harvesting circuit, therefore, we require here only 5 or 7 reactive elements with L and Π-type topologies, respectively. From Figure 2(a), it can be seen that the resultant matching network consists of five elements, where the inductor L_3 and capacitor C_2 results after the transformation of capacitor C_1 and inductor L_1, respectively. Besides, the inductor L_2 occurrs due to the diode reactive element, which is generally a capacitor.

In this work, two frequencies 0.9 and 1.8 GHz that correspond to the maximum signal strength are chosen for dual-band harvesting circuit. According to this method, it is necessary to assign the frequencies in descending order e.g. $\omega_1 = 1.8, \omega_2 = 0.9$. Therefore, from (3) single-band matching network frequency is equal to $\omega_1 - \omega_2 = 2\pi(1.8 - 0.9) \times 10^9 = 0.9 \times 2\pi \times 10^9$. In order to match the source impedance with the rectifier at the calculated frequency 0.9 GHz, the chosen matching topology is L-type as shown by the encircled portion in Figure 2(a). The corresponding element values can be approximated using the various methods some of which are described in Pozar (2010). Subsequently, this single-band matching network is transformed to dual-band matching network using (1)–(7). The detailed design steps of the dual-band rectifier circuit are summarized as follows:

(1) As we are interested in matching the diode to 50 Ω at two frequencies (0.9 and 1.8 GHz) so, the order of transformation is equal to 2 or $n = 2$.

(2) In the first step, single-band matching network is designed at the frequency f calculated as: $f = f_2 - f_1 = 1.8 - 0.9 = 0.9$ GHz. In this case, any matching topology that matches the diode to 50 Ω, at 0.9 GHz for an input power $P_{in} = -20$ dBm, and load resistance 4.7 kΩ can be used. The chosen single-band matching network is shown by the encircled portion in Figure 2(a).

(3) Afterwards, this single-band matching network is transformed into dual-band using the (1)–(7) as shown below:

Since n = 2 therefore, from (2)

$$\omega = \omega_t + \frac{1}{\frac{\omega_t}{a_2}} \tag{8}$$

From (4) a_2 can be calculated as:

$$a_2 = (-1)^{2+2} \sum (-1)^{1+2} \omega_1 \omega_2 = \omega_1 \omega_2 \tag{9}$$

$$a_2 = -1.62 \times 4\pi^2 \times 10^8 = 0.64 \times 10^{20} \tag{10}$$

Thus, inductor L_1 (=66 nH) is transformed to impedance as:

$$j66 \times 10^9 \omega = j66 \times 10^9 \omega_t + \frac{1}{j0.23 \times 10^{-12} \omega_t} \tag{11}$$

Similarly, capacitors (=0.5 pF) are transformed to the admittance as:

$$j5 \times 10^{-13} \omega = j5 \times 10^{-13} \omega_t + \frac{1}{j32 \times 10^{-9} \omega_t} \tag{12}$$

The circuit schematic of the dual-band harvesting circuit is shown in Figure 2(a). It can be seen that resultant matching network consists of five reactive elements according to $3n - 1$. In order to reduce the circuit complexity and sensitivity due to reactive elements, a parametric study has been carried out to eliminate the elements showing minimum influence on the circuit performance.

Figure 4 shows the simulated $|S_{11}|$ for the different combination of matching elements. The simulated results demonstrate that $|S_{11}|$ experiences maximum change when inductor L_2 and capacitor C_2 are removed from the circuit, whereas it remains almost unaffected when L_3 is not present in the circuit. Therefore, inductor L_3 can be extruded from the circuit and the resultant matching circuit requires only $2n$ and $3n$ reactive elements in place of $3n - 1$ and $4n - 1$ elements. In this way, for each topology, the proposed circuit reduces $n - 1$ elements compared to the conventional method. Figure 2(b) demonstrates the optimized circuit diagram of the dual-band rectifier. It can be observed that circuit requires large inductors value of 32 and 66 nH. Thus, it is quite difficult to realize the practical rectifier circuit whose response is similar to the response of simulated result. In order to avoid any impedance mismatch due to the small difference in elements value, the meander line inductor and open stub are used to realize the inductors and capacitors, respectively. In this case, not only fabrication and optimization process become so easy but the cost will also reduced.

Figure 5, shows the layout of the dual-band rectifier circuit. In Nintanavongsa et al. (2012) and Agrawal et al. (2014), it has been demonstrated that the number of rectifying diodes or equivalently voltage multiplier stages are very much sensitive to the RF-to-dc conversion efficiency. In low-power region (≤ -20 dBm), efficiency decreases if voltage multiplier stages increase, whereas in higher power region (≥ -20 dBm), an opposite effect occurs. As the demand is to harvest energy in low-power region, single-series circuit with a double diode is used to convert received RF energy into dc voltage. From the left side of the circuit, the first meander line corresponds to the inductor L_1, while the second meander line represents the inductor L_2, of the Figure 2(b). The shunt stub is accounted

Figure 4. Simulated $|S_{11}|$ vs. frequency for different combination of circuit elements.

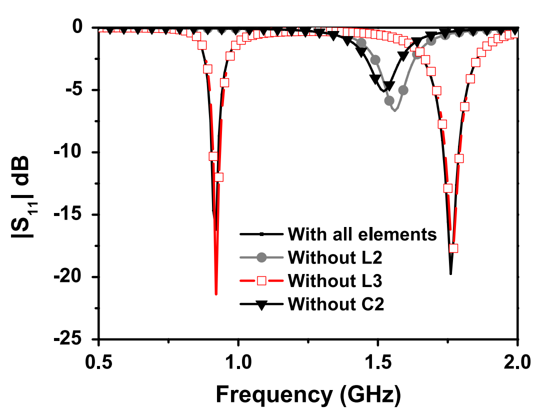

Figure 5. Layout of the proposed dual-band RF energy harvesting circuit.

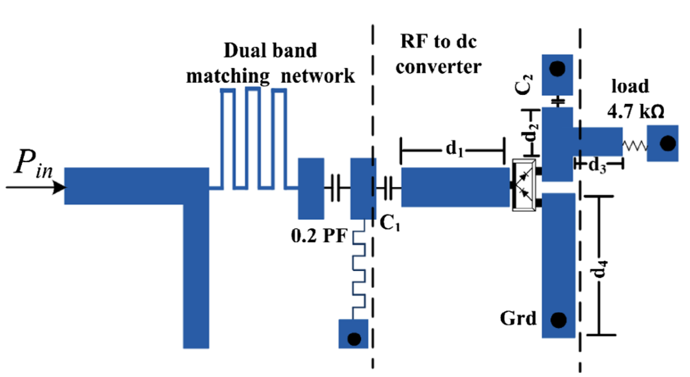

for the shunt capacitor C_1 of Figure 2(b). The dimensions of each element are calculated according to their respective reactive element value and the substrate on which circuit has to be fabricated. In Assimonis, Daskalakis, and Bletsas (2016), it has been demonstrated that traces (microstrips) connected to the rectifier terminals (e.g. distance between the diode and via and diode and load) are highly sensitive for RF-to-dc efficiency. Therefore, traces d_1, d_2 between diode and capacitor C_1 and C_2, d_3 between diode and load and d_4 between diode and ground are adjusted to optimize the impedance matching as well as the conversion efficiency of the rectifier. Due to nonlinear behavior of the diode, harvesting circuit itself exhibits nonlinearity i.e. its input impedance varies with received RF power, therefore harmonic-balance (HB) and large signal analysis (LSSP) were employed to take into consideration the nonlinear behavior of the rectifier.

The photograph of the fabricated dual-band rectifier is shown in Figure 6. It is fabricated on a 1.54 mm thick FR-4 substrate with a dielectric constant (ϵ_r) of 4.3 using chemical etching method. The rectifier performance is evaluated in terms of $|S_{11}|$ and output voltage using the Agilent vector network analyzer (VNA). The simulated and measured $|S_{11}|$ is illustrated in Figure 7(a). The measured result shows reasonable agreement with the simulated one; the slight difference can be accounted for the fabrication imperfections. It is well known that impedance matching is a function of frequency and input power, due to the nonlinearity of the diode. Such a characteristic is examined in Figure 7(b), where the measured $|S_{11}|$ is demonstrated as a function of input power level for three different load impedance values. From results, it is clear that impedance matching of the harvesting circuit is greatly affected by the input power and the load impedance. Figure 7(b) demonstrates that as power increases, the impedance matching at 0.9 GHz degraded drastically, while at 1.8 GHz, it improves. Moreover, it is noticed that the impedance matching at higher power level is more sensitive to the variation of load impedance (*RL*).

The measured RF-to-dc conversion efficiency and output voltage vs. input power for both frequencies are demonstrated in Figure 8(a). For 0.9 GHz, efficiency is equal to 25.7 and 65.1% for an input power of −20 and 0 dBm, respectively. However, at 1.8 GHz the efficiency is relatively small that might be due to the increased parasitic losses in the rectifier diode. Figure 8(b) shows the relation between the output voltage and frequency for various input power levels at fixed load resistance value of 4.7 kΩ. It can be seen that maximum output voltage is achieved in the frequency range of 860–900 and 1770–1800 MHz, showing the rectifier's capability to harvest RF energy in the GSM-900 and 1800 bands.

Figure 9, depicts the measured conversion for various values of load resistance. It can be noticed that the circuit yields maximum efficiency when the load impedance is 4.7 kΩ. It starts decreasing as the load impedance varies from 4.7 kΩ. Table 1 shows the comparison of the conversion efficiency and the size of the proposed rectifier with the similar works reported previously. Only measured results are compared in Table 1. It can be seen that in low-power condition maximum efficiency is achieved in Sun et al. (2013), but the expense of bulky circuit size. However, the proposed rectifier offers an optimal conversion efficiency with compact circuit size.

Figure 6. Photograph of the fabricated dual-band RF energy harvesting circuit.

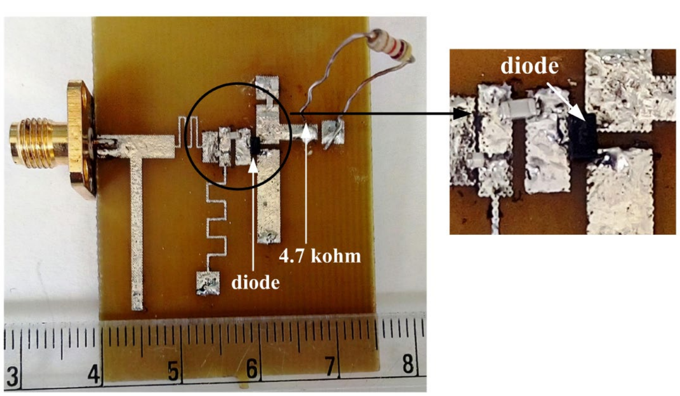

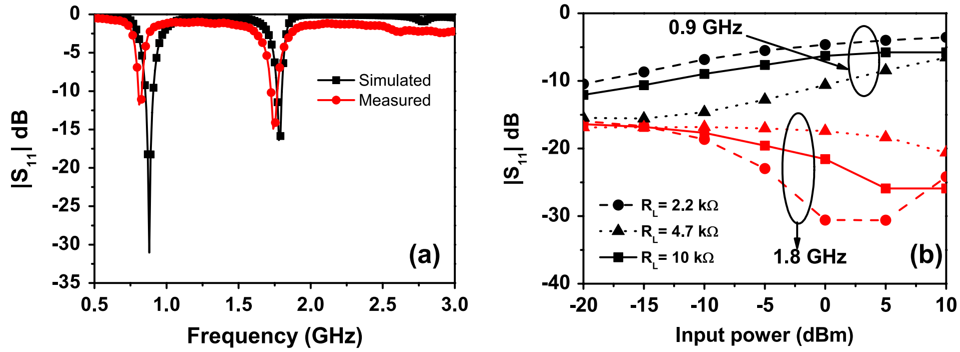

Figure 7. (a) Simulated and measured $|S_{11}|$ vs. frequency and (b) measured $|S_{11}|$ for various power levels.

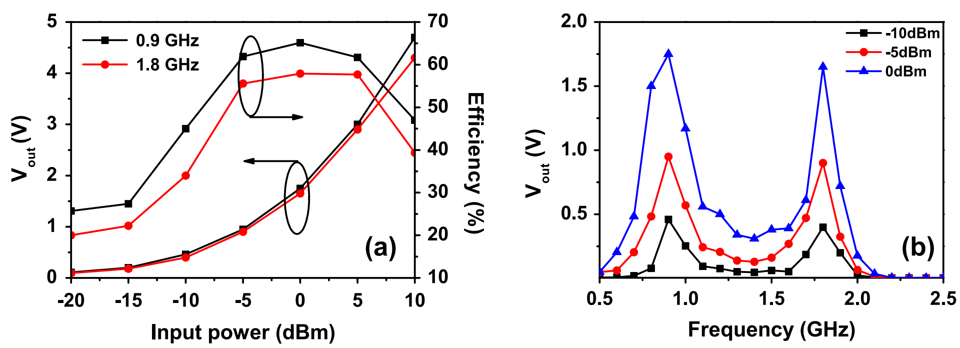

Figure 8. (a) Measured output dc voltage and RF-to-dc conversion efficiency and (b) measured dc voltage vs. frequency.

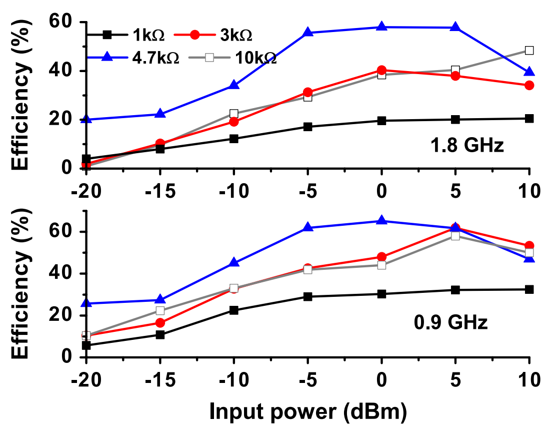

Figure 9. Measured RF-to-dc conversion efficiency for different load impedance.

Table 1. Performance comparison of the proposed dual rectifier with recently published works

Ref.	Measured rectifier efficiency (%)	Input power (dBm)	Rectifier size
Ho et al. (2016)	15.8 @ 0.89 GHz	−20	100 × 65 mm²
	11.2 @ 1.76 GHz		
Hamano et al. (2016)	10 @ 2.15 GHz	−10	37 × 71 mm²
	15 @ 5.84 GHz		
Bergès et al. (2015)	27 @ 0.91/2.4 GHz	−16	78 × 88 mm²
Sun et al. (2013)	30 @ 2.14 GHz	−20	145 mm
	35 @ 1.84 GHz		
Liu et al. (15)	20 @ (0.91+1.8) GHz	−20	23 × 37 mm²
This work	27.5 @ 0.9 GHz	−20	30 × 35 mm²
	20 @ 1.8 GHz		

3. Conclusion

A new compact 4th order dual-band rectifier has been designed to harvest the RF power of GSM-900 and 1800 bands. In order to reduce the circuit complexity and sensitivity due to reactive elements, the meander line and the open stub are used to fabricate the matching network. For $P_{in} = -20$ dBm, the measured RF-to-dc conversion efficiency of 27.5 and 20% is achieved at 0.9 and 1.8 GHz, respectively. Further, more than 45 and 34% conversion efficiency is maintained from -10 to 10 dBm for 0.9 and 1.8 GHz, respectively.

Funding
The authors received no direct funding for this research.

Author details
Sachin Agrawal[1]
E-mail: bitssachin.agrawal@gmail.com
Manoj S. Parihar[1]
E-mail: mparihar@iiitdmj.ac.in
P.N. Kondekar[1]
E-mail: pnkondekar@iiitdmj.ac.in
[1] PDPM-Indian Institute of Information Technology, Design and Manufacturing, Jabalpur 482005, India.

Citation information
Cite this article as: A dual-band RF energy harvesting circuit using 4th order dual-band matching network, Sachin Agrawal, Manoj S. Parihar & P.N. Kondekar, *Cogent Engineering* (2017), 4: 1332705.

References

Agrawal, S., Pandey, S. K., Singh, J., & Parihar, M. S. (2014). *Realization of efficient RF energy harvesting circuits employing different matching technique* (pp. 754–761). Fifteenth International Symposium on Quality Electronic Design, Santa Clara, CA.

Assimonis, S. D., Daskalakis, S. N., & Bletsas, A. (2016). Sensitive and efficient rf harvesting supply for batteryless backscatter sensor networks. *IEEE Transactions on Microwave Theory and Techniques, 64*, 1327–1338.

Bergès, R., Fadel, L., Oyhenart, L., Vigneras, V., & Taris, T. (2015). A dual band 915MHz/2.44 GHz RF energy harvester. *Microwave Conference (EuMC), 2015 European*. IEEE.

Collado, A., & Georgiadis, A. (2013). Conformal hybrid solar and electromagnetic (EM) energy harvesting rectenna. *IEEE Transactions on Circuits and Systems I: Regular Papers, 60*, p. 10.

Hamano, K., Tanaka, R., Yoshida, S., Miyachi, A., Nishikawa, K., & Kawasaki, S. (2016). Design of dual-band rectifier using microstrip spurline notch filter. *Radio-Frequency Integration Technology (RFIT), 2016 IEEE International Symposium on*. IEEE.

Ho, D. K., Kharrat, I., Ngo, V. D., Vuong, T. P., Nguyen, Q. C., & Le, M. T. (2016). *Dual-band rectenna for ambient RF energy harvesting at GSM 900 MHz and 1800 MHz* (pp. 306–310). 2016 IEEE International Conference on Sustainable Energy Technologies (ICSET), Hanoi.

Keyrouz, S., Visser, H., & Tijhuis, A. (2013, April). Multi-band simultaneous radio frequency energy harvesting. *In Antennas and Propagation (EuCAP), 2013 7th European Conference on*, 3058–3061.

Kuhn, V., Lahuec, C., Seguin, F., & Person, C. (2015). A multi-band stacked RF energy harvester with RF-to-DC efficiency up to 84\%. *IEEE Transactions on Microwave Theory and Techniques, 63*, 1768–1778.

Liu, Z., Zhong, Z., & Guo, Y.-X. (2015). Enhanced dual-band ambient RF energy harvesting with ultra-wide power range. *IEEE Microwave and Wireless Components Letters, 25*, 630–632.

Nallam, N., & Chatterjee, S. (2013, June). Multi-band frequency transformations, matching networks and amplifiers. *Circuits and Systems I: Regular Papers, IEEE Transactions on, 60*, 1635–1647.

Nintanavongsa, P., Muncuk, U., Lewis, D., & Chowdhury, K. (2012, March). Design optimization and implementation for rf energy harvesting circuits. *IEEE Journal on Emerging and Selected Topics in Circuits and Systems, 2*, 24–33.

Niotaki, K., Georgiadis, A., Collado, A., & Vardakas, J. S. (2014). Dual-band resistance compression networks for improved rectifier performance. *IEEE Transactions on Microwave Theory and Techniques, 62*, 3512–3521.

Pinuela, M., Mitcheson, P., & Lucyszyn, S. (2013, July). Ambient rf energy harvesting in urban and semi-urban environments. *Microwave Theory and Techniques, IEEE Transactions on, 61*, 2715–2726.

Pozar, D. M. (2010). *Microwave engineering* (3rd ed.). New Delhi: Wiley.

Scheeler, R., Korhummel, S., & Popovic, Z. (2014). A dual-frequency ultralowpower efficient 0.5-g rectenna. *IEEE Microwave Magazine, 15*, 109–114.

Shariati, N., Rowe, W. S., Scott, J. R., & Ghorban, K. (2015). Multi-service highly sensitive rectifier for enhanced RF energy scavenging. *Scientific Reports, 5*, 9655

Song, C., Huang, Y., Zhou, J., & Carter, P. (2014). Improved ultrawideband rectennas using hybrid resistance compression technique. *IEEE Transactions on Antennas and Propagation, 65*, 2057–2062.

Sun, H., Guo, Y. X., He, M., & Zhong, Z. (2013). A dual-band rectenna using broadband Yagi antenna array for ambient RF power harvesting. *IEEE Antennas and Wireless Propagation Letters, 12*, 918–921. doi:10.1109/LAWP.2013.2272873.

Circuits and Systems, **2012, 3, 216-222**
http://dx.doi.org/10.4236/cs.2012.33030 Published Online July 2012 (http://www.SciRP.org/journal/cs)

Optimization of the Voltage Doubler Stages in an RF-DC Convertor Module for Energy Harvesting

Kavuri Kasi Annapurna Devi[1*], Norashidah Md. Din[2], Chandan Kumar Chakrabarty[2]
[1]Department of Electrical and Electronic Engineering, INTI International University, Nilai, Malaysia
[2]Department of Electronics and Communication Engineering, Universiti Tenega Nasional, Kajang, Malaysia
Email: {[*]kavurik.adevi., chandan}@newinti.edu.my, norashidah@uniten.edu.my

Received August 25, 2011; revised March 26, 2012; accepted April 4, 2012

ABSTRACT

This paper presents an optimization of the voltage doubler stages in an energy conversion module for Radio Frequency (RF) energy harvesting system at 900 MHz band. The function of the energy conversion module is to convert the (RF) signals into direct-current (DC) voltage at the given frequency band to power the low power devices/circuits. The design is based on the Villard voltage doubler circuit. A 7 stage Schottky diode voltage doubler circuit is designed, modeled, simulated, fabricated and tested in this work. Multisim was used for the modeling and simulation work. Simulation and measurement were carried out for various input power levels at the specified frequency band. For an equivalent incident signal of –40 dBm, the circuit can produce 3 mV across a 100 kΩ load. The results also show that there is a multiplication factor of 22 at 0 dBm and produces DC output voltage of 5.0 V in measurement. This voltage can be used to power low power sensors in sensor networks ultimately in place of batteries.

Keywords: Energy Conversion; RF; Schottky Diode; Villard; Energy Harvesting

1. Introduction

RF energy harvesting is one type of energy harvesting that can be potentially harvested such as solar, vibration and wind. The RF energy harvesting uses the idea of capturing transmitted RF energy at ambient and either using it directly to power a low power circuit or storing it for later use. The concept needs an efficient antenna along with a circuit capable of converting RF signals to DC voltage. The efficiency of an antenna mainly depends on its impedance and the impedance of the energy converting circuit. If the two impedances aren't matched then it will be unable to receive all the available power from the free space at the desired frequency band. Matching of the impedances means that the impedance of the antenna is the complex conjugate of the impedance of the circuit (voltage doubler circuit).

The concept of energy harvesting system is shown in **Figure 1**, which consists of matching network, RF-DC conversion and load circuits. The authors in [1], used a 2.4 GHz operating frequency with an integrated zero bias detector circuit using BiCMOS technology which produced an output voltage of 1 V into a 1 MΩ load at an input power level of 0 dBm. H. Yan and co-authors revealed that a DC voltage of 0.8 volts can be achieved from a –20 dBm RF input signal at 868.3 MHz through simulation results [2]. In [3], work was carried out on a firm frequency of 900 MHz by matching to a 50 Ω impedance and resonance circuit transformation in front of the Schottky diode which yields an output voltage of over 300 mV at an input power level of 2.5 µ. W. J. Wang, L. Dong and Y. Fu [4] used a Cockcroft-Walton multiplier circuit that produced a voltage level of 1.0 V into a 200 MΩ load for an input power level of less than –30 dBm at a fixed frequency of 2.4 GHz.

The energy conversion module designed in this paper is based on a voltage doubler circuit which can be able to output a DC voltage typically larger than a simple diode rectifier circuit as in [5], in which switched capacitor charge pump circuits are used to design two phase voltage doubler and a multiphase voltage doubler. The module presented in this can function as an AC to DC converter that not only rectifies the input AC signal but also elevates the DC voltage level. The output voltage of the

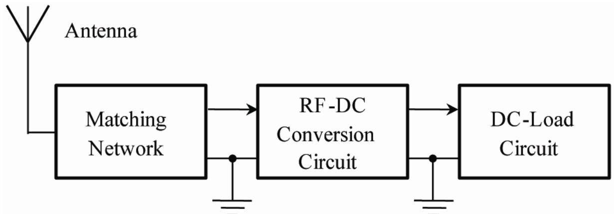

Figure 1. Schematic view of a RF energy harvesting system.

[*]Corresponding author.

energy conversion module can be used to energize the low power devices for example sensors for a sensor network in application to agriculture.

Section 2 of this paper discusses on the theoretical background of the voltage doubler circuit. Section 3 presents the simulation study and implementation of the circuit design. Section 4 provides the results and analysis. Section 5 concludes with a discussion on the findings from the simulated and measured results.

2. Voltage Multiplier

There are various voltage multiplier circuit topologies. The design used in this module is derived from the function of peak detector or a half wave peak rectifier. The Villard voltage multiplier circuit was chosen in the circuit design of this paper because it produces two times of the input signal voltage towards ground at a single output and can be cascaded to form a voltage multiplier with an arbitrary output voltage and its design simplicity.

2.1. Diode Modeling

The voltage multiplier circuit in this design uses zero bias Schottky diode HSMS-2850 from Agilent. The attractive feature of these Schottky diodes are low substrate losses and very fast switching but leads to a fabrication overhead. This diode has been modeled for the energy harvesting circuit which comes in a one-diode configuration. The modeling parameters for these diodes are given by Agilent in their data sheets. These parameters are used in Multisim for its own modeling purposes. The modeling is done by transforming the diode into an equivalent circuit using passive components which are described by the SPICE parameters in **Table 1** [6].

The diode used in this design is shown in **Figure 2** and its equivalent model is shown in **Figure 3**. The special features of HSMS-2850 diode is that it provides a low forward voltage, low substrate leakage and uses the non symmetric properties of a diode that allows unidirectional flow of current under ideal condition.

Table 1. SPICE parameters.

Parameters	Units	HSMS 2850
B_V	V	3.8
C_{J0}	pF	0.18
E_G	Ev	0.69
I_{BV}	A	3E–4
I_S	A	3E–6
N	No unite	1.06
R_S	Ω	25
P_B (V_J)	V	0.35
P_T (XTI)	No units	2
M	No units	0.5

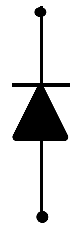

Figure 2. Schottky diode.

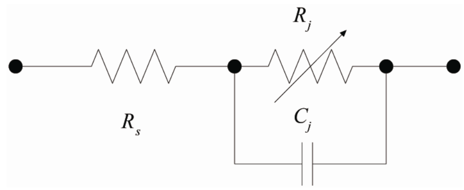

Figure 3. Linear circuit model of the Schottky diode [6].

The diodes are fixed and are not subject of optimization or tuning. This is described using the following derivations. By neglecting the effect of diode substrate, an equivalent linear model that can be used for the diode as shown in **Figure 3**. When C_j is the junction capacitance and R_j is the junction resistance, the admittance Y_z of the linear model is given by

$$Y_Z = Y_{C_j} + Y_{R_j} \tag{1}$$

Equation (1) related to the frequency of operation is given by

$$Y_Z = jwC_j + \frac{1}{R_j} \tag{2}$$

$$= \frac{jwC_jR_j + 1}{R_j} \tag{3}$$

The impedance Z of the linear model is given by

$$Z = \frac{R_j}{1 + jwR_jC_j} \tag{4}$$

The total impedance Z_T is given by

$$Z_T = R_S + \frac{R_j}{1 + jwR_jC_j} \tag{5}$$

where R_S is the series resistance of the circuit and R_j is given by

$$R_j = \frac{8.33 \times 10^{-5} \times N \times T}{I_b + I_S}$$

where:

I_b = bias current in μA;
I_s = saturation current in μA;
T = temperature (K);

N = ideality factor.

In Equation (5), R_j and C_j are constants and the frequency of operation (w) is the only variable parameter. As the frequency increases, the value of Z is almost negligible compared to the series resistance R_S of the diode. From this it is concluded that the function of the diode is independent of the frequency of operation.

2.2. Single Stage Voltage Multiplier

Figure 4 represents a single stage voltage multiplier circuit. The circuit is also called as a voltage doubler because in theory, the voltage that is arrived on the output is approximately twice that at the input. The circuit consists of two sections; each comprises a diode and a capacitor for rectification. The RF input signal is rectified in the positive half of the input cycle, followed by the negative half of the input cycle. But, the voltage stored on the input capacitor during one half cycle is transferred to the output capacitor during the next half cycle of the input signal. Thus, the voltage on output capacitor is roughly two times the peak voltage of the RF source minus the turn-on voltage of the diode.

The most interesting feature of this circuit is that when these stages are connected in series. This method behaves akin to the principle of stacking batteries in series to get more voltage at the output. The output of the first stage is not exactly pure DC voltage and it is basically an AC signal with a DC offset voltage. This is equivalent to a DC signal superimposed by ripple content. Due to this distinctive feature, succeeding stages in the circuit can get more voltage than the preceding stages. If a second stage is added on top of the first multiplier circuit, the only waveform that the second stage receives is the noise of the first stage. This noise is then doubled and added to the DC voltage of the first stage. Therefore, the more stages that are added, theoretically, more voltage will come from the system regardless of the input. Each independent stage with its dedicated voltage doubler circuit can be seen as a single battery with open circuit output voltage V_0, internal resistance R_0 with load resistance R_L, the output voltage, V_{out} is expressed as in Equation (7).

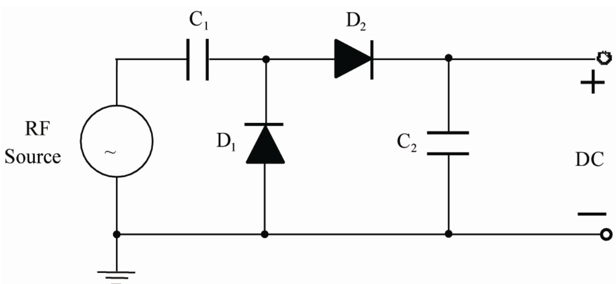

Figure 4. Single stage voltage multiplier circuit [7].

$$V_{out} = \frac{V_0}{R_0 + R_L} R_L \tag{6}$$

When n number of these circuits are put in series and connected to a load of R_L in Equation (6) the output voltage V_{out} obtained is given by this change in RC value will make the time constant longer which in turn retains the multiplication effect of two in this design of seven stage voltage doubler.

$$V_{out} = \frac{nV_0}{nR_0 + R_L} = V_0 \frac{1}{\frac{R_0}{R_L} + \frac{1}{n}} \tag{7}$$

The number of stages in the system has the greatest effect on the DC output voltage, as shown from Equations (6) and (7).

It is inferred that the output voltage V_{out} is determined by the addition of R_0/R_L and $1/n$, if V_0 is fixed. From this analysis it is observed that V_0, R_0 and R_L are all constants. Assume that V_0 = 1 V, R_0/R_L = 0.25, n = 2, 3, 4, 5, 6 and 7, the output voltage V_{out} = 1.33 V, 1.72 V, 2.0 V, 2.22 V, 2.43 V and 2.56 V respectively when substituted analytically in the Equation (7). This analysis can be compared with the results obtained in the circuit design of this module. In simulation at n = 4, V_{out} = 1.42 V, n = 5, V_{out} = 1.67 V; n = 6, V_{out} = 1.92; n = 7, V_{out} = 2.15 V; n = 8, V_{out} = 1.92 V; n = 9, V_{out} = 1.81 V. Also in measurement, for n = 4, V_{out} = 2.1 V; n = 5, V_{out} =2.9 V; n = 6, V_{out} = 3.72 V; and n = 7, V_{out} = 5 V. As n increases, the increase in output voltage will be almost double the input voltage up to some number of stages. But at some point, *i.e.* beyond seven stages, in this circuit the output voltage gained (8 and 9 stages) will be negligible as shown in **Figure 5**.

The capacitors are charged to the peak value of the input RF signal and discharge to the series resistance (R_s) of the diode. Thus the output voltage across the capacitor of the first stage is approximately twice that of the input signal. As the signal swings from one stage to other, there is an additive resistance in the discharge path of the

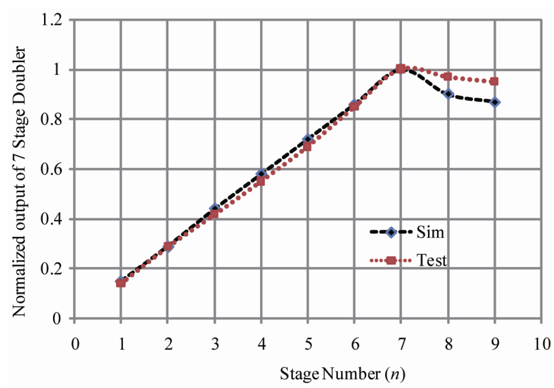

Figure 5. Normalized output voltage multiplier versus number of stages.

diode and increase of capacitance due to the stage capacitors.

2.3. Seven Stage Voltage Multiplier

The seven stage voltage multiplier circuit design implemented in this paper is shown in **Figure 6**. Starting on the left side, there is a RF signal source for the circuit followed by the first stage of the voltage multiplier circuit. Each stage is stacked onto the previous stage as shown in the **Figure 6**. Stacking was done from left to right for simplicity instead of conventional stacking from bottom to top.

The circuit uses eight zero bias Schottky surface-mount Agilent HSMS-285X series, HSMS-2850 diodes. The special features of these diode is that, it provides a low forward voltage, low substrate leakage and uses the non-symmetric properties of a diode that allows unidirectional flow of current under ideal conditions. The diodes are fixed and are not subject of optimization or tuning. This type of multiplier produces a DC voltage which depends on the incident RF voltage. Input to the circuit is a predefined RF source. The voltage conversion can be effective only if the input voltage is higher than the Schottky forward voltage.

The other components associated with the circuit are the stage capacitors. The chosen capacitors for this circuit are of through-hole type, which make it easier to modify for optimization, where in [8] the optimization was accomplished at the input impedance of the CMOS chip for a three stage voltage multiplier. The circuit design in this paper uses a capacitor across the load to store and provide DC leveling of the output voltage and its value only affects the speed of the transient response. Without a capacitor across the load, the output is not a good DC signal, but more of an offset AC signal.

In addition to the above, an equivalent load resistor is connected at the final node. The output voltage across the load decreases during the negative half cycle of the AC input signal. The voltage decreases is inversely proportional to the product of resistance and capacitance across the load. Without the load resistor on the circuit, the voltage would be hold indefinitely on the capacitor and look like a DC signal, assuming ideal components. In the design, the individual components of the stages need not to be rated to withstand the entire output voltage. Each component only needs to be concerned with the relative voltage differences directly across its own terminals and of the components immediately adjacent to it. In this type of circuitry, the circuit does not change the output voltage but increases the possible output current by a factor of two. The number of stages in the system is directly proportional to the amount of voltage obtained and has the greatest effect on the output voltage as explained in the Equation (7) and shown in **Figure 5**.

3. Simulation and Implementation

Multisim software was chosen for modeling and simulation which is a circuit simulation tool by Texas Instruments. The simulation and practical implementation were carried out with fixed RF at 945 MHz ± 100 MHz, which are close to the down link center radio frequency (947.5 MHz) of the GSM-900 transmitter. The voltages obtained at the final node V_{DC} of the multiplier circuit were recorded for various input power levels from –40 dBm - +5 dBm with power level interval (spacing) of 5 dBm.

The simulations were also carried out using same stage capacitance value (3.3 nF) and then with a varied capacitance value for all stages from 4 stages through 9 stages [9]. The capacitance value was varied in such a way that, from one stage to the next, it was halved. For example, if the first stage was 3.3 nF, the second stage was 1.65 nF, third stage was 825 pF, fourth stage was 415 pF and so on. But keeping in view of testing, the capacitance values were chosen to have a close match with the standard available values in the market.

Simulation was carried out through 4 to 9 voltage doubler stages. Based on results obtained a 7 stage doubler is best to implemented for this application.

The design of the printed circuit board (PCB) was carried out using DipTrace software. The material used to

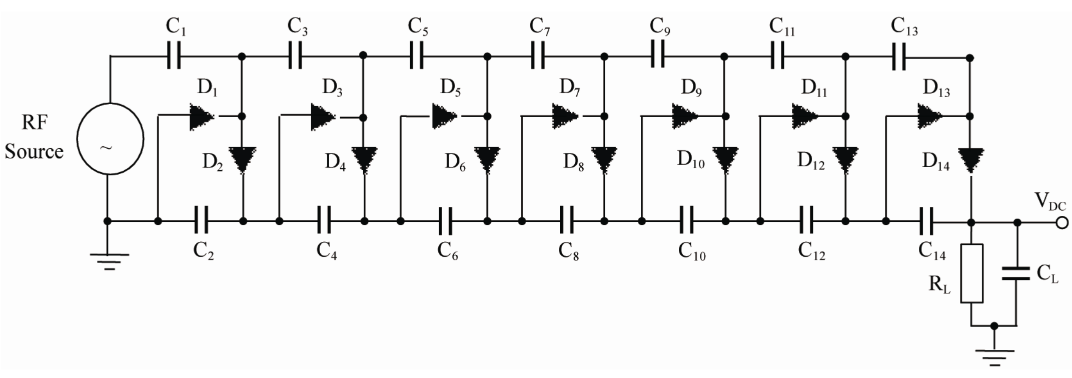

Figure 6. Schematic of 7 stage voltage multiplier.

manufacture the printed circuit board (PCB) is the standard Fiberglass Reinforced Epoxy (FR4), with the thickness of 1.6 mm and dielectric constant of 3.9. The topology is constructed on the PCB with the dimensions of 98 mm × 34 mm (W × H). The Sub Miniature version A (SMA) connectors are used at the input and output of PCB to carry out the measurements. The circuit components consist of active and passive components. The component used in circuit is shown in **Table 2**.

Special handling precautions have been taken to avoid Electro Static Discharge (ESD), while assembling of the surface-mount zero bias Schottky diodes. Also special attention has been given to mount other components and the SMA connectors on to the PCB. The Photograph of Assembled circuit board I shown in **Figure 7**.

4. Results and Analysis

The simulated and measured results at the output voltage of voltage multiplier circuit are shown graphically in **Figure 8**. From the graph analysis, the simulated and the measured results agree considerably with each other. The measured results are shown to be better than the simulation results. The reason behind this may be due to the uncertainty in series resistance value of the diode obtained from SPICE parameters in modeling as explained in Equation (5). This resistance vale of diodes in practical circuit may be lower than in the model, which provides fast discharge path, in turn rise in voltage as passes through the stages and reaches to final output. In this work, the DC output voltages obtained through simulation and measurement at 0 dBm re 2.12 V and 5.0 V respectively. These results are comparatively much better than in ref. [9], where in at 0 dBm, 900 MHz they achieved 0.5 V and 0.8 V through simulation and measurement respectively.

Figures 9 and **10** show the result of a 4 stage voltage doubler circuit with equal and varied capacitance values between the stages as described in Section 3.

From the analysis of these two simulations, it can be observed that the resulting output voltages are equal. The only difference between these two graphs is the rise time of the circuit with varied capacitance value is a little bit slower. But, overall result on the performance of rise time is still under 20 µs to 24 µs and the difference is negligible. From these results, the use of equal stage capacitance of each being 3.3 nF was hence considered for the design of the multiplier.

The results from **Figure 11**, shows that the output voltage reaches to 1.0 V within 20 µS and then uniformly increasing to 1.4 V, 1.67 V, 1.87 V and 2.12 V for 4, 5, 6 and 7 stages respectively compared to 2 mS as shown in [10]. **Figure 12** shows that the conversion ratio of 22 is achieved at 0 dBm input power and drops to 2.5 at –40 dBm. The highest value at 0 dBm is due to the innate characteristics of the zero bias Schottky diodes which conduct fairly well at higher input voltages.

5. Conclusion

From the experimental results, it is found that the pro-

Table 2. Component used in 7 stage voltage multiplier.

Name of component	Label	Value
Stage capacitors	C_1 - C_{14}	3.3 nF
Stage diodes	D_1 - D_{14}	HSMS 2850
Filter capacitor	C_L	100 nF
Load resister	R_L	100 kΩ

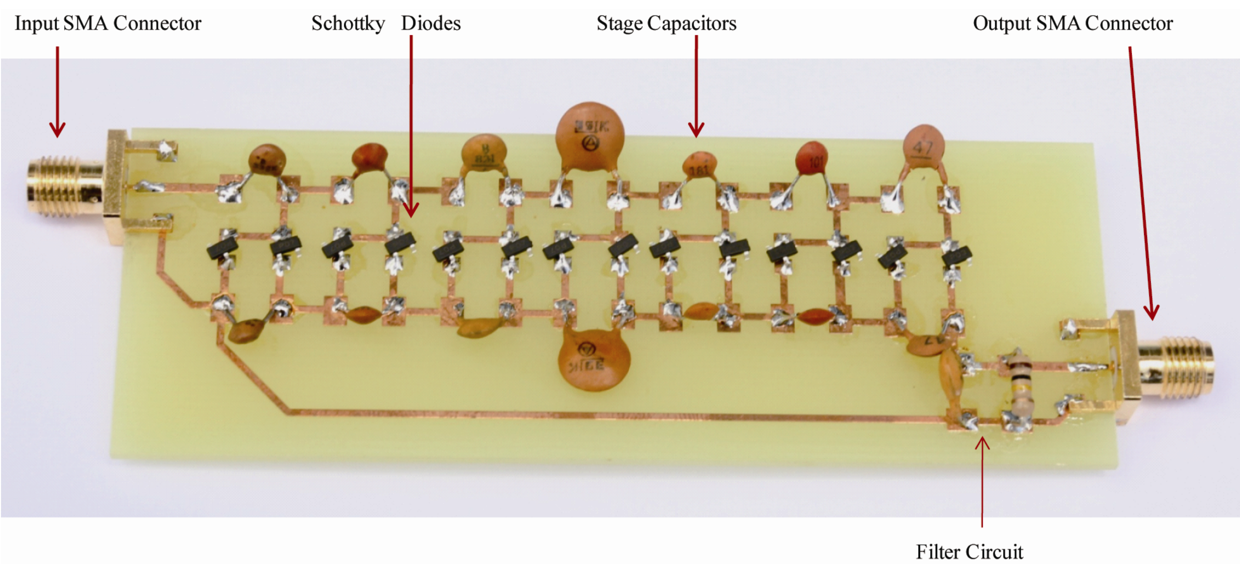

Figure 7. Photograph of assembled circuit board.

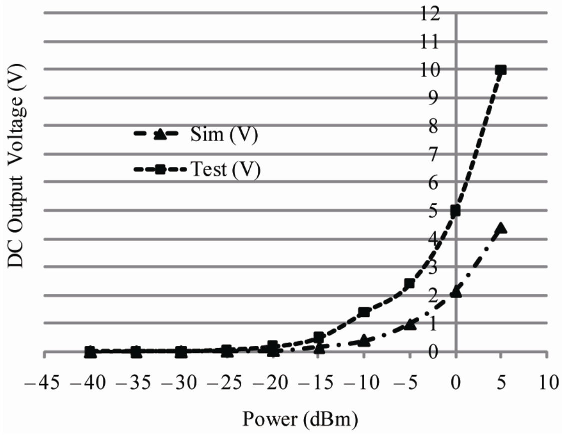

Figure 8. Simulated and test DC output voltage of multiplier as a function of input power.

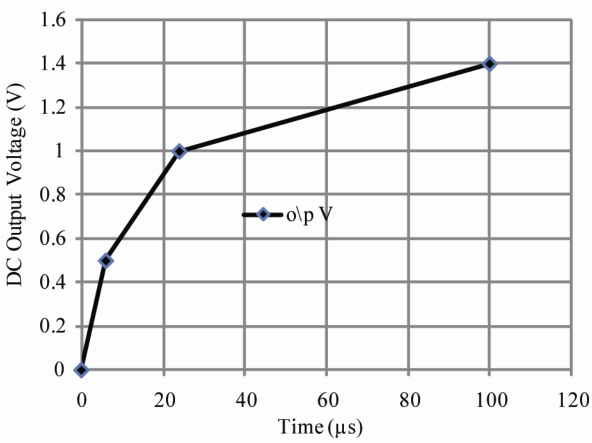

Figure 9. DC output voltage verses rise time of 4 stage voltage doubler circuit with equal stage capacitance [8].

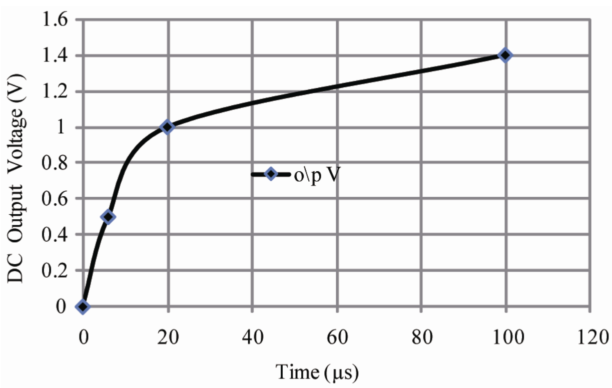

Figure 10. DC output voltage verses rise time of 4 stage voltage doubler with varied stage capacitance [8].

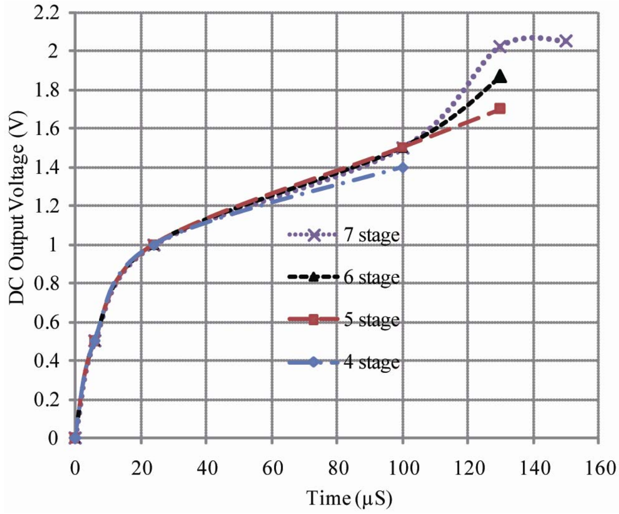

Figure 11. DC output voltage verses rise time of voltage doubler circuit through 4 - 7 stages with equal stage capacitance.

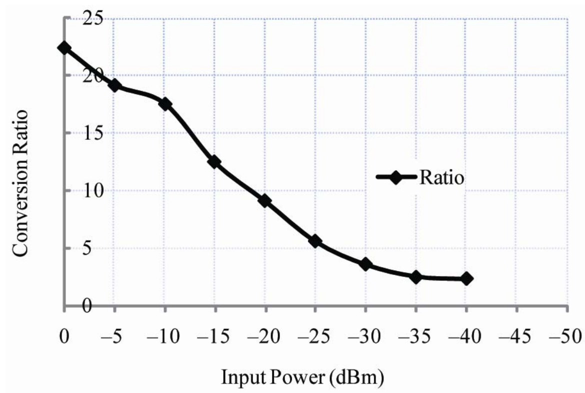

Figure 12. Conversion ratio as a function of input power.

posed voltage multiplier circuit operates at the frequency of 945 MHz with the specified input power levels. The results have shown that there is multiplication of the input voltage. From **Figure 12**, it is shown that at 0 dBm input power, the multiplication factor is 22. This is significant, as the work shows that RF energy in the GSM-900 band can be harvested from the ambient RF source using the Villard circuit topology. The power density levels from a GSM base station is expected from 0.1 mW/m^2 to 1 mW/m^2 for a distance ranging from 25 m - 100 m. These power levels may be elevated by a factor between one and three for the GSM-900 downlink frequency bands depending on the traffic density [10]. The next phase of the research work is to interface the voltage multiplier circuit through a matching network to the antenna at the input side and a low power device to power from the system at the output side to complete the RF energy harvesting system.

6. Acknowledgements

We would like to acknowledge and thank the Ministry of Higher Education Malaysia for funding this project under Fundamental Research Grant: FRGS/1/10/TK/UNITEN/02/13.

REFERENCES

[1] S. von der Mark and G. Boeck, "Ultra Low Power Wakeup Detector for Sensor Networks," *SBMO/IEEE MTT-S International Microwave & Optoelectronics Conference* (*IMOC* 2007), Berlin, 29 October-1 November 2007, pp. 865-868. doi:10.1109/IMOC.2007.4404394

[2] H. Yan, J. G. M. Montero, A. Akhnoukh, L. C. N. de Vreede and J. N. Burghartz, "An Integration Scheme for RF Power Harvesting," *Proceedings of STW Annual Workshop on Semiconductor Advances for Future Electronics and Sensors*, Veldhoven, November 2005, pp. 64-66. doi:10.1.1.126.5786

[3] T. Ungan and L. M. Reindl, "Concept for Harvesting Low Ambient RF-Sources for Microsystems," 2007. http://www.imtek.de/content/pdf/public/2007/powermems_2007_paper_ungan.pdf

[4] J. Wang, L. Dong and Y. Z. Fu, "Modeling of UHF Voltage Multiplier for Radio-Triggered Wake-Up Circuits," *International Journal of Circuit Theory and Application*, Vol. 39, No. 11, 2010, pp. 1189-1197. doi:10.1002/cta.692

[5] J. A. Starzyk, Y.-W. Jan and F. J. Qiu, "A DC-DC Charge Pump Design Based on Voltage Doublers," *IEEE Transactions on Circuits and Systems-I*: *Fundamental Theory and Applications*, Vol. 48, No. 3, 2001, pp. 350-359.

[6] HSMS-2850, "Surface Mount Zero Bias Schottky Detector Diodes." http://www.crystal-radio.eu/hsms285xdata.pdf

[7] D. W. Harrist, "Wireless Battery Charging System Using Radio Frequency Energy Harvesting," M.S. Thesis, University of Pittsburgh, Pittsburgh, 2004.

[8] E. Bergeret, J. Gaubert, P. Pannie and J. M. Gaultierr, "Modeling and Design of CMOS UHF Voltage Multiplier for RFID in an EEPROM Compatible Process," *IEEE Transactions on Circuits and Systems-I*, Vol. 54, No. 10, 2007, pp. 833-837. doi:10.1109/TCSII.2007.902222

[9] B. Emmanuel, J. Gaubert, P. Pannier and J. M. Gaultier, "Conception of UHF Voltage Multiplier for RFID Circui," *IEEE North-East Workshop on Circuits and Systems*, Gatineau, June 2006, pp. 217-220. doi:10.1109/NEWCAS.2006.250961

[10] H. J. Visser, A. C. F. Reniers and J. A. C. Theeuwes, "Ambient RF Energy Scavenging: GSM and WLAN Power Density Measurements," *Proceedings of the* 38*th European Microwave Conference*, Eindhoven, 27-31 October 2008, pp. 721-724. doi:10.1109/EUMC.2008.4751554

Homebrew at ACØC
Combo Analog+DSP Filter
A Few Good CW Keyers
Preamps
RF Current Meter
100W Speaker Amp
The Ultimate Audio Filter
2xSi570 RF Gen
SB200 Sleeper
SB-200 Tank Mods
High Perf Xtal Osc
CW-Skimmer Array
Leakage Tester
XR2206 Sig Gen
Fixed Bench PS
Dual Variable Bench PS
Station Interface
Speaker/Paddle Switching

RF Current Meter

Stop Guessing and Built This Simple Meter Making Measurements Easy to Take

Why a Hand Held RF Current Meter

There are two things that I wanted to do which would be made easy with a current meter... Both are related to the unusual nature of the antenna here at AC0C.

1. Checking common mode surface current on coax and control cables up in the attic antennas.

With the high cost of ferrites, placing them with the aid of a current meter is very helpful in that you can compare the before (no ferrite) and after (with ferrites attached) - and know that you have addressed the current problem on a given bit of line.

Otherwise, it seemed to me, that ferrite placement was more of a guess than a science.

2. Measuring relative antenna currents along an element

With the W8WWV RVM system, I can measure element currents where ever a current sensor is placed. This is typically at the center of a dipole element.

However, the center may or may not be the actual high-current point for the element depending on the frequency. My EZNEC models can indicate where the current peaks are - and by looking along these lines manually - comparing them with readings taken from the driven element, I can make current checks even in non-standard location of the array.

The meter described below accomplishes these two tasks very nicely.

Design Idea

The design follows an old RSGB design that I found on G3SEK's excellent web site:

http://www.ifwtech.co.uk/g3sek/clamp-on/clamp-on.htm

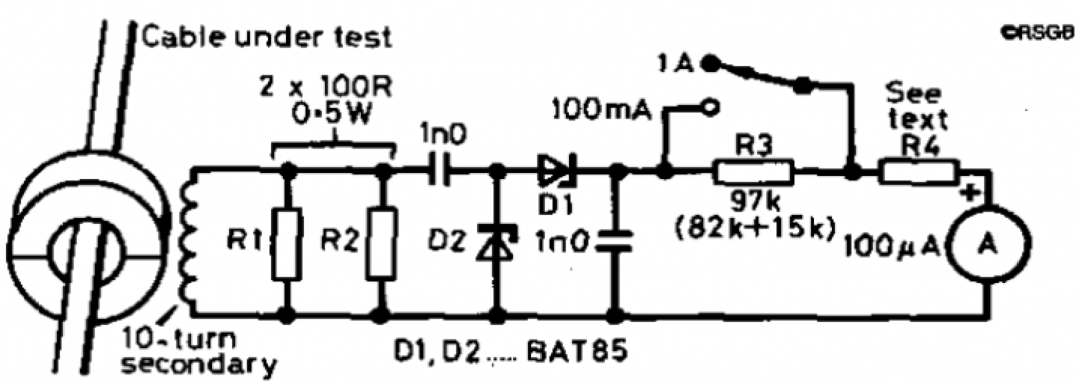

I followed this design pretty close except for the R3/R4 which I used variable trim pots. Due to the voltage-doubler nature of the circuit, it's capable of exceptional sensitivity.

The meter was calibrated for full-scale @ 1A on the higher scale, but I have left the lower scale set on a very high sensitivity setting which I find very handy for the common mode checking. Here, a sensitive meter providing a relative

current indication is needed.

Construction Details

Once parts were in hand, construction was very easy and took perhaps an hour.

No attempt was made to beautify the work - it's 100% orientated toward functionality and utility.

I had a 100 uA meter in the junk box along with the other parts needed and orienting them on the back-side of the meter was really the most time consuming aspect.

The switch is held in position with hot-glue. And a bit of hot glue is applied to the meter terminations as a safety precaution - just in case I were to brush the meter up against something carrying high levels of current.

Wraps around the toroid were made with wire-wrap type wire, 30 Gage.

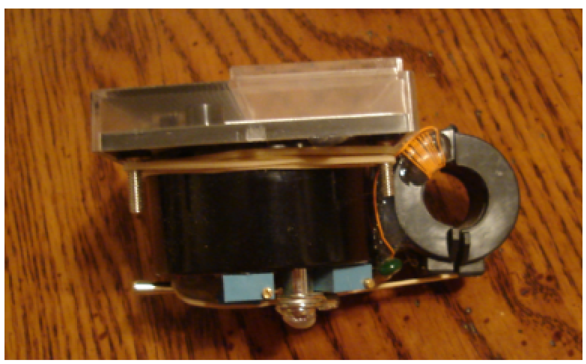

Selection of the toroid used was based on what would physically fit around the RG-213 sized cable and could be easily opened and closed.

The rubber band shown in the picture makes for a very convenient closing mechanism - and in a lot of applications, I simply hold the toroid closed with my finger pressure which makes moving the meter along a wire - and moving from cable to cable - very quick and easy.

For more ideas, check out Frank N4SPP's very nice RF current meter [found HERE.]

Bread board Arrangement:

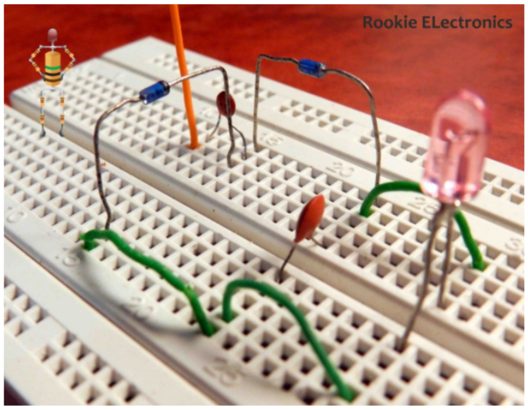

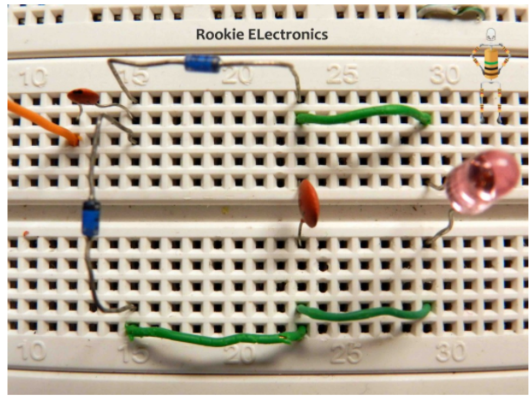

Strip Board:

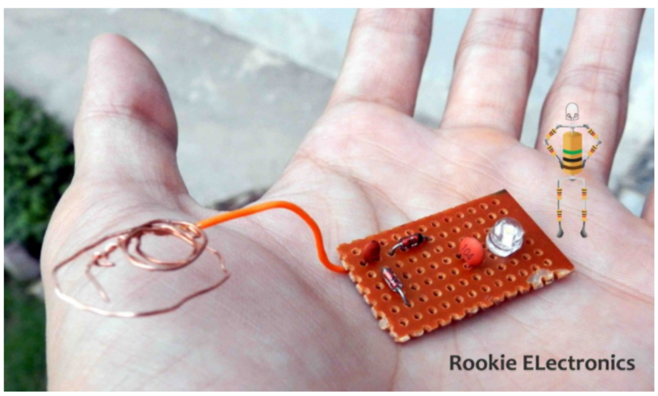

RF Diagnostics, LLC

WELCOME TO RF DIAGNOSTICS

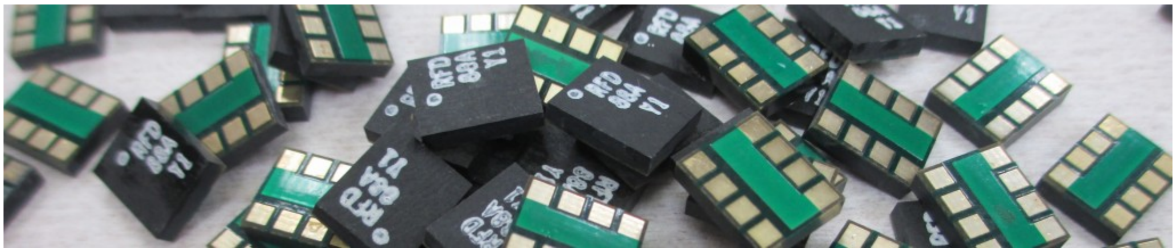

Energy Harvesting Modules

WIRELESS ENERGY HARVESTING PRODUCTS RF Diagnostics, LLC designs and sells surface mount RF to DC converters and other building block modules for energy harvesting systems. With our products you can harvest ambient AC/AM/FM/Wireless Energy to power your IoT battery free system. We also provide custom designs for RF/microwave and general electrical engineering products and design contracting services to clients in the commercial wireless and defense electronics businesses. We strive to be a high quality and cost effective design resource for your design team.

OUR PRODUCTS

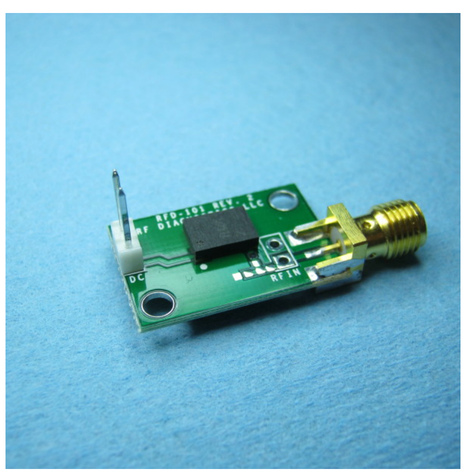

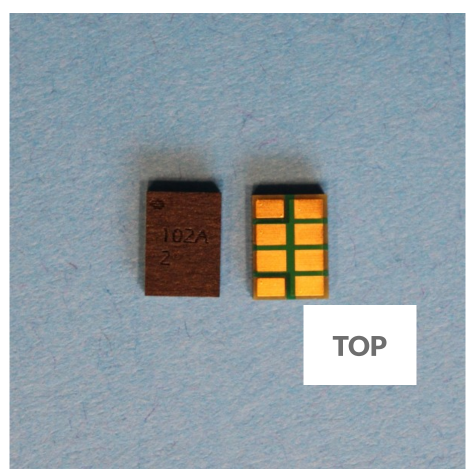

TOP

RFD102A-DET: Microwave Energy Detector

$18.00

Add to cart

RFD102A-TB: 60Hz…6GHz Energy Harvesting Test Board

$33.00

Add to cart

RFD102A: Wireless Energy Harvesting Module

$12.00

Add to cart

OUR DESIGN SERVICES

Energy Harvesting Module & System Design

Any of our standard products can be customized for your application. We can support your application with matching, testing, antenna design, assembly and many other tasks. Have a new idea for a product? We can help you realize it. We are developing new products and are always interested in your feedback to guide our product development.

MMIC Design

We use Agilent's Advanced Design System for MMIC design and PCB design. Previous designs completed are quad-band GSM power amplifier modules, 2.4-2.5GHz/5-6GHz wireless LAN power amplifiers, broadband power amplifiers, switch-filter designs, RFID detectors, RF/DC converters and filter designs.

Front End Module Design

We use Agilent's Advanced Design System and Orcad PCB Editor for Front-End Module designs. Previous design examples are high-volume switch filter modules, dual-band 802.11a/b/g front end modules, 76GHz car radar module, RFID card design.

RFID Detector System

On an NSF Phase I & II grant to one of our clients, operating as a subcontractor, the RF Diagnostics design team created a complete RFID MEMS resonator detection system. Both hardware and software were developed under this contract. The work was published at an SPIE conference in July 2010.

LEARN MORE

NISKAYUNA, NY 12309 USA
518-810-6560
INFO@RFDIAGNOSTICS.COM

TOP

Sebs World

- Home
- DA14 Asteriod
- Secret space plane
- Solar storm
- End of the world?
- UK monitoring
- Tracking
- Save money
- Get out of the EU
- UFO's
- Magnetic energy
- RF energy
- Radiant energy
- Perpetual
- Easy Steam!
- Irony- defined
- Funny Pics
- Internet Problems
- Star Wars
- Chat room
- Live music
- Kevzone
- Facebook Cheats
- Crashes

About us
Private Policy

RF energy..

This can extract some electricity from the air!

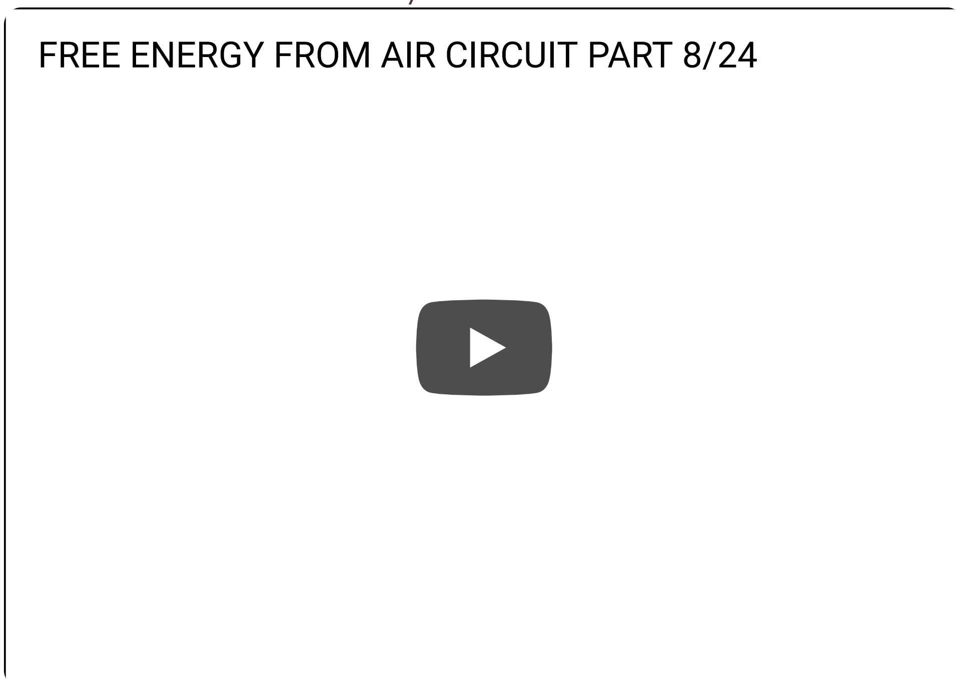

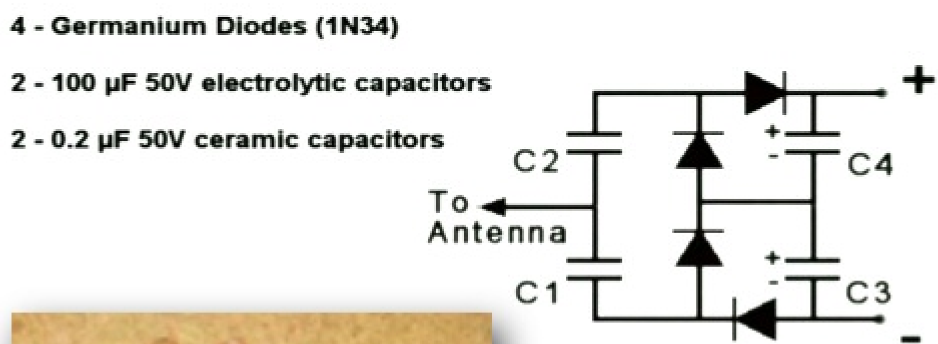

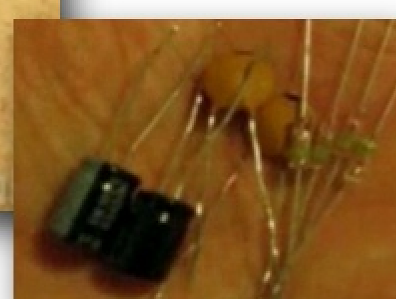

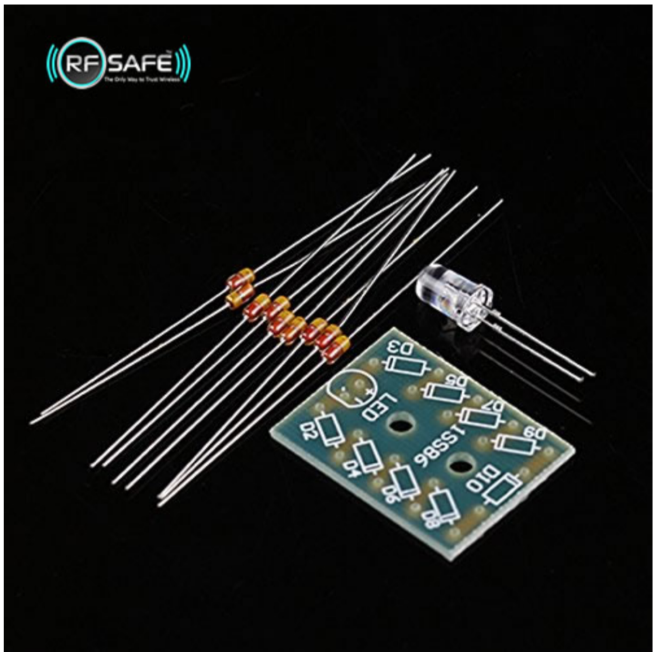

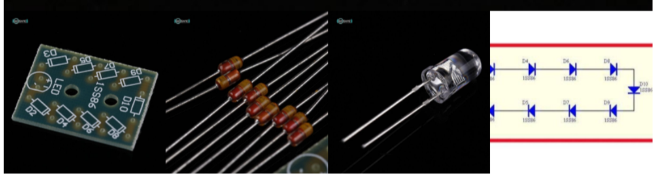

DIY RF METER: LED IS 100% POWERED BY RF RADIATION USING DETECTOR DIODES

$8.99

1 Add to cart

SAFE KIDS: LED Cell Phone Radiation Detector For DIY Science Project & Experiments || Test Phone Shields

NO batteries. it uses ONLY RF radiation power from cell phone. Yes, see with your own eyes how powerful cell phone radiation is when it powers a light from thin air.   RF Safe's DIY circuit is the simplest detector for microwave radiation. The RF diodes convert microwaves from a cell phone to DC current to power an LED which emits visible light warning you of possible danger.

SKU: 636684233801 Categories: Cell Phone Radiation Safety, D-I-Y Tags: 1SS86 detector diode, Cell Phone Radiation Meter, germanium diode, LED RF Meter

A concurrent 915/2440 MHz RF energy harvester

L Fadel, L Oyhenart, R Bergès, V Vigneras, T Taris

A concurrent 915 MHz / 2440 MHz RF Energy Harvester

L. Fadel[1], L. Oyhenart[1], R. Bergès[1], V. Vigneras[1], T.Taris[1]

[1] Laboratoire IMS, UMR - 5218, Université de Bordeaux, 33405 Talence Cedex, France.

This paper presents the development of two dual-band RF harvesters optimized to convert far-field RF energy to DC voltage at very low received power. The first one is based on a patch antenna and the second on a dipole antenna. They are both implemented on a standard FR4 substrate with commercially off-the-shelf (COTS) devices. The two RF harvesters provide a rectified voltage of 1V for a combined power respectively of -19.5 dBm at 915 MHz and -25 dBm at 2.44 GHz and of -20 dBm at 915 MHz and -15 dBm at 2.44 GHz. The remote powering of a clock consuming 1V/5µA is demonstrated, and the rectenna yields a power efficiency of 12 %.

Keywords: Antennas and Propagation for Wireless Systems, Applications and Standards (mobile, Wireless, networks), Circuit Design and Applications.

Corresponding author: email: ludivine.fadel@ims-bordeaux.fr; phone: +33 540 002 615

I. INTRODUCTION

Today's the society is evolving toward creating smart environments where a multitude of sensors and devices are interacting to deliver an abundance of useful information. Essential to the implementation of this Internet Of Things (IOT) is the design of energy efficient solutions aiming toward a low-carbon-emission, namely green, society. Within this context, the energy harvesting appears as an alternative to provide systems with self-sustained operation. Many electronic devices operate in conditions where it is costly, inconvenient, or impossible to replace the battery. Examples include sensors for health monitoring of patients [1],[2], aircraft or building structural monitoring [3],[4], sensors in natural, industrial or hazardous environments, etc. The scavenging of natural ambient energy requires some specific conditions such as: daylight for solar energy [5], breeze for wind energy or motion for kinetic energy [6] to name a few. As consequences the exploitation of natural source does not fit with many cases of applications. On the other hand the electromagnetic (EM) [7], or Radio-Frequency (RF), energy is a human made source that is not dependent of weather conditions nor the daytime. It is so very attractive for wireless powering of remote devices. Furthermore the ever growing of commercial and personal wireless installations opens up to a 24 hour a day available energy in the vicinity of any human activity areas. The schematic of a general Wireless RF Power Transmission (WPT) system is shown in Fig.1. We talk here about far-field RF energy transmission [8], which is different from near-field RF energy transmission [9]. This later including inductive, capacitive or resonant coupling is a close contact transmission and is not relevant for remote devices. In Fig. 1, the receiver antenna

collects the EM energy radiated by a RF source, and converts it into a RF signal. This RF signal is transferred to the rectifier by an impedance matching network, to be converted into DC power, which is further accumulated in a storage element. The main purpose in the deployment of WPT systems is the development of compact and efficient solutions. Most of the challenge concerns the implementation of harvesting modules, especially the antenna as its design defines the scavenging capability and the size of the RF harvester. At low frequency the transfer of energy is efficient, but the antenna footprint is large. To address the trade off between the efficiency of the WPT and the size of the modules, the frequency band located in the 433 MHz to 6 GHz frequency spectrums are preferred.

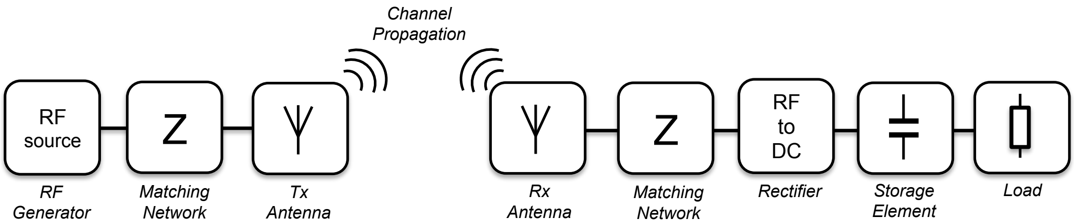

Fig. 1: Schematic of a Wireless RF Power Transmission (WPT) system

Over the last decade the research effort has focused on the development of WPT systems according two scenarios: the RF energy scavenging [10] and the RF energy transfer [11]. The two RF energy scavenging is an opportunistic collection of the RF ambient energy from the surrounding communication traffic. To improve the harvesting capability the scavenging RF harvesters are of wide-band type [12] and cover popular standards such as: DTV (470-610 MHz), GSM900, GSM1800, 3G (2.1GHz) and WiFi (2.4 GHz). Unfortunately these standards dedicated to convey wireless communications do not radiate a large RF power. As consequences the collected energy is weak, unpredictable and out of control. The RF energy scavenging remains a promising solution in the future as the increase of communication traffic could make it more reliable, and consistent with IOT applications. The second concept, namely RF energy transfer, assumes an identified source that is dedicated to perform the WPT. The amount of transmitted power is controlled by the source and the collected energy is larger than in scavenging approach. The licence-free Industry-Science-Medical (ISM) frequency bands located at 0.9, 2.4 and 5.8 GHz are usually exploited to support such a WPT scenario. Today the RF energy transfer in ISM Bands is not only promising, it becomes a reality as some pioneer companies propose some full kits: Powercast Corporation, AnSem and MicroChip to name a few. However there is still a lot of work to make the RF energy transfer an appropriate, low cost and easy-to-use solution for remote powering. One of the most critical point concerns the harvesting capability of the RF modules. So far the commercial kits referenced above only explore the 900 MHz ISM allocations to perform the WPT. This work proposes to demonstrate the interest of a concurrent harvesting at 915 MHz and 2.44 GHz. The design and implementation of a modified 4-stage doubler RF to DC converter, including a concurrent matching network, is first presented. The section III details the design of two types of multi-band antenna. The comparison between a single frequency and a multi-band WPT is exposed and the demonstration of the remote powering of a clock is reported as a case of application. To conclude a comparison of our results with the state of the art is exposed.

II. CONCURRENT RF TO DC CONVERTER

The Radio-Frequency IDentification (RFID) applications are the most popular systems exploiting the principle of RF energy transport. In passive RFID applications the reader transmits the RF power to the tag, and also sets up the communication. The RF to DC converter is designed to yield a maximum of power efficiency to the tag. Most of the time the reader and the tag are in line of sight and close to each other, these conditions improve the transmission of RF energy, the amount of power available at the tag antenna is large, typically between -15 dBm and -20 dBm. In RF energy harvesting the scenario is different. The distance between the RF source and the RF harvester ranges from 0.5 meter to 10 meters. The amount of collectable power is low, from -10 dBm to -25 dBm, and the remote powering is difficult. The RF harvesters are supposed to collect and to store the energy during a long period of time. Once the level of stored energy is large enough, it can be released to the application. For these reasons a rectifier dedicated to RF energy harvesting is first designed to yield a maximum of sensitive to increase its scavenging time and capability.

A) Rectifier Architecture

The rectifier architecture is based on voltage multipliers to provide an adequate output DC voltage. The architecture of the RF to DC converter, reported in Fig.2, includes a matching network based on a L-section, and a N-stage voltage multiplier based on Schottky diodes from Avago (HSMS285). The choice of the Schottky diode is very important in the design of the rectifier. A key parameter is its threshold voltage $V_{TH.}$ When only low power levels are available in the environment, the amplitude of the incident signal may be close to or even below this voltage. Below this voltage value, the diode will no longer conduct and the losses become predominant. For COTS devices the two Schottky diodes performing the best conversion efficiency in a 2.4 GHz range are HSMS-2850 from Avago and SMS-7630 from Skyworks [13].

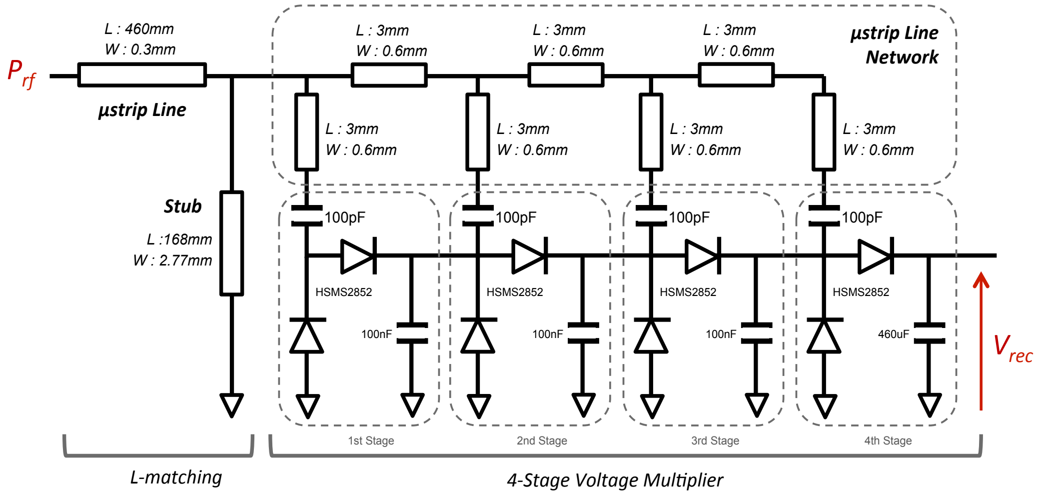

Fig. 2: Architecture of the RF to DC converter

Focusing on the sensitivity, the RF to DC converter is designed to maximize the rectified voltage for an input power close to -20 dBm. The optimum number of stage is fixed to four according [14]. The footprint of each voltage doubler imposes the micro-strip line network. The micro-strip lines namely "junction" is set to minimum length, the micro-strip lines "access" are used as an additional degree to tune the input-matching network. Indeed, the L section in combination with the micro-strip distributed network is equivalent to a T section (Fig.3). Many combinations of Z_1, Z_2, Z_3 can achieve input matching at 900 MHz or 2.4 GHz. Some of them are very close for each frequency, so we choose one that allows a return loss (< - 10 dB at least) both at 900 MHz and 2.4 GHz.

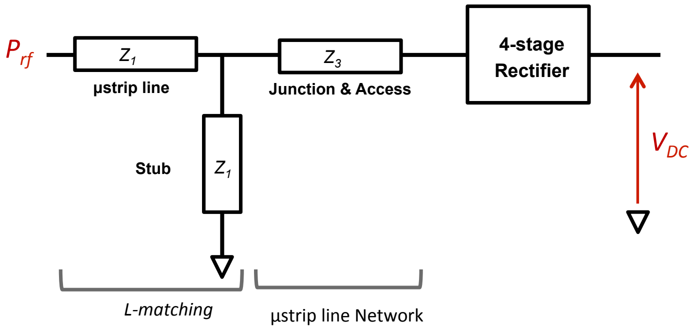

Fig. 3: Topology of the input-matching network

The equivalent narrow band model of the matching network is proposed for each frequency (Fig.4). At 915 MHz, the voltage multiplier, including the rectification stages and the micro-strip line network, is modelled with a shunt capacitor (5pF) and a shunt resistor of 270 Ω (Fig.4a). The stub, (Fig.3) is equivalent to an inductor (Fig.4a), which compensates the shunt capacitor. The input micro-strip line, (Fig.3), is a quarter wave impedance transformer, (Fig.4a) it converts the 270 Ω into 50 Ω. At 2.44 GHz the micro-strip line network distributing the RF signal to the voltage doublers (Fig.3), becomes inductive (Fig.4b). The stub is equivalent to a shunt capacitor of 120fF, its effect is negligible. The impedance transformation is actually performed by the input micro-strip line, which is modelled by a shunt capacitor (0,6 pF) and a series inductor of 5.6 nH.

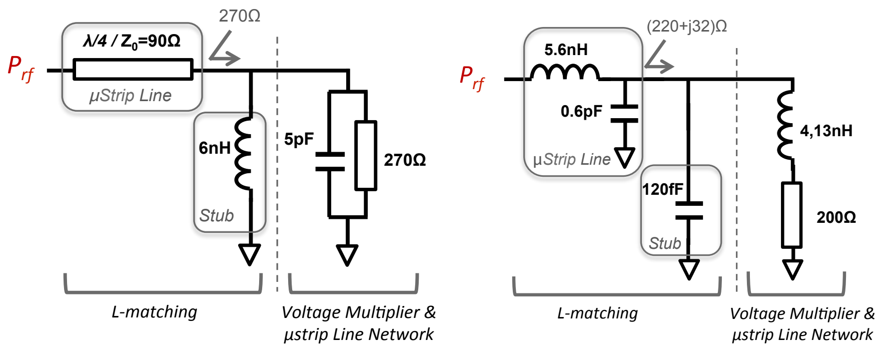

(a) *(b)*

Fig. 4: Equivalent model of the input matching network at 915 MHz (a) at 2,44 GHz (b)

To study the impact of the power on the diode, and input matching, behaviour the return loss of the 4-stage rectifier has been measured and plotted (Fig.5) for various input power P_{rf} at 9000MHz.

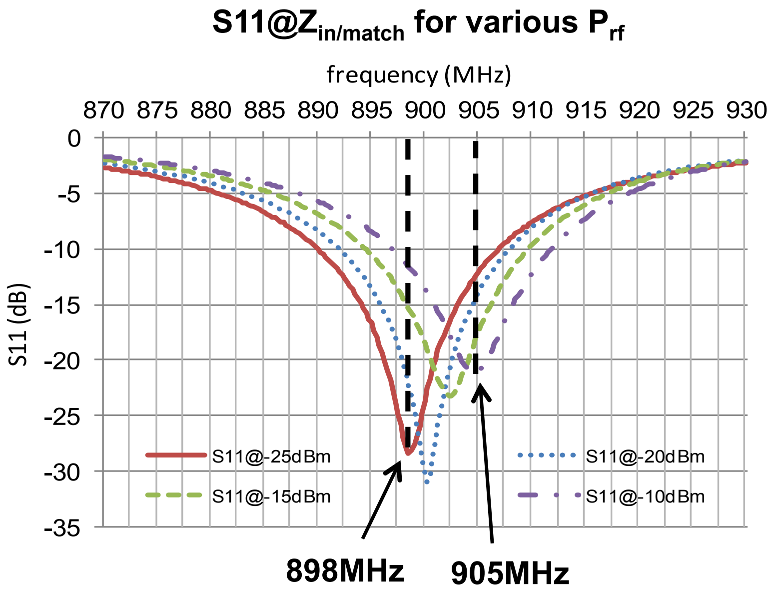

Fig. 5: Measured S_{11} of a 4-stage voltage multiplier with a L section at 900 MHz for various input power P_{rf}

As illustrated in the figure 5, the input return loss is not strongly affected by the input power if $P_{rf} < -15$ dBm. The RF harvesters developed in this work are dedicated to collect power from – 15 to – 25 dBm. Over this range the diode model can be considered as stable, and the slight frequency shift is still covered by the antenna bandwidth.

B) Rectifier Characterization

The power efficiency and the power sensitivity are two conversion characteristics of importance in RF harvesters. However, the RF harvester operating at low power level accumulates the energy in a storage element, to further release it to the application. In such accumulation mode the power sensitivity becomes more important than the power efficiency.

For the characterization the rectifier is not connected to a load. The load represents the equivalent impedance of the application (clock, sensor) to power. The effectiveness of RF-DC conversion of the rectenna and its DC ouput voltage varies depending on the load value. The rectifier is first characterized in a single tone mode, 915 MHz and 2.44 GHz respectively, and then in a dual-band mode. Measurements of the unloaded rectified voltage versus various input power P_{rf} are reported in Figure 6.

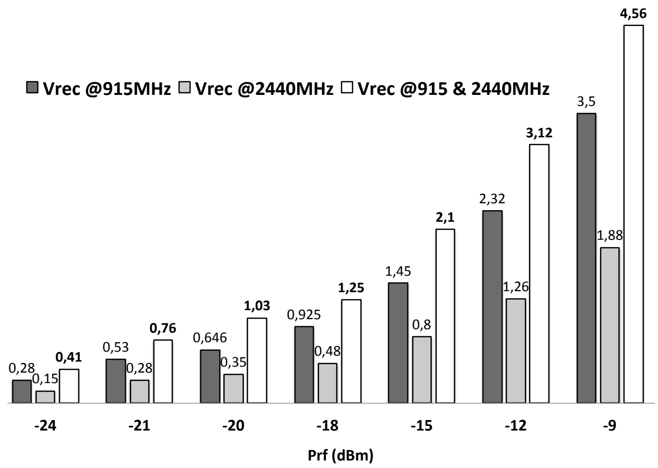

Fig. 6: Unloaded rectified voltage for various input power

To compare the results of the two considered tones, the target is fixed to a value of 1V. In a single tone mode, the required P_{rf} to rectify 1V is close to -18 dBm at 915 MHz, and would be larger than -15 dBm at 2.44 GHz. In a dual-band mode the circuit only needs a power P_{rf} of -20 dBm at each frequency. The dual-band rectification significantly improves the power sensitivity. The reverse breakdown voltage of the HSMS285 Schottky diode limits the input power to - 9 dBm, for which V_{rec} is 4,56 V.

III. ANTENNA DESIGN

To meet the low-cost constraints, the RF energy harvester will be implemented on a single low cost substrate, an FR4 PCB. For the antenna, there are more efficient substrates with a higher permittivity to reduce the size of the antenna or a lower losses but their cost is much higher than the improved performance. These powerful substrates fail to build low cost energy harvesters. This section exposes the design of two dual-band antennas implemented on a 1.6 mm FR4 printed circuit board. The fabrication uses a mechanical etching process with a 200µm resolution. We have chosen two complementary antenna topologies with a directional and omnidirectional radiation pattern.

A) Dual - band patch antenna

Emitting and receiving antennas do not usually meet the same constraints. Mobile devices such as smartphones and tablets use compact antennas (ifa, pifa…) to address the trade off between performance and size. Base stations can afford large efficient radiating elements (omnidirectional or directional antennas depending on the application). For energy harvesting purpose, micro-strip patch antennas are commonly used [15-17]. A rectangular micro-strip patch antenna (RMPA) is first developed to suit with both low cost technology of implementation and co-integration with the rectifier. Based on the cavity-model approximation, the resonant frequencies of the RMPA for the TM_{mn} mode is described in (1).

$$f_{mn} = \frac{c}{2\sqrt{\varepsilon_r}}\sqrt{\left(\frac{m}{L}\right)^2 + \left(\frac{n}{W}\right)^2} \quad (1)$$

W, L are the patch dimensions, $c = 3.10^8$m/s

The antenna dimensions, 68 cm^2 (8.8 x 7.8 cm), described Fig.7a are dependent to the frequency bands and the feed location is selected to only excite the fundamental modes TM_{01} and TM_{10}. Those modes permit to obtain a large aspect ratio (W/L = 2,7) but reduce the performance of the RMPA. On the other hand, TM_{01} and TM_{30} modes require an aspect ratio close to one but offer beneficial radiation patterns for our application. The RMPA is fed by a probe whose position (x,y) adjusts the matching both at 915 MHz and 2.44 GHz. This two operating bands of the proposed antenna are on cross polarization planes. The geometric parameters of RMPA have been optimized with an approximate model, the TL model [18], and with a full wave method. Details of the two approaches have been studied in [19]. The return loss of the RMPA is better at 915 MHz than 2.44 GHz because the maximum impedance of TM30 mode is 31 Ω [19]. The TM30 mode does not achieve 50 Ω because it is not a fundamental mode. This antenna has a maximum gain of 1.3 dB at 915 MHz (Fig.7b) and 2.5 dB at 2.44 GHz (Fig.7c). This two operating bands of the proposed antenna are on cross polarization planes.

The realized gains of the dual band patch antenna are lower than the classical patch antenna because the radiating efficiency is low, 60% for the TM_{01} mode and 30% for the TM_{30} mode. The FR4 substrate has a loss tangent of 0.02. The radiation efficiency of the dual band patch antenna is highly dependent of the substrate losses.

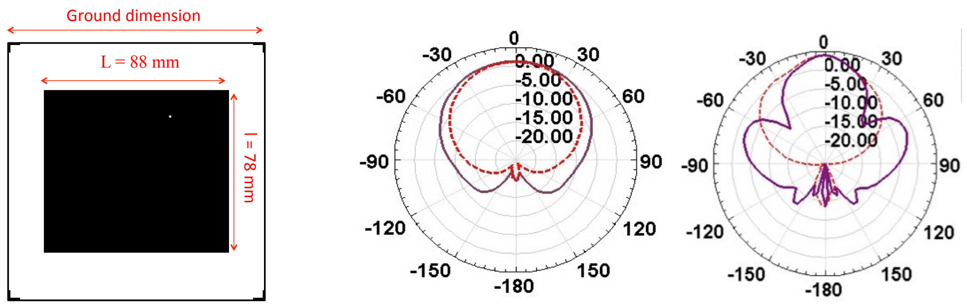

(a) *(b)* *(c)*

Fig. 7. Layout of the RMPA antenna (a) - Radiation pattern at 915MHz (b) and 2.44 GHz (c) Solid and dashed lines correspond to E-plane and H-plane respectively

B) Multi-band arm dipole antenna

The second antenna is a multi-band dipole type composed of three arms. Its dimension is about 23 cm^2 (11.1x2.1 cm), Fig.8a. Each arm is designed to work at one band of frequency. The longer one is for the 915 MHz, the middle one, not useful in our case, is for the 1.4 GHz and the last one, the smaller, is dedicated to 2.4 GHz [20].

All the geometric parameters have been optimized with a full-wave method in order to be matched both at 915/ 2440MHz. On Fig.6b and 6c, the radiation pattern is plotted for the elevation plane (orthogonal to substrate) of the simulated antenna. The maximum gain is 0.5 dB at 915 MHz and 3.4 dB at 2.44 GHz at 90°, on the substrate plane. The radiation efficiency is 99% at 915 MHz and 95% at 2.44 GHz.

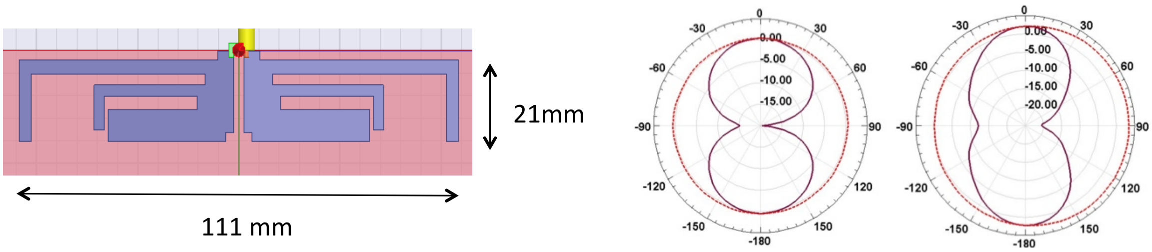

(a) *(b)* *(c)*

Fig. 8. Layout of the multi-band arms dipole antenna (a) - Radiation pattern at 915 MHz (b) and 2.44 GHz (c). Solid and dashed lines correspond to E-plane and H-plane respectively

It is interesting to compare the characteristics and performances of the two types of antennas. Although the radiation efficiency of the dipole antenna is better than the patch antenna, the antenna gains are similar because the high directivity of the RMPA antenna compensates the low values of radiation efficiency. When there are no cost constraints, it is interesting to use high performance substrates for the design of RMPA antennas because they improve the radiation efficiency and consequently antenna gain.

Moreover, the integration of the antenna with the rectifier will not be made in the same way. Considering the patch antenna, the rectifier can be integrated on the ground plane allowing a more compact solution. The dipole antenna, which is ground plane free, is less sensitive to the surrounding environment in our case. The performance of the dipole antenna and especially the radiation efficiency are very weakly dependent of the substrate characteristics. The design of a dipole antenna can be easily reuse with other material such as Kapton®, paper, Plexiglas to name a few.

IV. WIRELESS POWER TRANSMISSION

This part presents the measurement results of the assembled RF harvesters in the context of Wireless Power transfer. The two dual-band harvesters are realized with COTS devices such as HSMS diodes and capacitors. Those elements are reported by heat-treating. The RF to DC converter board, including the matching network and the rectifier, is reported on the backside and connected to the radiation part, on the front side, through a via (Fig.9a). The dipole antenna is connected to the rectifier circuit using SMA connector (Fig.9b).

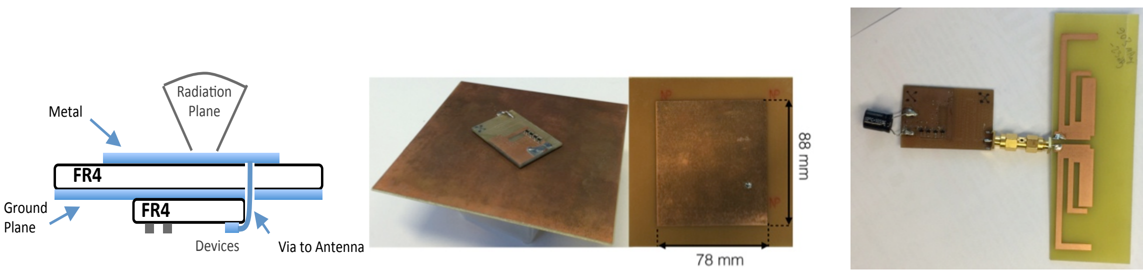

(a) *(b)*

Fig. 9. Dual-band RF harvesters based on patch antenna (a) – arms dipole antenna (b)

For the dual-band RF harvester based on patch antenna, the return loss, S_{11}, is measured for an input power of -20 dBm with a HP8720 network analyser. The patch antenna, the rectifier and the dipole antenna are centered at 915 MHz and 2.44 GHz with a low return loss ($S_{11} < -15$ dB), Fig.10. The return loss of the RMPA antenna is better at 915 MHz than 2.44 GHz because the maximum impedance of TM30 mode is 31 Ω (Fig. 6 and Fig. 7 of [16]). The TM30 mode does not achieve 50 Ω because it is not a fundamental mode.

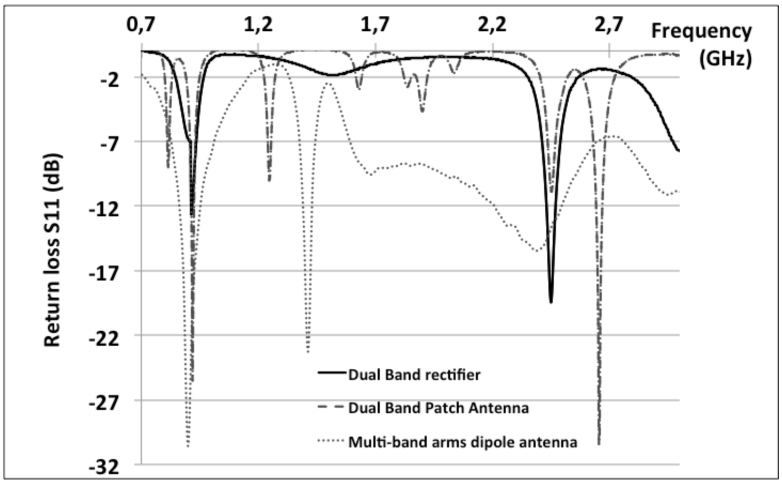

Fig. 10. Measured return loss S_{11} of the dual-band rectfier, patch and arms dipole antenna

A) Remote Powering and Power Efficiency

The rectenna is connected to a clock, which mimics a low power application. The remote powering of this clock is performed in a furnished room of the lab according the schematic of Fig.11. The distance between the source and the antenna is fixed to 2 m. The clock is turned on for different scenarios of transmitted power. For each combination of power proposed in Fig.12, the RF power is first measured with a calibrated antenna and a power meter. Then, the rectenna is measured and P_{eff} is the ration between the power delivered to the load (here the clock) and the power available at the antenna.

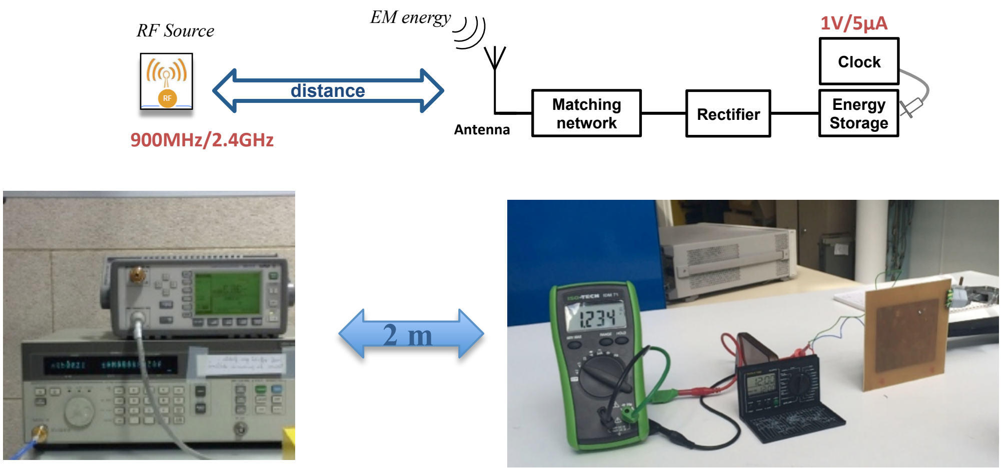

Fig. 11. Schematic and picture of the scene of remote powering of a clock

The power efficiency of the patch and the dipole rectenna is worked out from these experiments and reported in Fig.12. The power efficiency η is defined as the ratio between the DC power delivered to the clock and the RF power collected by the antenna.

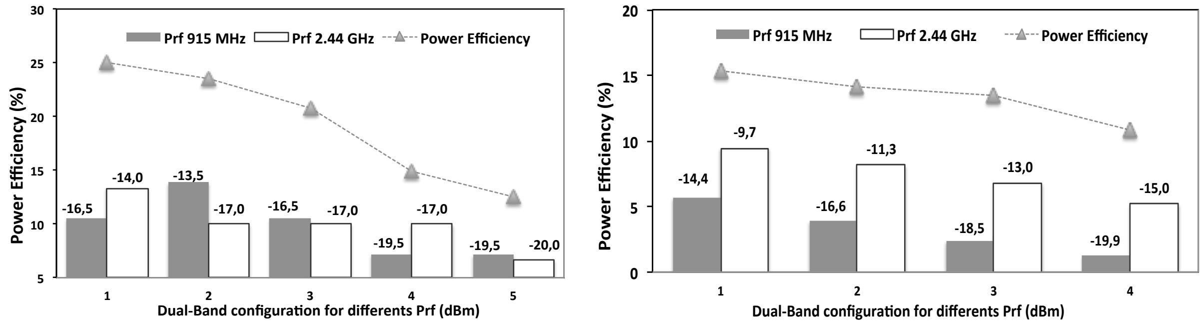

(a) *(b)*

Fig. 12. Power efficiency of the dual-band RF harvester based on the patch (a) and the arms dipole (b) antenna

The minimum power required to turn on the clock with the patch-based harvester, Fig. 10.a, is a two tone signal featuring: -19.5 dBm at 915 MHz and -20 dBm at 2.44 GHz. At this point, the power efficiency is 12.5 %, which corresponds to a DC output power of 2.7 μW/1V.

A maximum efficiency of 24 % occurs for a combined power of -16.5 dBm at 915 MHz and -14 dBm at 2.44 GHz. The harvester is able to deliver a DC ouput power of 15 μW. The harvester based on the arm dipole antenna needs a minimum power of -19.9 dBm at 915 MHz and -15 dBm at 2.44 GHz at the antenna to turn on the clock. For these conditions of remote powering, the efficiency of the harvester is 11 %. It delivers a DC power of 3.8 μW/1.15 V. The maximum power efficiency, 15.5 %, yields for an input power of -14.4 dBm at 915 MHz and -9.7 dBm at 2.44 GHz, the DC output power is 21 μW.

This scenario of remote powering figures out that the harvester based on the patch antenna exhibits a better power efficiency than the harvester combined with the dipole element. This difference is due to the antenna gains. Referring to Fig. 7 and Fig. 8, the gain of the patch antenna is larger (+0.8dB) at 915 MHz and lower (-0.9 dB) at 2.44 GHz than the dipole element. However the rectifier, referenced in [16], achieves a power efficiency of 17% at 915 MHz and only 5% at 2.44 GHz for an input signal of -15 dBm. As consequences the patch-based harvester is able to extract more power from a 915 MHz signal than the dipole-based harvester can do at 2.44 GHz. For this reason the overall efficiency of the patch harvester is better.

B) Power Sensitivity

The power sensitivity is measured with the same scenario of Fig.11 but the clock is disconnected. The output voltage is reported for different combination of collectable power at the antenna in a dual-band configuration.

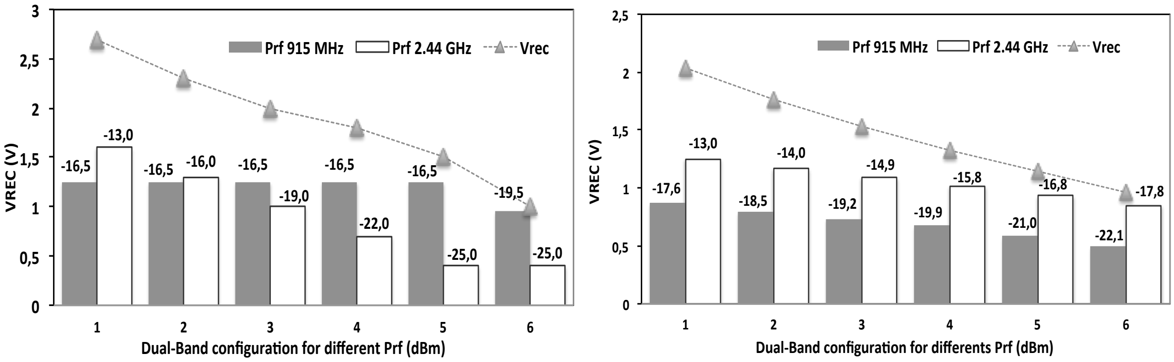

(a) *(b)*

Fig. 13. Rectified voltage of the RF harvester based on patch (a) and arm dipole (b) antenna

To rectify a 1V DC voltage, the patch-based harvester, Fig.13a, requires a two dual-band configuration: -19.5 dBm at 915 MHz and -25 dBm at 2.44 GHz, which is equivalent to an input power of -18.4 dBm (or 14 µW). For the same purpose the dipole-based harvester, Fig.13b, needs a dual-tone of -22.1 dBm at 915 MHz and -17.8 dBm at 2.44 GHz. The equivalent input power of this 2-tone signal is -16.5 dBm (or 22 µW). The patch-based harvester exhibits a better sensitivity than the dipole harvester for the same reason exposed in the part A of this section. In Fig.6, which reports the power sensitivity of the rectifier part only, the overall sensitivity is almost the same for the dipole harvester. It is improved by 1.8 dB for the patch harvester due to the additional gain of the antenna at 915 MHz.

C) Discussion and Comparison with the state of the art

An important characteristic of a remote powered device is its size. Indeed it is expected to be as small as possible to make it unobtrusive to our closest environment. In a scenario of RF harvesting the antenna footprint determines the compactness of a harvester operating Ultra High Frequency (UHF) bands. To complete the comparison between the two harvesting modules developed in this work, two figures of merit, FOM_{sens} and FOM_{eff}, including the size of the antenna, are proposed in (2) and (3).

$$FOM_{sens} = \frac{V_{REC@Psens}(V)}{\frac{P_{sens}(\mu W)}{100\mu W}.\frac{A_{ant}(cm^2)}{100cm^2}} \tag{2}$$

With: P_{sens} the input RF power required to provide $V_{REC@Psens}$ the unloaded rectified output DC voltage, and A_{ant} the area of the antenna.

$$FOM_{eff} = \frac{\eta(\%)}{\frac{P_{eff}(\mu W)}{100\mu W}.\frac{A_{ant}(cm^2)}{100cm^2}} \tag{3}$$

With: P_{eff} the input RF power required to achieve η the overall power efficiency.

FOM_{sens} and FOM_{eff} do not represent the same scenario of application. The FOM_{sens} illustrates the capability of the rectenna to start collecting energy and store it in an element such as a capacitor or a battery to further release it. FOM_{eff} demonstrates the capability of the RF harvester to yield "on time powering": the rectenna is connected to an application and

supply it on time. Both are reported in the Table I, which also includes some references of the state of the art. The ability of the proposed rectenna to simultaneously operate in two frequency bands, significantly improves the power sensitivity.

Table I. Comparison with the state of the art

Ref.	Freq (GHz)	Efficiency (%@P_{rf})	Sensitivity (V_{rec}@Prf)	Number of stage	Schottky diodes	Size (cm^2)	FOM Sens	FOM Eff
[21]	0.9	15% @ -10dBm	0.75V @ -10dBm	1	SMS-7630	15×15	1.9	6.6
[21]	2.4	9% @ -13dBm	0.9V @ -13dBm	1	SMS-7630	15×15	1.25	8
[22]	2.45	10.5% @ -20dBm	0.075V @ -20dBm	1	SMS-7630	3.4×3.4	6.5	905
[23]	0.915/ 2.45	14%@ -20/-20	0,36V@ -10/-10	1	SMS-7630	6×6	0.5	185
[24]	1.8/2.2 /2.5	55%@ -10dBm	300mV@ -32dBm 3tones	1	SMS-7630	7×7	20	112
This work Dipole	0.915/ 2.44	**11% @ -20/-15dBm**	**1V @ -22/-18dBm**	4	HSMS-2850	2.1×11	**19.8**	**136**
This work Patch	0.915/ 2.44	**12.5% @ - 19.5 dBm/ -20dBm**	**1V @ -19.5dBm/ -25dBm**	4	HSMS-2850	7.8×8.8	**10.5**	**100**

According the Table I, the patch-based harvester exhibits the highest sensitivity to rectify 1V with a dual-tone featuring: -19.5 dBm at 915 MHz and only -25 dBm at 2440 MHz. The FOM_{sens} represents the trade-off between the sensitivity performances of a rectenna and the antenna area. The FOM_{eff} rates the efficiency performances to the antenna area. For these two figures of merit, the rectenna based on the multi-arm dipole element yields the best trade-off, both for FOM_{sens} and FOM_{eff}, compared to the patch-based solution. This dual tone and multi-arm dipole harvester is close to the work proposed in [24] which exhibits the highest FOM_{sens} reported so far in the literature to our knowledge.

V. CONCLUSION

The range of power collectable in a scenario of RF harvesting varies from -15dBm to -25dBm. To address this purpose the rectenna proposed in this work are optimized to operate at a RF input power close to -20 dBm (or 10 µW). To further improve the ability to collect the RF energy, these rectenna, developed with Schottky diodes HSMS285 from Avago, perform a concurrent harvesting in the 915 MHz and 2.44 GHz ISM bands. The harvester including a patch antenna implemented on a 1.6mm FR4 PCB achieves the highest sensitivity. It provides a 1V-rectified voltage for a dual-tone excitation of -19.5 dBm at 915 MHz and -25 dBm at 2.44 GHz. For these conditions of operation the rectenna yields a power efficiency of 12.5%. To take into account the dimensions of the haverster, two figures of merit, FOM_{sens} and FOM_{eff} including the size of the antenna, respectively related to the power sensitivity and the power efficiency are proposed. The rectenna developed with the arm dipole element exhibits the highest figures of merit. A case of application is proposed with the remote powering of a

digital clock consuming 1V/5µA. The patch based harvester turns on the device with a dual tone excitation at the antenna of -19.5 dBm at 915 MHz and -20 dBm at 2.44 GHz. For the same scenario the harvester connected to the multi-arm dipole element needs a power of -22.1 dBm at 915 MHz and -17.8 dBm at 2.44 GHz.

REFERENCES

[1] T. Paing, A. Dolgov, J. Shin, J. Morroni, J. Brannan, R. Zane, and Z. Popovic, "Wirelessly powered wireless sensor platform'' in Eur. Microw. Conf. Dig, Munich, Germany, Oct. 2007, pp. 241-244.

[2] J. Bernhard, K. Hietpas, E. George, D. Kuchima, and H. Reis, ''An interdisciplinary effort to develop a wireless embedded sensor system to monitor and assess corrosion in the tendons of pre-stressed concrete girders,'' in Proc. IEEE Top. Conf. Wireless Commun, 2003, pp. 241-243.

[3] C. Walsh, S. Rondineau, M. Jankovic, G. Zhao, and Z. Popovic, ''A conformal 10-GHz rectenna for wireless powering of piezoelectric sensor electronics,'' in IEEE MTT-S Int. Microw. Symp. Dig, Jun. 2005, pp. 143-146.

[4] X. Zhao, T. Qian, G. Mei, C. Kwan, R. Zane, C. Walsh, T. Paing, and Z. Popovic, ''Active health monitoring of an aircraft wing with an embedded piezoelectric sensor/actuator network,'' Smart Mater. Struct, vol. 16, no. 2007, Jun. 2007, pp. 1218-1225.

[5] K. Lin, J. Yu, J. Hsu, S. Zahedi, D. Lee, J. Friedman, A. Kansal, V. Raghunathan, and M. Srivastava, "Heliomote: Enabling long-lived sensor networks through solar energy harvesting," in 3rd Int. Conf. Embedded Networked Sensor Syst., Nov. 2005, p. 309.

[6] J.A. Paradiso and T. Starner, "Energy scavenging for mobile and wireless electronics," IEEE Pervasive Computing, Vol. 4, and Issue: 1, Jan-March 2005, pp. 18- 27.

[7] K. R. Foster, "A world awash with wireless devices", IEEE Microwave magazine, vol. 14, Issue 2, March 2013, pp. 73-84.

[8] T. Le, K. Mayaram, and T. Fiez, "Efficient far-field radio frequency energy harvesting for passively powered sensor networks," IEEE J. Solid-State Circuits, vol. 43, no. 5, May 2008, pp. 1287-1302.

[9] J. Hirai, T.W. Kim, and A. Kawamura, ''Wireless transmission of power and information for cableless linear motor drive,'' IEEE Trans. Power Electron, vol. 15, 2000, pp. 21-27.

[10] H. Nishimoto, Y. Kawahara, and T. Asami, "Prototype implementation of ambient RF energy harvesting wireless sensor networks," IEEE Sens. J., Nov. 2010, pp. 1282-1287.

[11] BN. Shinohara, "Power without wires," IEEE Microw. Mag, vol. 12, no. 7, Dec. 2011, pp. S64-S73.

[12] M. Pinuela, P.D. Mitcheson, S. Lucyszyn, “Ambient RF Energy Harvesting in Urban and Semi-Urban Environments”, IEEE Trans. On Microwave Theory and Techniques, vol. 61, N°7, July 2013.

[13] Simon Hemour, Ke Wu “Radio-Frequency Rectifier for Electromagnetic Energy Harvesting : Developement Path and Future Outlook”, Proceeding of the IEEE, Vol.102, No.11, November 2014.

[14] T. Taris, L.Fadel, L.Oyhenart, V. Vigneras, “COTS-Based Modules for Far-Field Radio Frequency ”, IEEE NEWCAS, Paris, France, June 2013, pp. 1-4.

[15] Sika Shrestha, Sun-Kuk Noh, and Dong-You Choi, « Comparative Study of Antenna Designs for RF Energy Harvesting » International Journal of Antennas and Propagation Volume 2013, 10 pages.

[16] Z. W. Sim, R. Shuttleworth, M. J. Alexander, B. D. Grieve, « Compact patch antenna design for outdoor RF energy harvesting in wireless sensor networks, Progress In Electromagnetics Research, Vol. 105, 273–294, 2010.

[17] Naimul Hasan, Santu Kumar Giri, « Design of low power RF to DC generator for energy harvesting application », International Journal of Applied Sciences and Engineering Research, Vol 1, Issue 4, 2012.

[18] H. J. Visser, "Approximate Antenna Analysis for CAD", Wiley, 2009.

[19] R. Berges, L.Fadel, L. Oyhenart, V. Vigneras, T. Taris, “A dual Band 915MHz/2.44GHz RF Energy Harvester”, EUMW, Paris France, Sept 2015.

[20] Y-Y.Lu, J. Guo, H-C. Huang, “Design of Triple Symmetric Arms Dipole Antenna for 900/1800/2450MHz Applications”, Conf on Intelligent Information Hiding and Multimedia Signal Processing”, 2014.

[21] D. Masotti, A. Costanzo, M. Del Prete, V. Rizzoli, “Genetic-based design of a tetra-band high-efficiency radio-frequency energy harvesting system,” IET Microwaves, Antennas Propagation, vol.7, no. 15, June 2013, pp. 1254-1263.

[22] G. Vera, A. Georgiadis, A. Collado, and S. Via, “Design of a 2.45GHz rectenna for electromagnetic (EM) energy scavenging”, Proc. IEEE Radio and Wireless Symp, 2010, pp. 61-64.

[23] K. Niotaki, S. Kim, S. Jeong, A. Collado, A. Georgiadis, and M. Tentzeris, “A compact dual-band rectenna using slot-loaded dual band folded dipole antenna,” IEEE Antennas and Wireless Propagation. Lett. vol. 12, pp. 1634–1637, 2013.

[24] C. Song, Y. Huang, J. Zhou, J. Zhang, S. Yuan, and P. Carter, “A High-efficiency Broadband Rectenna for Ambient Wireless Energy Harvesting”, IEEE Transactions on Antennas and Propagation, accepted May 2015.

Bibliographies

Ludivine FADEL received the Ph.D in electrical engineering from the University of Bordeaux, France, in 2004. She is an Associate Professor at Bordeaux University and her main research interests include wireless power transfer and energy harvesting, materials and printing technologies for RF application.

Laurent Oyhenart received the Ph.D. degree in electrical engineering from the University of Bordeaux, Bordeaux, France, in 2005. He is currently an Associate Professor with the University of Bordeaux and develops his research activities in the IMS laboratory. His research interests include computational electromagnetics, photonic crystals and antenna synthesis.

Romain Bergès is a PhD student at IMS Laboratory. He received his Master from Bordeaux University in Electronic, in 2014. His current research focuses on RF Energy Harvesting.

Valérie Vigneras is a full professor in the Polytechnic Institute of Bordeaux and conducts research in the IMS Laboratory on complex structures (mixtures, structured media, self-assembled media) both by simulation to predict or optimize their properties and by characterization before their integration in high frequency systems (antennas, electromagnetic compatibility, radar shieldness…).

Thierry Taris is a full professor at the Bordeaux Institute of Technolgy (Bx-INP). He joined the IMS lab in 2005 where is research interests are related to the Radio-frequency Integrated Circuits in Silicon technologies.

List of figures and tables

Fun with Less Kilowatts: The Lectenna

By Vernon Trollinger, March 14, 2017, Energy Efficiency, Events & Fun, Family

Welcome to Fun with Less Kilowatts! We believe that science experiments at home can be a creative way to engage kids in learning while having fun. They can be educational AND great activities to keep your kids busy and away from the television. Each month, we'll feature a new science experiment that can be a great resource for parents and teachers.

The Lectenna

Did you know you that the energy from radio waves can be converted back into electric energy? It's true and you can make a *simple* two-component circuit that you and your kids can use to find 2.45 Ghz radio waves around your home. These are the same radio waves used by microwaves, WiFi network routers, bluetooth devices, smart phones, cordless phones, smart meters, and smart home systems that use Zigbee.

YouTuber pjaffeva posted this brilliant project showing how. Plus, there's also a link to a PDF set of instructions on Google Drive that you can download.

The Materials

- One HLMP-D150 Avago low current LED. Costs about 50¢/each. Available from: Amazon, Digikey, Mouser
- One Hitachi 1SS106 low capacitance Schottky diode. Pjaffeva recommends this Hitachi-made diode as being the only one in this shape that will work. But they're also hard to find. Currently, you can get them from LittleDiode's ebay store in the UK. Costs $6.38 but the bulk of that price is shipping from the UK.

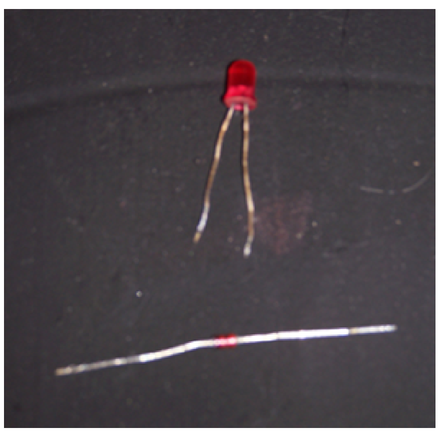

You'll also need:

- An operating WiFi router
- A bamboo kabob skewer
- Two pieces of tape

The Directions

1) Look on the base of the LED and find the side with the flat edge. This marks the negative or cathode side. Carefully splay the two wire leads away from each other as far as they will go. Make sure the one adjacent to the negative side gets bent over the flat edge so identify it. You can also mark it with a little spot of colored nail polish.

Categories

Careers/Jobs
Charity & Community
Energy Efficiency
Events & Fun
Family
FAQs
Green
Home Improvement
Hurricane Prep
Moving
News
Recipes
Save Money
Small Biz
Special Offers

Subscribe via Email

Subscribe

Subscribe via Email

Subscribe

Subscribe

Subscribe in a reader

Archives

December 2017
November 2017
October 2017
September 2017
August 2017
July 2017
June 2017
May 2017
April 2017
March 2017
February 2017
January 2017
all archives

Featured Articles

Prepare for Christmas With Green Cleaning Methods

Holiday Kitchen Safety – Cooking with Kids
How to Shop for Old Window Repairs
How Do I Clean A Clothes Dryer?
Gobble Up These Convenient Thanksgiving Deals on Meals

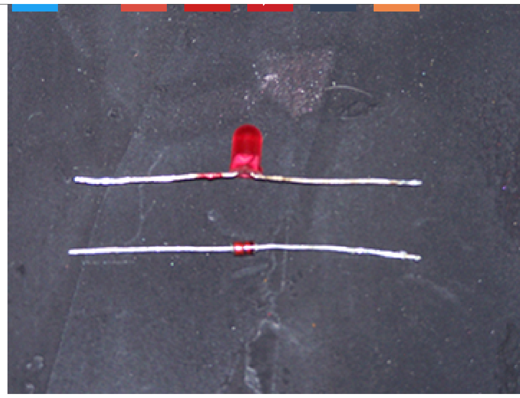

2) Next, find the band that runs around the Schottky diode. This identifies the negative end of this diode. The other end is the positive or anode end.

Using your fingers:

3) Twist the end of the negative or cathode wire from the LED onto to the positive or anode end of the Schottky diode.

4) Then twist the end of the negative or cathode end of the Schottky diode onto to the positive or anode end of the LED.

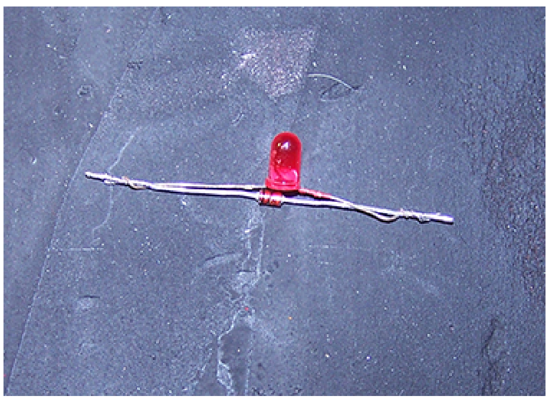

You have just made a "rectenna" and you'll need to keep the assembly and the wires straight as possible. The length of the wires should be about 6 cm long (a hair short of 2 3/8 inches).

5) Tape the two diodes to one end of the bamboo skewer.

6) With a WiFi router on and running, hold the diode near an antenna on the WiFi router.

The Result

The LED should light up as it draws closer to the antenna (signal). The further away it is, the weaker the signal and the less it can grab to light up.

The Science

The WiFi routers uses radio waves to transmit data to and from computers and other devices in your home. Radio waves behave like water in a glass, they ripple or oscillate at a certain number of times or frequency per second. A radio wave's wavelength is the distance covered by one complete cycle of a radio wave — from peak to valley.

Radio waves used by WiFi routers, bluetooth devices, microwaves, etc., broadcast signals in the 2.45 gigaherz (Ghz) range or 2.45 billion oscillations per second. That means the signal wavelength is about 12 cm. To pick up signal, however, you only need an antenna that's half as big— 6 cm. When the radio waves strike this antenna, called a 1/2 dipole ("di"=two), the energy excites the antenna's

The "Rectenna": Because the radio waves cause voltage to flow one direction and then the opposite direction, the current is called an alternating current (AC). By connecting a diode to both poles of the antenna it converts the AC current to flow only in one direction, called direct current (DC). The antenna becomes a "rectenna".

How the diodes work: The diodes work as one-way valves for electricity, allowing voltage to flow forward but not back. In the case of the rectenna, AC current caused by the radio wave sends a positive charge down one of the antenna poles and then the other. By putting the Hitachi 1SS106 diode across both poles, the diode only lets the positive charge coming down one of the antenna poles through. The LED is actually a Light Emitting Diode and works the same way as a regular diode except that when it's on, it lights up. Meanwhile, Schottky diodes turn on at a lower voltage than other diodesand because the rectenna can only catch a fraction of the WiFi's broadcast power, the Schottky diode can rectify that little bit of AC to DC.

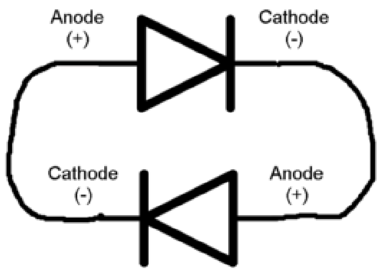

When we connected our diodes together, their polarity formed a loop that only allowed voltage to flow one way and thus light the LED. Brilliant job, pjaffeva!

Do you have any fun and kid-friendly science experiments you'd like to see us try for Fun with Less Kilowatts? Share with us in the comments!

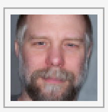

About Vernon Trollinger
A native of Wyomissing Hills, PA, Vernon Trollinger studied writing and film at the University of Iowa, later earning his MA in writing there as well. Following a decade of digging in CRM archaeology, he now writes about green energy technology, home energy efficiency, DIY projects, the natural gas industry, and the electrical grid.

Tags: family fun, Fun with Less Kilowatts, kids, science experiments

0 Comments Bounce Energy Blog 1 Login

Recommend Share Sort by Best

Start the discussion…

LOG IN WITH

OR SIGN UP WITH DISQUS ?

Name

Be the first to comment.

ALSO ON **BOUNCE ENERGY BLOG**

Choosing the Best Home Generator for Your Emergency Needs

1 comment • 3 years ago

T&B Electric LTD — Nice article covering the difference between portable and permanent generators. Some homeowners "back feed" …

Career Opportunity with Bounce Energy | PHP/Integration Developer

1 comment • 3 years ago

Chris Jones — Sounds like a great opportunity.

Take Care of Your Favorite Gadgets with Great Waterproof Tech

1 comment • 2 years ago

erna — Vermon thanks for your post, great as always! Coolest is cool I got one of this :) what's funny I also have swimmo watch for swimmers …

5 Quick DIY Home Improvement Fixes to Get Your Home Through Winter

1 comment • 3 years ago

Steve Veach — Excellent and informative blog post! I am a HVAC Contractor in Chicago and have found a new site to check in on. Thank …

Subscribe Add Disqus to your siteAdd DisqusAdd Privacy DISQUS

Follow Bounce: Share this on:

K3OPS® | HOME |

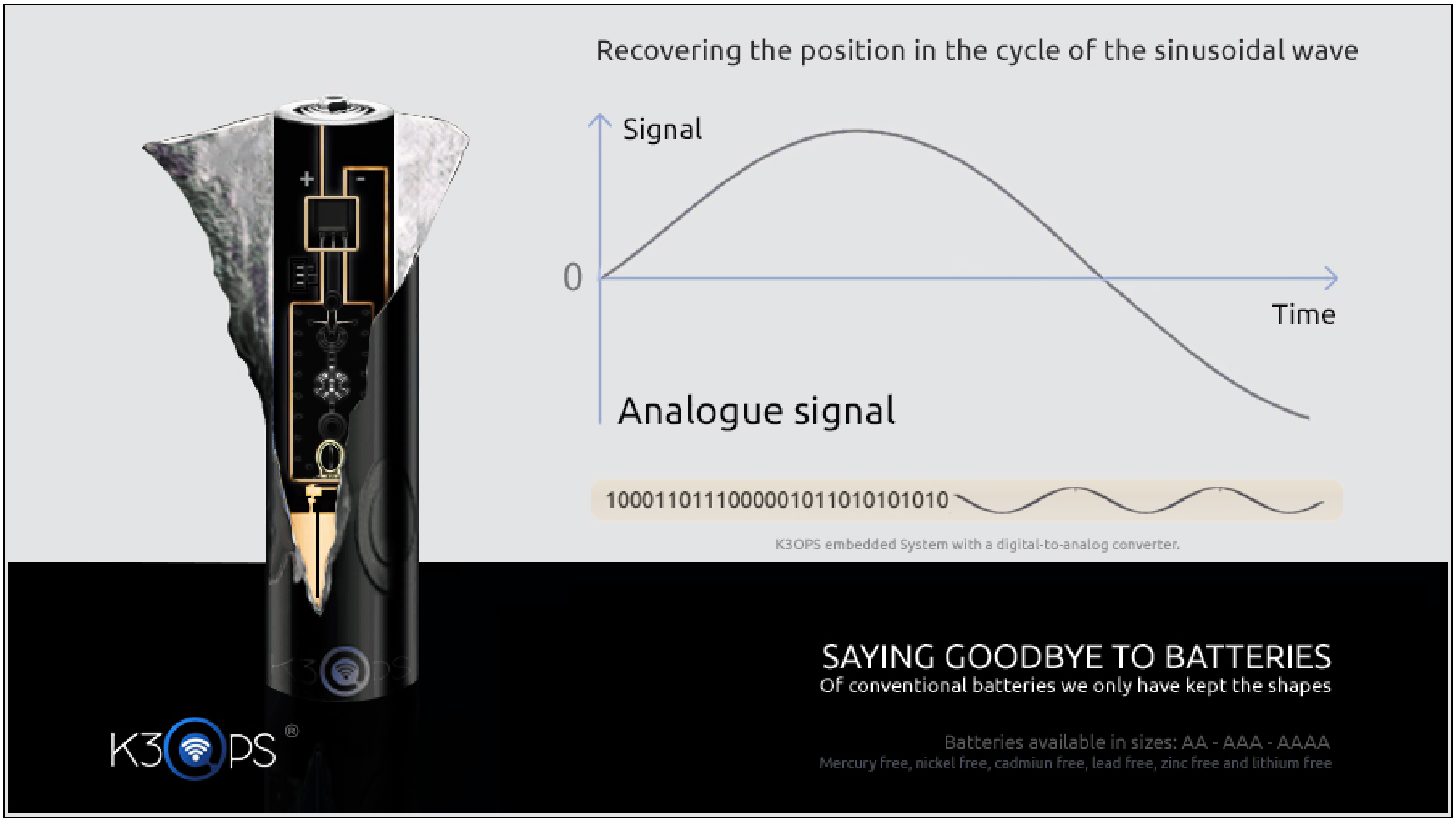

An electromagnetic field uses the photon as an elementary particle to transmit force. It combines:

- **A magnetic field** *force resulting from the movement of loads µT.*
- **An electric field** *force created by the attraction of repulsion loads, measured in volts per meter - V/m.*

With an energy determined according to the speed of light, the RF are by far the best medium to transmit any kind of information.

The multiplication of wireless communications systems in our environment ensures sufficient microwave leakages to harvest from the ambiant and enough energy to convert into DC electricity. Electromagnetic fields are everywhere and since they carry energy, they became the best candidate to deliver an endless source of renewable energy.

$\vec{B}$ is the magnetic induction expressed in T refered to **Nikola Tesla**, "Father of Free Energy", which is at the origin of the electromagnetism.

Using meta-materials combined with nanotechnology has deeply increased the performance and miniaturization of rectennas embedded in K3OPS system. Our products operate autonomously, offering an endless supply of green energy in a respectful and environment-friendly approach.

principles and beautiful sentences. At that point in time I would have simply been Xin, a child like any other...

But one day I dreamed. I woke up far away, somewhere else, in another past. I decided to change my destiny and even if I was supposed to become a mathematician, I eventually decided to create, because already as a child my heart was chasing the stars.

Of the hundreds of directions shown to me after graduating, only one captured my attention: a single goal... Build the impossible for a safer world. So, over the past 3 years, our real challenge to overcome for all RF Energy Harvesting technics was to optimize electricity conversion. The massive proliferation of wireless telecommunication systems since the past two decades brought a saturation of the electromagnetic fields with a constant growth of 15% every year in our environments. As a result, this situation reversed the base problem that makes today Harvesting RF Energy a game changer. The key was the Power Management System.

We are far beyond the conversion constraint and performance by controlling "RF-interferences", by harvesting different frequencies *from near and far*, by using Metamaterials combined with nanotechnologies. We dramatically have improved power conversion efficiency and reduced the size of our Energy Harvesting systems embedded in all K3OPS' products.

Thanks to Nikola Tesla, my inspiring mentor, K3OPS' products have reached by far their objectives in terms of converting and performance, offering an endless efficient source of green energy, reliable in an environmentally friendly approach.

Xin WEI Co-Founder of K3OPS technology with Alexandre Despallieres

The Rectenna was invented in 1964 by William C. Brown, patented in 1969. It is a rectifying antenna used to convert microwave energy into DC. A simple Rectenna consists of a dipole antenna with an RF diode connected across the dipole elements. The diode rectifies the AC current induced in the antenna to produce DC power.

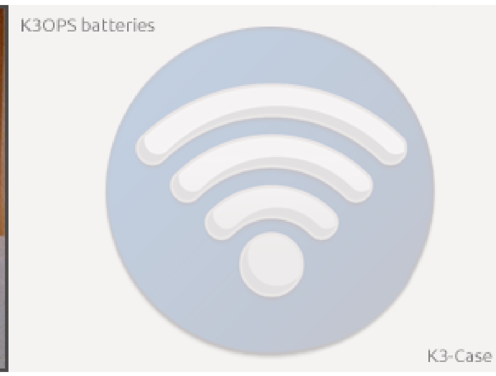

Centre for Collaboration in Electromagnetics and Antenna Engineering is a centre for research collaboration established to foster research in electromagnetics and engineering conducted by Macquarie University researchers and prominent collaborators from external institutions, including people from industry and overseas ins We have state of the art research ficilities including a NSI-700S-50 spherical nearfield anechoic chamber, 3 Vector Network Analyzers (capable up to 22GHz, 50GHz, and respectively), state-of-the-art embroidery machine DreamCreator-XE-VM5100 for embroided antennas, Dielectric Characterization Kit - High Temperature Probe (2(20GHz), as well as several in-house and commercial licenced softwares.

Our recent and ongoing research projects are:

- Wireless Implantable Bio-Telemetry System and Miniature Antenna Design
- Wireless Freedom for Lab Rats
- Flexible and Wearable Antennas for Biomedical and Healthcare Applications
- Characterizing Properties of Carbon nano Tubes at Microwave Frequencies
- Electromagnetic Band Gap (EBG) Resonator Antennas
- Leaky-Wave Antennas for Advanced Wireless Systems
- Shared Aperture Arrays for Space Borne Applications
- Novel Dielectric Resonator Antennas
- Super Wideband Antennas
- Focal Plane Arrays for Radio Astronomy
- Archimedian Spiral Metamaterials
- Frequency Selective Surfaces for Energy-Saving Glass Panels
- Dual-Band Artificial Magnetic Conductor (AMC) Surfaces
- Antenna Technologies for Ultrawideband (UWB) Systems
- High Gain Antennas with Planar Surface-Mounted Short Horns
- Photonic Crystal/EBG Based Horn Antennas
- Broadband Microstrip Patch Antennas for Wireless Computer Networks
- Theoretical Analysis of Photonic Crystal Structures
- New Closed-form Green's Functions for Microstrip Circuits and other Layered Structures
- Integrated-design of Hybrid-resonator Antennas for Broadband Wireless and other Communication Systems
- Singularity-enhanced Finite-different Time-domain (FDTD) Method for Diagonal Metal Edges, Strips and Films
- Low-profile Dielectric-resonator (DR) Antennas

Wireless Implantable Bio-Telemetry System and Miniature Antenna Design

The two major challenges associated with the conversion of a wireless system operating in air to an implantable version, antenna detuning and biocompatibility, are a in a coherent way. An RFID-based biomedical telemetry system designed for free-space operation was chosen as the starting reference. A new, pin-compatible, spa antenna with a ground plane was designed, fabricated and tested, to replace the original “free-space” antenna in the active RFID tag without making any other chang tag circuit, such that the tag would function well when it is placed under rat skin and fat. Biocompatibility and potential antenna detuning due to rat tissue variati addressed in the design process, without significantly increasing the tag physical height, by applying a thin coating of biocompatible material directly over the ante operation of the medical telemetry system was successfully demonstrated, with the tag placed under rat skin and fat, and its range of 60-72 cm was found to be sut support medical research experiments conducted with rats in cages. Due to the biocompatible coating over the antenna, antenna matching is very insensitive to cl tissue dielectric constants and thickness. The footprint of the new antenna is 33% less than that of the original antenna, its measured 10 dB return-loss bandwidth is 1(11%, and overall efficiency is 0.82% at 920 MHz.

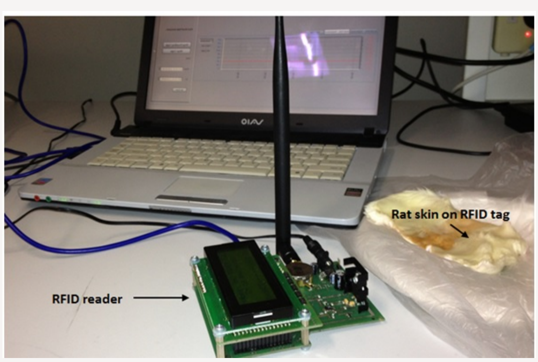

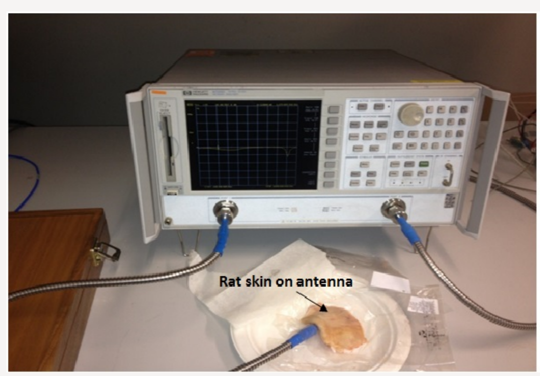

Wireless Freedom for Lab Rats

We are developing a fully implantable wireless telemetry system. This is a joint research project with BCS Innovations and the Australian School of Advanced Medicine (will be first used in the research conducted in ASAM, with rats, on hypertension. To date the major method of controlling hypertension is through the use o pharmaceuticals. The pathway to approval for most drugs for human use involves pre-clinical (animal) trials. Lab rats are considered biologically similar to humans, pa

in terms of their social behaviour. Therefore, it is very important to not compromise the pharmaceutical trials by unnecessarily stressing the rats by harnessing the monitoring equipment. One of the technical challenges of developing an implantable system that monitors the various signals, is the relatively small size requ implantable telemetry system is a miniature transceiver implanted in an animal that senses, processes and transmits data via a wireless link to monitor vital signals of c freely moving laboratory animals. This is crucial in giving researchers flexibility and reliability, especially in studies with special experimental settings using mazes wheels and treadmills. We have plans to develop a fully implantable telemetry system for subcutaneous or intraperitoneal placement in rats that monitors th parameters as well as blood pH and chemistry, nerve activity and circadian respiratory rate rhythms. The aim of this project is to eventually develop a system with e capabilities that costs less than what is currently available, to provide more universities and researchers with the opportunity to use this technology.

In this sequel, initially, when a module of our original system was placed under the skin of a rat, the wireless link failed completely. It could not send a temperature read a centimetre! The point of failure was the commercial antenna in the module that had been designed to work outside the body, in air. Such antennas do not work unde because the electrical characteristics of skin (rat or human) are significantly different from that of air. Hence the main challenge was to design an antenna that works v placed under the skin. In addition, it was necessary to cover the module and the antenna by biocompatible material, which also affects antenna performance. Possible v of skin characteristics from one rat to another or one person to another were considered. Unlike the commercial antenna, we wanted our antenna to radiate less into th the rat/person and more away from the body because that not only increases the quality of the wireless link, maximum range (distance between implanted mo monitoring station) and battery life but also reduces the exposure of the body to radio-frequency waves. Indeed we had to consider the electromagnetic effects of fat a material around the antenna. We were able to meet all these requirements with a novel compact antenna design that is approx. one third the size of the original co antenna. We successfully demonstrated wireless telemetry transmission of temperature with the new module placed under rat skin and the monitoring station pla distance of up to 80 cm! This range is sufficient for our immediate target application supporting new medical research by Professor Paul Pilowsky's team. If necessary, further extended by increasing the power level at the monitoring station.

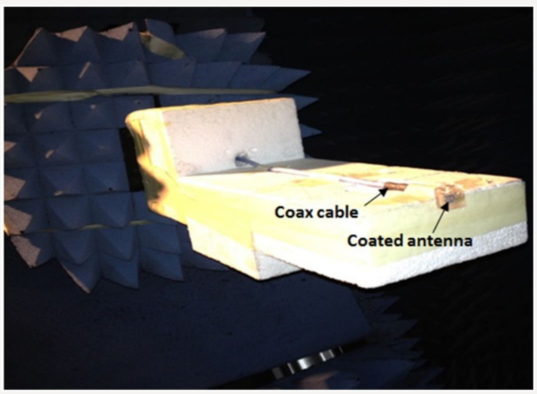

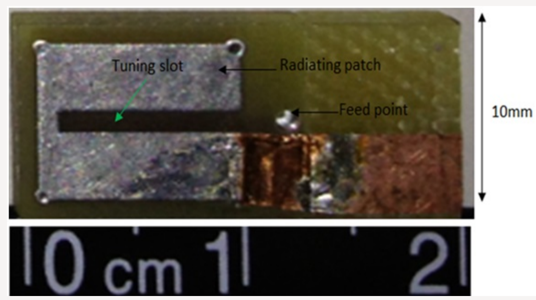

Flexible and Wearable Antennas for Bio-Medical and Healthcare Applications

Body Centric Wireless Communication is a rapidly growing research area targeted for medical, healthcare, public safety and defense applications. The need to address transceiver specifications and real-time scenarios in close proximity to human body is continuously evolving antenna system research. Several novel miniature antennas havi dual- and wide-band operations have been designed and tested for Wireless Body Area Network (WBAN). They have significant advantages of small size, wide radiation patt the human body for maximum coverage and are less sensitive to the gap variation between human body and antenna.

A compact ultra wideband antenna is shown below with strong notch-band rejections up to VSWR = 26, that is tunable over a wide frequency range from 3.55GHz to 6.8 been designed. To estimate the stub length to notch frequency for a given interfering application, analytical expressions for the normalized stub length which is indep substrate dielectric constant is also presented. This helps to avoid hit-an-trail method and gives a good estimate of initial design parameters for notch. Proposed antenna radiation patterns and yields a measured 10dB return-loss bandwidth from 3GHz to 10.5GHz.

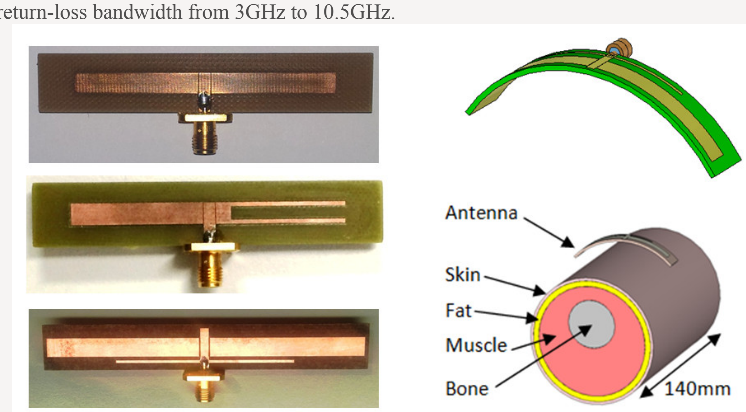

Characterizing Properties of Carbon Nano Tubes at Microwave Frequencies

Carbon Nanotube (CNT) yarns are novel CNT-based materials that extend the advantages of CNT from the nano-scale to macro-scale applications. We have modelled CNT potential data transmission lines. Test structures have been designed to measure electrical properties of CNT yarns, which are attached to these test structures using gold p testing and microwave S-parameter measurements have been conducted for characterisation. The observed frequency independent resistive behaviour of the CNT yarn promising indicator that this material, with its added values of mechanical resilience and thermal conductivity, could be invaluable for a range of applications such as B Networks (BAN). A model is developed for CNT yarn, which fits the measured data collected and agrees in general with similar data for non-yarn CNTs.

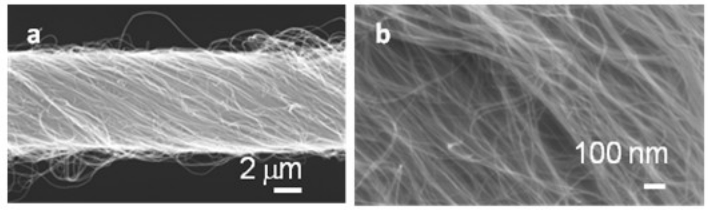

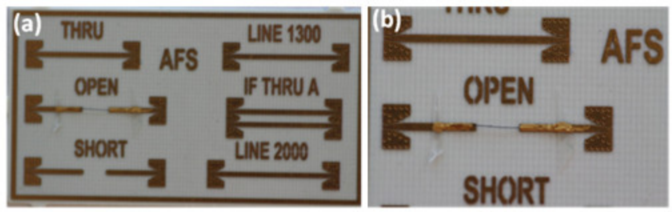

Electromagnetic Band Gap (EBG) Resonator Antennas (ERA)

We have designed, fabricated, and measured antennas based on 3D, planar and 1D EBG structures (i.e. photonic crystals). These flat microwave antennas, known as EBG antennas or Fabry-Perot cavity antennas, can give gains of about 20dB and very good efficiencies.

Enhancing Radiation Characteristics of ERAs by Improving Aperture Phase Distribution

This work focuses on achieving superior radiation characteristics of ERAs by improving their aperture phase distributions. A unique method, utilizing full-wave simula analytical analysis, has been developed to design Phase Correcting Structures (PCS) for ERAs. This method uses actual phase distribution on the physical aperture of ERAs relying on geometric optics. Several Phase Correcting Structures (PCSs) have been designed, which were later validated with the measurements of their fabricated p Tremendous improvement in the radiation performance is witnessed in both simulated and measured results. These exciting initial results validate our proposed methodo indicate an existence of a great potential to be explored. The figure below shows the field propagation above an ERA: (a) without PCS, and (b) with PCS. It is clear that the the PCS is much more uniform and the energy is focussed towards broadside direction, thus, resulting in increased directivity.

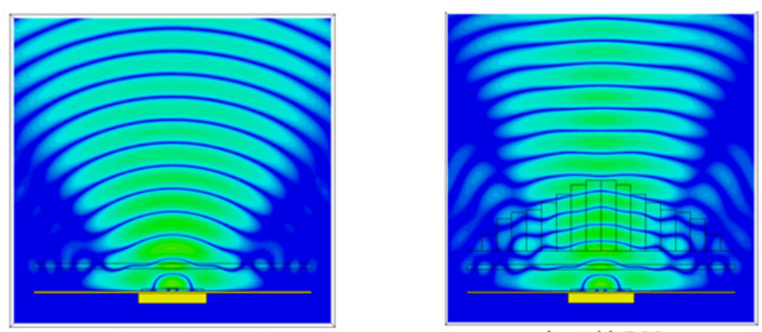

a. without PCS b. with PCS

Extremely Wideband High-Gain ERAs (Gain~15-20dBi, Bandwidths >50%)

In 2014-15, we invented an innovative class of electromagnetic band-gap (EBG) resonator antennas which provide high gain and wide bandwidth with an extremely r footprint. One of the prototype developed has only 8% of the area as compared to conventional EBG resonator antennas but its performance (gain bandwidth) is a record hi for this class of antennas, while providing gain in the range of 15-20 dBi. This represents an improvement of nearly two orders of magnitude in the bandwidth compared to EBG resonator antennas. Thanks to its practical advantages of flat shape and low-cost manufacturability, it can be easily attached to a wall of a building, for example, to co building wirelessly to the National Broadband Network.

Our most recent results on such wideband high gain antennas can be found in: "Achieving high gain-bandwidth through flat GRIN superstrates in Fabry-Perot cavity antenn 2014 IEEE International Symposium on Antennas and Propagation (AP-S/USNC-URSI), pp. 1748 – 1749, Memphis, Tennessee, USA, July 6-11, 2014.

Detailed antenna design along with experimental data of another of our wideband EBG resonator antenna having composite multi-layer superstrate, is published in the pa "Wideband high-gain EBG resonator antenna with a small footprint and all-dielectric superstructures" in IEEE Transactions on Antennas and Propagation, vol. 62, no. 6, 201

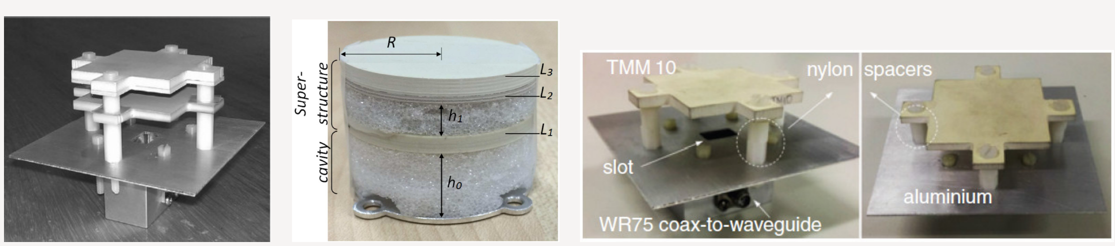

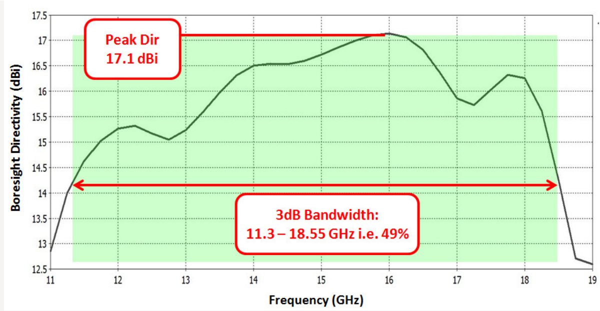

Frequency response of one of our Wideband ERA Prototypes

Simple Dual-Band ERAs

We developed a new method to obtain dual-band operation from a simple electromagnetic band gap resonator antenna. The antenna is based on a one-dimensional EBG made out of two low-cost unprinted dielectric slabs. The EBG structure is implemented as the antenna superstrate, which has been designed to provide a locally-inverted reflection phase gradient with high reflectivity, in two pre-determined frequency bands. The linearly polarised antenna design and experimental results are described in entitled: "A simple dual-band electromagnetic band gap resonator antenna based on inverted reflection phase gradient" published in IEEE Transactions on Antennas and Pro vol. 60, no. 10, pp. 4522-4529, 2012.

We have extended this concept for dual-band, dual-polarised and circularly-polarised antennas. We also designed a tri-band antenna following this concept. It needs only t cost unprinted dielectric slabs.

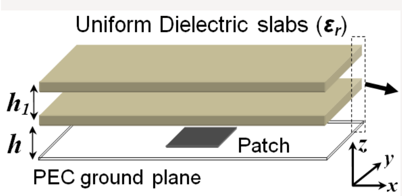

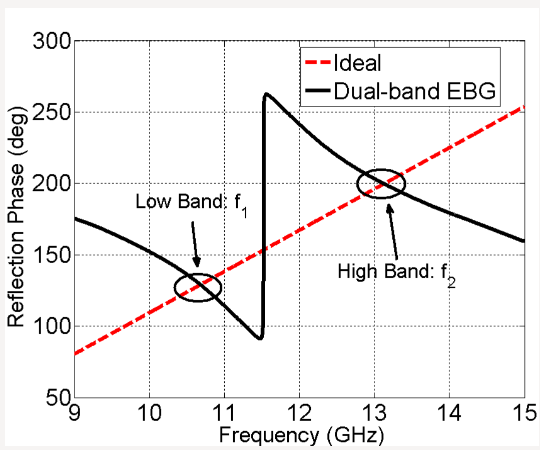

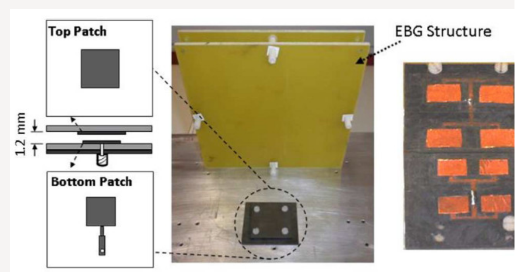

Low-Profile Wideband ERAs

We have designed and successfully tested wideband low-profile (thin) EBG resonator antennas. The breakthrough that contributed to this success is our design of a partially surface (PRS) with a positive reflection phase gradient. Thin single-dielectric-slab PRSs with printed patterns on both sides were investigated to minimise the PRS thickn simplify fabrication. Three such surfaces, each with printed dipoles on both sides, have been designed to obtain different positive reflection phase gradients and reflection r levels in the operating frequency bands. These surfaces, and the EBG resonator antennas formed from them, were analysed theoretically and experimentally to highlight t compromises involved and to reveal the relationships between the antenna peak gain, gain bandwidth, the reflection profile (i.e. positive phase gradient and magnitude) of th and the relative dimensions of dipoles. A small feed antenna, designed to operate in the cavity field environment, provides good impedance matching (|S11|< -10 dB) a operating frequency bands of all three EBG resonator antennas. Experimental results confirmed the wideband performance of a simple, low-profile EBG resonator antenna thickness is only 1.6mm, effective bandwidth is 12.6%, measured peak gain is 16.2 dBi at 11.5 GHz and 3dB gain bandwidth is 15.7%. Please find details in a paper entitled of Simple Thin Partially Reflective Surfaces with Positive Reflection Phase Gradients to Design Wideband, Low-Profile EBG Resonator Antennas," published in IEEE Tra on Antennas and Propagation in 2012.

Low-Profile Dual-Band ERAs

We have achieved dual-band operation in a low-profile EBGRA using a single dielectric superstate with a printed pattern only on one side. This also made use of our r inverting the gradient of the PRS reflection coefficient.

Woodpile EBG Material and Antennas

In 2003, we designed and built a woodpile 3D photonic crystal, also known as a EBG crystal, operating in microwave frequencies, and demonstrated experimentally the ex the electromagnetic band gap. The crystal is made out of cermain material.

Then we designed a planar EBG resonator antenna. Shown below, it has a resonant cavity between a ground place and a 3D woodpile photonic crystal. We employed both m and slots to feed the cavity, and investigated both linearly and circularly polarised antennas. The linearly polarised antenna design and experimental results are described in entitled "A planar resonator antenna based on a woodpile EBG material," published in IEEE Transactions on Antennas and Propagation,vol. 53, no. 1, pp. 216-223, January 2

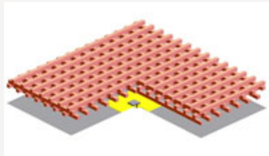
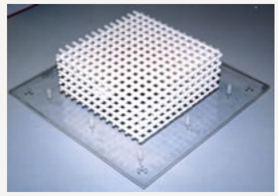
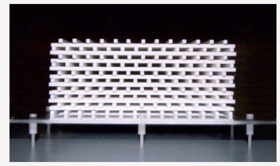
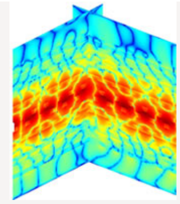

Leaky-Wave Antennas for Advanced Wireless Systems

Antenna beam steering can bring significant benefits to advanced wireless systems. Microstrip leaky-wave antennas (MLWAs) are of particular practical interest becaus planar low-profile configuration, ease of fabrication, and beam-scanning capabilities. In this research several planar MLWAs and arrays are developed to radiate at bores conical beam around the boresight, with simultaneous dual-side-beam scanning, dual-band forward and backward beam-scanning, and continuous beam scanning from the to the forward direction. Moreover, methods and antenna designs are proposed to steer the beam at a fixed frequency, shifting beam-steering range, and fixed-frequency bean in forward and backward directions.

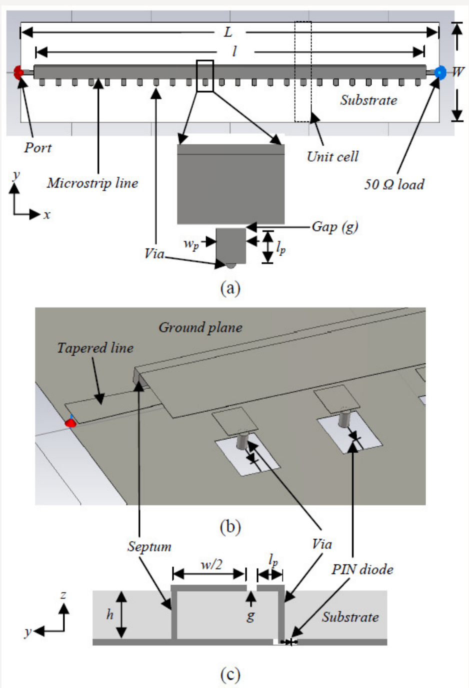

Figure 1. Proposed reconfigurable HW-MLWA: (a) top view, (b) perspective view, and (c) side view.

TABLE I. SWITCH CONFIGURATIONS AND CORRESPONDING MAIN BEAM DIRECTIONS AT 6.5 GHZ

	Switch Configuration	Main Beam Direction (θ)
1	11111111111111111111111	21°
2	11110011110011110011100	26°
3	00001100001100001100011	32°
4	00000000000000000000000	37°

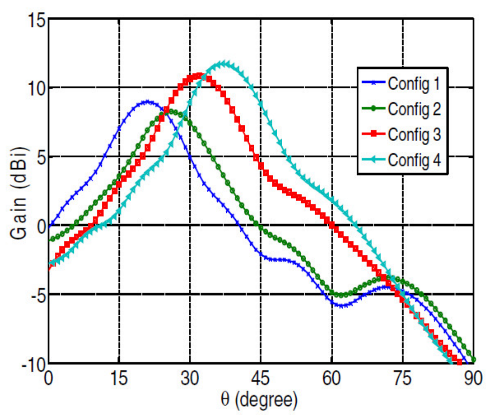

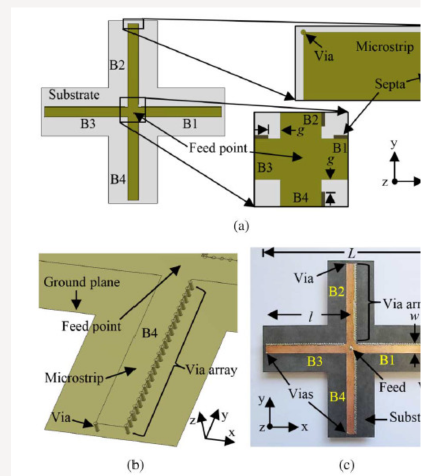

Fig. 1. HW-MLWA array design steps: (a) top view of the initial de septa, (b) perspective view of one branch of the final design with v (substrate omitted, not to scale), and (c) top view of the fabricated pro

Multi-band Dual-Polarized Shared Aperture Array

Multi-band dual-polarized shared-aperture (MBDP-SA) arrays are antenna arrays that operate in two (or more) frequency bands with dual-polarization in each band, a elements are integrated together into a common physical space by sharing the single aperture. The MBDP-SA array is of great interest in space-borne SAR system, bec technique can effectively reduce the payload and size of the antenna sub-system. In this research project, main efforts are focussed on three aspects: 1) improve the specifi current Dual-Band Dual-Polarized Shared-Aperture (DBDP-SA) array; 2) construct Tri-Band Dual-Polarized Shared-Aperture (TBDP-SA) array; and 3) explore some new for DBDP-SA antenna.

(a) Rear (b) Front

Fig.1 Improved DBDP-SA array.

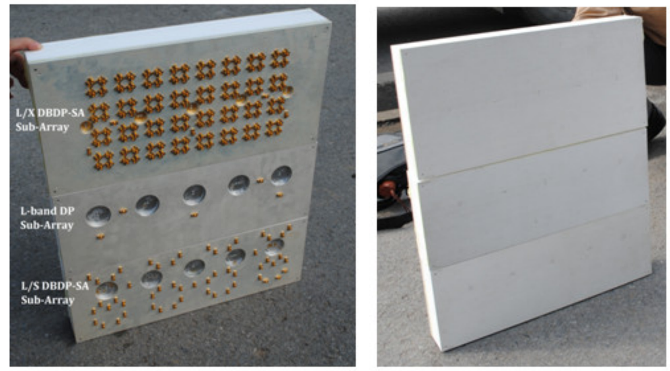

(a) Rear (b) Front

Fig.2 Photos of the TBDP shared aperture prototype array.

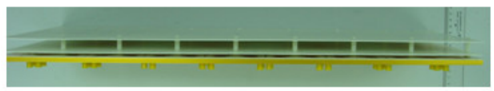

Side view

Fig.3 Novel structure DBDP-SA array

Compact Dielectric Resonator Antennas with Ultra-Wide 60%-110% Bandwidths

We have recently made a significant achievement in the emerging ultra wide-band (UWB) wireless communication systems, which require antennas with bandwidths gr 106%. In the past, the only way antenna engineers knew how to get such a bandwidth from a thin antenna was by removing the metal sheet underneath the antenna (known a plane"). This is not an acceptable solution for practical systems because the lack of it allows the antenna to radiate both upwards and (unnecessarily) downwards (i.e. electronic device on which the antenna is installed), wasting about half of its power. Saving power is crucial in UWB systems due to the severe power limits imposed by regu 2011, we made a breakthrough in dielectric-resonator (DR) antenna research, by inventing a novel DR antenna with a full ground plane and a 110% bandwidth. This disp myth that such bandwidths cannot be achieved with full ground planes. This antenna, published in the prestigious IEEE Transactions on Antennas and Propagation in Decem is 29% smaller but has a 30% greater bandwidth than the next-best DR antenna, which does not even have a full ground plane. Hence it is ideal for next-generation ultra-fas and sensor applications.

We theoretically and experimentally demonstrated that, by introducing a lower-permittivity full-length insert between the ground plane and a higher-permittivity dielectric dielectric resonator antennas (DRA) with ultra-wide bandwidths, in the range of 60%-110%, can be designed. Furthermore, the volume of such DRAs is reduced by appr 50% using a finite planar conducting wall. Unlike vertical monopole-type hybrid UWB DRAs, these antennas radiate sufficiently in the upward direction. Unlike in printed UWB antennas, the power radiated into the lower hemisphere is significantly less. An example prototype antenna, designed to operate in the FCC UWB band, has a dielectr of 12 x 8 x 15.2 mm3 (or 0.124 x 0.083 x 0.157 lambda3 at 3.1 GHz), and an average measured gain of 5 dBi from 3.1 to 10.6 GHz. These antennas exploit multiple low with overlapping bandwidths to form an ultra-wide contiguous bandwidth. With the proposed dielectric arrangement, it is possible to efficiently couple a sufficient numbe overlapping modes to a 50 ohm feedline using a single, simple feed.

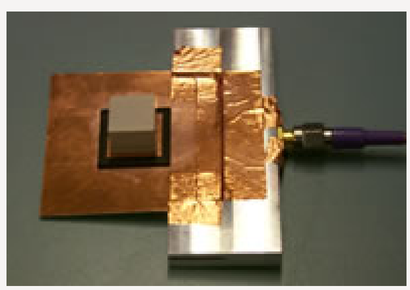

The antenna has a remarkably small footprint of 12x8 mm2 at 3.1 GHz - the lowest frequency of the FCC UWB band. Its dielectric volume is 1459 mm3, or 1.7x10-3 lamb lowest operating frequency of 3.1 GHz, and overall height is 15.2 mm or 0.157 lambda0. To place these results in perspective, it is worth comparing the new designs with wideband DR designs available in the literature. To the best of our knowledge, prior to this, the widest bandwidth ever obtained from a pure DRA design is 84% . The volu DR in that design is 0.225 x 0.172 x 0.062 lambda3 (= 2.4x10-3 lambda3) at its lowest operating frequency of 3.69 GHz. In that DRA, the DR is positioned in a non-traditi close to the edge of an orthogonal, "vertical" ground plane, which does not block radiation towards the lower hemisphere. The widest bandwidth demonstrated by a pure DI traditional "horizontal" ground plane, (which can be employed to shield the rest from the antenna, as discussed previously) is 78%. The dielectric volume of that design is 0. x 0.21 lambda3 (= 5.8x10-3 lambda3) at its lowest operating frequency of 6.7 GHz.

Super Wide-band Antennas

We have demonstrated that extremely wide bandwidths (ratio-bandwidths up to 1:25) can be obtained from a specially designed printed antenna with a tapered semi-ring design is described in "A Printed Elliptical Monopole Antenna with Modified feeding Structure for Bandwidth Enhancement," in IEEE Transactions on Antennas and Pro vol. 59, no. 2, pp. 667-670, Feb. 2011.

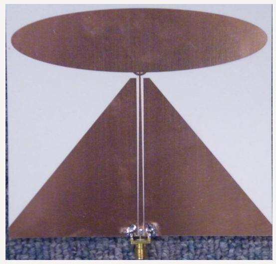

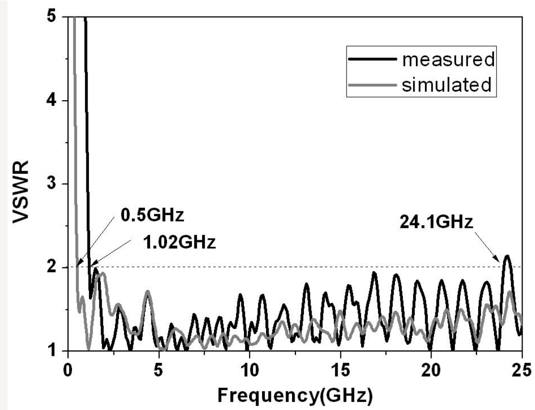

Focal Plane Arrays for Radio Astronomy

Dense focal plane arrays (FPAs) are a key technology for a new generation of Radio-telescopes. Their primary benefit is the rapid survey speed facilitated by the wide fiel provided by multiple beams. Recent advances have brought dense FPAs within reach of radio astronomy applications. A number of institutions have significant research pr this field. This technology is being considered for the Square Kilometre Array (SKA) (www.skatelescope.org). The PhD project of Douglas Hayman, conducted with CS Centre and Division of Astronomy and Space Science, investigated beamforming aspects of FPAs and evaluated their performance in Radio Astronomy. A prototype interf radiotelescope, built at CSIRO's Radiophysics Laboratory in Sydney, is used to demonstrate a suite of techniques forFPA beamforming and evaluation for this thesis. Bea solutions were experimentally demonstrated in our paper in IEEE Transactions on Antennas and Propagation, entitled “Experimental Demonstration of Beamforming Sol Focal Plane Arrays”.The THEA tile, shown below, is designed by ASTRON and used for the experimental component of this research.

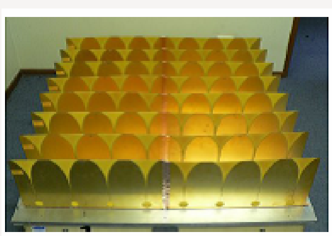

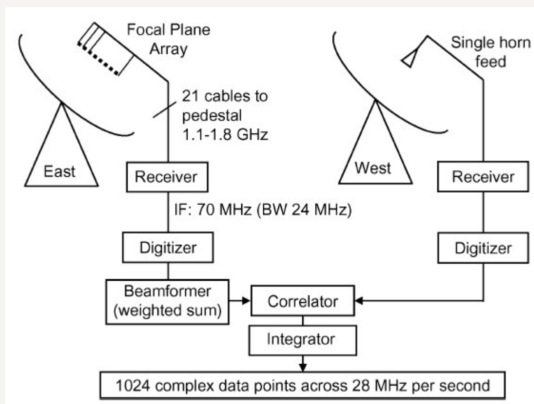

Negative Permeability of Spiral Metamaterials

Archimedean spirals and complementary Archimedean spirals are super-compact metamaterial particles. Thanks to their convoluted geometry, unit cells can be made electri small. We theoretically analysed monofilar, bifilar, trifilar and quadrifilar Archimedean spiral metamaterial particles using point group theory and crystallography. From the s properties electromagnetic response was determined. Magnetic, electric and magnetoelectric modes of the particles were identified along with their isotropy characteristics. shown that all the particles, except monofilar spiral, are nonbianisotropic. Further, effective medium theory was applied to extract the effective permeability of the spiral med results indicated negative values for permeability in certain frequency ranges. Detailed theory and numerical simulation results are available in the paper entitled “Analysis metamaterials by use of group theory,” published in the Metamaterials Journal, vol. 3, no. 1, pp. 33-43, March 2009.

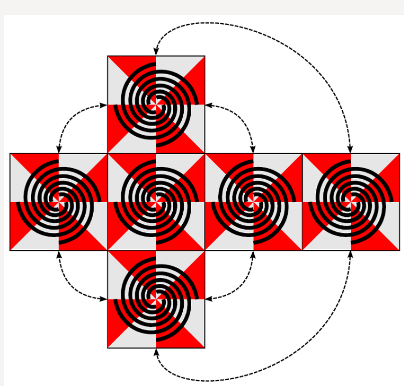

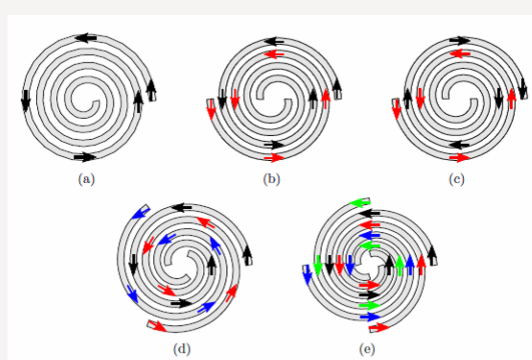

Archimedean Spiral Metamaterials and Backward Waves

We have shown backward wave propagation and double negative parameters over a 19% bandwidth in a microstrip line loaded with series gap discontinuities and super complementary Archimedean spiral resonator metamaterial particles. Moreover, our equivalent-circuit model for such unit cells almost perfectly described the structu practically important frequencies (by comparison with full-wave results). We also fabricated and tested compact filter circuits with only one or two complementary spiral met particles. Our results sre summarized in the paper entitled "Backward Wave Microstrip Lines with Complementary Spiral Resonators," published in IEEE Transactions on and Propagation, Vol. 56, Issue: 10, pp. 3173-3178, Oct 2008.

We derived design equations for Archimedean spiral resonators and tested them against full-wave simulations. The details are in the paper entitled "Design of monofilar a Archimedean spiral resonators for metamaterial applications," published in IET Microwaves, Antennas & Propagation, vol. 3, no.6, p. 929-935, Sep.2009.

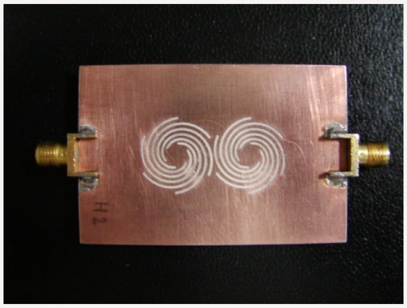

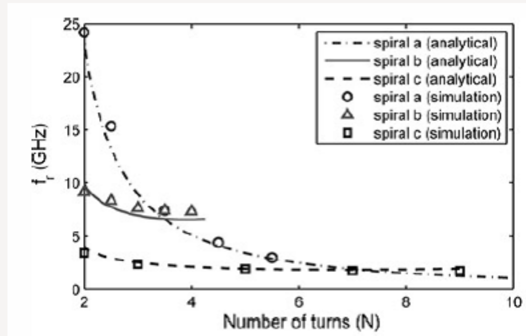

Frequency Selective Surfaces for Energy-Saving Glass Panel

Energy-saving glass is becoming very popular in building design due to their effective shielding of building interior against heat entering the building with infrared (IR) wave obtained by depositing a thin layer of metallic-oxide on the glass surface using special sputtering processes. This layer attenuates IR waves and hence keeps buildings summer and warmer in winter. However, this resistive coating also attenuates useful microwave/RF signals required for mobile phone, GPS and personal communication sy by as much as 30 dB. To overcome this drawback, we designed and tested a bandpass aperture type cross-dipole frequency selective surface (FSS), etched in the coatings o saving glass to improve the transmission of useful signals while preserving IR attenuation as much as possible. With this FSS, 15-18 dB peak transmission improveme achieved, for waves incident with 45 degrees from normal for both TE and TM polarizations.

Measurements and other results of this research, conducted in collaboration with the Lund University in Sweden, are available in the paper entitled "Cross-Dipole Frequency Selective Surface for Energy-Saving Glass Used in Buildings," published in IEEE Transactions on Antennas and Propagation, vol. 59, no. 2, pp. 520-525, Feb. effect of these FSSs on the transmission of infrared and visible wavelengths through energy-saving glass was investigated theoretically and experimentally in another pap Microwaves, Antennas & Propagation, Vol. 4, Iss. 7, pp. 955–961, 2010.

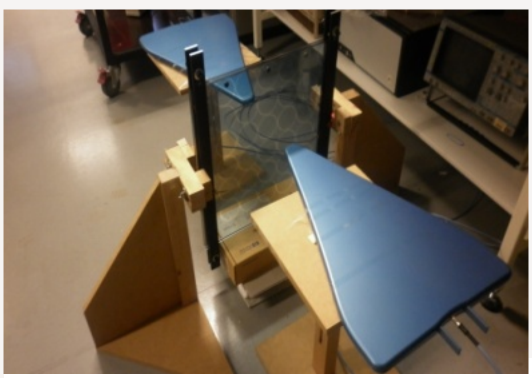

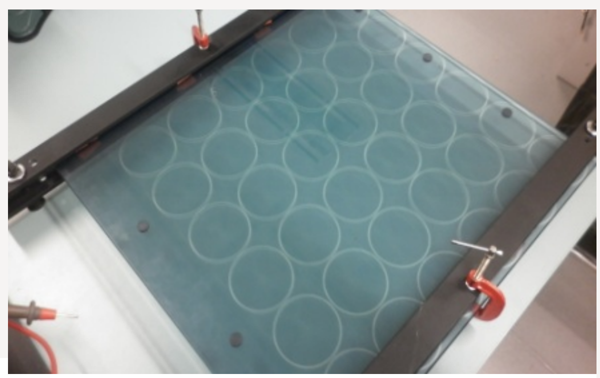

Switchable Frequency Selective Surfaces to Reconfigure Electromagnetic Architecture of Buildings

In large buildings and offices, frequency re-use methods will be required to enhance the spectral efficiency and capacity of wireless communication systems. This observatio to the concept of electromagnetic architecture of buildings. Passive bandstop FSSs can be used to enhance the electromagnetic architecture of a building, and hence to spectral efficiency and system capacity, but switchable FSSs can provide a better reconfigurable solution. If switchable FSSs are placed in strategic locations of a building, th reconfigured remotely and rapidly, which is not possible with passive FSSs.

With collaborators in UK and Sweden, we designed and successfully tested a single-layer active Frequency Selective Surface (FSS) that is electronically switchable between and transparent states. It can be used to provide a spatial filter solution to reconfigure the electromagnetic architecture of buildings. The FSS measurements show that the response of the filter does not change significantly when the wave polarization changes or the angle of incidence changes up to ±45º from normal. The FSS is based on sq aperture geometry, with each unit cell having four PIN diodes across the aperture at 90 degree intervals. Experiments demonstrated that almost 10 dB additional transmissio be introduced on average at the resonance frequency, for both polarizations, by switching PIN diodes to ON from OFF state.

For details, please refer to "Switchable Frequency Selective Surface for Reconfigurable Electromagnetic Architecture of Buildings," in IEEE Transactions on Ante Propagation, Vol. 58, Issue 2, pp 581-584, February 2010.

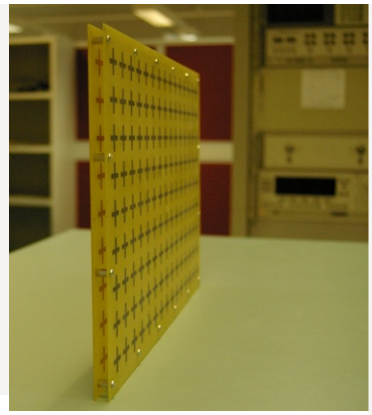

Absorb/Transit FSS

We designed and tested a novel absorb/transmit frequency selective surface (FSS) for 5-GHz wireless local area network (WLAN) applications. The novelty of the design i capable of absorbing, as opposed to rejecting, WLAN signals while passing mobile signals. The absorption of the WLAN signal is important to reduce additional multipa spread and resultant fading caused by typical reflect/transmit FSSs. Our FSS consists of two layers, one with conventional conducting cross dipoles and the other with resis dipoles. The FSS has good transmission characteristics for 900/ 1800/1900-MHz mobile bands and performs well for both horizontal and vertical polarizations.

Later we modified the FSS to obtain even better performance, for example, for both horizontal and vertical polarizations at oblique angles of incidence. The distance betwee layers has been successfully reduced to one eighth of free-space wavelength. This small distance makes it more compact as compared to the conventional Salisbury screen achieving an acceptable absorption in the stopband.

The details of our designs and test results can be found at "Oblique Incidence Performance of a Novel Frequency Selective Surface Absorber," in IEEE Transactions on Ant Propagation, Vol. 55, no. 10, pp. 2931 – 2934, Oct. 2007, and "A Novel Absorb/Transmit FSS for Secure Indoor Wireless Networks with Reduced Multi-path Fadin Microwave and Wireless Component Letters, Vol. 16 (6), pp. 378 - 380, June 2006.

Dual-Band Artificial Magnetic Conductor (AMC) Surfaces

AMC surfaces have many advantages and interesting properties due to their unique reflection characteristics, with near zero reflection phase. We have designed and pro novel dual-band AMC surface, which has a very wide upper AMC band and a narrow lower AMC band, and therefore suitable for multi-band wireless/mobile applications.

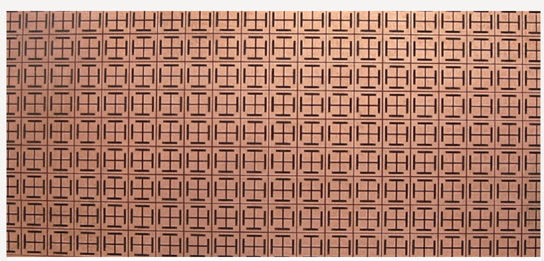

Fully Printed Quad-band Antennas for Wi-Fi IEEE802.11 and other WLAN Applications

Our fully-printed antennas can be fabricated and integrated to WLAN systems at almost zero cost by printing them on the same circuit board (e.g. FR4) with the radio circuit same standard fabrication methods. They are extremely compact: an antenna with a radiating element of 1cmx1cm covers all four IEEE standards (802.11a, 802.11b, 80 802.11n) as well as HiperLAN2 with a VSWR less than 2. We have also developed a packaging solution where the rest of the circuit can be shielded to satisfy EMC regulati leaving the antenna (on the same board) open for radiation. The advantages of the antennas based on this technology are: Lightweight; Radiates almost every direction in shadow region); Microstrip and co-planar waveguide (CPW) designs available; Compatible with all printed microwave circuits, including stripline circuits; Excellent because no cables, connectors, soldering or any mechanical attachments are required to connect the antenna to the radio; No protruding parts that are likely to break; Covers WLAN bands with one antenna (e.g. Wi-Fi IEEE 802.11 a, b, g, n, HiperLAN2 etc.); Excellent matching, i.e. input reflection < -10 dB (VSWR < 2) in all WLAN bands (e. GHz, 4.9-5.1 GHz, 5.15-5.35 GHz, 5.725 – 5.825 GHz); High efficiency (~60-70% on FR4; can be increased to over 90% on Duroid.); Ideal for internal mounting in a c device, to achieve very wide beam coverage; diversity reception or MIMO arrangements available; can be dsigned to cover other multiple bands (e.g. multiple mobile/c bands) and other applications.

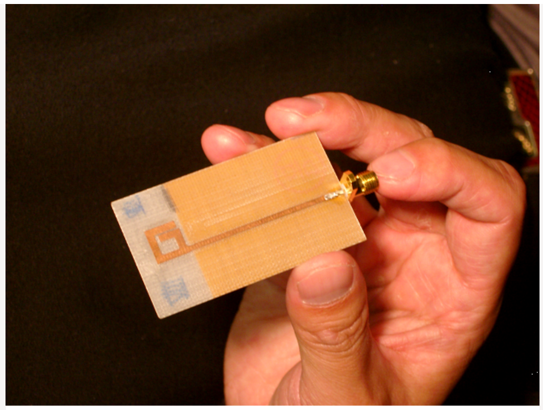

How can I optimise a UWB System to operate well over a range of directions?

Emerging ultra-wideband (UWB) communication devices will need to operate well, not just in one direction but over a range of directions. However previous UWB system optimisation techni been limited to one direction only. A system optimised in one direction may not work well in other directions due to pattern instability, or direction-dependent transfer function, of the an developed the concept of frequency-domain correlation patterns and proposed a figure of merit, the pattern stability factor (PSF), which can be determined from simulation of experimen With these new concepts, we have demonstrated the optimisation of UWB systems to operate well over a range of directions. The concepts and their applications are available in the PhD papers by Tharaka Dissanayake.

Antenna Techniques and Technologies for Ultrawideband (UWB) Systems

We developed antenna solutions for emerging UWB systems with very high data rates. Our research includes investigation of band-notching techniques to reduce UWB inference wi wireless systems and studies of antenna dispersion and pattern stability in the time domain.

High Gain Antennas with Planar Surface-Mounted Short Horns

In collaboration with University of Delhi, we have developed compact rectangular dielectric resonator antennas with surface mounted planar horns for gain enhancement. One configuration an aperture-fed rectangular dielectric resonator antenna and a planar surface mounted horn. We have achieved 10 dBi gain and a good efficiency from this configuration. The surface mou increases the gain of the standard dielectric resonator antenna by 4.9 dB. Total height of the prototype antenna shown in the figure is only 0.172 lambda and the aperture size is 0.96 lamb antennas can be easily adapted to low-profile, high-gain and array applications.

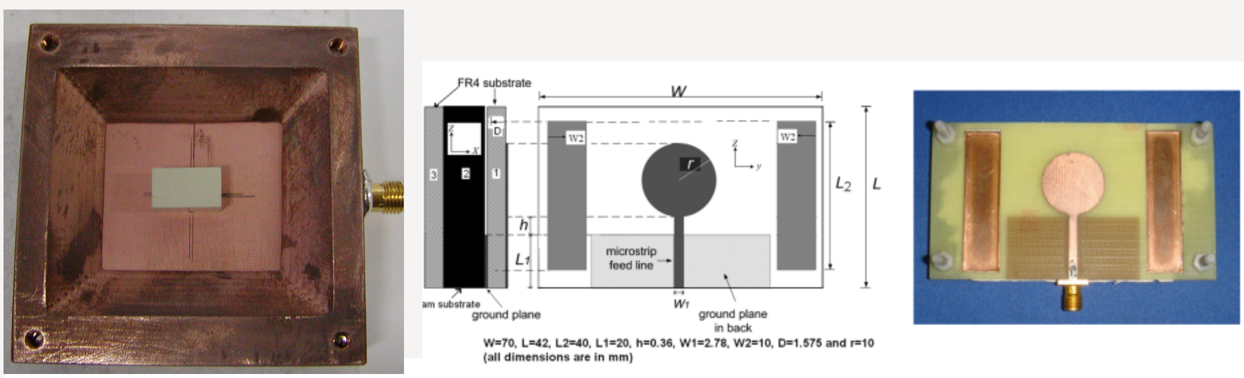

Photonic Crystal/EBG Based Horn Antennas

Waveguides and antennas made out of dielectric, as opposed to metal, are expected to perform better at Terahertz frequencies, as they do not suffer from the skin-effect loss of metal investigated horn antennas, horn arrays, waveguides, bends and junctions made out of 3D woodpile photonic crystals, which can be implemented at THz frequencies in high-resistivity S other materials. Our concepts have been tested by fabricating and measuring scaled-up prototypes operating in microwave frequencies. We have also designed a special broadband couple a photonic crystal waveguide to a rectangular waveguide or a coaxial cable, for example for testing using a vector network analyser. We demonstrated > 6% bandwidth both theore experimentally.

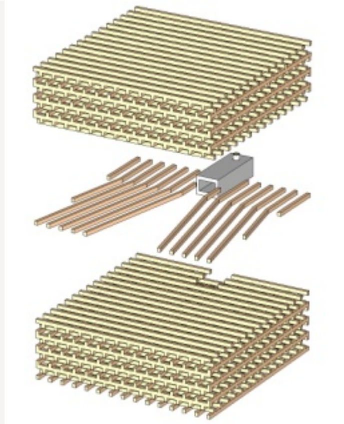

Broadband Microstrip Patch Antennas for Wireless Computer Networks

We have designed and tested broadband, compact E-shaped patch antennas for wireless communication networks, operating in frequencies from 4.9 GHz to 6.0 GHz. We made two achievements. First, we designed an E-shaped antenna, which is intrinsically compatible with a printed microstrip circuit. It can be made out of a single sheet of metal and can be mou microstrip circuit without expensive coaxial connector. Second, we designed a unique E-shaped antenna with corrugation to reduce the width of antenna. We successfully miniaturised the a fit it inside a thin (4mm) PC (or PCMCIA) card extension. In fact, we were able to squeeze in two of these antennas into a single PC card of standard width (54mm), for diversity communica achieve excellent isolation (>20 dB) and matching (<-10 dB) over the whole WLAN frequency band.

Theoretical Analysis of Photonic Crystal Structures

We have developed and successfully implemented, in both personal computers and supercomputers, efficient theoretical methods to analyse and design complex electromagnetic (micro optical) circuits based on photonic crystals (PC). Among our novel techniques is a PC-based Perfectly Matched Layer (PML) absorbing boundary for use with the finite difference time doma method in the analysis of waveguides in 3D photonic crystals.

We have applied these techniques to model wave propagation in various guiding structures such as bends, junctions and tapers in 2D and 3D crystals. From this analysis, we can transmission and reflection coefficients, propagation characteristics, phase and delay response, etc., of a component or a system.

New Closed-form Green's Functions for Microstrip Circuits and other Layered Structures

When combined with the spatial-domain Method of Moments (MoM), our new closed-form functions now enable efficient and accurate analysis of microstrip circuits and antennas with approximations. The key feature in this new MoM is that the four-dimensional integrations in MoM matrix elements can be solved analytically, completely eliminating the need for expensive integrations. Our new closed-form functions are simpler and more flexible than previous such functions, and (unlike previous ones) they do not require additional (Taylor series approximations. The computer time required for the analysis of an example microstrip line using the new MoM was three times less than the next best method, which required some integrations.

Integrated-design of Hybrid-resonator Antennas for Broadband Wireless and other Communication Systems

Shown below is the first baby of our recent project on broadband hybrid-resonator antennas. This first prototype of a Dielectric Resonator on Patch (DRoP) antenna demonstrated a ba 24%. This design also proved, both theoretically and experimentally, that the electromagnetic fields in a dielectric resonator can be efficiently coupled to the fields in a patch resona perturbing the radiation characteristics of each resonator.

Singularity-enhanced Finite-different Time-domain (FDTD) Method for Diagonal Metal Edges, Strips and Films

We developed the world's first and still the only singularity-enhanced FDTD method for metal edges not parallel to the grid. The edges were assumed to be diagonal to cell faces. Compare conventional spit-cell model, the computer memory required for an FDTD analysis of a structure could be reduced by up to 27 times and the computing time could be reduced by up to without sacrificing the accuracy of results. On the other hand, when the same grid was used, the accuracy of results improved by a factor of more than 3 compared to the split-cell model, a of more than 7 compared to the staircase model. The new equations were stable in all tests, and even in most demanding tests when the computational speed was further maximised by the time step (Dt) to the maximum allowed by the FDTD method! (i.e. stability factor of 1!)

The key to this success was the derivation of enhanced FDTD equations for nodes near the edges by considering rigorously the singular nature of the electromagnetic fields. The table here improvement of accuracy achieved by using the enhanced FDTD equations. The new equations are simple to implement in a standard FDTD code. They are ideal for the analysis and microstrip components and high-speed digital circuits where thin metal films or strips with diagonal edges are encountered.

Low-profile Dielectric-resonator (DR) Antennas

We designed and tested the world's first low-profile, circularly polarised, rectangular dielectric-resonator antenna (DRA) in 1995. The radiating element of this antenna is shown in the photo have also designed many other dielectric-resonator antennas, including a low-profile linearly polarised DRA, for various applications (see publications). We pioneered the FDTD analy antennas and published the first radiation patterns of a DR antenna obtained using the FDTD method in 1995.

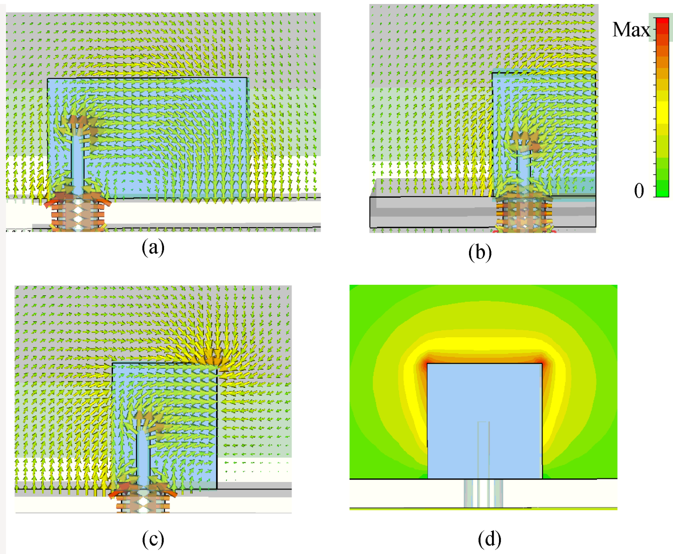

Australian Antenna Measurement Facility (AusAMF)

AusAMF is operated by a consortium of Australian Universities, Industry and CSIRO. The facility provides access to a shielded anechoic chamber offeri spherical near-field measurement capability for small antennas operating in the frequency range of 1-20 GHz, primarily for research purposes.

The facility was established under an ARC LIEF (Australian Research Council Linkage-Infrastructure Equipment and Facilities) grant and is hosted by C ICT Centre located in the Sydney suburb of Marsfield.

The facility currently consists of a spherical near-field turn-key NSI-700S-50 system within a 6m x 3.3m x 3.3m anechoic chamber. It has been designed to operate up to fre of 20 GHz, and uses an Agilent PNA (E8362B) as a receiver. The measurement system is capable of supporting a ~40kg antenna under test (AUT) up to a diameter of approximately 1.2m. I the standard gain horns and the probes available at AusAMF are as follows:

Waveguide Band	Frequency (GHz)	Probe	Standard Gain Horn
WR975	0.75 - 1.12	x	x
WR650	1.12 – 1.70	x	x
WR430	1.70 – 2.60	x	x
WR340	2.20 - 3.30	x	x
WR229	3.30 – 4.90	x	x
WR159	4.90 – 7.05	x	x
WR112	7.05 – 10.00	x	x
WR90	8.20 – 12.40	x	
WR75	10.00 - 15.00	x	x
WR51	15.00 - 22.00	x	x

Smart Surfaces: Large Area Electronics Systems for Internet of Things Enabled by Energy Harvesting

Article *in* Proceedings of the IEEE · November 2014

DOI: 10.1109/JPROC.2014.2357493

Luca Roselli
Università degli Studi di Perugia

Federico Alimenti
Università degli Studi di Perugia

Paolo Mezzanotte
Università degli Studi di Perugia

Giulia Orecchini
Università degli Studi di Perugia

INVITED PAPER

Smart Surfaces: Large Area Electronics Systems for Internet of Things Enabled by Energy Harvesting

This paper focuses on large-area "smart surfaces," RFID systems, and wearable RF electronics that could substantially benefit from multisource energy harvesting.

By LUCA ROSELLI, *Senior Member IEEE*, NUNO BORGES CARVALHO, *Senior Member IEEE*, FEDERICO ALIMENTI, *Senior Member IEEE*, PAOLO MEZZANOTTE, *Member IEEE*, GIULIA ORECCHINI, MARCO VIRILI, *Student Member IEEE*, CHIARA MARIOTTI, *Student Member IEEE*, RICARDO GONÇALVES, *Student Member IEEE*, AND PEDRO PINHO, *Member IEEE*

ABSTRACT | Energy harvesting is well established as one of the prominent enabling technologies [along with radio-frequency identification (RFID), wireless power transfer, and green electronics] for the pervasive development of Internet of Things (IoT). This paper focuses on a particular, yet broad, class of systems that falls in the IoT category of large area electronics (LAE). This class is represented by "smart surfaces." The paper, after an introductory overview about how smart surfaces are collocated in the IoT and LAE scenario, first deals with technologies and architectures involved, namely, materials, antennas, RFID systems, and chipless structures; then, some exemplifying solutions are illustrated to show the present development of these concurrent technologies in this area and to stimulate further solutions. Conclusions and future trends are then drawn.

KEYWORDS | Energy harvesting; green electronics; Internet of Things (IoT); large area electronics (LAE); radio-frequency identification (RFID) systems

I. INTRODUCTION

Looking at the telecommunication (TLC) market development worldwide in the last five years, we see an average decrease of about 5% per year, in both gross domestic product (GDP) contribution and employment [1]. Against this trend, the global information and communication technology (ICT) market has remained grossly constant. Some compartments, in fact, are experiencing an opposite trend. Beside some sectors related to new consumer products, such as tablets and smartphones, new Internet of Things (IoT) related products are growing at two digits per year and some estimations from big players report a market value in the order of trillions of dollars in the next decade [2], [3].

The vision behind IoT is in fact to connect objects directly to the Internet so as to allow them to provide information directly to the web without any human intermediation [4]. This vision will have a great impact on several electrical and electronic technologies, ranging from the basic physical layers (technology platforms) to the highest ones: communication protocols, software, human interface, and information management.

Manuscript received May 4, 2014; revised September 1, 2014; accepted September 5, 2014. Date of publication October 13, 2014; date of current version October 16, 2014.

L. Roselli, **F. Alimenti**, **P. Mezzanotte**, **G. Orecchini**, **M. Virili**, and **C. Mariotti** are with the Department of Engineering, University of Perugia, Perugia 06123, Italy (e-mail: roselli@ieee.org).

N. Borges Carvalho and **R. Gonçalves** are with the Instituto de Telecomunicações-Dep. Electrónica Telecomunicações e Informática, Universidade de Aveiro, Aveiro 3810-193, Portugal.

P. Pinho is with the Instituto de Telecomunicações, Instituto Superior de Engenharia de Lisboa, Lisboa 1959-007, Portugal.

Digital Object Identifier: 10.1109/JPROC.2014.2357493

In terms of physical layer, IoT actually inherits the technologies developed for wireless sensor networks (WSNs), bringing the distributed nature of that to the extreme. WSN, in fact, can be synthetically seen as a mesh of sensor nodes purposely conceived to build and communicate a sensed image of a monitored area. Within IoT, the sensing nodes are not purposely deployed to monitor something specific; instead, they are simply hosted by "objects" in order to provide the information they are able to collect and make it available on the web. Conceptually speaking, there is not a big difference, but in terms of related technological challenges, there is. Nodes must be hostable by objects; objects are of many types, and the better the nodes fit themselves transparently to the hosting objects, the denser and more reliable the information they are able to provide.

Several challenges can be envisioned in this evolution: first, electronic systems must be mechanically flexible, thin, and miniaturized in order to conform to the shape of as many objects as possible; second, the adopted materials have to be as recyclable as the hosting objects in order to avoid pollution from guest apparatuses; last but not least, hosted nodes must be autonomous, because they cannot be either connected to the grid or powered by life batteries.

A great technological paradigm shift is going to be pulled by the development of IoT; green materials, autonomous systems, ultralow-power circuits, energy saving protocols, and energy harvesting (EH) are concurrently mandatory.

Conversely, this technological evolution is pushing new solutions and architectures, so far constrained by the limits of conventional technologies. The development of inkjet printing techniques, the introduction of very cheap and eco-friendly materials compatible with roll-to-roll (R2R) circuit realization techniques [5] and so forth, open new horizons also to large area electronics (LAE).

LAE, first applied to printed photovoltaic and organic screens [6], is actually at the onset of its development. The development of R2R techniques and related materials, in fact, is allowing for tremendously increasing the dimensions of LAE circuits and systems, from the present tens of centimeters to meters and beyond. Along this evolutionary scenario, new configurations and architectures, based on massive integration of large circuits over conformable surfaces, can be envisioned, opening the way to what can be called the smart surfaces (SSs) approach.

SS, in turn, can be seen as a branch of IoT evolution. Large 2-D arrays of autonomous sensor nodes, for instance, make possible granular tracking of whatever parameter, ultimately providing augmented imaging of the environment; large 2-D arrays of tags can provide a very low-cost platform for precise localization and location-based services (LBS), thus enabling the realization, for instance, of smart floors [7] and smart wallpapers [8]; inheriting quasi-optical approach [9] contact-less electromagnetic (EM) wave processing (filtering, frequency conversion, selective shielding, etc.) can be conceived even at low frequencies.

On the one hand, SS is thus an approach stimulated by technologies pulled by IoT; on the other hand, it contributes to a class of architectures, within LAE, that can even widen the huge horizons of IoT applications in a sort of virtuous circle.

According to this wide vision, the paper is organized as follows. A review of the technologies suitable for distributed systems implementation to a large extent is given in Section II; then, the explanation about how radio-frequency identification (RFID) can be considered one of the most suitable technologies for the implementation of IoT architecture, and how it can be naturally integrated with SSs, is provided (Section III). In order to deal with the implications of the development of RFID systems compatible with SS and LAE evolution of IoT, two specific sessions have been provided: the first relates to antenna implications (Section IV), and the second relates to electronic architectures for RFID tags (mainly chipless ones; Section V). In order to smoothly bring the reader from relevant technologies to applications, quasi-optics, as an example of general approach concurrently exploiting the mentioned technologies to provide a platform suitable for LAE, is described in Section VI. After this, some application examples of how SS concept can be articulated, according to the IoT paradigm, are described; specifically, smart floor (Section VII), smart shoes as useful subsystems for the implementation of smart floors (Section VIII), and energy skin (Section IX). In order to have a vision of the logical links behind the many topics dealt with in this paper, a synoptic picture can be found in Fig. 1.

II. TECHNOLOGY FOR LAE DISTRIBUTED SYSTEMS

Given the described scenarios of SS, it is clear that the technologies involved have to be compatible with LAE

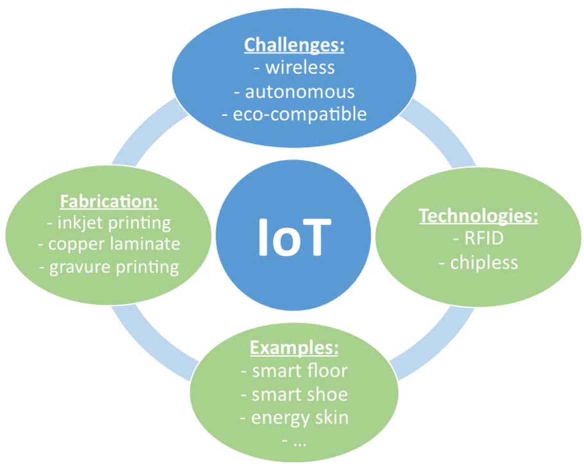

Fig. 1. ***Synoptic view of the paper structure reflecting the IoT vision described in the Introduction.***

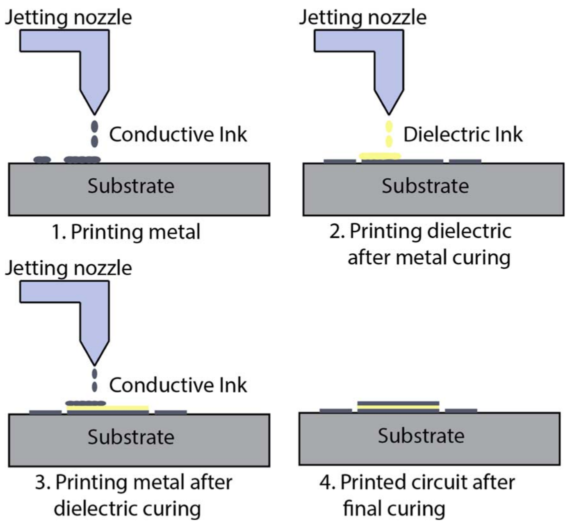

Fig. 2. ***Inkjet printing technique, synoptic description. The ink is deposited on the substrate with the desired pattern and after a curing procedure the next layer can be printed. The thickness of each film depends on the number of passes.***

approach, as described in the Introduction; according to [6], for example, the eco-compatibility of the materials, the mechanical flexibility of the substrates to make the device conformable to the hosting surface, and the life cycle (operability and biodegradability) have to be accounted for.

The new techniques proposed from different research groups [10]–[12] focus mostly on the printing techniques that can be industrialized easily with R2R methods, already investigated for the traditional printing on paper. Within the printing methods, one of the most attractive and investigated in the last decade is the inkjet printing of conductive and dielectric layers (Fig. 2). This technique allows circuits to be printed on almost any kind of substrate: from the photographic paper to liquid crystalline polymers (LCP) or Kapton, that are flexible, thin, and eco-compatible; to glass or poly methyl meta acrylate (PMMA, commonly referred to as Plexiglas) that are usually thicker but not flexible.

A first proof of concept for the inkjet printing technique at radio frequency (RF) and microwaves has been obtained on photographic paper by printing simple structures, such as antennas and other planar circuits and devices [10], [13]–[22], with a technology stack simply composed by the substrate and the conductive layer (usually realized by means of nanoparticle silver ink).

Recently, this method has been improved thanks to the development of new inks, usually composed by a polymer and a solvent (i.e., SU-8, PVP, PMMA, PEDOT, etc.); more complex fabrication procedures of multilayer structures are now possible, as shown in [23] and [24]. Another noticeable feature of this technology is represented by the resolution: conductive tracks of 50 μm of width and space gaps of 50 μm can be printed, allowing the design of millimeter-wave (mm-wave) frequency devices [25]. The combination of the quite high resolution (considering the simplicity of the technology) with the multilayer featuring also gives the opportunity to manufacture very easily matrix of passive and active devices that can be used in the SS development. It is worth noting that the process can be developed in a few steps based on the design and mostly on the number of layers needed. For example, a metal–insulator–metal (MIM) device can be realized by printing silver on the substrate [26], curing it in the oven in order to create a surface that, with the proper treatment (for instance, UV–Ozone exposure or preheating), is ready for the insulator printing. Then, the dielectric is cured as well and the last metal layer can be printed on top of it. The entire structure can be then cured at temperatures ranging between 130 °C and 200 °C.

In a perspective of industrialization of the inkjet printing technology, the hypothesis of R2R manufacturing of circuits is being investigated and some examples are already reported in literature for solar cells and other devices [27], [28].

Today, many pros have been mentioned for the inkjet printing method, and others can be found in the non-use of wasted chemicals (as is for the traditional lithographic technologies), in the no-need of clean-room environment for the fabrications, in the low-cost and rapidity of manufacture, and in a R2R perspective compatibility. However, the necessity of a curing procedure after the printing of a layer still represents the biggest inkjet limit for two main reasons: first, the time and type of curing are dependent on the inkjeted materials and on the material stack-up; second, especially on a laboratory level, the curing can cause misalignment issues, given the fact that the sample is removed and then replaced in the printer after the last layer curing.

Currently, the platform mostly used worldwide by researchers is the Dimatix 2800 DMP. In terms of inks, it is possible either to buy printable solutions or mix solutions in labs; for example, the combination of polymers and solvents allows layers to be printed with different electrical properties and thicknesses.

Besides the inkjet printing method, in [11], a new technique, suitable for LAE, has been proposed. It uses a metal (copper in that case) adhesive laminate technology based on the application of the standard etching process to an adhesive copper laminate material. This technique was already adopted to produce mm-wave circuits and to characterize the resulting compound substrates, as reported in [29]–[31]. A brief illustration of the metal laminate technique is here reported referring to Fig. 3.

The production process can be divided in five steps. The first step consists of the deposition of a (positive) photoresist film on the copper surface; then, the circuit layout is transferred to the photoresist by means of a photomask and ultraviolet exposure. After that, the unimpressed film of photoresist is removed using a NaOH

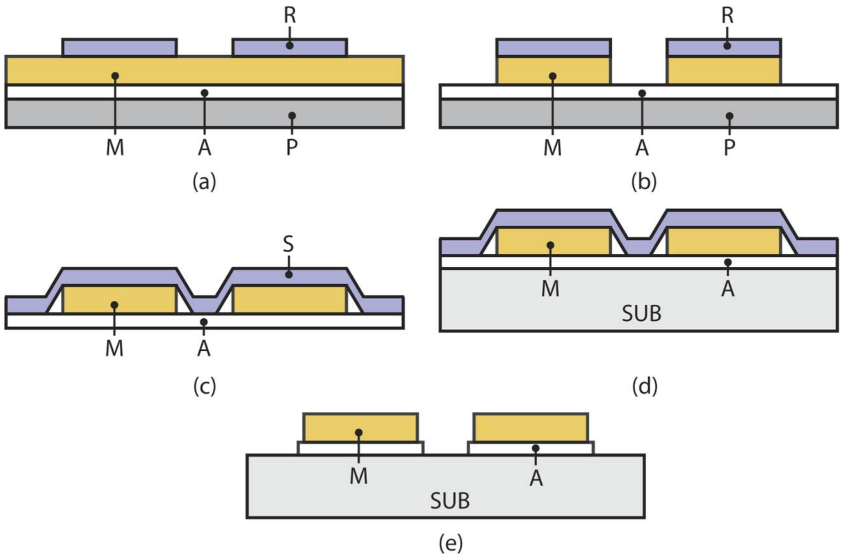

Fig. 3. ***Process steps for the circuit fabrication using the adhesive metal laminate. M: metal, A: adhesive, P: protection, R: photoresist, S: sacrificial layer, SUB: hosting substrate. After the standard lithographic procedure, the copper pattern can be transferred on top of any substrate by means of a sacrificial layer and exploiting the adhesive face of the copper tape.***

developer solution [Fig. 3(a)]. In the second step, the copper tape is wet etched. As can be seen in Fig. 3(b), in this way, the adhesive layer is exposed where the copper was removed, while it remains everywhere else covered by the original copper tape that serves as protection for the adhesive underneath.

The first two steps are, in this example, similar to those adopted in standard photolithographic technology. Moreover, different ways to remove the not needed metal can be used, as, for example, by means of numerical control pattern cutting plotters.

In the third step, depicted in Fig. 3(c), a sacrificial layer is stuck on the top copper side and, finally, the protection layer on the bottom is removed. The sacrificial layer is very important because it keeps the relative distances among the layout features constant even when these are not physically connected.

The fourth step is characterized by the transfer of the etched metal to the hosting paper substrate and, finally, the sacrificial layer can be removed [see Fig. 3(d) and (e)]. The last step is also useful to remove most of the exposed adhesive material.

With this method, quasi-fully-organic circuits and devices can be realized. The performance in terms of tracks width and pitch are, at present, a bit lower than what can be obtained with the inkjet printing, with the advantages of no curing processes, the possibility to fix devices on the circuit using standard soldering techniques, and a better conductivity (the conductivity of copper laminate, in fact, is one order of magnitude higher than that of the cured nanoparticle silver ink: 5.8×10^7 S/m versus about $6 \times 10^6 - 1 \times 10^7$S/m obtained with at least five layers of silver).

To verify the validity of the metal laminate technology at microwave frequencies, a 50-Ω microstrip line was manufactured exploiting the Mitsubishi photografic paper as the substrate (thickness 250 μm, relative permittivity $\varepsilon_r = 3.2$, and loss tangent $\tan\delta = 0.08$). The line is 30 mm long, and the measured scattering parameters are shown in Fig. 4. The same graph also compares the performance of a similar transmission line manufactured with an inkjet printing process. The performance of the

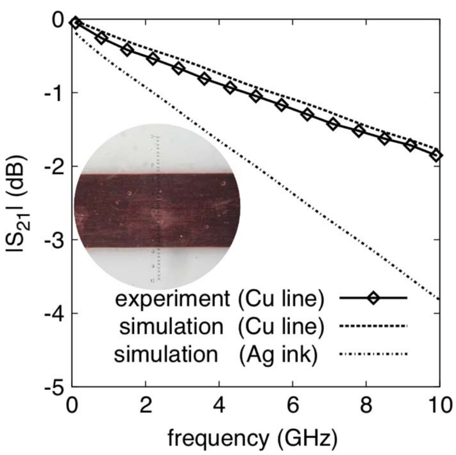

Fig. 4. ***Measured scattering parameters versus frequency for a 50-Ω microstrip line on paper substrate. The line, shown in the inset, is 30 mm long; the ruler division corresponds to 17.2 μm. The graph also reports a comparison with a microstrip line of equal dimensions made with an inkjet printing process (Ag ink, 3-μm thickness, $\sigma_{ink} = 1.1 \times 10^7$ S/m after curing). After [11].***

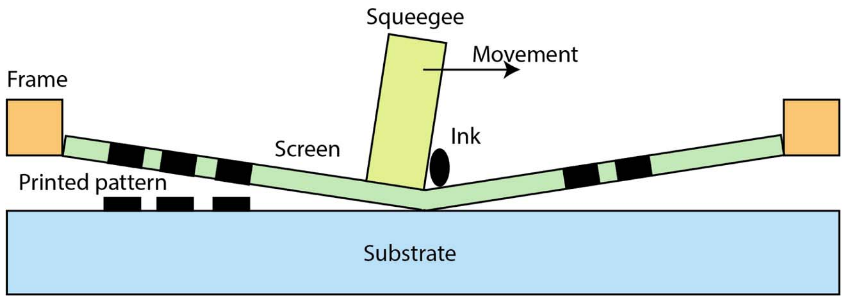

Fig. 5. ***Screen printing technique. The squeegee is used to press the screen with impressed pattern and transfer it on top of the substrate.***

metal laminate structure is superior compared to that of the inkjet printed line. At 10 GHz, the measured specific losses for the metal laminate microstrip are about 0.6 dB/cm [11]. Results at higher frequencies are also reported in [31]; in particular, an insertion loss of about 1.8 dBm/cm at 30 GHz is demonstrated.

The tradeoff is the adoption of a photolithographic step; it is worth mentioning, however, that the process is still compatible with R2R implementation.

Other possibilities for LAE are the screen printing [12] and the gravure printing [12], both of them adaptable to R2R industrialization techniques.

Screen printing consists of dragging a layer of ink across the surface of a screen and squeezing it through the open pores of the patterned mesh onto the substrate (Fig. 5). In general, the thickness of the printed layer and the achievable resolution depend on the density of the mesh and on the ink properties. Usually, the ink viscosity is in a range of 1–50 Pa $\times$ s, and this allows for printing with a resolution of about 100 μm and a thickness up to 100 μm. Until now screen printing has been adopted to realize low-resistance structures, solar cells, and field effect transistors (FETs), exploiting the possibility of printing very thick layers.

Gravure printing, also known as rotogravure, is considered a very high volume printing (Fig. 6) process, and it is being adopted to produce very conductive structures as, for example, capacitors, antennas, and organic devices such as pentacene-based diodes, organic light-emitting diodes (OLEDs), organic field effect transistors (OFETs), and organic thin film transistors (OTFTs).

The resolution can be of about 20 μm. The method is implemented by engraving the patterns into a metallic cylinder by a laser, by chemical etching, or electromechanically (as separate cells or intaglio trenches). Typically, the print pressure is high (1–5 MPa) in order to achieve a good ink transfer and to reduce the percentage of unprinted dots caused by the surface roughness of the flexible substrate. However, this high pressure of printing makes this technique suitable only for robust substrates with no soft, previously printed, layers that could be damaged.

To summarize, the technologies described in this section are characterized by some common features, such as: flexibility and conformability, compatibility with large area realization of circuits and interconnections, use of additive or mixed (subtractive/additive) deposition techniques, easy use of eco-friendly materials and, in some cases, compatibility with classical bond wiring as well as soldering techniques for electronic device placement.

Table 1 summarizes the main features of the described technologies.

III. RFID: A MIX OF CONCURRENT TECHNOLOGIES FOR SS IMPLEMENTATION

As mentioned in the outline paragraph at the end of the Introduction, after describing the technologies enabling SS development (Section II), here we illustrate RFID as a suitable means to transfer information through EM transmission between tags and readers to the Internet.

An RFID tag has a unique identification code and a memory used to store information, while the reader can

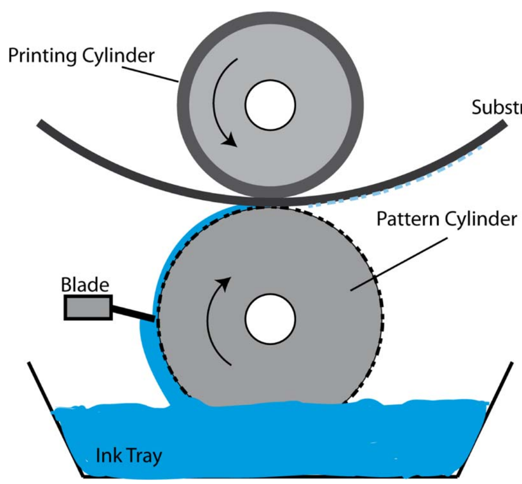

Fig. 6. ***Gravure printing process. Note that these machines can be from 20 cm to 3 m wide with a diameter ranging from 5 cm to 5 m.***

Table 1 Technologies Comparison

Technology	Resolution	Cost	Waste	Speed
Inkjet	50 μm	Low	Low	Fast
Copper	100 μm	Low	High	Medium
Gravure	20 μm	High	Medium	Very fast
Screen	100 μm	Medium	Low	Very fast

write or read data on and from the tag through RF transmissions. The tag is usually attached to an object that needs to be identified and monitored, or contains information to be read. In typical RFID applications [32], the main goal is to provide mapping of physical objects that are equipped with an RFID tag attached or embedded. In this way, RFID technology inherently leads to identifying, tracking, and localizing, but it can also enable the storage and transmission of information regarding object status and surrounding environments by embedding sensing capabilities.

As mentioned previously, IoT is most commonly described as a structured system of technologies concurrently working to capture meaningful data from objects and communicate them through networks to a decision-taking level. Useful keywords, whenever a definition of IoT is given, include: smart objects, autonomous logistics, machine-to-machine communication, RF technologies, centralized information, and so on.

In order to implement these functionalities, an IoT platform, an SS for instance, has to provide at least unique object identification together with wireless communication for data management.

The IoT physical layer can thus be naturally thought of as meshes of RFID and sensor nodes. The RFID tag that embeds a sensor can use the same working principles and protocols of the conventional RFID tags; a differentiation can be made, considering the way sensor tags are powered up, in active, semipassive, and passive tags; actually, the difference consists of the way they are powered.

Active tag sensors may use customarily conceived communication protocols or rely on RFID standards enabling the tag to be easily integrated into the existing wireless infrastructures so that they will not require expensive readers. In [33], a system architecture was developed to integrate WSNs and the RFID systems. Bluetooth and ZigBee technologies are adopted as the communication protocol of WSNs to meet the requirements of a large number of sensor nodes, large areas, and low cost.

Active tags with integrated sensors are used in several applications, including temperature and position monitoring, vibration detection, blood pressure, heart beat monitoring, and more. This type of sensor tags, besides having larger amount of energy provided by batteries, affords both a large range and multiple functionalities; some of them have also external buses that enable the use of connected external sensors [34].

Passive tags with an integrated sensor operate without battery, collecting the needed operational energy from external environment sources. The main requirements of this class are high energy conversion efficiency, large storage capability, and overall low-power consumption. Passive systems have usually low operating range and limited processing capability.

In this field, research activities are directed toward ultralow-power design of integrated sensor tags [35], antenna design for improving reading range [36], sensor overall performance optimization [37], and development of optimum protocols allowing for additional power saving [38], [39].

Typical applications are, for instance, temperature monitoring [40], photodetection [41], motion detections [42], etc.

Semipassive tags use both batteries and energy sources coming from the environment; they can integrate more operational capabilities than the passive ones, since they can exploit a higher amount of energy. For the same reason, semipassive RFID tags are more suitable to integrate a sensor; the operational methodology is similar to the passive one, using the reader signal to interrogate and cause a response from the tag. The primary difference is that the semipassive tag does have a battery used not to generate a response, but only to power electronics, like sensors incorporated in the tag, while exploiting RF circulation to reply to the reader interrogation. Just like passive tags, semipassive ones are limited in terms of slow reading speeds and short reading distances. In [43], the design, realization, and experimental validation of a battery-assisted RFID tag with sensing and computing capabilities, conceived to explore heterogeneous RFID-based sensor network applications, was presented.

Dealing with battery-less devices that are, by far, the most interesting ones for IoT, LAE, and SS applications, we can now focus on the typical energy sources adopted. No battery devices can exploit solar scavenging [44], [45], vibrational [46], [47], or RF radiations [48]–[52].

In many cases, wirelessly powered systems can harvest energy from the incident RF waves, thus generating the required direct current (dc) voltage to power the system. The EM energy present in the environment may be significant in some regions (some urban areas or indoor sites); here the use of proper conversion devices may allow enough energy to be scavenged. RF power harvesters usually consist of an antenna, an impedance transformation network, a rectifier, and a storage element. In [53], a design example of integrated rectifier antennas (rectennas) for wireless powering at low incident power densities, from 25 to 200 $\mu W/cm^2$, is given.

Regarding mechanical energy scavengers, they may be categorized upon the kind of energy source exploited; there are scavengers providing energy from a constant motion over extended periods of time (e.g., turbine air flow) or others based on intermittent motion (e.g., human

step). Particular attention is given to vibrational energy sources; in this case, the amount of energy that can be harvested depends mainly on the vibration amplitude and frequency and on the vibrating mass (mass of the harvesting device) [54]–[56].

In order to power the systems by using energy sources available in the working environment, proper energy transducers thus have to be chosen. Focusing on distributed systems (IoT, LAE, and SS), it is worth referring to typical parameters for optimum transducer design since, in these applications, the different kinds of energy available in the various scenarios may lead to the need of integrating more than one energy conversion system into the same device, in order to take advantage of all the accessible energies. The main design parameters are the available power output, the electrical impedance, and the operating voltage. Table 2 summarizes them for the most common energy transductions [57], [58].

To conclude this section, the mentioned reasons why RFID can be considered a useful technology for the implementation and development of LAE and, more specifically for SSs, are summarized. RFID systems, especially in the passive version of tags, are communication systems characterized by the following characteristics: compatibility with very low-power communication protocols, compatibility with the constrains posed by the hosting objects, especially when they are implemented by adopting the technologies described in Section II, inherent capability to gather information from the environment (sensor tags) and from the hosting objects, a low number of electronic devices (inherent circuital simplicity) and, finally, proven compatibility with printing technologies.

For all these reasons, RFID technology has to be considered the leading one to pursue the development of LAE and SSs as a communication platform for the evolution of IoT.

IV. ANTENNA DESIGN FOR NODES

Distributed systems for ubiquitous electronics (UE) and WSNs [59], [60] are, today, increasingly employed for monitoring and sensing applications. These systems can be seen as networks of nodes, massively distributed in the environment and communicating wirelessly with a base station. This massive deployment can be designed and structured to monitor a set of specified parameters by means of purposely conceived sensor nodes, as in the classical WSNs, or it can be obtained by integrating nodes into existing objects, which is the vision of IoT evolution. In general, the nodes can have different functionalities, however they have to provide information collected by embedded sensors (such as, for instance, identification codes, position and monitored environment parameters as well as object status) whenever it is required.

In this scenario, the RFID technology, summarized in Section III, is attractive. When RFID technology meets sensor nodes, information goes from the node to the Internet via a question-and-reply protocol between nodes, hosted by tagged objects, and readers.

Thinking about distributed systems and specifically SS, it is natural to think about radiative coupling in the available industrial–scientific–medical (ISM) frequency bands, including mainly the ultrahigh frequency (UHF) and microwave frequencies (around 0.9, 2.4, 5.8 GHz, and higher), exploiting the communication standard such as the WiFi [61]. Recently, also the ultrawideband (UWB) has been considered in order to minimize the limitations of narrowband systems (mainly localization accuracy and sensitivity to interference) [62].

Multistandard systems are often adopted for large compatibility and higher use flexibility. An example of this recent approach is given in [61] where near-field UHF nodes are combined with far-field transceivers. This allows application fields with compromised radiation capability,

Table 2 Transducer Characteristics for Several Forms of Ambient EH [57], [58]

Energy Source	Typical Electrical Impedance	Typical Voltage	Typical output power
Light	From low to 10s of KΩ	DC: 0.5 V to 5 V	Outdoors: 100*s* mW/cm^2 Indoors: < 500 μmW/cm^2
Vibrational	Constant Impedance 10s of kΩ to 100 kΩ	AC: 10s of Volts	100*s* μW/cm^2
Thermal	Constant Impedance 1 Ω to 100s of Ω	DC: 10s of mV to 10 V	10*s* μW/cm^2 (20° gradient)
Radio Frequency	Constant Impedance Low KΩs	AC: Varies with distance and power 0.5 V to 5 V	Wide-range

such as in proximity of metal and liquids at short ranges, to be improved.

It is clear that antenna systems are key elements in these apparatuses. The foundation of antenna design rules can be found in [63]. The antenna design specific for distributed systems, in turn, has to take into account several instances. Beyond the typical design criteria, other aspects are: the communication standard, the form and the size in agreement with the application, the communication range as a function of the equivalent isotropic radiated power (EIRP) limits, of the environment and of the orientation, the reliability under several conditions and processes, and the material cost considering massive production [64]–[67]. Among them, the operating environment is the most critical aspect that influences the node behavior [68].

As a consequence, antenna topology and materials for SS and IoT systems, in general, have to be chosen in order to make the antennas capable of operating in variable environmental conditions and to be integrated into objects. As an example, let us think about wearable antennas for body area networks (BANs): they must be washable, flexible, and able to shield the body from radiation [69].

In general, antennas for SS should be flexible, planar, and low profile; moreover, by adopting low-cost materials and technologies (see Section II), cost per unit surface is low, thus large arrays and big elements can be adopted more easily, ultimately allowing for easy developments of LAE distributed systems and SS, even at low frequency.

Materials compliant with SS implementations must be, in turn, mechanically robust, flexible, and very low cost, while exhibiting acceptable EM performance. These materials must also exhibit high tolerance levels in terms of bending repeatability. Flexible materials, often used, are polymers and polymer-ceramics composites such as the poly-di-methyl-siloxane (PDMS) and the titanate-based ceramic [68], which provide flexibility, robustness, and resistance to harsh environments in order to protect antenna and circuit. Moreover, when eco-compatibility has to be guaranteed, recyclable materials and related technologies have to be adopted; among them, cellulose substrates in combination with inkjet printing of conductive inks [18], [70] or with conductive adhesive laminate technology [11] are increasingly frequently adopted. The aforementioned techniques, compatible with the well-known industrial printing and the R2R processes [5], are in agreement with the low-cost fabrication and are expected to facilitate widespread and very low-cost electronics for distributed systems. These fabrication technologies can also be adopted for electronic devices on flexible polymeric substrates. An example of cellulose-based antenna for smart floor applications, such as indoor localization, is documented in [71]: a low-profile planar loop antenna is realized on cellulose substrate exploiting adhesive copper tape.

Although beyond the scope of this paper, which focuses on SS, it is worth mentioning here that this evolution toward the development of more and more sophisticated "unconventional" materials for electronics has a great impact on other IoT related developments such as, for instance, implantable systems.

When applications require devices with soft visual impact (think about SS, such as smart windows, glass integrated inside and outside buildings and glass for automotive applications, or smart skins [72]), transparent and conductive materials, such as transparent conducting oxides (TCOs), and in particular indium-tin-oxide (ITO) and ITO-based multilayers, have been proposed [73]. These materials afford a good compromise between minimum electrical resistivity and high optical transmittivity in the visible light spectrum when patterned on see-through materials such as glass or transparent polymers. A technique to improve the efficiency of the transparent antennas, without affecting their transparency, is the application of a layer of highly conductive coating or metallization strips on the antenna edges where the current density is high [72].

Among SSs, or in general distributed systems within the IoT vision, a fast growing field of research is represented by wearable electronics for BANs [74]. In this case, the integration of electronic devices in the garments requires the development of wearable and washable antennas and antenna arrays on fabrics. Washable antennas can be realized by covering textile antennas by a breathable thermoplastic polyurethane coating in order to protect the device against water absorption and corrosion [69].

Although dimension constraints are not very critical for distributed systems on cheap materials, they cannot be neglected thoroughly. At RF, for example, high permittivity materials [68] and magnetic composite substrates [75] can be adopted. Artificial magnetic conductors (AMC) can be employed alternatively to the magnetic composites with similar results [76]. These approaches are simply demonstrated from the wavelength equation: wavelength is a function of the relative permittivity and permeability and adopting suitable materials to increase these values, the effective wavelength, and therefore the antenna size, decreases. Anyway, the use of these materials introduces a tradeoff between dimensions and performance: generally the substrate losses decrease the antenna radiation efficiency, thus affecting the communication range of the overall wireless system, as documented in [68], [75], and [76].

In terms of design methodology, the introduction of unconventional materials as well as the environmental constraints posed by distributed systems and systems for IoT influence and drive the design strategies. Some solutions are proposed in the literature to cope simultaneously with these constraints; in [68], shielded configurations have been analyzed to mitigate environmental sensitivity. In [69], an example of robust patch antenna for BAN application that reduces the effect of the body on the performance is illustrated; in [77], the use of broadband antennas, such as the Chebyshev monopoles with a fractional bandwidth of about 40%, is proposed to reduce the frequency

shift introduced by the background materials or by the bending effects.

In SSs, and in general in IoT applications, antennas are used both to transmit and receive information and to harvest the necessary energy from the surrounding environment. Regardless of the fact that the available energy is randomly released in the environment by existing services (GSM, WiFi, and so on, in urban and semi-urban environments [78], [79]) or purposely delivered to empower a distributed population of nodes [80], antennas have to be able to harvest EM energy. This kind of "double effect" antenna is widely referred to in the literature as "rectenna": it combines rectifying circuitry with EM to electrical energy transduction.

The fundamental codesign techniques of antennas and rectifiers, focusing on the improvement of the conversion efficiency exploiting matching circuits, are described in [53]. Harmonic-balance and load-pull simulations are often used in order to find the optimal impedances that allow best efficiency to be obtained as a function of the EM incident power.

Multiband, broadband, and circularly polarized antennas are often adopted in EH applications to reduce the overall sensitivity to the environment. An example of planar antenna array for EH applications, in agreement with the SS principle, is documented in [81]: spiral antennas are proposed in order to provide a wide operating frequency band, and the rectification circuitry is optimized and characterized for low incident power levels. Similar antenna array for UWB EH is shown in Fig. 7.

A rectenna can be used in addition to the communication antenna or, alternatively, the same antenna can be used for both EH and data transmission. The use of different antennas is generally adopted if harvesting and communication are carried out at different frequencies

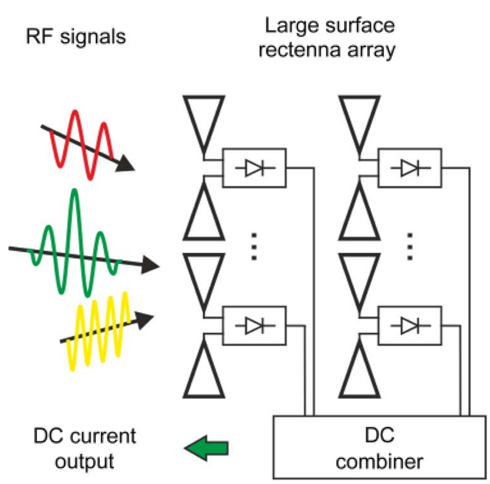

Fig. 7. ***Scheme of the rectenna array able to collect RF energy even in a broadband (depending of the kind of receiving antenna element), according to the solution adopted in [81].***

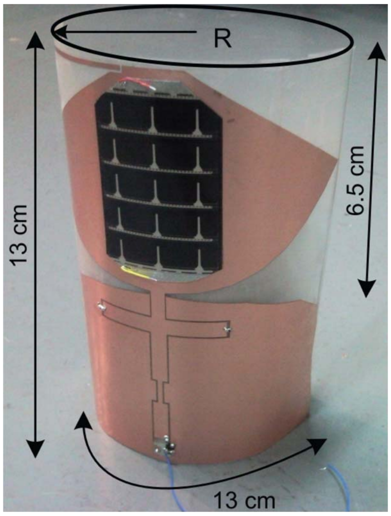

Fig. 8. ***Hybrid rectenna for solar and EM–EH. The hybrid rectenna consists of a broadband antenna and a solar cell combined in the same structure. After [82].***

and, mainly, in order to enhance harvesting efficiency without decreasing communication performance. In any case, this requires a codesign and can affect the node dimension and complexity. Alternatively, a single antenna can be a feasible compromise if communication and harvesting share the same frequency band and if the antenna harvesting efficiency is not the main issue; examples are the passive RFID tags empowered by the reader with a standard RFID antenna able to provide both EH and communication capability, as documented in [64] and [65].

However, the EM–EH is not the only solution to energize nodes and SS elements: hybrid EH, in fact, can be performed by exploiting different energy sources; that is, combining the rectennas with other sources of energy.

Recently, a low-cost and conformal structure for hybrid EH, based on low-cost and flexible poly-ethylene terephthalate (PET) substrate and an amorphous silicon solar cell, has been proposed in [82]; other examples are discussed in [20] and [83]. The use of low-cost, printable photovoltaics deposited on flexible substrates to form part of the antenna radiating structure is documented in [84]. In all these contributions, the main challenge appears to be the codesign of the antenna and solar cell in order to avoid reciprocal detrimental effects. The antenna is designed with a solar cell integrated on top of the radiating surface to obtain good radiation characteristics and to incorporate connections for the extraction of the dc provided by the solar cell. In [82], it was demonstrated that, by adopting thin film solar cells and paying attention to not exceeding the perimeter of the RF antenna, the solar cell can be integrated so as not to significantly affect the performance of the antenna. The hybrid rectenna for solar and EM–EH documented in [82] is shown in Fig. 8.

In terms of industrial assembly, the use of new materials and the need for low-cost and large-scale fabrication techniques would be fostered by architectures more insensitive against geometrical errors and placement misalignments. Following this direction, EM coupling can be exploited instead of ohmic contact to connect antennas on a flexible substrate to Si chips or, more generally, to the active circuitry [85]. This technique exploits a planar heterogeneous transformer, with the primary and secondary windings implemented on the antenna substrate and the Si chip, respectively. In this way, the galvanic contacts and the soldering process are avoided, and the final structures have been proven much more robust to alignment errors than traditional ohmic techniques without any significant performance degradation. By artificially applying a misalignment of 150 μm, which is the common dimension of a soldering pad, the technology proposed in [85] causes a loss increment of only 0.1 dB, due to the applied misalignment, while the same misalignment, when adopting ball grid arrays, would have implied missing the contact. This approach is quite attractive especially in combination with nonrigid materials where mechanical stress can result in significant substrate deformations. Recent contributions show the application of the aforementioned approach to inkjet printed antenna on PET substrate coupled to the chip for wireless nodes [86] and a textile patch antenna, magnetically coupled to the active circuitry, suitable for garment integration (see Fig. 9) [87], the reflection coefficient of which is shown in Fig. 10.

In order to testify the robustness of the proposed solution against uncertainties inherent to textile and garment electronics assembly, the radiation efficiency of the antenna, as a function of horizontal and vertical misalignment of the two transformer windings, used to perform the magnetic coupling, is plotted in Fig. 11(a) and (b), respectively. This technique can be extended also to interlayer communications of multilayer devices, and an example is documented in [88], where the circuitry fabricated on different garments communicates by means of overlapped coils.

V. CHIPLESS APPROACH

It has already been discussed that SS represents a possible technology for the development of killer applications within the IoT paradigm. Thanks to the convergence of several technologies, ranging from EH and sensing to RFID and LAE, SS can afford complex functions. For example, SSs can be used in intelligent buildings for structural monitoring and alarms (fire, for instance). To achieve these goals, SS must be equipped with a huge number of tags, each one monitoring a small portion of the surface itself.

The passive RFID systems can be divided into two families, namely, chip-based and chipless tags. The first family usually exploits a low-power complementary metal–oxide–semiconductor (CMOS) chip to implement the main tag functions [RF carrier rectification, dc voltage regulation, amplitude shift-keying (ASK) demodulation, IDentification code (ID) decoding, load modulation, etc.] and thus can be adapted to sensor applications by a few additional circuit blocks [signal conditioning,

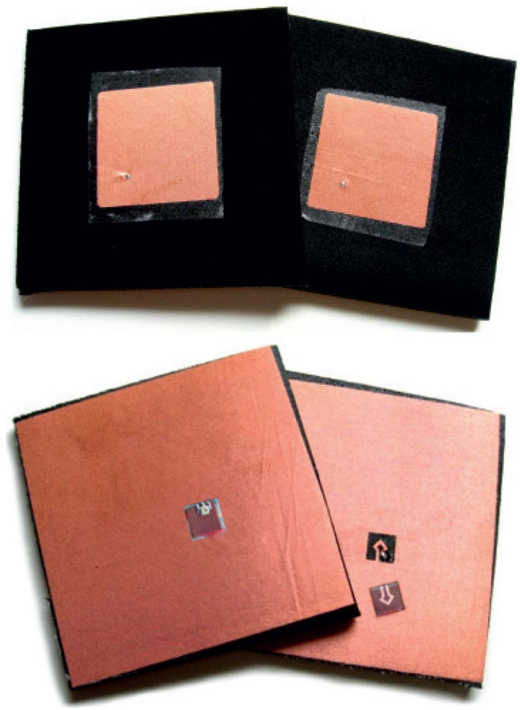

Fig. 9. ***Example of textile patch antennas operating at 2.4 GHz. The antenna and the ground plane are made of Flectron, a conductive textile, and the substrate is black foam. These materials are flexible and integrable in the garments. Magnetic coupling is exploited to connect the antenna and the active circuitry on flexible substrate. After [87].***

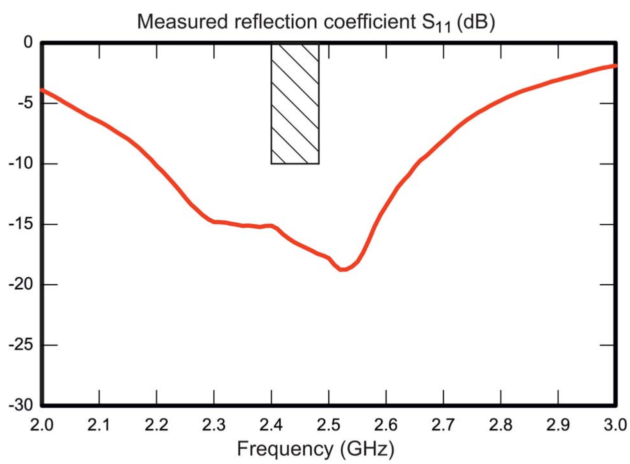

Fig. 10. ***Measured reflection coefficient of the previous textile antenna in the frequency band 2.4–2.48 GHz. After [87].***

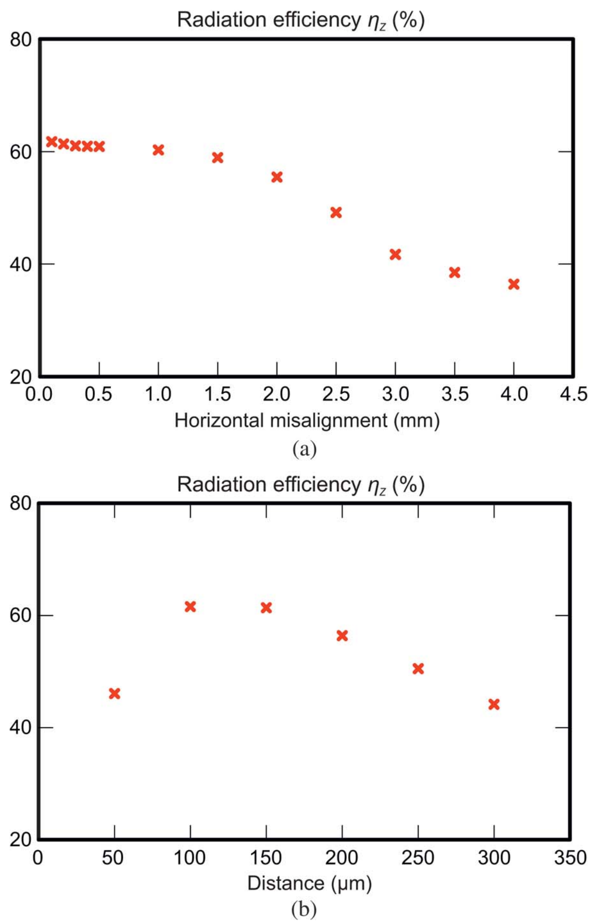

Fig. 11. ***Variation of the radiation efficiency evaluated versus (a) horizontal and (b) vertical misalignment between the antenna and the circuit windings. This test allows the robustness of the antenna performances against mounting uncertainties inherent to textile electronics to be evaluated at glance. After [87].***

analog-to-digital converter (ADC), etc.]. The main advantage of such an approach is the digital modulation of the transmitted signal, and thus the flexibility of the related data treatment, as shown in [89] and [90]. The production costs of chip-based tags are mostly associated with the heterogeneous integration of the silicon chip with the antenna [85], [91], the latter being manufactured typically on a flexible substrate or a textile substrate [92]–[97].

In order to reduce the aforementioned costs and to save as much energy as possible, solutions requiring minimum amount of electronics must be pursued. For this purpose, the chipless tag family was introduced and applied to wireless sensing in the recent years [98]–[103]. It is worth recalling here that the introduced buzzword "chipless" stands for a family of tags that are actually able to implement their functionalities by using only a few lumped components and passive distributed elements, without requiring any electronic integrated circuit (IC), the chip indeed, to be mounted.

The standard chipless tags (i.e., only coding and no sensing) exploit, basically, two mechanisms, namely, time-domain and frequency-domain scattering [64]. In the first case, the elapsed time between multiple reflections is used for coding. These reflections are obtained, at tag level, by connecting the antenna to a transmission line structure with several discontinuities. In the second case, instead, the tag has a specific frequency signature that is decoded at the reader level; to implement such a behavior, a coded series of resonators is realized on the tag antenna in order to reflect or not the corresponding frequency. Both approaches (time and frequency domain) lead to tag circuits that are not necessarily easy to miniaturize; nevertheless, it is worth noting that they are compliant with the LAE paradigm.

When dynamic sensor information has to be added to the static identification, we talk about chipless RFID sensor tags; these exploit an antenna, the electrical properties of which are controlled by the change of the physical parameter to be detected. There are, mostly, two proposed approaches for this. The first one is to induce a permanent change in the antenna property when a certain critical threshold (acceleration, temperature, fluid level, etc.) is exceeded [104]; this is useful for alarm type operations. The second one exploits a sensing load, i.e., a load the impedance of which is controlled by the sensed variable, connected to an antenna [105]. In both cases, the whole wireless sensor system (tag and reader) needs to have absolute accuracy, thus limiting the system performance with respect to both distance and fabrication tolerances.

A different method has been recently introduced in [106]. In this paper, a novel sensing principle is associated to the generation of an intermodulation signal from a tag, the latter being illuminated by two waves at different frequencies. The advantage of this idea is that the tag response is generated at a known frequency, thus the presence or the absence of such a signal can hardly be misinterpreted. Similar techniques have been used in harmonic radar systems [107] and in one-bit frequency doubling tags [108].

In line with the above ideas, a novel and completely original approach was proposed in [20] and [109] to solve the issue of absolute accuracy of the most of the passive chipless RFID sensors. The chipless tag described in [109] is based on the harmonic radar concept [110], [111], i.e., on a tag that, being illuminated by a carrier at frequency f_0, is capable of generating the second harmonic $2f_0$.

A simplified block diagram of the tag is illustrated in Fig. 12. For this purpose, the sensor information is encoded as the phase difference between two signals, one acting as the reference signal for the other one. First, the tag receives a carrier at frequency f_0. Then, two equal signals at frequency $2f_0$ are generated by means of a diode-based frequency doubler and a power divider. At this point, one of the two signals is phase-shifted using a passive sensing element. Finally, the $2f_0$ signals are reirradiated by

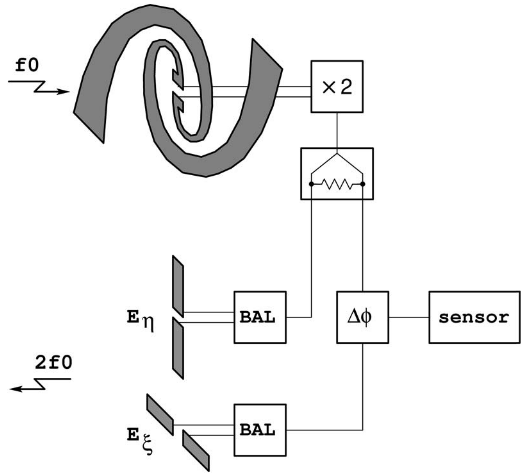

Fig. 12. ***Simplified block diagram of a harmonic chipless tag with sensing capabilities. After [109].***

exploiting two orthogonally polarized antennas. With this approach, the sensor information can be extracted by a suitable reader equipped with two complex (I/Q) receivers.

It must be observed that chipless tags, due to their inherent simplicity and extremely low number of lumped components, are easily realizable on flexible substrates by means of metal laminate [29], [30] and inkjet printing technologies. In particular, antennas [112], diodes [113], and passive sensing elements [114]–[117], i.e., all the main tag components, have already been experimented in cellulose-based materials. This will soon make SSs, equipped with sensing chipless tags, feasible at affordable prices.

VI. QUASI-OPTICS

"Quasi-optics concerns the propagation of EM radiation when the size of the wavelength is comparable to the size of the optical components (e.g., lenses, mirrors, and apertures) and hence diffraction effects become significant" [118].

In optics, operations are usually performed by using lenses. At EM frequencies, by following the quasi-optics analogy, lenses become large arrays, several wavelengths in size, of unconnected elements, each of them being able to get part of the signal incident on the array (usually focused by using a Gaussian beam), to carry out an operation and to irradiate the modified signal. The sum of the radiated signals modified by the array elements ends up in a radiated beacon elaborated with respect to the incident one [118]–[120]. From a historical point of view, quasi-optics was first introduced experimentally by Heinrich Hertz in the late 1880s [120] when he demonstrated the possibility of collimating EM signals on a multiwavelength surface by using cylindrical reflectors and studying effects that, until that time, were observed only at infrared and visible EM spectrum.

After more than 70 years, owing to the increasing demand for bandwidth and to the development of optical wavelength systems, quasi-optics experienced its palingenesis at the millimeter and submillimeter wavelengths.

We can classify the quasi-optical components into three main categories: frequency independent, frequency selective, and active devices. Frequency-independent surfaces include: delay lines, polarizing grids, hybrid junctions [121], attenuators [122], power dividers [123] and combiners [124], nonreciprocal devices [125], [126], absorbers, and calibration loads. Frequency-selective surfaces [127]–[129] include: inductive grids, capacitive grids, resonant grids, thick structures (perforated plates), and interferometers. Active devices include: oscillators [129], [130], amplifiers [131], [132], mixers [133], [134], phase shifters [135], [136], multipliers [108], [137]–[139], and switches [140]. This approach has been used so far mainly at millimeter and submillimeter frequencies because, being the size of the apparatuses proportional to the wavelength of the radiated wave, lower frequencies would have been prohibitive due to the very large size required. With the present development of technologies for LAE, however, quasi-optics has become a feasible approach even at RF and microwave bands, where large arrays of operational elements can be conceived.

Inheriting the quasi-optical approach, contact-less EM wave processing (filtering, frequency conversion, selective shielding, etc.) can be implemented even at low frequencies (in the order of megahertz). Two pioneer examples are switches [140] and the cross-dipole frequency doubler, proposed in [108], and implemented in [141], where, among various operating principles, the generation of harmonics is chosen to demonstrate the feasibility of such a component at microwave frequencies.

The layout of the proposed quasi-optical frequency doubler is shown in Fig. 13. The structure is inkjet printed on a cellulose-based substrate (a piece of photografic paper from Kodak). It consists of two crossed $\lambda/2$ dipoles. The longest dipole receives the incoming power at the fundamental frequency $f_0 = 3.5$ GHz, while the shortest one transmits the generated power at the doubled frequency $2f_0$ in an orthogonally polarized orientation. The length of the dipole operating at f_0 is 32 mm, while the $2f_0$ dipole is 16 mm long. The width of the tracks used to implement the dipoles is about 2 mm. The multiplication is provided by four diodes in a bridge configuration, thus forming a fully balanced multiplier unit.

Due to the omnidirectional nature of the dipole antenna, the harmonic signal is irradiated with the same intensity in the azimuthal plane (small differences are due to both the dielectric substrate and the planar nature of the dipole conductors). This means that the harmonic signal is reflected toward the reader and the transmitter toward other directions at the same time. A measurement of the received power at $2f_0 = 7$ GHz is reported in Fig. 13(b). Here the interrogation distance is 10 cm and the

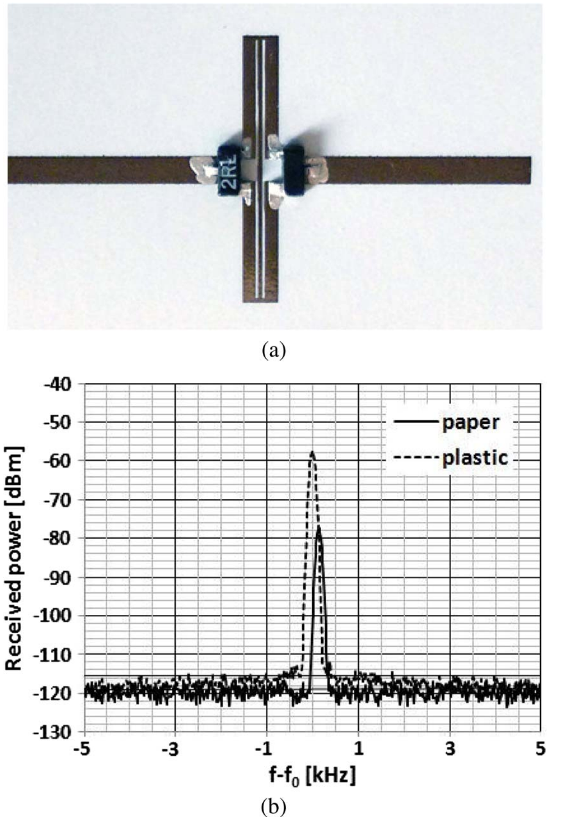

Fig. 13. ***Cellulose-based prototype of the (a) crossed-dipole frequency doubling tag and (b) measured second-harmonic response. The measurements have been carried out interrogating the tag at $f_0 = 3.5$ GHz and receiving the $2f_0 = 7$ GHz frequency component. The interrogation distance is 10 cm, and the transmitted power is equal to 20 dBm. The transmitter is equipped with a two-element Yagi antenna at f_0, while the receiver uses a helix antenna at $2f_0$. The fundamental frequency dipole is 32 mm long. After [141].***

transmitted power is equal to 20 dBm. The transmitter (reader side) is equipped with a two-element Yagi antenna at f_0, while the receiver (reader side) uses a helix antenna at $2f_0$. In these conditions, the power received from the cellulose-based (paper) tag prototype at $2f_0$ is about -80 dBm. The same structure implemented on a plastic substrate produces more power, mainly because of a better frequency tuning. An improved efficiency could be achieved by: 1) adopting a frequency multiplier with better harmonic terminations; and 2) using directive antennas in order to address the power only toward the reader.

In the frame of the IoT, the crossed-dipole tag is a very simple one-bit tag that can alarm a system when it is placed within the range of the reader. However, with very simple modifications, this idea can be used to implement a variety of on/off sensors (the paper substrate can be easily torn when a certain mechanical strain is exceeded).

The crossed-dipole structure can also be used as a building block to form arrays, an example being shown in Fig. 14. These arrays are mainly intended for LAE applications where a complete surface can be interrogated and answered by generating a harmonic signal. The fabricated prototype uses a Rogers substrate, thus it is not flexible. However, adopting a cellulose-based substrate, a flexible structure can be built. The bending capability of cellulose-based circuits is quite good and only limited by the discrete components mounted on them.

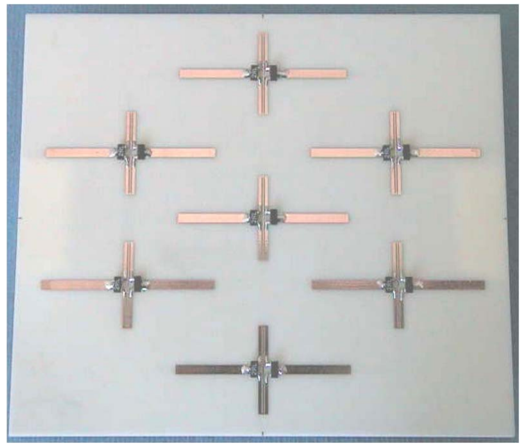

Fig. 14. ***Example of quasi-optical frequency doubler based on an array of crossed dipoles. This structure is implemented on a Rogers substrate, but this can be substituted with a cellulose-based material to reduce costs and obtain mechanical flexibility.***

The second example consists of a paper-based contactless frequency doubler for harmonic RFID applications [142]. The doubler, realized on paper substrate, generates the harmonic signal by means of a single Schottky diode. The system operates at 7.5 and 15 MHz, and these frequencies are chosen, without lack of generality, to accomplish the realization of a fully organic frequency doubler exploiting paper printed coils and organic diode (pentacene-based), the present frequency limit of which is around 15 MHz [143]. Fig. 15 shows a picture of the organic tag, while Fig. 16 shows the doubling efficiency of the organic tag versus transmitting/receiving (TX/RX) distance, assuming TX power as a parameter (for the sake of completeness, it is worth noting that TX and RX antennas of the reader are equal to the RX and TX antennas of the tag, respectively).

As a final remark, it is worth noting that, to the authors' knowledge, only planar developments of quasi-optical arrays have been proposed so far; reasonably, combining quasi-optics with LAE related technologies can lead, in the near future, to new SS solutions only in a limited planar extent.

VII. SMART FLOOR

The new concept of smart cities is generating a group of new scenarios that will impose a new way people interact with the environment. This immersion brings the IoT to a new level of relationship with people and environment,

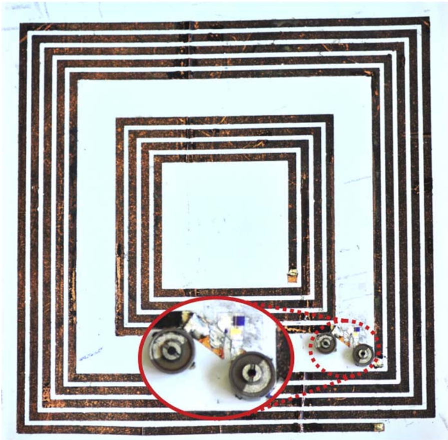

Fig. 15. ***Fully organic tag prototype of the frequency doubling tag operating at 7.5–15 MHz. After [142].***

where the scenario around is aware of people's needs and can interact with their way of living.

This new concept brings IoT to areas that cover broad topics, including transportation, energy distribution, data communications, and all technologies in a sense that they will become transparent to the normal users and citizens.

The growth of smart cities will significantly increase the quality of life, the reduction of energy waste, and the availability of information by using ICT. All these developments have, as a motivation, the overall inclusion of people into the city in a way that ICT should become completely embedded into our surroundings.

These new concepts are viable only if the smart environments are enabled by IoT. IoT is actually taking shape and is growing everyday through the number of devices that get connected to each other.

Nevertheless, most of these devices that team up with each other to build up the IoT world are powered by some kind of power sources. This is actually the main limitation of present IoT solutions. In order to be able to create real IoT environments, RFID, wireless power transfer (WPT), and EH devices appear as a major enabling technology for the IoT, due to their inherent simplicity and ability to provide sensing to remote objects without the need for constant powering.

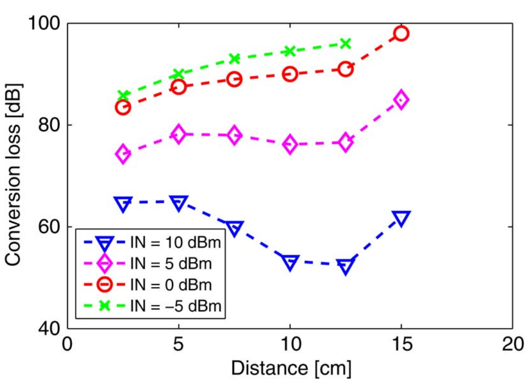

Fig. 16. ***Conversion (doubling) loss of the reader tag harmonic RFID system as a function of the reader tag distance, assuming the output reader power as a parameter. After [142].***

In this scenario, the concept of a smart floor becomes real. Smart floors should be capable of interacting with the environment seamlessly and be aware of persons and objects on top of them.

The focus of this section is going to be smart floors as an information system, where RFID capabilities are used to provide an identification and information source embedded into the floor. This massive RFID immersion will allow to create low-power high accuracy location, navigation, and, generally speaking, an information system that can team up with passers in a noninvasive way.

In this approach, the system uses passive RFID tags that are spread beneath a flooring in order to create a map that can be read with a mobile unit that might be self-powered through energy harvested from the movements of the subject to be located [144], [145].

This new location system based on smart floors can actually be extremely competitive when compared with existing solutions; among them, we can take into consideration those based on image processing [146]; they provide a high level of information at the price of high cost, power consumption, and intrusiveness. Another approach is based on pressure sensors [146], [147], providing actually a different type of smart floors; pressure sensors are nonintrusive and can be less expensive in terms of equipment when compared to the imaging systems; however, they can still be quite expensive to install into the floors; moreover, they do not allow for seamless identification of an individual in a given space. Eventually, ultrasounds [148] and RF localization system detection [149] have to be listed; although very flexible, they require dedicated communication infrastructures, additional complexity and costs, and they are mostly sensitive to environmental changes, both in terms of accuracy and functionalities.

The just mentioned smart-floor-based system tackles most of these challenges as it is very low cost, able to have a good, and precisely predictable, accuracy, and able to detect different users in a given space.

A. RFID-Based Smart Floor Including Material Aspects

Smart environments and floors should be completely seamless to the users. This entails the need to embed electronic devices into the environment in a noninvasive way. Nevertheless, this embedding of electronic devices, mainly wireless transceivers into the floor, is not a simple matter. Floors, in fact, have been made by almost the same kind of materials for centuries; tile industries are weakly available to introduce new materials to match

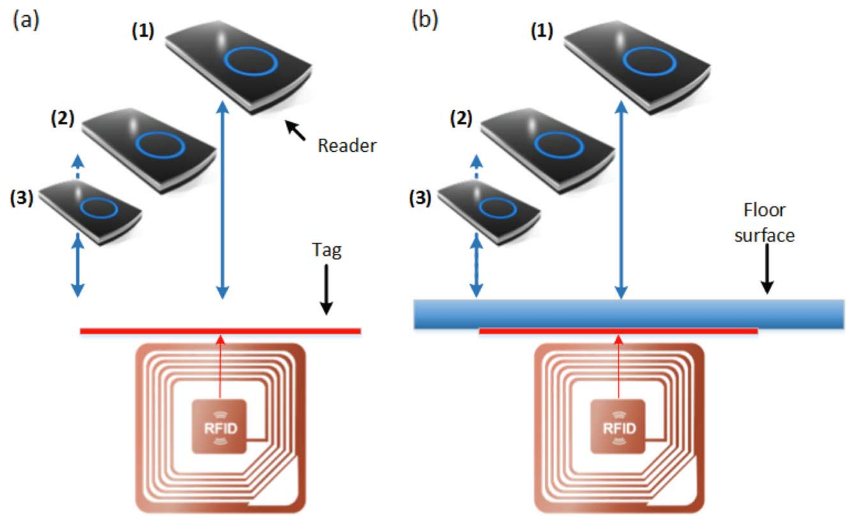

Fig. 17. ***Readable distance test scheme (a) without and (b) with tile. After [144].***

requirements posed by embedded electronics. Similar considerations can be made about the consolidated techniques to build apartments and houses: they are quite mature and whatever adaptation of them to embedded electronic systems is unrealistic. The consequence of this is that constitutive elements of SSs embedded into the floors must be suitable to materials and technologies already present: materials available are those adopted for tiles and SSs must be adapted to building constraints.

In this section, we focus on the most important approaches for the characterization of the EM properties of the materials, commonly adopted in floors, and their interactions with our electronic radio systems. As an example, ceramic tiles are going to be selected as the floor element where electronic tags have to be embedded.

Ceramic tiles have been used for ages to pave floors. These make up a great deal of most floor types in public buildings, from airports to banks, therefore, they are the most interesting flooring elements to investigate.

As the first approach, the study of the influence of some materials for floor surfaces, such as ceramic, cork laminates, and wood, in the communication between the transmitter and receiver devices has to be made; in this case, low-frequency (13 MHz) inductors are going to be used as the wireless interface.

In order to do the measurements, traditional RFIDs are used, which simplify the measurement approach significantly. A test setup is shown in Fig. 17, and experimental results are summarized in Table 3. What can be seen from the results presented in the table is that none of the tested materials affect the electrical characteristics of the RFID propagation significantly.

Another approach to the measurement is to evaluate the impact of the presence of metal inclusions beneath the ground; these can appear from pipes or from buildings supporting structures. In order to test this scenario, the presence of a metal sheet close to the coil was tested to verify its impact on the RFID reading distance. The test setup is presented in Fig. 18. In this case, when the reader is aligned (1) with the center of the coil beneath the tile, a minimum distance of 10 mm between the metallic sheet and the tag must be guaranteed in order to allow for the proper reading of the tag. In the other approach, the edge aligned scenario (2), the minimum distance between the metallic sheet and the tag increases to 30 mm to allow for communication.

Table 3 Results From Average Readable Distance Test

Tile type	Aligned (1)	Edge aligned (2)	Unaligned (3)
Without tile	4.5 cm	4.3 cm	2.4cm
Ceramic tile 4 mm thick	4.5 cm	4.3 cm	2.4cm
Ceramic tile 6 mm thick	4.5 cm	4.3 cm	2.4cm
Ceramic tile 7 mm thick	4.5 cm	4.3 cm	2.4cm
Cork laminate 5 mm thick	4.5 cm	4.3 cm	2.2cm
Wooden floor 8 mm thick	4.3 cm	4.2 cm	2.2cm

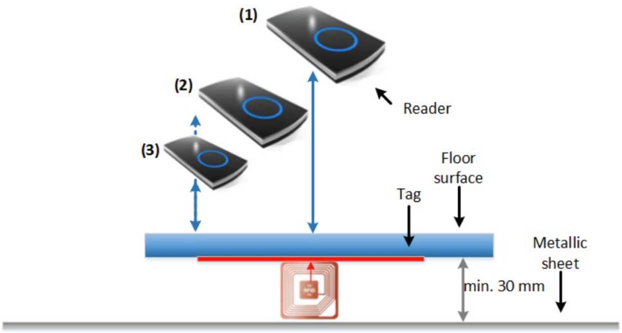

Fig. 18. ***Readable distance test scheme with metallic sheet presence. After [144].***

This test allows us to conclude that, in a real scenario, when considering the typical distance from the antenna to the floor, where the reader is usually embedded into a mobile device, a minimum distance from the tile to any metal inclusions in the ground has to be guaranteed. As seen, this safe distance should be at least 30 mm.

B. Navigation Approach Based on Smart Floors

A meaningful example of the applications of the smart floor concept is the demonstrator developed at the University of Aveiro, Aveiro, Portugal. It allows a nomadic RFID reader on top of it to be identified and localized by means of a smart floor.

The prototype in the present state is composed of four main components: a set of tagged tiles forming the smart floor, the nomadic reader, a wireless communication device to connect the reader to the information system, and a computer on which the location and navigation software is installed. A potential scenario of application for the monitoring of elderly housing is shown in Fig. 19. In the demonstrator presented, the RFID reader is connected to the radio unit and inserted into the user's shoes in order to read the passive tags as the user walks around a given area. The tile IDs are detected by the reader and sent to a centralized information system using, without lack of generality, a nonstandard wireless communication system, purposely developed in the laboratory.

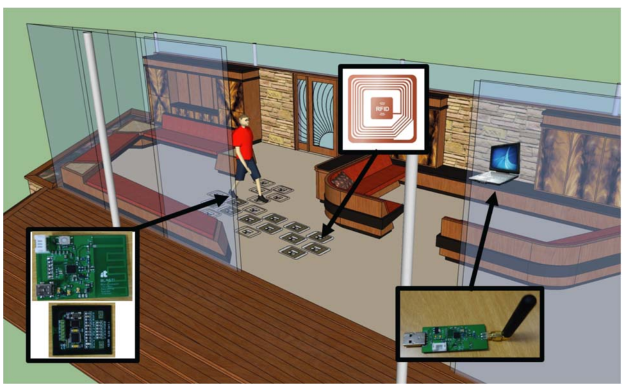

Fig. 19. ***Example of smart floor application scenario.***

The software in the computer then decodes the ID of the smart tile, and correlates it with a preloaded referenced map, thus being able to provide the precise position of the walker in the environment.

The location can be subsequently translated to a navigation system, and combined with artificial intelligence to allow navigation, situation awareness, etc.

Plenty of applications and related solutions can be envisioned on the basis of this smart floor approach: robot control, automatic pallet managements, prevention in harsh environments, and so forth.

VIII. SMART SHOES AND BAN

The aforementioned smart floor (Section VII), initially proposed to localize moving subjects in a given area, actually allows for the implementation of a very low-cost, accurate, and reliable system able to provide each kind of detectable information from an equipped area to the Internet.

To exploit the potentiality of a smart floor, it is obvious that developing purposely conceived communication units acting, on the one hand, as readers for tag tiles and, on the other hand, as communication systems with the web is needed.

One of the investigated systems for this is the so-called smart shoe [21]. Smart shoes are intended as shoes incorporating a reader able to illuminate the tag embedded into the tile and a wireless interface to communicate data to the web. To this extent, smart shoes can be seen as hubs of BANs able, on the one hand, to get information from the surrounding environment (body included) and, on the other hand, to communicate the collected information to the Internet. According to common buzzwords, they can be seen as the second technological layer, just above the first physical one consisting of tagged objects, in a hierarchical picture of IoT. Alternatively, they provide the cloud of nomadic readers with networking capabilities required for the implementation of the so-called networked RFID (N–RFID) [150] strategies. In the referred structure [21], the necessary antenna system is inkjet printed on paper, thus exploiting the process described in Section II, and it is a trademark-logo-shaped dual-band antenna working at 900 MHz and 2.4 GHz. A block diagram and its equivalent realization are shown in Fig. 20: it is worth noting that the reader itself works at 13.5 MHz exploiting the near-field communication (NFC) concept, according to what is stated in the smart floor section; as a consequence, there are no issues about the interference between the dual-band antenna and the NFC reader. Moreover, an approach similar to [145] is proposed to power the reader: the idea here is as well to harvest the energy produced by the human walking by means of piezoelectric materials embedded into the sole of the shoe.

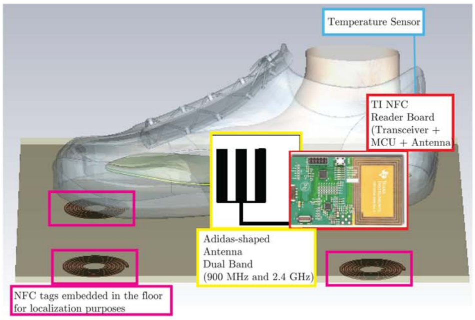

(a)

(b)

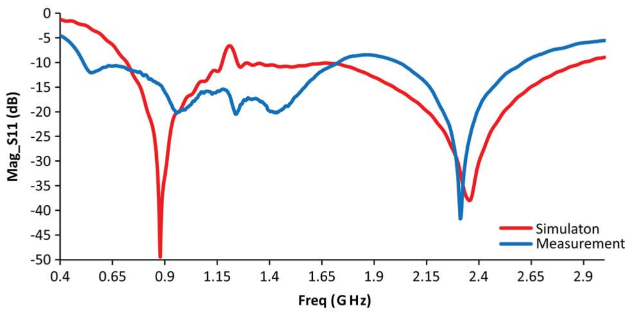

(c)

Fig. 20. ***(a) Block diagram, (b) photo, and (c) dual-band antenna results of the smart shoe that works as an energy autonomous reader for smart floors able to collect the localization data from the smart tiles and send them to a centralized system. After [21].***

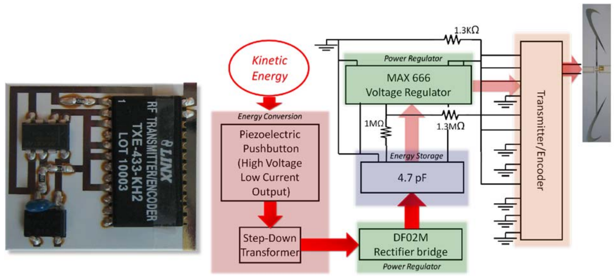

(a)

(b)

Fig. 21. ***(a) Mounted electronics on shoe with piezoelectric energy harvester and block diagram of the transmitting tag, driven by the EH unit. (b) Photograph of the assembled prototype showing the key components packaged on an organic flexible substrate. After [145].***

Fig. 21(a) shows the shoe with the mounted electronics consisting of a trademark-logo antenna inkjet printed on a flexible paper substrate together with the circuits in which the components [Fig. 21(b)] are fixed by conductive epoxy glue. A piezoelectric push button was embedded in the shoe to scavenge energy from human walking strike. This energy is then collected by a simple electronic circuit based on off-the-shelf components and used to supply the RFID transmitter. As reported in [145], the system is composed by the power-generator/energy-conversion device, the energy storage device, the power regulator circuit, and the RF transmitter that can broadcast the tag ID and the stored information.

When the push button is pressed, an inner spring is compressed and when the pressure exceeds a fixed threshold, the spring-loaded hammer will be released to deliver the dynamic mechanical force to the piezoelectric component; once the hammer strikes the piezoelectric element, a pressure wave is generated and reflected a few times between the hammer and the element, creating a mechanical resonance [151]. As a result, the generated output voltage follows closely an alternating current (ac) signal course. The signal out of the piezoelectric element is characterized by high voltage and low current; therefore, since this RF circuitry requires lower voltages at higher currents, a step-down transformer is used for better impedance matching to the following circuitry.

An energy storage device is adopted to collect the electrical energy and to provide it to the transmitter even when the external power source is temporarily unavailable; in fact, the RF transmitter takes tens of milliseconds to transmit one complete word, while the piezoelectric push button harvests energy in a transient time. To store the collected energy, a 4.7-μF tank capacitor was chosen. An ac–dc full wave diode bridge rectifier is used to convert the ac voltage from a piezoelectric element into a dc source and a dc linear regulator is added to adapt the dc voltage across the capacitor to 3-V transmitter operating voltage. For this purpose, a MAX666 low-dropout linear regulator, providing a stable 3-V supply until the tank capacitor charge is drained below the reference level of the dc linear regulator itself, is chosen. The transmitter used, the LINX

Table 4 Shoe Energy Performance Summary

Energy provided by the pushbutton	stored in the capacitor	848.4 μJ
Utilized energy	below 2.7 V capacitor voltage, the active RFID tag stops transmitting	17.1 μJ
Available energy	848.4 μJ − 17.1 μJ	831.3 μJ
Energy required by the circuit for a one-word transmission	Power Needed for 50 ms operation: 9 mW	450 μJ

TXE-433-KH2 [152], is able to combine a highly optimized RF transmitter with an onboard encoder.

The maximum voltage across the capacitor is 19 V; therefore, the energy stored in the capacitor can be calculated to be close to 850 μJ. After the strike, the regulator becomes active, providing power to the tag circuitry; its 3-V output remains constant before it starts to drop to zero according to the capacitor discharge rate. When the voltage across the capacitor drops below 2.7 V, the active tag stops transmitting. The resulting energy left in the capacitor and not used is about 17 μJ. The required time for successful completion has been measured to be close to 50 ms; the total circuit energy consumption for a 50-ms transmission is then approximately 9 mW (Section IV). Consequently, the energy required for a one word transmission is approximately 450 μJ, much less than the power collected by the energy conversion and regulation unit. The energy performance of the smart shoe is summarized in Table 4.

"Smart" solutions like smart shoes are suitable for smart floor interaction and for collecting information (position included) from them. The smart shoe has actually a double functionality: on the one hand, it is a means to collect information from the environment (smart floor included) and from the on-body sensors and apparatuses; on the other hand, it transfers data to the Internet, via WiFi, for instance, while likely receiving control and feedback signals. To this extent, it contributes to the development of wearable electronics for body-centric communication systems, according to the scheme of Fig. 22. This class of devices is based on the BAN concept (see Fig. 22): a network of wearable computational units, sensors, energy harvesters, and transceivers networked and implemented around the human body. The information is acquired by means of several sensors and, after processing and digital modulation, is transmitted by means of off-body transceivers. The most attractive application of BANs and wearable systems, so far, is probably health monitoring [88], but the number of foreseeable applications is constantly increasing (personal fitness monitoring, personal audio system, personal alarm set, and so on). Today, a big contribution to the BANs is being given by the interaction with portable devices such as smartphones which can be exploited as gateways.

Low-power ICs, sensors, and wireless communications are key elements of the BANs, and the use of EH techniques and mixed technologies such as RFID, as in the above described smart shoe, can contribute to the development of autonomous BANs. According to the notation adopted in [74] and [153], BANs can exploit wireless communication not only for off-body communications with other systems, but also for on-body and in-body communications to interconnect networked devices [wireless body area networks (WBANs)]. Generally, the proposed WBAN solutions are based on existing communication standards; but, recently, the IEEE 802.15.6 working group has provided a standard for short-range, wireless communications in the vicinity of, or inside, a human body based on ISM bands for BANs [154]. In this rapidly evolving scenario, smart shoes can be seen, in turn, as a promising mean to interface information coming from smart floors to the BANs and ultimately to the Internet, directly or via portable devices.

IX. ENERGY SKIN

Within SSs, another area is emerging, which requires dc energy. The availability of devices that can actually increase the battery life of our electronic gadgets [155] is the holy grail of IoT; the idea is actually to convert energy from

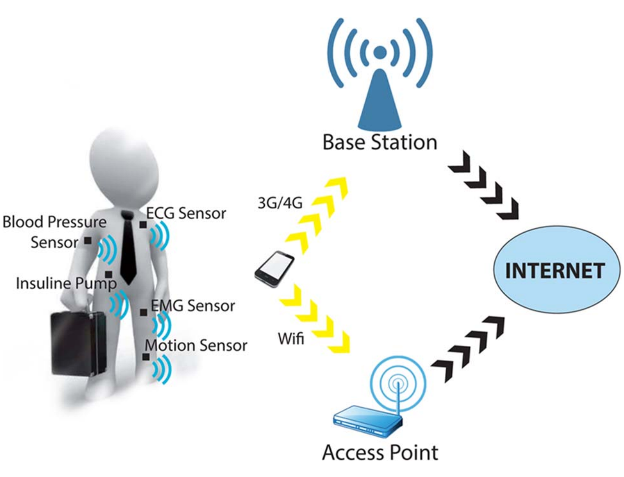

Fig. 22. *BAN integrated with IoT: the data sensed on the human body and collected by smart devices are sent to the Internet through the standard protocols like third generation/fourth generation (3G/4G) and WiFi.*

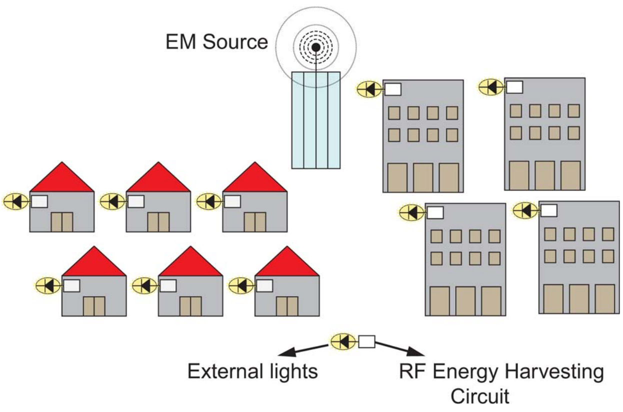

Fig. 23. ***EM source, likely supplied by solar energy in order to keep eco-friendliness, is used to broadcast energy to the urban neighborhood where houses are equipped with local RF–dc converters able to power supply local devices (external lamps in the example).***

different sources, as solar to dc [156], EM radio signals to dc, thermal to dc [156], vibration to dc [157], etc. [158].

Portable converters from solar to dc are today commonly available on the market at very low prize. Similar portable scavengers can be easily envisioned even for other energy converters. On this basis, plenty of sophisticated and more complex solutions are being proposed. Just as an example, we report the solution in Fig. 23, where the solar energy is used to supply an EM source that broadcasts RF energy in the surrounding urban environment; this energy is converted to dc energy at building level and, in turn, exploited to supply external local lamps. This approach was conceived for space applications [159], [160], but could be used in certain conditions in earth stations as well. The concept can actually move forward and be integrated into a smart skin, in the sense that all devices could be powered up by the skin energy conversion that a person can carry (vibrational, thermal, RF, etc.). This will become possible by integrating paper and textile radio electronic circuits in the smart skin surfaces of our clothes.

X. CONCLUSION

This paper focused on smart surfaces concept. This concept was introduced as a way to provide solutions to societal instances by means of technologies and techniques that today are gaining great momentum thanks to IoT development. The foreseeable IoT evolution, in fact, calls for systems and subsystems that are more and more energy conservative, fully autonomous (battery-less and not connected to the grid), as recyclable as possible (ultimately 100% biodegradable), flexible, and extremely low cost to be embedded in as many objects as possible. In order to meet these expectations, several technologies have to be implemented concurrently. This paper illustrates some of them, namely, recyclable and reliable materials, printing and R2R compatible techniques, conformal antennas on unconventional materials, and chipless RFID.

Subsequently, it has been shown how these technologies enable a fairly new branch of IoT development, represented just by SSs.

SSs are in their infancy; nevertheless, some examples, enabled by the aforementioned technologies, can be cited. Among them, the way to inherit "quasi-optics" and extend them to RF frequencies even below gigahertz is shown, and the smart floor implementation as a means to provide precise localization as well as assisted paths platforms has been reported. Energy skin as a means to convert several energy sources (solar, thermal, vibrational, EM, etc.) in electric one is described as well.

The reported examples must be researched as a new paradigm for potential promising developments aiming at providing new LAE solutions for the future networked society. ■

REFERENCES

[1] European Union (EU), "The ICT sector and RDI," Digital Agenda Scoreboard, 2012. [Online]. Available: http://ec.europa.eu/digital-agenda/sites/digital-agenda/files/scoreboard_ict_sector_and_rdi.pdf

[2] J. Manyika *et al.*, "How the Internet of Things is more like the Industrial Revolution than the Digital Revolution," MGI Rep., 2013. [Online]. Available: http://www.mckinsey.com/insights/business_technology/disruptive_technologies

[3] D. Evans, "The Internet of Things: How the next evolution of the internet is changing everything," CISCO White papers, 2011. [Online]. Available: http://www.cisco.com/web/about/ac79/docs/innov/IoT_IBSG_0411FINAL.pdf

[4] I. G. Smith, "The Internet of Things 2012 New Horizons," IERC European Research Cluster on the Internet of Things, 2012.

[5] J. Morse, "Nanofabrication technologies for roll-to-roll processing," in *Proc. NIST-NNN Workshop*, Boston, MA, USA, Sep. 2011, pp. 1–31.

[6] A. Arias, J. MacKenzie, I. McCulloch, J. Rivnay, and A. Salleo, "Materials and applications for large area electronics: Solution-based approaches," *Chem. Rev.*, vol. 110, no. 1, pp. 3–24, Jan. 2010.

[7] T. Kampke, B. Kluge, and M. Strobel, *Field and Service Robotics*. New York, NY, USA: Springer-Verlag, 2008, ser. Springer Tracts in Advanced Robotics.

[8] M. Shur, "Giant area and flexible electronics," in *Proc. IEEE Nanotechnol. Mater. Devices Conf.*, Oct. 2006, vol. 1, pp. 264–265.

[9] M. Steer *et al.*, "Global modeling of spatially distributed microwave and millimeter-wave systems," *IEEE Trans. Microw. Theory Tech.*, vol. 47, no. 6, pp. 830–838, Jun. 1999.

[10] A. Rida, L. Yang, R. Vyas, and M. Tentzeris, "Conductive inkjet-printed antennas on flexible low-cost paper-based substrates for RFID and WSN applications," *IEEE Antennas Propag. Mag.*, vol. 51, no. 3, pp. 13–23, Jun. 2009.

[11] F. Alimenti, P. Mezzanotte, M. Dionigi, M. Virili, and L. Roselli, "Microwave circuits in paper substrates exploiting conductive adhesive tapes," *IEEE Microw. Wireless Compon. Lett.*, vol. 22, no. 12, pp. 660–662, Dec. 2012.

[12] D. Tobjörk and R. Österbackaa, "Paper electronics," *Adv. Mater.*, vol. 23, no. 17, pp. 1935–1961, 2011.

[13] P. Calvert, "Inkjet printing for materials and devices," *Chem. Mater.*, vol. 13, no. 10, pp. 3299–3305, 2001.

[14] G. Orecchini *et al.*, "Inkjet printed organic transistors for sustainable electronics," in *Proc. 60th Electron. Compon. Technol. Conf.*, Jun. 2010, pp. 985–989.

[15] L. Yang, G. Orecchini, G. Shaker, H.-S. Lee, and M. Tentzeris, "Battery-free RFID-enabled wireless sensors," in *IEEE MTT-S Int. Microw. Symp. Dig.*, May 2010, pp. 1528–1531.

[16] G. Shaker, S. Safavi-Naeini, N. Sangary, and M. Tentzeris, "Inkjet printing of ultrawideband (UWB) antennas on paper-based substrates," *IEEE Antennas*

Wireless Propag. Lett., vol. 10, pp. 111–114, 2011.

[17] R. Vyas *et al.*, "Inkjet printed, self powered, wireless sensors for environmental, gas, and authentication-based sensing," *IEEE Sensors J.*, vol. 11, no. 12, pp. 3139–3152, Dec. 2011.

[18] G. Orecchini *et al.*, "Design and fabrication of ultra-low cost radio frequency identification antennas and tags exploiting paper substrates and inkjet printing technology," *IET Microw. Antennas Propag.*, vol. 5, no. 8, pp. 993–1001, Jun. 2011.

[19] S. Kim *et al.*, "Monopole antenna with inkjet-printed EBG array on paper substrate for wearable applications," *IEEE Antennas Wireless Propag. Lett.*, vol. 11, pp. 663–666, 2012.

[20] S. Kim *et al.*, "No battery required: Perpetual RFID-enabled wireless sensors for cognitive intelligence applications," *IEEE Microw. Mag.*, vol. 14, no. 5, pp. 66–77, Jul. 2013.

[21] C. Mariotti, V. Lakafosis, M. Tentzeris, and L. Roselli, "An IPv6-enabled wireless shoe-mounted platform for health-monitoring," in *Proc. IEEE Top. Conf. Wireless Sensors Sensor Netw.*, Jan. 2013, pp. 46–48.

[22] K. Sangkil *et al.*, "Inkjet-printed antennas, sensors and circuits on paper substrate," *IET Microw. Antennas Propag.*, vol. 7, no. 10, pp. 858–868, 2013.

[23] B. Cook, J. Cooper, and M. Tentzeris, "Multi-layer RF capacitors on flexible substrates utilizing inkjet printed dielectric polymers," *IEEE Microw. Wireless Compon. Lett.*, vol. 23, no. 7, pp. 353–355, Jul. 2013.

[24] B. Cook, J. Cooper, S. Kim, and M. Tentzeris, "A novel inkjet-printed passive microfluidic RFID-based sensing platform," in *IEEE MTT-S Int. Microw. Symp. Dig.*, Jun. 2013, DOI: 10.1109/MWSYM.2013.6697592.

[25] B. Cook, B. Tehrani, J. Cooper, and M. Tentzeris, "Multilayer inkjet printing of millimeter-wave proximity-fed patch arrays on flexible substrates," *IEEE Antennas Wireless Propag. Lett.*, vol. 12, pp. 1351–1354, 2013.

[26] C. Mariotti, B. Cook, L. Roselli, and M. Tentzeris, "High-performance inkjet-printed metal-insulator-metal (MIM) capacitors on lossy silicon substrate *IEEE Microw. Wireless Compon. Lett.*, 2014.

[27] D. Angmo, T. T. Larsen-Olsen, M. Jorgensen, R. R. Sazndergaard, and F. C. Krebs, "Roll-to-roll inkjet printing and photonic sintering of electrodes for ITO free polymer solar cell modules and facile product integration," *Adv. Energy Mater.*, vol. 3, no. 2, pp. 172–175, 2013.

[28] R. Sazndergaard, M. Hessel, D. Angmo, T. T. Larsen-Olsen, and F. C. Krebs, "Roll-to-roll fabrication of polymer solar cells," *Mater. Today*, vol. 15, no. 1–2, pp. 36–49, 2012.

[29] F. Alimenti *et al.*, "A 1.2 v, 0.9 mW UHF VCO based on hairpin resonator in paper substrate and Cu adhesive tape," *IEEE Microw. Wireless Compon. Lett.*, vol. 23, no. 4, pp. 214–216, Apr. 2013.

[30] F. Alimenti *et al.*, "24 GHz single-balanced diode mixer exploiting cellulose-based materials," *IEEE Microw. Wireless Compon. Lett.*, vol. 23, no. 11, pp. 596–598, Nov. 2013.

[31] C. Mariotti *et al.*, "Modeling and characterization of copper tape microstrips on paper substrate and application to 24 GHz branch-line couplers," in *Proc. Eur. Microw. Conf.*, Oct. 2013, pp. 794–797.

[32] L. Guoyu and W. Zhenkai, "Summarize of rfid technology and typical application," in *Proc. Cross Strait Quad-Regional Radio Sci. Wireless Technol. Conf.*, Jul. 2011, vol. 2, pp. 1032–1036.

[33] L. Wang, L. D. Xu, Z. Bi, and Y. Xu, "Data cleaning for RFID and WSN integration," *IEEE Trans. Ind. Inf.*, vol. 10, no. 1, pp. 408–418, Feb. 2014.

[34] H. Deng *et al.*, "Design of sensor-embedded radio frequency identification (SE-RFID) systems," in *Proc. IEEE Int. Conf. Mechatron. Autom.*, Jun. 2006, pp. 792–796.

[35] S. Mohamad, F. Tang, A. Amira, A. Bermak, and M. Benammar, "A low power oscillator based temperature sensor for RFID applications," in *Proc. 5th Asia Symp. Quality Electron. Design*, Aug. 2013, pp. 50–54.

[36] D. Hotte, R. Siragusa, Y. Duroc, and S. Tedjini, "Performance optimization for the choice of impedances in the design of passive RFID tags," in *Proc. IEEE-APS Top. Conf. Antennas Propag. Wireless Commun.*, Sep. 2013, pp. 1349–1352.

[37] M. Donelli, "Guidelines for the design and optimization of wireless sensors based on the modulated scattering technique," *IEEE Trans. Instrum. Meas.*, vol. 63, no. 7, pp. 1824–1833, Jul. 2014.

[38] A. Ricci, M. Grisanti, I. De Munari, and P. Ciampolini, "Improved pervasive sensing with RFID: An ultra-low power baseband processor for UHF tags," *IEEE Trans. Very Large Scale Integr. (VLSI) Syst.*, vol. 17, no. 12, pp. 1719–1729, Dec. 2009.

[39] L. Chen *et al.*, "Range extension of passive wake-up radio systems through energy harvesting," in *Proc. IEEE Int. Conf. Commun.*, Jun. 2013, pp. 1549–1554.

[40] S. Sauer, A. Turke, A. Weder, and W.-J. Fischer, "Inkjet printed humidity threshold monitoring sensor solution with irreversible resistance change for passive RFID applications," in *Proc. IEEE Sensors*, Nov. 2013, DOI: 10.1109/ICSENS.2013.6688307.

[41] N. Cho, S.-J. Song, S. Kim, S. Kim, and H.-J. Yoo, "A 5.1-uW UHF RFID tag chip integrated with sensors for wireless environmental monitoring," in *Proc. 31st Eur. Solid-State Circuits Conf.*, Sep. 2005, pp. 279–282.

[42] M. Philipose *et al.*, "Battery-free wireless identification and sensing," *IEEE Perv. Comput.*, vol. 4, no. 1, pp. 37–45, Jan. 2005.

[43] D. De Donno, L. Catarinucci, and L. Tarricone, "A battery-assisted sensor-enhanced RFID tag enabling heterogeneous wireless sensor networks," *IEEE Sensors J.*, vol. 14, no. 4, pp. 1048–1055, Apr. 2014.

[44] N. Guilar, T. Kleeburg, A. Chen, D. Yankelevich, and R. Amirtharajah, "Integrated solar energy harvesting and storage," *IEEE Trans. Very Large Scale Integr. (VLSI) Syst.*, vol. 17, no. 5, pp. 627–637, May 2009.

[45] D. Brunelli, C. Moser, L. Thiele, and L. Benini, "Design of a solar-harvesting circuit for batteryless embedded systems," *IEEE Trans. Circuits Syst. I, Reg. Papers*, vol. 56, no. 11, pp. 2519–2528, Nov. 2009.

[46] D. Kwon, G. Rincon-Mora, and E. Torres, "Harvesting ambient kinetic energy with switched-inductor converters," *IEEE Trans. Circuits Syst. I, Reg. Papers*, vol. 58, no. 7, pp. 1551–1560, Jul. 2011.

[47] S. Mehraeen, S. Jagannathan, and K. Corzine, "Energy harvesting from vibration with alternate scavenging circuitry and tapered cantilever beam," *IEEE Trans. Ind. Electron.*, vol. 57, no. 3, pp. 820–830, Mar. 2010.

[48] T. Le, K. Mayaram, and T. Fiez, "Efficient far-field radio frequency energy harvesting for passively powered sensor networks," *IEEE J. Solid-State Circuits*, vol. 43, no. 5, pp. 1287–1302, May 2008.

[49] G. Papotto, F. Carrara, and G. Palmisano, "A 90-nm CMOS threshold-compensated RF energy harvester," *IEEE J. Solid-State Circuits*, vol. 46, no. 9, pp. 1985–1997, Sep. 2011.

[50] S. Rahimizadeh, S. Korhummel, B. Kaslon, and Z. Popovic, "Scalable adaptive wireless powering of multiple electronic devices in an over-moded cavity," in *Proc. IEEE Wireless Power Transfer*, May 2013, pp. 84–87.

[51] S. Scorcioni, L. Larcher, A. Bertacchini, L. Vincetti, and M. Maini, "An integrated RF energy harvester for UHF wireless powering applications," in *Proc. IEEE Wireless Power Transfer*, May 2013, pp. 92–95.

[52] Z. Popovic, "Far-field wireless power delivery and power management for low-power sensors," in *Proc. IEEE Wireless Power Transfer*, May 2013, DOI: 10.1109/WPT.2013.6556867.

[53] E. Falkenstein, M. Roberg, and Z. Popovic, "Low-power wireless power delivery," *IEEE Trans. Microw. Theory Tech.*, vol. 60, no. 7, pp. 2277–2286, Jul. 2012.

[54] S. Roundy, P. K. Wright, and J. Rabaey, "A study of low level vibrations as a power source for wireless sensor nodes," *Comput. Commun.*, vol. 26, no. 11, pp. 1131–1144, 2003.

[55] C. D. Richards, M. J. Anderson, D. F. Bahr, and R. F. Richards, "Efficiency of energy conversion for devices containing a piezoelectric component," *J. Micromech. Microeng.*, vol. 14, no. 5, 2004, DOI: 10.1088/0960-1317/14/5/009.

[56] S. R. Anton and H. A. Sodano, "A review of power harvesting using piezoelectric materials (2003–2006)," *Smart Mater. Struct.*, vol. 16, no. 3, 2007, DOI: 10.1088/0964-1726/16/3/R01.

[57] Cymbet Corporation, "Energy harvesting and storage." [Online]. Available: http://www.cymbet.com/design-center/energy-harvesting.php#

[58] T. Armstrong, "Energy harvesting applications are everywhere," RTC, May 2011. [Online]. Available: http://www.rtcmagazine.com/articles/view/102133

[59] D. Puccinelli and M. Haenggi, "Wireless sensor networks: Applications and challenges of ubiquitous sensing," *IEEE Circuits Syst. Mag.*, vol. 5, no. 3, pp. 19–31, 2005.

[60] L. Roselli *et al.*, "WPT, RFID and energy harvesting: Concurrent technologies for the future networked society," in *Proc. Asia-Pacific Microw. Conf.*, Nov. 2013, pp. 462–464.

[61] H. Liu, M. Bolic, A. Nayak, and I. Stojmenovic, "Taxonomy and challenges of the integration of RFID and wireless sensor networks," *IEEE Network*, vol. 22, no. 6, pp. 26–35, Nov. 2008.

[62] D. Dardari, R. D'Errico, C. Roblin, A. Sibille, and M. Win, "Ultrawide bandwidth RFID: The next generation?" *Proc. IEEE*, vol. 98, no. 9, pp. 1570–1582, Sep. 2010.

[63] C. Balanis, *Antenna Theory: Analysis and Design*. New York, NY, USA: Wiley, 2005, ser. Knovel Library.

[64] K. Finkenzeller and D. Müller, *RFID Handbook: Fundamentals and Applications*

in Contactless Smart Cards, Radio Frequency Identification and Near-Field Communication. New York, NY, USA: Wiley, 2010.

[65] E. Perret, S. Tedjini, and R. Nair, "Design of antennas for UHF RFID tags," *Proc. IEEE*, vol. 100, no. 7, pp. 2330–2340, Jul. 2012.

[66] K. V. S. Rao, P. Nikitin, and S. Lam, "Antenna design for UHF RFID tags: A review and a practical application," *IEEE Trans. Antennas Propag.*, vol. 53, no. 12, pp. 3870–3876, Dec. 2005.

[67] H. Chaabane, E. Perret, and S. Tedjini, "A methodology for the design of frequency and environment robust UHF RFID tags," *IEEE Trans. Antennas Propag.*, vol. 59, no. 9, pp. 3436–3441, Sep. 2011.

[68] A. Babar, A. Elsherbeni, L. Sydanheimo, and L. Ukkonen, "RFID tags for challenging environments: Flexible high-dielectric materials and ink-jet printing technology for compact platform tolerant RFID tags," *IEEE Microw. Mag.*, vol. 14, no. 5, pp. 26–35, Jul. 2013.

[69] M. Scarpello, I. Kazani, C. Hertleer, H. Rogier, and D. Vande Ginste, "Stability and efficiency of screen-printed wearable and washable antennas," *IEEE Antennas Wireless Propag. Lett.*, vol. 11, pp. 838–841, 2012.

[70] V. Lakafosis *et al.*, "Progress towards the first wireless sensor networks consisting of inkjet-printed, paper-based RFID-enabled sensor tags," *Proc. IEEE*, vol. 98, no. 9, pp. 1601–1609, Sep. 2010.

[71] C. Mariotti, G. Orecchini, M. Virili, F. Alimenti, and L. Roselli, "Wireless localization in buildings by smart tiles," in *Proc. IEEE Workshop Environ. Energy Struct. Monitoring Syst.*, Sep. 2012, pp. 7–11.

[72] H. J. Song *et al.*, "A method for improving the efficiency of transparent film antennas," *IEEE Antennas Wireless Propag. Lett.*, vol. 7, pp. 753–756, 2008.

[73] F. Colombel *et al.*, "Ultra-thin metal layer, ITO film and ITO/Cu/ITO multilayer towards transparent antenna," *IET Sci. Meas. Technol.*, vol. 3, no. 3, pp. 229–234, May 2009.

[74] D. Zito and D. Pepe, "System-on-a-chip radio transceivers for 60-GHz wireless body-centric communications," in *Ultra-Wideband and 60 GHz Communications*. New York, NY, USA: Springer-Verlag, 2014, pp. 177–187.

[75] L. Martin *et al.*, "Effect of permittivity and permeability of a flexible magnetic composite material on the performance and miniaturization capability of planar antennas for RFID and wearable wireless applications," *IEEE Trans. Compon. Packag. Technol.*, vol. 32, no. 4, pp. 849–858, Dec. 2009.

[76] D. Kim and J. Yeo, "Low-profile RFID tag antenna using compact AMC substrate for metallic objects," *IEEE Antennas Wireless Propag. Lett.*, vol. 7, pp. 718–720, 2008.

[77] C. Kakoyiannis and P. Constantinou, "Compact WSN antennas of analytic geometry based on Chebyshev polynomials," in *Proc. Antennas Propag. Conf.*, Nov. 2012, DOI: 10.1109/LAPC.2012.6402976.

[78] H. Visser and R. Vullers, "RF energy harvesting and transport for wireless sensor network applications: Principles and requirements," *Proc. IEEE*, vol. 101, no. 6, pp. 1410–1423, Jun. 2013.

[79] M. Pinuela, P. Mitcheson, and S. Lucyszyn, "Ambient RF energy harvesting in urban and semi-urban environments," *IEEE Trans. Microw. Theory Tech.*, vol. 61, no. 7, pp. 2715–2726, Jul. 2013.

[80] K. M. Farinholt, G. Park, and C. Farrar, "RF energy transmission for a low-power wireless impedance sensor node," *IEEE Sensors J.*, vol. 9, no. 7, pp. 793–800, Jul. 2009.

[81] J. Hagerty, F. Helmbrecht, W. McCalpin, R. Zane, and Z. Popovic, "Recycling ambient microwave energy with broad-band rectenna arrays," *IEEE Trans. Microw. Theory Tech.*, vol. 52, no. 3, pp. 1014–1024, Mar. 2004.

[82] A. Collado and A. Georgiadis, "Conformal hybrid solar and electromagnetic (EM) energy harvesting rectenna," *IEEE Trans. Circuits Syst. I, Reg. Papers*, vol. 60, no. 8, pp. 2225–2234, Aug. 2013.

[83] T. Wu, R. Li, and M. Tentzeris, "A scalable solar antenna for autonomous integrated wireless sensor nodes," *IEEE Antennas Wireless Propag. Lett.*, vol. 10, pp. 510–513, 2011.

[84] A. Sample, J. Braun, A. Parks, and J. Smith, "Photovoltaic enhanced UHF RFID tag antennas for dual purpose energy harvesting," in *Proc. IEEE Int. Con. RFID*, Apr. 2011, pp. 146–153.

[85] F. Alimenti *et al.*, "A new contactless assembly method for paper substrate antennas and UHF RFID chips," *IEEE Trans. Microw. Theory Tech.*, vol. 59, no. 3, pp. 627–637, Mar. 2011.

[86] W. Pachler *et al.*, "A silver ink-jet printed UHF booster antenna on flexible substratum with magnetically coupled RFID die on-chip antenna," in *Proc. 7th Eur. Conf. Antennas Propag.*, Apr. 2013, pp. 1730–1733.

[87] M. Virili, H. Rogier, F. Alimenti, P. Mezzanotte, and L. Roselli, "Wearable textile antenna magnetically coupled to flexible active electronic circuits," *IEEE Antennas Wireless Propag. Lett.*, vol. 13, pp. 209–212, 2014.

[88] H.-J. Yoo, "Your heart on your sleeve: Advances in textile-based electronics are weaving computers right into the clothes we wear," *IEEE Solid-State Circuits Mag.*, vol. 5, no. 1, pp. 59–70, Mar. 2013.

[89] X. Jingtian *et al.*, "Low-cost low-power UHF RFID tag with on-chip antenna," *J. Semicond.*, vol. 30, no. 7, pp. 075012/1–075012/6, Jul. 2009.

[90] M. Law, A. Bermak, and H. Luong, "A sub-μW embedded CMOS temperature sensor for RFID food monitoring application," *IEEE J. Solid-State Circuits*, vol. 45, no. 6, pp. 1246–1255, Jun. 2010.

[91] Alien Technology Corporation, "Fluidic self assembly," White Paper, 1999. [Online]. Available: http://www.alientechnology.com

[92] C. Hertleer, H. Rogier, L. Vallozzi, and L. V. Langenhove, "A textile antenna for off-body communication integrated into protective clothing for firefighters," *IEEE Trans. Antennas Propag.*, vol. 57, no. 4, pp. 919–925, Apr. 2009.

[93] X. Li, J. Liao, Y. Yuan, and D. Yu, "Eye-shaped segmented reader antenna for near-field UHF RFID applications," *Progr. Electromagn. Res.*, vol. 114, pp. 481–493, 2011.

[94] J.-J. Tiang, M. Islam, N. Misran, and J. S. Mandeep, "Circular microstrip slot antenna for dual-frequency RFID application," *Progr. Electromagn. Res.*, vol. 120, pp. 499–512, 2011.

[95] Y. Amin, Q. Chen, H. Tenhunen, and L.-R. Zheng, "Performance-optimized quadrate bowtie RFID antennas for cost-effective and eco-friendly industrial applications," *Progr. Electromagn. Res.*, vol. 126, pp. 49–64, 2012.

[96] Y. Amin, Q. Chen, L.-R. Zheng, and H. Tenhunen, "Development and analysis of flexible UHF RFID antennas for "green" electronics," *Progr. Electromagn. Res.*, vol. 130, pp. 1–15, 2012.

[97] F. Viani, M. Salucci, G. Olivieri, F. Robol, and A. Massa, "Design of UHF RFID/GPS fractal antenna for logistic management," *J. Electromagn. Waves Appl.*, vol. 26, no. 4, pp. 480–492, 2012.

[98] A. Springer, R. Weigel, A. Pohl, and F. Seifert, "Wireless identification and sensing using surface acoustic wave devices," *Mechatronics*, vol. 9, no. 7, pp. 745–756, Oct. 1999.

[99] K. Chang, Y. Kim, Y. Kim, and Y. Yoon, "Functional antenna integrated with relative humidity sensor using synthetised polymide for passive RFID sensing," *Electron. Lett.*, vol. 43, no. 5, pp. 1918–1923, May 2007.

[100] S. Shrestha, M. Balachandran, M. Agarwal, V. Phoha, and K. Varahramyan, "A chipless RFID sensor system for cyber centric monitoring applications," *IEEE Trans. Microw. Theory Tech.*, vol. 57, no. 5, pp. 1303–1309, May 2009.

[101] C. Occhiuzzi, S. Cippitelli, and G. Marrocco, "Modeling, design and experimentation of wearable RFID sensor tag," *IEEE Trans. Antennas Propag.*, vol. 58, no. 8, pp. 2490–2498, Aug. 2010.

[102] A. Ramos, A. Lazaro, D. Girbau, and R. Villarino, "Time-domain measurement of time-coded UWB chipless RFID tags," *Progr. Electromagn. Res.*, vol. 116, pp. 313–331, 2011.

[103] R. Nair, E. Perret, and S. Tedjini, "Temporal multi-frequency encoding technique for chipless RFID applications," in *IEEE MTT-S Int. Microw. Symp. Dig.*, Montreal, QC, Canada, Jun. 2012, DOI: 10.1109/MWSYM.2012.6259483.

[104] R. Bhattacharyya, C. Floerkemeier, and S. Sarma, "Low-cost, ubiquitous RFID-tag-antenna-based sensing," *Proc. IEEE*, vol. 98, no. 9, pp. 1593–1600, Sep. 2010.

[105] R. Potyrailo *et al.*, "Development of radio-frequency identification sensors based on organic electronic sensing materials for selective detection of toxic vapors," *J. Appl. Phys.*, vol. 106, no. 12, pp. 124 902–124 902-6, Dec. 2009.

[106] V. Viikari and H. Seppa, "RFID MEMS sensor concept based on intermodulation distortion," *IEEE Sensor J.*, vol. 9, no. 12, pp. 1918–1923, Dec. 2009.

[107] J. Riley *et al.*, "Tracking bees with harmonic radar," *Nature*, vol. 379, pp. 29–30, Jan. 1996.

[108] S. Helbing *et al.*, "Design and verification of a novel crossed dipole structure for quasi-optical frequency doublers," *IEEE Microw. Guided Wave Lett.*, vol. 10, no. 3, pp. 105–107, Mar. 2000.

[109] F. Alimenti and L. Roselli, "Theory of zero-power RFID sensors based on harmonic generation and orthogonally polarized antennas," *Progr. Electromagn. Res.*, vol. 134, pp. 337–357, 2013.

[110] G. Lovei, I. Stringer, C. Devine, and M. Cartellieri, "Harmonic radar—A method using inexpensive tags to study invertebrate movement on land," *New Zealand J. Ecology*, vol. 21, no. 2, pp. 187–193, 1997.

[111] B. Colpitts and G. Boiteau, "Harmonic radar transceiver design: Miniature tags for insect tracking," *IEEE Trans. Antennas Propag.*, vol. 52, no. 11, pp. 2825–2832, Nov. 2004.

[112] G. Orecchini *et al.*, "Green technologies and RFID: Present and future," *Appl. Comput. Electromagn. Soc. J.*, vol. 25, no. 3, pp. 230–238, Mar. 2010.

[113] S. Steudel *et al.*, "Comparison of organic diode structures regarding high-frequency rectification behavior in radio-frequency identification tags," *J. Appl. Phy.*, vol. 99, no. 11, Jun. 2006, 114519.

[114] L. Valentini and J. Kenny, "Novel approaches to developing carbon nanotube based polymer composites: Fundamental studies and nanotech applications," *Polymer*, vol. 46, no. 17, pp. 6715–6718, Aug. 2005.

[115] V. Marinov *et al.*, "Direct-write vapor sensors on FR4 plastic substrates," *IEEE Sensor J.*, vol. 7, no. 6, pp. 937–944, Jun. 2007.

[116] T. Unander and H.-E. Nilsson, "Characterization of printed moisture sensors in packaging surveillance applications," *IEEE Sensor J.*, vol. 9, no. 8, pp. 922–928, Aug. 2009.

[117] S. Couderc, B. Kim, and T. Someya, "Cellulose-based composite as a raw material for flexible ANS ultra-lightweight mechanical switch devices," in *Proc. IEEE 22nd Int. Conf. Micro Electro Mech. Syst.*, Sorrento, Italy, Jan. 2009, pp. 646–649.

[118] P. F. Goldsmith, "Quasioptics in millimeterwave systems," in *Proc. 12th Eur. Microw. Conf.*, Sep. 1982, pp. 16–24.

[119] P. Goldsmith, "Quasi-optical techniques," *Proc. IEEE*, vol. 80, no. 11, pp. 1729–1747, Nov. 1992.

[120] P. F. Goldsmith, *Quasioptical Systems*. New York, NY, USA: IEEE Press, 1998.

[121] T. Djerafi, K. Wu, and S. Tatu, "3 dB 90° hybrid quasi-optical coupler with air field slab in SIW technology," *IEEE Microw. Wireless Compon. Lett.*, vol. 24, no. 4, pp. 221–223, Apr. 2014.

[122] A. Gonzalez, Y. Fujii, K. Kaneko, and Y. Uzawa, "Quasi-optical attenuators for alma band 10 receiver," in *Proc. Asia-Pacific Microw. Conf. Proc.*, Dec. 2011, pp. 1977–1980.

[123] K. Song, F. Zhang, S. Hu, and Y. Fan, "Millimeter-wave-wave quasi-optical low-loss power combiner based on dipole antenna," *Electron. Lett.*, vol. 49, no. 18, pp. 1160–1162, Aug. 2013.

[124] S. Kawasaki and T. Itoh, "Quasi-optical planar arrays with fets and slots," *IEEE Trans. Microw. Theory Tech.*, vol. 41, no. 10, pp. 1838–1844, Oct. 1993.

[125] S. Hollung, W. Shiroma, M. Markovic, and Z. Popovic, "A quasi-optical isolator," *IEEE Microw. Guided Wave Lett.*, vol. 6, no. 5, pp. 205–206, May 1996.

[126] N. Gagnon and J. Shaker, "Accurate phase measurement of passive non-reciprocal quasi-optical components," *IEE Proc.—Microw. Antennas Propag.*, vol. 152, no. 2, pp. 111–116, Apr. 2005.

[127] R. Dickie, R. Cahill, V. Fusco, H. Gamble, and N. Mitchell, "THz frequency selective surface filters for earth observation remote sensing instruments," *IEEE Trans. Terahertz Sci. Technol.*, vol. 1, no. 2, pp. 450–461, Nov. 2011.

[128] M. Euler and V. Fusco, "Quasi optical circulator X-band scale model utilizing a circular polarization frequency selective surface," in *Proc. 4th Eur. Conf. Antennas Propag.*, Apr. 2010, pp. 1–4.

[129] W. Shiroma, S. Bundy, S. Hollung, B. Bauernfeind, and Z. Popovic, "Cascaded active and passive quasi-optical grids," *IEEE Trans. Microw. Theory Tech.*, vol. 43, no. 12, pp. 2904–2909, Dec. 1995.

[130] J. Birkeland and T. Itoh, "A 16 element quasi-optical fet oscillator power combining array with external injection locking," *IEEE Trans. Microw. Theory Tech.*, vol. 40, no. 3, pp. 475–481, Mar. 1992.

[131] M. Forman, T. Marshall, and Z. Popovic, "Two Ka-band quasi-optical amplifier arrays," in *IEEE MTT-S Int. Microw. Symp. Dig.*, Jun. 1999, vol. 4, pp. 1829–1832.

[132] S. Hollung, A. Cox, and Z. Popovic, "A bi-directional quasi-optical lens amplifier," *IEEE Trans. Microw. Theory Tech.*, vol. 45, no. 12, pp. 2352–2357, Dec. 1997.

[133] J. Hacker, R. Weikle, M. Kim, P. De Lisio, and D. Rutledge, "A 100-element planar Schottky diode grid mixer," *IEEE Trans. Microw. Theory Tech.*, vol. 40, no. 3, pp. 557–562, Mar. 1992.

[134] G. Chattopadhyay, D. Miller, H. LeDuc, and J. Zmuidzinas, "A dual-polarized quasi-optical SIS mixer at 550 GHz," *IEEE Trans. Microw. Theory Tech.*, vol. 48, no. 10, pp. 1680–1686, Oct. 2000.

[135] V. Bezborodov, V. Kiseliov, Y. Kuleshov, and M. Yanovsky, "A terahertz quasi-optical polarization phase shifter with the crystal quartz phase sections," in *Proc. 5th Int. Kharkov Symp. Phys. Eng. Microw. Millimeter Submillimeter Waves*, Jun. 2004, vol. 2, pp. 603–605.

[136] G. Denisov *et al.*, "Fast quasi-optical phase shifter based on induced photoconductivity in silicon," in *Proc. Joint 32nd Int. Conf. Infrared Millimeter Waves/15th Int. Conf. Terahertz Electron.*, Sep. 2007, pp. 795–796.

[137] N. Camilleri, "A quasi-optical multiplying slot array," *IEEE Trans. Microw. Theory Tech.*, vol. 33, no. 11, pp. 1189–1195, Nov. 1985.

[138] A. Moussessian *et al.*, "A terahertz grid frequency doubler," *IEEE Trans. Microw. Theory Tech.*, vol. 46, no. 11, pp. 1976–1981, Nov. 1998.

[139] M. Cryan *et al.*, "Simulation and measurement of quasi-optical multipliers," *IEEE Trans. Microw. Theory Tech.*, vol. 49, no. 3, pp. 451–464, Mar. 2001.

[140] F. Jiang *et al.*, "High-speed monolithic millimeter-wave switch array," *IEEE Microw. Guided Wave Lett.*, vol. 8, no. 3, pp. 112–114, Mar. 1998.

[141] F. Alimenti *et al.*, "Crossed dipole frequency doubling RFID TAG based on paper substrate and ink-jet printing technology," in *Proc. IEEE MTT-S Int. Microw. Symp. Dig.*, May 2010, pp. 840–842.

[142] M. Virili *et al.*, "7.5–15 MHz organic frequency doubler made with pentacene-based diode and paper substrate," in *IEEE MTT-S Int. Microw. Symp. Dig.*, Tampa, FL, USA, Jun. 2014, DOI: 10.1109/MWSYM.2014.6848395.

[143] L. Roselli *et al.*, "Feasibility study of a fully organic frequency doubler for harmonic RFID applications," in *Proc. IEEE 12th Top. Meeting Silicon Monolithic Integr. Circuits RF Syst.*, Jan. 2012, pp. 203–206.

[144] R. Gonalves *et al.*, "Smart floor: Indoor navigation based on RFID," in *Proc. IEEE Wireless Power Transfer*, May 2013, pp. 103–106.

[145] G. Orecchini, L. Yang, M. Tentzeris, and L. Roselli, "Wearable battery-free active paper printed RFID tag with human-energy scavenger," in *IEEE MTT-S Int. Microw. Symp. Dig.*, Jun. 2011, DOI: 10.1109/MWSYM.2011.5973290.

[146] C.-R. Yu, C.-L. Wu, C.-H. Lu, and L.-C. Fu, "Human localization via multi-cameras and floor sensors in smart home," in *Proc. IEEE Int. Conf. Syst. Man Cybern.*, Oct. 2006, vol. 5, pp. 3822–3827.

[147] S. Chang, S. Ham, S. Kim, D. Suh, and H. Kim, "Ubi-floor: Design and pilot implementation of an interactive floor system," in *Proc. 2nd Int. Conf. Intell. Human-Mach. Syst. Cybern.*, Aug. 2010, vol. 2, pp. 290–293.

[148] J. Morgado and A. Konig, "Low-power concept and prototype of distributed resistive pressure sensor array for smart floor and surfaces in intelligent environments," in *Proc. 9th Int. Multi-Conf. Syst. Signals Devices*, Mar. 2012, DOI: 10.1109/SSD.2012.6198020.

[149] J. Zhao and Y. Wang, "Autonomous ultrasonic indoor tracking system," in *Proc. Int. Symp. Parallel Distrib. Process. Appl.*, Dec. 2008, pp. 532–539.

[150] R. Imura, "The role of networked RFID for driving the ubiquitous," in *Proc. IEEE Conf. Emerging Technol. Factory Autom.*, Sep. 2006, pp. 1115–1118.

[151] Y. Tan, K. Y. Hoe, and S. Panda, "Energy harvesting using piezoelectric igniter for self-powered radio frequency (RF) wireless sensors," in *Proc. IEEE Int. Conf. Ind. Technol.*, Dec. 2006, pp. 1711–1716.

[152] Linx Technologies, "KH2 series transmitter/encoder data guide." [Online]. Available: https://www.linxtechnologies.com/resources/data-guides/txe-xxx-kh2.pdf

[153] D. Smith, D. Miniutti, T. Lamahewa, and L. Hanlen, "Propagation models for body-area networks: A survey and new outlook," *IEEE Antennas Propag. Mag.*, vol. 55, no. 5, pp. 97–117, Oct. 2013.

[154] *IEEE Standard for Local and Metropolitan Area Networks—Part 15.6: Wireless Body Area Networks*, IEEE Std. 802.15.6-2012, Feb. 2012.

[155] J. Thomas and M. Qidwai, "The design and application of multifunctional structure-battery materials systems," *JOM*, vol. 57, no. 3, pp. 18–24, Mar. 2005.

[156] A. Bonfiglio and D. De Rossi, *Wearable Monitoring Systems*. New York, NY, USA: Springer-Verlag, 2011.

[157] S. Lee and B. Youn, "A design and experimental verification methodology for an energy harvester skin structure," *Smart Mater. Struct.*, vol. 20, no. 5, May 2011, DOI: 10.1088/0964-1726/20/5/057001.

[158] R. Vullers, R. van Schaijk, I. Doms, C. van Hoof, and R. Mertens, "Microwave energy harvesting," *Solid-State Electron.*, vol. 53, no. 4, pp. 684–693, Apr. 2009.

[159] P. Jaffe and J. McSpadden, "Energy conversion and transmission modules for space solar power," *Proc. IEEE*, vol. 101, no. 6, pp. 1424–1437, Jun. 2013.

[160] J. McSpadden and J. Mankins, "Space solar power programs and microwave wireless power transmission technology," *IEEE Microw. Mag.*, vol. 3, no. 4, pp. 46–57, Dec. 2002.

ABOUT THE AUTHORS

Luca Roselli (Senior Member, IEEE) was born in Florence, Italy, in 1962. He received the ''Laurea'' degree in electronic engineering from the University of Florence, Florence, Italy, in 1988.

From 1988 to 1991, he worked at the University of Florence on SAW devices. In November 1991, he joined the University of Perugia, Perugia, Italy, where he is currently working as an Associate Professor and where he has been teaching several classes on electronic devices, microwave electronics, high-frequency (HF) electronic components, and applied electronics. Since 2000, he has been coordinating research activity at the High Frequency Electronics (HFE) Laboratory. In that year, he also founded the spin-off company WiS (Wireless Solutions) Srl, operating in the field of microwave electronic systems with which he cooperated as a consultant until it joined the new company ART Srl. in 2008. From 2008 to 2012, he was the Director of the Technical and Scientific Committee of ART Srl and a member of the Board of Directors. In 2005, he founded a second spin-off company: DiES (Digital Electronic Solutions) Srl. His research interests mainly focus on the design of high-frequency electronic circuits and systems, including the development of numerical methods for electronic circuit analysis with special attention to RFID–NFC systems, new materials (including organic and recyclable ones), and far-field wireless power transfer. In these fields, he published more than 220 contributions in international reviews and peer-reviewed conferences, the interest in which is testified by an HF index of 20 (source Google Scholar) and more than 1350 citations.

Mr. Roselli was the Chairman of the VII Computational Electromagnetic in Time Domain Workshop in 2007. In 2013, he was the Chairman of the First IEEE Wireless Power Transfer Conference (WPTC). Currently, he is member of the list of experts of Italian Ministry of Research and University (MIUR); member of several IEEE Technical Committees [MTT-24 RFID Technologies (past chair), MTT-25 RF nanotechnolgies, MTT-26 Wireless Power Transfer]; member of the Sub Committee 32 RFID Technologies of International Microwave Symposium (IMS) (past chair); member of the European Research Council (ERC) Panel PE7; member of the Advisory Committee of IEEE WPTC. He is involved in the boards of several international conference (RWCOM, RFID-TA, EuCAP, MAREW). He is a reviewer for many international conferences and journals (the PROCEEDINGS OF THE IEEE, the IEEE TRANSACTIONS ON MICROWAVE THEORY AND TECHNIQUES, IEEE MICROWAVE AND WIRELESS COMPONENTS LETTERS, *ACES Journal*, *Radioengineering Journal*, Hindawi publishing corporation, *Elsevier Organic Electronics*, *ASP Nanoscience and Nanotechnology Letters*).

Nuno Borges Carvalho (Senior Member, IEEE) was born in Luanda, Angola, in 1972. He received the Diploma and Doctoral degrees in electronics and telecommunications engineering from the University of Aveiro, Aveiro, Portugal, in 1995 and 2000, respectively.

He is a Full Professor at the Universidade de Aveiro, Aveiro, Portugal and a Senior Research Scientist with the Instituto de Telecomunicações (IT), Universidade de Aveiro, where he coordinates the wireless communication thematic area and the Radio Systems Group. He coauthored *Intermodulation in Microwave and Wireless Circuits* (Reading, MA, USA: Artech House, 2003) and *Microwave and Wireless Measurement Techniques* (Cambridge, U.K.: Cambridge Univ. Press, 2013). He has been a reviewer and author of over 200 papers in magazines and conferences. He coholds four patents. His main research interests include software-defined radio front-ends, wireless power transmission, nonlinear distortion analysis in microwave/wireless circuits and systems, and measurement of nonlinear phenomena. He has recently been involved in the design of dedicated radios and systems for newly emerging wireless technologies.

Dr. Borges Carvalho is the Chair of the IEEE MTT-11 Technical Committee. He is a member of IEEE MTT-20, MTT-24, and MTT-26 and the IEEE Portugal Section Chair. He is an Associate Editor for the IEEE TRANSACTIONS ON MICROWAVE THEORY AND TECHNIQUES, IEEE MICROWAVE MAGAZINE, *Cambridge Journal on Wireless Power Transmission* and the Chair of the URSI–Portugal Metrology Group.

Federico Alimenti (Senior Member, IEEE) was born in Foligno, Italy, in 1968. He received the Laurea degree (*magna cum laude*) and the Ph.D. degree from the University of Perugia, Perugia, Italy, in 1993 and 1997 respectively, both in electronic engineering.

In 1993, he held an internship at Daimler-Benz Aerospace, Ulm, Germany. In 1996, he was recipient of the URSI young scientist award and visiting scientist at the Technical University of Munich, Munich, Germany. Since 2001, he has been with the Department of Engineering, University of Perugia, as an Aggregate Professor, teaching the class of microwave electronics. Between 2006 and 2010, he was a member of the Academic Senate in the same university. He authored more than 150 papers in refereed journals and conference proceedings. He coauthored several book chapters and a European patent (EP13161946.2) on zero-power wireless sensors. His scientific interests concern the design and the experimental characterization of radio-frequency (RF)-integrated circuits in complementary metal–oxide–semiconductor (CMOS) and BiCMOS technologies.

Prof. Alimenti was a recipient of the IET Premium (Best Paper) Award in 2013 and was the Technical Program Committee (TPC) Chair of the IEEE Wireless Power Transfer (WPT) Conference. He has been a local coordinator of the ARTEMOS project, ENIAC, call 3, 2010. His H-index is equal to 14 (source: Google Scholar).

Paolo Mezzanotte (Member, IEEE) was born in Perugia, Italy, in 1965. He received the Ph.D. degree in electrical engineering from the University of Perugia, Perugia, Italy, in 1997.

Since 1992, he has been involved with FDTD analysis of microwave structures in cooperation with the Department of Electronic and Information Engineering (DIEI), University of Perugia. In 1999, he was appointed Research Associate. Since January 2007, he has been an Associate Professor with the same university, teaching the classes on radio-frequency engineering. His research activities concern numerical methods and computer-aided design (CAD) techniques for passive microwave structures and the analysis and design of microwave and millimeter-wave circuits. More recently his research interests have mainly focused on the study of advanced technologies such as LTCC, RF-MEMS, and microwave circuits printed on green substrates. These research activities are testified by more than 100 publications in the most important specialized journals and at the main conferences of the microwave scientific community.

Prof. Mezzanotte serves as a Reviewer of a number of IEEE journals and belongs to the Top Amplifier Research Group in a European Team (TARGET) and to the Advanced MEMS for RF and Millimeterwave Communications (AMICOM) Networks of Excellence. He is a member of the IMS Technical Program Review Committee and of the Technical Committee MTT-24 RFID Technologies. He serves as an Associate Editor of the *ACES Journal*. He was the Co-Chairman of the Seventh International Workshop on Computational Electromagnetics in Time Domain (CEM–TD 2007). His present H-index (ISI journals) is equal to 13.

Giulia Orecchini received the Laurea degree in electronic engineering and the Ph.D. degree in electronic and information engineering from the University of Perugia, Perugia, Italy, in 2008 and 2012, respectively.

During her Ph.D. studies she joined the ATHENA Research Group, Georgia Institute of Technology, Atlanta, GA, USA. Her research interests concern the development of radio-frequency identification (RFID) electronic systems and technologies. She is currently working as a Research Assistant at the University of Perugia.

Marco Virili (Student Member, IEEE) was born in Terni, Italy, in 1983. He received the Laurea degree in electronic engineering from the University of Perugia, Perugia, Italy, in 2009, where he is currently working toward the Ph.D. degree at the Department of Engineering.

His scientific interests concern the design and the experimental validation of radio-frequency (RF) and microwave circuits. He has a strong experience in using the main electromagnetic computer-aided design (CAD) tools for characterization and design of microwave devices. He is focused on chipless radio-frequency identification (RFID) tags and green electronics.

Chiara Mariotti (Student Member, IEEE) was born in Assisi, Italy, in 1987. She received the Laurea degree (*magna cum laude*) in electronic and telecommunication engineering from the University of Perugia, Perugia, Italy, in 2011, where she is currently working toward the Ph.D. degree at the High Frequency Electronics (HFE) Laboratory, working on green technologies for passive and energetically autonomous radio-frequency identification (RFID) tags.

In Spring 2012, she joined the ATHENA Research Group, Georgia Institute of Technology, Atlanta, GA, USA, for six months, working on eco-compatible indoor localization systems and other types of sensors fabricated by means of inkjet printing technology. At the end of 2013, she again joined the ATHENA Research Group for six months to work on multilayer inkjet printed systems and devices such as passives and microfluidics sensors.

Ricardo Gonçalves (Student Member, IEEE) was born in Lisbon, Portugal, in 1988. He received the B.Sc. and M.Sc. (*magna cum laude*) degrees in electronics and telecommunications engineering from the Instituto Superior de Engenharia de Lisboa, Lisbon, Portugal, in 2010 and 2012, respectively. He is currently working toward the Ph.D. degree in electrical engineering at the University of Aveiro, Aveiro, Portugal.

He is a Researcher at the Instituto de Telecomunicações, Aveiro, Portugal. In 2011, he was awarded with merit scholarship for exceptional academic performances. From 2010 to 2012, he worked at Dailywork I&D as a Developer Engineer in Embedded Electronic Systems for Vehicular Location Systems and Healthcare Platforms. His main research interests include wireless power transfer systems, radio-frequency identification (RFID), and wireless passive sensor networks. His current focus is on the development of printed antennas and microwave circuits in nonconventional materials such as textiles, ceramics, plastic, paper, and cork, for the former applications.

Pedro Pinho (Member, IEEE) was born in Vale de Cambra, Portugal, in 1974. He received the Licenciado and M.S. degrees in electrical and telecommunications engineering and the Ph.D. degree in electrical engineering from the University of Aveiro, Aveiro, Portugal, in 1995 and 2000, respectively. from the University of Aveiro, Aveiro, Portugal, in 1997, 2000, and 2004, respectively.

He is currently a Professor Adjunto at the Department of Electrical Telecommunications and Computers Engineering, Instituto Superior de Engenharia de Lisboa, Instituto Politécnico de Lisboa, Lisbon, Portugal, and a Member of the Research Staff at the Institute for Telecommunications, Aveiro, Portugal (since 1997). He authored or coauthored more than 90 papers in conferences and international journals and four book chapters. His current research interest is in antennas for location systems, reconfigurable antennas, and antenna design for passive sensors in nonconventional materials.

RFID READER DETECTOR AND TILT-SENSITIVE RFID TAG

Technology (/technology/) > Science | by nmarquardt (/member/nmarquardt/) Follow

Posted Nov. 10, 2008 |

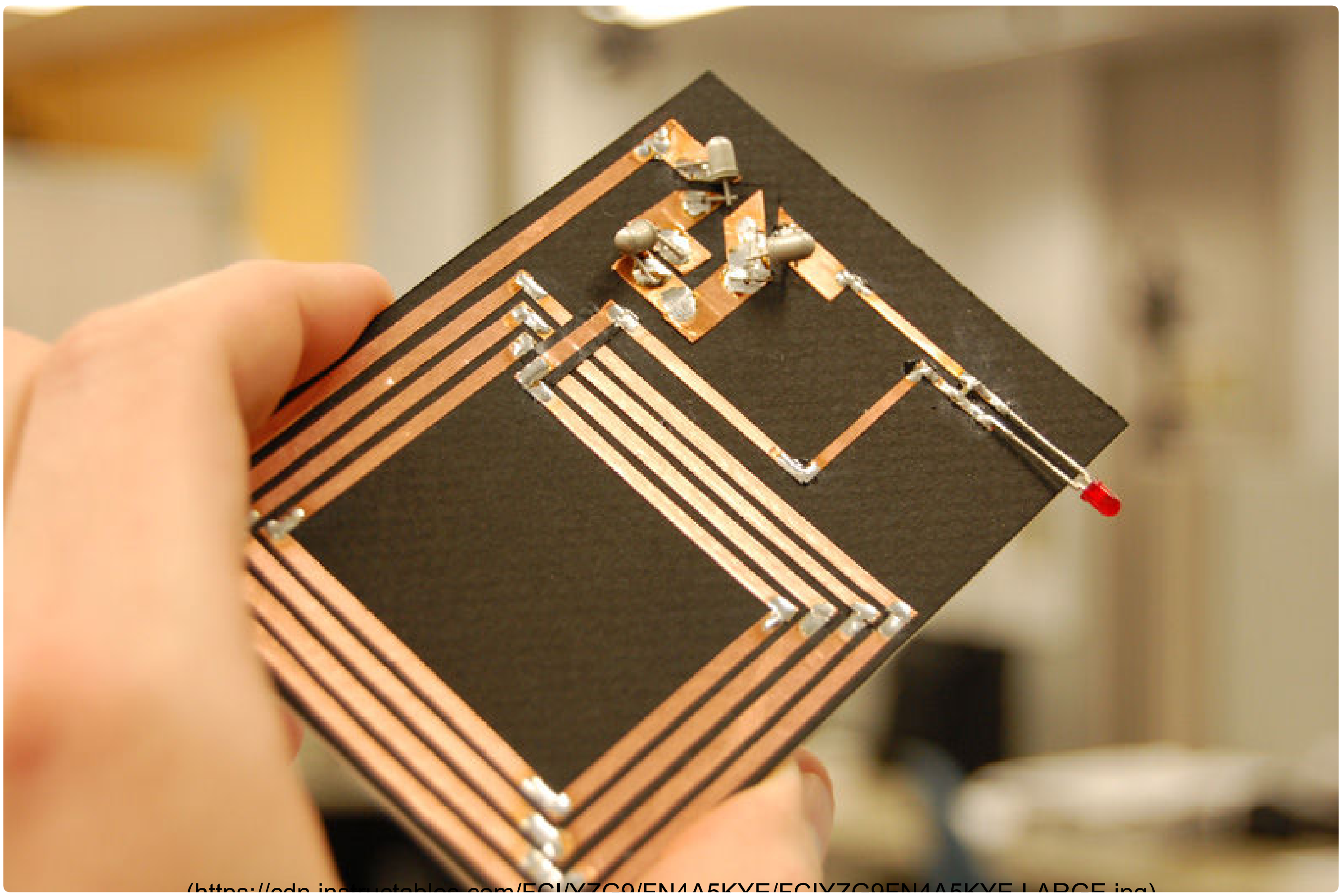

(https://cdn.instructables.com/FCIYZC9/FN4A5KYE/FCIYZC9FN4A5KYE.LARGE.jpg)

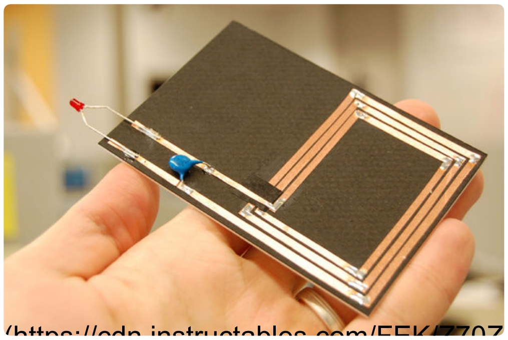  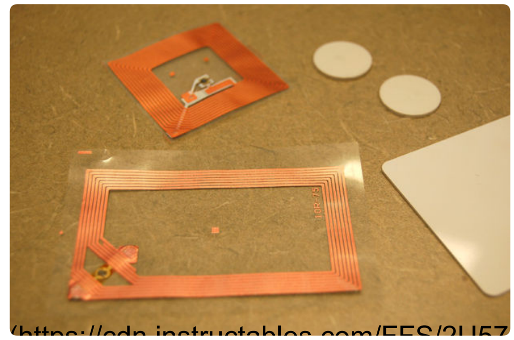

The 'rub' (http://www.usingenglish.com/reference/idioms/there%27s+the+rub.html)
Want to detect the presence of RFID readers? Want to control when a RFID tag is active or readable? We describe how to do both using bits of copper and card, and some readily available electronics hardware.

Longer preamble
Radio frequency identification (RFID (http://en.wikipedia.org/wiki/RFID)) is rapidly growing in popularity. RFID *tags* are found everywhere. They're attached to container freight, in those funny-looking white labels you find in newly purchased books, embedded in many corporate ID cards and passports, etc. The tags have a few common properties: they transmit a unique ID number, are optimized to be 'read' from predefined distances, and are usually small so they can remain unobtrusive or hidden.

RFID *readers* are used to track nearby tags by wirelessly reading a tag's unique ID (see Figure 4); a tag simply has to be brought into physical proximity with a reader to be read. Readers are mostly used for industrial or commercial purposes, e.g. asset tracking or electronic payment. Wal-mart use RFID tags and readers in their supply chain. The technology is also used in mass transit systems in cities like London (http://en.wikipedia.org/wiki/Oyster_card) and Hong Kong (http://en.wikipedia.org/wiki/Octopus_card). In Japan, many mobile phones incorporate readers to enable e-money payments in shops and vending machines.

For those of us who want to experiment with RFID, the problem is that the technology is almost always □black boxed (http://en.wikipedia.org/wiki/Black_box).

That is, the inner workings of a tag and its interaction with a reader is hidden from view, and thus difficult to have much control over.

In the two exercises that follow (building a RFID reader detector (https://www.instructables.com/id/SX28QZ1FN4H8QCG/) and a tilt-sensitive RFID tag (https://www.instructables.com/id/SGW3J0SFN49WUIF/)), we offer an example of how you can start revealing some of the workings of RFID and thus gain some control over the technology. The two exercises also hopefully show that the technology is relatively simple and how it can be extended to support some interesting interactions. We offer some other possibilities that build on our examples at the end (https://www.instructables.com/id/SQKIRD4FN49ZUS1/).

Add Tip Ask Question

Step 1: Material and Tools

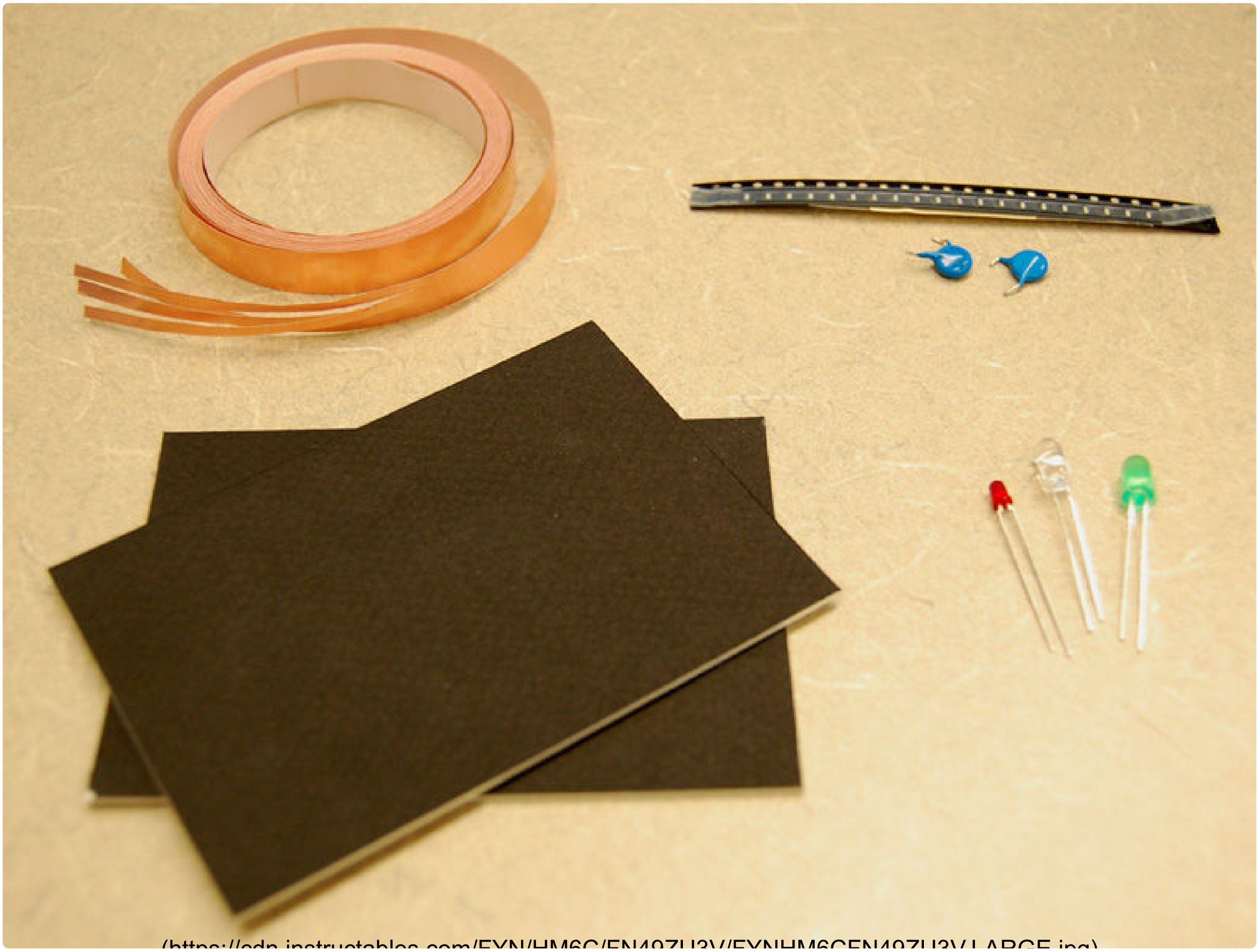

(https://cdn.instructables.com/FXN/HM6C/FN49ZU3V/FXNHM6CFN49ZU3V.LARGE.jpg)

(https://cdn.instructables.com/FIM/0KGJ/FN49ZU3U/FIM0KGJF

(https://cdn.instructables.com/F5C/CNJD/FN49ZU3T/F

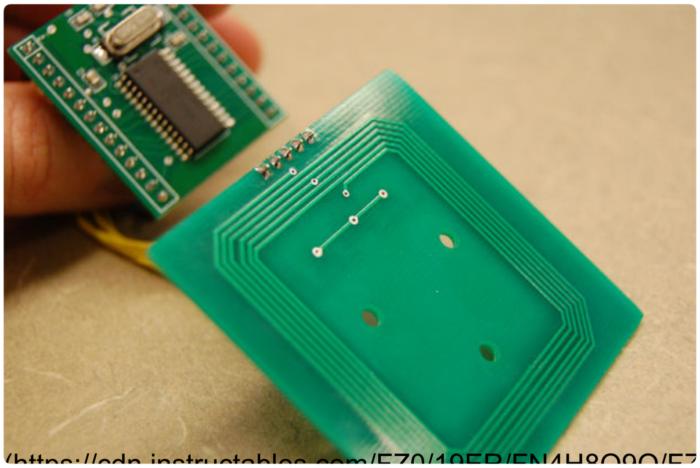

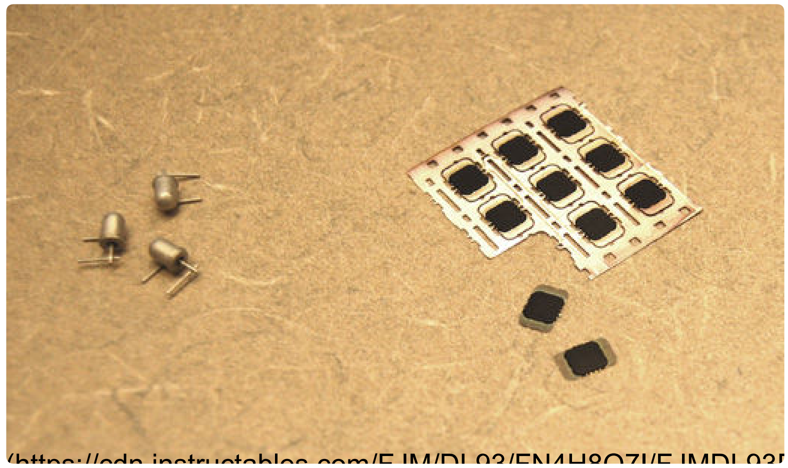

This section provides an overview of the necessary materials and tools.

Materials (see Figure 1):
We need the following material to built the basic RFID reader detector.
- Cardboard (around 100x70 mm)
- Conductive copper tape (e.g., order number 1218478 at www.farnell.com)
- Capacitor 82 pF (picofarad) (e.g., order number 1138852 at www.farnell.com)
- Low current LED (light-emitting diode) (e.g., order number 1003207at www.farnell.com)

Tools (see Figure 2 and 3):
- Craft knife and scissors
- Insulating tape (e.g., order number 1373979 at www.farnell.com)
- Soldering iron and solder

RFID reader for testing (see Figure 4):
To test our RFID tags we need an RFID reader that can operate at a frequency of 13.56 MHz.
There many readers for this widely used RFID standard, for instance the Sonmicro MIFARE USB reader (http://www.sonmicro.com/).
Note: The Phidget RFID reader does *not* work with the tags created in this project, as it uses a different frequency for communication with the tags (125 kHz).

Advanced material (see Figure 5):

The following material is necessary to build the second part of the project: the tilt-sensitive RFID tag.

- Micro tilt switches (e.g., www.digikey.com)
- RFID ICs (e.g., MIFARE Standard 1k, part no. 568-2219-1-ND at www.digikey.com)

Add Tip Ask Question

Step 2: Building the RFID Antenna

(https://cdn.instructables.com/FGI/0OXD/FN4A5N20/FGI0OXDFN4A5N20.LARGE.jpg)

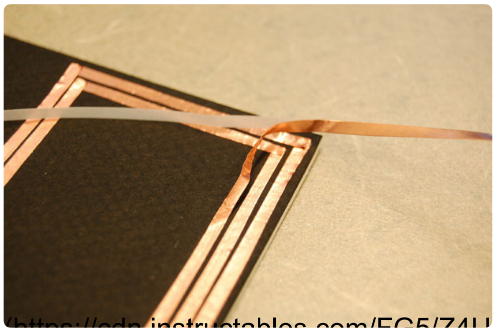

(https://cdn.instructables.com/FG5/Z4U

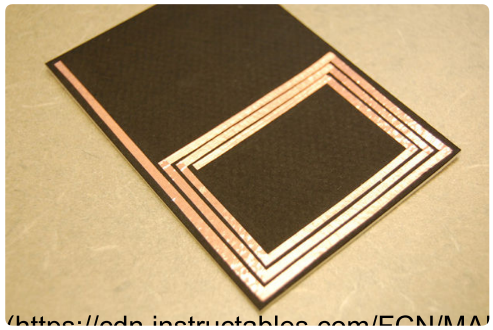

(https://cdn.instructables.com/FCN/MA

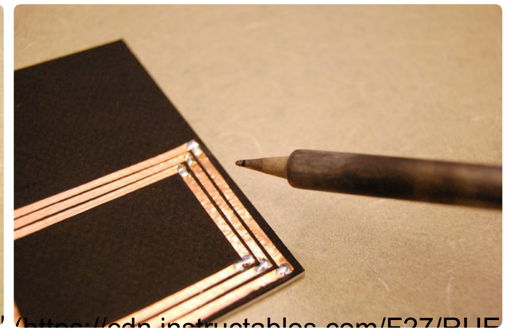

(https://cdn.instructables.com/F27/RUF

This step describes how to build the antenna for the RFID tag.

Building the RFID tag antenna

To build the tag's antenna follow these three steps.

1. Cut the conductive copper tape into thin stripes of around 2mm (see Figure 1).
2. Tape these stripes (see Figure 2) in loops around one half of the cardboard (see Figure 3 for the layout of the antenna). The tag should have between 3-4 loops for the antenna.
3. Solder all the connections between the copper tape. Sometimes, this isn't necessary as the tape's adhesive backing is conductive, but solder the connections if you want to be on the safe side.

Now we have created our RFID tag antenna, and we will add the "RFID reader detection" functionality in the following step.

A little background

RFID readers transmit an electromagnetic (EM) field with their reader antenna. This EM field induces a current in the antenna for all RFID tags within reading distance. This induced current activates the RFID chip that is connected to the tag's antenna. This chip then modulates a response (usually the unique ID number) that is transmitted back to the reader. The antenna of an RFID tag is usually a thin copper wire that is arranged in loops. The loops allow the emitted EM field of the RFID reader to induce current to the antenna of the tag.

Add Tip | Ask Question

Step 3: RFID Reader Detection

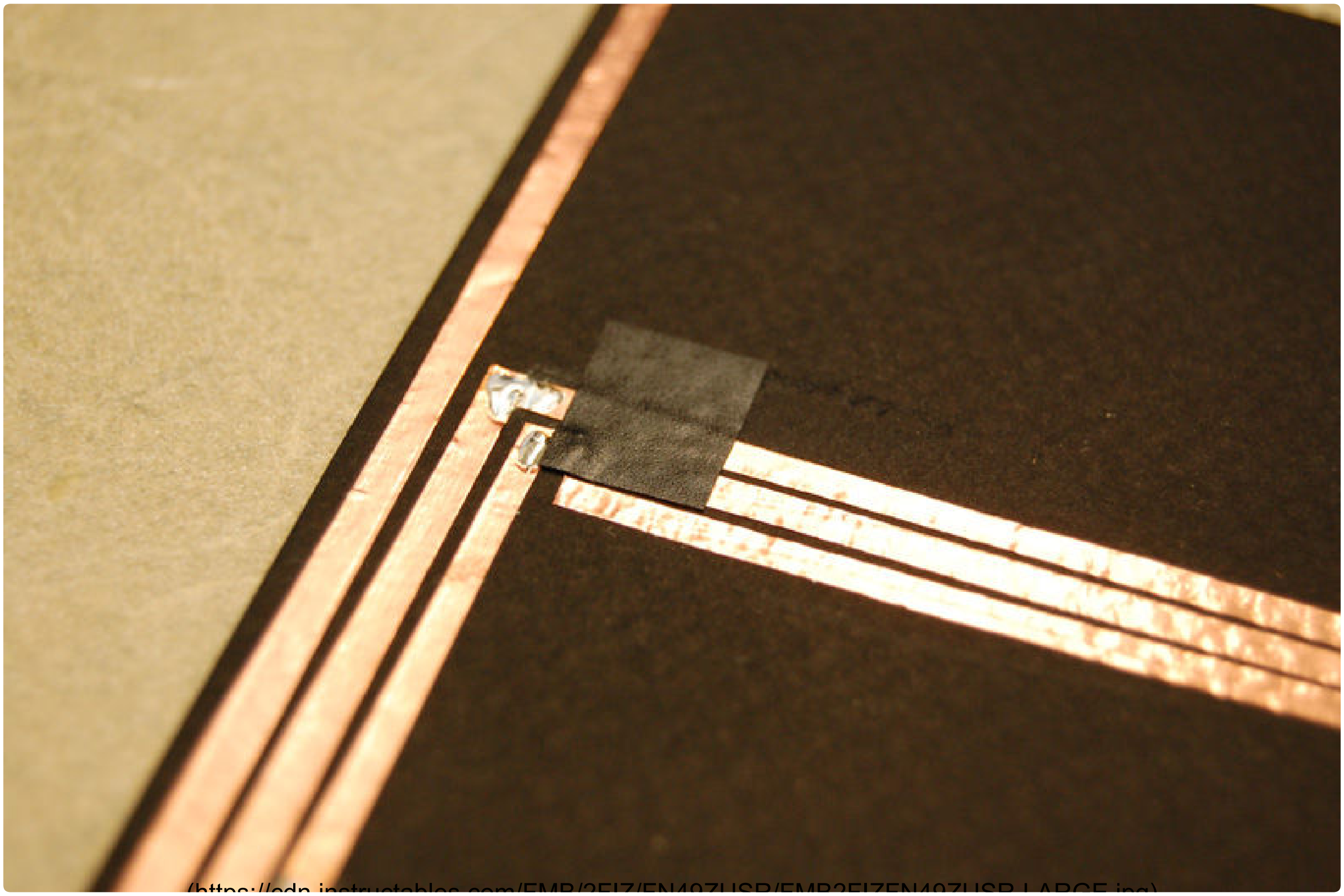
(https://cdn.instructables.com/FMR/2FIZ/FN49ZHSR/FMR2FIZFN49ZHSR.LARGE.jpg)

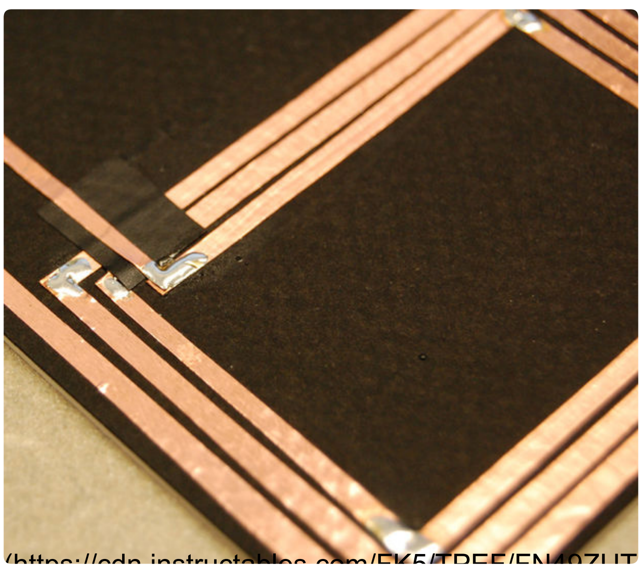
(https://cdn.instructables.com/FK5/TPFF/FN49ZHT

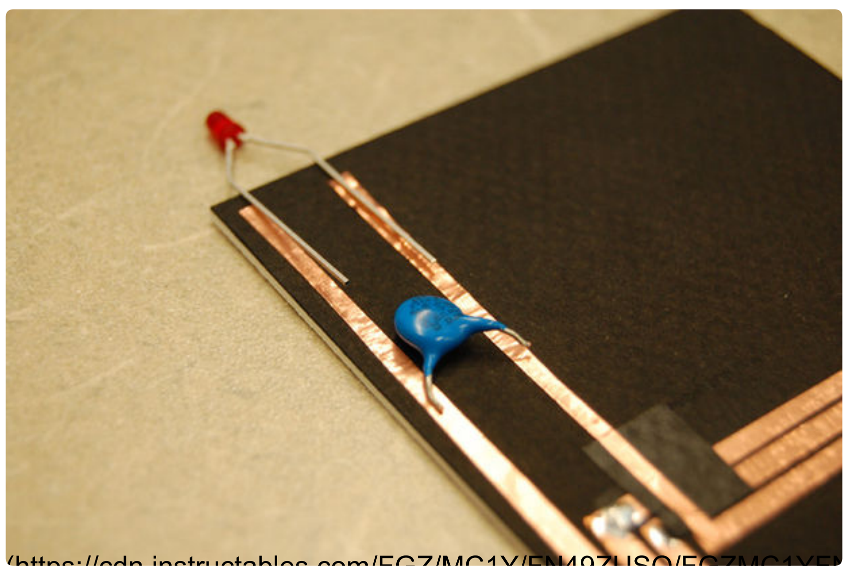
(https://cdn.instructables.com/FGZ/MC1X/FN49ZHSQ/FGZMC1XFN

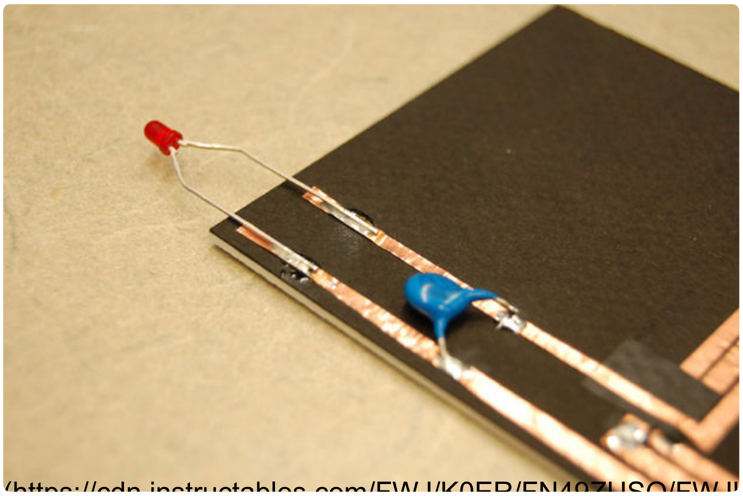
(https://cdn.instructables.com/FWJ/K0EB/FN49ZHSQ/FWJ

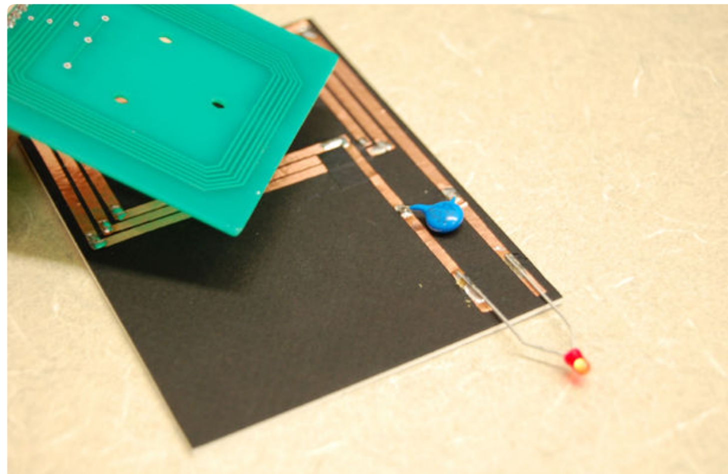
(https://cdn.instructables.com/F33/GPGW/FN49ZHSN/F33

This step describes how to add a simple mechanism to the RFID tag antenna that allows us detect nearby RFID readers.

Antenna connection

First, we add a small piece of insulation tape for the connection of the inner end of the antenna loop (as illustrated in Figure 1). This is to insulate the outer loops. Then we add another copper tape strip to the inner end of the antenna as shown in Figure 2. Here again we solder the two ends of the conductive copper tape together.

Capacitor and LED

Next, we add the capacitor (82 pF) and the low current LED to the tag as shown in Figure 3. They are connected in parallel. We also solder these two components to the copper tape (see Figure 4).

Testing

With these simple steps, our RFID reader detector is finished! By bringing our DIY RFID detector close to an RFID reader (as shown in Figure 5), the connected LED lights up. With the Sonmicro reader hardware the distance to the reader has to be below 8-10 cm; however, there are RFID readers available with a stronger EM field and therefore a higher maximum reading distance.

In the next step of the instructable we will show how to extend a basic RFID tag and make it tilt-sensitive.

Add Tip Ask Question

Step 4: Tilt-Sensitive RFID Tag

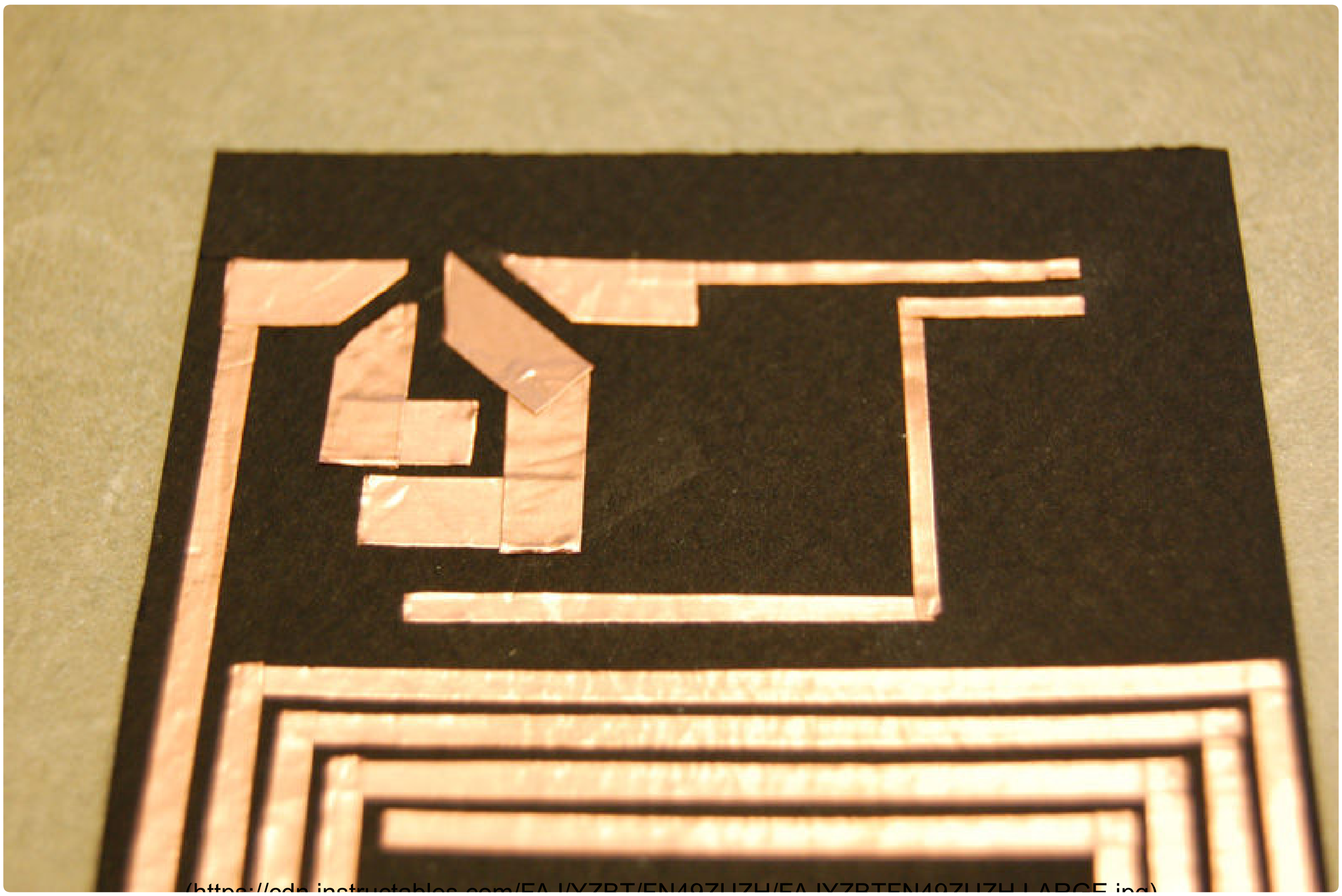

(https://cdn.instructables.com/FAJ/YZBT/FN49ZUZH/FAJYZBTFN49ZUZH.LARGE.jpg)

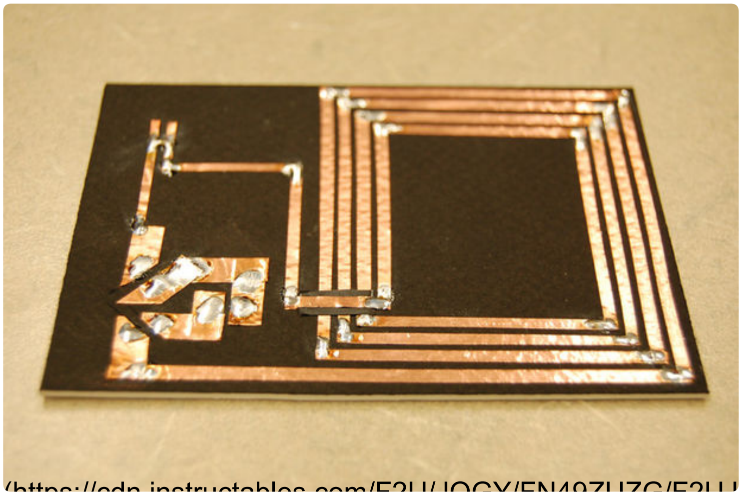
(https://cdn.instructables.com/F2U/JQGY/FN49ZUZG/F2U

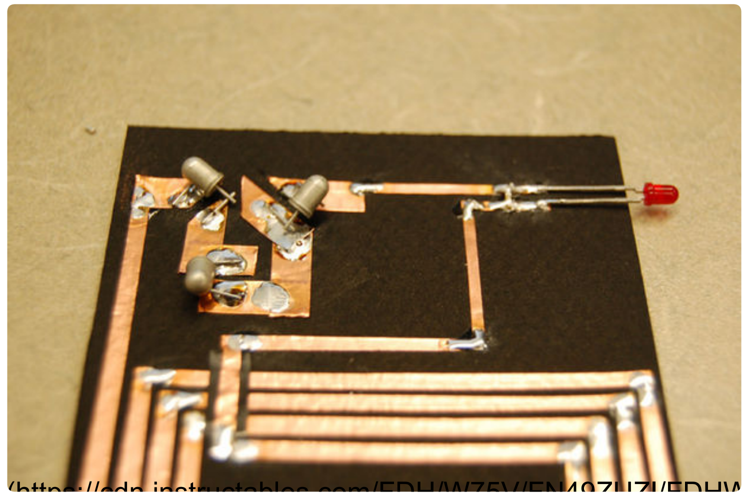
(https://cdn.instructables.com/FDH/W75V/FN49ZUZI/FDHW

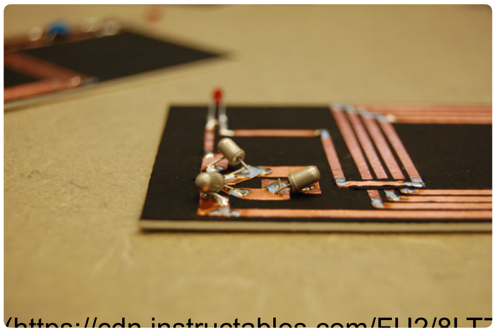
(https://cdn.instructables.com/FU2/8LT7

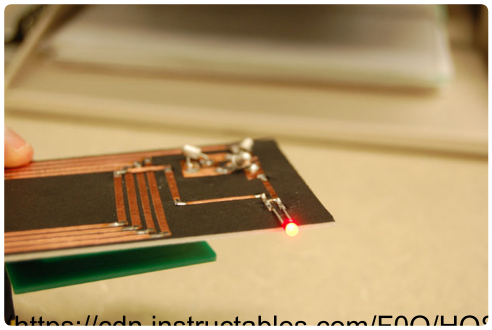
(https://cdn.instructables.com/F0Q/HQ9

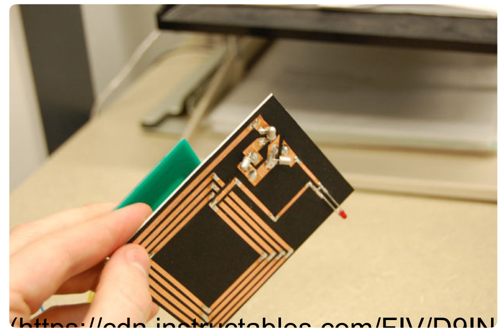
(https://cdn.instructables.com/FIV/D9IN

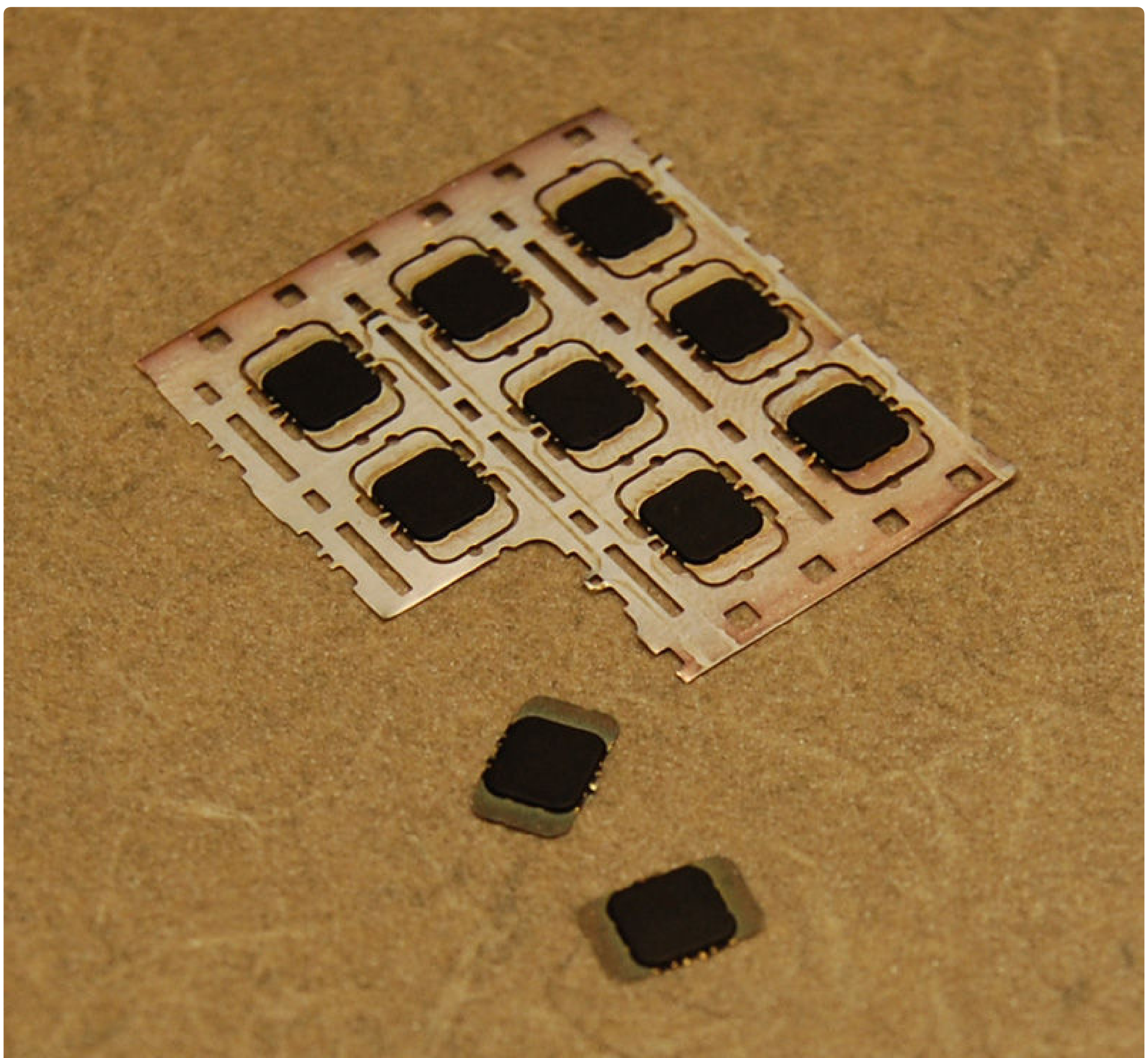
(https://cdn.instructables.com/F3Y/WGFU/FN49ZV73/F3YWGFUFN49ZV73.LARGE.jpg)

We now describe the process of how to build a tilt-sensitive RFID tag. This extends the previous exercise.

Antenna

The antenna for this second RFID tag is similar to the first antenna we built. We thus need another piece of cardboard and to repeat the steps described earlier in STEP 2 (https://www.instructables.com/id/S2YO8NWFN4H8Q8A/) of this instructable.

Tilt-sensitive tag

Next, we add additional copper tape connections to the tag, as shown in Figure 1. These connections allow us to connect three tilt switches, a capacitor, and the LED to the antenna. Again, all the connections of the copper tape are soldered together. We add the three tilt switches to the tag as shown in Figure 3. The tilt switches are soldered to the copper tape, and it is important to connect them in a slight angle (around 5-10 degrees) as shown in Figure 4. This makes sure that the silt switches are in a *closed* state while the RFID tag is in a horizontal position, and in a *open* state while the tag is in a vertical position.
Again, we also add an LED and a capacitor to the antenna as shown in Figure 3 (we use a different form factor of the capacitor here just to illustrate the alternative options).

Testing the tilt-sensitive tag

We can now use our Sonmicro RFID reader again to test our new tilt-sensitive RFID tag. The tag is activate while in a horizontal position as in Figure 5, and is inactive when in a vertical position as in Figure 6.

Using RFID chips

We can now replace the connected capacitor and LED from our tag with an RFID

MICROWAVE AND RADIO FREQUENCY ENGINEERING

INDEX

TRANSMISSION LINES

TELEGRAPHER'S EQUATIONS

$$(1)\quad \frac{\partial V}{\partial z} = -L\frac{\partial I}{\partial t} \qquad (2)\quad \frac{\partial I}{\partial z} = -C\frac{\partial V}{\partial t}$$

By taking the partial derivative with respect to z of equation 1 and partial with respect to t of equation 2, we can get:

$$(i)\quad \frac{\partial^2 V}{\partial z^2} = LC\frac{\partial^2 V}{\partial t^2} \qquad (ii)\quad \frac{\partial^2 I}{\partial z^2} = LC\frac{\partial^2 I}{\partial t^2}$$

SOLVING THE EQUATIONS

To solve the equations (i) and (ii) above, we guess that $F(u) = F(z \pm vt)$ is a solution to the equations. It is found that the unknown constant v is the wave propagation velocity.

$$\boxed{V_{total} = V_+(z - vt) + V_-(v + vt)}$$ where:

z is the position along the transmission line, where the load is at z=0 and the source is at z=-l, with l the length of the line.

v is the **velocity of propagation** $1/\sqrt{LC}$ or ω/β, the speed at which the waveform moves down the line; see p 2

t is time

THE COMPLEX WAVE EQUATION

The general solutions of equations (i) and (ii) above yield the complex wave equations for voltage and current. These are applicable when the excitation is sinusoidal and the circuit is under steady state conditions.

$$\boxed{V(z) = V^+e^{-j\beta z} + V^-e^{+j\beta z}}$$

$$\boxed{I(z) = I^+e^{-j\beta z} + I^-e^{+j\beta z}}$$

$$\boxed{I(z) = \frac{V^+e^{-j\beta z} + V^-e^{+j\beta z}}{Z_0}}$$ where:

$e^{-j\beta z}$ and $e^{+j\beta z}$ represent wave propagation in the $+z$ and $-z$ directions respectively,

$\beta = \omega\sqrt{LC} = \omega/v$ is the **phase constant,**

$Z_0 = \sqrt{L/C}$ is the **characteristic impedance** of the line. These equations represent the voltage and current **phasors**.

+/- WATCHING SIGNS

By convention z is the variable used to describe position along a transmission line with the origin z=0 set at the load so that all other points along the line are described by **negative** position values.

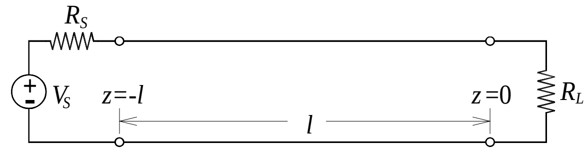

Ohm's law for right- and left-traveling disturbances:

$$V_+ = I_+Z_0 \qquad V_- = -I_-Z_0$$

v_p VELOCITY OF PROPAGATION [cm/s]

The velocity of propagation is the speed at which a wave moves down a transmission line. The velocity approaches the speed of light but may not exceed the speed of light since this is the maximum speed at which information can be transmitted. But v_p may exceed the speed of light mathematically in some calculations.

$$\boxed{v_p = \frac{1}{\sqrt{LC}} = \frac{1}{\sqrt{\varepsilon\mu}} = \frac{\omega}{\beta}}$$ where:

L = inductance per unit length [H/cm]
C = capacitance per unit length [F/cm]
ε = permittivity of the material [F/cm]
μ = permeability of the material [H/cm]
ω = frequency [radians/second]
β = phase constant

Phase Velocity The velocity of propagation of a TEM wave may also be referred to as the *phase velocity*. The phase velocity of a TEM wave in conducting material may be described by:

$$\boxed{v_p = \omega\delta = \frac{\omega}{k} = c\frac{2\pi\delta}{\lambda_0} = c\frac{1}{\sqrt{\varepsilon_{r\ \mathrm{eff}}}}}$$ where:

δ = skin depth [m]
c = speed of light 2.998×10^8 m/s
λ_0 = wavelength in the material [m]

Z_0 CHARACTERISTIC IMPEDANCE [Ω]

The **characteristic impedance** is the resistance initially *seen* when a signal is applied to the line. It is a physical characteristic resulting from the materials and geometry of the line.

Lossless line: $\boxed{Z_0 \equiv \sqrt{\frac{L}{C}}} = \frac{V_+}{I_+} = -\frac{V_-}{I_-}$

Lossy line: $\boxed{Z_0 \equiv \sqrt{\frac{R + j\omega L}{G + j\omega C}} = |Z_0| e^{j\phi_z}}$

L = inductance per unit length [H/cm]
C = capacitance per unit length [F/cm]
V_+ = the forward-traveling (left to right) voltage [V]
I_+ = the forward-traveling (left to right) current [I]
V_- = the reverse-traveling (right to left) voltage [V]
I_- = the reverse-traveling (right to left) current [I]
R = the line resistance per unit length [Ω/cm]
G = the conductance per unit length [Ω^{-1}/cm]
ϕ = phase angle of the complex impedance [radians]

y_0 CHARACTERISTIC ADMITTANCE [Ω^{-1}]

The **characteristic admittance** is the reciprocal of the characteristic impedance.

$$\boxed{y_0 \equiv \sqrt{\frac{C}{L}}} = \frac{I_+}{V_+} = -\frac{I_-}{V_-}$$

r REFLECTION COEFFICIENT

The **reflection coefficient** is the ratio of reflected voltage to the forward-traveling voltage, a value ranging from –1 to +1 which, when multiplied by the wave voltage, determines the amount of voltage reflected at one end of the transmission line.

$$\boxed{\rho \equiv \frac{V_-}{V_+} = -\frac{I_-}{I_+}}$$

A reflection coefficient is present at each end of the transmission line:

$$\boxed{\rho_{\text{source}} = \frac{R_S - z_0}{R_S + z_0}} \qquad \boxed{\rho_{\text{load}} = \frac{R_L - z_0}{R_L + z_0}}$$

t TRANSMISSION COEFFICIENT

The **transmission coefficient** is the ratio of total voltage to the forward-traveling voltage, a value ranging from 0 to 2.

$$\boxed{\tau \equiv \frac{V_{total}}{V_+}} = 1 + \rho$$

TOF TIME OF FLIGHT [s]

The **time of flight** is how long it takes a signal to travel the length of the transmission line

$$\boxed{TOF \equiv \frac{l}{v}} = l\sqrt{LC} = \sqrt{L_{TOT} C_{TOT}}$$

l = length of the transmission line [cm]
v = the velocity of propagation $1/\sqrt{LC}$, the speed at which the waveform moves down the line
L = inductance per unit length [H/cm]
C = capacitance per unit length [F/cm]
L_{TOT} = total inductance [H]
C_{TOT} = total capacitance [F]

DERIVED EQUATIONS

$$V_+ = z_0 I_+ = \left(V_{TOT} + I_{TOT} z_0\right)/2$$
$$V_- = -z_0 I_- = \left(V_{TOT} - I_{TOT} z_0\right)/2$$
$$I_+ = y_0 V_+ = \left(I_{TOT} + V_{TOT} y_0\right)/2$$
$$I_- = -y_0 V_- = \left(I_{TOT} - V_{TOT} y_0\right)/2$$

C_n FOURIER SERIES

The function $x(t)$ must be periodic in order to employ the Fourier series. The following is the exponential Fourier series, which involves simpler calculations than other forms but is not as easy to visualize as the trigonometric forms.

$$\boxed{C_n = \frac{1}{T}\int_{t_1}^{t_1+T} x(t)\, e^{-jn\omega_0 t}\, dt}$$

C_n = amplitude
T = period [s]
t = time [s]
n = the harmonic (an integer)
w_0 = frequency $2\pi/T$ [radians]

The function $x(t)$ may be delayed in time. All this does in a Fourier series is to shift the phase. If you know the C_ns for $x(t)$, then the C_ns for $x(t\text{-}\alpha)$ are just $C_n e^{-jn\omega 0\alpha}$. (Here, C_ns is just the plural of C_n.)

C CAPACITANCE [F]

$$v(t) = \frac{1}{C}\int_0^t i\,d\tau + v(0) \qquad I_{cap} = C\frac{dV_{cap}}{dt}$$

$$\boxed{v(t) = v_f + (v_0 - v_f)e^{-t/t}} \qquad i(t) = i_f + (i_0 - i_f)e^{-t/t}$$

$$P(t) = i_0^{\,2} R e^{-2t/\tau}$$

$v(t)$ = voltage across the capacitor, at time t [V]
v_f = final voltage across the capacitor, steady-state voltage [V]
v_0 = initial voltage across the capacitor [V]
t = time [s]
τ = the time constant, RC [seconds]
C = capacitance [F]
Natural log: $\ln x = b \Leftrightarrow e^b = x$

C PARALLEL PLATE CAPACITANCE

$$C = \frac{\varepsilon A}{h} \qquad C_{\text{per unit length}} = \frac{\varepsilon A}{lh} = \frac{\varepsilon wl}{lh} = \frac{\varepsilon w}{h}$$

ε = permittivity of the material [F/cm]
A = area of one of the capacitor plates [cm^2]
h = plate separation [cm]
w = plate width [cm]
l = plate length [cm]
C = capacitance [F]

CAPACITOR-TERMINATED LINE

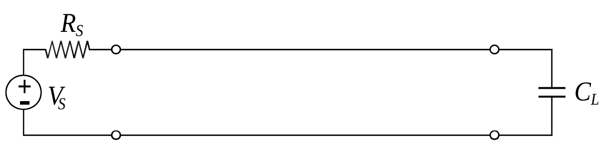

Where the incident voltage is $V_+ = V_0\left(1 - e^{-t/\tau_0}\right)$,

$$V_{cap} = V_+ + V_- = V_0\left(2 + \frac{2\tau_1}{\tau_0 - \tau_1}e^{-t/\tau_1} - \frac{2\tau_0}{\tau_0 - \tau_1}e^{-t/\tau_0}\right)$$

V_0 = final voltage across the capacitor [V]
t = time [s]
τ_0 = time constant of the incident wave, RC [s]
τ_1 = time constant effect due to the load, $Z_0 C_L$ [s]
C = capacitance [F]

SMITH CHART

First **normalize the load impedance** by dividing by the characteristic impedance, and find this point on the chart.

When working in terms of **reactance** X, an inductive load will be located on the top half of the chart, a capacitive load on the bottom half. It's the other way around when working in terms of **susceptance** B [Siemens].

Draw a straight line from the center of the chart through the normalized load impedance point to the edge of the chart.

Anchor a compass at the center of the chart and draw a circle through the normalized load impedance point. Points along this circle represent the normalized impedance at various points along the transmission line. Clockwise movement along the circle represents movement from the load toward the source with one full revolution representing 1/2 wavelength as marked on the outer circle. The two points where the circle intersects the horizontal axis are the voltage maxima (right) and the voltage minima (left).

The point opposite the impedance (180° around the circle) is the **admittance** Y [Siemens]. The reason admittance (or susceptibility) is useful is because admittances in parallel are simply added. (**Admittance** is the reciprocal of impedance; **susceptance** is the reciprocal of reactance.)

$$\boxed{\Gamma(z) = \Gamma_L e^{j2\beta z}}$$

$$e^{j2\beta z} = 1\angle 2\beta z$$

$$\mathbf{G}(z) = \frac{\mathbf{Z}(z) - 1}{\mathbf{Z}(z) + 1}$$

$$\mathbf{Z}_L = \frac{\Gamma_L - 1}{\Gamma_L + 1} \qquad \boxed{\mathbf{Z} = \frac{Z_L}{Z_0}}$$

z = distance from load [m]
$j = \sqrt{-1}$
ρ = magnitude of the reflection coefficient
β = phase constant
Γ = reflection coefficient
Z = normalized impedance [Ω]

SINGLE-STUB TUNING

The basic idea is to connect a line stub in parallel (shunt) or series a distance d from the load so that the imaginary part of the load impedance will be canceled.

Shunt-stub: Select d so that the admittance Y looking toward the load from a distance d is of the form $Y_0 + jB$. Then the stub susceptance is chosen as $-jB$, resulting in a matched condition.

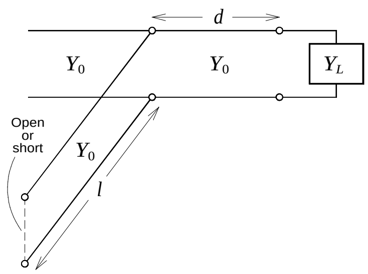

Series-stub: Select d so that the admittance Z looking toward the load from a distance d is of the form $Z_0 + jX$. Then the stub susceptance is chosen as $-jX$, resulting in a matched condition.

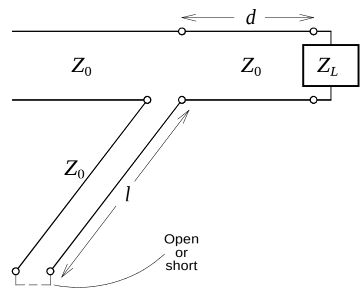

FINDING A STUB LENGTH

Example: Find the lengths of open and shorted shunt stubs to match an admittance of $1\text{-}j0.5$. The admittance of an open shunt (zero length) is $Y=0$; this point is located at the left end of the Smith Chart x-axis. We proceed clockwise around the Smith chart, i.e. away from the end of the stub, to the +j0.5 arc (the value needed to match –j0.5). The difference in the starting point and the end point on the wavelength scale is the length of the stub in wavelengths. The length of a shorted-type stub is found in the same manner but with the starting point at $Y=\infty$.

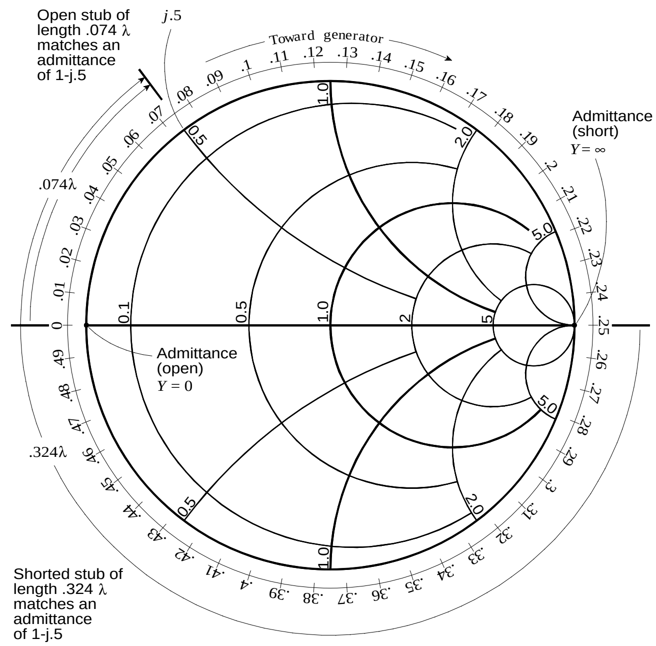

In this example, all values were in units of admittance. If we were interested in finding a stub length for a series stub problem, the units would be in impedance. The problem would be worked in exactly the same way. Of course in impedance, an open shunt (zero length) would have the value $Z=\infty$, representing a point at the right end of the x-axis.

LINE IMPEDANCE [Ω]

The impedance seen at the source end of a lossless transmission line:

$$Z_{in} = Z_0 \frac{1+\rho}{1-\rho} = Z_0 \frac{Z_L + jZ_0 \tan(\beta l)}{Z_0 + jZ_L \tan(\beta l)}$$

For a lossy transmission line:

$$Z_{in} = Z_0 \frac{Z_L + Z_0 \tanh(\gamma l)}{Z_0 + Z_L \tanh(\gamma l)}$$

Line impedance is periodic with spatial period λ/2.

$Z_0 = \sqrt{L/C}$, the characteristic impedance of the line. [Ω]
ρ = the reflection coefficient
Z_L = the load impedance [Ω]
β = 2π/λ, phase constant
γ = α+*j*β, complex propagation constant

l WAVELENGTH [cm]

The physical distance that a traveling wave moves during one period of its periodic cycle.

$$\boxed{\lambda = \frac{2\pi}{\beta} = \frac{2\pi}{k} = \frac{v_p}{f}}$$

$\beta = \omega\sqrt{LC}$ = 2π/λ, phase constant
$k = \omega\sqrt{\mu\varepsilon}$ = 2π/λ, wave number
v_p = velocity of propagation [m/s] see p 2.
f = frequency [Hz]

l/4 QUARTER-WAVE SECTION

A quarter-wave section of transmission line has the effect of inverting the <u>normalized</u> impedance of the load.

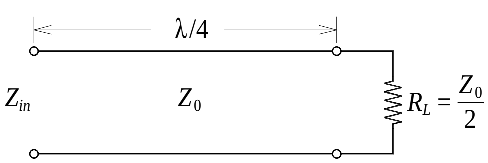

To find Z_{in}, we can normalize the load (by dividing by the characteristic impedance), invert the result, and "unnormalize" this value by multiplying by the characteristic impedance.

In this case, the normalized load is $\frac{Z_0}{2} \div Z_0 = \frac{1}{2}$

so the normalized input impedance is $\left(\frac{1}{2}\right)^{-1} = 2$

and the actual input impedance is $Z_{in} = 2Z_0$

g COMPLEX PROPAGATION CONSTANT

The propagation constant for lossy lines, taking into account the resistance along the line as well as the resistive path between the conductors.

$$\gamma = \alpha + j\beta = \sqrt{ZY} = \sqrt{(R + j\omega L)(G + j\omega C)}$$

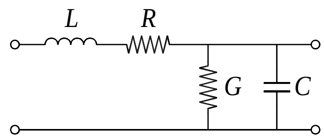

$\alpha = \sqrt{RG}$ **attenuation constant**, the real part of the complex propagation constant, describes the loss
β = 2π/λ, **phase constant**, the complex part of the complex propagation constant
Z = **series impedance** (complex, inductive) per unit length [Ω/cm]
Y = **shunt admittance** (complex, capacitive) per unit length [Ω^{-1}/cm]
R = the resistance per unit length along the transmission line [Ω/cm]
G = the conductance between conductors per unit length [Ω^{-1}/cm]
L = inductance per unit length [H/cm]
C = capacitance per unit length [F/cm]

MODULATED WAVE

Suppose we have a disturbance composed of two frequencies:

$$\sin\left[\left(\omega_0-\delta\omega\right)t-\left(\beta_0-\delta\beta\right)z\right]$$

and $$\sin\left[\left(\omega_0+\delta\omega\right)t-\left(\beta_0+\delta\beta\right)z\right]$$

where ω_0 is the average frequency and β_0 is the average phase.

Using the identity $2\cos\left(\frac{A-B}{2}\right)\sin\left(\frac{A+B}{2}\right)=\sin A+\sin B$

The combination (sum) of these two waves is

$$\boxed{2\underbrace{\cos\left(\delta\omega t-\delta\beta z\right)}_{\text{envelope}}\underbrace{\sin\left(\omega_0 t-\beta_0 z\right)}_{\text{carrier}}}$$

The envelope moves at the group velocity, see p 7.

δ = "the difference in"…
ω_0 = carrier frequency [radians/second]
ω = modulating frequency [radians/second]
β_0 = carrier frequency phase constant
β = phase constant

So the sum of two waves will be a modulated wave having a **carrier** frequency equal to the average frequency of the two waves, and an **envelope** with a frequency equal to half the difference between the two original wave frequencies.

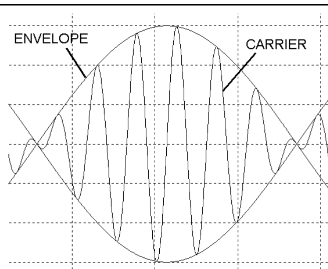

v_g GROUP VELOCITY [cm/s]

The velocity at which the envelope of a modulated wave moves.

$$\boxed{v_g=\frac{\delta\omega}{\delta\beta}=\frac{1}{\sqrt{LC_P}}\sqrt{1-\frac{\omega_c^{\,2}}{\omega^2}}}$$ where:

L = inductance per unit length [H/cm]
C_P = capacitance per unit length [F/cm]
ε = permittivity of the material [F/cm]
μ = permeability of the material, dielectric constant [H/cm]
ω_c = carrier frequency [radians/second]
ω = modulating frequency [radians/second]
β = phase constant

Also, since β may be given as a function of ω, remember

$$v_g=\left(\frac{d\beta}{d\omega}\right)^{-1}$$

OMEGA - BETA GRAPH

This representation is commonly used for modulated waves.

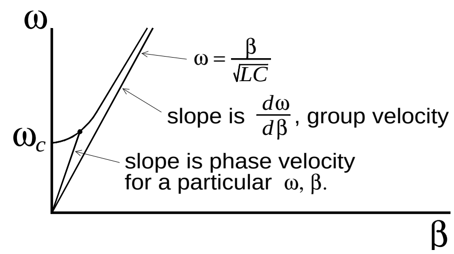

d SKIN DEPTH [cm]

The depth into a material at which a wave is attenuated by 1/e (about 36.8%) of its original intensity. This isn't the same δ that appears in the *loss tangent*, tan δ.

$$\boxed{\delta=\frac{1}{\alpha}=\sqrt{\frac{2}{\omega\mu\sigma}}}$$ where:

$\alpha=\sqrt{RG}$ **attenuation constant**, the real part of the complex propagation constant, describes loss
μ = permeability of the material, dielectric constant [H/cm]
ω = frequency [radians/second]
σ = (*sigma*) conductivity [Siemens/meter] see p12.

Skin Depths of Selected Materials

	60 Hz	1 MHz	1 GHz
silver	8.27 mm	0.064 mm	0.0020 mm
copper	8.53 mm	0.066 mm	0.0021 mm
gold	10.14 mm	0.079 mm	0.0025 mm
aluminum	10.92 mm	0.084 mm	0.0027 mm
iron	0.65 mm	0.005 mm	0.00016 mm

MAXWELL'S EQUATIONS

Maxwell's equations govern the principles of guiding and propagation of electromagnetic energy and provide the foundations of all electromagnetic phenomena and their applications. The time-harmonic expressions can be used only when the wave is sinusoidal.

	STANDARD FORM (Time Domain)	**TIME-HARMONIC** (Frequency Domain)
Faraday's Law	$\nabla \times \vec{\mathscr{E}} = -\dfrac{\partial \vec{\mathscr{B}}}{\partial t}$	$\nabla \times \vec{E} = -j\omega \vec{B}$
Ampere's Law*	$\nabla \times \vec{\mathscr{H}} = \vec{\mathscr{J}} + \dfrac{\partial \vec{\mathscr{D}}}{\partial t}$	$\nabla \times \vec{H} = j\omega \vec{D} + \vec{J}$
Gauss' Law	$\nabla \cdot \vec{\mathscr{D}} = \rho_v$	$\nabla \cdot \vec{D} = \rho_v$
no name law	$\nabla \cdot \vec{\mathscr{B}} = 0$	$\nabla \cdot \vec{B} = 0$

$\mathscr{E}$ = electric field [V/m]
$\mathscr{B}$ = magnetic flux density [W/m^2 or T] $\mathscr{B} = \mu_0 \mathscr{H}$
t = time [s]
$\mathscr{D}$ = electric flux density [C/m^2] $\mathscr{D} = \varepsilon_0 \mathscr{E}$
ρ = volume charge density [C/m^3]
$\mathscr{H}$ = magnetic field intensity [A/m]
$\mathscr{J}$ = current density [A/m^2]

*Maxwell added the $\dfrac{\partial \bar{\mathscr{D}}}{\partial t}$ term to Ampere's Law.

ELECTROMAGNETIC WAVES

MODELING MAXWELL'S EQUATIONS

This is a model of a wave, analogous to a transmission line model.

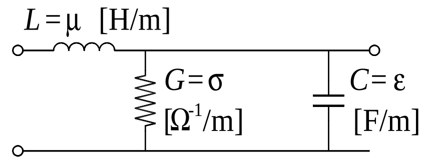

L = inductance per unit length [H/cm]
μ = permeability of the material, dielectric constant [H/cm]
G = the conductance per unit length [Ω^{-1}/cm]
σ = (*sigma*) conductivity [Siemens/meter]
C = capacitance per unit length [F/cm]
ε = permittivity of the material [F/cm]

propagation constant: $\gamma = \sqrt{(j\omega\mu)(j\omega\varepsilon + \sigma)}$

LOW FREQUENCY

At low frequencies, more materials behave as **conductors**. A wave is considered low frequency when

$\boxed{\omega \ll \dfrac{\sigma}{\varepsilon}}$ $\quad \dfrac{\sigma}{\varepsilon}$ is the dielectric relaxation frequency

$\boxed{\eta = \dfrac{1}{\sigma\delta}(1+j)}$ intrinsic wave impedance, see p 12.

What happens to the complex propagation constant at low frequency? From the wave model above, gamma is

$$\gamma = \sqrt{(j\omega\mu)(j\omega\varepsilon + \sigma)} = \sqrt{j\omega\mu\sigma}\sqrt{1 + \frac{j\omega\varepsilon}{\sigma}}$$

Since both ω and ε/σ are small

$$\gamma = \sqrt{j\omega\mu\sigma}\left(1 + \frac{1}{2}j\omega\frac{\varepsilon}{\sigma}\right) = \sqrt{j\omega\mu\sigma}\,(1)$$

Since $\sqrt{j} = \frac{1}{\sqrt{2}} + j\frac{1}{\sqrt{2}}$

$$\gamma = \sqrt{\omega\mu\sigma}\left(\frac{1}{\sqrt{2}} + j\frac{1}{\sqrt{2}}\right) = \sqrt{\frac{\omega\mu\sigma}{2}} + j\sqrt{\frac{\omega\mu\sigma}{2}}$$

So that, with $\gamma = \alpha + j\beta$

we get $\boxed{\alpha = \sqrt{\dfrac{\omega\mu\sigma}{2}}}$, $\boxed{\beta = \sqrt{\dfrac{\omega\mu\sigma}{2}}}$ or $\boxed{\gamma = \dfrac{1}{\delta}(1+j)}$

α = **attenuation constant**, the real part of the complex propagation constant, describes the loss
β = **phase constant**, the complex part of the complex propagation constant
σ = (*sigma*) conductivity [Siemens/cm]
δ = skin depth [cm]

So the wave is attenuating at the same rate that it is propagating.

HIGH FREQUENCY

At high frequencies, more materials behave as **dielectrics**, i.e. copper is a dielectric in the gamma ray range. A wave is considered high frequency when

$\boxed{\omega \gg \frac{\sigma}{\varepsilon}}$ $\frac{\sigma}{\varepsilon}$ is the dielectric relaxation frequency

$\boxed{\eta = \sqrt{\frac{\mu}{\varepsilon}}}$ intrinsic wave impedance, see p 12.

What happens to the complex propagation constant at high frequency?

$$\gamma = \sqrt{(j\omega\mu)(j\omega\varepsilon + \sigma)} = \sqrt{j\omega\mu\ j\omega\varepsilon\left(1 + \frac{\sigma}{j\omega\varepsilon}\right)}$$

Since both $1/\omega$ and σ/ε are small

$$\gamma = j\omega\sqrt{\mu\varepsilon}\left(1 + \frac{1}{2}\frac{\sigma}{j\omega\varepsilon}\right) \qquad \boxed{\gamma = \frac{\sigma}{2}\sqrt{\frac{\mu}{\varepsilon}} + j\omega\sqrt{\mu\varepsilon}}$$

With $\gamma = \alpha + j\beta$

we get $\boxed{\alpha = \frac{\sigma}{2}\sqrt{\frac{\mu}{\varepsilon}}}$, $\boxed{\beta = \omega\sqrt{\mu\varepsilon}}$,

tan d LOSS TANGENT

The loss tangent, a value between 0 and 1, is the loss coefficient of a wave after it has traveled one wavelength. This is the way data is usually presented in texts. This is not the same δ that is used for skin depth.

$$\boxed{\tan\delta = \frac{\sigma}{\omega\varepsilon}}$$

Graphical representation of loss tangent:

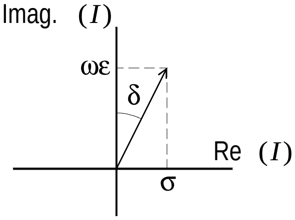

For a dielectric, $\tan\delta \ll 1$.

$$\alpha \approx \frac{1}{2}(\tan\delta)\beta = \frac{\pi}{\lambda}\tan\delta$$

$\omega\varepsilon$ is proportional to the amount of current going through the capacitance C.

σ is proportional to the amount current going through the conductance G.

TEM WAVES

Transverse Electromagnetic Waves

Electromagnetic waves that have single, orthogonal vector electric and magnetic field components (e.g., $\mathscr{E}_x$ and $\mathscr{H}_y$), both varying with a single coordinate of space (e.g., z), are known as *uniform plane waves* or *transverse electromagnetic (TEM) waves*. TEM calculations may be made using formulas from electrostatics; this is referred to as *quasi-static* solution.

Characteristics of TEM Waves

- The velocity of propagation (always in the *z* direction) is $v_p = 1/\sqrt{\mu\varepsilon}$, which is the speed of light in the material
- There is no electric or magnetic field in the direction of propagation. Since this means there is no voltage drop in the direction of propagation, it suggests that no current flows in that direction.
- The electric field is normal to the magnetic field
- The value of the electric field is η times that of the magnetic field at any instant.
- The direction of propagation is given by the direction of $\mathbf{E} \times \mathbf{H}$.
- The energy stored in the electric field per unit volume at any instant and any point is equal to the energy stored in the magnetic field.

TEM ASSUMPTIONS

Some assumptions are made for TEM waves.

$\mathscr{E}_z = 0$ $\mathscr{H}_z = 0$

$\sigma = 0$ time dependence $e^{j\omega t}$

WAVE ANALOGIES

Plane waves have many characteristics analogous to transmission line problems.

Transmission Lines	**Plane Waves**
Phase constant $\beta = \omega\sqrt{LC} = \dfrac{\omega}{v_p} = \dfrac{2\pi}{\lambda}$	Wave number $k = \omega\sqrt{\mu\varepsilon} = \dfrac{\omega}{v_p} = \dfrac{2\pi}{\lambda}$
Complex propagation const. $\gamma = \alpha + j\beta$ $= \sqrt{(R + j\omega L)(G + j\omega C)}$	Complex propagation constant $\gamma = \sqrt{(j\omega\mu)(j\omega\varepsilon + \sigma)}$
Velocity of propagation $v_p = \dfrac{1}{\sqrt{LC}} = \dfrac{\omega}{\beta}$	Phase velocity $v_p = \dfrac{1}{\sqrt{\mu\varepsilon}} = \dfrac{\omega}{k} = \omega\delta = c\dfrac{2\pi\delta}{\lambda}$
Characteristic impedance $Z_0 = \sqrt{\dfrac{L}{C}} = \dfrac{V_+}{I_+}$	Intrinsic impedance $\eta = \sqrt{\dfrac{\mu}{\varepsilon}} = \dfrac{E_{x+}}{H_{y+}}$
Voltage $V(z) = V_+ e^{-j\beta z} + V_- e^{j\beta z}$	Electric Field $E_x(z) = E_+ e^{-jkz} + E_- e^{jkz}$
Current $I(z) = \dfrac{1}{Z_0}\left[V_+ e^{-j\beta z} - V_- e^{j\beta z}\right]$	Magnetic Field $H_y(z) = \dfrac{1}{\eta}\left[E_+ e^{-jkz} - E_- e^{jkz}\right]$
Line input impedance $Z_{in} = Z_0 \dfrac{Z_L + jZ_0 \tan(\beta l)}{Z_0 + jZ_L \tan(\beta l)}$ $Z_{in} = Z_0 \dfrac{Z_L + Z_0 \tanh(\gamma l)}{Z_0 + Z_L \tanh(\gamma l)}$	Wave input impedance $\eta_{in} = \eta_0 \dfrac{\eta_L + j\eta_0 \tan(kl)}{\eta_0 + j\eta_L \tan(kl)}$ $\eta_{in} = \eta_0 \dfrac{\eta_L + \eta_0 \tanh(\gamma l)}{\eta_0 + \eta_L \tanh(\gamma l)}$
Reflection coefficient $\rho = \dfrac{Z_L - Z_0}{Z_L + Z_0}$	Reflection coefficient $\rho = \dfrac{\eta_L - \eta_0}{\eta_L + \eta_0}$

k WAVE NUMBER [rad./cm]

The phase constant for the uniform plane wave; the change in phase per unit length. It can be considered a constant for the medium at a particular frequency.

$$\boxed{k = \frac{\omega}{v} = \omega\sqrt{\mu\varepsilon} = \frac{2\pi}{\lambda}}$$

k appears in the phasor forms of the uniform plane wave

$E_x(z) = E_1 e^{-jkz} + E_2 e^{jkz}$, etc.

k has also been used as in the "*k* of a dielectric" meaning ε_r.

h (eta) INTRINSIC WAVE IMPEDANCE [Ω]

The ratio of electric to magnetic field components. Can be considered a constant of the medium. For free space, $\eta = 376.73\Omega$. The units of η are in ohms.

$$\eta = \frac{E_{x+}}{H_{y+}} = -\frac{E_{y+}}{H_{x+}} \qquad -\eta = \frac{E_{x-}}{H_{y-}} = -\frac{E_{y-}}{H_{x-}}$$

at low frequencies	**at high frequencies**
$\eta = \dfrac{1}{\sigma\delta}(1 + j)$	$\eta = \sqrt{\dfrac{\mu}{\varepsilon}}$

When an electromagnetic wave encounters a sheet of conductive material it sees an impedance. K is the direction of the wave, **H** is the magnetic component and **E** is the electrical field. **E** × **H** gives the direction of propagation K.

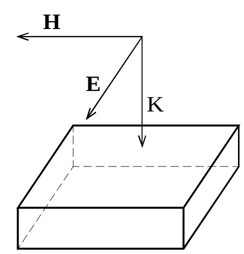

SHEET RESISTANCE [Ω]

Consider a block of material with conductivity σ.

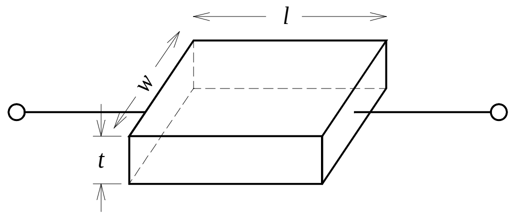

It's resistance is $R = \dfrac{l}{wt\sigma}$ Ω.

If the length is equal to the width, this reduces to

$$R = \frac{1}{t\sigma} \ \Omega.$$

And this is sheet resistance.

HIGH FREQUENCY RESISTANCE [Ω]

When a conductor carries current at high frequency, the electric field penetrates the outer surface only about 1 skin depth so that current travels near the surface of the conductor. Since the entire cross-section is not utilized, this affects the resistance of the conductor.

Cross-section of a conductor showing current flow near the surface:

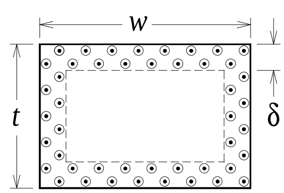

$$\boxed{R \approx \frac{1}{\sigma\delta(\text{perimeter})} = \sqrt{\frac{\omega\mu_0}{2\sigma}}\,\frac{1}{2w+2t}}$$

σ = (*sigma*) conductivity (5.8×10^{5} S/cm for copper) [Siemens/meter]
ω = frequency [radians/second]
δ = skin depth [cm]
μ_0 = permeability of free space $\mu_0 = 4\pi\times10^{-9}$ [H/cm]
w = width of the conductor [cm]
t = thickness of the conductor [cm]

h_{in} WAVE INPUT IMPEDANCE [Ω]

The impedance seen by a wave in a medium.

For example, the impedance of a metal sheet in a vacuum:

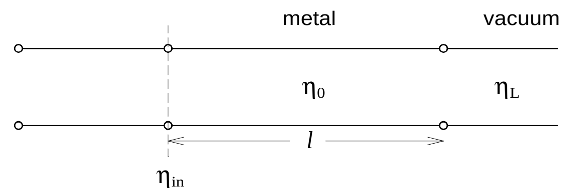

Note that a transmission line model is used here because it is <u>analogous</u> to a wave traveling in a medium. The "load" is the element most remote in the direction of propagation.

The input impedance is $\eta_{in} = \eta_0 \dfrac{\eta_L + \eta_0 \tanh(\gamma l)}{\eta_0 + \eta_L \tanh(\gamma l)}$ Ω.

In this example, *l* is the thickness of a metal sheet. If the metal thickness is much greater than the skin depth, then

$$\tanh(\lambda l) = \tanh\left[\frac{1}{\delta}(1+j)l\right] = \tanh[(\text{big number})(1+j)] \approx 1$$

If *l* is much less than the skin depth δ, then

$$\tanh(\lambda l) = \tanh\left[\frac{1}{\delta}(1+j)l\right] = \tanh[(\text{small number})(1+j)]$$

$$= (\text{same small number})(1+j) = \frac{l}{\delta}(1+j)$$

m MAGNETIC PERMEABILITY [H/m]

The relative increase or decrease in the resultant magnetic field inside a material compared with the magnetizing field in which the given material is located. The product of the permeability constant and the relative permeability of the material.

$\mu = \mu_0\mu_r$ where $\mu_0 = 4\pi\times10^{-7}$ H/m

Relative Permeabilities of Selected Materials

Air	1.00000037	Mercury	0.999968
Aluminum	1.000021	Nickel	600
Copper	0.9999833	Oxygen	1.000002
Gold	0.99996	Platinum	1.0003
Iron (99.96% pure)	280,000	Silver	0.9999736
Iron (motor grade)	5000	Titanium	1.00018
Lead	0.9999831	Tungsten	1.00008
Manganese	1.001	Water	0.9999912

e ELECTRIC PERMITTIVITY [F/m]

The property of a dielectric material that determines how much electrostatic energy can be stored per unit of volume when unit voltage is applied, also called the ***dielectric constant***. The product of the constant of permittivity and the relative permittivity of a material.

$$\varepsilon = \varepsilon_0 \varepsilon_r \quad \text{where } \varepsilon_0 = 8.85\times10^{-14} \text{ F/cm}$$

e$_c$ COMPLEX PERMITTIVITY

$$\varepsilon_c = \varepsilon' - j\varepsilon'' \quad \text{where} \quad \frac{\varepsilon''}{\varepsilon'} = \tan\delta_c$$

In general, both ε' and ε'' depend on frequency in complicated ways. ε' will typically have a constant maximum value at low frequencies, tapering off at higher frequencies with several peaks along the way. ε'' will typically have a peak at the frequency at which ε' begins to decline in magnitude as well as at frequencies where ε' has peaks, and will be zero at low frequencies and between peaks.

e$_r$ RELATIVE PERMITTIVITY

The permittivity of a material is the relative permittivity multiplied by the permittivity of free space

$$\varepsilon = \varepsilon_r \times \varepsilon_0$$

In old terminology, ε_r is called the "*k* of a dielectric". Glass (SiO_2) at ε_r = 4.5 is considered the division between low *k* and high *k* dielectrics.

Relative Permittivities of Selected Materials

Air (sea level)	1.0006	Polystyrene	2.6
Ammonia	22	Polyethylene	2.25
Bakelite	5	Rubber	2.2-4.1
Glass	4.5-10	Silicon	11.9
Ice	3.2	Soil, dry	2.5-3.5
Mica	5.4-6	Styrofoam	1.03
most metals	~1	Teflon	2.1
Plexiglass	3.4	Vacuum	1
Porcelain	5.7	Water, distilled	81
Paper	2-4	Water, seawater	72-80
Oil	2.1-2.3		

NOTE: Relative permittivity data is given for materials at **low or static frequency conditions**. The permittivity for most materials varies with frequency. The relative permittivities of most materials lie in the range of 1-25. At high frequencies, the permittivity of a material can be quite different (usually less), but will have resonant peaks.

s CONDUCTIVITY [S/m] or [1/(Ω·m)]

A measure of the ability of a material to conduct electricity, the higher the value the better the material conducts. The reciprocal is *resistivity*. Values for common materials vary over about 24 orders of magnitude. Conductivity may often be determined from skin depth or the loss tangent.

$$\sigma = \frac{n_c q_e^{\,2} \bar{l}}{m_e v_{th}} \text{ S/m} \quad \text{where}$$

n_c = density of conduction electrons (for copper this is 8.45×10^{28}) [m^{-3}]
q_e = electron charge? 1.602×10^{-23} [C]
$\bar{l}$ = $v_{th}t_c$ the product of the thermal speed and the mean free time between collisions of electrons, the average distance an electron travels between collisions [m]
m_e = the effective electron mass? [kg]
v_{th} = thermal speed, usually much larger than the drift velocity v_d. [m/s]

Conductivities of Selected Materials [1/(Ω·m)]

Aluminum	3.82×10^{7}	Mercury	1.04×10^{6}
Carbon	7.14×10^{4}	Nicrome	1.00×10^{6}
Copper (annealed)	5.80×10^{7}	Nickel	1.45×10^{7}
Copper (in class)	6.80×10^{7}	Seawater	4
Fresh water	$\sim10^{-2}$	Silicon	$\sim4.35\times10^{-4}$
Germanium	~2.13	Silver	6.17×10^{7}
Glass	$\sim10^{-12}$	Sodium	2.17×10^{7}
Gold	4.10×10^{7}	Stainless steel	1.11×10^{6}
Iron	1.03×10^{7}	Tin	8.77×10^{6}
Lead	4.57×10	Titanium	2.09×10^{6}
		Zinc	1.67×10^{7}

P POWER [W]

Power is the time rate of change of energy.

Power reflected at a discontinuity: $\%\text{ power} = |\rho|^2 \times 100$

Power transmitted at a discontinuity: $\%\text{ power} = \left(1 - |\rho|^2\right) \times 100$

MICROSTRIP CONDUCTORS

How fast does a wave travel in a microstrip? The question is complicated by the fact that the dielectric on one side of the strip may be different from the dielectric on the other side and a wave may travel at different speeds in different dielectrics. The solution is to find an **effective relative permittivity** $\varepsilon_{r\,\mathrm{eff}}$ for the combination.

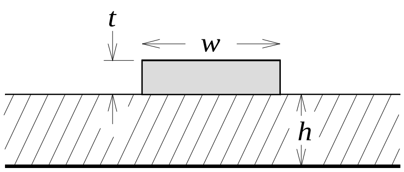

Some Microstrip Relations

$$Z_0^{\mathrm{air}} = Z_0\sqrt{\varepsilon_{r\,\mathrm{eff}}} \qquad C^{\mathrm{air}}Z_0^{\mathrm{air}} = \sqrt{\varepsilon_0\mu_0}$$

$$L = Z_0^{\mathrm{air}}\sqrt{\varepsilon_0\mu_0} = C^{\mathrm{total}}\left(Z_0\right)^2 \qquad L\,C^{\mathrm{air}} = \varepsilon_0\mu_0$$

$$Z_0 = \sqrt{\frac{L}{C^{\mathrm{total}}}} \qquad Z_0^{\mathrm{air}} = \sqrt{\frac{L}{C^{\mathrm{air}}}}$$

$$\gamma = j\beta = j\omega\sqrt{\varepsilon_0\mu_0}\sqrt{\varepsilon_{r\,\mathrm{eff}}} \qquad \varepsilon_{r\,\mathrm{eff}} = \frac{C^{\mathrm{total}}}{C^{\mathrm{air}}}$$

$$v_p = \frac{1}{\sqrt{\varepsilon_0\mu_0\varepsilon_{r\,\mathrm{eff}}}} = \frac{1}{\sqrt{L\,C^{\mathrm{total}}}}$$

It's difficult to get more than 200Ω for Z_0 in a microstrip.

Microstrip Approximations

$$\varepsilon_{r\,\mathrm{eff}} = \frac{\varepsilon_r+1}{2} + \frac{\varepsilon_r-1}{2\sqrt{1+12h/w}}$$

$$Z_0 = \begin{cases} \dfrac{60}{\sqrt{\varepsilon_{r\,\mathrm{eff}}}}\ln\left[\dfrac{8h}{w}+\dfrac{w}{4h}\right], & \text{for } \dfrac{w}{h}\le 1 \\[2ex] \dfrac{120\pi}{\sqrt{\varepsilon_{r\,\mathrm{eff}}}\left[\dfrac{w}{h}+1.393+0.667\ln\left(\dfrac{w}{h}+1.444\right)\right]}, & \text{for } \dfrac{w}{h}>1 \end{cases}$$

$$\frac{w}{h} = \begin{cases} \dfrac{8e^A}{e^{2A}-2}, & \dfrac{w}{h}<2 \\[2ex] \dfrac{2}{\pi}\left\{B-1-\ln\left(2B-1\right)+\dfrac{\varepsilon_r-1}{2\varepsilon_r}\left[\ln\left(B-1\right)+0.39-\dfrac{0.61}{\varepsilon_r}\right]\right\}, & \dfrac{w}{h}>2 \end{cases}$$

where $A = \dfrac{Z_0}{60}\sqrt{\dfrac{\varepsilon_r+1}{2}}+\dfrac{\varepsilon_r-1}{\varepsilon_r+1}\left(0.23+\dfrac{0.11}{\varepsilon_r}\right)$, $B = \dfrac{377\pi}{2Z_0\sqrt{\varepsilon_r}}$

STRIPLINE CONDUCTOR

Also called *shielded microstrip*. The effective relative permittivity is used in calculations.

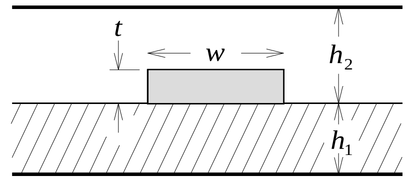

assuming $w \ge 10h$, $\quad \varepsilon_{r\,\mathrm{eff}} = \dfrac{\varepsilon_{r1}h_1+\varepsilon_{r2}h_2}{h_1+h_2}$ where

ε_{r1} = the relative permittivity of the dielectric of thickness h_1.
ε_{r2} = the relative permittivity of the dielectric of thickness h_2.

COPPER CLADDING

The thickness of copper on a circuit board is measured in ounces. 1-ounce cladding means that 1 square foot of the copper weighs 1 ounce. 1-ounce copper is 0.0014" or 35.6 μm thick.

a_d DIELECTRIC LOSS FACTOR [dB/cm]

$$\alpha_d = 8.68\frac{\beta_0\varepsilon_r\left(\varepsilon_{r\,\mathrm{eff}}-1\right)}{2\sqrt{\varepsilon_{r\,\mathrm{eff}}}\left(\varepsilon_r-1\right)}\tan\delta$$

a_c CONDUCTOR LOSS FACTOR [dB/cm]

$$\alpha_c = 8.68\frac{R}{2Z_0}, \qquad R = \frac{1}{\sigma\delta(\text{perimeter})} = \sqrt{\frac{\omega\mu_0}{2\sigma}}\,\frac{1}{(\text{perimeter})}$$

WHEELER'S EQUATION

Another approximation for microstrip calculations is Wheeler's equation.

$$Z_0 = \frac{42.4}{\sqrt{1+\varepsilon_r}} \ln\left(1+\left\{\frac{4h}{w'}\left[\frac{14+\frac{8}{\varepsilon_r}}{11}\times\frac{4h}{w'}+\sqrt{\left(\frac{14+\frac{8}{\varepsilon_r}}{11}\times\frac{4h}{w'}\right)^2+\pi^2\frac{1+\frac{1}{\varepsilon_r}}{2}}\right]\right\}\right)$$

where $$w' = \frac{8h\sqrt{\frac{7+\frac{4}{\varepsilon_r}}{11}\left[\exp\left(\frac{Z_0}{42.4}\sqrt{\varepsilon_r+1}\right)-1\right]+\frac{1+\frac{1}{\varepsilon_r}}{0.81}}}{\exp\left(\frac{Z_0}{42.4}\sqrt{\varepsilon_r+1}\right)-1}$$

NETWORK THEORY

S_{ij} SCATTERING PARAMETER

$S_{\mathrm{i\,j}}$

observation port excitation port

A scattering parameter, represented by S_{ij}, is a dimensionless value representing the fraction of wave amplitude transmitted from port j into port i, provided that all other ports are terminated with matched loads and only port j is receiving a signal. Under these same conditions, S_{ii} is the reflection coefficient at port i.

To experimentally determine the scattering parameters, attach an impedance-matched generator to one of the ports (***excitation port***), attach impedance-matched loads to the remaining ports, and observe the signal received at each of the ports (***observation ports***). The fractional amounts of signal amplitude received at each port i will make up one column j of the **scattering matrix**. Repeating the process for each column would require n^2 measurements to determine the scattering matrix for an n-port network.

S_{ij} SCATTERING MATRIX

$$\begin{bmatrix} S_{11} & S_{12} & \cdots & S_{1N} \\ S_{21} & S_{22} & \cdots & S_{2N} \\ \vdots & \vdots & \ddots & \vdots \\ S_{N1} & S_{N2} & \cdots & S_{NN} \end{bmatrix}$$

The scattering matrix is an $n \times n$ matrix composed of scattering parameters that describes an n-port network.

The elements of the diagonal of the scattering matrix are reflection coefficients of each port. The elements of the off-diagonal are transmission coefficients, under the conditions outlined in "SCATTERING PARAMETER".

If the network is **internally matched** or **self-matched**, then $S_{11} = S_{22} = \cdots = S_{NN} = 0$, that is, the diagonal is all zeros.

The sum of the squares of each column of a scattering matrix is equal to one, provided the network is lossless.

a_n, b_n INCIDENT/REFLECTED WAVE AMPLITUDES

The parameters a_n and b_n describe the incident and reflected waves respectively at each port n. These parameters are used for power and scattering matrix calculations.

The amplitude of the wave incident to port n is equal to the amplitude of the incident voltage at the port divided by the square root of the port impedance.	$a_n = \frac{V_n^+}{\sqrt{Z_{0n}}}$
Amplitude of the wave reflected at port n is equal to the amplitude of the reflected voltage at the port divided by the square root of the port impedance.	$b_n = \frac{V_n^-}{\sqrt{Z_{0n}}}$
The scattering parameter is equal to the wave amplitude output at port i divided by the wave amplitude input at port j provided the only source is a matched source at port j and all other ports are connected to matched loads.	$S_{ij} = \frac{b_i}{a_j}$
The relationship between the S-parameters and the a- and b-parameters can be written in matrix form where **S** is the scattering matrix and **a** and **b** are column vectors.	$\mathbf{b} = \mathbf{Sa}$
Power flow into any port is shown as a function of a- and b-parameters.	$P = \frac{1}{2}\left(\lvert a\rvert^2 - \lvert b\rvert^2\right)$
The ratio of the input power at port j to the output power at port I can be written as a function of a- and b-parameters or the S-parameter.	$\frac{P_{in\,j}}{P_{out\,i}} = \frac{\lvert a_j\rvert^2}{\lvert b_j\rvert^2} = \frac{1}{\lvert S_{ij}\rvert^2}$

RECIPROCITY

A network is reciprocal when $S_{ij} = S_{ji}$ in the scattering matrix, i.e. the matrix is symmetric across the diagonal. Also, $Z_{ij} = Z_{ji}$ and $Y_{ij} = Y_{ji}$. Networks constructed of “normal materials” exhibit reciprocity.

Reciprocity Theorem:

$$\oint_S \vec{E}_a \times \vec{H}_b \cdot ds = \oint_S \vec{E}_b \times \vec{H}_a \cdot ds$$

E_a and H_b are fields from two different sources.

LOSSLESS NETWORK

A network is lossless when

$$\underline{S}\ \underline{S}^{\dagger} = I$$

† means to take the complex conjugate and transpose the matrix. If the network is reciprocal, then the transpose is the same as the original matrix.

I = a unitary matrix. A **unitary matrix** has the properties:

$$\sum_{k=1}^{N} S_{ki} S_{ki}^{*} = 1 \qquad \sum_{k=1}^{N} S_{ki} S_{kj}^{*} = 0$$

In other words, a column of a unitary matrix multiplied by its complex conjugate equals one, and a column of a unitary matrix multiplied by the complex conjugate of a different column equals zero.

RAT RACE OR HYBRID RING NETWORK

The rat race or hybrid ring network is lossless, reciprocal, and internally matched.

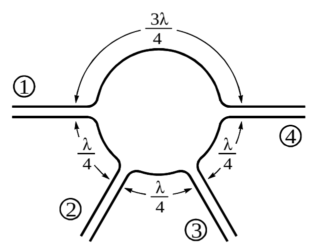

The signal splits upon entering the network and half travels around each side. A signal entering at port 1 and exiting at port 4 travels ¾ of a wavelength along each side, so the signals are in phase and additive. From port 1 to port 3 the signal travels one wavelength along one side and ½ wavelength along the other, arriving a port 3 out of phase and thus canceling. From port 1 to port 2 the paths are ¼ and 5/4 wavelengths respectively, thus they are in phase and additive.

DIRECTIONAL COUPLER

The directional coupler is a 4-port network similar to the rat race. It can be used to measure reflected and transmitted power to an antenna.

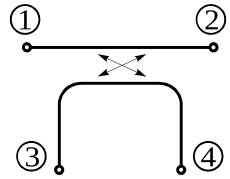

An input at one port is divided between two of the remaining ports. The **coupling factor**, measured in dB, describes the division of signal strength at the two ports. For example if the coupler has a coupling factor of –10 dB, then a signal input at port 1 would appear at port 4 attenuated by 10 dB with the majority of the signal passing to port 2. In other words, 90% of the signal would appear at port 2 and 10% at port 4. (-10 dB means "**10 dB down**" or 0.1 power, -6 dB means 0.25 power, and –3 dB means 0.5 power.) A reflection from port 2 would appear at port 3 attenuated by the same amount. Meters attached to ports 3 and 4 could be used to measure reflected and transmitted power for a system with a transmitter connected to port 1 and an antenna at port 2. The **directivity** of a coupler is a measurement of how well the coupler transfers the signal to the appropriate output without reflection due to the coupler itself; the directivity approaches infinity for a perfect coupler. $\text{directivity} = 10\log\left(p_3 / p_1\right)$, where the source is at port 1 and the load is at port 2.

The directional coupler is **lossless** and **reciprocal**. The scattering matrix looks like this. In a real coupler, the off-diagonal zeros would be near zero due to leakage.

$$\begin{bmatrix} 0 & p & 0 & -q \\ p & 0 & q & 0 \\ 0 & q & 0 & p \\ -q & 0 & p & 0 \end{bmatrix}$$

CIRCULATOR

The circulator is a 3-port network that can be used to prevent reflection at the antenna from returning to the source.

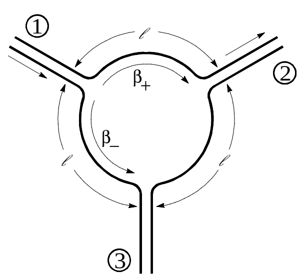

Port 3 is terminated internally by a matched load. With a source at 1 and a load at 2, any power reflected at the load is absorbed by the load resistance at port 3. A 3-port network cannot be both lossless and reciprocal, so the circulator is <u>not</u> reciprocal.

Schematically, the circulator may be depicted like this:

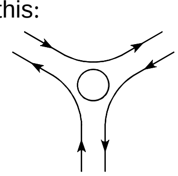

The circulator is **lossless** but is <u>not</u> **reciprocal**. The scattering matrix looks like this:

$$\begin{bmatrix} 0 & 0 & 1 \\ 1 & 0 & 0 \\ 0 & 1 & 0 \end{bmatrix}$$

MAXWELL'S EQUATIONS, TIME HARMONIC FORM

$$\nabla \times \bar{\mathscr{E}} = -j\omega\mu\mathbf{H} \qquad \text{"curl on E"}$$

$$\nabla \times \bar{\mathscr{H}} = -j\omega\mu\mathbf{E} \qquad \text{"curl on H"}$$

$$\bar{\mathscr{E}} = \left[E_x(x,y)\hat{\mathbf{x}} + E_y(x,y)\hat{\mathbf{y}} + E_z(x,y)\hat{\mathbf{z}}\right]e^{j\omega t-\gamma z}$$

$$\bar{\mathscr{H}} = \left[H_x(x,y)\hat{\mathbf{x}} + H_y(x,y)\hat{\mathbf{y}} + H_z(x,y)\hat{\mathbf{z}}\right]e^{j\omega t-\gamma z}$$

From the curl equations we can derive:

(1) $\dfrac{\partial E_z}{\partial y} + \gamma E_y = -j\omega\mu H_x$ (4) $\dfrac{\partial H_z}{\partial y} + \gamma H_y = j\omega\varepsilon E_x$

(2) $-\dfrac{\partial E_z}{\partial x} - \gamma E_x = -j\omega\mu H_y$ (5) $-\dfrac{\partial H_z}{\partial x} - \gamma H_x = j\omega\varepsilon E_y$

(3) $\dfrac{\partial E_y}{\partial x} - \dfrac{\partial E_x}{\partial y} = -j\omega\mu H_z$ (6) $\dfrac{\partial H_y}{\partial x} - \dfrac{\partial H_x}{\partial y} = j\omega\varepsilon E_z$

From the above equations we can obtain:

(1) & (5) $H_x = \dfrac{1}{\gamma^2 + \omega^2\mu\varepsilon}\left(j\omega\varepsilon\dfrac{\partial E_z}{\partial y} - \gamma\dfrac{\partial H_z}{\partial x}\right)$

(2) & (4) $H_y = \dfrac{1}{\gamma^2 + \omega^2\mu\varepsilon}\left(j\omega\varepsilon\dfrac{\partial E_z}{\partial x} - \gamma\dfrac{\partial H_z}{\partial y}\right)$

(2) & (4) $E_x = -\dfrac{1}{\gamma^2 + \omega^2\mu\varepsilon}\left(-\gamma\dfrac{\partial E_z}{\partial x} + j\omega\mu\dfrac{\partial H_z}{\partial y}\right)$

(1) & (5) $E_y = -\dfrac{1}{\gamma^2 + \omega^2\mu\varepsilon}\left(-\gamma\dfrac{\partial E_z}{\partial y} + j\omega\mu\dfrac{\partial H_z}{\partial x}\right)$

This makes it look like if E_z and H_z are zero, then H_x, H_y, E_x, and E_y are all zero. But since $\infty \times 0 \neq 0$, we could have non-zero result for the TEM wave if $\gamma^2 = -\omega^2\mu\varepsilon \Rightarrow \gamma = j\omega\sqrt{\mu\varepsilon}$. This should look familiar.

WAVE EQUATIONS

From Maxwell's equations and a vector identity on curl, we can get the following wave equations:

$$\nabla^2 \overline{\mathscr{E}} = -\omega^2 \mu\varepsilon \overline{\mathscr{E}} \qquad \text{"del squared on E"}$$

$$\nabla^2 \overline{\mathscr{H}} = \omega^2 \mu\varepsilon \overline{\mathscr{H}} \qquad \text{"del squared on H"}$$

The z part or "del squared on E_z" is:

$$\nabla^2 E_z = \frac{\gamma^2 E_z}{\partial x^2} + \frac{\gamma^2 E_z}{\partial y^2} + \frac{\gamma^2 E_z}{\partial z^2} = -\omega^2 \mu\varepsilon E_z$$

Using the separation of variables, we can let:

$$E_z = X(x) \cdot Y(y) \cdot Z(z)$$

We substitute this into the previous equation and divide by $X \cdot Y \cdot Z$ to get:

$$\underbrace{\frac{1}{X}\frac{d^2 X}{dx^2}}_{-k_x{}^2} + \underbrace{\frac{1}{Y}\frac{d^2 Y}{dy^2}}_{-k_y{}^2} + \underbrace{\frac{1}{Z}\frac{d^2 Z}{dz^2}}_{-k_z{}^2} = \underbrace{-\omega^2 \mu\varepsilon}_{\text{a constant}}$$

Since X, Y, and Z are independent variables, the only way the sum of these 3 expressions can equal a constant is if all 3 expressions are constants.

So we are letting $\frac{1}{Z}\frac{d^2 Z}{dz^2} = -k_z{}^2 \Rightarrow \frac{d^2 Z}{dz^2} = -Z k_z{}^2$

A solution could be $Z = e^{-\gamma z}$

so that $\gamma^2 e^{-\gamma z} = -k_z{}^2 e^{-\gamma z}$ and $-k_z{}^2 = \gamma^2$

Solutions for X and Y are found

$$\frac{1}{X}\frac{d^2 X}{dx^2} = -k_x{}^2 \Rightarrow X = A\sin(k_x x) + B\cos(k_x x)$$

$$\frac{1}{Y}\frac{d^2 Y}{dy^2} = -k_y{}^2 \Rightarrow Y = C\sin(k_y y) + D\cos(k_y y)$$

giving us the general solution $k_x{}^2 + k_y{}^2 - \gamma^2 = \omega^2 \mu\varepsilon$

For a particular solution we need to specify initial conditions and boundary conditions. For some reason, initial conditions are not an issue. The unknowns are k_x, k_y, A, B, C, D. The boundary conditions are

$$E_{\tan} = 0 \qquad \frac{\partial H_{\tan}}{\partial n} = 0$$

$E_{\tan}$ = the electric field tangential to a conducting surface
$H_{\tan}$ = the magnetic field tangential to a conducting surface
n = I don't know

TM, TE WAVES IN PARALLEL PLATES

TM, or transverse magnetic, means that magnetic waves are confined to the *transverse plane*. Similarly, TE (transverse electric) means that electrical waves are confined to the transverse plane.

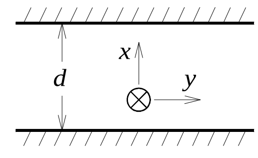

(z direction is into page)

Transverse plane means the plane that is transverse to (perpendicular to) the direction of propagation. The direction of propagation is taken to be in the z direction, so the transverse plane is the x-y plane. So for a TM wave, there is no H_z component (magnetic component in the z direction) but there is an E_z component.

$$\boxed{E_z = A\sin(k_x x)\, e^{-\gamma z}}$$

A = amplitude [V]

$k_x = \frac{m\pi}{d}$ The magnetic field must be zero at the plate boundaries. This value provides that characteristic. [cm^{-1}]

x = position; perpendicular distance from one plate. [cm]
d = plate separation [cm]
γ = propagation constant
z = position along the direction of propagation [cm]
m = mode number; an integer greater than or equal to 1

$$\boxed{\gamma = \sqrt{-\omega^2 \mu\varepsilon + (kx)^2}}$$

Notice than when $(kx)^2 \geq \omega^2 \mu\varepsilon$, the quantity under the square root sign will be positive and γ will be purely real. In this circumstance, the wave is said to be evanescent. The wavelength goes to infinity; there is no oscillation or propagation. On the other hand, when $(kx)^2 < \omega^2 \mu\varepsilon$, γ is purely imaginary.

The magnitude of E_z is related to its position between the plates and the mode number m. Note that for m = 2 that $d = \lambda$.

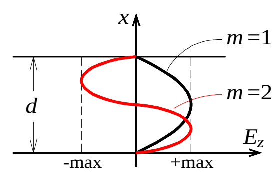

GENERAL MATHEMATICAL

COMPLEX TO POLAR NOTATION

j in polar notation:

$$j = e^{j\frac{\pi}{2}}$$

So we can find the square root of j:

$$\sqrt{j} = \sqrt{e^{j\frac{\pi}{2}}} = e^{j\frac{\pi}{4}} = \frac{1}{\sqrt{2}} + j\frac{1}{\sqrt{2}}$$

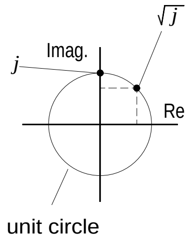

dBm DECIBELS RELATIVE TO 1 mW

The decibel expression for power. The logarithmic nature of decibel units translates the multiplication and division associated with gains and losses into addition and subtraction.

0 dBm = 1 mW
20 dBm = 100 mW
-20 dBm = 0.01 mW

$$P(\mathrm{dBm}) = 10\log\left[P(\mathrm{mW})\right]$$

$$P(\mathrm{mW}) = 10^{P(\mathrm{dBm})/10}$$

PHASOR NOTATION

To express a derivative in phasor notation, replace $\frac{\partial}{\partial t}$ with $j\omega$. For example, the

Telegrapher's equation $\frac{\partial V}{\partial z} = -L\frac{\partial I}{\partial t}$

becomes $\frac{\partial V}{\partial z} = -Lj\omega I$.

Ñ NABLA, DEL OR GRAD OPERATOR

Compare the ∇ operation to taking the time derivative. Where $\partial/\partial t$ means to take the derivative with respect to time and introduces a s^{-1} component to the units of the result, the ∇ operation means to take the derivative with respect to distance (in 3 dimensions) and introduces a m^{-1} component to the units of the result. ∇ terms may be called space derivatives and an equation which contains the ∇ operator may be called a vector differential equation. In other words $\nabla\mathbf{A}$ is how fast $\mathbf{A}$ changes as you move through space.

in rectangular coordinates: $\nabla\mathbf{A} = \hat{x}\frac{\partial A}{\partial x} + \hat{y}\frac{\partial A}{\partial y} + \hat{z}\frac{\partial A}{\partial z}$

in cylindrical coordinates: $\nabla\mathbf{A} = \hat{r}\frac{\partial A}{\partial r} + \hat{\phi}\frac{1}{r}\frac{\partial A}{\partial \phi} + \hat{z}\frac{\partial A}{\partial z}$

in spherical coordinates: $\nabla\mathbf{A} = \hat{r}\frac{\partial A}{\partial r} + \hat{\theta}\frac{1}{r}\frac{\partial A}{\partial \theta} + \hat{\phi}\frac{1}{r\sin\theta}\frac{\partial A}{\partial \phi}$

∇ GRADIENT

$$\boxed{\nabla\vec{\Phi} = -\mathbf{E}}$$

"The gradient of the vector Φ" or "del Φ" is equal to the negative of the electric field vector.

$\nabla\Phi$ is a vector giving the direction and magnitude of the maximum spatial variation of the scalar function Φ at a point in space.

$$\nabla\vec{\Phi} = \hat{\mathbf{x}}\frac{\partial\Phi}{\partial x} + \hat{\mathbf{y}}\frac{\partial\Phi}{\partial y} + \hat{\mathbf{z}}\frac{\partial\Phi}{\partial z}$$

Ñx DIVERGENCE

$\nabla\cdot$ is also a vector operator, combining the "del" or "grad" operator with the dot product operator and is read as "the divergence of". In this form of Gauss' law, where $\mathbf{D}$ is a density per unit area, with the operators applied, $\nabla\cdot\mathbf{D}$ becomes a density per unit volume.

$$\boxed{\mathrm{div}\,\mathbf{D} = \nabla\cdot\mathbf{D} = \frac{\partial D_x}{\partial x} + \frac{\partial D_y}{\partial y} + \frac{\partial D_z}{\partial z} = \rho}$$

$\mathbf{D}$ = electric flux density vector $\mathbf{D} = \varepsilon\mathbf{E}$ [C/m^2]
ρ = source charge density [C/m^3]

Ñ^2 THE LAPLACIAN

∇^2 is a combination of the divergence and del operations, i.e. $\mathrm{div}(\mathrm{grad}\ \Phi) = \nabla \cdot \nabla\ \Phi = \nabla^2\ \Phi$. It is read as "the LaPlacian of" or "del squared".

$$\boxed{\nabla^2 \mathbf{F} = \frac{\partial^2 \Phi}{\partial x^2} + \frac{\partial^2 \Phi}{\partial y^2} + \frac{\partial^2 \Phi}{\partial z^2}}$$

F = electric potential [V]

GRAPHING TERMINOLOGY

With *x* being the horizontal axis and *y* the vertical, we have a graph of ***y* versus *x*** or ***y* as a function of *x***. The *x*-axis represents the **independent variable** and the *y*-axis represents the **dependent variable**, so that when a graph is used to illustrate data, the data of regular interval (often this is time) is plotted on the *x*-axis and the corresponding data is dependent on those values and is plotted on the *y*-axis.

HYPERBOLIC FUNCTIONS

$$j \sin\theta = \sinh(j\theta)$$

$$j \cos\theta = \cosh(j\theta)$$

$$j \tan\theta = \tanh(j\theta)$$

TAYLOR SERIES

$$\sqrt{1+x} \approx 1 + \frac{1}{2}x, \quad x \ll 1$$

$$\frac{1}{1-x^2} \approx 1 + x^2 + x^4 + x^6 + \cdots, \quad |x| < 1$$

$$\frac{1}{1 \pm x} \approx 1 \mp x, \quad x \ll 1$$

ELECTROMAGNETIC SPECTRUM

FREQUENCY	WAVELENGTH (free space)	DESIGNATION	APPLICATIONS
< 3 Hz	> 100 Mm		Geophysical prospecting
3-30 Hz	10-100 Mm	ELF	Detection of buried metals
30-300 Hz	1-10 Mm	SLF	Power transmission, submarine communications
0.3-3 kHz	0.1-1 Mm	ULF	Telephone, audio
3-30 kHz	10-100 km	VLF	Navigation, positioning, naval communications
30-300 kHz	1-10 km	LF	Navigation, radio beacons
0.3-3 MHz	0.1-1 km	MF	AM broadcasting
3-30 MHz	10-100 m	HF	Short wave, citizens' band
30-300 MHz 54-72 76-88 88-108 174-216	1-10 m	VHF	TV, FM, police TV channels 2-4 TV channels 5-6 FM radio TV channels 7-13
0.3-3 GHz 470-890 MHz 915 MHz 800-2500 MHz 1-2 2.45 2-4	10-100 cm	UHF "money band"	Radar, TV, GPS, cellular phone TV channels 14-83 Microwave ovens (Europe) PCS cellular phones, analog at 900 MHz, GSM/CDMA at 1900 L-band, GPS system Microwave ovens (U.S.) S-band
3-30 GHz 4-8 8-12 12-18 18-27	1-10 cm	SHF	Radar, satellite communications C-band X-band (Police radar at 11 GHz) K_u-band (dBS Primestar at 14 GHz) K-band (Police radar at 22 GHz)
30-300 GHz 27-40 40-60 60-80 80-100	0.1-1 cm	EHF	Radar, remote sensing K_a-band (Police radar at 35 GHz) U-band V-band W-band
0.3-1 THz	0.3-1 mm	Millimeter	Astromony, meteorology
10^{12}-10^{14} Hz	3-300 μm	Infrared	Heating, night vision, optical communications
3.95×10^{14}- 7.7×10^{14} Hz	390-760 nm 625-760 600-625 577-600 492-577 455-492 390-455	Visible light	Vision, astronomy, optical communications Red Orange Yellow Green Blue Violet
10^{15}-10^{18} Hz	0.3-300 nm	Ultraviolet	Sterilization
10^{16}-10^{21} Hz		X-rays	Medical diagnosis
10^{18}-10^{22} Hz		γ-rays	Cancer therapy, astrophysics
> 10^{22} Hz		Cosmic rays	Astrophysics

GLOSSARY

anisotropic materials materials in which the electric polarization vector is not in the same direction as the electric field. The values of ε, μ, and σ are dependent on the field direction. Examples are crystal structures and ionized gases.

complex permittivity ϵ The imaginary part accounts for heat loss in the medium due to damping of the vibrating dipole moments.

dielectric An insulator. When the presence of an applied field displaces electrons within a molecule away from their average positions, the material is said to be polarized. When we consider the polarizations of insulators, we refer to them as *dielectrics*.

empirical A result based on observation or experience rather than theory, e.g. *empirical data*, *empirical formulas*. Capable of being verified or disproved by observation or experiment, e.g. *empirical laws*.

evanescent wave A wave for which $\beta=0$. α will be negative. That is, γ is purely real. The wave has infinite wavelength—there is no oscillation.

isotropic materials materials in which the electric polarization vector is in the same direction as the electric field. The material responds in the same way for all directions of an electric field vector, i.e. the values of ε, μ, and σ are constant regardless of the field direction.

linear materials materials which respond proportionally to increased field levels. The value of μ is not related to $\mathbf{H}$ and the value of ε is not related to $\mathbf{E}$. Glass is linear, iron is non-linear.

overdamped system in the case of a transmission line, this means that when the source voltage is applied the line voltage rises to the final voltage without exceeding it.

time variable materials materials whose response to an electric field changes over time, e.g. when a sound wave passes through them.

transverse plane perpendicular, e.g. the x-y plane is *transverse* to z.

underdamped system in the case of a transmission line, this means that after the source voltage is applied the line voltage periodically exceeds the final voltage.

wave number k The phase constant for the uniform plane wave. k may be considered a constant of the medium at a particular frequency.

LEARNING MADE EASY

Ixia Special Edition

5G for dummies®

A Wiley Brand

Innovations that make 5G possible

Achieve scale through network virtualization

See the future of the IoT and New Radio

Compliments of ixia

Kalyan Sundhar

Lawrence C. Miller

About Ixia

Ixia, recently acquired by Keysight Technologies, provides testing, visibility, and security solutions, strengthening applications across networks and cloud environments for enterprises, service providers, and network equipment manufacturers. Ixia offers companies trusted environments in which to develop, deploy, and operate. Customers worldwide rely on Ixia to verify their designs, optimize their performance, and ensure protection of their networks and cloud environments to make their applications stronger. Learn more at **www.ixiacom.com**.

About Keysight Technologies

Keysight Technologies is a leading technology company that helps its engineering, enterprise, and service provider customers optimize networks and bring electronic products to market faster and at a lower cost. Keysight's solutions go where the electronic signal goes, from design simulation, to prototype validation, to manufacturing test, to optimization in networks and cloud environments. Customers span the worldwide communications ecosystem, aerospace and defense, automotive, energy, semiconductor, and general electronics end markets. Keysight generated revenues of $2.9 billion in fiscal year 2016. In April 2017, Keysight acquired Ixia, a leader in network test, visibility, and security. More information is available at **www.keysight.com**.

5G

Ixia Special Edition

by Kalyan Sundhar and Lawrence C. Miller

for dummies®
A Wiley Brand

5G For Dummies®, Ixia Special Edition

Published by
John Wiley & Sons, Inc.
111 River St.
Hoboken, NJ 07030-5774
www.wiley.com

For general information on our other products and services, or how to create a custom *For Dummies* book for your business or organization, please contact our Business Development Department in the U.S. at 877-409-4177, contact info@dummies.biz, or visit www.wiley.com/go/custompub. For information about licensing the *For Dummies* brand for products or services, contact BrandedRights&Licenses@Wiley.com.

ISBN 978-1-119-42415-4 (pbk); ISBN 978-1-119-42416-1 (ebk)

Manufactured in the United States of America

10 9 8 7 6 5 4 3 2 1

Publisher's Acknowledgments

We're proud of this book and of the people who worked on it. Some of the people who helped bring this book to market include the following:

Project Editor: Martin V. Minner

Senior Acquisitions Editor: Amy Fandrei

Editorial Manager: Rev Mengle

Business Development Representative: Karen Hattan

Production Editor: Vasanth Koilraj

Table of Contents

Introduction

The next-generation mobile network (NGMN) is on the horizon. 5G, the next iteration of 4G Long Term Evolution (LTE) networks, will enable significantly greater mobile speeds — as much as 20 gigabits per second (Gbps) with less than one millisecond (ms) latency — to enable real-time connectivity for mission-critical and potentially lifesaving devices and applications. 5G will also provide truly ubiquitous connectivity in the most challenging and remote areas of the world whether on land, in the air, or at sea — even on the 42nd floor of an office building in downtown Chicago! Finally, 5G networks will connect billions of Internet of Things (IoT) devices with a wide variety of speed and data volume requirements.

But 5G is an ambitious goal. Work on key technologies to enable 5G has already begun. In much the same way that 4G LTE was rolled out in 2008, but is only now achieving the 4G LTE goal of 1 Gbps speeds with the 4G LTE Advanced standard, 5G will be a steady evolution that begins with commercial availability expected in 2020. Many technologies that have emerged in the evolution of 4G LTE, such as carrier aggregation (CA) and multiple input multiple output (MIMO), will continue to develop to achieve the massive speed and scale required in 5G. Innovative new technologies will leverage unlicensed spectrum — where Wi-Fi operates — to offload certain traffic from the carrier networks to create more capacity in their data pipes. Low-power technologies such as NarrowBand IoT (NB-IoT), LTE for Machines (LTE-M), Long Range Wide Area Network (LoRaWAN), Sigfox, and others, will be used in billions of IoT devices, and a new radio interface technology — 5G New Radio (5G NR) — will be developed for connections between User Equipment (UE) and carrier enhanced Node B (eNodeB) stations. Finally, carriers will fully embrace virtualization technologies in their core networks to enable massive scale and efficiency.

In this book, you learn about the technological innovations that are being developed today to enable a 5G future. You also learn about potential use cases that will transform entire businesses and industries, and create new business models and opportunities.

About This Book

5G For Dummies, Ixia Special Edition, consists of eight short chapters that explore

- How wireless communications technology has evolved and where it's going next (Chapter 1).
- How developments in today's networks are blazing the 5G trail to higher speeds (Chapter 2).
- Which technologies in unlicensed spectrum will be leveraged in the 5G networks of the future (Chapter 3).
- Why the Internet of Things requires 5G connectivity (Chapter 4).
- Where virtualization in mobile networks can help address the need for scale and elasticity (Chapter 5).
- What 5G New Radio (5G NR) is and how it will help create a 5G future (Chapter 6).
- How 5G will be used in various use case scenarios (Chapter 7).
- Ten common myths and the reality of 5G (Chapter 8).

Foolish Assumptions

It's been said that most assumptions have outlived their uselessness, but we assume a few things nonetheless!

Mainly, we assume that you either work in a technology profession or you're an avid user of wireless communications technology — if you have a smartphone within arm's distance of you, we're talking about you!

Beyond a basic knowledge of wireless communications and mobile technology in general, we don't assume you have a particularly strong technical background. As such, this book is written primarily for nontechnical readers — we explain any technical terms and concepts that come up in this book.

If any of these assumptions describe you, this book is for you! If none of these assumptions describe you, keep reading anyway. It's a great book, and when you finish reading it, you'll know enough about 5G to be dangerous!

Icons Used in This Book

Throughout this book, we occasionally use special icons to call attention to important information. Here's what to expect:

REMEMBER

This icon points out information you should commit to your non-volatile memory, your gray matter, or your noggin' – along with anniversaries and birthdays!

TECHNICAL STUFF

You won't find a map of the human genome here, but if you seek to attain the seventh level of NERD-vana, perk up! This icon explains the jargon beneath the jargon.

TIP

Tips are appreciated, never expected — and we sure hope you'll appreciate these tips! This icon points out useful nuggets of information.

Beyond the Book

There's only so much we can cover in 48 short pages, so if you find yourself at the end of this book thinking "gosh, this is a great book; where can I learn more?" just go to `www.ixiacom.com`.

Where to Go from Here

With our apologies to Lewis Carroll, Alice, and the Cheshire cat:

"Would you tell me, please, which way I ought to go from here?"

"That depends a good deal on where you want to get to," said the Cat — er, the Dummies Man.

"I don't much care where . . . ," said Alice.

"Then it doesn't matter which way you go!"

That's certainly true of *5G For Dummies*, which, like Alice in Wonderland, is also destined to become a timeless classic!

If you don't know where you're going, any chapter will get you there — but Chapter 1 might be a good place to start! However, if you see a particular topic that piques your interest, feel free to jump ahead to that chapter. Each chapter is written to stand on its own, so you can read this book in any order that suits you (though we don't recommend upside down or backward).

We promise you won't get lost falling down the rabbit hole!

IN THIS CHAPTER

» Recapping a century of innovation in wireless communications

» Addressing speed, scale, and responsiveness with 5G networks

» Unlocking the five key fundamentals of 5G

Chapter 1 Understanding the Journey to a 5G Future

In this chapter, you take a glimpse back at the evolution of wireless communications and a look ahead to the 5G future.

Tracing the Evolution of Wireless Communications

For more than a century, radio technology has been enabling wireless communications over ever greater distances and with ever greater capabilities.

In the late nineteenth century, Guglielmo Marconi built the first wireless telegraphy system, capable of transmitting Morse code via radio signals up to one-half mile. Today, more than seven billion mobile devices enable us to communicate with anyone, anywhere in the world.

The first truly mobile two-way radio was developed in 1923 and used in Australian police cars — although it took up the entire back seat of a patrol car. Hand-held radios — "walkie-talkies" — were first used in World War II.

In 1973, the first call on a hand-held cellular phone was made — the cellular phone was described as a "brick" weighing nearly two pounds, with just 30 minutes of talk time and a ten-hour battery recharge time. Ten years later, Motorola introduced the DynaTAC phone, weighing just one pound and costing $3,500.

To support modern wireless communications, cellular networks have evolved over several generations, as follows:

- **1G (analog cellular):** The first analog cellular service was launched in Japan in 1979. In 1983, the Advanced Mobile Phone Service (AMPS) was launched in North America. Analog cellular signals permitted only voice traffic and were not encrypted, so they could be easily intercepted.

  TECHNICAL STUFF

  1G service consumed lots of spectrum and used the frequency division multiple access (FDMA) channel access method. FDMA allocates one or more frequency bands (or channels) to a user for communication.

- **2G (digital cellular):** The second generation of cellular technology was launched in 1991 with the commercial release of the Global Standard for Mobile Communications (GSM) in Finland. Major innovations in 2G networks included:
  - **Digital:** Digital signals generally have less static and background noise, and they use available spectrum more efficiently than do analog signals.
  - **Encryption:** 2G digital calls can be encrypted to make eavesdropping and intercept more difficult.
  - **Data:** Short message service (SMS) text messages were first introduced in 2G networks — O-M-2G!

  TECHNICAL STUFF

  2G technologies use either time division multiple access (TDMA) or code division multiple access (CDMA) channel access methods. TDMA divides a signal into different time slots, enabling multiple callers to share the same frequency channel. CDMA assigns a code to each caller and uses spread-spectrum technology to create a signal with a wider bandwidth.

  In 2000, the European Telecommunications Standards Institute (ETSI) created the General Packet Radio Service (GPRS), which implemented packet-switched domains, in addition to existing circuit-switched domains. GPRS was

dubbed "2.5G" and had nothing to do with *Two and a Half Men,* introduced by CBS three years later.

- **3G (data driven):** Apple and Google brought smartphones to the masses with iPhones and Android devices, respectively, in the early 21st century. These powerful devices — and the mobile apps installed on them (including Global Positioning System or GPS, location-based services, and on-demand video) — created an insatiable appetite for faster download speeds. The first 3G networks, introduced in 1998, provided minimum information transfer rates of 200 kilobits per second (Kbps). The International Telecommunication Union (ITU) has never formally defined a standard for 3G data rates, so downlink data speeds vary widely — from 384 Kbps in a moving vehicle for Wideband Code Division Multiple Access (W-CDMA) to 42.2 megabits per second (Mbps) for Evolved High Speed Packet Access (HSPA+), also known as 3.5G, and 168 Mbps for Advanced HSPA+.
- **4G (Long Term Evolution):** Commercially available 4G mobile networks were rolled out in 2008, and 4G LTE followed in 2010. However, unlike 3G, the ITU Radiocommunication Sector (ITU-R) defined minimum 4G standards — but neither "4G" nor "4G LTE" meets those standards! The ITU-R International Mobile Telecommunications Advanced (IMT-Advanced) requirements include (among other things):
  - Packet-switched all-IP core networks
  - Peak data rates of approximately 100 Mbps for high mobility (such as moving vehicles)
  - Peak data rates of approximately 1 gigabit per second (Gbps) for low mobility (such as walking — or your authors sprinting)

  With the introduction of LTE Advanced, true 4G speeds of up to 1 Gbps finally arrived. LTE Advanced Pro is the next evolution of LTE technology, and it establishes the foundation for 5G. LTE Advanced Pro will deliver speeds in excess of 3 Gbps with less than 2 milliseconds (ms) of latency.

REMEMBER

At this point you may be thinking, "Long Term Evolution — no kidding! Will 5G ever get here?" However, the trend has been for each generation of mobile technology innovation to take about a decade — most of us just didn't pay attention before we got our first smartphones midway through the 3G era.

Focusing on the 5G Vision

The vision for the 5G future is bold: It is much more than just the next iteration of mobile networks. 5G will achieve three main goals:

- **Speed (ultra-high speed radio access):** 5G will provide download speeds of up to 20 Gbps. If you're wondering "Why would anyone ever need that much speed?" first answer this question: When have you ever heard anyone complain that their phone was *too fast*? It's also important to remember that bandwidth is shared by all the users on a cell tower. Today, if a few users are streaming a video at the airport or watching replays of a touchdown in a stadium, chances are that the download is choppy with lots of buffering, and the experience isn't so great. With 5G, you could theoretically download a 40 gigabyte (GB) 4K Ultra-High-Definition (UHD) movie (like *Jaws*) in less than a minute — you're gonna need a bigger data plan!
- **Responsiveness (ultra-low latency):** 5G networks will be used to control autonomous cars and high precision, mission-critical industrial devices in real-time. High reliability and availability at all times is a necessity for these use cases. For this to happen safely, end-to-end latency — the time it takes for data or commands to travel across the network — has to be extremely low. Latency in 5G networks will be five times faster than today's networks — less than 1ms.
- **Scale (massive connectivity):** By 2020, Gartner conservatively forecasts that there will be more than 21 billion connected devices in the Internet of Things (IoT). Some estimates predict more than 50 billion connected IoT devices by 2020. That's anywhere from three to seven connected devices for every person on the planet in 2020 — not including smartphones, tablets, and computers! These devices will have widely varying network requirements — from environmental sensors for agricultural applications installed in remote areas that might send a few bits of data every few days or weeks, to extremely high-precision, low-latency devices in nanobiotechnology, autonomous cars, and mission-critical industrial environments that rely on real-time communication for potentially lifesaving functions. 5G networks will need to handle the massive scale and

challenging connectivity requirements for all these diverse devices, sensors, and applications.

Ordering Up 5G in Five Easy Pieces

5G will be a quantum leap beyond today's networks and will require many technological innovations. We serve them up here in five easy pieces (easier than making wheat toast for Jack Nicholson — "hold the butter, the lettuce, the mayonnaise . . . and the chicken") in this section and the chapters that follow (see Figure 1-1):

- **Speeds and feeds.** Speeds of up to 20 Gbps will be achieved using a combination of innovations such as carrier aggregation (CA), massive multiple input multiple output (MIMO), and quadrature amplitude modulation (QAM). You learn about speeds and feeds in Chapter 2.
- **Unlicensed spectrum:** MNOs are increasingly using unlicensed spectrum in the 2.4 and 5 Gigahertz (GHz) frequency bands. 5G networks will need to tap into the vast amount of spectrum available in these unlicensed bands to offload traffic in heavily congested areas and provide connectivity for billions of IoT devices. Advancements in Wi-Fi, LTE in Unlicensed spectrum (LTE-U), License Assisted Access (LAA), and MulteFire, among others, provide better quality and regulated access to unlicensed spectrum. You learn about these advancements in Chapter 3.
- **Internet of Things (IoT):** IoT devices pose a diverse set of requirements and challenges for 5G networks. It's only fair that IoT should likewise pose a diverse set of solutions as well! You learn about a few of these solutions — including NarrowBand IoT (NB-IoT), LTE Category M1 (LTE-M), Long Range (LoRa) and Sigfox — in Chapter 4.
- **Virtualization:** Network functions virtualization (NFV) enables the massive scale and rapid elasticity that MNOs will require in their 5G networks. Virtualization enables a virtual evolved packet core (vEPC), centralized radio access network (C-RAN), mobile edge computing (MEC), and network slicing — all explained in Chapter 5.

» **New Radio (NR):** Although the other 5G innovations introduced in this section all have strong starting points in LTE Advanced Pro, 5G NR is a true 5G native technology that has yet to be standardized. 5G NR addresses the need for a new radio access technology that will enable access speeds up to 20 Gbps — and you learn about it in Chapter 6!

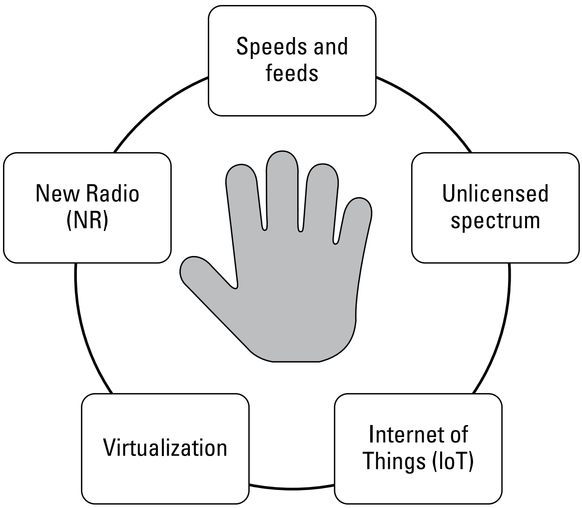

FIGURE 1-1: The five keys to 5G.

IN THIS CHAPTER

» Issuing a license to thrill — with higher speeds

» Cobbling together spectrum with carrier aggregation

» Going well beyond "rabbit ears" with massive antenna arrays

» Seeing stars with quadrature amplitude modulation

Chapter 2
Achieving Faster Speeds and Larger Feeds

Over the past decade, the need for speed in mobile networks has increased dramatically. To address this need, 5G will increase the speeds of today's most advanced Long Term Evolution (LTE) networks by an order of magnitude — from a few gigabits per second (Gbps) to as much as 20 Gbps. In this chapter, you get a glimpse of the engine — or, more correctly, the parts and components of the engine — that will power the 5G networks of the future.

Fattening the Data Pipe

Wireless spectrum is limited and highly regulated throughout the world. The International Telecommunication Union (ITU) allocates frequency spectrum worldwide, and governing bodies within the respective countries then license that spectrum for use by individual mobile network operators (MNOs). The ITU has identified three International Telecommunication Regions

throughout the world with distinct frequency bands allocated to each region (see Figure 2-1).

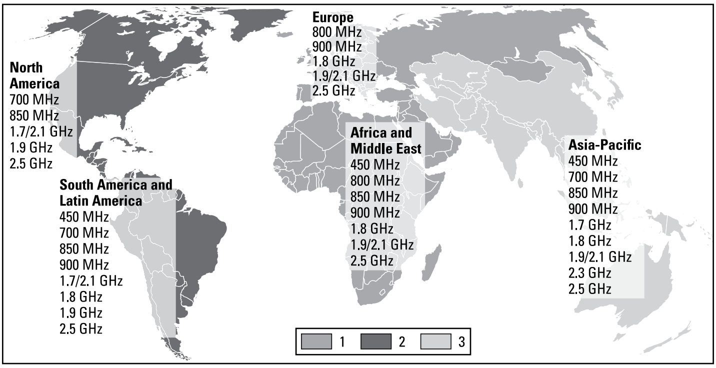

FIGURE 2-1: ITU International Telecommunication Regions and spectrum allocations.

MNOs must pay for the right to transmit and receive data using this shared medium in each country in which they operate. To fatten a wireless data pipe, an MNO must procure additional licenses to use a designated frequency spectrum.

In the U.S., the Federal Communications Commission (FCC) auctions spectrum to MNOs — and we aren't talking about eBay auctions here! In the U.S. alone, spectrum auctions have raised more than 60 billion dollars since 1994. Another challenge for MNOs is that available spectrum is limited and going once . . . going twice . . . sold!

Thus, MNOs must find new ways to use existing spectrum more efficiently. LTE Advanced and LTE Advanced Pro are pioneering the path to 5G, using several innovations to get more data through existing spectrum, including:

- Carrier aggregation (CA)
- Multiple input multiple output (MIMO)
- Quadrature amplitude modulation (QAM)

We All Bundle — with CA

As you might imagine, the process of buying and selling spectrum, over time, causes spectrum to be sliced and diced in some pretty creative ways. MNOs also come and go, or get merged, acquired, and divested (for example, Cingular Wireless and MCI). All of this causes yet another challenge — contiguous spectrum is hard to find and MNOs must cobble together different bands to maximize their available bandwidth. It's sort of like a business being so unreasonable as to want a continuous range of direct inward dialing (DID) phone numbers to simplify its phone switch programming, company directories, and business cards! Except that in the case of frequency spectrum, non-contiguous bands aren't just a messy inconvenience — they limit available bandwidth.

For LTE networks, including LTE Advanced and LTE Advanced Pro, four carrier bandwidths (or sizes) are available for transporting data:

- 5 megahertz (MHz)
- 10 MHz
- 15 MHz
- 20 MHz

Larger bandwidths can transport more data. For example, 10 MHz can transport data at 37.5 megabits per second (Mbps) and 20 MHz can transport data at 75 Mbps. These data transfer rates assume a single antenna on the user equipment (UE) side and on the Evolved Node B (eNodeB) side. This is known as single input single output (SISO).

TECHNICAL STUFF

User equipment (UE) refers to an end-user device in a mobile network, such as a smartphone. *Evolved Node B (eNodeB)* is the MNO hardware — for example, a base transceiver station (BTS) — that wirelessly communicates directly with the UE.

Carrier aggregation (CA) is a technique that allows an MNO to use more than one component carrier (CC) — known as the *secondary carrier* — as an additional data pipe. For example, 2CA enables any of the four carrier bandwidths (5, 10, 15, or 20 MHz) to be used as the primary carrier and any of the other four carrier bandwidths to be used as the secondary carrier.

In the simplest deployment scenario, known as *intra-band contiguous CA*, a 20 MHz primary and a 20 MHz secondary carrier (totaling 40 MHz) would provide twice the maximum possible bandwidth and throughput of a single carrier.

For SISO, a 2CA of 20+20 MHz would provide 150 Mbps of data throughput.

TIP

MNOs in the U.S. are currently deploying 3CA and some are already moving to 4CA (see Figure 2-2). The challenge for MNOs now is to find three or more CCs that they own the license to operate in and can aggregate. The LTE Advanced standard specifies 5CA totaling 100 MHz, while LTE Advanced Pro calls for 32CA totaling 640 MHz of aggregated carrier bandwidth.

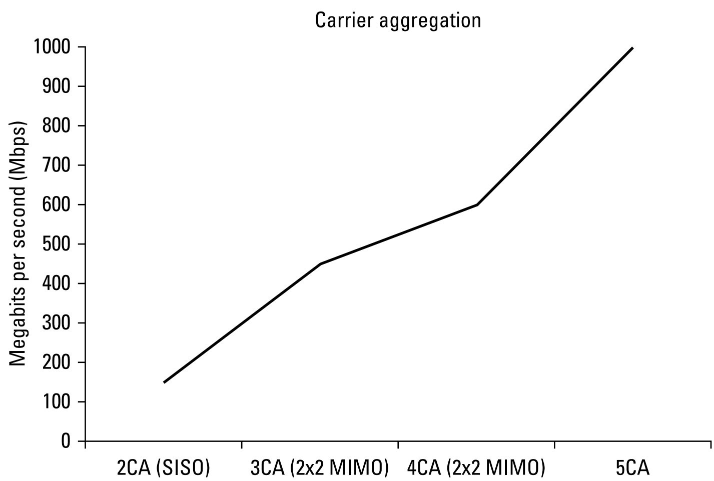

FIGURE 2-2: Carrier aggregation (CA) increases available bandwidth and data throughput.

Eeny, Meeny, Miny, MIMO

One of the techniques for fattening the data pipe defined from day one in 4G LTE networks is multiple input multiple output (MIMO) — using multiple antennas on the transmit and receive side in the wireless network. Using a technique called *spatial multiplexing*, it's possible to send a different data stream on each antenna, thereby increasing the throughput to the cell tower and to the user device.

While 2x2 MIMO deployments (two antennas in, two antennas out) are common today, 4x4 MIMO (four antennas in, four antennas out) is becoming more practical. 4x4 MIMO effectively enables four independent data streams, thereby increasing the throughput by four times. Thus, the 2CA deployment example (described in the previous section) with two 20 MHz channels and a 2x2 MIMO configuration would increase the data throughput from 150 Mbps to 300 Mbps. The same scenario with a 4x4 MIMO configuration would theoretically increase data throughput to 600 Mbps.

LTE Advanced specifications for MIMO accommodate 8-, 16-, and 32-antenna configurations. LTE Advanced Pro specifications increase MIMO configurations to 64 antenna elements. Realistically, using 64 antenna streams to increase the throughput of a single UE isn't practical. However, using a technique called *beamforming,* the eNodeB can focus energy (that is, steer beams of data) to a particular UE, thereby increasing the throughput of that UE while simultaneously handling other UEs through a different set of beams. Massive MIMO will utilize massive antenna arrays — comprised of hundreds of antennas — to provide efficient signal coverage and higher data rates with lower latency in 5G networks.

No Qualms About QAM

Quadrature amplitude modulation (QAM) is a technique widely used to vary data signals on a carrier used for radio communication. When used for digital transmission of radio communication applications, QAM can carry higher data rates than ordinary amplitude modulated and phase modulated schemes. In QAM, the constellation points are normally arranged in a square grid with equal vertical and horizontal spacing. As a result, the most common forms of QAM use a constellation with the number of points equal to a power of 2 (such as 4, 16, and 64). Thus, 16-QAM uses a 16-point constellation while 256-QAM uses a 256-point constellation.

By using higher order modulation formats (that is, more points on the constellation), it is possible to transmit more bits per symbol. So, 64-QAM has six bits per symbol (more data transmitted), whereas 16-QAM uses only four bits per symbol (less data transmitted). However, the points for a higher QAM are closer together and are therefore more susceptible to noise and data errors. 256-QAM has been used for data in digital cable

communications and is now starting to be used for radio communications. 256-QAM is included as part of the LTE Advanced Release 12 standard from the Third Generation Partnership Project (3GPP) because it is likely to work with small cell towers. T-Mobile has achieved 400Mbps downlink speeds in trials through a combination of 4x4 MIMO and 256-QAM.

REMEMBER

5CA and beyond, massive MIMO, and higher-order QAM are all techniques defined as part of the LTE Advanced and LTE Advance Pro standards. With LTE Advanced deployments in full swing, 1 Gbps download speeds are getting closer to becoming a reality in operational networks. 5G will use all these techniques to achieve 20 Gbps data speeds. For example, these are a few of the developments on the 5G horizon:

- CA on very large bandwidths, leading to aggregate totals of 800 MHz (and even 1 GHz) carrier bandwidth
- Massive MIMO antenna arrays of 128 elements or more
- 1024-QAM, and even 4096-QAM

IN THIS CHAPTER

» Expanding cellular traffic to unlicensed spectrum

» Getting LTE-U and LAA to coexist with Wi-Fi in unlicensed spectrum

» Going it alone in unlicensed spectrum with MulteFire

Chapter 3
Tapping into Unlicensed Spectrum

Unlicensed spectrum is used by low-power devices to transmit and receive wireless signals over short distances — typically a few meters. Although specific devices are permitted to operate only in specific bands, the process of getting certifications is not time-consuming or costly, compared to getting a cellular operator license. Some common devices in this category include garage door openers, nursery monitors, home security systems, cordless phones, and Bluetooth speakers/headsets. In this chapter, you learn about the role of unlicensed spectrum in the 5G future.

Giving a "High 5(G)" to Wi-Fi Advancements

Wi-Fi operates in the unlicensed 2.4 gigahertz (GHz) and 5 GHz spectrums. There are fewer rules on who can access these bands and more available spectrum compared to licensed frequency bands. Wi-Fi devices must therefore compete to use the same spectrum as other devices.

Over the past few years, improvements in speed and the advancement of new capabilities have made Wi-Fi viable (and lucrative) for many mobile network operators (MNOs).

MNOs now regularly use Wi-Fi to offload their cellular networks wherever possible. Newer Wi-Fi standards enable massive speed increases. The standards utilize many of the latest multiple input multiple output (MIMO) beamforming techniques and higher quadrature amplitude modulation (QAM) schemes as those used in the licensed spectrum (discussed in Chapter 2).

For example, 802.11ac delivers Wi-Fi speeds of up to several gigabits per second (Gbps) operating in the 5 GHz band, using 80 or 160 megahertz (MHz) wide channels, advanced beamforming techniques, eight spatial streams (MIMO), multi-user MIMO (MU-MIMO), and 256-QAM (which produces four times the spectral efficiency of the previous 802.11n Wi-Fi standard).

The next wave in Wi-Fi is 802.11ax. 802.11ax will use orthogonal frequency-division multiple access (OFDMA) — the same technique used in Long Term Evolution (LTE) networks — in which different subcarriers within a carrier can be used to transport data for different users. As a result, more than one user equipment (UE) device can access the same medium at a given instant without having to back off or concede the medium to another UE device.

TIP

In case you're wondering, other standards exist between 802.11ac and 802.11ax, but they define Wi-Fi standards in unlicensed spectrum other than 2.4 GHz and 5 GHz — and they don't sound as cool as "A-X"!

LTE in Unlicensed Spectrum

LTE in Unlicensed spectrum (LTE-U) is a proposal that was originally developed by Qualcomm for LTE to co-exist with Wi-Fi in shared unlicensed spectrum. In LTE-U, calls are initially set up using licensed LTE spectrum. Additional carriers (for data) can then be aggregated from the unlicensed spectrum. This method will allow the operators to use unlicensed spectrum to "fatten the data pipe."

The Wi-Fi Alliance developed a Wi-Fi co-existence test plan to ensure that Wi-Fi and LTE could peacefully co-exist, and MNOs (including T-Mobile, AT&T, and Verizon) began experimenting with unlicensed spectrum in addition to their licensed spectrum.

LTE-U has also generated a lot of interest from a small cell perspective because this approach potentially makes small cells a viable alternative to Wi-Fi hot spots.

As you might imagine, strong reservations about LTE-U exist, because of concerns that it will unfairly use the unlicensed spectrum and potentially interfere with other Wi-Fi users. Cable companies, such as Comcast, Charter Communications, and Time Warner Cable (TWC), as well as Google and Microsoft, are opposed to LTE-U. As of February 2017, the U.S. Federal Communications Commission (FCC) has approved Ericsson and Nokia equipment as LTE-U certified.

License Assisted Access

Unlike LTE-U, License Assisted Access (LAA) is a standard defined in the Release 13 specification from the Third Generation Partnership Project (3GPP). LAA attempts to resolve contention issues with Wi-Fi in unlicensed spectrum using a protocol many of us learned as children — Listen Before Talk (LBT). The LBT contention protocol requires LAA to listen to the unlicensed channel first, and then, if there is no other active Wi-Fi user (the channel is silent), the LTE user can use the channel.

TIP

A recent report by Strategy Analytics states that only 16 percent of operators can achieve gigabit LTE without using unlicensed spectrum. Using LTE-U and LAA, 64 percent of operators can achieve gigabit LTE.

Qualcomm's over-the-air trials with Deutsche Telecom in Germany showed that LAA had increased coverage and capacity compared to Wi-Fi on the same spectrum. By respecting the LBT maxim (uh, protocol), the behavior of LAA is more closely modeled to the principle "love thy neighbor" and is a better neighbor to Wi-Fi than Wi-Fi is to LTE. Wi-Fi was more of an imp during its formative years and ignores LBT, trying to access the same medium at the same time as others.

Enhanced LAA (eLAA), which aggregates the uplink on unlicensed spectrum, is the next step in the evolution of LAA. eLAA will be defined in the 3GPP Release 14 specification.

REMEMBER

Both LAA and eLAA require the initial call to be set up on LTE licensed spectrum as the primary channel. Unlicensed spectrum is only used to "fatten" the data pipes.

MulteFire

MulteFire goes beyond LTE-U and LAA by enabling the LTE primary channel on unlicensed spectrum. In fact, MulteFire uses unlicensed spectrum exclusively. This means MulteFire can be deployed for LTE by anyone — without owning licensed spectrum — such as Internet service providers (ISPs) and commercial enterprises. MulteFire also benefits MNOs by providing new deployment opportunities for offloading and augmenting their cellular networks.

In January 2017, the MulteFire Alliance released version 1.0, defining an LTE-like network that can run entirely on unlicensed spectrum and, in some cases, may be an alternative to Wi-Fi with more capacity, better security, and easier handoffs across carrier networks.

REMEMBER

Today's 4G spectrum has around 500 MHz of unlicensed spectrum available to deploy LTE-U, LAA, and MulteFire. In July 2016, the FCC opened up 5G spectrum in the U.S., which has 10.85 GHz of total spectrum (3.85 GHz of licensed spectrum and 7 GHz of unlicensed spectrum). The techniques that are now evolving in LTE Advanced Pro (Releases 13 and 14) — LTE-U, LAA (and eLAA), MulteFire, and others (see Figure 3-1) — will be vital as even more unlicensed spectrum becomes available in 5G. The key goal will be to provide users with a seamless experience, irrespective of whether they are operating on a licensed or unlicensed band.

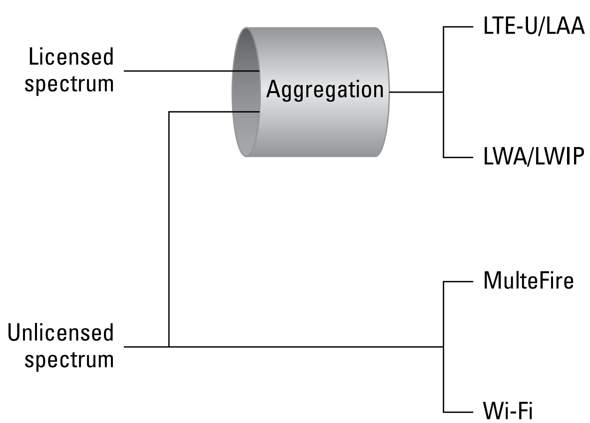

FIGURE 3-1: Leveraging licensed and unlicensed spectrum.

IN THIS CHAPTER

- » Defining IoT connectivity requirements
- » Handling massive scale with NB-IoT
- » Slicing up spectrum for the rise of the machines
- » Exploring LoRaWAN and Sigfox for low-power networks

Chapter 4
Enabling Massive IoT

When 4G networks were introduced in 2008, there were close to 700 million mobile subscribers worldwide. Today, there are more than 7 billion mobile subscribers worldwide. By 2020, according to the most conservative estimates, there will be approximately 20 billion Internet of Things (IoT) devices, in addition to the 9 billion mobile subscribers that are expected worldwide.

Thus, 5G networks must not only deliver extreme speeds and feeds, they must provide massive scale, predictability, and reliability to eventually support as many as a trillion connected devices, including mission-critical and potentially lifesaving applications and scenarios. In this chapter, you learn about the key requirements for IoT device connectivity and the innovations that are being developed to support IoT.

Key Connectivity Requirements for IoT Devices

Unlike smartphones and other cellular devices, IoT device communications can be sporadic in nature. Many of these devices "sleep" (to extend battery life for ten or more years in some cases)

for long periods of time — hours, days, or weeks — before transmitting a few bytes of data, and thus needn't always be connected to the network. 5G networks must be designed to handle infrequent, but important communications from these types of IoT devices. Although the amount of data these devices send may be significantly lower, they may still be of a time-critical nature. For example, a sensor that detects a hazardous condition may instruct an Evolved Node B (eNodeB) element to shut down equipment in an industrial plant or building. These types of communication, though extremely rare, must be handled with the utmost responsiveness and reliability.

Additionally, eNodeB elements will require massive capacity to scale to support tens of thousands of IoT devices — all with different communications requirements and characteristics — in a single cell.

Finally, a wide variety of security threats and new attack vectors will be surfaced in IoT devices. Unlike many of today's threats — identity theft and credit card fraud, for example — many IoT security threats will be potentially life threatening. Future threats may include hacked control systems in autonomous vehicles and smart grids, or compromised medical devices such as insulin pumps and pacemakers. Thus, 5G technologies will need to provide secure end-to-end communications throughout the network.

NarrowBand IoT (NB-IoT)

The Third Generation Partnership Project (3GPP) Long Term Evolution (LTE) Advanced Pro Release 13 specification defines a new standard — NarrowBand IoT (NB-IoT) — for handling low volumes of data (similar to 2G) from tens of thousands of devices in a single cell (tower, not amoeba).

NB-IoT extends LTE to even narrower bandwidths optimized for low data rate, latency-tolerant IoT applications. NB-IoT reduces device complexity, enables multiyear battery life, and provides deeper coverage to reach sensors in challenging locations, such as remote rural areas or inside buildings.

Perhaps one of the most attractive features of NB-IoT is its ability to leverage already ubiquitous LTE networks, in addition to providing high quality of service (QoS) and comprehensive security.

NB-IoT can be deployed in three different modes:

- **Standalone as a dedicated carrier:** Can use GSM frequencies in a bandwidth of 200 kHz. This does not require LTE.
- **Guard band:** Uses a free resource block within the LTE guard band. This allows the IoT devices to not compete with other LTE devices for the resource blocks within the carrier.
- **LTE in-band:** Uses a resource block within the LTE frequency band. The rest of the blocks are used by the regular LTE devices.

Long Term Evolution for Machines (LTE-M)

Like NB-IoT, Long Term Evolution for Machines (LTE-M or LTE Category M1) leverages a narrow slice of existing LTE spectrum to send and receive data for IoT devices. LTE-M has the same benefits as NB-IoT, but uses a larger network slice than NB-IoT (1.4 MHz compared to 180 KHz in NB-IoT) and leverages the LTE protocol more than the NB-IoT in terms of reusing the same control, data, and transport channels.

TIP

Verizon launched the first LTE-M network in the U.S. on March 31, 2017, and ATT Wireless was expected to follow shortly after.

LoRaWAN and Sigfox

Long Range Wide Area Network (LoRaWAN) is a Low Power Wide Area Network (LPWAN) specification for wireless, battery-operated IoT devices. LoRaWAN operates in the sub-1 GHz unlicensed spectrum band. This limits the volume and frequency of traffic, as well as the ability of the base station to control the network and send traffic down. However, LoRaWAN has great advantages in terms of battery life and cost, and communication is bi-directional.

Sigfox is a French company that created a technology similar to LoRaWAN for IoT device communication. Sigfox technology uses

very low bandwidth connections. It is not bi-directional and is only used for sending sparse uplink data with very limited downlink. Like LoRaWAN, Sigfox operates in the sub-1 GHz space and thus uses very low power.

LoRaWAN and Sigfox will be used with certain types of sensors, smart meters, and other low data IoT devices. A disadvantage for these technologies is that, unlike NB-IoT, which is built on top of existing LTE infrastructure, LoRaWAN and Sigfox are not integrated with LTE. However, the cost of deploying a LoRaWAN or Sigfox based IoT device is far less than for an NB-IoT or LTE-M device — by an order of magnitude, since NB-IoT and LTE-M devices must integrate LTE modules into their devices.

REMEMBER

As countries and mobile network operators (MNOs) make IoT technology decisions, it is likely that many standards, protocols, and technologies will need to co-exist. Factors such as cost, coverage, battery life, and integration with older 4G networks will determine which standards, protocols, and technologies are best for each use case.

The 3GPP specifications for IoT technologies are just starting to come out as part of the LTE-A Pro standards. Many IoT devices will need to operate at very low power, ideally suited for sub-1 GHz spectrum rather than the millimeter wave (mmWave) spectrum (discussed in Chapter 6). That said, there are some compelling 5G techniques, like resource spread multiple access (RSMA) waveforms that allow grant-free transmissions for “things” to send their data without prior scheduling by the eNodeB. As a result, the scheduling algorithm becomes less complex. 5G will also enable multi-hop mesh for these low-power devices, allowing out-of-coverage devices to relay to other connected devices in order to send data to the eNodeB.

IN THIS CHAPTER

» Virtualizing the network for 5G and IoT

» Knowing which network elements to virtualize

Chapter 5
Getting Real About the Need to Virtualize

Virtualization has been a hot topic in the technology industry for many years and its advantages transcend the cellular industry. In this chapter, you learn about the network elements that can be virtualized and the essential role of virtualization in 5G.

Driving 5G and IoT with Virtualization

Telecommunications companies and mobile network operators (MNOs) have invested heavily in their 4G and Long Term Evolution (LTE) networks. These organizations have embraced virtualization to enable faster, more agile, and scalable deployments that can keep pace with the explosion in subscriber data traffic and consumption, all while keeping control of their overall capital and operating costs. Even though these investments have already given users mobile connectivity of unprecedented speed and pervasiveness, they have only laid the foundation of what's to come, as 5G and smart, connected devices start to roll out.

A recent study by a division of Nokia Bell Labs provides a glimpse of what's coming. The study found that the number of Internet of Things (IoT) connected devices is expected to expand from 1.6 billion in 2014 to well over 20 billion by 2020. Also, by 2020, global consumption demand for digital content and services on portable devices will see an average increase of 30 to 45 times the

levels seen in 2014. Thus, MNOs will need to further accelerate their technology investments to meet ever-increasing consumer and business connectivity demands.

Recognizing the IoT explosion

Although MNOs in the U.S. are starting to embrace "pre-standard" 5G, vying for the first mover's advantage, the standards are not expected until 2018. This has echoes of the early days of 3G in the late 1990s and early 2000s, before proprietary implementations were standardized. It isn't surprising that some operators in the U.S. have already announced their plans to deploy 5G later this year, and some of the early adopters in Korea, Japan, and China are also ready to roll out 5G. Because of the rapid deployment, many 5G concepts are being solidified quickly.

5G is sometimes narrowly classified as a higher bandwidth radio access technology. But it is much more than that. It will also be the network for low-power devices and sensors that are classified as IoT devices, as well as low-latency applications. One example is the low latency required for some mission-critical devices, such as autonomous vehicles. The need for low latency will dictate that key LTE base station functions are distributed, with some moving closer to the edge and others being pooled in the cloud.

Another example is that vertical sectors will require different types of services from the 5G network. Some will need high bandwidth, while others will need low power. Some will need very low latency, and others will need very high availability. The vast volume of IoT devices will range from those that send multiple gigabits of data per second to those that will only send a few bits every month. This flexibility and elasticity can be supported only by advanced network virtualization.

Focusing on service

To support such varying 5G use cases across multiple verticals, MNOs need to shift from being network-centric to being more service-oriented.

To understand this shift, consider the concept of network slicing (see Figure 5-1). Here are a few typical cases:

- Mobile broadband with higher bandwidth video requiring high availability everywhere

- Low-power sensors that can operate on a pair of AA batteries for 10 years
- Autonomous vehicles that can zip through crowded city streets but brake within microseconds when they sense potential obstructions in their paths

TECHNICAL STUFF

Each of these scenarios requires a different configuration of the requirements and parameters in the network, potentially including:

- Home Subscriber Server (HSS)
- Mobility Management Entity (MME)
- User equipment (UE)
- Enhanced Node B (ENB or eNodeB)
- Serving Gateway (SGW)
- Packet Data Network Gateway (PGW)
- Policy and Charging Rules Function (PCRF)
- LTE Evolved Packet Core (EPC) interfaces (S1-MME, S11, S1-U, SGi)

In essence, each use case requires its own network slice. Networks must be built in a manner that allows speed, availability, capacity, and coverage to be allocated in logical slices to meet the demands of each use case.

The best way to implement network slices will be via virtualization — to use service provider software-defined networking (SDN), network functions virtualization (NFV), and network orchestration (see Figure 5-2). In each of these cases, the SDN controller will configure and build network slices that include service chains such as deep packet inspection (DPI), emails, and security scans per user or per service. The network services — including the Centralized Radio Access Network (C-RAN), Virtual Evolved Packet Core (vEPC), and Virtual IP Multimedia Subsystem (vIMS) — are virtualized as virtual network functions (VNFs) that allow MNOs to set up services rapidly, and scale them in response to network and service demands.

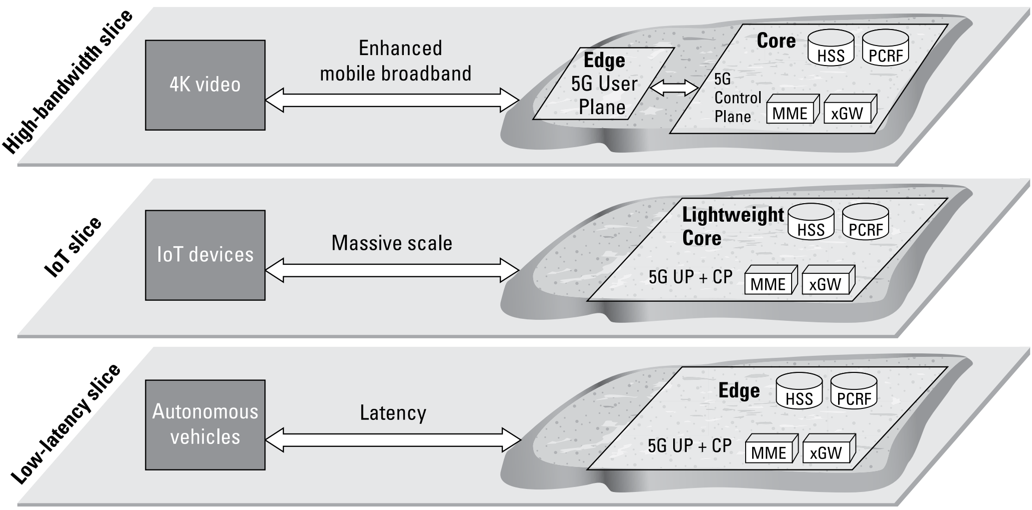

FIGURE 5-1: 5G network slices.

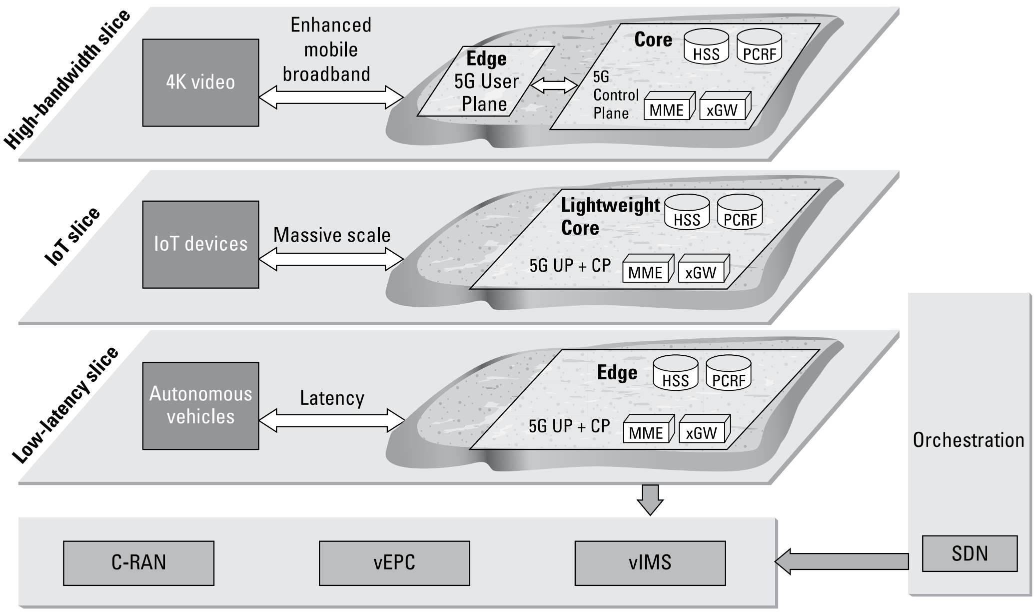

FIGURE 5-2: Network slices, VNFs, and management and orchestration in a 5G architecture.

Managing the migration

Thus, virtualization will be a vital piece of the puzzle as 5G is rolled out and the IoT grows. But the speed and agility that virtualization enables must be balanced against the need for network visibility, resilience, manageability and security, throughout the development, roll-out, and mass usage of each service.

MNOs and service providers must weigh the trade-offs between

- Quality and cost.
- Flexibility and control.
- Moving too quickly and not moving fast enough.

REMEMBER

As a result, the demand for simple, end-to-end solutions that can efficiently test and validate the effectiveness and benefits of virtualization at every stage is only going to increase. Network virtualization will be a key driver of the IoT ecosystem as it develops — and full-lifecycle reliability and performance testing will be a key element of this shift.

Virtualizing Network Components

When LTE networks were conceptualized, one notable difference from earlier 3G architectures was the idea of a central "brain" — the evolved Node B (eNodeB). From the eNodeB — the point at which the cellular network wirelessly connects directly to user equipment (UE) — to the Internet, the connectivity would all be Internet Protocol (IP) based.

When data centers and other wired network components (such as routers, switches, and firewalls) started being virtualized on standard off-the-shelf servers, it was only natural for the wireless, IP-based 4G evolved packet core (EPC) to follow.

Virtual EPC (vEPC)

Because packet gateways, policy servers, and subscriber databases are all IP-based in the LTE network, the EPC is an excellent

candidate for replacing proprietary hardware with virtualized functions hosted on standard, off-the-shelf servers. The benefit for MNOs is the elasticity this model enables — no more dedicated hardware and no need to oversubscribe every part of the network. Servers can be quickly and easily provisioned or de-provisioned based on real-time subscriber capacity needs. With SDN controllers and EPC functions migrated to NFV, and orchestration schemes added to manage it all, the wireless core could be fully virtualized and cloud ready!

Centralized Radio Access Network (C-RAN)

Virtualization in the radio access network (RAN) requires separating out latency-sensitive elements and the radio itself, then pooling the rest of the baseband functions into centralized baseband units (BBUs). Which functions should stay with the remote radio head (RRH) and which ones should move to centralized BBUs has been extensively studied, and a few options exist.

The C-RAN model, which requires a fiber connection between the RRH and the BBUs, is popular in some regions of the world, such as China and Korea. This front-haul interface is challenging because it has distance limitations and is bandwidth limited. It uses a protocol known as the Common Public Radio Interface (CPRI). China Mobile has been in the forefront of the C-RAN architecture. Other countries such as Japan and Korea have also adopted C-RAN. In the U.S., Verizon is looking at implementing C-RAN for small cells.

Mobile Edge Computing (MEC)

Mobile Edge Computing (MEC) offers an important balance as cellular networks move to a central model. MEC allows certain latency-sensitive components to be moved to the network edge. For example, even though it may make business sense for MNOs to centralize several functions into VNFs running on standard off-the-shelf servers, some critical functions may need to be

closer to the edge of the network to ensure high availability, low latency, and higher levels of security.

TIP

The network edge is also a good place to host application servers that require local context. For example, if you are driving around and you receive restaurant ads on your mobile device based on your current location, you need the application service to be close to the edge to avoid a lengthy delay in the app that could render the information obsolete.

IN THIS CHAPTER

- Tuning in to the basic functions of 5G New Radio
- Catching the millimeter wave

Chapter 6

Creating a New 5G World Order with New Radio (NR)

In this chapter, you learn about a completely new technology that creates the foundation for 5G — the 5G New Radio (NR) physical air interface.

5G NR Basics

Unlike the other 5G elements (covered in previous chapters), that advance the industry toward the goals of 5G networks, 5G New Radio (NR) is not an evolution of 4G Long Term Evolution (LTE) innovations. 5G NR is a completely new technology specification — a physical air interface — that is required to achieve the extreme bandwidth, low latency, and massive scalability requirements of 5G.

REMEMBER

The other four areas of 4G LTE innovation that are being further developed for 5G include:

- **Speeds and feeds:** Discussed in Chapter 2, innovations such as carrier aggregation (CA), massive multiple input multiple output (MIMO), and quadrature amplitude modulation (QAM), among others, enables carriers to "fatten" the data pipe.

- **Unlicensed spectrum:** Discussed in Chapter 3, LTE in unlicensed spectrum (LTE-U), License Assisted Access (LAA and enhanced LAA, or eLAA), and MulteFire enable carriers to leverage unlicensed spectrum as additional data pipes.
- **Internet of Things (IoT):** Discussed in Chapter 4, IoT developments include NarrowBand IoT (NB-IoT), LTE for Machines (LTE-M or LTE Category M1), and Low Power Wide Area Network (LPWAN) specifications such as Long Range WAN (LoRaWAN) and Sigfox. These developments enable wireless communication with a diverse array of billions of IoT devices.
- **Virtualization:** Discussed in Chapter 5, software-defined networking (SDN) and network functions virtualization (NFV) enable mobile network operators (MNOs) to achieve cost-effective scalability and elasticity in their core networks with innovations that include network slicing, virtual evolved packet core (vEPC), centralized radio access network (C-RAN), and mobile edge computing (MEC).

The 5G NR specification enables the following goals of 5G:

- **Extreme bandwidths:** 5G NR aggregates eight component carriers (CCs). The carrier width specifications are still in development, but will likely be 100 megahertz (MHz) or greater, providing a total of approximately one gigahertz (GHz) of aggregated bandwidth — wide enough to carry 20 gigabits of data per second.
- **Low latency:** In LTE Advanced, each subframe (there are 10 subframes) is handled in one millisecond (ms). 5G will be five to ten times faster — each subframe is handled in 100 to 200 microseconds (µs). 5G NR will use new channel coding techniques, such as low density parity check (LDPC), that are more efficient than existing techniques, resulting in shorter transmission time intervals (TTIs).

  TECHNICAL STUFF

  A technique called *scalable orthogonal frequency-division multiplexing (OFDM) numerology* will be used to support different use cases and scenarios within the same frame. Effectively, shorter TTIs will be used for low latency, high reliability use cases, and longer TTIs for higher spectral efficiency, higher bandwidth use cases. 5G NR can also effectively multiplex between short and long TTIs, thereby allowing a diverse set of users to simultaneously use the system.

- **Massive MIMO:** 5G NR extends MIMO up to 256 antenna elements and enables massive MIMO. This is a key enabler for higher spectrum bands. The antenna elements in this case are smaller, thereby making it less complex to build a massive array.
- **Massive IoT:** 5G NR will use resource spread multiple access (RSMA) on the uplink to enable grant-free transmission of data on the uplink. A device does not need an enhanced Node B (eNodeB) to give it a grant (or slot) in the pipe to transmit data. This capability eliminates the need for signaling and allows devices to send small packets asynchronously. 5G NR will also address distance and location challenges in low-power IoT devices, using a technique called *multi-hop mesh* to relay uplink data via nearby devices.

5G NR is part of the Release 15 specification from the Third Generation Partnership Project (3GPP). Two versions of 5G NR exist:

- **Non-standalone (NSA) 5G NR:** NSA will use the existing LTE radio and core network as the control plane anchor for mobility management and coverage, while adding a new 5G carrier. Early 2019 deployments of 5G NR will use this configuration. In this mode, the connection is anchored in 4G LTE while 5G NR carriers are used to boost data rates and reduce latency.
- **Standalone (SA) 5G NR:** SA will use the new 5G core network (5GCN) architecture, including the full control and user plane offered by 5G.

An interim release of the 5G NR NSA specification was accelerated to the end of 2017 to enable large-scale trials and deployments for enhanced mobile broadband (eMBB) use cases to begin in 2019. The 5G NR SA specification is expected in mid-2018.

More Spectrum — mmWave Bands

In the U.S., the Federal Communications Commission (FCC) has opened a total of 10.85 GHz of spectrum above 24 GHz to enable 5G use cases. The new spectrum includes 3.85 GHz of licensed spectrum from 27.5 to 28.35 GHz and 37 to 40 GHz, and 7 GHz of unlicensed spectrum from 64 to 71 GHz.

These bands — between 30 GHz and 300 GHz — are known as millimeter wave bands (mmWave). These high frequency bands translate to narrow wavelengths in the range of one to ten millimeters. There are some challenges with mmWave, including:

- Short transmission paths and high propagation losses over long distances and anything that is not line of sight
- Weakened signals in gases and precipitation

However, the short transmission paths and propagation loss characteristics of mmWave enable spectrum reuse, by limiting the interference between adjacent cells. Additionally, because of the extremely short wavelengths of mmWave signals, transmission paths can be extended using small, multi-element dynamic beamforming antennas that can be installed in user equipment (UE) such as smartphones.

TIP

5G NR, operating at very high frequencies with small coverage areas (because of propagation and line-of-sight issues), is ideal for dense urban locations, where cell sizes are generally small (approximately 200 meters).

IN THIS CHAPTER

» Bringing 5G home

» Staying entertained on the move

» Getting a dose of virtual and augmented reality

» Driving 5G for smart cars and autonomous vehicles

» Living in a connected world

» Assimilating humans and machines

Chapter 7
Exploring 5G Use Cases

In this chapter, you learn about some of the key use cases that will be enabled by 5G.

Fixed Wireless Broadband Service

5G will begin its commercial drive with the fixed wireless broadband use case in the U.S. AT&T and Verizon are racing to be the first to deliver fixed wireless broadband service to their customers.

Verizon acquired XO Communications, which included the 28 gigahertz (GHz) spectrum, in 2016. One of the primary drivers for Verizon will be to offer 5G as an alternative to cable/advanced digital subscriber line (ADSL) for high-speed broadband access to residential customers for gigabit speed Internet, 4K content, virtual reality (VR), and more. The goal is to achieve greater than one gigabit per second (Gbps) speeds without digging trenches to get fiber to your home.

AT&T is also pursuing 5G on fixed wireless in both the 28 GHz and 37 GHz spectrum bands. 5G video trials are currently underway for some residential customers, allowing them to stream DIRECTV NOW video service over a fixed wireless 5G connection. In its internal testing, AT&T Wireless claims it can now achieve 13 Gbps over a 5G connection. Like Verizon, AT&T is also looking at 5G to replace home broadband connections delivered by cable companies.

If successful, these use case trials could signal the end of the "cable guy" coming out "sometime between 1 p.m. and 4 p.m." to route a coaxial cable through your home. In areas where there is currently only one option for home broadband or television service, this technology could also lead to more competition, better service, and lower rates for subscribers.

Cable companies, such as Charter Communications, are also exploring 5G technologies. Charter is planning to conduct 28 GHz 5G experiments in the near future with antennas mounted on a mobile trailer and van with hydraulic masts, which will be moved to each of the test locations.

TIP

The motivation for a company like Charter is that 5G will enable a host of new products that take advantage of low-latency, high-capacity networks, including virtual reality (VR) and augmented reality (AR) applications, many of which will be used in a fixed home or office location.

Entertainment Everywhere

The natural progression of the fixed wireless broadband use case (discussed in the previous section) enables mobile broadband at extreme data rates "everywhere" — not only to a fixed home or office location.

Although some of the envisioned mobile broadband experience started in Long Term Evolution (LTE) networks, 5G takes it to a different level with 4K (and subsequently 8K) television, high dynamic range video streaming, 3D videos, and more. All these applications require very high bandwidth, and many require always-on connectivity to push real-time information to the users. The transformation from fixed wireless to wireless everywhere

requires several mobility-specific factors to be addressed, such as fast handoffs, seamless connectivity at very high speeds and low latency, high reliability when mobile, and others.

REMEMBER

Cloud storage is also driving the growth of uplink data rates. In the past, content was mostly downloaded and thus required a "fat" pipe in only one direction: the downlink from the base station to the mobile device. However, content is increasingly being uploaded to different cloud storage platforms, requiring robust data pipes in both the downlink and uplink directions. Cloud gaming is another 5G driver that requires fast responsiveness and high broadband capacity.

Virtual Reality (VR) and Augmented Reality (AR)

Virtual reality (VR) technology creates a fully immersive, computer-generated experience that simulates or re-creates real-life situations and environments. In contrast to VR, augmented reality (AR) layers computer-generated images and enhancements onto a real-world situation or environment to provide a more meaningful context for user interaction.

Although current 4G networks are sufficient for some early-adopter VR and AR experiences, the introduction of 5G will enable more novel VR and AR experiences and make them available for mass adoption by consumers. Offering much more capacity, lower latency, and a more uniform experience, 5G will not only improve, but will also be a requirement for some of the most exciting AR and VR use cases, including:

- Sharing live streaming content on social media from event venues along with 50,000 other people in a stadium becomes even more challenging with 4K 360-degree video because each user is uploading 25 Mbps at the same time.
- Next-generation VR and AR experiences will have "six degrees of freedom" (6DoF) — the next level of immersion — allowing users to move within and intuitively interact with the environment. 6DoF content is an order of magnitude richer in naturalness and interactivity than current "three degrees of freedom" (3DoF) video. 3DoF experiences, such as 360-degree

video, allow the user to look around rotationally from a fixed position. 6DoF experiences, which are available in video games today, allow the user to move spatially through the environment just by walking or leaning their head forward.

6DoF head-motion tracking is required to enjoy 6DoF content in an intuitive manner. Many industries such as tourism, education, and other forms of immersive video will flourish as 6DoF technologies evolve. Most components of the video delivery pipeline are currently ill-suited for 6DoF video, including capture devices, production software, codecs, compression algorithms, the network, and players. 6DoF video also demands bit rates in the range of 200 Mbps to 1Gbps, depending on the end-to-end latency.

Connected and Autonomous Vehicles

Smart, connected cars are already here — and some security risks have already been notoriously demonstrated — and self-driving autonomous vehicles are beginning to appear on our roads. Other applications that 5G will enable for smart, connected cars include:

- **Traffic safety:** This includes the ability to detect hazardous road conditions, such as inclement weather or nearby accidents, and provide real-time guidance for appropriate courses of action to enable safer driving and reduce the risk of accidents. For example, imagine a situation in which your driverless car gets a real-time message (in microseconds) that a truck is rapidly approaching the intersection that you are about to cross. Your car then automatically slows down to let the truck pass the intersection, thereby avoiding a possible accident.
- **Entertainment (for passengers):** Live video and music streaming (including 4K ultra high-definition movies), interactive video games, cloud connectivity, and data exchange elaborate the need for high capacity and high mobility mobile broadband.
- **Augmented reality (AR):** Displaying key information in near real-time for drivers requires low latency so that the information is timely and relevant. In the earlier truck

example, a live situation is being tracked by the involved IoT devices and infrastructure, and relayed in real-time to the users — vehicle and human.

- **Self-driving, autonomous vehicles:** These will require ultra-reliable, high-speed communication between different driverless cars, and between cars and infrastructure.

The Connected World

Smart homes, smart cities, multiple industries (such as health, retail, smart grids, and remote factories) have a common thread — they are using more and more devices and sensors that communicate with one another and the rest of the world.

Many of these devices are mission critical; others may send high-definition video, requiring high availability and very low latency. Yet another set of devices may send small data packets relatively infrequently (for example, every few hours, days, or weeks). Some examples of common use cases with diverse connectivity requirements include:

- **Logistics and freight:** These devices and sensors typically require lower data rates, but need wide coverage and reliable location information.
- **Smart grid:** A smart grid requires low latency sensors to regulate the use of utilities such as electricity, natural gas, and water. Leveraging digital information, such as the behaviors of suppliers and consumers, allows the smart grid to improve the efficiency, reliability, economics, and sustainability of the production and distribution of these resources.
- **Remote medical:** Collaborating about a medical case with other surgeons located thousands of miles away was a use case scenario discussed as part of the Long Term Evolution (LTE) rollout. It can become a reality with the extreme bandwidth, low latency, and high availability of 5G networks.
- **Hazardous areas:** The ability to remotely explore mining areas or shut down a nuclear power plant during an emergency — in a fraction of the time required for human interaction, and without risk to human life — is possible with 5G.

Augmented Humans

Looking ahead to the more distant future — perhaps 30 years from now — Google futurist Ray Kurzweil predicts humans will be able to upload their entire minds to computers and become "digitally immortal" — an event called *singularity.*

In 2011, IBM's Watson beat former winners on the television game show *Jeopardy!*, proving that computers can outperform the best of humans when it comes to synthesizing information and beating them to the buzzer. Google Home and Amazon Echo are becoming more common in homes — perhaps a bit unnerving at first as they start entering our private lives, and increasingly taking center stage when we want them to tell us more about the weather, play our favorite song, read us our favorite *5G For Dummies* book, or tell a few jokes. As machine learning and artificial intelligence develop further, these intelligent devices will better understand human behavior and evolve beyond databases of information. Eventually, they will also become more mobile and intrinsic in our lives, rather than sitting on a shelf in our living rooms.

REMEMBER

5G — with its extreme bandwidths, very low latency, and massive scale support — will be a critical component in creating these real-time experiences, initially as an assistant to humans, and eventually even "thinking" for humans (in some cases). Shopping for clothes with your kids or selecting your next car will become a more immersive experience. 5G technology might also assist humans as an augmented partner, offloading some of the tasks humans don't want to "expend their own brain cells" on. Although it may sound like science fiction, 5G might be a starting point for the next evolution of humans and machines.

IN THIS CHAPTER

» **Going beyond speed and latency**

» **Looking at drivers and timelines**

» **Overcoming misconceptions about limitations**

» **Recognizing complementary technologies**

» **Transforming entire industries**

Chapter 8
Ten Myths About 5G — Debunked

In this chapter, we expose ten common myths about 5G — and we clue you in to the reality behind them. Keep these points in mind:

- **5G is all about higher speeds to the user.** Although one of the key goals of 5G is to provide extreme bandwidth (high-speed data) to users, low latency and massive scale are other key goals of 5G. So, 5G isn't just about speed!
- **5G requires less than one millisecond latency.** Although less than one millisecond of latency is a goal of 5G, 5G networks will be deployed before that target is actually achieved.
- **Smartphones will lead the charge to 5G.** The iPhone and Android were born in the 3G era and virtually exploded (literally, in some cases) during the 4G LTE era. However, 5G will not only enable faster and better smartphones — it will also lead to mass-market consumer VR and AR devices, sensors and applications for smart homes and cars, industrial robots, and billions of other Internet of Things (IoT) devices yet to be conceived.

- **5G will be commercially available in 2017.** Although Verizon plans to roll out 5G fixed mobility in 2017 and Olympic 5G trials will be underway during the 2018 Winter Olympics, 5G standards will not be finalized until the end of 2017. Thus, although some early, pre-standard versions of 5G will be coming soon, the 5G standard is not complete. Standards-compliant 5G will be coming much later.
- **5G is only for short-range, line-of-sight communication.** In addition to other frequency bands, 5G uses mmWave bands, which are ideal for very short ranges. However, plenty of ongoing experiments demonstrate how techniques such as beamforming can achieve greater ranges to users in challenging environments beyond line-of-sight.
- **5G will be used only in very high bands.** Although 5G will be deployed in very high millimeter wave (mmWave) bands, it will also re-use spectrum in lower bands, both licensed and unlicensed.
- **5G will replace 4G LTE.** 5G will coexist with 4G LTE for a long time to come. 4G has plenty to offer for many current applications such as voice, data, and even IoT.
- **5G will be a revolution, not an evolution.** Although 5G brings in a new physical layer (in 5G New Radio, or 5G NR), there is plenty of evolution from LTE-A Pro technologies such as carrier aggregation (CA), massive multiple input/multiple output (MIMO), quadrature amplitude modulation (QAM), unlicensed spectrum (LTE in unlicensed spectrum or LTE-U, License Assisted Access or LAA, and MulteFire, among others), IoT, and virtualization.
- **5G will be required to drive IoT.** IoT will initially be driven by LTE-A Pro where NarrowBand IoT (NB-IoT) is specified. In addition, other low-power technologies, such as Long Range Wide Area Network (LoRaWAN) and Sigfox, have been defined for IoT.
- **The 5G winners will be the operators and vendors.** Mobile network operators (MNOs), network equipment manufacturers (NEMs), and smartphone manufacturers were the primary business beneficiaries of 4G LTE. However, 5G will transform many industries, including car manufacturing, agriculture, health and medicine, transportation and logistics, and many more.

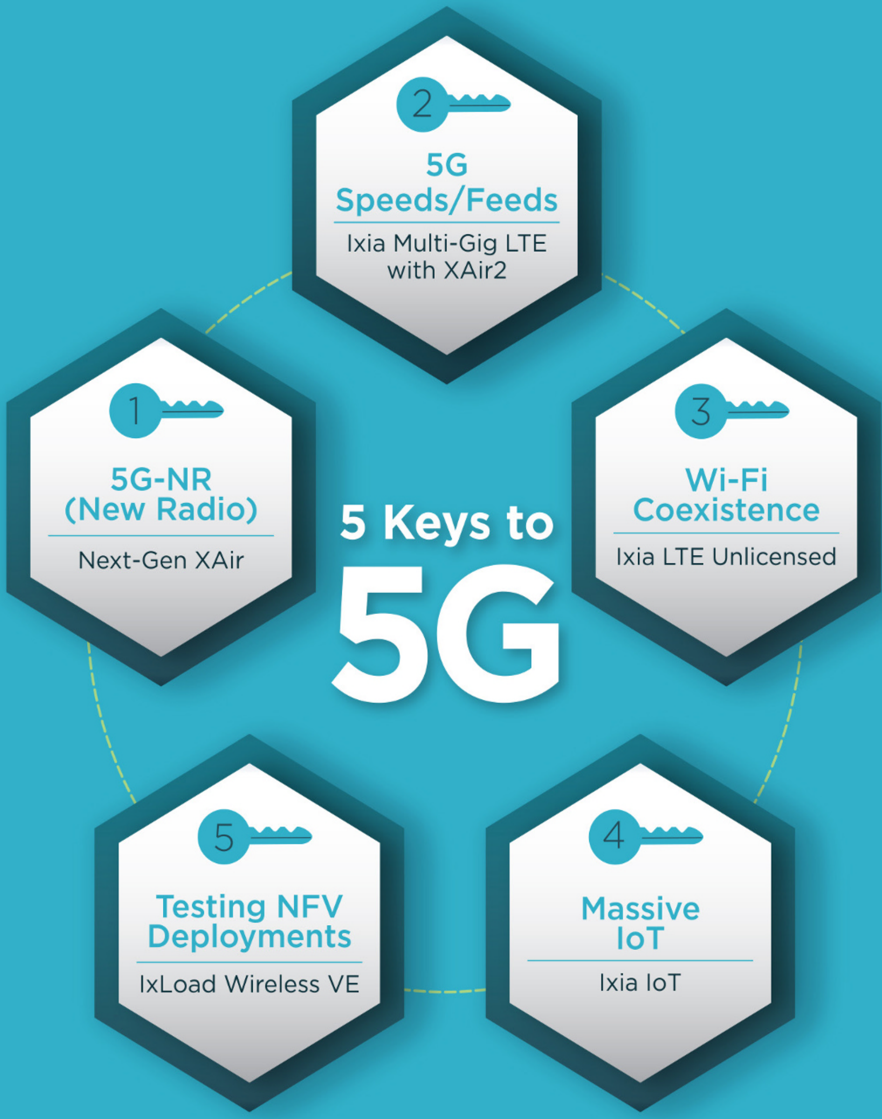
5 Keys to
5G
1
5G-NR (New Radio)
Next-Gen XAir
2
5G Speeds/Feeds
Ixia Multi-Gig LTE with XAir2
3
Wi-Fi Coexistence
Ixia LTE Unlicensed
4
Massive IoT
Ixia IoT
5
Testing NFV Deployments
IxLoad Wireless VE

Dream up new opportunities in the 5G future

The next-generation mobile network is on the horizon. 5G, the successor to 4G LTE networks, will enable significantly greater mobile speeds — as much as 20 gigabits per second — with very low latency. 5G will support a massive array of devices, from smart phones to virtual reality devices to small sensors. In this book, you learn about the technological innovations being developed today to enable a 5G future. You also learn about potential use cases that will transform entire industries and create new business models and opportunities.

Inside...

- Where wireless communication is headed
- Why higher speeds are the future
- How the IoT will employ 5G connectivity
- Why the unlicensed spectrum matters
- Why New Radio is a starting point for 5G
- How 5G will enable new business models

ixia

Kalyan Sundhar is Vice President — Mobility, Virtualization, and Applications at Ixia. He has more than 25 years experience in the industry, building cutting-edge products. **Lawrence C. Miller** has worked in information technology for more than 25 years. He has written more than 60 *For Dummies* books.

for dummies®
A Wiley Brand

ISBN: 978-1-119-42415-4
Ixia part number:
915-8156-01
Not for resale

WILEY END USER LICENSE AGREEMENT

AUGUST 2017

LTE to 5G: Cellular and Broadband Innovation

This white paper was written for 5G Americas by Rysavy Research (http://www.rysavy.com) and utilized a composite of statistical information from multiple resources.

Table of Contents

Introduction

Mobile computing with wireless communications has already changed how people socialize and how companies do business. Yet, we are still in the nascent stages of the transformation that ubiquitous connectivity is enabling. Early examples of this exciting future include virtual and augmented reality, autonomous driving, smart cities, wearable computers, and connected devices throughout our environment. While no one can predict the full extent of innovation that the new global broadband fabric, aided by complementary innovations such as AI, will unleash, one thing is certain: We are rushing toward an extraordinary time.

The step from 3G to 4G was dramatic, and industry advances occurring now in LTE and 5G will be even greater. Standards bodies are standardizing 5G, a process that will continue through the 2020 timeframe, with ongoing enhancements continuing during the next decade. Some operators are deploying pre-standard 5G in trials this year, and initial standards-based networks could be deployed as early as 2019. 5G will not replace LTE; in most deployments, the two technologies will be tightly integrated and co-exist through at least the late-2020s.

Many of the capabilities that will make 5G so effective are appearing in advanced forms of LTE. With carrier aggregation, for example, operators have not only harnessed the potential of their spectrum holdings to augment capacity and performance, but the technology is also the foundation for entirely new capabilities, such as operating LTE in unlicensed bands.

The computing power of today’s handheld computers rivals that of past mainframe computers, powering intuitive operating systems and millions of applications. Coupled with affordable mobile broadband connectivity, these devices provide such unprecedented utility that billions of people are using them.

With long term growth in smartphone and other mobile device use limited by population, innovators are increasingly turning their attention to the Internet of Things (IoT), which already encompasses a wide array of applications. Enhancements to LTE, followed by 5G IoT capabilities, will connect wearable computers, sensors, and other devices, leading to better health, economic gains, and other advantages. 5G addresses not only IoT deployments on a massive scale but also enables applications previously not possible that depend on ultra-reliable and low-latency communications, sometimes called “mission-critical applications.” Although a far more fragmented market than smartphones, the benefits will be so great that the realization of IoT on a massive scale is inevitable.

Regulatory policies are striving to keep pace, addressing complex issues that include how best to allocate and manage new spectrum, network neutrality, and privacy. Policy decisions will have a major impact on the evolution of mobile broadband.

These are exciting times for both people working in the industry and those who use the technology—which today is nearly everybody. This paper attempts to capture the scope of what the industry is developing, beginning with Table 1, which summarizes some of the most important advances.

Table 1: Most Important Wireless Industry Developments in 2017

Development	Summary
5G Research and Development Accelerates	5G, in early stages of definition through global efforts and many proposed technical approaches, could be deployed in non-standalone versions as early as 2019. Deployment will continue through 2030. Some operators will deploy pre-standard networks for fixed-wireless access in 2017. 5G is being designed to integrate with LTE, and some 5G features may be implemented as LTE-Advanced Pro extensions prior to full 5G availability.
5G New Radio (NR) Being Defined	Key aspects of the 5G NR have been determined, such as radio channel widths and use of OFDMA. The first version, specified in Release 15, will support low-latency, beam-based channels, massive Multiple Input Multiple Output (MIMO) with large numbers of controllable antenna elements, scalable-width subchannels, carrier aggregation, Cloud Radio-Access Network (RAN) capability, and dynamic co-existence with LTE.
LTE Has Become the Global Cellular Standard	A previously fragmented wireless industry has consolidated globally on LTE. LTE is being deployed more quickly than any previous-generation wireless technology.
LTE-Advanced Provides Dramatic Advantages	LTE capabilities continue to improve with carrier aggregation, 1 Gbps peak throughputs, higher-order MIMO, multiple methods for expanding capacity in unlicensed spectrum, new IoT capabilities, vehicle-based communications, small-cell support including Enhanced Inter-Cell Interference Coordination (eICIC), lower latency, Self-Organizing Network (SON) capabilities and Enhanced Coordinated Multi Point (eCoMP).
Internet of Things Poised for Massive Adoption	IoT, evolving from machine-to-machine (M2M) communications, is seeing rapid adoption, with tens of billions of new connected devices expected over the next decade. Drivers include improved LTE support, such as low-cost and low-power modems, enhanced coverage, higher capacity, and service-layer standardization, such as oneM2M.
Unlicensed Spectrum Becomes More Tightly Integrated with Cellular	The industry has developed increasingly sophisticated means for integrating Wi-Fi and cellular networks, such as LTE-WLAN Aggregation (LWA) and LTE-WLAN Aggregation with IPSec Tunnel (LWIP), making the user experience ever more seamless. The industry has also developed and is now deploying versions of LTE that can operate in unlicensed spectrum, such as LTE-Unlicensed (LTE-U), LTE-Licensed Assisted Access (LTE-LAA), and

Development	Summary
	MulteFire. Cellular and Wi-Fi industry members are successfully collaborating to ensure fair spectrum co-existence.
Spectrum Still Precious	Spectrum in general, and in particular licensed spectrum, remains a precious commodity for the industry. Recently added spectrum in the United States includes the 600 MHz band, auctioned in 2017, and the 3.5 GHz Citizens Broadband Radio Service (CBRS) "small-cell" band, which could see initial deployments in 2018. 5G spectrum will include bands above 6 GHz, including "mmWave" (30 GHz to 100 GHz), with the potential of ten times (or more) as much spectrum as is currently available for cellular. Radio channels of 200 MHz and 400 MHz, and even wider in the future, will enable multi-Gbps peak throughput.
Small Cells Take Baby Steps, Preparing to Stride	Operators have begun installing small cells, which now number in the tens of thousands. Eventually, hundreds of thousands if not millions of small cells will lead to massive increases in capacity. The industry is slowly overcoming challenges that include restrictive regulations, site acquisition, self-organization, interference management, power, and backhaul.
Network Function Virtualization (NFV) Emerges	Network function virtualization (NFV) and software-defined networking (SDN) tools and architectures are enabling operators to reduce network costs, simplify deployment of new services, reduce deployment time, and scale their networks. Some operators are also virtualizing the radio-access network, as well as pursuing a related development called cloud radio-access network (cloud RAN). NFV and cloud RAN will be integral components of 5G.

The main part of this paper covers the transformation of broadband, exploding demand for wireless services, the path to 5G including planned and expected capabilities, new LTE innovations, supporting technologies and architectures, voice over LTE (VoLTE), Wi-Fi Calling, LTE for public safety, options to expand capacity, and spectrum developments.

The appendix delves into more technical aspects of the following topics: 3GPP Releases, Data Throughput, latency, 5G, LTE, LTE-Advanced, LTE-Advanced Pro, HetNets and small cells, IoT, cloud RANs, Unlicensed Spectrum Integration, self-organizing networks, the IP Multimedia Subsystem, broadcast/multicast services, backhaul, UMTS/WCDMA,[1] HSPA, HSPA+, UMTS TDD, and EDGE/EGPRS.

[1] Although many use the terms "UMTS" and "WCDMA" interchangeably, in this paper "WCDMA" refers to the radio interface technology used within UMTS, and "UMTS" refers to the complete system. HSPA is an enhancement to WCDMA.

Broadband Transformation

Broadband networks rely on a fiber core with various access technologies, such as fiber to the premises, coaxial cable, digital subscriber line (DSL), or wireless connections. LTE provides a broadband experience, but capacity limitations prevent it from being the only broadband connection for most users. As a result, a majority of consumers in developed countries have both mobile broadband and fixed broadband accounts.

Two developments will transform the current situation:

1. **Fiber Densification**. Multiple companies are investing to extend the reach of fiber, decreasing the distance from the fiber network to the end node.

2. **5G Standardization and Deployment.** As 5G mmWave technology, including massive MIMO and beamforming, becomes commoditized, it will increasingly be a viable alternative to fixed-access technologies such as coaxial, DSL, and even fiber connections. 5G commercial services will enable a new innovation cycle. The ability to create new applications and services with fewer limitations will take the connected society to a new level.

Consequently, the companies that provide broadband service may change, and eventually, fixed and mobile broadband services may converge. For a more detailed discussion of trends in broadband, including the disruptive role of mmWave, refer to the 2017 Datacomm Research and Rysavy Research report, *Broadband Disruption: How 5G Will Reshape the Competitive Landscape*.[2]

As shown in Figure 1, the emerging broadband network is one with denser fiber and competing access technologies in which wireless connectivity plays a larger role.

[2] Details at https://datacommresearch.com/reports-broadband/.

Figure 1: Fiber Densification with Multiple Access Technologies, including mmWave

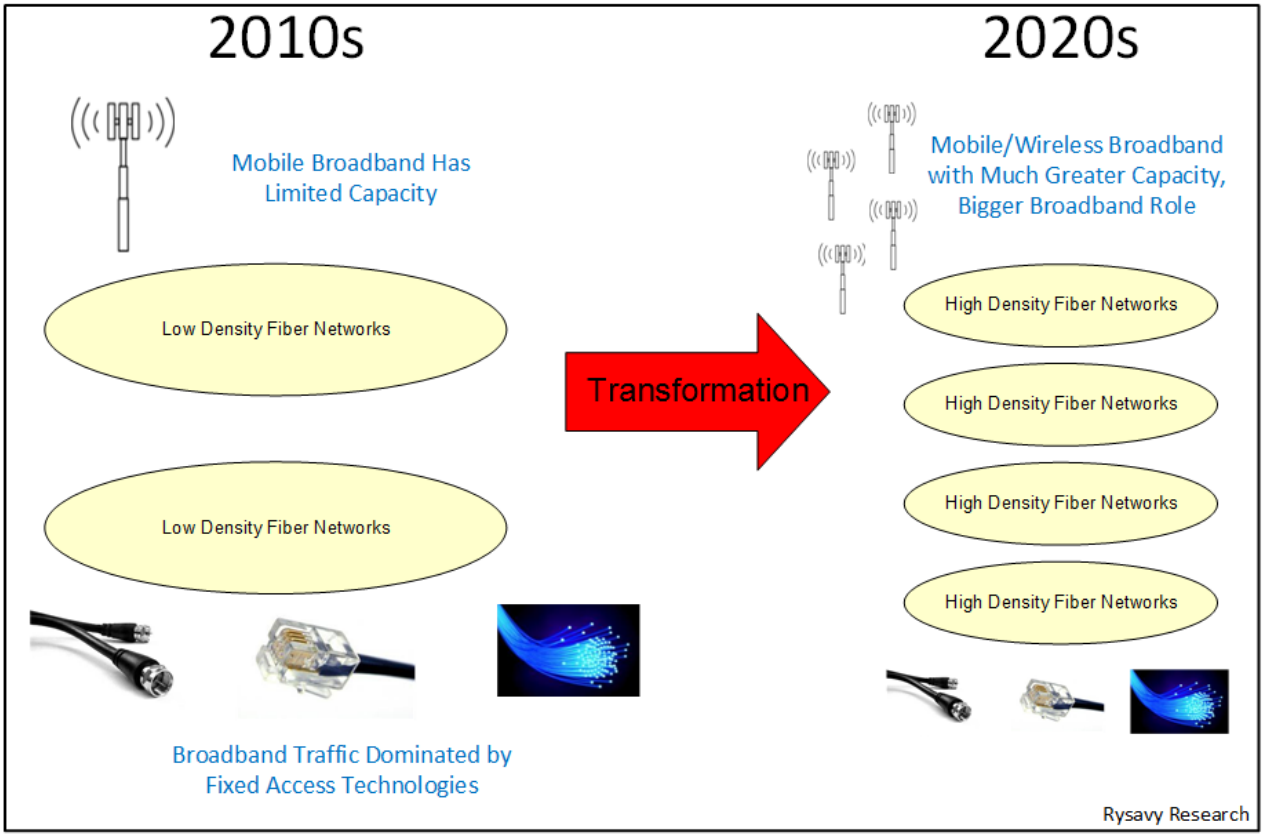

Many elements are interacting to transform mobile broadband, but the factors playing the most important roles are emerging capabilities for IoT, radio advances granting access to far more spectrum, small cells, new network architectures that leverage network function virtualization and software-defined networking, and new means to employ unlicensed spectrum. Except for access to high-band spectrum, a 5G objective, these advances apply to both LTE and 5G.

Figure 2: Fundamental Mobile Broadband Transformational Elements

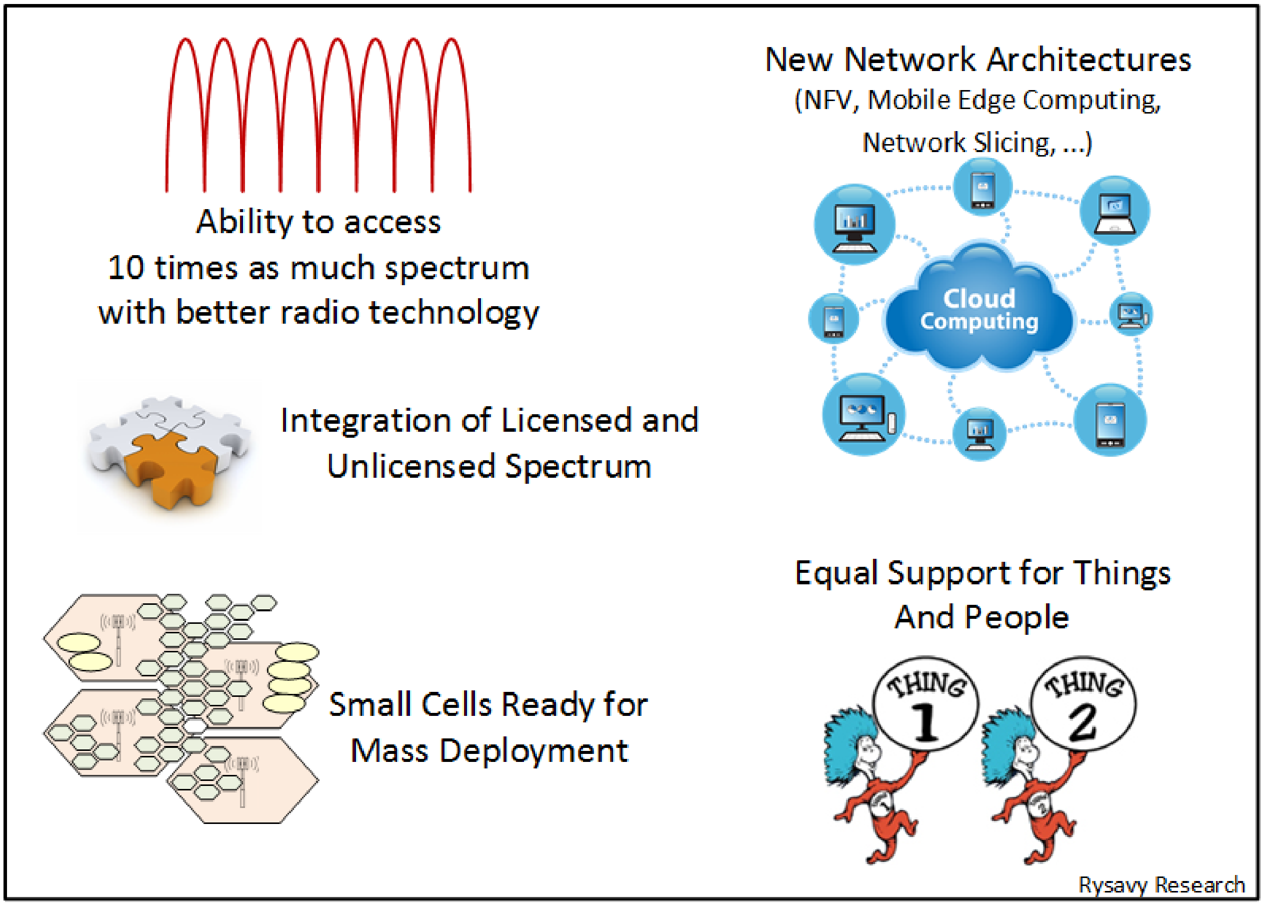

In the past, developers used modems and networks designed for human communication for machine-type applications. But now, new modes of network operation, initially in LTE then enhanced further in 5G, will cater to the unique needs of a wide variety of machine applications, addressing low-cost, long battery life, long communications range, and a wide variety of throughputs. For instance, some IoT applications need only low-throughput communications, some sending only a small number of bits per day.

As for spectrum, throughout radio history, technology has climbed up a ladder to use higher frequencies. What were called “ultra-high frequencies” when made available for television are now considered low-band frequencies for cellular. Frequencies above 6 GHz, particularly mmWave frequencies, are the new frontier. Networks will ultimately take advantage of ten times as much spectrum as they use now, and likely even more over time. Although challenging to use because of propagation limitations and higher penetration loss, massive MIMO, beam steering, beam tracking, dual connectivity, carrier aggregation, small-cell architectures with self-backhauling, and other methods will help mitigate the challenges at these frequencies. The result: massive increases in capacity in localized areas.

In addition to accessing higher bands, cellular technologies are integrating unlicensed spectrum more efficiently, using technologies such as LTE-U, LAA, MulteFire, LWA, and LWIP. This integration will immediately augment small-cell capacity, improving the business case for small cells.

Small cells, on the roadmap for many years but held back by implementation difficulties, such as backhaul, are on the verge of large scale deployment, leading ultimately to densities as high as ten small cells or more for every macro cell. Paving the way are better wireless backhaul solutions, neutral-host capabilities enabled by new technologies, and soon, access to mmWave bands.

Facilitating the capabilities listed above, networks are becoming programmable. Using a distributed, software-enabled network based on virtualization and new architectural approaches such as Multi-access Edge Computing (MEC) and network slicing, operators and third parties will be able to deploy new services and applications more rapidly, and in a more scalable fashion. Centralizing RAN signal processing will also play a huge role; depending on the deployment scenario, such centralization will increase RAN efficiency and decrease deployment cost.

This paper lists the dozens of other innovations also fueling mobile and cellular technology transformation. Together, these transformed networks will mean that for millions, and ultimately billions, of people, wireless connections will be the only connections that they need. These networks will also provide the foundation for entire new industries, ones not yet even conceived.

Exploding Demand

Two technology trajectories have created critical mass: handheld computing and fast wireless connections. This combined computing and communications platform inspires the innovation that has produced millions of mobile applications.

IoT is a third trajectory. LTE, and eventually 5G, will connect tens of billions of devices. And fixed-wireless access could be a fourth. 5G, with expected network capacity a hundred times greater than 4G networks, will make wireless connections not only a viable substitute for wireline broadband connections for tens of millions of users over the next ten years, but make that broadband connection the only connection that many users need.

Figure 3: Exploding Demand from Critical Mass of Factors

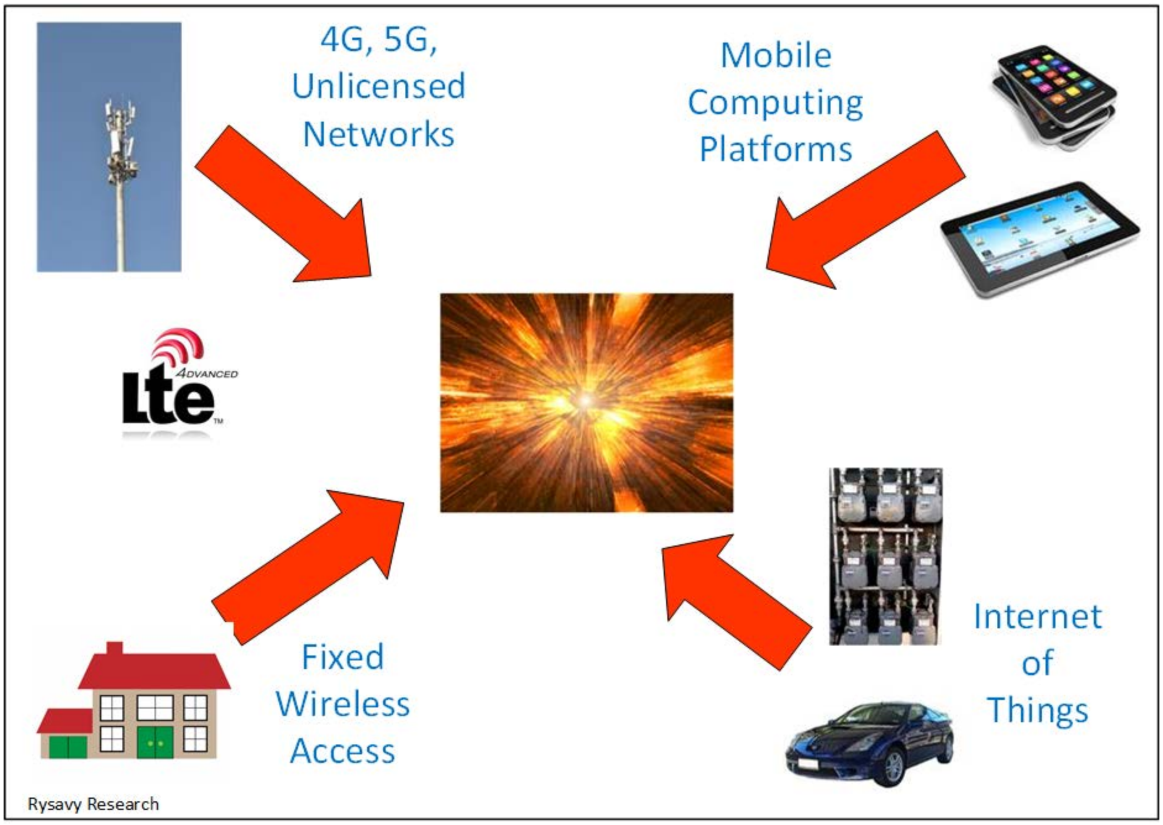

This section analyzes some of these demand factors.

Application Innovation

When planning 4G network technology, who could have predicted applications such as Uber and Lyft, which combine location information with mapping and online payment and are now disrupting the taxi industry and even challenging notions of private vehicle ownership? While some applications of new technology can be predicted, many cannot.

More efficient technology not only addresses escalating demand, it also provides higher performance, thus encouraging new usage models and further increasing demand.

Today's smartphones and tablets, dominated by the iOS and Android ecosystems, in combination with sophisticated cloud-based services, provide a stable, well-defined application environment, allowing developers to target billions of users. Developers have rich platform-specific development tools; web-based tools such as HTML5; application programming interfaces (APIs) for mobile-specific functions, such as WebRTC (Web Real-Time Communications); and cloud-based services for applications and application services, such as notifications, IoT support, and mobile-commerce.

Of concern to some companies in the wireless industry, however, are current network neutrality rules that could possibly hamper innovation. By restricting prioritization, for example, the rules seem to fail to recognize that traffic streams from different applications have inherently different quality of service requirements.[3]

Internet of Things

Current M2M and Internet of Things applications include vehicle infotainment, connected healthcare, transportation and logistics, connected cars, home security and automation, manufacturing, construction and heavy equipment, energy management, video surveillance, environmental monitoring, smart buildings, wearable computing, object tracking, and digital signage. Municipalities, evaluating the concept of "smart cities," are exploring how to optimize pedestrian and vehicular traffic, connect utility meters, and deploy trash containers that can report when they need emptying.

Although promising, the IoT market is also challenging, with varying communications requirements, long installation lifetimes, power demands that challenge current battery technology, cost sensitivity, security and data privacy concerns, unsuitability of conventional networking protocols for some applications, and other factors that developers must address. Consequently, the IoT opportunity is not uniform; it will eventually comprise thousands of markets. Success will occur one sector at a time, with advances in one area providing building blocks for the next.

Cloud-based support platforms and standardized interfaces are essential for development and deployment of IoT applications. For example, oneM2M has developed a service-layer that can be embedded in hardware and software to simplify communications with application servers.[4]

To address the IoT opportunity, 3GPP is defining progressive LTE refinements that will occur over multiple 3GPP releases. These refinements include low-cost modules that approach 2G module pricing and enable multi-year battery life. See the section "Internet of Things and Machine-to-Machine" in the appendix for more details.

Video Streaming

Video represents the greatest usage of data on smartphones. Just an hour a day of mobile video at 1.0 Mbps throughput, common with YouTube or Netflix, consumes 13.5 GB per month. Many streams, now available in high-definition (HD), consume even more data.

---

[3] For further discussion, see Rysavy Research, *How "Title II" Net Neutrality Undermines 5G*, April 19, 2017. Available at http://www.rysavy.com/Articles/2017-04-How-Title-II-Net-Neutrality-Undermines-5G.pdf. Also see *How Wireless is Different – Considerations for the Open Internet Rulemaking*, September 12, 2014. Available at http://www.rysavy.com/Articles/2014-09-Wireless-Open-Internet.pdf.

[4] OneM2M home page: http://onem2m.org/.

See the Appendix section “Data Consumed by Video” for a quantification of data consumed by video for multiple usage scenarios.

An increasing number of video applications adapt their streaming rates based on available bandwidth. By doing so, they can continue to operate even when throughput rates drop. Conversely, they take advantage of higher available bandwidth to present video at higher resolution. Fortunately, application developers are becoming sensitive to bandwidth constraints and are offering options for users to reduce consumption.

Nevertheless, video can consume so much data that cutting the broadband cord at the same time as the television cord is not possible for most consumers. With 5G’s massive increase in capacity, however, an increasing percentage of users will use wireless connections as their only broadband connections, including for all their entertainment needs.

Cloud Computing

Cloud computing inherently increases data consumption because it requires communications for all operations. Examples include data synchronization and backup, cloud-based applications (such as email, word processing, and spreadsheets), automatic photo uploads, and music and video streaming.

5G Data Drivers

Futurists can predict some 5G applications, but many others will arise as industries evolve or come into existence to take advantage of new network capabilities. Some potential applications of 5G include:

- Ultra-high-definition, such as 4K and 8K, and 3D video.
- Augmented and immersive virtual reality. Ultra-high-fidelity virtual reality can consume 50 times the bandwidth of a high-definition video stream.
- Realization of the tactile internet—real-time, immediate sensing and control, enabling a vast array of new applications.
- Automotive, including autonomous vehicles, driver-assistance systems, vehicular internet, infotainment, inter-vehicle information exchange, and vehicle pre-crash sensing and mitigation.
- Monitoring of critical infrastructure, such as transmission lines, using long battery life and low-latency sensors.
- Smart transportation using data from vehicles, road sensors, and cameras to optimize traffic flow.
- Mobile health and telemedicine systems that rely on ready availability of high-resolution and detailed medical records, imaging, and diagnostic video.
- Public safety, including broadband data and mission-critical voice.
- Sports and fitness enhancement through biometric sensing, real-time monitoring, and data analysis.
- Fixed broadband replacement.